

N O T I C E

THIS DOCUMENT HAS BEEN REPRODUCED FROM
MICROFICHE. ALTHOUGH IT IS RECOGNIZED THAT
CERTAIN PORTIONS ARE ILLEGIBLE, IT IS BEING RELEASED
IN THE INTEREST OF MAKING AVAILABLE AS MUCH
INFORMATION AS POSSIBLE

(NASA-TM-82838) BIBLIOGRAPHY OF LEWIS
RESEARCH CENTER TECHNICAL PUBLICATIONS
ANNOUNCED IN 1981 (NASA) 295 P
HC A13/MF A01

N82-27191

CSCL 05B

G3/85

Unclas

28107

Bibliography of Lewis Research Center Technical Publications Announced in 1981

May 1982



NASA

PREFACE

In 1981, Lewis Research Center's 899 research authors published 384 technical publications which were announced to and reached the worldwide scientific community. Although the number of reports published this year has decreased just as the staff has decreased, the number of reports published per person per year has increased slightly. Each year the number of technical presentations given at seminars, society symposia, and Lewis-hosted conferences increases. In 1981, Lewis authors published approximately 66 percent of their research contributions in outside publications and the remainder as NASA research reports. Lewis authors primarily use society proceedings, seminar presentations, journal articles, and transactions to describe their work. Many have received awards for their contributions; among them are the following:

The 1981 Lewis Distinguished Paper Award was presented to Krishna Rao V. Kaza and Robert E. Kielb for their paper entitled "Effects of Mistuning on Bending-Torsion Flutter and Response of a Cascade in Incompressible Flow." This paper was presented at the Dynamics Specialists Conference sponsored by the American Institute of Aeronautics and Astronautics held in Atlanta, Georgia, April 9-11, 1981. A description of the paper is given in abstract A81-29465 (p. 92) in this bibliography.

The Society for the Advancement of Material and Process Engineering (SAMPE) presented its "1981 Best Paper by a SAMPE Member Award" to Ruth H. Pater for the paper she presented at the Thirteenth National SAMPE Technical Conference held in Mount Pocono, Pennsylvania, October 13-15, 1981. The paper entitled "The Properties of Novel Bisimide Amine Cured Epoxy/Cellon 6000 Graphite Fiber Composites" by Daniel A. Scola and Ruth H. Pater was published in the January/February 1982 issue of the SAMPE Journal. The report is described in International Aerospace Abstracts, vol. 22, no. 6, p. 828 (March 15, 1982).

The Society of Automotive Engineers' Oral Presentation Award was given to Brent A. Miller for his outstanding presentation of the paper "The NASA High-Speed Turboprop Program" by J. F. Dugan, B. A. Miller, E. J. Graber, and D. A. Sagerser at the SAE Aerospace Congress and Exposition in Los Angeles, California, October 13-16, 1980. The paper is described in abstract A81-34156 (p. 21) of this bibliography.

In 1981, 312 contractor-authored research reports were produced, an increase over the previous year's output of 307. In addition, 25 patent applications were filed and 18 patents were issued.

All the publications in this collection were announced in the 1981 issues of STAR (Scientific and Technical Aerospace Reports) and IAA (International Aerospace Abstracts).

The arrangement of the material is by NASA subject category, as noted in the Contents. The Lewis-authored items are listed first, followed by the contractor items. Within each of these groups is listed report literature, in N-number sequence, followed by the journal and conference presentations, in A-number sequence.

The various indexes will help locate specific publications by subject, author, contractor organization, contract number, and report number.

George Mandel
Chief, Management Services Division

CONTENTS

	Page
AERONAUTICS (GENERAL)	1
AERODYNAMICS	3
AIR TRANSPORTATION AND SAFETY	9
AIRCRAFT COMMUNICATIONS AND NAVIGATION	10
AIRCRAFT DESIGN, TESTING AND PERFORMANCE	11
AIRCRAFT INSTRUMENTATION	12
AIRCRAFT PROPULSION AND POWER	13
RESEARCH AND SUPPORT FACILITIES (AIR)	31
ASTRONAUTICS (GENERAL)	32
LAUNCH VEHICLES AND SPACE VEHICLES	33
SPACE TRANSPORTATION	34
SPACECRAFT COMMUNICATIONS, COMMAND AND TRACKING	35
SPACECRAFT DESIGN, TESTING AND PERFORMANCE	36
SPACECRAFT INSTRUMENTATION	37
SPACECRAFT PROPULSION AND POWER	38
CHEMISTRY AND MATERIALS (GENERAL)	44
COMPOSITE MATERIALS	45
INORGANIC AND PHYSICAL CHEMISTRY	49
METALLIC MATERIALS	51
NONMETALLIC MATERIALS	60
PROPELLANTS AND FUELS	66
ENGINEERING (GENERAL)	68
COMMUNICATIONS	69
ELECTRONICS AND ELECTRICAL ENGINEERING	71
FLUID MECHANICS AND HEAT TRANSFER	74
INSTRUMENTATION AND PHOTOGRAPHY	79
MECHANICAL ENGINEERING	80
QUALITY ASSURANCE AND RELIABILITY	90
STRUCTURAL MECHANICS	91
EARTH RESOURCES	94
ENERGY PRODUCTION AND CONVERSION	96
ENVIRONMENT POLLUTION	115
GEOPHYSICS	116
METEOROLOGY AND CLIMATOLOGY	117
AEROSPACE MEDICINE	118
MATHEMATICAL AND COMPUTER SCIENCES (GENERAL)	119
COMPUTER PROGRAMMING AND SOFTWARE	120
COMPUTER SYSTEMS	121
NUMERICAL ANALYSIS	122
STATISTICS AND PROBABILITY	123
PHYSICS (GENERAL)	124
ACOUSTICS	125
ATOMIC AND MOLECULAR PHYSICS	130
OPTICS	131
PLASMA PHYSICS	132

SOLID-STATE PHYSICS	135
THERMODYNAMICS AND STATISTICAL PHYSICS	136
DOCUMENTATION AND INFORMATION SCIENCE	137
ECONOMICS AND COST ANALYSIS	138
LAW AND POLITICAL SCIENCE	139
URBAN TECHNOLOGY AND TRANSPORTATION	140
GENERAL	142
SUBJECT INDEX (KEYWORDS)	A-1
PERSONAL AUTHOR INDEX (INCLUDES LEWIS AND CONTRACTOR AUTHORS)	B-1
CORPORATE SOURCE INDEX (CONTRACTOR ORGANIZATIONS)	C-1
CONTRACT NUMBER INDEX	D-1
REPORT/ACCESSION NUMBER INDEX (INCLUDES PATENTS)	E-1

01 AERONAUTICS (GENERAL)

N81-18002* National Aeronautics and Space Administration. Lewis Research Center, Cleveland, Ohio.

STATUS OF NOISE TECHNOLOGY FOR ADVANCED SUPERSONIC CRUISE AIRCRAFT

c71
James R. Stone and Orlando A. Gutierrez / In NASA. Langley Research Center. Supersonic Cruise Res. 1979, Pt. 1. Mar. 1980 p 493-518 refs (For primary document see N81-17981 09-01)

Avail: NTIS HC A23/MF A01 CSCL 20A

Developments in acoustic technology applicable to advanced supersonic cruise aircraft, particularly those which relate to jet noise and its suppression are reviewed. The noise reducing potential of high radius ratio, inverted velocity profile coannular jets is demonstrated by model scale results from a wide range of nozzle geometries, including some simulated flight cases. These results were verified statistically at large scale on a variable cycle engine (VCE) testbed. A preliminary assessment of potential VCE noise sources such as fan and core noise is made based on the testbed data. Recent advances in the understanding of flight effects are reviewed. The status of computerized noise prediction methods is assessed on the basis of recent test data, and the remaining problem areas are outlined. M.G.

N81-18004* National Aeronautics and Space Administration. Lewis Research Center, Cleveland, Ohio.

ADVANCED TECHNOLOGY FOR CONTROLLING POLLUTANT EMISSIONS FROM SUPERSONIC CRUISE AIRCRAFT

c45
Robert A. Duerr and Larry A. Diehl / In NASA. Langley Research Center. Supersonic Cruise Res. 1979, Pt. 1. Mar. 1980 p 535-549 (For primary document see N81-17981 09-01)

Avail: NTIS HC A23/MF A01 CSCL 13B

Gas turbine engine combustor technology for the reduction of pollutant emissions is summarized. Variations of conventional combustion systems and advanced combustor concepts are discussed. Projected results from far term technology efforts aimed at applying the premixed prevaporized and catalytic combustion techniques to aircraft combustion systems indicate a potential for significant reductions in pollutant emission levels. M.G.

A81-29052 * The future of aeronautical propulsion. W. L. Stewart (NASA, Lewis Research Center, Cleveland, Ohio). In: International Symposium on Air Breathing Engines, 5th, Bangalore, India, February 16-22, 1981, Proceedings. (A81-29051 12-07) Bangalore, National Aeronautical Laboratory, 1981, p. KN-1 to KN-11.

This keynote address discusses some of the future challenges and opportunities confronting aeronautics where propulsion is a key factor. The discussion covers various aircraft types including commercial transports, general aviation and military aircraft and identifies propulsion technology required to accommodate further advancements in these types of aircraft. This is then followed by a discussion of some of the emerging technologies that, if properly exploited, will have significant effect on the engines of the '90's. Some comments on further advancements in the traditional technologies are also included. (Author)

A81-30003 * NASA research in aeropropulsion. W. L. Stewart and R. J. Weber (NASA, Lewis Research Center, Cleveland, Ohio). *American Society of Mechanical Engineers, Gas Turbine Conference and Products Show, Houston, Tex., Mar. 9-12, 1981, Paper 81-GT-96*. 11 p. Members, \$2.00; nonmembers, \$4.00.

NASA research activities in the development of civilian and military aircraft are discussed. The advances made in subsonic and supersonic transports, commuter aircraft, rotorcraft, V/STOL, and high-performance engines are reviewed, and the problems facing general aviation are considered. Comments on some new areas of technology are also presented. L.S.

N81-17986* Pratt and Whitney Aircraft, East Hartford, Conn. Commercial Products Div.

VARIABLE STREAM CONTROL ENGINE FOR ADVANCED SUPERSONIC AIRCRAFT DESIGN UPDATE

c07
Richard B. Hunt and Robert A. Howlett / In NASA. Langley Research Center. Supersonic Cruise Res. 1979, Pt. 1. Mar. 1980 p 347-370 refs (For primary document see N81-17981 09-01)

(Contract NAS3-21389)

Avail: NTIS HC A23/MF A01 CSCL 21E

The updating of the engine concept for a second-generation supersonic transport, the variable stream control engine (VSCE), in terms of mechanical design definition and estimated performance is discussed. The design definition reflects technology advancements that improve system efficiency, durability and environments were established. The components unique to the VSCE concept, a high performance duct burner and a low noise coannular nozzle, and the high temperature components are identified as critical technologies. Technology advances for the high temperature components (main combustor and turbines) are also discussed. To address the requirements in this area, the technical approach for undertaking a high temperature validation program is defined. The multi-phased effort would include assorted rig and laboratory tests, then culminate with the demonstration of a flight-type main combustor and single-stage high pressure turbine at operating conditions envisioned for a VSCE. M.G.

N81-17997* Pratt and Whitney Aircraft, East Hartford, Conn. Commercial Products Div.

PROGRESS WITH VARIABLE CYCLE ENGINES

c07
John S. Westmoreland / In NASA. Langley Research Center. Supersonic Cruise Res. 1979, Pt. 1. Mar. 1980 p 371-390 refs (For primary document see N81-17981 09-01)

(Contracts NAS3-20048; NAS3-20061; NAS3-20602)

Avail: NTIS HC A23/MF A01 CSCL 21E

The evaluation of components of an advanced propulsion system for a future supersonic cruise vehicle is discussed. These components, a high performance duct burner for thrust augmentation and a low jet noise coannular exhaust nozzle, are part of the variable stream control engine. An experimental test program involving both isolated component and complete engine tests was conducted for the high performance, low emissions duct burner with excellent results. Nozzle model tests were completed which substantiate the inherent jet noise benefit associated with the unique velocity profile possible of a coannular exhaust nozzle system on a variable stream control engine. Additional nozzle model performance tests have established high thrust efficiency levels at takeoff and supersonic cruise for this nozzle system. Large scale testing of these two critical components is conducted using an F100 engine as the testbed for simulating the variable stream control engine. M.G.

N81-22012* Nielsen Engineering and Research, Inc., Mountain View, Calif.

A RAPID PERTURBATION PROCEDURE FOR DETERMINING NONLINEAR FLOW SOLUTIONS: APPLICATION TO TRANSONIC TURBOMACHINERY FLOWS

Final Report
Stephen S. Stahara, James P. Elliott, and John R. Spreiter
Washington NASA May 1981 95 p refs

(Contract NAS3-20835)

(NASA-CR-3425; NEAR-TR-227)

Avail: NTIS

HC A05/MF A01 CSCL 20D

Perturbation procedures and associated computational codes for determining nonlinear flow solutions were developed to establish a method for minimizing computational requirements associated with parametric studies of transonic flows in turbomachines. The procedure that was developed and evaluated was found to be capable of determining highly accurate approximations to families of strongly nonlinear solutions which are either continuous or discontinuous, and which represent variations in some arbitrary parameter. Coordinate straining is employed to account for the movement of discontinuities and maxima of high gradient regions due to the perturbation. The development and results reported are for the single parameter perturbation problem. Flows past both isolated airfoils and compressor cascades involving a wide variety of flow and geometry

parameter changes are reported. Attention is focused in particular on transonic flows which are strongly supercritical and exhibit large surface shock movement over the parametric range studied; and on subsonic flows which display large pressure variations in the stagnation and peak suction pressure regions. Comparisons with the corresponding 'exact' nonlinear solutions indicate a remarkable accuracy and range of validity of such a procedure.

J.M.S.

02 AERODYNAMICS

Includes aerodynamics of bodies, combinations, wings, rotors, and control surfaces; and internal flow in ducts and turbomachinery.

For related information see also 34 *Fluid Mechanics and Heat Transfer*.

N81-13019* National Aeronautics and Space Administration, Lewis Research Center, Cleveland, Ohio.

NASA CONTRIBUTIONS TO RADIAL TURBINE AERODYNAMIC ANALYSES

Arthur J. Glassman 1980 20 p refs Presented at Automotive Technol. Develop. Contractor Coord. Meeting, Dearborn, Mich., 11-13 Nov. 1980

(NASA-TM-81644; E-9356-1) Avail: NTIS HC A02/MF A01 CSCI 01A

A brief description of the radial turbine and its analysis needs is followed by discussions of five analytical areas: design geometry and performance, off design performance, blade row flow, scroll flow, and duct flow. The functions of the programs, areas of applicability, and limitations and uncertainties are emphasized. Both past contributions and current activities are discussed.

Author

N81-14977* National Aeronautics and Space Administration, Lewis Research Center, Cleveland, Ohio.

FINITE ELEMENT ANALYSIS OF INVISCID SUBSONIC BOATTAIL FLOW

R. V. Chima and P. M. Gerhart (Akron Univ., Ohio) 1981 16 p refs Presented at the Nineteenth Aerospace Sci. Meeting, St. Louis, 12-15 Jan. 1981; sponsored by Am. Inst. of Aeronautics and Astronautics

(NASA-TM-81650; E-651) Avail: NTIS HC A02/MF A01 CSCI 01A

A finite element code for analysis of inviscid subsonic flows over arbitrary nonlifting planar or axisymmetric bodies is described. The code solves a novel primitive variable formulation of the coupled irrotationality and compressible continuity equations. Results for flow over a cylinder, a sphere, and a NACA 0012 airfoil verify the code. Computed subcritical flows over an axisymmetric boattailed afterbody compare well with finite difference results and experimental data. Interactive coupling with an integral turbulent boundary layer code shows strong viscous effects on the inviscid flow. Improvements in code efficiency and extensions to transonic flows are discussed.

Author

N81-14978* National Aeronautics and Space Administration, Lewis Research Center, Cleveland, Ohio.

SUPERSONIC STALL FLUTTER OF HIGH SPEED FANS

J. J. Adamczyk, W. Stevens, and R. Jutras (GE Co., Evendale, Ohio) 1981 15 p refs Proposed for presentation at 26th Ann. Intern. Gas Turbine Conf., Houston, 8-12 Mar. 1981; sponsored by Am. Soc. of Mech. Engr.

(NASA-TM-81613; E-612) Avail: NTIS HC A02/MF A01 CSCI 01A

An analytical model is developed for predicting the onset of supersonic stall bending flutter in axial flow compressors. The analysis is based on a modified two dimensional, compressible, unsteady actuator disk theory. It is applied to a rotor blade row by considering a cascade of airfoils whose geometry and dynamic response coincide with those of a rotor blade element at 85 percent of the span height (measured from the hub). The rotor blades are assumed to be unshrouded (i.e., free standing) and to vibrate in their first flexural mode. The effects of shock waves and flow separation are included in the model through quasi-steady, empirical, rotor total-pressure-loss and deviation-angle correlations. The actuator disk model predicts the unsteady aerodynamic force acting on the cascade blading as a function of the steady flow field entering the cascade and the geometry and dynamic response of the cascade. Calculations show that the present model predicts the existence of a bending flutter mode at supersonic inlet Mach numbers. This flutter mode is suppressed by increasing the reduced frequency of the system

or by reducing the steady state aerodynamic loading on the cascade. The validity of the model for predicting flutter is demonstrated by correlating the measured flutter boundary of a high speed fan stage with its predicted boundary. This correlation uses a level of damping for the blade row (i.e., the log decrement of the rotor system) that is estimated from the experimental flutter data. The predicted flutter boundary is shown to be in good agreement with the measured boundary.

Author

N81-14979* National Aeronautics and Space Administration, Lewis Research Center, Cleveland, Ohio.

SOLUTION OF PLANE CASCADE FLOW USING IMPROVED SURFACE SINGULARITY METHODS

Eric R. McFarland 1981 14 p refs Presented for presentation at 26th Ann. Intern. Gas Turbine Conf., Houston 8-12 Mar. 1981; sponsored by Am. Soc. of Mech. Engr.

(NASA-TM-81589; E-568) Avail: NTIS HC A02/MF A01 CSCI 01A

A solution method was developed for calculating compressible inviscid flow through a linear cascade of arbitrary blade shapes. The method uses advanced surface singularity formulations which were adapted from those in current external flow analyses. The resulting solution technique provides a fast flexible calculation for flows through turbomachinery blade rows. The solution method and some examples of the method's capabilities are presented.

Author

N81-21027* National Aeronautics and Space Administration, Langley Research Center, Hampton, Va.

FLUID MECHANICS MECHANISMS IN THE STALL PROCESS OF HELICOPTERS

Warren H. Young, Jr. Mar. 1981 12 p refs Presented at Symp. on Numerical and Phys. Aspects of Aerodyn. Flows, Long Beach, Calif., 10-21 Jan. 1981 Prepared in cooperation with Army Aviation Research and Development Command, Hampton, Va.

(NASA-TM-81956; USAAVRADCOM-TR-81-8-1) Avail: NTIS HC A02/MF A01 CSCI 01A

Recent experimental results from airfoils in the Mach number, Reynolds number, or reduced frequency ranges typical of helicopter rotor blades have identified the most influential flow mechanisms in the dynamic stall process. The importance of secondary shed vortices, downstream wake action, and the flow in the separated region is generally acknowledged but poorly understood. By means of surface pressure cross-correlations and flow field measurements in static stall, several new hypotheses have been generated. It is proposed that vortex shedding may be caused by acoustic disturbances propagating forward in the lower (pressure) surface boundary layer, that wake closure is a misnomer, and that the shed vortex leaves a trail of vorticity that forms a turbulent free shear layer. The known dynamic stall flow mechanisms are reviewed and the potential importance of recently proposed and hypothetical flow phenomena with respect to helicopter blade aeroelastic response are assessed.

J.D.H.

N81-21028* National Aeronautics and Space Administration, Lewis Research Center, Cleveland, Ohio.

LOW AND HIGH SPEED PROPELLERS FOR GENERAL AVIATION: PERFORMANCE POTENTIAL AND RECENT WIND TUNNEL TEST RESULTS

Robert J. Jeracki and Glenn A. Mitchell 1981 29 p refs Presented at the Natl. Business Aircraft Meeting, Wichita, Kan., 7-10 Apr. 1981; sponsored by SAE

(NASA-TM-81745; E-799) Avail: NTIS HC A03/MF A01 CSCI 01A

The performance of lower speed, 5 foot diameter model general aviation propellers, was tested in the Lewis wind tunnel. Performance was evaluated for various levels of airfoil technology and activity factor. The difference was associated with inadequate modeling of blade and spinner losses for propellers round shank blade designs. Suggested concepts for improvement are: (1) advanced blade shapes (airfoils and sweep); (2) tip devices (proplets); (3) integrated propeller/nacelles; and (4) composites.

Several advanced aerodynamic concepts were evaluated in the Lewis wind tunnel. Results show that high propeller performance can be obtained to at least Mach 0.8. E.A.K.

N81-22017* National Aeronautics and Space Administration, Lewis Research Center, Cleveland, Ohio.

IMPROVED METHOD FOR CALCULATING TRANSONIC VELOCITIES ON BLADE-TO-BLADE STREAM SURFACES OF A TURBOMACHINE

Jerry R. Wood Apr. 1981 28 p refs
(NASA-TP-1772; E-128) Avail: NTIS HC A03/MF A01 CSCL 01A

A method was developed to improve the accuracy of an existing computer program used to calculate transonic velocities on a blade-to-blade surface of a turbomachine. The method eliminates problems encountered in obtaining solutions with the velocity gradient equation when large gradients in velocity occur through the blade row. With the improved method, results indicate that the transonic solution can be obtained by scaling the velocities obtained at the reduced mass flow rate where all velocities are subsonic thereby eliminating the need for a solution of the velocity gradient equation. Solutions obtained with the scaling method on a two dimensional compressor cascade and an axial turbine stator show good agreement with experimental data. The results obtained for the stationary blade rows and comparison of analytical results obtained with and without the present method suggest that the method will yield an improved solution for centrifugal compressor impellers. Author

N81-25036* National Aeronautics and Space Administration, Lewis Research Center, Cleveland, Ohio.

SHOCKLESS DESIGN AND ANALYSIS OF TRANSONIC BLADE SHAPES

Djordje S. Dulikravich and Helmut Sobieczky (DFVLR) 1981 13 p refs Presented at the 14th Fluid and Plasma Dyn. Conf., Palo Alto, Calif., 23-25 Jun. 1981; sponsored by the American Inst. of Aeronautics and Astronautics
(NASA-TM-82611; E-861) Avail: NTIS HC A02/MF A01 CSCL 01A

A fast computer program was developed to eliminate the shocks by slightly altering portions of the contour of a given airfoil in the cascade. The program can be used in two basic modes: (1) An analysis for steady, transonic, potential flow through a given planar cascade of airfoils and (2) a design for converting a given cascade into a shockless transonic cascade. The design mode can automatically be followed by the analysis mode, which confirms that the flow field is shock free. The program generates its own multilevel boundary conforming computational grids and solves a full potential equation in a fully conservative form. The shockless design is performed by implementing Sobieczky's fictitious-gas elliptic continuation concept. E.A.K.

N81-27041* National Aeronautics and Space Administration, Lewis Research Center, Cleveland, Ohio.

LASER-VELOCIMETER FLOW-FIELD MEASUREMENTS OF AN ADVANCED TURBOPROP

J. S. Serafini, J. P. Sullivan (Purdue Univ., West Lafayette, Ind.), and H. E. Neumann 1981 31 p refs Presented at the 17th Joint Propulsion Conf., Colorado Springs, 27-29 Jul. 1981; sponsored by AIAA, SAE and ASME
(NASA-TM-82677; E-943) Avail: NTIS HC A03/MF A01 CSCL 01A

Non-intrusive measurements of velocity about a spinner-propeller-nacelle configuration at a Mach number of 0.8 were performed. A laser velocimeter, specifically developed for these measurements in the NASA Lewis 8-foot by 6-foot Supersonic Wind Tunnel, was used to measure the flow-field of the advanced swept SR-3 turboprop. The laser velocimeter uses an argon ion laser and a 2-color optics system to allow simultaneous measurements of 2-components of velocity. The axisymmetric nature of the propeller-nacelle flow-field permits two separate 2 dimensional measurements to be combined into 3 dimensional velocity data. Presented are data ahead of and behind the prop

blades and also a limited set in between the blades. Aspects of the observed flow-field such as the tip vortex are discussed.

Author

N81-27042* National Aeronautics and Space Administration, Lewis Research Center, Cleveland, Ohio.

FACTORS INFLUENCING THE PREDICTED PERFORMANCE OF ADVANCED PROPELLER DESIGNS

Lawrence J. Bober and Li-Ko Chang (Purdue Univ., Lafayette, Ind.) 1981 20 p refs Presented at the 17th Joint Propulsion Conf., Colorado Springs, Colo., 27-29 Jul. 1981; sponsored by AIAA, SAE, and ASME
(NASA-TM-82676; E-942; AIAA-Paper-81-1564) Avail: NTIS HC A02/MF A01 CSCL 01A

The assumptions on which conventional propeller aerodynamic performance analyses are based can be seriously violated when advanced high speed propellers are analyzed. Studies were performed using a lifting line representation for the propeller to determine the sensitivity of predicted propeller performance to various assumptions in the analysis. Items studied include the method of determining blade section lift and the effects of blade section drag, camber and blade sweep. The effects of nonuniform flow into the propeller and compressibility were also studied. Comparisons of analytical and experimental results are presented to demonstrate the overall validity of the results. Author

N81-28053* National Aeronautics and Space Administration, Lewis Research Center, Cleveland, Ohio.

COLD-AIR PERFORMANCE OF COMPRESSOR-DRIVE TURBINE OF DEPARTMENT OF ENERGY UPGRADED AUTOMOBILE GAS TURBINE ENGINE. 1: VOLUTE-MANIFOLD AND STATOR PERFORMANCE

Richard J. Roelke and Jeffrey E. Haas (Army Aviation Research and Development Command) Jun. 1981 17 p refs
(Contract EC-77-A-31-1011)
(NASA-TM-82682; DOE/NA/1011-34; E-572; AVRADCOM-TR-80-C-20) Avail: NTIS HC A02/MF A01 CSCL 01A

The aerodynamic performance of the inlet manifold and stator assembly of the compressor drive turbine was experimentally determined with cold air as the working fluid. The investigation included measurements of mass flow and stator-exit fluid torque as well as radial surveys of total pressure and flow angle at the stator inlet and annulus surveys of total pressure and flow angle at the stator exit. The stator-exit aftermixed flow conditions and overall stator efficiency were obtained and compared with their design values and the experimental results from three other stators. In addition, an analysis was made to determine the constituent aerodynamic losses that made up the stator kinetic energy loss.

Author

N81-28054* National Aeronautics and Space Administration, Lewis Research Center, Cleveland, Ohio.

SOME ASPECTS OF CALCULATING FLOWS ABOUT THREE-DIMENSIONAL SUBSONIC INLETS

H. C. Kao 1981 20 p refs Presented at the 17th Joint Propulsion Conf., Colorado Springs, Colo., 27-29 Jul. 1981; sponsored by AIAA, SAE, and ASME
(NASA-TM-82678; E-941) Avail: NTIS HC A02/MF A01 CSCL 01A

Based on the potential flow model, computations were carried out for various three-dimensional inlet models. Some of these calculated results are presented in the forms of surface static pressure, flow angularity, surface flow pattern, and inlet flow field. Comparisons with experimental data are also made. M.G.

N81-31126* National Aeronautics and Space Administration, Lewis Research Center, Cleveland, Ohio.

STALL FLUTTER EXPERIMENT IN A TRANSONIC OSCIL-

LATING LINEAR CASCADE

Donald R. Boldman, Alvin E. Buggele, and George M. Michelson
1981 19 p refs Presented at Wint. Ann. Meeting of the
Am. Soc. of Mech. Engrs., Washington, D.C., 15-20 Nov. 1981
(NASA-TM-82655; E-918) Avail: NTIS HC A02/MF A01 CSCL
01A

Two dimensional biconvex airfoils were oscillated at reduced frequencies up to 0.5 based on semi-chord and a free stream Mach number of 0.80 to simulate transonic stall flutter in rotors. Steady-state periodicity was confirmed through end-wall pressure measurements, exit flow traverses, and flow visualization. The initial flow visualization results from flutter tests indicated that the oscillating shock on the airfoils lagged the airfoil motion by as much as 80 deg. These initial data exhibited an appreciable amount of scatter; however, a linear fit of the results indicated that the greatest shock phase lag occurred at a positive interblade phase angle. Photographs of the steady-state and unsteady flow fields reveal some of the features of the lambda shock wave on the suction surface of the airfoils. T.M.

NS1-31128* National Aeronautics and Space Administration, Lewis Research Center, Cleveland, Ohio.
GRID30: COMPUTER PROGRAM FOR FAST GENERATION OF MULTILEVEL, THREE-DIMENSIONAL BOUNDARY-CONFORMING O-TYPE COMPUTATIONAL GRIDS
Djordje S. Dulikravich Sep. 1981 13 p refs
(NASA-TP-1920; E-590) Avail: NTIS HC A02/MF A01 CSCL 01A

A fast algorithm was developed for accurately generating boundary conforming, three-dimensional consecutively refined computational grids applicable to arbitrary wing-body and axial turbomachinery geometries. The method is based on using an analytic function to generate two-dimensional grids on a number of coaxial axisymmetric surfaces positioned between the centerbody and the outer radial boundary. These grids are of the C type and are characterized by quasi-orthogonality, geometric periodicity, and an adequate resolution throughout the flow field. Because the built-in nonorthogonal coordinate stretching and shearing cause the grid lines leaving the blade or wing trailing edge to end at downstream infinity, the numerical treatment of the three-dimensional trailing vortex sheets is simplified. Author

NS1-31129* National Aeronautics and Space Administration, Lewis Research Center, Cleveland, Ohio.
SURROGATE-EQUATION TECHNIQUE FOR SIMULATION OF STEADY INVISCID FLOW Final Report
Gary M. Johnson Washington NASA Sep. 1981 40 p refs
(NASA-TP-1866; E-583) Avail: NTIS HC A03/MF A01 CSCL 01A

A numerical procedure for the iterative solution of inviscid flow problems is described, and its utility for the calculation of steady subsonic and transonic flow fields is demonstrated. Application of the surrogate equation technique defined herein allows the formulation of stable, fully conservative, type dependent finite difference equations for use in obtaining numerical solutions to systems of first order partial differential equations, such as the steady state Euler equations. Steady, two dimensional solutions to the Euler equations for both subsonic, rotational flow and supersonic flow and to the small disturbance equations for transonic flow are presented. Author

A81-11646* Optimum subsonic, high-angle-of-attack nacelles. R. W. Luidens, N. O. Stockman, and J. H. Diedrich (NASA, Lewis Research Center, Cleveland, Ohio). In: International Council of the Aeronautical Sciences, Congress, 12th, Munich, West Germany, October 12-17, 1980, Proceedings. (A81-11601 02-01) New York, American Institute of Aeronautics and Astronautics, Inc., 1980, p. 530-541, 16 refs.

Many proposed advanced aircraft - but especially tilt-nacelle, subsonic-cruise, V/STOL aircraft - require nacelles that operate over a wide range of aerodynamic conditions. The optimum design of such nacelles and their inlets is described, including how the inlet

low-speed design conditions are selected, the conditions for which the various regions of the inlet are designed, and appropriate criteria of merit. For low-speed operation the optimum internal surface velocity distributions and skin friction distributions are described for three categories of inlets: those without boundary-layer control (BLC), those with BLC, and those with blow-in door slots and retractable slats. Experimental results are presented that show the performance of the various types of inlets. At cruise speed the effect of factors that reduce the nacelle external surface area and the local skin friction is illustrated. These factors are cruise Mach number, inlet throat size, fan-face Mach number, and nacelle contour. The interrelation of these cruise-speed factors with the design requirements for good low-speed performance is discussed. Finally an inlet design without BLC and an optimized inlet design with slots and slats are compared to illustrate the possible reductions in nacelle size.

(Author)

A81-17852* Inlet flow distortion in turbomachinery. B. S. Seidel, M. D. Matwey (Delaware University, Newark, Del.), and J. J. Adamczyk (NASA, Lewis Research Center, Cleveland, Ohio). *American Society of Mechanical Engineers, Gas Turbine Conference and Products Show, New Orleans, La., Mar. 10-13, 1980, Paper 80-GT-20*. 6 p. 12 refs. Members, \$1.50; nonmembers, \$3.00. Grant No. NSG-3189.

A single stage axial compressor with distorted inflow is studied. The inflow distortion occurs far upstream and may be a distortion in stagnation temperature, stagnation pressure or both. The blade rows are modeled as semi-actuator disks. Losses, quasi-steady deviation angles, and reference incidence correlations are included in the analysis. Both subsonic and transonic relative Mach numbers are considered. A parameter study is made to determine the influence of such variables as Mach number and swirl angle on the attenuation of the distortion. (Author)

A81-20703* Three-dimensional turbulent boundary layer development and separation in V/STOL engine inlets at incidence with small-cross flow and curvature influences. D. C. Chou, Z.-J. Yang (New Mexico University, Albuquerque, N. Mex.), R. W. Luidens, and N. O. Stockman (NASA, Lewis Research Center, Wind Tunnel and Flight Div., Cleveland, Ohio). *American Institute of Aeronautics and Astronautics, Aerospace Sciences Meeting, 19th, St. Louis, Mo., Jan. 12-15, 1981, Paper 81-0254*. 12 p. 33 refs.

The study concerns the influence of the three-dimensional cross flows on the compressible turbulent boundary layer development and flow separation prediction around V/STOL engine inlets at high incidence. The governing equations for the three-dimensional boundary layer flow with small-cross approximation are solved numerically on an intrinsic streamline coordinate system. Results are presented to illustrate the effects of small cross-flow, compressibility and streamline curvatures on the flow. Comparisons of the results with the wind tunnel data for scaled model and with data obtained from another existing compressible axisymmetric turbulent boundary layer scheme are included in the analysis. (Author)

A81-20782* The experimental verification of a streamline curvature numerical analysis method applied to the flow through an axial flow fan. M. J. Pierzga (NASA, Lewis Research Center, Cleveland, Ohio). *American Institute of Aeronautics and Astronautics, Aerospace Sciences Meeting, 19th, St. Louis, Mo., Jan. 12-15, 1981, Paper 81-0363*. 10 p. 7 refs. Navy-supported research.

The experimental verification of an inviscid, incompressible through-flow analysis method is presented. The primary component of this method is an axisymmetric streamline curvature technique which is used to compute the hub-to-tip flow field of a given turbomachine. To analyze the flow field in the blade-to-blade plane of the machine, the potential flow solution of an infinite cascade of airfoils is also computed using a source model technique. To verify the accuracy of such an analysis method an extensive experimental

verification investigation was conducted using an axial flow research fan. Detailed surveys of the blade-free regions of the machine along with intra-blade surveys using rotating pressure sensing probes and blade surface static pressure taps provide a one-to-one relationship between measured and predicted data. The results of this investigation indicate the ability of this inviscid analysis method to predict the design flow field of the axial flow fan test rotor to within a few percent of the measured values. (Author)

A81-20830 * # Mean rotor wake characteristics of an aerodynamically loaded 0.5 m diameter fan. L. M. Shaw and F. W. Glaser (NASA, Lewis Research Center, Cleveland, Ohio). *American Institute of Aeronautics and Astronautics, Aerospace Sciences Meeting, 19th, St. Louis, Mo., Jan. 12-15, 1981, Paper 81-0208*. 16 p. 15 refs.

Mean rotor wake properties at several downstream distances behind the rotor of a loaded 1.2 pressure ratio fan were measured with a cross film anemometer in an anechoic wind tunnel. Mean wake characteristics in the midspan and near tip region were determined utilizing an ensemble averaging technique. The upwash and streamwise components of the velocity behind the rotor indicate a complex structure superimposed on the major velocity defects at a downstream spacing of 0.5 rotor chords. Spectral analysis indicates high levels of the second and fourth harmonics of the blade passage frequency in the midspan region while the blade passage frequency and its second and third harmonic are predominant in the tip region. (Author)

A81-20831 * # Finite element analysis of inviscid subsonic boattail flow. R. V. Chima (NASA, Lewis Research Center, Cleveland, Ohio) and P. M. Gerhart (Akron, University, Akron, Ohio). *American Institute of Aeronautics and Astronautics, Aerospace Sciences Meeting, 19th, St. Louis, Mo., Jan. 12-15, 1981, Paper 81-0276*. 15 p. 32 refs. Grants No. DAHC04-75-G-0026; No. DAAG29-77-G-0030.

A finite element code for analysis of inviscid subsonic flows over arbitrary nonlifting planar or axisymmetric bodies is described. The code solves a novel primitive variable formulation of the coupled irrotationality and compressible continuity equations. Results for flows over a cylinder, a sphere, and a NACA 0012 airfoil verify the code. Computed subcritical flows over an axisymmetric boattailed afterbody compare well with finite difference results and experimental data. Iterative coupling with an integral turbulent boundary layer code shows strong viscous effects on the inviscid flow. Improvements in code efficiency and extensions to transonic flows are discussed. (Author)

A81-21212 * Calculation of the flow field in supersonic inlets using a bicharacteristics method with shock wave fitting. J. Vadyak, J. D. Hoffman (Purdue University, West Lafayette, Ind.), and A. R. Bishop (NASA, Lewis Research Center, Cleveland, Ohio). In: *International Conference on Numerical Methods in Fluid Dynamics, 6th, Tiflis, Georgian SSR, June 21-24, 1978, Proceedings*. (A81-21169 07-02) Berlin, Springer-Verlag, 1979, p. 523-529. 8 refs. Grants No. NGR-15-005-162; No. NGR-15-005-191.

The results of weakly viscous flow analysis are presented. The flow field, including molecular transport, is computed with the aid of a bicharacteristic method. The bow shock wave and the internal shock wave are computed with the aid of a three-dimensional shock wave fitting procedure. Characteristic equations are presented, and numerical integration procedure is discussed. Here, an inverse marching scheme is employed in which the solution is obtained on space-like planes of constant x and on space curves defined by the intersections of the internal shock wave with the solid boundaries. The distance between solution planes is arrived at by the Courant-Friedrichs-Lewy stability criterion. C.R.

A81-29114 * # Flow separation in inlets at incidence angles. A. K. Jakubowski (Virginia Polytechnic Institute and State University, Blacksburg, Va.) and R. W. Luidens (NASA, Lewis Research Center, Cleveland, Ohio). In: *International Symposium on Air Breathing Engines, 5th, Bangalore, India, February 16-22, 1981, Proceedings*. Symposium sponsored by ICAS, AIAA, UNESCO, et al. Bangalore, India, National Aeronautical Laboratory, 1981. 13 p. 13 refs. Grant No. NSG-3073.

Wind-tunnel pressure data and flow pictures obtained for two two-dimensional inlet models have been examined to study the internal flow structure and separation at large incidence angles. The inlet models were 12-in. high (diffuser exit height) and had internal contraction ratio of 1.21 and 1.17. They were tested at low forward speeds over a wide range of throat Mach numbers (inlet mass flow rates) and angles of incidence. Characteristic features of the internal flow such as a drastic change of pressure gradient near the highlight, local separation bubbles and shock/boundary-layer interactions have been indicated and discussed. For a few specific cases, the experimental surface pressure distributions have been compared with theoretical predictions. (Author)

A81-29979 * # Full potential solution of a transonic quasi-3-D flow through a cascade using artificial compressibility. C. Farrell and J. Adamczyk (NASA, Lewis Research Center, Cleveland, Ohio). *American Society of Mechanical Engineers, Gas Turbine Conference and Products Show, Houston, Tex., Mar. 9-12, 1981, Paper 81-GT-70*. 11 p. 12 refs. Members, \$2.00; nonmembers, \$4.00.

A reliable method is presented for calculating the flowfield about a cascade of arbitrary 2-D airfoils. The method approximates the three-dimensional flow in a turbomachinery blade row by correcting for streamtube convergence and radius change in the throughflow direction. The method is a fully conservative solution of the full potential equation incorporating the finite volume technique on a body-fitted periodic mesh, with an artificial density imposed in the transonic region to ensure stability and the capture of shock waves. Comparison of results for several supercritical blades shows good agreement with their hodograph solutions. Other calculations for these profiles as well as standard NACA blade sections indicate that this is a useful scheme for analyzing both the design and off-design performance of turbomachinery blading. (Author)

A81-30068 * # Solution of plane cascade flow using improved surface singularity methods. E. R. McFarland (NASA, Lewis Research Center, Cleveland, Ohio). *American Society of Mechanical Engineers, Gas Turbine Conference and Products Show, Houston, Tex., Mar. 9-12, 1981, Paper 81-GT-169*. 9 p. 13 refs. Members, \$2.00; nonmembers, \$4.00.

A solution method has been developed for calculating compressible inviscid flow through a linear cascade of arbitrary blade shapes. The method uses advanced surface singularity formulations which were adapted from those found in current external flow analyses. The resulting solution technique provides a fast flexible calculation for flows through turbomachinery blade rows. The solution method and some examples of the method's capabilities are presented. (Author)

A81-39874 * # Application of unsteady airfoil theory to rotary wings. K. R. V. Kaza (NASA, Lewis Research Center, Cleveland; Toledo, University, Toledo, OH) and R. G. Kvaternik (NASA, Langley Research Center, Hampton, VA). *Journal of Aircraft*, vol. 18, July 1981, p. 604, 605. 5 refs.

A clarification is presented on recent work concerning the application of unsteady airfoil theory to rotary wings. The application of this theory may be seen as consisting of four steps: (1) the selection of an appropriate unsteady airfoil theory; (2) the resolution

of that velocity which is the resultant of aerodynamic and dynamic velocities at a point on the elastic axis into radial, tangential and perpendicular components, and the angular velocity of a blade section about the deformed axis; (3) the expression of lift and pitching moments in terms of the three components; and (4) the derivation of explicit expressions for the components in terms of flight velocity, induced flow, rotor rotational speed, blade motion variables, etc. O.C.

A81-42177 * # **Some aspects of calculating flows about three-dimensional subsonic inlets.** H. C. Kao (NASA, Lewis Research Center, Cleveland, OH), AIAA, SAE, and ASME, *Joint Propulsion Conference, 17th, Colorado Springs, CO, July 27-29, 1981, AIAA Paper 81-1361*, 17 p, 10 refs.

As a consequence of the growing interest in the development of V/STOL aircraft technology, efforts are being made to create new designs for a propulsion system which can be operated over a wide range of flight speeds, incidence angles, and throttle settings. In connection with these efforts, various inlet configurations have been proposed. The high experimental costs incurred in the study of various inlet geometries, led to the employment of a computational method for the investigation of inlets. Attention is given to the computer program, paneling and surface static pressure, surface flow pattern, and the inlet flow field. The reported investigation demonstrates that useful information for initial screenings may be obtained from potential flow calculations. G.R.

A81-42210 * # **Factors influencing the predicted performance of advanced propeller designs.** L. J. Bober (NASA, Lewis Research Center, Cleveland, OH) and L.-K. Chang (Purdue University, West Lafayette, IN), AIAA, SAE, and ASME, *Joint Propulsion Conference, 17th, Colorado Springs, CO, July 27-29, 1981, AIAA Paper 81-1564*, 19 p, 9 refs.

The assumptions on which conventional propeller aerodynamic performance analyses are based can be seriously violated when advanced high speed propellers are analyzed. Studies have been performed using a lifting line representation for the propeller to determine the sensitivity of predicted propeller performance to various assumptions in the analysis. Items which have been studied include the method of determining blade section lift and the effects of blade section drag, camber and blade sweep. The effects of nonuniform flow into the propeller and compressibility have also been studied. Comparisons of analytical and experimental results are presented to demonstrate the overall validity of the results. (Author)

A81-42211 * # **Laser-velocimeter flow-field measurements of an advanced turboprop.** J. S. Serafini, H. E. Neumann (NASA, Lewis Research Center, Cleveland, OH), and J. P. Sullivan (Purdue University, West Lafayette, IN), AIAA, SAE, and ASME, *Joint Propulsion Conference, 17th, Colorado Springs, CO, July 27-29, 1981, AIAA Paper 81-1568*, 29 p, 18 refs.

Non-intrusive measurements of velocity about a spinner-propeller-nacelle configuration at a Mach number of 0.8 have been performed. A laser velocimeter, specifically developed for these measurements in the NASA Lewis 8- by 6-foot Supersonic Wind Tunnel, was used to measure the flow-field of the advanced swept SR-3 propeller. The laser velocimeter uses an argon ion laser and a 2-color optics system to allow simultaneous measurements of 2-components of velocity. The axisymmetric nature of the propeller-nacelle flow-field permits two separate 2-dimensional measurements to be combined into 3-dimensional velocity data. Presented are data ahead of and behind the propeller blades and also a limited set in between the blades. Aspects of the observed flow-field such as the tip vortex are discussed. (Author)

N81-14876* # **Detroit Diesel Allison, Indianapolis, Ind. EXPERIMENTAL DETERMINATION OF UNSTEADY BLADE ELEMENT AERODYNAMICS IN CASCADES. VOLUME 2: TRANSLATION MODE CASCADE Final Report** R. E. Riffel and M. D. Rothrock Dec. 1980 183 p refs (Contract NAS3-20055) (NASA-CR-165166; EDR-10361-Vol-2) Avail: NTIS HC A09/MF A01 CSCL 01A

A two dimensional cascade of harmonically oscillating airfoils was designed to model a near tip section from a rotor which was known to have experienced supersonic translational model flutter. This five bladed cascade had a solidity of 1.52 and a setting angle of 0.90 rad. Unique graphite epoxy airfoils were fabricated to achieve the realistic high reduced frequency level of 0.15. The cascade was tested over a range of static pressure ratios approximating the blade element operating conditions of the rotor along a constant speed line which penetrated the flutter boundary. The time steady and time unsteady flow field surrounding the center cascade airfoil were investigated. Author

N81-16876* # **Scientific Research Associates, Inc., Glastonbury, Conn.**

PREDICTION OF LAMINAR AND TURBULENT PRIMARY AND SECONDARY FLOWS IN STRONGLY CURVED DUCTS Final Report

J. P. Kreskovsky, W. R. Briley, and H. McDonald Washington NASA Feb. 1981 59 p refs (Contract NAS3-22014) (NASA-CR-3388; R80-900007-12) Avail: NTIS HC A04/MF A01 CSCL 01A

The analysis is based on a primary secondary velocity decomposition in a given coordinate system, and leads to approximate governing equations which correct an a priori inviscid solution for viscous effects, secondary flows, total pressure distortion, heat transfer, and internal flow blockage and losses. Solution of the correction equations is accomplished as an initial value problem in space using an implicit forward marching technique. The overall solution procedure requires significantly less computational effort than Navier-Stokes algorithms. The solution procedure is effective even with the extreme local mesh resolution which is necessary to solve near wall sublayer regions in turbulent flow calculations. Computed solutions for both laminar and turbulent flow compared very favorably with available analytical and experimental results. The overall method appears very promising as an economical procedure for making detailed predictions of viscous primary and secondary flows in highly curved passages. T.M.

A81-11628 * **A rapid method for the approximate determination of nonlinear solutions - Application to aerodynamic flows.** S. S. Stahara, J. P. Elliott (Nielsen Engineering and Research, Inc., Mountain View, Calif.), and J. R. Spreiter (Stanford University, Stanford, Calif.), In: *International Council of the Aeronautical Sciences, Congress, 12th, Munich, West Germany, October 12-17, 1980, Proceedings*, (A81-11601 02-01) New York, American Institute of Aeronautics and Astronautics, Inc., 1980, p. 324-337, 12 refs. Contract No. NAS3-20836.

A method for determining highly accurate approximations to families of strongly nonlinear solutions which are either continuous or discontinuous, and which represent variations in some arbitrary parameters, is developed and evaluated. The procedure consists of defining a unit perturbation by employing two or more nonlinear solutions which differ from one another by a nominal change in some geometric or flow parameter, and then using that unit perturbation to predict a family of related nonlinear solutions over a range of parameter variation. Coordinate straining is used in determining the unit perturbation to account for the movement of discontinuities and maxima of high-gradient regions due to the perturbation. Although the procedure is generally applicable, results are presented here for nonlinear aerodynamic applications. Attention

is focused in particular on transonic flows which are strongly supercritical and exhibit large surface shock movement over the parametric range studied; and on subsonic flows which display large pressure variations in the stagnation and peak suction pressure regions. Flows past both isolated airfoils and compressor cascades involving a variety of flow and geometry parameter changes are considered. Comparisons with the corresponding 'exact' nonlinear solutions indicate a remarkable accuracy and range of validity of such a procedure. Computational time is trivial. (Author)

A81-21199 Calculation of three-dimensional turbulent subsonic flows in transition ducts. R. Levy, H. McDonald, and W. R. Briley (Scientific Research Associates, Inc., Glastonbury, Conn.). In: *International Conference on Numerical Methods in Fluid Dynamics*, 6th, Tiflis, Georgian SSR, June 21-24, 1978, Proceedings. (A81-21169 07-02) Berlin, Springer-Verlag, 1979, p. 361-369. 10 refs. Contracts No. NAS3-17522; No. NAS3-19856.

A method for computing three-dimensional turbulent subsonic flow in curved ducts is being developed. A set of tube-like surface oriented coordinates is employed for a general class of geometries applicable to subsonic diffusers with offset bends. The geometric formulation is complex and no previous treatment of this class of viscous flow problems is known to the authors. The duct centerline is a space curve specified by piecewise polynomials. A Frenet frame is located on the centerline at each axial location. The cross sections are described by superellipses imbedded in the Frenet frame. Duct surfaces are also coordinate surfaces, which greatly simplifies the boundary conditions. The resulting coordinates are nonorthogonal. An approximate set of governing equations is employed for viscous flows having strong flow in a primary flow direction. The derivation is coordinate invariant and the resulting equations are expressed in tensor form. These equations are solved by an efficient alternating direction implicit (ADI) method. This numerical method is generally stable and permits solution in difficult geometries using the general tensor formulation. (Author)

A81-30094 * # Boundary layer development on turbine airfoil suction surfaces. O. P. Sharma, R. A. Wells (United Technologies Corp., Commercial Products Div., East Hartford, Conn.), R. H. Schlinker, and D. A. Bailey (United Technologies Research Center, East Hartford, Conn.). *American Society of Mechanical Engineers, Gas Turbine Conference and Products Show, Houston, Tex., Mar. 9-12, 1981, Paper 81-GT-204*. 12 p. 20 refs. Members, \$2.00; nonmembers, \$4.00. Contract No. NAS3-20646.

The results of a study supported by NASA under the Energy Efficient Engine Program, conducted to investigate the development of boundary layers under the influence of velocity distributions that simulate the suction sides of two state-of-the-art turbine airfoils, are presented. One velocity distribution represented a forward loaded airfoil ('squared-off' design), while the other represented an aft loaded airfoil ('aft loaded' design). These velocity distributions were simulated in a low-speed, high-aspect-ratio wind tunnel specifically designed for boundary layer investigations. It is intended that the detailed data presented in this paper be used to develop improved turbulence model suitable for application to turbine airfoil design.

(Author)

03 AIR TRANSPORTATION AND SAFETY

Includes passenger and cargo air transport operations, and aircraft accidents.

For related information see also 16 Space Transportation and 85 Urban Technology and Transportation.

N81-19021* National Aeronautics and Space Administration, Lewis Research Center, Cleveland, Ohio.

OZONE CONTAMINATION IN AIRCRAFT CABINS: RESULTS FROM GASP DATA AND ANALYSES

J. D. Holdeman and G. D. Nastro (Control Data Corp., Minneapolis, Minn.) 1981 15 p refs Presented at the 19th Aerospace Sci. Meeting, St. Louis, 12-15 Jan. 1981; sponsored by the American Inst. of Aeronautics and Astronautics (NASA-TM-81671; E-693) Avail: NTIS HC A02/MF A01 CSCL 01C

The global atmospheric sampling program pertaining to the problem of ozone contamination in commercial airplane cabins is described. Specifically, analyses of GASP data have confirmed the occurrence of high ozone levels in aircraft cabins and documented the ratio of ozone inside and outside the cabins of two B747 airliners, including the effects of air conditioning modifications on that ratio; defined ambient ozone climatology at commercial airplane cruise altitudes, including tabulation of encounter frequency data which were not available before GASP; and outlined procedures for estimating the frequency of flights encountering high cabin ozone levels using climatological ambient ozone data, and verified these procedures against cabin measurements.

Author

N81-19059* National Aeronautics and Space Administration, Lewis Research Center, Cleveland, Ohio.

PNEUMATIC BOOT FOR HELICOPTER ROTOR DEICING

Bernard J. Blaha and Peggy L. Evanich /in NASA, Langley Research Center The 1980 Aircraft Safety and Operating Probl., Pt. 2 Mar. 1981 p 425-443 refs (For primary document see N81-19056 10-03)

Avail: NTIS HC A17/MF A01 CSCL 01C

Pneumatic deicer boots for helicopter rotor blades were tested. The tests were conducted in the 6 by 9 ft icing research tunnel on a stationary section of a UH-1H helicopter main rotor blade. The boots were effective in removing ice and in reducing aerodynamic drag due to ice.

E.D.K.

N81-19080* National Aeronautics and Space Administration, Lewis Research Center, Cleveland, Ohio.

AIRCRAFT OPERATING EFFICIENCY ON THE NORTH ATLANTIC, A CHALLENGE FOR THE 1990'S

Robert Steinberg /in NASA, Langley Research Center The 1980 Aircraft Safety and Operating Probl., Pt. 2 Mar. 1981 p 445-451 (For primary document see N81-19036 10-03)

Avail: NTIS HC A17/MF A01 CSCL 01C

A number of changes are expected to occur in the near future which could have important consequences for Atlantic flight operations for the next decade. These changes are identified and their impact on aircraft operating efficiency is discussed. Possible alternatives for North Atlantic air carriers are reviewed and strategies and actions are suggested which may give a considerable impact on fuel savings for years to come.

E.D.K.

N81-19083* National Aeronautics and Space Administration, Lewis Research Center, Cleveland, Ohio.

THE USE OF ANTIMISTING KEROSENE (AMK) IN TURBOJET ENGINES

Harold W. Schmidt /in NASA, Langley Research Center The 1980 Aircraft Safety and Operating Probl., Pt. 2 Mar. 1981 p 499-510 (For primary document see N81-19056 10-03)

Avail: NTIS HC A17/MF A01 CSCL 01C

The effect of antimisting kerosene (AMK) flow characteristics

on fan jet engines and the impact of degradation requirements on the fuel system was evaluated. It was determined from the present program that AMK fuel cannot be used without predegradation, although some degradation occurs throughout the fuel feed system, especially in the fuel pumps. There is a tendency toward FM-9 AMK additive agglomeration and gel formation when the liquid flows at a critical velocity through very small passages. The data indicate this phenomenon to be a function of the degree of degradation, the passage size, the differential pressure, the fluid temperature, and the accumulated flow time. Additionally, test results indicate that the long term cumulative effects of this phenomenon may require more degradation than the theoretical requirement determined from short term tests.

E.D.K.

N81-19072* National Aeronautics and Space Administration, Lewis Research Center, Cleveland, Ohio.

RECENT DEVELOPMENTS IN AIRCRAFT ENGINE NOISE REDUCTION TECHNOLOGY

James R. Stone and Charles E. Feiler /in NASA, Langley Research Center The 1980 Aircraft Safety and Operating Probl., Pt. 2 Mar. 1981 p 671-698 refs (For primary document see N81-19056 10-03)

Avail: NTIS HCA17/MF A01 CSCL 01C

Some of the more important developments and progress in jet and fan noise reduction and flight effects are reviewed. Experiments are reported which show that nonaxisymmetric conical nozzles have the potential to reduce jet noise for conventional and inverted velocity profiles. It is shown that an improved understanding of suppressive linear behavior, coupled with the new understanding of fan source noise, will soon allow the joint optimization of acoustic liner and fan design for low noise. It is also shown that fan noise source reduction concepts are applicable to advanced turboprops. Advances in inflow control device design are reviewed that appear to offer an adequate approach to the ground simulation of inflight fan noise.

R.C.T.

N81-19078* National Aeronautics and Space Administration, Lewis Research Center, Cleveland, Ohio.

SURVEY OF AIRCRAFT ICING SIMULATION TEST FACILITIES IN NORTH AMERICA

William Olsen Feb. 1981 26 p refs

(NASA-TM-81707; E-736) Avail: NTIS HC A03/MF A01 CSCL 01C

A survey was made of the aircraft icing simulation facilities in North America: there are 12 wind tunnels, 20 engine test facilities, 6 aircraft tankers and 14 low velocity facilities that perform aircraft icing tests full or part time. The location and size of the facility, its speed and temperature range, icing cloud parameters, and the technical person to contact are surveyed. Results are presented in tabular form. The capabilities of each facility were estimated by its technical contact person. The adequacy of these facilities for various types of icing tests is discussed.

S.F.

04 AIRCRAFT COMMUNICATIONS AND NAVIGATION

Includes digital and voice communication with aircraft; air navigation systems (satellite and ground based); and air traffic control.

For related information see also 17 *Spacecraft Communications, Command, and Tracking* and 32 *Communications*.

A81-20740 * # Ozone contamination in aircraft cabins - Results from GASP data and analyses. J. D. Holdeman (NASA, Lewis Research Center, Combustion and Pollution Research Branch, Cleveland, Ohio) and G. D. Nastrom (Central Data Corp., Minneapolis, Minn.). *American Institute of Aeronautics and Astronautics, Aerospace Sciences Meeting, 19th, St. Louis, Mo., Jan. 12-15, 1981, Paper 81-0305*. 10 p. 21 refs. U.S. Department of Transportation Contract No. FA78WAI-893.

The paper reviews results from the NASA Global Atmospheric Sampling Program (GASP) pertaining to the problem of ozone contamination in commercial aircraft cabins. Specifically, analyses of GASP data have (1) confirmed the high ozone levels in aircraft cabins and documented the ratio of ozone inside and outside the cabins of two B747 airliners, including the effects of air conditioning modifications on that ratio; (2) defined ambient ozone climatology at commercial aircraft cruise altitudes, including tabulation of encounter frequency data; and (3) outlined procedures for estimating the frequency of flights encountering high cabin ozone levels using climatological ambient ozone data and verified these procedures against cabin measurements. (Author)

A81-28682 * The coupling between flow instabilities and incident disturbances at a leading edge. M. E. Goldstein (NASA, Lewis Research Center, Cleveland, Ohio). *Journal of Fluid Mechanics*, vol. 104, Mar. 1981, p. 217-246. 25 refs.

It is now generally agreed that an external disturbance field, such as an incident acoustic wave, can effectively couple to instabilities of a flow past a trailing edge. One purpose of the present paper is to show that there are situations where a similar coupling can occur at a leading edge. The process is analyzed and the effects of experimentally controllable parameters are assessed. It is important to account for such phenomena when evaluating the effect of external disturbances on transition. (Author)

N81-19079* # Rockwell International Corp., Los Angeles, Calif. Thermodynamics Group.

LIGHT TRANSPORT AND GENERAL AVIATION AIRCRAFT ICING RESEARCH REQUIREMENTS Final Report

R. K. Breeze and G. M. Clark 20 Mar. 1981 348 p refs

(Contract NAS3-22186)

(NASA-CR-165290)

NA-81-110)

Avail: NTIS

HC A15/MF A01 CSCL 01C

A short term and a long term icing research and technology program plan was drafted for NASA LeRC based on 33 separate research items. The specific items listed resulted from a comprehensive literature search, organized and assisted by a computer management file and an industry/Government agency survey. Assessment of the current facilities and icing technology was accomplished by presenting summaries of ice sensitive components and protection methods, and assessments of penalty evaluation, the experimental data base, ice accretion prediction methods, research facilities, new protection methods, ice protection requirements, and icing instrumentation. The intent of the research plan was to determine what icing research NASA LeRC must do or sponsor to ultimately provide for increased utilization and safety of light transport and general aviation aircraft. Author

05 AIRCRAFT DESIGN, TESTING AND PERFORMANCE

Includes aircraft simulation technology
For related information see also 18 *Spacecraft Design,
Testing and Performance* and 39 *Structural Mechanics*

N81-25065* # National Aeronautics and Space Administration,
Lewis Research Center, Cleveland, Ohio

EVALUATION OF A PNEUMATIC BOOT DEICING SYSTEM ON A GENERAL AVIATION WING MODEL

Alan E. Albright (Kansas Univ., Lawrence), David L. Kohlman
(Kansas Univ., Lawrence), William G. Schweikhard (Kansas Univ.,
Lawrence), and Peggy Evanich Jun. 1981 35 p refs
(Grant NAS3-71)

(NASA-TM-82363; KU-FRL-464-2) Avail: NTIS
HC A03/MF A01 CSCL 01C

The aerodynamic characteristics of a typical modern general
aviation airfoil were investigated with and without a pneumatic
boot ice protection system. The ice protection effectiveness of
the boot was studied. This includes the change in drag on the
airfoil with the boot inflated and deflated, the change in drag
due to primary and residual ice formation, drag change due to
cumulative residual ice formation, and parameters affecting boot
effectiveness. Boot performance was not affected by tunnel total
temperature or velocity. Marginal effect in performance was
associated with angle of attack. Significant effects on performance
were caused by variations in droplet size, LWC, ice cap thickness
inflation pressure, and surface treatment. T.M.

A81-20837 * # Icing tunnel tests of a glycol-exuding porous
leading edge ice protection system on a general aviation airfoil. D. L.
Kohlman, W. G. Schweikhard (Kansas, University, Lawrence, Kan.),
and P. Evanich (NASA, Lewis Research Center, Cleveland, Ohio).
*American Institute of Aeronautics and Astronautics, Aerospace
Sciences Meeting, 19th, St. Louis, Mo., Jan. 12-15, 1981, Paper
81-0405*, 10 p.

Tests were conducted in the Icing Research Tunnel at the NASA
Lewis Research Center to determine the characteristics of an ice
protection system that distributes a glycol solution onto the leading
edge of an airfoil through a porous surface material. Minimum fluid
flow rates required to achieve anti-icing (no ice formation) were
determined for various flight conditions and angles of attack. The
ability of the system to remove ice formed on the airfoil before
system activation was also investigated. (Author)

06 AIRCRAFT INSTRUMENTATION

¹Includes cockpit and cabin display devices; and flight instruments.

For related information see also 19 *Spacecraft Instrumentation* and 35 *Instrumentation and Photography*.

NS1-31190* National Aeronautics and Space Administration, Lewis Research Center, Cleveland, Ohio.

FIBER OPTICS FOR AIRCRAFT ENGINE/INLET CONTROL

Robert J. Baumbick 1981 13 p refs Presented at the Intern. Symp. and Instrument Display, San Diego, Calif., 24-28 Aug. 1981; sponsored by the Society of Photo-Optical Instrumentation Engineers

(NASA-TM-82654; E-917) Avail: NTIS HC A02/MF A01 CSCL 01D

NASA programs that focus on the use of fiber optics for aircraft engine/inlet control are reviewed. Fiber optics for aircraft control is attractive because of its inherent immunity to EMI and RFI noise. Optical signals can be safely transmitted through areas that contain flammable or explosive materials. The use of optics also makes remote sensing feasible by eliminating the need for electrical wires to be connected between sensors and computers. Using low-level optical signals to control actuators is also feasible when power is generated at the actuator. Each application of fiber optics for aircraft control has different requirements for both the optical cables and the optical connectors. Sensors that measure position and speed by using slotted plates can use lossy cables and bundle connectors if data transfer is in the parallel mode. If position and speed signals are multiplexed, cable and connector requirements change. Other sensors that depend on changes in transmission through materials require dependable characteristics of both the optical cables and the optical connectors. A variety of sensor types are reviewed, including rotary position encoders, tachometers, temperature sensors, and blade tip clearance sensors for compressors and turbines. Research on a gallium arsenide photoswitch for optically switched actuators that operate at 250 C is also described.

Author

07 AIRCRAFT PROPULSION AND POWER

Includes prime propulsion systems and systems components, e.g., gas turbine engines and compressors; and on-board auxiliary power plants for aircraft.

For related information see also 20 *Spacecraft Propulsion and Power*, 28 *Propellants and Fuels*, and 44 *Energy Production and Conversion*.

N81-10067* National Aeronautics and Space Administration, Lewis Research Center, Cleveland, Ohio.

COMPARISONS OF FOUR ALTERNATIVE POWERPLANT TYPES FOR FUTURE GENERAL AVIATION AIRCRAFT

T. J. Wickenheiser, G. Knip, R. M. Plencner, and W. C. Strack

Oct. 1980 50 p refs
(NASA-TM-81584; E-561) Avail: NTIS HC A03/MF A01 CSCL 21E

Recently completed NASA sponsored conceptual studies were culminated in the identification of promising new technologies for future spark ignition, diesel, rotary, and turbine engines. The results of a NASA in-house preliminary assessment study that compares these four powerplants types in several general aviation applications are reported. The evaluation consisted of installing each powerplant type in rubberized aircraft which are sized to accomplish fixed missions. The primary evaluation criteria include projected aircraft cost, total ownership cost, and mission fuel.

Author

N81-11037* National Aeronautics and Space Administration, Lewis Research Center, Cleveland, Ohio.

LOW-SPEED AERODYNAMIC PERFORMANCE OF 50.8-CENTIMETER-DIAMETER NOISE-SUPPRESSING INLETS FOR THE QUIET, CLEAN, SHORT-HAUL EXPERIMENTAL ENGINE (QCSEE)

John M. Abbott, James H. Diedrich, and Robert C. Williams

Aug. 1978 37 p refs
(NASA-TP-1178; E-9542) Avail: NTIS HC A03/MF A01 CSCL 21E

Two basic inlet concepts, a high throat Mach number (0.79) design and a low throat Mach number (0.60) design, were tested with four diffuser acoustical treatment designs that had face sheet porosity ranging from 0 to 24 percent for the high Mach number inlet and 0 to 28 percent for the low Mach number inlet. The tests were conducted in a low speed wind tunnel at free stream velocities of 0, 41, and 62 m/sec and angles of attack to 50 deg. Inlet throat Mach number was varied about the design value. Increasing the inlet diffuser face sheet porosity resulted in an increase in total pressure loss in the boundary layer for both the high and low Mach number inlet designs, however, the overall effect on inlet total pressure recovery of 0.991 at the design throat Mach number, a free stream velocity of 41 m/sec, and an angle of attack of 50 deg; inlet flow separation at an angle of attack of 50 deg was encountered with only one inlet configuration the high Mach number design with the highest diffuser face sheet porosity (24 percent). A.R.H.

N81-11038* National Aeronautics and Space Administration, Lewis Research Center, Cleveland, Ohio. Propulsion Lab.

OFF-DESIGN PERFORMANCE LOSS MODEL FOR RADIAL TURBINES WITH PIVOTING, VARIABLE-AREA STATORS

Peter L. Meitner and Arthur J. Glassman Nov. 1980 15 p refs

(NASA-TP-1708; AVRADCOM-TR-80-C-13; E-455) Avail: NTIS HC A02/MF A01 CSCL 21E

An off-design performance loss model was developed for variable stator (pivoted vane), radial turbines through analytical modeling and experimental data analysis. Stator loss is determined by a viscous loss model; stator vane end-clearance leakage effects are determined by a clearance flow model. Rotor loss coefficient were obtained by analyzing the experimental data from a turbine rotor previously tested with six stators having throat areas from 20 to 144 percent of design area and were correlated with

stator-to-rotor throat area ratio. An incidence loss model was selected to obtain best agreement with experimental results. Predicted turbine performance is compared with experimental results for the design rotor as well as with results for extended and cutback versions of the rotor. Sample calculations were made to show the effects of stator vane end-clearance leakage.

Author

N81-11039* National Aeronautics and Space Administration, Lewis Research Center, Cleveland, Ohio.

SURFACE PYROMETRY IN PRESENCE OF RADIATION FROM OTHER SOURCES WITH APPLICATION TO TURBINE BLADE TEMPERATURE MEASUREMENT

Donald R. Buchele Nov. 1980 19 p refs
(NASA-TP-1754; E-396) Avail: NTIS HC A02/MF A01 CSCL 21E

Surface pyrometry is feasible even when the amount of surface radiation is exceeded by radiation from surrounding sources. To measure and correct for this interfering radiation, several methods that use multiple wavelength pyrometry were compared by an error analysis. For a specific application of turbine blade temperature measurement in a turbofan engine, a two wavelength method was best. Auxiliary measurements at the same wavelengths substantially improve the accuracy of the method. S.F.

N81-12084* National Aeronautics and Space Administration, Lewis Research Center, Cleveland, Ohio.

LOW-SPEED AERODYNAMIC PERFORMANCE OF 50.8-CENTIMETER-DIAMETER NOISE-SUPPRESSING INLETS FOR THE QUIET, CLEAN, SHORT-HAUL EXPERIMENTAL ENGINE (QCSEE)

John M. Abbott, James H. Diedrich, and Robert C. Williams

Aug. 1978 37 p refs
(NASA-TP-1178; E-9542) Avail: NTIS HC A03/MF A01 CSCL 21E

Two basic inlet concepts, a high throat Mach number (0.79) design and a low throat Mach number (0.60) design, were tested with four diffuser acoustical treatment designs that had face sheet porosity ranging from 0 to 24 percent for the high Mach number inlet and 0 to 28 percent for the low Mach number inlet. The tests were conducted in a low speed wind tunnel at free stream velocities of 0, 41, and 62 m/sec and angles of attack to 50 deg. Inlet throat Mach number was varied about the design value. Increasing the inlet diffuser face sheet porosity resulted in an increase in total pressure loss in the boundary layer for both the high and low Mach number inlet designs, however, the overall effect on inlet total pressure recovery of 0.991 at the design throat Mach number, a free stream velocity of 41 m/sec, and an angle of attack of 50 deg; inlet flow separation at an angle of attack of 50 deg was encountered with only one inlet configuration the high Mach number design with the highest diffuser face sheet porosity (24 percent). A.R.H.

N81-12089* National Aeronautics and Space Administration, Lewis Research Center, Cleveland, Ohio.

EFFECT OF HOLE GEOMETRY AND ELECTRIC-DISCHARGE MACHINING (EDM) ON AIRFLOW RATES THROUGH SMALL DIAMETER HOLES IN TURBINE BLADE MATERIAL

Steven A. Hippensteele and Reeves P. Cochran Nov. 1980 14 p

(NASA-TP-1716; E-417) Avail: NTIS HC A02/MF A01 CSCL 21E

The effects of two design parameters, electrode diameter and hole angle, and two machine parameters, electrode current and current-on time, on air flow rates through small-diameter (0.257 to 0.462 mm) electric-discharge-machined holes were measured. The holes were machined individually in rows of 14 each through 1.6 mm thick IN-100 strips. The data showed linear increase in air flow rate with increases in electrode cross sectional area and current-on time and little change with changes in hole angle and electrode current. The average flow-rate deviation (from the mean flow rate for a given row) decreased linearly

with electrode diameter and increased with hole angle. Burn time and finished hole diameter were also measured. Author

N81-12090* National Aeronautics and Space Administration. Lewis Research Center, Cleveland, Ohio.

PROPULSION CONTROLS, 1979

Oct. 1980 147 p refs Proc. of symp. held in Cleveland, 17-19 May 1979

(NASA-CP-2137; E-477) Avail: NTIS HC A07/MF A01 CSCL 21E

The state of the art of multivariable engine control is examined in order to determine future needs and problem areas and to establish the appropriate roles of government, industries, and universities in addressing these problems. For individual titles, see N81-12091 through N81-12104.

N81-12091* National Aeronautics and Space Administration. Lewis Research Center, Cleveland, Ohio.

MULTIVARIABLE IDENTIFICATION USING CENTRALIZED FIXED MODES

Walter C. Merrill In its Propulsion Controls, 1979 Oct. 1980 p 3-10 refs (For primary document see N81-12090 03-07) Avail: NTIS HC A07/MF A01 CSCL 21E

A procedure to determine a state space model of a multivariable system (λ inputs, m outputs) is presented. The model is suitable for control studies and uses single input, single output (SISO) system data in the identification procedure. The procedure can be defined in three distinct steps. First, the system's $\lambda \times m$ SISO transfer functions are identified by using any standard or known identification technique for SISO systems. One objective of this step is to identify SISO transfer functions with as few distinct modes as possible between any two functions. Second, the time domain realization of each SISO transfer function is obtained in a straightforward manner and combined into a total multivariable realization. This total realization, in all probability, has more state variables than are required to define system response. In the third step, these excess or redundant states are removed by using minimal realization theory. The remaining states are related to system centralized fixed modes. Eigenvalue-eigenvector techniques were recently reported that yield a computationally feasible solution to the problem posed in step three. The procedure is applied to QCSSE data to demonstrate its feasibility. Author

N81-12092* National Aeronautics and Space Administration. Lewis Research Center, Cleveland, Ohio.

PERFORMANCE SEEKING CONTROLS

Kurt Seldner In its Propulsion Controls, 1979 Oct. 1980 p 11-17 refs (For primary document see N81-12090 03-07)

Avail: NTIS HC A07/MF A01 CSCL 21E

A performance logic algorithm (PSL) was developed to optimize the performance of propulsion systems for component and sensor degradations by monitoring the performance of the engine system and minimizing thrust specific fuel consumption (TSFC) while retaining a constant engine net thrust. Engine constraints such as surge margin, speed, pressure, and temperature are observed. The PSL algorithm was applied to the quiet, clean, short haul experimental engine. Engine control set points were modified for component degradations in order to restore the nominal net thrust. Results show convergence to the optimum value can be obtained within 60 to 90 seconds, which makes the program acceptable to on line operation with present state of the art minicomputers. Tests indicate that in most cases the PSL algorithm offers some improvement in thrust specific fuel consumption over the manual throttle. A.R.H.

N81-12093* National Aeronautics and Space Administration. Lewis Research Center, Cleveland, Ohio.

F100 MULTIVARIABLE CONTROL SYNTHESIS PROGRAM: A REVIEW OF FULL SCALE ENGINE ALTITUDE TESTS

Bruce Lehtinen and James F. Soeder In its Propulsion Controls, 1979 Oct. 1980 p 20-34 refs (For primary document see N81-12090 03-07)

Avail: NTIS HC A07/MF A01 CSCL 21E

The benefits of linear quadratic regulator synthesis methods in designing a multivariable engine control capable of operating an engine throughout its flight envelope were demonstrated. The entire multivariable control synthesis program is reviewed with particular emphasis on engine tests conducted in the NASA Lewis propulsion systems laboratory altitude facility. The multivariable control has basically a proportional plus integral, model following structure with gains scheduled as functions of flight condition. The multivariable control logic design is described, along with control computer implementation aspects. Altitude tests demonstrated that the multivariable control logic could control an engine over a wide range of test conditions. Representative transient responses are presented to demonstrate engine behavior and the functioning of the control logic. A.R.H.

N81-12099* National Aeronautics and Space Administration. Lewis Research Center, Cleveland, Ohio.

PROPULSION CONTROL AND CONTROL THEORY: A NEW RESEARCH FOCUS

John R. Zeller In its Propulsion Controls, 1979 Oct. 1980 p 89-95 (For primary document see N81-12090 03-07)

Avail: NTIS HC A07/MF A01 CSCL 21E

Technological developments necessary for the implementation of advanced digital control concepts for aircraft propulsion are identified and discussed. Developments associated with the replacement analog controllers with digital control systems, sensors and actuators, and control modes and software are reported. M.G.

N81-13066* National Aeronautics and Space Administration. Lewis Research Center, Cleveland, Ohio.

NASA RESEARCH IN AEROPROPULSION

Warner L. Stewart and Richard J. Weber 1981 24 p Proposed for presentation at the 26th Ann. Intern. Gas Turbine Conf., Houston, Tex., 8-12 Mar. 1981; sponsored by the ASME (NASA-TM-81633; E-645) Avail: NTIS HC A02/MF A01 CSCL 21E

Selected examples of recent accomplishments and current activities that are relevant to the principal classes of civil and military vehicles: subsonic transports, commutators, supersonic transports, general aviation, rotorcraft, V/STOL, and high performance. Some instances of emerging technologies with potential high impact on further progress are discussed. E.D.K.

N81-14199* National Aeronautics and Space Administration. Lewis Research Center, Cleveland, Ohio.

CURVED CENTERLINE AIR INTAKE FOR A GAS TURBINE ENGINE Patent

William C. Ruehr (GE, Cincinnati), James L. Youngmans (GE, Cincinnati), and Edwin B. Smith, inventors (to NASA) (GE, Cincinnati) Issued 2 Sep. 1980 6 p Filed 14 May 1979 Sponsored by NASA (NASA-Case-LEW-13201-1; US-Patent-4,220,171; US-Patent-Appl-SN-038980; US-Patent-Class-137-15.1; US-Patent-Class-181-214) Avail: US Patent and Trademark Office CSCL 21E

An inlet for a gas turbine engine was disposed about a curved centerline for the purpose of accepting intake air that is flowing at an angle to engine centerline and progressively turning that intake airflow along a curved path into alignment with the engine. This curved inlet is intended for use in under the wing locations and similar regions where airflow direction is altered by aerodynamic characteristics of the airplane. By curving the inlet, aerodynamic loss and acoustic generation and emission are decreased.

Official Gazette of the U.S. Patent and Trademark Office

N81-16050* National Aeronautics and Space Administration, Lewis Research Center, Cleveland, Ohio.

COLD-AIR INVESTIGATION OF FIRST STAGE OF 4-1/2-STAGE, FAN DRIVE TURBINE WITH AVERAGE STAGE LOADING FACTOR OF 4.86

Warren J. Whitney, Thomas P. Moffitt, and Frank P. Behning
JAN. 1981 15 p refs
(N.SA-TP-1780; E-461) Avail. NTIS HC A02/MF A01 CSCL 21E

The design procedure and the development of the blading geometry for the 4 and 1/2 stage turbine are discussed. Results obtained with the first stage, operated as a single stage turbine, are presented. A free vortex design meets the design requirements without incurring problems such as excessive turning, negative reaction, or high Mach number. Cold air tests of the single stage turbine showed that the turbine developed design work (stage loading factor of 5.26) at an efficiency of 0.86, which was the efficiency predicted by a reference method. The mass flow at this condition was 0.88, which occurred at design speed and a pressure ratio of 1.407, corresponding to a stage loading factor of 4.35. The efficiency at this condition was 0.003 higher than that predicted by the reference method. Author

N81-16052* National Aeronautics and Space Administration, Lewis Research Center, Cleveland, Ohio.

AN OVERVIEW OF GENERAL AVIATION PROPULSION RESEARCH PROGRAMS AT NASA LEWIS RESEARCH CENTER

Edward A. Willis and William C. Strack 1981 48 p refs
Proposed for presentation at the Natl. Business Aircraft Meeting, 13-15 Apr. 1981, Wichita, Kansas; sponsored by SAE
(NASA-TM-81666; E-686) Avail. NTIS HC A03/MF A01 CSCL 21E

The review covers near-term improvements for current-type piston engines, as well as studies and limited corroborative research on several advanced g/a engine concepts, including diesels, small turboprops and both piston and rotary stratified-charge engines. Also described is basic combustion research, cycle modeling and diagnostic instrumentation work that is required to make new engines a reality. T.M.

N81-16053* National Aeronautics and Space Administration, Lewis Research Center, Cleveland, Ohio.

MEAN ROTOR WAKE CHARACTERISTICS OF AN AERODYNAMICALLY LOADED 0.5 m DIAMETER FAN

L. M. Shaw and F. W. Glaser 1981 18 p refs
Presented at 19th Aerospace Sci. Meeting, St. Louis, 12-15 Jan. 1981; sponsored by AIAA
(NASA-TM-81657; E-674) Avail. NTIS HC A02/MF A01 CSCL 01A

Mean rotor wake properties at several downstream distances behind the rotor of a loaded 1.2 pressure ratio fan were measured with a cross film anemometer in an anechoic wind tunnel. Mean wake characteristics in the midspan and near tip region were determined utilizing an ensemble averaging technique. The upwash and streamwise components of the velocity behind the rotor indicate a complex structure superimposed on the major velocity defects at a down stream spacing of 0.5 rotor chords. Spectral analysis indicates high levels of the second and fourth harmonics of the blade passage frequency in the midspan region while the blade passage frequency and its second and third harmonic are predominant in the tip region. Author

N81-16054* National Aeronautics and Space Administration, Lewis Research Center, Cleveland, Ohio.

EXPERIMENTAL ANALYSIS OF IMEP IN A ROTARY COMBUSTION ENGINE

H. J. Schock, W. J. Rice, and P. R. Meng 1981 44 p refs
Presented at Intern. Symp. of Automotive Engr., Detroit, 23-27 Feb. 1981
(NASA-TM-81662; E-680) Avail. NTIS HC A03/MF A01 CSCL 21E

A real time indicated mean effective pressure measurement system is described which is used to judge proposed improvements

in cycle efficiency of a rotary combustion engine. This is the first self-contained instrument that is capable of making real time measurements of IMEP in a rotary engine. Previous methods used require data recording and later processing using a digital computer. The unique features of this instrumentation include its ability to measure IMEP on a cycle by cycle, real time basis and the elimination of the need to differentiate volume function in real time. Measurements at two engine speeds (2000 and 3000 rpm) and a full range of loads are presented, although the instrument was designed to operate to speeds of 9000 rpm. Author

N81-16055* National Aeronautics and Space Administration, Lewis Research Center, Cleveland, Ohio.

PROPULSION SYSTEM MATHEMATICAL MODEL FOR A LIFT/CRUISE FAN V/STOL AIRCRAFT

Gary L. Cole, James F. Sellers, and Bruce E. Tining (NASA, Ames Research Center) Dec. 1980 48 p refs
(NASA-TM-81663; E-681) Avail. NTIS HC A03/MF A01 CSCL 21E

A propulsion system mathematical model is documented that allows calculation of internal engine parameters during transient operation. A non-realtime digital computer simulation of the model is presented. It is used to investigate thrust response and modulation requirements as well as the impact of duty cycle on engine life and design criteria. Comparison of simulation results with steady state cycle deck calculations showed good agreement. The model was developed for a specific 3-fan subsonic V/STOL aircraft application, but it can be adapted for use with any similar lift/cruise V/STOL configuration. Author

N81-19115* National Aeronautics and Space Administration, Lewis Research Center, Cleveland, Ohio.

APPARATUS FOR SENSOR FAILURE DETECTION AND CORRECTION IN A GAS TURBINE ENGINE CONTROL SYSTEM Patent

Henry A. Spang, III (GE, Cincinnati) and Robert P. Wenger, inventors (to NASA) (GE, Cincinnati) Issued 3 Feb. 1981 14 p
Filed 24 May 1978 Continuation in part of abandoned US Patent Appl. SN-752050, filed 20 Dec. 1976 Sponsored by NASA
(NASA-Case-LEW-12907-2; US-Patent-4,249,238;
US-Patent-Appl-SN-909235; US-Patent-Appl-SN-752050;
US-Patent-Class-364-106; US-Patent-Class-60-39,24;
US-Patent-Class-364-431) Avail. US Patent and Trademark Office CSCL 21E

A gas turbine engine control system maintains a selected level of engine performance despite the failure or abnormal operation of one or more engine parameter sensors. The control system employs a continuously updated engine model which simulates engine performance and generates signals representing real time estimates of the engine parameter sensor signals. The estimate signals are transmitted to a control computational unit which utilizes them in lieu of the actual engine parameter sensor signals to control the operation of the engine. The estimate signals are also compared with the corresponding actual engine parameter sensor signals and the resulting difference signals are utilized to update the engine model. If a particular difference signal exceeds specific tolerance limits, the difference signal is inhibited from updating the model and a sensor failure indication is provided to the engine operator.

Official Gazette of the U.S. Patent and Trademark Office

N81-19116* National Aeronautics and Space Administration, Lewis Research Center, Cleveland, Ohio.

INTEGRATED CONTROL SYSTEM FOR A GAS TURBINE ENGINE Patent

Jack E. Cornett (GE, Cincinnati), Andrew A. Saunders, Jr. (GE, Cincinnati), Ira E. Marvin (GE, Cincinnati), and Richard S. Beitler, inventors (to NASA) (GE, Cincinnati) Issued 6 Jan. 1981 10 p
Filed 25 May 1978 Continuation in part of abandoned US Patent Appl. SN-741056, filed 11 Nov. 1976 Sponsored by NASA
(NASA-Case-LEW-12594-2; US-Patent-4,242,864;
US-Patent-Appl-SN-909608; US-Patent-Appl-SN-741056;

US-Patent-Class-60-226R; US-Patent-Class-60-236;
US-Patent-Class-60-238; US-Patent-Class-60-239) Avail: US
Patent and Trademark Office CSCL 21E

A control system for a turbofan engine receives signals from a number of engine sensors and from the engine operator, and generates control signals. One control signal regulates the fan exhaust nozzle area in order to control inlet throat Mach number to maintain a low level of engine noise. Additional control signals regulate fuel flow to control engine thrust and fan pitch to control fan speed. A number of schedules are utilized to maintain a predetermined relationship between the controlled parameters and a number of fixed and calculated limits can override the control signals to prevent unsatisfactory engine performance.

Official Gazette of the U.S. Patent and Trademark Office

NS1-19121* National Aeronautics and Space Administration,
Lewis Research Center, Cleveland, Ohio.

SPECTRAL FLAME RADIANCE FROM A TUBULAR-CAN COMBUSTOR

Russell W. Claus Feb. 1981 15 p refs
(NASA-TP-1722; E-509) Avail: NTIS HC A02/MF A01 CSCL 21E

An experimental investigation was conducted to determine the effects of fuel type, fuel-air ratio, and inlet-air pressure on the spectral flame radiance emanating from a JT8D can combustor. Spectral radiance measurements from 1.55 to 5.5 micrometers of wavelength were recorded and analyzed to determine soot concentration and flame temperature at various axial locations in the combustor. Two fuels differing in volatility, viscosity, and chemical composition were used in this investigation. Author

NS1-20076* National Aeronautics and Space Administration,
Lewis Research Center, Cleveland, Ohio.

REASONS FOR LOW AERODYNAMIC PERFORMANCE OF 13.5-CENTIMETER-TIP-DIAMETER AIRCRAFT ENGINE STARTER TURBINE

Jeffrey E. Haas, Richard J. Roelke, and Paul Hermann (Sundstrand Corp., Rockford, Ill.) Mar. 1981 18 p Presented at the SAE Aerospace Meeting, Los Angeles, 13-16 Oct. 1980
(NASA-TP-1810; E-540; AVRADCOM-TR 80 C-17) Avail: NTIS HC A02/MF A01 CSCL 21E

The reasons for the low aerodynamic performance of a 13.5 cm tip diameter aircraft engine starter turbine were investigated. Both the stator and the stage were evaluated. Approximately 10 percent improvement in turbine efficiency was obtained when the honeycomb shroud over the rotor blade tips was filled to obtain a solid shroud surface. Efficiency improvements were obtained for three rotor configurations when the shroud was filled. It is suggested that the large loss associated with the open honeycomb shroud is due primarily to energy loss associated with gas transportation as a result of the blade to blade pressure differential at the tip section. E.A.K.

NS1-21078* National Aeronautics and Space Administration,
Lewis Research Center, Cleveland, Ohio.

EXHAUST EMISSION SURVEY OF AN F100 AFTERBURNING TURBOFAN ENGINE AT SIMULATED ALTITUDE FLIGHT CONDITIONS

John E. Moss and Richard R. Cullom Mar. 1981 28 p refs
(NASA-TM-81656; E-673) Avail: NTIS HC A03/MF A01 CSCL 21E

Emissions of carbon monoxide, total oxides of nitrogen, unburned hydrocarbons, and carbon dioxide from an F100, afterburning, two spool turbofan engine at simulated flight conditions are reported. For each flight condition emission measurements were made for two or three power levels from intermediate power (nonafterburning) through maximum afterburning. The data showed that emissions vary with flight speed, altitude, power level, and radial position across the nozzle. Carbon monoxide emissions were low for intermediate power (nonafterburning) and partial afterburning, but regions of high carbon monoxide were present downstream of the flame holder at maximum afterburning. Unburned hydrocarbon emissions were low for most of the simulated flight conditions. The local NOx concentrations and their variability with power level increased with increasing flight Mach number at constant altitude, and decreased with increasing altitude at constant Mach number. Carbon dioxide emissions were proportional to local fuel air ratio for all conditions. Author

NS1-22066* National Aeronautics and Space Administration,
Lewis Research Center, Cleveland, Ohio.

THERMAL AND FLOW ANALYSIS OF A CONVECTION AIR-COOLED CERAMIC COATED POROUS METAL CONCEPT FOR TURBINE VANES

Francis S. Stepka 1981 12 p refs Presented at the 20th Natl. Heat Transfer Conf., Milwaukee, 2-5 Aug. 1981; sponsored by the ASME and the American Inst. of Chemical Engineers (NASA-TM-81749; E-815) Avail: NTIS HC A02/MF A01 CSCL 21E

The heat transfer and pressure drop through turbine vanes made of a sintered, porous metal coated with a thin layer of ceramic and convection cooled by spanwise flow of cooling air were analyzed. The analysis was made to determine the feasibility of using this concept for cooling very small turbines, primarily for short duration applications such as in missile engines. The analysis was made for gas conditions of approximately 10 and 40 atm and 1644 K and with turbine vanes made of felt type porous metals with relative densities from 0.2 to 0.6 and ceramic coating thicknesses of 0.076 to 0.254 mm. J.M.S.

NS1-24063* National Aeronautics and Space Administration,
Lewis Research Center, Cleveland, Ohio.

FUNDAMENTAL HEAT TRANSFER RESEARCH FOR GAS TURBINE ENGINES

Darryl E. Metzger, ed. (Arizona State Univ.) 1980 68 p refs
Presented at a Workshop Held at Cleveland, 8-9 Oct. 1980
(NASA-CP-2178; E-666) Avail: NTIS HC A04/MF A01 CSCL 21E

Thirty-seven experts from industry and the universities joined 24 NASA Lewis staff members in an exchange of ideas on trends in aeropropulsion research and technology, basic analyses, computational analyses, basic experiments, near-engine environment experiments, fundamental fluid mechanics and heat transfer, and hot technology as related to gas turbine engines. The workshop proceedings described include pre-workshop input from participants, presentations of current activity by the Lewis staff, reports of the four working groups, and a workshop summary. A.R.H.

NS1-24065* National Aeronautics and Space Administration,
Lewis Research Center, Cleveland, Ohio.

ANALYSIS OF EFFECT OF FLAMEHOLDER CHARACTERISTICS ON LEAN, PREMIXED, PARTIALLY VAPORIZED FUEL-AIR MIXTURES QUALITY AND NITROGEN OXIDES EMISSIONS

Larry P. Cooper May 1981 18 p refs
(NASA-TP-1842; E-563) Avail: NTIS HC A02/MF A01 CSCL 21E

An analysis was conducted of the effect of flameholding devices on the precombustion fuel-air characteristics and on oxides of nitrogen (NOx) emissions for combustion of premixed partially vaporized mixtures. The analysis includes the interrelationships of flameholder droplet collection efficiency, reatomization efficiency and blockage, and the initial droplet size distribution and accounts for the contribution of droplet combustion in partially vaporized mixtures to NOx emissions. Application of the analytical procedures is illustrated and parametric predictions of NOx emissions are presented. Author

NS1-24066* National Aeronautics and Space Administration,
Lewis Research Center, Cleveland, Ohio.

INVESTIGATION OF PERFORMANCE DETERIORATION OF THE CF6/JT9D HIGH BYPASS RATIO TURBOFAN ENGINES

Joseph A. Ziemianski In AGARD Turbine Engine Testing Jan. 1981 14 p refs (For primary document see NS1-24071 15-07) Avail: NTIS HC A21/MF A01 CSCL 21E

The extent and magnitude of performance deterioration of the Pratt and Whitney JT9D, and the General Electric CF6 engine models is presented. Overall engine and contributing module performance deterioration with respect to flight cycles and/or time are analyzed. The overall engine performance deterioration analyses are based on data obtained from historical records.

special engine tests, and tests for specific effects. Hardware inspection data from overhaul shops and special module tests are the basis for the modular performance deterioration data used in the analyses. Various damage mechanisms such as seal rubs, erosion, surface roughness and thermal distortion, and how they contribute to performance deterioration are included in the modular analyses. Results indicate that early performance deterioration occurring within the first few flights of these engines is less than 1 percent in cruise specific fuel consumption (SFC), that it is event oriented, and that it is the result of increased blade tip clearances. This performance deterioration gradually increases to about 2.5 to 3.0 percent (including the initial short term deterioration) after 2500 to 3000 flights where increased blade tip clearances, airfoil quality degradation, and thermal distortion are the contributing causes. R.C.T.

N81-25079* National Aeronautics and Space Administration, Lewis Research Center, Cleveland, Ohio.
COMPARISON OF NASA AND CONTRACTOR RESULTS FROM AEROACOUSTIC TESTS OF QCSEE OTW ENGINE
 H. E. Bloomer, I. J. Loeffler, W. J. Kreim, and J. W. Coats
 Apr. 1981 27 p refs
 (NASA-TM-81761; E-824) Avail: NTIS HC A03/MF A01 CSCL 21E

The aerodynamics and acoustics of the over-the-wing (OTW) Quiet, Clean, Short Haul Experimental Engine (QCSEE) were tested. A boilerplate (nonflight weight), high-throat Mach number, acoustically treated inlet and a D-shaped OTW exhaust nozzle with variable position side doors were used. Some acoustic directivity results for the type 'D' nozzle and acoustic effects of variations in the nozzle side door positions are included. It was found that the results are in agreement with those previously obtained. E.A.K.

N81-25080* National Aeronautics and Space Administration, Lewis Research Center, Cleveland, Ohio.
MEASUREMENT OF AERODYNAMIC WORK DURING FAN FLUTTER
 A. P. Kurkov 1981 16 p refs Proposed for presentation at the 1981 Winter Ann. Meeting of the ASME, Washington, D.C., 15-20 Nov. 1981
 (NASA-TM-82652; E-911) Avail: NTIS HC A02/MF A01 CSCL 21E

Stationary high response pressure and displacement measurements are used to describe the flutter characteristics of the first fan rotor of a turbofan engine. Flutter occurred at part speed and at high incidence. Several forward and backward traveling waves were identified in a predominantly torsional flutter mode. Positive aerodynamic work contribution was confined to the region close to the leading edge and was mainly due to modes corresponding to forward traveling waves of nodal diameters in the range 3 to 5. Author

N81-25081* National Aeronautics and Space Administration, Lewis Research Center, Cleveland, Ohio.
EFFECT OF A PART-SPAN VARIABLE INLET GUIDE VANE ON THE PERFORMANCE OF A HIGH-BYPASS TURBOFAN ENGINE

George A. Bobula (AVRADCOM Research and Technology Labs., Cleveland), Ronald H. Soeder, and Leo A. Burkardt 1981 15 p refs Proposed for presentation at the 17th Joint Propulsion Conf., Colorado Springs, 27-29 Jul. 1981; sponsored by AIAA, ASME, and SAE
 (NASA-TM-82617; E-869, AVRADCOM-TR-81-C-10) Avail: NTIS HC A02/MF A01 CSCL 21E

The ability of a part span variable inlet guide vane (VIGV) to modulate the thrust of a high bypass turbofan engine was evaluated at altitude/Mach number conditions of 4572 m/0.6 and 9144 m/0.93. Fan tip, gas generator and supercharger performance were also determined, both on operating lines and during fan duct throttling. The evaluation was repeated with the bypass splitter extended forward to near the fan blade trailing edge. Gross thrust attenuation of over 50 percent was achieved

with 50 degree VIGV closure at 100 percent corrected fan speed. Gas generator supercharger performance fell off with VIGV closure, but this loss was reduced when a splitter extension was added. The effect of VIGV closure on gas generator performance was minimal. Author

N81-25082* National Aeronautics and Space Administration, Lewis Research Center, Cleveland, Ohio.
JT9D PERFORMANCE DETERIORATION RESULTS FROM A SIMULATED AERODYNAMIC LOAD TEST
 Edward G. Stakolich and William J. Stromberg (Pratt and Whitney Aircraft, East Hartford, Conn.) 1981 21 p refs Proposed for presentation at the 17th Joint Propulsion Conf., Colorado Springs, 27-29 Jul. 1981; sponsored by AIAA, SAE, and ASME
 (NASA-TM-82640; E-895) Avail: NTIS HC A02/MF A01 CSCL 21E

The results of testing to identify the effects of simulated aerodynamic flight loads on JT9D engine performance are presented. The test results were also used to refine previous analytical studies on the impact of aerodynamic flight loads on performance losses. To accomplish these objectives, a JT9D-7AH engine was assembled with average production clearances and new seals as well as extensive instrumentation to monitor engine performance, case temperatures, and blade tip clearance changes. A special loading device was designed and constructed to permit application of known moments and shear forces to the engine by the use of cables placed around the flight inlet. The test was conducted in the Pratt & Whitney Aircraft X-Ray Test Facility to permit the use of X-ray techniques in conjunction with laser blade tip proximity probes to monitor important engine clearance changes. Upon completion of the test program, the test engine was disassembled, and the condition of gas path parts and final clearances were documented. The test results indicate that the engine lost 1.1 percent in thrust specific fuel consumption (TSFC), as measured under sea level static conditions, due to increased operating clearances caused by simulated flight loads. This compares with 0.9 percent predicted by the analytical model and previous study efforts. Author

N81-25083* National Aeronautics and Space Administration, Lewis Research Center, Cleveland, Ohio.
SELECTED RESULTS FROM COMBUSTION RESEARCH AT THE LEWIS RESEARCH CENTER
 Robert E. Jones 1981 13 p refs Proposed for presentation at the 17th Joint Propulsion Conf., Colorado Springs, 27-29 Jul. 1981; sponsored by AIAA, SAE, and ASME
 (NASA-TM-82627; E-880) Avail: NTIS HC A02/MF A01 CSCL 21E

Combustion research at Lewis is organized to provide a balanced program responsive to national needs and the gas turbine industry. The results of this research is a technology base that assists the gas turbine engine manufacturers in developing new and improved combustion systems for advanced civil and military engines with significant improvements in performance, durability, fuel flexibility and control of exhaust emissions. Research efforts consist of fundamentals and modeling, and applied component and combustor research. T.M.

N81-25084* National Aeronautics and Space Administration, Lewis Research Center, Cleveland, Ohio.
HIGH-RESPONSE MEASUREMENTS OF A TURBOFAN ENGINE DURING NONRECOVERABLE STALL
 Doug Lee Apr. 1981 27 p refs
 (NASA-TM-81759; E-822) Avail: NTIS HC A03/MF A01 CSCL 21E

High response measurements of a Pratt and Whitney F100(3) turbofan engine at a simulated Mach number and altitude of 1.2 and 3000 m (10,000 ft) respectively were recorded during a nonrecoverable stall. The nonrecoverable stall occurred as a result of incorrect scheduling of the high compressor variable vanes (RCVV) during an experimental engine control investigation. Recorded data indicates rotating stall originating in the high

pressure compressor. From this region the disturbance propagates upstream into the fan and downstream throughout the core compressor. The rotating stall remained in the core compressor until the engine was shutdown. The fan exhibited some rotating stall, but the amplitude of the pressure oscillations were less severe. Data indicates that the fan was able to recover from the stall. Fan turbine inlet temperature (FTIT) had been decreasing until stall developed in the high-pressure compressor. From this time, FTIT increased towards its maximum temperature limit. The rising FTIT during nonrecoverable stall may be the result of incomplete combustion in the combustor and additional combustion occurring through the turbine. Author

N81-26145* National Aeronautics and Space Administration, Lewis Research Center, Cleveland, Ohio.
TURBINE BYPASS ENGINE: A NEW SUPERSONIC CRUISE PROPULSION CONCEPT

Leo C. Franciscus 1981 15 p. refs. Presented at the 17th Joint Propulsion Conf., Colorado Springs, Colo., 27-29 Jul. 1981, sponsored by AIAA, SAE, and ASME
 (NASA-TM-82608; E-855) Avail: NTIS HC A02/MF A01 CSCL 21E

Engine performance and mission studies were carried out for a single-spool Turbine Bypass Engine concept. Comparisons were made between the TBE, a conventional single-spool turbojet, and the Pratt & Whitney Variable Stream Control Engine. The airplane assumed for the study was a Mach 2.32 commercial supersonic transport. The nominal mission was a 4000-nautical miles total range with a 300-nautical miles subsonic cruise leg. The figure of merit was the minimum takeoff gross weight for the mission. Comparisons of the three engines were also made for the 4000-nautical miles total range with longer subsonic cruise legs. Author

N81-26146* National Aeronautics and Space Administration, Lewis Research Center, Cleveland, Ohio.
SMALL GAS-TURBINE COMBUSTOR STUDY: FUEL INJECTOR EVALUATION

Carl T. Norgren and Stephen M. Riddibaugh 1981 20 p. refs. Presented at the Joint Propulsion Conf., Colorado Springs, Colo., 27-29 Jul. 1981, sponsored by AIAA, SAE, and ASME
 (NASA-TM-82641; E-891) Avail: NTIS HC A02/MF A01 CSCL 21E

As part of a continuing effort at the Lewis Research Center to improve performance, emissions, and reliability of turbine machinery, an investigation of fuel injection technique and effect of fuel type on small gas turbine combustors was undertaken. Performance and pollutant emission levels are documented over a range of simulated flight conditions for a reverse flow combustor configuration using simplex pressure-atomizing, spill-flow return, and splash cone airblast injectors. A parametric evaluation of the effect of increased combustor loading with each of the fuel injector types was obtained. Jet A and an experimental referee broad specification fuel were used to determine the effect of fuel type. Author

N81-27094* National Aeronautics and Space Administration, Lewis Research Center, Cleveland, Ohio.
THE SUPERSONIC FAN ENGINE: AN ADVANCED CONCEPT IN SUPERSONIC CRUISE PROPULSION

Leo C. Franciscus 1981 13 p. refs. Presented at the 17th Joint Propulsion Conf., Colorado Springs, Colo., 27-29 Jul. 1981, sponsored by AIAA, SAE, and ASME
 (NASA-TM-82657; E-923) Avail: NTIS HC A02/MF A01 CSCL 21E

Engine performance and mission studies were carried out for turbofan engines equipped with supersonic through-flow fans. The mission was for a commercial supersonic transport with a Mach 2.32 capability. The advantages of the supersonic fan engines are discussed in terms of mission range comparisons with other engine types. The effects of fan efficiency, inlet losses, and engine weight on engine performance and mission range are shown. The range of a supersonic transport with supersonic fan engines could be 10 to 20 percent better than with other types having the same technology core. Author

N81-27095* National Aeronautics and Space Administration, Lewis Research Center, Cleveland, Ohio.

MIXING EFFECTIVENESS TEST OF AN EXHAUST GAS MIXER IN A HIGH BYPASS TURBOFAN AT ALTITUDE

R. R. Cullom, G. A. Bobula, and L. A. Burkardt 1981 13 p. refs. Presented at the 17th Joint Propulsion Conf., Colorado Springs, Colo., 27-29 Jul. 1981, sponsored by AIAA, SAE, and ASME
 (NASA-TM-82663; AVRADCOM-TR-81-C-24; E-938) Avail: NTIS HC A02/MF A01 CSCL 21E

Thermal mixing effectiveness characteristics of an eighteen lobe, scalloped and unscalloped, partial, forced mixer were measured in a high-bypass turbofan engine. Data were also obtained without the mixer installed, i.e., free mixing. Tests were conducted at four combinations of simulated flight conditions from: 0.3 to 0.8 Mach number and from 6,096 meters (20,000 ft) to 13,715 m (45,000 ft) altitude, mixing chamber lengths of L/D = 0.52 and 0.65 were tested. For this range of test conditions and mixer configurations, the forced mixing effectiveness varied from 59 to 68 percent. Values of mixing effectiveness and total pressure loss were calculated from temperature and pressure data obtained at the mixer inlet and exhaust nozzle exit. Author

N81-28095* National Aeronautics and Space Administration, Lewis Research Center, Cleveland, Ohio.

THE E3 COMBUSTORS: STATUS AND CHALLENGES

Daniel E. Sokolowski and John E. Rohde 1981 24 p. refs. Presented at 17th Joint Propulsion Conf., Colorado Springs, Colo., 27-29 Jul. 1981, sponsored by AIAA, SAE, and ASME
 (NASA-TM-82684; E-904) Avail: NTIS HC A02/MF A01 CSCL 21E

The design, fabrication, and initial testing of energy efficient engine combustors, developed for the next generation of turbofan engines for commercial aircraft, are described. The combustor designs utilize an annular configuration with two zone combustion for low emissions, advanced liners for improved durability, and short, curved-wall, dump prediffusers for compactness. Advanced cooling techniques and segmented construction characterize the advanced liners. Linear segments are made from castable, turbine-type materials. M.G.

N81-29129* National Aeronautics and Space Administration, Lewis Research Center, Cleveland, Ohio.

SUPERCritical FUEL INJECTION SYSTEM Patent

Cecil J. Marek and Larry P. Cooper, inventors (to NASA) Issued 26 Feb. 1980 4 p. Filed 19 Jun. 1978 Supersedes N78-27122 (16 - 18, p. 2353)

(NASA-Case-LEW-12990-1; US-Patent-4,189,914;
 US-Patent-Appl-SN-916654; US-Patent-Class-60-726;
 US-Patent-Class-60-39.06; US-Patent-Class-261-28;
 US-Patent-Class-431-2; US-Patent-Class-60-737) Avail: US Patent and Trademark Office CSCL 21E

A fuel injection system for gas turbines is described including a pair of high pressure pumps. The pumps provide fuel and a carrier fluid such as air at pressures above the critical pressure of the fuel. A supercritical mixing chamber mixes the fuel and carrier fluid and the mixture is sprayed into a combustion chamber. The use of fuel and a carrier fluid at supercritical pressures promotes rapid mixing of the fuel in the combustion chamber so as to reduce the formation of pollutants and promote cleaner burning. Official Gazette of the U.S. Patent and Trademark Office

N81-30130* National Aeronautics and Space Administration
Lewis Research Center, Cleveland, Ohio.
ROTOR WAKE CHARACTERISTICS RELEVANT TO ROTOR-STATOR INTERACTION NOISE GENERATION
Loretta M. Shaw and Joseph R. Balombin 1981 25 p refs
Presented at 7th Acoustic Conf., Palo Alto, Calif., 5-7 Oct. 1981.
Sponsored by AIAA
(NASA-TM-82703, E-984) Avail. NTIS HC A02/MF A01 CSCL 21E

Mean and turbulent wake properties at three axial locations behind the rotor of an aerodynamically loaded 1" pressure ratio fan were measured using a stationary cross film anemometer in an anechoic wind tunnel. Wake characteristics at four radial immersions across the duct at four different fan speeds were determined utilizing a signal enhancement technique. The shapes of the waveforms of the mean rotor relative and mean upwash velocities were shown to change significantly across the span of the blades. In addition, an increase in fan rotational speed caused an increase in the maximum wake turbulence intensity levels near the hub and tip. Spectral analysis was used to describe the complex nature of the rotor wake. Author

N81-31195* National Aeronautics and Space Administration
Lewis Research Center, Cleveland, Ohio.
ADVANCED SUBSONIC TRANSPORT PROPULSION
Donald L. Nored, Carl C. Ciepluch, Roger Chamberlain, Edward T. Meleason, and Gerald A. Kraft 1981 32 p refs
Presented at the Intern. Air Transportation Conf., Atlantic City, N.J., 26-28 May 1981; sponsored by AIAA and SAE
(NASA-TM-82696, E-979) Avail. NTIS HC A03/MF A01 CSCL 21E

A brief review of the current NASA Energy Efficient Engine (E(3)) Project is presented. Included in this review are the factors that influenced the design of these turbofan engines and the advanced technology incorporated in them to reduce fuel consumption and improve environmental characteristics. In addition, factors such as the continuing spiral in fuel cost, that could influence future aircraft propulsion systems beyond those represented by the E(3) engines, are also discussed. Advanced technologies that will address these influencing factors and provide viable future propulsion systems are described. The potential importance of other propulsion system types, such as geared fans and turboshaft engines, is presented. TM

N81-31196* National Aeronautics and Space Administration
Lewis Research Center, Cleveland, Ohio.
AIRCRAFT ENGINE DIAGNOSTICS
Jul. 1981 277 p refs
Conf. held at Cleveland, 6-7 May 1981
(NASA-CP-2190, E-845) Avail. NTIS HC A17/MF A01 CSCL 21E

Engine durability and performance retention concepts are discussed. Other topics include engine diagnostics for performance retention and engine condition monitoring systems. For individual titles, see N81-31197 through N81-31217.

N81-31208* National Aeronautics and Space Administration
Lewis Research Center, Cleveland, Ohio.
AN INTRODUCTION TO NASA'S TURBINE ENGINE HOT SECTION TECHNOLOGY (HOST) PROJECT
Daniel J. Gaunther and C. Robert Ensign. In: *Aircraft Engine Diagnostics* 1981 p. 153-173. (For primary document see N81-31196 22-07)
Avail. NTIS HC A17/MF A01 CSCL 21E

An overview of research to develop and improve the accuracy of current analysis methods so that increased durability can be designed into future engines is presented. Emphasis is placed on improved accuracy in life prediction. Component design, including description of the thermal and aerodynamic environments, the material's mechanical response, the interactions between environmental and structural response, and high

temperature instrumentation capable of measuring near-engine environment effects are addressed. Component tests, improved modeling of the physical phenomena, and tests to verify the proved models are also discussed. JMS

N81-31208* National Aeronautics and Space Administration
Lewis Research Center, Cleveland, Ohio.
CONSERVATION OF STRATEGIC AEROSPACE MATERIALS (COSAM)

Joseph R. Stephens. In: *Aircraft Engine Diagnostics* 1981 p. 189-207. refs. (For primary document see N81-31196 22-07)
Avail. NTIS HC A17/MF A01 CSCL 21E

Research efforts to reduce the dependence of the aerospace industry on strategic metals, such as cobalt (Co), columbium (Cb), tantalum (Ta), and chromium (Cr), by providing the materials technology needed to minimize the strategic metal content of critical aerospace components for gas turbine engines are addressed. Thrusts in three technology areas are identified: near term activities in the area of strategic element substitution; intermediate-range activities in the area of materials processing; and long term, high risk activities in the area of 'new classes' of high temperature metallic materials. Specifically, the role of cobalt in nickel-base and cobalt-base superalloys vital to the aerospace industry is examined along with the mechanical and physical properties of intermetallics that will contain a minimum of the strategic metals. JMS

A81-20834 * Fuel/air nonuniformity - Effect on nitric oxide emissions. V. J. Lyons (NASA, Lewis Research Center, Cleveland, Ohio). *American Institute of Aeronautics and Astronautics, Aerospace Sciences Meeting, 19th, St. Louis, Mo., Jan. 12-15, 1981, Paper 81-0327*. 12 p. 22 refs.

An analytical and experimental study was performed to determine the effect of inlet fuel/air profile nonuniformity on NO(x) emissions. The theoretical NO(x) levels were verified in a flame-tube rig at inlet air temperatures of 600, 700, and 800 K, 0.3 MPa rig pressure, 25 m/sec reference velocity, overall equivalence ratio of 0.6 and residence time near 0.002 sec. The theory predicts an increase in NO(x) emissions for increased fuel/air nonuniformity for average equivalence ratios less than 0.7, while for average equivalence ratios near stoichiometric, increasing the nonuniformity will decrease NO(x) emissions. The results can be used to predict the degree of uniformity of fuel/air profiles necessary to achieve NO(x) emissions goals for actual engines that use lean premixed, prevaporized combustion systems. (Author)

A81-22531 * Core noise measurements from a small, general aviation turbofan engine. M. Reshotko and A. Karchmer (NASA, Lewis Research Center, Fluid Mechanics and Acoustics Div., Cleveland, Ohio). *Acoustical Society of America, Meeting, 100th, Los Angeles, Calif., Nov. 17-21, 1980, Paper*. 27 p. 10 refs.

As part of a program to investigate combustor and other core noises, simultaneous measurements of internal fluctuating pressure and far field noise were made with a JT15D turbofan engine. Acoustic waveguide probes, located in the engine at the combustor, at the turbine exit and in the core nozzle wall, were used to measure internal fluctuating pressures. Low frequency acoustic power determined at the core nozzle exit corresponds in level to the far-field acoustic power at engine speeds below 65% of maximum, the approach condition. At engine speeds above 65% of maximum, the jet noise dominates in the far-field, greatly exceeding that of the core. From coherence measurements, it is shown that the combustor is the dominant source of the low frequency core noise. The results obtained from the JT15D engine were compared with those obtained previously from a YF102 engine, both engines having reverse flow annular combustors and being in the same size class. (Author)

A81-29940 * # Superhybrid composite blade impact studies. C. C. Chamis, R. F. Lark, and J. H. Sinclair (NASA, Lewis Research Center, Cleveland, Ohio). *American Society of Mechanical Engineers, Gas Turbine Conference and Products Show, Houston, Tex., Mar. 9-12, 1981, Paper 81-GT-24*. 8 p. 5 refs. Members, \$2.00; nonmembers, \$4.00.

An investigation was conducted to determine the feasibility of superhybrid composite blades for meeting the mechanical design and impact resistance requirements of large fan blades for aircraft turbine engine applications. Two design concepts were evaluated: (1) leading edge spar (TiCom) and (2) center spar (TiCore), both with superhybrid composite shells. The investigation was both analytical and experimental. The results obtained show promise that superhybrid composites can be used to make light-weight, high-quality, large fan blades with good structural integrity. The blades tested successfully demonstrated their ability to meet steady-state operating conditions, overspeed, and small bird impact requirements. (Author)

A81-29954 * # Development of a low NO_x/lean premixed annular combustor. P. B. Roberts, A. J. Kubasco (Solar Turbines International, San Diego, Calif.), and N. J. Sekas (NASA, Lewis Research Center, Cleveland, Ohio). *American Society of Mechanical Engineers, Gas Turbine Conference and Products Show, Houston, Tex., Mar. 9-12, 1981, Paper 81-GT-40*. 8 p. 9 refs. Members, \$2.00; nonmembers, \$4.00. NASA-supported research.

The results of an experimental atmospheric rig test program developed to define a low NO_x annular combustor of 0.66 m diameter for high-altitude aircraft applications are presented. The test program strategy adopted evaluates the emission characteristics of a baseline configuration and subsequently examines the sensitivity of the emission signatures to variations in the key design features. The lean premixed combustor in axisymmetric annular form demonstrates the capability of operating at reduced-pressure, simulated high-altitude, supersonic cruise conditions with NO_x emissions below 1.0 g NO₂/kg fuel. The testing shows that for the full range of low emissions operation from idle to cruise, a variable dilution port system is necessary, but that fuel-switching can be avoided and a single fuel injection system used. L.S.

A81-30006 * # Low NO_x/and fuel flexible gas turbine combustors. H. G. Lew, S. M. DeCorso, G. Vermes, D. Carl (Westinghouse Electric Corp., Concordville, Pa.), W. J. Havener (Westinghouse Electric Corp., Madison, Pa.), J. Schwab (Westinghouse Electric Corp., Pittsburgh, Pa.), and J. Notardonato (NASA, Lewis Research Center, Cleveland, Ohio). *American Society of Mechanical Engineers, Gas Turbine Conference and Products Show, Houston, Tex., Mar. 9-12, 1981, Paper 81-GT-99*. 13 p. 12 refs. Members, \$2.00; nonmembers, \$4.00. Research supported by the U.S. Department of Energy; Contract No. DEN3-146.

The feasibility of various low NO_x emission gas turbine combustor configurations was evaluated. The configurations selected for fabrication and testing at full pressure and temperature involved rich-lean staged combustion utilizing diffusion flames, rich-lean prevaporized/premix flames, and staged catalytic combustion. The test rig consisted of a rich burner module, a quench module, and a lean combustion module. Test results are obtained for the combustor while burning petroleum distillate fuel, a coal derived liquid, and a petroleum residual fuel. The results indicate that rich-lean diffusion flames with low fuel-bound nitrogen conversion are achievable with very high combustion efficiencies. L.S.

A81-30033 * # Design and development of the combustor inlet diffuser for the NASA/GE energy efficient engine. P. E. Sabla, J. R. Taylor (General Electric Co., Evendale, Ohio), and D. J. Gauntner (NASA, Lewis Research Center, Cleveland, Ohio). *American Society of Mechanical Engineers, Gas Turbine Conference and Products Show, Houston, Tex., Mar. 9-12, 1981, Paper 81-GT-129*. 9 p. Members, \$2.00; nonmembers, \$4.00. Contract No. NAS3-20643.

Results of an experimental investigation of the aerodynamic

performance of a split duct annular combustor inlet diffuser system are presented. Several diffuser configurations were investigated in 3X-scale water table tests and the preferred design was evaluated in full-scale annular airflow model tests. Pressure recovery and flow losses were determined as a function of prediffuser inlet velocity profile, flow extraction at the prediffuser exit, and distribution of flow in the combustor. Inlet velocity profile and turbulence levels were found to have a pronounced effect on system performance. Flow extraction at the prediffuser exit was found to have little influence on system performance. Generally, the annular split duct diffuser system was found to satisfy the performance objectives for the engine. (Author)

A81-30057 * # A study of external fuel vaporization. E. J. Szelc, L. Chiappetta (United Technologies Research Center, East Hartford, Conn.), and C. E. Baker (NASA, Lewis Research Center, Cleveland, Ohio). *American Society of Mechanical Engineers, Gas Turbine Conference and Products Show, Houston, Tex., Mar. 9-12, 1981, Paper 81-GT-158*. 9 p. 16 refs. Members, \$2.00; nonmembers, \$4.00. Contract No. NAS3-21971.

Candidate external vaporizer designs for an aircraft gas turbine engine are evaluated with respect to fuel thermal stability, integration of the vaporizer system into the aircraft engine, engine and vaporizer dynamic response, startup and altitude restart, engine performance, control requirements, safety, and maintenance. The selected concept is shown to offer potential gains in engine performance in terms of reduced specific fuel consumption and improved engine thrust/weight ratio. The thrust/weight improvement can be traded against vaporization system weight. V.L.

A81-30078 * # Supersonic stall flutter of high-speed fans. J. J. Adamczyk, W. Stevans (NASA, Lewis Research Center, Cleveland, Ohio), and R. Jutras (General Electric Co., Evendale, Ohio). *American Society of Mechanical Engineers, Gas Turbine Conference and Products Show, Houston, Tex., Mar. 9-12, 1981, Paper 81-GT-184*. 8 p. 11 refs. Members, \$2.00; nonmembers, \$4.00.

An analytical model is proposed for predicting the onset of supersonic stall bending flutter in high-speed rotors. The analysis is based on a modified two-dimensional, compressible, unsteady actuator disk theory. The stability boundary predicted by the analysis is shown to be in good agreement with the measured boundary of a high speed fan. The prediction that the flutter mode would be a forward traveling wave sensitive to wheel speed and aerodynamic loading is confirmed by experimental measurements. In addition, the analysis shows that reduced frequency and dynamic head also play a significant role in establishing the supersonic stall bending flutter boundary of an unshrouded fan. L.S.

A81-32544 * # An automated procedure for developing hybrid computer simulations of turbofan engines. J. R. Szuch, S. M. Krosel, and W. M. Bruton (NASA, Lewis Research Center, Cleveland, Ohio). *ACM, SCS, IEEE, and IMACS, Annual Simulation Symposium, 14th, Tampa, Fla., Mar. 18-20, 1981, Paper 17*. p. 10 refs.

This paper offers a systematic, computer-aided, self-documenting methodology for developing hybrid computer simulations of turbofan engines. The methodology that is presented makes use of a host program that can run on a large digital computer and a machine-dependent target (hybrid) program. The host program performs all of the calculations and data manipulations that are needed to transform user-supplied engine design information to a form suitable for the hybrid computer. The host program also trims the self-contained engine model to match specified design point information. A test case is described and comparisons between hybrid simulation and specified engine performance data are presented. (Author)

A81-32549 * **Factors which influence the behavior of turbofan forced mixer nozzles.** B. H. Anderson and L. A. Povinelli (NASA, Lewis Research Center, Aerodynamics Analysis Section, Cleveland, Ohio). *American Institute of Aeronautics and Astronautics, Aerospace Sciences Meeting, 19th, St. Louis, Mo., Jan. 12-15, 1981, Paper 81-0274*. 28 p. 14 refs.

A finite difference procedure was used to compute the mixing for three experimentally tested mixer geometries. Good agreement was obtained between analysis and experiment when the mechanisms responsible for secondary flow generation were properly modeled. Vorticity generation due to flow turning and vorticity generated within the centerbody-lobe passage were found to be important. Results are presented for two different temperature ratios between fan and core streams and for two different free-stream turbulence levels. It was concluded that the dominant mechanisms in turbofan mixers is associated with the secondary flows arising within the lobe region and their development within the mixing section. (Author)

A81-34152 * **Improved components for engine fuel savings.** R. J. Antl and J. E. McAulay (NASA, Lewis Research Center, Cleveland, Ohio). *Society of Automotive Engineers, Aerospace Congress and Exposition, Los Angeles, Calif., Oct. 13-16, 1980, Paper 801116*. 17 p. 11 refs.

NASA programs for developing fuel saving technology include the Engine Component Improvement Project for short term improvements in existing air engines. The Performance Improvement section is to define component technologies for improving fuel efficiency for CF6, JT9D and JT8D turbofan engines. Sixteen concepts were developed and nine were tested while four are already in use by airlines. If all sixteen concepts are successfully introduced the gain will be fuel savings of more than 6 billion gallons over the lifetime of the engines. The improvements include modifications in fans, mounts, exhaust nozzles, turbine clearance and turbine blades. D.B.

A81-34154 * **Performance deterioration of commercial high-bypass ratio turbofan engines.** C. M. Mehalic and J. A. Ziemanski (NASA, Lewis Research Center, Cleveland, Ohio). *Society of Automotive Engineers, Aerospace Congress and Exposition, Los Angeles, Calif., Oct. 13-16, 1980, Paper 801118*. 14 p. 17 refs.

NASA programs for improving aircraft engine fuel efficiency include the Engine Component Improvement Project of which the Engine Diagnostics section is to identify performance deterioration factors for the JT9D and CF6 high-bypass ratio turbofan engines and to develop technology for fuel consumption reduction. The program tests and inspects engines, examines deteriorated elements, formulates deterioration trends and models, identifies specific causative events or modules and determines mechanisms. Results show that short-term performance deterioration is less than 1% of cruise specific fuel consumption and is caused by flight loads or thermal damage due to rubbing of turbine blade tips against shrouds. Long-term deterioration is 2.5-3% of cruise specific fuel consumption after 2500-3000 flights and mechanisms are thermal damage to blade tips with rubbing and damaged airfoils and parts. D.B.

A81-34155 * **A status report on the Energy Efficient Engine Project.** L. E. Macioce, J. W. Schaefer, and N. T. Saunders (NASA, Lewis Research Center, Cleveland, Ohio). *Society of Automotive Engineers, Aerospace Congress and Exposition, Los Angeles, Calif., Oct. 13-16, 1980, Paper 801119*. 18 p. 18 refs.

The Energy Efficient Engine (E3) Project is directed at providing, by 1984, the advanced technologies which could be used for a new generation of fuel conservative turbofan engines. This paper summarizes the scope of the entire project and the current status of these efforts. Included is a description of the preliminary designs of the fully developed engines, the potential benefits of these advanced engines, and highlights of some of the component technology efforts conducted to date. (Author)

A81-34156 * **The NASA high-speed turboprop program.** J. F. Dugan, B. A. Miller, E. J. Graber, and D. A. Sagerser (NASA, Lewis Research Center, Cleveland, Ohio). *Society of Automotive Engineers, Aerospace Congress and Exposition, Los Angeles, Calif., Oct. 13-16, 1980, Paper 801120*. 21 p. 21 refs.

NASA's Advanced Turboprop Project is a three-phase effort initiated in 1978 to provide technology readiness for Mach 0.7 to 0.9 turboprop-powered aircraft; with the potential for fuel savings and DOC reductions of up to 30 and 15%, respectively, relative to current in-service aircraft. This paper reviews the status of Phase I in the areas of propeller aeroacoustics, propeller structures, turboprop installed performance, aircraft cabin environment, and turboprop engine and aircraft studies. Current plans to establish large-scale propeller characteristics and to conduct high-speed propeller flight research tests using a modified testbed aircraft are also presented.

(Author)

A81-34166 * **Loss model for off-design performance analysis of radial turbines with pivoting-vane, variable-area stators.** P. L. Meitner (U.S. Army, Propulsion Laboratory, Cleveland, Ohio) and A. J. Glassman (NASA, Lewis Research Center, Cleveland, Ohio). *Society of Automotive Engineers, Aerospace Congress and Exposition, Los Angeles, Calif., Oct. 13-16, 1980, Paper 801135*. 11 p. 6 refs.

An off-design performance loss model for a radial turbine with pivoting, variable-area stators is developed through a combination of analytical modeling and experimental data analysis. A viscous loss model is used for the variation in stator loss with setting angle, and stator vane end-clearance leakage effects are predicted by a clearance flow model. The variation of rotor loss coefficient with stator setting angle is obtained by means of an analytical matching of experimental data for a rotor that was tested with six stators, having throat areas from 20 to 144% of the design area. An incidence loss model is selected to obtain best agreement with experimental data. The stator vane end-clearance leakage model predicts increasing mass flow and decreasing efficiency as a result of end-clearances, with changes becoming significantly larger with decreasing stator area. O.C.

A81-34168 * **An experimental evaluation of the performance deficit of an aircraft engine starter turbine.** J. E. Haas (U.S. Army, Research and Technology Laboratories, Cleveland, Ohio), R. J. Roelke (NASA, Lewis Research Center, Cleveland, Ohio), and P. Hermann (Sundstrand Corp., Rockford, Ill.). *Society of Automotive Engineers, Aerospace Congress and Exposition, Los Angeles, Calif., Oct. 13-16, 1980, Paper 801137*. 10 p.

An experimental investigation is presented to determine the aerodynamic performance deficit of a 13.5-centimeter-tip-diameter aircraft engine starter turbine. The two-phased evaluation comprised both the stator and the stage performance, and the experimental design is described in detail. Data obtained from the investigation of three honeycomb shrouds clearly showed that the filled honeycomb reached a total efficiency of 0.868, 8.2 points higher than the open honeycomb shroud, at design equivalent conditions of speed and blade-jet speed ratio. It was concluded that the use of an open honeycomb shroud caused the large performance deficit for the starter turbine. Further research is suggested to ascertain stator inlet boundary layer measurements. E.B.

A81-34169 * **Composite wall concept for high-temperature turbine shrouds - Heat transfer analysis.** L. P. Ludwig and F. S. Stepka (NASA, Lewis Research Center, Cleveland, Ohio). *Society of Automotive Engineers, Aerospace Congress and Exposition, Los Angeles, Calif., Oct. 13-16, 1980, Paper 801138*. 9 p. 13 refs.

The variables affecting the design of a composite turbine shroud, consisting of a metal base, an interlayer of porous metal, and an outer layer of yttria-stabilized zirconia, are analyzed. Results show that significant reductions in the cooling-air to gas-flow ratio are

indicated for the composite shrouds compared to an all-metal shroud that was only impingement air cooled. The good insulating properties of the ceramic reduced the temperatures of the porous metal and support wall significantly. For a given porous metal density and coolant to gas-flow ratio, decreasing the thickness of the porous metal and increasing ceramic thickness resulted in lower support wall temperatures. To maintain given allowable inter-layer temperatures and coolant to gas-flow ratios, porous-metal density or thermal conductivity must increase as the ratio of the thickness of the ceramic-to-porous metal decreases. It is concluded that a 1.78 mm thickness of porous material with a density of 0.2 and a 1.78 mm thickness of ceramic appears to be a good composite wall configuration for the assumed conditions. E.B.

A81-34170 * Future challenges in V/STOL flight propulsion control integration. S. P. Roth, R. J. Miller (United Technologies Corp., Pratt and Whitney Aircraft Group, West Palm Beach, Fla.), and J. Mihalow (NASA, Lewis Research Center, Cleveland, Ohio). *Society of Automotive Engineers, Aerospace Congress and Exposition, Los Angeles, Calif., Oct. 13-16, 1980, Paper 801140*. 15 p. 6 refs.

A survey of propulsion control requirements forming part of an advanced V/STOL control requirements study has to date determined, among other findings: (1) that the dependence of V/STOL flying qualities on propulsive lift makes it necessary to identify propulsion control requirements early in a development program; (2) that V/STOL controls of the future should relieve the pilot of control functions and elevate him to the position of a flight operations manager, with substantial gains in capability and/or safety; and (3) that research is required to define the V/STOL control system reliability requirements and specific component reliability allocations. An interactive, integrated design process for the realization of these objectives is also described. O.C.

A81-34177 * Some advantages of methane in an aircraft gas turbine. R. W. Graham and A. J. Glassman (NASA, Lewis Research Center, Cleveland, Ohio). *Society of Automotive Engineers, Aerospace Congress and Exposition, Los Angeles, Calif., Oct. 13-16, 1980, Paper 801154*. 9 p. 22 refs.

Because liquid methane may be obtained from existing natural gas sources or produced synthetically from a range of other hydrocarbon sources (coal, biomass, shale, organic waste), it is considered as an aviation fuel in a simplified cycle analysis of the performance of a turboprop engine intended for operation at Mach 0.8 and 10,688 m altitude. Performance comparisons are given for four cases in which the turbine cooling air is either not cooled or cooled to -111, -222, and -333 K, and the advantages and problems that may be expected from direct use of the cryogenic fuel in turbine cooling are discussed. It is shown that while (1) methane combustion characteristics are appreciably different from those of Jet A fuel and will require the development of different combustor designs, and (2) the safe integration of methane cryotanks into transport aircraft structures poses a major design problem, a highly fuel-efficient turboprop engine fueled by methane appears to be feasible. O.C.

A81-38064 * A nonlinear propulsion system simulation technique for piloted simulators. J. R. Mihalow (NASA, Lewis Research Center, Cleveland, Ohio). *IEEE, ISA, SCS, SMCS, Annual Pittsburgh Conference on Modeling and Simulation, 12th, Pittsburgh, PA, Apr. 30-May 1, 1981, Paper*. 12 p. 6 refs.

A real time digital simulation technique providing the capabilities needed to evaluate propulsion system performance and aircraft system interaction on NASA manned flight simulators, is discussed. A parameter correlation technique is used with real and pseudo dynamics in a stable integration convergence loop. The cycle time reported was 2.0 ms on one computer and 5.7 ms on the simulator computer. The model was found to be stable and accurate with time up to 50 ms. It is concluded that the program has generated a

valuable simulation technology and flight simulator experience by providing an adequate level of detail to evaluate propulsion systems in a simulated flight environment. E.B.

A81-40842 * Effect of a part-span variable inlet guide vane on the performance of a high-bypass turbofan engine. G. A. Bobula (U.S. Army, Propulsion Laboratory, Cleveland, OH), R. H. Soeder, and L. A. Burkardt (NASA, Lewis Research Center, Cleveland, OH). *AIAA, SAE, and ASME, Joint Propulsion Conference, 17th, Colorado Springs, CO, July 27-29, 1981, AIAA Paper 81-1362*. 9 p. 7 refs.

The ability of a part-span variable inlet guide vane to modulate the thrust of a high bypass turbofan engine was evaluated at altitude/Mach number conditions of 4572 m/0.6 and 9144 m/0.93. Fan-tip, gas generator and supercharger performance were also determined, both on operating lines and during fan duct throttling. The evaluation was repeated with the bypass splitter extended forward to near the fan blade trailing edge. Gross thrust attenuation of over 50% was achieved with 50 deg variable inlet guide vane closure at 100% corrected fan speed. Gas generator supercharger performance fell off with variable inlet guide vane closure but this loss was reduced when a splitter extension was added. The effect of variable inlet guide vane closure on gas generator performance was minimal. (Author)

A81-40859 * Selected results from combustion research at the Lewis Research Center. R. E. Jones (NASA, Lewis Research Center, Cleveland, OH). *AIAA, SAE, and ASME, Joint Propulsion Conference, 17th, Colorado Springs, CO, July 27-29, 1981, AIAA Paper 81-1392*. 9 p. 13 refs.

Combustion research at Lewis is organized to provide a balanced program responsive to national needs and the gas turbine industry. The results of this research is a technology base that assists the gas turbine engine manufacturers in developing new and improved combustion systems for advanced civil and military engines with significant improvements in performance, durability, fuel flexibility and control of exhaust emissions. Research efforts consist of fundamentals and modeling, and applied component and combustor research. This paper reports on some of the progress and results that have been achieved recently in all three research areas. (Author)

A81-40963 * JT9D performance deterioration results from a simulated aerodynamic load test. E. G. Stakolich (NASA, Lewis Research Center, Cleveland, OH) and W. J. Stromberg (United Technologies Corp., Pratt and Whitney Aircraft Group, East Hartford, CT). *AIAA, SAE, and ASME, Joint Propulsion Conference, 17th, Colorado Springs, CO, July 27-29, 1981, AIAA Paper 81-1588*. 16 p.

This paper presents the results of testing to identify the effects of simulated aerodynamic flight loads on JT9D engine performance. The test results were also used to refine previous analytical studies on the impact of aerodynamic flight loads on performance losses. To accomplish these objectives, a JT9D-7AH engine was assembled with average production clearances and new seals as well as extensive instrumentation to monitor engine performance, case temperatures, and blade tip clearance changes. A special loading device was designed and constructed to permit application of known moments and shear forces to the engine by the use of cables placed around the flight inlet. The test was conducted in the Pratt and Whitney Aircraft X-Ray Test Facility to permit the use of X-ray techniques in conjunction with laser blade tip proximity probes to monitor important engine clearance changes. Upon completion of the test program, the test engine was disassembled, and the condition of gas path parts and final clearances were documented. The test results indicate that the engine lost 1.1 percent in thrust specific fuel consumption (TSFC), as measured under sea level static conditions, due to increased operating clearances caused by simulated flight loads. This compares with 0.9 percent predicted by the analytical model and previous study efforts. (Author)

A81-40971 * # Turbine bypass engine - A new supersonic cruise propulsion concept. L. C. Franciscus (NASA, Lewis Research Center, Cleveland, OH). *AIAA, SAE, and ASME, Joint Propulsion Conference, 17th, Colorado Springs, CO, July 27-29, 1981, AIAA Paper 81-1596.* 9 p. 7 refs.

Engine performance and mission studies were carried out for a single-spool turbine bypass engine (TBE) concept. Comparisons were made between the TBE, a conventional single-spool turbojet, and the Pratt and Whitney Variable Stream Control Engine (VSCE). The airplane assumed for the study was a Mach 2.32 commercial supersonic transport. The nominal mission was a 4000 n mi total range with a 300 n mi subsonic cruise leg. The figure of merit was the minimum takeoff gross weight for the mission. Comparisons of the three engines were also made for the 4000 n mi total range with longer subsonic cruise legs. (Author)

A81-40973 * # The supersonic fan engine - An advanced concept in supersonic cruise propulsion. L. C. Franciscus (NASA, Lewis Research Center, Mission Analysis Office, Cleveland, OH). *AIAA, SAE, and ASME, Joint Propulsion Conference, 17th, Colorado Springs, CO, July 27-29, 1981, AIAA Paper 81-1599.* 9 p. 11 refs.

Engine performance and mission studies were conducted for a novel turbofan engine concept incorporating a supersonic through-flow fan, and comparisons were made with two supersonic transport (SST) engine concepts of equivalent thrust and technological sophistication. It was found that in the case of an SST with a cruise speed of Mach 2.32, the through-flow fan engine may yield ranges 10 to 20% greater than the two alternatives considered. The engine has a conventional core, with the supersonic fan being driven by a concentric low-pressure turbine that is uncoupled with the single, high pressure turbine/compressor core spool. Among the topics discussed are the methods of analysis employed and perturbation studies concerning supersonic fan adiabatic efficiency, fan discharge characteristics and propulsion system weight. (Author)

A81-42176 * # The E3 combustors - Status and challenges. D. E. Sokolowski and J. E. Rohde (NASA, Lewis Research Center, Cleveland, OH). *AIAA, SAE, and ASME, Joint Propulsion Conference, 17th, Colorado Springs, CO, July 27-29, 1981, AIAA Paper 81-1353.* 23 p. 17 refs.

The technology programs for the Energy Efficient Engine (E3) combustors are outlined, status and test results to date are summarized, and present and future challenges indicated. The NASA-sponsored programs, which are being conducted at the General Electric Company and Pratt & Whitney Aircraft, are making important technology advances. Both combustor designs utilize an annular configuration with two-zone combustion for low emissions, advanced liners for improved durability, and short, curved-wall, dump prediffusers for compactness. Advanced cooling techniques and segmented construction characterize the advanced liners in both programs. Liner segments are made from castable, turbine-type materials. At this time, analysis and design activities have been completed; experimental evaluations are progressing. Test results are verifying both design concepts for combustion, cooling, and mechanical integrity. All goals appear capable of being met, with the exception of NO(x). (Author)

A81-42758 * Low and high speed propellers for general aviation - Performance potential and recent wind tunnel test results. R. J. Jeracki and G. A. Mitchell (NASA, Lewis Research Center, Cleveland, OH). *Society of Automotive Engineers, Business Aircraft Meeting and Exposition, Wichita, KS, Apr. 7-10, 1981, Paper 810601.* 27 p. 24 refs.

A survey is presented of current research efforts in general aviation, low-speed propeller design and high-speed propfan design, with attention on such features as (1) advanced blade shapes, with novel airfoils and sweep, (2) tip devices, (3) integrated propeller/nacelle designs, (4) area-ruled spinners, (5) lightweight, all-composite blade construction, and (6) contra-rotating propfan systems. The potential overall improvements associated with these design modifi-

cations are calculated to lie at 10-15% for low-speed rotors and 15-30% for high-speed ones. Emphasis is placed on noise reduction, blade drag, performance prediction methods and wind tunnel testing of alternative rotor configurations. Extensive use of graphs is made in performance comparisons between alternative blade and rotor designs. (Author)

A81-42778 * An overview of general aviation propulsion research programs at NASA-Lewis Research Center. E. A. Willis and W. C. Strack (NASA, Lewis Research Center, Cleveland, OH). *Society of Automotive Engineers, Business Aircraft Meeting and Exposition, Wichita, KS, Apr. 7-10, 1981, Paper 810624.* 21 p. 19 refs.

This paper presents a brief overview and technical highlights of general aviation (g/a) propulsion research efforts and studies which have been underway at NASA's Lewis Research Center (LeRC) for the past several years. The review covers near-term improvements for current-type piston engines, as well as studies and limited corroborative research on several advanced g/a engine concepts, including diesels, small turboprops and both piston and rotary stratified-charge engines. Also described is basic combustion research, cycle modeling and diagnostic instrumentation work that will be required to make the new engines a reality. The discussion emphasizes the most recently-completed studies and the basic underlying research work, which have not been reported previously. (Author)

A81-44225 * # Mixing effectiveness test of an exhaust gas mixer in a high bypass turbofan at altitude. R. R. Cullem, L. A. Burkardt (NASA, Lewis Research Center, Cleveland, OH), and G. A. Bobula (U.S. Army, Propulsion Laboratory, Cleveland, OH). *AIAA, SAE, and ASME, Joint Propulsion Conference, 17th, Colorado Springs, CO, July 27-29, 1981, AIAA Paper 81-1495.* 10 p. 6 refs.

Thermal mixing effectiveness characteristics of an eighteen lobe, scalloped and unscalloped, partial, forced mixer were measured in a high bypass turbofan engine. Data were also obtained without the mixer installed, i.e. free mixing. Tests were conducted at four combinations of simulated flight conditions from 0.3 to 0.8 Mach number and from 6,096 meters (20,000 ft) to 13,715 m (45,000 ft) altitude. Mixing chamber lengths of L/D = 0.52 and 0.65 were tested. For this range of test conditions and mixer configurations the forced mixing effectiveness varied from 59 to 68 percent. Values of mixing effectiveness and total pressure loss were calculated from temperature and pressure data obtained at the mixer inlet and exhaust nozzle exit. (Author)

A81-48621 * # Turbomachinery noise studies of the AiResearch OCGAT engine with inflow control. J. G. McArdle, L. Homyak, and D. D. Cnruiski (NASA, Lewis Research Center, Cleveland, OH). *American Institute of Aeronautics and Astronautics, Aeroacoustics Conference, 7th, Palo Alto, CA, Oct. 5-7, 1981, Paper 81-2049.* 16 p. 17 refs.

The AiResearch Quiet Clean General Aviation Turbofan engine was tested on a vertical lift fan facility to measure the acoustic performance of two inflow control devices (ICD) of similar design, and three inlet lips of different external shape. Far-field directivity patterns calculated by existing analyses were compared with the measured fan fundamental blade passing frequency (BPF/F) and broadband data. Installing an ICD on an engine with hardwall ducts reduced the BPF(F) tone everywhere in the far-field. When the ICD was installed on an engine with active acoustic panels, tone reduction in the forward quadrant was comparable to that in the hardwall tests; in the aft quadrant, however, tone noise was attenuated by the large acoustic panels in the bypass duct to such a degree that the ICD had little effect. Tests to compare performance of ICDs with hardwall inlet ducts showed only minor differences in the BPF(F) directivity patterns, while broadband noise was the same for both. Forward-quadrant BPF(F) and broadband directivity patterns were found to be similar for the inlet lips tested with a hardwall inlet duct. At high fan speeds, however, the shape of the analytical multimodal tone

pattern from the exhaust nozzle was flatter than the measured patterns. The sources of lobes from several propagating single modes found in the forward-quadrant BPF(F) data were attributed to rotor/strut interaction and the rotor-alone pressure field. J.F.

A81-48628 * # Effects of blade-vane ratio and rotor-stator spacing on fan noise with forward velocity. R. P. Woodward and F. W. Giasser (NASA, Lewis Research Center, Cleveland, OH). *American Institute of Aeronautics and Astronautics, Aeroacoustics Conference, 7th, Palo Alto, CA, Oct. 5-7, 1981, Paper 81-2032*. 12 p. 30 refs.

A research fan stage is acoustically tested in an anechoic wind tunnel with a 41 m/sec tunnel flow. Two stator vane numbers giving cut-on and cut-off conditions are tested at three rotor stator spacings ranging from 0.5 to 2.0 rotor chords. Hot-film anemometer turbulence measurements are made at the leading edge of the stator for each spacing, and a crossed film anemometer is radially transversed to define streamwise and upwash characteristics of the rotor blade wakes. Trends in the acoustic results are observed in the front and aft quadrants at 80% design fan speed. Aft quadrant results demonstrate a fundamental tone 9 dB lower for the 25 vane stator than for the 11 vane stator, while overtone levels are 3 dB higher. The cut-off criterion strongly controls fundamental tone level at all spacings, and spacing trends of the wake-defect upwash component show good agreement with corresponding cut-on acoustic tone levels.

D.L.G.

A81-48635 * # Comparison of predicted engine core noise with current and proposed aircraft noise certification requirements. U. H. von Glahn and D. E. Groesbeck (NASA, Lewis Research Center, Cleveland, OH). *American Institute of Aeronautics and Astronautics, Aeroacoustics Conference, 7th, Palo Alto, CA, Oct. 5-7, 1981, Paper 81-2053*. 11 p. 15 refs.

Predicted engine core noise levels for subsonic CTOL aircraft engines are compared with measured total aircraft noise levels and to current and proposed federal noise certification requirements. Comparisons are made at FAR-36 measuring stations and take into consideration both full and cutback power operations at takeoff. The spectral shape used for the prediction of core noise is identified as the spectral envelope, with a peak at 400 Hz which is assumed to be shifted in flight by a Doppler shift in frequency. Perceived noise levels are computed for appropriate engine power settings at desired flight conditions, and reductions in sideline noise levels are made to account for jet and airframe shielding effects. Results indicate that core noise can provide a barrier to the proposed EPA stage 4 and 5 federal noise rules for wide-body aircraft, with the most severe core noise problem occurring at takeoff and sideline measuring stations.

D.L.G.

N81-12085* # General Electric Co., Evendale, Ohio. Aircraft Engine Business Group.
ENGINE DIAGNOSTICS PROGRAM: CF6-50 ENGINE PERFORMANCE DETERIORATION
Ray H. Wulf Nov. 1980 208 p refs
(Contract NAS3-20631)
(NASA-CR-159867) Avail: NTIS HC A10/MF A01 CSCL 21E

Cockpit cruise recordings and test cell data in conjunction with hardware inspection results from airline overhaul shops were analyzed to define the extent and magnitude of performance deterioration of the General Electric CF6-50 high bypass turbofan engine. The magnitude of short term deterioration was isolated from the long term, and the individual damage mechanisms that were the cause for the majority of the performance deterioration was identified. It was determined that the long term engine performance deterioration characteristics were different for the 3 aircraft types currently powered by the CF6-50 engine, but these differences were due to operational considerations (flight length and takeoff derate) and not to differences associated with the aircraft type. Unrestored losses, that is, performance deterioration which remains after engine refurbishment, represents over 70 percent of the total performance deterioration at engine shop visit. Superficial damage, such as, increased surface

roughness, leading edge shape changes on airfoils, and increases in the average clearances between rotating and stationary components is the major contributor to these losses. Seventy one percent of the unrestored losses are cost effective to restore, and if implemented could reduce fuel consumed by CF6-50 engines by 26 million gallons in 1980. R.C.T.

N81-12086* # General Electric Co., Cincinnati, Ohio.
CORE COMPRESSOR EXIT STAGE STUDY. VOLUME 3: DATA AND PERFORMANCE REPORT FOR SCREENING TEST CONFIGURATIONS

D. C. Wisler Nov. 1980 53 p refs

(Contract NAS3-20070)

(NASA-CR-159499; R80AEG313-Vol-3)

Avail: NTIS

HC A04/MF A01 CSCL 21E

Rear stage blading designs that have lower losses in their endwall boundary layer regions were developed. Test data and performance results for rotor B, stator B, and stator C - blading designs that offer promise of reducing endwall losses relative to the baseline are given. A low speed research compressor was the principal investigative tool. The tests were conducted using four identical stages of blading so that the test data would be obtained in a true multistage environment. S.F.

N81-12087* # Pratt and Whitney Aircraft Group, East Hartford, Conn.

ROTOR REDESIGN FOR A HIGHLY LOADED 1800 FT/SEC TIP SPEED FAN. 2 Final Report

C. R. Bolt Dec. 1980 185 p refs

(Contract NAS3-20591)

(NASA-CR-159879; PWA-5523-92)

Avail: NTIS

HC A09/MF A01 CSCL 21E

Tests were conducted on a 0.5 hub/tip ratio single-stage fan designed to produce a pressure ratio of 2.280 at an efficiency of 83.8 percent with a rotor tip speed of 548.6 m/sec (1800 ft/sec). The rotor was designed utilizing a quasi three dimensional design system and four-part, multiple-circular-arc airfoil sections. The rotor is the third in a series of single-stage fans that have included a precompression airfoil design and a multiple-circular-arc airfoil design. The stage achieved a peak efficiency of 82.8 percent after performance had deteriorated by 0.6 of a point. The design mass flow was achieved at the peak efficiency point, and the stage total pressure ratio was 2.20, which is lower than the design goal of 2.28. The surge margin of 13% from the peak efficiency point exceeded the design goal of 7%. Author

N81-12088* # AiResearch Mfg. Co., Phoenix, Ariz.
LOW-COST DIRECTIONALLY-SOLIDIFIED TURBINE BLADES, VOLUME 2

R. E. Dennis, G. S. Hoppin, III, and L. G. Hurst Apr. 1979 41 p

(Contract NAS3-20073)

(NASA-CR-159562; AiResearch-21-2953-2-Vol-2) Avail: NTIS

HC A03/MF A01 CSCL 21E

An endothermically heated technology was used to manufacture low cost, directionally solidified, uncooled nickel-alloy blades for the TFE731-3 turbofan engine. The MAR-M 247 and MER-M 100+Hf blades were finish processed through heat treatment, machining, and coating operations prior to 150 hour engine tests consisting of the following sequences: (1) 50 hours of simulated cruise cycling (high fatigue evaluation); (2) 50 hours at the maximum continuous power rating (stress rupture endurance (low cycle fatigue). None of the blades visually showed any detrimental effects from the test. This was verified by post test metallurgical evaluation. The specific fuel consumption was reduced by 2.4% with the uncooled blades. A.R.H.

N81-12094* Pratt and Whitney Aircraft Group, East Hartford, Conn. Commercial Products Div.

DESIGN OF A MULTIVARIABLE INTEGRATED CONTROL FOR A SUPERSONIC PROPULSION SYSTEM

Edward C. Beattie / In NASA, Lewis Research Center Propulsion Controls, 1979 Oct. 1980 p 35-47 refs (For primary document see N81-12090 03-07)

Avail. NTIS HC A07/MF A01 CSCL 21E

An inlet/engine/nozzle integrated control mode for the propulsion system of an advanced supersonic commercial aircraft was studied. Results show that integration of these control functions can result in both operational and performance benefits for the propulsion system. For example, this integrated control mode may make it possible to minimize the use of inlet bypass doors for shock position control. This may be of benefit to the aircraft as a result of minimizing: (1) bypass bleed drag effects; (2) perturbations to the aircraft resulting from the side thrust effect of the bypass bleeds; and (3) potential unstarts of the inlet. A conceptual integrated control mode was developed which makes use of many cross coupling paths between inlet and engine control variables and inlet and engine sensed variables. A multivariable control design technique based upon linear quadratic regulator theory was applied to designing the feedback gains for this control to allow a simulation evaluation of the benefits of the integrated control mode. Author

N81-12095* Pratt and Whitney Aircraft Group, East Hartford, Conn. Government Products Div.

PROPULSION CONTROLS

Ronald D. Harkney / In NASA, Lewis Research Center Propulsion Controls, 1979 Oct. 1980 p 49-59 refs (For primary document see N81-12090 03-07)

Avail. NTIS HC A07/MF A01 CSCL 21E

Increased system requirements and functional integration with the aircraft have placed an increased demand on control system capability and reliability. To provide these at an affordable cost and weight and because of the rapid advances in electronic technology, hydromechanical systems are being phased out in favor of digital electronic systems. The transition is expected to be orderly from electronic trimming of hydromechanical controls to full authority digital electronic control. Future propulsion system controls will be highly reliable full authority digital electronic with selected component and circuit redundancy to provide the required safety and reliability. Redundancy may include a complete backup control of a different technology for single engine applications. The propulsion control will be required to communicate rapidly with the various flight and fire control avionics as part of an integrated control concept. A.R.H.

N81-12096* Air Force Aero Propulsion Lab., Wright-Patterson AFB, Ohio.

FUTURE AIR FORCE AIRCRAFT PROPULSION CONTROL SYSTEMS: THE EXTENDED SUMMARY PAPER

Charles A. Skira / In NASA, Lewis Research Center Propulsion Controls, 1979 Oct. 1980 p 63-67 (For primary document see N81-12090 03-07)

Avail. NTIS HC A07/MF A01 CSCL 21E

Hydromechanical control technology simply cannot compete against the performance benefits offered by electronics. Future military aircraft propulsion control systems will be full authority, digital electronic, microprocessor base systems. Anticipating the day when microprocessor technology will permit the integration and management of aircraft flight control, fire control and propulsion control systems, the Air Force Aero Propulsion Laboratory is developing control logic algorithms for a real time, adaptive control and diagnostic information system. A.R.H.

N81-12097* Boeing Military Airplane Development, Seattle, Wash.

SHOULD WE ATTEMPT GLOBAL (INLET ENGINE AIRFRAME) CONTROL DESIGN?

Christopher M. Carlin / In NASA, Lewis Research Center Propulsion Controls, 1979 Oct. 1980 p 71-82 (For primary document see N81-12090 03-07)

Avail. NTIS HC A07/MF A01 CSCL 21E

The feasibility of multivariable design of the entire airplane control system is briefly addressed. An intermediate step in that direction is to design a control for an inlet engine augmentor system by using multivariable techniques. The supersonic cruise large scale inlet research program is described which will provide an opportunity to develop, integrate, and wind tunnel test a control for a mixed compression inlet and variable cycle engine. The integrated propulsion airframe control program is also discussed which will introduce the problem of implementing MVC within a distributed processing avionics architecture, requiring real time decomposition of the global design into independent modules in response to hardware communication failures. M.G.

N81-12098* Detroit Diesel Allison, Indianapolis, Ind.

ROAD MAP TO ADAPTIVE OPTIMAL CONTROL

Robert Boyer / In NASA, Lewis Research Center Propulsion Controls, 1979 Oct. 1980 p 83-87 (For primary document see N81-12090 03-07)

Avail. NTIS HC A07/MF A01 CSCL 21E

A building block control structure leading toward adaptive, optimal control for jet engines is developed. This approach simplifies the addition of new features and allows for easier checkout of the control by providing a baseline system for comparison. Also, it is possible to eliminate certain features that do not have payoff by being selective in the addition of new building blocks to be added to the baseline system. The minimum risk approach specifically addresses the need for active identification of the plant to be controlled in real time and real time optimization of the control for the identified plant. M.G.

N81-12100* Virginia Polytechnic Inst. and State Univ., Blacksburg.

ENGINE IDENTIFICATION FOR ADAPTIVE CONTROL

Robert G. Leonard and Eric M. Arner / In NASA, Lewis Research Center Propulsion Controls, 1979 Oct. 1980 p 97-104 refs (For primary document see N81-12090 03-07) (Grant NsG-3119)

Avail. NTIS HC A07/MF A01 CSCL 21E

An attempt to obtain a dynamic model for a turbofan gas turbine engine for the purpose of adaptive control is described. The requirements for adaptive control indicate that a dynamic model should be identified from data sampled during engine operation. The dynamic model identified was of the form of linear differential equations with time varying coefficients. A turbine engine is, however, a highly nonlinear system, so the identified model would be valid only over a small area near the operating point, thus requiring frequent updating of the coefficients in the model. Therefore it is necessary that the identifier use only recent information to perform its function. The identifier selected minimized the square of the equation errors. Known linear systems were used to test the characteristics of the identifier. It was found that the performance was dependent on the number of data points used in the computations and upon the time interval over which the data points were obtained. Preliminary results using an engine deck for the quiet, clean, shorthaul experimental engine indicate that the identified model predicts the engine motion well when there is sufficient dynamic information, that is when the engine is in transient operation. M.G.

N81-12101* Purdue Univ., Lafayette, Ind. School of Mechanical Engineering

MULTIVARIABLE NYQUIST ARRAY METHOD WITH APPLICATION TO TURBOFAN ENGINE CONTROL

Gary G. Leininger / In NASA Lewis Research Center Propulsion Controls, 1979 Oct. 1980 p 105-110 refs (For primary document see N81-12090 03-07)

Avail: NTIS HC A07/MF A01 CSCL 21E

Extensions to the multivariable Nyquist array (MNA) method are used to design a feedback control system for the quiet clean shorthaul experimental engine. The results of this design are compared with those obtained from the deployment of an alternate control system design on a full scale nonlinear, real time digital simulation. The results clearly demonstrate the utility of the MNA synthesis procedures for highly nonlinear sophisticated design applications. M.G.

N81-12102* Bendix Corp., Detroit, Mich. Energy Control Div.

MULTIVARIABLE SYNTHESIS WITH TRANSFER FUNCTIONS

Joseph L. Peczkowski / In NASA Lewis Research Center Propulsion Controls, 1979 Oct. 1980 p 111-127 refs (For primary document see N81-12090 03-07)

Avail: NTIS HC A07/MF A01 CSCL 21E

A transfer function design theory for multivariable control synthesis is highlighted. The use of unique transfer function matrices and two simple, basic relationships - a synthesis equation and a design equation - are presented and illustrated. This multivariable transfer function approach provides the designer with a capability to specify directly desired dynamic relationships between command variables and controlled or response variables. At the same time, insight and influence over response, simplifications, and internal stability is afforded by the method. A general, comprehensive multivariable synthesis capability is indicated including nonminimum phase and unstable plants. Gas turbine engine examples are used to illustrate the ideas and method. M.G.

N81-13057* Pratt and Whitney Aircraft Group, East Hartford, Conn. Commercial Products Div.

MODEL AERODYNAMIC TEST RESULTS FOR TWO VARIABLE CYCLE ENGINE COANNULAR EXHAUST SYSTEMS AT SIMULATED TAKEOFF AND CRUISE CONDITIONS Final Report

D. P. Nelson 17 Dec. 1980 70 p refs

(Contract NAS3-20061)

(NASA-CR-159818; PWA-5550-37)

Avail: NTIS

HC A04/MF A01 CSCL 21E

Wind tunnel tests were conducted to evaluate the aerodynamic performance of a coannular exhaust nozzle for a proposed variable stream control supersonic propulsion system. Tests were conducted with two simulated configurations differing primarily in the fan duct flowpaths: a short flap mechanism for fan stream control with an isentropic contoured flow splitter, and an iris fan nozzle with a conical flow splitter. Both designs feature a translating primary plug and an auxiliary inlet ejector. Tests were conducted at takeoff and simulated cruise conditions. Data were acquired at Mach numbers of 0.036, 0.9, and 2.0 for a wide range of nozzle operating conditions. At simulated supersonic cruise, both configurations demonstrated good performance, comparable to levels assumed in earlier advanced supersonic propulsion studies. However, at subsonic cruise, both configurations exhibited performance that was 6 to 7.5 percent less than the study assumptions. At take off conditions, the iris configuration performance approached the assumed levels, while the short flap design was 4 to 6 percent less. Author

N81-13963* Teledyne Continental Motors, Mobile, Ala. Aircraft Products Div.

ADVANCED TECHNOLOGY SPARK-IGNITION AIRCRAFT PISTON ENGINE DESIGN STUDY Final Report

Kenneth J. Stuckas Nov. 1980 127 p refs

(Contract NAS3-21272)

(NASA-CR-165162) Avail: NTIS HC A07/MF A01 CSCL 21G

The advanced technology, spark ignition, aircraft piston engine design study was conducted to determine the improvements that could be made by taking advantage of technology that could reasonably be expected to be made available for an engine intended for production by January 1, 1990. Two engines were proposed to account for levels of technology considered to be moderate risk and high risk. The moderate risk technology engine is a homogeneous charge engine operating on avgas and offers a 40% improvement in transportation efficiency over present designs. The high risk technology engine, with a stratified charge combustion system using kerosene-based jet fuel, projects a 65% improvement in transportation efficiency. Technology enablement program plans are proposed herein to set a timetable for the successful integration of each item of required advanced technology into the engine design. Auth: r

N81-15002* Pratt and Whitney Aircraft, East Hartford, Conn. ENERGY EFFICIENT ENGINE DIFFUSER/COMBUSTOR MODEL TECHNOLOGY

W.B. Gardner Jun. 1980 62 p refs

(Contract NAS3-20646)

(NASA-CR-165157; PWA-5594-122)

Avail: NTIS

HC A04/MF A01 CSCL 21E

A full scale, full annular diffuser/combustor model test rig was tested to investigate how configurational changes affect pressure loss and flow separation characteristics. The rig was characterized by five major modules: inlet; prediffuser; strut; simulated combustor; and full combustor. The prediffuser featured a short, curved wall dump design. Performance goals included: (1) a separation-free prediffuser flow field; (2) total pressure loss limited to 3.0 percent in the prediffuser and shrouds; and (3) an overall section pressure loss of 5.5 percent P sub T3 at the design airflow distribution. The results indicated that the prediffuser configurations operate well within the program goals for pressure loss and demonstrate separation free operation over a wide range of inlet conditions. R.C.T.

N81-15003* Spectron Development Labs., Inc., Costa Mesa, Calif.

FUEL INJECTOR CHARACTERIZATION STUDIES Final Report

Michael J. Houser and William D. Bachalo Oct. 1980 54 p refs

(Contract NAS3-21288)

(NASA-CR-165200; SDL-80-2122-13F)

Avail: NTIS

HC A04/MF A01 CSCL 21E

The atomization of several general aviation piston engine manifold port fuel injectors was investigated. The injectors were installed in a test rig and operated under simulated conditions. Laser interferometric techniques were used to optically probe the spray droplet fields for droplet size and velocity at numerous spatial locations throughout the field. R.C.T.

N81-15004* General Electric Co., Cincinnati, Ohio. Aircraft Engine Group.

AERODYNAMIC STABILITY ANALYSIS OF NASA J85-13/ PLANAR PRESSURE PULSE GENERATOR INSTALLATION K. Chung, W. M. Hosny, and W. G. Steenken. Nov. 1980. 168 p refs.

(Contract NAS3-21259)

(NASA-CR-165141; R80AEG429) Avail. NTIS HC A08/MF A01 CSCL 21E

A digital computer simulation model for the J85-13/Planar Pressure Pulse Generator (P3 G) test installation was developed by modifying an existing General Electric compression system model. This modification included the incorporation of a novel method for describing the unsteady blade lift force. This approach significantly enhanced the capability of the model to handle unsteady flows. In addition, the frequency response characteristics of the J85-13/P3G test installation were analyzed in support of selecting instrumentation locations to avoid standing wave nodes within the test apparatus and thus, low signal levels. The feasibility of employing explicit analytical expression for surge prediction was also studied. J.M.S.

N81-15005* General Electric Co., Cincinnati, Ohio. Aircraft Engine Group.

TF34 ENGINE COMPRESSION SYSTEM COMPUTER STUDY

W. M. Hosny and W. G. Steenken. Jun. 1979. 93 p refs.

(Contract NAS3-20599)

(NASA-CR-159889; R78AEG612) Avail. NTIS HC A05/MF A01 CSCL 21E

The stability of the fan and the compressor components was examined individually using linearized and time dependent, one dimensional stability analysis techniques. The stability of the fan core integrated compression system was investigated using a two dimensional compression system model. The analytical equations on which this model was based satisfied the mass, axial momentum, radial momentum, and energy conservation equations for flow through a finite control volume. The results gave an accurate simulation of the flow through the compression system. The speed lines of the components were reproduced; the points of instability were accurately predicted; the locations where the instability was initiated in the fan and the core were indicated; and the variation of the bypass ratio during flow throttling was calculated. The validity of the analytical techniques was then established by comparing these results with test data and with results obtained from the steady state cycle deck. J.M.S.

N81-15006* Pratt and Whitney Aircraft Group, East Hartford, Conn. Commercial Products Div.

COST/BENEFIT ANALYSIS OF ADVANCED MATERIALS TECHNOLOGIES FOR FUTURE AIRCRAFT TURBINE ENGINES Final Report

G. E. Stephens. Aug. 1980. 49 p refs.

(Contract NAS3-20072)

(NASA-CR-165225; PWA-5755) Avail. NTIS HC A03/MF A01 CSCL 21E

The materials technologies studied included thermal barrier coatings for turbine airfoils, turbine disks, cases, turbine vanes and engine and nacelle composite materials. The cost/benefit of each technology was determined in terms of Relative Value defined as change in return on investment times probability of success divided by development cost. A recommended final ranking of technologies was based primarily on consideration of Relative Values with secondary consideration given to changes in other economic parameters. Technologies showing the most promising cost/benefits were thermal barrier coated temperature nacelle/engine system composites. T.M.

N81-16051* General Electric Co., Cincinnati, Ohio. Aircraft Engine Group.

CORE COMPRESSOR EXIT STAGE STUDY. VOLUME 2: DATA AND PERFORMANCE REPORT FOR THE BASELINE CONFIGURATION

D. C. Wisler. Nov. 1980. 178 p refs.

(Contract NAS3-20070)

(NASA-CR-159498; R80AEG312-Vol-2) Avail. NTIS HC A09/MF A01 CSCL 21E

The objective of the program is to develop rear stage blading designs that have lower losses in their endwall boundary layer regions. The overall technical approach in this efficiency improvement program utilized General Electric's Low Speed Research Compressor as the principal investigative tool. Tests were conducted in two ways: using four identical stages of blading so that test data would be obtained in a true multistage environment and using a single stage of blading so that comparison with the multistage test results could be made. T.M.

N81-16057* Avco Lycoming Div., Stratford, Conn.
DESIGN AND EVALUATION OF AN INTEGRATED QUIET CLEAN GENERAL AVIATION TURBOFAN (OCGAT) ENGINE AND AIRCRAFT PROPULSION SYSTEM Final Report, Dec. 1978 - Apr. 1980

Jon German, Philip Fogel, and Craig Wilson. Apr. 1980. 226 p refs.

(Contract NAS3-20584)

(NASA-CR-165185; LYC-80-27) Avail. NASA Industrial Application Center CSCL 21E

The engine and nacelle system design was to demonstrate the applicability of large turbofan engine technology to small turboprops suitable for the general aviation market. The design was based on the LTS-101 engine family for the core engine. A high bypass fan design (BPR = 9.4) was incorporated to provide reduced fuel consumption for the design mission. All acoustic and pollutant emissions goals were achieved. A discussion of the preliminary design of a business jet suitable for the developed propulsion system is also included. Large engine technology can be successfully applied to small turboprops, and noise or pollutant levels need not be constraints for the design of future small general aviation turbofan engines. T.M.

N81-17078* General Electric Co., Cincinnati, Ohio. Aircraft Engine Group.

TURBINE MODELING TECHNIQUE TO GENERATE OFF-DESIGN PERFORMANCE DATA FOR BOTH SINGLE AND MULTISTAGE AXIAL-FLOW TURBINES Contractor Report, Aug. 1979 - Aug. 1980

G. L. Converse. Feb. 1981. 46 p refs.

(Contract NAS3-21999)

(NASA-CR-165244; R81AEG219) Avail. NTIS HC A03/MF A01 CSCL 21E

This technique is applicable to larger axial flow turbines which may or may not incorporate variable geometry in the first stage stator. A user specified option will also permit the calculation of design point cooling flow levels and the corresponding change in turbine efficiency. The modeling technique was incorporated into a time sharing computer program in order to facilitate its use. Because this report contains a description of the input/output data, values of typical inputs, and example cases, it is suitable as a user's manual. T.M.

N81-17079* Pratt and Whitney Aircraft Group, East Hartford, Conn.

COMBUSTOR LINER DURABILITY ANALYSIS Final Report

V. Moreno. Feb. 1981. 84 p refs.

(Contract NAS3-21836)

(NASA-CR-165250; PWA-5684-19) Avail. NTIS HC A05/MF A01 CSCL 21E

An 18 month combustor liner durability analysis program was conducted to evaluate the use of advanced three dimensional transient heat transfer and nonlinear stress-strain analyses for

modeling the cyclic thermomechanical response of a simulated combustor liner specimen. Cyclic life prediction technology for creep/fatigue interaction is evaluated for a variety of state-of-the-art tools for crack initiation and propagation. The sensitivity of the initiation models to a change in the operating conditions is also assessed. A.R.H.

NS1-17080* Pratt and Whitney Aircraft Group, East Hartford, Conn. Commercial Products Div.

JT2-16/17 HIGH PRESSURE TURBINE ROOT DISCHARGED BLADE PERFORMANCE IMPROVEMENT
Contractor Report, Sep. 1978 - Aug. 1980

A. S. Janus 18 Feb. 1981 60 p refs

(Contract NAS3-20630)

(NASA-CR-165220; PWA-5515-138)

Avail: NTIS

HC A04/MF A01 CSCL 21E

The JTSD high pressure turbine blade and seal were modified, using a more efficient blade cooling system, improved airfoil aerodynamics, more effective control of secondary flows, and improved blade tip sealing. Engine testing was conducted to determine the effect of these improvements on performance. The modified turbine package demonstrated significant thrust specific fuel consumption and exhaust gas temperature improvements in sea level and altitude engine tests. Inspection of the improved blade and seal hardware after testing revealed no unusual wear or degradation. R.C.T.

NS1-17081* Pratt and Whitney Aircraft Group, East Hartford, Conn. Commercial Products Div.

MODEL AERODYNAMIC TEST RESULTS FOR TWO VARIABLE CYCLE ENGINE COANNULAR EXHAUST SYSTEMS AT SIMULATED TAKEOFF AND CRUISE CONDITIONS. COMPREHENSIVE DATA REPORT. VOLUME 1: DESIGN LAYOUTS

D. P. Nelson Jan. 1981 40 p refs

(Contract NAS3-20061)

(NASA-CR-159819-Vol-1; PWA-5550-50-Vol-1) Avail: NTIS

HC A03/MF A01 CSCL 21E

The design layouts and detailed design drawings of coannular exhaust nozzle models for a supersonic propulsion system are presented. The layout drawings show the assembly of the component parts for each configuration. A listing of the component parts is also given. M.G.

NS1-17082* Pratt and Whitney Aircraft Group, East Hartford, Conn. Commercial Products Div.

MODEL AERODYNAMIC TEST RESULTS FOR TWO VARIABLE CYCLE ENGINE COANNULAR EXHAUST SYSTEMS AT SIMULATED TAKEOFF AND CRUISE CONDITIONS. COMPREHENSIVE DATA REPORT. VOLUME 2: TABULATED AERODYNAMIC DATA BOOK 1

D. P. Nelson Jan. 1981 400 p refs

(Contract NAS3-20061)

(NASA-CR-159819-Vol-2-Bk-1; PWA-5550-50-Vol-2-Bk-1)

Avail: NTIS HC A17/MF A01 CSCL 21E

Tabulated data from wind tunnel tests conducted to evaluate the aerodynamic performance of an advanced coannular exhaust nozzle for a future supersonic propulsion system are presented. Tests were conducted with two test configurations: (1) a short flap mechanism for fan stream control with an isentropic contoured flow splitter, and (2) an iris fan nozzle with a conical flow splitter. Both designs feature a translating primary plug and an auxiliary inlet ejector. Tests were conducted at takeoff and simulated cruise conditions. Data were acquired at Mach numbers of 0.38, 0.9, and 2.0 for a wide range of nozzle operating conditions. At simulated supersonic cruise, both configurations demonstrated good performance, comparable to levels assumed in earlier advanced supersonic propulsion studies. However, at subsonic cruise, both configurations exhibited performance that was 6 to 7.5 percent less than the study assumptions. At takeoff conditions, the iris configuration performance approached the assumed levels, while the short flap design was 4 to 6 percent less. Data are provided through test run 25. M.G.

NS1-17083* Pratt and Whitney Aircraft Group, East Hartford, Conn. Commercial Products Div.

MODEL AERODYNAMIC TEST RESULTS FOR TWO VARIABLE CYCLE ENGINE COANNULAR EXHAUST SYSTEMS AT SIMULATED TAKEOFF AND CRUISE CONDITIONS. COMPREHENSIVE DATA REPORT. VOLUME 2: TABULATED AERODYNAMIC DATA BOOK 2

D. P. Nelson Jan. 1981 446 p refs

(Contract NAS3-20061)

(NASA-CR-159819-Vol-2-Bk-2; PWA-5550-50-Vol-2-Bk-2)

Avail: NTIS HC A18/MF A01 CSCL 21E

Tabulated aerodynamic data from coannular nozzle performance tests are given for test runs 28 through 37. The data include nozzle thrust coefficient parameters, nozzle discharge coefficients, and static pressure tap measurements. M.G.

NS1-17084* Pratt and Whitney Aircraft Group, East Hartford, Conn. Commercial Products Div.

MODEL AERODYNAMIC TEST RESULTS FOR TWO VARIABLE CYCLE ENGINE COANNULAR EXHAUST SYSTEMS AT SIMULATED TAKEOFF AND CRUISE CONDITIONS. COMPREHENSIVE DATA REPORT. VOLUME 2: TABULATED AERODYNAMIC DATA BOOK 3

D. P. Nelson Jan. 1981 467 p refs

(Contract NAS3-20061)

(NASA-CR-159819-Vol-2-Bk-3; PWA-5550-50-Vol-2-Bk-3) Avail:

NTIS HC A20/MF A01 CSCL 21E

Tabulated data from wind tunnel tests evaluating the aerodynamic performance of coannular exhaust nozzles are given for test runs 37 through 65. M.G.

NS1-17085* Pratt and Whitney Aircraft Group, East Hartford, Conn. Commercial Products Div.

MODEL AERODYNAMIC TEST RESULTS FOR TWO VARIABLE CYCLE ENGINE COANNULAR EXHAUST SYSTEMS AT SIMULATED TAKEOFF AND CRUISE CONDITIONS. COMPREHENSIVE DATA REPORT. VOLUME 3: GRAPHICAL DATA BOOK 1

D. P. Nelson Jan. 1981 411 p refs

(Contract NAS3-20061)

(NASA-CR-159819-Vol-3-Bk-1; PWA-5550-50-Vol-3-Bk-1)

Avail: NTIS HC A16/MF A01 CSCL 21E

A graphical presentation of the aerodynamic data acquired during coannular nozzle performance wind tunnel tests is given. The graphical data consist of plots of nozzle gross thrust coefficient, fan nozzle discharge coefficient, and primary nozzle discharge coefficient. Normalized model component static pressure distributions are presented as a function of primary total pressure, fan total pressure, and ambient static pressure for selected operating conditions. In addition, the supersonic cruise configuration data include plots of nozzle efficiency and secondary-to-fan total pressure pumping characteristics. Supersonic and subsonic cruise data are given. M.G.

NS1-17086* Pratt and Whitney Aircraft Group, East Hartford, Conn. Commercial Products Div.

MODEL AERODYNAMIC TEST RESULTS FOR TWO VARIABLE CYCLE ENGINE COANNULAR EXHAUST SYSTEMS AT SIMULATED TAKEOFF AND CRUISE CONDITIONS. COMPREHENSIVE DATA REPORT. VOLUME 3: GRAPHICAL DATA BOOK 2

D. P. Nelson Jan. 1981 482 p

(Contract NAS3-20061)

(NASA-CR-159819-Vol-3-Bk-2; PWA-5550-50-Vol-3-Bk-2)

Avail: NTIS HC A21/MF A01 CSCL 21E

Graphical data from wind tunnel tests of variable cycle engine coannular exhaust nozzles are given. Specifically, aerodynamic data for takeoff conditions are presented. M.G.

N81-17087# General Electric Co., Cincinnati, Ohio. Aircraft Engine Group.
SAMARIUM COBALT (SMCO) GENERATOR/ENGINE INTEGRATION STUDY Final Report, Aug. 1977 - Sep. 1979

Herbert F. Demel, Eike Richter, Charles F. Triebel, Robert C. Webb, and Max Baumgardner Wright-Patterson AFB, Ohio
AFWAL Apr. 1980 348 p refs
(Contract F33615-77-C-2018; AF Proj. 3145)
(AD-A092904; R79AEG123; AFWAL-TR-80-2022) Avail: NTIS HC A15/MF A01 CSCL 21/5

This study consists of integrating a generator/starter internally on the engine rotor shaft, providing both secondary electric power and engine starting. The integrated engine generator/starter (IEG/S) has been analyzed and conceptually designed for three power levels and three engine categories. The preliminary layouts and supporting analysis of the rate earth, permanent magnet machine indicate that the IEG/S concept is a technically feasible approach to secondary power extraction and engine starting.

GRA

N81-17989# General Electric Co., Cincinnati, Ohio.
VCE EARLY ACOUSTIC TEST RESULTS OF GENERAL ELECTRIC'S HIGH-RADIUS RATIO COANNULAR PLUG NOZZLE c71

Paul R. Knott, J. F. Brausch, P. K. Bhutiani, R. K. Majjigi, and V. L. Doyle In NASA, Langley Research Center Supersonic Cruise Res. 1979, Pt. 1 Mar. 1980 p 417-452 refs (For primary document see N81-17981 09-01)
(Contracts NAS3-20582; NAS3-21608)
Avail: NTIS HC A23/MF A01 CSCL 20A

Results of variable cycle engine (VCE) early acoustic engine and model scale tests are presented. A summary of an extensive series of far field acoustic, advanced acoustic, and exhaust plume velocity measurements with a laser velocimeter of inverted velocity and temperature profile, high radius ratio coannular plug nozzles on a YJ101 VCE static engine test vehicle are reviewed. Select model scale simulated flight acoustic measurements for an unsuppressed and a mechanical suppressed coannular plug nozzle are also discussed. The engine acoustic nozzle tests verify previous model scale noise reduction measurements. The engine measurements show 4 to 6 PNdB aft quadrant jet noise reduction and up to 7 PNdB forward quadrant shock noise reduction relative to a fully mixed conical nozzle at the same specific thrust and mixed pressure ratio. The influences of outer nozzle radius ratio, inner stream velocity ratio, and area ratio are discussed. Also, laser velocimeter measurements of mean velocity and turbulent velocity of the YJ101 engine are illustrated. Select model scale static and simulated flight acoustic measurements are shown which corroborate that coannular suppression is maintained in forward speed.

M.G.

N81-18066# General Electric Co., Evendale, Ohio. Aircraft Engine Group.

ENERGY EFFICIENT ENGINE: FLIGHT PROPULSION SYSTEM PRELIMINARY ANALYSIS AND DESIGN Topical Report, Jan. - Nov. 1978

R. P. Johnston, R. S. Beitler, R. O. Bobinger, C. L. Broman, R. D. Gravitt, H. Heineke, P. R. Holloway, J. S. Klem, D. O. Nash, and P. Ortiz Jun. 1980 276 p refs
(Contract NAS3-20643)

(NASA-CR-159583; R79AEG623) Avail: NTIS HC A12/MF A01 CSCL 21E

The characteristics of an advanced flight propulsion system (FPS), suitable for introduction in the late 1980's to early 1990's, was more fully defined. It was determined that all goals for efficiency, environmental considerations, and economics could be met or exceeded with the possible exception of NOx emission. In evaluating the FPS, all aspects were considered including component design, performance, weight, initial cost, maintenance cost, engine system integration (including nacelle), and aircraft integration considerations. The current FPS installed specific fuel consumption was reduced 14.2% from that of the CF6-50C reference engine. When integrated into an advanced, subsonic, study transport, the FPS produced a fuel burn savings of 15 to

23% and a direct operating cost reduction of 5 to 12% depending on the mission and study aircraft characteristics relative to the reference engine.

E.D.K.

N81-19117# AiResearch Mfg. Co., Phoenix, Ariz.
GENERAL AVIATION TURBINE ENGINE (GATE) STUDY Final Report

C. F. Baerst and D. G. Furst 5 Feb. 1979 274 p refs
(Contract NAS3-20755)

(NASA-CR-159482; AiResearch-21-2997) Avail: NTIS HC A12/MF A01 CSCL 21E

The feasibility of turbine engines for the smaller general aviation aircraft was investigated and a technology program for developing the necessary technology was identified. Major results included the definition of the 1980 general aviation market, the identification of turboprop and turbofan engines that meet the requirements of the aircraft studies, a benefit analysis showing the superiority of gas turbine engines for portions of the market studied, and detailed plans for the development of the necessary technology.

J.M.S.

N81-19118# Detroit Diesel Allison, Indianapolis, Ind.
CERAMIC APPLICATIONS IN TURBINE ENGINES Semianual Progress Report, 1 Jul. 1979 - 3 Dec. 1979

Michael S. Hudson, Michael A. Janovicz, and Franklin A. Rockwood May 1980 157 p refs

(Contracts DEN3-17; EC-77-A-31-1040)

(NASA-CR-159865; EDR-10156) Avail: NTIS HC A08/MF A01 CSCL 21E

Ceramic material characterization and testing of ceramic nozzle vanes, turbine tip shrouds, and regenerators disks at 36 C above the baseline engine TIT and the design, analysis, fabrication and development activities are described. The design of ceramic components for the next generation engine to be operated at 2070 F was completed. Coupons simulating the critical 2070 F rotor blade was hot spin tested for failure with sufficient margin to quality sintered silicon nitride and sintered silicon carbide, validating both the attachment design and finite element strength. Progress made in increasing strength, minimizing variability, and developing nondestructive evaluation techniques is reported.

E.A.K.

N81-19119# AiResearch Mfg. Co., Phoenix, Ariz.
QCGAT MIXER COMPOUND EXHAUST SYSTEM DESIGN AND STATIC BIG MODEL TEST REPORT

W. L. Blackmore and C. E. Thompson 31 Oct. 1978 336 p refs

(Contract NAS3-20585)

(NASA-CR-135386; AiResearch-21-2861) Avail: NTIS HC A15/MF A01 CSCL 21E

A mixer exhaust system was designed to meet the proposed performance and exhaust jet noise goals for the AiResearch QCGAT engine. Some 0.35 scale models of the various nozzles were fabricated and aerodynamically and acoustically tested. Preliminary optimization, engine cycle matching, model test data and analysis are presented. A final mixer exhaust system is selected for optimum performance for the overall flight regime.

A.R.H.

N81-19120# Avco Lycoming Div., Stratford, Conn.
DESIGN OF AN EXHAUST MIXER NOZZLE FOR THE AVCO-LYCOMING QUIET CLEAN GENERAL AVIATION TURBOFAN (QCGAT)

John F. Hurley, Leonard Anson, and Craig Wilson Aug. 1978 46 p refs

(Contract NAS3-20584)

(NASA-CR-159426; LYC-78-36)

Avail: NTIS HC A03/MF A01 CSCL 21E

This report describes the design configuration and method used to design the forced engine exhaust to bypass air mixing

system for Lycoming's QCGAT engine. This mixer is an integral part of the total engine and nacelle system and was configured to reduce the propulsion system noise and fuel consumption levels. Author

**NS1-20078*# Pratt and Whitney Aircraft, West Palm Beach, Fla. Government Products Div.
EXTENDED FREQUENCY TURBOFAN MODEL Final Report**

J. R. Mason, J. W. Park, and R. F. Jaekel 15 Dec. 1980
104 p refs
(Contract NAS3-21807)
(NASA-CR-185261; FR-13983) Avail: NTIS
HC A06/MF A01 CSCL 21E

The fan model was developed using two dimensional modeling techniques to add dynamic radial coupling between the core stream and the bypass stream of the fan. When incorporated into a complete TF-30 engine simulation, the fan model greatly improved compression system frequency response to planar inlet pressure disturbances up to 100 Hz. The improved simulation also matched engine stability limits at 15 Hz, whereas the one dimensional fan model required twice the inlet pressure amplitude to stall the simulation. With verification of the two dimensional fan model, this program formulated a high frequency F-100(3) engine simulation using row by row compression system characteristics. In addition to the F-100(3) remote splitter fan, the program modified the model fan characteristics to simulate a proximate splitter version of the F-100(3) engine. T.M.

**NS1-22061*# General Electric Co., Cincinnati, Ohio.
ENERGY EFFICIENT ENGINE FLIGHT PROPULSION
SYSTEM: AIRCRAFT/ENGINE INTEGRATION EVALUA-
TION Status Report, Jan. 1978 - Nov. 1978**

R. F. Patt Jun. 1980 328 p refs
(Contract NAS3-20643)
(NASA-CR-159584; R79AEG274) Avail: NTIS
HC A15/MF A01 CSCL 21E

Results of aircraft/engine integration studies conducted on an advanced flight propulsion system are reported. Economic evaluations of the preliminary design are included and indicate that program goals will be met. Installed sfc, DOC, noise, and emissions were evaluated. Aircraft installation considerations and growth were reviewed. J.M.S.

**NS1-22062*# General Electric Co., Lynn, Mass.
QUIET CLEAN GENERAL AVIATION TURBOFAN (QCGAT)
TECHNOLOGY STUDY, VOLUME 1 Final Report**

Dec. 1975 193 p refs
(Contract NAS3-19429)
(NASA-CR-164222; R75AEG026-Vol-1) Avail: NTIS
HC A09/MF A01 CSCL 21E

The preliminary design of an engine which satisfies the requirements of a quiet, clean, general aviation turbofan (QCGAT) engine is described. Also an experimental program to demonstrate performance is suggested. The T700 QCGAT engine preliminary design indicates that it will radiate noise at the same level as an aircraft without engine noise, have exhaust emissions within the EPA 1981 Standards, have lower fuel consumption than is available in comparable size engines, and have sufficient life for five years between overhauls. M.G.

**NS1-22063*# General Electric Co., Evendale, Ohio.
DESIGN CONCEPTS FOR LOW-COST COMPOSITE TUR-
BOFAN ENGINE FRAME Final Report**

S. C. Mitchell and L. J. Stoffer Oct. 1980 70 p refs
(Contract NAS3-22180)
(NASA-CR-165217; R81AEG311) Avail: NTIS
HC A04/MF A01 CSCL 21E

Design concepts for low cost, lightweight composite engine frames were applied to the design requirements for the frame of a commercial, high bypass engine. Four alternative composite frame design concepts identified which consisted of generic type

components and subcomponents that could be adapted to use in different locations in the engine and the different engine sizes. A variety of materials and manufacturing methods were projected with a goal for the lowest number of parts at the lowest possible cost. After a preliminary evaluation of all four frame concepts, two designs were selected for an extended design and evaluation which narrowed the final selection down to one frame that was significantly lower in cost and slightly lighter than the other frame. An implementation plan for this lowest cost frame is projected for future development and includes prospects for reducing its weight with proposed unproven, innovative fabrication techniques. Author

**A81-20767*# A model for the analysis of premixing-
prevaporizing fuel-air mixing passages. O. L. Anderson, L. M.
Chiappetta, and J. B. McVey (United Technologies Research Center,
East Hartford, Conn.). American Institute of Aeronautics and
Astronautics, Aerospace Sciences Meeting, 19th, St. Louis, Mo., Jan.
12-15, 1981, Paper 81-0345. 11 p. 16 refs. Contract No. NAS3-
21269.**

A model for predicting the distribution of liquid fuel droplets and fuel vapor in premixing-prevaporizing fuel-air mixing passages has been developed. The analysis involves successive application of computer codes which calculate the two dimensional or axisymmetric air flow field; calculate the three dimensional fuel droplet trajectories and evaporation rates; and calculate the fuel vapor diffusing through a moving air stream. A description of the more important features of the model and the results of a design study on two premixing fuel-air passages are presented. (Author)

**A81-29987*# Interactive multi-mode blade impact analysis.
A. Alexander (Hercules, Inc., Allegany Ballistics Laboratory, Cum-
berland, Md.). American Society of Mechanical Engineers, Gas
Turbine Conference and Products Show, Houston, Tex., Mar. 9-12,
1981, Paper 81-GT-79. 11 p. Members, \$2.00; nonmembers, \$4.00.
Contract No. NAS3-20091.**

This paper describes the theoretical methodology used in developing an analysis for the response of turbine engine fan blades subjected to soft body (bird) impacts and the computer program that was developed using this methodology as its basis. This computer program is an outgrowth of two programs that were previously developed for the purpose of studying problems of a similar nature (a three-mode beam impact analysis and a multi-mode beam impact analysis). The present program utilizes an improved missile model that is interactively coupled with blade motion which is more consistent with actual observations. It takes into account local deformation at the impact area, blade camber effects, and the spreading of the impacted missile mass on the blade surface. In addition, it accommodates plate-type mode shapes. The analysis capability in this computer program represents a significant improvement in the development of the methodology for evaluating potential fan blade materials and designs with regard to foreign object impact resistance. (Author)

**A81-30093*# Effect of time-dependent flight loads on tur-
bofan engine performance deterioration. B. L. Lewis (Teledyne, Inc.,
Teledyne CAE, Toledo, Ohio), A. Jay (United Technologies Corp.,
Commercial Products Div., East Hartford, Conn.), and E. G.
Stakolich (NASA, Lewis Research Center, Cleveland, Ohio). American
Society of Mechanical Engineers, Gas Turbine Conference and
Products Show, Houston, Tex., Mar. 9-12, 1981, Paper 81-GT-203. 6
p. 8 refs. Members, \$2.00; nonmembers, \$4.00. Contract No.
NAS3-20632.**

An analytic evaluation of the dynamic effects of two flight load conditions of the JT9D-7/747 propulsion system is conducted. Predicted performance changes associated with a once-per-flight vertical gust and a typical revenue service landing are calculated. The predicted dynamic load effects on thrust specific fuel consumption are found to be negligible. The results indicate that the quasi-steady state approach to flight loads modeling is adequate to investigate the factors important to the deterioration process. L.S.

09 RESEARCH AND SUPPORT FACILITIES (AIR)

Includes airports, hangars and runways; aircraft repair and overhaul facilities; wind tunnels; shock tube facilities; and engine test blocks.

For related information see also 14 *Ground Support Systems and Facilities (Space)*.

A81-34158 * Description of the warm core turbine facility and the warm annular cascade facility recently installed at NASA Lewis Research Center. W. J. Whitney, R. G. Stabe, and T. P. Moffitt (NASA, Lewis Research Center, Cleveland, Ohio). *Society of Automotive Engineers, Aerospace Congress and Exposition, Los Angeles, Calif., Oct. 13-16, 1980, Paper 801122*. 9 p.

The two new facilities have been installed and operated at their design or rated conditions. The important feature of both of these facilities is that the ratio of turbine inlet temperature to coolant temperature encountered in high temperature engines can be duplicated at moderate turbine inlet temperature. Included in the discussion are the limits of the facilities with regard to maximum temperature, maximum pressure, maximum mass flow rate, turbine size, and dynamometer torque-speed characteristics. (Author)

12 ASTRONAUTICS (GENERAL)

For extraterrestrial exploration see 91 *Lunar and Planetary Exploration*.

A81-20642 * # Requirements and preliminary concept of a Zero-Gravity Combustion Facility for Spacelab. R. L. DeWitt (NASA, Lewis Research Center, Cleveland, Ohio). *American Institute of Aeronautics and Astronautics, Aerospace Sciences Meeting, 19th, St. Louis, Mo., Jan. 12-15, 1981, Paper 81-0165*. 6 p. 17 refs.

This paper describes the preliminary concept, specifications, and requirements of a reusable Zero-Gravity Combustion Facility for use by experimenters aboard the Spacelab payload of the Space Transportation System Orbiter. The proposed facility allows a wide variety of combustion research experiments, from rapid burning to long term smoldering, in a low gravity environment. Included is the philosophy behind the design, the basic facility concept itself, and a description of the hardware required to implement the concept.

(Author)

A81-46059 * # Overview study of combustion experiments in a space laboratory. T. H. Cochran (NASA, Lewis Research Center, Systems Concepts and Space Experiments Branch, Cleveland, OH). In: *Combustion experiments in a zero-gravity laboratory*. (A81-46057 22-12) New York, American Institute of Aeronautics and Astronautics, 1981, p. 7-12.

A program of reduced gravity fluids research was initiated in the late 1950s. The primary motivations for this program was a need to characterize the behavior of propellants in a space environment. In the conduction of experiments, use was made of drop towers, aircraft, and ballistic rockets. There remained a core of problems which could not be solved with the aid of the employed approaches. Proposals for Spacelab experiments were, therefore, submitted. A committee came to the overall conclusion that there was a broad range of combustion experimentation that should be conducted in space. An examination of the analytical models which exist for numerous combustion phenomena reveals that these, are 'zero-G' theories. Experimentation in space will permit these theories to be tested and establish a firm basis upon which to build an understanding of more complicated combustion processes. Realistic in-space fire safety criteria are needed to eliminate the risk of major fire hazards in space. Such criteria can only be obtained through long-term reduced-gravity experimentation.

G.R.

A81-46068 * # Combustion experimentation aboard the space transportation system. R. L. DeWitt (NASA, Lewis Research Center, Space Propulsion Div., Cleveland, OH). In: *Combustion experiments in a zero-gravity laboratory*. (A81-46057 22-12) New York, American Institute of Aeronautics and Astronautics, 1981, p. 245-258.

A description is presented of the preliminary concept, specifications, and general requirements of a proposed Combustion Facility (CF) for the Spacelab payload of the Space Transportation System. The CF will permit an experimenter to use suitably contained liquid, gas, or solid fuels. He can specify and establish the composition and pressure level of the atmosphere in which the combustion will take place. It will be possible to characterize the experiment with common types of instrumentation as well as selected specialized equipment, to study the combustion process visually by direct observation and by motion picture coverage, and to obtain time histories of pertinent experimental parameters. During an experimental period, the CF will depend on Spacelab resources for power, heat rejection, and vacuum. Activating the CF and preparing it for the various experiments, performing the experiments, and shutting down the facility will be largely manual operations performed by flight personnel.

G.R.

15 LAUNCH VEHICLES AND SPACE VEHICLES

Includes boosters; manned orbital laboratories; reusable vehicles; and space stations.

N81-13079* National Aeronautics and Space Administration, Lewis Research Center, Cleveland, Ohio.

ELECTRIC PROPULSION - CHARACTERISTICS, APPLICATIONS, AND STATUS

Joseph E. Maloy, Carl R. Dulgeroff (Hughes Research Labs., Malibu, Calif.), and Robert E. Poeschel (Hughes Research Labs., Malibu, Calif.) 1981 14 p refs

(NASA-TM-81630; E-640) Avail: NTIS HC A02/MF A01 CSCL 20C

A comparative review of the principles of ion thruster and chemical rocket operations is presented. The 30cm mercury ion thruster development and the specifications imposed on it by the Solar Electric Propulsion System program are discussed. The 30cm thruster operating range, efficiency, wear out lifetime, and interface requirements are described. T.M.

N81-12135* Dayton Univ., Ohio.

APPLICATIONS TECHNOLOGY SATELLITE AND COMMUNICATIONS TECHNOLOGY SATELLITE USER EXPERIMENTS FOR 1967 - 1980 REFERENCE BOOK, VOLUME 1 Final Report

Nicolas A. Engler, John F. Nash, and Jenny D. Strange Aug. 1980 263 p 4 Vol.

(Contracts NAS3-21370; NAS3-19699; NAS3-20392)

(NASA-CR-165169-Vol-1; UDR-TR-80-99-Vol-1) Avail: NTIS HC A12/MF A01 CSCL 22B

A description of each of the satellites is given and a brief summary of each user experiment is presented. A Cross Index of User Experiments sorted by various parameters and a listing of keywords versus Experiment Number are presented. Author

N81-12136* Dayton Univ., Ohio.

APPLICATIONS TECHNOLOGY SATELLITE AND COMMUNICATIONS TECHNOLOGY SATELLITE USER EXPERIMENTS FOR 1967-1980 REFERENCE BOOK, VOLUME 2 Final Report

Nicolas A. Engler, John F. Nash, and Jenny D. Strange Aug. 1980 370 p refs 4 Vol.

(Contracts NAS3-21370; NAS3-19699; NAS3-20392)

(NASA-CR-165169-Vol-2; UDR-TR-80-100-Vol-2) Avail: NTIS HC A16/MF A01 CSCL 22B

The experiments are grouped by type of service offered; for example, education, health services, and data transmission. A bibliography of reports by accession number and by author are also presented. A listing of keywords versus report number is presented. Author

N81-12137* Dayton Univ., Ohio.

APPLICATIONS TECHNOLOGY SATELLITE AND COMMUNICATIONS TECHNOLOGY SATELLITE USER EXPERIMENTS FOR 1967-1980 REFERENCE BOOK, VOLUME 3: USER FORM SURVEYS Final Report

Nicolas A. Engler, John F. Nash, and Jenny D. Strange Aug. 1980 340 p refs 4 Vol.

(Contracts NAS3-21370; NAS3-19699; NAS3-20392)

(NASA-CR-165169-Vol-3; UDR-TR-80-101-Vol-3) Avail: NTIS HC A15/MF A01 CSCL 22B

Questionnaires received from the satellite users are presented. Questionnaires were sent to users in 1976, 1977 and 1979. The forms reflect user viewpoints of the systems. Author

N81-12139* Columbia Univ., New York. Dept. of Electrical Engineering.

NEXT GENERATION COMMUNICATIONS SATELLITES:

MULTIPLE ACCESS AND NETWORK STUDIES Final Report

T. E. Stern, M. Schwartz, H. E. Meadows, H. K. Ahmat, J. G. Gadre, I. S. Gopal, and K. Matsmo Jul. 1980 174 p refs (Contract NAS5-25759)

(NASA-CR-165145; FR-1) Avail: NTIS HC A08/MF A01 CSCL 22B

Following an overview of issues involved in the choice of promising system architectures for efficient communication with multiple small inexpensive Earth stations serving heterogeneous user populations, performance evaluation via analysis and simulation for six SS/TDMA (satellite-switched/time-division multiple access) system architectures is discussed. These configurations are chosen to exemplify the essential alternatives available in system design. Although the performance evaluation analyses are of fairly general applicability, whenever possible they are considered in the context of NASA's 30/20 GHz studies. Packet switched systems are considered, with the assumption that only a part of transponder capacity is devoted to packets, the integration of circuit and packet switched traffic being reserved for further study. Three types of station access are distinguished: fixed (FA), demand (DA), and random access (RA). Similarly, switching in the satellite can be assigned on a fixed (FS) or demand (DS) basis, or replaced by a buffered store-and-forward system (SF) onboard the satellite. Since not all access/switching combinations are practical, six systems are analyzed in detail: three FS SYSTEMS, FA/FS, DA/FS, RA/FS; one DS system, DA/DS; and two SF systems, FA/SF, DA/SF. Results are presented primarily in terms of delay-throughput characteristics. J.M.S.

N81-21106* Vought Corp., Dallas, Tex.

STUDY OF THERMAL MANAGEMENT FOR SPACE PLATFORM APPLICATIONS

John A. Oren Dec. 1980 184 p refs Prepared in cooperation with Hughes Aircraft Co., Los Angeles, TRW Systems, Redondo Beach, Calif., Hamilton Standard, Hartford, Conn., General Dynamics/Astronautics, San Diego, Calif., and Lockheed Missiles and Space Co., Sunnyvale, Calif.

(Contract NAS3-22270)

(NASA-CR-165238; Rept-2-63020/OR-62678) Avail: NTIS HC A08/MF A01 CSCL 22B

Techniques for the management of the thermal energy of large space platforms using many hundreds of kilowatts over a 10 year life span were evaluated. Concepts for heat rejection, heat transport within the vehicle, and interfacing were analyzed and compared. The heat rejection systems were parametrically weight optimized over conditions for heat pipe and pumped fluid approaches. Two approaches to achieve reliability were compared for: performance, weight, volume, projected area, reliability, cost, and operational characteristics. Technology needs are assessed and technology advancement recommendations are made. E.A.K.

N81-27169* Systems Science and Software, La Jolla, Calif.

ANALYSIS OF THE CHARGING OF THE SCATHA (P78-2) SATELLITE Final Report, Mar. 1979 - Oct. 1980

P. R. Stannard, I. Katz, M. J. Mandell, J. J. Cassidy, D. E. Parks, M. Rotenberg, and P. G. Steen Dec. 1980 249 p refs

Sponsored in cooperation with AFGL

(Contract NAS3-21762)

(NASA-CR-165348; SSS-R-81-4798)

Avail: NTIS HC A11/MF A01 CSCL 22B

The charging of a large object in polar Earth orbit was investigated in order to obtain a preliminary indication of the response of the shuttle orbiter to such an environment. Two NASCAP (NASA Charging Analyzer Program) models of SCATHA (Satellite Charging at High Altitudes) were used in simulations of charging events. The properties of the satellite's constituent materials were compiled and representations of the experimentally observed plasma spectra were constructed. Actual charging events, as well as those using test environments, were simulated. Numerical models for the simulation of particle emitters and detectors were used to analyze the operation of these devices onboard SCATHA. The effect of highly charged surface regions on the charging conductivity within a photosheath was used to interpret results from the onboard electric field experiment. Shadowing calculations were carried out for the satellite and a table of effective illuminated areas was compiled. J.D.H.

16 SPACE TRANSPORTATION

Includes passenger and cargo space transportation e.g. shuttle operations, and rescue techniques.

For related information see also 03 Air Transportation and Safety and 85 Urban Technology and Transportation.

A81-19936 * # Modelling of environmentally induced discharges in geosynchronous satellites. N. J. Stevens (NASA, Lewis Research Center, Cleveland, Ohio). (*IEEE, U.S. Defense Nuclear Agency, Jet Propulsion Laboratory, and DOE. Annual Conference on Nuclear and Space Radiation Effects, 17th, Ithaca, N.Y., July 15-18, 1980.*) *IEEE Transactions on Nuclear Science*, vol. NS-27, Dec. 1980, p. 1792-1796. 29 refs.

The NASCAP computer code is used to compute the charging and discharging characteristics of a typical communications satellite in geosynchronous orbit. For the case of a severe substorm, satellite surface differential charging in sunlight is found to be substantially less than that required to produce discharges in ground simulation studies. A discharge process is postulated involving discharges triggered at edges (or imperfection) followed by discharges to space. The characteristics of such discharges are parametrically varied to evaluate the possible effects on the satellite. It has been found that discharge characteristics inferred from satellite monitors could be caused by predicted space discharges, that single cell discharges to space can reduce surface potential over entire satellite, and that low-density electron trajectory computations indicate that discharge generated electrons may not return to the satellite by long trajectories. Current transients predicted do not agree with the available ground simulation results indicating that additional work must be done both analytically and experimentally to understand and fully explain these discrepancies. (Author)

17 SPACECRAFT COMMUNICATIONS, COMMAND AND TRACKING

Includes telemetry, space communications networks,
astronavigation, and radio blackout

For related information see also *04 Aircraft Commu-
nications and Navigation* and *32 Communications*

N81-30172* National Aeronautics and Space Administration
Lewis Research Center, Cleveland, Ohio

THE 30/20 GHz EXPERIMENTAL COMMUNICATIONS SATELLITE SYSTEM

Joseph N Sivo 1981 10 p refs Proposed for presentation
at 1981 Natl Telecommun Conf., New Orleans, 29 Nov - 3 Dec
1981, sponsored by IEEE

(NASA TM-82683, E-966) Avail NTIS HC A02/MF A01 CSCL
22A

NASA is continuing to pursue an aggressive satellite com-
munications technology development program focused on the
30/20 GHz frequency band. A review of the program progress
to date is presented. Included is a discussion of the technology
program status as well as a description of the experimental
system concept under study. Expected system performance
characteristics together with spacecraft and payload configuration
details including weight and power budget is presented. Overall
program schedules of both the technology development and the
flight system development are included. Author

18 SPACECRAFT DESIGN, TESTING AND PERFORMANCE

Includes spacecraft thermal and environmental control,
and attitude control.

For life support systems see 54 *Man/System Technology
and Life Support* For related information see also 05
Aircraft Design, Testing and Performance and 39 *Structural
Mechanics*

N81-32187* National Aeronautics and Space Administration,
Lewis Research Center, Cleveland, Ohio

REVIEW OF BIASED SOLAR ARRAY. PLASMA INTERAC- TION STUDIES

N John Stevens 1981 17 p refs Presented at Fifteenth
Intern Elec Propulsion Conf., Las Vegas, Nev., 21-23 Apr 1981;
sponsored by AIAA, Japan Society for Aeronautical and Space
Sciences and DGLR
(NASA-TM-82693; E-973) Avail NTIS HC A02/MF A01 CSCL
21C

The Solar Electric Propulsion System (SEPS) is proposed
for a variety of space missions. Power for operating SEPS is
obtained from large solar array wings capable of generating tens
of kilowatts of power. To minimize resistive losses in the solar
array bus lines, the array is designed to operate at voltages up
to 400 volts. This use of high voltage can increase interaction
between the biased solar cell interconnects and plasma environ-
ments. With thrusters operating, the system ground is maintained
at space plasma potential which exposes large areas of the
arrays at the operating voltages. This can increase interactions
with both the natural and enhanced charged particle environments.
Available data on interactions between biased solar array surfaces
and plasma environments are summarized. The apparent
relationship between collection phenomena and solar cell size
and effects of array size on interactions are discussed. The impact
of these interactions on SEPS performance is presented. T.M.

A81-20400 * # Engineering management and innovation. R.
W. Graham (NASA, Lewis Research Center, Cleveland, Ohio).
Mechanical Engineering, vol. 102, Oct. 1980, p. 26-28.

Although improved management methods can enhance the
performance of some enterprises, they can lower that of research
organizations. The prevalent use of cost-effectiveness criteria as a
management tool overvalues identifiable short-term accomplishment
at the expense of long-term research efforts, which often serve as the
antecedents upon which a new, seemingly unrelated technology is
later founded. Medical instruments used in the treatment of
emphysema, for example, evolved from NASA-sponsored research
devoted to the measurement of the composition of the atmospheres
of the planets. The best manager is the manager who creates an
environment that enables his research engineers to pursue ideas with
a minimum of interference. Such an environment consists of broad
research objectives, adequate facilities, and proper technical support.
Within a framework of prudent spending, the manager's aim is to
cultivate innovation. R.S.

19 SPACECRAFT INSTRUMENTATION

For related information see also 06 Aircraft Instrumentation and 35 Instrumentation and Photography.

NS1-11688* National Aeronautics and Space Administration, Lewis Research Center, Cleveland, Ohio.

AN AUTOMATED PROCEDURE FOR DEVELOPING HYBRID COMPUTER SIMULATIONS OF TURBOFAN ENGINES

John R. Szuch and Susan M. Krosel 1980 19 p refs Proposed for presentation at the 14th Ann. Simulation Symp. Tampa, Fla., 18-20 Mar. 1981

(NASA-TM-81605; E-598) Avail: NTIS HC A02/MF A01 CSCL 05B

A systematic, computer-aided, self-documenting methodology for developing hybrid computer simulations of turbofan engines is presented. The methodology makes use of a host program that can run on a large digital computer and a machine-dependent target (hybrid) program. The host program performs all of the calculations and data manipulations needed to transform user-supplied engine design information to a form suitable for the hybrid computer. The host program also trims the self contained engine model to match specified design point information. A test case is described and comparisons between hybrid simulation and specified engine performance data are presented. S.F.

NS1-16119* National Aeronautics and Space Administration, Lewis Research Center, Cleveland, Ohio.

SPACECRAFT TRANSMITTER RELIABILITY

1980 18 p refs Synopsis of Workshop, held in Cleveland, 25-26 Sep. 1979; sponsored by NASA and Air Force (NASA-CP-2159; E-662) Avail: NTIS HC A06/MF A01 CSCL 17B

A workshop on spacecraft transmitter reliability was held at the NASA Lewis Research Center on September 25 and 26, 1979, to discuss present knowledge and to plan future research areas. Since formal papers were not submitted, this synopsis was derived from audio tapes of the workshop. The following subjects were covered: users' experience with space transmitters; cathodes; power supplies and interfaces; and specifications and quality assurance. A panel discussion ended the workshop. T.M.

NS1-17127* National Aeronautics and Space Administration, Lewis Research Center, Cleveland, Ohio.

ENVIRONMENTAL CHARGING EFFECTS MONITORS FOR OPERATIONAL SATELLITES

John C. Sturman 1981 11 p refs Proposed for presentation at the 1981 Aerospace Ind./Test Meas. Symp., Sponsored by the Instr. Soc. of Am., Indianapolis, 26-30 Apr. 1981

(NASA-TM-81669; E-691) Avail: NTIS HC A02/MF A01 CSCL 22B

A set of three instruments was developed that can provide early detection of potentially dangerous geomagnetic substorm conditions, and monitor the spacecraft response. The set consists of three instruments: A Surface Voltage Sensor that measures the characteristic energy of collected electrons or ions from +100 to -20,000 volts; a logarithmic current density sensor or Nanoammeter that measures local electron flux by measuring currents from 10 to the minus 9th power to 10 to the minus 5th power A; and a Transient Events Counter that counts the spurious pulses from electrostatic discharges that are coupled into the spacecraft wiring harness. An amplitude threshold can be set to count only pulses that are large enough to cause circuit malfunction. Performance characteristics, specifications, and application of these instruments are discussed. Size, weight, and power requirements were minimized. The Surface Voltage Sensor and Nanoammeter are packaged together in a box that is 10.1 by 11.3 by 9.5 cm and weighs 0.82 kg. The transient Events Counter measures 10.1 by 11.3 by 5.4 cm and weighs 0.55 kg. Both operate from a nominal 28 V dc input and require a total of 3/4 watt for both. Although designed for flight use, these instruments are also suitable for laboratory use. T.M.

NS1-20172* National Aeronautics and Space Administration, Lewis Research Center, Cleveland, Ohio.

DIAGNOSTIC SYSTEM DESIGN FOR THE ION AUXILIARY PROPULSION SYSTEM (IAPS). FLIGHT TESTS OF TWO 8 cm MERCURY ION

E. B. Hurst and G. Z. Thomas (Hughes Aircraft Co., Los Angeles) 1981, 33 p Presented at the 18th Intern. Elec. Propulsion Conf., Las Vegas, Nev., 21-23 Apr. 1981; sponsored by A/AA, Japan Society for Aeronautical and Space Sciences and DGLR (NASA-TM-81702; E-727) Avail: NTIS HC A03/MF A01 CSCL 21C

The mechanical, thermal, electrical design and the ground test results of four types of detectors are explained. The DSS is designed to measure the thruster efflux material deposition and S/C potential relative to the local plasma in the vicinity of two 8 cm mercury ion thrusters. The DSS consists of two quartz crystal microbalance (QCM) detectors, one potential probe, nine solar cell arrays, seven ion collectors and two electronic packages. T.M.

A81-38057* Environmental charging effects monitors for operational satellites. J. C. Sturman (NASA, Lewis Research Center, Cleveland, OH). *Instrument Society of America, International Aerospace Instrumentation Symposium, Indianapolis, IN, Apr. 26-30, 1981, Paper. 9 p.* 11 refs.

A set of three instruments has been developed that can provide early detection of potentially dangerous geomagnetic substorm conditions, and monitor the spacecraft response. The set consists of three instruments: (1) a 'surface voltage sensor' that measures the characteristic energy of collected electrons or ions from +100 to -20,000 volts; (2) a 'nanoammeter' or logarithmic current density sensor that measures local electron flux by measuring currents from 10 to the -9th to 10 to the -5th A; and (3) a 'transient events counter' that counts the spurious pulses from electrostatic discharges that are coupled into the spacecraft wiring harness. Performance characteristics, specifications, and application of these instruments are discussed. (Author)

A81-42207* Shuttle compatible cryogenic liquid storage instrumentation/data needs. W. L. Allen (Thiokol Corp., Wasatch Div., Brigham City, UT). *AIAA, SAE, and ASME, Joint Propulsion Conference, 17th, Colorado Springs, CO, July 27-29, 1981, AIAA Paper 81-1550. 10 p.* 12 refs.

Results of an assessment of a designer's data needs for solid rocket motor instrumentation is described, along with the state-of-the-art and specialized instrumentation used to date. It is determined that solid rocket motor data obtained during static testing does not always agree with flight test data, and more quantitative data is necessary for motor design. The most promising new flight test instrumentation/data techniques for future flight programs are presented: microwave horns, ultrasonics, thermovision, in situ transducers, isotopes, and parachute recovery of flight hardware. It is noted that a development effort (minimum one to two years) and adequate funding will be required to have these concepts available for the design of future solid rocket motors. J.F.

20 SPACECRAFT PROPULSION AND POWER

Includes main propulsion systems and components e.g. rocket engines; and spacecraft auxiliary power sources.

For related information see also 07 Aircraft Propulsion, 28 Propellants and Fuels, and 44 Energy Production and Conversion.

N81-19219* National Aeronautics and Space Administration, Lewis Research Center, Cleveland, Ohio.

PERFORMANCE OF A MAGNETIC MULTIPOLE LINE-CUSP ARGON ION THRUSTER

James S. Sovey 1981 12 p refs Proposed for presentation at the 15th Intern. Elec. Propulsion Conf., Las Vegas, Nev., 21-23 Apr. 1981; cosponsored by the AIAA, the Japan Soc. for Aeronautical and Space Sciences, and Deutsche Gesellschaft fuer Luft- und Raumfahrt.

(NASA-TM-81703; E-2) Avail: NTIS HC A02/MF A01 CSCL 21C

A 17 cm diameter line cusp ion thruster was evaluated with inert gases which are candidate propellants for on orbit and orbit transfer propulsion functions for Large Space Systems. A semiempirical relationship was generated to predict thruster beam current in terms of plasma parameters which would allow initial thruster optimization without ion extraction and the associated large vacuum facilities. The sensitivity of performance to changes in discharge electrode configurations and magnetic circuit was evaluated and is presented. After final optimization a propellant utilization efficiency of 0.8 at a discharge chamber power expenditure of about 260 w per beam ampere was obtained. These performance parameters are the highest yet achieved with argon propellant. Author

N81-19220* National Aeronautics and Space Administration, Lewis Research Center, Cleveland, Ohio.

PERFORMANCE CAPABILITIES OF THE 8-CM MERCURY ION THRUSTER

M. A. Mantieniks 1981 13 p refs Proposed for Presentation at the 15th Intern. Elec. Propulsion Conf., Las Vegas, Nev., 21-23 Apr. 1981; cosponsored by the AIAA, the Japan Soc. for Aeronautical and Space Sciences, and Deutsche Gesellschaft fuer Luft- und Raumfahrt.

(NASA-TM-81720; E-755) Avail: NTIS HC A02/MF A01 CSCL 21C

A preliminary characterization of the performance capabilities of the 8-cm thruster in order to initiate an evaluation of its application to LSS propulsion requirements is presented. With minor thruster modifications, the thrust was increased by about a factor of four while the discharge voltage was reduced from 39 to 22 volts. The thruster was operated over a range of specific impulse of 1950 to 3040 seconds and a maximum total efficiency of about 54 percent was attained. Preliminary analysis of component lifetimes, as determined by temperature and spectroscopic line intensity measurements, indicated acceptable thruster lifetimes are anticipated at the high power level operation. T.M.

N81-19221* National Aeronautics and Space Administration, Lewis Research Center, Cleveland, Ohio.

ION BEAM DEPOSITED PROTECTIVE FILMS

Michael J. Mirtich 1981 16 p refs Proposed for presentation at the 15th Intern. Elec. Propulsion Conf., Las Vegas, Nev., 21-23 Apr. 1981; sponsored by the AIAA, the Japan Society for Aeronautical and Space Sciences, and Deutsche Gesellschaft fuer Luft- und Raumfahrt.

(NASA-TM-81722; E-759) Avail: NTIS HC A02/MF A01 CSCL 21C

Single or dual ion beam sources were used to deposit thin films for different applications. Metal and metal oxide films were evaluated as protective coatings for the materials. Film adherence was measured and the most promising films were then tested under environments similar to operating conditions. It was shown

that some materials do protect the material (H-13 steel) and do reduce thermal fatigue. Diamondlike films have many useful applications. A series of experiments were conducted to define and optimize new approaches to the manufacture of such films. A dual beam system using argon and methane gases was developed to generate these films. T.M.

N81-19222* National Aeronautics and Space Administration, Lewis Research Center, Cleveland, Ohio.

SERT II 1980 EXTENDED FLIGHT THRUSTER EXPERIMENTS

W. R. Kerslake and L. R. Ignaczak 1981 27 p refs Presented at 15th Intern. Elec. Propulsion Conf., Las Vegas, Nevada, 21-23 Apr. 1981; sponsored by Japan Society for Aeronautical and Space Sciences and PGLR.

(NASA-TM-81685; E-695) Avail: NTIS HC A03/MF A01 CSCL 21C

The flight results obtained from mid 1979 through December 1980 are presented. Near continuous solar power in 1979 and 1980 has enabled long periods of thruster endurance testing. Three of four propellant tanks were exhausted with no significant change in thruster system operation before being empty. A new plasma mode thrust was characterized and direct thrust measurements obtained. Other tests, including beam neutralization by various neutralizer sources, give insight to electron conduction across plasmas in space and provide a basis to model neutralization of thruster arrays. E.D.K.

N81-20173* National Aeronautics and Space Administration, Lewis Research Center, Cleveland, Ohio.

ANALYSIS OF COSTS OF GALLIUM ARSENIDE AND SILICON SOLAR ARRAYS FOR SPACE POWER APPLICATIONS

Kent S. Jefferies Mar. 1981 16 p refs

(NASA-TP-1811; E-536) Avail: NTIS HC A02/MF A01 CSCL 10A

A parametric analysis was performed to compare the costs of silicon and gallium arsenide arrays for Earth orbital missions. The missions included electric power in low Earth orbit (LEO), electric power in geosynchronous Earth orbit (GEO), and power for electric propulsion of a LEO to GEO orbit transfer mission. Inputs to the analysis for all missions included launch and purchase costs of the array. For the orbit transfer mission, the launch and purchase costs of the electric propulsion system were added. Radiation flux as a function of altitude and radiation tolerance as a function of cell type were used to determine power degradation for each mission. Curves were generated that show the sensitivity of launch-array cost and total mission cost to a variety of input parameters for each mission. These parameters included mission duration, cover glass thickness, array specific cost, array specific mass, and solar cell efficiency. Solar concentration was considered and the sensitivities of cost to concentration ratio, concentrator costs, and concentrator mass were also evaluated. Results indicate that solar cell development should give a high priority to reducing array costs and that the development of low cost, lightweight, solar concentrators should be pursued. Author

N81-20176* National Aeronautics and Space Administration, Lewis Research Center, Cleveland, Ohio.

SOME EFFECTS OF THERMAL-CYCLE-INDUCED DEFORMATION IN ROCKET THRUST CHAMBERS

Ned P. Hannum and Raymond G. Price, Jr. Apr. 1981 24 p refs

(NASA-TP-1834; E-553) Avail: NTIS HC A02/MF A01 CSCL 21H

The deformation process observed in the hot gas side wall of rocket combustion chambers was investigated for three different liner materials. Five thrust chambers were cycled to failure by using hydrogen and oxygen as propellants at a chamber pressure of 4.14 MN/cu m. The deformation was observed nondestructively at midlife points and destructively after failure occurred. The cyclic life results are presented with an accompanying discussion about the problems of life prediction associated with

the types of failures encountered in the present work. Data indicating the deformation of the thrust chamber liner as cycles are accumulated are presented for each of the test thrust chambers. From these deformation data and observation of the failure sites it is evident that modeling the failure process as classic low cycle thermal fatigue is inadequate as a life prediction method. R.C.T.

NS1-20177* National Aeronautics and Space Administration, Lewis Research Center, Cleveland, Ohio.

SIMPLIFIED POWER SUPPLIES FOR ION THRUSTERS

Robert P. Gruber 1981 24 p refs Presented at the 15th Intern. Elec. Propulsion Conf., Las Vegas, Nev., 21-23 Apr. 1981 (NASA-TM-81725; E-765) Avail: NTIS HC A02/MF A01 CSCL 21C

The initial development and demonstration of power supplies with an order of magnitude reduction in parts count, leading to increased reliability at lower weight, while still maintaining thrust system performance are discussed. Two new self-regulating keeper power supply circuits were developed and tested. One supply comprises 14 parts and uses an input voltage range of 18 to 36 volts, the other operates from 200 to 400 volts and requires 22 components. A technique for controlling heater power is also demonstrated. T.M.

NS1-20178* National Aeronautics and Space Administration, Lewis Research Center, Cleveland, Ohio.

RECENT WORK ON AN RF ION THRUSTER

Richard Q. Lee and Shigeo Nakanishi 1981 12 p refs Presented at the 15th Intern. Elec. Propulsion Conf., Las Vegas, Nev., 21-23 Apr. 1981; sponsored by AIAA, Japan Society for Aeronautical and Space Sciences and DGLR (NASA-TM-81734; E-802) Avail: NTIS HC A02/MF A01 CSCL 21C

An experimental investigation of an rf ion thruster using an immersed coupler in an argon discharge is reported. The conical coil, used to couple rf power into the discharge, is placed inside the discharge vessel. The discharge was self-sustained by 100-150 MHz rf power at low environmental pressures. The ion extraction was accomplished by conventional accelerated grid optics from an unoptimized 8 cm diameter ion thruster. T.M.

NS1-20179* National Aeronautics and Space Administration, Lewis Research Center, Cleveland, Ohio.

EXTENDED OPERATING RANGE OF THE 30-cm ION THRUSTER WITH SIMPLIFIED POWER PROCESSOR REQUIREMENTS

V. K. Rawlin 1981 15 p refs Presented at the 15th 1981; cosponsored by the AIAA, Japan Soc. for Aeron. and Space Sci. and DGLR and Space Sci. and Deut. Ges. fur Luft- und Raumfahrt (NASA-TM-81729; E-772) Avail: NTIS HC A02/MF A01 CSCL 21C

A two grid 30 cm diameter mercury ion thruster was operated with only six power supplies over the baseline J series thruster power throttle range with negligible impact on thruster performance. An analysis of the functional model power processor showed that the component mass and parts count could be reduced considerably and the electrical efficiency increased slightly by only replacing power supplies with relays. The input power, output thrust, and specific impulse of the thruster were then extended, still using six supplier from 2660 watts, 0.13 newtons, and 2980 seconds to 9130 watts, 0.37 newtons, and 3820 seconds, respectively. Increases in thrust and power density enable reductions in the number of thrusters and power processors required for most missions. Preliminary assessments of the impact of thruster operation at increased thrust and power density on the discharge characteristics, performance, and lifetime of the thruster were also made. E.D.K.

NS1-20180* National Aeronautics and Space Administration, Lewis Research Center, Cleveland, Ohio.

FREE RADICAL PROPULSION CONCEPT

C. E. Hawkins and S. Nakanishi 1981 25 p refs Presented at 15th Intern. Elec. Propulsion Conf., Las Vegas, Nevada, 21-23 Apr. 1981; sponsored by AIAA, Japan Society for Aeronautical and Space Sciences and DGLR (NASA-TM-81770; E-813) Avail: NTIS HC A02/MF A01 CSCL 21C

A free radical propulsion concept utilizing the recombination energy of dissociated low molecular weight gases to produce thrust was examined. The concept offered promise of a propulsion system operating at a theoretical impulse, with hydrogen, as high as 2200 seconds at high thrust to power ratio, thus filling the gap existing between chemical and electrostatic propulsion capabilities. Microwave energy used to dissociate a continuously flowing gas was transferred to the propellant via three body recombination for conversion to propellant kinetic energy. Power absorption by the microwave plasma discharge was in excess of 90 percent over a broad range of pressures. Gas temperatures inferred from gas dynamic equations showed much higher temperatures from microwave heating than from electrothermal heating. Spectroscopic analysis appeared to corroborate the inferred temperatures of one of the gases tested. R.C.T.

NS1-21121* National Aeronautics and Space Administration, Lewis Research Center, Cleveland, Ohio.

CHARACTERISTICS OF 30-CENTIMETER MERCURY ION THRUSTERS

Joseph E. Maloy, Robert L. Foeschel (Hughes Research Lab., Malibu, Calif.), and Carl R. Duggeroff (Hughes Research Lab., Malibu, Calif.) 1981 24 p refs Presented at 15th Intern. Elec. Propulsion Conf., Las Vegas, Nevada, 21-23 Apr. 1981; sponsored by AIAA, Japan Society for Aeronautical and Space Sciences and DGLR (NASA-TM-81706; E-735) Avail: NTIS HC A02/MF A01 CSCL 21C

The technology development of the 30 centimeter J series mercury ion thruster for prime propulsion application in solar electric propulsion systems is described. Thruster design is reviewed. A standardized set of test and data recording procedures formulated to allow for the characterization of the J series thruster is described. Characteristics measured are the magnetic baffle characterization, the neutralizer characterization, pervance, the minimum eV/ion measurement, and the electrical and propellant utilization efficiency measurements. Test results are presented. J.D.H.

NS1-22084* National Aeronautics and Space Administration, Lewis Research Center, Cleveland, Ohio.

PARTICLE AND FIELD MEASUREMENTS ON TWO J-SERIES 30 CENTIMETER THRUSTERS

Walter C. Lathe 1981 27 p refs Presented at the 15th Intern. Elec. Propulsion Conf., Las Vegas, Nev., 21-23 Apr. 1981; sponsored by AIAA, Japan Society for Aeronautical and Space Sciences and DGLR (NASA-TM-81741; E-794) Avail: NTIS HC A03/MF A01 CSCL 21H

Tests were performed to characterize the particles and fields associated with two 30 cm mercury ion thrusters operating independently and simultaneously. Flux rates and energies of ions and their distribution around the thrusters were determined. Facility effect ions were measured and their effect on thruster created flux measurements was assessed. The flux rate and distribution of sputtered metal atoms was determined and compared with theory and previous measurements. Mapping of the potential fields in the near vicinity of the thrusters was accomplished. Author

N81-26173*# National Aeronautics and Space Administration.
Lewis Research Center, Cleveland, Ohio.
DETERMINATION OF OPTIMUM SUNLIGHT CONCENTRATION LEVEL IN SPACE FOR GALLIUM ARSENIDE SOLAR CELLS

Henry B. Curtis 1981 8 p refs Presented at the 15th Photovoltaic Spec. Conf., Kissimmee, Fla., 12-15 May 1981; sponsored by the Inst. of Electrical and Electronics Engineers (NASA-TM-82643; E-898) Avail: NTIS HC A02/MF A01 CSCL 10A

The solar cell diode equation was used to calculate the optimum values, or range of values of concentration ratios. A variety of temperature vs. concentration assumptions were used and cell area and series resistance were varied. The coefficients of the diffusion and recombination terms vary strongly with temperature while the light generated current is a weak function of temperature and proportional to concentration. The study indicates that the cell temperature vs. concentration ratio assumption is critical. It appears that concentration levels of approximately 100X are feasible in space. T.M.

N81-26174*# National Aeronautics and Space Administration.
Lewis Research Center, Cleveland, Ohio.

SERT 2 THRUSTERS: STILL TICKING AFTER ELEVEN YEARS

W. R. Kerslake 1981 23 p refs Presented at the 17th Joint Propulsion Conf., Colorado Springs, Colo., 27-29 Jul. 1981; sponsored by AIAA, SAE and ASME (NASA-TM-81774; E-835) Avail: NTIS HC A02/MF A01 CSCL 21C

The performance and durability of the ion thruster system and components are discussed. Interactions between the ion thruster and the space plasma-spacecraft interfaces were examined. The application of the results of testing the thruster to designing future ion thrusters is emphasized. T.M.

N81-30182*# National Aeronautics and Space Administration.
Lewis Research Center, Cleveland, Ohio.

A CASE HISTORY OF TECHNOLOGY TRANSFER

Aug. 1981 28 p refs
(NASA-TM-82618; E-870) Avail: NTIS HC A03/MF A01 CSCL 21H

A sequence of events, occurring over the last 25 years, are described that chronicle the evolution of ion-bombardment electric propulsion technology. Emphasis is placed on the latter phases of this evolution, where special efforts were made to pave the way toward the use of this technology in operational space flight systems. These efforts consisted of a planned program to focus the technology toward its end applications and an organized process that was followed to transfer the technology from the research-technology NASA Center to the user-development NASA Center and its industry team. Major milestones in this evolution, which are described, include the development of thruster technology across a large size range, the successful completion of two space electric rocket tests, SERT I and SERT II, development of power-processing technology for electric propulsion, completion of a program to make the technology ready for flight system development, and finally the technology transfer events. Author

N81-31282*# National Aeronautics and Space Administration.
Lewis Research Center, Cleveland, Ohio.

DEVELOPMENT AND DESIGN OF THREE MONITORING INSTRUMENTS FOR SPACECRAFT CHARGING

John C. Sturman Sep. 1981 28 p refs
(NASA-TP-1800; E-603) Avail: NTIS HC A03/MF A01 CSCL 22B

A set of instruments which provide early detection of potentially dangerous geomagnetic substorm conditions and monitor the spacecraft response are discussed. The set consists of a sensor that measures the characteristic energy of collected electrons or ions from +100 to 20,000 V, a logarithmic current density sensor that measures local electron flux and a transient events counter that counts the spurious pulses from electrostatic discharges that couple into the spacecraft wiring

harness. Design details and performance characteristics of the three instruments are given. Size, weight, and power requirements are minimized. E.A.K.

A81-27207*# Radiation damage annealing mechanisms and possible low temperature annealing in silicon solar cells. I. Weinberg and C. K. Swartz (NASA, Lewis Research Center, Cleveland, Ohio). In: Photovoltaic Specialists Conference, 14th, San Diego, Calif., January 7-10, 1980, Conference Record. (A81-27076 11-44) New York, Institute of Electrical and Electronics Engineers, Inc., 1980, p. 858-862. 9 refs.

Deep level transient spectroscopy and the Shockley-Read-Hall recombination theory are used to identify the defect responsible for reverse annealing in 2 ohm-cm n+p silicon solar cells. This defect, with energy level at $E_v + 0.30$ eV, has been tentatively identified as a boron-oxygen-vacancy complex. It has been also determined by calculation that the removal of this defect could result in significant annealing at temperatures as low as 200 C for 2 ohm-cm and lower resistivity cells. V.L.

A81-29528*# SERT II 1980 extended flight thruster experiments. W. R. Kerslake and L. R. Ignaczak (NASA, Lewis Research Center, Cleveland, Ohio). *AIAA, Japan Society for Aeronautical and Space Sciences, and DGLR, International Electric Propulsion Conference, 15th, Las Vegas, Nev., Apr. 21-23, 1981, AIAA Paper 81-0665*. 18 p. 14 refs.

The SERT II spacecraft, launched in 1970, has been maintained in an operational, but intermittent status since 1971. This paper presents the flight results obtained from mid 1979 through December 1980. Near continuous solar power in 1979 and 1980 has enabled long periods of thruster endurance testing. Three of four propellant tanks have been exhausted with no significant change in thruster system operation before being empty. A new plasma mode thrust has been characterized and direct thrust measurements obtained. Other tests, including beam neutralization by various neutralizer sources, give insight to electron conduction across plasmas in space and provide a basis to model neutralization of thruster arrays. (Author)

A81-29542*# Simplified power supplies for ion thrusters. R. P. Gruber (NASA, Lewis Research Center, Cleveland, Ohio). *AIAA, Japan Society for Aeronautical and Space Sciences, and DGLR, International Electric Propulsion Conference, 15th, Las Vegas, Nev., Apr. 21-23, 1981, AIAA Paper 81-0693*. 12 p. 22 refs.

A program addressing less complex and potentially lower cost ion thruster systems has been started at the NASA Lewis Research Center. This paper discusses the initial development and demonstration of power supplies with an order of magnitude reduction in parts count, leading to increased reliability at lower weight, while still maintaining thrust system performance. Two new self-regulating keeper power supply circuits were developed and tested. One supply comprises 14 parts and uses an input voltage range of 18 to 36 volts, the other operates from 200 to 400 volts and requires 22 components. A new technique for controlling heater power is also demonstrated. (Author)

A81-32897*# Extended operating range of the 30-cm ion thruster with simplified power processor requirements. V. K. Rawlin (NASA, Lewis Research Center, Cleveland, Ohio). *AIAA, Japan Society for Aeronautical and Space Sciences, and DGLR, International Electric Propulsion Conference, 15th, Las Vegas, Nev., Apr. 21-23, 1981, AIAA Paper 81-0692*. 13 p. 25 refs.

A 30-cm-diameter Hg ion thruster similar in design to the J-series thruster was operated at fixed conditions with only five power supplies and was throttled over the baseline power range with six supplies. An analysis of the functional model power processor showed that the component mass and parts count would be reduced

by about 14 and 35% respectively, and the electrical efficiency would be increased about 1.5% by replacing power supplies with relays. By introducing new circuit designs, additional reductions in the component mass and parts, as well as an increase in electrical efficiency would be expected. The impact on thruster performance of reducing the number of power supplies was to lower the propellant utilization efficiency about 1.0% and raise the electrical efficiency values from 0.2 to 1.3% over the throttle range. L.S.

A81-32905 * # Free radical propulsion concept. C. E. Hawkins and S. Nakanishi (NASA, Lewis Research Center, Cleveland, Ohio). *AIAA, Japan Society for Aeronautical and Space Sciences, and DGLR, International Electric Propulsion Conference, 15th, Las Vegas, Nev., Apr. 21-23, 1981, AIAA Paper 81-0676*. 24 p.

The concept of a free radical propulsion system, utilizing the recombination energy of dissociated low molecular weight gases to produce thrust, is analyzed. The system, operating at a theoretical impulse with hydrogen, as high as 2200 seconds at high thrust to power ratio, is hypothesized to bridge the gap between chemical and electrostatic propulsion capabilities. A comparative methodology is outlined by which characteristics of chemical and electric propulsion for orbit raising mission can be investigated. It is noted that free radicals proposed in rockets previously met with difficulty and complexity in terms of storage requirements; the present study proposes to eliminate the storage requirements by using electric energy to achieve a continuous-flow product of free radicals which are recombined to produce a high velocity propellant. Microwave energy used to dissociate a continuously flowing gas is transferred to the propellant via three-body-recombination for conversion to propellant kinetic energy. Microwave plasma discharge was found in excess of 90 percent over a broad range of pressure in preliminary experiments, and microwave heating compared to electrothermal heating showed much higher temperatures in gasdynamic equations. E.B.

A81-35625 * # Recent work on an RF ion thruster. R. Q. Lee and S. Nakanishi (NASA, Lewis Research Center, Cleveland, Ohio). *AIAA, Japan Society for Aeronautical and Space Sciences, and DGLR, International Electric Propulsion Conference, 15th, Las Vegas, Nev., Apr. 21-23, 1981, AIAA Paper 81-0678*. 12 p, 17 refs.

Preliminary results of an RF ion thruster using an immersed coupler in an argon discharge are presented. Conventional ion accelerator optics are used to extract an ion beam. An account is given of the operation of an unoptimized thruster over a range of input powers, propellant flow rates, frequencies, and magnetic field strengths. It is noted that lifetime and overall efficiency factors have not yet been extensively investigated. The results obtained establish the feasibility of this approach and the potential for future improvements. The conical coil employed to couple RF power into the discharge is placed inside the discharge vessel. The discharge is self-sustained by 100-150 MHz RF power at low environmental pressures (approximately 0.00001 torr). The ion extraction is accomplished by conventional accelerator grid optics from an unoptimized 8 cm diameter ion thruster. C.R.

A81-37569 * # Characteristics of 30-centimeter mercury ion thrusters. J. E. Maloy (NASA, Lewis Research Center, Cleveland, Ohio), R. L. Poeschel, and C. R. Dulgeroff (Hughes Research Laboratories, Malibu, Calif.). *AIAA, Japan Society for Aeronautical and Space Sciences, and DGLR, International Electric Propulsion Conference, 15th, Las Vegas, Nev., Apr. 21-23, 1981, AIAA Paper 81-0715*. 22 p, 9 refs.

The technology development of the 30-cm J-series mercury ion thruster for prime propulsion application in solar electric propulsion systems has been conducted at NASA-Lewis Research Center. This development included the fabrication and testing of the 30-cm thruster. The present J-series thruster design is the result of an intensive effort to eliminate real and potential design deficiencies that were uncovered during initial endurance, structural, and performance tests. A standardized set of test and data recording

procedure was formulated to allow for the characterization of the J-series thruster. This paper briefly reviews the design of the J-series thruster and presents a compilation of recent test results that define the J-series thruster characteristics. (Author)

A81-38068 * # Ion beam applications research - A 1981 summary of Lewis Research Center programs. B. A. Banks (NASA, Lewis Research Center, Cleveland, OH). *AIAA, Japan Society for Aeronautical and Space Sciences, and DGLR, International Electric Propulsion Conference, 15th, Las Vegas, NV, Apr. 21-23, 1981, AIAA Paper 81-0669*. 71 p, 101 refs.

In 1975 the NASA's Lewis Research Center initiated a technology specific spinoff program to more broadly utilize benefits resulting from ion thruster technology. An Ion Beam Applications Research (IBAR) program was organized to enable the development of new or improved materials, products, and processes through the nonpropulsive application of ion thruster technology. Focused efforts to identify, evaluate, develop and transfer applications to the user community were conducted. A summary of the NASA Lewis Research Center's in-house, grant, and contract projects involving IBAR is given. Specific application efforts utilizing ion beam sputter etching, deposition, and texturing are discussed as well as ion source and component technology applications. (Author)

A81-33070 * # Diagnostic system design for the Ion Auxiliary Propulsion System (IAPS) - Flight test of two 8 cm mercury ion thrusters. E. B. Hurst (NASA, Lewis Research Center, Cleveland, OH) and G. Z. Thomas (Hughes Aircraft Co., Los Angeles, CA). *AIAA, Japan Society for Aeronautical and Space Sciences, and DGLR, International Electric Propulsion Conference, 15th, Las Vegas, NV, Apr. 21-23, 1981, AIAA Paper 81-0666*. 31 p.

The experimental design of a Diagnostic Subsystem (DSS) as part of an Ion Auxiliary Propulsion System (IAPS) to be flown on P80-1 spacecraft in May 1983, is discussed. The DSS is composed of several detectors measuring thruster efflux, material deposition and spacecraft potential relative to the local space plasma in the vicinity of two 8 cm mercury ion thrusters. The detectors consist of two QCM units measuring frequency in the range of two to 65 KHz. Nine solar cell arrays have the capability of measuring current and voltage from 0-600 mA and 0-0.9 V. Seven ion collectors can measure ion currents with bias voltages of 0, 25, 55 and 96 V. The potential probe can measure current at 16 different commandable levels varying from one to 5 K microamperes within a voltage range of -25 to 175 V. The analysis of the ground-based data indicates that the hardware is qualified for flight, with the detectors and electronic units having passed all functional and environmental tests. Block diagrams are given and the functional parameters of the different design configurations are described. E.B.

A81-38071 * # Performance of a magnetic multipole line-cusp argon ion thruster. J. S. Sovey (NASA, Lewis Research Center, Cleveland, OH). *AIAA, Japan Society for Aeronautical and Space Sciences, and DGLR, International Electric Propulsion Conference, 15th, Las Vegas, NV, Apr. 21-23, 1981, AIAA Paper 81-0745*. 10 p, 11 refs.

The performance of a 17-cm diameter line-cusp ion thruster, using argon and xenon propellants, is investigated. Basic optimization of the thruster was accomplished without ion extraction and tests were conducted with small vacuum facilities and power supplies. The evaluation of the sensitivity of the performance to changes in discharge electrode configurations and the magnetic circuit is discussed. Final optimization results show that an argon propellant utilization efficiency of 0.9, at 260 W of discharge power per beam ampere, was obtained with a thruster having 20 rows of magnets and 10 tubular anodes. The average ion beam current densities were as high as 13 mA/sq cm. The results are considered to be the highest yet achieved with argon propellant. E.B.

A81-38072 * # Particle and field measurements on two J-series 30-centimeter thrusters. W. C. Lathem (NASA, Lewis Research Center, Cleveland, OH). *AIAA, Japan Society for Aeronautical and Space Sciences, and DGLR, International Electric Propulsion Conference, 15th, Las Vegas, NV, Apr. 21-23, 1981, AIAA Paper 81-0728*. 25 p. 13 refs.

An experimental investigation under complete computer control of the characteristics of particles and fields emanating from mercury bombardment ion thrusters (J-series, 30 cm diameter), operating independently and simultaneously, is discussed. Results show that the flux rate of sputtered metal atoms leaving a single thruster has been determined and the data is in agreement with previous test results. The flux rate and energies of ions leaving single and two-thruster configurations have been established for a variety of beam current levels and combinations involving the two thrusters, and the data are sufficient to establish upper bounds. Floating potential measurements made in the near vicinity of the thrusters indicate that the fields are weak, plus or minus a few volts. The tests may be significant for the Solar Electric Propulsion System (SEPS) planners. E.B.

A81-40934 * # SERT II thrusters - Still ticking after eleven years. W. R. Kerslake (NASA, Lewis Research Center, Cleveland, OH). *AIAA, SAE, and ASME, Joint Propulsion Conference, 17th, Colorado Springs, CO, July 27-29, 1981, AIAA Paper 81-1539*. 13 p. 14 refs.

The Space Electric Rocket Test II (SERT II) spacecraft was launched in 1970 with a primary objective of demonstrating long-term operation of a space electric thruster system. An overview is presented of all the SERT II testing conducted during the time from 1970 to 1981. Thruster testing and interaction results are considered, taking into account ion beam thrusting, distant neutralization, and the plasma beam thrust. In a discussion of durability testing, attention is given to the main cathodes, the neutralizer cathodes, the main keeper insulator, the H.V. grid insulators, the neutralizer propellant tanks, and the main propellant tanks. The most important result of the study is related to the confidence gained that mercury bombardment ion thruster systems can be built and operated in space on a routine basis with the same lifetime and performance as measured in ground testing. G.R.

A81-42198 * # Propellant management for low thrust chemical propulsion systems. K. M. Hamlyn, R. H. Dergance (Martin Marietta Aerospace, Denver, CO), and J. C. Aydelott (NASA, Lewis Research Center, Cleveland, OH). *AIAA, SAE, and ASME, Joint Propulsion Conference, 17th, Colorado Springs, CO, July 27-29, 1981, AIAA Paper 81-1453*. 9 p. 8 refs.

Low-thrust chemical propulsion systems (LTPS) will be required for orbital transfer of large space systems (LSS). The work reported in this paper was conducted to determine the propellant requirements, preferred propellant management technique, and propulsion system sizes for the LTPS. Propellants were liquid oxygen (LO2) combined with liquid hydrogen (LH2), liquid methane or kerosene. Thrust levels of 100, 500, and 1000 lbf were combined with 1, 4, and 8 perigee burns for transfer from low earth orbit to geosynchronous earth orbit. This matrix of systems was evaluated with a multilayer insulation (MLI) or a spray-on-foam insulation. Vehicle sizing results indicate that a toroidal tank configuration is needed for the LO2/LH2 system. Multiple perigee burns and MLI allow for superior LSS payload capability. Propellant settling, combined with a single screen device, was found to be the lightest and least complex propellant management technique. (Author)

N81-20174* # Hughes Research Labs., Malibu, Calif. **RETROFIT AND VERIFICATION TEST OF A 30-cm ION THRUSTER** Final Report, 6 Dec. 1977 - 16 Jun. 1980. C. R. Dulgeroff and R. L. Poeschel. Dec. 1980. 140 p. (Contract NAS3-21052) (NASA-CR-165233) Avail: NTIS HC A07/MF A01 CSCL 21H

Twenty modifications were found to be necessary and were approved by design review. These design modifications were incorporated in the thruster documents (drawings and procedures) to define the J series thruster. Sixteen of the design revisions were implemented in a 900 series thruster by retrofit modification. A standardized set of test procedures was formulated, and the retrofit J series thruster design was verified by test. Some difficulty was observed with the modification to the ion optics assembly, but the overall effect of the design modification satisfies the design objectives. The thruster was tested over a wide range of operating parameters to demonstrate its capabilities. T.M.

N81-21122* # Aerojet Liquid Rocket Co., Sacramento, Calif. **LOW-THRUST CHEMICAL ROCKET ENGINE STUDY** Final Contractor Report. J. A. Mellish. Mar. 1981. 152 p. refs. (Contract NAS3-21940) (NASA-CR-165276) Avail: NTIS HC A08/MF A01 CSCL 21H

Engine data and information are presented to perform system studies on cargo orbit-transfer vehicles which would deliver large space structures to geosynchronous equatorial orbit. Low-thrust engine performance, weight, and envelope parametric data were established, preliminary design information was generated, and technologies for liquid rocket engines were identified. Two major engine design drivers were considered in the study: cooling and engine cycle options. Both film-cooled and regeneratively cooled engines were evaluated. The propellant combinations studied were hydrogen/oxygen, methane/oxygen, and kerosene/oxygen. T.M.

N81-21125* # Rocketdyne, Canoga Park, Calif. **LOW-THRUST CHEMICAL ROCKET ENGINE STUDY** Final Progress Report, Jul. 1979 - Nov. 1980. J. M. Shoji. Mar. 1981. 340 p. refs. (Contract NAS3-21941) (NASA-CR-165275) RI/RD80-237 Avail: NTIS HC A15/MF A01 CSCL 21H

An analytical study evaluating thrust chamber cooling engine cycles and preliminary engine design for low thrust chemical rocket engines for orbit transfer vehicles is described. Oxygen/hydrogen, oxygen/methane, and oxygen/RP-1 engines with thrust levels from 444.8 N to 13345 N, and chamber pressures from 13.8 N/sq cm to 689.5 N/sq cm were evaluated. The physical and thermodynamic properties of the propellant theoretical performance data, and transport properties are documented. The thrust chamber cooling limits for regenerative/radiation and film/radiation cooling are defined and parametric heat transfer data presented. A conceptual evaluation of a number of engine cycles was performed and a 2224.1 N oxygen/hydrogen engine cycle configuration and a 2224.1 N oxygen/methane configuration chosen for preliminary engine design. Updated parametric engine data, engine design drawings, and an assessment of technology required are presented. J.D.H.

N81-22075* # International Applied Physics, Inc., Dayton, Ohio. **THE ELECTRIC RAIL GUN FOR SPACE PROPULSION** Final Report, 24 Jun. 1980 - 30 Jan. 1981. David P. Bauer, John P. Barber, and C. Julian Vahlberg. Feb. 1981. 160 p. (Contract NAS3-22475) (NASA-CR-165312) Avail: NTIS HC A08/MF A01 CSCL 21H

An analytic feasibility investigation of an electric propulsion concept for space application is described. In this concept,

quasistatic thrust due to inertial reaction to repetitively accelerated pellets by an electric rail gun is used to propel a spacecraft. The study encompasses the major subsystems required in an electric rail gun propulsion system. The mass, performance, and configuration of each subsystem are described. Based on an analytic model of the system mass and performance, the electric rail gun mission performance as a reusable orbital transfer vehicle (OTV) is analyzed and compared to a 30 cm ion thruster system (BIMOD) and a chemical propulsion system (IUS) for payloads with masses of 1150 kg and 2300 kg. For system power levels in the range from 25 kW(e) to 100 kW(e) an electric rail gun OTV is more attractive than a BIMOD system for low Earth orbit to geosynchronous orbit transfer durations in the range from 20 to 120 days. E.D.K.

A81-18363 * High performance cryogenic engines for orbit transfer vehicles. L. B. Basham (Aerojet Liquid Rocket Co., Sacramento, Calif.). *International Astronautical Federation, International Astronautical Congress, 31st, Tokyo, Japan, Sept. 22-28, 1980, Paper 80-F-253*. 25 p. 8 refs. Contracts No. NAS8-32999; No. NAS8-33574; No. NAS3-21940; No. NAS3-21960.

Evaluations of O₂/H₂ engine candidates in the 10K to 30K lb thrust class for Manned Orbit Transfer Vehicles (MOTV) and engine candidates using O₂/H₂, O₂/RP-1, and O₂/CH₄ in the 100 to 3,000 lb thrust range for Cargo Orbit Transfer Vehicles (COTV) are discussed. Both space vehicles are part of the larger SPS concept. It is shown that the Advanced Expander Cycle O₂/H₂ engine for MOTV merits further study and investigations. COTV engine study has so far indicated that conventionally cooled O₂/H₂ and O₂/CH₄ engine candidates should be evaluated further, while advanced cooling schemes are required for O₂/RP-1 concepts. With regard to MOTV, it is concluded that while no existing system meets the requirements of the Orbit Transfer Vehicles, the need for twin expander cycle engines is established because a single engine cannot provide a tolerable man-safety profile. With regard to COTV, it is stressed that advanced cooling concepts must be considered if other propellant combinations are to become competitive with O₂/H₂. Multistage centrifugal pumps are seen as the most promising concept. C.R.

A81-19937 * The effect of solar array voltage patterns on plasma power losses. M. J. Mandell, I. Katz, P. G. Steen, and G. W. Schnuelle (Systems, Science and Software, La Jolla, Calif.). (*IEEE, U.S. Defense Nuclear Agency, Jet Propulsion Laboratory, and DOE, Annual Conference on Nuclear and Space Radiation Effects, 17th, Ithaca, N.Y., July 15-18, 1980*) *IEEE Transactions on Nuclear Science*, vol. NS-27, Dec. 1980, p. 1797-1800. Contract No. NAS3-21762.

The use of high-voltage solar arrays in space is discussed in connection with the draining of array power by currents flowing between exposed surfaces through the surrounding plasma. The possibility of reducing the power loss by arranging solar cell strings in repeated small-area modules to eliminate any large areas at high potentials is investigated. It is found that the difference in power loss between modular and linear patterned high-voltage arrays is fairly small. Although the use of modular patterns can reduce the effective mean potential by about 10%, for the type of configuration being considered there is also a 10% increase in sheath area, leading to only a few percent change in total power loss. It is concluded that plasma power loss should not be a primary consideration in designing the physical arrangement of high-voltage arrays. C.R.

A81-20625 * Adapting magnetoelectrostatic containment to inert gas thrusters. W. D. Ramsey and E. L. James (Xerox Electro-Optical Systems, Pasadena, Calif.). *American Institute of Aeronautics and Astronautics, Aerospace Sciences Meeting, 19th, St. Louis, Mo., Jan. 12-15, 1981, Paper 81-0140*. 6 p. 6 refs. Contract No. NAS3-21345.

Two different types of 12 cm magnetoelectrostatic containment (MESCC) ion thrusters have been adapted to argon-xenon operation. Discharge chamber optimization produced excellent performance

with both the hexagonal and hemispherical shaped thrusters. The hemispherical thruster design yielded the best performance, ionizing 75 to 96 percent of the xenon propellant with a discharge energy consumption rate of 185 to 320 eV/ion. Argon operation of the same thruster achieved 60 to 80 percent propellant ionization at 215 to 370 eV/ion. (Author)

A81-29552 * Results of the Mission Profile Life Test first test segment - Thruster J1. E. L. James (Xerox Electro-Optical Systems, Pasadena, Calif.) and R. T. Bechtel (NASA, Marshall Space Flight Center, Huntsville, Ala.). *AIAA, Japan Society for Aeronautical and Space Sciences, and DGLR, International Electric Propulsion Conference, 15th, Las Vegas, Nev., Apr. 21-23, 1981, AIAA Paper 81-0716*. 13 p. 8 refs. Contract No. NAS3-20399.

A series of long term test segments of 30 cm diameter mercury bombardment thrusters is being conducted as the Mission Profile Life Test. The first 4000 hour segment has been completed with the J series thruster, J1. Thruster and power processing units were controlled by computer with software algorithms governing normal functions of startup, throttle, and shutdown as well as automatically handling a variety of off-normal conditions. Thruster operation includes a discussion of the test chronology describing notable events and their significance. Post-test examination provides insight into thruster lifetime. Results are consistent with mission requirements of 15,000 hours at 2A. (Author)

A81-29561 * Parasitic current losses due to solar electric propulsion generated plasmas. I. Katz, D. E. Parks, M. J. Mandell, and G. W. Schnuelle (Systems, Science and Software, La Jolla, Calif.). *AIAA, Japan Society for Aeronautical and Space Sciences, and DGLR, International Electric Propulsion Conference, 15th, Las Vegas, Nev., Apr. 21-23, 1981, AIAA Paper 81-0740*. 7 p. 9 refs. Contract No. NAS3-21762.

Solar electric propulsion is a leading candidate for many upcoming space missions. Under many circumstances plasma produced by charge-exchange reactions within the ion beam dominates the ambient environment near the spacecraft. The calculations presented here contain a predictive hydrodynamic model for the charge-exchange plasma expansion, and a fully three-dimensional model for the structure of the plasma sheath around the solar array wing. Results of calculations for several configurations and voltage levels indicate that with kilovolt biases power losses of approximately 10 percent or more are likely, even with only one engine in operation, and that ameliorative measures should focus on the inboard portion of the solar arrays. (Author)

23 CHEMISTRY AND MATERIALS (GENERAL)

Includes biochemistry and organic chemistry.

N81-18123* National Aeronautics and Space Administration.
Lewis Research Center, Cleveland, Ohio.

NEW ION EXCHANGE MEMBRANES

Warren H. Philipp, Charles E. May, and Li-Chen Hsu 1980
14 p refs Presented at Fall Meeting of Electrochem. Soc.,
Hollywood, Fla., 5-10 Oct. 1980

(NASA-TM-81670; E-641) Avail: NTIS HC A02/MF A01 CSCL
07B

A technique for the preparation of ion exchange films composed of radiation crosslinked polyacrylic acid and crosslinked polyacrylate salts is presented. Results suggest that radiolytic crosslinking occurs at the alpha carbon on polyacrylic acid via hydrogen abstraction by hydrogen atoms produced by the radiolytic decomposition of water. Conditions of reaction media and radiation dose are discussed for optimum crosslinking. Practical use of crosslinked polyacrylate ion exchange films for the removal of metal cations from dilute solution was demonstrated on a laboratory scale. The wet strength of membranes comprising various polyacrylate salts is correlated with water content of the swelled membrane.

J.M.S.

N81-21129* National Aeronautics and Space Administration.
Lewis Research Center, Cleveland, Ohio.

ION BEAM APPLICATIONS RESEARCH. A SUMMARY OF LEWIS RESEARCH CENTER PROGRAMS

Bruce A. Banks 1981 73 p refs Presented at 15th Intern. Elec. Propulsion Conf., Las Vegas, 21-23 Apr. 1981; sponsored by AIAA, Japan Soc. for Aeron. and Space Sci., and DGLR (NASA-TM-81721; E-756) Avail: NTIS HC A04/MF A01 CSCL
20H

A summary of the ion beam applications research (IBAR) program organized to enable the development of materials, products, and processes through the nonpropulsive application of ion thruster technology is given. Specific application efforts utilizing ion beam sputter etching, deposition, and texturing are discussed as well as ion source and component technology applications.

E.D.K.

N81-29180* National Aeronautics and Space Administration.
Lewis Research Center, Cleveland, Ohio.

CROSS-LINKED POLYVINYL ALCOHOL AND METHOD OF MAKING SAME Patent

Li-Chen Hsu, Dean W. Sheibley, and Warren H. Philipp, inventors
(to NASA) Issued 9 Jun. 1981 4 p Filed 30 Apr. 1980
(NASA-Case-LEW-13101-2; US-Patent-4,272,470.

US-Patent-Appl-SN-145271; US-Patent-Appl-SN-971473;

US-Patent-Class-264-104; US-Patent-Class-260-174UC;

US-Patent-Class-429-27; US-Patent-Class-429-28;

US-Patent-Class-428-139; US-Patent-Class-429-249;

US-Patent-Class-429-253; US-Patent-Class-525-56;

US-Patent-Class-525-61) Avail: U.S. Patent and Trademark
Office CSCL 07C

A film-forming polyvinyl alcohol polymer is mixed with a polyaldehyde-polysaccharide cross-linking agent having at least two monosaccharide units and a plurality of aldehyde groups per molecule, preferably an average of at least one aldehyde group per monosaccharide units. The cross-linking agent, such as a polydialdehyde starch, is used in an amount of about 2.5 to 20% of the theoretical amount required to cross-link all of the available hydroxyl groups of the polyvinyl alcohol polymer. Reaction between the polymer and cross-linking agent is effected in aqueous acidic solution to produce the cross-linked polymer. The polymer product has low electrical resistivity and other properties rendering it suitable for making separators for alkaline batteries.

Official Gazette of the U.S. Patent and Trademark Office

A81-29566 * # Magneto-electrostatic thruster physical geometry tests. W. D. Ramsey (Xerox Electro-Optical Systems, Pasadena, Calif.). AIAA, Japan Society for Aeronautical and Space Sciences, and DGLR, International Electric Propulsion Conference, 15th, Las Vegas, Nev., Apr. 21-23, 1981, AIAA Paper 81-0753. 11 p. Contract No. NAS3-21345.

Inert gas tests are conducted with several magneto-electrostatic containment discharge chamber geometries. The configurations tested include three discharge chamber lengths; three boundary magnet patterns; two different flux density magnet materials; hemispherical and conical shaped thrusters having different surface-to-volume ratios; and two and three grid ion optics. Argon mass utilizations of 60 to 79% are attained at 210 to 280 eV/ion in different test configurations. Short hemi thruster configurations are found to produce 70 to 92% xenon mass utilization at 185 to 220 eV/ion.

C.R.

A81-29567 * # Performance capabilities of the 8-cm Mercury ion thruster. M. A. Manteniks (NASA, Lewis Research Center, Cleveland, Ohio). AIAA, Japan Society for Aeronautical and Space Sciences, and DGLR, International Electric Propulsion Conference, 15th, Las Vegas, Nev., Apr. 21-23, 1981, AIAA Paper 81-0754. 9 p. 11 refs.

The paper presents an initial characterization of the performance capabilities and constraints of the 8-cm Hg ion thruster system with a view to evaluating its application to large space system propulsion requirements. With minor thruster modifications, the thrust was increased by about a factor of four, while the discharge voltage was reduced from 39 to 22 volts. The thruster was operated over a range of specific impulse of 1950 to 3040 seconds, and a maximum total efficiency of about 54% was attained at a discharge voltage of 24 volts and thruster input power of 0.49 kW.

V.L.

24 COMPOSITE MATERIALS

Includes laminates

NS1-12171* National Aeronautics and Space Administration, Lewis Research Center, Cleveland, Ohio.

LAMINATES AND REINFORCED METALS

C. C. Chamis Oct. 1980 47 p refs
(NASA-TM-81591; E-570) Avail: NTIS HC A03/MF A01 CSCL 11D

A selective review is presented of the state of the art of metallic laminates and fiber reinforced metals called metallic matrix laminates (MMLs). Design and analysis procedures that are used for, and typical structural components that have been made from MMLs are emphasized. Selected MMLs, constituent materials, typical material properties and fabrication procedures are briefly described, including hybrids and superhybrids. Advantages, disadvantages, and special considerations required during design, analysis, and fabrication of MMLs are examined. Tabular and graphical data are included to illustrate key aspects of MMLs. Appropriate references are cited to provide a selective bibliography of a rapidly expanding and very promising research and development field.

J.M.S.

NS1-16132* National Aeronautics and Space Administration, Lewis Research Center, Cleveland, Ohio.

PREDICTION OF COMPOSITE THERMAL BEHAVIOR MADE SIMPLE

Christos C. Chamis 1981 33 p refs Presented at the 36th Ann. Conf. of the Soc. of the Plastics Ind. (SPI) Reinforced Plastics/Composites Inst., Washington, D.C., 16-20 Feb. 1981
(NASA-TM-81618; E-624) Avail: NTIS HC A03/MF A01 CSCL 11D

A convenient procedure is described to determine the thermal behavior (thermal expansion coefficients and thermal stresses) of angleply fiber composites using a pocket calculator. The procedure consists of equations and appropriate graphs for various (+ or - theta) ply combinations. These graphs present reduced stiffness and thermal expansion coefficients as functions of (+ or - theta) in order to simplify and expedite the use of the equations. The procedure is applicable to all types of balanced, symmetric fiber composites including interply and intraply hybrids. The versatility and generality of the procedure is illustrated using several step-by-step numerical examples.

Author

NS1-17170* National Aeronautics and Space Administration, Lewis Research Center, Cleveland, Ohio.

METHOD FOR ALLEVIATING THERMAL STRESS DAMAGE IN LAMINATES Patent

Charles A. Hoffman, John W. Weeton, and Norman W. Orth, inventors (to NASA) Issued 8 Jul. 1980 6 p Filed 6 Apr. 1978 Supersedes N78-22163 (16 - 13, p 1675)
(N.A. Case-LEW-12493-1; US-Patent-4,211,354;
US-Patent-Appl-SN-893857; US-Patent-Class-228-118;
US-Patent-Class-228-170; US-Patent-Class-228-174;
US-Patent-Class-228-190; US-Patent-Class-156-292) Avail: US Patent and Trademark Office CSCL 11D

A method is provided for alleviating the stress damage in metallic matrix composites, such as laminated sheet or foil composites. Discontinuities are positively introduced into the interface between the layers so as to reduce the thermal stress produced by unequal expansion of the materials making up the composite. Although a number of discrete elements could be used to form one of the layers and thus carry out this purpose, the discontinuities are preferably produced by simply drilling holes in the metallic matrix layer or by forming grooves in a grid pattern in this layer.

Official Gazette of the U.S. Patent and Trademark Office

NS1-17174* National Aeronautics and Space Administration, Lewis Research Center, Cleveland, Ohio.

LOWER-CURING-TEMPERATURE PMR POLYIMIDES

T. T. Serafini, P. Delvige, and R. D. Vannucci 1981 17 p refs Presented at Thirty-Sixth Ann. Conf. of the Reinforced Plastics/Composites Inst. of the Soc. of the Plastics Ind., Inc., Washington, D.C., 16-20 Feb. 1981
(NASA-TM-81705; E-734) Avail: NTIS HC A02/MF A01 CSCL 11D

Studies were performed to achieve a lower-curing-temperature PMR polyimide. The use of m-aminostyrene as the end-cap instead of the monoalkyl ester of 5-norbornene-2,3 dicarboxylic acid was investigated in typical PMR formulations. Model compound studies were also performed. Differential scanning calorimetry studies were performed on model compounds and neat resins to establish their melting and curing characteristics. The elevated temperature weight loss characteristics of neat resins and graphite fiber composites were determined. The room temperature and short-time 280 C (500 F) mechanical properties of the composites were also determined. The use of m-aminostyrene end-caps reduced the final cure temperature of PMR resins by about 55 C (100 F), but the composites prepared with these resins are limited to use temperatures of about 260 C (500 F).

Author

NS1-21174* National Aeronautics and Space Administration, Lewis Research Center, Cleveland, Ohio.

ION BEAM SPUTTER ETCHING OF ORTHOPEDIC IMPLANTED ALLOY MP35N AND RESULTING EFFECTS ON FATIGUE

Edwin G. Wintucky, Mark Christopher, Eugene Bahnuk, and Simon Wang Mar. 1981 35 p refs Presented at 15th Intern. Electric Propulsion Conf., Las Vegas, 21-23 Apr. 1981; sponsored by AIAA, Japan Soc. for Aeron. and Space Sci. and DGLR
(NASA-TM-81747; E-782) Avail: NTIS HC A03/MF A01 CSCL 11F

The effects of two types of argon ion sputter etched surface structures on the tensile stress fatigue properties of orthopedic implant alloy MP35N were investigated. One surface structure was a natural texture resulting from direct bombardment by 1 keV argon ions. The other structure was a pattern of square holes milled into the surface by a 1 keV argon ion beam through a Ni screen mask. The etched surfaces were subjected to tensile stress only in fatigue tests designed to simulate the cyclic load conditions experienced by the stems of artificial hip joint implants. Both types of sputter etched surface structures were found to reduce the fatigue strength below that of smooth surface MP35N.

Author

NS1-25148* National Aeronautics and Space Administration, Lewis Research Center, Cleveland, Ohio.

TUNGSTEN FIBER REINFORCED SUPERALLOYS: A STATUS REVIEW

Donald W. Petrusek and Robert A. Signorelli 1981 70 p refs Presented at the 5th Ann. Conf. on Composites and Advan. Ceram. Mater., Merritt Island, Fla., 18-22 Jan. 1981; sponsored by the American Ceramic Society
(NASA-TM-82590; E-837) Avail: NTIS HC A04/MF A01 CSCL 11D

Improved performance of heat engines is largely dependent upon maximum cycle temperatures. Tungsten fiber reinforced superalloys (TFRS) are the first of a family of high temperature composites that offer the potential for significantly raising hot component operating temperatures and thus leading to improved heat engine performance. This status review of TFRS research emphasizes the promising property data developed to date, the status of TFRS composite airfoil fabrication technology, and the areas requiring more attention to assure their applicability to hot section components of aircraft gas turbine engines.

Author

N81-26149* National Aeronautics and Space Administration, Lewis Research Center, Cleveland, Ohio.
NONLINEAR LAMINATE ANALYSIS FOR METAL MATRIX FIBER COMPOSITES

C. C. Chamis and J. H. Sinclair 1981 18 p refs Presented at the 22d Structural Dyn. and Mater. Conf., Atlanta 6-8 Apr. 1981; sponsored by AIAA, ASME, American Society of Civil Engineers and AHS
(NASA-TM-82596; E-763) Avail: NTIS HC A02/MF A01 CSCL 11D

A nonlinear laminate analysis is described for predicting the mechanical behavior (stress-strain relationships) of angle-ply laminates in which the matrix is strained nonlinearly by both the residual stress and the mechanical load and in which additional nonlinearities are induced due to progressive fiber fractures and ply relative rotations. The nonlinear laminate analysis (NLA) is based on linear composite mechanics and a piecewise linear laminate analysis to handle the nonlinear responses. Results obtained by using this nonlinear analysis on boron fiber/aluminum matrix angle-ply laminates agree well with experimental data. The results shown illustrate the *in situ* ply stress-strain behavior and synergistic strength enhancement. Author

N81-26150* National Aeronautics and Space Administration, Lewis Research Center, Cleveland, Ohio.

OXIDATION-INDUCED CONTRACTION AND STRENGTHENING OF BORON FIBERS

James A. DiCarlo and Timothy C. Wagner 1981 35 p refs Presented at the 5th Ann. Conf. on Composites and Advanced Mater., Merritt Island, Fla., 18-22 Jan. 1981; sponsored by the American Ceramic Society
(NASA-TM-82599; E-846) Avail: NTIS HC A03/MF A01 CSCL 11D

An investigation was conducted to measure and understand the physical and mechanical effects that occur in boron fibers during and after thermal treatment in a controlled oxygen argon gaseous mixture. Of principal concern was the optimization of this treatment as a secondary processing method for significantly improving fiber tensile strength. Strengthening was accomplished by an oxidation induced axial contraction of the fiber and a resulting axial compression of strength limiting flaws within the fiber's tungsten boride core. Various physical observations were used to develop mechanistic models for oxidation, contraction, and flow formation. Processing guidelines are discussed for possibly exceeding the 5.5 GN/sq m strength limit and also for achieving fiber strengthening during application of boron containing diffusion barrier coatings. E.D.K.

N81-26151* National Aeronautics and Space Administration, Lewis Research Center, Cleveland, Ohio.

COMPUTER CODE FOR INTRAPLY HYBRID COMPOSITE DESIGN

C. C. Chamis and J. H. Sinclair 1981 15 p refs Presented at the 5th Conf. on Fibrous Composites in Struct. Design, New Orleans, 27-29 Jan. 1981; sponsored by DOD and NASA
(NASA-TM-82593; E-841) Avail: NTIS HC A02/MF A01 CSCL 11D

A computer program is described for intraply hybrid composite design (INHYPD). The program includes several composite micromechanics theories, intraply hybrid composite theories, and a hygrothermomechanical theory. These theories provide INHYPD with considerable flexibility and capability which the user can exercise through several available options. Key features and capabilities of INHYPD are illustrated through selected samples. E.D.K.

N81-26179* National Aeronautics and Space Administration, Lewis Research Center, Cleveland, Ohio.

METHOD FOR ALLEVIATING THERMAL STRESS DAMAGE IN LAMINATES Patent

Charles A. Hoffman, John W. Weston, and Norman W. Orth, inventors (to NASA) Issued 19 May 1981 5 p Filed 20 Feb. 1980 Division of US Patent Appl. SN-893857, filed 6 Apr. 1979, US Patent-4,211,354
(NASA-Case-LEW-12493-2; US-Patent-4,267,953;

US-Patent-Appl-SN-122967; US-Patent-4,211,354;

US-Patent-Appl-SN-893857; US-Patent-Class-228-118;

US-Patent-Class-228-190) Avail: US Patent and Trademark Office CSCL 11D

The method is for metallic matrix composites, such as laminated sheet or foil composites. Non-intersecting discrete discontinuities are positively introduced into the interface between the layers so as to reduce the thermal stress produced by unequal expansion of the materials making up the composite. The discontinuities are preferably produced by drilling holes in the metallic matrix layer. However, a plurality of discrete elements may be used between the layers to carry out this purpose.

Official Gazette of the U.S. Patent and Trademark Office

N81-27198* National Aeronautics and Space Administration, Lewis Research Center, Cleveland, Ohio.

ION SPUTTER TEXTURED GRAPHITE Patent Application

James S. Sovey, Ralph Forman, Arthur N. Curren, and Edwin G. Wintucky, inventors (to NASA) Filed 15 May 1981 14 p
(NASA-Case-LEW-12919-1; US-Patent-Appl-SN-264378) Avail: NTIS HC A02/MF A01 CSCL 11D

A specially textured surface of pyrolytic graphite which exhibits extremely low yields of secondary electrons and reduced numbers of reflected primary electrons after impingement of high energy primary electrons is described. An ion flux having an energy between 500 eV and 1000 eV and a current density between 1.0 mA/sq cm and 6.0 mA/sq cm produces surface roughening or texturing which is in the form of needles or spires. Such textured surfaces are especially useful as anode collector plates in high efficiency electron tube devices. NASA

N81-32194* National Aeronautics and Space Administration, Lewis Research Center, Cleveland, Ohio.

ENVIRONMENTAL EFFECTS ON GRAPHITE FIBER REINFORCED PMR-15 POLYIMIDE

Tito T. Serafini and Morgan P. Hanson 1980 23 p refs Presented at Symp. Composites for Extreme Environ., Bal Harbor, Fla., 11-12 Nov. 1980; Sponsored by Am Soc. for Testing and Materials
(NASA-TM-82625; E-883) Avail: NTIS HC A02/MF A01 CSCL 11D

Studies were conducted to establish the effects of thermo-oxidative and hydrothermal exposure on the mechanical properties of T300 graphite fabric reinforced PMR-15 composites. The effects of hydrothermal exposure on the mechanical properties of HTS-2 continuous graphite fiber composites were also investigated. The thermo-oxidative stability characteristics of T300 fabric and T300 fabric/PMR-15 composites were determined. Flexural strengths of specimens were determined. The useful lifetime of T300 fabric/PMR-15 composites in air at 316 C was found to be about 100 hours. The useful lifetimes in air at 228 and 260 C were determined to be 500 and 1000 hours, respectively. Absorbed moisture was found to reduce the elevated temperature properties of both the T300 fabricate and HTS-2 continuous fiber composites. The moisture effect was found to be reversible. Author

A81-29411 * Nonlinear laminate analysis for metal matrix

fiber composites. C. C. Chamis and J. H. Sinclair (NASA, Lewis Research Center, Structures and Mechanical Technologies Div., Cleveland, Ohio). In: Structures, Structural Dynamics and Materials Conference, 22nd, Atlanta, Ga., April 6-8, 1981, Technical Papers, Part 1. (A81-29377 12-39) New York, American Institute of Aeronautics and Astronautics, Inc., 1981, p. 313-324. 11 refs. (AIAA 81-0579)

A nonlinear laminate analysis is described for predicting the mechanical behavior (stress-strain relationships) of angle-ply laminates in which the matrix is strained nonlinearly by both the residual stress and the mechanical load and in which additional nonlinearities are induced due to progressive fiber fractures and ply relative rotations. The nonlinear laminate analysis is based on linear composite mechanics and a piecewise linear laminate analysis to handle the nonlinear responses. Results obtained by using this

nonlinear analysis on boron-fiber/aluminum-matrix angle-ply laminates agree well with experimental data. The results shown illustrate the in situ ply stress-strain behavior and synergistic strength enhancement. (Author)

A81-43602 * **Feasibility of Kevlar 49/PMR-15 polyimide for high temperature applications.** M. P. Hanson (NASA, Lewis Research Center, Cleveland, OH). In: *Materials 1980; Proceedings of the Twelfth National Technical Conference*, Seattle, WA, October 7-9, 1980. (A81-43601 20-23) Azusa, CA, Society for the Advancement of Material and Process Engineering, 1980, p. 1-14. 6 refs.

Kevlar 49 aramid organic fiber reinforced PMR-15 polyimide laminates were characterized to determine the applicability of the material to high temperature aerospace structures. Kevlar 49/3501-6 epoxy laminates were fabricated and characterized for comparison with the Kevlar 49/PMR-15 polyimide material. Flexural strengths and moduli and interlaminar shear strengths were determined from 75 to 600 F for the PMR-15 and from 75 to 450 F for the Kevlar 49/3501-6 epoxy material. The study also included the effects of hydrothermal and long-term elevated temperature exposures on the flexural strengths and moduli and the interlaminar shear strengths.

(Author)

A81-43603 * **Properties of PMR polyimide composites made with improved high strength graphite fibers.** R. D. Vannucci (NASA, Lewis Research Center, Cleveland, OH). In: *Materials 1980; Proceedings of the Twelfth National Technical Conference*, Seattle, WA, October 7-9, 1980. (A81-43601 20-23) Azusa, CA, Society for the Advancement of Material and Process Engineering, 1980, p. 15-30. 7 refs.

Recent graphite fiber developments have resulted in high strength, intermediate modulus graphite fibers having improved thermo-oxidative resistance. These improved fibers, obtained from various commercial suppliers, were used to fabricate PMR-15 and PMR-11 polyimide composites. Studies were performed to investigate the effects of the improved high strength graphite fibers on composite properties after exposure in air at 600 F. The use of the more oxidatively resistant fibers did not result in improved performance at 600 F. Two of the improved fibers were found to have an adverse effect on the long-term performance of PMR composites. The influence of various factors such as fiber physical properties, surface morphology and chemical composition are also discussed.

(Author)

A81-43635 * **Influence of excess diamine on properties of PMR polyimide resins and composites.** F. I. Hurwitz (NASA, Lewis Research Center, Cleveland, OH). In: *Materials 1980; Proceedings of the Twelfth National Technical Conference*, Seattle, WA, October 7-9, 1980. (A81-43601 20-23) Azusa, CA, Society for the Advancement of Material and Process Engineering, 1980, p. 517-530. 6 refs.

This preliminary study explores the influence of 1-10 percent molar excess MDA on the molecular weight distribution and rheological properties of an imidized PMR system. Molecular weight distribution is characterized by gel permeation chromatography of the imidized molding compound; shear viscosity is related to changes in average molecular weight. The thermo-oxidative stability at 600 F glass transition temperature, flexural and interlaminar shear properties of PMR polyimide/Celion 6000 graphite fiber composites are compared as a function of the percent excess MDA in the monomer reactant mixture.

(Author)

A81-44662 * **Computer code for intraply hybrid composite design.** C. C. Chamis and J. H. Sinclair (NASA, Lewis Research Center, Cleveland, OH). *U.S. Department of Defense and NASA, Conference on Fibrous Composites in Structural Design*, 5th, New Orleans, LA, Jan. 27-29, 1981, Paper. 13 p. 9 refs.

A computer program has been developed and is described herein

for intraply hybrid composite design (INHYD). The program includes several composite micromechanics theories, intraply hybrid composite theories and a hygrothermomechanical theory. These theories provide INHYD with considerable flexibility and capability which the user can exercise through several available options. Key features and capabilities of INHYD are illustrated through selected samples. (Author)

A81-44664 * **Oxidation-induced contraction and strengthening of boron fibers.** J. A. DiCarlo and T. C. Wagner (NASA, Lewis Research Center, Cleveland, OH). *American Ceramic Society, Annual Conference on Composites and Advanced Ceramic Materials*, 5th, Merritt Island, FL, Jan. 18-22, 1981, Paper. 33 p. 16 refs.

An investigation of the physical and mechanical effects of thermal treatment in a controlled oxygen-argon atmosphere on boron fibers is reported, with attention to the optimization of such treatment as a secondary processing method for improvement of fiber strength. The strengthening mechanism is comprised of an oxidation-induced axial contraction of the fiber, accompanied by axial compression of strength-limiting flaws within the fiber's tungsten boride core. It was found that after an oxidation contraction of 0.3% near 900 C, and a slight surface etch near 100 C, the average tensile strength of 203-micron fibers increased from 500 to 800 ksi. Various physical observations are used to develop mechanistic models of oxidation, contraction, and the formation of new flaws in the boron sheath at contractions greater than 0.3%. O.C.

A81-44665 * **Tungsten fiber reinforced superalloys - A status review.** D. W. Petrasek and R. A. Signorelli (NASA, Lewis Research Center, Cleveland, OH). *American Ceramic Society, Annual Conference on Composites and Advanced Ceramic Materials*, 5th, Merritt Island, FL, Jan. 18-22, 1981, Paper. 68 p. 58 refs.

After a review of refractory metal fiber/alloy matrix composite development, a discussion is presented of the fabrication techniques used in production of tungsten fiber reinforced superalloys (TFRS), their most significant properties, and their potential applications in the hot section components of gas turbine engines. Emphasis is given the development of airfoil-fabrication technology, with a view to the production of TFRS turbine blades, and attention is given the first-generation TFRS material, a tungsten alloy fiber/FeCrAlY composite currently under evaluation. Detailed properties, design criteria and cost data are presented for this material. Among the properties covered are stress-rupture strength, high and low cycle fatigue, thermal fatigue, impact strength, oxidation and corrosion and thermal conductivity. O.C.

N81-10112* # TRW, Inc., Cleveland, Ohio. Materials Technology Lab.

TUNGSTEN WIRE-REINFORCED SUPERALLOYS FOR 1093 C (2000 F) TURBINE BLADE APPLICATIONS Final Report

G. I. Friedman and J. N. Fleck Oct. 1979 72 p refs

(Contract NAS3-20084)

(NASA-CR-153720 TRW-ER-8135)

Avail. NTIS

HC A04/MF A01 CSCL 11D

Various combinations of fiber and matrix materials were fabricated and evaluated for the purpose of selecting a specific combination that exhibited the best overall properties for a turbine blade application. A total of seven matrix alloys, including Hestelloy X, Nimonic 80A, Inconel 600, Inconel 625, IN-102, FeCrAlY, were investigated reinforced with either 218CS tungsten, or W-Hf-C fibers. Based on preliminary screening studies, FeCrAlY, Inconel 600 and Inconel 625 matrix composites systems were selected for extended thermal cycle tests and for property evaluations which included stress rupture, impact, and oxidation resistance. Of those investigated, the FeCrAlY matrix composite system exhibited the best overall properties required for a turbine blade application. The W-Hf-C/FeCrAlY system was selected for further property evaluation. Tensile strength values of up to 724 MPa (105,000 psi) were obtained for this material at 982 C and 607 MPa at 1093 C. (Author)

NS1-12172* Purdue Univ., Lafayette, Ind. School of Aeronautics and Astronautics.

CONTACT LAW AND IMPACT RESPONSES OF LAMINATED COMPOSITES Interim Report

C. T. Sun and S. H. Yang Feb. 1980 112 p refs

(Grant' NSG-3185)

(NASA-CR-159884; CML-80-1)

Avail: NTIS

HC A06/MF A01 CSCL 11D

Static indentation tests were performed to determine the law of contact between a steel ball and glass/epoxy and graphite/epoxy laminated composites. For both composites the power law with an index of 1.5 was found to be adequate for the loading curve. Substantial permanent deformations were noted after the unloading. A high order beam finite element was used to compute the dynamic contact force and response of the laminated composite subjected to the impact of an elastic sphere. This program can be used with either the classical Hertzian contact law or the measured contact law. A simple method is introduced for estimating the contact force and contact duration in elastic impacts.

Author

NS1-18229* Fiber Materials, Inc., Biddeford, Maine.

FABRICATION OF ALUMINA OXIDE FIBER REINFORCED ALUMINUM MATRIX COMPOSITES Final Report

J. E. Hack and G. C. Strempek Nov. 1980 89 p refs

(Contract NAS3-21013)

(NASA-CR-185184) Avail: Issuing Activity CSCL 11D

The mechanical fabrication of polycrystalline alumina fiber reinforced aluminum composites was accomplished. Wire preform material was prepared by liquid metal infiltration of alumina fiber bundles. The wires were subsequently fabricated into bulk composite material by hot drawing. Extensive mechanical, thermal and chemical testing was conducted on preform bulk material to develop a process and materials data base. In addition, a preliminary investigation of mechanical forming of bulk alumina fiber reinforced aluminum composite material was conducted.

Author

NS1-18233* Fiber Materials, Inc., Biddeford, Maine.

FABRICATION DEVELOPMENT OF ALUMINA/ALUMINUM COMPOSITES Final Report

G. C. Strempek and D. E. Kizer Nov. 1980 41 p refs

(Contract NAS3-21844)

(NASA-CR-185195) Avail: Issuing Activity CSCL 11D

The mechanical fabrication of polycrystalline alumina fiber reinforced A201 aluminum alloy composite hat and angle shapes is described. Wire preform material was prepared by liquid metal infiltration of alumina fiber bundles. The wire was made into test samples by hot pressing, hot isostatic pressing, and pultrusion. Samples were examined for metallographic and mechanic quality and hot pressing was selected for fabricating hat and angle shapes. A series of processing iterations was performed and A1203/A201 hat and angle sections were produced for testing.

J.M.S.

NS1-21130* Du Pont de Nemours (E. I.) and Co., Wilmington, Del. Textile Fibers Dept.

ULTRA-HIGH MODULUS ORGANIC FIBER HYBRID COMPOSITES

A. R. Champion 15 Mar. 1981 103 p refs

(Contract NAS3-21837)

(NASA-CR-185228; RSC-3697-6)

Avail: NTIS

HC A06/MF A01 CSCL 11D

An experimental organic fiber, designated Fiber D, was characterized, and its performance as a reinforcement for composites was investigated. The fiber has a modulus of 172 GPa, tensile strength of 3.14 GPa, and density of 1.46 gm/cu cm. Unidirectional Fiber D/epoxy laminates containing 60 percent fiber by volume were evaluated in flexure, shear, and compression, at room temperature and 121 C in both the as fabricated condition and after humidity aging for 14 days at 95 percent RH and 82 C. A modulus of 94.1 GPa, flexure strength of 700 MPa,

shear strength of 54 MPa, and compressive strength of 232 MPa were observed at room temperature. The as-fabricated composites at elevated temperature and humidity aged material at room temperature had properties 1 to 20 percent below these values. Combined humidity aging plus elevated temperature testing resulted in even lower mechanical properties. Hybrid composite laminate of Fiber D with Fiber FP alumina or Thornel 300 graphite fiber were also evaluated and significant increases in modulus, flexure, and compressive strengths were observed.

E.D.K.

AB1-11336 *

CVD-produced boron filaments. F. E. Wawner

(Virginia, University, Charlottesville, Va.), H. E. DeBolt, and R. D. Suplinskas (Avco Corp., Avco Specialty Materials Div., Lowell, Mass.). (*American Ceramic Society, Annual Conferences on Composites and Advanced Materials, 2nd and 3rd, Cocoa Beach, Fla., Jan. 22-25, 1978 and Jan. 21-24, 1979.*) *Ceramic Engineering and Science Proceedings*, vol. 1, July-Aug. 1980, p. 348-355. 11 refs. Contract No. NAS3-20577.

A technique for producing boron filaments with an average tensile strength of 6.89 GPa has been developed which involves longitudinal splitting of the filament and core (substrate) removal by etching. Splitting is accomplished by a pinch wheel device which continuously splits filaments in lengths of 3.0 m by applying a force to the side of the filament to create a crack which is then propagated along the axis by a gentle sliding action. To facilitate the splitting, a single 10 mil tungsten substrate is used instead of the usual 0.5 mil substrate. A solution of hot 30% hydrogen peroxide is used to remove the core without attacking the boron. An alternative technique is to alter the residual stress by heavily etching the filament. Average strengths in the 4.83-5.52 GPa range have been obtained by etching an 8 mil filament to 4 mil.

V.L.

25 INORGANIC AND PHYSICAL CHEMISTRY

Includes chemical analysis, e.g., chromatography; combustion theory; electrochemistry; and photochemistry.

For related information see also 77 *Thermodynamics and Statistical Physics*.

N81-13106* National Aeronautics and Space Administration, Lewis Research Center, Cleveland, Ohio. **IMPROVEMENT AND SCALE-UP OF THE NASA REDOX STORAGE SYSTEM**

Margaret A. Reid and Lawrence H. Thaller 1980 9 p refs Presented at 15th Intersoc. Energy Conversion Engineering Conf., Seattle, 18-21 Aug. 1980 (Contract DE-A104-80AL-12726) (NASA-TM-81632; DOE/NASA/12726-6; E-644) Avail: NTIS HC A02/MF A01 CSCL 10C

A preprototype 1.0 kW redox system (2 kW peak) with 11 kWh storage capacity was built and integrated with the NASA/DOE photovoltaic test facility at NASA Lewis. This full function redox system includes four substacks of 39 cells each (1/3 cu ft active area) which are connected hydraulically in parallel and electrically in series. An open circuit voltage cell and a set of rebalance cells are used to continuously monitor the system state of charge and automatically maintain the anode and cathode reactants electrochemically in balance. Recent membrane and electrode advances are summarized and the results of multicell stack tests of 1 cu ft are described. R.C.T.

N81-13106* National Aeronautics and Space Administration, Lewis Research Center, Cleveland, Ohio. **ACCURACY OF TRACE ELEMENT DETERMINATIONS IN ALTERNATE FUELS**

Leslie A. Greenbauer-Seng 28 May 1980 22 p refs Presented at May Conf. of the Soc. of Appl. Spectry. of Cleveland and the Am. Chem. Soc. Anal. Topics Group of Cleveland, Ohio, 28 May 1980 (NASA-TM-81609; E-605) Avail: NTIS HC A02/MF A01 CSCL 07D

A review of the techniques used at Lewis Research Center (LeRC) in trace metals analysis is presented, including the results of Atomic Absorption Spectrometry and DC Arc Emission Spectrometry of blank levels and recovery experiments for several metals. The design of an Interlaboratory Study conducted by LeRC is presented. Several factors were investigated, including: laboratory, analytical technique, fuel type, concentration, and ashing additive. Conclusions drawn from the statistical analysis will help direct research efforts toward those areas most responsible for the poor interlaboratory analytical results. Author

N81-17188* National Aeronautics and Space Administration, Lewis Research Center, Cleveland, Ohio. **ACCEPTANCE TESTS AND MANUFACTURER RELATIONSHIPS FOR 20 AMPERE-HOUR SEALED NICKEL-CADMIUM CELLS USING DISCHARGE PARAMETERS**

Harold F. Laibecki Nov. 1980 31 p refs (NASA-TM-81619; E-625) Avail: NTIS HC A03/MF A01 CSCL 10C

One hundred and forty-six 20 ampere-hour sealed nickel cadmium cells from five manufacturers were detected using preliminary tests which do not require life testing and do not reduce the expected life of the cells. Differences between individual cells were also detected, using these tests, allowing a comparison of variability of cell construction by and between manufacturers. Author

N81-19245* National Aeronautics and Space Administration, Lewis Research Center, Cleveland, Ohio. **HEAT PIPES TO REDUCE ENGINE EXHAUST EMISSIONS** Patent Application

Donald F. Schultz, inventor (to NASA) Filed 30 Jan. 1980 17 p (NASA-Case-LEW-12590-1; US-Patent-Appl-SN-229693) Avail: NTIS HC A02/MF A01 CSCL 21B

A fuel combustor employing heat transfer devices for improving combustion efficiency and reducing engine exhaust emissions is described. The fuel combustor consists of an elongated casing with an air inlet conduit portion at one end. An elongated heat pipe is mounted longitudinally in the casing and is offset from and extends alongside an intermediate combustion space. The heat pipe is in heating transmitting relationship with the air intake conduit for heating incoming air. A fuel conduit has a portion engaged in heat transfer relationship of the heat pipe for preheating the fuel. The offset position of the heat pipe relative to the combustion space minimizes the quenching effect of the heat pipe on the gaseous products of combustion, as well as reducing coking of the fuel on the heat pipe, thereby improving the efficiency of the combustor. NASA

N81-25168* National Aeronautics and Space Administration, Lewis Research Center, Cleveland, Ohio. **SYNTHETIC BATTERY CYCLING**

Lawrence H. Thaller 1981 13 p refs Proposed for presentation at the 16th Intersoc. Energy Conversion Eng. Conf., Atlanta, 9-14 Aug. 1981; sponsored by the American Society of Mechanical Engineering (NASA-TM-81757; E-820) Avail: NTIS HC A02/MF A01 CSCL 10C

The use of interactive computer graphics is suggested as an aid in battery system development. Mathematical representations of simplistic but fully representative functions of many electrochemical concepts of current practical interest will permit battery level charge and discharge phenomena to be analyzed in a qualitative manner prior to the assembly and testing of actual hardware. This technique is a useful addition to the variety of tools available to the battery system designer as he bridges the gap between interesting single cell life test data and reliable energy storage subsystems. E.D.K.

N81-26203* National Aeronautics and Space Administration, Lewis Research Center, Cleveland, Ohio. **ZIRCONIUM CARBIDE AS AN ELECTROCATALYST FOR THE CHROMOUS/CHROMIC REDOX COUPLE** Patent Application

Randall F. Gahn, Margaret A. Reid, and Chiang Yuan Yang, inventors (to NASA) Filed 22 May 1981 17 p (NASA-Case-LEW-13246-1; US-Patent-Appl-SN-266255) Avail: NTIS HC A02/MF A01 CSCL 07D

Zirconium carbide is used as a catalyst in a REDOX cell for the oxidation of chromous ions to chromic ions and for the reduction of chromic ions to chromous ions. The zirconium carbide is coated on an inert electronically conductive electrode which is present in the anode fluid of the cell. NASA

N81-31308* National Aeronautics and Space Administration, Lewis Research Center, Cleveland, Ohio. **DESIGN AND ASSEMBLY CONSIDERATIONS FOR REDOX CELLS AND STACKS**

Dale K. Stalnaker and Arthur Lieberman Sep 1981 13 p refs (Contract DE-A104-80AL-12726) (NASA-TM-82672; DOE/NASA/12726-10; E-954) Avail: NTIS HC A02/MF A01 CSCL 10B

Individual redox flow cells are arranged electrically in series and hydraulically in parallel to form a single assembly called a stack. The hardware currently being tested in the laboratory has an active electrode area of either 310 sq cm or 929 sq cm. Four 310 sq cm stacks, each consisting of 39 active cells, were

incorporated into a 1.0 kW preprototype system. The physical design of the stack is very critical to the performance and efficiency of the redox storage system. This report will discuss the mechanical aspects of the cell and stack design for the current Redox hardware, with regard to sealing the stack internally as well as externally, minimizing shunt currents and minimizing the electrical resistance of the stack.

E.D.K.

NS1-16176* Tennessee Technological Univ., Cookeville. Dept. of Engineering Science and Mechanics and Mechanical Engineering.

Perturbation Solutions of Combustion Instability Problems

A. Googerdy, J. Perdiesson, Jr., and M. Ventrice Oct. 1979
66 p refs

(Grant NGR-43-003-015)

(NASA-CR-159643) Avail: NTIS HC A04/MF A01 CSCI
21B

A method involving approximate modal analysis using the Galerkin method followed by an approximate solution of the resulting modal-amplitude equations by the two-variable perturbation method (method of multiple scales) is applied to two problems of pressure-sensitive nonlinear combustion instability in liquid-fuel rocket motors. One problem exhibits self-coupled instability while the other exhibits mode-coupled instability. In both cases it is possible to carry out the entire linear stability analysis and significant portions of the nonlinear stability analysis in closed form. In the problem of self-coupled instability the nonlinear stability boundary and approximate forms of the limit-cycle amplitudes and growth and decay rates are determined in closed form while the exact limit-cycle amplitudes and growth and decay rates are found numerically. In the problem of mode-coupled instability the limit-cycle amplitudes are found in closed form while the growth and decay rates are found numerically. The behavior of the solutions found by the perturbation method are in agreement with solutions obtained using complex numerical methods.

Author

NS1-16177* Aerojet Liquid Rocket Co., Sacramento, Calif.
HIGH-DENSITY FUEL COMBUSTION AND COOLING INVESTIGATION Final Report, Oct. 1977 - Aug. 1980

Rich J. LaBotz, Don C. Rousar, and Harry W. Valler Sep. 1980
114 p refs

(Contract NAS3-21030)

(NASA-CR-165177) Avail: NTIS HC A06/MF A01 CSCI
21B

The analysis, design, fabrication and testing of several engine configurations are discussed with respect to the combustion and heat transfer characteristics of LOX/RP-1 at chamber pressures between 6895 and 13790 kPa (1000 and 2000 psia). The different engine configurations discussed include: 8274 kPa and 13790 kPa (1200 psia and 2000 psia) chamber pressure injectors with like doublet and preatomized triplet elements; cooled and uncooled acoustic resonators; and graphite, regeneratively cooled and calorimetric chambers ranging in length from 27.9 to 37.5 cm (11 to 15 in.). A high pressure LOX/RP-1 spark igniter is also evaluated.

R.C.T.

26 METALLIC MATERIALS

Includes physical, chemical, and mechanical properties of metals, e.g. corrosion, and metallurgy.

N81-11111* National Aeronautics and Space Administration, Lewis Research Center, Cleveland, Ohio.

COMPLETION OF EVALUATION OF MANUFACTURING PROCESSES FOR B/Al COMPOSITES CONTAINING 0.2mm DIAMETER BORON FIBERS

Thomas J. Moore and Paul E. Moorhead Sep. 1980 39 p refs

(NASA-TM-81573; E-543) Avail. NTIS HC A03/MF A01 CSCL 11D

Four fabricators produced a total of 54 B/1:00 Al, B/6061 Al, and B/2024 Al panels for evaluation. The 3 ply unidirectional, 45 to 50 volume percent, panels were made using 0.20 mm diameter boron fibers which were obtained from a single supplier. Hot press consolidation was carried out in vacuum except for one set of dry woven tape panels which were hot pressed in air. A single testing contractor conducted nondestructive inspection, metallography, fractography and mechanical property tests. The mechanical property tests included 21 and 260 C tensile tests and 21 C shear tests. Panel quality, as measured by nondestructive evaluation, was generally good as were the 21 C tensile properties. The panels hot pressed in air delaminated in the shear tests. Shear strength values were lower in these panels. But tensile strengths were not affected by the delaminations because of the relation between the tensile loading direction and the delaminations. Composite tensile strength was found to be proportional to the volume percent boron and the aluminum matrix rather than to the tape used or fabrication technique. Suitability of these composites for 260 C service was confirmed by tensile tests. R.K.G.

N81-11178* National Aeronautics and Space Administration, Lewis Research Center, Cleveland, Ohio.

EFFECT OF MECHANICAL SURFACE AND HEAT TREATMENTS ON EROSION RESISTANCE

Joshua Salik and Donald H. Buckley 1980 10 p refs Proposed for presentation at the Intern. Conf. on Wear of Materials, San Francisco, 30 Mar. - 1 Apr. 1980

(NASA-TM-81540; E-326) Avail. NTIS HC A02/MF A01 CSCL 11F

The effects of mechanical surface treatments as well as heat treatments on the erosion resistance of 6061 aluminum alloy and 1045 steel were studied. Mechanical surface treatments were found to have little or no effect on the erosion resistance. This is due to the formation by particle impact of a work hardened surface layer regardless of the initial surface condition. The erosion resistance of Al single crystals is found to be independent of orientation. This is due to destruction of the surface microstructure and formation of a polycrystalline surface layer by the impact of erodent particles as observed by X-ray diffraction. While upon solution treatment of annealed 6061 aluminum the increase in hardness is accompanied by an increase in erosion resistance, precipitation treatment which causes a further increase in hardness results in slightly lower erosion resistance. Using two types of erodent particles, glass beads and crushed glass, the erosion rate is found to be strongly dependent on erodent particle shape, being an order of magnitude higher for erosion with crushed glass as compared to glass beads. While for erosion with glass beads heat treatment of 1045 steel had a profound effect on its erosion resistance, little or no such effect was observed for erosion with crushed glass. R.K.G.

N81-12210* National Aeronautics and Space Administration, Lewis Research Center, Cleveland, Ohio.

THE ROLE OF OXIDATION IN THE FRETTING WEAR PROCESS

Robert C. Bill 1980 25 p refs Proposed for presentation at the Intern. Conf. on Wear of Mater. San Francisco, 30 Mar. - 1 Apr. 1981, sponsored by AMSE and Japan Soc. of Mech. Engr. Prepared in cooperation with Army Aviation Research and

N81-12211* National Aeronautics and Space Administration, Lewis Research Center, Cleveland, Ohio.

NiCrAl TERNARY ALLOY HAVING IMPROVED CYCLIC OXIDATION RESISTANCE Patent Application

C. A. Barrett, inventor (to NASA) Filed 23 Oct. 1980 6 p (NASA Case-LEW-13339-1; US-Patent-Appl-SN-199769) Avail. NTIS HC A02/MF A01 CSCL 11F

NiCrAl alloys were improved by the addition of zirconium. These alloys are in the beta or gamma/gamma prime + beta region of the ternary system. Zirconium was added in a very low amount between 0.06 and 0.20 weight percent. There was a narrow optimum zirconium level at the low value of 0.13 weight percent. Maximum resistance to cyclic oxidation was achieved when the zirconium addition was at the optimum value. NASA Development Command, Cleveland

(NASA-TM-81570; AVRADCOM-TR-80-C-15; E-538) Avail. NTIS HC A02/MF A01 CSCL 11F

Fretting experiments were conducted on titanium, a series of Ni-Cr-Al alloys and on some high temperature turbine alloys at room temperature and at elevated temperatures in air and in various inert environments. It was found that, depending on temperature and environment, the fretting behavior of the materials examined could be classified according to four general types of behavior. Briefly, these types of behavior were: (1) the complete absence of oxidation, as in inert environments, generally leading to low rates of fretting wear but high fretting friction; (2) gradual attrition of surface oxide with each fretting stroke, found in these experiments to operate in concert with other dominating mechanisms; (3) rapid oxidation at surface fatigue damage sites, resulting in undermining and rapid disintegration of the load bearing surface; and (4) the formation of coherent, protective oxide film, resulting in low rates of fretting wear. An analytical model predicting conditions favorable to the fourth type of behavior was outlined. Author

N81-15088* National Aeronautics and Space Administration, Lewis Research Center, Cleveland, Ohio.

EVALUATION OF CANDIDATE STIRLING ENGINE HEATER TUBE ALLOYS FOR 1000 HOURS AT 760 C Final Report

John A. Misencik Nov. 1980 35 p refs

(Contract EC-77-A-31-1040)

(NASA-TM-81578; E-548; DOE/NASA/1040-18) Avail. NTIS HC A03/MF A01 CSCL 11F

Six tubing alloys were endurance tested in a diesel fired, Stirling engine simulator materials test rig for 1000 hours of 760 C while pressurized at 17 to 21 MPa with either hydrogen or helium. The alloys tested were N 155, A 286, Incoloy 800, 19 9DL, Nitronic 40 and 316 stainless steel. The alloys were in the form of thin wall tubing. Hydrogen permeated rapidly through the tube walls of all six alloys when they were heated to 760 C. Helium was readily contained. Creep rupture failures occurred in four of the six alloys pressurized with hydrogen. Only two alloys survived the 1000 hour endurance test with no failures. Simultaneous exposure to either hydrogen or helium and the combustion environment did not seriously degrade the tensile strength of the six alloys in room temperature or 760 C tests after exposure. Decreases in room temperature ductility were observed and are attributed to aging rather than to hydrogen embrittlement in three of the alloys. However, there may be a hydrogen embrittlement effect in the N 155, 19 9DL and Nitronic 40 alloys. Author

N81-15089* National Aeronautics and Space Administration, Lewis Research Center, Cleveland, Ohio.

DEPOSITION AND MATERIAL RESPONSE FROM MACH 0.3 BURNER RIG COMBUSTION OF SRC 2 FUELS Final Report

G. J. Santoro, F. J. Kohi, C. A. Stearns, G. C. Fryburg, and J. R. Johnson Oct. 1980 47 p refs

(Contract EF-77-A-01-2593)

(NASA-TM-81634; E-647; DOE/NASA/2593-20) Avail. NTIS HC A03/MF A01 CSCL 11F

Collectors at 1173K (900 C) were exposed to the combustion products of a Mach 0.3 burner rig fueled with various industrial turbine liquid fuels from solvent refined coals. Four fuels were employed: a naphtha, a light oil, a wash solvent and a mid-heavy

distillate blend. The response of four superalloys (IN-100, U 700, IN 792 and M-509) to exposure to the combustion gases from the SRC-2 naphtha and resultant deposits was also determined. The SRC-2 fuel analysis and insights obtained during the combustion experience are discussed. Particular problems encountered were fuel instability and reactions of the fuel with hardware components. The major metallic elements which contributed to the deposits were copper, iron, chromium, calcium, aluminum, nickel, silicon, titanium, zinc, and sodium. The deposits were found to be mainly metal oxides. An equilibrium thermodynamic analysis was employed to predict the chemical composition of the deposits. The agreement between the predicted and observed compounds was excellent. No hot corrosion was observed. This was expected because the deposits contained very little sodium or potassium and consisted mainly of the unreactive oxides. However, the amounts of deposits formed indicated that fouling is a potential problem with the use of these fuels. Author

N81-16209* National Aeronautics and Space Administration, Lewis Research Center, Cleveland, Ohio.

IMPROVED REFRACTORY COATINGS Patent Application William A. Brainard, inventor (to NASA) Filed 29 Sep. 1980 8 p (NASA-Case-LEW-23169-2, US-Patent-Appl-SN-191746) Avail: NTIS HC A02/MF A01 CSCL 11F

The adhesion, friction and wear properties of sputtered refractory coatings on substrates of materials that form stable nitrides are enhanced by placing each substrate directly below a titanium carbide target of a commercial radiofrequency diode apparatus in a vacuum chamber. Nitrogen is bled into the system through a nozzle resulting in a small partial pressure of about 0.5% to 2.5% during the first two minutes of deposition. The flow of nitrogen is then stopped, and the sputtering is reduced to pure argon through a nozzle without interrupting the sputtering process. When nitrogen is deliberately introduced during the crucial interface formation, some of the titanium at the interface reacts to form titanium nitride while the metal of the substrate also forms the nitride. These two nitrides atomically mixed together in the interfacial region act to more strongly bond the growing titanium carbide coating as it forms on the substrate. NASA

N81-16210* National Aeronautics and Space Administration, Lewis Research Center, Cleveland, Ohio.

EFFECTS OF ERODANT PARTICLE SHAPE AND VARIOUS HEAT TREATMENTS ON EROSION RESISTANCE OF PLAIN CARBON STEEL

Joshua Salik and Donald H. Buckley Jan. 1981 10 p refs (NASA-TP-1755; E-326) Avail: NTIS HC A02/MF A01 CSCL 11F

Erosion tests were conducted on 1045 steel samples which had been subjected to different heat treatments. The weight of material removed upon erosion with glass beads and crushed glass was measured. The data show that there is no correlation between hardness and erosion resistance. The erosion rate was strongly dependent on the shape of erodant particles, being an order of magnitude higher for erosion with crushed glass than with glass beads. Heat treatment had a profound effect on the erosion resistance when the erodant particles were glass beads but little or no effect when the particles were crushed glass. It is thus concluded that different mechanisms of material removal are involved with these two erodants. This conclusion is supported by the surface morphology of annealed 1045 steel samples which had been eroded by these two types of erodant particles. SEM micrographs of the eroded surfaces show that for erosion with glass beads it is deformation induced fracture of surface layers. Author

N81-16211* National Aeronautics and Space Administration, Lewis Research Center, Cleveland, Ohio.

THE EFFECTS OF TRACE IMPURITIES IN COAL-DERIVED LIQUID FUELS ON DEPOSITION AND ACCELERATED HIGH TEMPERATURE CORROSION OF CAST SUPERALLOYS

Carl E. Lowell, Daniel J. Deadmore, Gilbert J. Santoro, and Fred

J. Kohl 1981 19 p refs Presented at the 26th Ann. Intern. Gas Turbine Conf., Houston, Tex., 8-12 Mar. 1981; Sponsored by ASME

(Contract EF-77-A-01-2593)

(NASA-TM-81678; DOE/NASA/2593-22) Avail: NTIS HC A02/MF A01 CSCL 11F

The effects of trace metal impurities in coal-derived liquids on deposition, high temperature corrosion and fouling were examined. Alloys were burner rig tested from 800 to 1100 C and corrosion was evaluated as a function of potential impurities. Actual and doped fuel test were used to define an empirical life prediction equation. An evaluation of inhibitors to reduce or eliminate accelerated corrosion was made. Barium and strontium were found to limit attack. Intermittent application of the inhibitors or silicon additions were found to be effective techniques for controlling deposition without losing the inhibitor benefits. A computer program was used to predict the dew points and compositions of deposits. These predictions were confirmed in deposition test. The potential for such deposits to plug cooling holes of turbine airfoils was evaluated. Tests indicated that, while a potential problem exists, it strongly depended on minor impurity variations. M.G.

N81-16212* National Aeronautics and Space Administration, Lewis Research Center, Cleveland, Ohio.

MICROSTRUCTURE OF Al₂O₃ SCALES FORMED ON NiCrAl ALLOYS Ph.D. Thesis - Case Western Reserve Univ.

James Leo Smialek Jan. 1981 287 p refs

(NASA-TM-81676; E-664) Avail: NTIS HC A13/MF A01 CSCL 11F

The structure of transient scales formed on pure and Y or Zr-doped Ni-15Cr-13Al alloys oxidized for 0.1 hr at 1100 C was studied by the use of transmission electron microscopy. Crystallographically oriented scales were found on all three alloys, but especially for the Zr-doped NiCrAl. The oriented scales consisted of alpha-(Al,Cr)2O3, Ni(Al,Cr)2O4 and gamma-Al2O3. They were often found in intimate contact with each other such that the close-packed planes and directions of one oxide phase were aligned with those of another. The prominent structural features of the oriented scales were approximately equal to micrometer subgrains; voids, antiphase domain boundaries and aligned precipitates were also prevalent. Randomly oriented alpha-Al2O3 was also found and was the only oxide ever observed at the immediate oxide metal interface. These approximately 0.15 micrometer grains were populated by intragranular voids which decreased in size and number towards the oxide metal interface. A sequence of oxidation was proposed in which the composition of the growing scale changed from oriented oxides rich in Ni and Cr to oriented oxides rich in Al. At the same time the structure changed from cubic spinels to hexagonal corundums with apparent precipitates of one phase in the matrix of the other. Eventually randomly oriented pure alpha-Al2O3 formed as the stable oxide with an abrupt transition: there was no gradual loss of orientation, no gradual compositional change or no gradual decrease in precipitate density. R.C.T.

N81-16165* National Aeronautics and Space Administration, Lewis Research Center, Cleveland, Ohio.

THE EFFECT OF THERMAL CYCLING TO 1100 DEGREE C ON THE ALPHA (MO) PHASE IN DIRECTIONALLY SOLIDIFIED GAMMA/GAMMA PRIME-ALPHA ALLOYS

Fredric H. Harf 1981 15 p refs Presented at the 110th Ann. Meeting of the Am. Inst. of Mining, Met. and Petrol. Eng., Chicago, 22-26 Feb. 1981

(NASA-TM-81F88; E-725) Avail: NTIS HC A02/MF A01 CSCL 11F

In gamma/gamma prime - alpha eutectic alloys (Ni-Mo-Al), the resistance of the alpha phase to morphological changes during thermal cycling was found to be dependent on the structure formed during directional solidification. Fine, smooth alpha fibers survived up to 1000 five minute cycles to 1100 C with minor microstructural contour changes, while coarser and irregularly shaped alpha fibers tended to spheroidize. A mechanism to explain

this phenomenon is proposed. It is suggested that on heating to 1100 C, the alpha phase is likely to undergo morphological changes, until differential thermal expansion creates a stress free interface between the alpha phase and the gamma/gamma prime matrix.

Author

N81-19273* National Aeronautics and Space Administration
Lewis Research Center, Cleveland, Ohio.

CREEP AND RESIDUAL MECHANICAL PROPERTIES OF CAST SUPERALLOYS AND OXIDE DISPERSION STRENGTHENED ALLOYS

J. Daniel Whittenberger Feb. 1981 69 p refs
(NASA-TP-1781; E-472) Avail: NTIS HC A04/MF A01 CSCL 11F

Tensile, stress-rupture, creep, and residual tensile properties after creep testing were determined for two typical cast superalloys and four advanced oxide dispersion strengthened (ODS) alloys. The superalloys examined included the nickel-base alloy B-1900 and the cobalt-base alloy MAR-M509. The nickel-base ODS MA-757 (Ni-16Cr-4Al-0.6Y2O3) and the iron-base ODS alloy MA-956 (Fe-20Cr-5Al-0.8Y2O3) were extensively studied, while limited testing was conducted on the ODS nickel-base alloys STCA (Ni-16Cr-4.5Al-2Y2O3) with and without Ta and YD-NiCrAl (Ni-16Cr-5Al-2Y2O3). Elevated temperature testing was conducted from 114 to 1477 K except for STCA and YD-NiCrAl alloys, which were only tested at 1366 K. The residual tensile properties of B-1900 and MAR-M509 are not reduced by prior creep testing (strains at least up to 1 percent), while the room temperature tensile properties of ODS nickel-base alloys can be reduced by small amounts of prior creep strain (less than 0.5 percent). The iron-base ODS alloy MA-956 does not appear to be susceptible to creep degradation at least up to strains of about 0.25 percent. However, MA-956 exhibits unusual creep behavior which apparently involves crack nucleation and growth.

Author

N81-19278* National Aeronautics and Space Administration
Lewis Research Center, Cleveland, Ohio.

SIMULTANEOUS ION SPUTTER POLISHING AND DEPOSITION

Sharon Rutledge, Bruce Banks, and Marko Brdar (Akron Univ.)
Jan. 1981 20 p refs
(NASA-TM-81679; E-705) Avail: NTIS HC A02/MF A01 CSCL 11F

Results of experiments to study ion beam sputter polishing in conjunction with simultaneous deposition as a means of polishing copper surfaces are presented. Two types of simultaneous ion sputter polishing and deposition were used in these experiments. The first type utilized sputter polishing simultaneous with vapor deposition, and the second type utilized sputter polishing simultaneous with sputter deposition. The etch and deposition rates of both techniques were studied, as well as the surface morphology and surface roughness.

Author

N81-20245* National Aeronautics and Space Administration
Lewis Research Center, Cleveland, Ohio.

EFFECTS OF GEOMETRIC VARIABLES ON RUB CHARACTERISTICS OF Ti-6Al-4V

Robert C. Bill, Jan Wolek (Washington Univ., Seattle), and Donald W. Wisander Apr. 1981 21 p refs Prepared in cooperation with Army Aviation Research and Development Command, Cleveland, Ohio
(NASA-TP-1835; AVRADCOM-TR-80-C-19; E-449) Avail: NTIS HC A02/MF A01 CSCL 11F

Experiments simulating rub interactions between Ti-6Al-4V blade tips and various seal materials were conducted. The number of blade tips and the blade tip geometry were varied to determine their effects on rub forces and on wear phenomena. Contact was found to be quite unsteady for all blade tip geometries except for those incorporating deliberately rounded blade tips. The unsteady contact was characterized by long periods of rubbing contact and increasing blade tip that terminated in sudden rapid metal removal, sometimes accompanied by tearing and disruption

of porous seal material under the rub surface. A model describing the blade tip loading is proposed and is based on the propagation of an elastic stress wave through the seal material as the seal material is dynamically compressed by the blade tip leading edge.

E.D.K.

N81-21173* National Aeronautics and Space Administration
Lewis Research Center, Cleveland, Ohio.

SPUTTERED PROTECTIVE COATINGS FOR DIE CASTING DIES

Michael J. Mirtich, Cuo-Yo Nieh (Case Western Reserve Univ.), and John F. Wallace (Case Western Reserve Univ.) 1981 14 p refs Presented at the 1981 Intern. Conf. on Met. Coatings, San Francisco, 6 - 10 Apr. 1981
(NASA-TM-81735; E-803) Avail: NTIS HC A02/MF A01 CSCL 11F

This investigation determined whether selected ion beam sputtered coatings on H-13 die steel would have the potential of improving the thermal fatigue behavior of the steel used as a die in aluminum die casting. The coatings were selected to test candidate insulators and metals capable of providing protection of the die surface. The studies indicate that 1 micrometer thick W and Pt coatings reduced the thermal fatigue more than any other coating tested and are candidates to be used on a die surface to increase die life.

E.D.K.

N81-21193* National Aeronautics and Space Administration
Lewis Research Center, Cleveland, Ohio.

STEADY-STATE BOUNDARY LUBRICATION WITH FORMULATED C-ETHERS TO 260 C

William R. Loomis Apr. 1981 16 p refs
(NASA-TP-1812; E-480) Avail: NTIS HC A02/MF A01 CSCL 07C

Steady state wear and friction studies were made at boundary lubrication conditions in a pin on disk (pure iron on rotating CVM M 50 steel) sliding friction apparatus with five C ether formulated fluids (modified polyphenyl ether containing phosphorus ester, organic acid, and other additives). Conditions included 20, 150, and 260 C disk temperatures, dry air test atmosphere, 1 kilogram load, 50 rpm disk speed, and test times to 130 minutes. Results were compared with those obtained with a formulated MIL L 27502 candidate ester and the C ether base fluid. Three of the C ether formulations gave better lubrication than both reference fluids under most conditions. The other two C ether formulations yielded higher wear rates and friction coefficients than the C ether base fluid for most of the temperature range. Only one C ether formulation showed consistently higher steady state wear rates than the ester.

M.G.

N81-22161* National Aeronautics and Space Administration
Lewis Research Center, Cleveland, Ohio.

EFFECTS OF PLASMA SPRAY PARAMETERS ON TWO LAYER THERMAL BARRIER

Stephen Stacura Mar. 1981 22 p refs
(NASA-TM-81724; E-764) Avail: NTIS HC A02/MF A01 CSCL 11F

The power level and the type of arc gas used during plasma spraying of a two layer thermal barrier system (TBS) were found to affect the life of the system. Life at 1095 C in a cyclic furnace test was improved by about 140 percent by increasing the power during plasma spray applications of the bond and thermal barrier coatings. This improvement is due to increases in the densities of the bond and thermal barrier coatings by 3 and 5 percent, respectively. These increases in densities are equivalent to about 45 and 30 percent reduction in mean porosities, respectively. The addition of hydrogen to the argon arc gas had the same effect as the reduction in power level and caused a reduction in TBS life.

Author

NS1-24230* National Aeronautics and Space Administration, Lewis Research Center, Cleveland, Ohio.

METHOD FOR DEPOSITING AN OXIDE COATING Patent Application

G. E. McDonald, inventor (to NASA) Filed 23 Mar. 1981 8 p (NASA-Case-LEW-13131-1; US-Patent-Appl-SN-246772) Avail: NTIS HC A02/MF A01 CSCL 11F

A metal oxide coating is plated onto a metal substrate at the cathode from an acid solution which contains an oxidizing agent. The process is particularly useful for producing solar panels. Conventional plating at the cathode avoids the presence of oxidizing agents. Coatings made in accordance with the invention are stable both at high temperatures and while under the influence of high photon flux in the visible range. NASA

NS1-25188* National Aeronautics and Space Administration, Lewis Research Center, Cleveland, Ohio.

CORROSION RESISTANT THERMAL BARRIER COATING Patent

Stanley R. Levine, Robert A. Miller, and Philip E. Hodge, inventors (to NASA) Issued 10 Mar. 1981 3 p Filed 31 Oct. 1979 Supersedes N80-11142 (18 - 02, p 0160)

(NASA-Case-LEW-13088-1; US-Patent-4,255,495;

US-Patent-Appl-SN-089779; US-Patent-Class-428-632;

US-Patent-Class-428-471; US-Patent-Class-428-678;

US-Patent-Class-428-679; US-Patent-Class-428-680) Avail: US Patent and Trademark Office CSCL 11F

A thermal barrier coating system for protecting metal surfaces at high temperature in normally corrosive environments is described. The thermal barrier coating system includes a metal alloy bond coating, the alloy containing nickel, cobalt, iron, or a combination of these metals. The system further includes a corrosion resistant thermal barrier oxide coating containing at least one alkaline earth silicate. The preferred oxides are calcium silicate, barium silicate, magnesium silicate, or combinations of these silicates.

Official Gazette of the U.S. Patent and Trademark Office

NS1-26189* National Aeronautics and Space Administration, Lewis Research Center, Cleveland, Ohio.

ION PLATING FOR THE FUTURE

Talivaldis Spalvins 1981 9 p refs Presented at the 24th Ann. Tech. Conf. of the Soc. of Vacuum Coaters, Dearborn, Mich., 12-14 May 1981

(NASA-TM-82630; E-884) Avail: NTIS HC A02/MF A01 CSCL 11F

The ion plating techniques are classified relative to the instrumental set up, evaporation media, and mode of transport. A distinction is drawn between the low vacuum (plasma) and high vacuum (ion beam) techniques. Ion plating technology is discussed at the fundamental and industrial level. At the fundamental level, the capabilities and limitations of the plasma (evaporant flux) and film characteristics are evaluated. And on the industrial level, the performance and potential uses of ion plated films are discussed. Author

NS1-26191* National Aeronautics and Space Administration, Lewis Research Center, Cleveland, Ohio.

HIGH TEMPERATURE ALKALI CORROSION IN HIGH VELOCITY GASES

Carl E. Lowell, Steven M. Sidik, and Daniel L. Deadmore May 1981 37 p refs

(Contract EF-77-A-01-2593)

(NASA-TM-82591; DOE/NASA/2593-26; E-838) Avail: NTIS HC A03/MF A01 CSCL 11F

The effects of potential impurities in coal derived liquids such as Na, K, Mg, Ca and Cl on the accelerated corrosion of IN-100, U-700, IN-792 and Mar-M509 were investigated using a Mach 0.3 burner rig for times to 1000 hours in one hour cycles. These impurities were injected in combination as aqueous solutions into the combustor of the burner rig. The experimental matrix utilized was designed statistically. The extent of corrosion was determined by metal recession. The metal recession data were fitted by linear regression to a polynomial expression which

allows both interpolation and extrapolation of the data. As anticipated, corrosion increased rapidly with Na and K, and a marked maximum in the temperature response was noted for many conditions. In contrast, corrosion decreased somewhat as the Ca, Mg and Cl contents increased. Extensive corrosion was observed at concentrations of Na and K as low as 0.1 PPM at long times. Author

NS1-26234* National Aeronautics and Space Administration, Lewis Research Center, Cleveland, Ohio.

HIGH TEMPERATURE CYCLIC OXIDATION FURNACE TESTING AT NASA LEWIS RESEARCH CENTER

Charles A. Barrett and Carl E. Lowell 1981 15 p refs Presented at the Symp. on Ind. Methods for Testing at High Temp. Environ., Phoenix, Ariz., 12 May 1981; sponsored by American Society for Testing and Materials

(NASA-TM-21773; E833) Avail: NTIS HC A02/MF A01 CSCL 11F

A standardized method of testing the cyclic oxidation resistance of various alloys in static air to 1200 C was developed and is routinely used at NASA Lewis Research Center. Test samples are automatically raised and lowered into a resistance wound furnace for a series of fixed interval heating and cooling cycles. Spall catchers collect the accumulated spall from each sample. The samples are weighed intermittently to generate specific weight change/time data. At various test times the samples and the accumulated spall are analyzed by X-ray diffraction. A computer program uses this gravimetric and X-ray data as input to print out the oxidation curves and specific

NS1-26235* National Aeronautics and Space Administration, Lewis Research Center, Cleveland, Ohio.

FRETTING WEAR AND FRETTING FATIGUE: HOW ARE THEY RELATED?

Robert C. Bill 1981 25 p refs Proposed for presentation at the Joint Lubrication Conf., New Orleans, 4-7 Oct. 1981; sponsored by American Society of Lubrication Engineer and ASME Prepared in cooperation with Army Aviation Research and Development Command, Cleveland, Ohio

(NASA-TM-82633; AVRADCOM-TR-81-C-16; E-715) Avail: NTIS HC A02/MF A01 CSCL 11F

Results from published literature, and results obtained experimentally using a fretting wear apparatus are examined to determine how fretting wear and fretting fatigue are related. The effects of various experimental parameters including slip amplitude, number of fretting cycles, frequency of fretting motion, experimental atmosphere, temperature, and the performance of coatings and surface treatments are surveyed. All of the results examined indicate that fretting wear and fretting fatigue are influenced in a consistent and analogous manner by controlled variations in experimental conditions. That is, conditions that tend to accelerate fretting wear also accelerate fretting fatigue failures. Correlation of the performance of coatings on material under fretting wear and fretting fatigue conditions is rather tenuous, partly because similar contact conditions for fretting fatigue and fretting wear are not available for very many materials. A.R.H.

NS1-26236* National Aeronautics and Space Administration, Lewis Research Center, Cleveland, Ohio.

HOSTILE ENVIRONMENTAL CONDITIONS FACING CANDIDATE ALLOYS FOR THE AUTOMOTIVE STIRLING ENGINE

Joseph R. Stephens 1981 12 p refs Proposed for presentation at the Environ. Degradation of Eng. Mater. Conf., Blackburn, Va., 21-23 Sep. 1981

(Contract DE-AI01-77CS-51040)

(NASA-TM-82632; DOE/NASA/51040-29; E-887)

Avail: NTIS HC A02/MF A01 CSCL 11F

The materials research program in support of the Automotive Stirling Engine Project focuses on the hot heater head of the engine including the heater head tubes, cylinders, and regenerator housings, which are considered to be the most critical components from a materials viewpoint. The specific areas of investigation

in the program involve hydrogen permeability testing, doping of the hydrogen working fluid to reduce permeability rates, oxidation/corrosion studies, creep-rupture evaluation, and assessing effects of hydrogen environment on mechanical properties. Emphasis is placed on the materials challenges that result from the use of hydrogen as the working fluid. S.F.

N81-27258* National Aeronautics and Space Administration, Lewis Research Center, Cleveland, Ohio.

MATERIAL RESPONSE FROM MACH 0.3 BURNER RIG COMBUSTION OF A COAL-OIL MIXTURE

G. J. Santoro, F. D. Calfo, and F. J. Kohl. Jun. 1981. 24 p. refs.

(Contract EF-77-A-01-2593)

(NASA-TM-81686; DOE/NASA/2593-23; E-718) Avail: NTIS HC A02/MF A01 CSCL 11F

Wedge shaped specimens were exposed to the combustion gases of a Mach 0.3 burner rig fueled with a mixture of 40 weight percent micron size coal particles dispersed in No. 2 fuel oil. Exposure temperature was about 900 C and the test duration was about 44 one hour cycles. The alloys tested were the nickel base superalloys, IN-100, U-700 and IN-792, and the cobalt base superalloy, Mar-M509. The deposits on the specimens were analyzed and the extent of corrosion/erosion was measured. The chemical compositions of the deposits were compared with the predictions from an equilibrium thermodynamic analysis. The experimental results were in very good agreement with the predictions. Author

N81-27259* National Aeronautics and Space Administration, Lewis Research Center, Cleveland, Ohio.

ADVANCED AIRCRAFT ENGINE MATERIALS TRENDS

R. L. Dreshfield, Hugh R. Gray, Stanley R. Levine, and Robert Signorelli. 1981. 16 p. refs. Presented at the 26th Ann. Intern. Gas Turbine Conf., Houston, Tex., 8-12 Mar. 1981; sponsored by ASME.

(NASA-TM-82626; E-879) Avail: NTIS HC A22/MF A01 CSCL 11F

Recent activities of the Lewis Research Center are reviewed which are directed toward developing materials for rotating hot section components for aircraft gas turbines. Turbine blade materials activities are directed at increasing metal temperatures approximately 100 C compared to current directionally solidified alloys by use of oxide dispersion strengthening or tungsten alloy wire reinforcement of nickel or iron base superalloys. The application of thermal barrier coatings offers a promise of increasing gas temperatures an additional 100 C with current cooling technology. For turbine disk alloys, activities are directed toward reducing the cost of turbine disks by 50 percent through near net shape fabrication of prealloyed powders as well as towards improved performance. In addition, advanced alloy concepts and fabrication methods for dual alloy disks are being studied as having potential for improving the life of future high performance disks and reducing the amount of strategic materials required in these components. E.D.K.

N81-28231* National Aeronautics and Space Administration, Lewis Research Center, Cleveland, Ohio.

BURNER RIG EVALUATION OF THERMAL BARRIER COATING

Michael A. Gedwill. Feb. 1981. 23 p. refs.

(Contract EF-77-A-01-2593)

(NASA-TM-81684; DOE/NASA/2593-26; E-712) Avail: NTIS HC A02/MF A01 CSCL 11F

Eight plasma sprayed bond coatings were evaluated for potential use with ZrO₂-Y₂O₃ thermal barrier coatings (TBCs) which are being developed for coal derived fuel fired gas turbines. Longer TBC lives in cyclic burner rig oxidation to 1050 C were achieved with the more oxidation resistant bond coatings. These were Ni-14.1Cr-13.4Al-0.10Ar, Ni-14.1Cr-14.4Al-0.16Y, and Ni-15.8Cr-12.8Al-0.36Y on Rene 41. The TBC systems performed best when 0.015-cm thick bond coatings were employed that were sprayed at 20 kW using argon 3.5v/o hydrogen. Cycling had a more life limiting influence on the TBC than accumulated time at 1050 C. Author

N81-28233* National Aeronautics and Space Administration, Lewis Research Center, Cleveland, Ohio.

ADHESION AND FRICTION OF TRANSITION METALS IN CONTACT WITH NONMETALLIC HARD MATERIALS

Kazuhisa Miyoshi and Donald H. Buckley. 1981. 19 p. refs. Presented at Intern. Conf. on the Sci. of Hard Mater., Moran, Wyoming, 23-28 Aug. 1981.

(NASA-TM-82605; E-853) Avail: NTIS HC A02/MF A01 CSCL 11F

Sliding friction experiments were conducted with the metals yttrium, titanium, tantalum, zirconium, vanadium, neodymium, iron, cobalt, nickel, tungsten, platinum, rhenium, ruthenium, and rhodium in sliding contact with single crystal diamond, silicon carbide, pyrolytic boron nitride, and ferrite. Auger electron spectroscopy analysis was conducted with the metals and nonmetals to determine the surface chemistry and the degree of surface cleanliness. The results of the investigation indicate the adhesion and friction of the transition metals in contact with diamond, silicon carbide, boron nitride, and ferrite are related to the relative chemical activity of the metals. The more chemically active the metal, the higher the coefficient of friction and the greater amount of transfer to the nonmetals. E.D.K.

N81-29206* National Aeronautics and Space Administration, Lewis Research Center, Cleveland, Ohio.

NASA'S ACTIVITIES IN THE CONSERVATION OF STRATEGIC AEROSPACE MATERIALS

Joseph R. Stephens. 1980. 24 p. refs.

(NASA-TM-81617; E-623) Avail: NTIS HC A02/MF A01 CSCL 11F

The primary objective of the Conservation of Strategic Aerospace Materials (COSAM) Program is to help reduce the dependence of the United States aerospace industry on strategic metals by providing the materials technology needed to minimize the strategic metal content of critical aerospace components with prime emphasis on components for gas turbine engines. Initial emphasis was placed in the area of strategic element substitution. Specifically, the role of cobalt in nickel base and cobalt base superalloys vital to the aerospace industry is being examined in great detail by means of cooperative university-industry-government research efforts. Investigations are underway in the area of 'new classes' of alloys. Specifically, a study was undertaken to investigate the mechanical and physical properties of intermetallics that contain a minimum of the strategic metals. Current plans for the much larger COSAM Program are also presented. E.D.K.

N81-29208* National Aeronautics and Space Administration, Lewis Research Center, Cleveland, Ohio.

COBALT: A VITAL ELEMENT IN THE AIRCRAFT ENGINE INDUSTRY

Joseph R. Stephens. 1981. 15 p. refs. Presented at the Workshop Conserv. Technol. for Critical Mater., 15-17 Jun. 1981; sponsored by Dept. of Commerce.

(NASA-TM-82662; E-934) Avail: NTIS HC A02/MF A01 CSCL 11F

Recent trends in the United States consumption of cobalt indicate that superalloys for aircraft engine manufacture require increasing amounts of this strategic element. Superalloys consume a lion's share of total U.S. cobalt usage which was about 16 million pounds in 1980. In excess of 90 percent of the cobalt used in this country was imported, principally from the African countries of Zaire and Zambia. Early studies on the roles of cobalt as an alloying element in high temperature alloys concentrated on the simple Ni-Cr and Nimonic alloy series. The role of cobalt in current complex nickel base superalloys is not well defined and indeed, the need for the high concentration of cobalt in widely used nickel base superalloys is not firmly established. The current cobalt situation is reviewed as it applies to superalloys and the opportunities for research to reduce the consumption of cobalt in the aircraft engine industry are described. E.D.K.

A81-33273* # National Aeronautics and Space Administration, Lewis Research Center, Cleveland, Ohio.
A NEW DIFFUSION-INHIBITED OXIDATION-RESISTANT COATING FOR SUPERALLOYS
 Michael A. Gedwill, Thomas K. Glasgow, and Stanley R. Levine
 Aug. 1981 21 p refs
 (NASA-TM-82687; E-988) Avail: NTIS HC A02/MF A01 CSCL 11F

A concept for enhanced protection of superalloys consists of adding an oxidation- and diffusion-resistant cermet layer between the superalloy and the outer oxidation-resistant metallic alloy coating. Such a duplex coating was compared with a physical-vapor-deposited (PVD) NiCrAlY coating in cyclic oxidation at 1150 C. The substrate alloy was MA 754 - an oxide-dispersion-strengthened superalloy that is difficult to coat. The duplex coating, applied by plasma spraying, outperformed the PVD coating on the basis of weight change and both macroscopic and metallographic observations. Author

A81-10765 * The influence of isothermal annealing on the molybdenum fibers of a directed solid gamma/gamma prime - alpha alloy (Der Einfluss isothermer Glühung auf die Molybdänfasern einer gerichtet erstarrten gamma/gamma prime - alpha-Legierung). J. D. Whittenberger (NASA, Lewis Research Center, Cleveland, Ohio), G. Wirth (Deutsche Forschungs- und Versuchsanstalt für Luft- und Raumfahrt, Cologne, West Germany), and R. Owen (Gould Laboratories, Cleveland, Ohio). *Scripta Metallurgica*, vol. 14, Oct. 1980, p. 1115-1118. 7 refs. In German.

The mechanical characteristics of the directed solid eutectic Ni-Al-Mo (gamma/gamma prime)-alpha alloy at high temperatures make it useful in the blades of gas turbines. Structural changes are observed for the alloy under isothermal annealing, particularly the formation of molybdenum plates at the grain boundary and an increase of the gamma phase in relation to the gamma prime phase. Molybdenum lamellae appear at the grain boundary above 1100 C which can have a negative influence on the mechanical properties. The change in the structure near the grain boundary with the increase in temperature is illustrated through a sequence of pictures. R.C.

A81-12266 * # Cyclic behavior of turbine disk alloys at 650 C. B. A. Cowles, D. L. Sims, J. R. Warren (United Technologies Corp. Pratt and Whitney Aircraft Group, West Palm Beach, Fla.), and R. V. Miner, Jr. (NASA, Lewis Research Center, Cleveland, Ohio). *ASME, Transactions, Journal of Engineering Materials and Technology*, vol. 102, Oct. 1980, p. 356-363. 12 refs.

Five gas turbine disk alloys representing a range of strengths and processing methods were tested for resistance to both cyclic crack initiation and propagation at 650 C using a 0.33 Hz fatigue cycle and a cycle incorporating a 900 s tensile dwell. At the low strain ranges pertinent to disks, resistance to crack initiation increased with increasing tensile yield strength among the alloys, though the advantage was somewhat smaller for the creep fatigue cycle. Cyclic crack growth resistance, however, decreased with increasing strength and very markedly so for the dwell cycle. (Author)

A81-12920 * Thermal barrier coatings for heat engine components. S. R. Levine, R. A. Miller, and P. E. Hodge (NASA, Lewis Research Center, Cleveland, Ohio). *SAMPE Quarterly*, vol. 12, Oct. 1980, p. 20-26. 25 refs.

A comprehensive NASA-Lewis program of coating development for aircraft gas turbine blades and vanes is presented. Improved ceramic layer compositions are investigated, along the MCrAlY bond films and the methods of uniform deposition of the coatings; the thermomechanical and fuel impurity tolerance limits of the coatings are being studied. Materials include the ZrO₂-Y₂O₃/NiCrAlY system; the effects of the bond coat and zirconia composition on coating life and Mach 1 burner rig test results are discussed. It is concluded that Diesel engines can also utilize thermal barrier coatings; they have been used successfully on piston crowns and exhaust valves of shipboard engines to combat lower grade fuel combustion corrosion. A.T.

A81-14998 * # Adherence of on beam sputter deposited metal films on H-13 steel. M. J. Mirtich (NASA, Lewis Research Center, Cleveland, Ohio). *American Vacuum Society, National Symposium, 27th, Detroit, Mich., Oct. 14-17, 1980, Paper*. 15 p. 6 refs.

An electron bombardment argon ion source sputter deposited 17 metals and metal oxides on H-13 steel. The films ranged 1 to 8 micrometers in thickness and their adherence was generally greater than the capacity of the measuring device; adherence quality depended on proper precleaning of the substrate before deposition. N₂ or air was introduced for correct stoichiometry in metallic compounds. Au, Ag, MgO, and TaSi₃ films 8 microns thick have bond strength equal to 1 micron coatings; the bond strength of pure metallic films up to 5 microns thick was greater than the epoxy to film bond (8000 psi). The results of exposures of coated material to temperatures up to 700 C are presented. A.T.

A81-18559 * The effect of zirconium on the cyclic oxidation of NiCrAl alloys. C. A. Barrett, A. S. Khan, and C. E. Lowell (NASA, Lewis Research Center, Cleveland, Ohio). *Electrochemical Society, Journal*, vol. 128, Jan. 1981, p. 25-32. 18 refs.

This paper examines results with cyclic oxidation tests of Ni(9-20) Cr(15-30) Al-(x)Zr alloys carried out at 1100 C and 1200 C in static air. The concentration of zirconium varies from 0 to 0.63 atomic percent. Significant aluminum penetration is found in metallographic and electron microscopic examination of oxidized surfaces. Small amounts of zirconium lead to minimal penetration, and with increased zirconium content pronounced oxide penetration is observed. R.C.

A81-22530 * # Accuracy of trace element determinations in alternate fuels. L. A. Greenbauer-Seng (NASA, Lewis Research Center, Cleveland, Ohio). *Society for Applied Spectroscopy and American Chemical Society, May Conference, Cleveland, Ohio, May 28, 1980, Paper*. 20 p. 36 refs.

NASA-Lewis Research Center's work on accurate measurement of trace level of metals in various fuels is presented. The differences between laboratories and between analytical techniques especially for concentrations below 10 ppm, are discussed, detailing the Atomic Absorption Spectrometry (AAS) and DC Arc Emission Spectrometry (dc arc) techniques used by NASA-Lewis. Also presented is the design of an Interlaboratory Study which is considering the following factors: laboratory, analytical technique, fuel type, concentration and ashing additive. N.D.

A81-22535 * # NASA's activities in the conservation of strategic aerospace materials. J. R. Stephens (NASA, Lewis Research Center, Cleveland, Ohio). *American Society for Metals, Fall Meeting, Cleveland, Ohio, Oct. 28-30, 1980, Paper*. 22 p. 7 refs.

The United States imports 50-100 percent of certain metals critical to the aerospace industry, namely, cobalt, columbium, chromium, and tantalum. In an effort to reduce this dependence on foreign sources, NASA is planning a program called Conservation of Strategic Aerospace Materials (COSAM), which will provide technology minimizing strategic metal content in the components of aerospace structures such as aircraft engines. With a proposed starting date of October 1981, the program will consist of strategic element substitution, process technology development, and alternate materials research. NASA's two-fold pre-COSAM studies center on, first, substitution research involving nickel-base and cobalt-base superalloys (Waspaloy, Udimet-700, MAE-M247, René 150, HA-188) used in turbine disks, low-pressure blades, turbine blades, and combustors; and, second, alternate materials research devoted initially to investigating possible structural applications of the intermetallic alloys nickel aluminide and iron aluminide. R.S.

A81-24104 * # Elevated temperature mechanical properties and residual tensile properties of two cast superalloys and several nickel-base oxide dispersion strengthened alloys. J. D. Whittenberger (NASA, Lewis Research Center, Cleveland, Ohio). *Metallurgical Transactions A - Physical Metallurgy and Materials Science*, vol. 12A, Feb. 1981, p. 193-206. 14 refs.

The elevated temperature tensile, stress-rupture and creep properties and residual tensile properties after creep straining have been determined for two cast superalloys and several wrought Ni-16Cr-4Al-yttria oxide dispersion strengthened (ODS) alloys. The creep behavior of the ODS alloys is similar to that of previously studied ODS nickel alloys. In general, the longitudinal direction is stronger than the long transverse direction, and creep is at least partially due to a diffusional creep mechanism as dispersoid-free zones were observed after creep-rupture testing. The tensile properties of the nickel-base superalloy B-1900 and cobalt-base superalloy MAR-M509 are not degraded by prior elevated temperature creep straining (at least up to 1 pct) between 1144 and 1366 K. On the other hand, the room temperature tensile properties of ODS nickel-base alloys can be reduced by prior creep strains of 0.5 pct or less between 1144 and 1477 K, with the long transverse direction being more susceptible to degradation than the longitudinal direction. (Author)

A81-27944 * The effect of mechanical surface and heat treatments on the erosion resistance of 6061 aluminum alloy. J. Salik, D. Buckley, and W. A. Brainard (NASA, Lewis Research Center, Cleveland, Ohio). *Wear*, vol. 65, Jan. 1, 1981, p. 351-358. 17 refs.

The effects of both mechanical surface treatments and heat treatments on the erosion resistance of 6061 aluminum alloy were studied in order to gain a better understanding of material properties which affect erosion behavior. It was found that mechanical surface treatments have little or no effect on the erosion resistance. This is due to the formation by particle impact of a work-hardened surface layer, independent of the initial surface condition. The erosion resistance of aluminum single crystals was found to be independent of orientation, which is due to destruction of the surface microstructure and formation of a polycrystalline surface layer by the particle impact as observed by X-ray diffraction. Although on solution treatment of annealed aluminum 6061 the increase in hardness is accompanied by an increase in erosion resistance, precipitation treatment (which causes a further increase in hardness) results in a slightly lower erosion resistance. (Author)

A81-29973 * # Effect of fuel nitrogen and hydrogen content on emissions in hydrocarbon combustion. D. A. Bittker and G. Wolfbrandt (NASA, Lewis Research Center, Cleveland, Ohio). *American Society of Mechanical Engineers, Gas Turbine Conference and Products Show, Houston, Tex., Mar. 9-12, 1981, Paper 81-GT-63*. 13 p. 22 refs. Members, \$2.00; nonmembers, \$4.00. Contract No. DE-AI01-77ET-10350.

The results of an investigation of the effect of operating conditions and fuel properties on emission for the two-stage combustion of fuels with significant organic nitrogen content are presented. The way in which the emissions of nitrogen oxides and carbon monoxide are affected by the decreased hydrogen content and the increased organic nitrogen content of coal-derived fuels is discussed. Limited measurements of smoke from the rich-lean combustion of simulated syncrude fuels indicate relatively high smoke emissions in spite of the very lean second-stage burning. This fact, together with the high observed carbon monoxide emissions, suggests that trade-offs will be necessary between the conditions that minimize NOx and those that control CO and smoke emissions. C.R.

A81-32546 * # The effect of thermal cycling to 1100 C on the alpha /Mo/ phase in directionally solidified gamma/gamma-prime-alpha alloys. F. H. Harf (NASA, Lewis Research Center, Cleveland, Ohio). *American Institute of Mining, Metallurgical and Petroleum Engineers, Annual Meeting, 110th, Chicago, Ill., Feb. 22-26, 1981, Paper*. 13 p. 16 refs.

Specimens of gamma/gamma-prime-alpha (Mo) eutectic alloy were thermally cycled or isothermally exposed at temperatures of 1075 to 1100 C. Transmission electron microscopy examination of cycled specimens indicated that even an exposure of 10 minutes effected noticeable changes in the shape of the alpha phase, and that the changes were cumulative as more cycles were added. The cross sections of fine, smooth fibers changed from rectangles to octagons, while lamellae and irregular shapes spheroidized. These effects are attributed to the differences in thermal expansion coefficients between the alpha phase and the gamma/gamma-prime matrix, and to the higher diffusion rates prevailing at elevated temperatures. Where the configuration of the alpha phase is a simple shape, such as a fiber, increasing the temperature eventually brings about a stress free interface between the alpha phase and the matrix by differential thermal expansion. Where the shape of the alpha phase is more complex, a stressed interface persists to higher temperatures where diffusion produces the more drastic morphological changes. (Author)

A81-38066 * # Frictional and morphological characteristics of ion plated soft, metallic films. T. Spalvins and B. Buzek (NASA, Lewis Research Center, Cleveland, OH). *American Vacuum Society, International Conference on Metallurgical Coatings, San Francisco, CA, Apr. 6-10, 1981, Paper*. 12 p. 6 refs.

Ion plated metallic films in contrast to films applied by other deposition techniques offer a lower friction coefficient, longer endurance lives and exhibit a gradual increase in friction coefficient after the film has been worn off. The friction coefficients of metallic films are affected by the degree of adherence, thickness and nucleation and growth characteristics. The effective film thickness for the minimum friction coefficient was established for Au and Pb films. The nucleation and growth characteristics during ion plating lead to a fine, continuous crystalline structure, which contributes to a lower friction coefficient. (Author)

A81-38067 * # Sputtered protective coatings for die casting dies. M. J. Mirtich (NASA, Lewis Research Center, Cleveland, OH), C.-Y. Nieh, and J. F. Wallace (Case Western Reserve University, Cleveland, OH). *American Vacuum Society, International Conference on Metallurgical Coatings, San Francisco, CA, Apr. 6-10, 1981, Paper*. 12 p. 5 refs.

Three experimental research designs investigating candidate materials and processes involved in protective die surface coating procedures by sputter deposition, using ion beam technologies, are discussed. Various pre-test results show that none of the coatings remained completely intact for 15,000 test cycles. The longest lifetime was observed for coatings such as tungsten, platinum, and molybdenum which reduced thermal fatigue, but exhibited oxidation and suppressed crack initiation only as long as the coating did not fracture. Final test results confirmed earlier findings and coatings with Pt and W proved to be the candidate materials to be used on a die surface to increase die life. In the W-coated specimens, which remained intact on the surface after thermal fatigue testing, no oxidation was found under the coating, although a few cracks formed on the surface where the coating broke down. Further research is planned. E.B.

A81-38069 * # Ion beam sputter etching of orthopedic implant alloy MP35N and resulting effects on fatigue properties. E. G. Wintucky, M. Christopher (NASA, Lewis Research Center, Cleveland, OH), E. Bahnuk (Case Western Reserve University, Cleveland, OH), and S. Wang. *AIAA, Japan Society for Aeronautical and Space Sciences, and DGLR, International Electric Propulsion Conference, 15th, Las Vegas, NV, Apr. 21-23, 1981, AIAA Paper 81-0671*. 31 p. 13 refs.

A81-43384 * Oxidation and hot corrosion of coated and bare oxide dispersion strengthened superalloy MA-755E. T. K. Glasgow and G. J. Santoro (NASA, Lewis Research Center, Cleveland, OH). *Oxidation of Metals*, vol. 15, Apr. 1981, p. 251-276. 9 refs.

Cyclic hot corrosion and oxidation of an experimental oxide dispersion strengthened (ODS) superalloy MA-755E were conducted in a hot gas stream at Mach 0.3. The response of the ODS alloy, bare or with protective coatings, was similar to that of a conventional cast alloy, IF-792, in hot corrosion at 900 C. However, during oxidation at 1100 and 1150 C the ODS alloy differed from the cast alloy by developing a greater amount of subsurface porosity. Compared with a diffused aluminide coating, an electron beam vapor deposited NiCrAlY coating offered superior oxidation protection and decreased porosity formation. In additional testing, the tendency to form porosity was associated with the large grains of recrystallized powder metallurgy alloys but was independent of the presence of an oxide dispersion. (Author)

A81-44653 * # High temperature cyclic oxidation furnace testing at NASA Lewis Research Center. C. A. Barrett and C. E. Lowell (NASA, Lewis Research Center, Cleveland, OH). *American Society for Testing and Materials, Symposium on Industrial Methods for Testing at High Temperature Environments, Phoenix, AZ, May 12, 1981, Paper*. 13 p. 18 refs.

A standardized method of testing the cyclic oxidation resistance of various alloys in static air up to 1200 C has been developed and routinely used at the NASA Lewis Research Center. Test samples are automatically raised and lowered into a resistance wound furnace for a series of fixed-interval heating and cooling cycles. Spall catchers collect the accumulated spall from each sample. The samples are weighed intermittently to generate specific weight change with time data. At various test times the samples and the accumulated spall are analyzed by X-ray diffraction. A computer program is used to print out the specific weight change versus time data and the X-ray data in tabular form and to plot the specific weight change versus time data in a publishable format. The data are also organized and indexed. So far several hundred Fe-, Ni-, and Co-base alloys have been tested using this basic procedure and will form the basis of a series of cyclic oxidation handbooks to be published by NASA. Such specific weight change/time data have been used to estimate the oxidative metal consumption by several computer modeling techniques both to rank alloys and to estimate life. (Author)

A81-44657 * # Assessment of variations in thermal cycle life data of thermal barrier coated rods. R. C. Hendricks and G. McDonald (NASA, Lewis Research Center, Cleveland, OH). *American Vacuum Society, International Conference on Metallurgical Coatings, San Francisco, CA, Apr. 6-10, 1981, Paper*. 11 p. 10 refs.

The reported study had the purpose to examine variations in cyclic life and in adhesive/cohesive coating strength. Possible effects of heating rate, stress reversal, temperature level, and ceramic deposition methods on coating life were also investigated. Life cycle data for 22 thermal barrier coated rods were examined and found to be statistically modeled by normal or log-normal distributions. The sample mean was 1330 cycles with a standard deviation of 520 cycles. Adhesive/cohesive pull-off strength data for 20 thermal barrier coated flat head piston specimens were taken. The average pull-off stress was 9 MPa with a standard deviation of 4.2 MPa. It was found that variations in heating rate can produce significant variations in the life cycle data. G.R.

A81-44663 * # Synergistic erosion/corrosion of superalloys in PFB coal combustor effluent. S. M. Benford, G. R. Zellars, and C. E. Lowell (NASA, Lewis Research Center, Cleveland, OH). *American Ceramic Society, Annual Meeting, 82nd, Chicago, IL, Apr. 28-30, 1980, Paper*. 25 p. 13 refs.

Two Ni-based superalloys were exposed to the high velocity effluent of a pressurized fluidized bed coal combustor (PFBC). Targets were 15-cm diameter rotors operating at 40,000 rpm and

small flat plate specimens. Above an erosion rate threshold (approximately 10 microns/hr), the targets were eroded to bare metal. The presence of accelerated oxidation at lower erosion rates suggests erosion/corrosion synergism. Various mechanisms which may contribute to the observed oxide growth enhancement include erosive removal of protective oxide layers, oxide and subsurface cracking, and chemical interaction with sulfur in the gas and deposits through damaged surface layers. (Author)

A81-48143 * Mechanical properties of weldments in experimental Fe-12Mn-0.2Ti and Fe-12Mn-1Mo-0.2Ti alloys for cryogenic service. J. R. Stephens, W. R. Witzke (NASA, Lewis Research Center, Cleveland, OH), and J. H. Devletian (Oregon Graduate Center, Beaverton, OR). (*American Welding Society, Annual Meeting, 62nd, Cleveland, OH, Apr. 5-10, 1981, Welding Journal, Research Supplement*, vol. 60, Sept. 1981, p. 177-s to 184-s, 16 refs.

Mechanical properties of weldments in two Fe-12Mn experimental alloys designed for cryogenic service were evaluated. Weldments were made using the GTA welding process. Tests to evaluate the weldments were conducted at -196 C and included: equivalent energy fracture toughness tests; autogenous transverse weld, notched transverse weld, and longitudinal weld tensile tests; and all-weld-metal tensile tests. The Fe-12Mn-0.2Ti and Fe-12Mn-1Mo-0.2Ti alloys proved weldable for cryogenic service, with weld metal and heat-affected zone properties comparable with those of the base metal. Optimum properties were achieved in the base alloys, weld metals, and heat-affected zones after a two-step heat treatment consisting of austenitizing at 900 C followed by tempering at 500 C. The Mo-containing alloy offered a marked improvement in cryogenic properties over those of the Mo-free alloy. Molybdenum increased the amount of retained austenite and reduced the amount of epsilon martensite observed in the microstructure of the two alloys. (Author)

A81-49217 * Thermal barrier coatings for superalloys. R. A. Miller, S. R. Levine, and P. E. Hodge (NASA, Lewis Research Center, Cleveland, OH). In: *Superalloys 1980, Proceedings of the Fourth International Symposium, Champion, PA, September 21-25, 1980*. (A81-49176 24-26) Metals Park, OH, American Society for Metals, 1980, p. 473-480. 15 refs.

The current status of ceramic thermal barrier coatings for protection of turbine airfoil components is reviewed. Test results for an early duplex coating system ZrO₂-12% Y₂O₃/Ni-16% Cr-6% Al-0.6% Y, improved system ZrO₂-8% Y₂O₃/Ni-17% Cr-5% Al-0.35% Y, and air/fuel impurity tolerant systems based on ZrO₂-8% Y₂O₃, 2CaO-SiO₂, and a MgO-NiCrAlY cermet are discussed. Preliminary test results at 800 C for a graded ZrO₂-8% Y₂O₃/Ni-20% Cr-11% Al-0.4% Y coating system show that the coating can survive at least 500 hr in the presence of 50 ppm V plus other fuel contaminants and additives. V.L.

N81-16208 Pittsburgh Univ., Pa.
AN INVESTIGATION OF HOT CORROSION MECHANISMS IN NICKEL BASE ALLOYS Ph.D. Thesis
Tai Tsu Huang 1980 218 p
Avail: Univ. Microfilms Order No. 8028015

The mechanisms by which metals and alloys are attacked by gaseous environments when deposits are present on their surface were determined. A large number of different metal and alloy specimens were exposed to an oxygen atmosphere with various salt coatings, and oxidized specimens were examined by ordinary light and scanning electron microscopy to characterize the morphology and structure of the scale developed at various stages of oxidation. Alloy microstructure and oxidation products were identified through X-ray diffraction, electron diffraction and EDAX analysis techniques in order to obtain a more conclusive picture of the mechanism of hot corrosion. Dissert. Abstr.

N81-19277* Pratt and Whitney Aircraft Group, East Hartford, Conn.

TURBINE BLADE TEMPERATURE MEASUREMENTS USING THIN FILM TEMPERATURE SENSORS

H. P. Grant, J. S. Przybyszewski, and R. G. Claing 17 Mar. 1981 65 p refs

(Contract NAS3-20831)

(NASA-CR-185201; PWA-5604-31)

Avail: NTIS

HC A04/MF A01 CSCL 11F

The development of thin film temperature sensors is discussed. The technology for sputtering 2 micron thin film platinum versus platinum 10 percent rhodium thermocouples on alumina forming coatings was improved and extended to applications on actual turbine blades. Good adherence was found to depend upon achieving a proper morphology of the alumina surface. Problems of adapting fabrication procedures to turbine blades were uncovered, and improvements were recommended. Testing at 1250 K at one atmosphere pressure was then extended to a higher Mach No. (0.5) in combustor flow for 60 hours and 71 thermal cycles. The mean time to failure was 47 hours accumulated during 1 hour exposures in the combustor. Calibration drift was about 0.1 percent per hour, attributable to oxidation of the rhodium in the thin films. An increase in film thickness and application of a protective overcoat are recommended to reduce drift in actual engine testing. M.G.

N81-20244* Colorado State Univ., Fort Collins. Dept. of Mechanical Engineering.

PASSIVATION OF CARBON STEEL THROUGH MERCURY IMPLANTATION Final Report, 1 Feb. 1980 - 1 Feb. 1981

Paul J. Wilbur and Raymond S. Robinson Feb. 1981 36 p refs

(Contract NAG3-25)

(NASA-CR-165292) Avail: NTIS HC A03/MF A01 CSCL 11F

An experiment, in which carbon steel samples were implanted with mercury ions from a broad beam ion source and their corrosion characteristics in air were evaluated, is described. Mercury doses of a few mA min/square cm at energies of a few hundred electron volts are shown to effect significant improvements in the corrosion resistance of the treated surfaces. In a warm moist environment the onset of rusting was extended from 15 min. for an untreated sample to approximately 30 hrs. for one implanted at a dose of 33 mA min/square cm with 1000 eV mercury ions. Author

N81-22156* Case Western Reserve Univ., Cleveland, Ohio. **MICROSTRUCTURE AND MECHANICAL PROPERTIES OF BULK AND PLASMA-SPRAYED Y2O3-PARTIALLY STABILIZED ZIRCONIA Annual Report**

Peter G. Valentine and Ralph D. Maier Aug. 1980 45 p refs (Grant NSG-3252)

(NASA-CR-165126) Avail: NTIS HC A03/MF 01 CSCL 11F

Bulk 8.0 weight percent yttria partially stabilized zirconia (PSZ) was studied by light microscopy, transmission electron microscopy, X-ray analysis, microhardness testing, and fracture toughness testing. The as received PSZ contained spheroidal and grain boundary precipitates up to 4 micrometers in size. Spheroids up to 1.26 micrometers were metastable tetragonal; large spheroids were monoclinic. Grinding the PSZ into powder did not cause a significant amount of tetragonal to transform to monoclinic. This indicates that transformation toughness is not a significant mechanism in PSZ. Aging the PSZ at 1500 C caused the fine tetragonal precipitates to grow from 0.06 to 0.12 micrometers, in 250 minutes. A peak hardness of 1400 kg/sq mm was attained after 50 minutes. Solution annealing and quenching the as received PSZ eliminated the large precipitates, but fine tetragonal precipitates reformed on quenching. Aging at 1500 C caused the fine 0.02 micrometers tetragonal precipitates to grow into plates about 0.10 by 0.50 micrometers. A peak hardness of 1517 kg/sq mm was obtained after 250 minutes. On further aging, monoclinic precipitates formed along grain boundaries. The fracture toughness of the aged and unaged solution annealed and quenched PSZ was found to be between 2 and 3 MN/square root of m cubed. This range of fracture toughness is consistent with PSZ's that do not undergo transformation toughening. Author

A81-10706 * Effect of TMP variables upon structure and properties in ODS alloy HDA 8077 sheet. M. F. Rothman and H. M. Tawancy (Cabot Corp., Kokomo, Ind.). *International Conference on Superalloys, 4th, Champion, Pa., Sept. 21-25, 1980, Paper. 10 p.* Contract No. NAS3-20072.

The effects of oxide content level and variations in thermo-mechanical processing upon the final structure and properties of HDA 8077 sheet have been systematically examined. It was found that creep strength and formability are substantially influenced by both oxide content and TMP schedule. Variations in creep properties obtained appear to correlate with observed microstructures. (Author)

27 NONMETALLIC MATERIALS

Includes physical, chemical, and mechanical properties of plastics, elastomers, lubricants, polymers, textiles, adhesives, and ceramic materials

N81-10170* National Aeronautics and Space Administration, Lewis Research Center, Cleveland, Ohio

EFFECT OF SUBSTRATE SURFACE FINISH ON THE LUBRICATION AND FAILURE MECHANISMS OF MOLYBDENUM DISULFIDE FILMS

Robert L. Fusaro 1980 40 p refs Proposed for presentation at Annual Meeting of the Am. Soc. of Lubrication Engr., Pittsburgh, 11-14 May 1981 (NASA-TM-81595; E-9715) Avail: NTIS HC A03/MF A01 CSCL 11H

An optical microscope was used to study the lubrication and failure mechanisms of rubbed (burnished) MoS₂ films applied to three substrate surface finishes - polished, sanded, and sandblasted - as a function of sliding distance. The lubrication mechanism was the plastic flow of thin films of MoS₂ between flat plateaus on the rider and on the metallic substrate. If the substrates were rough, flat plateaus were created during 'run in' and the MoS₂ flowed across them. Wear life was extended by increasing surface roughness since valleys in the roughened substrate served as reservoirs for MoS₂ and a deposit site for wear debris. In moist air, the failure mechanism was the transformation of metallic colored MoS₂ films to a black, powdery material that was found by X ray diffraction to consist primarily of alpha iron and MoO₃ powders. In dry argon, the failure mechanism was the gradual depletion of the MoS₂ film from the contact region by transverse flow. Analysis of the wear debris on the wear track at failure showed it consisted mainly of alpha iron and some residual MoS₂. No molybdenum oxides were found. M.G.

N81-11214* National Aeronautics and Space Administration, Lewis Research Center, Cleveland, Ohio

POLYTETRAFLUOROETHYLENE TRANSFER FILM STUDIED WITH X-RAY PHOTOELECTRON SPECTROSCOPY

Donald R. Wheeler Nov. 1980 11 p refs (NASA-TP-1728; E-414) Avail: NTIS HC A02/MF A01 CSCL 11G

Polytetrafluoroethylene (PTFE) was rubbed against nickel in ultrahigh vacuum at loads up to 3.9 N and speeds up to 94 mm/sec. The transfer film formed on the nickel was analyzed using X-ray photoelectron spectroscopy. The film was indistinguishable from bulk PTFE except for the possible presence of a small amount of NiF₂. The transfer film was found to be about 1 molecule (0.5 nm) thick under all conditions; but at speeds above 10 mm/sec, there was evidence of bulk transfer in the form of fragments as well. The thickness measurements required a choice among conflicting published values of the inelastic mean free path for electrons in polymers. The values chosen gave internally consistent results. Author

N81-12226* National Aeronautics and Space Administration, Lewis Research Center, Cleveland, Ohio

EFFECT OF LOAD, AREA OF CONTACT, AND CONTACT STRESS ON THE WEAR MECHANISMS OF A BONDED SOLID LUBRICANT FILM

Robert L. Fusaro 1980 22 p refs Prepared for the 3d Intern. Conf. on Wear of Mater., San Francisco, 30 Mar - 1 Apr. 1981, sponsored by the Am. Soc. of Mech. Eng. (NASA-TM-81563; E-525) Avail: NTIS HC A02/MF A01 CSCL 11H

A pin on disk type of friction and wear apparatus was used to study the effect of load, contact stress and rider area of contact on the friction and wear properties of polyimide bonded graphite fluoride films. Different rider area contacts were obtained by initially generating flats (with areas of 0.0035, 0.0071, 0.0145, and 0.0240 cm) on 0.476-cm radius hemispherically tipped riders. Different projected contact stresses were obtained by applying loads of 2.5- to 58.8-N to the flats. Two film wear mechanisms

were observed. The first was found to be a linear function of contact stress and was independent of rider area of contact. The second was found to increase exponentially as the stress increased. The second also appeared to be a function of rider contact area. Wear equations for each mechanism were empirically derived from the experimental data. In general, friction coefficients increased with increasing rider contact area and with sliding duration. This was related to the build up of thick rider transfer films. Author

N81-13186* National Aeronautics and Space Administration, Lewis Research Center, Cleveland, Ohio

EFFECT OF MILLING AND LEACHING ON THE STRUCTURE OF SINTERED SILICON

H. C. Yeh (Cleveland State Univ., Ohio), T. K. Glasgow, and T. P. Herbell 1980 15 p refs Presented at Ann. Meeting of the Am. Ceram. Soc., Chicago, 28-30 Apr. 1980 (NASA-TM-81602; E-591) Avail: NTIS HC A02/MF A01 CSCL 07D

Sintering was performed in He for 16 hours at 1200, 1250, and 1300 C. Compacts of as-received Si did not densify during sintering. Milling reduced the average particle size to below 0.5 micrometer and enhanced densification (1.75 g/cc). Leaching milled Si further enhanced densification (1.90 g/cc max.) and decreased structural coarsening. After sintering, the structure of the milled and leached powder compacts appears favorable for the production of reaction bonded silicon nitride. Author

N81-14079* National Aeronautics and Space Administration, Lewis Research Center, Cleveland, Ohio

CHANGES IN SURFACE CHEMISTRY OF SILICON CARBIDE (0001) SURFACE WITH TEMPERATURE AND THEIR EFFECT ON FRICTION

Kazuhisa Miyoshi and Donald H. Buckley Nov. 1980 12 p refs (NASA-TP-1756; E-475) Avail: NTIS HC A02/MF A01 CSCL 07D

Friction studies were conducted with a silicon carbide (0001) surface contacting polycrystalline iron. The surface of silicon carbide was pretreated: (1) by bombarding it with argon ions for 30 minutes at a pressure of 1.3 pascals; (2) by heating it at 800 C for 3 hours in vacuum at a pressure of 10 to the minus eighth power pascal; or (3) by heating it at 1500 C for 3 hours in a vacuum of 10 to the minus eighth power pascal. Auger emission spectroscopy was used to determine the presence of silicon and carbon and the form of the carbon. The surfaces of silicon carbide bombarded with argon ions or preheated to 800 C revealed the main Si peak and a carbide type of C peak in the Auger spectra. The surfaces preheated to 1500 C revealed only a graphite type of C peak in the Auger spectra, and the Si peak had diminished to a barely perceptible amount. The surfaces of silicon carbide preheated to 800 C gave a 1.5 to 3 times higher coefficient of friction than did the surfaces of silicon carbide preheated to 1500 C. The coefficient of friction was lower in the <11(-2)0> direction than in the <10(-1)0> direction; that is, it was lower in the preferred crystallographic slip direction. Author

N81-17280* National Aeronautics and Space Administration, Lewis Research Center, Cleveland, Ohio

CURING AGENT FOR POLYEPIDOXES AND EPOXY RESINS AND COMPOSITES CURED THEREWITH Patent

Tito T. Serafini, Peter Delvigs, and Raymond D. Vannucci, inventors (to NASA) Issued 13 Jan. 1981 5 p Filed 30 Aug. 1979 Supersedes N79-31345 (17 - 22, p2926) (NASA-Case-LEW-13226-1; US-Patent-4,244,857; US-Patent-Appl-SN-070771; US-Patent-Class-260-37EP; US-Patent-Class-260-326S; US-Patent-Class-260-326N; US-Patent-Class-538-117; US-Patent-Class-524-118; US-Patent-Class-528-322) Avail: US Patent and Trademark Office CSCL 07C

A curing for a polyepoxide is described which contains a divalent aryl radical such as phenylene a tetravalent aryl radical such as a tetravalent benzene radical. An epoxide is cured by

admixture with the curing agent. The cured epoxy product retains the usual properties of cured epoxides and, in addition, has a higher char residue after burning, on the order of 45% by weight. The higher char residue is of value in preventing release to the atmosphere of carbon fibers from carbon fiber-epoxy resin composites in the event of burning of the composite.

Official Gazette of the U.S. Patent and Trademark Office

N81-17284* National Aeronautics and Space Administration, Lewis Research Center, Cleveland, Ohio.

DYNAMICS OF SOLID DISPERSIONS IN OIL DURING THE LUBRICATION OF POINT CONTACTS. PART 1: GRAPHITE

C. Cusano (Illinois Univ., Urbana) and H. E. Sliney 1981 29 p refs Proposed for presentation at the Ann. Meeting of the Am. Soc. of Lubrication Eng., Pittsburgh, 11-14 May 1981 (NASA-TM-81683; E-410-1) Avail: NTIS HC A03/MF A01 CSCL 11H

A Hertzian contact was lubricated with dispersed graphite in mineral oils under boundary lubrication conditions. The contact was optically observed under pure rolling, combined rolling and sliding, and pure sliding conditions. The contact was formed with a steel ball on the flat surface of a glass disk. Photomicrographs are presented which show the distribution of the graphite in and around the contact. Friction and surface damage are also shown for conditions when the base oils are used alone and when graphite is added to the base oils. Under pure rolling and combined rolling and sliding conditions, it is found that, for low speeds, a graphite film can form which will separate the contacting surfaces. Under pure sliding conditions, graphite accumulates at the inlet and sweeps around the contact, but very little of the graphite passes through the contact. The accumulated graphite appears to act as a barrier which reduces the supply of oil available to the contact for boundary lubrication. Friction data show no clear short term beneficial or detrimental effect caused by addition of graphite to the base oil. However, during pure sliding, more abrasion occurs on the polished balls lubricated with the dispersion than on those lubricated with the base oil alone. All observations were for the special case of a highly-polished ball on a glass surface and may not be applicable to other geometries and materials, or to rougher surfaces.

Author

N81-17285* National Aeronautics and Space Administration, Lewis Research Center, Cleveland, Ohio.

EVALUATION OF BOUNDARY LUBRICANTS USING STEADY-STATE WEAR AND FRICTION

William R. Loomis and William R. Jones, Jr. 1981 26 p refs Proposed for presentation at the 36th Ann. Meeting of the Am. Soc. of Lubrication Eng., Pittsburgh, 11-14 May 1981 (NASA-TM-81601; E-716) Avail: NTIS HC A03/MF A01 CSCL 11H

A friction and wear study was made at 20 C to establish operating limits and procedures for obtaining improved reproducibility and reliability in boundary lubrication testing. Ester base and C-ether base fluids were used to lubricate a pure iron rider in sliding contact with a rotating M-50 steel disk in a pin-on-disk apparatus. Results of a parametric study with varying loads and speeds showed that satisfactory test conditions for studying the direction and wear characteristics in the boundary lubrication regime with this test device were found to be 1 kilogram load; 7 to 9 meters-per-minute (50 rpm) surface speed; dry air test atmosphere (less than 100 ppm H₂O); and use of a time stepwise procedure for measuring wear. Highly reproducible steady-state wear rates resulted from the two fluid studies which had a linearity of about 99 percent after initially higher wear rates and friction coefficients during run-in periods of 20 to 40 minutes.

Author

N81-17286* National Aeronautics and Space Administration, Lewis Research Center, Cleveland, Ohio.

COMMERCIAL (TERRESTRIAL) AND MODIFIED SOLAR ARRAY DESIGN STUDIES FOR LOW COST, LOW POWER SPACE APPLICATIONS

Joseph C. Kolecki and Thomas J. Riley Dec. 1980 21 p refs (NASA-TM-81622; E-632) Avail: NTIS HC A02/MF A01 CSCL 10A

The suitability of commercial (terrestrial) solar arrays for use in low Earth orbit is examined. It is shown that commercial solar arrays degrade under thermal cycling because of material flexure, and that certain types of silicones used in the construction of these arrays outgas severely. Based on the results, modifications were made. The modified array retains the essential features of typical commercial arrays and can be easily built by commercial fabrication techniques at low cost. The modified array uses a metal tray for containment, but eliminates the high outgassing potting materials and glass cover sheets. Cells are individually mounted with an adhesive and individually covered with glass cover slips, or clear plastic tape. The modified array is found to withstand severe thermal cycling for long intervals of time. M.G.

N81-18296* National Aeronautics and Space Administration, Lewis Research Center, Cleveland, Ohio.

COMPOSITION AND METHOD FOR MAKING POLYIMIDE RESIN-REINFORCED FABRIC Patent

Tito T. Serafini and Peter Delvigs, inventors (to NASA) Issued 13 Jan. 1981 4 p Filed 6 Apr. 1979 Supersedes N79-24061 (17 - 15, p 1947)

(NASA-Case-LEW-12933-1; US-Patent-4,244,853; US-Patent-Appl-SN-027557; US-Patent-Class-260-33.4R; US-Patent-Class-427-221; US-Patent-Class-427-379; US-Patent-Class-528-353) Avail: US Patent and Trademark Office CSCL 11E

A composition for making polyimide resin reinforced fibers or fabric is discussed. The composition includes a polyfunctional ester, a polyfunctional amine, and an end capping agent. The composition is impregnated into fibers or fabric and heated to form prepreg material. The tack retention characteristics of this prepreg material are improved by incorporating into the composition a liquid olefinic material compatible with the other ingredients of the composition. The prepreg material is heated at a higher temperature to effect formation of the polyimide resin and the monomeric additive is incorporated in the polyimide polymer structure.

Official Gazette of the U.S. Patent and Trademark Office

N81-19300* National Aeronautics and Space Administration, Lewis Research Center, Cleveland, Ohio.

SURFACE CHEMISTRY AND FRICTION BEHAVIOR OF THE SILICON CARBIDE (0001) SURFACE AT TEMPERATURES TO 1500 DEG C

Kazuhide Miyoshi and Donald H. Buckley Mar. 1981 14 p refs (NASA-TP-1813; E-542) Avail: NTIS HC A02/MF A01 CSCL 11C

X-ray photoelectron and Auger electron spectroscopy analyses and friction studies were conducted with a silicon carbide (0001) surface in contact with iron at various temperatures to 1200 or 1500 C in a vacuum of 10 to the minus 8th power Pa. The results indicate that there is a significant temperature influence on both the surface chemistry and friction properties of silicon carbide. The principal contaminant of adsorbed amorphous carbon on the silicon carbide surface in the as received state is removed by simply heating to 400 C. Above 400 C, graphite and carbide type carbene are the primary species on the silicon carbide surface, in addition to silicon. The coefficients of friction of polycrystalline iron sliding against a single crystal silicon carbide (0001) surface were high at temperatures to 800 C. Similar coefficients of friction were obtained at room temperature after the silicon carbide was preheated at various temperatures up to 800 C. When the friction experiments were conducted above 800 C or when the specimens were preheated to above 800 C, the coefficients of friction were dramatically lower. At 800 C the silicon and carbide type carbon are at a maximum intensity in the XPS spectra. With increasing temperature above 800 C, the concentration of the graphite increases rapidly on the surface, whereas those of the carbide type carbon and silicon decrease rapidly.

Author

N81-20275* National Aeronautics and Space Administration, Lewis Research Center, Cleveland, Ohio.
DYNAMICS OF SOLID DISPERSIONS IN OIL DURING THE LUBRICATION OF POINT OF CONTACTS. PART 2: MOLYBDENUM DISULFIDE

C. Cusano (Illinois Univ., Urbana-Champaign) and H. E. Sliney 1981 27 p refs Proposed for presentation at Ann. Meeting of the Am. Soc. of Lubrication Engr., Pittsburgh, 11-14 May 1981

(NASA-TM-81709; E-410-2) Avail: NTIS HC A03/MF A01 CSCL 11H

A Hertzian contact consisting of a steel ball in contact with a glass disk is lubricated with MoS₂ dispersions and observed by optical microscopy at various slide/roll conditions. In general the behavior of MoS₂ and graphite are similar. That is, the solids tend to enter the contact and form a film on the contacting surfaces whenever a rolling component of motion is used, but solid particles seldom enter the contact during pure sliding. The MoS₂ has more pronounced plastic flow behavior than graphite. However, the polished steel ball is more readily scratched by MoS₂ than by graphite. Under the conditions of these studies, lower friction and wear are observed with pure oil rather than with the dispersions. However under other conditions (such as different contact geometry or rougher surfaces) the solid lubricant dispersions might be beneficial. E.D.K.

N81-21198* National Aeronautics and Space Administration, Lewis Research Center, Cleveland, Ohio

A SPUTTERED ZIRCONIA PRIMER FOR IMPROVED THERMAL SHOCK RESISTANCE OF PLASMA SPRAYED CERAMIC TURBINE SEALS

R. C. Bill, J. Sovey, and G. P. Allen 1981 14 p refs Presented at the 3d Intern. Conf. on Wear of Mater., San Francisco, 30 Mar. - 1 Apr. 1981 Prepared in cooperation with Army Aviation Research and Development Command, Cleveland (NASA-TM-81732; AVRADCOM-TR-81-C-6; E-742) Avail: NTIS HC A02/MF A01 CSCL 07C

The development of plasma-sprayed yttria stabilized zirconia (YSZ) ceramic turbine blade tip seal components is discussed. The YSZ layers are quite thick (0.040 to 0.090 in.). The service potential of seal components with such thick ceramic layers is cyclic thermal shock limited. The most usual failure mode is ceramic layer delamination at or very near the interface between the plasma sprayed YSZ layer and the NiCrAlY bondcoat. Deposition of a thin RF sputtered YSZ primer to the bondcoat prior to deposition of the thick plasma sprayed YSZ layer was found to reduce laminar cracking in cyclic thermal shock testing. The cyclic thermal shock life of one ceramic seal design was increased by a factor of 5 to 6 when the sputtered YSZ primer was incorporated. A model based on thermal response of plasma sprayed YSZ particles impinging on the bondcoat surface with and without the sputtered YSZ primer provides a basis for understanding the function of the primer. M.G.

N81-22190* National Aeronautics and Space Administration, Lewis Research Center, Cleveland, Ohio

LASER SURFACE FUSION OF PLASMA SPRAYED CERAMIC TURBINE SEALS Patent Application

Donald W. Wisender and Robert C. Bill, inventors (to NASA) Filed 11 Mar. 1981 11 p

(NASA-Case-LEW-13269-1; US-Patent-Appl-SN-242795) Avail: NTIS HC A02/MF A01 CSCL 07C

An abradable lining that is deposited on a shroud forming a gas path seal in turbomachinery is described. Improved thermal shock resistance is effected through the deliberate introduction of microcracks which will not propagate appreciably upon exposure to the thermal shock environment in which a turbine seal must function. The microcracks are introduced by laser surface fusion treatment of the ceramic. The ceramic surface is laser scanned to form a continuous dense layer. As this layer cools and solidifies, shrinkage results in the formation of a very fine crack network which precludes the formation of a catastrophic crack during thermal shock exposure. J.D.H.

N81-22193* National Aeronautics and Space Administration, Lewis Research Center, Cleveland, Ohio

ELECTRON REFLECTION AND SECONDARY EMISSION CHARACTERISTICS OF SPUTTER-TEXTURED PYROLYTIC GRAPHITE SURFACES

Edwin G. Wintucky, Arthur N. Curren, and James S. Sovey 1981 18 p refs Presented at the Intern. Conf. on Met. Coatings, San Francisco, 6-10 Apr. 1981; sponsored by AVS (NASA-TM-81755; E-818) Avail: NTIS HC A02/MF A01 CSCL 11D

Low secondary and reflected primary electron emission from the collector electrode surfaces is important for optimum collector efficiency and hence for high overall efficiency of microwave amplifier tubes used in communication satellites and in military systems. Ion sputter texturing of the surface effectively suppresses electron emission from pyrolytic graphite, which is a promising collector electrode material. Secondary and reflected primary electron emission characteristics of sputter textured pyrolytic graphite surfaces with microstructures of various sizes and densities are presented. The microstructure with the lowest electron emission levels, less than those of soot, consists of a dense array of tall, thin spires. E.D.K.

N81-24257* National Aeronautics and Space Administration, Lewis Research Center, Cleveland, Ohio

IN-SITU CROSS LINKING OF POLYVINYL ALCOHOL Patent

Warren H. Philipp, L-Chen Hsu, and Dean W. Sheibley, inventors (to NASA) Issued 14 Apr. 1981 4 p Filed 18 Jan. 1980 Continuation of abandoned US Patent Appl. SN971475, filed 20 Dec. 1978

(NASA-Case-LEW-13135-2; US-Patent-4,262,067;

US-Patent-Appl-SN-113014; US-Patent-Class-429-139;

US-Patent-Class-429-27; US-Patent-Class-429-28;

US-Patent-Class-429-249; US-Patent-Class-429-253;

US-Patent-Class-264-104; US-Patent-Class-264-105;

US-Patent-Class-525-61; US-Patent-Appl-SN-971475) Avail: US Patent and Trademark Office CSCL 07C

A method of producing a crosslinked polyvinyl alcohol structure, such as a battery separator membrane or electrode envelope is described. An aqueous solution of a film-forming polyvinyl alcohol is admixed with an aldehyde crosslinking agent at a basic pH to inhibit crosslinking. The crosslinking agent, preferably a dialdehyde such as glutaraldehyde, is used in an amount of from about 1/2 to about 20% of the theoretical amount required to crosslink all of the hydroxyl groups of the polymer. The aqueous admixture is formed into a desired physical shape, such as by casting a sheet of the solution. The sheet is then dried to form a self-supporting film. Crosslinking is then effected by immersing the film in aqueous acid solution. The resultant product has excellent properties for use as a battery separator.

Official Gazette of the U.S. Patent and Trademark Office

N81-24265* National Aeronautics and Space Administration, Lewis Research Center, Cleveland, Ohio

THERMAL BARRIER COATING SYSTEM HAVING IMPROVED ADHESION Patent Application

R. C. Bill and J. S. Sovey, inventors (to NASA) Filed 28 Jan. 1981 7 p

(NASA-Case-LEW-13359-1; US-Patent-Appl-SN-229233) Avail: NTIS HC A02/MF A01 CSCL 11A

A metallic bond coat on a substrate is primer coated by depositing an ion sputtered ceramic film. A ceramic thermal barrier coating is then plasma-sprayed onto this primer film. The sputter deposited primer coating improves the integrity and strength of the interface between the plasma-sprayed ceramic layer and metallic bond coat. Improvement of the integrity of the interface insures stronger adherence between the metal and the ceramic. NASA

N81-27277* National Aeronautics and Space Administration, Lewis Research Center, Cleveland, Ohio
CONTACT ANGLE MEASUREMENTS OF A POLYPHENYL ETHER TO 190 C ON M-50 STEEL
William R. Jones, Jr. Jun. 1981 16 p refs
(NASA-TM-82628; E-831) Avail. NTIS HC A02/MF A01 CSCL 07C

Contact angle measurements were performed for a polyphenyl ether on steel in nitrogen. A tilting plate and a sessile drop apparatus were used. Surface tension was measured with a maximum bubble pressure apparatus. Critical surface energies of spreading were found to be 30.1 and 31.3 dynes/cm. It was concluded that the polyphenyl ether is inherently autophobic and will not spread on its own surface film. Author

N81-27279* National Aeronautics and Space Administration, Lewis Research Center, Cleveland, Ohio
CROSS-LINKED POLYVINYL ALCOHOL AND METHOD OF MAKING SAME Patent Application
Dean W. Sheibley, Lora L. Rieker, Li-Chen Hsu, and Michelle A. Manzo, inventors (to NASA) Filed 10 Jun. 1981 14 p
(NASA-Case-LEW-13504-1; US-Patent-Appl-SN-272234) Avail. NTIS HC A02/MF A01 CSCL 07C

A method is described for producing cross-linked polyvinyl alcohol battery separators. A film-forming polyvinyl alcohol resin is admixed, in aqueous solution, with a dialdehyde cross-linking agent which is capable of cross-linking the polyvinyl alcohol resin and a water soluble acid aldehyde. The acid aldehyde contains a reactive aldehyde group capable of reacting with hydroxyl groups in the polyvinyl alcohol resin, and an ionizable acid hydrogen atom. The amount of acid aldehyde is from 1 to 5% by weight and is sufficient to reduce the pH of the aqueous admixture to 5 or less. The admixture is then formed into a desired physical shape, such as by casting a sheet or film and the shaped material is then heated to simultaneously dry and cross-link the article. NASA

N81-27282* National Aeronautics and Space Administration, Lewis Research Center, Cleveland, Ohio
CORRELATION OF IDEAL AND ACTUAL SHEAR STRENGTHS OF METALS WITH THEIR FRICTION PROPERTIES

Kazuhisa Miyoshi and Donald H. Buckley Jul. 1981 12 p refs
(NASA-TP-1891; E-701) Avail. NTIS HC A02/MF A01 CSCL 11F

The relation between the ideal and actual shear strengths and friction properties of clean metals in contact with clean diamond, boron nitride, silicon carbide, manganese-zinc ferrite, and the metals themselves in vacuum is discussed. An estimate of the ideal shear strength for metals is obtained from the shear modulus, the repeat distance of atoms in the direction of shear of the metal, and the interplanar spacing of the shearing planes. The coefficient of friction for metals is shown to be correlated with both the ideal and actual shear strength of metals. The higher the strength of the metal, the lower the coefficient of friction occurs. Author

N81-31366* National Aeronautics and Space Administration, Lewis Research Center, Cleveland, Ohio
EFFECT OF YTTRIA ADDITIVES ON PROPERTIES OF PRESSURELESS-SINTERED SILICON NITRIDE
Alan Arias Sep. 1981 11 p refs
(NASA-TP-1899; E-751) Avail. NTIS HC A02/MF A01 CSCL 11G

Si₃N₄-base ceramics were made from milled Si₃N₄ containing 11.1 wt% SiO₂ and oxide additives by pressureless sintering at 1760 C. The four-point-average moduli of rupture were 460, 515, and 515 MPa at room temperature and 270, 256, and 227 MPa at 1400 C for compositions with 3.67, 7.22, and 14 C wt% Y₂O₃, respectively. The oxidation resistance of these compositions decreased with increasing Y₂O₃ in the 600 to 1400 C range, and no surface oxide cracking or spalling was noted. Partial substitution of Al₂O₃ for Y₂O₃ reduced both strength and oxidation resistance. Author

N81-32269* National Aeronautics and Space Administration, Lewis Research Center, Cleveland, Ohio
EFFECT OF ELECTRONIC STRUCTURE OF THE DIAMOND SURFACE ON THE STRENGTH OF THE DIAMOND-METAL INTERFACE

Stephen V. Pepper 1981 16 p refs. Proposed for presentation at the 28th Natl. Symp. of the Am. Vacuum Soc., Anaheim, Calif., 2-6 Nov. 1981
(NASA-TM-82714; E-998) Avail. NTIS HC A02/MF A01 CSCL 11G

A diamond surface undergoes a transformation in its electronic structure by a vacuum anneal at approximately 900 C. The polished surface has no electronic states in the band gap, whereas the annealed surface has both occupied and unoccupied states in the gap and exhibits some electrical conductivity. The effect of this transformation on the strength of the diamond-metal interface was investigated by measuring the static friction force of an atomically clean metal sphere on a diamond flat in ultrahigh vacuum. It was found that low friction (weak bonding) is associated with the diamond surface devoid of gap states whereas high friction (strong bonding) is associated with the diamond surface with gap states. Exposure of the annealed surface to excited hydrogen also leads to weak bonding. The interfacial bond is discussed in terms of interaction of the metal conduction band electrons with the band gap states on the diamond surface. Effects of surface electrical conductivity on the interfacial bond are also considered. A.R.H.

N81-33293* National Aeronautics and Space Administration, Lewis Research Center, Cleveland, Ohio
RELATIONSHIP BETWEEN THE IDEAL TENSILE STRENGTH AND THE FRICTION PROPERTIES OF METALS IN CONTACT WITH NONMETALS AND THEMSELVES Final Report

Kazuhisa Miyoshi and Donald H. Buckley Washington NASA Sep. 1981 10 p refs
(NASA-TP-1883; E-587) Avail. NTIS HC A02/MF A01 CSCL 11H

The adhesion and friction properties of metals in contact with diamond, boron nitride, silicon carbide, manganese-zinc ferrite, and the metals themselves in vacuum was investigated. An estimate of the ideal uniaxial tensile was obtained in terms of the equilibrium surface energy, interplanar spacing of the planes perpendicular to the tensile axis, and the Young's modulus of elasticity. The coefficient of friction for metals was found to be related to the ideal tensile strength of metals. The higher the strength of the metal, the lower the coefficient of friction. A.R.H.

A81-12630* Thermal barrier coatings - Burner rig hot corrosion test results. P. E. Hodge, S. Stcura, M. A. Gedwill, I. Zaplatynsky, and S. R. Levine (NASA, Lewis Research Center, Cleveland, Ohio). *Journal of Materials for Energy Systems*, vol. 1, Mar. 1980, p. 47-58. 14 refs. Contract No. EF-A-31-2593.

A Mach 0.3 burner rig test program was conducted to examine the sensitivity of thermal barrier coatings to Na- and V-contaminated combustion gases simulating potential utility gas turbine environments. Coating life of the standard ZrO₂-12Y₂O₃/Ni-16.2Cr-5.6Al-0.6Y (composition in wt %) NASA thermal barrier coating system which was developed for aircraft gas turbines was significantly reduced in such environments. Two thermal barrier coating systems, Ca₂SiO₄/Ni-16.2Cr-5.6Al-0.6Y and ZrO₂-8Y₂O₃/Ni-16.4Cr-5.1Al-0.15Y and a less insulative cermet coating system, 50 vol % MgO-50 vol % Ni-19.6Cr-17.1Al-0.97Y/Ni-16.2Cr-5.6Al-0.6Y, were identified as having much improved corrosion resistance compared to the standard coating. (Author)

A81-15984 * Comparative evaluation of insulating properties of plasma-sprayed ceramic coatings. I. Zaplatynsky (NASA, Lewis Research Center, Cleveland, Ohio). (*American Ceramic Society, Annual Conference on Composites and Advanced Materials, 4th, Cocoa Beach, Fla., Jan. 20-24, 1980.*) *Ceramic Engineering and Science Proceedings*, vol. 1, no. 7-8 (B), July-Aug. 1980, p. 609-623. 15 refs.

A simple method for evaluating the thermal insulating capability of ceramic coatings was devised. It is based on monitoring the temperature of the uncoated back surface of a thin superalloy disk while its front surface, coated with the ceramic material, is exposed to the high-temperature environment of an electric muffle furnace. The results obtained indicate that zirconia containing 8 wt% Y₂O₃ is a better thermal insulator than barium zirconate or calcium orthosilicate. (Author)

A81-22529 * # Effect of milling and leaching on the structure of sintered silicon. H. C. Yeh (Cleveland State University, Cleveland, Ohio), T. K. Glasgow, and T. P. Herbell (NASA, Lewis Research Center, Cleveland, Ohio). *American Ceramic Society, Annual Meeting, Chicago, Ill., Apr. 28-30, 1980, Paper*, 13 p. 7 refs.

The effects of attrition milling and acid leaching on the sintering behavior and the resultant structures of two commercial silicon powders were investigated. Sintering was performed in He for 16 hours at 1200, 1250, and 1300 C. Compacts of as-received Si did not densify during sintering. Milling reduced the average particle size to below 0.5 microns and enhanced densification (1.75 g/cc). Leaching milled Si further enhanced densification (1.90 g/cc max.) and decreased structural coarsening. After sintering, the structure of the milled and leached powder compacts appears favorable for the production of reaction bonded silicon nitride. (Author)

A81-28974 * Effect of CeO₂, MgO and Y₂O₃ additions on the sinterability of a milled Si₃N₄ with 14.5 wt% SiO₂. A. Arias (NASA, Lewis Research Center, Cleveland, Ohio). *Journal of Materials Science*, vol. 16, Mar. 1981, p. 787-793. 20 refs.

The sinterability of alpha Si₃N₄ with 0.5-0.7 equivalent per cent of CeO₂, MgO, or Y₂O₃ has been studied in the temperature range 1650-1820 C by density measurements and X-ray diffraction analysis. Maximum densities were obtained in the range 1765-1820 C and were 99.5% of theoretical with 2.5% CeO₂; 98.5% of theoretical with 1.24 to 1.87% MgO, and 99.2% of theoretical with 2.5% Y₂O₃. Densities 94% or more of theoretical value were obtained with as little as 0.62 equivalent per cent additive. V.L.

A81-32545 * # Fracture toughness of brittle materials determined with chevron notch specimens. J. L. Shannon, Jr., R. T. Bubsey, W. S. Pierce (NASA, Lewis Research Center, Cleveland, Ohio), and D. Munz (Karlsruhe, Universität; Kernforschungszentrum Karlsruhe GmbH, Karlsruhe, West Germany). *Société Française de Métallurgie, International Conference on Fracture, 5th, Cannes, France, Mar. 29-Apr. 3, 1981, Paper*, 15 p. 11 refs.

Short bar, short rod, and four-point-bend chevron-notch specimens were used to determine the plane strain fracture toughness of hot-pressed silicon nitride and sintered aluminum oxide brittle ceramics. The unique advantages of this specimen type are: (1) the production of a sharp natural crack during the early stage of test loading, so that no precracking is required; and (2) the load passes through a maximum at a constant, material-independent crack length-to-width ratio for a specific geometry, so that no post-test crack measurement is required. The plane strain fracture toughness is proportional to the maximum test load and functions of the specimen geometry and elastic compliance. Although results obtained for silicon nitride are in good mutual agreement and relatively free of geometry and size effects, aluminum oxide results were affected in both these respects by the rising crack growth resistance curve of the material. O.C.

A81-33859 * Effect of substrate surface finish on the lubrication and failure mechanisms of molybdenum disulfide films. R. L. Fusaro (NASA, Lewis Research Center, Cleveland, Ohio). *American Society of Lubrication Engineers, Annual Meeting, 36th, Pittsburgh, Pa., May 11-14, 1981, Preprint 81-AM-5D-1*, 12 p. 17 refs.

An optical microscope was used to study the lubrication and failure mechanisms of rubbed (burnished) MoS₂ films applied to three substrate surface finishes - polished, sanded, and sandblasted - as a function of sliding distance. The lubrication mechanism was the plastic flow of thin films of MoS₂ between flat plateaus on the rider and on the metallic substrate. If the substrate was rough, flat plateaus were created during 'run-in' and the MoS₂ flowed across them. Wear life was extended by increasing surface roughness since valleys in the roughened substrate served as reservoirs for MoS₂ and a deposit site for wear debris. In moist air the failure mechanism was the transformation of metallic-colored MoS₂ films to a black, powdery material that was found by X-ray diffraction to consist primarily of alpha-iron and MoO₃ powders. In dry argon, the failure mechanism was the gradual depletion of the MoS₂ film from the contact region by transverse flow. Analysis of the wear debris on the wear track at failure showed it consisted mainly of alpha-iron and some residual MoS₂. No molybdenum oxides were found. (Author)

A81-33260 * Dynamics of solid dispersions in oil during the lubrication of point contacts. I - Graphite. C. Cusano (Illinois, University, Urbana, Ill.) and H. E. Stiney (NASA, Lewis Research Center, Cleveland, Ohio). *American Society of Lubrication Engineers, Annual Meeting, 36th, Pittsburgh, Pa., May 11-14, 1981, Preprint 81-AM-5D-3*, 7 p. 10 refs.

A Hertzian contact is lubricated with dispersed graphite in mineral oils under boundary lubrication conditions. The contacts are optically observed under pure rolling, combined rolling and sliding, and pure sliding conditions. The contact is formed with a steel ball on the flat surface of a glass disk. Under pure rolling and combined rolling and sliding conditions, it is found that, for low speeds, a graphite film can form which will separate the contacting surfaces. In contrast, under pure sliding conditions, graphite accumulates at the inlet and sweeps around the contact, but very little of graphite passes through the contact. The accumulated graphite appears to act as a barrier which reduces the supply of oil available to the contact for boundary lubrication. Friction data show no clear short-term beneficial or detrimental effect caused by addition of graphite to the base oil. However, during pure sliding, more abrasion occurs on the polished balls lubricated with the dispersion than on those lubricated with the base oil alone. (Author)

A81-35045 * The generation and morphology of single-crystal silicon carbide wear particles under adhesive conditions. K. Miyoshi and D. H. Buckley (NASA, Lewis Research Center, Cleveland, Ohio). *Wear*, vol. 67, Apr. 1, 1981, p. 303-319. 22 refs.

Sliding friction experiments were performed in vacuum at room temperature on a plane-type SiC surface in contact with iron-based binary alloys. Multiangular and spherical wear particles were found to form as a result of multipass sliding. The multiangular particles were produced by primary and secondary cracking of the 0001, 10(-)10, and 11(-)20 plane-type cleavage planes under the Hertzian stress field or local inelastic deformation zone. When alloy surfaces are in contact with silicon carbide under a load of 0.2 N, the alloy around the contact area is subjected to stresses that are close to the elastic limit in the elastic deformation region and/or exceed it. It was also found that spherical wear particles may be produced by two mechanisms: a penny-shaped fracture along the circular stress trajectories under the local inelastic deformation zone, and the attrition and fatigue of wear particles. E.B.

A81-38065 * # **Electron reflection and secondary emission characteristics of sputter-textured pyrolytic graphite surfaces.** E. G. Wintucky, A. N. Curren, and J. S. Sovey (NASA, Lewis Research Center, Cleveland, OH). *American Vacuum Society, International Conference on Metallurgical Coatings, San Francisco, CA, Apr. 6-10, 1981, Paper*, 16 p. 7 refs.

Measurements are presented of secondary electron emission and reflected primary electron characteristics of sputter-textured pyrolytic graphite surfaces with microstructures of various sizes and densities, made with an Auger cylindrical mirror analyzer in a high-vacuum chamber at pressures below 1.33×10^{-7} to 10^{-9} torr. A dense, tall, thin, spire like microstructure, obtained at ion energies of 1000 eV and ion current densities of 5 mA/sq cm, is the most effective. The secondary electron emission from such a surface is lower than that of soot, whose secondary emission is among the lowest of any material. At a primary electron energy of 1000 eV, the secondary electron emission yield of smooth Cu is about 350% greater than the lowest value obtained for sputter-textured pyrolytic graphite. The reflected primary electron index of smooth Cu is a factor of 80 greater. If the secondary electron emission yield is reduced to 0.3, which is possible with sputter-textured pyrolytic graphite, the traveling wave tube collector efficiency could be improved by as much as 4% over that for smooth copper. K.S.

A81-42024 * **Dissolution of bulk specimens of silicon nitride.** W. F. Davis and E. J. Merkle (NASA, Lewis Research Center, Cleveland, OH). *Analytical Chemistry*, June 1981, p. 1139.

An accurate chemical characterization of silicon nitride has become important in connection with current efforts to incorporate components of this material into advanced heat engines. However, there are problems concerning a chemical analysis of bulk silicon nitride. Current analytical methods require the pulverization of bulk specimens. A pulverization procedure making use of grinding media, on the other hand, will introduce contaminants. A description is given of a dissolution procedure which overcomes these difficulties. It has been found that up to at least 0.6 g solid pieces of various samples of hot pressed and reaction bonded silicon nitride can be decomposed in a mixture of 3 mL hydrofluoric acid and 1 mL nitric acid overnight at 150 C in a Parr bomb. High-purity silicon nitride is completely soluble in nitric acid after treatment in the bomb. Following decomposition, silicon and hydrofluoric acid are volatilized and insoluble fluorides are converted to a soluble form. G.R.

A81-44658 * # **Prolonging thermal barrier coated specimen life by thermal cycle management.** R. C. Hendrick, G. McDonald (NASA, Lewis Research Center, Cleveland, OH), and R. P. Poolos (Harvard University, Cambridge, MA). *American Vacuum Society, International Conference on Metallurgical Coatings, San Francisco, CA, Apr. 6-10, 1981, Paper*, 10 p. 17 refs.

Thermal barrier coatings applied to the heated side of engine components such as seals, combustor, and blades of a gas turbine offer a potential increase in efficiency through the use of higher gas temperatures or less cooling air or benefits arising from extended component life by reducing component metal temperatures. The considered investigation has the objective to show that while a thermal barrier coated (TBC) specimen can be brought to a fixed temperature using various fuel-air ratio (F/A) values, lower calculated stresses are associated with lower (F/A) values. This implies that control of (F/A) values (i.e., rate of heat input) during the starting transient and to a lesser extent during shutdown and operation, offers a potential method of improving TBC lifetime through thermal cycle management. G.R.

N81-10189# Ultrasonics, Inc., Irvine, Calif.
PHOSPHAZENE DIAMINES Contractor Report, Jun. 1979
Apr. 1980

K. L. Paciorek, D. H. Harris, T. I. Ito, and R. H. Kratzer Oct 1980 61 p refs
(Contract NAS3-22019)
(NASA-CR-165147; SN-8342-F) Avail NTIS

HC A04/MF A01 CSCL 11G

The synthesis of a specific phosphazene diamine was optimized, other phosphorus-containing diamines were prepared, and their effect upon certain characteristics of epoxy resins, prepared via reaction with MY 720, in particular, char yield at elevated temperatures was evaluated. The synthesis of the phosphazene diamine resulting from the interaction of methylenedianiline with 4,4'-bis(diphenylphosphino)biphenyl was simplified into a one step process giving 77 percent yield of the pure product. Using this procedure, a related diamine containing bis(diphenylphosphino)methane was obtained in a 70 percent yield. Preparation of another class of phosphorus containing amines based upon p-aminophenyldiphenyl-phosphine was unsuccessful; the inability to produce p-aminophenyl lithium was responsible for this failure. Seven epoxy resins employing Araldite MY 720, diaminodiphenylsulfone, and two of the phosphorus containing diamines were prepared, characterized, and their char yield capacity at elevated temperatures assessed. Based on these investigations, the resins containing phosphorus appear to exhibit significantly better char formation characteristics than materials hardened using conventional amines, without impairing the other properties measured. R.K.G.

N81-14082# General Electric Co., Philadelphia, Pa. Advanced Energy Programs Dept.

IMPROVED CERAMIC HEAT EXCHANGER MATERIALS
Final Report

Harry W. Rauch Dec. 1980 39 p
(Contracts NAS3-19698 EC-77-A-31-1011;
DE-A101-77CS-51040)

(NASA-CR-159678; DOE/NASA/9698-2) Avail NTIS
HC A03/MF A01 CSCL 07C

The development and evaluation of materials for potential application as heat exchanger structures in automotive gas turbine engines is discussed. Test specimens in the form of small monolithic bars were evaluated for thermal expansion and dimensional stability before and after exposure to sea salt and sulfuric acid, followed by short and long term cycling at temperatures up to 1200 C. The material finally selected, GE-7808, consists of the oxides, ZrO₂-MgO-Al₂O₃-SiO₂, and is described generically as ZrMAS. The original version was based on a commercially available cordierite (MAS) frit. However, a clay/talc mixture was demonstrated to be a satisfactory very low cost source of the cordierite (MAS) phase. Several full size honeycomb regenerator cores, about 10.2 cm thick and 55 cm diameter were fabricated from both the frit and mineral versions of GE-7808. The honeycomb cells in these cores had rectangular dimensions of about 0.5 mm x 2.5 mm and a wall thickness of approximately 0.2 mm. The test data show that GE-7808 is significantly more stable at 1100 C in the presence of sodium than the aluminosilicate reference materials. In addition, thermal exposure up to 1100 C, with and without sodium present, results in essentially no change in thermal expansion of GE-7808. M.G.

N81-17283# Acurex Corp., Mountain View, Calif. Aerotherm Div.

SYNTHESIS OF IMPROVED PHENOLIC AND POLYESTER RESINS Final Report

C. B. Delano 27 Sep. 1980 79 p refs
(Contract NAS3-22025)

(NASA-CR-165180; FR-80-42/AS) Avail NTIS
HC A05/MF A01 CSCL 07C

Thirty-seven cured phenolic resin compositions were prepared and tested for their ability to provide improved char residues and moisture resistance over state of the art epoxy resin composite matrices. Cyanate, epoxy novolac and vinyl ester resins were investigated. Char promoter additives were found to increase the anaerobic char yield at 800 C of epoxy novolacs and vinyl esters. Moisture resistant cyanate and vinyl ester compositions were investigated as composite matrices with Thorne 300 graphite fiber. A cyanate composite matrix provided state of the art composite mechanical properties before and after humidity exposure and an anaerobic char yield of 46 percent at 800 C. The outstanding moisture resistance of the matrix was not completely realized in the composite. Vinyl ester resins showed promise as candidates for improved composite matrix systems. Author

28 PROPELLANTS AND FUELS

Includes rocket propellants, igniters, and oxidizers, storage and handling, and aircraft fuels.

For related information see also 07 Aircraft Propulsion and Power, 20 Spacecraft Propulsion and Power, and 44 Energy Production and Conversion.

N81-14103* National Aeronautics and Space Administration, Lewis Research Center, Cleveland, Ohio.

ATOMIC HYDROGEN STORAGE METHOD AND APPARATUS Patent

John A. Woollam, inventor (to NASA) Issued 21 Oct. 1980 4 p Filed 6 Feb. 1979 Supersedes N79-18455 (17-09, p 1157) Division of US Patent Appl. SN-837794, filed 29 Sep. 1977, US Patent-4,193,827, which is a division of US Patent Appl. SN-875432, filed 13 Apr. 1976, US Patent-4,077,788 (NASA-Case-LEW-12081-3; US-Patent-4,229,196; US-Patent-4,193,827; US-Patent-4,077,788; US-Patent-Appl-SN-009887; US-Patent-Appl-SN-837794; US-Patent-Appl-SN-676432; US-Patent-Class-62-40; US-Patent-Class-62-47; US-Patent-Class-62-18; US-Patent-Class-62-12; US-Patent-Class-55-2; US-Patent-Class-423-648R; US-Patent-Class-156-344; US-Patent-Class-149-1; US-Patent-Class-44-7R) Avail: US Patent and Trademark Office CSCL 21D

Atomic hydrogen, for use as a fuel or as an explosive, is stored in the presence of a strong magnetic field in exfoliated layered compounds such as molybdenum disulfide or an elemental layer material such as graphite. The compounds maintained at liquid helium temperatures and the atomic hydrogen is collected on the surfaces of the layered compound which are exposed during delamination (exfoliation). The strong magnetic field and the low temperature combine to prevent the atoms of hydrogen from recombining to form molecules.

Official Gazette of the U.S. Patent and Trademark Office

N81-24283* National Aeronautics and Space Administration, Lewis Research Center, Cleveland, Ohio.

EFFECT OF HYDROPROCESSING SEVERITY ON CHARACTERISTICS OF JET FUEL FROM OSCO 2 AND PARAHIO DISTILLATES

George M. Prok, Francisco J. Flores, and Gary T. Seng Jun. 1981 20 p refs (NASA-TP-1768; E-617) Avail: NTIS HC A02/MF A01 CSCL 21D

Jet A boiling range fuels and broad-property research fuels were produced by hydroprocessing shale oil distillates, and their properties were measured to characterize the fuels. The distillates were the fraction of whole shale oil boiling below 343 C from TOSCO 2 and Paraho syn-crudes. The TOSCO 2 was hydroprocessed at medium severity, and the Paraho was hydroprocessed at high, medium, and low severities. Fuels meeting Jet A requirements except for the freezing point were produced from the medium severity TOSCO 2 and the high severity Paraho. Target properties of a broad property research fuel were met by the medium severity TOSCO 2 and the high severity Paraho except for the freezing point and a high hydrogen content. Medium and low severity Paraho jet fuels did not meet thermal stability and freezing point requirements. E.D.K.

N81-25232* National Aeronautics and Space Administration, Lewis Research Center, Cleveland, Ohio.

AVIATION TURBINE FUEL PROPERTIES AND THEIR TRENDS

Robert Friedman 1981 27 p refs Proposed for presentation at the West Coast Intern. Meeting, Seattle, 3-6 Aug. 1981; sponsored by the Society of Automotive Engineers (NASA-TM-82603; E-851) Avail: NTIS HC A03/MF A01 CSCL 21D

Fuel property values and their trends were studied through a review of a recognized, wide ranging sample population from actual fuel inspection data. A total of 676 fuel samples of Jet A aviation turbine fuel were compiled over an eleven year

period. Results indicate that most fuel samples have one to three near-specification properties, the most common being aromatics, smoke point, and freezing point. R.C.T.

N81-29246* National Aeronautics and Space Administration, Lewis Research Center, Cleveland, Ohio.

PERFORMANCE TESTS OF A GAS BLENDING SYSTEM BASED ON MASS-FLOW CONTROLLERS

Albert Evans, Jr. Aug. 1981 16 p refs (NASA-TP-1896; E-629) Avail: NTIS HC A02/MF A01 CSCL 21D

The system provides many of the gas mixtures required for calibrating analytical instruments used in engine exhaust gas analysis and is capable of blending from one to four additive gases with either of two carrier gases in concentrations from 20 ppm to 50%. Two mixtures can be flowing simultaneously. Performance tests were made to determine the stability accuracy of the system while it was in limited use for a period of 2 years. The accuracy of the blender was measured by comparing binary mixtures from the blender with National Bureau of Standards standard reference materials. Analytical instruments were used to make these comparisons. The expected accuracy of 2% was obtained in some of the tests, by the majority showed a systematic bias of -5%. Although these tests revealed subtle instabilities in the flow controllers that contributed to the random scatter of data, the accuracy of wet test meters and bubble flowmeters used for calibration is marginal for this purpose. A simple procedure is recommended that should enable the full potential of the system to be realized. E.D.K.

N81-31380* National Aeronautics and Space Administration, Lewis Research Center, Cleveland, Ohio.

INFRARED SPECTROSCOPY FOR THE DETERMINATION OF HYDROCARBON TYPES IN JET FUELS

Constance S. Bucher Aug. 1981 10 p refs (NASA-TM-82674; E-957) Avail: NTIS HC A02/MF A01 CSCL 21D

The concentration of hydrocarbon types in conventional jet fuels and synfuels can be measured using a computerized infrared spectrophotometer. The computerized spectrophotometer is calibrated using a fuel of known aromatic and olefinic content. Once calibration is completed, other fuels can be rapidly analyzed using an analytical program built into the computer. The concentration of saturates can be calculated as 100 percent minus the sum of the aromatic and olefinic concentrations. The analysis of a number of jet fuels produced an average standard deviation of 1.76 percent for aromatic type, and one of 3.99 percent for olefinic types. Other substances such as alcohols and organic mixtures can be analyzed for their hydrocarbon content. Author

A81-11612* Advanced fuel system technology for utilizing broadened property aircraft fuels. G. M. Reck (NASA, Lewis Research Center, Cleveland, Ohio). In: International Council of the Aeronautical Sciences, Congress, 12th, Munich, West Germany, October 12-17, 1980, Proceedings. (A81-11601 02-01) New York, American Institute of Aeronautics and Astronautics, Inc., 1980, p. 129-143, 28 refs.

Factors which will determine the future supply and cost of aviation turbine fuels are discussed. The most significant fuel properties of volatility, fluidity, composition, and thermal stability are discussed along with the boiling ranges of gasoline, naphtha jet fuels, kerosene, and diesel oil. Tests were made to simulate the low temperature of an aircraft fuel tank to determine fuel tank temperatures for a 9100-km flight with and without fuel heating; the effect of N content in oil-shale derived fuels on the Jet Fuel Thermal Oxidation Tester breakpoint temperature was measured. Finally, compatibility of non-metallic gaskets, sealants, and coatings with increased aromatic content jet fuels was examined. A.T.

A81-30056 * # Evaluation of concepts for controlling exhaust emissions from minimally processed petroleum and synthetic fuels. Z. L. Russell, G. W. Beal (United Technologies Corp., Government Products Div., West Palm Beach, Fla.), R. A. Sederquist (United Technologies Corp., Power Systems Div., South Windsor, Conn.), and D. Shultz (NASA, Lewis Research Center, Cleveland, Ohio). *American Society of Mechanical Engineers, Gas Turbine Conference and Products Show, Houston, Tex., Mar. 9-12, 1981, Paper 81-GT-157*. 8 p. Members, \$2.00; nonmembers, \$4.00. Research supported by the U.S. Department of Energy and NASA.

Rich-lean combustion concepts designed to enhance rich combustion chemistry and increase combustor flexibility for NO(x) reduction with minimally processed fuels are examined. Processes such as rich product recirculation in the rich chamber, rich-lean annihilation, and graduated air addition or staged rich combustion to release bound nitrogen in steps of reduced equivalence ratio are discussed. Variations to the baseline rapid quench section are considered, and the effect of residence time in the rich zone is investigated. The feasibility of using uncooled non-metallic materials for the rich zone combustion construction is also addressed. The preliminary results indicate that rich primary zone staged combustion provides environmentally acceptable operation with residual and/or synthetic coal-derived liquid fuels. L.S.

A81-44661 * # Safety management of complex research operations. W. J. Brown (NASA, Lewis Research Center, Cleveland, OH). *American Nuclear Society, International System Safety Conference, 5th, Denver, CO, July 26-31, 1981, Paper*. 18 p.

Complex research and technology operations present many varied potential hazards which must be addressed in a disciplined independent safety review and approval process. The research and technology effort at the Lewis Research Center is divided into programmatic areas of aeronautics, space and energy. Potential hazards vary from high energy fuels to hydrocarbon fuels, high pressure systems to high voltage systems, toxic chemicals to radioactive materials and high speed rotating machinery to high powered lasers. A Safety Permit System presently covers about 600 potentially hazardous operations. The Safety Management Program described in this paper is believed to be a major factor in maintaining an excellent safety record at the Lewis Research Center. (Author)

N81-12255*# United Technologies Corp., East Hartford, Conn. **EXPERIMENTAL STUDY OF THE STABILITY OF AIRCRAFT FUELS AT ELEVATED TEMPERATURES**

Alexander Vranos and Pierre J. Marteney Dec. 1980 31 p refs
(Contract NAS3-21593)
(NASA-CR-165165, R80-954440-17) Avail: NTIS
HC A03/MF A01 CSCL 21D

An experimental study of fuel stability was conducted in an apparatus which simulated an aircraft gas turbine fuel system. Two fuels were tested: Jet A and Number 2 Home Heating oil. Jet A is an aircraft gas turbine fuel currently in wide use. No. 2 HH was selected to represent the properties of future turbine fuels, particularly experimental Reference Broad Specification, which, under NASA sponsorship, was considered as a possible next generation fuel. Tests were conducted with varying fuel flow rate, delivery pressures and fuel pretreatments (including preheating and deoxygenation). Simulator wall temperatures were varied between 422K and 672K at fuel flows of 0.022 to 0.22 Kg/sec. Coking rate was determined at four equally-spaced locations along the length of the simulator. Fuel samples were collected for infrared analysis. The dependence of coking rate in Jet A may be correlated with surface temperature via an activation energy of 9 to 10 kcal/mole, although the results indicate that both bulk fluid and surface temperature affect the rate of decomposition. As a consequence, flow rate, which controls bulk temperature, must also be considered. Taken together, these results suggest that the decomposition reactions are initiated on the surface and continue in the bulk fluid. The coking rate data for No. 2 HH oil are very highly temperature dependent above approximately 533K. This suggests that bulk phase reactions can become controlling in the formation of coke. Author

N81-19316*# Pratt and Whitney Aircraft Group, East Hartford, Conn. Commercial Products Div.

AN ASSESSMENT OF THE USE OF ANTIMISTING FUEL IN TURBOFAN ENGINES Final Report, Sep. 1979 - Nov. 1980

A. Fiorentino, R. DeSaro, and T. Franz Nov. 1980 146 p refs

(Contract NAS3-22045)

(NASA-CR-165258, PWA-5697-29)

Avail: NTIS

HC A07/MF A01 CSCL 21D

The effects of antimisting kerosene on the performance of the components from the fuel system and the combustor of a JT8D aircraft engine were evaluated. The problems associated with antimisting kerosene were identified and the extent of shearing or degradation required to allow the engine components to achieve satisfactory operation were determined. The performance of the combustor was assessed in a high pressure facility and in an altitude reflight/cold ignition facility. The performance of the fuel pump and control system was evaluated in an open loop simulation. R.C.T.

N81-21213*# Beech Aircraft Corp., Boulder, Colo. **CONCEPTUAL DESIGN OF AN IN-SPACE CRYOGENIC FLUID MANAGEMENT FACILITY**

G. S. Willen, D. H. Riemer, and D. C. Hustvedt Apr. 1981 229 p refs

(Contract NAS3-22260)

(NASA-CR-165279, BAC-ER-14967)

Avail: NTIS

HC A11/MF A01 CSCL 21H

The conceptual design of a Spacelab experiment to develop the technology associated with low gravity propellant management is presented. The proposed facility consisting of a supply tank, receiver tank, pressurization system, instrumentation, and supporting hardware, is described. The experimental objectives, the receiver tank to be modeled, and constraints imposed on the design by the space shuttle, Spacelab, and scaling requirements, are described. The conceptual design, including the general configurations, flow schematics, insulation systems, instrumentation requirements, and internal tank configurations for the supply tank and the receiver tank, is described. Thermal, structural, fluid, and safety and reliability aspects of the facility are analyzed. The facility development plan, including schedule and cost estimates for the facility, is presented. A program work breakdown structure and master program schedule for a seven year program are included. J.D.H.

31 ENGINEERING (GENERAL)

Includes vacuum technology; control engineering; display engineering; and cryogenics.

N81-16327* National Aeronautics and Space Administration, Lewis Research Center, Cleveland, Ohio.

TEXTURING POLYMER SURFACES BY TRANSFER CASTING Patent Application

Bruce A. Banks, Albert J. Weigand, and James S. Sovey, inventors (to NASA) Filed 19 Dec. 1980 7 p (NASA-Case-LEW-13120-1; US-Patent-Appl-SN-218587) Avail: NTIS HC A02/MF A01 CSCL 13H

A surface of a fluorocarbon polymer is exposed to a beam of ions from a source to texture it. The polymer which is to be surface roughened is then cast over the textured surface of the fluorocarbon polymer. After curing, the cast polymer is peeled off the textured fluorocarbon polymer and the peeled off surface has a negative replica of the textured surface. The microscopic surface texture provides large surface area for adhesive bonding. In cardiovascular prosthesis applications the surfaces are relied on for the development of a thin adherent well nourished thrombus.

NASA

N81-16329* National Aeronautics and Space Administration, Lewis Research Center, Cleveland, Ohio.

MECHANICAL BONDING OF METAL Patent Application

Bruce A. Banks, inventor (to NASA) Filed 26 Nov. 1980 8 p (NASA-Case-LEW-12941-1; US-Patent-Appl-SN-210632) Avail: NTIS HC A02/MF A01 CSCL 13H

The metal surfaces of the structures that are to be bonded are exposed to an ion beam together with a target of low sputtering yield material. This material deposits on the surfaces and creates sites of sputter resistance which evolve into peaks of a conelike surface microstructure. The textured metal surfaces are arranged in face-to-face relationship and compressed together with plastic deformation which mechanically interlocks the cone. A large interface area is produced which minimizes thermal and electrical losses. Also, no electrical power or heat is required during metal joining. The process can be performed in either air or vacuum.

NASA

N81-25263* National Aeronautics and Space Administration, Lewis Research Center, Cleveland, Ohio.

SAFETY MANAGEMENT OF COMPLEX RESEARCH OPERATORS

William J. Brown 30 Jul. 1981 20 p refs Proposed for presentation at the 5th Intern. System Safety Conf., Denver, 30 Jul. 1981 (NASA-TM-81772, E-832) Avail: NTIS HC A02/MF A01 CSCL 13L

Complex research and technology operations present varied potential hazards which are addressed in a disciplined, independent safety review and approval process. Potential hazards vary from high energy fuels to hydrocarbon fuels, high pressure systems to high voltage systems, toxic chemicals to radioactive materials and high speed rotating machinery to high powered lasers. A Safety Permit System presently covers about 600 potentially hazardous operations. The Safety Management Program described is believed to be a major factor in maintaining an excellent safety record.

S F

A81-27148 * Global calibration of terrestrial reference cells and errors involved in using different irradiance monitoring techniques. H. B. Curtis (NASA, Lewis Research Center, Cleveland, Ohio). In: Photovoltaic Specialists Conference, 14th, San Diego, Calif., January 7-10, 1980, Conference Record. (A81-27076 11-44) New York, Institute of Electrical and Electronics Engineers, Inc., 1980, p. 500-505. 7 refs.

A81-18667 * Some limitations in applying classical EHD film thickness formulas to a high-speed bearing. J. J. Coy (U.S. Army, Propulsion Laboratory, Cleveland, Ohio) and E. V. Zaretsky (NASA, Lewis Research Center, Cleveland, Ohio). *American Society of Mechanical Engineers and American Society of Lubrication Engineers, Century 2 International Lubrication Conference, San Francisco, Calif., Aug. 18-21, 1980, ASME Paper 80-C2/Lub-13*. 7 p. 28 refs. Members, \$1.50; nonmembers, \$3.00.

Elastohydrodynamic film thickness was measured for a 20-mm ball bearing using the capacitance technique. The bearing was thrust loaded to 90, 448, and 778 N. The corresponding maximum stresses on the inner race were 1.28, 2.09, and 2.45 GPa. Test speeds ranged from 400 to 14,000 rpm. Film thickness measurements were taken with four different lubricants: (a) synthetic paraffinic, (b) synthetic paraffinic with additives, (c) neopentylpolyol (tetra) ester meeting MIL-L-23699A specifications, and (d) synthetic cycloaliphatic hydrocarbon traction fluid. The test bearing was mist lubricated. Test temperatures were 300, 338, and 393 K. The measured results were compared to theoretical predictions using the formulas of Grubin, Archard and Cowking, Dowson and Higginson, and Hamrock and Dowson. There was good agreement with theory at low dimensionless speed, but the film was much smaller than theory predicts at higher speeds. This was due to kinematic starvation and inlet shear heating effects.

(Author)

32 COMMUNICATIONS

Includes land and global communications, communications theory, and optical communications.

For related information see also 04 Aircraft Communications and Navigation and 17 Spacecraft Communications, Command and Tracking.

N81-10239* National Aeronautics and Space Administration, Lewis Research Center, Cleveland, Ohio.

AN ECONOMICS SYSTEMS ANALYSIS OF LAND MOBILE RADIO TELEPHONE SERVICES

B. E. Leroy and S. M. Stevenson 13 Nov. 1980 15 p. refs. Presented at INTELCOM 80/Los Angeles Conf., Los Angeles, 10-13 Nov. 1980.

(NASA-TM-81476, E-589) Avail: NTIS HC A02/MF A01 CSCL 17B

The economic interaction of the terrestrial and satellite systems is considered. Parametric equations are formulated to allow examination of necessary user thresholds and growth rates as a function of system costs. Conversely, first order allowable systems costs are found as a function of user thresholds and growth rates. Transitions between satellite and terrestrial service systems are examined. User growth rate density (user/year/sq km) is shown to be a key parameter in the analysis of systems compatibility. The concept of system design matching the price/demand curves is introduced and examples are given. The role of satellite systems is critically examined and the economic conditions necessary for the introduction of satellite service are identified. Author

N81-10240* National Aeronautics and Space Administration, Lewis Research Center, Cleveland, Ohio.

EXPERIMENTAL INVESTIGATION OF INTERMODULATION EFFECTS AND RELATED EFFICIENCIES ASSOCIATED WITH TWO- AND THREE-SIGNAL OPERATION OF A TRAVELING WAVE TUBE

Thomas A. Fox Oct. 1980 30 p. refs.

(NASA-TM-81576, E-546) Avail: NTIS HC A03/MF A01 CSCL 17B

An experimental investigation of multiple signal operations using an octave bandwidth traveling wave tube (TWT) was conducted in order to approximate the behavior of a TWT being developed for multichannel digital communication. Test results include the intermodulation effects as well as collector and overall efficiencies associated with two and three discrete signal operations. Data are presented for operations that cover approximately a 4 dB range in combined signal output power up to the maximum RF power achievable in each case. (For multiple signal operation the term maximum power is more appropriate than saturation). The power associated with intermodulation products was very small at operating levels 4 dB below maximum power, but it approached 15 percent of the total combined output at maximum power for the two signal case and 20 percent for the three signal case. The maximum RF output powers in the multiple signal cases were 20 to 25 percent lower than the saturated output level for any of the signals inserted individually. In general, both the collector (a five stage depressed collector was used) and overall tube efficiencies were adversely affected during multiple signal operation in a manner related to the power levels involved. At 4 dB below maximum, where the intermodulation effects were small, it was possible to achieve collector and overall efficiencies with multiple signals that are comparable to single signal efficiencies. This changed gradually until at maximum RF output the collector efficiencies were several percentage points less and the overall efficiency as much as 10 percentage points less (a change of 25 percent) than single frequency values. The large overall efficiency loss is partially due to the loss in collector efficiency but largely due to the loss in usable RF power that is associated with the intermodulation power. The three signal tests were always the more severely affected. Author

N81-10241* National Aeronautics and Space Administration, Lewis Research Center, Cleveland, Ohio.

SATELLITES USING THE 30/20 GHz BAND

Joseph N. Sivo 1980 16 p. To be presented at the 1980 Natl. Telecommunications Conf., Houston, Texas, 30 Nov. - 4 Dec.; Sponsored by IEEE.

(NASA-TM-81600, E-586) Avail: NTIS HC A02/MF A01 CSCL 17B

A review of the future options open to satellite system planners focuses attention on the use of the 30/20 GHz band. Very broad bandwidths available, coupled with a primary allocation for fixed satellite service, make the band very attractive. NASA, in concert with the system and service supplier industries, is planning a research and development program aimed at flight demonstration of 30/20 satellite systems which it is hoped will lead to operational system use in the early 1990's. The communication system concepts and the spacecraft systems necessary to support these for operational use in 1990 and beyond are discussed. Author

A81-21911* Carrier Interference Ratio for frequency sharing between satellite systems transmitting frequency modulated and digital television signals. S. P. Barnes (NASA, Lewis Research Center, Cleveland, Ohio). In: NTC '79; National Telecommunications Conference, Washington, D.C., November 27-29, 1979, Conference Record, Volume 3. (A81-21831 08-32) Piscataway, N.J., Institute of Electrical and Electronics Engineers, Inc., 1979, p. 57.5.1-57.5.6.

As the data rates required for digitally encoded television are reduced, satellite systems employing the transmission of digitally encoded television will become attractive. It is likely that television transmitted in this format will be adjacent to or in the same frequency band as television transmissions in other modulation formats, so a knowledge of carrier to interference power ratios as a function of assessed picture quality will be required for frequency sharing between these different modulation formats. This paper presents the results of subjective and quantitative tests describing the results of interference to a particular digital television system from a frequency modulated (FM) television system, and for interference to an FM television system from a digital television system. (Author)

A81-22528* An economic systems analysis of land mobile radio telephone services. B. E. LeRoy and S. M. Stevenson (NASA, Lewis Research Center, Cleveland, Ohio). *Horizon House, INTEL-COM 80/Los Angeles Conference, Los Angeles, Calif., Nov. 10-13, 1980, Paper*. 14 p. 7 refs.

This paper deals with the economic interaction of the terrestrial and satellite land-mobile radio service systems. The cellular, trunked and satellite land-mobile systems are described. Parametric equations are formulated to allow examination of necessary user thresholds and growth rates as functions of system costs. Conversely, first order allowable systems costs are found as a function of user thresholds and growth rates. Transitions between satellite and terrestrial service systems are examined. User growth rate density (user/year/km squared) is shown to be a key parameter in the analysis of systems compatibility. The concept of system design matching the price demand curves is introduced and examples are given. The role of satellite systems is critically examined and the economic conditions necessary for the introduction of satellite service are identified. L.S.

A81-33532* Advanced communications satellites. J. N. Sivo (NASA, Lewis Research Center, Cleveland, Ohio). *American Astronautical Society and American Institute of Aeronautics and Astronautics, Annual Meeting on Space Enhancing Technology Leadership, Boston, Mass., Oct. 20-23, 1980, AAS Paper 80-206*. 18 p. 9 refs.

The paper presents satellite system concepts that are likely in the 1990's and may bring a new dimension to satellite communication services. The NASA 30/20 GHz communications satellite demonstration program is discussed with emphasis on the related technology development. Two general types of services are examined: trunking services and customer premises services. P.T.H.

A81-39144 * # High power densities from high-temperature material interactions. J. F. Morris (NASA, Lewis Research Center, Cleveland, OH). *American Institute of Aeronautics and Astronautics, Thermophysics Conference, 16th, Palo Alto, CA, June 23-25, 1981, Paper 81-1161*. 15 p. 84 refs. Contract No. EC-77-A-31-1062.

Thermionic energy conversion (TEC) and metallic-fluid heat pipes (MFHPs), offering unique advantages in terrestrial and space energy processing by virtue of operating on working-fluid vaporization/condensation cycles that accept great thermal power densities at high temperatures, share complex materials problems. Simplified equations are presented that verify and solve such problems, suggesting the possibility of cost-effective applications in the near term for TEC and MFHP devices. Among the problems discussed are: the limitation of alkali-metal corrosion, protection against hot external gases, external and internal vaporization, interfacial reactions and diffusion, expansion coefficient matching, and creep deformation. O.C.

NS1-10242*# Mitre Corp., Bedford, Mass.

SECOND YEAR TECHNICAL REPORT ON-BOARD PROCESSING FOR FUTURE SATELLITE COMMUNICATIONS SYSTEMS

William T. Brandon, Warren K. Green, Murray Hoffman, Paul N. Jean, William R. Neal, and Brian E. White Oct. 1980 255 p refs

(Contract F19628-80-C-0001)

(NASA-CR-165155; MTR-8164; TR-2) Avail: NTIS HC A10/MF A01 CSCL 17B

Advanced baseband and microwave switching techniques for large domestic communications satellites operating in the 30/20 GHz frequency bands are discussed. The nominal baseband processor throughput is one million packets per second (1.6 Gb/s) from one thousand T1 carrier rate customer premises terminals. A frequency reuse factor of sixteen is assumed by using 16 spot antenna beams with the same 100 MHz bandwidth per beam and a modulation with a one b/s per Hz bandwidth efficiency. Eight of the beams are fixed on major metropolitan areas and eight are scanning beams which periodically cover the remainder of the U.S. under dynamic control. User signals are regenerated (demodulated/remodulated) and message packages are reformatted on board. Frequency division multiple access and time division multiplex are employed on the uplinks and downlinks, respectively, for terminals within the coverage area and dwell interval of a scanning beam. Link establishment and packet routing protocols are defined. Also described is a detailed design of a separate 100 x 100 microwave switch capable of handling nonregenerated signals occupying the remaining 2.4 GHz bandwidth with 60 dB of isolation, at an estimated weight and power consumption of approximately 400 kg and 100 W, respectively. M.G.

33 ELECTRONICS AND ELECTRICAL ENGINEERING

Includes test equipment and maintainability components, e.g. tunnel diodes and transistors; microminiaturization; and integrated circuitry.

For related information see also 60 *Computer Operations and Hardware* and 76 *Solid-State Physics*.

N81-11315* National Aeronautics and Space Administration, Lewis Research Center, Cleveland, Ohio.

MODULAR INSTRUMENTATION SYSTEM FOR REAL-TIME MEASUREMENTS AND CONTROL ON RECIPROCATING ENGINES

William J. Rice and Arthur G. Birchenough Nov. 1980 14 p refs
(NASA-TP-1757; E-455) Avail: NTIS HC A02/MF A01 CSCL 148

An instrumentation system was developed for reciprocating engines. Among the parameters measured are the indicated mean effective pressure, or theoretical work per cycle, and the mass fraction burn rate, a measure of the combustion rate in the cylinder. These computations are performed from measured cylinder pressure and crankshaft angle and are available in real time for the experimenter. A 100 or 200 consecutive-cycle sample is analyzed to reduce the effect of cyclic variations in the engine. Data are displayed in bargraph form, and the mean and standard deviation are computed. Other instruments are also described.

Author

N81-16384* National Aeronautics and Space Administration, Lewis Research Center, Cleveland, Ohio.

GYROTRON TRANSMITTING TUBE Patent Application

Henry G. Kosmahl, inventor (to NASA) Filed 24 Dec. 1980 9 p

(NASA-Case-LEW-13429-1; US-Patent-Appl-SN-220212) Avail: NTIS HC A02/MF A01 CSCL 09A

An R.F. transmitting tube for the 20 GHz to 500 GHz range comprises a gyrotron and a multistage depressed collector. A winding provides a magnetic field which acts on spent, spinning or orbiting electrons changing their motion to substantially forward linear motion in a downstream direction. The spent electrons then pass through a focuser into the collector. Nearly all of the electrons injected into the collector will remain within an imaginary envelope as they travel forward toward the end collector plate. The apertures in the collector plates are at least as large in diameter as the 5 envelope at any particular axial position.

NASA

N81-16388* National Aeronautics and Space Administration, Lewis Research Center, Cleveland, Ohio.

HIGH TEMPERATURE ELECTRONIC REQUIREMENTS IN AEROPROPULSION SYSTEMS

William C. Nieberding and J. Anthony Powell 1981 5 p refs
Proposed for presentation at High-Temp. Electron. Conf., Tucson, Ariz., 25-27 Mar. 1981; sponsored by NASA, DOE and IEEE (NASA-TM-81682; E-708) Avail: NTIS HC A02/MF A01 CSCL 09C

This paper discusses the needs for high temperature electronic and electrooptic devices as they would be used on aircraft engines in either research and development applications, or operational applications. The conclusion reached is that the temperature at which the devices must be able to function is in the neighborhood of 500 to 600 C either for research and development or for operational applications. In research and development applications, the devices must function in this temperature range when in the engine but only for a moderate period of time. On an operational engine, the reliability requirements dictate that the devices be able to be burned-in at temperatures significantly higher than those at which they will function on the engine. The major point made is that semiconductor technology must be pushed well beyond the level at which silicon will be able to function.

Author

N81-20359* National Aeronautics and Space Administration, Lewis Research Center, Cleveland, Ohio.

THREE-AXIS ELECTRON-BEAM TEST FACILITY

James A. Dayton, Jr. and Ben T. Ebihara Mar. 1981 8 p
(NASA-TP-1836; E-582) Avail: NTIS HC A02/MF A01 CSCL 09C

An electron beam test facility, which consists of a precision multidimensional manipulator built into an ultra-high-vacuum bell jar, was designed, fabricated, and operated at Lewis Research Center. The position within the bell jar of a Faraday cup which samples current in the electron beam under test, is controlled by the manipulator. Three orthogonal axes of motion are controlled by stepping motors driven by digital indexers, and the positions are displayed on electronic totalizers. In the transverse directions, the limits of travel are approximately ± 2.5 cm from the center with a precision of 2.54 micron (0.0001 in.); in the axial direction, approximately 15.0 cm of travel are permitted with an accuracy of 12.7 micron (0.0005 in.). In addition, two manually operated motions are provided, the pitch and yaw of the Faraday cup with respect to the electron beam can be adjusted to within a few degrees. The current is sensed by pulse transformers and the data are processed by a dual channel box car averager with a digital output. The beam tester can be operated manually or it can be programmed for automated operation. In the automated mode, the beam tester is controlled by a microcomputer (installed at the test site) which communicates with a minicomputer at the central computing facility. The data are recorded and later processed by computer to obtain the desired graphical presentations.

Author

N81-21281* National Aeronautics and Space Administration, Lewis Research Center, Cleveland, Ohio.

ELECTRIC VEHICLE MOTORS AND CONTROLLERS

Richard R. Secunde 1981 33 p refs Presented at the 5th Intern. Workshop on Rare Earth: Cobalt Magnets and their Applications, Roanoke, Va., 7-10 Jun. 1981

(Contract DE-AI01-77CS-51044)

(NASA-TM-81780; DOE/NASA/51044-18; E-823) Avail: NTIS HC A03/MF A01 CSCL 09C

Improved and advanced components being developed include electronically commutated permanent magnet motors of both drum and disk configuration, an unconventional brush commutated motor, and ac induction motors and various controllers. Test results on developmental motors, controllers, and combinations thereof indicate that efficiencies of 90% and higher for individual components, and 80% to 90% for motor/controller combinations can be obtained at rated power. The simplicity of the developmental motors and the potential for ultimately low cost electronics indicate that one or more of these approaches to electric vehicle propulsion may eventually displace presently used controllers and brush commutated dc motors.

E.D.K.

N81-24348* National Aeronautics and Space Administration, Lewis Research Center, Cleveland, Ohio.

LADDER SUPPORTED RING BAR CIRCUIT Patent Application

H. G. Kosmahl, inventor (to NASA) Filed 3 Apr. 1981 11 p
(NASA-Case-LEW-13570-1; US-Patent-Appl-SN-251009) Avail: NTIS HC A02/MF A01 CSCL 09A

An improved slow wave circuit especially useful in backward wave oscillators is comprised of rings disposed between and attached to respective stubs which are themselves attached to opposing sidewalls of the waveguide. To the end that opposed, interacting magnetic fields will be established to provide a very high coupling impedance for the slow wave structure, axially orientated bars are connected between rings in alternate spaces and adjacent to the attachment points of stubs. Similarly, axial bars are connected between rings in the spaces which do not include bars and at points adjacent to the attachments of bars. The rings may be half rings of 180 deg arc and may be formed of flat metal ribbons.

NASA

N81-28352* National Aeronautics and Space Administration, Lewis Research Center, Cleveland, Ohio.

ANALYTICAL PREDICTION AND EXPERIMENTAL VERIFICATION OF PERFORMANCE AT VARIOUS OPERATING CONDITIONS OF A DUAL-MODE TRAVELING WAVE TUBE WITH MULTISTAGE DEPRESSED COLLECTORS

James A. Dayton, Jr., Henry G. Kosmahl, Peter Ramins, and Norbert Stankiewicz Jul. 1981 27 p refs

(NASA-TP-1831; E-577) Avail: NTIS HC A03/MF A01 CSCL 09C

A comparison of analytical and experimental results is presented for a high performance dual-mode traveling wave tube (TWT) operated over a wide range conditions. The computations are carried out with advanced multidimensional computer programs. These programs model the electron beam as a series of disks or rings of charge and follow their trajectories from the rf input of the TWT through the slow-wave structure refocusing system to their points of impacts in the depressed collector. TWT performance, collector efficiency, and collector current distribution are computed and compared with measurements. Very good agreement was obtained between computed and measured TWT performance and collector efficiencies, and the computer design of a highly efficient collector was demonstrated. Author

N81-30360* National Aeronautics and Space Administration, Lewis Research Center, Cleveland, Ohio.

PERFORMANCE OF COMPUTER-DESIGNED SMALL-SIZED FOUR-STAGE DEPRESSED COLLECTOR FOR OPERATION OF DUAL-MODE TRAVELING WAVE TUBE

Peter Ramins and Thomas A. Fox Aug. 1981 14 p refs (NASA-TP-1832; E-643) Avail: NTIS HC A02/MF A01 CSCL 09C

A computer-designed axisymmetric 2.4-cm-diameter four-stage depressed collectors was evaluated in conjunction with an octave bandwidth, dual-mode traveling wave tube (TWT). The TWT was operated over a wide range of conditions to simulate different applications. The collector performance was optimized (within the constraint of fixed collector geometry which was designed for operation of the TWT at saturation) over the range of TWT operating conditions covered. For operation of the dual-mode TWT at saturation, average collector efficiencies of 81 1/2 and 82 percent for the high and low modes, respectively, were obtained across an octave bandwidth, leading to a three-fold increase in the TWT overall efficiency. For operation of the TWT in the linear, low distortion range, collector efficiencies of 87 to 92 percent were obtained, leading to TWT overall efficiencies as high as 35 percent. For operation of the dual-mode TWT over a 10 to 1 range in output power, overall efficiencies of 14 to 41 percent were obtained. Author

A81-32547* High temperature electronic requirements in aeropropulsion systems. W. C. Nieberding and J. A. Powell (NASA, Lewis Research Center, Cleveland, Ohio). NASA, DOE, and IEEE, High-Temperature Electronics Conference, Tucson, Ariz., Mar. 25-27, 1981, Paper. 3 p.

This paper discusses the needs for high temperature electronic and electro-optic devices as they would be used on aircraft engines in either research and development applications, or operational applications. The conclusion reached is that the temperature at which the devices must be able to function is in the neighborhood of 500 to 600 C either for R&D or for operational applications. In R&D applications the devices must function in this temperature range when in the engine but only for a moderate period of time. On an operational engine, the reliability requirements dictate that the devices be able to be burned-in at temperatures significantly higher than those at which they will function on the engine. The major point made is that semiconductor technology must be pushed well beyond the level at which silicon will be able to function. (Author)

N81-10301* TRW Defense and Space Systems Group, Redondo Beach, Calif. Power Conversion Electronics Dept.

APPLICATION HANDBOOK FOR A STANDARDIZED CONTROL MODULE (SCM) FOR DC-DC CONVERTERS, VOLUME 1 Final Report, Jun. 1976 - Jan. 1980

Fred C. Lee, M. F. Mahmoud, and Yuan Yu Apr. 1980 240 p refs Prepared in cooperation with Virginia Polytechnic Inst. and State Univ., Blacksburg 2 Vol. (Contract NAS3-20102)

(NASA-CR-165172; TRW-29922-6001-RU-01) Avail: NTIS HC A11/MF A01 CSCL 09C

The standardized control module (SCM) was developed for application in the buck, boost and buck/boost DC-DC converters. The SCM used multiple feedback loops to provide improved input line and output load regulation, stable feedback control system, good dynamic transient response and adaptive compensation of the control loop for changes in open loop gain and output filter time constraints. The necessary modeling and analysis tools to aid the design engineer in the application of the SCM to DC-DC Converters were developed. The SCM functional block diagram and the different analysis techniques were examined. The average time domain analysis technique was chosen as the basic analytical tool. The power stage transfer functions were developed for the buck, boost and buck/boost converters. The analog signal and digital signal processor transfer functions were developed for the three DC-DC Converter types using the constant on time, constant off time and constant frequency control laws. R.C.T.

N81-11314* TRW Defense and Space Systems Group, Redondo Beach, Calif. Power Conversion Electronics Dept.

USER'S DESIGN HANDBOOK FOR A STANDARDIZED CONTROL MODULE (SCM) FOR DC TO DC CONVERTERS, VOLUME 2 Final Report, Jun. 1976 - Jan. 1980

Fred C. Lee (Virginia Polytechnic Inst. and State Univ.) Apr. 1980 162 p refs Prepared by Virginia Polytechnic Inst. and State Univ. (Contract NAS3-20102)

(NASA-CR-165173; TRW-29922-6001-RU-01-Vol-2) Avail: NTIS HC A08/MF A01 CSCL 09C

A unified design procedure is presented for selecting the key SCM control parameters for an arbitrarily given power stage configuration and parameter values, such that all regulator performance specifications can be met and optimized concurrently in a single design attempt. All key results and performance indices, for buck, boost, and buck/boost switching regulators which are relevant to SCM design considerations are included to facilitate frequent references. A.R.H.

N81-14227* Siemens A.G., Munich (West Germany). Unternehmensbereich Bauelemente und Zentralbereich Technik.

INTEGRATED RC-CIRCUITS IN ALTA-TECHNOLOGY ON ONE SUBSTRATE Final Report

Helmold Kausche, Wolf-Dieter Muenz, and Hans Werner Poetzberger Bonn Bundesministerium fuer Forschung und Technologie Dec. 1979 60 p refs In GERMAN; ENGLISH summary Sponsored by Bundesministerium fuer Forschung und Technologie

(BMFT-FB-T-79-107; ISSN-0340-7608) Avail: NTIS HC A04/MF A01 Fachinformationszentrum, Karlsruhe, West Germany DM 12.60

To reach the goals of this program - i.e., the realization of integrated RC circuits in ALTA-technology on one substrate - two ways were investigated: first the 'single layer technique' with resistors and capacitors from one layer and then the 'double layer technique' with a Ta-rich layer for the resistors and an Al-rich layer for the capacitors. The compensation of temperature coefficients of R and C is done by reactive sputtering (AlTa-O) or by use of a sandwich dielectric of AlTa-oxide and SiO₂. The double layer technique was optimized with production equipment and reached preproduction standards. Samples of highly stable RC-circuits (active filters) were realized. The technology also includes the integration of crossovers. Author

NS1-16389* TRW Systems Group, Redondo Beach, Calif.
K-BAND HIGH POWER LATCHING SWITCH Final Report
M. J. Minar, W. S. Piotrowski, and J. E. Raue 19 Dec. 1980
49 p refs

(Contract NAS3-21761)

(NASA-CR-165159; Rept-34037)

Avail: NTIS

HC A03/MF A01 CSCL 09A

A 19 GHz waveguide latching switch with a bandwidth of 1400 MHz and an exceptionally low insertion loss of 0.25 dB was demonstrated. The RF and driver ferrites are separate structures and can be optimized individually. This analysis for each structure is separately detailed. Basically, the RF section features a dual turnstile junction. The circulator consists of a dielectric tube which contains two ferrite rods, and a dielectric spacer separating the ferrite parts along the center of symmetry of the waveguide to form two turnstiles. This subassembly is indexed and locked in the center of symmetry of a uniform junction of three waveguides by the metallic transformers installed in the top and bottom walls of the housing. The switching junction and its actuating circuitry met all RF performance objectives and all shock and vibration requirements with no physical damage or performance degradation. It exceeds thermal requirements by operating over a 100 C temperature range (-44 C to +56 C) and has a high power handling capability allowing up to 100 W of CW input power.

A.R.H.

A81-21675 * # Analysis and design of an adaptive multi-loop controlled two winding buck/boost regulator. M. F. Mahmoud and F. C. Lee (Virginia Polytechnic Institute and State University, Blacksburg, Va.). *Institute of Electrical and Electronics Engineers, International Telecommunications Energy Conference, Washington, D.C., Nov. 26-29, 1979, Paper.* 10 p. 8 refs. Contract No. NAS3-20102.

Small signal low frequency linear average model is derived for a multi-loop controlled two-winding buck/boost converter employing average techniques and the describing function method. The model reveals that a well-designed multi-loop control can provide a second-order zero adaptive to output filter parameter changes due to component tolerances, temperature changes, aging, and the effect of duty cycle modulation. It also can provide stabilization effect by shifting the positive zero to the left-half S-plane. Design guidelines are formulated to optimize regulator-loop dependent characteristics.

(Author)

NS1-16385* SRI International Corp., Menlo Park, Calif.
Physical Electronics Group.

DEVELOPMENT PROGRAM ON A COLD CATHODE ELECTRON GUN Final Report

C. A. Spindt May 1979 82 p refs

(Contract NAS3-20096; SRI Proj. 5413)

(NASA-CR-159570; SRI-5413)

Avail: NTIS

HC A05/MF A01 CSCL 09A

A prototype electron gun with a field emitter cathode capable of producing 95 mA in a 1/4 mm diameter beam at 12 kV was produced. Achievement of this goal required supporting studies in cathode fabrication, cathode performance, gun design, cathode mounting and gun fabrication. A series of empirical investigations advanced fabrication technology. More stable emitters were produced and multiple cone failure caused by chain reaction discharges were reduced. The cathode is capable of producing well over 95 mA, but a substantial collector development effort was required to demonstrate emission levels in the 100 mA region. Space charge problems made these levels difficult to achieve. Recommendations are made for future process and materials investigation. Electron gun designs were modeled and tested. A pair of two-electrode gun structures were fabricated and tested; one gun was delivered to NASA. Cathodes were pretested up to 100 mA at SRI and delivered to NASA for test in the gun structure.

Author

NS1-22278* Hughes Aircraft Co., Culver City, Calif. Electro-Optical and Data Systems Group.

FABRICATION AND TESTING OF POLYVINYLIDENE FLUORIDE CAPACITORS

Robert S. Buritz Jun 1980 115 p refs

(Contract NAS3-21042)

(NASA-CR-159501; FR-80-76-952)

Avail: NTIS

HC A06/MF A01 CSCL 09A

High energy density capacitors made from metallized polyvinylidene fluoride film were built and tested. Terminations of aluminum-babbitt, tin-babbitt, and all-babbitt were evaluated. All-babbitt terminations appeared to be better. The 0.1 microfarad and 2 microfarad capacitors were made of 6 micrometer material. Capacitance, dissipation factor, and insulation resistance measurements were made over the ranges -55 C to 125 C and 10 Hz to 100 kHz. Twelve of forty-one 0.1 microfarad capacitors survived a 5000 hour dc plus ac life test. Under the same conditions, the 2 microfarad capacitors exhibited overheating because of excessive power loss. Some failures occurred after low temperature exposures for 48 hours. No failures were caused by vibration or temperature cycling.

J.M.S.

34 FLUID MECHANICS AND HEAT TRANSFER

Includes boundary layers; hydrodynamics; fluidics; mass transfer; and ablation cooling.

For related information see also 02 Aerodynamics and 77 Thermodynamics and Statistical Physics.

N81-12358* National Aeronautics and Space Administration, Lewis Research Center, Cleveland, Ohio.

TURBULENT SOLUTION OF THE NAVIER-STOKES EQUATIONS

R. G. Deissler 1980 23 p refs Presented at Thirty-Third Ann. Meeting of the Div. of Fluid Dyn. of the Am. Phys. Soc., Ithaca, N.Y., 23-25 Nov. 1980

(NASA-TM-81621; E-631) Avail: NTIS HC A02/MF A01 CSCL 20D

The unaveraged Navier-Stokes equations are solved numerically in order to study the nonlinear physics of incompressible turbulent flow. Initial three dimensional cosine velocity fluctuations and periodic boundary conditions are used. No mean gradients are present. The three components of the mean square velocity fluctuations are equal for the initial conditions chosen. The resulting solution shows characteristics of turbulence, such as the nonlinear excitation of small scale fluctuations. For the higher Reynolds numbers the initially nonrandom flow develops into an apparently random turbulence. J.M.S.

N81-12363* National Aeronautics and Space Administration, Lewis Research Center, Cleveland, Ohio.

CURVED FILM COOLING ADMISSION TUBE Patent Application

R. W. Graham and S. S. Papell, inventors (to NASA) Filed 27 Oct. 1980 12 p

(NASA-Case-LEW-13174-1; US-Patent-Appl-SN-200634) Avail: NTIS HC A02/MF A01 CSCL 20D

Effective film cooling to protect a wall surface from a hot fluid which impinges on or flows along the surface is proposed. A film of cooling fluid having increased area is provided by changing the direction of a stream of cooling fluid through an angle of from 135 degrees to 165 degrees before injecting it through the wall into a hot flowing gas at an angle to form a cooling fluid film. Cooling fluid is supplied to the orifice from a cooling fluid source via a turbulence control passageway having a curved portion between two straight portions. The angle through which the direction of the cooling fluid is turned results in less mixing of the cooling fluid with the hot gas, thereby substantially increasing the length of the film in a downstream direction.

NASA

N81-13301* National Aeronautics and Space Administration, Lewis Research Center, Cleveland, Ohio.

ANALYSIS FOR PREDICTING ADIABATIC WALL TEMPERATURES WITH SINGLE HOLE COOLANT INJECTION INTO A LOW SPEED CROSSFLOW

C. R. Wang, S. S. Papell, and R. W. Graham 1981 10 p refs Proposed for presentation at the 26th Ann. Intern. Gas Turbine Conf., Houston, Tex., 8-12 Mar. 1981

(NASA-TM-81620; E-628) Avail: NTIS HC A02/MF A01 CSCL 20D

Assuming the local adiabatic wall temperature equals the local total temperature in a low speed coolant mixing layer, integral conservation equations with and without the boundary layer effects are formulated for the mixing layer downstream of a single coolant injection hole oriented at a 30 degree angle to the crossflow. These equations are solved numerically to determine the center line local adiabatic wall temperature and the effective coolant coverage area. Comparison of the numerical results with an existing film cooling experiment indicates that the present analysis permits a simplified but reasonably accurate prediction of the centerline effectiveness and coolant coverage area downstream of a single hole crossflow streamwise injection at 30 degree inclination angle. Author

N81-13302* National Aeronautics and Space Administration, Lewis Research Center, Cleveland, Ohio.

HEAT TRANSFER COEFFICIENTS FOR STAGGERED ARRAYS OF SHORT PIN FINS

G. James VanFossen 1981 15 p refs Proposed for presentation at the 26th Ann. Intern. Gas Turbine Conf., Houston, Tex., 8-12 Mar. 1981; sponsored by the ASME

(NASA-TM-81596; E-658) Avail: NTIS HC A02/MF A01 CSCL 20D

Short pin fins are often used to increase that heat transfer to the coolant in the trailing edge of a turbine blade. Due primarily to limits of casting technology, it is not possible to manufacture pins of optimum length for heat transfer purposes in the trailing edge region. In many cases the pins are so short that they actually decrease the total heat transfer surface area compared to a plain wall. A heat transfer data base for these short pins is not available in the literature. Heat transfer coefficients on pin and endwall surfaces were measured for several staggered arrays of short pin fins. The measured Nusselt numbers when plotted versus Reynolds numbers were found to fall on a single curve for all surfaces tested. The heat transfer coefficients for the short pin fins (length to diameter ratios of 1/2 and 2) were found to be about a factor of two lower than data from the literature for longer pin arrays (length to diameter ratios of about 8). Author

N81-15239* National Aeronautics and Space Administration, Lewis Research Center, Cleveland, Ohio.

NUMERICAL SIMULATION OF FLOWS IN CURVED DIFFUSERS WITH CROSS-SECTIONAL TRANSITIONING USING A THREE-DIMENSIONAL VISCOUS ANALYSIS

C. E. Towne and B. H. Anderson 1981 19 p refs Presented at 19th Aerospace Sci. Meeting, St. Louis, 12-15 Jan. 1981; sponsored by AIAA

(NASA-TM-81672; E-696) Avail: NTIS HC A02/MF A01 CSCL 20D

A three dimensional analysis for fully viscous, subsonic, compressible flow is evaluated. An approximate form of the Navier Stokes equations is solved by an implicit spatial marching technique. Calculations were made for flow in a circular S duct and in the F 16 inlet duct. The computed total pressure contours and secondary flow velocity vectors are presented. Qualitative comparisons with experiment are shown for both ducts. The analysis is used to show how the cross section transitioning in the F 16 inlet suppresses the development of a secondary flow vortex. Author

N81-15240* National Aeronautics and Space Administration, Lewis Research Center, Cleveland, Ohio.

FACTORS WHICH INFLUENCE THE BEHAVIOR OF TURBOFAN FORCED MIXER NOZZLES

B. H. Anderson and L. A. Povinelli 1981 30 p refs Prepared for 19th Aerospace Sci. Meeting, St. Louis, 12-15 Jan. 1981; sponsored by AIAA

(NASA-TM-81668; E-689) Avail: NTIS HC A03/MF A01 CSCL 20D

A finite difference procedure was used to compute the mixing for three experimentally tested mixer geometries. Good agreement was obtained between analysis and experiment when the mechanisms responsible for secondary flow generation were properly modeled. Vorticity generation due to flow turning and vorticity generated within the centerbody lobe passage were found to be important. Results are presented for two different temperature ratios between fan and core streams and for two different free stream turbulence levels. It was concluded that the dominant mechanisms in turbofan mixers is associated with the secondary flows arising within the lobe region and their development within the mixing section. Author

N81-15241* National Aeronautics and Space Administration, Lewis Research Center, Cleveland, Ohio.

A FOUR-CYLINDER STIRLING ENGINE CONTROLS MODEL

Carl F. Lorenzo and Carl J. Daniele 1980 25 p refs Presented at Automotive Technol. Develop. Contractor Coordination Meeting, Dearborn, Mich., 11-13 Nov. 1980

(Contract DE-A101-77CS-51040)

(NASA-TM-81648; E-9356-7; DOE/NASA/51040-21) Avail: NTIS HC A02/MF A01 CSCL 10B

A four working space, double acting piston, Stirling engine simulation was developed for controls studies. Two simulations, one for detailed fluid behavior, and a second model with simple fluid behavior but containing the four working space aspects and engine inertias, validate these models separately, then upgrade the four working space model by incorporating the detailed fluid behavior model for all four working spaces. The single working space model contains the detailed fluid dynamics. The four working space (FWS) model was built to observe the behavior of the whole engine. The drive dynamics and vehicle inertia effects are simulated. The capabilities of the model are exercised to look at working fluid supply transients, short circuit transients, and piston ring leakage effects. S F

N81-19417* National Aeronautics and Space Administration, Lewis Research Center, Cleveland, Ohio.

CAPILLARY AND ACCELERATION WAVE BREAKUP OF LIQUID JETS IN AXIAL-FLOW AIRSTREAMS

Robert D. Ingebo 1981 13 p refs

(NASA-TP-1791; E-537) Avail: NTIS HC A02/MF A01 CSCL 20D

Empirical correlations of reciprocal mean drop diameter with airstream momentum were derived from capillary and acceleration wave breakup of liquid jets atomized by cross stream injection into axial flow airstreams. A scanning radiometer was used to obtain data over an airstream momentum range of 3.7 to 25.7 g/sq cm sec. Transition from capillary to acceleration wave breakup was obtained at a critical Weber-Reynolds number of 1,000,000. E.D.K.

N81-16421* National Aeronautics and Space Administration, Lewis Research Center, Cleveland, Ohio.

THE EFFECT OF INFLOW VELOCITY PROFILES ON THE PERFORMANCE OF SUPERSONIC EJECTOR NOZZLES

Allen R. Bishop 1981 8 p refs Presented at the 19th Aerospace Sci. Meeting, St. Louis, 12-15 Jan. 1981; sponsored by AIAA

(NASA-TM-81673; E-697) Avail: NTIS HC A02/MF A01 CSCL 20D

The effect of initial velocity profile on the performance of axisymmetric supersonic ejector nozzles is discussed. Two different initial profiles in each of two different geometries are analyzed, and the importance of using realistic starting conditions to predict supersonic nozzle performance is demonstrated. Author

N81-18331* National Aeronautics and Space Administration, Langley Research Center, Hampton, Va.

GEOMETRIC METHODS IN COMPUTATIONAL FLUID DYNAMICS

Peter R. Eiseman In Von Karman Inst. for Fluid Dyn. Shock-Boundary Layer Interaction in Turbomachines, Vol. 2 1980 181 p refs (For primary document see N81-18328 09-34)

(Contracts NAS3-22117; NAS1-15810;

AGARD-OTAN-DPP-80-11007)

Avail: NTIS HC A14/MF A01 CSCL 20D

General methods for the construction of geometric computational fluid dynamic algorithms are presented which simulate a variety of flow fields in various nontrivial regions. Included are: basic developments with tensors; various forms for the equations of motion; generalized numerical methods and boundary conditions; and methods for mesh generation to meet the strong geometric constraints of turbomachines. Coordinate generation is shown generally to yield mesh descriptions from one or more transformations that are smoothly joined together to form a composite mesh. Author (ESA)

N81-21310* National Aeronautics and Space Administration, Lewis Research Center, Cleveland, Ohio.

ACCELERATION WAVE BREAKUP OF LIQUID JETS WITH AIRSTREAMS

Robert D. Ingebo 1981 10 p refs Proposed for presentation at the Symp. on Fluid Mech., Boulder, Colo., 22-24 Jun. 1981; sponsored by ASME

(NASA-TM-81717; E-750) Avail: NTIS HC A02/MF A01 CSCL 20D

Characteristic mean drop diameters were determined for downstream and upstream injection into nonswirling and swirling airflows. The effects of the aerodynamic and liquid surface forces on the mean drop size were obtained with a scanning radiometer. Water jet breakup was studied primarily in the acceleration wave regime with values of $WeRe > 10$ to the 6th power and the following empirical expression was obtained: $D(o)/D(m) = C (WeRe)^{0.4}$, power where $D(o)$ and $D(m)$ are the orifice and mean drop diameters, respectively. We and Re are the Weber and Reynolds numbers defined as respectively, $We = \rho(a)D(o)V(r)/\sigma$ and $Re = D(o)V(r)/\nu$, where $V(r)$ and $\rho(a)$ are airstream relative velocity and density, respectively, and σ and ν are surface tension and kinematic viscosity of the liquid, respectively. The proportionality constant C was evaluated as follows: for downstream injection, $C = 0.023$ with nonswirling airflow, and $C = 0.027$ with swirling airflow. For upstream injection, the empirical expression $D(o)/D(m) = 0.0045 (WeRe)^{0.5}$ to the 0.5 power was obtained with nonswirling airflow. Experimental conditions included a water flow rate of 68 liter per hour and an airflow rate per unit area range of 4.6 to 25.2 gm/sq cm sec at 293 K and atmospheric pressure. A.R.H.

N81-21313* National Aeronautics and Space Administration, Lewis Research Center, Cleveland, Ohio.

EVALUATION OF A METHOD FOR HEAT TRANSFER MEASUREMENTS AND THERMAL VISUALIZATION USING A COMPOSITE OF A HEATER ELEMENT AND LIQUID CRYSTALS

Steven A. Hippensteele, Louis M. Russell, and Francis S. Stepka Apr. 1981 22 p refs Presented at the 26th Ann. Intern. Gas Turbine Conf., Houston, Tex., 8-12 Mar. 1981; sponsored by ASME Original contains color illustrations

(NASA-TM-81639; E-656) Avail: NTIS HC A02/MF A01 CSCL 20D

Commercially available elements of a composite consisting of a plastic sheet coated with liquid crystal, another sheet with a thin layer of a conducting material (gold or carbon), and copper bus bar strips were evaluated and found to provide a simple, convenient, accurate, and low-cost measuring device for use in heat transfer research. The particular feature of the composite is its ability to obtain local heat transfer coefficients and isotherm patterns that provide visual evaluation of the thermal performances of turbine blade cooling configurations. Examples of the use of the composite are presented. Author

N81-21314* National Aeronautics and Space Administration, Lewis Research Center, Cleveland, Ohio.

FLOW THROUGH AXIALLY ALIGNED SEQUENTIAL APERTURES OF THE ORIFICE AND BORDA TYPES

R. C. Hendricks and T. Trent Stetz 1981 17 p refs Proposed for presentation at the 20th Natl. Heat Transfer Conf., Milwaukee, 2-5 Aug. 1981; sponsored by ASME and AICHE

(NASA-TM-81681; E-707) Avail: NTIS HC A02/MF A01 CSCL 20D

Choked flow rate and pressure profile data were obtained and studied for two axially aligned sequential configurations consisting of four Borda type inlets of 1.9 1/D with two separation distances of 0.8 and 30 diameters and four orifice type inlets of 0.5 1/D with two separation distances of 0.66 and 32 diameters. Data were obtained using fluid nitrogen over the reduced inlet temperature and pressure range $0.68 < T/T_{sub c} < 1$ and $P/P_{sub c} < 2$. A flow coefficient reduced temperature plot can be used to represent the flow rate data for each geometry. At the larger separation distances, the pressure profiles dropped sharply at the entrance and partially recovered within each of the Borda and orifice inlet configurations; the exception being the last inlet where at low entrance temperatures, fluid jetting

could occur. For the smaller spacings fluid jetting was prevalent throughout each of the inlet configurations at lower inlet temperatures. These results are in qualitative agreement with data of tubes with single Borda or sharp edge orifice type inlets to 105 1/D and water flow visualization studies. DOE

N81-22310* National Aeronautics and Space Administration, Lewis Research Center, Cleveland, Ohio.

HEAT PIPES CONTAINING ALKALI METAL WORKING FLUID Patent Application

James F. Morris, inventor (to NASA) Filed 16 Mar. 1981 8 p (NASA-Case-LEW-12253-1; US-Patent-Appl-EN-243682) Avail: NTIS HC A02/MF A01 CSCL 20D

The improvement of high temperature evaporation condensation heat transfer devices which have important and unique advantages in terrestrial and space energy processing is discussed. The device is in the form of a heat pipe comprising a sealed container or envelope which contains a capillary wick. The temperature of one end of the heat pipe is raised by the input of extremely hot and corrosive heat from an external heat source. A working fluid of a corrosive alkali metal, transfers this heat to a heat receiver remote from the heat source. The container and wick are fabricated from a superalloy containing a small percentage of corrosion inhibiting or gettering element. Lanthanum, scandium, yttrium, thorium, and hafnium are utilized as the alloying metal.

NASA

N81-24387* National Aeronautics and Space Administration, Lewis Research Center, Cleveland, Ohio.

SOME FLOW PHENOMENA ASSOCIATED WITH ALIGNED, SEQUENTIAL APERTURES WITH BORDA-TYPE INLETS

Robert C. Hendericks and T. Trent Stetz May 1981 63 p refs (NASA-TP-1792; E-479) Avail: NTIS HC A04/MF A01 CSCL 20D

Choked flow rate and pressure profile data were taken and studied for a configuration consisting of four axially aligned, sequential Borda tubes of 1.9 length diameter ratio with separation distances of 0.8 and 30 tube diameters. For either case the flow rate data could be represented by a flow coefficient reduced temperature plot. At a separation distance of 30 tube diameters the pressure profiles dropped sharply at the entrance and recovered within each Borda tube; except at low temperatures, where fluid jetting through the last Borda tube occurred. At a separation distance of 0.8 tube jetting was prevalent, and application of a significant backpressure did not alter the jetting. These results agree with other data for tubes with Borda or sharp edge orifice inlets and with a water flow visualization study reported herein.

Author

N81-24388* National Aeronautics and Space Administration, Lewis Research Center, Cleveland, Ohio.

FORCED AND NATURAL CONVECTION IN LAMINAR-JET DIFFUSION FLAMES

John B. Haggard, Jr. Jun. 1981 24 p refs (NASA-TP-1841; E-487) Avail: NTIS HC A02/MF A01 CSCL 20D

An experimental investigation was conducted on methane, laminar-jet, diffusion flames with coaxial, forced-air flow to examine flame shapes in zero-gravity and in situations where buoyancy aids (normal-gravity flames) or hinders (inverted-gravity flames) the flow velocities. Fuel nozzles ranged in size from 0.051 to 0.305 cm inside radius, while the coaxial, convergent, air nozzle had a 1.4 cm inside radius at the fuel exit plane. Fuel flows ranged from 1.55 to 10.3 cu cm/sec and air flows from 0 to 597 cu cm/sec. A computer program developed under a previous government contract was used to calculate the characteristic dimensions of normal and zero-gravity flames only. The results include a comparison between the experimental data and the computed axial flame lengths for normal gravity and zero gravity which showed good agreement. Inverted-gravity flame width was correlated with the ratio of fuel nozzle radius to average fuel velocity. Flame extinguishment upon entry into weightlessness was studied, and it was found that relatively

low forced-air velocities (approximately 10 cm/sec) are sufficient to sustain methane flame combustion in zero gravity. Flame color is also discussed. Author

N81-28389* National Aeronautics and Space Administration, Lewis Research Center, Cleveland, Ohio.

DEPRESSURIZATION AND TWO-PHASE FLOW OF WATER CONTAINING HIGH LEVELS OF DISSOLVED NITROGEN GAS

Robert J. Simoneau Jul. 1981 46 p refs (NASA-TP-1839; E-218) Avail: NTIS HC A03/MF A01 CSCL 20D

Depressurization of water containing various concentrations of dissolved nitrogen gas was studied. In a nonflow depressurization experiment, water with very high nitrogen content was depressurized at rates from 0.09 to 0.50 MPa per second and a metastable behavior which was a strong function of the depressurization rate was observed. Flow experiments were performed in an axisymmetric, converging diverging nozzle, a two dimensional, converging nozzle with glass sidewalls, and a sharp edge orifice. The converging diverging nozzle exhibited choked flow behavior even at nitrogen concentration levels as low as 4 percent of the saturation level. The flow rates were independent of concentration level. Flow in the two dimensional, converging, visual nozzle appeared to have a sufficient pressure drop at the throat to cause nitrogen to come out of solution, but choking occurred further downstream. The orifice flow motion pictures showed considerable oscillation downstream of the orifice and parallel to the flow. Nitrogen bubbles appeared in the flow at back pressures as high as 3.28 MPa, and the level at which bubbles were no longer visible was a function of nitrogen concentration. E.A.K.

N81-29384* National Aeronautics and Space Administration, Lewis Research Center, Cleveland, Ohio.

INFLUENCE OF THERMAL BOUNDARY CONDITIONS ON HEAT TRANSFER FROM A CYLINDER IN CROSS FLOW

S. Stephen Papell Aug. 1981 10 p refs (NASA-TP-1894; E-627) Avail: NTIS HC A02/MF A01 CSCL 20D

Local heat transfer data over the leading surface of a cylinder in crossflow were obtained for a Reynolds number range of 50,000. The cylinder was operated at both uniform-wall-temperature and uniform-heat-flux thermal ances of 80 deg from the front stagnation point, the uniform-wall-temperature heat transfer coefficients were as much as 56 percent lower than the uniform-heat-flux data. Between the stagnation point and 60 deg around the cylinder, there were no significant differences in the data. This region of the cylinder is within the cylindrical curvature region of the front end of a real turbine so it was concluded that either thermal boundary condition could be used to model turbine flow over that region of the blade. Results of evaluating the exponent x in the fundamental relationship $Nu = f(Re) \sup x$, which is used in data correlation show the exponent varies as a function of local position on the cylinder even in the laminar flow region. The value of x increases linearly from 0.50 at the stagnation point to 0.59 at 60 deg around the cylinder. This linear trend continued into the separation region at 80 deg for the uniform-wall-temperature data, but x increased markedly in the separation region for the uniform-heat-flux data. A.R.H.

N81-30390* National Aeronautics and Space Administration, Lewis Research Center, Cleveland, Ohio.

SEP BIMOD VARIABLE CONDUCTANCE HEAT PIPES ACCEPTANCE AND CHARACTERIZATION TESTS

Joseph A. Hemminger Aug. 1981 175 p refs (NASA-TM-82635; E-857) Avail: NTIS HC A08/MF A01 CSCL 20D

A series of six heat pipes, similar in design to those flown on the Communications Technology Satellite Hermes, for use in a prototype Solar Electric Propulsion JMOD thrust module are evaluated. The results of acceptance and characterization tests performed on the heat pipe subassembly are reported. The performance of all the heat pipes met, or exceeded, design specifications. J.D.H.

N81-30391* # National Aeronautics and Space Administration Lewis Research Center, Cleveland, Ohio
EXPERIMENTS ON FLOW THROUGH ONE TO FOUR INLETS OF THE ORIFICE AND BORDA TYPE
 R. C. Hendricks and T. Trent Stetz 1981 18 p. refs. Presented at the Cryogenic Eng. Conf./Intern. Cryogenic Mater. Conf., San Diego, Calif., 10-14 Aug. 1981; sponsored by NBS (NASA-TM-82680; E-963) Avail: NTIS HC A02/MF A01 CSCL 20D

Choked flow rate and pressure profile data were taken on sequential axially aligned inlets of the orifice and Borda type. The configuration consisted of from two to four inlets spaced at two nominal separation distances of 0.7 and 30 diameters. At the nominal 30 diameter spacing, the reduced flow rate follows a simple empirical relation based on the reduced flow rate for a single inlet. At the nominal 0.7 diameter spacing, fluid jetting was prevalent at low temperatures and flow rates were the same as for a single inlet. Author

A81-29983* # Heat transfer coefficients for staggered arrays of short pin fins. G. J. VanFossen (NASA, Lewis Research Center, Cleveland, Ohio). *American Society of Mechanical Engineers, Gas Turbine Conference and Products Show, Houston, Tex., Mar. 9-12, 1981, Paper 81-GT-75*. 11 p. 14 refs. Members, \$2.00; nonmembers, \$4.00.

Short pin fins are often used to increase the heat transfer to the coolant in the trailing edge of a turbine blade. Due primarily to limits of casting technology, it is not possible to manufacture pins of optimum length for heat transfer purposes in the trailing edge region. In many cases the pins are so short that they actually decrease the total heat transfer surface area compared to a plain wall. A heat transfer data base for these short pins is not available in the literature. Heat transfer coefficients on pin and endwall surfaces were measured for several staggered arrays of short pin fins. The measured Nusselt numbers when plotted versus Reynolds numbers were found to fall on a single curve for all surfaces tested. The heat transfer coefficients for the short pin fins (length to diameter ratios of 1/2 and 2) were found to be about a factor of two lower than data from the literature for longer pin arrays (length to diameter ratios of about 8). Author

A81-29998* # Analysis for predicting adiabatic wall temperatures with single hole coolant injection into a low speed crossflow. C. R. Wang, S. S. Papell, and R. W. Graham (NASA, Lewis Research Center, Cleveland, Ohio). *American Society of Mechanical Engineers, Gas Turbine Conference and Products Show, Houston, Tex., Mar. 9-12, 1981, Paper 81-GT-91*. 7 p. 12 refs. Members, \$2.00; nonmembers, \$4.00.

Assuming the local adiabatic wall temperature equals the local total temperature in a low speed coolant mixing layer, integral conservation equations with and without the boundary layer effects are formulated for the mixing layer downstream of a single coolant injection hole oriented at a 30 degree angle to the crossflow. These equations are solved numerically to determine the center-line local adiabatic wall temperature and the effective coolant coverage area. Comparison of the numerical results with an existing film cooling experiment indicates that the present analysis permits a simplified but reasonably accurate prediction of the centerline effectiveness and coolant coverage area downstream of a single hole crossflow streamwise injection at 30-deg inclination angle. Author

A81-18638* # Pressure spectra and cross spectra at an area contraction in a ducted combustion system. J. H. Miles (NASA, Lewis Research Center, Cleveland, Ohio) and D. D. Raftopoulos (Toledo, University, Toledo, Ohio). *American Society of Mechanical Engineers, Century 2 Aerospace Conference, San Francisco, Calif., Aug. 13-15, 1980, Paper 80-C2/Aero-9*. 7 p. Members, \$1.50; nonmembers, \$3.00.

Pressure spectra and cross-spectra at an area contraction in a liquid fuel, ducted, combustion noise test facility are analyzed.

Measurements made over a range of air and fuel flows are discussed. Measured spectra are compared with spectra calculated using a simple analytical model. Author

A81-19284* # Turbulent solution of the Navier-Stokes equations. R. G. Deissler (NASA, Lewis Research Center, Cleveland, Ohio). *American Physical Society, Annual Meeting, 33rd, Ithaca, N.Y., Nov. 23-25, 1980, Paper*. 21 p. 16 refs.

To study the nonlinear physics of incompressible turbulent flow, the unaveraged Navier-Stokes equations are solved numerically. Initial three-dimensional cosine velocity fluctuations and periodic boundary conditions are used. No mean gradients are present. The three components of the mean-square velocity fluctuations are equal for the initial conditions chosen. The resulting solution shows characteristics of turbulence, such as the nonlinear excitation of small-scale fluctuations. For the higher Reynolds numbers the initially nonrandom flow develops into an apparently random turbulence. Author

A81-29996* # Some modifications to, and operational experiences with, the two-dimensional, finite-difference, boundary-layer code, STAN5. R. E. Gaugler (NASA, Lewis Research Center, Cleveland, Ohio). *American Society of Mechanical Engineers, Gas Turbine Conference and Products Show, Houston, Tex., Mar. 9-12, 1981, Paper 81-GT-89*. 5 p. 16 refs. Members, \$2.00; nonmembers, \$4.00.

The two-dimensional, finite-difference boundary-layer code, STAN5, is the primary tool used at the NASA-Lewis Research Center for predicting turbine blade gas-side heat-transfer coefficients. A number of modifications have been made to the program to enhance its usefulness for these calculations. Experience in using STAN5 has identified some problems in the program that can be treated through program input, without modifying the program. These include the presence of a small separation bubble near the leading edge, and the effect of full-coverage film cooling on transition to turbulence. Some of the techniques used to treat these problems are described. Author

N81-20383* # Scientific Research Associates, Inc., Glastonbury, Conn.

A THREE-DIMENSIONAL TURBULENT COMPRESSIBLE SUBSONIC DUCT FLOW ANALYSIS FOR USE WITH CONSTRUCTED COORDINATE SYSTEMS Final Report
 R. Levy, H. McDonald, W. R. Briley, and J. P. Kreskovsky
 Washington NASA Apr. 1981 40 p. refs
 (Contract NAS3-21735)

(NASA-CR-3389) Avail: NTIS HC A03/MF A01 CSCL 20D

An approximate analysis is presented which is applicable to non-orthogonal coordinate systems having a curved centerline and planar transverse coordinate surfaces normal to the centerline. The primary flow direction is taken to coincide with the local direction of the duct centerline and is hence normal to transverse coordinate planes. The formulation utilizes vector components (velocity, vorticity, transport equations) defined in terms of local Cartesian directions aligned with the centerline tangent, although the governing equations themselves are expressed in general nonorthogonal coordinates. For curved centerlines, these vector quantities are redefined in new local Cartesian directions at each streamwise location. The use of local Cartesian variables and fluxes leads to governing equations which require only first derivatives of the coordinate transformation, and this provides for the aforementioned ease in using constructed coordinates.

A.R.H.

NS1-22313*# Martini Engineering, Richland, Wash.
A COMPUTER SIMULATION OF THE TRANSIENT RESPONSE OF A 4 CYLINDER STIRLING ENGINE WITH BURNER AND AIR PREHEATER IN A VEHICLE Final Report

W. R. Martini Mar. 1981 182 p refs
(Contracts DEN3-226; DE-A101-77CS-51040)
(NASA-CR-185262; DOE/NASA/0226-1) Avail: NTIS
HC A09/MF A01 CSCL 10B

A series of computer programs are presented with full documentation which simulate the transient behavior of a modern 4 cylinder Siemens arrangement Stirling engine with burner and air preheater. Cold start, cranking, idling, acceleration through 3 gear changes and steady speed operation are simulated. Sample results and complete operating instructions are given. A full source code listing of all programs are included. Author

A81-15537* Full-coverage film cooling. I - Three-dimensional measurements of turbulence structure. II - Prediction of the recovery-region hydrodynamics. S. Yavuzkurt, R. J. Moffat, and W. M. Kays (Stanford University, Stanford, Calif.). *Journal of Fluid Mechanics*, vol. 101, Nov. 13, 1980, p. 129-178. 46 refs. Research sponsored by the Scientific and Technical Research Council of Turkey; Contract No. NAS3-14336.

Hydrodynamic measurements of turbulence structure were performed with a triaxial hot wire in the full coverage and the recovery regions following an array of injection holes under isothermal conditions at ambient temperature and pressure for blowing ratios of 0.9 and 0.4. High levels of turbulence kinetic energy (TKE) were determined for low blowing, and low TKE levels were found for the high blowing levels; in the recovery region, the flow can be represented by a model with an outer boundary layer and a 2-dimensional inner boundary layer. Recovery region hydrodynamics can be modelled by considering that a new boundary layer started to grow immediately after the end of blowing; the Prandtl mixing length distributions calculated from the values of mean velocity and turbulent shear stresses were consistent with the presence of a dual boundary layer structure in the recovery region. The program used here contains a one-equation model of turbulence, using turbulence kinetic energy with an algebraic mixing length; this 2-dimensional, finite difference program can predict the mean velocity and turbulence kinetic energy profiles based on: initial values, boundary conditions, and a closure condition. A.T.

A81-18021*# Evacuation-induced pressure differentials in multilayer insulation systems. A. P. M. Glassford (Lockheed Research Laboratories, Palo Alto, Calif.). *AIAA Journal*, vol. 19, Jan. 1981, p. 104-112. 5 refs. Contract No. NAS3-14377.

The pressure differentials induced across three types of multilayer insulation systems during evacuation have been measured and compared with values predicted using an idealized parallel plate geometric model. The systems tested were double-aluminized Mylar with a Tissuglas or silk net spacer and crinkled single-aluminized Mylar. Test samples were circular. The influence of purge gas type, layer density, sample diameter, and temperature was systematically investigated. The experimental approach was to measure the absolute pressure history and corresponding pressure differential induced across the insulation during evacuation. The measured pressure differentials were nondimensionalized and compared with those predicted by the parallel plate model as a function of Knudsen number. It was concluded that the parallel plate model is adequate for making engineering analyses. The influence of all parameters, except layer density, is well represented by the model. Representation of the influence of layer density is less satisfactory, but can be improved by modification of the flat plate model to allow for the more obvious practical nonidealities, such as crinkling, or the presence of a net spacer. (Author)

A81-24924* Heat transfer from a row of impinging jets to concave cylindrical surfaces. P. Hrycak (New Jersey Institute of Technology, Newark, N.J.). *International Journal of Heat and Mass Transfer*, vol. 24, Mar. 1981, p. 407-419. 39 refs. Contract No. NAS3-11175.

Starting from the first principles, and with one experimentally obtained parameter, an expression for stagnation heat transfer is derived, applicable to round, impinging jets. The results obtained with a row of air jets impinging on an electrically-heated surface in a small-scale setup characteristic of a typical turbine blade have been found compatible with the average heat transfer from a geometrically similar, steam-heated surface scaled up ten times, and comparable with the results of other investigators. These findings were linked to the flow fields likely to exist in the gas turbine blades, internally cooled by a row of round jets or a single jet of equivalent width. The magnitude of heat-transfer coefficients obtained here with impinging jets approaches that normally associated with forced convection of water and evaporative cooling. (Author)

35 INSTRUMENTATION AND PHOTOGRAPHY

Includes remote sensors, measuring instruments and gages, detectors, cameras and photographic supplies, and holography.

For aerial photography see 43 *Earth Resources*. For related information see also 06 *Aircraft Instrumentation*, and 19 *Spacecraft Instrumentation*.

N81-18428* # National Aeronautics and Space Administration, Lewis Research Center, Cleveland, Ohio.

MINIATURE DRAG-FORCE ANEMOMETER

L. N. Krause and G. C. Fralick 1981 17 p refs. Proposed for presentation at the 2nd Intern. Symp. and Ind., St. Louis, 6-10 Apr. 1981; sponsored by ASME, the ISA and NBS (NASA-TM-81680; E-706) Avail: NTIS HC A02/MF A01 CSCL 14B

A miniature drag force anemometer is described which is capable of measuring unsteady as well as steady state velocity head and flow direction. It consists of a cantilevered beam with strain gages located at the base of the beam as the force measuring element. The dynamics of the beam are like those of lightly damped second order system with a natural frequency as high as 40 kilohertz depending on beam geometry and material. The anemometer is used in both forward and reversed flow. Anemometer characteristics and several designs are presented along with discussions of several applications. Author

N81-18429* # National Aeronautics and Space Administration, Lewis Research Center, Cleveland, Ohio.

SPECIFYING AND CALIBRATING INSTRUMENTATIONS

FOR WIDEBAND ELECTRONIC POWER MEASUREMENTS

Daniel J. Lesco and Donald H. Weikle Dec. 1980 20 p refs (Contract EC-77-A-31-1044)

(NASA-TM-81545; DOE/NASA/1044-II) Avail: NTIS HC A02/MF A01 CSCL 14B

The wideband electric power measurement related topics of electronic wattmeter calibration and specification are discussed. Tested calibration techniques are described in detail. Analytical methods used to determine the bandwidth requirements of instrumentation for switching circuit waveforms are presented and illustrated with examples from electric vehicle type applications. Analog multiplier wattmeters, digital wattmeters and calculating digital oscilloscopes are compared. The instrumentation characteristics which are critical to accurate wideband power measurement are described. J.M.S.

A81-41732* Experimental analysis of IMEP in a rotary combustion engine. H. J. Schock, W. J. Rice, and P. R. Meng (NASA, Lewis Research Center, Cleveland, OH). *Society of Automotive Engineers, International Congress and Exposition, Detroit, MI, Feb. 23-27, 1981, Paper 810150*. 42 p. 14 refs.

This experimental work demonstrates the use of a NASA designed, real time Indicated Mean Effective Pressure (IMEP) measurement system which will be used to judge proposed improvements in cycle efficiency of a rotary combustion engine. This is the first self-contained instrument that is capable of making real time measurements of IMEP in a rotary engine. Previous methods used require data recording and later processing using a digital computer. The unique features of this instrumentation include its ability to measure IMEP on a cycle by cycle, real time basis and the elimination of the need to differentiate the volume function in real time. Measurements at two engine speeds (2000 and 3000 RPM) and a full range of loads are presented, although the instrument was designed to operate to speeds of 9000 RPM. (Author)

A81-47642* # Holographic flow visualization of time-varying shock waves. A. J. Decker (NASA, Lewis Research Center, Cleveland, OH). *Applied Optics*, vol. 20, Sept. 15, 1981, p. 3120-3127, 8 refs.

Rapid-double exposure, diffuse-illumination holography is evaluated analytically and experimentally as a flow visualization method for time-varying shock waves. Conditions are determined that minimize the distance (localization error) between the surface or curve of interference-fringe localization and the shock surface. Treated specifically are the cases of shock waves in a transonic compressor rotor for which there is laser anemometer data for comparison and shock waves in a flutter cascade. (Author)

A81-48950* Gauge calibration system based on piston manometer. I. Warshawsky (NASA, Lewis Research Center, Cleveland, OH). *Journal of Vacuum Science and Technology*, vol. 19, July-Aug. 1981, p. 243-249, 12 refs.

An unbaked calibration system is described that permits absolute calibration with a piston manometer in the range 0.0002 to 6 Pa, with a probable error of 5 microPa + 0.8%, or in the range 0.00008 to 0.02 Pa, with a probable error of 2 microPa + 1%. Procedures and techniques that permit this performance are detailed. For hot-cathode ion gauges, the magnitudes of systematic corrections for envelope temperature and grid current are also indicated. (Author)

A81-17906* Surface flaw detection in structural ceramics

by scanning photoacoustic spectroscopy. P. K. Khandelwal, P. W. Heitman (General Motors Corp., Detroit Diesel Allison Div., Indianapolis, Ind.), T. D. Wakefield (Gilford Instrument Laboratories, Inc., Oberlin, Ohio), and A. J. Silversmith. *Applied Physics Letters*, vol. 37, Nov. 1, 1980, p. 779-781, 9 refs. Research supported by the U.S. Department of Energy; Contract No. DEN3-17.

Laser-scanned photoacoustic spectroscopy has been used to detect tightly closed surface cracks in three structural ceramic materials: sintered silicon nitride, reaction-bonded silicon nitride, and sintered silicon carbide. It is found that the amplitude of the photoacoustic signal from the flaws is greater for the silicon nitrides than for silicon carbide, which is attributed to the lower thermal diffusivity of silicon nitride as well as differences in the grain size distribution and chemical composition. Signal amplitude, reproducibility, and signal-to-noise ratio are acceptable for effective flaw detection. V.L.

A81-30000* # Evaluation of a method for heat transfer measurements and thermal visualization using a composite of a heater element and liquid crystals. S. A. Hippensteel, L. M. Russell, and F. S. Stepka (NASA, Lewis Research Center, Cleveland, Ohio). *American Society of Mechanical Engineers, Gas Turbine Conference and Products Show, Houston, Tex., Mar. 9-12, 1981, Paper 81-GT-93*. 9 p. 16 refs. Members, \$2.00; nonmembers, \$4.00.

Commercially available elements of a composite consisting of a plastic sheet coated with liquid crystal, another sheet with a thin layer of a conducting material (gold or carbon), and copper bus bars strips were evaluated and found to provide a simple, convenient, accurate, and low-cost measuring device for use in heat transfer research. The particular feature of the composite is its ability to obtain local heat transfer coefficients and isotherm patterns that provide visual evaluation of the thermal performances of turbine blade cooling configurations. Examples of the use of the composite are presented. (Author)

37 MECHANICAL ENGINEERING

Includes auxiliary systems (non-power); machine elements and processes; and mechanical equipment.

N81-11334* National Aeronautics and Space Administration, Lewis Research Center, Cleveland, Ohio.

ANISOTROPIC TRIBOLOGICAL PROPERTIES OF SILICON CARBIDE

Kazuhisa Miyoshi and Donald H. Buckley 1980 20 p refs Proposed for presentation at the Intern. Conf. on Wear of Materials, San Francisco, 30 Mar. - 1 Apr. 1980 (NASA-TM-81547; E-505) Avail: NTIS HC A02/MF A01 CSCL 11D

The anisotropic friction, deformation and fracture behavior of single crystal silicon carbide surfaces were investigated in two categories. The categories were called adhesive and abrasive wear processes, respectively. In the adhesive wear process, the adhesion, friction and wear of silicon carbide were markedly dependent on crystallographic orientation. The force to reestablish the shearing fracture of adhesive bond at the interface between silicon carbide and metal was the lowest in the preferred orientation of silicon carbide slip system. The fracturing of silicon carbide occurred near the adhesive bond to metal and it was due to primary cleavages of both prismatic (10-110) and basal (0001) planes. R.C.T.

N81-11395* National Aeronautics and Space Administration, Lewis Research Center, Cleveland, Ohio.

EFFECT OF TANGENTIAL TRACTION AND ROUGHNESS ON CRACK INITIATION/PROPAGATION DURING ROLLING CONTACT

Norimune Soda (Tokyo Univ. Japan) and Takashi Yamamoto (Tokyo Univ. of Agriculture and Technology, Japan) 1980 37 p refs Proposed for presentation at the 36th Ann. Meeting of ASLE, Pittsburgh, 11-14 May 1981 (NASA-TM-81608; E-604) Avail: NTIS HC A03/MF A01 CSCL 20K

Rolling fatigue tests of 0.45 percent carbon steel rollers were carried out using a four roller type rolling contact fatigue tester. Tangential traction and surface roughness of the harder mating rollers were varied and their effect was studied. The results indicate that the fatigue life decreases when fraction is applied in the same direction as that of rolling. When the direction of fraction is reversed, the life increases over that obtained with zero traction. The roughness of harder mating roller also has a marked influence on life. The smoother the mating roller, the longer the life. Microscopic observation of specimens revealed that the initiation of cracks during the early stages of life is more strongly influenced by the surface roughness, while the propagation of these cracks in the latter stages is affected mainly by the tangential traction. Author

N81-13357* National Aeronautics and Space Administration, Lewis Research Center, Cleveland, Ohio.

DESIGN STUDIES OF CONTINUOUSLY VARIABLE TRANSMISSIONS FOR ELECTRIC VEHICLES

Richard J. Parker, Stuart H. Loewenthal, and George K. Fischer 1981 18 p refs Presented at SAE Congr., Detroit, 23-27 Feb. 1981 (Contract EC-77-A-31-1044)

(NASA-TM-81642; E-588; DOE/NASA/1044-12) Avail: NTIS HC A02/MF A01 CSCL 13I

Preliminary design studies were performed on four continuously variable transmission (CVT) concepts for use with a flywheel equipped electric vehicle of 1700 kg gross weight. Requirements of the CVTs were a maximum torque of 450 N-m (330 lb-ft), a maximum output power of 75 kW (100 hp), and a flywheel speed range of 28,000 to 14,000 rpm. Efficiency, size, weight, cost, reliability, maintainability, and controls were evaluated for each of the four concepts which included a steel V-belt type, a flat rubber belt type, a toroidal traction type, and a cone roller traction type. All CVTs exhibited relatively high calculated efficiencies (68 percent to 97 percent) over a broad range of

vehicle operating conditions. Estimated weight and size of these transmissions were comparable to or less than equivalent automatic transmission. The design of each concept was carried through the design layout stage. A.R.H.

N81-13358* National Aeronautics and Space Administration, Lewis Research Center, Cleveland, Ohio.

ELASTOHYDRODYNAMIC LUBRICATION OF ELLIPTICAL CONTACTS

Bernard J. Hamrock 1981 13 p refs Proposed for presentation at the 1st Symp. INTERTRIBO '81, Stbske Pleso, Czechoslovakia, 27-29 Apr. 1981 (NASA-TM-81647; E-663) Avail: NTIS HC A02/MF A01 CSCL 11H

The determination of the minimum film thickness within contact is considered for both fully flooded and starved conditions. A fully flooded conjunction is one in which the film thickness is not significantly changed when the amount of lubricant is increased. The fully flooded results presented show the influence of contact geometry on minimum film thickness as expressed by the ellipticity parameter and the dimensionless speed, load, and materials parameters. These results are applied to materials of high elastic modulus (hard EHL), such as metal, and to materials of low elastic modulus (soft EHL), such as rubber. In addition to the film thickness equations that are developed, contour plots of pressure and film thickness are given which show the essential features of elastohydrodynamically lubricated conjunctions. The crescent shaped region of minimum film thickness, with its side lobes in which the separation between the solids is a minimum, clearly emerges in the numerical solutions. In addition to the 3 presented for the fully flooded results, 15 more cases are used for hard EHL contacts and 18 cases are used for soft EHL contacts in a theoretical study of the influence of lubricant starvation on film thickness and pressure. From the starved results for both hard and soft EHL contacts, a simple and important dimensionless inlet boundary distance is specified. This inlet boundary distance defines whether a fully flooded or a starved damage and phase change processes. Classes of useful experiments in this area are given. Author

N81-14322* National Aeronautics and Space Administration, Lewis Research Center, Cleveland, Ohio.

COMPARISONS OF MODIFIED VASCO X-2 AND AISI 9310 GEAR STEELS

Dennis P. Townsend and Erwin V. Zuretsky Nov. 1980 19 p refs (NASA-TP-1731; E-070) Avail: NTIS HC A02/MF A01 CSCL 13I

Endurance tests were conducted with four groups of spur gears manufactured from three heats of consumable electrode vacuum melted (CVM) modified Vasco X-2. Endurance tests were also conducted with gears manufactured from CVM AISI 9310. Bench type rolling element fatigue tests were conducted with both materials. Hardness measurements were made to 811 K. There was no statistically significant life difference between the two materials. Life differences between the different heats of modified Vasco X-2 can be attributed to heat treat variation and resultant hardness. Carburization of gear flanks only can eliminate tooth fracture as a primary failure mode for modified Vasco X-2. However, a tooth surface fatigue spall can act as a nucleus of a tooth fracture failure for the modified Vasco X-2. Author

N81-15367* National Aeronautics and Space Administration, Lewis Research Center, Cleveland, Ohio.

AXIAL FORCE AND EFFICIENCY TESTS OF FIXED CENTER VARIABLE SPEED BELT DRIVE

David J. Bents 1981 31 p refs Proposed for presentation at Snc of Automotive Engr. Intern. Congr. and Exposition, Detroit, 23-27 Feb. 1981 (Contract DE-A101-77CS-51044)

(NASA-TM-81652; DOE/NASA/51044-13; E-669) Avail: NTIS HC A03/MF A01 CSCL 13I

An investigation of how the axial force varies with the centerline force at different speed ratios, speeds, and loads, and

how the drive's transmission efficiency is affected by these related forces is described. The tests, intended to provide a preliminary performance and controls characterization for a variable speed belt drive continuously variable transmission (CVT), consisted of the design and construction of an experimental test rig geometrically similar to the CVT, and operation of that rig at selected speed ratios and power levels. Data are presented which show: how axial forces exerted on the driver and driven sheaves vary with the centerline force at constant values of speed ratio, speed, and output power; how the transmission efficiency varies with centerline force and how it is also a function of the V belt coefficient; and the axial forces on both sheaves as normalized functions of the traction coefficient. T.M.

N81-18474* National Aeronautics and Space Administration. Lewis Research Center, Cleveland, Ohio.

SELF-ACTING GEOMETRY FOR NONCONTACT SEALS

G. P. Allen 1981 19 p refs Proposed for presentation at Ann. Meeting of ASLE Pittsburgh, 11-14 May 1981 (NASA-TM-81659; E-473) Avail: NTIS HC A02/MF A01 CSCL 11A

Performance of two self acting seal designs for a liquid oxygen (LOX) turbopump was predicted over ranges of pressure differential and speed. Predictions were compared with test results. Performance of a radial face seal for LOX was predicted up to 448 N/cu cm and 147 m/sec. Performance of a segmented circumferential seal for helium was predicted up to 69 N/cu cm and 189 m/sec. Results confirmed predictions of noncontact operation. Qualitative agreement between test and analysis was found. The LOX face seal evidently operated with mostly liquid in the self acting geometry and mostly gas across the dam.

Author

N81-17435* National Aeronautics and Space Administration. Lewis Research Center, Cleveland, Ohio.

COMPUTER PROGRAM DOCUMENTATION FOR THE DYNAMIC ANALYSIS OF A NONCONTACTING MECHANICAL FACE SEAL

B. M. Auer and I. Etsion Nov. 1980 47 p refs (NASA-TM-81636; E-650) Avail: NTIS HC A03/MF A01 CSCL 11A

A computer program is presented which achieves a numerical solution for the equations of motion of a noncontacting mechanical face seal. The flexibly-mounted primary seal ring motion is expressed by a set of second order differential equations for three degrees of freedom. These equations are reduced to a set of first order equations and the GEAR software package is used to solve the set of first order equations. Program input includes seal design parameters and seal operating conditions. Output from the program include: velocities and displacements of the seal ring about the axis of an inertial reference system. One example problem is described. M.G.

N81-17436* National Aeronautics and Space Administration. Lewis Research Center, Cleveland, Ohio.

DESIGN OF SPUR GEARS FOR IMPROVED EFFICIENCY

Neil E. Anderson (Army Aviation Research and Development Command, Cleveland) and Stuart H. Loewenthal 1981 17 p refs Presented at ASME Western Design Eng. Conf., Anaheim, Calif., 9-11 Dec. 1980 and proposed for presentation at ASME Design Eng. Conf., Chicago, 27-30 Apr. 1981 Prepared in cooperation with Army Aviation Research and Development Command, Cleveland

(NASA-TM-81625; E-630; AVRADCOM-TR-81-C-3) Avail: NTIS HC A02/MF A01 CSCL 13I

A method to calculate spur gear system loss for a wide range of gear geometries and operating conditions was used to determine design requirements for an efficient gearset. The effects of spur gear size, pitch, ratio, pitch line velocity and load on efficiency were determined. Peak efficiencies were found to be greater for large diameter and fine pitched gears and tare (no-load) losses were found to be significant. R.C.T.

N81-18391* National Aeronautics and Space Administration. Lewis Research Center, Cleveland, Ohio.

HISTORY OF BALL BEARINGS

Duncan Dowson (Leeds Univ., England) and Bernard J. Hamrock Feb. 1981 84 p refs (NASA-TM-81689; E-209) Avail: NTIS HC A05/MF A01 CSCL 13I

The familiar precision rolling-element bearings of the twentieth century are products of exacting technology and sophisticated science. Their very effectiveness and basic simplicity of form may discourage further interest in their history and development. Yet the full story covers a large portion of recorded history and surprising evidence of an early recognition of the advantages of rolling motion over sliding action and progress toward the development of rolling-element bearings. The development of rolling-element bearings is followed from the earliest civilizations to the end of the eighteenth century. The influence of general technological developments, particularly those concerned with the movement of large building blocks, road transportation, instruments, water-raising equipment, and windmills are discussed, together with the emergence of studies of the nature of rolling friction and the impact of economic factors. By 1800 the essential features of ball and rolling-element bearings had emerged and it only remained for precision manufacture and mass production to confirm the value of these fascinating machine elements. Author

N81-18392* National Aeronautics and Space Administration. Lewis Research Center, Cleveland, Ohio.

INTRODUCTION TO BALL BEARINGS

Bernard J. Hamrock and Duncan Dowson Feb. 1981 86 p refs (NASA-TM-81690; E-209) Avail: NTIS HC A05/MF A01 CSCL 13I

The purpose of a ball bearing is to provide a relative positioning and rotational freedom while transmitting a load between two structures, usually a shaft and a housing. For high rotational speeds (e.g. in gyroscope ball bearings) the purpose can be expanded to include rotational freedom with practically no wear in the bearing. This condition can be achieved by separating the bearing parts with a coherent film of fluid known as an elastohydrodynamic film. This film can be maintained not only when the bearing carries the load on a shaft, but also when the bearing is preloaded to position the shaft to within micro- or nano-inch accuracy and stability. Background information on ball bearings is provided, different types of ball bearings and their geometry and kinematics are defined, bearing materials, manufacturing processes, and separators are discussed. It is assumed, for the purposes of analysis, that the bearing carries no load. Author

N81-19455* National Aeronautics and Space Administration. Lewis Research Center, Cleveland, Ohio.

METHOD OF COLD WELDING USING ION BEAM TECHNOLOGY Patent

Bernard L. Sater inventor (to NASA) Issued 20 Jan. 1981 5 p Filed 28 Jul. 1978 Superseded: N78-28459 (16 - 19, p 2534)

(NASA-Case-LEW-12982-1; US-Patent-4,245,768;

US-Patent-Appl-SN-929084; US-Patent-Class-228-116;

US-Patent-Class-228-205; US-Patent-Class-204-192E) Avail

US Patent and Trademark Office CSCL 13H

A method for cold welding metal joints is described. In order to remove the contamination layer on the surface of the metal, an ion beam generator is used in a vacuum environment. A gas, such as xenon or argon, is ionized and accelerated toward the metal surface. The beam of gas effectively sputters away the surface oxides and contamination layer so that clean underlying metal is exposed in the area to be welded. The use of this method allows cold welding with minimal deformation. Both similar and dissimilar metals can be cold welded with this method Official Gazette of the U.S. Patent and Trademark Office

N81-19455* National Aeronautics and Space Administration, Lewis Research Center, Cleveland, Ohio.

PERFORMANCE OF JET- AND INNER-RING-LUBRICATED 35 MILLIMETER BORE BALL BEARINGS OPERATING TO 2.5 MILLION DN

Fredrick Schuller, T. and Hans R. Signer Feb. 1981 15 p refs
(NASA-TP-1808; E-515) Avail: NTIS HC A02/MF A01 CSCL 131

Parametric tests were conducted with a 35 millimeter bore, angular contact ball bearing having a single outer land guided cage. Lubrication was achieved by flowing oil through axial grooves and radial holes machined in the inner ring of the bearing. Test conditions were a thrust load of 667 N (150 lb), shaft speeds from 48,000 to 72,000 rpm, and an oil inlet temperature of 394 K (250 F). Data from tests where the distribution of the total oil supplied to the inner ring was 50 percent for bearing lubrication and 50 percent for bearing inner ring cooling were compared with those where the distribution pattern was 25 percent lubrication and 75 percent cooling. Successful operation was experienced with both the 50-50 and 25-75 percent flow distribution patterns to 2.5 million DN. The 50-50 percent flow pattern provided the cooler bearing operation of the two inner ring lubricated bearings. The jet lubricated bearing had lower outer ring and higher inner ring temperatures than the inner ring lubricated bearings. Maximum power loss of 2.8 kW (3.7 hp) was experienced with the 25-75 percent flow distribution, and maximum percent cage slip of 7.0 occurred at 72,300 rpm with the 50-50 percent flow distribution. Author

N81-19459* National Aeronautics and Space Administration, Lewis Research Center, Cleveland, Ohio.

ADVANCED CONTINUOUSLY VARIABLE TRANSMISSIONS FOR ELECTRIC AND HYBRID VEHICLES

Stuart H. Loewenthal 1980 29 p refs Presented at Electric and Hybrid Vehicle Advanced Vehicle Seminar, Pasadena, Calif., 8-9 Dec. 1980

(Contract DE-AI01-77CS-51044)

(NASA-TM-81718; DOE/NASA/51044-17; E-752) Avail: NTIS HC A03/MF A01 CSCL 13F

A brief survey of past and present continuously variable transmissions (CVT) which are potentially suitable for application with electric and hybrid vehicles is presented. Discussion of general transmission requirements and benefits attainable with a CVT for electric vehicle use is given. The arrangement and function of several specific CVT concepts are cited along with their current development status. Lastly, the results of preliminary design studies conducted under a NASA contract for DOE on four CVT concepts for use in advanced electric vehicles are reviewed.

Author

N81-20423* National Aeronautics and Space Administration, Lewis Research Center, Cleveland, Ohio.

LIFE ANALYSIS OF MULTIROLLER PLANETARY TRACTION DRIVE

John J. Coy (Army Aviation Research and Development Command, Cleveland, Ohio), Douglas A. Rohn, and Stuart H. Loewenthal Apr. 1981 16 p refs Prepared in cooperation with Army Aviation Research and Development Command, Cleveland
(NASA-TP-1710; AVRADCOM-TR-80-C-16; E-484) Avail: NTIS HC A02/MF A01 CSCL 13I

A contact fatigue life analysis was performed for a constant ratio, Nasvytis Multiroller Traction Drive. The analysis was based on the Lundberg-Palmgren method for rolling element bearing life prediction. Life adjustment factors for materials, processing, lubrication and traction were included. The 14.7 to 1 ratio drive consisted of a single stage planetary configuration with two rows of stepped planet rollers of five rollers per row, having a roller cluster diameter of approximately 0.21 m, a width of 0.06 m and a weight of 9 kg. Drive system 10 percent life ranged from 18,800 hours at 16.6 kW (22.2 hp) and 25,000 rpm sun roller speed, to 305 hours at maximum operating conditions of 149 kW (200 hp) and 75,000 rpm sun roller speed. The effect of roller diameter and roller center location on life were determined. It was found that an optimum life geometry exists.

Author

N81-20424* National Aeronautics and Space Administration, Lewis Research Center, Cleveland, Ohio.

SPUTTERING AND ION PLATING FOR AEROSPACE APPLICATIONS

T. Spelvin 1981 14 p refs Proposed for presentation at Natl. Conf. of the Am. Electroplaters Soc., Boston, 28 Jun. - 2 Jul. 1981

(NASA-TM-81726; E-778) Avail: NTIS HC A02/MF A01 CSCL 13H

Sputtering and ion plating technologies are reviewed in terms of their potential and present uses in the aerospace industry. Sputtering offers great universality and flexibility in depositing any material or in the synthesis of new ones. The sputter deposition process has two areas of interest: thin film and fabrication technology. Thin film sputtering technology is primarily used for aerospace mechanical components to reduce friction, wear, erosion, corrosion, high temperature oxidation, diffusion and fatigue, and also to sputter-construct temperature and strain sensors for aircraft engines. Sputter fabrication is used in intricate aircraft component manufacturing. Ion plating applications are discussed in terms of the high energy evaporant flux and the high throwing power. Excellent adherence and 3 dimensional coverage are the primary attributes of this technology. Author

N81-21356* National Aeronautics and Space Administration, Lewis Research Center, Cleveland, Ohio.

EFFECT OF SURFACE ROUGHNESS ON HYDRODYNAMIC BEARINGS

Bankim C. Majumdar and Bernard J. Hamrock 1981 24 p refs Proposed for presentation at Joint Lubrication Conf., New Orleans, 5-7 Oct. 1981; sponsored by ASME and ASLE
(NASA-TM-81711; E-698) Avail: NTIS HC A02/MF A01 CSCL 13I

A theoretical analysis on the performance of hydrodynamic oil bearings is made considering surface roughness effect. The hydrodynamic as well as asperity contact load is found. The contact pressure was calculated with the assumption that the surface height distribution was Gaussian. The average Reynolds equation of partially lubricated surface was used to calculate hydrodynamic load. An analytical expression for average gap was found and was introduced to modify the average Reynolds equation. The resulting boundary value problem was then solved numerically by finite difference methods using the method of successive over relaxation. The pressure distribution and hydrodynamic load capacity of plane slider and journal bearings were calculated for various design data. The effects of attitude and roughness of surface on the bearing performance were shown. The results are compared with similar available solution of rough surface bearings. It is shown that: (1) the contribution of contact load is not significant; and (2) the hydrodynamic and contact load increase with surface roughness. Author

N81-22317* National Aeronautics and Space Administration, Lewis Research Center, Cleveland, Ohio.

COMBUSTION OF SOLID CARBON RODS IN ZERO AND NORMAL GRAVITY Ph.D. Thesis - Toledo Univ., Ohio

Charles M. Spuckler May 1981 181 p refs
(NASA-TM-81728; E-771) Avail: NTIS HC A09/MF A01 CSCL 21B

In order to investigate the mechanism of carbon combustion and to assess the importance of gravitational induced convection on the process, zero and normal gravity experiments were conducted in which spectroscopic carbon rods were resistance ignited and burned in dry oxygen environments. In the zero-gravity drop tower tests, a blue flame surrounded the rod, showing that a gas phase reaction in which carbon monoxide was oxidized to carbon dioxide was taking place. The ratio of flame diameter to rod diameter was obtained as a function of time. It was found that this ratio was inversely proportional to both the oxygen pressure and the rod diameter. In the normal gravity tests, direct mass spectrometric sampling was used to measure gas phase concentrations. The gas sampling probe was positioned near the circumference of a horizontally mounted 0.615 cm diameter carbon rod, either at the top or at angles of 45 deg to 90 deg from the top, and yielded concentration profiles of

CO₂, CO, and O₂ as a function of distance from the surface. The mechanism controlling the combustion process was found to change from chemical process control at the 90 deg and 45 deg probe positions to mass transfer control at the 0 deg probe position at the top of the rod. Under the experimental conditions used, carbon combustion was characterized by two surface reactions, 2C + O₂ yields 2CO and CO₂ + C yields 2CO, and a gas phase reaction, 2CO + O₂ yields 2CO₂. J.M.S.

N81-22380* National Aeronautics and Space Administration, Lewis Research Center, Cleveland, Ohio
MULTIPLE PLATE HYDROSTATIC VISCOUS DAMPER
 Patent Application

L. P. Ludwig, inventor (to NASA). Filed 27 Feb. 1981. 7 p (NASA-Case-LEW-12445-1; US-Patent-Appl-SN-238887). Avail. NTIS HC A02/MF A01 CSCL 131

A device for damping radial motion of a rotating shaft is described. The damper comprises a series of spaced plates extending in a radial direction. A hydraulic piston is utilized to place a load in these plates. Each annular plate is provided with a suitable hydrostatic bearing geometry on at least one of its faces. This structure provides a high degree of dampening in a rotor case system of turbomachinery in general. The damper is particularly useful in gas turbine engines. NASA

N81-24442* National Aeronautics and Space Administration, Lewis Research Center, Cleveland, Ohio

SELF-STABILIZING RADIAL FACE SEAL Patent

Izhak Etsion, inventor (to NASA) (Technion Research and Development Foundation Ltd., Haifa, Israel). Issued 7 Jan. 1981. 6 p. Filed 17 Nov. 1978. Supersedes N79-12445 (17-03, p. 0333). Sponsored by NASA.

(NASA-Case-LEW-12991-1; US-Patent-4,260,166; US-Patent-Appl-SN-961-832; US-Patent-Class-277-96.) Avail. US Patent and Trademark Office CSCL 11A

A self-stabilizing radial face seal comprises an axial member and a primary seal ring juxtapositioned to a seal seat. At least one primary seal ring and seal seat unit is affixed to the axial member so as to rotate with it. The primary seal ring has a front face which opposes a face of the seal seat. The seal has both high-pressure and low-pressure regions of fluid, and seal seat is provided with a porous ring-like circumferential structure in the face of the seal seat opposite the front face of the primary seal ring.

Official Gazette of the U.S. Patent and Trademark Office

N81-26447* National Aeronautics and Space Administration, Lewis Research Center, Cleveland, Ohio

CIRCUMFERENTIAL SHAFT SEAL Patent

Lawrence P. Ludwig, inventor (to NASA). Issued 12 May 1981. 4 p. Filed 7 Dec. 1979. Supersedes N80-18401 (18-09, p. 1145). Division of US Patent Appl. SN-672219, filed 21 Mar. 1976. US-Patent-4,212,477

(NASA-Case-LEW-12119-2; US-Patent-4,266,788; US-Patent-Appl-SN-102004; US-Patent-Class-277-193; US-Patent-Class-277-153; US-Patent-4,212,477; US-Patent-Appl-SN-672219). Avail. US Patent and Trademark Office CSCL 11A

A circumferential shaft seal comprising two sealing rings held to a rotating shaft by means of a surrounding elastomeric band is disclosed. The rings are segmented and are of a rigid sealing material such as carbon or a polyimide and graphite fiber composite.

Official Gazette of the U.S. Patent and Trademark Office

N81-26488* National Aeronautics and Space Administration, Lewis Research Center, Cleveland, Ohio

SURFACE GEOMETRY OF CIRCULAR CUT SPIRAL BEVEL GEARS

R. L. Huston (Cincinnati Univ.) and John J. Coy. 1981. 23 p. refs. Presented at the NASA-AVRADCOM Symp. on Advan.

Power Transmission Technol., Cleveland, 9-11 Jun. 1981 and proposed for presentation at the Design Eng. Tech. Conf., Hartford, Conn., 20-23 Sep. 1981; sponsored by the American Society of Mechanical Engineers

(Grant NAG-3188)

(NASA-TM-82622; E-873; AVRADCOM-TR-81-C-13). Avail. NTIS HC A02/MF A01 CSCL 131

The tooth surface principal radii of curvature of crown (flat) gears were determined. Specific results are presented for involute, straight, and hyperbolic cutter profiles. It is shown that the geometry of circular cut spiral bevel gears is somewhat simpler than a theoretical logarithmic spiral bevel gear. A.R.H.

N81-27523* National Aeronautics and Space Administration, Lewis Research Center, Cleveland, Ohio

SURFACE FILMS AND METALLURGY RELATED TO LUBRICATION AND WEAR Ph.D. Thesis - Tokyo Inst. of Technology

Donald H. Buckley. Jul. 1981. 218 p. refs.

(NASA-TM-82645; E-900). Avail. NTIS HC A08/MF A01 CSCL 11H

The nature of the tribological surface is identified and characterized with respect to adhesion, friction, wear, and lubricating properties. Surface analysis is used to identify the role of environmental constituents on tribological behavior. The effect of solid to solid interactions for metals in contact with metals, ceramics, semiconductors, carbons, and polymers is discussed. The data presented indicate that the tribological surface is markedly different than an ideal solid surface. The environment is shown to affect strongly the behavior of two solids in contact. Results also show that small amounts of alloying elements in base metals can alter markedly adhesion, friction, and wear by segregating to the solid surface. A.R.H.

N81-27524* National Aeronautics and Space Administration, Lewis Research Center, Cleveland, Ohio

OPTIMAL TOOTH NUMBERS FOR COMPACT STANDARD SPUR GEAR SETS

Michael Savage (Akron Univ.), John J. Coy, and Dennis P. Townsend. 1981. 33 p. refs. Proposed for presentation at the Design Eng. Tech. Meeting, Hartford, Conn., 20-23 Sep. 1981; Sponsored by ASME and presented at the NASA-AVRADCOM Symp. on Advan. Power Transmission Technol., Cleveland, 9-11 Jun. 1981. Prepared in cooperation with Army Aviation Research and Development Command, Cleveland

(Grant NAG3-55)

(NASA-TM-82614; E-865; AVRADCOM-TR-81-C-15). Avail. NTIS HC A03/MF A01 CSCL 131

The design of a standard gear mesh is treated with the objective of minimizing the gear size for a given ratio, pinion torque, and allowable tooth strength. Scoring, pitting fatigue, bending fatigue, and the kinematic limits of contact ratio and interference are considered. A design space is defined in terms of the number of teeth on the pinion and the diametral pitch. This space is then combined with the objective function of minimum center distance to obtain an optimal design region. This region defines the number of pinion teeth for the most compact design. The number is a function of the gear ratio only. A design example illustrating this procedure is also given.

Author

N81-27525* National Aeronautics and Space Administration, Lewis Research Center, Cleveland, Ohio

A METHOD OF SELECTING GRID SIZE TO ACCOUNT FOR HERTZ DEFORMATION IN FINITE ELEMENT ANALYSIS OF SPUR GEARS

John J. Coy and Charles Hu-Chih Chao (Northwestern Univ.). 1981. 27 p. refs. Proposed for presentation at the Design Eng. Tech. Conf., Hartford, Conn., 20-23 Sep. 1981; sponsored by ASME. Prepared in cooperation with Army Aviation Research and Development Command, Cleveland

(NASA-TM-82623; E-728; AVRADCOM-TR-81-C-14). Avail.

NTIS HC A03/MF A01 CSCL 131

A method of selecting grid size for the finite element analysis of gear tooth deflection is presented. The method is based on a finite element study of two cylinders in line contact, where the criterion for establishing element size was that there be agreement with the classical Hertzian solution for deflection. The results are applied to calculate deflection for the gear specimen used in the NASA spur gear test rig. Comparisons are made between the present results and the results of two other methods of calculation. The results have application in design of gear tooth profile modifications to reduce noise and dynamic loads.

S.F.

N81-27526* National Aeronautics and Space Administration
Lewis Research Center, Cleveland, Ohio.

SURFACE ROUGHNESS EFFECT ON FINITE OIL JOURNAL BEARINGS

B. C. Majumdar and B. J. Hamrock 1981 27 p refs Proposed for presentation at the Intern Conf on Optimum Resources Utilization through Tribo-Terrotechnol and Maintenance Management at the Indian Inst. of Technol., New Delhi, 30 Nov. 6 Dec 1981

(NASA-TM-82639; E-894) Avail. NTIS HC A03/MF A01 CSCL 131

A theoretical study of the performance of finite oil journal bearings is made, considering the surface roughness effect. The total load supporting ability under such a condition derives from the hydrodynamic as well as asperity contact pressure. These two components of load are calculated separately. The average Reynolds equation for partially lubricated surfaces is used to evaluate hydrodynamic pressure. An analytical expression for average film thickness is obtained and introduced to modify the average Reynolds equation. The resulting differential equation is then solved numerically by finite difference methods for mean hydrodynamic pressure, which in turn gives the hydrodynamic load. Assuming the surface height distribution as Gaussian, the asperity contact pressure is found. The effect of surface roughness parameter, surface pattern, eccentricity ratio, and length to diameter ratio on hydrodynamic load and on side leakage is investigated. It is shown that hydrodynamic load increases with increasing surface roughness when both journal and bearing surfaces have identical roughness structures or when the journal only has a rough surface. The trend of hydrodynamic load is reversed if the journal surface is smooth and the bearing surface is rough.

Author

N81-28443* National Aeronautics and Space Administration
Lewis Research Center, Cleveland, Ohio.

STRESS CONCENTRATION IN THE VICINITY OF A HOLE DEFECT UNDER CONDITIONS OF HERTZIAN CONTACT

Takashi Yamamoto (Tokyo Univ. of Agriculture and Technology), Masao Eguchi (Tokyo Univ. of Agriculture and Technology), and Kosho Murayama (Tokyo Univ. of Agriculture and Technology) 1981 25 p refs Proposed for presentation at the Joint Lubrication Conf., New Orleans, 5-7 Oct. 1981; sponsored by ASME and the American Society of Lubrication Engineers

(NASA-TM-82649; E-907) Avail. NTIS HC A02/MF A01 CSCL 20K

Two dimensional photoelastic stress analyses were conducted for epoxy resin models containing a hole defect under the conditions of Hertzian contact. Stress concentrations around the defect were determined as a function of several parameters. The effect of tangential traction on the stress concentration was also determined. Sharp stress concentrations occur in the vicinity of both the left and the right side of the hole. The stress concentration becomes more distinct the larger the hole diameter and the smaller distance between the hole and the contact surface. The stress concentration is greatest when the disk imposing a normal load is located at the contact surface directly over the hole. The magnitude and the location of stress concentration varies with the distance between the Hertzian contact area and the hole. The area involved in a process of rolling contact fatigue is confined to a shallow region at both sides of the hole. It was found that the effect of tangential traction is comparatively small on the stress concentration around the hole.

E.A.K.

N81-28444* National Aeronautics and Space Administration
Lewis Research Center, Cleveland, Ohio.

SIMPLIFIED SOLUTION FOR STRESSES AND DEFORMATION

Bernard J. Hamrock and David E. Brewe 1981 25 p refs Proposed for presentation at the Joint Lubrication Conf., New Orleans, 5-7 Oct. 1981; sponsored by the Am. Soc. of Lubrication Eng. and ASME. Prepared in cooperation with Army Aviation Research and Development Command, Cleveland
(NASA-TM-82647; E-905; AVRADCOM-TR-81-C-14) Avail. NTIS HC A02/MF A01 CSCL 20K

Conventional contact deformation analysis for ball bearings, gears, and cams involves tedious iterative procedures or the use of design charts. A simplified approach that makes the elastic deformation at the center of contact easy to calculate was previously reported. The range of validity in which these equations can be used is extended. A simplified approach to the calculation of the location and magnitude of subsurface stresses developed in machine element applications is included.

S.F.

N81-29438* National Aeronautics and Space Administration
Lewis Research Center, Cleveland, Ohio.

ANALYSIS OF STARVATION EFFECTS ON HYDRODYNAMIC LUBRICATION IN NONCONFORMING CONTACTS

David E. Brewe and Bernard J. Hamrock 1981 32 p refs To be presented at the Joint Propulsion Conf. of Lubrication Engr. and ASME, New Orleans, 5-7 Oct. 1981. Prepared in cooperation with Army Aviation Research and Development Command, Cleveland

(NASA-TM-82668; E-773; AVRADCOM-81-C-17) Avail. NTIS HC A03/MF A01 CSCL 131

Numerical methods were used to determine the effects of lubricant starvation on the minimum film thickness under conditions of a hydrodynamic point contact. Starvation was effected by varying the fluid inlet level. The Reynolds boundary conditions were applied at the cavitation boundary and zero pressure was stipulated at the meniscus or inlet boundary. A minimum-fill-thickness equation as a function of both the ratio of dimensionless load to dimensionless speed and inlet supply level was determined. By comparing the film generated under the starved inlet condition with the film generated from the fully flooded inlet, an expression for the film reduction factor was obtained. Based on this factor a starvation threshold was defined as well as a critically starved inlet. The changes in the inlet pressure buildup due to changing the available lubricant supply are presented in the form of three dimensional isometric plots and also in the form of contour plots.

Author

N81-29439* National Aeronautics and Space Administration
Lewis Research Center, Cleveland, Ohio.

ENDURANCE TESTS WITH LARGE-BORE TAPERED-ROLLER BEARINGS TO 2.2 MILLION DN

Richard J. Parker, H. R. Signer (Industrial Tectonics, Inc.), and S. I. Pintel (Industrial Tectonics, Inc.) 1981 23 p refs Proposed for presentation at the Joint Lubrication Conf., New Orleans, 5-7 Oct. 1981; sponsored by Am. Soc. of Lubrication Engr. and ASME

(NASA-TM-82669; E-726) Avail. NTIS HC A02/MF A01 CSCL 131

Endurance life tests were run with standard design and optimized high-speed design 120.65-mm-(4.750-in.-) bore tapered-roller bearings at shaft speeds of 12,500 and 18,500 rpm, respectively. Standard design bearings of vacuum melted AISI 4320 and CBS-1000M, and high-speed design bearings of CBS-1000M and through-hardened AISI M-50 were run under heavy combined radial and thrust load until fatigue failure or until a preset cutoff time of 1100 hours was reached. Standard design bearings made from CBS 1000M material ran to a 10 percent life approximately six times rated catalog life. Twelve identical bearings of AISI 4320 material ran to ten times rated catalog life without failure. Cracking and fracture of the cones of AISI M-50 high-speed design bearings occurred at 18,500 rpm due to high tensile hoop stresses. Four CBS 1000M high-speed design bearings ran to twenty-four times rated catalog life without any spalling, cracking or fracture failures.

Author

N81-29440* # National Aeronautics and Space Administration, Lewis Research Center, Cleveland, Ohio.

EFFECTS OF ULTRA-CLEAN AND CENTRIFUGAL FILTRATION ON ROLLING-ELEMENT BEARING LIFE

Stuart H. Loewenthal, Donald W. Moyer (Tribon Bearing Co.), and William M. Needelman (Pall Corp., Glen Cove, N.Y.) 1981 34 p refs. Proposed for presentation at the Joint Lubrication Conf., New Orleans, 5-7 Oct. 1981; sponsored by ASME and Am. Soc. of Lubrication Engr. (NASA-TM-82660; E-929) Avail: NTIS HC A03/MF A01 CSCL 131

Fatigue tests were conducted on groups of 65-millimeter bore diameter deep-groove ball bearings in a MIL-L-23699 lubricant under two levels of filtration. In one test series, the oil cleanliness was maintained at an exceptionally high level (better than a class '000' per NAS 1638) with a 3 micron absolute barrier filter. These tests were intended to determine the 'upper limit' in bearing life under the strictest possible lubricant cleanliness conditions. In the tests using a centrifugal oil filter, contaminants of the type found in aircraft engine filters were injected into the filters' supply line at 125 milligrams per bearing-hour. 'Ultra-clean' lubrication produced bearing fatigue lives that were approximately twice that obtained in previous tests with contaminated oil using 3 micron absolute filtration and approximately three times that obtained with 49 micron filtration. It was also observed that the centrifugal oil filter had approximately the same effectiveness as a 30 micron absolute filter in preventing bearing surface damage. Author

N81-31550* # National Aeronautics and Space Administration, Lewis Research Center, Cleveland, Ohio

BALL BEARING MECHANICS

Bernard J. Hamrock and Duncan Dowson (Leeds Univ.) Jun. 1981 105 p refs. Repr. from Ball Bearing Lubrication, Chapter 3, Sep. 1981 (NASA-TM-81691; E-209) Avail: NTIS HC A06/MF A01 CSCL 131

Load-deflection relationships for different types of elliptical contacts such as those found in a ball bearing are developed. Simplified expressions that allow quick calculations of deformation to be made simply from a knowledge of the applied load, the material properties, and the geometry of the contacting elements are presented. Ball bearings subjected to radial, thrust and combined ball loads are analyzed. A design criterion for fatigue life of ball bearings is developed. The selection of a satisfactory lubricant, as well as describing systems that provide a constant flow of lubricant to the contact, is considered. Author

N81-33434* # National Aeronautics and Space Administration, Lewis Research Center, Cleveland, Ohio

CONTINUOUSLY VARIABLE TRANSMISSION: ASSESSMENT OF APPLICABILITY TO ADVANCE ELECTRIC VEHICLES

Stuart H. Loewenthal and Richard J. Parker 1981 32 p refs. Presented at the 4th Electric Vehicle Council Symp., Baltimore, 21-23 Oct. 1981

(Contract DE-AI01-77CS-51044)

(NASA-TM-82700; DOE/NASA/51044-23; E-983) Avail: NTIS HC A03/MF A01 CSCL 13F

A brief historical account of the evolution of continuously variable transmissions (CVT) for automotive use is given. The CVT concepts which are potentially suitable for application with electric and hybrid vehicles are discussed. The arrangement and function of several CVT concepts are cited along with their current developmental status. The results of preliminary design studies conducted on four CVT concepts for use in advanced electric vehicles are discussed. RCT

A81-17900* # Tribological properties of silicon carbide in metal removal process. K. Miyoshi and D. H. Buckley (NASA, Lewis Research Center, Cleveland, Ohio). *American Society of Mechanical Engineers, International Symposium on Metalworking Lubrication, San Francisco, Calif., Aug. 18, 19, 1980, Paper*. 16 p. 21 refs.

This paper reviews material properties of adhesion, friction and wear of single-crystal silicon carbide in contact with metals and alloys involved in a metal removal process such as grinding. The tribological properties in the metal removal processes are divided into properties which remove metal by adhesion between sliding surfaces, and metal removal by silicon carbide sliding against a metal, indenting it, and plowing a series of grooves or furrows. The paper also deals with fracture and deformation characteristics of the silicon carbide surface; the adhesion, friction and metal transfer to silicon carbide is related to the relative chemical activity of the metals. Atomic size and content of alloying elements play a dominant role in controlling adhesion and friction properties of alloys. The friction and abrasive wear decrease as the shear strength of the bulk metal increases. (Author)

A81-18647* # Kinematic correction for roller skewing. M. Savage (Akron, University, Akron, Ohio) and S. H. Loewenthal (NASA, Lewis Research Center, Cleveland, Ohio). *American Society of Mechanical Engineers, Design Engineering Technical Conference, Beverly Hills, Calif., Sept. 28-Oct. 1, 1980, Paper 80-DET-76*. 10 p. 14 refs. Members, \$1.50; nonmembers, \$3.00. Grant No. NSG-3077.

A theory of kinematic stabilization of rolling cylinders is developed for high-speed cylindrical roller bearings. This stabilization requires race and roller crowning to produce changes in the rolling geometry as the roller shifts axially. These changes put a reverse skew in the rolling elements by changing the rolling taper. Twelve basic possible bearing modifications are identified in this paper. Four have single transverse convex curvature in the rollers while eight have rollers with compound transverse curvature composed of a central cylindrical band of constant radius surrounded by symmetric bands with both slope and transverse curvature. (Author)

A81-18668* # Calculated and experimental data for a 118-mm bore roller bearing to 3 million DN. H. H. Coe and F. T. Schuller (NASA, Lewis Research Center, Cleveland, Ohio). *American Society of Mechanical Engineers and American Society of Lubrication Engineers, Century 2 International Lubrication Conference, San Francisco, Calif., Aug. 18-21, 1980, ASME Paper 80-C2/Lub-14*. 8 p. 16 refs. Members, \$1.50; nonmembers, \$3.00.

Operating characteristics for a 118-mm bore cylindrical roller bearing were calculated using the computer program CYBEAN. The predicted results of inner and outer-race temperatures and heat transferred to the lubricant generally compared well with experimental data for shaft speeds to 3 million DN (25,500 rpm), radial loads to 8900 N (2000 lb), and total lubricant flow rates to 0.0102 cu m/min (2.7 gal/min). (Author)

A81-18683* # Dynamic characteristics of a high-speed rotor with radial and axial foil-bearing supports. L. Licht, W. J. Anderson (NASA, Lewis Research Center, Cleveland, Ohio), and S. W. Doroff (U.S. Navy, Office of Naval Research, Arlington, Va.). *American Society of Mechanical Engineers and American Society of Lubrication Engineers, Century 2 International Lubrication Conference, San Francisco, Calif., Aug. 18-21, 1980, ASME Paper 80-C2/Lub-35*. 10 p. 15 refs. Members, \$1.50; nonmembers, \$3.00. NASA-Navy-sponsored research.

An asymmetric rotor (19N; 4.3 lb), supported radially and axially by compliant bearings is subjected to severe excitation by rotating unbalance in the 'pitching' mode at speeds to 50,000 rpm. The resilient, air-lubricated bearings provide very effective damping, so that regions of resonance and instability can be traversed with amplitudes and limit-trajectories within acceptable bounds. A novel journal bearing is introduced, in which a resilient support is furnished

by the outer turn of the coiled foil-element bent to form an open polygon. The experimental apparatus and procedure are described, and the response of the rotor and flexible support system are documented by oscilloscope records of motion. (Author)

A81-18684 * # Design and performance of compliant thrust bearing with spiral-groove membranes on resilient supports. L. Licht, W. J. Anderson (NASA, Lewis Research Center, Cleveland, Ohio), and S. W. Doroff (U.S. Navy, Office of Naval Research, Arlington, Va.). *American Society of Mechanical Engineers and American Society of Lubrication Engineers, Century 2 International Lubrication Conference, San Francisco, Calif., Aug. 18-21, 1980, ASME Paper 80-C2/Lub-36*. 12 p. 20 refs. Members, \$1.50; nonmembers, \$3.00. NASA-Navy-sponsored research.

Novel thrust bearings with spiral-groove flexible membranes mounted on resilient supports were designed and their performance demonstrated. Advantages of surface compliance were combined with the superior load-capacity of the spiral-groove geometry. Loads of 127-150N were supported on an area 42 sq cm, at speeds of 43,000-45,000 rpm and mean clearances of 15-20 microns. Support-worthiness was proved when tested in conjunction with foil journal-bearings and a 19N rotor, excited in a pitching mode by a total unbalance of 43 micron-N. (Author)

A81-18695 * # The adhesion, friction, and wear of binary alloys in contact with single-crystal silicon carbide. K. Miyoshi and D. H. Buckley (NASA, Lewis Research Center, Cleveland, Ohio). *American Society of Mechanical Engineers and American Society of Lubrication Engineers, Century 2 International Lubrication Conference, San Francisco, Calif., Aug. 18-21, 1980, ASME Paper 80-C2/Lub-53*. 8 p. 10 refs. Members, \$1.50; nonmembers, \$3.00.

Sliding friction experiments were conducted with various iron-base alloys (alloying elements were Ti, Cr, Ni, Rh, and W) in contact with a single-crystal silicon carbide (0001) surface in vacuum. Results indicate atomic size misfit and concentration of alloying elements play a dominant role in controlling adhesion, friction, and wear properties of iron-base binary alloys. The controlling mechanism of the alloy properties is an intrinsic effect involving the resistance to shear fracture of cohesive bonding in the alloy. The coefficient of friction generally increases with an increase in solute concentration. The coefficient of friction increases as the solute-to-iron atomic radius ratio increases or decreases from unity. Alloys having higher solute concentration produce more transfer to silicon carbide than do alloys having low solute concentrations. The chemical activity of the alloying element is also an important parameter in controlling adhesion and friction of alloys. (Author)

A81-18738 * # Lubrication of rolling element bearings. R. J. Parker (NASA, Lewis Research Center, Cleveland, Ohio). *American Society of Mechanical Engineers and American Society of Lubrication Engineers, Century 2 International Lubrication Conference, San Francisco, Calif., Aug. 18-21, 1980, Paper*. 24 p. 47 refs.

This paper is a broad survey of the lubrication of rolling-element bearings. Emphasis is on the critical design aspects related to speed, temperature, and ambient pressure environment. Types of lubrication including grease, jets, mist, wick, and through-the-race are discussed. The paper covers the historical development, present state of technology, and the future problems of rolling-element bearing lubrication. (Author)

A81-18739 * # Practical applications of surface analytic tools in tribology. J. Ferrante (NASA, Lewis Research Center, Cleveland, Ohio). *American Society of Mechanical Engineers and American Society of Lubrication Engineers, Century 2 International Lubrication Conference, San Francisco, Calif., Aug. 18-21, 1980, Paper*. 43 p. 34 refs.

Many of the currently, widely used tools available for surface

analysis are described. Those which have the highest applicability for giving elemental and/or compound analysis for problems of interest in tribology and are truly surface sensitive (that is, less than 10 atomic layers) are presented. The latter group is evaluated in detail in terms of strengths and weaknesses. Emphasis is placed on post facto analysis of experiments performed under 'real' conditions (e.g., in air with lubricants). It is further indicated that such equipment could be used for screening and quality control. (Author)

A81-29531 * # Ion beam texturing of heat transfer surfaces. P. K. Agarwal, E. L. Park, Jr. (Mississippi University, University, Miss.), and A. J. Weigand (NASA, Lewis Research Center, Cleveland, Ohio). *AIAA, Japan Society for Aeronautical and Space Sciences, and DGLR, International Electric Propulsion Conference, 15th, Las Vegas, Nev., Apr. 21-23, 1981, AIAA Paper 81-0670*. 7 p. 21 refs. NASA-supported research.

Nucleate boiling heat transfer is examined as a means of energy conservation. Nucleate boiling curves were obtained for ion beam textured copper surfaces, untreated cooper surfaces, copper surfaces which had been polished and surfaces which had been coated with a plasma deposited polymer. Results show that texturing aids heat transfer while polishing has the opposite effect. The polymer coatings did not change nucleate boiling behavior. Aging effects were observed for untreated and for polished surfaces, while no such effects were noticed for textured surfaces. These data suggest that aging may be dependent on surface microgeometry, which is important in nucleate boiling heat transfer. D.K.

A81-29532 * # Ion beam deposited protective films. M. J. Mirtich (NASA, Lewis Research Center, Cleveland, Ohio). *AIAA, Japan Society for Aeronautical and Space Sciences, and DGLR, International Electric Propulsion Conference, 15th, Las Vegas, Nev., Apr. 21-23, 1981, AIAA Paper 81-0672*. 11 p. 13 refs.

Sputter deposition of adherent thin films on complex geometric surfaces by ion beam sources is examined in order to evaluate three different types of protective coatings for die materials. In the first experiment, a 30 cm diameter argon ion source was used to sputter deposit adherent metallic films up to eight microns thick on H-13 steel, and a thermal fatigue test specimen sputter deposited with metallic coatings one micron thick was immersed in liquid aluminum and cooled by water for 15,000 cycles to simulate operational environments. Results show that these materials do protect the steel by reducing thermal fatigue and thereby increasing die lifetime. The second experiment generated diamond-like carbon films using a dual beam ion source system that directed an eight cm argon ion source beam at the substrates. These films are still in the process of being evaluated for crystallinity, hardness and infrared absorption. The third experiment coated a fiber glass beam shield incorporated in the eight-cm diameter mercury ion thruster with molybdenum to ensure proper electrical and thermal properties. The coating maintained its integrity even under acceleration tests. D.K.

A81-29958 * # Ultra-lean combustion at high inlet temperatures. D. N. Anderson (NASA, Lewis Research Center, Cleveland, Ohio). *American Society of Mechanical Engineers, Gas Turbine Conference and Products Show, Houston, Tex., Mar. 9-12, 1981, Paper 81-GT-44*. 9 p. 13 refs. Members, \$2.00; nonmembers, \$4.00.

Combustion at inlet-air temperatures of 1100 to 1250 K was studied for application to advanced automotive gas turbine engines. Combustion was initiated by the hot environment, and therefore no external ignition source was used. Combustion was stabilized without a flameholder. The tests were performed in a 12-cm-diameter test section at a pressure of 250,000 Pa, with reference velocities of 32 to 60 m/s and at maximum combustion temperatures of 1350 to 1850 K. Number 2 diesel fuel was injected by means of a multiple-source fuel injector. Unburned hydrocarbon emissions were negligible for all test conditions. Nitrogen oxide emissions were less than 1.9 g NO₂/kg fuel for combustion temperatures below 1680 K. Carbon

monoxide emissions were less than 16 g CO/kg fuel for combustion temperatures greater than 1600 K, inlet-air temperatures higher than 1150 K, and residence times greater than 4.3 ms. (Author)

A81-30013 * # **Design and preliminary results of a fuel flexible industrial gas turbine combustor.** A. S. Novick, D. L. Troth (General Motors Corp., Detroit Diesel Allison Div., Indianapolis, Ind.), and H. G. Yacubucci (NASA, Lewis Research Center, Cleveland, Ohio). *American Society of Mechanical Engineers, Gas Turbine Conference and Products Show, Houston, Tex., Mar. 9-12, 1981, Paper 81-GT-108.* 10 p. 15 refs. Members, \$2.00; nonmembers, \$4.00. Research supported by the U.S. Department of Energy.

The design characteristics are presented of a fuel tolerant variable geometry staged air combustor using regenerative/convective cooling. The rich/quench/lean variable geometry combustor is designed to achieve low NO(x) emission from fuels containing fuel bound nitrogen. The physical size of the combustor was calculated for a can-annular combustion system with associated operating conditions for the Allison 570-K engine. Preliminary test results indicate that the concept has the potential to meet emission requirements at maximum continuous power operation. However, airflow sealing and improved fuel/air mixing are necessary to meet Department of Energy program goals. L.S.

A81-30029 * # **Evaluation of advanced combustors for dry NO_x suppression with nitrogen bearing fuels in utility and industrial gas turbines.** M. B. Cutrone, M. B. Hilt (General Electric Co., Schenectady, N.Y.), A. Goyal, E. E. Ekstedt (General Electric Co., Evendale, Ohio), and J. Notardonato (NASA, Lewis Research Center, Cleveland, Ohio). *American Society of Mechanical Engineers, Gas Turbine Conference and Products Show, Houston, Tex., Mar. 9-12, 1981, Paper 81-GT-125.* 10 p. Members, \$2.00; nonmembers, \$4.00. Research supported by the U.S. Department of Energy.

A81-31238 * **The transfer of polytetrafluoroethylene studied by X-ray photoelectron spectroscopy.** D. R. Wheeler (NASA, Lewis Research Center, Cleveland, Ohio). *Wear*, vol. 66, Feb. 16, 1981, p. 355-365. 19 refs.

A polytetrafluoroethylene (PTFE) sphere of radius 4.8 mm was rubbed against nickel and S-Monel at speeds from 0.94 to 94 mm/s and at loads from 0.19 to 3.9 N. The transfer film of PTFE on the metal was examined with X-ray photoelectron spectroscopy. In all cases the film was found to be indistinguishable from bulk PTFE. A trace of metal fluoride was observed whether the rubbing took place on oxidized or atomically clean metal. The film was of the order of a molecule thick for the entire range of loads and did not increase with repeated passes over the same rubbed area. An erratic increase in thickness at rubbing speeds above 10 mm/s was taken as evidence of random transfer of bulk material. (Author)

A81-38059 * # **Simulation and visualization of face seal motion stability by means of computer generated movies.** I. Etsion and B. M. Auer (NASA, Lewis Research Center, Cleveland, OH). *British Hydrodynamic Research Association, Fluid Sealing Conference, Leeuwenhorst, Netherlands, Apr. 1-3, 1981, Paper.* 17 p. 6 refs.

A computer aided design method for mechanical face seals is described. Based on computer simulation, the actual motion of the flexibly mounted element of the seal can be visualized. This is achieved by solving the equations of motion of this element, calculating the displacements in its various degrees of freedom vs. time, and displaying the transient behavior in the form of a motion picture. Incorporating such a method in the design phase allows one to detect instabilities and to correct undesirable behavior of the seal. A theoretical background is presented. Details of the motion display technique are described, and the usefulness of the method is demonstrated by an example of a noncontacting conical face seal. (Author)

A81-44654 * # **Ion plating for the future.** T. Spalvins (NASA, Lewis Research Center, Cleveland, OH). *Society of Vacuum Coaters, Annual Technical Conference, 24th, Dearborn, MI, May 12-14, 1981, Paper.* 7 p. 12 refs.

The ion plating techniques are classified relative to the instrumental set up, evaporation media and mode of transport. Distinction is drawn between the low vacuum (plasma) and high vacuum (ion beam) techniques. Ion plating technology is discussed at the fundamental and industrial level. At the fundamental level, the capabilities and limitations of the plasma (evaporant flux) and film characteristics are evaluated. On the industrial level, the performance and potential uses of ion plated films are discussed. (Author)

A81-44655 * # **Sputtering and ion plating for aerospace applications.** T. Spalvins (NASA, Lewis Research Center, Cleveland, OH). *American Electroplaters Society, National Conference, Boston, MA, June 28-July 2, 1981, Paper.* 12 p. 13 refs.

Sputtering and ion plating technologies are reviewed in terms of their potential and present uses in the aerospace industry. Sputtering offers great universality and flexibility in depositing any material or in the synthesis of new ones. The sputter deposition process has two areas of interest: thin film and fabrication technology. Thin film sputtering technology is primarily used for aerospace mechanical components to reduce friction, wear, erosion, corrosion, high temperature oxidation, diffusion and fatigue, and also to sputter-construct temperature and strain sensors for aircraft engines. Sputter fabrication is used in intricate aircraft component manufacturing. Ion plating applications are discussed in terms of the high energy evaporant flux and the high throwing power. Excellent adherence and 3-dimensional coverage are the primary attributes of this technology. (Author)

A81-44659 * # **NASA five-ball fatigue tester - Over 20 years of research.** E. V. Zaretsky, R. J. Parker, and W. J. Anderson (NASA, Lewis Research Center, Cleveland, OH). *American Society for Testing and Materials, International Symposium on Contact Rolling Fatigue Testing of Bearing Steel, Phoenix, AZ, May 12-14, 1981, Paper.* 55 p. 60 refs.

The paper reviews, from both a technical and historic perspective, the results of research conducted using the NASA Five-Ball Fatigue Tester. The test rig was conceived by W. J. Anderson in late 1958. The first data was generated in March 1959. Since then a total of approximately 500,000 test hours have been accumulated on a group of eight test rigs which are capable of running 24 hours a day, 7 days a week. Studies have been conducted to determine the effect on rolling-element fatigue life of contact angle, material hardness, chemistry, heat treatment, and processing, lubricant type and chemistry, elastohydrodynamic film thickness, deformation and wear, vacuum, and temperature as well as Hertzian and residual stresses. Correlation was established between the results obtained using the five-ball tester and those obtained with full-scale rolling-element bearings. (Author)

A81-46493 * # **The role of the micro environment on the tribological behavior of materials.** D. H. Buckley (NASA, Lewis Research Center, Cleveland, OH). In: *Life cycle problems and environmental technology. Proceedings of the Twenty-sixth Annual Technical Meeting, Philadelphia, PA, May 12-14, 1980.* (A81-46476 22-38) Mt. Prospect, IL, Institute of Environmental Sciences, 1980, p. 124-130. 10 refs.

The paper reviews studies of the role of the microenvironment in the adhesion, friction, and wear behavior of materials in solid-state contact. The microenvironment is defined as the environment on the surface of solids in solid-state contact. Properties of the environment are discussed which exert an influence on the adhesion, friction, wear, and lubrication of materials in contact. The effect of the environment on lubricants and their properties is considered with respect to the interaction of lubricants with material surfaces in contact; the effect on the ability of lubricants to provide protective surface films is also considered. It is concluded that naturally

N81-13359* Shaker Research Corp., Ballston Lake, N. Y.
MEASUREMENT OF ROD SEAL LUBRICATION FOR STIRLING ENGINE Final Report, Mar. 1979 - Jun. 1980
 Allan I. Krauter Jul. 1980 62 p refs
 (Contract DEN-3-22; EC-77-A-31-1040)
 (NASA-CR-165157; DOE/NASA/022-2; SRC-80TR-62) Avail:
 NTIS HC A04/MF A01 CSCL 11A

The elastohydrodynamic behavior of sliding elastomeric seals for the Stirling engine, was analyzed using an experimental apparatus to determine the instantaneous oil film thickness throughout the cyclic reciprocating motion. Tests were conducted on two commercial elastomeric seals: a 'T' seal (76 mm O.D. and 3.8 mm between backing rings) and an 'O' ring (76 mm O.D. and 5.3 mm diameter). Testing conditions included seal diameters of 70 and 90, sliding velocities of 0.8, 2.0, and 3.6 m/s, and no pressure gradient across the seal. Both acrylic and aluminum cylinders were used. Measured oil film thickness profiles were compared to results of the elastohydrodynamic analysis. The comparison shows an overall qualitative agreement. Friction and oil leakage measurements were also made at these sliding speeds. The fluid used was a typical synthetic base automotive lubricant. It is concluded that this first time experimental analytical comparison for oil film thickness indicates the need for some improvements in the analytical model and in the experimental technique. A.R.H.

N81-15366* Eaton Engineering and Research Center, Southfield, Mich. Engineering and Research Center.
SMALL PASSENGER CAR TRANSMISSION TEST: DODGE OMNI A-404 TRANSMISSION Final Report
 M. P. Bujold Sep. 1980 355 p
 (Contracts DEN3-124; DE-A101-77CS-51044; EC-77-A-31-1044)
 (NASA-CR-165181; DOE/NASA/0124-5; ERC-LIB-80173)
 Avail: NTIS HC A16/MF A01 CSCL 13F

The small passenger car transmission test was initiated to supply electric vehicle manufacturers with technical information regarding the performance of commercially available transmissions. This transmission was tested in accordance with a passenger car automatic transmission test code (SAE J651b) which required drive performance, coast performance, and no load test conditions. Under these test conditions, the transmission attained maximum efficiencies in the mid eighty percent range for both drive performance test and coast performance tests. R.C.T.

N81-17434* General Electric Co., Cincinnati, Ohio.
PROGRAM TO DEVELOP SPRAYED, PLASTICALLY DEFORMABLE COMPRESSOR SHROUD SEAL MATERIALS Final Report, Jul. 1976 - Aug. 1980
 J. D. Schell and J. D. Schell Jan. 1980 148 p refs
 (Contract NAS3-20054)
 (NASA-CR-165237; R80AEG458) Avail: NTIS
 HC A07/MF A01 CSCL 11A

A study of fundamental rub behavior for 10 dense, sprayed materials and eight current compressor clearance materials was conducted. A literature survey of a wide variety of metallurgical and thermophysical properties was conducted and correlated to rub behavior. Based on the results, the most promising dense rub material was Cu-9Al. Additional studies on the effects of porosity, incursion rate, blade solidity, and ambient temperature were carried out on aluminum bronze (Cu-9Al-1Fe) with and without a 515B Feltmetal underlayer. A further development effort was conducted to assess the property requirements of a porous, aluminum bronze, seal material. Strength, thermal cycle capabilities, erosion and oxidation resistance, machinability, and abrasability at several porosity levels were examined. T.M.

N81-17437* Rocketdyne, Canoga Park, Calif.
LOW-THRUST CHEMICAL PROPULSION SYSTEM PUMP TECHNOLOGY Final Report, Oct. 1979 - Sep. 1980
 J. W. Meadville 20 Oct. 1980 411 p
 (Contract NAS3-21958)
 (NASA-CR-165210; RI/RD80-222) Avail: NTIS

HC A18/MF A01 CSCL 13K

A study was conducted within the thrust range 450 to 9000 N (100 to 2000 pounds). Performance analyses were made on centrifugal, pitot, Barake, drag, Tesla, gear, piston, lobe, and vane pumps with liquid hydrogen, liquid methane, and liquid oxygen as propellants. Gaseous methane and hydrogen driven axial impulse turbines, vane expanders, piston expanders, and electric motors were studied as drivers. Data are presented on performance, sizes, weights, and estimated service lives and costs. T.M.

N81-21355* Mechanical Technology, Inc., Latham, N. Y.
AN EXPERIMENTAL EVALUATION OF OIL PUMPING RINGS
 Martin W. Eusepi, Jed Walowit, and Maurice Cohen Apr. 1981 117 p refs
 (Contracts DEN3-119; EC-77-A-31-1040)
 (NASA-CR-165271; DOE/NASA/0119-81/1; MTI-81TR3)
 Avail: NTIS HC A06/MF A01 CSCL 13I

The design and construction of a reciprocating test vehicle to be used in evaluating hydrodynamic oil pumping rings are discussed. In addition, experimental test data are presented for three pumping ring designs that were constructed from Tin-Based Babbitt (SAE 11), Bearing Bronze (SAE 680), and Mechanical Carbon Graphite (Union Carbide Grade CNF-J). Data of pumped flow rate versus delivered pressure, as well as friction loss, are reported for the following conditions: frequencies of 10, 25 and 45 Hz; strokes of 25.4 mm (1.00 in.), 38.1 mm (1.50 in.) and 50.8 mm (2.00 in.) oil inlet temperature of 49 degrees (120 degrees); and pumping ring close-in pressures of 10.3 MPa (1500 lb/square inch. A 20W40 automotive oil was used for all tests. The maximum delivered pressure was 11 MPa (1600 lb/square inch. An analysis of hydrodynamic oil pumping rings was performed and the results of the analysis were compared to measured test data. S.F.

A81-10707 * Development of low-cost directionally-solidified turbine blades. G. S. Hoppin, III, M. Fujii (AirResearch Manufacturing Company of Arizona, Phoenix, Ariz.), and L. W. Sink (Tiernay Manufacturing, Phoenix, Ariz.). *International Symposium on Superalloys, 4th, Champion, Pa., Sept. 21-25, 1980, Paper. 10 p.* Contract No. NAS3-20073.

A low-cost directionally solidified (DS) casting of turbine blades of high stress rupture is discussed. The process uses an exothermically heated mold; a newly designed solid blade was cast for the high-pressure turbine of the TFE731-3 turbofan engine. Ni-based alloys Mar-M 247 and Mar-M 200 + Hf were used. The solid DS blade replaced a conventionally cast IN100 component; a 40% cost saving is expected, with a 2.4% reduction in the takeoff specific fuel consumption. The DS Mar-M 247 blade has been selected for production in the TFE731-3B-100, and advanced version of the TFE731-3. A.T.

A81-15796 * Computer-aided roll pass design in rolling of airfoil shapes. N. Akgerman, G. D. Lahoti, and T. Altan (Battelle Columbus Laboratories, Columbus, Ohio). *Journal of Applied Metalworking*, vol. 1, July 1980, p. 30-40. 9 refs. Contract No. NAS3-20380.

This paper describes two computer-aided design (CAD) programs developed for modeling the shape rolling process for airfoil sections. The first program, SHPROL, uses a modular upper-bound method of analysis and predicts the lateral spread, elongation, and roll torque. The second program, ROLPAS, predicts the stresses, roll separating force, the roll torque and the details of metal flow by simulating the rolling process, using the slab method of analysis. ROLPAS is an interactive program; it offers graphic display capabilities and allows the user to interact with the computer via a keyboard, CRT, and a light pen. The accuracy of the computerized models was evaluated by (a) rolling a selected airfoil shape at room temperature from 1018 steel and isothermally at high temperature from Ti-6Al-4V, and (b) comparing the experimental results with

computer predictions. The comparisons indicated that the CAD systems, described here, are useful for practical engineering purposes and can be utilized in roll pass design and analysis for airfoil and similar shapes. (Author)

A81-18680 * # Structural and compositional characterization of RF sputter-deposited Ni-Cr + Cr₂O₃ films. B. Bhushan (Mechanical Technology, Inc., Latham, N.Y.). *American Society of Mechanical Engineers and American Society of Lubrication Engineers, Century 2 International Lubrication Conference, San Francisco, Calif., Aug. 18-21, 1980, ASME Paper 80-C2/Lub-31.* 7 p. 9 refs. Member, \$1.50; nonmembers, \$3.00. Research sponsored by the U.S. Department of Energy; Contract No. DEN3-43.

An RF-sputtered chrome oxide coating with metallic binders was developed. The chrome oxide coating has high-temperature capabilities and is wear resistant, and has some self-lubricating properties. A nichrome metallic binder was added in the coating to improve its ductility without significant loss in the hardness. The sputtering parameters were optimized to obtain a smooth coating with the maximum adherence. The coatings were applied using bias-sputter and sputter-deposit modes on the heat treated and annealed foil substrates. The coating applied on annealed foils using the sputter-deposit mode was smooth and had the best adherence. Metallurgical examinations showed that the coating was Ni-Cr + Cr₂O₃. The coating as applied was amorphous and it crystallized during substrate heat treatment. (Author)

A81-18693 * # Friction and wear results from sputter-deposited chrome oxide with and without nichrome metallic binders and interlayers. B. Bhushan (Mechanical Technology, Inc., Latham, N.Y.). *American Society of Mechanical Engineers and American Society of Lubrication Engineers, Century 2 International Lubrication Conference, San Francisco, Calif., Aug. 18-21, 1980, ASME Paper 80-C2/Lub-49.* 10 p. 8 refs. Member, \$1.50; nonmembers, \$3.00. Research sponsored by the U.S. Department of Energy; Contract No. DEN3-43.

Friction and wear tests were conducted on optimized sputtered Cr₂O₃ and Cr₂O₃ with metallic binder coatings. The coatings were applied on the bearing surface of journal foil air bearings and were tested against chrome-carbide-coated journal surfaces. The objective of the study was to develop a coating system which would withstand 9000 start-stops and high-speed runs (maximum acceleration, 100 g) in temperatures ranging from room temperature to 650 C. The Cr₂O₃ coating completed the test sequence and the coating consisting of Cr₂O₃ with metallic binders completed 3000 start-stops. The coefficient of friction of the coatings at 650 C was found to be about half that at room temperature. It was concluded, therefore, that the coatings should perform much better in a high temperature environment alone. The decrease in friction at high temperature is attributed to oxidation and interactions of the coatings and substrates at the interface temperature. (Author)

A81-22664 * Design, durability and low cost processing technology for composite fan exit guide vanes. S. S. Blecherman (United Technologies Corp., Pratt and Whitney Aircraft Group, Middletown, Conn.). In: *The 1980's - Payoff decade for advanced materials. Proceedings of the Twenty-fifth National Symposium and Exhibition, San Diego, Calif., May 6-8, 1980.* (A81-22636 08-27) Azusa, Calif., Society for the Advancement of Material and Process Engineering, 1980, p. 403-417. 5 refs. Contract No. NAS3-21037.

A program was conducted to design, fabricate and test a durable, low cost, lightweight composite fan exit guide vane for high bypass ratio gas turbine engine application. Eight candidate material/design combinations were evaluated by NASTRAN finite element analysis. Four of these candidate systems were selected for composite vane fabrication by two vendors. A core and shell vane design was chosen in which the unidirectional graphite core fiber was the same for all candidates. The shell material, fiber orientation and ply configuration were varied. Material tests were performed on raw

material and composite specimens to establish specification requirements. Composite vanes were nondestructively inspected and subsequently fatigue tested in both dry and 'wet' conditions. The program provided relevant data with respect to design analysis, materials properties, inspection standards, improved durability, weight benefits and part price of the composite fan exit guide vane. (Author)

A81-30014 * # Low NO_x/ combustion systems for burning heavy residual fuels and high-fuel-bound nitrogen fuels. D. J. White, A. Batakis, R. T. LeCren (Solar Turbines International, San Diego, Calif.), and H. G. Yacoubucci (NASA, Lewis Research Center, Cleveland, Ohio). *American Society of Mechanical Engineers, Gas Turbine Conference and Products Show, Houston, Tex., Mar. 9-12, 1981, Paper 81-GT-109.* 11 p. Member, \$2.00; nonmembers, \$4.00. Research supported by the U.S. Department of Energy.

Design concepts are presented for lean-lean and staged rich-lean combustors. The combustors are designed for the dry reduction of thermal NO_x, control of NO_x from fuels containing high levels of organic nitrogen, and control of smoke from low hydrogen content fuels. The combustor concepts are tested with a wide variety of fuels including a middle distillate, a petroleum based heavy residual, a coal derived synthetic, and ratios of blends of these fuels. The configurations of the lean-lean and rich-lean combustion systems are provided along with a description of the test rig and test procedure. L.S.

A81-30060 * # Fabrication of injection molded sintered alpha SiC turbine components. R. S. Storm, R. W. Ohnsorg, and F. J. Frechette (Carborundum Co., Niagara Falls, N.Y.). *American Society of Mechanical Engineers, Gas Turbine Conference and Products Show, Houston, Tex., Mar. 9-12, 1981, Paper 81-GT-161.* 6 p. 5 refs. Member, \$2.00; nonmembers, \$4.00. Research supported by the U.S. Department of Energy Contracts No. DEN3-17; No. DEN3-168; No. DEN3-167.

Fabrication of a sintered alpha silicon carbide turbine blade by injection molding is described. An extensive process variation matrix was carried out to define the optimum fabrication conditions. Variation of molding parameters had a significant impact on yield. Turbine blades were produced in a reasonable yield which met a rigid quality and dimensional specification. Application of injection molding technology to more complex components such as integral rotors is also described. (Author)

38 QUALITY ASSURANCE AND RELIABILITY

Includes product sampling procedures and techniques and quality control.

N81-28458* # National Aeronautics and Space Administration. Lewis Research Center, Cleveland, Ohio.

ACOUSTO-ULTRASONIC CHARACTERIZATION OF FIBER REINFORCED COMPOSITES

Alex Vary 1981 14 p refs Presented at the Office of Naval Res. Conf. A Critical Rev: Tech. for the Characterization of Composite Mater., Cambridge, Mass., 8-10 Jun. 1981 (NASA-TM-82651; E-910) Avail: NTIS HC A02/MF A01 CSCI 14D

The acousto-ultrasonic technique combines advantageous aspects of acoustic emission and ultrasonic methodologies. Acousto-ultrasonics operates by introducing a repeating series of ultrasonic pulses into a material. The waves introduced simulate the spontaneous stress waves that would arise if the material were put under stress as in the case of acoustic emission measurements. These benign stress waves are detected by an acoustic emission sensor. The physical arrangement of the ultrasonic (input) transducer and acoustic emission (output) sensor is such that the resultant waveform carries an imprint of morphological factors that govern or contribute to material performance. The output waveform is complex, but it can be quantitized in terms of a 'stress wave factor'. The stress wave factor, which can be defined in a number of ways, is a relative measure of the efficiency of energy dissipation in a material. If flaws or other material anomalies exist in the volume being examined, their combined effect appears in the stress wave factor. S.F.

N81-33492* # National Aeronautics and Space Administration. Lewis Research Center, Cleveland, Ohio.

RELIABILITY AND QUALITY ASSURANCE ON THE MOD 2 WIND SYSTEM

W. E. B. Mason and B. G. Jones (Boding Engineering and Construction Co., Seattle, Wash.) 1981 16 p refs Presented at 5th Biennial Wind Energy Conf. and Workshop, Washington, 5-7 Oct. 1981; sponsored by Solar Energy Res. Inst. and DOE (Contract DE-A101-79ET-20305) (NASA-TM-82717; DOE/NASA/20305-6; E-1015) Avail: NTIS HC A02/MF A01 CSCI 14D

The Safety, Reliability, and Quality Assurance (R&QA) approach developed for the largest wind turbine generator, the Mod 2, is described. The R&QA approach assures that the machine is not hazardous to the public or to the operating personnel, is operated unattended on a utility grid, demonstrates reliable operation, and helps establish the quality assurance and maintainability requirements for future wind turbine projects. The significant guideline consisted of a failure modes and effects analysis (FMEA) during the design phase, hardware inspections during parts fabrication, and three simple documents to control activities during machine construction and operation. E.A.K.

A81-19656* Ultrasonic measurement of material properties. A. Vary (NASA, Lewis Research Center, Materials and Structures Div., Cleveland, Ohio). In: Research techniques in nondestructive testing. Volume 4. (A81-19651 00-38) London, Academic Press, 1980, p. 159-204, 121 refs.

The state-of-the-art of ultrasonic methods is reviewed with reference to the basic measurements, signal acquisition and processing, strength property and morphological condition measurements, and industrial applications. The emphasis is placed on techniques that indicate quantitative ultrasonic correlations with material strength and morphology relevant to the reliability of load-bearing structures. V.L.

A81-33867* Self-acting geometry for noncontact seals. G. P. Allen (NASA, Lewis Research Center, Cleveland, Ohio). *American Society of Lubrication Engineers, Annual Meeting, 36th, Pittsburgh, Pa., May 11-14, 1981, Preprint 81-AM-58-2*, 5 p, 6 refs.

Two hydrodynamic self-acting seal designs for a LOX turbo-pump were analyzed in order to predict performance. A radial face seal-to-seal LOX at 310 N/sq cm and 32,000 rpm (130 m/s) was analyzed for pressure differentials of 17 to 448 N/sq cm and speeds from 98 to 147 m/s. A segmented circumferential seal-to-seal helium at 34.5 or 69 N/sq cm and 157 m/s was analyzed for pressures of 35 to 86 N/sq cm (10 N/sq cm ambient) and speeds from 94 to 189 m/s. Test results confirmed noncontact operation near the design speed and pressure, and relatively good qualitative agreement between test and analysis. The face seal was found to operate with mostly liquid in the pads and mostly gas across the dam. E.B.

A81-44660* # Acousto-ultrasonic characterization of fiber reinforced composites. A. Vary (NASA, Lewis Research Center, Cleveland, OH). *U.S. Navy, Conference on a Critical Review: Technique for the Characterization of Composite Materials, Cambridge, MA, June 8-10, 1981, Paper*, 13 p, 12 refs.

The acousto-ultrasonic technique combines advantageous aspects of acoustic emission and ultrasonic methodologies. Acousto-ultrasonics operates by introducing a repeating series of ultrasonic pulses into a material. The waves introduced simulate the spontaneous stress waves that would arise if the material were put under stress as in the case of acoustic emission measurements. These benign stress waves are detected by an acoustic emission sensor. The physical arrangement of the ultrasonic (input) transducer and acoustic emission (output) sensor is such that the resultant waveform carries an imprint of morphological factors that govern or contribute to material performance. The output waveform is quite complex, but it can be quantitized in terms of a 'stress wave factor'. The stress wave factor, which can be defined in a number of ways, is essentially a relative measure of the efficiency of energy dissipation in a material. If flaws or other material anomalies exist in the volume being examined, their combined effect will appear in the stress wave factor. (Author)

39 STRUCTURAL MECHANICS

Includes structural element design and weight analysis, fatigue, and thermal stress.

For applications see 05 Aircraft Design, Testing and Performance and 18 Spacecraft Design, Testing and Performance.

N81-11412* National Aeronautics and Space Administration, Lewis Research Center, Cleveland, Ohio.

SUPERHYBRID COMPOSITE BLADE IMPACT STUDIES

C. C. Chamis, R. F. Lark, and J. H. Sinclair [1980] 16 p refs. Proposed for presentation at the 26th Ann. Intern. Gas Turbine Conf., Houston, Tex., 9-12 Mar. 1981. (NASA-TM-81597; E-580) Avail: NTIS HC A02/MF A01 CSCL 20K

The feasibility of superhybrid composite blades for meeting the mechanical design and impact resistance requirements of large fan blades for aircraft turbine engine applications was investigated. Two design concepts were evaluated: leading edge spar (TiCom) and center spar (TiCore), both with superhybrid composite shells. The investigation was both analytical and experimental. The results obtained show promise that superhybrid composites can be used to make light weight, high quality, large fan blades with good structural integrity. The blades tested successfully demonstrated their ability to meet steady state operating conditions, overspeed, and small bird impact requirements.

A.R.H.

N81-11417* National Aeronautics and Space Administration, Lewis Research Center, Cleveland, Ohio.

METHOD FOR ESTIMATING CRACK-EXTENSION RESISTANCE CURVE FROM RESIDUAL STRENGTH DATA

Thomas W. Orange. Nov. 1980 15 p refs. (NASA-TP-1753; E-439) Avail: NTIS HC A02/MF A01 CSCL 20K

A method is presented for estimating the crack extension resistance curve (R curve) from residual strength (maximum load against initial crack length) data for precracked fracture specimens. The method allows additional information to be inferred from simple test results, and that information is used to estimate the failure loads of more complicated structures. Numerical differentiation of the residual strength data is required, and the problems that it may present are discussed.

R.C.T.

N81-12446* National Aeronautics and Space Administration, Lewis Research Center, Cleveland, Ohio.

STABILITY OF LARGE HORIZONTAL-AXIS AXISYMMETRIC WIND TURBINES Ph.D. Thesis - Delaware Univ.

M. S. Hirschbein and M. I. Young (Delaware Univ., Newark) 1980 37 p refs. Presented at 3d Miami Conf. on Alternative Energy Sources, Miami, 15-17 Dec. 1980. (NASA-TM-81623; E-633) Avail: NTIS HC A03/MF A01 CSCL 20K

The stability of large horizontal axis, axis-symmetric, power producing wind turbines was examined. The analytical model used included the dynamic coupling of the rotor, tower and power generating system. The aerodynamic loading was derived from blade element theory. Each rotor blade was permitted two principal elastic bending degrees of freedom, one degree of freedom in torsion and controlled pitch as a rigid body. The rotor hub was mounted in a rigid nacelle which may yaw freely or in a controlled manner. The tower can bend in two principal directions and may twist. Also, the rotor speed can vary and may induce perturbation reactions within the power generating equipment. Stability was determined by the eigenvalues of a set of linearized constant coefficient differential equations. All results presented are based on a 3 bladed, 300 ft. diameter, 2.5 megawatt wind turbine. Some of the parameters varied were: wind speed, rotor speed, structural stiffness and damping, the effective stiffness and damping of the power generating system and the principal bending directions of the rotor blades. Unstable or weakly stable behavior can be caused by aerodynamic forces

due to motion of the rotor blades and tower in the plane of rotation or by mechanical coupling between the rotor system and the tower.

Author

N81-18492* National Aeronautics and Space Administration, Lewis Research Center, Cleveland, Ohio.

EXPERIMENTAL COMPLIANCE CALIBRATION OF THE COMPACT FRACTURE TOUGHNESS SPECIMEN

D. M. Fisher and R. J. Buzzard. Dec. 1980 11 p refs. (NASA-TM-81865; E-685) Avail: NTIS HC A02/MF A01 CSCL 20K

Compliance and stress intensity coefficients were determined over crack length to width ratios from 0.1 to 0.8. Displacements were measured at the load points, load line, and crack mouth. Special fixturing was devised to permit accurate measurement of load point displacement. The results are in agreement with the currently used results of boundary collocation analyses. The errors which occur in stress intensity coefficients or specimen energy input determinations made from load line displacement measurements rather than from load point measurements are emphasized.

Author

N81-18494* National Aeronautics and Space Administration, Lewis Research Center, Cleveland, Ohio.

EFFECTS OF MISTUNING ON BENDING-TORSION FLUTTER AND RESPONSE OF A CASCADE IN IN-COMPRESSIBLE FLOW

Krishna Rao V. Kaza (Toledo Univ., Ohio) and Robert E. Kielb. 1981 20 p refs. Proposed for presentation at Dyn. Specialists Conf., Atlanta, 9-11 Apr. 1981; sponsored by AIAA (Contract EX-76-1-01-1028). (NASA-TM-81674; DOE/NASA/1028-29; E-699) Avail: NTIS HC A02/MF A01 CSCL 20K

The effect of small differences between the individual blades (mistuning) on the aeroelastic stability and response of a cascade were studied. The aerodynamic, inertial, and structural coupling between the bending and torsional motions of each blade and the aerodynamic coupling between the blades was considered. A digital computer program was developed to conduct parametric studies. Results indicate that the mistuning has a beneficial effect on the coupled bending torsion and uncoupled torsion flutter. On forced response, however, the effect may be either beneficial or adverse, depending on the engine order of the forcing function. The results also illustrate that it may be feasible to utilize mistuning as a passive control to increase flutter speed while maintaining forced response at an acceptable level.

A.R.H.

N81-28492* National Aeronautics and Space Administration, Lewis Research Center, Cleveland, Ohio.

AEROELASTIC CHARACTERISTICS OF A CASCADE OF MISTUNED BLADES IN SUBSONIC AND SUPERSONIC FLOWS

Robert E. Kielb and Krishna Rao V. Kaza (Toledo Univ.) 1981 18 p refs. Proposed for presentation at the 8th Biennial Eng. Div. Conf., Hartford, Conn., 20-23 Sep. 1981; sponsored by the American Society of Mechanical Engineers (Grant NSG-3139).

(NASA-TM-82631; E-886) Avail: NTIS HC A02/MF A01 CSCL 20K

The effects of mistuning on flutter and forced response of a cascade in subsonic in subsonic and supersonic flow were investigated. The aerodynamic and structural coupling between the bending and torsional motions and the aerodynamic coupling between the blades were studied. It is shown that frequency mistuning always has a beneficial effect on flutter. For the cascade considered, the potential for raising flutter speed is greater in subsonic than in supersonic flow. Preliminary results for structural damping mistuning show that there are no additional benefits over adding damping mistuning may have either a beneficial or an adverse effect on forced response, depending on the engine order of the excitation and Mach number.

A.R.H.

N81-33497* National Aeronautics and Space Administration, Lewis Research Center, Cleveland, Ohio.

STRUCTURAL DYNAMICS VERIFICATION FACILITY STUDY

Louis J. Kiraly, Murray S. Hirschbein, James M. McAleese, and David P. Fleming. Aug. 1981. 21 p. refs. (NASA-TM-82675; E-958) Avail. NTIS HC A02/MF A01 CSCL 20K

The need for a structural dynamics verification facility to support structures programs was studied. Most of the industry operated facilities are used for highly focused research, component development, and problem solving, and are not used for the generic understanding of the coupled dynamic response of major engine subsystems. Capabilities for the proposed facility include: the ability to both excite and measure coupled structural dynamic response of elastic blades on elastic shafting, the mechanical simulation of various dynamic loadings representative of those seen in operating engines, and the measurement of engine dynamic deflections and interface forces caused by alternative engine mounting configurations and compliances.

E. A. K.

A81-18792* On the equivalence between semiempirical fracture analyses and R-curves. T. W. Orange (NASA, Lewis Research Center, Cleveland, Ohio). In: Fracture mechanics: Proceedings of the Twelfth National Symposium, Washington University, St. Louis, Mo., May 21-23, 1979. (A81-18776 06-39) Philadelphia, Pa., American Society for Testing and Materials, 1980, p. 478-499. 11 refs.

The relationship between the R-curves and semiempirical fracture analyses (SEFA) is investigated theoretically using a hypothetical material. Equivalent R-curves (ERC) are developed for real materials using data from the literature. It is shown that for each SEFA there is an ERC whose magnitude and shape are determined by the SEFA formulation and its empirical parameters. The ERC is equivalent in that it predicts exactly the same relationship between the fracture stress and the initial crack length (residual strength) as the SEFA. If the effective R-curve is unique, then the various empirical parameters cannot be constant, and vice versa. However, for one of the SEFA examined, Newman's SEFA, parameter variations are small enough to be within the range of normal data scatter for real materials.

V. L.

A81-22526* Stability of large horizontal-axis axisymmetric wind turbines. M. S. Hirschbein (NASA, Lewis Research Center, Cleveland, Ohio) and M. I. Young (Delaware University, Newark, Del.). *Miami International Conference on Alternative Energy Sources*, 3rd, Miami, Fla., Dec. 15-17, 1980, Paper. 35 p. 19 refs.

The stability of large horizontal-axis, axisymmetric, power producing wind turbines is examined within the framework of an analytical model which includes dynamic coupling of the rotor, tower, and power generating system. The aerodynamic loading is derived from blade element theory. Stability is determined by the eigenvalues of a set of linearized constant-coefficient differential equations. All results presented are based on a 3-bladed, 300-ft diameter, 2.0-MW wind turbine. It is shown that unstable or weakly stable behavior can be caused by aerodynamic forces due to motion of the rotor blades and tower in the plane of rotation or by mechanical coupling between the rotor system and the tower.

V. L.

A81-29095* Effects of mistuning on blade torsional flutter.

A. V. Srinivasan (United Technologies Research Center, East Hartford, Conn.) and A. Kurkov (NASA, Lewis Research Center, Cleveland, Ohio). In: International Symposium on Air Breathing Engines, 5th, Bangalore, India, February 16-22, 1981, Proceedings. (A81-29051 12-07) Bangalore, National Aeronautical Laboratory, 1981, p. 59-1 to 59-8. 9 refs. Contract No. NAS3-21603.

An analytical model for the prediction of fan blade flutter is presented and evaluated using data from NASA tests on an advanced high performance engine. For the cascade conditions appropriate to the test points studied, the aerodynamic theory cannot predict subcritical flutter. Under the assumptions of a tuned assembly, the

imaginary part of the aerodynamic coefficients does indicate flutter for a limited number of interblade phase angles, but these interblade phase angles are close to those at which the acoustic resonance is predicted. Upon using the individual blade frequencies and solving the mistuned system with aerodynamic coupling only, the results show a stable system. Eigenvectors calculated for the mistuned system demonstrate the presence of several harmonics in each mistuned mode. Inclusion of both mechanical and aerodynamic coupling in the solution of the eigenproblem influences not only the frequencies but also damping in the system with a trend toward stability.

L. S.

A81-29465* Effects of mistuning on bending-torsion flutter and response of a cascade in incompressible flow. K. R. V. Kaza (NASA, Lewis Research Center, Cleveland; Toledo, University, Toledo, Ohio) and R. E. Kiehl (NASA, Lewis Research Center, Structures Branch, Cleveland, Ohio). In: Structures, Structural Dynamics and Materials Conference, 22nd, Atlanta, Ga., April 6-8, 1981, and AIAA Dynamics Specialists Conference, Atlanta, Ga., April 9, 10, 1981, Technical Papers, Part 2. (A81-29428 12-01) New York, American Institute of Aeronautics and Astronautics, Inc., 1981, p. 320-331. 21 refs. (AIAA 81-0602)

This paper presents an investigation of the effects of blade mistuning on the aeroelastic stability and response of a cascade in incompressible flow. The aerodynamic, inertial, and structural coupling between the bending and torsional motions of each blade and the aerodynamic coupling between the blades are included in the formulation. A digital computer program was developed to conduct parametric studies. Results indicate that the mistuning has a beneficial effect on the coupled bending-torsion and uncoupled torsion flutter. The effect of mistuning on forced response, however, may be either beneficial or adverse, depending on the engine order of the forcing function. Additionally, the results illustrate that it may be feasible to utilize mistuning as a passive control to increase flutter speed while maintaining forced response at an acceptable level.

(Author)

N81-17480* National Aeronautics and Space Administration, Lewis Research Center, Cleveland, Ohio.

COMPOSITE CONTAINMENT SYSTEMS FOR JET ENGINE FAN BLADES

G. T. Smith. 1981. 18 p. refs. Presented at the 36th Ann. Conf. of the Reinforced Plastics/Composites Inst. of the Soc. of the Plastics Ind., Inc., Washington, D.C., 16-20 Feb. 1981. (NASA-TM-81675; E-700) Avail. NTIS HC A02/MF A01 CSCL 21E

The use of composites in fan blade containment systems is investigated and the associated structural benefits of the composite system design are identified. Two basic types of containment structures were investigated. The short finned concept was evaluated using Kevlar/epoxy laminates for fins which were mounted in a 6061 T-6 aluminum ring. The long fin concept was evaluated with Kevlar/epoxy, 6Al4V titanium, and 2024 T-3 aluminum fins. The unfinned configurations consisted of the base-line steel sheet, a circumferentially oriented aluminum honeycomb, and a Kevlar cloth filled ring. Results obtained show that a substantial reduction in the fan blade containment system weight is possible. Minimization of damage within the engine arising from impact interaction between blade debris and the engine structure is also achieved.

M. G.

N81-19479* Textron Bell Aerospace Co., Buffalo, N. Y. **AEROELASTIC AND DYNAMIC FINITE ELEMENT ANALYSES OF A BLADDER SHROUDED DISK**

G. C. C. Smith and V. Elchuri. Mar. 1980. 152 p. refs. (Contract NAS3-20382)

(NASA-CR-159728; D2536-941001) Avail. NTIS HC A08/MF A01 CSCL 20K

The delivery and demonstration of a computer program for the analysis of aeroelastic and dynamic properties is reported. Approaches to flutter and forced vibration of mistuned disks, and transient aerothermoelasticity are described.

R. C. T.

NS1-19480* Textron Bell Aerospace Co., Buffalo, N. Y.
NASTRAN LEVEL 16 THEORETICAL MANUAL UPDATES FOR AEROELASTIC ANALYSIS OF BLADED DISCS
 V. Elchuri and G. C. C. Smith Mar. 1980 24 p refs
 (Contract NAS3-20382)
 (NASA-CR-159823; D2536-941002) Avail: NTIS
 HC A02/MF A01 CSCL 20K

A computer program based on state of the art compressor and structural technologies applied to bladed shrouded disc was developed and made operational in NASTRAN Level 16. Aeroelastic analyses, modes and flutter. Theoretical manual updates are included. S.F.

NS1-19481* Textron Bell Aerospace Co., Buffalo, N. Y.
NASTRAN LEVEL 16 USER'S MANUAL UPDATES FOR AEROELASTIC ANALYSIS OF BLADED DISCS
 V. Elchuri and A. M. Gallo Mar. 1980 167 p refs
 (Contract NAS3-20382)
 (NASA-CR-159824; D2536-941003) Avail: NTIS
 HC A08/MF A01 CSCL 20K

The NASTRAN aeroelastic and flutter capability was extended to solve a class of problems associated with axial flow turbomachines. The capabilities of the program are briefly discussed. The aerodynamic data pertaining to the bladed disc sector, the associated aerodynamic modeling, the steady aerothermoelastic 'design/analysis' formulations, and the modal, flutter, and subcritical roots analyses are described. Sample problems and their solutions are included. R.C.T.

NS1-19482* Textron Bell Aerospace Co., Buffalo, N. Y.
NASTRAN LEVEL 16 PROGRAMMER'S MANUAL UPDATES FOR AEROELASTIC ANALYSIS OF BLADED DISCS
 A. M. Gallo and B. Dale Mar. 1980 88 p refs
 (Contract NAS3-20382)
 (NASA-CR-159825; D2536-941004) Avail: NTIS
 HC A05/MF A01 CSCL 20K

The programming routines for the NASTRAN Level 16 program are presented. Particular emphasis is placed on its application to aeroelastic analyses, mode development, and flutter analysis for turbomachine blades. R.C.T.

NS1-19483* Textron Bell Aerospace Co., Buffalo, N. Y.
NASTRAN LEVEL 16 DEMONSTRATION MANUAL UPDATES FOR AEROELASTIC ANALYSIS OF BLADED DISCS
 V. Elchuri and A. M. Gallo Mar. '80 15 p refs
 (Contract NAS3-20382)
 (NASA-CR-159826; D2536-941005) Avail: NTIS
 HC A02/MF A01 CSCL 20K

A computer program based on state of the art compressor and structural technologies applied to bladed shrouded discs was developed and made operational in NASTRAN Level 16. The problems encompassed include aeroelastic analyses, modes, and flutter. The demonstration manual updates are described. L.F.M.

A81-14162 * Continuous analysis of stresses from arbitrary surface loads on a half space. J. C. Bell (Battelle Columbus Laboratories, Columbus, Ohio). *International Journal of Solids and Structures*, vol. 16, no. 12, 1980, p. 1069-1091. 11 refs. Research supported by Battelle Memorial Institute and Bell Aerospace Co.; Contracts No. F33615-72-C-1739; No. NAS3-17760; No. NAS3-21020.

A new form of elemental surface load on a half space is introduced, presuming a quasi-pyramidal variation of load which is doubly linear in each of four rectangular parts of a surface rectangle. Approximations of arbitrary load distributions by sums of such elements are continuous, piecewise linear in two directions and well adaptable. The loads may be normal or tangential. The explicit solutions obtained for all stress and displacement components due to each elemental load involve only elementary functions, are free of

the discontinuities which arise with stepwise elements, and are suitable for computing. Some illustrative stress distributions are presented for elemental loads and for multiple pyramidal loads involving both normal and tangential loads. The value of the load continuity in the more complicated analyses of surface cracks is also illustrated. (Author)

43 EARTH RESOURCES

Includes remote sensing of earth resources by aircraft and spacecraft; photogrammetry; and aerial photography. For instrumentation see 35 *Instrumentation and Photography*.

N81-28517* National Aeronautics and Space Administration. Lewis Research Center, Cleveland, Ohio.
DESIGN DESCRIPTION OF THE SCHUCHULI VILLAGE PHOTOVOLTAIC POWER SYSTEM Final Report
Anthony F. Ratajczak, Richard W. Vasicek, and Richard DeLembard
May 1981 100 p
(Contract DE-AI01-79ET-20485)
(NASA-TM-82650; DOE/NASA/20485-10) Avail: NTIS HC A05/MF A01 CSCL 10B

A stand alone photovoltaic (PV) power system for the village of Schuchuli (Gunsight), Arizona, on the Papago Indian Reservation is a limited energy, all 120 V (d.c.) system to which loads cannot be arbitrarily added and consists of a 3.5 kW (peak) PV array, 2380 ampere-hours of battery storage, an electrical equipment building, a 120 V (d.c.) electrical distribution network, and equipment and automatic controls to provide control power for pumping water into an existing water system; operating 15 refrigerators, a clothes washing machine, a sewing machine, and lights for each of the homes and communal buildings. A solar hot water heater supplies hot water for the washing machine and communal laundry. Automatic control systems provide voltage control by limiting the number of PV strings supplying power during system operation and battery charging, and load management for operating high priority at the expense of low priority loads as the main battery becomes depleted. A.R.H.

N81-13425* Houston Univ., Tex. Dept. of Mathematics.
NUMERICAL TRIALS OF HISSE
Charles Peters and Frank Kampe, Principal Investigators 5 Aug. 1980 28 p refs Sponsored by NASA, USDA, Dept. of Commerce, Dept. of Interior, and Agency for International Development ERTS
(Contract NAS9-14689; Proj. AgRISTARS)
(E81-10069; NASA-CR-160881; SR-HO-00477) Avail: NTIS HC A03/MF A01 CSCL 02C

The mathematical description and implementation of the statistical estimation procedure known as the Houston integrated spatial/spectral estimator (HISSE) is discussed. HISSE is based on a normal mixture model and is designed to take advantage of spectral and spatial information of LANDSAT data pixels, utilizing the initial classification and clustering information provided by the AMOEBA algorithm. The HISSE calculates parametric estimates of class proportions which reduce the error inherent in estimates derived from typical classify and count procedures common to nonparametric clustering algorithms. It also singles out spatial groupings of pixels which are most suitable for labeling classes. These calculations are designed to aid the analyst/interpreter in labeling patches with a crop class label. Finally, HISSE's initial performance on an actual LANDSAT agricultural ground truth data set is reported. E.D.K.

N81-13426* Lockheed Engineering and Management Services Co., Inc., Houston, Tex.
NORMAL CROP CALENDARS. VOLUME 2: THE SPRING WHEAT STATES OF MINNESOTA, MONTANA, NORTH DAKOTA, AND SOUTH DAKOTA
William L. West, III, Principal Investigator Aug. 1980 24 p refs Sponsored by NASA, USDA, Dept. of Commerce, Dept. of Interior, and Agency for International Development ERTS
(Contract NAS9-15800; Proj. AgRISTARS)
(E81-10070; NASA-CR-160867; SR-LO-00485; LEMSCO-15034; JSC-16814) Avail: NTIS HC A02/MF A01 CSCL 02C

The state crop calendars for the principal spring wheat producing states within the United States are presented. These crop calendars are an update of those produced for the large area crop inventory experiment multilabeling task during 1978 and

are compiled for the foreign commodity production forecasting (FCPF) project of the agriculture and resources inventory surveys through aerospace remote sensing program. R.C.T.

N81-13427* Lockheed Engineering and Management Services Co., Inc., Houston, Tex.
PRELIMINARY EVALUATION OF THE ENVIRONMENTAL RESEARCH INSTITUTE OF MICHIGAN CROP CALENDAR SHIFT ALGORITHM FOR ESTIMATION OF SPRING WHEAT DEVELOPMENT STAGE
D. E. Phinney, Principal Investigator Sep. 1980 20 p refs Sponsored by NASA, USDA, Dept. of Commerce, Dept. of Interior, and Agency for International Development ERTS
(Contract NAS9-15800; Proj. AgRISTARS)
(E81-10071; NASA-CR-160865; SR-LO-00476; LEMSCO-15115; JSC-16377) Avail: NTIS HC A02/MF A01 CSCL 02C

An algorithm for estimating spectral crop calendar shifts of spring small grains was applied to 1978 spring wheat fields. The algorithm provides estimates of the date of peak spectral response by maximizing the cross correlation between a reference profile and the observed multitemporal pattern of Kauth-Thomas greenness for a field. A methodology was developed for estimation of crop development stage from the date of peak spectral response. Evaluation studies showed that the algorithm provided stable estimates with no geographical bias. Crop development stage estimates had a root mean square error near 10 days. The algorithm was recommended for comparative testing against other models which are candidates for use in AgRISTARS experiments. E.D.K.

N81-13428* Lockheed Engineering and Management Services Co., Inc., Houston, Tex.
LIMITED AREA COVERAGE/HIGH RESOLUTION PICTURE TRANSMISSION (LAC/HRPT) TAPE IJ GRID PIXEL EXTRACTION PROCESSOR USER'S MANUAL
S. O. O'Brien, Principal Investigator Sep. 1980 14 p Sponsored by NASA, USDA, Dept. of Commerce, Dept. of Interior, and Agency for International Development ERTS
(Contract NAS9-15800; Proj. AgRISTARS)
(E81-10072; NASA-CR-160866; EW-LO-00702; LEMSCO-15326; JSC-16374) Avail: NTIS HC A02/MF A01 CSCL 05B

The program, LACREG, extracted all pixels that are contained in a specific IJ grid section. The pixels, along with a header record are stored in a disk file defined by the user. The program will extract up to 99 IJ grid sections. Author

N81-13429* Lockheed Engineering and Management Services Co., Inc., Houston, Tex.
LIMITED AREA COVERAGE/HIGH RESOLUTION PICTURE TRANSMISSION (LAC/HRPT) DATA VEGETATIVE INDEX CALCULATION PROCESSOR USER'S MANUAL
S. O. O'Brien, Principal Investigator Sep. 1980 14 p Sponsored by NASA, USDA, Dept. of Commerce, Dept. of Interior, and Agency for International Development ERTS
(Contract NAS9-15800; Proj. AgRISTARS)
(E81-10073; NASA-CR-160870; EW-LO-00703; LEMSCO-15327; JSC-16375) Avail: NTIS HC A02/MF A01 CSCL 08F

The program, LACVIN, calculates vegetative indexes numbers on limited area coverage/high resolution picture transmission data for selected IJ grid sections. The IJ grid sections were previously extracted from the full resolution data tapes and stored on disk files. Author

C-2

N81-13430* Lockheed Engineering and Management Services Co., Inc., Houston, Tex.

EROS TO UNIVERSAL TAPE CONVERSION PROCESSOR
S. O. O'Brien, Principal Investigator Sep. 1980 11 p Sponsored by NASA, USDA, Dept. of Commerce, Dept. of Interior, and Agency for International Development ERTS
(Contract NAS9-15800; Proj. AgRISTARS)
(E81-10074; NASA-CR-160869; EW-LO-00705;
LEMSCO-15357; JSC-16382) Avail: NTIS HC A02/MF A01
CSCL 05B

The function of the EROS processor is to allow a user to select a specific area from a full frame LANDSAT image which is written on tape in the EROS format. The area of interest is read from the EROS formatted tape and converted to the JSC Universal format and written onto another tape. This tape can then be read by the IMDACS processing system and normal analysis can be performed. Author

N81-13431* Lockheed Engineering and Management Services Co., Inc., Houston, Tex.

NORMAL CROP CALENDARS. VOLUME 1: ASSEMBLY AND APPLICATION OF HISTORICAL CROP DATA TO A STANDARD PRODUCT

William L. West, III, Principal Investigator Aug. 1980 21 p refs Sponsored by NASA, USDA, Dept. of Commerce, Dept. of Interior, and Agency for International Development ERTS
(Contract NAS9-15800; Proj. AgRISTARS)
(E81-10075; NASA-CR-160868; SR-LO-00484;
LEMSCO-15033; JSC-16813) Avail: NTIS HC A02/MF A01
CSCL 02C

The approach used in the collection, collation, and compilation of normal crop calendar for the foreign commodity production forecasting (FCPF) project of the AgRISTARS program is described. A.R.H.

N81-13432* Lockheed Engineering and Management Services Co., Inc., Houston, Tex.

EVALUATION OF RESULTS OF US CORN AND SOYBEANS EXPLORATORY EXPERIMENT: CLASSIFICATION PROCEDURES VERIFICATION TEST

J. G. Carnes and J. E. Baird, Principal Investigators Sep. 1980 39 p refs Sponsored by NASA, USDA, Dept. of Commerce, Dept. of Interior, and Agency for International Development ERTS
(Contract NAS9-15800; Proj. AgRISTARS)
(E81-10076; NASA-CR-160873; SR-LO-00423;
LEMSCO-14386; JSC-16339) Avail: NTIS HC A03/MF A01
CSCL 02C

The classification procedure utilized in making crop proportion estimates for corn and soybeans using remotely sensed data was evaluated. The procedure was derived during the transition year of the Large Area Crop Inventory Experiment. Analysis of variance techniques were applied to classifications performed by 3 groups of analysts who processed 25 segments selected from 4 agrophysical units (APUs). Group and APU effects were assessed to determine factors which affected the quality of the classifications. The classification results were studied to determine the effectiveness of the procedure in producing corn and soybeans proportion estimates. A.R.H.

N81-13433* Lockheed Engineering and Management Services Co., Inc., Houston, Tex.

LIMITED AREA COVERAGE/HIGH RESOLUTION PICTURE TRANSMISSION, LAC/HRPT TAPE CONVERSION PROCESSOR USER'S MANUAL

S. O. O'Brien, Principal Investigator Sep. 1980 14 p Sponsored by NASA, USDA, Dept. of Commerce, Dept. of Interior, and Agency for International Development ERTS
(Contract NAS9-15800; Proj. AgRISTARS)
(E81-10077; NASA-CR-160871; EW-LO-00701;
LEMSCO-15325; JSC-16373) Avail: NTIS HC A02/MF A01
CSCL 05B

The program, LACSEG, converts LAC/HRPT data tapes to

the CSC defined Universal format. The Universal formatted data tape is then processed the normal way by the FAS IMDACS system. Author

N81-33539* Environmental Research and Technology, Inc., Concord, Mass.

COMPARATIVE ANALYSIS OF SEA ICE FEATURES USING SIDE-LOOKING AIRBORNE RADAR (SLAR) AND LANDSAT IMAGERY Final Report

James C. Barnes and Clinton J. Bowley, Principal Investigators Cleveland NASA Lewis Research Center Mar. 1981 71 p refs Original contains imagery. Original photography may be purchased from the EROS Data Center, Sioux Falls, S.D. 57198. ERTS

(Contract NAS3-21924)
(E81-10044; NASA-CR-165335; P-3970-F) Avail: NTIS
HC A04/MF A01 CSCL 08L

A comparative analysis of sea ice features was carried out using X-Band, real aperture side-looking airborne radar (SLAR) and LANDSAT imagery. The SLAR data were collected by the NASA/LeRC C-131 aircraft on flights over the Mackenzie Delta and Prudhoe-Barrow areas of the southern Beaufort Sea and the Norton Sound area of the eastern Bering Sea. The LANDSAT data were for dates as near as possible to the dates of the SLAR missions. The analysis of the data sample available for the investigation indicates the SLAR imagery has distinct advantages over LANDSAT for identifying certain features and ice types. It is further indicated that the capability for SLAR observe ice through clouds is essential for an operational ice information system. R.C.T.

44 ENERGY PRODUCTION AND CONVERSION

Includes specific energy conversion systems, e.g. fuel cells and batteries; global sources of energy; fossil fuels; geophysical conversion; hydroelectric power; and wind power.

For related information see also 07 Aircraft Propulsion and Power, 20 Spacecraft Propulsion and Power, 28 Propellants and Fuels, and 85 Urban Technology and Transportation.

N81-11448* National Aeronautics and Space Administration, Lewis Research Center, Cleveland, Ohio.

PERFORMANCE OF A STEEL SPAR WIND TURBINE BLADE ON THE MOD-0 100 kW EXPERIMENTAL WIND TURBINE Final Report

Theo G. Keith, Jr. (Toledo Univ.), Timothy L. Sullivan, and Larry A. Viterna Sep. 1980 24 p refs
(Contract EX-76-1-01-1028)

(NASA-TM-81588; DOE/NASA/1028-27; E-567) Avail: NTIS HC A02/MF A01 CSCL 10B

The performance and loading of a large wind rotor, 38.4 m in diameter and composed of two low-cost steel spar blades were examined. Two blades were fabricated at Lewis Research Center and successfully operated on the Mod-0 wind turbine at Plum Brook. The blades were operated on a tower on which the natural bending frequency were altered by placing the tower on a leaf-spring apparatus. It was found that neither blade performance nor loading were affected significantly by this tower softening technique. Rotor performance exceeded prediction while blade loads were found to be in reasonable agreement with those predicted. Seventy-five hours of operation over a five month period resulted in no deterioration in the blade.

Author

N81-11449* National Aeronautics and Space Administration, Lewis Research Center, Cleveland, Ohio.

ELECTRIC AND HYBRID VEHICLE SYSTEM R/D

Harvey J. Schwartz 17 Sep. 1980 15 p refs Presented at Intern. Conf. on Transportation Electron., Dearborn, Michigan, 15-17 Sep. 1980; sponsored by the Vehicle Technol. Soc. and Int. of Elec. and Electron. Engr. and Soc. of Automotive Engr. and Inst. of Elec. Engr.

(Contract DE-AI01-77CS-51044)

(NASA-TM-81606; E-599; DOE/NASA/51044-11) Avail: NTIS HC A02/MF A01 CSCL 10B

The work being done to characterize the level of current propulsion technology through component testing is described. Important interactions between the battery and the propulsion system will be discussed. Component development work, involving traction motors, motor controllers and transmissions are described and current results are presented. Studies of advanced electric and hybrid propulsion system studies are summarized and the status of propulsion system development work supported by the project is described. A strategy for fostering joint industry/government projects for commercialization of propulsion components and systems is described briefly. T.M.

N81-12542* National Aeronautics and Space Administration, Lewis Research Center, Cleveland, Ohio.

SOLAR CELL SYSTEM HAVING ALTERNATING CURRENT OUTPUT Patent

John C. Evans, Jr., inventor (to NASA) Issued 12 Aug. 1980 6 p Filed 10 Aug. 1979 Continuation-in-part of abandoned US Patent Appl. SN 915050, filed 9 Jun. 1978

(NASA-Case-LEW-12806-2; US-Patent-4,217,633;

US-Patent-Appl-SN-065676; US-Patent-Class-363-27;

US-Patent-Class-136-249; US-Patent-Class-136-291;

US-Patent-Class-363-60; US-Patent-Class-363-147;

US-Patent-Appl-SN-915050) Avail: US Patent and Trademark Office CSCL 10A

A monolithic multijunction solar cell was modified by fabricating an integrated circuit inverter on the back of the cell to produce a device capable of generating an alternating current

output. In another embodiment, integrated circuit power conditioning electronics was incorporated in a module containing a solar cell power supply.

Official Gazette of the U.S. Patent and Trademark Office

N81-13463* National Aeronautics and Space Administration, Lewis Research Center, Cleveland, Ohio.

DATA ACQUISITION AND ANALYSIS IN THE DOE/NASA WIND ENERGY PROGRAM

Harold E. Neustadter 1980 18 p refs Presented at Symp. on Detection Diagnosis and Prognosis, Santa Monica, Calif., 7-9 Oct. 1980; sponsored by NBS

(Contract EX-76-1-01-1028)

(NASA-TM-81603; E-594) Avail: NTIS HC A02/MF A01 CSCL 10B

Four categories of data systems, each responding to a distinct information need are presented. The categories are: control, technology, engineering and performance. The focus is on the technology data system which consists of the following elements: sensors which measure critical parameters such as wind speed and direction, output power, blade loads and strains, and tower vibrations; remote multiplexing units (RMU) mounted on each wind turbine which frequency modulate, multiplex and transmit sensor outputs; the instrumentation available to record, process and display these signals; and centralized computer analysis of data. The RMU characteristics and multiplexing techniques are presented. Data processing is illustrated by following a typical signal through instruments such as the analog tape recorder, analog to digital converter, data compressor, digital tape recorder, video (CRT) display, and strip chart recorder. Author

N81-13464* National Aeronautics and Space Administration, Lewis Research Center, Cleveland, Ohio.

STATUS OF COMMERCIAL PHOSPHORIC ACID FUEL CELL SYSTEM DEVELOPMENT

Marvin Warshaw, Paul R. Prokopus, Steven N. Simons, and Robert B. King 1981 12 p refs Proposed for presentation at 19th Aerospace Sci. Meeting, St. Louis, 12-15 Jan. 1981; sponsored by AIAA

(Contract DE-AI03-79ET-11272)

(NASA-TM-81641; E-659; DOE/NASA/11272-2) Avail: NTIS HC A02/MF A01 CSCL 10A

In both the electric utility and onsite integrated energy system applications, reducing cost and increasing reliability are the main technology drivers. The longstanding barrier to the attainment of these goals, which manifests itself in a number of ways, was materials. The differences in approach among the three major participants (United Technologies Corporation, Westinghouse Electric Corporation/Energy Research Corporation, and Engelhard Industries) and their unique technological features, including electrodes, matrices, intercell cooling, bipolar/seperator plates, electrolyte management, fuel selection and system design philosophy are discussed. Author

N81-13465* National Aeronautics and Space Administration, Lewis Research Center, Cleveland, Ohio.

IGNITION OF LEAN FUEL-AIR MIXTURES IN A PREMIXING-PREVAPOORIZING DUCT AT TEMPERATURES UP TO 1000 K

Robert R. Tacine Dec. 1980 16 p refs

(Contract DE-AI01-77CS-51040)

(NASA-TM-81645; E-9356-3; DOE/NASA/51040-19) Avail: NTIS HC A02/MF A01 CSCL 21B

Conditions were determined in a premixing prevaporizing fuel preparation duct at which ignition occurred. An air blast type fuel injector with nineteen fuel injection points was used to provide a uniform spatial fuel air mixture. The range of inlet conditions where ignition occurred were: inlet air temperatures of 600 to 1000 K air pressures of 180 to 660 kPa, equivalence ratios (fuel air ratio divided by stoichiometric fuel air ratio) from 0.12 to 1.05, and velocities from 3.5 to 30 m/s. The duct was insulated and the diameter was 12 cm. Mixing lengths were varied from 16.5 to 47.6 and residence times ranged from 4.6 to 107 ms. The fuel was no. 2 diesel. Results show a strong effect of equivalence ratio, pressure and temperature on the

conditions where ignition occurred. The data did not fit the most commonly used model of auto-ignition. A correlation of the conditions where ignition would occur which apply to this test apparatus over the conditions tested is $(p/V)\phi$ to the 1.3 power = 0.62 e to the 2804/T power where p is the pressure in kPa, V is the velocity in m/s, ϕ is the equivalence ratio, and T is the temperature in K. The data scatter was considerable, varying by a maximum value of 5 at a given temperature and equivalence ratio. There was wide spread in the autoignition data contained in the references. A.R.H.

N81-14396* National Aeronautics and Space Administration, Lewis Research Center, Cleveland, Ohio

CATALYTIC COMBUSTION OF COAL-DERIVED LIQUIDS

Daniel L. Bulzan and Robert R. Tacina 1981 25 p refs Presented at 26th Ann. Intern. Gas Turbine Conf., Houston, Tex., 8-12 Mar. 1981; sponsored by ASME (Contract DE-AI01-77ET-10350) (NASA-TM-81594; E-661; DOE/NASA/10350-21) Avail: NTIS HC A02/MF A01 CSCL 10B

A noble metal catalytic reactor was tested with three grades of SRC 2 coal derived liquids, naphtha, middle distillate, and a blend of three parts middle distillate to one part heavy distillate. A petroleum derived number 2 diesel fuel was also tested to provide a direct comparison. The catalytic reactor was tested at inlet temperatures from 600 to 800 K, reference velocities from 10 to 20 m/s, lean fuel air ratios, and a pressure of 3×10 to the 5th power Pa. Compared to the diesel, the naphtha gave slightly better combustion efficiency, the middle distillate was almost identical, and the middle heavy blend was slightly poorer. The coal derived liquid fuels contained from 0.58 to 0.95 percent nitrogen by weight. Conversion of fuel nitrogen to NOx was approximately 75 percent for all three grades of the coal derived liquids. Author

N81-14397* National Aeronautics and Space Administration, Lewis Research Center, Cleveland, Ohio

APPLICABILITY OF ADVANCED AUTOMOTIVE HEAT ENGINES TO SOLAR THERMAL POWER

Donald G. Beremand, David G. Evans, and Donald L. Alger 1981 26 p refs Presented at SAE Intern. Eng. Congr. and Exposition, Detroit, 23-27 Feb. 1981 (Contract EX-76-A-29-1060) (NASA-TM-81658; E-675; DOE/NASA/1060-4) Avail: NTIS HC A03/MF A01 CSCL 10B

The requirements of a solar thermal power system are reviewed and compared with the predicted characteristics of automobile engines under development. A good match is found in terms of power level and efficiency when the automobile engines, designed for maximum powers of 65-100 kW (87 to 133 hp) are operated to the nominal 20-40 kW electric output requirement of the solar thermal application. At these reduced power levels it appears that the automotive gas turbine and Stirling engines have the potential to deliver the 40+ percent efficiency goal of the solar thermal program. M.G.

N81-14398* National Aeronautics and Space Administration, Lewis Research Center, Cleveland, Ohio

ULTRA-LEAN COMBUSTION AT HIGH INLET TEMPERATURES

David N. Anderson 1981 20 p refs Presented at 26th Intern. Gas Turbine Conf., Houston, Tex., 8-12 Mar. 1981; sponsored by ASME (Contract EC-77-A-31-1101) (NASA-TM-81640; E-677; DOE/NASA/1011-33) Avail: NTIS HC A02/MF A01 CSCL 21B

Combustion at inlet air temperatures of 1100 to 1250 K was studied for application to advanced automotive gas turbine engines. Combustion was initiated by the hot environment, and therefore no external ignition source was used. Combustion was stabilized without a flameholder. The tests were performed in a 12 cm diameter test section at a pressure of 2.5×10 to the 5th power Pa, with reference velocities of 32 to 60 m/sec and at maximum combustion temperatures of 1350 to 1850 K. Number 2 diesel fuel was injected by means of a multiple source

fuel injector. Unburned hydrocarbons emissions were negligible for all test conditions. Nitrogen oxides emissions were less than 1.9 g NO2/kg fuel for combustion temperatures below 1680 K. Carbon monoxide emissions were less than 16 g CO/kg fuel for combustion temperatures greater than 1600 K, inlet air temperatures higher than 1150 K, and residence times greater than 4.3 microseconds. Author

N81-14399* National Aeronautics and Space Administration, Lewis Research Center, Cleveland, Ohio

EFFECT OF FUEL NITROGEN AND HYDROGEN CONTENT ON EMISSIONS IN HYDROCARBON COMBUSTION

David A. Bittker and Gary Wollbrandt 1981 24 p refs Presented at 26th Ann. Intern. Gas Turbine Conf., Houston, Tex., 8-12 Mar. 1981; sponsored by ASME (Contract DE-AI01-77ET-10350) (NASA-TM-81612; E-614; DOE/NASA-10350-19) Avail: NTIS HC A02/MF A01 CSCL 10B

How the emissions of nitrogen oxides and carbon monoxide are affected by: (1) the decreased hydrogen content and (2) the increased organic nitrogen content of coal derived fuels is investigated. Previous CRT experimental work in a two stage flame tube has shown the effectiveness of rich lean two stage combustion in reducing fuel nitrogen conversion to nitrogen oxides. Previous theoretical work gave preliminary indications that emissions trends from the flame tube experiment could be predicted by a two stage, well stirred reactor combustor model using a detailed chemical mechanism for propane oxidation and nitrogen oxide formation. Additional computations are reported and comparisons with experimental results for two additional fuels and a wide range of operating conditions are given. Fuels used in the modeling are pure propane, a propane toluene mixture and pure toluene. These give hydrogen contents 18, 11 and 9 percent by weight, respectively. Fuel bound nitrogen contents of 0.5 and 1.0 percent were used. Results are presented for oxides of nitrogen and also carbon monoxide concentrations as a function of primary equivalence ratio, hydrogen content and fuel bound nitrogen content. Author

N81-15484* National Aeronautics and Space Administration, Lewis Research Center, Cleveland, Ohio

ELECTRONICALLY COMMUTATED dc MOTORS FOR ELECTRIC VEHICLES

Edward A. Maslowski 1981 18 p refs Prepared for presentation at Soc. of Automotive Engr. Intern. Congr. and Exposition, Detroit, 23-27 Feb. 1981 (Contract DE-AI01-77CS-51044) (NASA-TM-81654; E-657; DOE/NASA/51044-14) Avail: NTIS HC A02/MF A01 CSCL 09C

A motor development program to explore the feasibility of electronically commutated dc motors (also known as brushless) for electric cars is described. Two different design concepts and a number of design variations based on these concepts are discussed. One design concept is based on a permanent magnet, medium speed, machine rated at 7000 to 9000 rpm, and powered via a transistor inverter power conditioner. The other concept is based on a permanent magnet, high speed, machine rated at 22,000 to 26,000 rpm, and powered via a thyristor inverter power conditioner. Test results are presented for a medium speed motor and a high speed motor each of which have been fabricated using samarium cobalt permanent magnet material. Author

N81-15485* National Aeronautics and Space Administration, Lewis Research Center, Cleveland, Ohio

CHARACTERIZATION OF THE NEAR-TERM ELECTRIC VEHICLE (ETV-1) BREADBOARD PROPULSION SYSTEM OVER THE SAE J227a DRIVING SCHEDULE D

Noel B. Sargent and Miles O. Dustin 1981 15 p refs Prepared for presentation at Soc. of Automotive Engr. Intern. Congr. and Exposition, Detroit, 23-27 Feb. 1981 (Contract DE-AI01-77CS-51044) (NASA-TM-81664; E-684; DOE/NASA/51044-15) Avail: NTIS HC A02/MF A01 CSCL 10B

The electric test vehicle one (ETV-1) was built from the ground up with present state of the art technology. Two vehicles

were built and are presently being evaluated by NASA's Jet Propulsion Laboratory (JPL). A duplicate set of propulsion system components was built, mounted on a breadboard, and delivered to NASA's Lewis Research Center for testing on the road load simulator (RLS). Driving cycle tests completed on the system are described. E.D.K.

N81-16528* National Aeronautics and Space Administration, Lewis Research Center, Cleveland, Ohio.

HIGH VOLTAGE PLANAR MULTIJUNCTION Patent Application

J. C. Evans, Jr., A. T. Chai, inventors (to NASA), and C. P. Goradia Filed 24 Dec. 1980 15 p (NASA-Case-LEW-13400-1; US-Patent-Appl-SN-219677) Avail: NTIS HC A02/MF A01 CSCL 10A

A solar cell which provides high output voltages, comprises a semiconductor wafer in which a number or array of voltage generating regions or unit cells are formed. Each of the unit cells has two regions of opposite conductivity type (e.g., n+ and p+) which are separated by a gap region. The unit cells are connected together by metal contacts so that their outputs are additive. Field regions, separated by gaps, overlie the unit cells. Cells are formed in both faces of the wafer; a circular wafer is employed. NASA

N81-16529* National Aeronautics and Space Administration, Lewis Research Center, Cleveland, Ohio.

HIGH VOLTAGE V-GROOVE SOLAR CELL Patent Application

John C. Evans, Jr., An-Ti Chai, and Chandra P. Goradia Filed 24 Dec. 1980 11 p (NASA-Case-LEW-13401-1; US-Patent-Appl-SN-219678) Avail: NTIS HC A02/MF A01 CSCL 10A

The fabrication of the cell is described. The solar cell features a plurality of discrete voltage generating regions or unit cells which are formed in a single, generally planar semiconductor body. The unit cells comprise doped regions of opposite conductivity type separated by a gap or indiffused regions. Metal contacts connect adjacent cells together in series so that the output voltages of the individual cells are additive. In some embodiments, doped field regions separated by gaps overlie the unit cells but the cells may be formed in both faces of the wafer. T.M.

N81-16532* National Aeronautics and Space Administration, Lewis Research Center, Cleveland, Ohio.

ANALYTICAL INVESTIGATION OF EFFICIENCY AND PERFORMANCE LIMITS IN KLYSTRON AMPLIFIERS USING MULTIDIMENSIONAL COMPUTER PROGRAMS; MULTI-STAGE DEPRESSED COLLECTORS; AND THERMIONIC CATHODE LIFE STUDIES

H. G. Kosmahl In NASA, Johnson Space Center Solar Power Satellite Microwave Transmission and Reception Dec. 1980 p 206-213 refs (For primary document see N81-16533 07-44) Avail: NTIS HC A16/MF A01 CSCL 10A

An extensive parametric investigation was performed of the extraction of energy in output gaps of klystron amplifiers, using 3-D computer programs. Due to complexity of the program which used a hydrodynamic, axially and radially deformable disk ring model and the resulting long computing time, the investigation was limited to the output gap, by far the most important and difficult part of the klystron interaction. Results show that, for a confined flow focused beam throughout the penultimate cavity, radial velocities remain very small and the beam is highly laminar. It was, therefore, concluded that possible errors resulting from treating only the output cavity in 3-D would remain small. T.M.

N81-16570* National Aeronautics and Space Administration, Lewis Research Center, Cleveland, Ohio.

PERFORMANCE CALCULATIONS FOR 1000 MWe MHD/STEAM POWER PLANTS

C. C. P. Pian 1981 15 p refs Presented at the 19th Aerospace

Sci. Meeting, St. Louis, 12-15 Jan. 1981; sponsored by AIAA (Contract DE-A101-77ET-10769)

(NASA-TM-81687; DOE/NASA/10769-13; E-588) Avail: NTIS HC A02/MF A01 CSCL 10B

The effects of MHD generator operating conditions and constraints on the performance of MHD/steam power plants are investigated. Power plants using high temperature combustion air preheat (2500 F) and plants using intermediate temperature preheat (1100 F) with oxygen enrichment are considered. Variations of these two types of power plants are compared on the basis of fixed total electrical output (1000 MWe). Results are presented to show the effects of generator plant length and level of oxygen enrichment on the plant thermodynamic efficiency and on the required generator mass flow rate. Factors affecting the optimum levels of oxygen enrichment are analyzed. It is shown that oxygen enrichment can reduce magnet stored energy requirement. Author

N81-16571* National Aeronautics and Space Administration, Lewis Research Center, Cleveland, Ohio.

OFF-DESIGN ANALYSIS OF A GAS TURBINE POWER-PLANT AUGMENTED BY STEAM INJECTION USING VARIOUS FUELS

Robert J. Stochl Nov. 1980 29 p refs (NASA-TM-81611; E-609) Avail: NTIS HC A03/MF A01 CSCL 10B

Results are compared using coal derived low and intermediate heating value fuel gases and a conventional distillate. The results indicate that steam injection provides substantial increases in both power and efficiency within the available compressor surge margin. The results also indicate that these performance gains are relatively insensitive as to the type of fuel. Also, in a cogeneration application, steam injection could provide some degree of flexibility by varying the split between power and process steam. T.M.

N81-16584* National Aeronautics and Space Administration, Marshall Space Flight Center, Huntsville, Ala.

DEVELOPMENT AND TESTING OF HEAT TRANSPORT FLUIDS FOR USE IN ACTIVE SOLAR HEATING AND COOLING SYSTEMS Final Report

John C. Parker Jan. 1981 43 p Sponsored in cooperation with DOE Prepared in part by Houston Chemical Corp., Corpus Christi, Tex.

(Contract NAS8-32255)

(NASA-TM-82395) Avail: NTIS HC A03/MF A01 CSCL 10B

Work on heat transport fluids for use with active solar heating and cooling systems is described. Program objectives and how they were accomplished including problems encountered during testing are discussed. S.F.

N81-17531* National Aeronautics and Space Administration, Lewis Research Center, Cleveland, Ohio.

SPACE PHOTOVOLTAIC RESEARCH AND TECHNOLOGY 1980. HIGH EFFICIENCY, RADIATION DAMAGE AND BLANKET TECHNOLOGY

1980 395 p refs Conf. held in Cleveland, 15-17 Oct. 1980 (NASA-CP-2169; E-469) Avail: NTIS HC A17/MF A01 CSCL 10A

The application of silicon solar cells are discussed with respect to their importance in the exploration of space. Several aspects of the technology associated with the development of photovoltaic devices are reported. For individual titles, see N81-17532 through N81-17576.

N81-17536* National Aeronautics and Space Administration, Lewis Research Center, Cleveland, Ohio.

THE EFFECT OF MINORITY CARRIER MOBILITY VARIATIONS ON THE PERFORMANCE OF HIGH VOLTAGE SILICON SOLAR CELLS

V. G. Weizer and M. P. Godlewski In its Space Photovoltaic Res. and Technol. 1980 p 29-35 refs (For primary document

see N81-17531 08-44)

Avail: NTIS HC A17/MF A01 CSCL 10A

A multistep diffusion processing schedule is described which allows the attainment of high open circuit voltages in 0.1 ohm/cm silicon cells. The schedule consists of a deep primary diffusion, followed by an acid etch of emitter surface which is then followed by a shallow secondary diffusion. A correlation is made between the observed voltage increases and the time of primary diffusion. Results indicate that as the primary diffusion time increases, the voltage rises monotonically. R.C.T.

N81-17536*# National Aeronautics and Space Administration, Lewis Research Center, Cleveland, Ohio.

THEORETICAL RESULTS ON THE DOUBLE-COLLECTING TANDEM JUNCTION SOLAR CELL

Chandra Goradia (Cleveland State Univ.), John Vaughn (Cleveland State Univ.), and Cosmo R. Barone *In its* Lewis Research Center Space Photovoltaic Res. and Technol. 1980 p 51-59 refs (For primary document see N81-17531 08-44)

Avail: NTIS HC A17/MF A01 CSCL 10A

Results of computer calculations using a one dimensional model of the silicon tandem junction solar cell with both front and back current collection are presented. Using realistically achievable geometrical and material parameters, the model predicts that with base widths of 50 micrometers and 100 micrometers and base resistivities between 1 ohm/cm and 20 ohm/cm, beginning of life efficiencies of 14% to 17% and end of life efficiencies of 12% to 14%, after about seven years in synchronous orbit, can be obtained. Author

N81-17554*# National Aeronautics and Space Administration, Lewis Research Center, Cleveland, Ohio.

ANNEALING OF RADIATION DAMAGE IN LOW RESISTIVITY SILICON SOLAR CELLS

I. Weinberg and C. K. Swartz *In its* Space Photovoltaic Res. and Technol. 1980 p 181-186 (For primary document see N81-17531 08-44)

Avail: NTIS HC A17/MF A01 CSCL 10A

The reduction of the temperatures required to restore cell performance after irradiation was investigated with emphasis on the annealing characteristics of two groups of cells containing different amounts of oxygen and carbon. Examination of defect behavior in irradiated boron doped silicon leads to the tentative conclusion that further reduction in annealing temperature could be achieved by decreasing the carbon concentration and either neutralizing the divacancy and/or minimizing its formation as a result of irradiation. A significant reduction in the temperature required to remove radiation induced degradation in 0.1 ohm centimeter silicon solar cells was achieved. A.R.H.

N81-17557*# National Aeronautics and Space Administration, Lewis Research Center, Cleveland, Ohio.

RADIATION DAMAGE IN SILICON NIP SOLAR CELLS

I. Weinberg, C. Goradia (Cleveland State Univ.), C. K. Swartz, and A. M. Hermann *In its* Space Photovoltaic Res. and Technol. 1980 p 199-206 refs (For primary document see N81-17531 08-44)

Avail: NTIS HC A17/MF A01 CSCL 10A

The performance parameters of n(+)-p p(+) silicon solar cells of varying thicknesses with boron doped p base resistivities of 1250 and 84 ohm centimeters were determined. High injection theory was used to analyze the experimental data. Results from an analysis of open circuit voltages show a much greater contribution to V_{oc} from the back junction than is the case for the lower resistivity in common use. The base minority carrier distribution is seen to be significant in determining the contribution of $V(B)$, the base contribution to V_{oc} . Although $V(B)$ is small, its value increases with increasing radiation fluence. In this connection it is noted that, with illumination from the p(+) side, the sign of $V(B)$ becomes positive, and $V(B)$ itself becomes an additive term to V_{oc} . Diffusion lengths determined under high injection conditions are significantly greater than those obtained under low injection, while damage coefficients under low injection are higher than those obtained under high injection conditions. A.R.H.

N81-17561*# National Aeronautics and Space Administration, Lewis Research Center, Cleveland, Ohio.

GaAs HOMOJUNCTION IN SOLAR CELL DEVELOPMENT

Dennis J. Flood, Clifford K. Swartz, and Russell E. Hart, Jr. *In its* Space Photovoltaic Res. and Technol. 1980 p 239-247 refs (For primary document see N81-17531 08-44)

Avail: NTIS HC A17/MF A01 CSCL 10A

The Lincoln Laboratory n(+)/p/p(+) GaAs shallow homojunction cell structure was successfully demonstrated on 2 by 2 cm GaAs substrates. Air mass zero efficiencies of the seven cells produced to date range from 13.6 to 15.6 percent. Current voltage (I-V) characteristics, spectral response, and measurements were made on all seven cells. Preliminary analysis of 1 MeV electron radiation damage data indicate excellent radiation resistance for these cells. Author

N81-17564*# National Aeronautics and Space Administration, Lewis Research Center, Cleveland, Ohio.

PROTON RADIATION DAMAGE IN BULK N-GaAs

D. C. Liu, J. W. Blue, D. J. Flood, and W. E. Stanchina *In its* Space Photovoltaic Res. and Technol. 1980 p 265-275 refs Prepared in cooperation with Notre Dame Univ., Ind. (For primary document see N81-17531 08-44)

Avail: NTIS HC A17/MF A01 CSCL 10A

Bulk samples of Te-doped n-type GaAs were irradiated using 10 MeV to 24 MeV protons to fluences between 2×10 to the 11th power protons/sq cm and 2×10 to the 14th power protons/sq cm. Majority carrier electrical effects were measured using the vanderPauw techniques and it was observed that radiation damage was minimal at the 10 to the 11th power proton/sq cm fluence. For the higher fluences, carrier removal was proportional to $\Delta E/\Delta x$ for the protons indicating ionization interactions between the protons and atoms. Thermal annealing was observed at 155 C. Author

N81-17571*# National Aeronautics and Space Administration, Lewis Research Center, Cleveland, Ohio.

RECENT DEVELOPMENTS IN LIGHTWEIGHT SOLAR CELL MODULES

J. D. Broder and A. F. Forestieri *In its* Space Photovoltaic Res. and Technol. 1980 p 345-349 refs (For primary document see N81-17531 08-44)

Avail: NTIS HC A17/MF A01 CSCL 10A

Two types of lightweight solar cell modules were prepared. The goal is to achieve a module with a power to weight ratio of 350 watts per kilogram. Both structures use thin cells approximately 50 micrometers thick and glass covers approximately 75 micrometers thick. In one structure the glass is bonded to the module using 93-500 silicone adhesive; while the other relies on heat and pressure bonding using FEP as the adhesive. Specific powers of about 335 watts per kilogram were achieved. J.M.S.

N81-19561*# National Aeronautics and Space Administration, Lewis Research Center, Cleveland, Ohio.

IMPROVED THERMIONIC ENERGY CONVERTERS Patent Application

James F. Morris, inventor (to NASA) Filed 19 Feb. 1981 11 p

(NASA-Case-LEW-12443-1; US-Patent-Appl-SN-235797) Avail: NTIS HC A02/MF A01 CSCL 10A

The efficiency of thermionic energy converters is improved by reducing plasma losses. This is achieved by internal distribution of tiny shorted cesium diodes driven by the thermal gradient between the primary emitter and the collector. The tiny, shorted diode distribution comprises protrusions of the emitter material from the main emitter face which contact the main collector face thermally but not electrically. The main collector ends of the protrusions are separated from the main collector by a thin layer of insulation, such as aluminum oxide. The diode effect will increase with the use of metals that adsorb cesium less readily for the main emitter ends of the tiny protrusions and metals that adsorb cesium more readily for the main collector ends of the protrusions. Author

N81-21515* National Aeronautics and Space Administration, Lewis Research Center, Cleveland, Ohio.
ACCEPTANCE TESTS AND MANUFACTURER RELATIONSHIPS FROM THE 20A H STANDARD CELL DATA
Harold F. Leiback / in NASA, Goddard Space Flight Center The 1980 Goddard Space Flight Center Battery Workshop Mar. 1981 p 243-255 (For primary document see N81-21493 12-44) Avail: NTIS HC A19/MF A01 CSCL 10C

Seventeen performance tests were used to classify spacecraft batteries in four standard groups established by manufacturers. Tests included capacity delivered values, end of charge voltage values, and internal shorts. Variance ratios are listed. S.F.

N81-21537* National Aeronautics and Space Administration, Lewis Research Center, Cleveland, Ohio.
THE NASA-LERC WIND TURBINE SOUND PREDICTION CODE

Larry A. Viterna 1981 10 p refs Presented at Second DOE/NASA Wind Turbine Dyn. Workshop, Cleveland, 24-26 Feb. 1981

(Contract DE-AI01-76ET-20366)

(NASA-TM-81737; DOE/NASA/20366-1; E-808) Avail: NTIS HC A02/MF A01 CSCL 10B

Development of the wind turbine sound prediction code began as part of an effort understand and reduce the noise generated by Mod-1. Tone sound levels predicted with this code are in good agreement with measured data taken in the vicinity Mod-1 wind turbine (less than 2 rotor diameters). Comparison in the far field indicates that propagation effects due to terrain and atmospheric conditions may amplify the actual sound levels by 6 dB. Parametric analysis using the code shows that the predominant contributors to Mod-1 rotor noise are (1) the velocity deficit in the wake of the support tower, (2) the high rotor speed, and (3) off-optimum operation. S.F.

N81-22486* National Aeronautics and Space Administration, Lewis Research Center, Cleveland, Ohio.

ADVANCED INORGANIC SEPARATORS FOR ALKALINE BATTERIES AND METHOD OF MAKING SAME Patent Application

Dean W. Sheibley, inventor (to NASA) Filed 27 Feb. 1981 18 p

(NASA-Case-LEW-13171-1; US-Patent-Appl-SN-238790) Avail: NTIS HC A02/MF A01 CSCL 10C

A method of forming a flexible, porous battery separator comprising a coating applied to a porous, flexible substrate is discussed. The coating comprises: (1) a thermoplastic rubber based resin which is insoluble and unreactive in the alkaline electrolyte; (2) a polar organic plasticizer which is reactive with the alkaline electrolyte to produce a reaction product which contains a hydroxyl group and/or a carboxylic acid group; and (3) a mixture of polar particulate filler materials which are unreactive with the electrolyte. The mixture comprises at least one first filler material, wherein the volume of the mixture of filler materials is less than 45% of the total volume of the fillers and the binder, the filler surface area per gram of binder is about 20 to 60 sq m/gr, and the amount of plasticizer is sufficient to coat each filler particle. NASA

N81-22472* National Aeronautics and Space Administration, Lewis Research Center, Cleveland, Ohio.

COMPARISON OF UPWIND AND DOWNWIND ROTOR OPERATIONS OF THE DOE/NASA 100-kW MOD-0 WIND TURBINE

John C. Glasgow, Dean R. Miller, and Robert D. Corrigan 1981 12 p refs Presented at the 2nd DOE/NASA Wind Turbine Dyn. Workshop, Cleveland, 24-26 Feb. 1981

(NASA-TM-81744; E-798; DOE/NASA1028-31) Avail: NTIS HC A02/MF A01 CSCL 10B

Three aspects of the test results are compared: rotor blade bending loads, rotor teeter response, and nacelle yaw moments. As a result of the tests, it is shown that while mean flatwise bending moments were unaffected by the placement of the rotor, cyclic flatwise bending tended to increase with wind speed for the downwind rotor while remaining somewhat uniform with

wind speed for the upwind rotor, reflecting the effects of increased flow disturbance for a downwind rotor. Rotor teeter response was not significantly affected by the rotor location relative to the tower, but appears to reflect reduced teeter stability near rated wind speed for both configurations. Teeter stability appears to return above wind speed, however. Nacelle yaw moments are higher for the upwind rotor but do not indicate significant design problems for either configuration. T.M.

N81-22476* National Aeronautics and Space Administration, Lewis Research Center, Cleveland, Ohio.

PERFORMANCE CALCULATIONS FOR 200-1000 MW MHD/STEAM POWER PLANTS

Peter J. Staiger 1981 11 p refs Presented at the Nineteenth Symp. on the Eng. Aspects of Magnetohydrodyn., Tullahoma, Tenn., 15-17 Jun. 1981

(NASA-TM-81775; DOE/NASA/10769-18; E-836) Avail: NTIS HC A02/MF A01 CSCL 10B

The effects of MHD generator length, level of oxygen enrichment, and oxygen production power on the performance of MHD/steam power plants ranging from 200 to 1000 MW in electrical output are investigated. The plants considered use oxygen enriched combustion air preheated to 1100 F. Both plants in which the MHD generator is cooled with low temperature and pressure boiler feedwater and plants in which the generator is cooled with high temperature and pressure boiler feedwater are considered. For plants using low temperature boiler feedwater for generator cooling the maximum thermodynamic efficiency is obtained with shorter generators and a lower level of oxygen enrichment compared to plants using high temperature boiler feedwater for generator cooling. The generator length at which the maximum plant efficiency occurs increases with power plant size for plants with a generator cooled by low temperature feedwater. Also shown is the relationship of the magnet stored energy requirement of the generator length and the power plant performance. Possible cost/performance tradeoffs between magnet cost and plant performance are indicated. Author

N81-22477* National Aeronautics and Space Administration, Lewis Research Center, Cleveland, Ohio.

REVIEW OF STAND-ALONE PHOTOVOLTAIC APPLICATION PROJECTS SPONSORED BY US DOE AND US AID

William J. Bifano 1981 12 p refs Presented at the Ann. Conf. of the Am. Sect. of the Intern. Solar Energy Soc., Inc., Philadelphia, 26-30 May 1981

(Contract DE-AI01-79ET-20485)

(NASA-TM-81738; DOE/NASA/20485-8; E-808) Avail: NTIS HC A02/MF A01 CSCL 10A

Experience with dc photovoltaic systems (without backup power) and ranging in output from 23 to 3,500 peak watts, in a wide range of environmental conditions and with a wide range of insolation, is described. Cooperation of NASA with other government agencies resulted in the installation of an air pollution monitor in New Jersey, a seismic sensor in Hawaii, power for lookout towers in national forests in California, an electric power system for a Papago Indian village in Arizona, and a power system for a grain mill and water pump in Tangaye, Upper Volta. Significant operational results are discussed and system reliability is assessed for the 20 experimental systems installed since 1976. Additional systems to be installed overseas are highlighted, and economic factors are considered. A.R.H.

N81-22478* National Aeronautics and Space Administration, Lewis Research Center, Cleveland, Ohio.

AN EXPERIMENTAL INVESTIGATION OF SILICON WAFER SURFACE ROUGHNESS AND ITS EFFECT ON THE FULL STRENGTH OF PLATED METALS

Guy D. Spiers 1981 8 p refs Presented at the 15th Photovoltaic Specialists Conf., Kissimmee, Fla., 12-15 May 1981

(NASA-TM-81763; E-826) Avail: NTIS HC A02/MF A01 CSCL 10A

Plated silicon wafers with surface roughness ranging from 0.4 to 130 microinches were subjected to tensile pull strength tests. Electroless Ni/electroless Cu/electroplated Cu and

electroless Ni/electroplated Cu were the two types of plate contacts tested. It was found that smoother surfaces had higher pull strength than rougher, chemically etched surfaces. The presence of the electroless Cu layer was found to be important to adhesion. The mode of fracture of the contact as it left the silicon was studied, and it was found that in almost all cases separation was due to fracture of the bulk silicon phase. The correlation between surface roughness and mode of contact failure is presented and interpreted. Author

N81-23086* National Aeronautics and Space Administration, Lewis Research Center, Cleveland, Ohio.

A NONLINEAR PROPULSION SYSTEM SIMULATION TECHNIQUE FOR PILOTED SIMULATORS

James R. Mihalow 1981 14 p refs Presented at the 12th Ann. Pittsburgh Conf. on Modeling and Simulation, 30 Apr. - 1 May 1981; sponsored by IEEE, ISA, SCS, SMCS (NASA-TM-82600; E-847) Avail: NTIS HC A02/MF A01 CSCL 21E

In the past, propulsion system simulations used in flight simulators have been extremely simple. This resulted in a loss of simulation realism since significant engine and aircraft interactions were neglected and important internal engine parameters were not computed. More detailed propulsion system simulators are needed to permit evaluations of modern aircraft propulsion systems in a simulated flight environment. A real time digital simulation technique has been developed which provides the capabilities needed to evaluate propulsion system performance and aircraft system interaction on manned flight simulators. A parameter correlation technique is used with real and pseudo dynamics in a stable integration convergence loop. The technique has been applied to a multivariable propulsion system for use in a piloted NASA flight simulator program. Cycle time is 2.0 ms on a Univac 1110 computer and 5.7 ms on the simulator computer, a Xerox Sigma 8. The model is stable and accurate with time steps up to 50 ms. The program evaluated the simulation technique and the propulsion system digital control. The simulation technique and model used in that program are described and results from the simulation are presented. Author

N81-23188* National Aeronautics and Space Administration, Lewis Research Center, Cleveland, Ohio.

TRACTION DRIVE FOR CRYOGENIC BOOST PUMP

Scott Meyer and R. E. Connelly Mar. 1981 23 p refs (NASA-TM-81704; E-730) Avail: NTIS HC A02/MF A01 CSCL 21H

Two versions of a Nasvitis multiroller traction drive were tested in liquid oxygen for possible application as cryogenic boost pump speed reduction drives for advanced hydrogen-oxygen rocket engines. The roller drive, with a 108:1 reduction ratio, was successfully run at up to 70,000 rpm input speed and up to 14.9 kW (20 hp) input power level. Three drive assemblies were tested for a total of about three hours of which approximately one hour was at nominal full speed and full power conditions. Peak efficiency of 60 percent was determined. There was no evidence of slippage between rollers for any of the conditions tested. The ball drive, a version using balls instead of one row of rollers, and having a 325:1 reduction ratio, failed to perform satisfactorily. M.G.

N81-23205* National Aeronautics and Space Administration, Lewis Research Center, Cleveland, Ohio.

INEXPENSIVE CROSS-LINKED POLYMERIC SEPARATORS MADE FROM WATER SOLUBLE POLYMERS

Li-Chen Hsu and Dean W. Sheibley 1979 16 p refs Presented at Ann. Meeting of the Electrochem. Soc., Inc., Los Angeles, 14-19 Oct. 1979 (NASA-TM-82619; E-767) Avail: NTIS HC A02/MF A01 CSCL 07D

Polyvinyl alcohol (PVA) crosslinked chemically with aldehyde reagents produces membranes which demonstrate oxidation resistance, dimensional stability, low ionic resistivity, low zincate diffusivity, and low zinc dendrite penetration rate which make them suitable for use as alkaline battery separators. They are

intrinsically low in cost and environmental health and safety problems associated with commercial production appear minimal. Preparation, property measurements, and cell test results in Ni/Zn and Ag/Zn cells are described and discussed. Author

N81-23243* National Aeronautics and Space Administration, Lewis Research Center, Cleveland, Ohio.

COMBUSTION SYSTEM PROCESSES LEADING TO CORROSIVE DEPOSITS

Carl A. Stearns, Fred J. Kohl, and Daniel E. Rosner (Yale Univ.) 1981 25 p refs Presented at the NACE Intern. Conf. on High Temp. Corrosion, San Diego, Calif., 2-6 Mar. 1981 (Contract EF-77-A-01-2593) (NASA-TM-81752; DOE/NASA/2593-27; E-744) Avail: NTIS HC A02/MF A01 CSCL 11F

Degradation of turbine engine hot gas path components by high temperature corrosion can usually be associated with deposits even though other factors may also play a significant role. The origins of the corrosive deposits are traceable to chemical reactions which take place during the combustion process. In the case of hot corrosion/sulfidation, sodium sulfate was established as the deposited corrosive agent even when none of this salt enters the engine directly. The sodium sulfate is formed during the combustion and deposition processes from compounds of sulfur contained in the fuel as low level impurities and sodium compounds, such as sodium chloride, ingested with intake air. In other turbine and power generation situations, corrosive and/or fouling deposits can result from such metals as potassium, iron, calcium, vanadium, magnesium, and silicon. Author

N81-23244* National Aeronautics and Space Administration, Lewis Research Center, Cleveland, Ohio.

THE FRACTURE MORPHOLOGY OF NICKEL-BASE SUPERALLOYS TESTED IN FATIGUE AND CREEP-FATIGUE AT 650 C

John Gayda and Robert V. Miner Apr. 1981 26 p refs (NASA-TM-81740; E-793) Avail: NTIS HC A03/MF A01 CSCL 11F

The fracture surfaces of compact tension specimens from seven nickel-base superalloys fatigue tested at 650 C were studied by scanning electron microscopy and optical metallography to determine the nature and morphology of the crack surface in the region of stable growth. Crack propagation testing was performed as part of an earlier study at 650 C in air using a 0.33 Hz fatigue cycle and a creep-fatigue cycle incorporating a 900 second dwell at maximum load. In fatigue, alloys with a grain size greater than 20 micrometers, HIP Astrology, Waspaloy, and MERL 76, exhibited transgranular fracture. MERL 76 also displayed numerous fracture sites which were associated with boundaries of prior powder particles. The two high strength, fine grain alloys, IN 100 and NASA IIB-7, exhibited intergranular fracture. Rene 95 and HIP plus forged Astrology displayed a mixed failure mode that was transgranular in the coarse grains and intergranular in the fine grains. Under creep-fatigue conditions, fracture was found to be predominantly intergranular in all seven alloys. L.F.M.

N81-23245* National Aeronautics and Space Administration, Lewis Research Center, Cleveland, Ohio.

SYNERGISTIC EROSION/CORROSION OF SUPERALLOYS IN PFB COAL COMBUSTOR EFFLUENT

S. M. Benford, G. R. Zellars, and C. E. Lowell 1981 27 p refs Presented at 82d Ann. Meeting of the Am. Ceram. Soc., Chicago, 28-30 Apr. 1981 (NASA-TM-81715; E-748) Avail: NTIS HC A03/MF A01 CSCL 11F

Two Ni-based superalloys were exposed to the high velocity effluent of a pressurized fluidized bed coal combustor. Targets were 15 cm diameter rotors operating at 40,000 rpm and small flat plate specimens. Above an erosion rate threshold, the targets were eroded to bare metal. The presence of accelerated oxidation at lower erosion rates suggests erosion/corrosion synergism. Various mechanisms which may contribute to the observed oxide

growth enhancement include erosive removal of protective oxide layers, oxide and subsurface cracking, and chemical interaction with sulfur in the gas and deposits through damaged surface layers. Author

N81-23275* National Aeronautics and Space Administration, Lewis Research Center, Cleveland, Ohio

TRIBOLOGICAL PROPERTIES AND THERMAL STABILITY OF VARIOUS TYPES OF POLYIMIDE FILMS

Robert L. Furiaro 1981 23 p refs Proposed for Presentation at Joint Lubrication Conf., New Orleans, 4-7 Oct. 1981; sponsored by Am. Soc. of Lubrication Engr. (NASA-TM-81765; E-710) Avail: NTIS HC A02/MF A01 CSCL 07C

Thermal exposure experiments at 315 and 350 C were conducted on seven different types of polyimide films to determine which was the most thermally stable and adherent. The polyimides were ranked according to the rate at which they lost weight and how well they adhered to the metallic substrate. Friction and wear experiments were conducted at 25 C (room temperature) on films bonded to 440C HT stainless steel. Friction, film wear rates, wear mechanisms, and transfer films of the seven films were investigated and compared. The polyimides were found to fall into two groups as far as friction and wear properties were concerned. Group one had lower friction but an order of magnitude higher film wear rate than did group two. The wear mechanism was predominately adhesive, but the size of the wear particles were larger for group one polyimides. Author

N81-23417* National Aeronautics and Space Administration, Lewis Research Center, Cleveland, Ohio

PROLONGING THERMAL BARRIER COATED SPECIMEN LIFE BY THERMAL CYCLE MANAGEMENT

Robert C. Hendricks, G. McDonald, and Nicholas P. Poolos (Harvard Univ.) 1981 12 p refs Presented at the Intern. Conf. on Met. Coatings, San Francisco, 6-10 Apr. 1981; sponsored by the Am. Vacuum Soc. (NASA-TM-81742; E-795) Avail: NTIS HC A02/MF A01 CSCL 20D

Measurements were made of the rate of increase in temperature of a ZrO₂-8Y₂O₃ thermal barrier coated (TBC) specimen for various values of fuel/air (F/A) ratios when the specimen is exposed to a 0.3 Mach burner flame. For rod specimens in a carousel, the heating rates increased with (F/A) ratio and were higher at the inward facing surface for a given (F/A). Plate specimens were more sensitive to burner variations. Calculated results are given for the radial stress in the coated rod specimens for variations in (F/A) ratios from 0.04 to 0.065. Over this range, the radial stress varies from 4.3 to 5.3 MPa. The results indicate that controlling the heating rate of a TBC by controlling the (F/A) ratio offers a potential method to prolong TBC cyclic life; uncontrolled (F/A) ratios will produce scatter in experimental results. Geometric arrangement can have an equivalent effect, but is usually fixed by design. R.C.T.

N81-23418* National Aeronautics and Space Administration, Lewis Research Center, Cleveland, Ohio

ASSESSMENT OF VARIATIONS IN THERMAL CYCLE LIFE DATA OF THERMAL BARRIER COATED RODS

Robert C. Hendricks and G. McDonald 1981 13 p refs Presented at the Intern. Conf. on Met. Coatings, San Francisco, 6-10 Apr. 1981; sponsored by the Am. Vacuum Soc. (NASA-TM-81743; E-796) Avail: NTIS HC A02/MF A01 CSCL 20D

An analysis of thermal cycle life data for 22 thermal barrier coated (TBC) specimens was conducted. The ZrO₂-8Y₂O₃/NiCrAlY plasma spray coated Rene 41 rods were tested in a Mach 0.3 Jet A/air burner flame. All specimens were subjected to the same coating and subsequent test procedures in an effort to control three parametric groups: material properties, geometry and heat flux. Statistically, the data sample space had a mean of 1330 cycles with a standard deviation of 520 cycles. The data were described by normal or log-normal distributions, but other models could also apply; the sample size must be increased to clearly

delineate a statistical failure model. The statistical methods were also applied to adhesive/cohesive strength data for 20 TBC discs of the same composition, with similar results. The sample space had a mean of 9 MPa with a standard deviation of 4.2 MPa. R.C.T.

N81-23435* National Aeronautics and Space Administration, Lewis Research Center, Cleveland, Ohio

AN INTEGRATED EXHAUST GAS ANALYSIS SYSTEM WITH SELF-CONTAINED DATA PROCESSING AND AUTOMATIC CALIBRATION

R. C. Anderson and R. L. Summers 1981 15 p refs Presented at the Aerospace/Test Meas. Symp., Indianapolis, 27-30 Apr. 1981; sponsored by Instrument Soc. of Am. (NASA-TM-81592; E-786) Avail: NTIS HC A02/MF A01 CSCL 14B

An integrated gas analysis system designed to operate in automatic, semiautomatic, and manual modes from a remote control panel is described. The system measures the carbon monoxide, oxygen, water vapor, total hydrocarbons, carbon dioxide, and oxides of nitrogen. A pull through design provides increased reliability and eliminates the need for manual flow rate adjustment and pressure correction. The system contains two microprocessors to range the analyzers, calibrate the system, process the raw data to units of concentration, and provides information to the facility research computer and to the operator through terminal and the control panels. After initial setup, the system operates for several hours without significant operator attention. E.A.K.

N81-23462* National Aeronautics and Space Administration, Lewis Research Center, Cleveland, Ohio

NASA FIVE-BALL FATIGUE TESTER: OVER 20 YEARS OF RESEARCH

Erwin V. Zaretsky, Richard J. Parker, and William J. Anderson 1981 57 p refs Presented at the Intern. Symp. on Contact Rolling Fatigue Testing of Bearing Steel, Phoenix, Ariz., 12-14 May 1981; sponsored by the Am. Soc. for Testing and Mater. (NASA-TM-82589; E-720) Avail: NTIS HC A04/MF A01 CSCL 14B

Studies were conducted to determine the effect on rolling-element fatigue life of contact angle, material hardness, chemistry, heat treatment and processing, lubricant type and chemistry, elastohydrodynamic film thickness, deformation and wear, vacuum, and temperature as well as Hertzian and residual stresses. Correlation was established between the results obtained using the five-ball tester and those obtained with full scale rolling-element bearings. E.D.K.

N81-23486* National Aeronautics and Space Administration, Lewis Research Center, Cleveland, Ohio

MEGA16 - COMPUTER PROGRAM FOR ANALYSIS AND EXTRAPOLATION OF STRESS-RUPTURE DATA

C. Robert Ensign May 1981 46 p refs (NASA-TP-1809; E-495) Avail: NTIS HC A03/MF A01 CSCL 20K

The computerized form of the minimum commitment method of interpolating and extrapolating stress versus time to failure data, MEGA16, is described. Examples are given of its many plots and tabular outputs for a typical set of data. The program assumes a specific model equation and then provides a family of predicted isothermals for any set of data with at least 12 stress-rupture results from three different temperatures spread over reasonable stress and time ranges. It is written in FORTRAN 4 using IBM plotting subroutines and its runs on an IBM 370 time sharing system. M.G.

N81-23490* National Aeronautics and Space Administration, Lewis Research Center, Cleveland, Ohio.
LUBRICATION FUNDAMENTALS
Bernard J. Hamrock Apr. 1981 8 p refs
(NASA-TM-81762; E-825) Avail: NTIS HC A02/MF A01 CSCL 11H

A lubricant is any substance that is used to reduce friction and wear and to provide smooth running and a satisfactory life for machine components. Lubrication fundamentals are discussed and the various lubrication mechanisms are defined. These include: hydrodynamic, elastohydrodynamic, mixed, boundary, and extreme pressure. Before the various lubrication mechanisms are presented, it is desirable to define conformal and nonconformal surfaces.

J.M.S.

N81-23608* National Aeronautics and Space Administration, Lewis Research Center, Cleveland, Ohio.
RESPONSE OF NICKEL TO ZINC CELLS TO ELECTRIC VEHICLE CHOPPER DISCHARGE WAVEFORMS

Robert L. Cataldo 1981 10 p refs Presented at the Elec. Vehicle Council Symp. 6, Baltimore, 21-23 May 1981; sponsored by the Elec. Vehicle Council

(Contract DE-AI01-77CS-51044)

(NASA-TM-81713; DOE/NASA/51044-16; E-746) Avail: NTIS HC A02/MF A01 CSCL 10C

The preliminary results of simulated electric vehicle chopper controlled discharge of a Nickel/Zinc battery shows delivered energy increases of 5 to 25 percent compared to constant current discharges of the same average current. The percentage increase was a function of chopper frequency, the ratio of peak to average current, and the magnitude of the discharge current. Because the chopper effects are of a complex nature, electric vehicle battery/speed controller interaction must be carefully

N81-23609* National Aeronautics and Space Administration, Lewis Research Center, Cleveland, Ohio.

EXPERIMENTAL EVALUATION OF CATALYTIC COMBUSTION WITH HEAT REMOVAL AT NEAR STOICHIOMETRIC CONDITIONS

Daniel L. Bulzan 1980 16 p refs Presented at the 4th Workshop on Catalytic Combust., Cincinnati, 14-15 May 1980 (Contract DE-AI01-77CS-51040)

(NASA-TM-81748; DOE/NASA/51044-23; E-814) Avail: NTIS HC A02/MF A01 CSCL 10A

Two concentric tube configurations were tested. Tests were conducted at an inlet pressure of 150,000 Pa, inlet fuel air mixture temperatures from 780 to 960 K, combustion air flow rates from 0.78 to 1.5 g/s, equivalence ratios up to 0.90, and a range of cooling air flow rates. Propane and propylene fuels were used. Both configurations used air flowing through the center tube for cooling and combustion in the annulus on the catalytic surface. One configuration had the catalyst applied to the outside surface of the inner tube. Conversion of the fuel was very low for this configuration. The other configuration had the catalyst applied to the inside surface of the outer tube. Conversion of the fuel was considerably better in this configuration.

T.M.

N81-23610* National Aeronautics and Space Administration, Lewis Research Center, Cleveland, Ohio.

PRELIMINARY INVESTIGATION OF ACOUSTIC OSCILLATIONS IN AN H₂-O₂ FIRED HALL GENERATOR

Bert Phillips 1981 13 p refs Presented at the 19th Symp. on the Eng. Aspects of Magnetohydrodyn., Tullahoma, Tenn., 15-17 Jun. 1981

(Contract DE-AI01-77ET-10769)

(NASA-TM-81756; DOE/NASA/10769-15; E-819) Avail: NTIS HC A02/MF A01 CSCL 10A

Burner pressure oscillations and interelectrode voltage oscillations measured in an open-cycle supersonic flow Hall generator are presented. The ionized gas for the channel was supplied by seeding the approximately 1 lb/sec of hydrogen-oxygen combustion products with cesium. Since both the burner and the channel were located within magnetic fields exceeding 4 Tesla during operation, an infinite probe pressure measurement technique was used to measure burner pressure

oscillations. Calibration of the burner pressure transducer using a resonance tube technique is presented. Evidence is presented for the existence of the first longitudinal mode of oscillations (5000 Hz) within the burner. Interelectrode voltage oscillations were simultaneously measured at two separate axial stations. The magnitude change and the phase shift between the two signals was interpreted as a decaying magnetoacoustic wave driven by the burner that propagates at local gas plus sonic velocities. The amplitude of the electrical voltage oscillations at the start of the power producing region of the channel varied with the magnetic field. This variation is compared with the results of a simple perturbation analysis. Arguments are presented for using an unsteady model for analyzing wave processes in channels.

Author

N81-23611* National Aeronautics and Space Administration, Lewis Research Center, Cleveland, Ohio.

ASSESSMENT OF DISK MHD GENERATORS FOR A BASE LOAD POWERPLANT

Donald L. Chubb, F. D. Retallick (Westinghouse Electric Corp., Pittsburgh), C. L. Lu (Westinghouse Electric Corp., Pittsburgh), M. Stella (Westinghouse Electric Corp., Pittsburgh), J. D. Teare (MIT), W. J. Loubsky (MIT), J. F. Louis (MIT), and B. J. Teare (MIT) 1981 17 p refs Presented at the 19th Symp. on Engr. Aspects of Magnetohydrodyn., Tullahoma, Tenn., 15-17 Jun. 1981

(Contract DE-AI01-77ET-10769)

(NASA-TM-82609; DOE/NASA/10769-17; E-849) Avail: NTIS HC A02/MF A01 CSCL 10A

Results from a study of the disk MHD generator are presented. Both open and closed cycle disk systems were investigated. Costing of the open cycle disk components (nozzle, channel, diffuser, radiant boiler, magnet and power management) was

N81-23625* National Aeronautics and Space Administration, Lewis Research Center, Cleveland, Ohio.

THE EFFECT OF MINORITY CARRIER MOBILITY VARIATIONS ON SOLAR CELL SPECTRAL RESPONSE

V. G. Weizer, M. P. Godlewski, and R. J. Trivisonno 1981 12 p refs Presented at the 15th Photovoltaic Spec. Conf., Kissimmee, Fla., 12-15 May 1981; sponsored by the IEEE (NASA-TM-82604; E-852) Avail: NTIS HC A02/MF A01 CSCL 10A

Analysis of multistep diffused, high voltage 0.1 ohm-cm solar cells suggests that the increased voltage capability of these cells is correlated with localized variations in the base minority carrier mobility. An attempt to calculate the behavior of those cells revealed unexpected results. It is shown, contrary to what was expected, that spatial variations in the mobility effects severe changes in the short-circuit current and the spectral response. Variations in cell output as a result of imposing abrupt, linear, and exponential mobility variations are presented.

Author

N81-23626* National Aeronautics and Space Administration, Lewis Research Center, Cleveland, Ohio.

PERFORMANCE OF HIGH RESISTIVITY n+pp+ SILICON SOLAR CELLS UNDER 1 MeV ELECTRON IRRADIATION

I. Weinberg, C. Goradia, C. K. Swartz, and A. M. Hermann 1981 12 p refs Presented at the 15th Photovoltaic Specialists Conf., Kissimmee, Fla. 12-15 May 1981; sponsored by the IEEE (NASA-TM-82610; E-856) Avail: NTIS HC A02/MF A01 CSCL 10A

High resistivity (1250 and 84 ohm-cm) n(+)/pp(+) silicon solar cells were irradiated and their performance evaluated as a function of fluence. The greatest degradation in power occurred for the higher resistivity cell. The data were analyzed under open circuit conditions, and the components of $V_{sub oc}$ determined as a function of fluence. It was found that the voltage contributions from the front and back junctions decreased while the base component ($V_{sub B}$) increased with fluence. The anomalous behavior of $V_{sub B}$ was attributed to an increase in the base minority carrier gradient with fluence. An argument that the increased power degradation in the 1250 ohm-cm cells was attributable to an increased voltage drop in the base is presented.

Diffusion lengths calculated under high injection conditions were significantly greater than those determined under low injection. This was attributed to a saturation of recombination centers under high injection conditions. Author

NTIS-23627* National Aeronautics and Space Administration, Lewis Research Center, Cleveland, Ohio.
REDUCED ANNEALING TEMPERATURES IN SILICON SOLAR CELLS

I. Weinberg and C. K. Swartz 1981 10 p refs Presented at the 15th Photovoltaic Spec. Conf., Kissimmee, Fla., 12-15 May 1981; sponsored by the IEEE (NASA-TM-82597; E-842) Avail: NTIS HC A02/MF A01 CSCL 10A

Cells irradiated to a fluence of $5 \times 10,000,000,000,000/\text{square cm}$ showed short circuit current on annealing at 200 C, with complete annealing occurring at 275 C. Cells irradiated to $100,000,000,000,000/\text{square cm}$ showed a reduction in annealing temperature from the usual 500 to 300 C. Annealing kinetic studies yield an activation energy of $(1.5 + \text{ or } - 2) \text{ eV}$ for the low fluence, low temperature anneal. Comparison with activation energies previously obtained indicate that the presently obtained activation energy is consistent with the presence of either the divacancy or the carbon interstitial carbon substitutional pair, a result which agrees with the conclusion based on defect behavior in boron-doped silicon. S.F.

NTIS-24519* National Aeronautics and Space Administration, Lewis Research Center, Cleveland, Ohio.
HEAT EXCHANGER AND METHOD OF MAKING Patent

Anthony Fortini and John M. Kazaroff, inventors (to NASA) Issued 20 Jan. 1981 5 p Filed 23 Apr. 1979 Supersedes N79-23383 (17 - 14, p 1850) Division of US Patent Appl. SN-856482, US Patent-4,199,937, filed 30 Nov. 1977 (NASA-Case-LEW-12441-3; US-Patent-4,245,489; US-Patent-Appl-SN-032307; US-Patent-Class-60-204; US-Patent-Class-60-257; US-Patent-Class-239-127.1; US-Patent-4,199,937, US-Patent-Appl-SN-856462) Avail: US Patent and Trademark Office CSCL 10B

A heat exchanger of increased effectiveness is disclosed. A porous metal matrix is disposed in a metal chamber or between walls through which a heat transfer fluid is directed. The porous metal matrix has internal bonds and is bonded to the chamber in order to remove all thermal contact resistance within the composite structure. Utilization of the invention in a rocket chamber is disclosed as a specific use. Also disclosed is a method of constructing the heat exchanger.

Official Gazette of the U.S. Patent and Trademark Office

NTIS-24521* National Aeronautics and Space Administration, Lewis Research Center, Cleveland, Ohio.
TOROIDAL CELL AND BATTERY Patent

William J. Nagle, inventor (to NASA) Issued 14 Apr. 1981 7 p Filed 28 Mar. 1980 Supersedes N80-33857 (18 - 24, p 3299) (NASA-Case-LEW-12918-1; US-Patent-4,262,064; US-Patent-Appl-SN-134855; US-Patent-Class-429-94; US-Patent-Class-429-120; US-Patent-Class-429-180; US-Patent-Class-429-184) Avail: US Patent and Trademark Office CSCL 10C

A toroidal storage battery designed to handle relatively high amp-hour loads is described. The cell includes a wound core disposed within a pair of toroidal channel shaped electrodes spaced apart by nylon insulator. The shape of the case electrodes of this toroidal cell allows a first planar doughnut shaped surface and the inner cylindrical case wall to be used as a first electrode and a second planar doughnut shaped surface and the outer cylindrical case wall to be used as a second electrode. Connectors may be used to stack two or more toroidal cells together by connecting substantially the entire surface area of the first electrode of a first cell to substantially the entire surface area of the second electrode of a second cell. The central cavity of each toroidal cell may be used as a conduit for pumping a fluid through the toroidal cell to thereby cool the cell.

Official Gazette of the U.S. Patent and Trademark Office

NTIS-24533* National Aeronautics and Space Administration, Lewis Research Center, Cleveland, Ohio.

EFFECTS OF FUEL-INJECTOR DESIGN ON ULTRA-LEAN COMBUSTION PERFORMANCE

David N. Anderson 1981 14 p refs Proposed for presentation at the 16th Intersoc. Energy Conversion Eng. Conf., Atlanta, 9-14 Aug. 1981

(Contract DE-A101-77CS-51040)

(NASA-TM-82624; DOE/NASA/51040-2R; E-877) Avail: NTIS HC A02/MF A01 CSCL 10A

Emissions data were obtained for six fuel injector configurations tested with ultra lean combustion. Fuel injectors included three multiple source designs and three configurations using a single air assist injector. Only the multiple source fuel injectors provided acceptable emissions. Values of 16 g CO/kg fuel , 1.9 g HC/kg fuel , and $19 \text{ g NO}_2/\text{kg fuel}$ were obtained for the combustion temperature range of 1450 to 1700 K for both a high blockage 19 source injector and a low blockage 41 source injector. It was shown that high fuel injector pressure drop may not be required to achieve low emissions performance at high inlet air temperature when the fuel is well dispersed in the airstream. E.A.K.

NTIS-24534* National Aeronautics and Space Administration, Lewis Research Center, Cleveland, Ohio.

NASA PREPROTOTYPE REDOX STORAGE SYSTEM FOR A PHOTOVOLTAIC STAND-ALONE APPLICATION

Norman H. Hagedorn 1981 13 p To be presented at the Intersociety Energy Conversion Eng. Conf., Atlanta, 9-14 Aug. 1981; sponsored by ASME

(NASA-TM-82607; DOE/NASA/12726-B; E-854) Avail: NTIS HC A02/MF A01 CSCL 10C

A 1 kW preprototype redox storage system underwent characterization tests and was operated as the storage device for a 5 kW (peak) photovoltaic array. The system is described and performance data are presented. Loss mechanisms are discussed and simple design changes leading to significant increases in efficiency are suggested. The effects on system performance of nonequilibrium between the predominant species of complexed chromic ion in the negative electrode reactant solution are indicated. Author

NTIS-24535* National Aeronautics and Space Administration, Lewis Research Center, Cleveland, Ohio.

TEST EVALUATION OF A LAMINATED WOOD WIND TURBINE BLADE CONCEPT Final Report

James R. Faddoul May 1981 48 p refs

(Contract DE-A101-76ET-20320)

(NASA-TM-81719; DOE/NASA/20320-30; E-753) Avail: NTIS HC A03/MF A01 CSCL 10B

A series of tests conducted on a root end section of a laminated wood wind turbine blade are reported. The blade to hub transition of the wood blade uses steel studs cast into the wood D spar with a filled epoxy. Both individual studs and a full scale, short length, root section were tested. Results indicate that the bonded stud concept is more than adequate for both the 30 year life fatigue loads and for the high wind or hurricane gust loads. E.A.K.

NTIS-24536* National Aeronautics and Space Administration, Lewis Research Center, Cleveland, Ohio.

LABORATORY EVALUATION OF A PILOT CELL BATTERY PROTECTION SYSTEM FOR PHOTOVOLTAIC APPLICATIONS

Robert L. Cataldo and Ralph D. Thomas 1981 14 p refs Proposed for presentation at the 16th Intersoc. Energy Conversion Eng. Conf., Atlanta, 9-14 Aug. 1981

(Contract DE-A101-79ET-20485)

(NASA-TM-81714; DOE/NASA/20485-7; E-747) Avail: NTIS HC A02/MF A01 CSCL 10C

An energy storage method for the 3.5 kW battery power system was investigated. The Pilot Cell Battery Protection System was tested for use in photovoltaic power systems and results show that this is a viable method of storage battery control. The method of limiting battery depth of discharge has the following

advantages: (1) temperature sensitivity; (2) rate sensitivity; and (3) state of charge indication. The pilot cell concept is of interest in remote stand alone photovoltaic power systems. The battery can be protected from damaging overdischarge by using the proper ratio of pilot cell capacities to main battery capacity.

E.A.K.

NS1-24530* National Aeronautics and Space Administration, Lewis Research Center, Cleveland, Ohio.

LIGHTNING ACCOMMODATION SYSTEMS FOR WIND TURBINE GENERATOR SAFETY

H. Bankaitis 1981 16 p. refs. Proposed for presentation at the 5th Intern. System Safety Conf., Denver, 26-31 Jul. 1981 (Contract DE-AI01-76ET-20320) (NASA-TM-7601; DOE/NASA/20320-31; E-848) Avail: NTIS HC A02/MF A01 CSCL 10B

The wind turbine safety program identifies the naturally occurring lightning phenomenon as a hazard with the potential to cause loss of program objectives, injure personnel, damage system instrumentation, structure or support equipment and facilities. Several candidate methods of lightning accommodation for each blade were designed, analyzed, and tested by submitting sample blade sections to simulated lightning. Lightning accommodation systems for composite blades were individually developed. Their effectiveness was evaluated by submitting the systems to simulated lightning strikes. The test data were analyzed and system designs were reviewed on the basis of the analysis.

NS1-25487* National Aeronautics and Space Administration, Lewis Research Center, Cleveland, Ohio.

OVERVIEW: DOE/NASA AUTOMOTIVE GAS TURBINE AND STIRLING PROJECTS

Donald G. Beremand 1981 17 p. Presented at the Heat Pump Contractors' Program Integration Meeting, McLean, Va., 2-4 Jun. 1981

(Contract DE-AI01-77CS-51040)

(NASA-TM-82637; DOE/NASA/51040-28; E-890) Avail: NTIS HC A02/MF A01 CSCL 10B

An overview on the progress of the automotive gas turbine and automotive Stirling engine technology projects is presented. The following items are reported: (1) formulation and execution of projects in accordance with the Auto Propulsion Research and Development Act of 1978; (2) substantive technology accomplishments; and (3) future path options of the programs.

E.A.K.

NS1-25488* National Aeronautics and Space Administration, Lewis Research Center, Cleveland, Ohio.

CONCEPTUAL DESIGN STUDY OF A COAL GASIFICATION COMBINED-CYCLE POWERPLANT FOR INDUSTRIAL COGENERATION

Harvey S. Bloomfield, S. G. Nelson (McKee (Davy) Corp.), H. F. Straight (McKee (Davy) Corp.), T. K. Subramaniam (McKee (Davy) Corp.), and R. G. Winklepleck (McKee (Davy) Corp.) Mar. 1981 49 p.

(Contract NAS3-22105-AE)

(NASA-TM-81687; E-723) Avail: NTIS HC A03/MF A01 CSCL 10B

A conceptual design study was conducted to assess technical feasibility, environmental characteristics, and economics of coal gasification. The feasibility of a coal gasification combined cycle cogeneration powerplant was examined in response to energy needs and to national policy aimed at decreasing dependence on oil and natural gas. The powerplant provides the steam heating and baseload electrical requirements while serving as a prototype for industrial cogeneration and a modular building block for utility applications. The following topics are discussed: (1) screening of candidate gasification, sulfur removal and power conversion components; (2) definition of a reference system; (3) quantification of plant emissions and waste streams; (4) estimates of capital and operating costs; and (5) a procurement and construction schedule. It is concluded that the proposed powerplant is technically feasible and environmentally superior.

E.A.K.

NS1-27587* National Aeronautics and Space Administration, Lewis Research Center, Cleveland, Ohio.

ADDITIVE FOR ZINC ELECTRODES Patent Application

D. G. Soltis, D. W. Sheibley, and W. J. Nagle, inventors (to NASA) Filed 10 Jun. 1981 7 p.

(NASA-Case-LEW-13286-1; US-Patent-Appl-SN-272406) Avail: NTIS HC A02/MF A01 CSCL 10C

An improved zinc electrode for alkaline cells includes up to about ten percent by weight of Ba(OH)2.8H2O with about five percent being preferred. The zinc electrode may or may not be amalgamated with mercury.

NASA

NS1-27588* National Aeronautics and Space Administration, Lewis Research Center, Cleveland, Ohio.

HEAT TRANSPARENT HIGH INTENSITY HIGH EFFICIENCY SOLAR CELL Patent Application

J. C. Evans, Jr., inventor (to NASA) Filed 15 May 1981 13 p.

(NASA-Case-LEW-12892-1; US-Patent-Appl-SN-264380) Avail: NTIS HC A02/MF A01 CSCL 10A

A heat transparent high intensity solar cell with improved efficiency is described. The surface of each solar cell has a plurality of grooves. Each groove has a vertical face and a slanted face that is covered by a reflecting metal. Light rays are reflected from the slanted face through the vertical face where they traverse a photovoltaic junction. As the light rays travel to the slanted face of an adjacent groove, they again traverse the junction. The underside of the reflecting coating directs the light rays toward the opposite surface of solar cell as they traverse the junction again. When the light rays travel through the solar cell and reach the saw toothed grooves on the under side, the process of reflection and repeatedly traversing the junction again takes place. The light rays ultimately emerge from the solar cell. These solar cells are particularly useful at very high levels of insolation because the infrared or heat radiation passes through the cells without being appreciably absorbed to heat the cell.

NASA

NS1-27604* National Aeronautics and Space Administration, Lewis Research Center, Cleveland, Ohio.

COMPATIBILITY OF ALTERNATIVE FUELS WITH ADVANCED AUTOMOTIVE GAS TURBINE AND STIRLING ENGINES. A LITERATURE SURVEY Final Report

James Carrelli and David Horvath May 1981 44 p. refs.

(Contract DE-AI01-77CS-51040)

(NASA-TM-81754; DOE/NASA/51040-24; E-792) Avail: NTIS HC A03/MF A01 CSCL 10B

The application of alternative fuels in advanced automotive gas turbine and Stirling engines is discussed on the basis of a literature survey. These alternative engines are briefly described, and the aspects that will influence fuel selection are identified. Fuel properties and combustion properties are discussed, with consideration given to advanced materials and components. Alternative fuels from petroleum, coal, oil shale, alcohol, and hydrogen are discussed, and some background is given about the origin and production of these fuels. Fuel requirements for automotive gas turbine and Stirling engines are developed, and the need for certain research efforts is discussed. Future research efforts planned at Lewis are described.

Author

NS1-27605* National Aeronautics and Space Administration, Lewis Research Center, Cleveland, Ohio.

COMPARATIVE RADIATION TESTING OF SOLAR CELLS FOR THE SHUTTLE POWER EXTENSION PACKAGE

Cosmo R. Barona, Clifford K. Swartz, and Russell E. Hart, Jr. 1981 4 p. refs. Presented at the 15th Photovoltaic Spec. Conf., Kissimmee, Fla., 12-15 May 1982; sponsored by IEEE (NASA-TM-82656; E-922) Avail: NTIS HC A02/MF A01 CSCL 10A

The Power Extension Package (PEP) is the prime focus of a development program to produce low cost solar cells. The PEP is a 32 kilowatt flexible substrate, retrievable, solar array system for use on the Space Shuttle. Solar cell cost will be reduced by increasing cell area and simplifying cell and coverglass fabrication processes and specifications. The cost goal is to produce cells below \$30 per watt. Two and ten ohm-cm silicon cells

were investigated. This paper describes a unique radiation damage test and side-by-side comparison of candidate cell types with pre- and post-irradiation airplane calibration of outer space short-circuit current. Author

NS1-27606* National Aeronautics and Space Administration, Lewis Research Center, Cleveland, Ohio.

THE MOD-2 WIND TURBINE DEVELOPMENT PROJECT Final Report

Bradford S. Linscott, Joann T. Dennett (RDD Consultants Inc.), and Larry H. Gordon Jul 1981 24 p refs (Contract DE-A101-79ET-20305)

(NASA-TM-82681; DOE/NASA/20305-5; E-965) Avail: NTIS HC A02/MF A01 CSCL 10B

A major phase of the Federal Wind Energy Program, the Mod-2 wind turbine, a second-generation machine developed by the Boeing Engineering and Construction Co. for the U.S. Department of Energy and the Lewis Research Center of the National Aeronautics and Space Administration, is described. The Mod-2 is a large (2.5-MW power rating) horizontal-axis wind turbine designed for the generation of electrical power on utility networks. Three machines were built and are located in a cluster at Goodnoe Hills, Washington. All technical aspects of the project are described: design approach, significant innovation features, the mechanical system, the electrical power system, the control system, and the safety system. Author

NS1-27615* National Aeronautics and Space Administration, Lewis Research Center, Cleveland, Ohio.

POLYVINYL ALCOHOL BATTERY SEPARATOR CONTAINING INERT FILLER Patent Application

Dean W. Sheibley, Li-Chen Hsu, and Michelle A. Manzo, inventors (to NASA) Filed 10 Jun 1981 14 p

(NASA-Case-LEW-13556-1; US-Patent-Appl-SN-272233) Avail: NTIS HC A02/MF A01 CSCL 10C

A cross-linked polyvinyl alcohol battery separator is disclosed. A particulate filler, inert to alkaline electrolyte of an alkaline battery, is incorporated in the separator in an amount of 1-20% by weight, based on the weight of the polyvinyl alcohol, and is dispersed throughout the product. Incorporation of the filler enhances performance and increases cycle life of alkaline batteries when compared with batteries containing a similar separator not containing filler. Suitable fillers include titanates, silicates, zirconates, aluminates, wood flour, lignin, and titania. Particle size is not greater than about 50 microns. NASA

NS1-27616* National Aeronautics and Space Administration, Lewis Research Center, Cleveland, Ohio.

METHOD OF FORMING OXIDE COATINGS Patent Application

G. E. McDonald, inventor (to NASA) Filed 10 Jun 1981 7 p (NASA-Case-Lew-13132-1; US-Patent-Appl-SN-272152) Avail: NTIS HC A02/MF A01 CSCL 10A

This invention is concerned with an improved plating process for covering a substrate with a black metal oxide film. The invention is particularly directed to making a heating panel for a solar collector. A compound is electrodeposited from an aqueous solution containing cobalt metal salts onto a metal substrate. This compound is converted during plating into a black, highly absorbing oxide coating which contains hydrated oxides. This is achieved by the inclusion of an oxidizing agent in the plating bath. The inclusion of an oxidizing agent in the plating bath is contrary to standard electroplating practice. The hydrated oxides are converted to oxides by treatment in a hot bath, such as boiling water. An oxidizing agent may be added to the hot liquid treating bath. NASA

NS1-28519* National Aeronautics and Space Administration, Lewis Research Center, Cleveland, Ohio.

PUMPING POWER CONSIDERATIONS IN THE DESIGNS OF NASA-REDOX FLOW CELLS Final Report

Mark A. Hobericht Jun 1981 12 p refs (Contract DE-A104-80AL-12726)

(NASA-TM-82598; DOE/NASA/12726-7) Avail: NTIS HC A02/MF A01 CSCL 10C

Pressure drop data for six different cell geometries of various flow port, manifold, and cavity dimensions are presented. The redox/energy/storage system uses two fully soluble redox couples as anode and cathode fluids. Both fluids are pumped through a redox cell, or stack of cells, where the electrochemical reactions take place at porous carbon felt electrodes. Pressure drops are therefore associated with this system due to the continuous flow of reactant solutions. The exact pressure drop within a redox flow cell is directly dependent on the flow rate as well as the various cell dimensions. Pumping power requirements for a specific set of cell operating conditions are found for various cell geometries once the flow rate and pressure drop are determined. These pumping power requirements contribute to the overall system parasitic energy losses which must be minimized, the choice of cell geometry becomes critical. E.D.K.

NS1-28520* National Aeronautics and Space Administration, Lewis Research Center, Cleveland, Ohio.

COMPARISON OF PHOTOVOLTAIC CELL TEMPERATURES IN MODULES OPERATING WITH EXPOSED AND ENCLOSED BACK SURFACES Final Report

David Namkoong and Frederick F. Simon May 1981 21 p refs (Contract DE-A101-79ET-20485)

(NASA-TM-81769; DOE/NASA/20485-9; E-831) Avail: NTIS HC A02/MF A01 CSCL 10C

Four different photovoltaic module designs were tested to determine the cell temperature of each design. The cell temperatures were compared to those obtained on identical design, using the same nominal operating cell temperature (NOCT) concept. The results showed that the NOCT procedure does not apply to the enclosed configurations due to continuous transient conditions. The enclosed modules had higher cell temperatures than the open modules, and insulated modules higher than the uninsulated. The severest performance loss - when translated from cell temperatures - 17.5 % for one enclosed, insulated module as compared to that module mounted openly. E.A.K.

NS1-28522* National Aeronautics and Space Administration, Lewis Research Center, Cleveland, Ohio.

COMPARISON OF INTEGRATED GASIFIER-COMBINED CYCLE AND AFB-STEAM TURBINE SYSTEMS FOR INDUSTRIAL COGENERATION

Joseph J. Fainiger, John M. Abbott, and Raymond K. Burns 1981 27 p refs Presented at 16th Intersoc. Energy Conversion Engr. Conf., Atlanta, 9-14 Aug 1981; sponsored by ASME (NASA-TM-82648; E-908) Avail: NTIS HC A03/MF A01 CSCL 10B

In the cogeneration technology alternatives study (CTAS) a number of advanced coal fired systems were examined and systems using an integrated coal gasifier IGCC or a fluid bed combustor AFB were found to yield attractive cogeneration results in industrial cogeneration applications. A range of site requirements and cogeneration sizing strategies using ground rules based on CTAS were used in comparing an IGCC and an AFB. The effect of time variations in site requirements and the sensitivity to fuel and electricity price assumptions are examined. The economic alternatives of industrial or utility ownership are also considered. The results indicate that the IGCC system has potentially higher fuel and emission savings and could be an attractive option for utility ownership. The AFB steam turbine system has a potentially higher return on investment and could be attractive assuming industrial ownership. A.R.H.

NS1-28523* National Aeronautics and Space Administration, Lewis Research Center, Cleveland, Ohio.

CHARACTERIZATION, PERFORMANCE, AND PREDICTION OF A LEAD-ACID BATTERY UNDER SIMULATED ELECTRIC VEHICLE DRIVING REQUIREMENTS Final Report

John G. Ewashinski and John M. Borek May 1981 26 p refs (Contract DE-A101-77CS-51044)

(NASA-TM-81771; DOE/NASA/51044-19; E-717) Avail: NTIS HC A03/MF A01 CSCL 10C

A state-of-the-art 6-V battery module in current use by the electric vehicle industry was tested at the NASA Lewis Re-

search Center to determine its performance characteristics under the SAE J227a driving schedules B, C, and D. The primary objective of the tests was to determine the effects of periods of recuperation and long and short periods of electrical regeneration in improving the performance of the battery module and hence extending the vehicle range. A secondary objective was to formulate a computer program that would predict the performance of this battery module for the above driving schedules. The results show excellent correlation between the laboratory tests and predicted results. The predicted performance compared with laboratory tests was within +2.4 to -3.7 percent for the D schedule, +0.5 to -7.1 percent for the C schedule, and better than -11.4 percent for the B schedule. Author

N81-28524* National Aeronautics and Space Administration, Lewis Research Center, Cleveland, Ohio.

SOLAR THERMAL POWER SYSTEMS PARABOLIC DISH PROJECT Annual Technical Report

V. C. Truscillo 15 May 1981 94 p refs Prepared in cooperation with JPL, California Inst. of Technology, Pasadena (Contracts NAS7-100; DE-AT04-81AL-18228) (NASA-TM-82371; JPL-PUB-81-39; DOE/JPL-1060-45) Avail: NTIS HC A05/MF A01 CSCL 10A

The status of the Solar Thermal Power Systems Project for FY 1980 is summarized. Included is: a discussion of the project's goals, program structure, and progress in parabolic dish technology. Analyses and test results of concentrators, receivers, and power converters are discussed. Progress toward the objectives of technology feasibility, technology readiness, system feasibility, and system readiness are covered. E.A.K.

N81-29524* National Aeronautics and Space Administration, Lewis Research Center, Cleveland, Ohio.

CATALYST SURFACES FOR THE CHROMOUS/CHROMIC REDOX COUPLE Patent

Jose D. Giner (Giner, Inc., Waltham, Mass.) and Kathleen J. Cahill, inventors (to NASA) (Giner, Inc., Waltham, Mass.) Issued 2 Jun. 1981 8 p Filed 27 Jul. 1979 Supersedes N80-18557 (18 - 09, p 1165) Sponsored by NASA (NASA-Case-LEW-13148-2; US-Patent-4,270,984; US-Patent-Appl-SN-061555; US-Patent-4,192,910; US-Patent-Appl-SN-964754; US-Patent-Class-204-2.1) Avail: U.S. Patent and Trademark Office CSCL 10C

An electricity producing cell of the reduction-oxidation (REDOX) type divided into two compartments by a membrane is disclosed. A ferrous/ferric couple in a chloride solution serves as a cathode fluid to produce a positive electric potential. A chromic/chromous couple in a chloride solution serves as an anode fluid to produce a negative potential. The electrode is an electrically conductive, inert material plated with copper, silver or gold. A thin layer of lead plates onto the copper, silver or gold layer when the cell is being charged, the lead ions being available from lead chloride which has been added to the anode fluid. If the REDOX cell is then discharged, the lead deplates from the negative electrode and the metal coating on the electrode acts as a catalyst to increase current density.

Official Gazette of the U.S. Patent and Trademark Office

N81-29528* National Aeronautics and Space Administration, Lewis Research Center, Cleveland, Ohio.

TESTS OF AN OVERRUNNING CLUTCH IN A WIND TURBINE Final Report

Robert C. Seidel and Henry G. Pfanner Jul. 1981 13 p refs (Contract DE-AI01-76ET-20320) (NASA-TM-82653; DOE/NASA/20320-32; E-914) Avail: NTIS HC A02/MF A01 CSCL 10A

An overrunning clutch that slipped freely under reverse torque was tested in the drive train of the Mod-O wind turbine. In low variable wind conditions, the clutch engaged and disengaged smoothly without perturbation or oscillations. The clutch permitted the generator to be connected to the line using a relay instead of an automatic synchronizer. The alternator was connected to the line when the rpm reached 95% of synchronous speed and it motored to synchronous speed in about 0.15 seconds with a momentary power spike of 50 kW. The performance of the clutch was the same with and without the fluid coupling. The ideal

power with the clutch was 5 to 7 kW compared to up to 50 kW without the clutch. The overrunning clutch merits consideration in future wind turbine designs as a means of simplifying the control system, increasing energy capture, and increasing the life of blades and electrical switch gear. A.R.H.

N81-29531* National Aeronautics and Space Administration, Lewis Research Center, Cleveland, Ohio.

ALKALINE BATTERY CONTAINING A SEPARATOR OF A CROSS-LINKED COPOLYMER OF VINYL ALCOHOL AND UNSATURATED CARBOXYLIC ACID Patent Application

Li-Chen Hsu, Warren H. Philipp, Deen W. Sheibley, and Olga D. Gonzalez-Sanabria, inventors (to NASA) Filed 10 Jul. 1981 12 p

(NASA-Case-LEW-13102-1; US-Patent-Appl-SN-282298) Avail: NTIS HC A02/MF A01 CSCL 10C

A battery separator for an alkaline battery separator comprises a crosslinked copolymer of vinyl alcohol units and unsaturated carboxylic acid units. The crosslinked copolymer is insoluble in water, has excellent zincate diffusion and oxygen gas barrier properties and a low electrical resistivity. A polyaldehyde crosslinking agent is preferred. NASA

N81-30522* National Aeronautics and Space Administration, Lewis Research Center, Cleveland, Ohio.

PREPARATION AND CHARACTERIZATION OF ELECTRODES FOR THE NASA REDOX STORAGE SYSTEM

Margaret A. Reid, Randall F. Gahn, Jerri S. L'ng, and JoAnn Charleston Sep. 1980 17 p refs Prepared for Electrochem. Soc. Meeting, Hollywood, Fla., 5-10 Sep. 1980

(Contract DE-AI04-80AL-12726)

(NASA-TM-82702; DOE/NASA/12726-13; E-739) Avail: NTIS HC A02/MF A01 CSCL 10C

Electrodes for the Redox energy storage system based on iron and chromium chloride reactants is discussed. The physical properties of several lots of felt were determined. Procedures were developed for evaluating electrode performance in lab scale cells. Experimental procedures for evaluating electrodes by cyclic voltammetry are described which minimize the IR losses due to the high internal resistance in the felt (distributed resistance). Methods to prepare electrodes which reduced the coevolution of hydrogen at the chromium electrode and eliminate the drop in voltage on discharge occasionally seen with previous electrodes were discussed. Single cells of 0.3329 ft area with improved membranes and electrodes are operating at over 80% voltage efficiency and coulombic efficiencies of over 98% at current densities of 16 to 20 amp % ft. E.A.K.

N81-30562* National Aeronautics and Space Administration, Lewis Research Center, Cleveland, Ohio.

TEST RESULTS OF THE CHRYSLER UPGRADED AUTOMOTIVE GAS TURBINE ENGINE: INITIAL DESIGN Final Report

David Horvath, Guy H. Ribble, Jr., Edward L. Warren, and James C. Wood Jul. 1981 66 p refs (Contract DE-AI01-77CS-51040)

(NASA-TM-81660; DOE/NASA/51040-22; E-676) Avail: NTIS HC A04/MF A01 CSCL 10B

The upgraded engine as built to the original design was deficient in power and had excessive specific fuel consumption. A high instrumented version of the engine was tested to identify the sources of the engine problems. Analysis of the data shows the major problems to be low compressor and power turbine efficiency and excessive interstage duct losses. In addition, high HC and CO emission were measured at idle, and high NOx emissions at high energy speeds. T.M.

N81-30563* National Aeronautics and Space Administration. Lewis Research Center, Cleveland, Ohio.

QUALIFICATION TESTING OF SECONDARY STERILIZABLE SILVER-ZINC CELLS FOR USE IN THE JUPITER ATMOSPHERIC ENTRY PROBE

Michelle A. Manzo J.L. 1981 16 p

(NASA-TM-82638; E-893) Avail: NTIS HC A02/MF A01 CSCL 10C

A series of qualification tests were run on the secondary, sterilizable silver oxide - zinc cell developed at the NASA Lewis Research Center to determine if the cell was capable of providing mission power requirements for the Jupiter atmospheric entry probe. The cells were tested for their ability to survive radiation at the levels predicted for the Jovian atmosphere with no loss of performance. Cell performance was evaluated under various temperature and loading conditions, and the cells were tested under various environmental conditions related to launch and to deceleration into the Jovian atmosphere. The cell performed acceptably except under the required loading at low temperatures. The cell was redesigned to improve low-temperature performance and energy density. The modified cells improved performance at all temperatures. Results of testing cells of both the original and modified designs are discussed. Author

N81-31627* National Aeronautics and Space Administration. Lewis Research Center, Cleveland, Ohio.

RESULTS OF THE ETV-1 BREADBOARD TESTS UNDER STEADY-STATE AND TRANSIENT CONDITIONS

Noel B. Sargent and Miles O. Dustin Aug. 1981 16 p refs Presented at the Elec. Vehicle Council Symp. 6, Baltimore, 21-23 Oct. 1981

(Contract DE-A101-77CS-51044)

(NASA-TM-82667; E-944. DOE/NASA/51044-21) Avail: NTIS HC A02/MF A01 CSCL 10A

Steady state tests were run to characterize the system and component efficiencies over the complete speed-torque capabilities of the propulsion system in both motoring and regenerative modes of operation. The steady state data were obtained using a battery simulator to separate the effects on efficiency caused by changing battery state-of-charge and component temperature. Transient tests were performed to determine the energy profiles of the propulsion system operating over the SAE J227a driving schedules. T.M.

N81-32608* National Aeronautics and Space Administration. Lewis Research Center, Cleveland, Ohio.

A REDOX SYSTEM DESIGN FOR SOLAR STORAGE APPLICATIONS

A. W. Nice and Norman H. Hagedorn 1981 9 p refs Presented at the 4th Battery and Electrochem. Contractors' Conf., Washington, D.C., 2-4 Jun. 1981 Sponsored by DOE

(Contract DE-A104-80AL-12726)

(NASA-TM-82720; DOE/NASA/12726-14; E-1019) Avail: NTIS CSCL 10A

Redox energy storage systems developed for solar power applications and utility load leveling applications are described. The technology readiness of Redox energy storage for transfer of the technology to industry for product development and commercialization by industry is addressed. The design features of Redox systems for application to stand alone or residential storage requirements are described. Redox system designs with 3 to 10 kW power output and storage times of 6 to 250 hours are summarized and performance characteristics presented. J.M.S.

N81-33631* National Aeronautics and Space Administration. Lewis Research Center, Cleveland, Ohio.

ADVANCES IN MEMBRANE TECHNOLOGY FOR THE NASA REDOX ENERGY STORAGE SYSTEM

Jerri S. Ling and JoAnn Charleston 1980 18 p refs Presented at Electrochem. Soc. Meeting, Hollywood, Fla., 5-10 Sep. 1980

(Contract DE-A104-80AL-12726)

(NASA-TM-82701; DOE/NASA/12726-12; E-738) Avail: NTIS HC A02/MF A01 CSCL 10A

Anion exchange membranes used in the system serve as a charge transferring medium as well as a reactant separator and

are the key enabling component in this storage technology. Each membrane formulation undergoes a series of screening tests for area-resistivity, static (non-flow) diffusion rate determination, and performance in Redox systems. The CDIL series of membranes has, by virtue of its chemical stability and high ion exchange capacity, demonstrated superior properties in the redox environment. Additional resistivity results at several acid and iron solution concentrations, iron diffusion rates, and time dependent iron fouling of the various membrane formulations are presented in comparison to past standard formulations. T.M.

A81-11034 * Control of volume resistivity in inorganic-organic separators. D. W. Sheibley and M. A. Manzo (NASA, Lewis Research Center, Cleveland, Ohio). *Electrochemical Society, Journal*, vol. 127, Nov. 1980, p. 2392-2397. 9 refs.

Control of resistivity in NASA inorganic-organic separators is achieved by incorporating small percentages of high surface area, fine-particle silica with other ingredients in the separator coating. The volume resistivity appears to be predictable from coating composition, that is, from the surface area of filler particles in the coating. The approach has been applied to two polymer-'plasticizer'-filler coating systems, where the filler content of each is below the generally acknowledged critical pigment volume concentration of the coating. Application of these coating systems to 0.0254 cm thick (10 mil) fuel-cell grade asbestos sheet produces inexpensive, flexible, microporous separators that perform at least as well as the original inorganic-organic concept, the Astropower separator. (Author)

A81-20805 * Status of commercial phosphoric acid fuel cell system development. M. Warshaw, P. R. Prokopius, S. N. Simons, and R. B. King (NASA, Lewis Research Center, Phosphoric Acid Fuel Cell Program Lead Center Office, Cleveland, Ohio). *American Institute of Aeronautics and Astronautics, Aerospace Sciences Meeting, 19th, St. Louis, Mo., Jan. 12-15, 1981, Paper 81-0396*. 9 p. 12 refs.

A review of the current commercial phosphoric acid fuel cell system development efforts is presented. In both the electric utility and on-site integrated energy system applications, reducing cost and increasing reliability are important. The barrier to the attainment of these goals has been materials. The differences in approach among the three major participants are their technological features, including electrodes, matrices, intercell cooling, bipolar/separator plates, electrolyte management, fuel selection and system design philosophy. (Author)

A81-23694 * Large wind-turbine projects in the United States wind energy program. R. L. Thomas and W. H. Robbins (NASA, Lewis Research Center, Cleveland, Ohio). *Journal of Industrial Aerodynamics*, vol. 5, May 1980, p. 323-335.

The technological development of large, horizontal-axis wind turbines (100 kW-2500 kW) is surveyed with attention to prototype projects managed by NASA. Technical feasibility has been demonstrated in utility service for systems with a rated power of up to 200 kW and a rotor diameter of 125 ft (Mod-OA). Current designs of large wind turbines such as the 2500 kW Mod-2 are projected to be cost competitive for utility applications when produced in quantity, with capital costs of 600 to 700 dollars per kW (in 1977 dollars). L.S.

A81-27174 * Space solar cells - High efficiency and radiation damage. H. W. Brandhorst, Jr. and D. T. Bernatowicz (NASA, Lewis Research Center, Cleveland, Ohio.). In: *Photovoltaic Specialists Conference, 14th, San Diego, Calif., January 7-10, 1980, Conference Record*. (A81-27076 11-44) New York, Institute of Electrical and Electronics Engineers, Inc., 1980, p. 667-673. 22 refs.

The proceedings of the Third Solar Cell High Efficiency and Radiation Damage Meeting are outlined. The topics covered included high efficiency silicon solar cells, silicon solar cell radiation damage, GaAs solar cell performance, and 30 percent conversion devices. The

study of radiation damage from a fundamental defect-centered basis is discussed and evaluated as a focus of future work. 18% AMO efficiency and 0.7 V open-circuit voltages are designated as achievable goals for silicon solar cells, and the potential for 30% AMO efficiencies from monolithic tandem cell designs without sunlight concentration is noted. In addition to its potential for 20% AMO efficiencies, the GaAs cell offers the possibility of a radiation-insensitive power supply when operated at temperatures near 200 C. L.S.

A81-27204 * **Radiation damage in lithium-counterdoped N/P silicon solar cells.** A. M. Hermann, C. K. Swartz, H. W. Brandhorst, Jr., and I. Weinberg (NASA, Lewis Research Center, Cleveland, Ohio). In: Photovoltaic Specialists Conference, 14th, San Diego, Calif., January 7-10, 1980, Conference Record. (A81-27076 11-44) New York, Institute of Electrical and Electronics Engineers, Inc., 1980, p. 840-846. 14 refs.

The radiation resistance and low-temperature annealing properties of lithium-counterdoped n(+)-p silicon solar cells are investigated. Cells fabricated from float zone and Czochralski grown silicon were irradiated with 1 MeV electrons and their performance compared to that of 0.35 ohm-cm control cells. The float zone cells demonstrated superior radiation resistance compared to the control cells, while no improvement was noted for the Czochralski grown cells. Annealing kinetics were found to lie between first and second order for relatively short times, and the most likely annealing mechanism was found to be the diffusion of lithium to defects with the subsequent neutralization of defects by combination with lithium. Cells with zero lithium gradients exhibited the best radiation resistance. L.S.

A81-27231 * **Photovoltaic applications - Past and future.** H. L. Macomber (Monegon, Ltd., Gaithersburg, Md.), D. Faehn (U.S. Army, Mobility Equipment Research and Development Command, Fort Belvoir, Va.), S. I. Kaplan (Oak Ridge National Laboratory, Oak Ridge, Tenn.), J. N. Deyo (NASA, Lewis Research Center, Cleveland, Ohio), M. D. Pope (MIT, Lincoln Laboratory, Lexington, Mass.), and D. G. Schueler (Sandia Laboratories, Albuquerque, N. Mex.). In: Photovoltaic Specialists Conference, 14th, San Diego, Calif., January 7-10, 1980, Conference Record. (A81-27076 11-44) New York, Institute of Electrical and Electronics Engineers, Inc., 1980, p. 1004-1017. 25 refs.

This paper presents an overview of photovoltaic systems applications since the initiation of the U.S. National Photovoltaic Program in 1975. Experiences with these applications are summarized and some conclusions are drawn. Implications for future research, technology development and application experiments are drawn from the experiences to date. (Author)

A81-27254 * **Analysis of GaAs and Si solar cell arrays for earth orbital and orbit transfer missions.** K. S. Jefferies (NASA, Lewis Research Center, Space Propulsion and Power Div., Cleveland, Ohio). In: Photovoltaic Specialists Conference, 14th, San Diego, Calif., January 7-10, 1980, Conference Record. (A81-27076 11-44) New York, Institute of Electrical and Electronics Engineers, Inc., 1980, p. 1164-1168. 6 refs.

Solar array systems have been studied and compared for earth orbital and orbit transfer missions with the principal objective of quantifying the cost tradeoffs between gallium arsenide and silicon array for specific classes of missions and system characteristics. For the missions considered, it is found that the purchase cost advantage of Si arrays is not overcome by the greater radiation resistance of GaAs arrays. The use of reflectors for concentration may significantly reduce the power system cost. However, GaAs arrays benefit considerably more from solar concentration than Si arrays in terms of mission cost because of their higher allowable temperature. In the case of orbit transfer missions, a cover glass thickness of at least 0.05 cm is recommended to reduce total mission cost. V.L.

A81-38063 * **An experimental investigation of silicon wafer surface roughness and its effect on the pull-strength of plated metals.** G. D. Spiers (NASA, Lewis Research Center, Cleveland, OH). *Institute of Electrical and Electronics Engineers, Photovoltaic Specialists Conference, 15th, Kissimmee, FL, May 12-15, 1981, Paper.* 6 p. 14 refs.

Plated silicon wafers with surface roughness ranging from 0.4 to 130 microinches, subjected to tensile pull-strength tests, were analyzed. Results show that the measured pull-strength of plated metals decrease with increasing silicon surface roughness, effecting a weakening of the cohesive strength of the wafer, possibly caused by microcracks or 'etch pits' in the silicon surface. The mean value of pull-strength for all wafers plated with the Ni-Cu-Cu sequence exceeded the required 450 g/0.02 sq cm, and at Ra = 0.4 microinches, the mean pull-strength for the Ni-Cu-Cu and Ni-Cu wafers were 2290 and 850 g/0.02 sq cm, respectively. The development of standardized methods for measuring contact pull-strength is suggested. These results may have some bearing on solar cell arrays problems. E.B.

N81-10517* **United Technologies Corp., South Windsor, Conn. Power Systems Div.**

COGENERATION TECHNOLOGY ALTERNATIVES STUDY (CTAS) VOLUME 5: ANALYTICAL APPROACH AND RESULTS Final Report

Jan. 1980 176 p refs

(Contracts DEN3-30; EC-77-A-31-1062)

(NASA-CR-159763; DOE/NASA/0030-80/5; UTC-FCR-1333)

Avail: NTIS HC A09/MF A01 CSCL 10B

Data and information in the area of advanced energy conversion systems for industrial cogeneration applications in the 1985 to 2000 time period are provided. Six current and thirty-six advanced energy conversion systems were defined and combined with appropriate balance of plant equipment. Twenty-six industrial processes were selected from among the high energy consuming industries to serve as a framework for the study. Each conversion system was analyzed as a cogenerator with each industrial plant. Fuel consumption, costs, and environmental intrusion were evaluated and compared to corresponding traditional values. Various cogeneration strategies were analyzed and both topping and bottoming (using industrial by-product heat) applications were included. The advanced energy conversion technologies indicated reduced fuel consumption, costs, and emissions. Typically fuel energy savings of 10 to 25 percent were predicted compared to traditional on site furnaces and utility electricity. Gas turbines and combined cycles indicated high overall annual cost savings. Steam turbines and gas turbines produced high estimated returns. In some applications, diesels were most efficient. The advanced technologies used coal derived fuels, or coal with advanced fluid bed combustion or on site gasification systems. R.K.G.

N81-12546* **STD Research Corp., Arcadia, Calif. ANALYTICAL INVESTIGATION OF CRITICAL PHENOMENA IN MHD POWER GENERATORS Final Report**

31 Jul. 1980 375 p refs

(Contracts DEN3-179; SC-77-AA-012674)

(NASA-CR-165143; DOE/NASA/O179-1; STDR-80-22) Avail:

NTIS HC A16/MF A01 CSCL 10A

Critical phenomena in the Arnold Engineering Development Center (AEDC) High Performance Demonstration Experiment (HPDE) and the U.S. U-25 Experiment, are analyzed. The performance of a NASA specified 500 MW(th) flow train is analyzed. Critical phenomena analyzed include: Hall voltage overshoots; optimal load schedules; parametric dependence of the electrode voltage drops; boundary layer behavior; near electrode phenomena with finite electrode segmentation; current distribution in the end regions; scale up rules; optimum Mach number distribution; and the effects of alternative cross sectional shapes. R.C.T.

N81-13466* Burns and Roe, Inc., Woodbury, N. Y.
ENGINEERING SUPPORT FOR MAGNETOHYDRODYNAMIC POWER PLANT ANALYSIS AND DESIGN STUDIES
 A. W. Carlson, I. L. Chait, G. Marchmont, R. Rogali, and D. Shikar Aug. 1980 288 p refs
 (Contracts DEN3-107; EC-77-A-01-2674)
 (NASA-CR-159690; DOE/NASA/O197-1) Avail: NTIS HC A13/MF A01 CSCL 10B

The major factors which influence the economic engineering selection of stack inlet temperatures in combined cycle MHD powerplants are identified and the range of suitable stack inlet temperatures under typical operating conditions is indicated. Engineering data and cost estimates are provided for four separately fired high temperature air heater (HTAH) system designs for HTAH system thermal capacity levels of 100, 250, 500 and 1000 MWt. An engineering survey of coal drying and pulverizing equipment for MHD powerplant application is presented as well as capital and operating cost estimates for varying degrees of coal pulverization. A.R.H.

N81-13467* Burns and Roe, Inc., Woodbury, N. Y.
MODIFICATION OF THE ECAS REFERENCE STEAM POWER GENERATING PLANT TO COMPLY WITH THE EPA 1979 NEW SOURCE PERFORMANCE STANDARDS Final Report
 S. A. Fogelson, I. L. Chait, W. J. Bradley, and W. Benson Aug. 1980 246 p refs
 (Contracts DEN3-107; DE-A101-77ET-10769)
 (NASA-CR-159853; DOE/NASA/O107-2) Avail: NTIS HC A11/MF A01 CSCL 10B

Detailed capital cost estimates for the ECAS and modified reference plants in mid-1978 dollars for both 250 and 175 F (394 and 353 K) stack gas reheat temperatures based on the cost estimates developed for the ECAS study are presented. The scope of the work included technical assessment of sulfur dioxide scrubber system design, on site calcination versus purchased lime, reheat of stack gas, effect of sulfur dioxide scrubber on particulate emission, and control of nitrogen oxides. Author

N81-14391* Motorola, Inc., Phoenix, Ariz.
MARKET DEFINITION STUDY OF PHOTOVOLTAIC POWER FOR REMOTE VILLAGES IN DEVELOPING COUNTRIES
 Clyde Ragsdale and Prosper Quashie Oct. 1980 208 p refs
 (Contracts DEN3-49; DE-A101-79ET-20485)
 (NASA-CR-159880; DOE/NASA/O049-80/2; EDR-1110) Avail: NTIS HC A10/MF A01 CSCL 10B

The potential market of photovoltaic systems in remote village applications in developing countries is assessed. It is indicated that photovoltaic technology is cost-competitive with diesel generators in many remote village applications. The major barriers to development of this market are the limited financial resources on the part of developing countries, and lack of awareness of photovoltaics as a viable option in rural electrification. A comprehensive information, education and demonstration program should be established as soon as possible to convince the potential customer countries and the various financial institutions of the viability of photovoltaics as an electricity option for developing countries. J.M.S.

N81-15461* Little (Arthur D.), Inc., Cambridge, Mass.
STUDY OF COMPONENT TECHNOLOGIES FOR FUEL CELL ON-SITE INTEGRATED ENERGY SYSTEMS Final Report
 W. David Lee and Siegfried Mathias Dec. 1980 129 p refs
 (Contracts DEN3-121; DE-A103-80ET-11272)
 (NASA-CR-165152-Vol. 1; DOE/NASA/O121-80/1-Vol. 1; ADL-83613) Avail: NTIS HC A07/MF A01 CSCL 10A

Heating, ventilation and air conditioning equipment are integrated with three types of fuel cells. System design and computer simulations are developed to utilize the thermal energy discharge of the fuel in the most cost effective manner. The fuel provides all of the electric needs and a loss of load probability analysis is used to ensure adequate power plant reliability. Equipment cost is estimated for each of the systems analyzed. A leveled annual cost reflecting owning and operating costs including the cost of money was used to select the most

promising integrated system configurations. Cash flows are presented for the most promising 16 systems. Several systems for the 96 unit apartment complex (a retail store was also studied) were cost competitive with both gas and electric based conventional systems. Thermal storage is shown to be beneficial and the optimum absorption chiller sizing (waste heat recovery) in connection with electric chillers are developed. Battery storage was analyzed since the system is not electric grid connected. Advanced absorption chillers were analyzed as well. Recommendations covering financing, technical development, and policy issues are given to accelerate the commercialization of the fuel cell for on-site power generation in buildings. Author

N81-15462* Little (Arthur D.), Inc., Cambridge, Mass.
STUDY OF COMPONENT TECHNOLOGIES FOR FUEL CELL ON-SITE INTEGRATED ENERGY SYSTEM. VOLUME 2: APPENDICES Final Report
 W. David Lee and Siegfried Mathias Dec. 1980 143 p refs
 (Contracts DEN3-121; DE-A103-80ET-11272)
 (NASA-CR-165152-Vol. 2; DOE/NASA/O121-80/1-Vol. 2; ADL-83613) Avail: NTIS HC A07/MF A01 CSCL 10A

This data base catalogue was compiled in order to facilitate the analysis of various on site integrated energy system with fuel cell power plants. The catalogue is divided into two sections. The first characterizes individual components in terms of their performance profiles as a function of design parameters. The second characterizes total heating and cooling systems in terms of energy output as a function of input and control variables. The integrated fuel cell systems diagrams and the computer analysis of systems are included as well as the cash flows series for baseline systems. E.D.K.

N81-15463* Lincoln Lab., Mass. Inst. of Tech., Lexington.
GaAs SHALLOW-HOMOJUNCTION SOLAR CELLS Final Report
 John C. Fan 30 Jun. 1980 29 p refs
 (NASA Order C-30969-D)
 (NASA-CR-165167) Avail: NTIS HC A03/MF A01 CSCL 10A

With the objective of demonstrating the feasibility of fabricating 2 x 2 cm efficient, shallow homojunction GaAs solar cells for space applications, this program addresses the basic problems of material preparation and device fabrication. Significant progress was made and conversion efficiencies close to 16 percent at AM0 were obtained on 2 x 2 cm cells. Measurements and computer analyses on the n(+)/p/p(+) shallow homojunction cells indicate that such cell configuration should be very resistant to 1 MeV electron irradiation. E.D.K.

N81-16579* Westinghouse Electric Corp., Pittsburgh, Pa.
CELL MODULE AND FUEL CONDITIONER DEVELOPMENT Quarterly Report, Jul. - Sep. 1980
 D. Q. Hoover, Jr. Oct. 1980 68 p
 (Contracts DEN3-161; DE-A103-79ET-11272)
 (NASA-CR-165189; DOE/NASA/O161-5; Rept-80-9E6-MARE-R4; QR-4) Avail: NTIS HC A04/MF A01 CSCL 10A

Measurements of stack height changes with temperature and cell material characteristics were made. Stack 559 was assembled and components were fabricated for 560, 561, and 562. Stack 425 was transferred from the parallel DOE program and installed in the OS/IES simulation loop for mechanical and electrical testing. Construction and preliminary checkout of the 2 kW test facility was completed and design and procurement of the 8 kW test facility was initiated. The fuel conditioning subsystem design continued to evolve, and the state points for the current design were calculated at full and part load conditions. Steam reforming catalyst activity tests were essentially completed and aging tests and CO shift converter tests were initiated. Author

N81-16582* Boeing Aerospace Co., Seattle, Wash.
ELECTROSTATIC BONDING OF THIN (CYCLE SINE 3 MIL) 7070 COVER GLASS TO Ta2O5 AR-COATED THIN (CYCLE SINE 2 MIL) SILICON WAFERS AND SOLAR CELLS
 D. W. Egelkroun Jan. 1981 77 p refs
 (Contract NAS3-22216)
 (NASA-CR-165240; D180-26200-1) Avail: NTIS
 HC A05/MF A01 CSCL 10A

Electrostatic bonding of thin cover glass to thin solar cells was researched. Silicon solar cells, wafers, and Corning 7070 glass of from about 0.002' to about 0.003' in thickness were used in the investigation to establish optimum parameters for producing mechanically acceptable bonds while minimizing thermal stresses and resultant solar cell electrical parameter degradation. E.D.K.

N81-16583* Ionics, Inc., Watertown, Mass.
ANION PERMSELECTIVE MEMBRANE Summary Report
 Russell B. Hodgdon and Warren A. Waite Nov. 1980 54 p refs
 (Contracts DEN3-137; DE-A104-80AL-12726)
 (NASA-CR-165223; DOE/NASA/O137-1) Avail: NTIS
 HC A04/MF A01 CSCL 10A

The efforts on the synthesis of polymer anion redox membranes were mainly concentrated in two areas, membrane development and membrane fabrication. Membrane development covered the preparation and evaluation of experimental membranes systems with improved resistance stability and/or lower permeability. Membrane fabrication covered the laboratory scale production of prime candidate membranes in quantities of up to two hundred and sizes up to 18 inches x 18 inches (46 cm x 46 cm). These small (10 in x 11 in) and medium sized membranes were mainly for assembly into multicell units. Improvements in processing procedures and techniques for preparing such membrane sets lifted yields to over 90 percent. T.M.

N81-17527* Stonehart Associates, Inc., Madison, Conn.
PREPARATION AND EVALUATION OF ADVANCED ELECTROCATALYSTS FOR PHOSPHORIC ACID FUEL CELLS Quarterly Report, Jul. - Sep. 1980
 Paul Stonehart, John Baris, and Peter Pagliaro Sep. 1980 30 p refs
 (Contract DEN3-176)
 (NASA-CR-165179; DOE/NASA/O176-80/3; QR-3) Avail:
 NTIS HC A03/MF A01 CSCL 10A

Results are presented for hydrogen oxidation and hydrogen oxidation poisoned by carbon monoxide at levels between 0 and 30%. Due to the high activities that are now being observed for our platinum based electrocatalysts, the hydrogen concentrations were reduced to 10% levels in the gas supplies. Perturbation techniques were used to determine that a mechanism for the efficient operation of our porous gas diffusion electrodes is diffusion of the carbon monoxide out of the electrode structure through the electrolyte film on the electro-catalyst. A survey of the literature on platinum group materials (PGM) was carried out so that an identification of successful electrocatalysts could be made. Two PGM electrocatalysts were prepared and performance data for hydrogen oxidation in hot phosphoric acid in the presence of high carbon monoxide concentrations showed that they matched the best platinum on carbon electrocatalysts but with an electrocatalyst cost that was half of the platinum catalyst cost. Author

N81-17588* Boeing Aerospace Co., Seattle, Wash.
EVALUATION OF SOLAR CELL COVERS AND ENCAPSULANT MATERIALS FOR SPACE APPLICATION
 Dennis A. Russell In NASA. Lewis Research Center Space Photovoltaic Res. and Technol. 1980 p 293-315 ref (For primary document see N81-17531 08-44)
 (Contract NAS3-22222)
 Avail: NTIS HC A17/MF A01 CSCL 10A

The effects of space radiation (electrons and protons), vacuum, and thermal cycling on a variety of solar cell covers are investigated. Cover materials evaluated include glass resins, 2 mil glass applied with adhesives or electrostatically bonded, and thin

plastic films of FEP or PFA applied with adhesive. Solar cells were exposed to environmental conditions simulating those encountered in outer space. These test conditions include 1 MeV electrons, 0.5 MeV protons, and thermal cycling in vacuum. During testing the solar cells were monitored for variations in electrical characteristics and structural changes. M.G.

N81-17589* Boeing Aerospace Co., Seattle, Wash.
ELECTROSTATIC BONDING OF THIN (APPROXIMATELY 3 MIL) 7070 COVER GLASS TO Ta2O5 AR-COATED THIN (APPROXIMATELY 2 MIL) SILICON WAFERS AND SOLAR CELLS
 D. W. Egelkroun and W. E. Horne In NASA. Lewis Research Center Space Photovoltaic Res. and Technol. 1980 p 317-336 refs (For primary document see N81-17531 08-44)
 (Contract NAS3-22216)
 Avail: NTIS HC A17/MF A01 CSCL 10A

Electrostatic bonding (ESB) of thin (3 mil) Corning 7070 cover glasses to Ta2O5 AR-coated thin (2 mil) silicon wafers and solar cells is investigated. An experimental program was conducted to establish the effects of variations in pressure, voltage, temperature, time, Ta2O5 thickness, and various prebond glass treatments. Flat wafers without contact grids were used to study the basic effects for bonding to semiconductor surfaces typical of solar cells. Solar cells with three different grid patterns were used to determine additional requirements caused by the raised metallic contacts. M.G.

N81-17574* Spectrolab, Inc., Sylmar, Calif.
THE HEWAC PILOT LINE EXPERIENCE
 M. Gillanders and R. Opjorden In NASA. Lewis Research Center Space Photovoltaic Res. and Technol. 1980 p 379-386 (For primary document see N81-17531 08-44)
 (Contract NAS3-21270)
 Avail: NTIS HC A17/MF A01 CSCL 10A

Advanced silicon solar cells with both electrical contacts on the back side of the cell are described. These high efficiency wrap around contact solar cells (HEWACS) utilize a screen printed dielectric insulation layer to isolate the 'n' and 'p' contacts from each other. Development of a device exhibiting high AMO conversion efficiencies is addressed along with the processing of such cells to a point where cell fabrication can be carried out by production personnel under operating production line conditions. J.M.S.

N81-18482 Rensselaer Polytechnic Inst., Troy, N. Y.
A METHODOLOGY FOR THE DESIGN AND CALIBRATION OF DATA BASED MODELS OF AGGREGATE LAKE ECOSYSTEM DYNAMICS Ph.D. Thesis
 Glenn Foster Roberts 1980 284 p
 Avail: Univ. Microfilms Order No. 8103762
 (NASA-CR-159588; DOE/NASA/0056-79/2) Avail: NTIS
 HC A06/MF A01 CSCL 10B

The concept evaluation shows that the four cylinder double acting U type Stirling engine with annular regenerators is the most suitable engine type for the 15 kW solar application with respect to design, performance and cost. Results show that near term performance for a metallic Stirling engine is 42% efficiency. Further improved components show an impact on efficiency of the future metallic engine to 45%. Increase of heater temperature, through the introduction of ceramic components, contribute the greatest amount to achieve high efficiency goals. Future ceramic Stirling engines for solar applications show an efficiency of around 50%. T.M.

N81-18491* Westinghouse Electric Corp., Pittsburgh, Pa.
 Advanced Energy Systems Div.
DISK MHD GENERATOR STUDY Final Report
 F. D. Retallick et al Oct. 1980 424 p refs
 (Contract DEN3-139; DE-A101-77ET-10769)
 (NASA-CR-159872; DOE/NASA/O139-1; AESD-TME-3064)
 Avail: NTIS HC A18/MF A01 CSCL 10A
 Directly-fired, separately-fired, and oxygen-augmented MHD power plants incorporating a disk geometry for the MHD generator

were studied. The base parameters defined for four near-optimum-performance MHD steam power systems of various types are presented. The finally selected systems consisted of (1) two directly fired cases, one at 1920 K (2996F) preheat and the other at 1650 K (2500 F) preheat, (2) a separately-fired case where the air is preheated to the same level as the higher temperature directly-fired cases, and (3) an oxygen augmented case with the same generator inlet temperature of 2839 (4650F) as the high temperature directly-fired and separately-fired cases. Supersonic Mach numbers at the generator inlet, gas inlet swirl, and constant Hall field operation were specified based on disk generator optimization. System pressures were based on optimization of MHD net power. Supercritical reheat steam plants were used in all cases. Open and closed cycle component costs are summarized and compared. A.R.H.

NS1-18494* Westinghouse Research and Development Center, Pittsburgh, Pa.

CELL MODULE AND FUEL CONDITIONER Quarterly Report, Jul. - Sep. 1980

D. Q. Hoover, Jr. Oct. 1980 72 p

(Contracts DEN3-161; DE-A103-79ET-11272)

(NASA CR-165189; DOE/NASA/0161-5;

Rept-80-9E6-MAREC-R4; QR-4)

Avail: NTIS

HC A04/MF A01 CSCL 10A

Measurements of stack height changes with temperature and cell material characteristics were made. Stack 559 was assembled and components were fabricated for 560, 561, and 562. Stack 425 was transferred from the parallel DOE program and installed in the OS/IES simulation loop for mechanical and electrical testing. Construction and preliminary checkout of the 2 kW test facility was completed and design and procurement of the 8 kW test facility was initiated. The fuel conditioning subsystem design continued to evolve and the state points for the current design were calculated at full and part load conditions. Steam reforming catalyst activity tests were essentially completed and aging tests and CO shift converter tests were initiated. Author

NS1-18495* Solarex Corp., Rockville, Md.

COPLANAR BACK CONTACTS FOR THIN SILICON SOLAR CELLS Final Report, 24 Jul. 1978 - 15 Jul. 1980

G. Storti, A. Scheinine, D. Whitehouse, J. Wohlgemuth, C. Wrigley, and M. Giuliano Jan. 1981 38 p refs

(Contract NAS3-21250)

(NASA-CR-165272) Avail: NTIS HC A03/MF A01 CSCL 10A

The type of coplanar back contact solar cell described was constructed with interdigitated n(+) and p(+) type regions on the back of the cell, such that both contacts are made on the back with no metallization grid on the front. This cell construction has several potential advantages over conventional cells for space use namely, convenience of interconnects, lower operating temperatures and higher efficiency due to the elimination of grid shadowing. However, the processing is more complex, and the cell is inherently more radiation sensitive. The latter problem can be reduced substantially by making the cells very thin (approximately 50 micrometers). Two types of interdigitated back contact cells are possible, the types being dependent on the character of the front surface. The front surface field cell has a front surface region that is of the same conductivity type as the bulk but is more heavily doped. This creates an electric field at the surface which repels the minority carriers. The tandem junction cell has a front surface region of a conductivity type that is opposite to that of the bulk. The junction thus created floats to open circuit voltage on illumination and injects carriers into the bulk which then can be collected at the rear junction. For space use, the front surface field cell is potentially more radiation resistant than the tandem junction cell because the flow of minority carriers (electrons) into the bulk will be less sensitive to the production of recombination centers, particularly in the space charge region at the front surface. T.M.

NS1-18496* Stonehart Associates, Inc., Madison, Conn.
PREPARATION AND EVALUATION OF ADVANCED ELECTROCATALYSTS FOR PHOSPHORIC ACID FUEL

CELLS Quarterly Report, Oct. - Dec. 1980

Paul Stonehart, John Baris, John Hochmuth, and Peter Pagliaro 31 Dec. 1980 35 p

(Contracts DEN3-176; DE-A101-80ET-17088)

(NASA-CR-185245; DOE/NASA/0176-80/4; GR-4) Avail: NTIS HC A03/MF A01 CSCL 10A

Alloy electrocatalysts on carbon supports were developed for hydrogen oxidation in the presence of carbon monoxide. These electrocatalysts match the best platinum on carbon catalysts for performance yet cost half as much. The results demonstrate that a significant reduction in anode electrocatalyst material cost can be achieved by replacing the platinum. Since surface characterization of this catalyst is important to explain its performance, several approaches and pitfalls to the elucidation of the surface characterization are presented. T.M.

NS1-18497* National Bureau of Standards, Washington, D.C. Metallurgy Div.

NON-NOBLE CATALYSTS AND CATALYST SUPPORTS FOR PHOSPHORIC ACID FUEL CELLS Quarterly Report, Aug. - Nov. 1980

A. J. McAlister Nov. 1980 13 p refs

(NASA Order C-46229D; Contract DE-A101-80ET-17088)

(NASA-CR-165221; DOE/NASA/6229-1; QR-1) Avail: NTIS HC A02/MF A01 CSCL 10A

Tungsten carbide, which is known to be active for hydrogen oxidation and CO tolerant has a hexagonal structure. Titanium carbide is inactive and has a cubic structure. Four different samples of the cubic alloys Wx-1Ti_{1-x}C were prepared and found to be active and CO tolerant. These alloys are of interest as possible phosphoric acid fuel cell catalysts. They also are of interest as opportunities to study the activity of W in a different crystalline environment and to correlate the activities of the surface sites with surface composition. Author

NS1-19573* Westinghouse Research and Development Center, Pittsburgh, Pa. Research and Development Center.

CELL MODULE AND FUEL CONDITIONER DEVELOPMENT Quarterly Report, Oct. - Dec. 1980

D. Q. Hoover, Jr. Jan. 1981 72 p refs

(Contracts DEN3-161; DE-A101-80ET-17088)

(NASA-CR-165190; DOE/NASA/0161-6;

Rept-80-9E6-MAREC-R5; QR-5)

Avail: NTIS

HC A04/MF A01 CSCL 10A

The test results of and post test analysis of Stack 559 are reported. The design features and construction status of Stacks 560, 561, 562 and 563 are described. The measurements of cell materials compressibility are rationalized and summarized and an explanation of their uses is given. Preliminary results of a manifold material/coating survey are given. The results of shift converter catalyst performance tests and reforming catalyst aging tests are reported. State points for full load and part load operation of the fuel conditioning subsystem tabulated. Work on the data base for the fuel conditioner ancillary subsystems is summarized. T.M.

NS1-21633* Mathtech, Inc., Arlington, Va.

STUDY OF FUEL CELL ON-SITE, INTEGRATED ENERGY SYSTEMS IN RESIDENTIAL/COMMERCIAL APPLICATIONS Final Report

R. A. Wakefield, S. Karamchetty, R. H. Rand, W. S. Ku, and V. Tekumalla Oct. 1980 310 p refs

(Contracts DEN3-89; DE-A103-79ET-11272)

(NASA-CR-165144; DOE/NASA-0089-80/1; E-FC-002) Avail: NTIS HC A14/MF A01 CSCL 10A

Three building applications were selected for a detailed study: a low rise apartment building; a retail store, and a hospital. Building design data were then specified for each application, based on the design and construction of typical, actual buildings. Finally, a computerized building loads analysis program was used to estimate hourly end use load profiles for each building. Conventional and fuel cell based energy systems were designed and simulated for each building in each location. Based on the results of a computer simulation of each energy system, levelized annual costs and annual energy consumptions were calculated for all systems. T.M.

NS1-21536* Energy Research Corp., Danbury, Conn.
TECHNOLOGY DEVELOPMENT FOR PHOSPHORIC ACID FUEL CELL POWERPLANT, PHASE 2 Quarterly Report
 Larry Christner Mar. 1980 74 p
 (Contracts DEN3-67; DE-AL03-79ET-11272)
 (NASA-CR-185317; DOE/NASA/0067-79-3; ERC-18; QR-6)
 Avail: NTIS HC A04/MF A01 CSCL 10A

The technology development for materials, cells, and reformers for on site integrated energy systems is described. The carbonization of 25 cu cm, 350 cu cm, and 1200 cu cm cell test hardware was accomplished and the performance of 25 cu cm fuel cells was improved. Electrochemical corrosion rates of graphite/phenolic resin composites in phosphoric acid were determined. Three cells (5 in by 15 in stacks) were operated for longer than 7000 hours. Specified endurance stacks completed a total of 4000 hours. An electrically heated reformer was tested and is to provide hydrogen for 23 cell fuel cell stack. R.C.T.

NS1-21547* Energy Research Corp., Danbury, Conn.
TECHNOLOGY DEVELOPMENT FOR PHOSPHORIC ACID FUEL CELL POWERPLANT (PHASE 2) Quarterly Report
 Larry Christner Dec. 1979 52 p refs
 (Contracts DEN3-67; DE-AI03-79ET-11272)
 (NASA-CR-185316; DOE/NASA/0067-79-2; QR-5) Avail:
 NTIS HC A04/MF A01 CSCL 10A

The status of technology for the manufacturing and testing of 1200 sq. cm cell materials, components, and stacks for on-site integrated energy systems is assessed. Topics covered include: (1) preparation of thin layers of silicon carbide; (2) definition and control schemes for volume changes in phosphoric acid fuel cells; (3) preparation of low resin content graphite phenolic resin composites; (4) chemical corrosion of graphite-phenolic resin composites in hot phosphoric acid; (5) analysis of electrical resistance of composite materials for fuel cells; and (6) fuel cell performance and testing. A.R.H.

NS1-21548* Energy Research Corp., Danbury, Conn.
TECHNOLOGY DEVELOPMENT FOR PHOSPHORIC ACID FUEL CELL POWERPLANT (PHASE 2) Quarterly Report
 Larry Christner Mar. 1980 75 p refs
 (Contracts DEN3-67; DE-AI03-79ET-11272)
 (NASA-CR-185317; DOE/NASA/0067-79-3; QR-6) Avail:
 NTIS HC A04/MF A01 CSCL 10A

Progress is reported in the development of technology for materials, cell components, and reformers for on-site integrated energy systems. Carbonization of 25 sq. cm, 350 sq. cm, and 1200 sq. cm cell test hardware was accomplished. The performance of 25 sq. cm fuel cells was improved by using this material. Electrochemical corrosion rates of graphite phenolic resin composites in phosphoric acid were determined. Three cell, 5 in. by 15 in. stacks operated for more than 7,000 hours. Specified endurance stacks completed 4,000 hours. A electrically heated reformer to provide hydrogen for a 23 cell fuel cell stack was tested. A.R.H.

NS1-22467* Thermo Electron Corp., Waltham, Mass.
THERMAL ENERGY STORAGE FOR THE STIRLING ENGINE POWERED AUTOMOBILE Final Report
 Dean T Morgan, ed. Mar. 1979 319 p refs Prepared for Argonne National Lab.
 (NASA Order C-2325; Contract W-31-109-38-4135)
 (NASA-CR-159561; ANL-K78-4135-1; TE5484-66-79) Avail:
 NTIS HC A14/MF A01 CSCL 10C

A thermal energy storage (TES) system developed for use with the Stirling engine as an automotive power system has gravimetric and volumetric storage densities which are competitive with electric battery storage systems, meets all operational requirements for a practical vehicle, and can be packaged in compact sized automobiles with minimum impact on passenger and freight volume. The TES/Stirling system is the only storage approach for direct use of combustion heat from fuel sources not suitable for direct transport and use on the vehicle. The particular concept described is also useful for a dual mode TES/liquid fuel system in which the TES (recharged from an external energy source) is used for short duration trips (ap-

proximately 10 miles or less) and liquid fuel carried on board the vehicle used for long duration trips. The dual mode approach offers the potential of 50 percent savings in the consumption of premium liquid fuels for automotive propulsion in the United States. A.R.H.

NS1-22473* Institute of Gas Technology, Chicago, Ill.
 Engineering Research Div.
STABILIZING PLATINUM IN PHOSPHORIC ACID FUEL CELLS Quarterly Report, Dec. 1980 - Mar. 1981
 Robert J. Remick Apr. 1981 25 p refs
 (Contracts DEN3-208; DE-AI01-80ET-17088)
 (NASA-CR-185311; DOE/NASA/0208-1; Rept-61051; QR-1)
 Avail: NTIS HC A02/MF A01 CSCL 10A

The cathode of the phosphoric acid fuel cell uses a high surface area platinum catalyst supported on a carbon substrate. During operation, the small platinum crystallites sinter, causing loss in cell performance. A support was developed that stabilizes platinum in the high surface area condition by retarding or preventing the sintering process. The approach is to form etch pits in the carbon by oxidizing the carbon in the presence of a metal oxide catalyst, remove the metal oxide by an acid wash, and then deposit platinum in these pits. Results confirm the formation of etch pits in each of the three supports chosen for investigation: Vulcan XC-72R, Vulcan XC-72 that was graphitized at 2500 C, and Shawinigan Acetylene Black. T.M.

NS1-22475* Energy Research Corp., Danbury, Conn.
TECHNOLOGY DEVELOPMENT FOR PHOSPHORIC ACID FUEL CELL POWERPLANT (PHASE 2) Quarterly Report
 Larry Christner Jun. 1980 49 p refs
 (Contract DEN3-67; DE-AI03-79ET-11272)
 (NASA-CR-185318; DOE/NASA/0067-79-6; QR-7) Avail:
 NTIS HC A03/MF A01 CSCL 10A

Progress is reported in the development of material, cell components, and reformers for on site integrated energy systems. Internal resistance and contact resistance were improved. Dissolved gases (O₂, N₂, and CO₂) were found to have no effect on the electrochemical corrosion of phenolic composites. Stack performance was increased by 100 mV over the average 1979 level. A.R.H.

AB1-15027 * Moderate temperature sodium cells. I - Transition metal disulfide cathodes. K. M. Abraham, L. Pitts, and R. Schiff (EIC Corp., Newton, Mass.). *Electrochemical Society, Journal*, vol. 127, Dec. 1980, p. 2545-2550. 19 refs. Contract No. NAS3-21726.
 TiS₂, VS₂, and Nb(1.1)S₂ transition metal disulfides were evaluated as cathode materials for a moderate temperature rechargeable Na cell operating at 130 C. The 1st discharge of TiS₂ results in a capacity of 0.85 eq/mole; approximately half of the Na in the 1st phase spanning the Na range from zero to 0.30 and almost all the Na in the 2nd phase spanning the 0.37 to 0.80 range are rechargeable. VS₂ intercalates up to one mole of Na/mole of VS₂ in the 1st discharge; the resulting Na(x)VS₂ ternary consists of 3 phases in the 3 ranges of Na from zero to 1. Niobium disulfide undergoes a phase change in the 1st discharge; the average rechargeable capacity in extended cycling of this cathode is 0.50 eq/mole. A.T.

AB1-27089 * Silicon solar cells with high open-circuit voltage. J. A. Minnucci, K. W. Matthei, A. R. Kirkpatrick, and A. McCrosky (Spire Corp., Bedford, Mass.). In: *Photovoltaic Specialists Conference*, 14th, San Diego, Calif., January 7-10, 1980, Conference Record. (AB1-27076 11-44) New York, Institute of Electrical and Electronics Engineers, Inc., 1980, p. 93-96. Contract No. NAS3-20823.

Open-circuit voltages as high as 0.645 V (AM0-25 C) have been obtained by a new process developed for low-resistivity silicon. The method utilizes high-dose phosphorus implantation, followed by furnace annealing and simultaneous oxide growth to form high efficiency, shallow junctions. The effect of the thermally grown

oxide is a reduction of surface recombination velocity; the oxide also acts as a moderately efficient AR coating. Boron doped silicon with resistivities from 0.1 to 0.3 ohm-cm has been processed according to this sequence; results show highest open-circuit voltage is attained with 0.1-ohm-cm starting material. The effects of bandgap narrowing, caused by high doping concentrations in the junction, were also investigated by implanting phosphorus over a wide range of dose levels. (Author)

A81-27092 * **High efficiency ultrathin coplanar back contact cells.** G. Storti, C. Wrigley, J. Wohlgemuth, D. Whitehouse, and A. Scheinine (Solarex Corp., Rockville, Md.). In: Photovoltaic Specialists Conference, 14th, San Diego, Calif., January 7-10, 1980, Conference Record. (A81-27076 11-44) New York, Institute of Electrical and Electronics Engineers, Inc., 1980, p. 137-140. Contract No. NAS3-21250.

Efforts to fabricate high efficiency, ultrathin coplanar back contact cells are described. Included is a description of design considerations, cell fabrication, and theoretical and experimental analyses of loss mechanisms. The results of these efforts has been the fabrication of a 11.8% AMO efficient, 50 micron cell when measured at 25 C. Design and process changes required to increase the efficiency are indicated. (Author)

A81-27094 * **High efficiency wraparound contact solar cells /HEWACS/.** M. Gillanders and R. Opjorden (Spectrolab, Inc., Sylmar, Calif.). In: Photovoltaic Specialists Conference, 14th, San Diego, Calif., January 7-10, 1980, Conference Record. (A81-27076 11-44) New York, Institute of Electrical and Electronics Engineers, Inc., 1980, p. 146-150. Contracts No. NAS3-20065; No. NAS3-21270.

A cell technology, producing high efficiency wrap-around contact solar cells (HEWACS), with both electrical contacts on the back and AMO conversion efficiencies of almost 15%, is presented. A flow chart indicating the baseline process sequence along with the process changes is given. Tests checking for coating delamination and contact integrity, those measuring contact strength, and thermal cycle tests, successfully demonstrated that this cell technology is ready to be moved to the pilot production stage. K.S.

A81-27097 * **Thin n-i-p silicon solar cell.** A. Meulenber, Jr., J. F. Allison, and R. A. Arndt (COMSAT Laboratories, Clarksburg, Md.). In: Photovoltaic Specialists Conference, 14th, San Diego, Calif., January 7-10, 1980, Conference Record. (A81-27076 11-44) New York, Institute of Electrical and Electronics Engineers, Inc., 1980, p. 161-165. Research sponsored by the Communications Satellite Corp.; Contract No. NAS3-21280.

A space solar cell concept which combines high cell output with low diffusion length damage coefficients is presented for the purpose of reducing solar cell susceptibility to degradation from the radiation environment. High resistivity n-i-p silicon solar cells ranging from upward of 83 micron-cm were exposed to AMO ultraviolet illumination. It is shown that high resistivity cells act as extrinsic devices under dark conditions and as intrinsic devices under AMO illumination. Resistive losses in thin n-i-p cells are found to be comparable to those in low resistivity cells. Present voltage limitations appear to be due to generation and recombination in the diffused regions. D.K.

45 ENVIRONMENT POLLUTION

Includes air, noise, thermal and water pollution;
environment monitoring; and contamination control.

NS1-30657* National Aeronautics and Space Administration
Lewis Research Center, Cleveland, Ohio.

**NASA GLOBAL ATMOSPHERIC SAMPLING PROGRAM
(GASP) DATA REPORT FOR TAPE VL0015, VL0016, VL0017,
VL0018, VL0019, AND VL0020**

Leonidas C. Papthakos and Daniel Briehl Jun. 1981 95 p
refs

(NASA-TM-81661; E-679) Avail NTIS HC A05/MF A01 CSCL
138

This is the twelfth of a series of reports which describes the data currently available from GASP, including flight routes and dates, instrumentation, data processing procedures, and data tape specifications. In-situ measurements of atmospheric ozone, cabin ozone, carbon monoxide, water vapor, particles, clouds, condensation nuclei, filter samples and related meteorological and flight information obtained during 1732 flights of aircraft N533PA, N4711U, N655PA, and VH-EBE from January 5, 1978 through October 9, 1978 are reported. These data are now available from the National Climatic Center, Asheville, NC, 22801. In addition to the GASP data, tropopause pressures obtained from time and space interpolation of National Meteorological Center archived data for the dates of the flights are included.

Author

46 GEOPHYSICS

Includes aeronomy; upper and lower atmosphere studies; ionospheric and magnetospheric physics; and geomagnetism.

For space radiation see 93 *Space Radiation*.

N81-13568* National Aeronautics and Space Administration, Lewis Research Center, Cleveland, Ohio.

TABULATIONS OF AMBIENT OZONE DATA OBTAINED BY GASP AIRLINERS, MARCH 1975 TO DECEMBER 1977

Gregory D. Nastrom (Control Data Corp., Minneapolis) and James D. Holdeman Sep. 1980 111 p refs
(Contract DOT-FA78WAI-893)

(NASA-TM-81528, E-481, FAA-EE-43)

Avail: NTIS

MC A06/MF A01 CSCL 04A

Tabulations are given of GASP ambient ozone mean, standard deviation, median, 84th percentile, and 98th percentile values, by season, flight level, and geographical region. In addition, selected empirical probability variations are highlighted to illustrate the types of curves which might be appropriate in specific analyses of the tabulated data, and an example-case calculation is presented to illustrate how the tables can be used to estimate the frequency of commercial airline flights encountering high cabin ozone levels.

Author

47 METEOROLOGY AND CLIMATOLOGY

Includes weather forecasting and modification

N81-14559* National Aeronautics and Space Administration, Lewis Research Center, Cleveland, Ohio.

ICING INSTRUMENTATION

William Olsen. In NASA. Marshall Space Flight Center. Proc. Fourth Ann. Workshop on Meteorol. and Environ. Inputs to Aviation Systems. Mar. 1980. p 49-60. refs (For primary document see N81-14555 05-47)

Avail. NTIS HC A13/MF A01 CSCL 048

The types and usage categories of icing instrumentation are discussed. The state-of-the-art for the technology governing the use of icing instrumentation is reported with particular emphasis on ground based facilities for icing tests. R.C.T.

N81-21686* National Aeronautics and Space Administration, Lewis Research Center, Cleveland, Ohio.

ANALYSIS OF ATMOSPHERIC OZONE LEVELS AT COMMERCIAL AIRPLANE CRUISE ALTITUDES IN WINTER AND SPRING, 1976 - 1977

James D. Holdeman and Gregory D. Nastrom (Control Data Corp., Minneapolis) Apr. 1981. 18 p. refs (Contract DOT-FA78WAI-893)

(NASA-TP-1807; FAA-EF-81-1; E-468) Avail. NTIS HC A02/MF A01 CSCL 048

It was speculated that the ozone sickness experienced by some airline passengers and crew members during the winter and spring of 1976-77 were induced by abnormally high concentrations of ambient atmospheric ozone. To investigate the possibility that 1976-77 was anomalous, ozone measurements from balloons for up to 13 years and from Global Atmospheric Sampling Program (GASP) equipped aircraft for 3 years were studied. The analyses presented show that the winter and spring seasons of 1976-77 were averaged statistically, and no evidence was found to suggest that there was more than a usual variation in the frequency that commercial airplanes encountered high ambient ozone concentrations. Author

A81-20742 * Cloud encounter and particle density variabilities from GASP data. G. D. Nastrom (Control Data Corp., Minneapolis, Minn.), J. D. Holdeman (NASA, Lewis Research Center, Cleveland, Ohio), and R. E. Davis (NASA, Langley Research Center, Hampton, Va.). *American Institute of Aeronautics and Astronautics, Aerospace Sciences Meeting, 19th, St. Louis, Mo., Jan. 12-15, 1981, Paper 81-0308*. 7 p. 17 refs.

Summary statistics and variability studies are presented for cloud encounter and particle number density data as part of the NASA Global Atmospheric Sampling Program (GASP) aboard commercial Boeing 747 airliners. On the average, cloud encounter is shown on about 15% of the 52,164 data samples available; this value varies with season, latitude, synoptic weather situation, and distance from the tropopause. The number density of particles (diameter greater than 3 microns) also varies with time and location, and depends on the horizontal extent of cloudiness. (Author)

A81-20810 * An analytical approach to airfoil icing. M. B. Bragg, G. M. Gregorek (Ohio State University, Columbus, Ohio), and R. J. Shaw (NASA, Lewis Research Center, Cleveland, Ohio). *American Institute of Aeronautics and Astronautics, Aerospace Sciences Meeting, 19th, St. Louis, Mo., Jan. 12-15, 1981, Paper 81-0403*. 18 p. 26 refs. Grant No. NAG3-28.

An analytical procedure has been developed to predict rime ice growth on unprotected airfoil sections and to evaluate the aerodynamic performance. A time stepping method is used in which: (1) water droplet trajectories are calculated, (2) a rime ice shape determined, (3) the flowfield around the iced airfoil is recalculated, and (4) the build-up process iterated upon until the desired icing

time is reached. The performance of the iced airfoil shapes are then determined from existing analytic methods. Rime ice shapes determined in the NASA Lewis Icing Research Tunnel on a modified NACA 64 series airfoil agree well with the shapes predicted by the analytical method. Measured and predicted increases in drag due to the rime ice also agree favorably. A simplified scaling analysis is also presented and verified which provides the duplication of full scale results of rime ice accretions in small scale model tests. (Author)

52 AEROSPACE MEDICINE

Includes physiological factors, biological effects of radiation, and weightlessness.

N81-27786* National Aeronautics and Space Administration, Lewis Research Center, Cleveland, Ohio

ION BEAM SPUTTER-ETCHED VENTRICULAR CATHETER FOR HYDROCEPHALUS SHUNT Patent Application

Bruc Banks, inventor (to NASA) Filed 10 Jun 1981 11 p (NASA Case-LEW-13107-1; US Patent Appl-SN-272407) Avail. NTIS HC A02/MF A01 CSCL 06B

A cerebrospinal fluid shunt in the form of a ventricular catheter for controlling the condition of hydrocephalus by relieving the excessive cerebrospinal fluid pressure is described. A method for fabrication of the catheter and shunting the cerebral fluid from the cerebral ventricles to other areas of the body is also considered. Shunt flow failure occurs if the ventricle collapses due to improper valve function causing overdrainage. The ventricular catheter comprises a multiplicity of inlet microtubules. Each microtubule has both a large opening at its inlet end and a multiplicity of microscopic openings along its lateral surfaces. The microtubules are perforated by an ion beam sputter etch technique. The holes are etched in microtubule by directing an ion beam through an electro formed metal mesh mask producing perforations NASA

59 MATHEMATICAL AND COMPUTER SCIENCES (GENERAL)

NS1-29782* National Aeronautics and Space Administration,
Lewis Research Center, Cleveland, Ohio.

APPLICATION OF COMPUTER GENERATED COLOR GRAPHIC TECHNIQUES TO THE PROCESSING AND DISPLAY OF THREE DIMENSIONAL FLUID DYNAMIC DATA

Bernhard H. Anderson, C. W. Putt, and C. C. Giamati 1981
15 p refs Presented at Winter Ann. Meeting of the AM. Soc.
of Mech. Engr., Washington, D.C., 15-20 Nov. 1981
(NASA-TM-82658; E-926) Avail: NTIS HC A02/MF A01 CSCL
20D

Color coding techniques used in the processing of remote
sensing imagery were adapted and applied to the fluid dynamics
problems associated with turbofan mixer nozzles. The computer
generated color graphics were found to be useful in reconstructing
the measured flow field from low resolution experimental data
to give more physical meaning to this information and in scanning
and interpreting the large volume of computer generated data
from the three dimensional viscous computer code used in the
analysis.

M.G.

61 COMPUTER PROGRAMMING AND SOFTWARE

Includes computer programs, routines, and algorithms.

NS1-28888* National Aeronautics and Space Administration,
Lewis Research Center, Cleveland, Ohio.

KONFIG AND REKONFIG: TWO INTERACTIVE PREPROCESSING TO THE NAVY/NASA ENGINE PROGRAM (NNEP)

Lawrence H. Fishbein May 1981 59 p
(NASA-TM-82633; E-889) Avail: NTIS HC A04/MF A01 CSCL
09B

The NNEP is a computer program that is currently being used to simulate the thermodynamic cycle performance of almost all types of turbine engines by many government, industry, and university personnel. The NNEP uses arrays of input data to set up the engine simulation and component matching method as well as to describe the characteristics of the components. A preprocessing program (KONFIG) is described in which the user at a terminal on a time shared computer can interactively prepare the arrays of data required. It is intended to make it easier for the occasional or new user to operate NNEP. Another preprocessing program (REKONFIG) in which the user can modify the component specifications of a previously configured NNEP dataset is also described. It is intended to aid in preparing data for parametric studies and/or studies of similar engines such as mixed flow turbofans, turboshafts, etc.

E.D.K.

NS1-33838* National Aeronautics and Space Administration,
Lewis Research Center, Cleveland, Ohio.

COMPUTER PROGRAM FOR PULSED THERMOCOUPLES WITH CORRECTIONS FOR RADIATION EFFECTS

Herbert A. Will Sep. 1981 42 p refs
(NASA-TP-1895; E-615) Avail: NTIS HC A03/MF A01 CSCL
09B

A pulsed thermocouple was used for measuring gas temperatures above the melting point of common thermocouples. This was done by allowing the thermocouple to heat until it approaches its melting point and then turning on the protective cooling gas. This method required a computer to extrapolate the thermocouple data to the higher gas temperatures. A method that includes the effect of radiation in the extrapolation is described. Computations of gas temperature are provided, along with the estimate of the final thermocouple wire temperature. Results from tests on high temperature combustor research rigs are presented.

R.C.T.

62 COMPUTER SYSTEMS

Includes computer networks.

NS1-21803* # National Aeronautics and Space Administration. Lewis Research Center, Cleveland, Ohio.

AN APPROACH TO REAL-TIME SIMULATION USING PARALLEL PROCESSING

Richard A. Blech and Dale J. Arpasi 1981 9 p refs Proposed for presentation at the 1981 Summer Computer Simulation Conf., Washington, D.C., 15-17 Jul. 1981; sponsored by ISA and the Soc. for Computer Simulation (NASA-TM-81731; E-787) Avail: NTIS HC A02/MF A01 CSCL 09B

A preliminary simulator design that uses a parallel computer organization to provide accuracy, portability, and low cost is presented. The hardware and software for this prototype simulator are discussed. A detailed discussion of the inter-computer data transfer mechanism is also presented. M.G.

A81-44652* # An approach to real-time simulation using parallel processing. R. A. Blech and D. J. Arpasi (NASA, Lewis Research Center, Cleveland, OH). *Instrument Society of America and Society for Computer Simulation, Summer Computer Simulation Conference, Washington, DC, July 15-17, 1981, Paper. 7 p. 13 refs.*

Current applications of real-time simulations to the development of complex aircraft propulsion system controls have demonstrated the need for accurate, portable, and low-cost simulators. This paper presents a preliminary simulator design that uses a parallel computer organization to provide these features. The hardware and software for this prototype simulator are discussed. A detailed discussion of the inter-computer data transfer mechanism is also presented.

(Author)

64 NUMERICAL ANALYSIS

Includes iteration, difference equations, and numerical approximation

N81-14695* National Aeronautics and Space Administration, Lewis Research Center, Cleveland, Ohio

AN ELECTROSTATIC ANALOG FOR GENERATING CASCADE GRIDS

John Jay Adamczyk / In NASA, Langley Research Center Numerical Grid Generation, 1980 p 129-142 (For primary document see N81-14690 05-64)

Avail: NTIS HC A24/MF A01 CSCL 12A

Accurate and efficient numerical simulation of flows through turbomachinery blade rows depends on the topology of the computational grids. These grids must reflect the periodic nature of turbomachinery blade row geometries and conform to the blade shapes. Three types of grids can be generated that meet these minimal requirements: through-flow grids, O-type grids, and C-type grids. A procedure which can be used to generate all three types of grids is presented. The resulting grids are orthogonal and can be stretched to capture the essential physics of the flow. A discussion is also presented detailing the extension of the generation procedure to three dimensional geometries.

Author

N81-14706* National Aeronautics and Space Administration, Lewis Research Center, Cleveland, Ohio

FAST GENERATION OF BODY CONFORMING GRIDS FOR 3-D

Ojordje Dulikravich / In NASA, Langley Research Center Numerical Grid Generation Tech. 1980 p 241-252 refs (For primary document see N81-14690 05-64)

Avail: NTIS HC A24/MF A01 CSCL 12A

A fast algorithm was developed for accurately generating boundary conforming, three dimensional, consecutively refined, computational grids applicable to arbitrary axial turbomachinery geometry. The method is based on using a single analytic function to generate two dimensional grids on a number of coaxial axisymmetric surfaces positioned between the hub and the shroud. These grids are of the 'O' type and are characterized by quasi-orthogonality, geometric periodicity, and an adequate resolution throughout the flowfield. Due to the built in additional nonorthogonal coordinate stretching and shearing, the grid lines leaving the trailing of the blade end at downstream infinity, thus simplifying the numerical treatment of the three dimensional trailing vortex sheet.

Author

N81-14721* National Aeronautics and Space Administration, Lewis Research Center, Cleveland, Ohio

GENERATION OF C-TYPE CASCADE GRIDS FOR VISCOUS FLOW COMPUTATION

Peter M. Sockol / In NASA, Langley Research Center Numerical Grid Generation Tech. 1980 p 437-448 refs (For primary document see N81-14690 05-64)

Avail: NTIS HC A24/MF A01 CSCL 12A

A rapid procedure for generating C-type cascade grids suitable for viscous flow computations in turbomachinery blade rows is presented. The resulting mesh is periodic from one blade passage to the next, nearly orthogonal, and continuous across the wake downstream of a blade. The procedure employs a pair of conformal mappings that take the exterior of the cascade into the interior of an infinite strip with curved boundaries. The final transformation to a rectangular computational domain is accomplished numerically. The boundary values are obtained from a panel solution of an integral equation and the interior values by a rapid ADI solution of Laplace's equation. Examples of C-type grids are presented for both compressor and turbine blades and the extension of the procedure to three dimensions is briefly outlined.

M.G.

A81-14999* Backward deletion to minimize prediction errors in models from factorial experiments with zero to six center points. A. G. Holms (NASA, Lewis Research Center, Cleveland, Ohio). *American Statistical Association, Annual Meeting, 140th, Houston, Tex., Aug. 11-14, 1980, Paper 61* p. 24 refs.

Population model coefficients were chosen to simulate a saturated 2 to the 4th fixed-effects experiment having an unfavorable distribution of relative values. Using random number studies, deletion strategies were compared that were based on the F-distribution, on an order statistics distribution of Cochran's, and on a combination of the two. The strategies were compared under the criterion of minimizing the maximum prediction error, wherever it occurred, among the two-level factorial points. The strategies were evaluated for each of the conditions of 0, 1, 2, 3, 4, 5, or 6 center points. Three classes of strategies were identified as being appropriate, depending on the extent of the experimenter's prior knowledge. In almost every case the best strategy was found to be unique according to the number of center points. Among the three classes of strategies, a security regret class of strategy was demonstrated as being widely useful in that over a range of coefficients of variation from 4 to 65%, the maximum predictive error was never increased by more than 12% over what it would have been if the best strategy had been used for the particular coefficient of variation. The relative efficiency of the experiment, when using the security regret strategy, was examined as a function of the number of center points, and was found to be best when the design used one center point. (Author)

65 STATISTICS AND PROBABILITY

Includes data sampling and smoothing; Monte Carlo method; and stochastic processes.

N81-10778* National Aeronautics and Space Administration, Lewis Research Center, Cleveland, Ohio.

BACKWARD DELETION TO MINIMIZE PREDICTION ERRORS IN MODELS FROM FACTORIAL EXPERIMENTS WITH ZERO TO SIX CENTER POINTS

Arthur G. Holms. 14 Aug. 1980. 63 p. refs. Presented at the 140th Annual Meeting of the Am. Statist. Assoc., Houston, Texas, 11-14 Aug. 1980.

(NASA-TM-81524; E-475) Avail: NTIS HC A04/MF A01 CSCL 124.

Population model coefficients were chosen to simulate a saturated 2 to the fourth power fixed effects experiment having an unfavorable distribution of relative values. Using random number studies, deletion strategies were compared that were based on the F distribution, on an order statistics distribution of Cochran's, and on a combination of the two. Results of the comparisons and a recommended strategy are given. Author

70 PHYSICS (GENERAL)

For geophysics see 46 *Geophysics*. For astrophysics see 90 *Astrophysics*. For solar physics see 92 *Solar physics*.

N81-12817* National Aeronautics and Space Administration. Lewis Research Center, Cleveland, Ohio.

THEORETICAL MODEL APPLICABLE TO THE EXPERIMENTAL DETERMINATION OF SURFACE ANCHORING ENERGIES OF NEMATIC LIQUID CRYSTALS M.S. Thesis

Edwin G. Wintucky Nov. 1980 34 p refs

(NASA-TM-81628; E-637) Avail: NTIS HC A03/MF A01 CSCL 208

For a cell configuration consisting of a thin nematic layer bounded by two parallel plane surfaces, with opposing surfaces suitably treated to produce dissimilar molecular orientations, the elastic continuum theory for nematic liquid crystals was applied to derive an expression relating surface anchoring energies to elastic constants, director orientations at the substrate surfaces, and cell thickness. A numerical comparison with the elastically isotropic result over a range $K_{sub 3} = 1.5 K_{sub 1}$ to $K_{sub 3} = 10 K_{sub 1}$ showed the effect of elastic anisotropy could be quite significant. Surface anchoring energies calculated for anisotropic of $K_{sub 3} = 2 K_{sub 1}$ and $K_{sub 3} = 10 K_{sub 1}$ were approximately 50% and 500%, respectively, than the isotropic values. Author

71 ACOUSTICS

Includes sound generation, transmission and attenuation.

For noise pollution see 45 Environment Pollution.

N81-10807* National Aeronautics and Space Administration, Lewis Research Center, Cleveland, Ohio.

NEW INTERPRETATIONS OF SHOCK-ASSOCIATED NOISE WITH AND WITHOUT SCREECH

U. vonGlahn 21 Nov. 1980 25 p refs To be presented at the 100th Meeting of the ASA, Los Angeles, 17-21 Nov. 1980 (NASA-TM-81590; E-569) Avail: NTIS HC A02/MF A01 CSCL 20A

Anomalous trends in present convergent nozzle (Mach 1) shock associated noise analyses and predictions, with particular emphasis on the roles of screech and jet temperature, are discussed. Experimentally measured values of shock associated noise are used to reassess data trends, including both frequency and sound pressure level. The data used includes model-scale nozzles, varying in nominal diameter from 5 cm to 13 cm, and full scale engine nozzles up to 48 cm. All data were obtained at static conditions. From this reassessment of the measured data, new empirical methods for the prediction of shock associated noise are developed. Separate procedures are presented for screech free and screech contaminated shock associated noise. In the present approach, shock associated noise spectra are developed from considerations that include the peak sound pressure level and its frequency, the low frequency sound pressure level slope, and the high frequency sound pressure level slope or roll-off; the latter is shown to vary with directivity angle.

Author

N81-11769* National Aeronautics and Space Administration, Lewis Research Center, Cleveland, Ohio. Fluid Mechanics and Acoustics Div.

CORE NOISE MEASUREMENTS FROM A SMALL, GENERAL AVIATION TURBOFAN ENGINE

Meyer Reshotko and Allen Karchmer 21 Nov. 1980 28 p refs Presented at the 100th Meeting of the Acoust. Soc. of Am., Los Angeles, 17-21 Nov. 1980 (NASA-TM-81610; E-607) Avail: NTIS HC A03/MF A01 CSCL 20A

As part of a program to investigate combustor and other core noises, simultaneous measurements of internal fluctuating pressure and far field noise were made with a JT15D turbofan engine. Acoustic waveguide probes, located in the engine at the combustor, at the turbine exit and in the core nozzle wall, were used to measure internal fluctuating pressures. Low frequency acoustic power determined at the core nozzle exit corresponds in level to the far field acoustic power at engine speeds below 65% of maximum, the approach condition. At engine speeds above 65% of maximum, the jet noise dominates in the far field, greatly exceeding that of the core. From coherence measurements, it is shown that the combustor is the dominant source of the low frequency core noise. The results obtained from the JT15D engine were compared with those obtained previously from a YF102 engine, both engines having reverse flow annular combustors and being in the same size class.

Author

N81-11770* National Aeronautics and Space Administration, Lewis Research Center, Cleveland, Ohio.

EFFECT OF A SEMI-ANNULAR THERMAL ACOUSTIC SHIELD ON JET EXHAUST NOISE

J. Goodykoontz 21 Nov. 1980 21 p refs Presented at the 100th Meeting of the Acoust. Soc. of Am., Los Angeles, 17-21 Nov. 1980 (NASA-TM-81615; E-616) Avail: NTIS HC A02/MF A01 CSCL 20A

Reductions in jet exhaust noise obtained by the use of an annular thermal acoustic shield consisting of a high temperature, low velocity gas stream surrounding a high velocity central jet exhaust appear to be limited by multiple reflections. The effect of a semi-annular shield on jet exhaust noise was investigated with the rationale that such a configuration would eliminate or reduce the multiple reflection mechanism. Noise measurements

for a 10 cm conical nozzle with a semi-annular acoustic shield are presented in terms of lossless free field data at various angular locations with respect to the nozzle. Measurements were made on both the shielded and unshielded sides of the nozzle. The results are presented parametrically, showing the effects of various shield and central system velocities and temperatures. Selected results are scaled up to a typical full scale engine size to determine the perceived noise level reductions. A.R.H.

N81-12821* National Aeronautics and Space Administration, Lewis Research Center, Cleveland, Ohio.

ACOUSTIC TRANSMISSION MATRIX OF A VARIABLE AREA DUCT OR NOZZLE CARRYING A COMPRESSIBLE SUBSONIC FLOW

J. H. Miles 1980 39 p refs Presented at the One-Hundredth Meeting of the Acoust. Soc. of Am., Los Angeles, 17-21 Nov. 1980

(NASA-TM-81614; E-613) Avail: NTIS HC A03/MF A01 CSCL 20A

The differential equations governing the propagation of sound in a variable area duct or nozzle carrying a one dimensional subsonic compressible fluid flow are derived and put in state variable form using acoustic pressure and particle velocity as the state variables. The duct or nozzle is divided into a number of regions. The region size is selected so that in each region the Mach number can be assumed constant and the area variation can be approximated by an exponential area variation. Consequently, the state variable equation in each region has constant coefficients. The transmission matrix for each region is obtained by solving the constant coefficient acoustic state variable differential equation. The transmission matrix for the duct or nozzle is the product of the individual transmission matrices of each region. Solutions are presented for several geometries with and without mean flow. J.M.S.

N81-15766* National Aeronautics and Space Administration, Lewis Research Center, Cleveland, Ohio.

ANALYSIS OF PRESSURE SPECTRA MEASUREMENTS IN A DUCTED COMBUSTION SYSTEM Ph.D. Thesis - Toledo Univ.

Jeffrey Hilton Miles Nov. 1980 138 p refs (NASA-TM-81583; E-558) Avail: NTIS HC A07/MF A01 CSCL 20A

Combustion noise propagation in an operating ducted liquid fuel combustion system is studied in relation to the development of combustion noise prediction and suppression techniques. The presence of combustor emissions in the duct is proposed as the primary mechanism producing the attenuation and dispersion of combustion noise propagating in an operating liquid fuel combustion system. First, a complex mathematical model for calculating attenuation and dispersion taking into account mass transfer, heat transfer, and viscosity effects due to the presence of liquid fuel droplets or solid soot particles is discussed. Next, a simpler single parameter model for calculating pressure auto-spectra and cross-spectra which takes into account dispersion and attenuation due to heat transfer between solid soot particles and air is developed. Then, auto-spectra and cross-spectra obtained from internal pressure measurements in a combustion system consisting of a J-47 combustor can, a spool piece, and a long duct are presented. Last, analytical results obtained with the single parameter model are compared with the experimental measurements. The single parameter model results are shown to be in excellent agreement with the measurements. J.M.S.

N81-19875* National Aeronautics and Space Administration, Lewis Research Center, Cleveland, Ohio.

ON THE PROPAGATION OF LONG WAVES IN ACOUSTICALLY TREATED, CURVED DUCTS

W. Rostafinski 1981 21 p refs Proposed for presentation at 101st Meeting of the Acoust. Soc. of Am., Ottawa, 18-22 May 1981

(NASA-TM-81712; E-745) Avail: NTIS HC A02/MF A01 CSCL 20A

A two dimensional study is presented on the behavior of long waves in lined, curved ducts. The analysis includes a

comparison between the propagation in curved and straight lined ducts. A parametric study was conducted over a range of wall admittance and duct wall separation. The complex eigenvalues of the characteristic equation, which in the case of a curved duct are also the angular wavenumbers, were obtained by successive approximations. Author

N81-20831* National Aeronautics and Space Administration. Lewis Research Center, Cleveland, Ohio.

HIGH-FREQUENCY SOUND PROPAGATION IN A SPATIALLY VARYING MEAN FLOW

Y. C. Cho and E. J. Rice 1980 29 p refs Presented at the 100th Meeting of ASA, Los Angeles, 17-21 Nov. 1980 (NASA-TM-81751; E-797) Avail: NTIS HC A03/MF A01 CSCL 20A

An equation for acoustic ray paths in a spatially varying mean flow was examined to determine some of the characteristics of the flow gradient effects on sound propagation. In a potential flow, the acoustic rays are deflected in the direction of increasing mean flow, and the gradient of the mean flow speed is the dominant factor causing the ray deflection. In contrast, in a sheared mean flow, the vorticity is the dominant factor in deflection of the acoustic rays. Author

N81-26844* National Aeronautics and Space Administration. Lewis Research Center, Cleveland, Ohio.

NEW TECHNIQUE FOR THE DIRECT MEASUREMENT OF CORE NOISE FROM AIRCRAFT ENGINES

Eugene A. Krejsa 1981 25 p refs Presented at the 17th Joint Propulsion Conf., Colorado Springs, 27-29 Jul. 1981; cosponsored by the AIAA, SAE, and ASME (NASA-TM-82634; E-859) Avail: NTIS HC A02/MF A01 CSCL 20A

The core noise levels from gas turbine aircraft engines were measured using a technique which requires that fluctuating pressures be measured in the far field and at two locations within the engine core. The cross spectra of these measurements are used to determine the levels of the far-field noise that propagated from the engine vore. The technique makes it possible to measure core noise levels even when other noise sources dominate. The technique was applied to signals measured from an Avco Lycoming YF102 turbofan engine. Core noise levels as a function of frequency and radiation angle were measured and are presented over a range of power settings. A.R.H.

N81-29922* National Aeronautics and Space Administration. Lewis Research Center, Cleveland, Ohio.

COMPARISON OF PREDICTED ENGINE CORE NOISE WITH CURRENT AND PROPOSED AIRCRAFT NOISE CERTIFICATION REQUIREMENTS

Uwe H. vonGlahn and Donald E. Groesbeck 1981 15 p refs Presented at the Seventh Aeroacoustic Conf., Palo Alto, Calif., 5-7 Oct. 1981; sponsored by AIAA (NASA-TM-82659; E-927) Avail: NTIS HC A02/MF A01 CSCL 20A

Predicted engine core noise levels are compared with measured total aircraft noise levels and with current and proposed federal noise certification requirements. Comparisons are made at the FAR-36 measuring stations and include consideration of both full- and cutback-power operation at takeoff. In general, core noise provides a barrier to achieving proposed EPA stage 5 noise levels for all types of aircraft. More specifically, core noise levels will limit further reductions in aircraft noise levels for current widebody commercial aircraft. Author

N81-30806* National Aeronautics and Space Administration. Lewis Research Center, Cleveland, Ohio.

INFLUENCE OF EXIT IMPEDANCE ON FINITE DIFFERENCE SOLUTIONS OF TRANSIENT ACOUSTIC MODE PROPAGATION IN DUCTS

K. J. Baumeister 1981 16 p refs Proposed for presentation at the Winter Ann. Meeting of the ASME, Washington, D.C., 15-20 Nov. 1981

(NASA-TM-82666; E-940) Avail: NTIS HC A02/MF A01 CSCL 20A

The time-dependent governing acoustic-difference equations and boundary conditions are developed and solved for sound propagation in an axisymmetric (cylindrical) hard-wall duct without flow and with spinning acoustic modes. The analysis begins with a harmonic sound source radiating into a quiescent duct. This explicit iteration method then calculates stepwise in real time to obtain the steady solutions of the acoustic field. The transient method did not converge to the steady-state solution for cutoff acoustic duct modes. This has implications as to its use in a variable-area duct, where modes may become cutoff in the small-area portion of the duct. For single cutoff mode propagation the steady-state impedance boundary condition produced acoustic reflections during the initial transient that caused finite instabilities in the numerical calculations. The stability problem is resolved by reformulating the exit boundary condition. Example calculations show good agreement with exact analytical and numerical results for forcing frequencies above, below, and nearly at the cutoff frequency. Author

N81-30808* National Aeronautics and Space Administration. Lewis Research Center, Cleveland, Ohio.

NOTE ON REFLECTION AND TRANSMISSION COEFFICIENTS FOR CONVERGING-DIVERGING DUCTS

Paul A. Durbin Sep. 1981 10 p refs (NASA-TM-82679; E-964) Avail: NTIS HC A02/MF A01 CSCL 20A

Simple formulas for calculating acoustic reflection and transmission coefficients for converging-diverging ducts are derived; they extend the method of Cho and Ingard to arbitrary, slowly varying ducts. These formulas involve two parameters. The first is a function of duct shape and the second is the ratio of the duct radius downstream of the throat to that upstream of the throat to the upstream of the throat. An extension of the method to include mean flow is made for symmetric ducts. M.G.

N81-30807* National Aeronautics and Space Administration. Lewis Research Center, Cleveland, Ohio.

CONDITIONED PRESSURE SPECTRA AND COHERENCE MEASUREMENTS IN THE CORE OF A TURBOFAN ENGINE

Allen Karchmer 1981 10 p refs Presented at 7th Aeroelastic Conf., Palo Alto, Calif., 5-7 Oct. 1981; sponsored by AIAA (NASA-TM-82688; E-970; AIAA-Paper-81-2052) Avail: NTIS HC A02/MF A01 CSCL 20A

Multiple and partial coherence functions and the corresponding conditioned coherent output spectra are computed between fluctuating pressures measured at two locations within the tailpipe of a turbofan engine and far-field acoustic pressure. The results are compared with the ordinary coherent output spectrum as obtained between a single tailpipe pressure measurement and the far-field acoustic pressure. The comparison indicates apparent additional 'coherent output' (i.e., core-noise) beyond that detectable with an ordinary coherent measurement, thus suggesting the tailpipe as a core-noise source region. Further evidence suggests, however, that these differences may be attributed to the presence of transverse acoustic modes in the tailpipe and that the tailpipe is not, in fact, a significant source region. Author

N81-31956* National Aeronautics and Space Administration. Lewis Research Center, Cleveland, Ohio.

EFFECTS OF BLADE-VANE RATIO AND ROTOR-STATOR SPACING OF FAN NOISE WITH FORWARD VELOCITY

Richard P. Woodward and Frederick W. Glaser Aug. 1981 21 p refs Presented at the 7th Aeroacoustic Conf., Palo Alto, Calif., 5-7 Oct. 1981; sponsored by AIAA (NASA-TM-82690; E-971) Avail: NTIS HC A02/MF A01 CSCL 20A

A research fan stage was acoustically tested in an anechoic wind tunnel with a 41 m/sec tunnel flow. Two stator vane numbers giving cut-on and cut-off conditions were tested at three rotor-stator spacings ranging from about 0.5 to 2.0 rotor chords. These two stators were designed for similar aerodynamic

performance. Hot film anemometer turbulence measurements were made at the leading edge of the stator for each spacing. The cut-off criterion strongly controlled the fundamental tone level at all spacings. The trends with spacing of the wake defect upwash component at the stator tip showed good agreement with the corresponding cut-on acoustic tone levels. Author

N81-31957* National Aeronautics and Space Administration, Lewis Research Center, Cleveland, Ohio.
TURBOMACHINERY NOISE STUDIES OF THE AIR-SEARCH QCGAT ENGINE WITH INFLOW CONTROL
 J. G. McArdle, L. Homyak, and D. D. Chruslki 1981 26 p refs Presented at the 7th Aeroacoustic Conf., Palo Alto, Calif., 5-7 Oct. 1981; sponsored by AIAA (NASA-TM-82694; E-977) Avail: NTIS HC A03/MF A01 CSCL 20A

The AirResearch Quiet Clean General Aviation Turbofan engine was tested on an outdoor test stand to compare the acoustic performance of two inflow control devices (ICD's) of similar design, and three inlet lips of different external shape. Only small performance differences were found. Far-field directivity patterns calculated by applicable existing analyses were compared with the measured tone and broadband patterns. For some of these comparisons, tests were made with an ICD to reduce rotor/inflow disturbance interaction noise, or with the acoustic suppression panels in the inlet or bypass duct covered with aluminum tape to determine hard wall acoustic performance. The comparisons showed that the analytical expressions used predict many directivity pattern features and trends, but can deviate in shape from the measured patterns under certain engine operating conditions. Some patterns showed lobes from modes attributable to rotor/engine strut interaction sources. Author

N81-32964* National Aeronautics and Space Administration, Lewis Research Center, Cleveland, Ohio.
AN IMPROVED PREDICTION METHOD FOR NOISE GENERATED BY CONVENTIONAL PROFILE COAXIAL JETS

James R. Stone, Donald E. Groesbeck, and Charles L. Zola 1981 32 p refs Presented at Seventh Aeroacoustics Conf., Palo Alto, Calif., 5-7 Oct. 1981; sponsored by AIAA (NASA-TM-82712; E-994; AIAA-Paper-81-1991) Avail: NTIS HC A03/MF A01 CSCL 20A

A semiempirical model for predicting the noise generated by conventional velocity profile jets exhausting from coaxial nozzles is presented and compared with small scale static and simulated flight data. Improvements to the basic circular jet noise prediction are developed which improve the accuracy, especially at high jet velocity and near the jet axis. R.C.T.

N81-32965* National Aeronautics and Space Administration, Lewis Research Center, Cleveland, Ohio.
A MODEL FOR THE ACOUSTIC IMPEDANCE OF LINEAR SUPPRESSOR MATERIALS BONDED ON PERFORATED PLATE

Edward J. Rice 1981 21 p refs Presented at Seventh Acoustic Conf., Palo Alto, Calif., 5-7 Oct. 1981; sponsored by AIAA (NASA-TM-82716; E-1014; AIAA-81-1999) Avail: NTIS HC A02/MF A01 CSCL 20A

An analytical model is presented which describes the impedance of a linear suppressor material, such as a fine wire screen, bonded to a perforated plate. This type of acoustic lining material has come into use in place of perforated plates because of its nominal linear properties. The model also describes the linear and nonlinear resistance of the screen and of the screen perforated plate composite. The effect of the perforated plate bonded to the screen is derived from basic hydrodynamic principles. Although a fine screen is much more linear and thus less amplitude sensitive than a perforated plate without grazing flow, some nonlinearity will always exist for any screen. The nonlinearity in the screen resistance is shown to depend on the square of the screen wire diameter. When the screen is bonded to a perforated plate, the linear resistance is increased as the inverse of the perforated open area as expected. When the

resistance is considered as a function of approach velocity the screen nonlinear term is increased as the inverse of the square of the perforated open area ratio. R.C.T.

N81-32968* National Aeronautics and Space Administration, Lewis Research Center, Cleveland, Ohio.
ACOUSTIC PERFORMANCE OF INLET SUPPRESSORS ON AN ENGINE GENERATING A SINGLE MODE

L. J. Heidelberg, E. J. Rice, and L. Homyak 1981 24 p refs Presented at the 7th Aeroacoustics Conf., Palo Alto, Calif., 5-7 Oct. 1981; sponsored by AIAA (NASA-TM-82697; E-980; AIAA-Paper-81-1965) Avail: NTIS HC A02/MF A01 CSCL 20A

Three single degree of freedom liners with different open area ratio face sheets were designed for a single spinning mode in order to evaluate an inlet suppressor design method based on mode cutoff ratio. This mode was generated by placing 41 rods in front of the 28 blade fan of a JT15D turbofan engine. At the liner design this near cutoff mode has a theoretical maximum attenuation of nearly 200 dB per L/D. The data show even higher attenuations at the design condition than predicted by the theory for dissipation of a single mode within the liner. This additional attenuation is large for high open area ratios and should be accounted for in the theory. The data show the additional attenuation to be inversely proportional to acoustic resistance. It was thought that the additional attenuation could be caused by reflection and modal scattering at the hard to soft wall interface. A reflection model was developed, and then modified to fit the data. This model was checked against independent (multiple pure tone) data with good agreement. M.G.

N81-33947* National Aeronautics and Space Administration, Lewis Research Center, Cleveland, Ohio.
COMPUTER PROGRAM TO PREDICT AIRCRAFT NOISE LEVELS

Bruce J. Clark Sep. 1981 146 p (NASA-TP-1913; E-733) Avail: NTIS HC A07/MF A01 CSCL 20A

Methods developed at the NASA Lewis Research Center for predicting the noise contributions from various aircraft noise sources were programmed to predict aircraft noise levels either in flight or in ground tests. The noise sources include fan inlet and exhaust, jet, flap (for powered lift), core (combustor), turbine, and airframe. Noise propagation corrections are available for atmospheric attenuation, ground reflections, extra ground attenuation, and shielding. Outputs can include spectra, overall sound pressure level, perceived noise level, tone-weighted perceived noise level, and effective perceived noise level at locations specified by the user. Footprint contour coordinates and approximate footprint areas can also be calculated. Inputs and outputs can be in either System International or U.S. customary units. The subroutines for each noise source and propagation correction are described. A complete listing is given. A.R.H.

A81-21120 * Numerical techniques in linear duct acoustics - A status report. K. J. Baumeister (NASA, Lewis Research Center, Cleveland, Ohio). *American Society of Mechanical Engineers, Winter Annual Meeting, Chicago, Ill., Nov. 16-21, 1980, Paper 80-WA/NC-2*. 16 p. 72 refs. Members, \$2.00; nonmembers, \$4.00.

A review is presented covering both finite difference and finite element analysis of small amplitude (linear) sound propagation in straight and variable area ducts with flow, as might be found in a typical turbojet engine duct, muffler, or industrial ventilation system. Both 'steady' state and transient theories are discussed. Emphasis is placed on the advantages and limitations associated with the various numerical techniques. Examples of practical problems are given for which the numerical techniques have been applied. (Author)

A81-22533 * # Acoustic transmission matrix of a variable area duct or nozzle carrying a compressible subsonic flow. J. H. Miles (NASA, Lewis Research Center, Cleveland, Ohio). *Acoustical Society of America, Meeting, 100th, Los Angeles, Calif., Nov. 17-21, 1980. Paper. 37 p. 30 refs.*

The differential equations governing the propagation of sound in a variable area duct or nozzle carrying a one-dimensional subsonic compressible fluid flow are derived and put in state variable form using acoustic pressure and particle velocity as the state variables. The duct or nozzle is divided into a number of regions. The region size is selected so that in each region the Mach number can be assumed constant and the area variation can be approximated by an exponential area variation. Consequently, the state variable equation in each region has constant coefficients. The transmission matrix for each region is obtained by solving the constant coefficient acoustic state variable differential equation. The transmission matrix for the duct or nozzle is the product of the individual transmission matrices of each region. Solutions are presented for several geometries with and without mean flow. (Author)

A81-38060 * # On the propagation of long waves in acoustically treated, curved ducts. W. Rostafinski (NASA, Lewis Research Center, Cleveland, OH). *Acoustical Society of America, Meeting, 101st, Ottawa, Canada, May 18-22, 1981, Paper. 19 p. 7 refs.*

A two-dimensional, detailed study is presented on the behavior of long waves in lined, curved ducts. The analysis includes a comparison between the propagation in curved and straight lined ducts. A parametric study was conducted over a range of wall admittance and duct wall separation. The complex eigenvalues of the characteristic equation, which in the case of a curved duct are also the angular wavenumbers, have been obtained by successive approximations. (Author)

A81-38061 * # A theoretical approach to sound propagation and radiation for ducts with suppressors. E. J. Rice (NASA, Lewis Research Center, Cleveland, OH) and D. T. Sawdy (Boeing Military Airplane Co., Wichita, KS). *Acoustical Society of America, Meeting, 101st, Ottawa, Canada, May 18-22, 1981, Paper. 42 p. 50 refs.*

The several phenomena involved in theoretical prediction of the far-field sound radiation attenuation from an acoustically lined duct have been studied. These include absorption by the suppressor, termination reflection, and far-field radiation. Extensive parametric studies have shown that the suppressor absorption performance can be correlated with mode cut-off ratio or angle of propagation. The other phenomena can be shown to depend explicitly upon mode cut-off ratio. A complete system can thus be generated which can be used to evaluate aircraft sound suppressors and which can be related to the sound source through the cut-off ratio-acoustic power distribution. Although the method is most fully developed for inlet suppressors, several aft radiated noise phenomena will also be discussed. This paper summarized this simplified suppressor design and evaluation method, presents the recent improvements in the technique and discusses areas where further refinement is necessary. Noise suppressor data from engine experiments are compared with the theoretical calculations. (Author)

A81-38062 * # Comparison of predicted engine core noise with proposed FAA helicopter noise certification requirements. U. von Glahn and D. Groesbeck (NASA, Lewis Research Center, Cleveland, OH). *Acoustical Society of America, Meeting, 101st, Ottawa, Canada, May 18-22, 1981, Paper. 17 p. 8 refs.*

Calculated engine core noise levels, based on NASA-Lewis prediction procedures, for five representative helicopter engines are compared with measured total helicopter noise levels and proposed FAA helicopter noise certification requirements. Comparisons are made for level flyover and approach procedures. The measured noise levels are generally significantly greater than those predicted for the core noise levels, except for the Sikorsky S-61 and S-64 helicopters. However, the predicted engine core noise levels are generally at or within 3 dB of the proposed FAA noise rules. Consequently,

helicopter engine core noise can be a significant contributor to the overall helicopter noise signature and, at this time, will provide a limiting floor to a further decrease in future noise regulations.

(Author)

A81-40962 * # New technique for the direct measurement of core noise from aircraft engines. E. A. Krejsa (NASA, Lewis Research Center, Fluid Mechanics and Acoustics Div., Cleveland, OH). *AIAA, SAE, and ASME, Joint Propulsion Conference, 17th, Colorado Springs, CO, July 27-29, 1981, AIAA Paper 81-1587. 15 p. 19 refs.*

A new technique is presented for directly measuring the core noise levels from gas turbine aircraft engines. The technique requires that fluctuating pressures be measured in the far-field and at two locations within the engine core. The cross-spectra of these measurements are used to determine the levels of the far-field noise that propagated from the engine core. The technique makes it possible to measure core noise levels even when other noise sources dominate. The technique was applied to signals measured from an AVCO Lycoming YF102 turbofan engine. Core noise levels as a function of frequency and radiation angle were measured and are presented over a range of power settings. (Author)

A81-48622 * # Application of 'steady' state finite element and transient finite difference theory to sound propagation in a variable duct - A comparison with experiment. K. J. Baumeister (NASA, Lewis Research Center, Cleveland, OH), W. Eversman, R. J. Astley (Missouri-Rolla, University, Rolla, MO), and J. W. White (Tennessee, University, Knoxville, TN). *American Institute of Aeronautics and Astronautics, Aeroacoustics Conference, 7th, Palo Alto, CA, Oct. 5-7, 1981, Paper 81-2016. 10 p. 19 refs.*

Experimental data are presented for sound propagation in a simulated infinite hard wall duct with a large change in duct cross sectional area. The data are conveniently tabulated for further use. The 'steady' state finite element theory of Astley and Eversman (1981) and the transient finite difference theory of White (1981) are in good agreement with the data for both the axial and transverse pressure profiles and the axial phase angle. Therefore, numerical finite difference and finite element theories appear to be ideally suited for handling duct propagation problems which encounter large axial gradients in acoustic parameters. The measured energy reflection coefficient agrees with the values from the Astley-Eversman modal coupling model. G.R.

A81-48639 * # Mixer nozzle aeroacoustic characteristics for the energy efficient engine. P. R. Gliebe, G. T. Sandusky (General Electric Co., Aircraft Engine Group, Cincinnati, OH), and R. Chamberlin (NASA, Lewis Research Center, Transport Propulsion Office, Cleveland, OH). *American Institute of Aeronautics and Astronautics, Aeroacoustics Conference, 7th, Palo Alto, CA, Oct. 5-7, 1981, Paper 81-1994. 11 p. NASA-supported research.*

Aeroacoustic tests are conducted on scale model mixer nozzle configurations, a separate flow nozzle, and a baseline conical nozzle in an anechoic chamber free-jet facility to investigate exhaust system designs. Far-field acoustic data and exhaust jet plume aerodynamic data are obtained for various combinations of exhaust jet velocity and simulated flight speed, with corrected microphone data at a constant 12.2 m arc distance, and scaled acoustic data at a sideline distance of 457 m. It is found that jet plume aerodynamic and acoustic characteristics of lobed mixer exhaust systems are similar to those of a conical nozzle operating at the same specific thrust, although differences occur at high frequencies, where the sound pressure level of the mixer nozzle is 1-5 dB higher than that of a conical nozzle. In addition, no direct correlation is found between exit plane turbulence levels and plume development or acoustic characteristics for mixer exhaust configurations. D.L.G.

A81-49913 * High-frequency sound propagation in a spatially varying mean flow. Y. C. Cho and E. J. Rice (NASA, Lewis Research Center, Cleveland, OH). *Acoustical Society of America, Journal*, vol. 70, Sept. 1981, p. 860-865. 14 refs.

An equation for acoustic ray paths in a spatially varying mean flow has been examined to determine some of the characteristics of the flow gradient effects on sound propagation. In a potential flow the acoustic rays are deflected in the direction of increasing mean flow, and the gradient of the mean flow speed is the dominant factor causing the ray deflection. In contrast, in a sheared mean flow, the vorticity is the dominant factor in deflection of the acoustic rays.

(Author)

A81-49741 * A model for the acoustic impedance of linear suppressor materials bonded on perforated plate. E. J. Rice (NASA, Lewis Research Center, Acoustics Section, Cleveland, OH). *American Institute of Aeronautics and Astronautics, Aeroacoustics Conference, 7th, Palo Alto, CA, Oct. 5-7, 1981, Paper 81-1999*. 21 p. 12 refs.

An analytical model is developed for the acoustic impedance of a composite made of a fine screen bonded to a perforated plate, the resistance having been modeled using steady flow theory and data, and including both linear and nonlinear components. The model of the screen resistance alone is derived first, and it is then extended to include a perforated plate bonded to the screen. Quantities such as effective open ratio and pressure recovery are evaluated. Conclusions are presented, including: (1) when the screen is bonded to a perforated plate, the linear resistance increases as the inverse of the perforate open area, (2) the nonlinearity in the screen resistance depends on the square of the screen wire diameter, and (3) when the resistance is considered as a function of approach velocity, the screen nonlinear term increases as the inverse of the square of the perforated plate open area ratio. The general theory can be applied to any screen structure, but final results are limited to a twilled square weave screen. Results can be applied to the study of sound absorbing materials used for lining the walls of aircraft engine duct suppressors.

K.S.

A81-49743 * An improved prediction method for noise generated by conventional profile coaxial jets. J. R. Stone, D. E. Groesbeck, and C. L. Zola (NASA, Lewis Research Center, Cleveland, OH). *American Institute of Aeronautics and Astronautics, Aeroacoustics Conference, 7th, Palo Alto, CA, Oct. 5-7, 1981, Paper 81-1991*. 33 p. 13 refs.

A semi-empirical model for predicting the noise generated by conventional-velocity-profile jets exhausting from coaxial nozzles is presented and compared with small-scale static and simulated flight data. The present method is an updated version of that part of the original NASA Aircraft Noise Prediction (ANOP) Program (1974) relating to coaxial jet noise. That method has been shown to agree reasonably well with model and full-scale experimental data except at high jet velocities in the region near the jet axis. Improvements to the basic circular jet noise prediction have been developed since that time which improve the accuracy, especially at high jet velocity and near the jet axis, and are incorporated into the coaxial jet procedure in this paper. The new procedure is more theoretically based and has also been improved by some empirical adjustments.

(Author)

N81-15769* Pratt and Whitney Aircraft Group. East Hartford, Conn. Commercial Products Div.
IMPROVED METHODS FOR FAN SOUND FIELD DETERMINATION

D. E. Cicon, T. G. Sofrin, and D. C. Mathews Jan 1981 180 p refs

(Contract NAS3-21391)

(NASA-CR-165188 PWA-5635-43)

Avail: NTIS

HC A09/MF A01 CSCL 20A

Several methods for determining acoustic mode structure in aircraft turbofan engines using wall microphone data were studied. A method for reducing data was devised and implemented which makes the definition of discrete coherent sound fields measured in the presence of engine speed fluctuation more accurate. For the analytical methods, algorithms were developed to define the

dominant circumferential modes from full and partial circumferential arrays of microphones. Axial arrays were explored to define mode structure as a function of cutoff ratio, and the use of data taken at several constant speeds was also evaluated in an attempt to reduce instrumentation requirements. Sensitivities of the various methods to microphone density, array size and measurement error were evaluated and results of these studies showed these new methods to be impractical. The data reduction method used to reduce the effects of engine speed variation consisted of an electronic circuit which windowed the data so that signal enhancement could occur only when the speed was within a narrow range.

T.M.

N81-17846* General Electric Co., Cincinnati, Ohio. Aircraft Engine Business Group.

AERODYNAMIC/ACOUSTIC PERFORMANCE OF YJ101/DOUBLE BYPASS VCE WITH COANNULAR PLUG NOZZLE
Final Report

John W. Vdovick, Paul R. Knott, and Jon J. Ebecker Jan. 1981 307 p refs

(Contract NAS3-20582)

(NASA-CR-159869; R80AEG369)

Avail: NTIS

HC A14/MF A01 CSCL 20A

Results of a forward Variable Area Bypass Injector test and a Coannular Nozzle test performed on a YJ101 Double Bypass Variable Cycle Engine are reported. These components are intended for use on a Variable Cycle Engine. The forward Variable Area Bypass Injector test demonstrated the mode shifting capability between single and double bypass operation with less than predicted aerodynamic losses in the bypass duct. The acoustic nozzle test demonstrated that coannular noise suppression was between 4 and 6 PNdB in the aft quadrant. The YJ101 VCE equipped with the forward VABI and the coannular exhaust nozzle performed as predicted with exhaust system aerodynamic losses lower than predicted both in single and double bypass modes. Extensive acoustic data were collected including far field, near field, sound separation/ internal probe measurements as Laser Velocimeter traverses.

Author

A81-28943 * An experimental study of transmission, reflection and scattering of sound in a free jet flight simulation facility and comparison with theory. K. K. Ahuja, H. K. Tanna, and B. J. Tester (Lockheed-Georgia Co., Marietta, Ga.). *Journal of Sound and Vibration*, vol. 75, Mar. 8, 1981, p. 51-85. 10 refs. Contract No. NAS3-20050.

When a free jet (or open jet) is used as a wind tunnel to simulate the effects of flight on model noise sources, it is necessary to calibrate out the effects of the free jet shear layer on the transmitted sound, since the shear layer is absent in the real flight case. In this paper, a theoretical calibration procedure for this purpose is first summarized; following this, the results of an experimental program, designed to test the validity of the various components of the calibration procedure, are described. The experiments are conducted by using a point sound source located at various axial positions within the free jet potential core. By using broadband excitation and cross-correlation methods, the angle changes associated with ray paths across the shear layer are first established. Measurements are then made simultaneously inside and outside the free jet along the proper ray paths to determine the amplitude changes across the shear layer. It is shown that both the angle and amplitude changes can be predicted accurately by theory. It is also found that internal reflection at the shear layer is significant only for large ray angles in the forward quadrant where total internal reflection occurs. Finally, the effects of sound absorption and scattering by the shear layer turbulence are also examined experimentally.

(Author)

72 ATOMIC AND MOLECULAR PHYSICS

Includes atomic structure and molecular spectra.

NS1-22836* National Aeronautics and Space Administration, Lewis Research Center, Cleveland, Ohio.
AN EVALUATION OF A SIMPLIFIED NEAR FIELD NOISE MODEL FOR SUPERSONIC HELICAL TIP SPEED PROPELLERS

James H. Dittmar Mar. 1981 24 p refs
 (NASA-TM-81727; E-768) Avail: NTIS HC A02/MF A01 CSCL 20A

Existing propeller noise models are versatile and complex but require large computational times, therefore a simplified noise model that could be used to obtain quick noise estimates for these propellers was evaluated. This simplified noise model compared favorably with a complex model for a straight blade propeller and for swept propeller blades when the propeller sweep was properly considered. The simplified model can thus be used as an approximation to the complex model. Comparisons of either the complex or simplified noise models with the available noise data are not good for supersonic propeller helical tip speeds. By adjusting various constants in the simplified model, the noise estimates can be brought into the same range as the data at the propeller design point but the variation of the model with helical tip Mach number remains different than the data. A.R.H.

NS1-22837* National Aeronautics and Space Administration, Lewis Research Center, Cleveland, Ohio.
A THEORETICAL APPROACH TO SOUND PROPAGATION AND RADIATION FOR DUCTS WITH SUPPRESSORS

Edward J. Rice and David T. Sawdy (Boeing Military Airplane Co., Wichita, Kas.) 1981 44 p refs Proposed for presentation at the 101st Meeting of the ASA Ottawa, Ontario, 18-22 May 1981
 (NASA-TM-82612; E-863) Avail: NTIS HC A03/MF A01 CSCL 20A

The several phenomena involved in theoretical prediction of the far-field sound radiation attenuation from an acoustically lined duct were studied. These include absorption by the suppressor, termination reflections, and far-field radiation. Extensive parametric studies show that the suppressor absorption performance can be correlated with mode cut-off ratio or angle of propagation. The other phenomena can be shown to depend explicitly upon mode cut-off ratio. A complete system can thus be generated which can be used to evaluate aircraft sound suppressors and which can be related to the sound source through the cut-off ratio-acoustic power distribution. Although the method is most fully developed for inlet suppressors, several aft radiated noise phenomena are also discussed. This simplified suppressor design and evaluation method is summarized, the recent improvements in the technique are presented, and areas where further refinement is necessary are discussed. Noise suppressor data from engine experiments are compared with the theoretical calculations.

A.R.H.

NS1-22838* National Aeronautics and Space Administration, Lewis Research Center, Cleveland, Ohio.
THE PROPELLER TIP VORTEX, A POSSIBLE CONTRIBUTOR TO AIRCRAFT CABIN NOISE

Brent A. Miller, James H. Dittmar, and Robert J. Jeracki Apr. 1981 11 p refs
 (NASA-TM-81788; E-821) Avail: NTIS HC A02/MF A01 CSCL 20A

Although the assumption is generally made that cabin noise levels are governed by the transmission of propeller generated noise through the fuselage sidewall, it was postulated that the propeller wake striking the wing, in particular pressure disturbances generated downstream of the propeller by the action of the propeller tip vortex, could be strong enough to excite the aircraft structure and contribute to the cabin noise level. Tests conducted to measure the strength of the propeller tip vortex support this hypothesis. It was found that the propeller tip vortex can produce a fluctuation pressure on a simulated wing surface in the wake of a propeller that exceeds by more than 15 dB the

maximum direct noise that would strike the fuselage. Wing surface response to propeller tip vortex induced excitations, and the effectiveness of this response in radiating noise to the cabin interior, must be established to assess the full significance of these results. A.R.H.

NS1-22839* National Aeronautics and Space Administration, Lewis Research Center, Cleveland, Ohio.

COMPARISON OF PREDICTED ENGINE CORE NOISE WITH PROPOSED FAA HELICOPTER NOISE CERTIFICATION REQUIREMENTS

U. vonGlahn and D. Grossbeck 1981 19 p refs Presented at the 101st Meeting of the ASA, Ottawa, Ontario, 18-22 May 1981
 (NASA-TM-81739; E-791) Avail: NTIS HC A02/MF A01 CSCL 20A

Calculated engine core noise levels, based on NASA-Lewis prediction procedures, for five representative helicopter engines are compared with measured total helicopter noise levels and proposed FAA helicopter noise certification requirements. Comparisons are made for level flyover and approach procedures. The measured noise levels are generally significantly greater than those predicted for the core noise levels, except for Sikorsky S-61 and S-64 helicopters. However, the predicted engine core noise levels are generally at or within 3 db of the proposed FAA noise rules. Consequently, helicopter engine core noise can be a significant contributor to the overall helicopter noise signature and, at this time, will provide a limiting floor to a further decrease in future noise regulations. Author

NS1-26779* National Aeronautics and Space Administration, Lewis Research Center, Cleveland, Ohio.

THE SELF-CONSISTENT CALCULATION OF PSEUDO-MOLECULE ENERGY LEVELS, CONSTRUCTION OF ENERGY LEVEL CORRELATION DIAGRAMS AND AN AUTOMATED COMPUTATION SYSTEM FOR SCF-X(ALPHA)-SW CALCULATIONS

Herbert Schlosser (Cleveland State Univ.) Mar. 1981 20 p refs
 (NASA-TM-81710; E-740) Avail: NTIS HC A02/MF A01 CSCL 20H

The self consistent calculation of the electronic energy levels of noble gas pseudomolecules formed when a metal surface is bombarded by noble gas ions is discussed along with the construction of energy level correlation diagrams as a function of interatomic spacing. The self consistent field \times alpha scattered wave (SCF-X(alpha)-SW) method is utilized. Preliminary results on the Ne-Mg system are given. An interactive \times alpha programming system, implemented on the LeRC IBM

A81-27031* Electron spectroscopy of the diamond surface. S. V. Pepper (NASA, Lewis Research Center, Cleveland, Ohio). *Applied Physics Letters*, vol. 38, Mar. 1, 1981, p. 344-346. 10 refs.

The diamond surface is studied by ionization loss spectroscopy and Auger electron spectroscopy. For surfaces heated to temperatures not exceeding 900 C, the band gap was found to be devoid of empty states in the absence of electron beam effects. The incident electron beam generates empty states in the band gap and loss of structure in the valence band for these surfaces. A cross section of 1.4×10 to the -19th sq cm was obtained for this effect. For surfaces heated to temperatures exceeding 900 C the spectra were identical to those from surfaces modified by the electron beam. The diamond surface undergoes a thermal conversion in its electronic structure at about 900 C. (Author)

74 OPTICS

includes light phenomena

NS1-16800* National Aeronautics and Space Administration,
Lewis Research Center, Cleveland, Ohio.

HIGH POWER DENSITIES FROM HIGH-TEMPERATURE MATERIALS INTERACTIONS

James F. Morris 1981 22 p refs Presented at 16th Thermophys.
Conf., High Temp. Mater. Session, Palo Alto, Calif., 23-25 Jun.
1981; sponsored by AIAA

(Contract EC-77-A-31-1062)

(NASA-TM-81626; DOE/NASA/1062-7)

Avail: NTIS

HC A02/MF A01 CSCL 201

Thermionic energy converters and metallic-fluid heat pipes
are well suited to serve together synergistically. The two operating
cycles appear as simple and isolated as their material problems
seem forbodingly deceptive and complicated. Simplified equations
verify material properties and interactions as primary influences
on the operational effectiveness of both. Each experiences flow
limitations in thermal emission and vaporization because of
temperature restrictions redounding from thermophysicochemical
stability considerations. Topics discussed include: (1) successful
limitation of alkali-metal corrosion; (2) protection against external
hot corrosive gases; (3) coping with external and internal
vaporization; (4) controlling interfacial reactions and diffusion;
and (5) meeting other thermophysical challenges: expansion
matches and creep.

A.R.H.

75 PLASMA PHYSICS

Includes magnetohydrodynamics and plasma fusion.
For ionospheric plasmas see 46 Geophysics. For space plasmas see 90 Astrophysics.

NS1-19920*# National Aeronautics and Space Administration, Lewis Research Center, Cleveland, Ohio. **THERMIONIC ENERGY CONVERSION (TEC) TOPPING THERMOELECTRICS**

James F. Morris 1981 16 p refs Proposed for presentation at Intern. Conf. on Plasma Sci., Santa Fe, N. Mex., 18-20 May 1981; sponsored by IEEE
(Contract EC-77-A-31-1062)
(NASA-TM-81677; E-702; DOE/NASA/1062-8) Avail: NTIS HC A02/MF A01 CSCL 20I

Performance expectations for thermionic and thermoelectric energy conversion systems are reviewed. It is noted that internal radiation effects diminish thermoelectric figures of merit significantly at 1000 K and substantially at 2000 K; the effective thermal conductivity contribution of intrathermoelectric radiative dissipation increases with the third power of temperature. It is argued that a consideration of thermoelectric power generation with high temperature heat sources should include utilization of thermionic energy conversion (TEC) topping thermoelectrics. However TEC alone or TEC topping more efficient conversion systems like steam or gas turbines, combined cycles, or Stirling engines would be more desirable generally. M.G.

NS1-24926*# National Aeronautics and Space Administration, Lewis Research Center, Cleveland, Ohio. **CONCEPTUAL DESIGN OF THE MHD ENGINEERING TEST FACILITY**

D. J. Bents, R. W. Bercaw, J. A. Burkhart, T. S. Mroz, H. S. Rigo, C. V. Pearson (Argonne National Lab., Ill.), D. K. Warinner (Argonne National Lab., Ill.), A. M. Hatch (MIT, Cambridge), M. Burden (Gilbert Associates, Inc., Reading, Pa.), D. A. Giza (Gilbert Associates, Inc., Reading, Pa.) et al 1981 15 p refs Presented at the 19th Symp. on Eng. Aspects of Magnetohydrodyn., Tullahoma, Tenn., 15-17 Jun. 1981
(Contracts DE-A101-77ET-10769; EF-77-A-01-2674)
(NASA-TM-82621; DOE/NASA/10769-18; E-872) Avail: NTIS HC A02/MF A01 CSCL 20I

The reference conceptual design of the MHD engineering test facility, a prototype 200 MWe coal-fired electric generating plant designed to demonstrate the commercial feasibility of open cycle MHD is summarized. Main elements of the design are identified and explained, and the rationale behind them is reviewed. Major systems and plant facilities are listed and discussed. Construction cost and schedule estimates are included and the engineering issues that should be reexamined are identified. A.R.H.

NS1-24927*# National Aeronautics and Space Administration, Lewis Research Center, Cleveland, Ohio. **A MHD CHANNEL STUDY FOR THE ETF CONCEPTUAL DESIGN**

S. Y. Wang, P. J. Staiger, and J. Marlin Smith 1981 13 p refs Presented at the 19th Symp. on Eng. Aspects of Magnetohydrodyn., Tullahoma, Tenn., 15-17 Jun. 1981
(Contract DE-A101-77ET-10769)
(NASA-TM-81784; DOE/NASA/10769-14; E-827) Avail: NTIS HC A02/MF A01 CSCL 20I

The procedures and computations used to identify an MHD channel for a 540 MW(l) EFT-scale plant are presented. Under the assumed constraints of maximum $E(x)$, $E(y)$, $J(y)$ and Beta; results show the best plant performance is obtained for active length, L is approximately 12 M, whereas in the initial ETF studies, L is approximately 16 M. As MHD channel length is reduced from 16 M, the channel enthalpy extraction falls off, slowly. This tends to reduce the MHD power output; however, the shorter channels result in lower heat losses to the MHD channel cooling water which allows for the incorporation of more low pressure boiler feedwater heaters into the system and an increase in steam plant efficiency. The net result of these changes

is a net increase in the over all MHD/steam plant efficiency. In addition to the sensitivity of various channel parameters, the trade-offs between the level of oxygen enrichment and the electrical stress on the channel are also discussed. A.R.H.

NS1-25808*# National Aeronautics and Space Administration, Lewis Research Center, Cleveland, Ohio.

GOALS OF THERMIONIC PROGRAM FOR SPACE POWER
Robert E. English 1981 11 p refs Presented at the Plasma Sci. Intern. Conf., Santa Fe, N. Mex., 18-20 May 1981; sponsored by IEEE
(NASA-TM-82616; E-868) Avail: NTIS HC A02/MF A01 CSCL 20I

The thermionic and Brayton reactor concepts were compared for application to space power. For a turbine inlet temperature of 15000 K the Brayton powerplant weighted 5 to 40% less than the thermionic concept. The out of core concept separates the thermionic converters from their reactor. Technical risks are diminished by: (1) moving the insulator out of the reactor; (2) allowing a higher thermal flux for the thermionic converters than is required of the reactor fuel; and (3) eliminating fuel swelling's threat against lifetime of the thermionic converters. Overall performance can be improved by including power processing in system optimization for design and technology on more efficient, higher temperature power processors. The thermionic reactors will be larger than those for competitive systems with higher conversion efficiency and lower reactor operating temperatures. It is concluded that although the effect of reactor size on shield weight will be modest for unmanned spacecraft, the penalty in shield weight will be large for manned or man-tended spacecraft. E.A.K.

NS1-30973*# National Aeronautics and Space Administration, Lewis Research Center, Cleveland, Ohio.

A PROGRAM-MANAGEMENT PLAN WITH CRITICAL-PATH DEFINITION FOR COMBUSTION AUGMENTATION WITH THERMIONIC ENERGY CONVERSION (CATEC)

James F. Morris, Owen S. Merrill (DOE, Washington, D.C.), and Harsha K. Reddy (The Aerospace Corp., Los Angeles) 1981 50 p refs Presented at Intern. Conf. on Plasma Sci., Santa Fe, N. Mex., 18-20 May 1981
(Contract EC-77-A-31-1062)
(NASA-TM-82670; E-950; DOE/NASA/1062-0) Avail: NTIS HC A03/MF A01 CSCL 20I

Thermionic energy conversion (TEC) is discussed in recent TEC-topping analyses, overall plant efficiency (OPE) and cost of electricity (COE) improved slightly with current capabilities and substantially with fully matured technologies. Enhanced credibility derives from proven hot-corrosion protection for TEC by silicon-carbide clads in fossil fuel combustion products. Combustion augmentation with TEC (CATEC) affords minimal cost and plant perturbation, but with smaller OPE and COE improvements than more conventional topping applications. Risk minimization as well as comparative simplicity and convenience, favor CATEC for early market penetration. A program-management plan is proposed. Inputs, characteristics, outputs and capabilities are discussed. S.F.

NS1-32026*# National Aeronautics and Space Administration, Lewis Research Center, Cleveland, Ohio.

HIGH B-FIELD, LARGE AREA RATIO MHD DUCT EXPERIMENTS

J. Marlin Smith, Shih-Ying Wang, and J. L. Morgan 1981 14 p refs Presented at the Intern. Conf. on Plasma Sci., Santa Fe, N. Mex. 18-20 May 1981; Sponsored by IEEE
(Contract DE-A101-77ET-10769)
(NASA-TM-82673; E-956; DOE/NASA/10769-10) Avail: NTIS HC A02/MF A01 CSCL 20I

Studies of the effect of area ratio variation on the performance of a supersonic Hall MHD duct were extended up to area ratios of 6.25/1. It is shown that for a given area ratio there is a combustion pressure above which the power generating region of the duct is shock free and the power output increases linearly

with the square of the magnetic field. Below this pressure a shock forms in the duct which moves upstream with increasing magnetic field strength and results in a less rapid rise in power output. Author

A81-44056 * # Goals of thermionic program for space power. R. E. English (NASA, Lewis Research Center, Cleveland, OH). *Institute of Electrical and Electronics Engineers, Plasma Science International Conference, Santa Fe, NM, May 18-20, 1981, Paper.* 9 p. 9 refs.

The considered investigation has the two objectives to assess the feasibility of operating a Brayton power-generating system at 1500 K and to explore the manner in which changing goals for the thermionic program may have resulted in the rise in specific mass that has been observed. Concerning the first objective, it is pointed out that to date no components have been built and evaluated for use in a Brayton space-power system to operate at 1500 K. On the other hand, the principles in design were successfully demonstrated at 1150 K with materials appropriate to that temperature. Long-time creep data for both the tantalum alloy ASTAR-811 C and the molybdenum alloy TZM support the performance predictions made by Harper (1979) with respect to a Brayton system providing a specific mass value of 21 kg/kWe at 1500 K. For the thermionics program, it is recommended to conduct an investigation of the original goals of high emitter temperature (1800-2000 K) and high power density. G.R.

N81-11833* # Wichita State Univ., Kans. Dept. of Mechanical Engineering.

PERFORMANCE PREDICTION OF STRAIGHT TWO DIMENSIONAL DIFFUSERS Final Report

Mahesh S. Greywall Sep. 1980 35 p refs

(Contract NSG-3186; Contract DE-AI01-77ET-10769)

(NASA-CR-165186; DOE/NASA/3186-1; ME-MG80-1) Avail: NTIS HC A03/MF A01 CSCL 201

A method, based on full viscous calculations, is presented to predict performance of straight two dimensional diffusers. The method predicts adequately the experimental pressure recovery data, up to the point of maximum pressure recovery, for small and large inlet boundary layer thicknesses. It is shown that at the point of maximum pressure recovery the streamwise velocity in the very near wall region varies as Z to the 0.22 power, where Z is the distance from the diffuser wall. Author

N81-11834* # Texas Univ., Arlington.

MHD GENERATOR OFF-DESIGN PERFORMANCE AND NO_x CHEMICAL KINETICS ANALYSIS. VOLUME 1: ANALYSIS OF THE OFF-DESIGN PERFORMANCE OF THE ENGINEERING TEST FACILITY ET F MHD GENERATOR FLOW TRAIN Donald R. Wilson and Gloyd A. Simmons Jun. 1980 77 p refs

(Grant NSG-3255)

(NASA-CR-165187; DOE/NASA/3255-1) Avail: NTIS CSCL 201

A computer code for performing parametric design point calculations, and evaluating the off design performance of magnetohydrodynamic generators was developed. Details of the computer codes are presented. An assessment of the effect of preheat, stoichiometry, and oxygen enrichment on the design point electrical performance of the generator, and the NO_x concentration at the exit of the radiant boiler are included. The off design study included variations in mass flow rate and oxygen enrichment. Maximum design point performance was achieved with a combination of high preheat, high stoichiometry, and no oxygen enrichment. The reduction in generator power was found to scale almost quadratically with the mass flow rate reduction. The power increased to a maximum level for off design operation at an oxygen enrichment value of 60 percent, then decreased with further increases in oxygen enrichment. The off design generator would not run at oxygen enrichment levels less than the 50 percent design level and simultaneously match the imposed thermal power input and downstream pressure constraints. S.F.

N81-12138* # Dayton Univ., Ohio.

APPLICATIONS TECHNOLOGY SATELLITE AND COMMUNICATIONS TECHNOLOGY SATELLITE USER EXPERIMENTS FOR 1987-1990 REFERENCE BOOK. VOLUME 4: ABSTRACTS Final Report

Nicholas A. Engler, John F. Nash, and Jerry D. Strange Aug. 1980 677 p refs

(Contract NAS3-21370)

(NASA-CR-165169-Vol-4; UDR-TR-80-102-Vol-4) Avail: NTIS HC A99/MF A01 CSCL 228

The important user experiments conducted during the fourteen year period from 1966 to 1980 are summarized. A description of each of the satellites and a brief summary of each user experiment is presented. A cross index of user experiments sorted by various parameters and a listing of keywords versus experiment number is included. The experiments are grouped by type of service offered: for example, education, health services, and data transmission. A bibliography of reports by accession number and by author is also presented. User viewpoints of the systems are presented. Author

A81-20649 * # The STD/MHD codes - Comparison of analyses

with experiments at AEDC/HPDE, Reynolds Metal Co., and Hercules, Inc. A. A. Vetter, C. D. Maxwell, T. F. Swean, Jr., S. T. Demetriades, D. A. Oliver, and C. D. Bangerter (STD Research Corp., Arcadia, Calif.). *American Institute of Aeronautics and Astronautics, Aerospace Sciences Meeting, 19th, St. Louis, Mo., Jan. 12-15, 1981, Paper 81-0173.* 16 p. 39 refs. Research supported by the Reynolds Metal Co. and U.S. Department of Energy; NSF Grant No. C-727; Contracts No. DEN3-179; No. DEN3-202.

Data from sufficiently well-instrumented, short-duration experiments at AEDC/HPDE, Reynolds Metal Co., and Hercules, Inc., are compared to analyses with multidimensional and time-dependent simulations with the STD/MHD computer codes. These analyses reveal detailed features of major transient events, severe loss mechanisms, and anomalous MHD behavior. In particular, these analyses predicted higher-than-design voltage drops, Hall voltage overshoots, and asymmetric voltage drops before the experimental data were available. The predictions obtained with these analyses are in excellent agreement with the experimental data and the failure predictions are consistent with the experiments. The design of large, high-interaction or advanced MHD experiments will require application of sophisticated, detailed and comprehensive computational procedures in order to account for the critical mechanisms which led to the observed behavior in these experiments. (Author)

A81-20698 * # On the magnetoaerothermal instability. S. T.

Demetriades, D. A. Oliver, T. F. Swean, Jr., and C. D. Maxwell (STD Research Corp., Arcadia, Calif.). *American Institute of Aeronautics and Astronautics, Aerospace Sciences Meeting, 19th, St. Louis, Mo., Jan. 12-15, 1981, Paper 81-0248.* 14 p. 18 refs. Research supported by the Northrop Corp., U.S. Department of the Interior, U.S. Department of Energy, and ERDA; NSF Grant No. C-727; Contracts No. AF-49(638)-1160; No. DEN3-179; No. DEN3-202.

A fundamental instability in MHD channel flow, hitherto unknown or unappreciated, is described. Lorentz force-driven secondary flow cells preferentially couple core temperature gradient modes into the near fields of the anode wall leading to a locally growing Lorentz force which eventually separates the anode boundary layer. The instability is described with both heuristic order-of-magnitude analyses and detailed three-dimensional, turbulent, MHD flow computations. This magnetoaerothermal instability will be manifested in commercial scale MHD generators of moderate MHD interaction parameter. Methods of control and prevention of the magnetoaerothermal instability exist. (Author)

A81-29560 * # Fluid model of plasma outside a hollow cathode neutralizer. D. E. Parks, M. J. Manfell, and I. Katz (Systems, Science and Software, La Jolla, Calif.). *AIAA, Japan Society for Aeronautical and Space Sciences, and DGLR, International Electric Propulsion Conference, 15th, Las Vegas, Nev., Apr. 21-23, 1981, AIAA Paper 81-0739*. 6 p. 12 refs. Contract No. NAS3-21762.

The present study analyzes the capability of a fluid model of electron transport to explain observed properties of the external plasma of a hollow cathode neutralizer used to neutralize beams emerging from ion thrusters. Calculations reported here show that when the effective collision frequency in such a model is near the plasma frequency, the resulting electric potential and electron temperature variations are in qualitative agreement with values measured in the plume mode of the hollow cathode. Both theory and experiment show strong variations of temperature and potential within a few centimeters of the cathode orifice. (Author)

76 SOLID-STATE PHYSICS

includes superconductivity.

For related information, see also 33 *Electronics and Electrical Engineering* and 36 *Lasers and Masers*.

A81-43004 * T-S diagram for gadolinium near the Curie temperature. S. M. Benford and G. V. Brown (NASA, Lewis Research Center, Cleveland, OH) (*American Institute of Physics and Institute of Electrical and Electronics Engineers, Annual Conference on Magnetism and Magnetic Materials, 26th, Dallas, TX, Nov. 11-14, 1980.*) *Journal of Applied Physics*, vol. 52, Mar. 1981, pt. 2, p. 2110-2112. 9 refs.

77 THERMODYNAMICS AND STATISTICAL PHYSICS

Includes quantum mechanics; and Bose and Fermi statistics.

For related information see also 25 *Inorganic and Physical Chemistry* and 34 *Fluid Mechanics and Heat Transfer*.

A81-31375 * **Thermodynamics. II - The extended thermodynamic system.** F. J. Zeleznik (NASA, Lewis Research Center, Cleveland, Ohio). *Journal of Mathematical Physics*, vol. 22, Jan. 1981, p. 161-178. 5 refs.

The algebraic theory of thermodynamics developed in a previous paper is extended to include the algebraic structure that arises from the introduction of a physical body into the theory. The extension is based on very general definitions of both the thermodynamic states of a body and subsystems of that body. The algebraic analysis, which includes bodies in nonuniform states, shows that the set of all thermodynamic states of a body has the same algebraic structure as the set of thermodynamic states and that composite systems are induced by the algebraic structure of thermodynamic states. The analysis also justifies a variational treatment of thermodynamic bodies in uniform as well as nonuniform states. The variational calculation includes all conventional methods of calculation as special cases and helps to illuminate the origin and interpretation of the electrochemical potential. (Author)

82 DOCUMENTATION AND INFORMATION SCIENCE

Includes information storage and retrieval technology,
micrography, and library science.

For computer documentation see 61 *Computer Program-
ming and Software*

N81-17942* National Aeronautics and Space Administration,
Lewis Research Center, Cleveland, Ohio.

BIBLIOGRAPHY OF LEWIS RESEARCH CENTER TECHNICAL PUBLICATIONS ANNOUNCED IN 1979

May 1980 376 p

(NASA-TM-81525; E-9449-4) Avail: NTIS HC A17/MF A01
CSCL 058

This compilation of over 1100 abstracts describes and
indexes the technical reporting that resulted from the scientific
and engineering work performed and managed by the Lewis
Research Center in 1979. All the publications were announced
in the 1979 issues of STAR (Scientific and Technical Aerospace
Reports) and/or IAA (International Aerospace Abstracts). Research
reports, journal articles, conference presentations, patents and
patent applications, and theses are included. Subject, author,
corporate source, contract number, and report number indexes
are provided. A.R.H.

N81-17943* National Aeronautics and Space Administration,
Lewis Research Center, Cleveland, Ohio.

BIBLIOGRAPHY OF LEWIS RESEARCH CENTER TECHNICAL PUBLICATIONS ANNOUNCED IN 1978

May 1979 367 p

(NASA-TM-79182; E-9449-3) Avail: NTIS HC A16/MF A01
CSCL 058

All the publications were announced in the 1978 issues of
STAR (Scientific and Technical Aerospace Reports) and/or IAA
(International Aerospace Abstracts). Included are research reports,
journal articles, conference presentations, patents and patent
applications, and theses. T.M.

N81-29026* National Aeronautics and Space Administration,
Lewis Research Center, Cleveland, Ohio.

BIBLIOGRAPHY OF LEWIS RESEARCH CENTER TECHNICAL PUBLICATIONS ANNOUNCED IN 1980

May 1981 373 p

(NASA-TM-82661; E-9449-5) Avail: NTIS HC A16/MF A01
CSCL 058

This compilation of abstracts describes and indexes over
780 research reports, journal articles, conference presentations,
patents and patent applications, and theses resulting from the
scientific and engineering work performed and managed by the
Lewis Research Center in 1980. All the publications were
announced in Scientific and Technical Aerospace Reports
and/or International Aerospace Abstracts. A.R.H.

N81-21212* Beech Aircraft Corp., Boulder, Colo.

CONCEPTUAL DESIGN OF AN IN-SPACE CRYOGENIC FLUID MANAGEMENT FACILITY, EXECUTIVE SUMMARY

Final Report

G. S. Willen, D. H. Riemer, and D. C. Hustvedt Apr. 1981
36 p refs

(Contract NAS3-22260)

(NASA-CR-165279-Exec-Summ; BAB-ER-14967-Exec-Summ)

Avail: NTIS HC A03/MF A01 CSCL 21H

The conceptual design of a Spacelab experiment to develop
the technology associated with low gravity propellant management
is summarized. The preliminary facility definition, conceptual design
and design analysis, and facility development plan, including
schedule and cost estimates for the facility, are presented. J.D.H.

83 ECONOMICS AND COST ANALYSIS

Includes cost effectiveness studies.

NS1-27976* National Aeronautics and Space Administration,
Lewis Research Center, Cleveland, Ohio.
**HIGHLIGHTS OF NASA/DOE PHOTOVOLTAIC MARKET
ASSESSMENT VISIT TO MOROCCO**
9 Jun. 1981 11 p refs
(NASA-TM-82288) Avail: NTIS HC A02/MF A01 CSC1
05C

A broad range of agricultural, rural development, and other power applications in various regions of Morocco were examined to determine the potential market for photovoltaic products in Moroccan development. The primary focus of the study was the agriculture sector which accounts for approximately 17% of the country's GNP. The country has a clear need for reliable remote power systems, but does not have the financial resources to invest in the relatively high capital cost PV equipment. A modest potential for PV use was identified in nonagricultural rural services, such as refrigerators for rural clinics and rural radio-telephones. The main potential for PV in Morocco in the next five years lies mainly in the telecommunications sector. Applications include rural TV sets, TV repeater stations, microwave relay stations, and railroad, marine, and airline signalling. Market size estimates were derived from development and expansion plans. At an average customer cost for complete installed systems from \$18/Wp to \$30/Wp the total potential market value is estimated in the range of \$6.6 to \$11 million over the 1981-1986 period.

A.R.H.

NS1-32081* National Aeronautics and Space Administration,
Lewis Research Center, Cleveland, Ohio.
**HIGHLIGHTS OF NASA/DOE PHOTOVOLTAICS MARKET
ASSESSMENT VISIT TO COLOMBIA**
[1981] 13 p
(NASA-TM-84011) Avail: NTIS HC A02/MF A01 CSC1
05C

A NASA/DOE sponsored photovoltaic market assessment team composed of representatives of NASA-Lewis Research Center, DHR Inc., and Associates in Rural Development, Inc. recently conducted a month-long study in Colombia (June 28 - July 23). The team contacted government officials and private sector representatives in Bogota and Cali, and visited rural development and agricultural sites in the departments of Cundinamarca, Caldas, Valle, and Chaco to determine the potential market for American photovoltaic products in the Colombia agricultural and rural sectors.

L.F.M.

84 LAW AND POLITICAL SCIENCE

Includes space law; international law; international cooperation; and patent policy.

N81-32087* National Aeronautics and Space Administration, Lewis Research Center, Cleveland, Ohio.

HIGH-POWER BASELINE AND MOTORING TEST RESULTS FOR THE GPU-3 STIRLING ENGINE Final Report

Lanny G Thiede Jun 1981 37 p refs

(Contract DE-AI01-77CS-51040)

(NASA-TM-82646; DOE/NASA-51040-31; E-902) Avail: NTIS

HC A03/MF A01 CSCL 13F

Test results are given for the full power range of the engine with both helium and hydrogen working fluids. Comparisons are made to previous testing using an alternator and resistance load bank to absorb the engine output. Indicated power results are presented as determined by several methods. Motoring tests were run to aid in determining engine mechanical losses. Comparisons are made between the results of motoring and energy-balance methods for finding mechanical losses. T M

N81-11952* Mechanical Technology, Inc., Latham, N. Y. Stirling Engine Systems Div.

AUTOMOTIVE STIRLING ENGINE DEVELOPMENT PROGRAM Quarterly Technical Progress Report, 30 Mar. - 28 Jun. 1980

Merton Allen, ed. Aug. 1980 96 p refs

(Contract DEN3-32; EC-77-A-31-1040)

(NASA-CR-165134; DOE/NASA/0032-80/8;

MTI-80ASE144QT9) Avail: NTIS HC A05/MF A01 CSCL 13F

Progress is reported in the following: the Stirling reference engine system design; components and subsystems; F-40 baseline Stirling engine installation and test; the first automotive engine to be built on the program; computer development activities; and technical assistance to the Government. The overall program philosophy is outlined, and data and results are given. A R H.

N81-11953* AiResearch Mfg. Co., Phoenix, Ariz.

COST/BENEFIT ANALYSIS OF ADVANCED MATERIALS TECHNOLOGY CANDIDATES FOR THE 1980'S, PART 2 Final Report

R. E. Dennis and H. F. Maertins Aug. 1980 106 p refs

(Contract NAS3-20C73)

(NASA-CR-165176; AIRESEARCH-21-3663-PT-2) Avail: NTIS

HC A06/MF A01 CSCL 05A

Cost/benefit analyses to evaluate advanced material technologies projects considered for general aviation and turboprop commuter aircraft through estimated life-cycle costs, direct operating costs, and development costs are discussed. Specifically addressed is the selection of technologies to be evaluated; development of property goals; assessment of candidate technologies on typical engines and aircraft; sensitivity analysis of the changes in property goals on performance and economics; cost, and risk analysis for each technology; and ranking of each technology by relative value. The cost/benefit analysis was applied to a domestic, nonrevenue producing, business-type jet aircraft configured with two TFE731-3 turbofan engines, and to a domestic, nonrevenue producing, business type turboprop aircraft configured with two TPE331-10 turboprop engines. In addition, a cost/benefit analysis was applied to a commercial turboprop aircraft configured with a growth version of the TPE331-10.

M G

85 URBAN TECHNOLOGY AND TRANSPORTATION

Includes applications of space technology to urban problems; technology transfer; technology assessment; and surface and mass transportation.

For related information see 03 Air Transportation and Safety, 16 Space Transportation, and 44 Energy Production and Conversion.

NS1-18933* National Aeronautics and Space Administration, Lewis Research Center, Cleveland, Ohio.

A METHODOLOGY FOR FOSTERING COMMERCIALIZATION OF ELECTRIC AND HYBRID VEHICLE PROPULSION SYSTEMS

Pierre A. Thollot and Norman T. Musial Oct. 1980 14 p refs (Contract EC-77-A-31-1044)

(NASA-TM-81575; E-545; DOE/NASA/1044-10) Avail: NTIS HC A02/MF A01 CSCL 13F

The rationale behind, and a proposed approach for, application of government assistance to accelerate the process of moving a new electric vehicle propulsion system product from technological readiness to profitable marketplace acceptance and utilization are described. Emphasis is on strategy, applicable incentives, and an implementation process. T.M.

NS1-24994* National Aeronautics and Space Administration, Lewis Research Center, Cleveland, Ohio.

SYSTEM SAFETY IN STIRLING ENGINE DEVELOPMENT

H. Bankaitis 1981 29 p refs Presented at the 5th. Intern. Systems Safety Conf., Denver, 26-31 Jul. 1981

(Contract DE-AI01-77CS-51040)

(NASA-TM-82615; DOE/NASA/51040-25; E-867) Avail: NTIS HC A03/MF A01 CSCL 10B

The DOE/NASA Stirling Engine Project Office has required that contractors make safety considerations an integral part of all phases of the Stirling engine development program. As an integral part of each engine design subtask, analyses are evolved to determine possible modes of failure. The accepted system safety analysis techniques (Fault Tree, FMEA, Hazards Analysis, etc.) are applied in various degrees of extent at the system, subsystem and component levels. The primary objectives are to identify critical failure areas, to enable removal of susceptibility to such failures or their effects from the system and to minimize risk. T.M.

NS1-26986* National Aeronautics and Space Administration, Lewis Research Center, Cleveland, Ohio.

EFFECT OF VOLTAGE ON THE COST OF AN ELECTRIC VEHICLE PROPULSION SYSTEM

Richard M. Schuh and Edward F. McBrien 1981 31 p refs

Proposed for presentation at the 91st Natl. Meeting of the Am. Inst. of Chem. Engrs., Detroit, 16-19 Aug. 1981

(Contract DE-AI01-77CS-51044)

(NASA-TM-82592; DOE/NASA/51044-20; E-839)

Avail: NTIS HC A03/MF A01 CSCL 13F

The life cycle cost and the purchase price of simple dc and ac propulsion systems are estimated as a function of battery voltage from 50 to 500 V. The results show a slight preference for a battery pack voltage of approximately 100 V. Three propulsion systems are examined: one has a series motor with a chopper controller, another an induction motor with an inverter controller, and the third a shunt motor using stepped-voltage control below base speed and field control above base speed. Motor power rating is assumed to be 20 kW continuous duty. The cost and the specific energy of a 24 kW-hr battery pack are estimated from 50 to 500 V by a battery manufacturer. The impact of system voltage variation on the efficiency, weight, and cost of the other electrical components is estimated from basic electrical considerations and informal discussions with manufacturers. Author

NS1-13903* Cummins Engine Co., Inc., Columbus, Ind. VEHICLE TESTING OF CUMMINS TURBOCOMPOUND DIESEL ENGINE Final Report

Michael C. Brands, John R. Werner, and John L. Hoehne Jun. 1980 64 p refs

(Contracts EM-78-C-02-4936; EC-77-A-31-1011)

(NASA-CR-159840; DOE/NASA/4936-80/1;

CTR-0746-80002) Avail: NTIS HC A04/MF A01 CSCL 13F

Two turbocompound diesel engines were installed in Class VII heavy-duty vehicles to determine the fuel consumption potential and performance characteristics. One turbocompound powered vehicle was evaluated at the Cummins Pilot Center where driveability, fuel consumption, torsional vibration, and noise were evaluated. Fuel consumption testing showed a 14.8% benefit for the turbocompound engine in comparison to a production NTC-400 used as a baseline. The turbocompound engine also achieved lower noise levels, improved driveability, improved gradeability, and marginally superior engine retardation. The second turbocompound engine was placed in commercial service and accumulated 50,000 miles on a cross-country route without malfunction. Tank mileage revealed a 15.92% improvement over a production NTCC-400 which was operating on the same route. Author

NS1-18935* Mechanical Technology, Inc., Latham, N. Y. ADVANCED PROPULSION SYSTEM CONCEPT FOR HYBRID VEHICLES

Suresh Bhat, Hsin Chen, and George Dochat Dec. 1980 169 p refs

(Contracts DEN3-92; EC-77-A-31-1044)

(NASA-CR-159772; DOE/NASA/0092-80/1; MTI-BOTR25)

Avail: NTIS HC A08/MF A01 CSCL 13F

A series hybrid system, utilizing a free piston Stirling engine with a linear alternator, and a parallel hybrid system, incorporating a kinematic Stirling engine, are analyzed for various specified reference missions/vehicles ranging from a small two passenger commuter vehicle to a van. Parametric studies for each configuration, detail tradeoff studies to determine engine, battery and system definition, short term energy storage evaluation, and detail life cycle cost studies were performed. Results indicate that the selection of a parallel Stirling engine/electric, hybrid propulsion system can significantly reduce petroleum consumption by 70 percent over present conventional vehicles. J.M.S.

NS1-20986* Garrett Corp., Phoenix, Ariz. Turbine Engine Co.

ANALYTICAL DESIGN OF AN ADVANCED RADIAL TURBINE Final Report, 1 Feb. 1979 - 1 Aug. 1980

Gerald D. Large, David G. Finger, and Charles G. Linder Feb. 1981 155 p refs

(Contracts DEN3-106; DE-AI01-77CS-51040)

(NASA-CR-185170; DOE/NASA/0106-1; Rept-31-1853) Avail: NTIS HC A08/MF A01 CSCL 13F

The aerodynamic and mechanical potential of a single stage ceramic radial inflow turbine was evaluated for a high temperature single stage automotive engine. The aerodynamic analysis utilizes a turbine system optimization technique to evaluate both radial and nonradial rotor blading. Selected turbine rotor configurations were evaluated mechanically with three dimensional finite element techniques. Results indicate that exceptionally high rotor tip speeds (2300 ft/sec) and performance potential are feasible with radial bladed rotors if the projected ceramic material properties are realized. Nonradial rotors reduced tip speed requirements (at constant turbine efficiency) but resulted in a lower cumulative probability of success due to higher blade and disk stresses. R.C.T.

NS1-22962* Ford Motor Co., Dearborn, Mich.
**CERAMIC REGENERATOR SYSTEMS DEVELOPMENT
PROGRAM Final Report, 1 Oct. 1976 - 31 Dec. 1979**
C. A. Fucinari, C. J. Rahnke, V. D. N. Rao, and J. K. Vallance
Oct. 1980 264 p refs Sponsored in part by DOE
(DEN3-8)

(NASA-CR-165139; DOE/NASA/0008-12) Avail: NTIS
HC A12/MF A01 CSCL 10B

The DOE/NASA Ceramic Regenerator Design and Reliability Program aims to develop ceramic regenerator cores that can be used in passenger car and industrial/truck gas turbine engines. The major cause of failure of early gas turbine regenerators was found to be chemical attack of the ceramic material. Improved materials and design concepts aimed at reducing or eliminating chemical attack were placed on durability test in Ford 707 industrial gas turbine engines late in 1974. Results of 53,065 hours of turbine engine durability testing are described. Two materials, aluminum silicate and magnesium aluminum silicate, show promise. Five aluminum silicate cores attained the durability objective of 10,000 hours at 800 C (1472 F). Another aluminum silicate core shows minimal evidence of chemical attack after 8071 hours at 982 C (1800 F). Results obtained in ceramic material screening tests, aerothermodynamic performance tests, stress analysis, cost studies, and material specifications are included. S.F.

99 GENERAL

N81-12978* National Aeronautics and Space Administration, Lewis Research Center, Cleveland, Ohio.

IMPACT FOR THE 80'S: PROCEEDINGS OF A CONFERENCE ON SELECTED TECHNOLOGY FOR BUSINESS AND INDUSTRY

Nov. 1980 238 p. Conf. held in Cleveland, 14-15 May 1980 (NASA-CP-2149; E-489) Avail: NTIS HC A11/MF A01 CSCL 05A

Various aspects of advanced energy technology are discussed. Specific emphasis is given to: aircraft propulsion; wind power commercialization; materials and structures; lubrication and bearings; Stirling and gas turbine engines; and electric and hybrid vehicles. For individual titles, see N81-12979 through N81-12991.

N81-12979* National Aeronautics and Space Administration, Lewis Research Center, Cleveland, Ohio.

ENERGY OVERVIEW

Henry O. Slone *In its Impact for the 80's: Proc. of a Conf. on Selected Technol. for Business and Ind.* Nov. 1980 p 1-9 (For primary document see N81-12978 03-99)
Avail: NTIS HC A11/MF A01 CSCL 10A

The experience, capabilities, and facilities being utilized at NASA Lewis in support of energy programs conducted by the Department of Energy and other agencies are discussed. Background information is given regarding NASA's involvement in solving energy problems. R.C.T.

N81-12980* National Aeronautics and Space Administration, Lewis Research Center, Cleveland, Ohio.

NASA RESEARCH IN AEROPROPULSION

Warner L. Stewart *In its Impact for the 80's: Proc. of a Conf. on Selected Technol. for Business and Ind.* Nov. 1980 p 11-26 (For primary document see N81-12978 03-99)
Avail: NTIS HC A11/MF A01 CSCL 21E

The role of the Lewis Research Center in aeronautical propulsion is described. The state of the art in engine systems and components are discussed and some of the problems that confront the civil and military aeronautic sectors are addressed. Some of the programs that are under way are summarized with emphasis on the future needs and opportunities in aeronautics. R.C.T.

N81-12981* National Aeronautics and Space Administration, Lewis Research Center, Cleveland, Ohio.

LARGE WIND TURBINES: A UTILITY OPTION FOR THE GENERATION OF ELECTRICITY

William H. Robbins, Ronald L. Thomas, and Darrell H. Baldwin *In its Impact for the 80's: Proc. of a Conf. on Selected Technol. for Business and Ind.* Nov. 1980 p 27-41 refs. Also presented at the Am. Power Conf., Chicago, 21-23 Apr. 1980 (For primary document see N81-12978 03-99)

Avail: NTIS HC A11/MF A01 CSCL 10B

The economic and technical potential of wind energy in the United States is discussed. Particular attention is given to the status of wind turbine operational experience as well as the environmental posture of the technology. R.C.T.

N81-12982* National Aeronautics and Space Administration, Lewis Research Center, Cleveland, Ohio.

PROGRESS IN MATERIALS AND STRUCTURES AT LEWIS RESEARCH CENTER

Thomas K. Glasgow, Richard W. Lauver, Gary R. Halford, and Robert L. Davies *In its Impact for the 80's: Proc. of a Conf. on Selected Technol. for Business and Ind.* Nov. 1980 p 43-64 refs (For primary document see N81-12978 03-99)

Avail: NTIS HC A11/MF A01 CSCL 11G

The development of power and propulsion system technology is discussed. Specific emphasis is placed on the following: high temperature materials; composite materials; advanced design and life prediction; and nondestructive evaluation. Future areas of research are also discussed. R.C.T.

N81-12983* National Aeronautics and Space Administration, Lewis Research Center, Cleveland, Ohio.

THIN-FILM COATINGS

Donald H. Buckley *In its Impact for the 80's: Proc. of a Conf. on Selected Technol. for Business and Ind.* Nov. 1980 p 65-74 (For primary document see N81-12978 03-99)
Avail: NTIS HC A11/MF A01 CSCL 11F

Thin, adherent, high density films are discussed with respect to their application in two plasma physics techniques (ion plating and sputtering). The operation of each technique is described as well as what surfaces can be coated, and what kind of materials can be applied. The effects of these films on the mechanical properties of solid surfaces are also discussed. R.C.T.

N81-12984* National Aeronautics and Space Administration, Lewis Research Center, Cleveland, Ohio.

SELF-LUBRICATING COMPOSITE MATERIALS

Harold E. Sliney *In its Impact for the 80's: Proc. of a Conf. on Selected Technol. for Business and Ind.* Nov. 1980 p 75-95 (For primary document see N81-12978 03-99)

Avail: NTIS HC A11/MF A01 CSCL 11D

The mechanical properties of two types of self lubricating composites (polymer matrix composites and inorganic composites) are discussed. Specific emphasis is given to the applicability of these composites in the aerospace industry. R.C.T.

N81-12985* National Aeronautics and Space Administration, Lewis Research Center, Cleveland, Ohio.

PROPULSION SYSTEM RESEARCH AND DEVELOPMENT FOR ELECTRIC AND HYBRID VEHICLES

Harvey J. Schwartz *In its Impact for the 80's: Proc. of a Conf. on Selected Technol. for Business and Ind.* Nov. 1980 p 97-103 (For primary document see N81-12978 03-99)

Avail: NTIS HC A11/MF A01 CSCL 13F

An approach to propulsion subsystem technology is presented. Various tests of component reliability are described to aid in the production of better quality vehicles. component characterization work is described to provide engineering data to manufacturers on component performance and on important component propulsion system interactions. R.C.T.

N81-12986* National Aeronautics and Space Administration, Lewis Research Center, Cleveland, Ohio.

THE FEDERAL ELECTRIC AND HYBRID VEHICLE PROGRAM

Harvey J. Schwartz *In its Impact for the 80's: Proc. of a Conf. on Selected Technol. for Business and Ind.* Nov. 1980 p 105-109 (For primary document see N81-12978 03-99)

Avail: NTIS HC A11/MF A01 CSCL 13F

The commercial development and use of electric and hybrid vehicles is discussed with respect to its application as a possible alternative transportation system. A market demonstration is described that seeks to place 10,000 electric hybrid vehicles into public and private sector demonstrations. R.C.T.

N81-12986* National Aeronautics and Space Administration, Lewis Research Center, Cleveland, Ohio.

COAL GASIFIER COGENERATION POWERPLANT PROJECT

Lloyd I. Shure and Harvey S. Bloomfield *In its Impact for the 80's: Proc. of a Conf. on Selected Technol. for Business and Ind. Nov. 1980 p 123-131 (For primary document see N81-12978 03-99)*

Avail: NTIS HC A11/MF A01 CSCL 21D

Industrial cogeneration and utility power systems were analyzed and a conceptual design study was conducted to evaluate the economic feasibility of a coal gasifier power plant for NASA Lewis Research Center. Site location, plant size, and electric power demand were considered in criteria developed for screening and selecting candidates that could use a wide variety of coals, including that from Ohio. A fluidized bed gasifier concept was chosen as the baseline design and key components of the powerplant were technically assessed. No barriers to environmental acceptability are foreseen. If funded, the powerplant will not only meet the needs of the research center, but will reduce the commercial risk for utilities and industries by fully verifying and demonstrating the technology, thus accelerating commercialization.

A.R.H.

N81-12990* National Aeronautics and Space Administration, Lewis Research Center, Cleveland, Ohio.

SOLAR PHOTOVOLTAICS: STAND ALONE APPLICATIONS

James N. Deyo *In its Impact for the 80's: Proc. of a Conf. on Selected Technol. for Business and Ind. Nov. 1980 p 145-156 (For primary document see N81-12978 03-99)*

Avail: NTIS HC A11/MF A01 CSCL 10A

The Lewis Research Center involvement in space photovoltaic research and development and in using photovoltaics for terrestrial applications is described with emphasis on applications in which the normal source of power may be a diesel generator, batteries, or other types of power not connected to a utility grid. Once an application is processed, technology is developed and demonstrated with a user who participates in the cost and furnishes the site. Projects completed related to instruments, communication, refrigeration, and highways, are described as well as warning systems, weather stations, fire lookouts, and village power systems. A commercially available photovoltaic powered electric fence charger is the result of Lewis research and development.

A.R.H.

N81-29063* National Aeronautics and Space Administration, Lewis Research Center, Cleveland, Ohio.

AEROSPACE IN THE FUTURE

John F. McCarthy, Jr. May 1980 34 p Presented at CECON, Cleveland, 20-21 May 1980 (NASA-TM-82664, E-575) Avail: NTIS HC A03/MF A01 CSCL 05A

National research and technology trends are introduced in the environment of accelerating change. NASA and the federal budget are discussed. The U.S. energy dependence on foreign oil, the increasing oil costs, and the U.S. petroleum use by class are presented. The \$10 billion aerospace industry positive contribution to the U.S. balance of trade of 1979 is given as an indicator of the positive contribution of NASA in research to industry. The research work of the NASA Lewis Research Center in the areas of space, aeronautics, and energy is discussed as a team effort of government, the areas of space, aeronautics, and energy is discussed as a team effort of government, industry, universities, and business to maintain U.S. world leadership in advanced technology.

A.R.H.

N81-12987* Jet Propulsion Lab., California Inst. of Tech., Pasadena.

JPL'S ELECTRIC AND HYBRID VEHICLES PROJECT: PROJECT ACTIVITIES AND PRELIMINARY TEST RESULTS

Thomas A. Barber *In NASA, Lewis Research Center Impact for the 80's: Proc. of a Conf. on Selected Technol. for Business and Ind. Nov. 1980 p 111-122 (For primary document see N81-12978 03-99)*

Avail: NTIS HC A11/MF A01 CSCL 13F

Efforts to achieve a 100 mile urban range, to reduce petroleum usage 40% to 70%, and to commercialize battery technology are discussed with emphasis on an all plastic body, four passenger car that is flywheel assisted and battery powered, and on an all metal body, four passenger car with front wheel drive and front motor. For the near term case, a parallel hybrid in which the electric motor and the internal combustion engine may directly power the drive wheels, is preferred to a series design. A five passenger car in which the electric motor and the gasoline engine both feed into the same transmission is discussed. Upgraded demonstration vehicles were tested using advanced lead acid, nickel zinc, nickel iron, and zinc chloride batteries to determine maximum acceleration, constant speed, and battery behavior. The near term batteries demonstrated significant improvement relative to current lead acid batteries. The increase in range was due to improved energy density, and ampere hour capacity, with relatively small weight and volume differences.

A.R.H.

N81-12989* Jet Propulsion Lab., California Inst. of Tech., Pasadena.

THE DOE PHOTOVOLTAICS PROGRAM

Robert R. Ferber *In NASA, Lewis Research Center Impact for the 80's: Proc. of a Conf. on Selected Technol. for Business and Ind. Nov. 1980 p 133-143 Sponsored in part by DOE (For primary document see N81-12978 03-99)*

Avail: NTIS HC A11/MF A01 CSCL 10A

As part of the National Solar Energy program, the U.S. Department of Energy is now engaged in the development of technically feasible, low cost candidate component and system technologies to the point where technical readiness can be demonstrated by 1982. The overall strategy is to pursue parallel options that continue to show promise of meeting the program goals, thus increasing the probability that at least one technology will be successful. Included in technology development are both flat plate solar collectors and concentrator solar collectors, as well as the balance of system components, such as structures, power conditioning, power controls, protection, and storage. Generally, these last items are common to both flat plate and concentrator systems, but otherwise there is considerable disparity in design philosophy, photovoltaic cell requirements, and possible applications between the two systems. Objectives for research activities at NASA Lewis for stand alone applications, and at Sandia Laboratories where intermediate load center applications are addressed, are highlighted as well as college projects directed by Oak Ridge National Laboratory, and international applications managed by the Solar Energy Research Institute. Joint DOD/DOE effects for military applications are also summarized.

A.R.H.

N81-12991* TRW Defense and Space Systems Group, Redondo Beach, Calif.

MATERIALS PROCESSING IN SPACE: FUTURE TECHNOLOGY TRENDS

Neville J. Barter *In NASA, Lewis Research Center Impact for the 80's: Proc. of a Conf. on Selected Technol. for Business and Ind. Nov. 1980 p 159-177 (For primary document see N81-12978 03-99)*

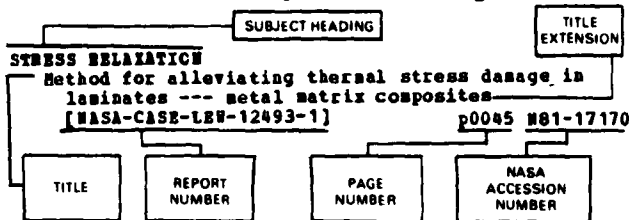
Avail: NTIS HC A11/MF A01 CSCL 22A

NASA's materials processing in space (MPS) program involves both ground and space-based research and looks to frequent and cost effective access to the space environment for necessary progress. The first generation payloads for research are under active design and development. They will be hosted by the Space Shuttle/Spacelab on Earth orbital flights in the early 1980's. These missions will focus on the acquisition of materials behavior research data, the potential enhancement of Earth based technology, and the implementation of space based processing for specialized, high value materials. Some materials to be studied in these payloads may provide future breakthroughs for stronger alloys, ultrapure glasses, superior electronic components, and new or better chemicals. An operational 25 kW power system is expected to be operational to support sustained, systematic space processing activity beyond shuttle capability for second generation payload systems for SPACELAB and free flyer missions to study solidification and crystal growth and to process metal/alloys, glasses/ceramics, and chemicals and biologicals.

A.R.H.

SUBJECT INDEX

Typical Subject Index Listing



The title is used to provide a description of the subject matter. When the title is insufficiently descriptive of the document content, a title extension is added, separated from the title by three hyphens. The STAR or IAA accession number is included in each entry to assist the user in locating the abstract in the abstract section. If applicable a report number is also included as an aid in identifying the document. The page and accession numbers are located beneath and to the right of the title. Under any one subject heading the accession numbers are arranged in sequence with the IAA accession numbers appearing first.

A

ABRASION RESISTANCE

Program to develop sprayed, plastically deformable compressor shroud seal materials [NASA-CR-165237] p0088 N81-17434

ABSORPTION SPECTROSCOPY

Accuracy of trace element determinations in alternate fuels [NASA-TN-81609] p0049 N81-13106

AC (CURRENT)

U ALTERNATING CURRENT

AC GENERATORS

Tests of an overrunning clutch in a wind turbine [NASA-TN-82653] p0107 N81-29528

ACCELERATING AGENTS

Preparation and characterization of electrodes for the NASA Redox storage system [NASA-TN-82702] p0107 N81-30522

ACCELERATION (PHYSICS)

NT ANGULAR ACCELERATION

ACCEPTABILITY

Acceptance tests and manufacturer relationships from the 20A h standard cell data p0100 N81-21515

ACCEPTANCE

U ACCEPTABILITY

ACCIDENT PREVENTION

Lightning accommodation systems for wind turbine generator safety [NASA-TN-82601] p0105 N81-24539

ACCIDENTS

NT BIRD-AIRCRAFT COLLISIONS

ACCRETION

U DEPOSITION

ACCUMULATORS

NT SOLAR COLLECTORS

Performance of computer-designed small-sized four-stage depressed collector for operation of dual-node traveling wave tube [NASA-TP-1832] p0072 N81-30360

ACIDS

NT PHOSPHORIC ACID

ACOUSTIC ATTENUATION

NT SHOCK WAVE ATTENUATION

On the propagation of long waves in acoustically treated, curved ducts p0128 N81-38060

Acoustic transmission matrix of a variable area duct or nozzle carrying a compressible subsonic flow [NASA-TN-81614] p0125 N81-12821

Analysis of pressure spectra measurements in a ducted combustion system [NASA-TN-81583] p0125 N81-15768

ACOUSTIC COMBUSTION

U COMBUSTION STABILITY

ACOUSTIC DUCTS

Numerical techniques in linear duct acoustics - A status report [ASME PAPER 80-WA/NC-2] p0127 N81-21120

Acoustic transmission matrix of a variable area duct or nozzle carrying a compressible subsonic flow p0128 N81-22533

On the propagation of long waves in acoustically treated, curved ducts p0128 N81-38060

A theoretical approach to sound propagation and radiation for ducts with suppressors p0128 N81-38061

Application of 'steady' state finite element and transient finite difference theory to sound propagation in a variable duct - A comparison with experiment [AIAA PAPER 81-2016] p0128 N81-48622

High-frequency sound propagation in a spatially varying mean flow p0129 N81-49913

On the propagation of long waves in acoustically treated, curved ducts [NASA-TN-81712] p0125 N81-19875

A theoretical approach to sound propagation and radiation for ducts with suppressors [NASA-TN-82612] p0130 N81-22837

Influence of exit impedance on finite difference solutions of transient acoustic mode propagation in ducts [NASA-TN-82666] p0126 N81-30905

ACOUSTIC EMISSION

Acousto-ultrasonic characterization of fiber reinforced composites p0090 N81-44660

VCE early acoustic test results of General Electric's high-radius ratio annular plug nozzle p0029 N81-17999

Acousto-ultrasonic characterization of fiber reinforced composites [NASA-TN-82651] p0090 N81-28458

ACOUSTIC IMPEDANCE

A model for the acoustic impedance of linear suppressor materials bonded on perforated plate [AIAA PAPER 81-1999] p0129 N81-49741

Effect of a semi-annular thermal acoustic shield on jet exhaust noise [NASA-TN-81615] p0125 N81-11770

A model for the acoustic impedance of linear suppressor materials bonded on perforated plate --- noise reduction in aircraft engines [NASA-TN-82716] p0127 N81-32965

ACOUSTIC MEASUREMENT

NT NOISE MEASUREMENT

Effects of blade-vane ratio and rotor-stator spacing on fan noise with forward velocity [AIAA PAPER 81-2032] p0024 N81-48628

Improved methods for fan sound field determination [NASA-CR-165188] p0129 N81-15769

Comparison of predicted engine core noise with proposed FAA helicopter noise certification requirements [NASA-TN-81739] p0130 N81-22839

ACOUSTIC NOISES

Acoustic transmission matrix of a variable area duct or nozzle carrying a compressible subsonic flow p0128 N81-22533

ACOUSTIC PROPAGATION

Acoustic transmission matrix of a variable area duct or nozzle carrying a compressible subsonic flow

p0128 A81-22533

The propeller tip vortex. A possible contributor to aircraft cabin noise

[NASA-TN-81768]

p0130 A81-22838

Influence of exit impedance on finite difference solutions of transient acoustic mode propagation in ducts

[NASA-TN-82666]

p0126 A81-30905

Note on reflection and transmission coefficients for converging-diverging ducts

[NASA-TN-82679]

p0126 A81-30906

ACOUSTIC PROPERTIES

NT ACOUSTIC IMPEDANCE

NT ACOUSTIC SCATTERING

NT SOUND INTENSITY

ACOUSTIC RADIATION

U SOUND WAVES

ACOUSTIC SCATTERING

An experimental study of transmission, reflection and scattering of sound in a free jet flight simulation facility and comparison with theory

p0129 A81-28943

ACOUSTIC VIBRATIONS

U SOUND WAVES

ACOUSTICS

NT AEROACOUSTICS

Acousto-ultrasonic characterization of fiber reinforced composites

[NASA-TN-82651]

p0090 A81-28458

Turbomachinery noise studies of the A10 research

QCSAT engine with inflow control

[NASA-TN-82694]

p0127 A81-31957

ACQUISITION

NT DATA ACQUISITION

ACRYLIC RESINS

New ion exchange membranes --- composed of radiation crosslinked polyacrylic resins

[NASA-TN-81670]

p0044 A81-16123

ACTINOMETERS

NT INFRARED SPECTROPHOTOMETERS

ACTIVATION ENERGY

Reduced annealing temperatures in silicon solar cells

[NASA-TN-82597]

p0104 A81-23627

ACTUATOR DISKS

Supersonic stall flutter of high-speed fans

[ASME PAPER 81-GT-184]

p0020 A81-30078

ACTUATORS

Fiber optics for aircraft engine/inlet control

[NASA-TN-82654]

p0012 A81-31190

ADAPTIVE CONTROL

Analysis and design of an adaptive multi-loop controlled two winding buck/boost regulator

[NASA-TN-82679]

p0073 A81-21675

Propulsion Controls, 1979 --- air breathing engine control

[NASA-CP-2137]

p0014 A81-12090

Future Air Force aircraft propulsion control systems: The extended summary paper

[NASA-CP-2137]

p0025 A81-12096

Road map to adaptive optimal control --- jet engine control

[NASA-CP-2137]

p0025 A81-12098

Engine identification for adaptive control

[NASA-CP-2137]

p0025 A81-12100

ADAPTIVE CONTROL SYSTEMS

U ADAPTIVE CONTROL

ADDITION RESINS

NT ACRYLIC RESINS

ADDITIVES

NT OIL ADDITIVES

NT ELASTICIZERS

Effect of CeO₂, MgO and Y₂O₃ additions on the sinterability of a milled Si₃N₄ with 14.5 wt% SiO₂

[NASA-TN-82679]

p0064 A81-28974

The use of Antikoking Kerosene (AKK) in turbojet engines

[NASA-TN-82679]

p0009 A81-19063

Additive for zinc electrodes

[NASA-CASE-LEN-13286-1]

p0105 A81-27557

Effect of Yttria additives on properties of pressureless-sintered silicon nitride

[NASA-TN-82679]

p0063 A81-31366

ADHESION

U ADHESION TESTS

ADHESION

The adhesion, friction, and wear of binary alloys in contact with single-crystal silicon carbide

[ASME PAPER 80-C2/LUB-53]

p0086 A81-18695

Improved refractory coatings --- sputtered coatings on substrates that form stable nitrides

[NASA-CASE-LEN-23169-2]

p0052 A81-16209

Adhesion and friction of transition metals in contact with nonmetallic hard materials

[NASA-TN-82605]

p0055 A81-28233

ADHESION TESTS

Adherence of ion beam sputter deposited metal films on S-13 steel

[NASA-TN-82605]

p0056 A81-14998

Tribological properties of silicon carbide in metal removal process

[NASA-TN-82605]

p0085 A81-17900

The generation and morphology of single-crystal silicon carbide wear particles under adhesive conditions

[NASA-TN-82605]

p0064 A81-35045

The role of the micro environment on the tribological behavior of materials

[NASA-TN-82605]

p0087 A81-46493

ADHESIVE BONDING

Thermal barrier coating system having improved adhesion

[NASA-CASE-LEN-13359-1]

p0062 A81-24265

ADIABATIC CONDITIONS

Analysis for predicting adiabatic wall temperatures with single hole coolant injection into a low speed crossflow

[ASME PAPER 81-GT-91]

p0077 A81-29998

Analysis for predicting adiabatic wall temperatures with single hole coolant injection into a low speed crossflow

[NASA-TN-81620]

p0074 A81-13301

AERIAL RECONNAISSANCE

Tabulations of ambient ozone data obtained by GASP airliners, March 1975 to December 1977

[NASA-TN-81528]

p0116 A81-13568

AEROACOUSTICS

The NASA high-speed turboprop program

[SAB PAPER 801120]

p0021 A81-34156

Mixer nozzle aeroacoustic characteristics for the energy efficient engine

[AIAA PAPER 81-1994]

p0128 A81-48639

Analysis of pressure spectra measurements in a ducted combustion system

[NASA-TN-81583]

p0125 A81-15768

Comparison of NASA and contractor results from aeroacoustic tests of QCSER OTN engine

[NASA-TN-81761]

p0017 A81-25079

New technique for the direct measurement of core noise from aircraft engines --- IF 102 turbofan engine

[NASA-TN-82634]

p0126 A81-26844

Acoustic performance of inlet suppressors on an engine generator; a single mode

[NASA-TN-82697]

p0127 A81-32968

AERODYNAMIC BUZZ

U FLUTTER

AERODYNAMIC CHARACTERISTICS

NT AERODYNAMIC STABILITY

An experimental evaluation of the performance deficit of an aircraft engine starter turbine

[SAB PAPER 801137]

p0021 A81-34168

Factors influencing the predicted performance of advanced propeller designs

[AIAA PAPER 81-1564]

p0007 A81-42210

Low-speed aerodynamic performance of 50.8-centimeter-diameter noise-suppressing inlets for the Quiet, Clean, Short-haul Experimental Engine (QCSER) --- Lewis 9- by 15-foot low speed wind tunnel tests

[NASA-TN-81776]

p0013 A81-11037

Model aerodynamic test results for two variable cycle engine coaxial exhaust systems at simulated takeoff and cruise conditions --- Lewis 8 by 6-foot supersonic wind tunnel tests

[NASA-CR-155818]

p0026 A81-13057

Curved centerline air intake for a gas turbine engine

[NASA-CASE-LEN-13201-1]

p0014 A81-14999

Model aerodynamic test results for two variable cycle engine coaxial exhaust systems at simulated takeoff and cruise conditions. Comprehensive data report. Volume 1: Design layouts

[NASA-CASE-LEN-13201-1]

p0014 A81-14999

- [NASA-CR-159819-VOL-1] p0028 N81-17081
Model aerodynamic test results for two variable
cycle engine coaxial exhaust systems at
simulated takeoff and cruise conditions.
Comprehensive data report. Volume 2: Tabulated
aerodynamic data book 1
- [NASA-CR-159819-VOL-2-BK-1] p0028 N81-17082
Model aerodynamic test results for two variable
cycle engine coaxial exhaust systems at
simulated takeoff and cruise conditions.
Comprehensive data report. Volume 2: Tabulated
aerodynamic data book 2
- [NASA-CR-159819-VOL-2-BK-2] p0028 N81-17083
Model aerodynamic test results for two variable
cycle engine coaxial exhaust systems at
simulated takeoff and cruise conditions.
Comprehensive data report. Volume 2: Tabulated
aerodynamic data book 3
- [NASA-CR-159819-VOL-2-BK-3] p0028 N81-17084
Model aerodynamic test results for two variable
cycle engine coaxial exhaust systems at
simulated takeoff and cruise conditions.
Comprehensive data report. Volume 3: Graphical
data book 1
- [NASA-CR-159819-VOL-3-BK-1] p0028 N81-17085
Model aerodynamic test results for two variable
cycle engine coaxial exhaust systems at
simulated takeoff and cruise conditions.
Comprehensive data report. Volume 3: Graphical
data book 2
- [NASA-CR-159819-VOL-3-BK-2] p0028 N81-17086
Reasons for low aerodynamic performance of
13.5-centimeter-tip-diameter aircraft engine
starter turbine
- [NASA-TP-1810] p0016 N81-20076
- AERODYNAMIC CHORDS**
U AIRFOIL PROFILES
- AERODYNAMIC CONFIGURATIONS**
MASTRAN level 16 user's annual updates for
aeroelastic analysis of bladed discs
[NASA-CR-159824] p0093 N81-19481
Low and high speed propellers for general
aviation: Performance potential and recent wind
tunnel test results
[NASA-TN-81745] p0003 N81-21028
- AERODYNAMIC FORCES**
NT AERODYNAMIC LOADS
Acceleration wave breakup of liquid jets with
airstreams
[NASA-TN-81717] p0075 N81-21310
- AERODYNAMIC LOADS**
Mean rotor wake characteristics of an
aerodynamically loaded 0.5 m diameter fan
[AIAA PAPER 81-0208] p0006 A81-26830
Effect of time-dependent flight loads on turbofan
engine performance deterioration
[ASME PAPER 81-GT-203] p0030 A81-36093
JT9D performance deterioration results from a
simulated aerodynamic load test
[AIAA PAPER 81-1588] p0022 A81-40963
Mean rotor wake characteristics of an
aerodynamically loaded 0.5 m diameter fan
[NASA-TN-81657] p0015 N81-16053
MASTRAN level 16 theoretical annual updates for
aeroelastic analysis of bladed discs
[NASA-CR-159823] p0093 N81-19480
- AERODYNAMIC NOISE**
Mean rotor wake characteristics of an
aerodynamically loaded 0.5 m diameter fan
[AIAA PAPER 81-0208] p0006 A81-26830
An improved prediction method for noise generated
by conventional profile coaxial jets
[AIAA PAPER 81-1991] p0129 A81-49743
Curved centerline air intake for a gas turbine
engine
[NASA-CASE-LEN-13201-1] p0014 N81-14999
- AERODYNAMIC STABILITY**
Stability of large horizontal-axis axisymmetric
wind turbines
[NASA-TN-81623] p0091 N81-12446
Aerodynamic stability analysis of NASA
J85-13/planar pressure pulse generator
installation
[NASA-CR-165141] p0027 N81-15004
TF34 engine compression system computer study ---
simulation of flow stability
[NASA-CR-159889] p0027 N81-15005
- AERODYNAMIC STALLING**
Supersonic stall flutter of high-speed fans
- [ASME PAPER 81-GT-184] p0020 A81-30078
Supersonic stall flutter of high speed fans --- in
turbofan engines
[NASA-TN-81613] p0003 N81-14978
Fluid mechanics mechanisms in the stall process of
helicopters
[NASA-TN-81956] p0003 N81-21027
High-response measurements of a turbofan engine
during nonrecoverable stall
[NASA-TN-81119] p0017 N81-25084
Stall flutter experiment in a transonic
oscillating linear cascade
[NASA-TN-82655] p0004 N81-31126
- AERODYNAMIC VEHICLES**
U AIRCRAFT
AERODYNAMICS
NT AEROTHERMODYNAMICS
NT SCOTCH AERODYNAMICS
Application of unsteady airfoil theory to rotary
wings
p0006 A81-39874
Experimental determination of unsteady blade
element aerodynamics in cascades. Volume 2:
Translation mode cascade
[NASA-CR-165166] p0007 N81-14976
Bibliography of Lewis Research Center Technical
Publications announced in 1979
[NASA-TN-81525] p0137 N81-17942
Measurement of aerodynamic work during fan flutter
[NASA-TN-82652] p0017 N81-25080
Cold-air performance of compressor-drive turbine
of Department of Energy upgraded automobile gas
turbine engine. 1: Volute-manifold and stator
performance
[NASA-TN-82682] p0004 N81-28053
Bibliography of Lewis Research Center technical
publications announced in 1980
[NASA-TN-82661] p0137 N81-29026
- AERONAUTICS**
NT AEROTHERMOELASTICITY
Effects of mistuning on bending-torsion flutter
and response of a cascade in incompressible flow
[AIAA 81-0602] p0092 A81-29465
Application of unsteady airfoil theory to rotary
wings
p0006 A81-39874
Effects of mistuning on bending-torsion flutter
and response of a cascade in incompressible flow
--- turbofan engines
[NASA-TN-81674] p0091 N81-16494
MASTRAN level 16 theoretical annual updates for
aeroelastic analysis of bladed discs
[NASA-CR-159823] p0093 N81-19480
MASTRAN level 16 user's annual updates for
aeroelastic analysis of bladed discs
[NASA-CR-159824] p0093 N81-19481
MASTRAN level 16 programmer's annual updates for
aeroelastic analysis of bladed discs
[NASA-CR-159825] p0093 N81-19482
MASTRAN level 16 demonstration annual updates for
aeroelastic analysis of bladed discs
[NASA-CR-159826] p0093 N81-19483
Aeroelastic characteristics of a cascade of
mistuned blades in subsonic and supersonic flows
--- turbofan engines
[NASA-TN-82631] p0091 N81-26492
Stall flutter experiment in a transonic
oscillating linear cascade
[NASA-TN-82655] p0004 N81-31126
- AERONAUTICS**
U GEOPHYSICS
AERONAUTIC FLUTTER
U FLUTTER
AERONAUTICAL ENGINEERING
NASA Research in aeropropulsion
[NASA-TN-81633] p0014 N81-13056
Bibliography of Lewis Research Center Technical
Publications announced in 1979
[NASA-TN-81525] p0137 N81-17942
Bibliography of Lewis Research Center technical
publications announced in 1980
[NASA-TN-82661] p0137 N81-29026
- AEROSPACE ENGINEERING**
NT AERONAUTICAL ENGINEERING
Bibliography of Lewis Research Center Technical
Publications announced in 1979
[NASA-TN-81525] p0137 N81-17942
Bibliography of Lewis Research Center technical
publications announced in 1980

- [NASA-TN-82661] p0137 N81-29026
Aerospace in the future
[NASA-TN-82664] p0143 N81-29063
AEROSPACE ENVIRONMENTS
Evaluation of solar cell covers and encapsulant materials for space applications p0111 N81-17568
Determination of optimum sunlight concentration level in space for gallium arsenide solar cells [NASA-TN-82643] p0040 N81-26173
AEROSPACE INDUSTRY
NASA's activities in the conservation of strategic aerospace materials p0056 N81-22535
Sputtering and ion plating for aerospace applications p0067 N81-44655
NASA's activities in the conservation of strategic aerospace materials [NASA-TN-81617] p0055 N81-29205
AEROSPACE TECHNOLOGY TRANSFER
Study of thermal management for space platform applications [NASA-CR-165238] p0033 N81-21106
AEROTHERMODYNAMICS
On the magnetoacoustic instability [AIAA PAPER 81-0248] p0133 N81-20658
AEROTHERMOELASTICITY
Aeroelastic and dynamic finite element analyses of a bladder shrouded disk [NASA-CR-159728] p0092 N81-19479
AEROSOL
HT LIQUID FUELS
AGE HARDENING
U PRECIPITATION HARDENING
AGING (MATERIALS)
Ultra-high modulus organic fiber hybrid composites [NASA-CR-165228] p0048 N81-21130
AGRICULTURE
Normal crop calendars. Volume 1: Assembly and application of historical crop data to a standard product [E81-10075] p0095 N81-13431
AGRICULTURE PROJECT
Numerical trials of HISSE [E81-10069] p0094 N81-13425
Normal crop calendars. Volume 2: The spring wheat states of Minnesota, Montana, North Dakota, and South Dakota [E81-10070] p0094 N81-13426
Preliminary evaluation of the Environmental Research Institute of Michigan crop calendar shift algorithm for estimation of spring wheat development stage --- North Dakota, South Dakota, Montana, and Minnesota [E81-10071] p0094 N81-13427
Limited Area Coverage/High Resolution Picture Transmission (LAC/HAPT) tape IX grid pixel extraction processor user's manual [E81-10072] p0094 N81-13428
Limited Area Coverage/High Resolution Picture Transmission (LAC/HAPT) data vegetative index calculation processor user's manual [E81-10073] p0094 N81-13429
EROS to universal tape conversion processor [E81-10074] p0095 N81-13430
Normal crop calendars. Volume 1: Assembly and application of historical crop data to a standard product [E81-10075] p0095 N81-13431
Evaluation of results of US corn and soybeans exploratory experiment: Classification procedures verification test --- Missouri, Iowa, Indiana, and Illinois [E81-10076] p0095 N81-13432
Limited Area Coverage/High Resolution Picture Transmission, LAC/HAPT tape conversion processor user's manual [E81-10077] p0095 N81-13433
AIR BREATHING DEVICES
HT GAS TURBINE ENGINES
HT J-85 ENGINE
HT JET ENGINES
HT TURBOFAN ENGINES
HT TURBOJET ENGINES
HT TURBOPROP ENGINES
The future of aeronautical propulsion p0001 N81-29052
Propulsion Controls, 1979 --- air breathing engine control [NASA-CR-2137] p0014 N81-12090
AIR COOLING
Thermal and flow analysis of a convection air-cooled ceramic coated porous metal concept for turbine vanes [NASA-TN-81749] p0016 N81-22056
AIR DUCTS
Prediction of laminar and turbulent primary and secondary flows in strongly curved ducts [NASA-CR-1388] p0007 N81-16976
AIR FLOW
A rapid method for the approximate determination of nonlinear solutions Application to aerodynamic flows p0007 N81-11628
Fluid mechanics mechanisms in the stall process of helicopters [NASA-TN-81956] p0003 N81-21027
Acceleration wave breakup of liquid jets with airstreams [NASA-TN-81717] p0075 N81-21310
AIR INLETS
U AIR INTAKES
AIR INTAKES
HT ENGINE INLETS
HT SUPERSONIC INLETS
Flow separation in inlets at incidence angles p0006 N81-29114
Curved centerline air intake for a gas turbine engine [NASA-CR-15U-13201-1] p0014 N81-14999
AIR POLLUTION
NASA Global Atmospheric Sampling Program (GASP) data report for tape VLO015, VLO016, VLO017, VLO018, VLO019, and VLO020 [NASA-TN-81661] p0115 N81-30657
AIR QUALITY
NASA Global Atmospheric Sampling Program (GASP) data report for tape VLO015, VLO016, VLO017, VLO018, VLO019, and VLO020 [NASA-TN-81661] p0115 N81-30657
AIR SAMPLING
Tabulations of ambient ozone data obtained by GASP airliners, March 1975 to December 1977 [NASA-TN-81528] p0116 N81-13568
Analysis of atmospheric ozone levels at commercial airplane cruise altitudes in winter and spring, 1976 - 1977 --- Global Atmospheric Sampling Program [NASA-TP-1807] p0117 N81-21685
NASA Global Atmospheric Sampling Program (GASP) data report for tape VLO015, VLO016, VLO017, VLO018, VLO019, and VLO020 [NASA-TN-81661] p0115 N81-30657
AIR TRAFFIC
Aircraft operating efficiency on the North Atlantic, a challenge for the 1980's p0009 N81-19060
AIRBORNE EQUIPMENT
High temperature electronic requirements in aeropropulsion systems p0072 N81-32547
AIRCRAFT
Design concepts for low-cost composite turbofan engine frame [NASA-CR-165217] p0030 N81-22053
GRID30: Computer program for fast generation of multilevel, three-dimensional boundary-conforming O-type computational grids [NASA-TP-1920] p0005 N81-31128
AIRCRAFT ACCIDENTS
HT BIRD-AIRCRAFT COLLISIONS
AIRCRAFT CABINS
U AIRCRAFT COMPARTMENTS
AIRCRAFT COMPARTMENTS
Ozone contamination in aircraft cabins - Results from GASP data and analyses [AIAA PAPER 81-0305] p0010 N81-20740
Analysis of atmospheric ozone levels at commercial airplane cruise altitudes in winter and spring, 1976 - 1977 --- Global Atmospheric Sampling Program [NASA-TP-1807] p0117 N81-21685
The propeller tip vortex. A possible contributor to aircraft cabin noise [NASA-TN-81768] p0130 N81-22838

AIRCRAFT CONSTRUCTION MATERIALS

Feasibility of Kevlar 49/EPR-15 polyimide for high temperature applications p0047 A81-83602

Cost/benefit analysis of advanced materials technology candidates for the 1980's, part 2 [NASA-CN-165176] p0139 A81-11953

Cobalt: A vital element in the aircraft engine industry [NASA-TN-82662] p0055 A81-29206

Conservation of Strategic Aerospace Materials (COSAM) p0019 A81-31208

AIRCRAFT CONTROL

Propulsion controls p0025 A81-12095

Should we attempt global (inlet engine airframe) control design? p0025 A81-12097

AIRCRAFT DESIGN

Optimum subsonic, high-angle-of-attack nacelles p0001 A81-11646

Future challenges in V/STOL flight propulsion control integration [SAR PAPER 801140] p0022 A81-34170

An approach to real-time simulation using parallel processing p0121 A81-44652

Should we attempt global (inlet engine airframe) control design? p0025 A81-12097

AIRCRAFT ENGINES

HT HELICOPTER ENGINES

HT TP-34 ENGINE

HT VARIABLE CYCLE ENGINES

HT VARIABLE STREAM CONTROL ENGINES

Calculated and experimental data for a 118-mm bore roller bearing to 3 silicon DN [ASME PAPER 80-C2/LUB-14] p0085 A81-18668

Core noise measurements from a small, general aviation turbofan engine p0019 A81-22531

The future of aeronautical propulsion p0001 A81-29052

Flow separation in inlets at incidence angles p0006 A81-29114

NASA research in aeropropulsion [ASME PAPER 81-G1-96] p0001 A81-30003

Low NO_x and fuel flexible gas turbine combustors [ASME PAPER 81-G1-99] p0020 A81-30006

Design and development of the combustor inlet diffuser for the NASA/G2 energy efficient engine [ASME PAPER 81-G1-129] p0020 A81-30033

High temperature electronic requirements in aeropropulsion systems p0072 A81-32547

Performance deterioration of commercial high-bypass ratio turbofan engines [SAR PAPER 801118] p0021 A81-34154

Description of the warm core turbine facility and the warm annular cascade facility recently installed at NASA Lewis Research Center [SAR PAPER 801122] p0031 A81-34158

An experimental evaluation of the performance deficit of an aircraft engine starter turbine [SAR PAPER 801137] p0021 A81-34168

Future challenges in V/STOL flight propulsion control integration [SAR PAPER 801140] p0022 A81-34170

Some advantages of methane in an aircraft gas turbine [SAR PAPER 801154] p0022 A81-34177

Selected results from combustion research at the Lewis Research Center [AIAA PAPER 81-1392] p0022 A81-46659

JT9D performance deterioration results from a simulated aerodynamic load test [AIAA PAPER 81-1588] p0022 A81-46963

Turbine bypass engine - A new supersonic cruise propulsion concept [AIAA PAPER 81-1556] p0023 A81-40971

The supersonic fan engine - An advanced concept in supersonic cruise propulsion [AIAA PAPER 81-1599] p0023 A81-46973

Experimental analysis of IHFP in a rotary combustion engine --- Indicated Mean Effective Pressure [SAR PAPER 810150] p0079 A81-41732

The B3 combustors - Status and challenges

[AIAA PAPER 81-1353] p0023 A81-42170

Some aspects of calculating flows about three-dimensional subsonic inlets [AIAA PAPER 81-1361] p0007 A81-42177

An overview of general aviation propulsion research programs at NASA-Lewis Research Center [SAR PAPER 810624] p0023 A81-42778

Mixing effectiveness test of an exhaust gas mixer in a high bypass turbofan at altitude [AIAA PAPER 81-1495] p0023 A81-44225

Turbomachinery noise studies of the Aikenshaw QCAT engine with inflow control --- acoustic performance [AIAA PAPER 81-2049] p0023 A81-48621

Mixer nozzle aeroacoustic characteristics for the energy efficient engine [AIAA PAPER 81-1994] p0128 A81-48639

Comparisons of four alternative powerplant types for future general aviation aircraft [NASA-TN-81584] p0013 A81-10067

Cost/benefit analysis of advanced materials technology candidates for the 1980's, part 2 [NASA-CN-165176] p0139 A81-11953

Propulsion Controls, 1979 --- air breathing engine control [NASA-CP-2137] p0014 A81-12090

Should we attempt global (inlet engine airframe) control design? p0025 A81-12097

Road map to adaptive optimal control --- jet engine control p0025 A81-12098

Propulsion control and control theory: A new research focus p0014 A81-12099

Engine identification for adaptive control p0025 A81-12100

Multivariable synthesis with transfer functions --- applications to gas turbine engines p0026 A81-12102

Advanced Technology Spark-Ignition Aircraft Piston Engine Design Study [NASA-CN-165162] p0026 A81-13963

Analysis of pressure spectra measurements in a ducted combustion system [NASA-TN-81583] p0125 A81-15768

An overview of general aviation propulsion research programs at NASA Lewis Research Center [NASA-TN-81666] p0015 A81-16052

Experimental analysis of IHFP in a rotary combustion engine [NASA-TN-81662] p0015 A81-16054

Propulsion system mathematical model for a lift/cruise fan V/STOL aircraft [NASA-TN-81663] p0015 A81-16055

High temperature electronic requirements in aeropropulsion systems [NASA-TN-81682] p0071 A81-16386

Recent developments in aircraft engine noise reduction technology p0009 A81-19072

General Aviation Turbine Engine (GATE) study [NASA-CN-159482] p0029 A81-19117

Reasons for low aerodynamic performance of 13.5-centimeter-tip-diameter aircraft engine starter turbine [NASA-TN-1810] p0016 A81-20076

Energy efficient engine flight propulsion system: Aircraft/engine integration evaluation [NASA-CN-159584] p0030 A81-22051

Quiet Clean General Aviation Turbofan (QCAT) technology study, volume 1 [NASA-CN-164222] p0030 A81-22052

The B3 combustors: Status and challenges --- energy efficient turbofan engines [NASA-TN-82684] p0018 A81-28095

Cobalt: A vital element in the aircraft engine industry [NASA-TN-82662] p0055 A81-29206

Comparison of predicted engine core noise with current and proposed aircraft noise certification requirements [NASA-TN-82659] p0126 A81-29922

Fiber optics for aircraft engine/inlet control [NASA-TN-82654] p0012 A81-31190

Aircraft Engine Diagnostics [NASA-CP-2190] p0019 A81-31196

Conservation of Strategic Aerospace Materials
(COSAM) p0019 N81-31208

A model for the acoustic impedance of linear
suppressor materials bonded on perforated plate
--- noise reduction in aircraft engines
[NASA-TN-82716] p0127 N81-32965

Acoustic performance of inlet suppressors on an
engine generating a single mode
[NASA-TN-82697] p0127 N81-32968

AIRCRAFT EQUIPMENT

A nonlinear propulsion system simulation technique
for piloted simulators p0022 A81-38064

AIRCRAFT FUELS

NT LIQUID FUELS

Advanced fuel system technology for utilizing
broadened property aircraft fuels p0066 A81-11612

A study of external fuel vaporization --- for
aircraft gas turbine engines
[ASME PAPER 81-GT-158] p0020 A81-30957

Improved components for engine fuel savings
[SAS PAPER 801116] p0021 A81-34152

Some advantages of methane in an aircraft gas
turbine
[SAS PAPER 801154] p0022 A81-34177

Experimental study of the stability of aircraft
fuels at elevated temperatures
[NASA-CR-165165] p0067 N81-12255

Aviation turbine fuel properties and
their trends
[NASA-TN-82603] p0066 N81-25232

AIRCRAFT HAZARDS

Cloud encounter and particle density variabilities
from GASP data
[AIAA PAPER 81-0308] p0117 A81-20742

AIRCRAFT INSTRUMENTS

NT DRAG FORCE ANEMOMETERS

AIRCRAFT NOISE

NT JET AIRCRAFT NOISE

Comparison of predicted engine core noise with
current and proposed aircraft noise
certification requirements
[AIAA PAPER 81-2053] p0024 A81-48635

The propeller tip vortex. A possible contributor
to aircraft cabin noise
[NASA-TN-81768] p0130 N81-22838

AIRCRAFT NOISE PREDICTION

U NOISE PREDICTION (AIRCRAFT)

AIRCRAFT PARTS

Sputtering and ion plating for aerospace
applications
[NASA-TN-81726] p0082 N81-20424

AIRCRAFT PERFORMANCE

Aircraft operating efficiency on the North
Atlantic, a challenge for the 1980's
p0009 N81-19060

AIRCRAFT POWER SOURCES

U AIRCRAFT ENGINES

AIRCRAFT WAKES

NT HELICOPTER WAKES

Mean rotor wake characteristics of an
aerodynamically loaded 0.5 m diameter fan
[NASA-TN-81657] p0015 N81-16053

AIRFOIL CHARACTERISTICS

U AIRFOILS

AIRFOIL PROFILES

Computer-aided roll pass design in rolling of
airfoil shapes p0088 A81-15796

An analytical approach to airfoil icing
[AIAA PAPER 81-0403] p0117 A81-20810

Icing tunnel tests of a glycol-exuding porous
leading edge ice protection system on a general
aviation airfoil
[AIAA PAPER 81-0405] p0011 A81-20837

Secondary layer development on turbine airfoil
suction surfaces
[ASME PAPER 81-GT-204] p0008 A81-30694

Application of unsteady airfoil theory to rotary
wings p0006 A81-39674

Rotor redesign for a highly loaded 1800 ft/sec tip
speed fan, 2
[NASA-CR-159879] p0024 N81-12067

AIRFOIL SECTIONS

U AIRFOIL PROFILES

AIRFOIL THICKNESS

U AIRFOIL PROFILES

AIRFOILS

NT PROPELLER BLADES

NT ROTARY WINGS

NT SUPERSONIC AIRFOILS

NT WINGS

Experimental determination of unsteady blade
element aerodynamics in cascades. Volume 2:
Translation mode cascade
[NASA-CR-165166] p0007 N81-14976

Low and high speed propellers for general
aviation: Performance potential and recent wind
tunnel test results
[NASA-TN-81745] p0003 N81-21028

A rapid perturbation procedure for determining
nonlinear flow solutions: Application to
transonic turbomachinery flows
[NASA-CR-1425] p0001 N81-22012

Shockless design and analysis of transonic blade
shapes
[NASA-TN-82611] p0004 N81-25036

ALCOHOLS

NT GLYCOLS

NT POLYVINYL ALCOHOL

ALDEHYDES

Cross-linked polyvinyl alcohol and method of
making same
[NASA-CASE-LEW-13504-1] p0063 N81-27279

ALPACA

Normal crop calendars. Volume 2: The spring
wheat states of Minnesota, Montana, North
Dakota, and South Dakota
[E81-10070] p0094 N81-13426

ALGEBRA

NT EIGENVALUES

NT LINEAR EQUATIONS

NT NONLINEAR EQUATIONS

Thermodynamics. II - The extended thermodynamic
system p0136 A81-31375

ALGORITHMS

Performance seeking controls p0014 N81-12092

Preliminary evaluation of the Environmental
Research Institute of Michigan crop calendar
shift algorithms for estimation of spring wheat
development stage --- North Dakota, South
Dakota, Montana, and Minnesota
[E81-10071] p0094 N81-13427

Past Generation of body conforming grids for 3-D
p0122 N81-14706

Geometric methods in computational fluid dynamics
--- turbomachinery p0075 N81-18331

ALIPHATIC COMPOUNDS

NT ALKENES

NT GLYCOLS

NT METHANE

NT PROPANE

ALKALI METALS

NT LIQUID SODIUM

NT LITHIUM

Heat pipes containing alkali metal working fluid
[NASA-CASE-LEW-12253-1] p0076 N81-22310

ALKALIES

High temperature alkali corrosion in high velocity
gases
[NASA-TN-82591] p0054 N81-25191

ALKALINE BATTERIES

Control of volume resistivity in inorganic-organic
separators --- for alkaline batteries
p0108 A81-11034

Advanced inorganic separators for alkaline
batteries and method of making same --- a
polymeric coating applied to a porous flexible
substrate
[NASA-CASE-LEW-13171-1] p0100 N81-22466

Inexpensive cross-linked polymeric separators made
from water soluble polymers
[NASA-TN-82619] p0101 N81-23205

Additive for zinc electrodes
[NASA-CASE-LEW-13286-1] p0105 N81-27597

Polyvinyl alcohol battery separator containing
inert filler --- alkaline batteries
[NASA-CASE-LEW-13556-1] p0106 N81-27615

Alkaline battery containing a separator of a
cross-linked copolymer of vinyl alcohol and
unsaturated carboxylic acid
[NASA-CASE-LEW-13102-1] p0107 N81-29531

ORIGINAL PAGE IS
OF POOR QUALITY

- ALKANES
NT METHANE
NT PROPANE
ALKENES
Infrared spectroscopy for the determination of hydrocarbon types in jet fuels
[NASA-TN-82674] p0066 N81-31380
- ALLOYS
NT ALUMINUM ALLOYS
NT BABBITT METAL
NT BINARY ALLOYS
NT CARBON STEELS
NT CAST ALLOYS
NT CHROMIUM ALLOYS
NT COBALT ALLOYS
NT EUTECTIC ALLOYS
NT HEAT RESISTANT ALLOYS
NT HIGH STRENGTH ALLOYS
NT IRON ALLOYS
NT MANGANESE ALLOYS
NT MOLYBDENUM ALLOYS
NT NICKEL ALLOYS
NT QUATERNARY ALLOYS
NT REFRACTORY METAL ALLOYS
NT BENE 41
NT STEELS
NT TERNARY ALLOYS
NT TITANIUM ALLOYS
NT TUNGSTEN ALLOYS
NT VANADIUM ALLOYS
Hostile environmental conditions facing candidate alloys for the automotive Stirling engine
[NASA-TN-82632] p0054 N81-26236
- ALTERNATING CURRENT
Solar cell system having alternating current output
[NASA-CASE-LBN-12806-2] p0096 N81-12542
- ALTERNATING CURRENT GENERATORS
U AC GENERATORS
ALTERNATORS (GENERATORS)
U AC GENERATORS
ALTITUDE SIMULATION
Mixing effectiveness test of an exhaust gas mixer in a high bypass turbofan at altitude
[AIAA PAPER 81-1495] p0023 A81-44225
- ALTITUDE TESTS
P100 multivariable control synthesis program: A review of full scale engine altitude tests --- P100 engine
p0014 N81-12093
- ALUMINA
U ALUMINUM OXIDES
ALUMINUM
Integrated RC-circuits in ALTA-technology on one substrate
[BAPT-FB-T-79-107] p0072 N81-14227
The effect of thermal cycling to 1100 degree C on the alpha (H0) phase in directionally solidified gamma/gamma prime-alpha alloys
[NASA-TN-81688] p0052 N81-18165
Fabrication of aluminum oxide fiber reinforced aluminum matrix composites
[NASA-CR-165184] p0048 N81-19229
- ALUMINUM ALLOYS
On the equivalence between semiempirical fracture analyses and R-curves
p0092 A81-18792
The effect of mechanical surface and heat treatments on the erosion resistance of 6061 aluminum alloy
p0057 A81-27944
Effect of mechanical surface and heat treatments on erosion resistance
[NASA-TN-81540] p0051 N81-11178
NiCrAl ternary alloy having improved cyclic oxidation resistance
[NASA-CASE-LBN-13339-1] p0051 N81-12211
Fabrication development of alumina/aluminum composites
[NASA-CR-165195] p0048 N81-19233
Effects of geometric variables on rub characteristics of Ti-6Al-4V
[NASA-TP-1835] p0053 N81-20245
- ALUMINUM COMPOUNDS
NT ALUMINUM OXIDES
NT ALUMINUM SILICATES
ALUMINUM OXIDES
Fracture toughness of brittle materials determined with chevron notch specimens
p0064 A81-32545
- Microstructure of Al2O3 scales formed on NiCrAl alloys
[NASA-TN-81676] p0052 N81-16212
Fabrication of aluminum oxide fiber reinforced aluminum matrix composites
[NASA-CR-165184] p0048 N81-19229
Fabrication development of alumina/aluminum composites
[NASA-CR-165195] p0048 N81-19233
- ALUMINUM SILICATES
Ceramic regenerator systems development program
[NASA-CR-165139] p0141 N81-22982
- AMERICAN INDIANS
Design description of the Schuchuli Village photovoltaic power system
[NASA-TN-82650] p0094 N81-28517
- ANIDES
NT POLYIMIDES
ANINES
NT DIANINES
ANISOTROPY
Environmental charging effects monitors for operational satellites
[NASA-TN-81669] p0037 N81-17127
- AMPLIFIERS
NT TRAVELING WAVE AMPLIFIERS
Analytical investigation of efficiency and performance limits in klystron amplifiers using multidimensional computer programs; multi-stage depressed collectors; and theraionic cathode life studies
p0098 N81-16552
- ANALYSIS (MATHEMATICS)
NT APPROXIMATION
NT COMPUTATIONAL FLUID DYNAMICS
NT COPLANARITY
NT DIFFERENTIAL EQUATIONS
NT ERROR ANALYSIS
NT FINITE DIFFERENCE THEORY
NT FINITE ELEMENT METHOD
NT LINEAR EQUATIONS
NT NONLINEAR EQUATIONS
NT NUMERICAL ANALYSIS
ANALYZERS
NT ENGINE ANALYZERS
ANATOMY
NT JOINTS (ANATOMY)
ANECNOIC CHANNELS
Effects of blade-vane ratio and rotor-stator spacing on fan noise with forward velocity
[AIAA PAPER 81-2032] p0024 A81-48628
- ANEMOMETERS
NT DRAG FORCE ANEMOMETERS
NT LASER ANEMOMETERS
ANEMOMETRY
U VELOCITY MEASUREMENT
ANGLE OF ATTACK
Optimum subsonic, high-angle-of-attack nacelles
p0005 A81-11646
- ANGLES (GEOMETRY)
NT ANGLE OF ATTACK
ANGULAR ACCELERATION
Calculated and experimental data for a 118-mm bore roller bearing to 3 million DN
[ASME PAPER 80-C2/LUB-14] p0085 A81-18668
- ANIONS
Anion permselective membrane
[NASA-CR-165223] p0111 N81-16583
Pneumatic boot for helicopter rotor deicing
p0009 N81-19059
- ANISOTROPY
NT ELASTIC ANISOTROPY
Anisotropic tribological properties of silicon carbide
[NASA-TN-81547] p0080 N81-11394
- ANNEALING
NT LASER ANNEALING
The influence of isothermal annealing on the molybdenum fibers of a directed solid gamma/gamma prime - alpha alloy
p0056 A81-10765
Radiation damage annealing mechanisms and possible low temperature annealing in silicon solar cells
p0040 A81-27207
Annealing of radiation damage in low resistivity silicon solar cells
p0099 N81-17554
Reduced annealing temperatures in silicon solar cells

[NASA-TN-82597] p0104 N81-23627
ANNUAL FLOW
Description of the ware core turbine facility and the ware annular cascade facility recently installed at NASA Lewis Research Center [SAS PAPER 801122] p0031 N81-34158
ANNUAL NOZZLES
Model aerodynamic test results for two variable cycle engine coannular exhaust systems at simulated takeoff and cruise conditions --- Lewis 8 by 6-foot supersonic wind tunnel tests [NASA-CR-159818] p0026 N81-13057
ANNUAL PLATES
Multiple plate hydrostatic viscous damper [NASA-CASE-LEN-12445-1] p0083 N81-22360
ANTI-FRICTION BEARINGS
NT BALL BEARINGS
NT ROLLER BEARINGS
ANTIMONY ALLOYS
NT BABBITT METAL
APERTURES
Flow through axially aligned sequential apertures of the orifice and Borda types [NASA-TN-81681] p0075 N81-21314
APPLICATIONS TECHNOLOGY SATELLITES
U ATS
APPROXIMATION
NT FINITE DIFFERENCE THEORY
NT FINITE ELEMENT METHOD
A rapid method for the approximate determination of nonlinear solutions Application to aerodynamic flows p0007 N81-11628
Comparison of photovoltaic cell temperatures in modules operating with exposed and enclosed back surfaces [NASA-TN-81769] p0106 N81-28520
APPROXIMATION METHODS
U APPROXIMATION
ARGON
Adapting magnetoelectrostatic containment to inert gas thrusters [AIAA PAPER 81-0140] p0043 N81-20625
Performance of a magnetic multiple line-cusp argon ion thruster [AIAA PAPER 81-0745] p0041 N81-38071
Ion beam sputter etching of orthopedic implanted alloy MP35N and resulting effects on fatigue [NASA-TN-81747] p0045 N81-21174
ARGON PLASMA
Recent work on an RF ion thruster [AIAA PAPER 81-0678] p0041 N81-35625
ARIP (IMPACT PREDICTION)
U COMPUTERIZED SIMULATION
ARMED FORCES
NT ARMED FORCES (UNITED STATES)
ARMED FORCES (UNITED STATES)
Future Air Force aircraft propulsion control systems: The extended summary paper p0025 N81-12096
AROMATIC COMPOUNDS
Curing agent for polyepoxides and epoxy resins and composites cured therewith --- preventing carbon fiber release [NASA-CASE-LEN-1226-1] p0060 N81-17260
ARRAYS
NT SOLAR ARRAYS
ARSENIC COMPOUNDS
NT GALLIUM ARSENIDES
ARSENIDES
NT GALLIUM ARSENIDES
ARTIFICIAL SATELLITES
NT ATS
NT COMMUNICATION SATELLITES
NT COMMUNICATIONS TECHNOLOGY SATELLITE
NT SCATHA SATELLITE
NT SOLAR POWER SATELLITES
NT SYNCHRONOUS SATELLITES
ARYL COMPOUNDS
U AROMATIC COMPOUNDS
ASSESSMENTS
NT TECHNOLOGY ASSESSMENT
ASTRONOMICS
Environmental charging effects monitors for operational satellites [NASA-TN-81669] p0037 N81-17127
ATLANTIC OCEAN
Aircraft operating efficiency on the North Atlantic, a challenge for the 1980's

p0009 N81-19060
ATMOSPHERIC CONDITIONS
U METEOROLOGY
ATMOSPHERIC DENSITY
Cloud encounter and particle density variabilities from GASP data [AIAA PAPER 81-0308] p0117 N81-20742
ATMOSPHERIC IMPURITIES
U AIR POLLUTION
ATMOSPHERIC MODELS
NT BRACKETBOARD MODELS
NT DYNAMIC MODELS
ATOMIC STRUCTURE
Electron spectroscopy of the diamond surface p0130 N81-27031
ATOMIZING
NT LIQUID ATOMIZATION
ATOMS
NT HYDROGEN ATOMS
ATS
Applications Technology Satellite and Communications Technology Satellite user experiments for 1967 - 1980 reference book, volume 1 [NASA-CR-165169-VOL-1] p0033 N81-12135
Applications Technology Satellite and Communications Technology Satellite user experiments for 1967-1980 reference book, volume 2 [NASA-CR-165169-VOL-2] p0033 N81-12136
Applications Technology Satellite and Communications Technology Satellite user experiments for 1967-1980 reference book, Volume 3: User form surveys [NASA-CR-165169-VOL-3] p0033 N81-12137
Applications Technology Satellite and Communications Technology Satellite user experiments for 1967-1980 reference book, Volume 4: Abstracts [NASA-CR-165169-VOL-4] p0133 N81-12138
ATTENUATION
NT ACOUSTIC ATTENUATION
NT SHOCK WAVE ATTENUATION
ATTENUATORS
NT RESISTORS
ATTENTION (MATERIALS)
U CORRUPTION
AUGER SPECTROSCOPY
Electron spectroscopy of the diamond surface p0130 N81-27031
Surface chemistry and friction behavior of the silicon carbide (3001) surface at temperatures to 1500 deg C [NASA-TN-1813] p0061 N81-19300
AUTOMATIC CONTROL
NT ADAPTIVE CONTROL
NT FEEDBACK CONTROL
NT NUMERICAL CONTROL
NT OPTIMAL CONTROL
Integrated control system for a gas turbine engine [NASA-CASE-LEN-12594-2] p0015 N81-19116
AUTOMATIC CONTROL VALVES
NT PRESSURE REGULATORS
NT RELIEF VALVES
AUTOMATIC DATA PROCESSING
U DATA PROCESSING
AUTOMATIC PATTERN RECOGNITION
U PATTERN RECOGNITION
AUTOMATIC ROCKET IMPACT PREDICTORS
U COMPUTERIZED SIMULATION
AUTOMATIC TEST EQUIPMENT
Three-axis electron-beam test facility [NASA-TN-1836] p0071 N81-20359
AUTOMOBILE ENGINES
Ultra-lean combustion at high inlet temperatures [ASME PAPER 81-GT-44] p0086 N81-29958
Automotive Stirling engine development program [NASA-CR-165134] p0139 N81-11952
Applicability of advanced automotive heat engines to solar thermal power [NASA-TN-81658] p0097 N81-14397
Advanced propulsion system concept for hybrid vehicles [NASA-CR-159772] p0140 N81-18935
Analytical design of an advanced radial turbine --- automobile engines [NASA-CR-165170] p0140 N81-20958
A computer simulation of the transient response of a 4 cylinder Stirling engine with burner and air preheater in a vehicle

[NASA-CR-165262] p0078 N81-22313
Thermal energy storage for the Stirling engine
powered automobile
[NASA-CR-159561] p0113 N81-22467
System safety in Stirling engine development
[NASA-TN-82615] p0140 N81-24994
Hostile environmental conditions facing candidate
alloys for the automotive Stirling engine
[NASA-TN-82632] p0054 N81-26236
Test results of the Chrysler upgraded automotive
gas turbine engine: Initial design
[NASA-TN-81660] p0107 N81-30562
High-power baseline and motoring test results for
the GPU-3 Stirling engine
[NASA-TN-82646] p0139 N81-32087

AUTOMOBILE FUELS
NT LIQUID FUELS
AUTOMOBILES
NT ELECTRIC AUTOMOBILES
The Federal electric and hybrid vehicle program
p0142 N81-12986
JPL's electric and hybrid vehicles project:
Project activities and preliminary test results
--- power conditioning and battery charge
efficiency
p0143 N81-12987
Small passenger car transmission test: Dodge Omni
A-404 transmission
[NASA-CR-165181] p0088 N81-15366
Characterization of the near-term electric vehicle
(RTV-1) breadboard propulsion system over the
SAB J227a driving schedule D
[NASA-TN-81664] p0097 N81-15465

AUXILIARY POWER SOURCES
NT CHEMICAL AUXILIARY POWER UNITS
NT SPACE POWER REACTIONS
AUXILIARY PROPULSION
Diagnostic system design for the Ion Auxiliary
Propulsion System /IAFS/ - Flight test of two 8
cm mercury ion thrusters
[AIAA PAPER 81-0666] p0041 N81-38070

AXES (COORDINATES)
U COORDINATES
AXES (REFERENCE LINES)
NT AXES OF ROTATION
AXES OF ROTATION
Three-axis electron-beam test facility
[NASA-TP-1836] p0071 N81-20359

AXIAL COMPRESSORS
U TURBOCOMPRESSORS
AXIAL FLOW
Capillary and acceleration wave breakup of liquid
jets in axial-flow airstreams
[NASA-TP-1791] p0075 N81-16417

AXIAL FLOW COMPRESSORS
U TURBOCOMPRESSORS
AXIAL FLOW PUMPS
NT TURBINE PUMPS
AXIAL FLOW TURBINES
Stability of large horizontal-axis axisymmetric
wind turbines
[NASA-TN-81623] p0091 N81-12446
NASA contributions to radial turbine aerodynamic
analyses
[NASA-TN-81644] p0003 N81-13019
Data acquisition and analysis in the DOE/NASA Wind
Energy Program
[NASA-TN-81603] p0096 N81-13463
Turbine modeling technique to generate off-design
performance data for both single and multistage
axial-flow turbines
[NASA-CR-165244] p0027 N81-17078
Improved method for calculating transonic
velocities on blade-to-blade stream surfaces of
a turbomachine
[NASA-TP-1772] p0004 N81-22017
Cold-air performance of compressor-drive turbine
of Department of Energy upgraded automobile gas
turbine engine. 1: Volute-manifold and stator
performance
[NASA-TN-82682] p0004 N81-28053

AXIAL STRESS
Axial force and efficiency tests of fixed center
variable speed belt drive
[NASA-TN-81652] p0080 N81-15367

AXISYMMETRIC BODIES
Finite element analysis of inviscid subsonic
boattail flow
[AIAA PAPER 81-0276] p0006 N81-20831

AXISYMMETRIC FLOW**NT AXIAL FLOW**

The experimental verification of a streamline
curvature numerical analysis method applied to
the flow through an axial flow fan
[AIAA PAPER 81-0363] p0005 N81-20782
Stability of large horizontal-axis axisymmetric
wind turbines
[NASA-TN-81623] p0091 N81-12446

AXLES**U SHAFTS (MACHINE ELEMENTS)****B****BABBITT METAL**

Fabrication and testing of polyvinylidene fluoride
capacitors
[NASA-CR-159501] p0073 N81-22278

BACKWARD WAVES

Ladder supported ring bar circuit
[NASA-CASE-LEW-13570-1] p0071 N81-24348
Measurement of aerodynamic work during fan flutter
[NASA-TN-82652] p0017 N81-25080

BALL BEARINGS

Some limitations in applying classical HBD film
thickness formulas to a high-speed bearing
[ASME PAPER 80-C2/LUB-13] p0068 N81-18667
History of ball bearings
[NASA-TN-81689] p0081 N81-18391
Introduction to ball bearings
[NASA-TN-81690] p0081 N81-18392
Performance of jet- and inner-ring-lubricated 35
millimeter bore ball bearings operating to 2.5
million DN
[NASA-TP-1808] p0082 N81-19458
Life analysis of multiroller planetary traction
drive
[NASA-TP-1710] p0082 N81-20423
Simplified solution for stresses and deformation
[NASA-TN-82647] p0084 N81-28444
Ball bearing mechanics
[NASA-TN-81691] p0085 N81-31550

BAND STRUCTURE OF SOLIDS

Effect of electronic structure of the diamond
surface on the strength of the diamond-metal
interface
[NASA-TN-82714] p0063 N81-32269

BANDWIDTH**NT BROADBAND****BANDS APPROXIMATION****U ELECTRICAL PROPERTIES****U SURFACE PROPERTIES****BARLEY**

Numerical trials of HISSE
[81-10069] p0094 N81-13425
Normal crop calendars. Volume 2: The spring
wheat states of Minnesota, Montana, North
Dakota, and South Dakota
[81-10070] p0094 N81-13426

BATTERIES**U ELECTRIC BATTERIES****BATTERY SEPARATORS****U SEPARATORS****BEAMS (RADIATION)****NT ELECTRON BEAMS****NT ION BEAMS****BEAMS (SUPPORTS)****NT CANTILEVER BEAMS****BEARINGS****NT BALL BEARINGS****NT JOURNAL BEARINGS****NT ROLLER BEARINGS****NT THRUST BEARINGS****BEAT****U SYNCHRONISM****BEAUFORT SEA (NORTH AMERICA)**

Comparative analysis of sea ice features using
Side-Looking Airborne Radar (SLAR) and LANDSAT
imagery --- Beaufort Sea and Bering Sea
[81-10044] p0095 N81-33539

BENDING VIBRATION

Effects of mistuning on bending-torsion flutter
and response of a cascade in incompressible flow
[AIAA 81-0602] p0092 N81-29465

BERING SEA

Comparative analysis of sea ice features using
Side-Looking Airborne Radar (SLAR) and LANDSAT
imagery --- Beaufort Sea and Bering Sea
[81-10044] p0095 N81-33539

BIAS

Review of biased solar array. Plasma interaction studies
[NASA-TN-82693] p0036 N81-32187

BIBLIOGRAPHIES

Bibliography of Lewis Research Center Technical Publications announced in 1979
[NASA-TN-81525] p0137 N81-17942
Bibliography of Lewis Research Center Technical Publications announced in 1978
[NASA-TN-79162] p0137 N81-17943
Bibliography of Lewis Research Center technical publications announced in 1980
[NASA-TN-82661] p0137 N81-29026

BINARY ALLOYS

The adhesion, friction, and wear of binary alloys in contact with single-crystal silicon carbide
[ASME PAPER 80-C2/LUE-53] p0086 A81-18695

BINARY MIXTURES

NT EUTECTIC ALLOYS

The effect of thermal cycling to 1100 degree C on the alpha (Ho) phase in directionally solidified gamma/gamma prime-alpha alloys
[NASA-TN-81688] p0052 N81-18165

BINARY SYSTEMS (DIGITAL)

U DIGITAL SYSTEMS

BINARY SYSTEMS (MATERIALS)

NT BINARY ALLOYS

NT BINARY MIXTURES

NT EUTECTIC ALLOYS

BINDERS (MATERIALS)

Friction and wear results from sputter-deposited chrome oxide with and without nichrome metallic binders and interlayers
[ASME PAPER 80-C2/LUE-49] p0089 A81-18693

BIPROPELLANTS

U LIQUID ROCKET PROPELLANTS

BIRD-AIRCRAFT COLLISIONS

Superhybrid composite blade impact studies
[ASME PAPER 81-GT-24] p0020 A81-29940
Interactive multi-node blade impact analysis
[ASME PAPER 81-GT-79] p0030 A81-29987

BIREFRINGENT COATINGS

Theoretical model applicable to the experimental determination of surface anchoring energies of nematic liquid crystals
[NASA-TN-81628] p0124 N81-12817

BLADE TIPS

Rotor redesign for a highly loaded 1600 ft/sec tip speed fan, 2
[NASA-CR-159879] p0024 N81-12087
Effects of geometric variables on rub characteristics of Ti-6Al-4V
[NASA-TP-1835] p0053 N81-20245
A sputtered zirconia primer for improved thermal shock resistance of plasma sprayed ceramic turbine seals
[NASA-TN-81732] p0062 N81-21198
An evaluation of a simplified near field noise model for supersonic helical tip speed propellers
[NASA-TN-81727] p0130 N81-22836

BLEED-OFF

U PRESSURE REDUCTION

BLOCK DIAGRAMS

An automated procedure for developing hybrid computer simulations of turbofan engines
p0020 A81-32544

BLOWING

Full-coverage film cooling. I - Three-dimensional measurements of turbulence structure. II - Prediction of the recovery-region hydrodynamics
p0078 A81-15537

BOATTAILS

Finite element analysis of inviscid subsonic boattail flow
[AIAA PAPER 81-0276] p0006 A81-20831

BODIES OF REVOLUTION

NT CYLINDRICAL BODIES

BODY FLUIDS

NT CEREBROSPINAL FLUID

BORING AIRCRAFT

NT BORING 747 AIRCRAFT

BORING MILITARY AIRCRAFT

U MILITARY AIRCRAFT

BORING 747 AIRCRAFT

Ozone contamination in aircraft cabins - Results from GASP data and analyses
[AIAA PAPER 81-0305] p0010 A81-20740

BOILERS

Modification of the ECAS reference steam power generating plant to comply with the EPA 1979 new source performance standards
[NASA-CR-159853] p0110 N81-13467
Performance calculations for 1000 MWe BHD/steam power plants
[NASA-TN-81667] p0098 N81-16570

BOILING

NT NUCLEATE BOILING

BONDING

NT ADHESIVE BONDING

NT METAL BONDING

NT METAL-METAL BONDING

NT RESIN BONDING

BORON

NT BORON FIBERS

BORON FIBERS

CVD-produced boron filaments

p0048 A81-11336

Oxidation-induced contraction and strengthening of boron fibers

p0047 A81-44664

Oxidation-induced contraction and strengthening of boron fibers

p0046 N81-25150

BORON REINFORCED MATERIALS

Oxidation-induced contraction and strengthening of boron fibers

p0047 A81-44664

BOUNDARIES

NT LIQUID-SOLID INTERFACES

Fast Generation of body conforming grids for 3-D

p0122 N81-14706

BOUNDARY LAYER CONTROL

Core compressor exit stage study. Volume 3: Data and performance report for screening test configurations
[NASA-CR-159499] p0024 N81-12086

BOUNDARY LAYER FLOW

NT BOUNDARY LAYER SEPARATION

NT SECCNARY FLOW

NT SEPARATED FLOW

Analysis for predicting adiabatic wall temperatures with single hole coolant injection into a low speed crossflow
[NASA-TN-81620] p0074 N81-13301

GRID30: Computer program for fast generation of multilevel, three-dimensional boundary-conforming O-type computational grids
[NASA-TP-1920] p0005 N81-31128

BOUNDARY LAYER NOISE

U AERODYNAMIC NOISE

BOUNDARY LAYER SEPARATION

Three-dimensional turbulent boundary layer development and separation in V/STOL engine inlets at incidence with small-cross flow and curvature influences
[AIAA PAPER 81-0254] p0005 A81-20703
Some flow phenomena associated with aligned, sequential apertures with Borda-type inlets --- inlet pressure and flow separation
[NASA-TP-1792] p0076 N81-24387

BOUNDARY LAYER TRANSITION

Boundary layer development on turbine airfoil suction surfaces
[ASME PAPER 81-GT-204] p0008 A81-30094
Core compressor exit stage study. Volume 2: Data and performance report for the baseline configuration
[NASA-CR-159498] p0027 N81-16051

BOUNDARY LAYERS

NT THERMAL BOUNDARY LAYER

NT THREE DIMENSIONAL BOUNDARY LAYER

NT TURBULENT BOUNDARY LAYER

NT TWO DIMENSIONAL BOUNDARY LAYER

BOUNDARY LUBRICATION

Dynamics of solid dispersions in oil during the lubrication of point contacts. Part 1: Graphite
[NASA-TN-81683] p0061 N81-17264
Evaluation of boundary lubricants using steady-state wear and friction
[NASA-TN-81601] p0061 N81-17265
Steady-state boundary lubrication with formulated C-ethers to 260 C
[NASA-TP-1812] p0053 N81-21193
Lubrication fundamentals
[NASA-TN-81762] p0103 N81-23490

- BOV SHOCK WAVES**
U SHOCK WAVES
BREADBOARD MODELS
Characterization of the near-term electric vehicle (ETV-1) breadboard propulsion system over the SAE J227a driving schedule D
[NASA-TN-81664] p0097 N81-15465
Results of the ETV-1 breadboard tests under steady-state and transient conditions --- conducted in the NASA-LeRC Road Load Simulator
[NASA-TN-82667] p0108 N81-31627
- BREAKAWAY**
U BOUNDARY LAYER SEPARATION
BRITTLE MATERIALS
Fracture toughness of brittle materials determined with chevron notch specimens
p0064 A81-32545
- BROADBAND**
Specifying and calibrating instrumentations for wideband electronic power measurements --- in switching circuits
[NASA-TN-81545] p0079 N81-16429
- BUILDING MATERIALS**
U CONSTRUCTION MATERIALS
BURNERS
Prolonging thermal barrier coated specimen life by thermal cycle management
p0065 A81-44658
A computer simulation of the transient response of a 4 cylinder Stirling engine with burner and air preheater in a vehicle
[NASA-CR-165262] p0078 N81-22313
- BURNING**
U COMBUSTION
BURNING PROCESS
U COMBUSTION
BYPASS RATIO
Effect of a part-span variable inlet guide vane on the performance of a high-bypass turbofan engine
[AIAA PAPER 81-1362] p0022 A81-40842
Turbine bypass engine - A new supersonic cruise propulsion concept
[AIAA PAPER 81-1596] p0023 A81-40971
Mixing effectiveness test of an exhaust gas mixer in a high bypass turbofan at altitude
[AIAA PAPER 81-1495] p0023 A81-44225
- C**
- CABIN ATMOSPHERES**
Ozone contamination in aircraft cabins - Results from GASP data and analyses
[AIAA PAPER 81-0305] p0010 A81-20740
Ozone contamination in aircraft cabins: Results from GASP data and analyses
[NASA-TN-81671] p0009 N81-16021
Analysis of atmospheric ozone levels at commercial airplane cruise altitudes in winter and spring, 1976 - 1977 --- Global Atmospheric Sampling Program
[NASA-TP-1807] p0117 N81-21685
- CADMIUM NICKEL BATTERIES**
U NICKEL CADMIUM BATTERIES
CALCULATION
U COMPUTATION
CALCULUS
U COPLANARITY
CALENDARS
U CROP CALENDARS
CALIBRATING
Global calibration of terrestrial reference cells and errors involved in using different irradiance monitoring techniques
p0068 A81-27148
Gauge calibration system based on piston manometer
p0079 A81-48950
Specifying and calibrating instrumentations for wideband electronic power measurements --- in switching circuits
[NASA-TN-81545] p0079 N81-16429
An integrated exhaust gas analysis system with self-contained data processing and automatic calibration
[NASA-TN-81592] p0102 N81-23435
- CANS**
Simplified solution for stresses and deformation
[NASA-TN-82647] p0084 N81-28444
- CANTILEVER BEAMS**
Miniature drag-force anemometer
[NASA-TN-81680] p0079 N81-16428
CANTILEVER MEMBERS
U CANTILEVER BEAMS
CANTILEVER RINGS
U RINGS
CAPACITORS
Integrated RC-circuits in ALTA-technology on one substrate
[BNFT-FN-T-79-107] p0072 N81-14227
Fabrication and testing of polyvinylidene fluoride capacitors
[NASA-CR-159501] p0073 N81-22278
- CAPILLARY CIRCULATION**
U CAPILLARY FLOW
CAPILLARY FLOW
Heat pipes containing alkali metal working fluid
[NASA-CASE-LEW-12253-1] p0076 N81-22310
CAPILLARY WAVES
Capillary and acceleration wave breakup of liquid jets in axial-flow airstreams
[NASA-TP-1791] p0075 N81-16417
- CARBIDES**
U SILICON CARBIDES
U ZIRCONIUM CARBIDES
CARBON
Combustion of solid carbon rods in zero and normal gravity
[NASA-TN-81728] p0082 N81-22317
CARBON COMPOUNDS
U FLUOROPOLYMERS
U SILICON CARBIDES
U ZIRCONIUM CARBIDES
CARBON DIOXIDE
Exhaust emission survey of an F100 afterburning turbofan engine at simulated altitude flight conditions
[NASA-TN-81656] p0016 N81-21078
CARBON FIBER REINFORCED PLASTICS
Curing agent for polyepoxides and epoxy resins and composites cured therewith --- preventing carbon fiber release
[NASA-CASE-LEW-13226-1] p0060 N81-17260
CARBON MONOXIDE
Preparation and evaluation of advanced electrocatalysts for phosphoric acid fuel cells
[NASA-CR-165179] p0111 N81-17527
Exhaust emission survey of an F100 afterburning turbofan engine at simulated altitude flight conditions
[NASA-TN-81656] p0016 N81-21078
- CARBON STEELS**
Computer-aided roll pass design in rolling of airfoil shapes
p0088 A81-15796
Effects of erodant particle shape and various heat treatments on erosion resistance of plain carbon steel
[NASA-TP-1755] p0052 N81-16210
Passivation of carbon steel through mercury implantation
[NASA-CR-165292] p0059 N81-20244
- CARRIER MOBILITY**
U ELECTRON MOBILITY
The effect of minority carrier mobility variations on the performance of high voltage silicon solar cells
p0098 N81-17536
The effect of minority carrier mobility variations on solar cell spectral response
[NASA-TN-82604] p0103 N81-23625
- CARTOGRAPHY**
U MAPPING
CARTRIDGE ACTUATED DEVICES
U ACTUATORS
CASCADE FLOW
Effects of mistuning on bending-torsion flutter and response of a cascade in incompressible flow
[AIAA 81-0602] p0092 A81-29465
Full potential solution of a transonic quasi-3-D flow through a cascade using artificial compressibility
[ASME PAPER 81-GT-70] p0006 A81-29979
Solution of plane cascade flow using improved surface singularity methods
[ASME PAPER 81-GT-109] p0006 A81-30068
Description of the vane core turbine facility and the vane annular cascade facility recently installed at NASA Lewis Research Center
[SAE PAPER 801122] p0031 A81-34158

- An electrostatic analog for generating cascade grids
p0122 N81-14695
- Generation of C-type cascade grids for viscous
flow computation
p0122 N81-14721
- Experimental determination of unsteady blade
element aerodynamics in cascades. Volume 2:
Translation mode cascade
[NASA-CR-165166] p0007 N81-14976
- Supersonic stall flutter of high speed fans --- in
turbofan engines
[NASA-TN-81613] p0003 N81-14978
- Solution of plane cascade flow using improved
surface singularity methods --- application of
panel method to internal aerodynamics
[NASA-TN-81589] p0003 N81-14979
- Effects of mistuning on bending-torsion flutter
and response of a cascade in incompressible flow
--- turbofan engines
[NASA-TN-81674] p0091 N81-16494
- Shockless design and analysis of transonic blade
shapes
[NASA-TN-82611] p0004 N81-25036
- Stall flutter experiment in a transonic
oscillating linear cascade
[NASA-TN-82655] p0004 N81-31126
- CASCADES (FLUID DYNAMICS)**
- U FLUID DYNAMICS**
- CASE HISTORIES**
- A case history of technology transfer
[NASA-TN-82618] p0040 N81-30182
- CASE ALLOYS**
- Development of low-cost directionally-solidified
turbine blades
p0088 N81-10707
- The effect of zirconium on the cyclic oxidation of
NiCrAl alloys
p0056 N81-18559
- CASTING**
- Texturing polymer surfaces by transfer casting ---
cardiovascular prosthesis
[NASA-CASE-LEW-13120-1] p0068 N81-16327
- Sputtered protective coatings for die casting dies
[NASA-TN-81735] p0053 N81-21173
- CASTING SOLVENTS**
- U PLASTICIZERS**
- CASTINGS**
- Sputtered protective coatings for die casting dies
p0057 N81-38067
- CATALYSIS**
- Preparation and characterization of electrodes for
the NASA Redox storage system
[NASA-TN-82702] p0107 N81-30522
- CATALYSTS**
- NT ELECTROCATALYSTS**
- Catalytic combustion of coal-derived liquids
[NASA-TN-81594] p0097 N81-14396
- CATALYTIC ACTIVITY**
- Cell module and fuel conditioner
[NASA-CR-165189] p0112 N81-18494
- Experimental evaluation of catalytic combustion
with heat removal at near stoichiometric
conditions
[NASA-TN-81748] p0103 N81-23609
- CATHETERIZATION**
- Ion beam sputter-etched ventricular catheter for
hydrocephalus shunt
[NASA-CASE-LEW-13107-1] p0118 N81-27786
- CATHODES**
- NT COLD CATHODES**
- NT HOLLOW CATHODES**
- NT THERMIONIC CATHODES**
- Moderate temperature sodium cells. I - Transition
metal disulfide cathodes
p0113 N81-15027
- Spacecraft transmitter reliability
[NASA-CP-2159] p0037 N81-16119
- CAUSTICS**
- U ALKALIES**
- CERAMAL PROTECTIVE COATINGS**
- U CEMENTS**
- U PROTECTIVE COATINGS**
- CERAMALS**
- U CEMENTS**
- CERAMIC COATINGS**
- Thermal barrier coatings for heat engine components
p0056 N81-12920
- Comparative evaluation of insulating properties of
plasma-sprayed ceramic coatings
- Thermal barrier coatings for superalloys
p0064 N81-15984
- Ceramic applications in turbine engines --- for
improved component performance and reduced fuel
usage
[NASA-CR-159865] p0029 N81-19118
- A sputtered zirconia primer for improved thermal
shock resistance of plasma sprayed ceramic
turbine seals
[NASA-TN-81732] p0062 N81-21198
- Thermal and flow analysis of a convection
air-cooled ceramic coated porous metal concept
for turbine vanes
[NASA-TN-81749] p0016 N81-22056
- Laser surface fusion of plasma sprayed ceramic
turbine seals
[NASA-CASE-LEW-13269-1] p0062 N81-22190
- Thermal barrier coating system having improved
adhesion
[NASA-CASE-LEW-13359-1] p0062 N81-24260
- CERAMIC ROCKETMOTORS**
- Improved ceramic heat exchanger materials
[NASA-CR-159678] p0065 N81-14082
- CERAMICS**
- Surface flaw detection in structural ceramics by
scanning photoacoustic spectroscopy
p0079 N81-17906
- Fracture toughness of brittle materials determined
with chevron notch specimens
p0064 N81-32545
- Dissolution of bulk specimens of silicon nitride
p0065 N81-42024
- Improved ceramic heat exchanger materials
[NASA-CR-159678] p0065 N81-14082
- Ceramic regenerator systems development program
[NASA-CR-165139] p0141 N81-22982
- Compatibility of alternative fuels with advanced
automotive gas turbine and stirling engines. A
literature survey
[NASA-TN-81754] p0105 N81-27604
- Effect of Yttria additives on properties of
pressureless-sintered silicon nitride
[NASA-TP-1899] p0063 N81-31366
- CEREBROSPINAL FLUID**
- Ion beam sputter-etched ventricular catheter for
hydrocephalus shunt
[NASA-CASE-LEW-13107-1] p0118 N81-27786
- CERRETS**
- A new diffusion-inhibited oxidation-resistant
coating for superalloys
[NASA-TN-82667] p0056 N81-33273
- CERTIFICATION**
- Comparison of predicted engine core noise with
proposed FAA helicopter noise certification
requirements
p0128 N81-38062
- Comparison of predicted engine core noise with
current and proposed aircraft noise
certification requirements
[AIAA PAPER 81-2053] p0024 N81-48635
- Comparison of predicted engine core noise with
proposed FAA helicopter noise certification
requirements
[NASA-TN-81739] p0130 N81-22839
- Comparison of predicted engine core noise with
current and proposed aircraft noise
certification requirements
[NASA-TN-82659] p0126 N81-29922
- CESIUM DIODES**
- Improved thermionic energy converters
[NASA-CASE-LEW-12443-1] p0099 N81-19561
- CHESNA MILITARY AIRCRAFT**
- U MILITARY AIRCRAFT**
- CFRP**
- U CARBON FIBER REINFORCED PLASTICS**
- CHALCOGENIDES**
- NT ALUMINUM OXIDES**
- NT CARBON DIOXIDE**
- NT CARBON MONOXIDE**
- NT CHROMIUM OXIDES**
- NT DISULFIDES**
- NT METAL OXIDES**
- NT MOLYBDENUM DISULFIDES**
- NT NICKEL OXIDES**
- NT NITRIC OXIDE**
- NT NITROGEN OXIDES**
- NT SILICON DIOXIDE**
- NT TANTALUM OXIDES**

- NT YTTRIUM OXIDES
 NT ZIRCONIUM OXIDES
 CHACCO-VOUGHT MILITARY AIRCRAFT
 U MILITARY AIRCRAFT
 CHANNEL FLOW
 On the magnetohydrothermal instability
 [AIAA PAPER 81-0248] p0133 881-20698
 CHARACTERISTIC EQUATIONS
 U HIGHVALUES
 CHARACTERISTIC FUNCTIONS
 U HIGHVALUES
 CHARACTERISTIC METHOD
 U METHOD OF CHARACTERISTICS
 CHARGE EFFICIENCY
 JPL's electric and hybrid vehicles project:
 Project activities and preliminary test results
 --- power conditioning and battery charge
 efficiency p0143 881-12987
 Characterization, performance, and prediction of a
 lead-acid battery under simulated electric
 vehicle driving requirements
 [NASA-TN-81771] p0106 881-2823
 CHARGE SEPARATION
 U POLARIZATION (CHARGE SEPARATION)
 CHARGED PARTICLES
 NT ANIONS
 NT ARGON PLASMA
 NT ELECTRON PLASMA
 NT ELECTRONS
 NT PLASMA SHEATHS
 Particle and field measurements on two J-series
 30-centimeter thrusters
 [AIAA PAPER 81-0728] p0042 881-38072
 CHECKOUT EQUIPMENT
 U TEST EQUIPMENT
 CHEMICAL ANALYSIS
 NT GAS ANALYSIS
 NT OZONOMETRY
 NT QUANTITATIVE ANALYSIS
 NT SPECTROSCOPIC ANALYSIS
 Dissolution of bulk specimens of silicon nitride
 p0065 881-42024
 Accuracy of trace element determinations in
 alternate fuels
 [NASA-TN-81609] p0049 881-13106
 Material response from Mach 0.3 burner rig
 combustion of a coal-oil mixture
 [NASA-TN-81686] p0055 881-27258
 Performance tests of a gas blending system based
 on mass-flow controllers
 [NASA-TP-1896] p0066 881-29246
 CHEMICAL AUXILIARY POWER UNITS
 Preparation and evaluation of advanced
 electrocatalysts for phosphoric acid fuel cells
 [NASA-CN-165245] p0112 881-18496
 CHEMICAL BONDS
 Effect of electronic structure of the diamond
 surface on the strength of the diamond-metal
 interface
 [NASA-TN-82714] p0063 881-32269
 CHEMICAL COMPOSITION
 Composition and method for making polyimide
 resin-reinforced fabric
 [NASA-CASE-LEW-12933-1] p0061 881-19296
 CHEMICAL ELEMENTS
 NT ALKALI METALS
 NT ALUMINUM
 NT ARGON
 NT CARBON
 NT COBALT
 NT COPPER
 NT GADOLINIUM
 NT HYDROGEN
 NT HYDROGEN ATOMS
 NT LEAD (METAL)
 NT LIQUID NITROGEN
 NT LIQUID SODIUM
 NT LITHIUM
 NT MERCURY (METAL)
 NT SOLIDBISMUTH
 NT NICKEL
 NT NITROGEN
 NT PHOSPHORUS
 NT PLATINUM
 NT RARE GASES
 NT SILICON
 NT TANTALUM
 NT TITANIUM
 NT TRACE ELEMENTS
 NT TUNGSTEN
 NT ZENON
 NT YTTRIUM
 NT ZIRCONIUM
 CHEMICAL FUELS
 NT AIRCRAFT FUELS
 NT DIESEL FUELS
 NT HIGH ENERGY FUELS
 NT HYDROCARBON FUELS
 NT JET ENGINE FUELS
 NT LIQUID FUELS
 NT SYNTHETIC FUELS
 Accuracy of trace element determinations in
 alternate fuels
 [NASA-TN-81609] p0049 881-13106
 CHEMICAL KINETICS
 U REACTION KINETICS
 CHEMICAL PROPERTIES
 NT THERMOCHEMICAL PROPERTIES
 Compatibility of alternate fuels with advanced
 automotive gas turbine and stirling engines. A
 literature survey
 [NASA-TN-81754] p0105 881-27604
 CHEMICAL PROPULSION
 Propellant management for low thrust chemical
 propulsion systems
 [AIAA PAPER 81-1453] p0042 881-42198
 CHEMICAL REACTIONS
 NT ELECTROCHEMICAL OXIDATION
 NT HYDROGENATION
 NT OXIDATION
 NT OXIDATION-REDUCTION REACTIONS
 NT RADIOLYSIS
 NT REDUCTION (CHEMISTRY)
 CHEMICAL REACTORS
 Catalytic combustion of coal-derived liquids
 [NASA-TN-81594] p0097 881-14396
 CHEMICAL TESTS
 NT CHEMICAL ANALYSIS
 NT GAS ANALYSIS
 NT OZONOMETRY
 NT QUANTITATIVE ANALYSIS
 NT SPECTROSCOPIC ANALYSIS
 Infrared spectroscopy for the determination of
 hydrocarbon types in jet fuels
 [NASA-TN-82674] p0066 881-31380
 CHEMONUCLEAR PROPULSION
 U CHEMICAL PROPULSION
 CHILLING
 U COOLING
 CHOKES (RESTRICTIONS)
 Experiments on flow through one to four inlets of
 the orifice and Borda type
 [NASA-TN-82680] p0077 881-30391
 CHOPPERS (ELECTRIC)
 U ELECTRIC CHOPPERS
 CHROMATOGRAPHY
 Influence of excess diamine on properties of PBR
 polyimide resins and composites
 p0047 881-43635
 CHROMIUM ALLOYS
 NT FE82 41
 NiCrAl ternary alloy having improved cyclic
 oxidation resistance
 [NASA-CASE-LEW-13339-1] p0051 881-12211
 CHROMIUM COMPOUNDS
 NT CHROMIUM OXIDES
 CHROMIUM OXIDES
 Friction and wear results from sputter-deposited
 chromium oxide with and without nichrome metallic
 binders and interlayers
 [ASME PAPER 80-C2/LUB-49] p0089 881-18693
 CHUGGING
 U COMBUSTION STABILITY
 CINEFLUOROGRAPHY
 U MOTION PICTURES
 CINEBADIOGRAPHY
 U MOTION PICTURES
 CIRCUIT PROTECTION
 Laboratory evaluation of a pilot cell battery
 protection system for photovoltaic applications
 [NASA-TN-81714] p0104 881-24536
 CIRCUITS
 NT INTEGRATED CIRCUITS
 NT POWER SUPPLY CIRCUITS
 NT RC CIRCUITS
 NT SWITCHING CIRCUITS

- Ladder supported ring bar circuit
[NASA-CASE-LBN-13570-1] p0071 N81-24348
- CITIES**
An economic systems analysis of land mobile radio
telephone services p0069 A81-22528
- CIVIL AVIATION**
NASA Research in aeropropulsion p0142 N81-12980
- An overview of general aviation propulsion
research programs at NASA Lewis Research Center
[NASA-TN-81666] p0015 N81-16052
- General Aviation Turbine Engine (GATE) study
[NASA-CR-159482] p0029 N81-19117
- CLARK I AIRFOIL**
U AIRFOIL PROFILES
- CLASSIFICATIONS**
NT INDICES (DOCUMENTATION)
- Numerical trials of HISSE
[E81-10069] p0094 N81-13425
- Preliminary evaluation of the Environmental
Research Institute of Michigan crop calendar
shift algorithm for estimation of spring wheat
development stage --- North Dakota, South
Dakota, Montana, and Minnesota
[E81-10071] p0094 N81-13427
- Evaluation of results of US corn and soybeans
exploratory experiment: Classification
procedures verification test --- Missouri, Iowa,
Indiana, and Illinois
[E81-10076] p0095 N81-13432
- Acceptance tests and manufacturer relationships
from the 20A h standard cell data p0100 N81-21515
- CLEAN FUELS**
NT FUEL OILS
- CLOSED CYCLES**
Disk MHD generator study
[NASA-CR-159872] p0111 N81-18491
- CLOSED LOOP SYSTEMS**
U FEEDBACK CONTROL
- CLOTH**
U FABRICS
- CLOUD COVER**
Cloud encounter and particle density variabilities
from GASP data
[AIAA PAPER 81-0308] p0117 A81-20742
- CLOUD GLACIATION**
Survey of aircraft icing simulation test
facilities in North America
[NASA-TN-81707] p0005 N81-19078
- CLUMPS**
Numerical trials of HISSE
[E81-10069] p0094 N81-13425
- CLUSTERS**
U CLUMPS
- CLUTCHES**
Tests of an overrunning clutch in a wind turbine
[NASA-TN-82653] p0107 N81-29528
- COAL DERIVED LIQUIDS**
Effect of fuel nitrogen and hydrogen content on
emissions in hydrocarbon combustion
[ASME PAPER 81-GT-63] p0057 A81-29973
- Catalytic combustion of coal-derived liquids
[NASA-TN-81594] p0097 N81-14396
- Deposition and material response from Mach 0.3
burner rig combustion of SRC 2 fuels
[NASA-TN-81634] p0051 N81-15069
- The effects of trace impurities in coal-derived
liquid fuels on deposition and accelerated high
temperature corrosion of cast superalloys
[NASA-TN-81678] p0052 N81-16211
- High temperature alkali corrosion in high velocity
gases
[NASA-TN-82591] p0054 N81-25191
- COAL GASIFICATION**
Coal gasifier cogeneration powerplant project
p0143 N81-12588
- Conceptual design study of a coal gasification
combined-cycle powerplant for industrial
cogeneration
[NASA-TN-81687] p0105 N81-25488
- Comparison of Integrated Gasifier-Combined Cycle
and APB-steam turbine systems for industrial
cogeneration
[NASA-TN-82648] p0106 N81-28522
- A program-management plan with critical-path
definition for Combustion Augmentation with
Thermionic Energy Conversion (CATIC)
- [NASA-TN-82670] p0132 N81-30973
- COAL UTILIZATION**
Synergistic erosion/corrosion of superalloys in
PFB coal combustor effluent p0058 A81-44663
- Coal gasifier cogeneration powerplant project
p0143 N81-12988
- Engineering support for magnetohydrodynamic power
plant analysis and design studies
[NASA-CR-159690] p0110 N81-13466
- Modification of the ECAS reference steam power
generating plant to comply with the EPA 1979 new
source performance standards
[NASA-CR-159853] p0110 N81-13467
- Effect of fuel nitrogen and hydrogen content on
emissions in hydrocarbon combustion
[NASA-TN-81612] p0047 N81-14399
- Material response from Mach 0.3 burner rig
combustion of a coal-oil mixture
[NASA-TN-81686] p0055 N81-27258
- COATING**
NT ELECTROPLATING
NT ENCAPSULATING
NT METALLIZING
- COATINGS**
NT BIREFRINGENT COATINGS
NT CERAMIC COATINGS
NT ELECTROPLATING
NT ENCAPSULATING
NT GLASS COATINGS
NT INORGANIC COATINGS
NT METAL COATINGS
NT METALLIZING
NT PRIMERES (COATINGS)
NT PROTECTIVE COATINGS
NT SPROAYED COATINGS
NT THERMAL CONTROL COATINGS
- Control of volume resistivity in inorganic-organic
separators --- for alkaline batteries p0108 A81-11034
- Ion plating for the future p0087 A81-44654
- Sputtering and ion plating for aerospace
applications
[NASA-TN-81726] p0082 N81-20424
- Fretting wear and fretting fatigue: How are they
related?
[NASA-TN-82633] p0054 N81-26235
- COAXIAL FLOW**
An improved prediction method for noise generated
by conventional profile coaxial jets
[AIAA PAPER 81-1991] p0129 A81-49743
- COAXIAL NOZZLES**
An improved prediction method for noise generated
by conventional profile coaxial jets
[NASA-TN-82712] p0127 N81-32964
- COAXIAL TRANSMISSION**
U TRANSMISSION
- COBALT**
Cobalt: A vital element in the aircraft engine
industry
[NASA-TN-82662] p0055 N81-29206
- COBALT ALLOYS**
NT BENE 41
NASA's activities in the conservation of strategic
aerospace materials
[NASA-TN-81617] p0055 N81-29205
- Conservation of Strategic Aerospace Materials
(COSAM) p0019 N81-31208
- COEFFICIENT OF FRICTION**
Frictional and morphological characteristics of
ion plated soft, metallic films p0057 A81-38066
- Correlation of ideal and actual shear strengths of
metals with their friction properties
[NASA-TN-1891] p0063 N81-27282
- Adhesion and friction of transition metals in
contact with nonmetallic hard materials
[NASA-TN-82605] p0055 N81-28233
- Relationship between the ideal tensile strength
and the friction properties of metals in contact
with nonmetals and themselves
[NASA-TN-18633] p0063 N81-33293
- COEFFICIENTS**
NT COEFFICIENT OF FRICTION
NT COHERENCE COEFFICIENT
NT HEAT TRANSFER COEFFICIENTS

COGENERATION

- Cogeneration Technology Alternatives Study (CTAS)
Volume 5: Analytical approach and results
[NASA-CR-159763] p0109 N81-10517
- Coal gasifier cogeneration powerplant project
p0143 N81-12988
- Conceptual design study of a coal gasification
combined-cycle powerplant for industrial
cogeneration
[NASA-TN-81687] p0105 N81-25488
- Comparison of Integrated Gasifier-Combined Cycle
and AFB-steam turbine systems for industrial
cogeneration
[NASA-TN-82648] p0106 N81-28522

COMBUSTION COEFFICIENT

- Conditioned pressure spectra and coherence
measurements in the core of a turbofan engine
[NASA-TN-82688] p0126 N81-30907

CONCURRENT ACOUSTIC RADIATION

- Improved methods for fan sound field determination
[NASA-CR-165188] p0129 N81-15769

CONCURRENT RADIATION

NET CONCURRENT ACOUSTIC RADIATION

COLD CATHODES

- Development program on a cold cathode electron gun
[NASA-CR-159570] p0073 N81-19395

COLD WELDING

- Method of cold welding using ion beam technology
[NASA-CASE-LBN-12982-1] p0081 N81-19455

COLLECTORS

U ACCUMULATORS

COLLISIONS

NET BIRD-AIRCRAFT COLLISIONS

COLOMBIA

- Highlights of NASA/DOE photovoltaics market
assessment visit to Colombia
[NASA-TN-84011] p0138 N81-32081

COLOR CODING

- Application of computer generated color graphic
techniques to the processing and display of
three dimensional fluid dynamic data
[NASA-TN-82658] p0119 N81-29782

COMBINED CYCLE POWER GENERATION

- Comparison of Integrated Gasifier-Combined Cycle
and AFB-steam turbine systems for industrial
cogeneration
[NASA-TN-82648] p0106 N81-28522

COMBUSTION

NET FUEL COMBUSTION

NET HYDROCARBON COMBUSTION

- Ultra-lean combustion at high inlet temperatures
[NASA-TN-81640] p0097 N81-14398

COMBUSTION CHAMBERS

- Pressure spectra and cross spectra at an area
contraction in a ducted combustion system
[ASME PAPER 80-C2/AT80-5] p0077 N81-18638
- Requirements and preliminary concept of a
Zero-Gravity Combustion Facility for Spacelab
[AIAA PAPER 81-1165] p0032 N81-20642
- Development of a low NO_x/lean premixed annular
combustor
[ASME PAPER 81-G1-40] p0020 N81-29954
- Low NO_x/and fuel flexible gas turbine combustors
[ASME PAPER 81-G1-99] p0020 N81-30006
- Design and preliminary results of a fuel flexible
industrial gas turbine combustor
[ASME PAPER 81-G1-108] p0087 N81-30013
- Low NO_x/combustion systems for burning heavy
residual fuels and high-fuel-bound nitrogen fuels
[ASME PAPER 81-G1-109] p0089 N81-30014
- Evaluation of advanced combustors for dry NO_x/
suppression with nitrogen bearing fuels in
utility and industrial gas turbines
[ASME PAPER 81-G1-125] p0087 N81-30029
- Design and development of the combustor inlet
diffuser for the NASA/G1 energy efficient engine
[ASME PAPER 81-G1-129] p0020 N81-30033
- Evaluation of concepts for controlling exhaust
emissions from minimally processed petroleum and
synthetic fuels
[ASME PAPER 81-G1-157] p0067 N81-30056
- The E3 combustors - Status and challenges
[AIAA PAPER 81-1353] p0023 N81-42176
- Energy efficient engine diffuser/combustor model
technology
[NASA-CR-165157] p0026 N81-15002
- Analysis of pressure spectra measurements in a
ducted combustion system
[NASA-TN-81583] p0125 N81-15768

Combustor liner durability analysis

- [NASA-CR-165250] p0027 N81-17079
 - Spectral flame radiance from a tubular-can combustor
[NASA-TN-1722] p0016 N81-19121
 - Heat pipes to reduce engine exhaust emissions
[NASA-CASE-LBN-12590-1] p0049 N81-19245
 - Analysis of effect of flameholder characteristics
on lean, premixed, partially vaporized fuel-air
mixtures quality and nitrogen oxides emissions
[NASA-TN-1842] p0016 N81-24065
 - Selected results from combustion research at the
Lewis Research Center
[NASA-TN-82627] p0017 N81-25083
 - Small gas-turbine combustor study: Fuel injector
evaluation
[NASA-TN-82641] p0018 N81-26146
 - The E3 combustors: Status and challenges ---
energy efficient turbofan engines
[NASA-TN-82684] p0018 N81-28095
- COMBUSTION CONTROL**
- Low NO_x/combustion systems for burning heavy
residual fuels and high-fuel-bound nitrogen fuels
[ASME PAPER 81-G1-109] p0089 N81-30014
- COMBUSTION EFFICIENCY**
- Low NO_x/and fuel flexible gas turbine combustors
[ASME PAPER 81-G1-99] p0020 N81-30006
 - Selected results from combustion research at the
Lewis Research Center
[AIAA PAPER 81-1392] p0022 N81-40859
 - The E3 combustors - Status and challenges
[AIAA PAPER 81-1353] p0023 N81-42176
 - Modular instrumentation system for real-time
measurements and control on reciprocating engines
[NASA-TN-1757] p0071 N81-11315
 - Catalytic combustion of coal-derived liquids
[NASA-TN-81594] p0097 N81-14396
 - Experimental evaluation of catalytic combustion
with heat removal at near stoichiometric
conditions
[NASA-TN-81748] p0103 N81-23609
 - Analysis of effect of flameholder characteristics
on lean, premixed, partially vaporized fuel-air
mixtures quality and nitrogen oxides emissions
[NASA-TN-1842] p0016 N81-24065
 - Effects of fuel-injector design on ultra-lean
combustion performance
[NASA-TN-82624] p0104 N81-24533
 - Small gas-turbine combustor study: Fuel injector
evaluation
[NASA-TN-82641] p0018 N81-26146
- COMBUSTION INSTABILITY**
- U COMBUSTION STABILITY**
- COMBUSTION PHYSICS**
- Overview study of combustion experiments in a
space laboratory
p0032 N81-46059
 - An overview of general aviation propulsion
research programs at NASA Lewis Research Center
[NASA-TN-81666] p0015 N81-16052
 - Combustion of solid carbon rods in zero and normal
gravity
[NASA-TN-81728] p0082 N81-22317
 - Selected results from combustion research at the
Lewis Research Center
[NASA-TN-82627] p0017 N81-25083
- COMBUSTION PRODUCTS**
- Synergistic erosion/corrosion of superalloys in
PFB coal combustor effluent
p0058 N81-44663
 - Ultra-lean combustion at high inlet temperatures
[NASA-TN-81640] p0097 N81-14398
 - Effect of fuel nitrogen and hydrogen content on
emissions in hydrocarbon combustion
[NASA-TN-81612] p0097 N81-14399
 - Deposition and material response from Mach 0.3
burner rig combustion of SBC 2 fuels
[NASA-TN-81634] p0051 N81-15069
 - Combustion system processes leading to corrosive
deposits
[NASA-TN-81752] p0101 N81-23243
 - Material response from Mach 0.3 burner rig
combustion of a coal-oil mixture
[NASA-TN-81686] p0055 N81-27258
- COMBUSTION STABILITY**
- Perturbation solutions of combustion instability
problems
[NASA-CR-159643] p0050 N81-16176
- COMBUSTORS**
- U COMBUSTION CHAMBERS**

COMMERCIAL AIRCRAFT

NT BORING 747 AIRCRAFT
 NT SUPERSONIC COMMERCIAL AIR TRANSPORT
 Performance deterioration of commercial
 high-bypass ratio turbofan engines
 [SAR PAPER 801118] p0021 A81-34154
 NASA Research in aeropropulsion p0142 A81-12980
 NASA Research in aeropropulsion
 [NASA-TN-81633] p0014 A81-13056
 Tabulations of ambient ozone data obtained by GASP
 airliners, March 1975 to December 1977
 [NASA-TN-81528] p0116 A81-13568
 Ozone contamination in aircraft cabins: Results
 from GASP data and analyses
 [NASA-TN-81671] p0009 A81-16021
 Analysis of atmospheric ozone levels at commercial
 airplane cruise altitudes in winter and spring,
 1976 - 1977 --- Global Atmospheric Sampling
 Program
 [NASA-TP-1807] p0117 A81-21685
 Advanced subsonic transport propulsion
 [NASA-TN-82696] p0019 A81-31195
 COMMERCIAL AVIATION
 U CIVIL AVIATION
 U COMMERCIAL AIRCRAFT
 COMMERCIAL ENERGY
 Status of commercial phosphoric acid fuel cell
 system development
 [NASA-TN-81641] p0096 A81-13464
 Study of fuel cell on-site, integrated energy
 systems in residential/commercial applications
 [NASA-CN-165144] p0112 A81-21533
 CORROSION
 Effect of milling and leaching on the structure of
 sintered silicon
 [NASA-TN-81602] p0060 A81-13166
 COMMUNICATION CABLES
 NT WAVEGUIDES
 COMMUNICATION EQUIPMENT
 NT SATELLITE TELEVISION
 COMMUNICATION NETWORKS
 Second year technical report on-board processing
 for future satellite communications systems
 [NASA-CN-165155] p0070 A81-10242
 COMMUNICATION SATELLITES
 NT COMMUNICATIONS TECHNOLOGY SATELLITE
 Modelling of environmentally induced discharges in
 geosynchronous satellites p0034 A81-19936
 Carrier - Interference ratios for frequency
 sharing between satellite systems transmitting
 frequency modulated and digital television signals
 p0069 A81-21911
 Advanced communications satellites
 [AAS PAPER 80-206] p0069 A81-33532
 Satellites using the 30/20 GHz band
 [NASA-TN-81600] p0069 A81-10241
 Second year technical report on-board processing
 for future satellite communications systems
 [NASA-CN-165155] p0070 A81-10242
 Next generation communications satellites:
 Multiple access and network studies
 [NASA-CN-165145] p0033 A81-12139
 K-band high power latching switch ---
 communication satellite system
 [NASA-CN-165159] p0073 A81-16389
 The 30/20 GHz experimental communications
 satellite system
 [NASA-TN-82683] p0035 A81-30172
 COMMUNICATION SYSTEMS
 U TELECOMMUNICATION
 COMMUNICATIONS TECHNOLOGY SATELLITE
 Applications Technology Satellite and
 Communications Technology Satellite user
 experiments for 1967 - 1980 reference book,
 volume 1
 [NASA-CN-165169-VOL-1] p0033 A81-12135
 Applications Technology Satellite and
 Communications Technology Satellite user
 experiments for 1967-1980 reference book, volume 2
 [NASA-CN-165169-VOL-2] p0033 A81-12136
 Applications Technology Satellite and
 Communications Technology Satellite user
 experiments for 1967-1980 reference book.
 Volume 3: User form surveys
 [NASA-CN-165169-VOL-3] p0033 A81-12137
 Applications Technology Satellite and
 Communications Technology Satellite user

experiments for 1967-1980 reference book.
 Volume 4: Abstracts
 [NASA-CN-165169-VOL-4] p0133 A81-12138
 COMBUSTION
 Electronically commutated dc motors for electric
 vehicles
 [NASA-TN-81654] p0097 A81-15464
 COMBUSTORS
 Electric vehicle motors and controllers
 [NASA-TN-81760] p0071 A81-21281
 COMPARISON
 Acceptance tests and manufacturer relationships
 for 20 ampere-hour sealed nickel-cadmium cells
 using discharge parameters
 [NASA-TN-81619] p0049 A81-17189
 COMPARTMENTS
 NT AIRCRAFT COMPARTMENTS
 NT ACOUSTIC CHAMBERS
 COMPONENT RELIABILITY
 Electric and hybrid vehicle system R/D
 [NASA-TN-81606] p0096 A81-11449
 Ceramic applications in turbine engines --- for
 improved component performance and reduced fuel
 usage
 [NASA-CN-159865] p0029 A81-19118
 COMPOSITE MATERIALS
 NT BORON REINFORCED MATERIALS
 NT CARBON FIBER REINFORCED PLASTICS
 NT CERAMICS
 NT FIBER COMPOSITES
 NT FIBER REINFORCED COMPOSITES
 NT GLASS FIBER REINFORCED PLASTICS
 NT GRAPHITE-EPOXY COMPOSITES
 NT GRAPHITE-POLYIMIDE COMPOSITES
 NT LAMINATES
 NT METAL MATRIX COMPOSITES
 NT POLYMER MATRIX COMPOSITES
 NT RESIN MATRIX COMPOSITES
 NT SUPERHYBRID MATERIALS
 A model for the acoustic impedance of linear
 suppressor materials bonded on perforated plate
 [AIAA PAPER 81-1999] p0129 A81-49741
 Completion of evaluation of manufacturing
 processes for B/A1 composites containing 0.2mm
 diameter boron fibers
 [NASA-TN-81573] p0051 A81-11111
 Progress in materials and structures at Lewis
 Research Center p0142 A81-12982
 Cost/benefit analysis of advanced materials
 technologies for future aircraft turbine engines
 [NASA-CN-165225] p0027 A81-15006
 Ultra-high modulus organic fiber hybrid composites
 [NASA-CN-165228] p0048 A81-21130
 Design concepts for low-cost composite turbofan
 engine frame
 [NASA-CN-165217] p0030 A81-22053
 COMPOSITE STRUCTURES
 NT LAMINATES
 Design, durability and low cost processing
 technology for composite fan exit guide vanes
 p0089 A81-22664
 Composite wall concept for high-temperature
 turbine shrouds - Heat transfer analysis
 [SAR PAPER 801138] p0021 A81-34169
 Contact law and impact responses of laminated
 composites
 [NASA-CN-159884] p0048 A81-12172
 Composite containment systems for jet engine fan
 blades
 [NASA-TN-81675] p0092 A81-17480
 Evaluation of a method for heat transfer
 measurements and thermal visualization using a
 composite of a heater element and liquid crystals
 --- thermal performance of turbine blade cooling
 configurations
 [NASA-TN-81639] p0075 A81-21313
 COMPOSITES
 U COMPOSITE MATERIALS
 COMPOSITION (PROPERTY)
 NT CHEMICAL COMPOSITION
 NT CONCENTRATION (COMPOSITION)
 COMPRESSIBILITY
 Solution of plane cascade flow using improved
 surface singularity methods --- application of
 panel method to internal aerodynamics
 [NASA-TN-81589] p0003 A81-14979
 COMPRESSIBILITY EFFECTS
 Full potential solution of a transonic quasi-3-D

- flow through a cascade using artificial compressibility
[ASME PAPER 81-21-70] p0006 A81-1 179
- COMPRESSIBLE FLOW**
- NT TRANSONIC FLOW**
- Inlet flow distortion in turbomachinery
[ASME PAPER 80-67-20] p0005 A81-17952
- Acoustic transmission matrix of a variable area duct or nozzle carrying a compressible subsonic flow
p0128 A81-22533
- Solution of plane cascade flow using improved surface singularity methods
[ASME PAPER 81-67-169] p0006 A81-30068
- A three-dimensional turbulent compressible subsonic duct flow analysis for use with constructed coordinate systems
[NASA-CR-3389] p0077 A81-20383
- COMPRESSING**
- Mechanical bonding of metal
[NASA-CR-12941-1] p0068 A81-16329
- COMPRESSOR BLADES**
- Core compressor exit stage study. Volume 3: Data and performance report for screening test configurations
[NASA-CR-159499] p0024 A81-12086
- Core compressor exit stage study. Volume 2: Data and performance report for the baseline configuration
[NASA-CR-159498] p0027 A81-16051
- COMPRESSOR MOTORS**
- Holographic flow visualization of time-varying shock waves
p0072 A81-47642
- Core compressor exit stage study. Volume 3: Data and performance report for screening test configurations
[NASA-CR-159499] p0024 A81-12086
- Rotor redesign for a highly loaded 1800 ft/sec tip speed fan, 2
[NASA-CR-159879] p0024 A81-12087
- COMPRESSORS**
- NT SUPERCHARGERS**
- NT TRANSONIC COMPRESSORS**
- NT TURBOCOMPRESSORS**
- Program to develop sprayed, plastically deformable compressor shroud seal materials
[NASA-CR-165237] p0088 A81-17438
- COMPUTATION**
- Generation of C-type cascade grids for viscous flow computation
p0122 A81-14721
- COMPUTATIONAL FLUID DYNAMICS**
- A rapid method for the approximate determination of nonlinear solutions Application to aerodynamic flows
p0007 A81-11628
- Turbulent solution of the Navier-Stokes equations
p0077 A81-19284
- Finite element analysis of inviscid subsonic boattail flow
[AIAA PAPER 81-0276] p0006 A81-20831
- Numerical techniques in linear duct acoustics - A status report
[ASME PAPER 80-WA/HC-2] p0127 A81-21120
- Calculation of three-dimensional turbulent subsonic flows in transition ducts
p0008 A81-21199
- Calculation of the flow field in supersonic inlets using a bi-characteristics method with shock wave fitting
p0006 A81-21212
- Solution of plane cascade flow using improved surface singularity methods
[ASME PAPER 81-67-169] p0006 A81-30068
- Some aspects of calculating flows about three-dimensional subsonic inlets
[AIAA PAPER 81-1361] p0007 A81-42177
- Numerical simulation of flows in curved diffusers with cross-sectional transition using a three-dimensional viscous analysis
[NASA-TN-81672] p0074 A81-15239
- Geometric methods in computational fluid dynamics --- turbomachinery
p0075 A81-18331
- A three-dimensional turbulent compressible subsonic duct flow analysis for use with constructed coordinate systems
[NASA-CR-3389] p0077 A81-20383
- A rapid perturbation procedure for determining nonlinear flow solutions: Application to transonic turbomachinery flows
[NASA-CR-3425] p0001 A81-22013
- Fundamental heat transfer research for gas turbine engines
[NASA-CR-2178] p0016 A81-24063
- Some aspects of calculating flows about three-dimensional subsonic inlets
[NASA-TN-82678] p0004 A81-28054
- COMPUTER COMPATIBLE TAPES**
- EBOS to universal tape conversion processor
[A81-10074] p0095 A81-13430
- Limited Area Coverage/High Resolution Picture Transmission, LAC/HREPT tape conversion processor user's manual
[A81-10077] p0095 A81-13433
- COMPUTER GRAPHICS**
- Simulation and visualization of face seal motion stability by means of computer generated movies
p0087 A81-38059
- Synthetic battery cycling
[NASA-TN-81757] p0049 A81-25168
- Application of computer generated color graphic techniques to the processing and display of three dimensional fluid dynamic data
[NASA-TN-82658] p0119 A81-29782
- COMPUTER METHODS**
- U COMPUTER PROGRAMS**
- COMPUTER PROGRAMMING**
- MASTRAN level 16 programmer's manual updates for aeroelastic analysis of bladed discs
[NASA-CR-155825] p0093 A81-19482
- COMPUTER PROGRAMS**
- NT MASTRAN**
- Some modifications to, and operational experiences with, the two-dimensional, finite-difference, boundary-layer code, STAN5
[ASME PAPER 81-GT-89] p0077 A81-29996
- Computer code for intraply hybrid composite design
p0047 A81-44662
- Performance seeking controls
p0014 A81-12092
- F100 multivariable control synthesis program: A review of full scale engine altitude tests --- F100 engine
p0014 A81-12093
- Numerical trials of HISS2
[A81-10069] p0094 A81-13425
- Limited Area Coverage/High Resolution Picture Transmission (LAC/HREPT) data vegetative index calculation processor user's manual
[A81-10073] p0094 A81-13429
- A four-cylinder Stirling engine controls model
[NASA-TN-81648] p0075 A81-15241
- Analytical investigation of efficiency and performance limits in klystron amplifiers using multidimensional computer programs; multi-stage depressed collectors; and theraionic cathode life studies
p0098 A81-16552
- Computer program documentation for the dynamic analysis of a noncontacting mechanical face seal
[NASA-TN-81636] p0081 A81-17435
- MASTRAN level 16 demonstration manual updates for aeroelastic analysis of bladed discs
[NASA-CR-159826] p0093 A81-19483
- The NASA-LeRC wind turbine sound prediction code
[NASA-TN-81737] p0100 A81-21537
- MEGA16 - Computer program for analysis and extrapolation of stress-rupture data
[NASA-TP-1809] p0102 A81-23486
- Computer code for intraply hybrid composite design
[NASA-TN-82593] p0046 A81-25151
- KONFIG and BEKONFIG: Two interactive preprocessing to the Navy/NASA Engine Program (NNEP)
[NASA-TN-82636] p0120 A81-25698
- GRID30: Computer program for fast generation of multilevel, three-dimensional boundary-conforming O-type computational grids
[NASA-TP-1920] p0005 A81-31128
- Computer program for pulsed thermocouples with corrections for radiation effects
[NASA-TP-1895] p0120 A81-33838
- Computer program to predict aircraft noise levels
[NASA-TP-1913] p0127 A81-33947
- COMPUTER SIMULATION**
- U COMPUTERIZED SIMULATION**

COMPUTER STORAGE DEVICES

NT COMPUTER COMPATIBLE TAPES

NT MAGNETIC DISKS

COMPUTERIZED CONTROL

U NUMERICAL CONTROL

COMPUTERIZED DESIGN

Computer-aided roll pass design in rolling of
airfoil shapes

p0088 A81-15796

Simulation and visualization of face seal action
stability by means of computer generated movies

p0087 A81-38059

Computer code for intraply hybrid composite design

p0047 A81-44662

K-band high power latching switch ---
communication satellite system

p0073 A81-16389

Performance of computer-designed small-sized
four-stage depressed collector for operation of
dual-node traveling wave tube

p0072 A81-30360

COMPUTERIZED SIMULATION

NT DIGITAL SIMULATION

Backward deletion to minimize prediction errors in
models from factorial experiments with zero to
six center points

p0122 A81-14999

The STD/HND codes - Comparison of analyses with
experiments at AEC/EPDR, Reynolds Metal Co.,
and Hercules, Inc. --- for HND generator flows

p0133 A81-20649

[AIAA PAPER 81-0173]

Interactive multi-node blade impact analysis

p0030 A81-29987

[ASME PAPER 81-GT-79]

An automated procedure for developing hybrid
computer simulations of turbofan engines

p0020 A81-32544

An approach to real-time simulation using parallel
processing

p0121 A81-44652

An automated procedure for developing hybrid
computer simulations of turbofan engines

p0037 A81-11688

[NASA-TN-81605]

Aerodynamic stability analysis of NASA
J85-13/planar pressure pulse generator
installation

p0027 A81-15004

[NASA-CR-165141]

Study of component technologies for fuel cell
on-site integrated energy systems

p0110 A81-15461

[NASA-CR-165152-VOL-1]

Study of component technologies for fuel cell
on-site integrated energy system. Volume 2:
Appendices

p0110 A81-15462

[NASA-CR-165152-VOL-2]

Propulsion system mathematical model for a
lift/cruise fan V/STOL aircraft

p0015 A81-16055

[NASA-TN-81663]

An approach to real-time simulation using parallel
processing

p0121 A81-21803

[NASA-TN-81731]

A computer simulation of the transient response of
a 4 cylinder Stirling engine with burner and air
preheater in a vehicle

p0078 A81-22313

[NASA-CR-165262]

KONFIG and REKNFIG: Two interactive
preprocessing to the Navy/NASA Engine Program
(NNEP)

p0120 A81-25658

[NASA-TN-82636]

Analysis of the charging of the SCATHA (P78-2)
satellite

p0033 A81-27169

[NASA-CR-165346]

Characterization, performance, and prediction of a
lead-acid battery under simulated electric
vehicle driving requirements

p0106 A81-28523

[NASA-TN-81771]

COMPUTERS

NT HYBRID COMPUTERS

CONCENTRATION (COMPOSITION)

Determination of optimum sunlight concentration
level in space for gallium arsenide solar cells

p0040 A81-26173

[NASA-TN-82643]

CONCENTRATION

The DOE photovoltaics program

p0143 A81-12989

CONDENSED RADIATORS

U HEAT RADIATORS

CONDITIONS

NT ADIABATIC CONDITIONS

NT FLIGHT CONDITIONS

CONDUCTORS

NT ELECTRIC CONDUCTORS

NT ION EXCHANGE MEMBRANE ELECTROLYTES

CONFERENCES

Propulsion Controls, 1979 --- air breathing engine
control

[NASA-CP-2137] p0014 A81-12090

Impact for the 80's: Proceedings of a Conference
on Selected Technology for Business and Industry

[NASA-CP-2149] p0142 A81-12978

Space Photovoltaic Research and Technology 1980.
High Efficiency, Radiation Damage and Blanket
Technology

[NASA-CP-2169] p0098 A81-17531

Fundamental heat transfer research for gas turbine
engines

[NASA-CP-2178] p0016 A81-24063

Aircraft Engine Diagnostics

[NASA-CP-2190] p0019 A81-31196

CONFLUENCE

U CONVERGENCE

CONSERVATION

NT ENERGY CONSERVATION

CONSTRUCTION MATERIALS

NASA's activities in the conservation of strategic
aerospace materials

[NASA-TN-81617] p0055 A81-29205

CONSUMPTION

NT ENERGY CONSUMPTION

NT FUEL CONSUMPTION

CONTACTS (ELECTRIC)

U ELECTRIC CONTACTS

CONTAINMENT

Composite containment systems for jet engine fan
blades

[NASA-TN-81675] p0092 A81-17480

CONTAMINANTS

NT TRACE CONTAMINANTS

CONTAMINATION

NT FUEL CONTAMINATION

CONTENT

Infrared spectroscopy for the determination of
hydrocarbon types in jet fuels

[NASA-TN-82674] p0066 A81-31380

CONTRACTION

Oxidation-induced contraction and strengthening of
boron fibers

[NASA-TN-82599] p0046 A81-25150

CONTROL EQUIPMENT

NT PRESSURE REGULATORS

CONTROL STABILITY

Apparatus for sensor failure detection and
correction in a gas turbine engine control system

[NASA-C/SE-LEM-12907-2] p0015 A81-19115

CONTROL SURFACES

NT GUIDE VANES

CONTROL THEORY

Propulsion Controls, 1979 --- air breathing engine
control

[NASA-CP-2137] p0014 A81-12090

Multivariable identification using centralized
fixed modes

p0014 A81-12091

F100 multivariable control synthesis program: A
review of full scale engine altitude tests ---
F100 engine

p0014 A81-12093

Design of a multivariable integrated control for a
supersonic propulsion system --- variable stream
control engine

p0025 A81-12094

Should we attempt global (inlet engine airframe)
control design?

p0025 A81-12097

Propulsion control and control theory: A new
research focus

p0014 A81-12099

Multivariable syquist array method with application
to turbofan engine control

p0026 A81-12101

Multivariable synthesis with transfer functions
--- applications to gas turbine engines

p0026 A81-12102

CONTROLLED ATMOSPHERES

NT CABIN ATMOSPHERES

CONTROLLERS

Electric vehicle motors and controllers

[NASA-TN-81760] p0071 A81-21281

SUBJECT INDEX

COMPLING

CONVAIR MILITARY AIRCRAFT

U MILITARY AIRCRAFT

CONVECTION

Forced and natural convection in laminaar-jet
diffusion flames --- normal-gravity,
inverted-gravity and zero-gravity flames
[NASA-TP-1841] p0076 N81-24388

CONVECTIVE FLOW

Thermal and flow analysis of a convection
air-cooled ceramic coated porous metal concept
for turbine vanes
[NASA-TN-81749] p0016 N81-22056

CONVERGENCE

Note on reflection and transmission coefficients
for converging-diverging ducts
[NASA-TN-82679] p0126 N81-30906

CONVEYMENT POSSIBILITIES

New interpretations of shock-associated noise with
and without screech
[NASA-TN-81590] p0125 N81-10807

CONVEYANCE

U V-STOL AIRCRAFT

COOLANTS

NT ENGINE COOLANTS

COOLING

NT AIR COOLING
NT FILM COOLING
NT MAGNETIC COOLING
NT SOLAR COOLING
NT SURFACE COOLING

Performance of jet- and inner-ring-lubricated 35
millimeter bore ball bearings operating to 2.5
million CM
[NASA-TP-1808] p0082 N81-19458

COOLING FILMS

Heat transfer coefficients for staggered arrays of
short pin fins
[ASME PAPER 81-GT-75] p0077 N81-29583

COOLING SYSTEMS

Heat exchanger and method of making
[NASA-CASE-LBN-12441-3] p0104 N81-24519

COORDINATE SYSTEMS

U COORDINATES

COORDINATE TRANSFORMATIONS

An electrostatic analog for generating cascade grids
p0122 N81-18695
Geometric methods in computational fluid dynamics
--- turbomachinery
p0075 N81-18331

A three-dimensional turbulent compressible
subsonic duct flow analysis for use with
constructed coordinate systems
[NASA-CN-3389] p0077 N81-20383

COORDINATES

Generation of C-type cascade grids for viscous
flow computation
p0122 N81-18721

COPLANARITY

High efficiency ultrathin coplanar back contact
cells
p0114 N81-27092

COPOLYMERS

Alkaline battery containing a separator of a
cross-linked copolymer of vinyl alcohol and
unsaturated carboxylic acid
[NASA-CASE-LBN-13102-1] p0107 N81-29531

COPPER

Simultaneous ion sputter polishing and deposition
[NASA-TN-81679] p0053 N81-19278

COPPER ALLOYS

NT HABBITY METAL

CORN

Normal crop calendars. Volume 2: The spring
wheat states of Minnesota, Montana, North
Dakota, and South Dakota
[N81-10070] p0094 N81-13426
Evaluation of results of US corn and soybeans
exploratory experiment: Classification
procedures verification test --- Missouri, Iowa,
Indiana, and Illinois
[N81-10076] p0095 N81-13432

CORPUSCULAR RADIATION

NT ELECTRON BEAMS

CORROSION

NT HOT CORROSION

NT SCALE (CORROSION)

Combustion system processes leading to corrosive
deposits
[NASA-TN-81752] p0101 N81-23243

Synergistic erosion/corrosion of superalloys in

PFB coal combustor effluent
[NASA-TN-81715] p0101 N81-23245

High temperature alkali corrosion in high velocity
gases
[NASA-TN-82591] p0054 N81-25191

CORROSION RESISTANCE

NT OXIDATION RESISTANCE

Thermal barrier coatings - Burner rig hot
corrosion test results
p0063 N81-12630

Synergistic erosion/corrosion of superalloys in
PFB coal combustor effluent
p0058 N81-44663

Self-lubricating composite materials
p0142 N81-12984

Development and testing of heat transport fluids
for use in active solar heating and cooling
systems
[NASA-TN-82395] p0098 N81-16584

Passivation of carbon steel through mercury
implantation
[NASA-CN-165292] p0059 N81-20244

Ceramic regenerator systems development program
[NASA-CN-165139] p0141 N81-22982

Corrosion resistant thermal barrier coating ---
protecting gas turbines and other engine parts
[NASA-CASE-LBN-13088-1] p0054 N81-25188

Hostile environmental conditions facing candidate
alloys for the automotive Stirling engine
[NASA-TN-82632] p0054 N81-26236

A program-management plan with critical-path
definition for Combustion Augmentation with
Thermionic Energy Conversion (CATEC)
[NASA-TN-82670] p0132 N81-30973

CORROSION TESTS

Thermal barrier coatings - Burner rig hot
corrosion test results
p0063 N81-12630

CORROSION

U ALUMINUM OXIDES

COST ANALYSIS

Cogeneration Technology Alternatives Study (CTAS)
Volume 5: Analytical approach and results
[NASA-CN-159763] p0109 N81-10517

Cost/benefit analysis of advanced materials
technology candidates for the 1980's, part 2
[NASA-CN-165176] p0139 N81-11953

Cost/benefit analysis of advanced materials
technologies for future aircraft turbine engines
[NASA-CN-165225] p0027 N81-15006

Analysis of costs of gallium arsenide and silicon
solar arrays for space power applications
[NASA-TP-1811] p0038 N81-20173

Assessment of disk MHD generators for a base load
powerplant
[NASA-TN-82609] p0103 N81-23611

Effect of voltage on the cost of an electric
vehicle propulsion system
[NASA-TN-82592] p0140 N81-26986

COST EFFECTIVENESS

Engineering management and innovation
p0036 N81-20400

Analysis of CAs and Si solar cell arrays for
earth orbital and orbit transfer missions
p0109 N81-27254

COST ESTIMATES

Modification of the ECAS reference steam power
generating plant to comply with the EPA 1979 new
source performance standards
[NASA-CN-159853] p0110 N81-13467

Effect of voltage on the cost of an electric
vehicle propulsion system
[NASA-TN-82592] p0140 N81-26986

COSTS

NT LIFE CYCLE COSTS

NT LCM COST

COTTON

Normal crop calendars. Volume 1: Assembly and
application of historical crop data to a
standard product
[N81-10075] p0095 N81-13431

COUPLED MODES

Perturbation solutions of combustion instability
problems
[NASA-CN-159643] p0050 N81-16176

COUPLING

The coupling between flow instabilities and
incident disturbances at a leading edge

- COVERINGS
- Evaluation of solar cell covers and encapsulant materials for space application p0111 N81-17568
- Electrostatic bonding of thin (approximately 3 mil) 7070 cover glass to Ta2O5 AB-coated thin (approximately 2 mil) silicon wafers and solar cells p0111 N81-17569
- CRACK FORMATION
- U CRACK INITIATION
- CRACK GROWTH
- On the equivalence between semiempirical fracture analyses and R-curves p0092 A81-18792
- CRACK INITIATION
- Cyclic behavior of turbine disk alloys at 650 C p0056 A81-12266
- Effect of tangential traction and roughness on crack initiation/propagation during rolling contact [NASA-TN-81608] p0080 N81-11395
- CRACK PROPAGATION
- On the equivalence between semiempirical fracture analyses and R-curves p0092 A81-18792
- Effect of tangential traction and roughness on crack initiation/propagation during rolling contact [NASA-TN-81608] p0080 N81-11395
- The fracture morphology of nickel-base superalloys tested in fatigue and creep-fatigue at 650 C [NASA-TN-81740] p0101 N81-23244
- CRACKING (FRACTURING)
- Method for estimating crack-extension resistance curve from residual strength data [NASA-TP-1753] p0091 N81-11417
- Experimental compliance calibration of the compact fracture toughness specimen [NASA-TN-81665] p0091 N81-16492
- CRACKS
- NT MICROCRACKS
- NT SURFACE CRACKS
- CRACKING
- U SURFACE CRACKS
- CREEP PROPERTIES
- Creep and residual mechanical properties of cast superalloys and oxide dispersion strengthened alloys [NASA-TP-1781] p0053 N81-19273
- CREEP RUPTURE STRENGTH
- Low-cost directionally-solidified turbine blades, volume 2 --- TFE731-3 turbofan engine [NASA-CN-159562] p0024 N81-12088
- MEGAT6 - Computer program for analysis and extrapolation of stress-rupture data [NASA-TP-1809] p0102 N81-23466
- Hostile environmental conditions facing candidate alloys for the automotive Stirling engine [NASA-TN-82632] p0054 N81-26236
- CRYSTALLITES
- U TRAVELING WAVE TUBES
- CRITERIA
- NT STRUCTURAL DESIGN CRITERIA
- CRITICAL FLOW
- Depressurization and two-phase flow of water containing high levels of dissolved nitrogen gas [NASA-TP-1839] p0076 N81-28389
- CRITICAL MACH NUMBER
- U CRITICAL VELOCITY
- CRITICAL REYNOLDS NUMBER
- U CRITICAL VELOCITY
- CRITICAL SPEED
- U CRITICAL VELOCITY
- CRITICAL VELOCITY
- Cold-air investigation of first stage of 4-1/2-stage, fan drive turbine with average stage-loading factor of 4.66 [NASA-TP-1780] p0015 N81-16050
- CROP CALENDARS
- Normal crop calendars. Volume 2: The spring wheat states of Minnesota, Montana, North Dakota, and South Dakota [881-10070] p0094 N81-13426
- Preliminary evaluation of the Environmental Research Institute of Michigan crop calendar shift algorithm for estimation of spring wheat development stage --- North Dakota, South Dakota, Montana, and Minnesota [881-10071] p0094 N81-13427
- Normal crop calendars. Volume 1: Assembly and application of historical crop data to a standard product [881-10075] p0095 N81-13431
- CROP IDENTIFICATION
- Numerical trials of HISSE [881-10069] p0094 N81-13425
- CROP INVENTORIES
- Limited Area Coverage/High Resolution Picture Transmission (LAC/HRPT) tape IJ grid pixel extraction processor user's manual [881-10072] p0094 N81-13428
- Limited Area Coverage/High Resolution Picture Transmission (LAC/HRPT) data vegetative index calculation processor user's manual [881-10073] p0094 N81-13429
- Evaluation of results of US corn and soybeans exploratory experiment: Classification procedures verification test --- Missouri, Iowa, Indiana, and Illinois [881-10076] p0095 N81-13432
- CROP INVENTORIES BY REMOTE SENSING
- U AGRISTARS PROJECT
- CROSS FLOW
- Analysis for predicting adiabatic wall temperatures with single hole coolant injection into a low speed crossflow [ASME PAPER 81-GT-91] p0077 A81-29998
- Influence of thermal boundary conditions on heat transfer from a cylinder in cross flow [NASA-TP-1894] p0076 N81-29384
- CROSSLINKING
- New ion exchange membranes --- composed of radiation crosslinked polyacrylic resins [NASA-TN-81670] p0044 N81-16123
- Inexpensive cross-linked polymeric separators made from water soluble polymers [NASA-TN-82619] p0101 N81-23205
- In-situ cross linking of polyvinyl alcohol --- application to battery separator films [NASA-CASE-LEW-13135-2] p0062 N81-24257
- Cross-linked polyvinyl alcohol and method of making same [NASA-CASE-LEW-13504-1] p0063 N81-27279
- Cross-linked polyvinyl alcohol and method of making same [NASA-CASE-LEW-13101-2] p0044 N81-29160
- Alkaline battery containing a separator of a cross-linked copolymer of vinyl alcohol and unsaturated carboxylic acid [NASA-CASE-LEW-13102-1] p0107 N81-29161
- CRUISING FLIGHT
- The supersonic fan engine - An advanced concept in supersonic cruise propulsion [AIAA PAPER 81-1599] p0023 A81-40973
- CRYOGENIC EQUIPMENT
- Traction drive for cryogenic boost pump --- hydrogen oxygen rocket engines [NASA-TN-81704] p0101 N81-23188
- CRYOGENIC FLUID STORAGE
- Shuttle compatible cryogenic liquid storage and supply systems [AIAA PAPER 81-1509] p0037 A81-42207
- CRYOGENIC FLUIDS
- NT LIQUID NITROGEN
- NT LIQUID OXYGEN
- CRYOGENIC ROCKET PROPELLANTS
- NT LIQUID FUELS
- High performance cryogenic engines for orbit transfer vehicles [IAF PAPER 80-P-253] p0043 A81-18363
- Low-thrust chemical propulsion system pump technology [NASA-CN-165210] p0088 N81-17437
- Conceptual design of an in-space cryogenic fluid management facility, executive summary [NASA-CN-165279-EXEC-SUMM] p0137 N81-21212
- Conceptual design of an in-space cryogenic fluid management facility [NASA-CN-165279] p0067 N81-21213
- CRYOGENICS
- Mechanical properties of weldments in experimental Fe-12Mn-0.2Ti and Fe-12Mn-18Co-0.2Ti alloys for cryogenic service p0058 A81-48143
- CRYSTAL DEFECTS
- NT VACANCIES (CRYSTAL DEFECTS)

CRYSTAL GROWTH
 NT DIRECTIONAL SOLIDIFICATION (CRYSTALS)
 CRYSTAL STRUCTURE
 Anisotropic tribological properties of silicon carbide
 [NASA-TN-81547] p0080 N81-11394
 Changes in surface chemistry of silicon carbide (0001) surface with temperature and their effect on friction
 [NASA-TP-1756] p0060 N81-14079
 CRYSTALLIZATION
 NT DIRECTIONAL SOLIDIFICATION (CRYSTALS)
 CRYSTALS
 NT DOPED CRYSTALS
 NT LIQUID CRYSTALS
 NT SINGLE CRYSTALS
 CURIE TEMPERATURE
 T-S diagram for gadolinium near the Curie temperature
 p0135 A81-43004
 CURING
 Lower-curing-temperature EEE polyimides
 [NASA-TN-81705] p0045 N81-17174
 Curing agent for polyepoxides and epoxy resins and composites cured therewith --- preventing carbon fiber release
 [NASA-CASE-LEW-15226-1] p0060 N81-17260
 CURRENT DENSITY
 Three-axis electron-beam test facility
 [NASA-TP-1836] p0071 N81-20359
 Catalyst surfaces for the chromous/chromic redox couple
 [NASA-CASE-LEW-13148-2] p0107 N81-29524
 CURRENT DISTRIBUTION
 Parasitic current losses due to solar electric propulsion generated plasmas
 [AIAA PAPER 81-0740] p0043 A81-29561
 Characterization, performance, and prediction of a lead-acid battery under simulated electric vehicle driving requirements
 [NASA-TN-81771] p0106 N81-28523
 Performance of computer-designed small-sized four-stage depressed collector for operation of dual-mode traveling wave tube
 [NASA-TP-1832] p0072 N81-30360
 CURTIS-WRIGHT MILITARY AIRCRAFT
 U MILITARY AIRCRAFT
 CURVATURE
 Surface geometry of circular cut spiral bevel gears
 [NASA-TN-82622] p0083 N81-26459
 CURVED SURFACES
 U SHAPES
 CUTTING
 NT MILLING (MACHINING)
 CYCLES
 NT STIRLING CYCLE
 NT THERMODYNAMIC CYCLES
 High temperature cyclic oxidation furnace testing at NASA Lewis Research Center
 [NASA-TN-81773] p0054 N81-26234
 CYCLIC LOADS
 Cyclic behavior of turbine disk alloys at 650 C
 p0056 A81-12266
 CYCLING
 U CYCLES
 CYCLOTRON RESONANCE DEVICES
 Gyrotr transmitting tube
 [NASA CASE-LEW-13429-1] p0071 N81-16384
 CYLINDRICAL AFTERBODIES
 U CYLINDRICAL RODS
 CYLINDRICAL RODS
 Heat transfer from a row of impinging jets to concave cylindrical surfaces
 p0078 A81-24924
 Influence of thermal boundary conditions on heat transfer from a cylinder in cross flow
 [NASA-TP-1894] p0076 N81-29384
 CYLINDROIDS
 U CYLINDRICAL RODS
 D
 DABNO (DATA ANALYSIS)
 U DATA PROCESSING
 U DATA TRANSMISSION
 DAMAGE
 NT RADIATION DAMAGE
 DAMPING
 NT VISCOUS DAMPING
 Miniature drag-force anemometer
 [NASA-TN-81680] p0079 N81-16428
 DAMPING FACTOR
 U DAMPING
 DAMPING IN FITCH
 U DAMPING
 DAMPING IN BOLL
 U DAMPING
 DAMPING IN TAN
 U DAMPING
 DART TURBOPROP ENGINES
 U TURBOPROP ENGINES
 DATA ACQUISITION
 Data acquisition and analysis in the DOE/NASA Wind Energy Program
 [NASA-TN-81603] p0096 N81-13463
 DATA ADAPTIVE EVALUATOR/MONITOR
 U DATA PROCESSING
 U DATA TRANSMISSION
 DATA ANALYSIS
 U DATA PROCESSING
 DATA BASES
 A methodology for the design and calibration of data based models of aggregate lake ecosystem dynamics
 p0111 N81-18482
 DATA CONVERSION ROUTINES
 Limited Area Coverage/High Resolution Picture Transmission, LAC/HRPT tape conversion processor user's manual
 [81-10077] p0095 N81-13433
 DATA PROCESSING
 NT PARALLEL PROCESSING (COMPUTERS)
 NT SIGNAL PROCESSING
 Preliminary evaluation of the Environmental Research Institute of Michigan crop calendar shift algorithm for estimation of spring wheat development stage --- North Dakota, South Dakota, Montana, and Minnesota
 [81-10071] p0094 N81-13427
 EGS to universal tape conversion processor
 [81-10074] p0095 N81-13430
 DATA PROCESSING EQUIPMENT
 NT HYBRID COMPUTERS
 An integrated exhaust gas analysis system with self-contained data processing and automatic calibration
 [NASA-TN-81592] p0102 N81-23435
 DATA PROCESSORS
 U DATA PROCESSING EQUIPMENT
 DATA SAMPLING
 Ozone contamination in aircraft cabins - Results from GASP data and analyses
 [AIAA PAPER 81-0305] p0010 A81-20740
 DATA TRANSMISSION
 Applications Technology Satellite and Communications Technology Satellite user experiments for 1967 - 1980 reference book, volume 1
 [NASA-CN-165169-VOL-1] p0033 N81-12135
 Applications Technology Satellite and Communications Technology Satellite user experiments for 1967-1980 reference book, volume 2
 [NASA-CN-165169-VOL-2] p0033 N81-12136
 Applications Technology Satellite and Communications Technology Satellite user experiments for 1967-1980 reference book, Volume 3: User form surveys
 [NASA-CN-165169-VOL-3] p0033 N81-12137
 DECAT
 NT ACOUSTIC EMISSION
 NT EXHAUST EMISSION
 NT SECONDARY EMISSION
 NT SPECTRAL EMISSION
 DECOMPOSITION
 NT RADICLYSIS
 DECOMPRESSION
 U PRESSURE REDUCTION
 DEFECTS
 NT SURFACE DEFECTS
 NT VACANCIES (CRYSTAL DEFECTS)
 DEFLATING
 U PRESSURE REDUCTION
 DEFLECTION
 A method of selecting grid size to account for Hertz deformation in finite element analysis of spur gears
 [NASA-TN-82623] p0083 N81-27525

DEFORMATION

NT ELASTIC DEFORMATION
NT PLASTIC DEFORMATION
Some effects of thermal-cycle-induced deformation
in rocket thrust chambers
[NASA-TP-1834] p0038 N81-20176

DEICERS
Evaluation of a pneumatic boot deicing system on a
general aviation wing model
[NASA-TN-82363] p0011 N81-25065

DEICING
Pneumatic boot for helicopter rotor deicing
p0009 N81-19059
Evaluation of a pneumatic boot deicing system on a
general aviation wing model
[NASA-TN-82363] p0011 N81-25065

DEICING SYSTEMS
U DEICERS
DELAMINATING
Completion of evaluation of manufacturing
processes for B/AI composites containing 0.2mm
diameter boron fibers
[NASA-TN-81573] p0051 N81-11111

DENSITY (MASS/VOLUME)
NT ATMOSPHERIC DENSITY
DENSITY (RATE/AREA)
U FLOW DENSITY
DEPENDENCE
NT TEMPERATURE DEPENDENCE
NT TIME DEPENDENCE
DEPOSITION
NT ELECTROLESS DEPOSITION
NT ELECTROPLATING
NT VAPOR DEPOSITION
Deposition and material response from Mach 0.3
burner rig combustion of SRC 2 fuels
[NASA-TN-81634] p0051 N81-15069
Ion beam deposited protective films
[NASA-TN-81722] p0038 N81-19221
Simultaneous ion sputter polishing and deposition
[NASA-TN-81679] p0053 N81-19278
Diagnostic system design for the Ion Auxiliary
Propulsion System (IAPS). Flight tests of two 8
cm mercury ion
[NASA-TN-81702] p0037 N81-20172
Combustion system processes leading to corrosive
deposits
[NASA-TN-81752] p0101 N81-23243

DEPRESSURIZATION
U PRESSURE REDUCTION
DESIGN ANALYSIS
Analysis and design of an adaptive multi-loop
controlled two winding buck/boost regulator
p0073 N81-21675
Factors influencing the predicted performance of
advanced propeller designs
[AIAA PAPER 81-1564] p0007 N81-42210
NASA contributions to radial turbine aerodynamic
analyses
[NASA-TN-81644] p0003 N81-13019
Modification of the ECAS reference steam power
generating plant to comply with the EPA 1979 new
source performance standards
[NASA-CR-159853] p0110 N81-13467
Energy efficient engine diffuser/combustor model
technology
[NASA-CR-165157] p0026 N81-15002
Cold-air investigation of first stage of
4-1/2-stage, fan drive turbine with average
stage-loading factor of 4.66
[NASA-TP-1780] p0015 N81-16050
Off-design analysis of a gas turbine powerplant
augmented by steam injection using various fuels
[NASA-TN-81611] p0098 N81-16571
Design of spur gears for improved efficiency
[NASA-TN-81625] p0081 N81-17436
Development program on a cold cathode electron gun
[NASA-CR-159570] p0073 N81-19395
Conceptual design of the MED Engineering Test
Facility
[NASA-TN-82621] p0132 N81-24926
System safety in Stirling engine development
[NASA-TN-82615] p0140 N81-24994
Overview: DOE/NASA automotive gas turbine and
stirling projects
[NASA-TN-82637] p0105 N81-25467
Optimal tooth numbers for compact standard spur
gear sets
[NASA-TN-82614] p0083 N81-27524

Effects of blade-vane ratio and rotor-stator
spacing of fan noise with forward velocity
[NASA-TN-82690] p0126 N81-31956

DESIGN OF EXPERIMENTS
U EXPERIMENTAL DESIGN
DETECTION
NT ULTRASONIC FLAW DETECTION
DEVELOPING NATIONS
Market definition study of photovoltaic power for
remote villages in developing countries
[NASA-CR-159880] p0110 N81-14391

DIAGRAMS
U CRYOGENIC EQUIPMENT
DIAGRAMS
NT BLOCK DIAGRAMS
NT NIQUIST DIAGRAM
DIAMINES
Influence of excess diamine on properties of PHR
polyimide resins and composites
p0047 N81-43635
Phosphazene diamines
[NASA-CR-165147] p0065 N81-10169

DIAMONDS
Electron spectroscopy of the diamond surface
p0130 N81-27031
Effect of electronic structure of the diamond
surface on the strength of the diamond-metal
interface
[NASA-TN-82714] p0063 N81-32269

DIELECTRIC PERMEABILITY
Anion permselective membrane
[NASA-CR-165223] p0111 N81-16583

DIES
Sputtered protective coatings for die casting dies
p0057 N81-38067
Sputtered protective coatings for die casting dies
[NASA-TN-81735] p0053 N81-21173

DIESEL ENGINES
Comparisons of four alternative powerplant types
for future general aviation aircraft
[NASA-TN-81584] p0013 N81-10067
Vehicle testing of Cummins turbocompound diesel
engine
[NASA-CR-155840] p0140 N81-13803

DIESEL FUELS
NT LIQUID FUELS
Ultra-lean combustion at high inlet temperatures
[NASA-TN-81640] p0097 N81-14398

DIFFERENTIAL EQUATIONS
A rapid method for the approximate determination
of nonlinear solutions Application to
aerodynamic flows
p0007 N81-11628

DIFFERENTIAL GEOMETRY
NT TENSOR ANALYSIS
Surface geometry of circular cut spiral bevel gears
[NASA-TN-82622] p0083 N81-26459

DIFFERENTIAL OPERATORS
U DIFFERENTIAL EQUATIONS
DIFFERENTIAL THERMAL ANALYSIS
Lower-curing-temperature PHR polyimides
[NASA-TN-81705] p0045 N81-17174

DIFFUSERS
Design and development of the combustor inlet
diffuser for the NASA/GE energy efficient engine
[ASME PAPER 81-GT-129] p0020 N81-30033
Performance prediction of straight two dimensional
diffusers
[NASA-CR-165186] p0133 N81-11833

DIFFUSION
Ion plating for the future
[NASA-TN-82630] p0054 N81-25189

DIFFUSION EFFECT
U DIFFUSION
DIFFUSION FLAMES
Forced and natural convection in laminar-jet
diffusion flames --- normal-gravity,
inverted-gravity and zero-gravity flames
[NASA-TP-1841] p0076 N81-24388

DIFFUSIVITY
A new diffusion-inhibited oxidation-resistant
coating for superalloys
[NASA-TN-82687] p0056 N81-33273

DIPLOMO COMPOUNDS
NT ICLETETRAFLUOROETHYLENE
DIGITAL SIMULATION
A nonlinear propulsion system simulation technique
for piloted simulators
p0022 N81-38064

- A nonlinear propulsion system simulation technique
for piloted simulators
[NASA-TN-82600] p0101 N81-23085
- DIGITAL SYSTEMS**
Propulsion controls p0025 N81-12095
- Future Air Force aircraft propulsion control
systems: The extended summary paper p0025 N81-12096
- DIGITAL TELEVISION**
Carrier - Interference ratios for frequency
sharing between satellite systems transmitting
frequency modulated and digital television signals p0069 A81-21911
- DIMENSIONAL STABILITY**
UT STRUCTURAL STABILITY
- DIMENSIONS**
UT FILM THICKNESS
- DIODES**
UT CESIUM DIODES
- DIOXIDES**
UT CARBON DIOXIDE
UT SILICON DIOXIDE
- DIRECT POWER GENERATORS**
UT ALKALINE BATTERIES
UT FUEL CELLS
UT MAGNETOHYDRODYNAMIC GENERATORS
UT NICKEL ZINC BATTERIES
UT SOLAR CELLS
UT THERMIONIC CONVERTERS
UT THERMOELECTRIC GENERATORS
- DIRECTIONAL SOLIDIFICATION (CRYSTALS)**
Development of low-cost directionally-solidified
turbine blades p0088 A81-10707
- The effect of thermal cycling to 1100 C on the
alpha /beta/ phase in directionally solidified
gamma/gamma-prime-alpha alloys p0057 A81-32546
- Low-cost directionally-solidified turbine blades,
volume 2 --- TPE731-3 turbofan engine
[NASA-CR-159562] p0024 N81-12088
- Advanced aircraft engine materials trends
[NASA-TN-82626] p0055 N81-27259
- DIRECTORIES**
U INDEXES (DOCUMENTATION)
- DISCHARGERS**
UT STATIC DISCHARGERS
- DISHES**
U PARABOLIC REFLECTORS
- DISKS (SHAPES)**
UT ACTUATOR DISKS
- DISPERSION PRECIPITATION HARDENING**
U PRECIPITATION HARDENING
- DISPERSIONS**
Dynamics of solid dispersions in oil during the
lubrication of point contacts. Part 1: Graphite
[NASA-TN-81683] p0061 N81-17264
- Dynamics of solid dispersions in oil during the
lubrication of point of contacts. Part 2:
Molybdenum disulfide
[NASA-TN-81709] p0062 N81-20275
- DISPLAY DEVICES**
UT DRAG FORCE ANEMOMETERS
- DISSIPATION**
UT ENERGY DISSIPATION
- DISSOCIATION**
UT GAS DISSOCIATION
- DISSOLUTION**
U DISSOLVING
- DISSOLVED GASES**
Depressurization and two-phase flow of water
containing high levels of dissolved nitrogen gas
[NASA-TP-1839] p0076 N81-28385
- DISSOLVING**
Dissolution of bulk specimens of silicon nitride
p0065 A81-42024
- DISTORTION**
UT FLOW DISTORTION
- DISTRIBUTION (PROPERTY)**
UT CURRENT DISTRIBUTION
UT FLOW DISTRIBUTION
UT HOLE DISTRIBUTION (ELECTRONICS)
UT HOLE DISTRIBUTION (MECHANICS)
UT LOAD DISTRIBUTION (FORCES)
UT PRESSURE DISTRIBUTION
UT STRESS CONCENTRATION
UT VELOCITY DISTRIBUTION
- DISTURBANCE THEORY**
U PERTURBATION THEORY
- DISULFIDES**
Moderate temperature sodium cells. I - Transition
metal disulfide cathodes p0113 A81-15027
- DOCUMENTATION**
Bibliography of Lewis Research Center Technical
Publications announced in 1979
[NASA-TN-81525] p0137 N81-17942
- DOCUMENTS**
UT BIBLIOGRAPHIES
UT USER MANUALS (COMPUTER PROGRAMS)
- DOMESTIC ENERGY**
Design description of the Schuchuli Village
photovoltaic power system
[NASA-TN-82650] p0094 N81-28517
- DOMESTIC SATELLITE COMMUNICATIONS SYSTEMS**
Satellites using the 30/20 GHz band
[NASA-TN-81600] p0069 N81-10241
- DOPED CRYSTALS**
Radiation damage in lithium-copperdoped N/P
silicon solar cells p0109 A81-27204
- DOPING (ADDITIVES)**
U ADDITIVES
- DOUGLAS MILITARY AIRCRAFT**
U MILITARY AIRCRAFT
- DRAG FORCE ANEMOMETERS**
Miniature drag-force anemometer
[NASA-TN-81680] p0079 N81-16428
- DRAG REDUCTION**
Pneumatic boot for helicopter rotor deicing
p0009 N81-19059
- DRONE HELICOPTERS**
U HELICOPTERS
- DROP SIZE**
Acceleration wave breakup of liquid jets with
airstreams
[NASA-TN-81717] p0075 N81-21310
- Evaluation of a pneumatic boot deicing system on a
general aviation wing model
[NASA-TN-82363] p0011 N81-25065
- DROPS (LIQUIDS)**
A model for the analysis of
premixing-prevaporizing fuel-air mixing passages
[AIAA PAPER 81-0345] p0030 A81-20767
- Fuel injector characterization studies
[NASA-CR-165200] p0026 N81-15003
- DRY CELLS**
UT NICKEL ZINC BATTERIES
- DTA (ANALYSIS)**
U DIFFERENTIAL THERMAL ANALYSIS
- DUCT GEOMETRY**
Numerical simulation of flows in curved diffusers
with cross-sectional transitioning using a
three-dimensional viscous analysis
[NASA-TN-81672] p0074 N81-15239
- On the propagation of long waves in acoustically
treated, curved ducts
[NASA-TN-81712] p0125 N81-19875
- Note on reflection and transmission coefficients
for converging-diverging ducts
[NASA-TN-82679] p0126 N81-30906
- DUCTED FLOW**
UT KNUDSEN FLOW
- Calculation of three-dimensional turbulent
subsonic flows in transition ducts p0008 A81-21199
- Acoustic transmission matrix of a variable area
duct or nozzle carrying a compressible subsonic
flow
[NASA-TN-81614] p0125 N81-12821
- NASA contributions to radial turbine aerodynamic
analyses
[NASA-TN-81644] p0003 N81-13019
- Analysis of pressure spectra measurements in a
ducted combustion system
[NASA-TN-81583] p0125 N81-15768
- Prediction of laminar and turbulent primary and
secondary flows in strongly curved ducts
[NASA-CR-3388] p0007 N81-16976
- A three-dimensional turbulent compressible
subsonic duct flow analysis for use with
constructed coordinate systems
[NASA-CR-3389] p0077 N81-20383
- DUCTED PROPELLERS**
U SHROUDED PROPELLERS

DUCTS

NT ACOUSTIC DUCTS
 NT AIR DUCTS
 Note on reflection and transmission coefficients
 for converging-diverging ducts
 [NASA-TN-82679] p0126 N81-30906
 High B-field, large area ratio MHD duct experiments
 [NASA-TN-82673] p0132 N81-32026
DURABILITY
 Endurance tests with large-bore tapered-roller
 bearings to 2.2 million LM
 [NASA-TN-82669] p0084 N81-29439
DYNAMIC CHARACTERISTICS
 NT AERODYNAMIC STABILITY
 NT COMBUSTION STABILITY
 NT CONTROL STABILITY
 NT DYNAMIC STABILITY
 NT FLOW CHARACTERISTICS
 NT FLOW DISTRIBUTION
 NT FLOW STABILITY
 NT FLOW VELOCITY
 NT MAGNETOHYDRODYNAMIC STABILITY
 NT MOTION STABILITY
 NT ROTARY STABILITY
 NT TRANSIENT RESPONSE
 Dynamic characteristics of a high-speed rotor with
 radial and axial roll-bearing supports
 [ASME PAPER 80-C2/LUB-35] p0085 N81-18683
DYNAMIC LOADS
 NT AERODYNAMIC LOADS
 NT CYCLIC LOADS
 NT ROLLING CONTACT LOADS
 NT THRUST LOADS
DYNAMIC MODELS
 Stability of large horizontal-axis axisymmetric
 wind turbines
 p0092 N81-22526
 A methodology for the design and calibration of
 data based models of aggregate lake ecosystem
 dynamics
 p0111 N81-18482
DYNAMIC PROPERTIES
 U DYNAMIC CHARACTERISTICS
DYNAMIC RESPONSE
 NT TRANSIENT RESPONSE
 Contact law and impact responses of laminated
 composites
 [NASA-CN-159884] p0048 N81-12172
 Combustor liner durability analysis
 [NASA-CN-165250] p0027 N81-17079
 Computer program documentation for the dynamic
 analysis of a noncontacting mechanical face seal
 [NASA-TN-81636] p0081 N81-17435
DYNAMIC STABILITY
 NT AERODYNAMIC STABILITY
 NT COMBUSTION STABILITY
 NT CONTROL STABILITY
 NT FLOW STABILITY
 NT MAGNETOHYDRODYNAMIC STABILITY
 NT MOTION STABILITY
 NT ROTARY STABILITY
 Kinematic correction for roller skewing
 [ASME PAPER 80-CET-76] p0085 N81-18647
DYNAMIC STRUCTURAL ANALYSIS
 Effects of mistuning on bending-torsion flutter
 and response of a cascade in incompressible flow
 [AIAA 81-0602] p0092 N81-29465
 Interactive multi-mode blade impact analysis
 [ASME PAPER 81-GT-79] p0030 N81-29987
 Structural dynamics verification facility study
 [NASA-TN-82675] p0092 N81-33497
E
EARTH ORBITS
 Analysis of costs of gallium arsenide and silicon
 solar arrays for space power applications
 [NASA-TP-1811] p0038 N81-20173
EARTH SATELLITES
 NT ATS
 NT COMMUNICATION SATELLITES
 NT COMMUNICATIONS TECHNOLOGY SATELLITE
 NT SCATHA SATELLITE
 NT SOLAR POWER SATELLITES
 NT SYNCHRONOUS SATELLITES
ECONOMIC ANALYSIS
 An economic systems analysis of land mobile radio
 telephone services
 p0069 N81-22528

An economic systems analysis of land mobile radio
 telephone services
 [NASA-TN-81476] p0069 N81-10239
ECOSYSTEMS
 A methodology for the design and calibration of
 data based models of aggregate lake ecosystem
 dynamics
 p0111 N81-18482
EDDIES
 U VORTICES
EDGES
 NT LEADING EDGES
 NT TRAILING EDGES
EFFECTIVENESS
 NT COST EFFECTIVENESS
EFFICIENCY
 NT CHARGE EFFICIENCY
 NT COMBUSTION EFFICIENCY
 NT ENERGY CONVERSION EFFICIENCY
 NT POWER EFFICIENCY
 NT PROPELLER EFFICIENCY
 NT PROPULSIVE EFFICIENCY
 NT THERMODYNAMIC EFFICIENCY
 Electric vehicle motors and controllers
 [NASA-TN-81760] p0071 N81-21281
EFFLUENTS
 Synergistic erosion/corrosion of superalloys in
 FFB coal combustor effluent
 [NASA-TN-81715] p0101 N81-23245
EIGENVALUES
 Stability of large horizontal-axis axisymmetric
 wind turbines
 p0092 N81-22526
 On the propagation of long waves in acoustically
 treated, curved ducts
 p0128 N81-38060
ELASTIC ANISOTROPY
 Theoretical model applicable to the experimental
 determination of surface anchoring energies of
 nematic liquid crystals
 [NASA-TN-81628] p0124 N81-12817
ELASTIC BODIES
 Continuous analysis of stresses from arbitrary
 surface loads on a half space
 p0053 N81-14162
 Simplified solution for stresses and
 deformation
 [NASA-TN-82647] p0084 N81-28444
ELASTIC CONSTANTS
 U ELASTIC PROPERTIES
ELASTIC DEFORMATION
 Simplified solution for stresses and deformation
 [NASA-TN-82647] p0084 N81-28444
ELASTIC PROPERTIES
 NT ANISOTROPY
 NT ANISOTROPY
 NT AEROELASTICITY
 NT AEROELASTICITY
 Structural dynamics verification facility study
 [NASA-TN-82675] p0092 N81-33497
ELASTIC STABILITY
 U DAMPING
ELASTIC WAVES
 NT AERODYNAMIC NOISE
 NT AIRCRAFT NOISE
 NT CAPILLARY WAVES
 NT COHERENT ACOUSTIC RADIATION
 NT ENGINE NOISE
 NT JET AIRCRAFT NOISE
 NT SHOCK WAVES
 NT SOUND WAVES
 NT STRESS WAVES
ELASTICITY
 U ELASTIC PROPERTIES
ELASTICISMS
 U PLASTICISMS
ELASTODYNAMICS
 NT ELASTOHYDRODYNAMICS
ELASTOHYDRODYNAMICS
 Some limitations in applying classical BHD film
 thickness formulas to a high-speed bearing
 [ASME PAPER 80-C2/LUB-13] p0068 N81-18667
 Lubrication of rolling element bearings
 p0086 N81-18738
 Elastohydrodynamic lubrication of elliptical
 contacts
 [NASA-TN-81647] p0080 N81-13358
 Measurement of rod seal lubrication for Stirling
 engine
 [NASA-CN-165158] p0088 N81-13359
 History of ball bearings
 [NASA-TN-81689] p0081 N81-18391

- Introduction to ball bearings
[NASA-TN-81690] p0081 N81-18392
- Lubrication fundamentals
[NASA-TN-81762] p0103 N81-23490
- ELASTOMERS**
- Circumferential shaft seal
[NASA-CASE-LEN-12119-2] p0083 N81-26447
- ELECTRIC AUTOMOBILES**
- Effect of voltage on the cost of an electric vehicle propulsion system
[NASA-TN-82592] p0140 N81-26986
- ELECTRIC BATTERIES**
- NT ALKALINE BATTERIES
- NT LEAD ACID BATTERIES
- NT NICKEL CADMIUM BATTERIES
- NT NICKEL ZINC BATTERIES
- NT REDOX CELLS
- NT SILVER ZINC BATTERIES
- NT SODIUM SULFUR BATTERIES
- NT STORAGE BATTERIES
- Acceptance tests and manufacturer relationships from the 20A standard cell data p0100 N81-21515
- In-situ cross linking of polyvinyl alcohol --- application to battery separator films
[NASA-CASE-LEN-13135-2] p0062 N81-24257
- Synthetic battery cycling
[NASA-TN-81757] p0049 N81-25168
- Effect of voltage on the cost of an electric vehicle propulsion system
[NASA-TN-82592] p0140 N81-26586
- ELECTRIC CHARGE**
- NT SPACE CHARGE
- ELECTRIC CHOPPERS**
- Response of nickel to zinc cells to electric vehicle chopper discharge waveforms
[NASA-TN-81713] p0103 N81-23608
- ELECTRIC CIRCUITS**
- U CIRCUITS
- ELECTRIC CONDUCTORS**
- The HEVAC pilot line experience p0111 N81-17574
- ELECTRIC CONTACTS**
- Coplanar back contacts for thin silicon solar cells
[NASA-CR-165272] p0112 N81-18495
- Fabrication and testing of polyvinylidene fluoride capacitors
[NASA-CR-159501] p0073 N81-22278
- ELECTRIC CONTROL**
- Control of volume resistivity in inorganic-organic separators --- for alkaline batteries p0108 N81-11034
- ELECTRIC CURRENT**
- NT ALTERNATING CURRENT
- NT ELECTRIC DISCHARGES
- NT GAS DISCHARGES
- NT LIGHTNING
- NT RADIO FREQUENCY DISCHARGE
- ELECTRIC DISCHARGES**
- NT GAS DISCHARGES
- NT LIGHTNING
- NT RADIO FREQUENCY DISCHARGE
- Modelling of environmentally induced discharges in geosynchronous satellites p0034 N81-19936
- Effect of hole geometry and Electric-Discharge Machining (EDM) on airflow rates through small diameter holes in turbine blade material
[NASA-TP-1716] p0013 N81-12089
- Environmental charging effects monitors for operational satellites
[NASA-TN-81669] p0037 N81-17127
- Response of nickel to zinc cells to electric vehicle chopper discharge waveforms
[NASA-TN-81713] p0103 N81-23608
- ELECTRIC ENERGY STORAGE**
- Response of nickel to zinc cells to electric vehicle chopper discharge waveforms
[NASA-TN-81713] p0103 N81-23608
- Toroidal cell and battery --- storage battery for high amp-hour load applications
[NASA-CASE-LEN-12918-1] p0104 N81-24521
- ELECTRIC FIELD STRENGTH**
- Analysis of the charging of the SCATHA (P78-2) satellite
[NASA-CR-165348] p0033 N81-27169
- ELECTRIC FIELDS**
- Particle and field measurements on two J-series 30 centimeter thrusters
- [NASA-TN-81741] p0039 N81-22084
- ELECTRIC GENERATORS**
- NT AC GENERATORS
- NT ALKALINE BATTERIES
- NT FUEL CELLS
- NT MAGNETOHYDRODYNAMIC GENERATORS
- NT NICKEL ZINC BATTERIES
- NT SOLAR CELLS
- NT SOLAR GENERATORS
- NT THERMIONIC CONVERTERS
- NT THERMOELECTRIC GENERATORS
- NT TURBOGENERATORS
- Large wind turbines: A utility option for the generation of electricity p0142 N81-12981
- Samarium cobalt (SMCO) generator/engine integration study
[AD-A092904] p0029 N81-17087
- ELECTRIC HYBRID VEHICLES**
- Impact for the 80's: Proceedings of a Conference on Selected Technology for Business and Industry
[NASA-CP-2149] p0142 N81-12978
- Propulsion system research and development for electric and hybrid vehicles p0142 N81-12985
- The Federal electric and hybrid vehicle program p0142 N81-12986
- JPL's electric and hybrid vehicles project: Project activities and preliminary test results --- power conditioning and battery charge efficiency p0143 N81-12987
- Design studies of continuously variable transmissions for electric vehicles
[NASA-TN-81642] p0080 N81-13357
- A methodology for fostering commercialization of electric and hybrid vehicle propulsion systems
[NASA-TN-81575] p0140 N81-18933
- Advanced propulsion system concept for hybrid vehicles
[NASA-CR-159772] p0140 N81-18935
- Advanced continuously variable transmissions for electric and hybrid vehicles
[NASA-TN-81718] p0082 N81-19459
- Results of the ETV-1 breadboard tests under steady-state and transient conditions --- conducted in the NASA-LaRC Road Load Simulator
[NASA-TN-82667] p0108 N81-31627
- ELECTRIC MOTOR VEHICLES**
- Electric and hybrid vehicle system R/D
[NASA-TN-81606] p0096 N81-11449
- Impact for the 80's: Proceedings of a Conference on Selected Technology for Business and Industry
[NASA-CP-2149] p0142 N81-12978
- Propulsion system research and development for electric and hybrid vehicles p0142 N81-12985
- The Federal electric and hybrid vehicle program p0142 N81-12986
- Small passenger car transmission test: Dodge Omni A-404 transmission
[NASA-CR-165181] p0088 N81-15366
- Electronically commutated dc motors for electric vehicles
[NASA-TN-81654] p0097 N81-15464
- Characterization of the near-term electric vehicle (ETV-1) breadboard propulsion system over the SAE J227a driving schedule D
[NASA-TN-81664] p0097 N81-15465
- A methodology for fostering commercialization of electric and hybrid vehicle propulsion systems
[NASA-TN-81575] p0140 N81-18933
- Characterization, performance, and prediction of a lead-acid battery under simulated electric vehicle driving requirements
[NASA-TN-81771] p0106 N81-28523
- Continuously variable transmission: Assessment of applicability to advance electric vehicles
[NASA-TN-82700] p0085 N81-33484
- ELECTRIC MOTORS**
- Electric vehicle motors and controllers
[NASA-TN-81760] p0071 N81-21281
- Effect of voltage on the cost of an electric vehicle propulsion system
[NASA-TN-82592] p0140 N81-26986
- ELECTRIC POTENTIAL**
- NT OPEN CIRCUIT VOLTAGE
- Laboratory evaluation of a pilot cell battery protection system for photovoltaic applications

- [NASA-TN-81714] p0104 N81-24536
Effect of voltage on the cost of an electric
vehicle propulsion system
[NASA-TN-82592] p0140 N81-26986
- ELECTRIC POWER CONVERSION**
U ELECTRIC GENERATORS
ELECTRIC POWER PLANTS
Status of commercial phosphoric acid fuel cell
system development
[AIAA PAPER 81-0396] p0108 N81-20805
Coal gasifier cogeneration powerplant project
[NASA-TN-81706] p0143 N81-12988
Engineering support for magnetohydrodynamic power
plant analysis and design studies
[NASA-CR-159690] p0110 N81-13466
Modification of the RCAS reference steam power
generating plant to comply with the EPA 1979 new
source performance standards
[NASA-CR-159853] p0110 N81-13467
Performance calculations for 1000 MWe MHD/steam
power plants
[NASA-TN-81667] p0098 N81-16570
Off-design analysis of a gas turbine powerplant
augmented by steam injection using various fuels
[NASA-TN-81611] p0098 N81-16571
Performance calculations for 200-1000 MWe
MHD/steam power plants
[NASA-TN-81775] p0100 N81-22476
Assessment of disk MHD generators for a base load
powerplant
[NASA-TN-82609] p0103 N81-23611
Conceptual design of the MHD Engineering Test
Facility
[NASA-TN-82621] p0132 N81-24926
A MHD channel study for the ETP conceptual design
[NASA-TN-81764] p0132 N81-24927
- ELECTRIC POWER SUPPLIES**
NT SPACECRAFT POWER SUPPLIES
Simplified power supplies for ion thrusters
[AIAA PAPER 81-0693] p0040 N81-29542
Extended operating range of the 30-cm ion thruster
with simplified power processor requirements
[AIAA PAPER 81-0692] p0040 N81-32897
Review of stand-alone photovoltaic application
projects sponsored by US DOE and US AID
[NASA-TN-81738] p0100 N81-22477
Effect of voltage on the cost of an electric
vehicle propulsion system
[NASA-TN-82592] p0140 N81-26986
- ELECTRIC POWER TRANSMISSION**
Design description of the Schuchuli Village
photovoltaic power system
[NASA-TN-82650] p0094 N81-28517
- ELECTRIC PROPULSION**
NT ELECTROSTATIC PROPULSION
NT ION PROPULSION
NT PLASMA PROPULSION
NT SOLAR ELECTRIC PROPULSION
Free radical propulsor concept
[AIAA PAPER 81-0676] p0041 N81-32905
Electric and hybrid vehicle system R/D
[NASA-TN-81606] p0096 N81-11449
Analysis of costs of gallium arsenide and silicon
solar arrays for space power applications
[NASA-TN-1811] p0038 N81-20173
Ion beam applications research. A summary of
Lewis Research Center Programs
[NASA-TN-81721] p0044 N81-21129
The electric rail gun for space propulsion
[NASA-CR-165312] p0042 N81-22078
SENT 2 thrusters: Still ticking after eleven years
[NASA-TN-81774] p0040 N81-26174
A case history of technology transfer
[NASA-TN-82618] p0040 N81-30182
Results of the BTU-1 breadboard tests under
steady-state and transient conditions ---
conducted in the NASA-LeRC Road load Simulator
[NASA-TN-82667] p0108 N81-31627
- ELECTRIC ROCKET ENGINES**
NT ELECTROSTATIC ENGINES
NT ION ENGINES
NT MERCURY ION ENGINES
NT RIT ENGINES
SENT II 1980 extended flight thruster experiments
[AIAA PAPER 81-0665] p0040 N81-29528
SENT II 1980 extended flight thruster experiments
[NASA-TN-81685] p0038 N81-19222
- ELECTRICAL CONDUCTIVITY**
U ELECTRICAL RESISTIVITY
- ELECTRICAL LEADS**
U ELECTRICAL CONDUCTORS
ELECTRICAL MEASUREMENT
Environmental charging effects monitors for
operational satellites p0037 N81-38057
Specifying and calibrating instrumentation for
wideband electronic power measurements --- in
switching circuits
[NASA-TN-81545] p0079 N81-16429
Characteristics of 30-centimeter mercury ion
thrusters
[NASA-TN-81706] p0039 N81-21121
- ELECTRICAL PROPERTIES**
NT CARRIER MOBILITY
NT ELECTRICAL RESISTIVITY
NT ELECTRON MOBILITY
NT PHOTOVOLTAIC EFFECT
The STD/MHD codes - Comparison of analyses with
experiments at AEDC/HPDE, Reynolds Metal Co.,
and Hercules, Inc --- for MHD generator flows
[AIAA PAPER 81-0173] p0133 N81-20649
- ELECTRICAL RESISTIVITY**
Control of volume resistivity in inorganic-organic
separators --- for alkaline batteries
p0108 N81-11034
Silicon solar cells with high open-circuit voltage
p0113 N81-27089
High voltage V-groove solar cell
[NASA-CASE-LEW-13401-1] p0098 N81-16529
Performance of high resistivity n++p silicon
solar cells under 1 MeV electron irradiation
[NASA-TN-82610] p0103 N81-23626
Effect of electronic structure of the diamond
surface on the strength of the diamond-metal
interface
[NASA-TN-82714] p0063 N81-32269
- ELECTRICITY**
NT ALTERNATING CURRENT
Market definition study of photovoltaic power for
remote villages in developing countries
[NASA-CR-159880] p0110 N81-14391
- ELECTRIFICATION**
Review of stand-alone photovoltaic application
projects sponsored by US DOE and US AID
[NASA-TN-81738] p0100 N81-22477
- ELECTRO-OPTICS**
High temperature electronic requirements in
aeropropulsion systems p0072 N81-32547
High temperature electronic requirements in
aeropropulsion systems
[NASA-TN-81682] p0071 N81-16388
- ELECTROCATALYSTS**
Preparation and evaluation of advanced
electrocatalysts for phosphoric acid fuel cells
[NASA-CR-165179] p0111 N81-17527
Preparation and evaluation of advanced
electrocatalysts for phosphoric acid fuel cells
[NASA-CR-165245] p0112 N81-18496
Non-noble catalysts and catalyst supports for
phosphoric acid fuel cells
[NASA-CR-165221] p0112 N81-18497
Stabilizing platinum in phosphoric acid fuel cells
[NASA-CR-165311] p0113 N81-22473
Zirconium carbide as an electrocatalyst for the
chromous/chronic redox couple
[NASA-CASE-LEW-13246-1] p0049 N81-26203
- ELECTROCHEMICAL CELLS**
NT ALKALINE BATTERIES
NT ELECTRIC BATTERIES
NT FUEL CELLS
NT LEAD ACID BATTERIES
NT NICKEL CADMIUM BATTERIES
NT NICKEL ZINC BATTERIES
NT REDOX CELLS
NT SILVER ZINC BATTERIES
NT SODIUM SULFUR BATTERIES
NT STORAGE BATTERIES
Improvement and scale-up of the NASA Redox storage
system
[NASA-TN-81632] p0049 N81-13105
- ELECTROCHEMICAL OXIDATION**
Method for depositing an oxide coating ---
producing solar panels
[NASA-CASE-LEW-13131-1] p0054 N81-24230
- ELECTROCHEMISTRY**
Anion permselective membrane
[NASA-CR-165223] p0111 N81-16583

Technology development for phosphoric acid fuel
cell powerplant (phase 2)
[NASA-CR-165316] p0113 N81-21547

Synthetic battery cycling
[NASA-TN-81757] p0049 N81-25168

ELECTRODEPOSITION
NT ELECTROPLATING

ELECTRODES
NT CATHODES
NT COLD CATHODES
NT HOLLOW CATHODES
NT PLASMA ELECTRODES
NT THERMIONIC CATHODES

Electron reflection and secondary emission
characteristics of sputter-textured pyrolytic
graphite surfaces
[NASA-TN-81755] p0062 N81-22193

Toroidal cell and battery --- storage battery for
high amp-hour load applications
[NASA-CASE-LEW-12918-1] p0104 N81-24521

Additive for zinc electrodes
[NASA-CASE-LEW-13286-1] p0105 N81-27557

Catalyst surfaces for the chromous/chromic redox
couple
[NASA-CASE-LEW-13148-2] p0107 N81-29524

Preparation and characterization of electrodes for
the NASA Redox storage system
[NASA-TN-82702] p0107 N81-30522

Design and assembly considerations for Redox cells
and stacks
[NASA-TN-82672] p0049 N81-31308

ELECTROGENERATORS
U ELECTRIC GENERATORS

ELECTROHYDRAULIC CONTROL
U ELECTRIC CONTROL

ELECTROLESS DEPOSITION
An experimental investigation of silicon wafer
surface roughness and its effect on the full
strength of plated metals
[NASA-TN-81763] p0100 N81-22478

ELECTROLYTES
NT ION EXCHANGE MEMBRANE ELECTROLYTES

ELECTROLYTIC CELLS
Toroidal cell and battery --- storage battery for
high amp-hour load applications
[NASA-CASE-LEW-12918-1] p0104 N81-24521

ELECTROMAGNETIC FIELDS
NT NEAR FIELDS
NT SYSTEM GENERATED ELECTROMAGNETIC PULSES

ELECTROMAGNETIC PROPAGATION
U ELECTROMAGNETIC WAVE TRANSMISSION

ELECTROMAGNETIC PROPERTIES
NT ELECTRICAL PROPERTIES
NT OPTICAL PROPERTIES
NT PHOTOVOLTAIC EFFECT
NT RADIANCE
NT TRANSPARENCY
Characteristics of 30-centimeter mercury ion
thrusters
[NASA-TN-81706] p0039 N81-21121

ELECTROMAGNETIC PULSES
NT SYSTEM GENERATED ELECTROMAGNETIC PULSES

ELECTROMAGNETIC PUMPS
Pumping power considerations in the designs of
NASA-Redox flow cells
[NASA-TN-82598] p0106 N81-28519

ELECTROMAGNETIC RADIATION
NT SUBMILLIMETER WAVES
NT SUNLIGHT
NT SYSTEM GENERATED ELECTROMAGNETIC PULSES

ELECTROMAGNETIC WAVE TRANSMISSION
NT MICROWAVE TRANSMISSION
NT TELEVISION TRANSMISSION
Gyrotron transmitting tube
[NASA-CASE-LEW-13429-1] p0071 N81-16384

ELECTRON BEAMS
Electron spectroscopy of the diamond surface
p0130 A81-27031

Three-axis electron-beam test facility
[NASA-TP-1836] p0071 N81-20359

Analytical prediction and experimental
verification of performance at various operating
conditions of a dual-node traveling wave tube
with multistage depressed collectors
[NASA-TP-1811] p0072 N81-28352

ELECTRON COLLISIONS
U ELECTRON SCATTERING

ELECTRON COMPOUNDS
U INTERMETALLICS

ELECTRON EMISSION
NT SECONDARY EMISSION

ELECTRON FLUX
U ELECTRONS
U FLUX (RATE)

ELECTRON GUNS
Development program on a cold cathode electron gun
[NASA-CR-159570] p0073 N81-19395

ELECTRON INTERACTIONS
U ELECTRON SCATTERING

ELECTRON IRRADIATION
Radiation damage in lithium-counterdoped N/P
silicon solar cells
p0109 A81-27204

GaAs shallow-homojunction solar cells
[NASA-CR-165167] p0110 N81-15463

Radiation damage in silicon NIP solar cells
p0099 N81-17557

Performance of high resistivity n⁺pp⁺ silicon
solar cells under 1 MeV electron irradiation
[NASA-TN-82610] p0103 N81-23626

ELECTRON MOBILITY
The effect of minority carrier mobility variations
on solar cell spectral response
[NASA-TN-82604] p0103 N81-23625

ELECTRON PLASMA
Fluid model of plasma outside a hollow cathode
neutralizer
[AIAA PAPER 81-0739] p0134 A81-29560

ELECTRON RADIATION
NT ELECTRON BEAMS

ELECTRON SCATTERING
Electron reflection and secondary emission
characteristics of sputter-textured pyrolytic
graphite surfaces
p0065 A81-38065

ELECTRON SPECTROSCOPY
Electron spectroscopy of the diamond surface
p0130 A81-27031

ELECTRON TRANSFER
Fluid model of plasma outside a hollow cathode
neutralizer
[AIAA PAPER 81-0739] p0134 A81-29560

ELECTRON TUBES
NT KLYSTRONS
NT MICROWAVE TUBES
NT TRAVELING WAVE TUBES
Gyrotron transmitting tube
[NASA-CASE-LEW-13429-1] p0071 N81-16384

Ion sputter textured graphite --- applications to
electron tube devices
[NASA-CASE-LEW-12919-1] p0046 N81-27198

ELECTRONIC AMPLIFIERS
U AMPLIFIERS

ELECTRONIC EQUIPMENT
NT CESIUM DIODES
NT ELECTRONIC MODULES
NT PHOTOVOLTAIC CELLS
NT SEMICONDUCTOR DEVICES
NT THYRISTORS
NT TRANSISTORS
High temperature electronic requirements in
aeropropulsion systems
p0072 A81-32547

Environmental charging effects monitors for
operational satellites
p0037 A81-38057

ELECTRONIC EQUIPMENT TESTS
Three-axis electron-beam test facility
[NASA-TP-1836] p0071 N81-20359

ELECTRONIC MODULES
Recent developments in lightweight solar cell
modules --- with protective glass cover
p0099 N81-17571

Comparison of photovoltaic cell temperatures in
modules operating with exposed and enclosed back
surfaces
[NASA-TN-81769] p0106 N81-28520

ELECTRONIC STRUCTURE
U ATOMIC STRUCTURE

ELECTRONIC SWITCHES
U SWITCHING CIRCUITS

ELECTRONS
Environmental charging effects monitors for
operational satellites
[NASA-TN-81669] p0037 N81-17127

ELECTROPHYSICS
NT ELECTRO-OPTICS

ELECTROPLATING

An experimental investigation of silicon wafer surface roughness and its effect on the pull-strength of plated metals p0109 A81-38063

An experimental investigation of silicon wafer surface roughness and its effect on the full strength of plated metals [NASA-TN-81763] p0100 N81-22478

Method for depositing an oxide coating --- producing solar panels [NASA-CASE-LEN-13131-1] p0054 N81-24230

Method of forming oxide coatings [NASA-CASE-LEN-13132-1] p0106 N81-27616

Catalyst surfaces for the chromous/chromic redox couple [NASA-CASE-LEN-13148-2] p0107 N81-29524

ELECTROSTATIC BONDING

Electrostatic bonding of thin (cycle sine 3 mil) 7070 cover glass to Ta2O5 AR-coat. 4 thin (cycle sine 2 mil) silicon wafers and solar cells [NASA-CR-165240] p0111 N81-16582

Electrostatic bonding of thin (approximately 3 mil) 7070 cover glass to Ta2O5 AR-coated thin (approximately 2 mil) silicon wafers and solar cells p0111 N81-17569

ELECTROSTATIC ENGINES

Adapting magnetoelectrostatic containment to inert gas thrusters [AIAA PAPER 81-0140] p0043 A81-20625

Magnetoelectrostatic thruster physical geometry tests [AIAA PAPER 81-0753] p0044 A81-29566

ELECTROSTATIC FIELDS

O ELECTRIC FIELDS

ELECTROSTATIC PROBES

Development and design of three monitoring instruments for spacecraft charging [NASA-TP-1800] p0040 N81-31282

ELECTROSTATIC PROPULSION

ET ION PROPULSION

Free radical propulsion concept [NASA-TN-81770] p0039 N81-20180

ELEMENTARY PARTICLES

ET ELECTRONS

ELLIPTICITY

Elastohydrodynamic lubrication of elliptical contacts [NASA-TN-81647] p0020 N81-13358
Simplified solution for stresses and deformation [NASA-TN-82647] p0084 N81-28444

EMISSION

ET ACOUSTIC EMISSION

ET EXHAUST EMISSION

ET SECONDARY EMISSION

ET SPECTRAL EMISSION

EMITTERS

ET THERMIONIC CATHODES

ENCAPSULATING

Evaluation of solar cell covers and encapsulant materials for space application p0111 N81-17568

ENERGETIC PARTICLES

ET ARGON FLASH

ET ELECTRON PLASMA

ET ELECTRONS

ENERGY CONSERVATION

A status report on the Energy Efficient Engine Project [SAE PAPER 801119] p0021 A81-34155

Vehicle testing of Cummins turbocompound diesel engine [NASA-CR-159840] p0140 N81-13803

Energy efficient engine: flight propulsion system preliminary analysis and design [NASA-CR-159583] p0029 N81-18056

Ceramic applications in turbine engines --- for improved component performance and reduced fuel usage [NASA-CR-159865] p0029 N81-19118

Energy efficient engine flight propulsion system: Aircraft/engine integration evaluation [NASA-CR-159584] p0030 N81-22051

ENERGY CONSUMPTION

Study of fuel cell on-site, integrated energy systems in residential/commercial applications [NASA-CR-165144] p0112 N81-21533

ENERGY CONVERSION

ET PHOTOTHERMAL CONVERSION

ET SATELLITE SOLAR ENERGY CONVERSION

ET SOLAR ENERGY CONVERSION

Cogeneration Technology Alternatives Study (CTAS) Volume 5: Analytical approach and results [NASA-CR-159763] p0109 N81-10517
Energy overview p0142 N81-12979

Large wind turbines: A utility option for the generation of electricity p0142 N81-12981

Cell module and fuel conditioner [NASA-CR-165189] p0112 N81-18494

Cell module and fuel conditioner development [NASA-CR-165190] p0112 N81-19573

Thermionic Energy Conversion (TEC) topping thermoelectrics [NASA-TN-81677] p0132 N81-19920

Technology development for phosphoric acid fuel cell powerplant (phase 2) [NASA-CR-165316] p0113 N81-21547

The electric rail gun for space propulsion [NASA-CR-165312] p0042 N81-22078

Technology development for phosphoric acid fuel cell powerplant (phase 2) --- on site integrated energy systems [NASA-CR-165318] p0113 N81-22475

Conceptual design study of a coal gasification combined-cycle powerplant for industrial cogeneration [NASA-TN-81687] p0105 N81-25488

A program-management plan with critical-path definition for Combustion Augmentation with Thermionic Energy Conversion (CATEC) [NASA-TN-82670] p0132 N81-30973

ENERGY CONVERSION EFFICIENCY

Silicon solar cells with high open-circuit voltage p0113 N81-27089

High efficiency wraparound contact solar cells /HEWACS/ p0114 N81-27094

Space solar cells - High efficiency and radiation damage p0108 N81-27174

Status of commercial phosphoric acid fuel cell system development [NASA-TN-81641] p0096 N81-13464

GaAs shallow-homojunction solar cells [NASA-CR-165167] p0110 N81-15463

Off-design analysis of a gas turbine powerplant augmented by steam injection using various fuels [NASA-TN-81611] p0098 N81-16571

Thermionic Energy Conversion (TEC) topping thermoelectrics [NASA-TN-81677] p0132 N81-19920

ENERGY DENSITY

O FLUX DENSITY

ENERGY DISSIPATION

The effect of solar array voltage patterns on plasma power losses p0043 A81-19937

Loss model for off-design performance analysis of radial turbines with pivoting-vane, variable-area stators [SAE PAPER 801135] p0021 A81-34166

Core compressor exit stage study. Volume 2: Data and performance report for the baseline configuration [NASA-CR-159498] p0027 N81-16051

ENERGY LEVELS

ET MOLECULAR ENERGY LEVELS

ENERGY LOSSES

O ENERGY DISSIPATION

ENERGY POLICY

Status of commercial phosphoric acid fuel cell system development [AIAA PAPER 81-0396] p0108 A81-20805

Large wind-turbine projects in the United States wind energy program p0108 A81-23694

Automotive Stirling engine development program [NASA-CR-165134] p0139 N81-11952

Energy overview p0142 N81-12979

JPL's electric and hybrid vehicles project: Project activities and preliminary test results --- power conditioning and battery charge efficiency

Coal gasifier cogeneration powerplant project p0143 N81-12987
 The DOE photovoltaics program p0143 N81-12988
 Solar photovoltaics: Stand alone applications --- NASA Lewis Research Center research and development p0143 N81-12989
 Data acquisition and analysis in the DOE/NASA Wind Energy Program [NASA-TN-81603] p0096 N81-13463
 Status of commercial phosphoric acid fuel cell system development [NASA-TN-81641] p0096 N81-13464
 Vehicle testing of Cummins turbocompound diesel engine [NASA-CR-159840] p0140 N81-13803
 Analytical investigation of efficiency and performance limits in klystron amplifiers using multidimensional computer programs; multi-stage depressed collectors; and thermionic cathode life studies p0098 N81-16552
 Off-design analysis of a gas turbine powerplant augmented by steam injection using various fuels [NASA-TN-81611] p0098 N81-16571
 Coplanar back contacts for thin silicon solar cells [NASA-CR-165272] p0112 N81-18495
 Cell module and fuel conditioner development [NASA-CR-165190] p0112 N81-19573
 Technology development for phosphoric acid fuel cell powerplant (phase 2) [NASA-CR-165316] p0113 N81-21547
 Thermal energy storage for the Stirling engine powered automobile [NASA-CR-159561] p0113 N81-22467
 Assessment of disk MHD generators for a base load powerplant [NASA-TN-82609] p0103 N81-23611
 Tests of an overrunning clutch in a wind turbine [NASA-TN-82653] p0107 N81-29528
ENERGY SOURCES
 Photovoltaic applications - Past and future p0109 A81-27231
ENERGY STORAGE
HT ELECTRIC ENERGY STORAGE
HT HEAT STORAGE
 Improvement and scale-up of the NASA Redox storage system [NASA-TN-81632] p0049 N81-13105
 Atomic hydrogen storage method and apparatus [NASA-CASE-LEN-12081-3] p0066 N81-14103
 Preparation and evaluation of advanced electrocatalysts for phosphoric acid fuel cells [NASA-CR-165245] p0112 N81-18496
 NASA preprototype redox storage system for a photovoltaic stand-alone application [NASA-TN-82607] p0104 N81-24534
 Laboratory evaluation of a pilot cell battery protection system for photovoltaic applications [NASA-TN-81714] p0104 N81-24536
 Synthetic battery cycling [NASA-TN-81757] p0049 N81-25168
 Pumping power considerations in the designs of NASA-Redox flow cells [NASA-TN-82598] p0106 N81-28519
 Preparation and characterization of electrodes for the NASA Redox storage system [NASA-TN-82702] p0107 N81-30522
 Design and assembly considerations for Redox cells and stacks [NASA-TN-82672] p0049 N81-31308
 A Redox system design for solar storage applications [NASA-TN-82720] p0108 N81-32608
 Advances in membrane technology for the NASA redox energy storage system [NASA-TN-82701] p0108 N81-33601
ENERGY STORAGE DEVICES
U ENERGY STORAGE
ENERGY TECHNOLOGY
 Analytical investigation of critical phenomena in MHD power generators [NASA-CR-165143] p0109 N81-12546
 Impact for the 80's: Proceedings of a Conference on Selected Technology for Business and Industry [NASA-CP-2149] p0142 N81-12978
 Energy overview p0142 N81-12979

Status of commercial phosphoric acid fuel cell system development [NASA-TN-81641] p0096 N81-13464
 Market definition study of photovoltaic power for remote villages in developing countries [NASA-CR-159880] p0110 N81-14391
 Reliability and quality assurance on the MOD 2 wind system [NASA-TN-82717] p0090 N81-33492
ENGINE ANALYSES
 Effect of time-dependent flight loads on turbofan engine performance deterioration [ASME PAPER 81-GT-203] p0030 A81-30093
 Modular instrumentation system for real-time measurements and control on reciprocating engines [NASA-TP-1757] p0071 N81-11315
ENGINE CONTROL
HT TURBOJET ENGINE CONTROL
 Simplified power supplies for ion thrusters [AIAA PAPER 81-0693] p0040 A81-29542
 Future challenges in V/STOL flight propulsion control integration [SAE PAPER 801140] p0022 A81-34170
 Turbomachinery noise studies of the AirResearch QCSAT engine with inflow control --- acoustic performance [AIAA PAPER 81-2049] p0023 A81-48621
 Propulsion Controls, 1979 --- air breathing engine control [NASA-CR-2137] p0014 N81-12090
 Multivariable identification using centralized fixed nodes p0014 N81-12091
 Performance seeking controls p0014 N81-12092
 F100 multivariable control synthesis program: A review of full scale engine altitude tests --- F100 engine p0014 N81-12093
 Design of a multivariable integrated control for a supersonic propulsion system --- variable stress control engine p0025 N81-12094
 Propulsion controls p0025 N81-12095
 Future Air Force aircraft propulsion control systems: The extended summary paper p0025 N81-12096
 Should we attempt global (inlet engine airframe) control design? p0025 N81-12097
 Road map to adaptive optimal control --- jet engine control p0025 N81-12098
 Propulsion control and control theory: A new research focus p0014 N81-12099
 Multivariable synthesis with transfer functions --- applications to gas turbine engines p0026 N81-12102
 Apparatus for sensor failure detection and correction in a gas turbine engine control system [NASA-CASE-LEN-12907-2] p0015 N81-19115
ENGINE COOLANTS
 Heat transfer from a row of impinging jets to concave cylindrical surfaces p0078 A81-24924
ENGINE DESIGN
HT ROCKET ENGINE DESIGN
 Design, durability and low cost processing technology for composite fan exit guide vanes p0089 A81-22664
 The future of aeronautical propulsion p0001 A81-29052
 Development of a low NO_x/ lean premixed annular combustor [ASME PAPER 81-GT-40] p0020 A81-29954
 Low NO_x/ and fuel flexible gas turbine combustors [ASME PAPER 81-GT-99] p0020 A81-30006
 Design and preliminary results of a fuel flexible industrial gas turbine combustor [ASME PAPER 81-GT-108] p0087 A81-30013
 Low NO_x/ combustion systems for burning heavy residual fuels and high-fuel-bound nitrogen fuels [ASME PAPER 81-GT-109] p0089 A81-30014
 Evaluation of advanced combustors for dry NO_x/ suppression with nitrogen bearing fuels in utility and industrial gas turbines [ASME PAPER 81-GT-125] p0087 A81-30029

- Design and development of the combustor inlet
diffuser for the NASA/G2 energy efficient engine
[ASME PAPER 81-GT-129] p0020 A81-30033
- Improved components for engine fuel savings
[SAE PAPER 801116] p0021 A81-34152
- A status report on the Energy Efficient Engine
Project
[SAE PAPER 801119] p0021 A81-34155
- Composite wall concept for high-temperature
turbine shrouds - Heat transfer analysis
[SAE PAPER 801139] p0021 A81-34169
- Selected results from combustion research at the
Lewis Research Center
[AIAA PAPER 81-1392] p0022 A81-40859
- The B3 combustors - Status and challenges
[AIAA PAPER 81-1353] p0023 A81-42176
- Low and high speed propellers for general aviation
- Performance potential and recent wind tunnel
test results
p0023 A81-42758
- An overview of general aviation propulsion
research programs at NASA-Lewis Research Center
[SAE PAPER 810624] p0023 A81-42778
- Automotive Stirling engine development program
[NASA-CR-165134] p0139 A81-11952
- Cost/benefit analysis of advanced materials
technology candidates for the 1980's, part 2
[NASA-CR-165176] p0139 A81-11953
- Road map to adaptive optimal control --- jet
engine control
p0025 A81-12098
- NASA contributions to radial turbine aerodynamic
analyses
[NASA-TN-81644] p0003 A81-13019
- Electric propulsion - characteristics,
applications, and status
[NASA-TN-81630] p0033 A81-13079
- Advanced Technology Spark-Ignition Aircraft Piston
Engine Design Study
[NASA-CR-165162] p0026 A81-13963
- An overview of general aviation propulsion
research programs at NASA Lewis Research Center
[NASA-TN-81666] p0015 A81-16052
- Propulsion system mathematical model for a
lift/cruise fan V/STOL aircraft
[NASA-TN-81663] p0015 A81-16055
- High-density fuel combustion and cooling
investigation --- engine design
[NASA-CR-165177] p0050 A81-16177
- JT8D-15/17 high pressure turbine root discharged
blade performance improvement --- engine design
[NASA-CR-165220] p0028 A81-17080
- Variable stream control engine for advanced
supersonic aircraft design update
p0001 A81-17996
- Progress with variable cycle engines
p0001 A81-17997
- Energy efficient engine: Flight propulsion system
preliminary analysis and design
[NASA-CR-159583] p0029 A81-18056
- Simplified power supplies for ion thrusters
[NASA-TN-81725] p0039 A81-20177
- Analytical design of an advanced radial turbine
--- automobile engines
[NASA-CR-165170] p0140 A81-20958
- Electric vehicle motors and controllers
[NASA-TN-81760] p0071 A81-21281
- Quiet Clean General Aviation Turbofan (QCGAT)
technology study, volume 1
[NASA-CR-164222] p0030 A81-22052
- Design concepts for low-cost composite turbofan
engine frame
[NASA-CR-165217] p0030 A81-22053
- System safety in Stirling engine development
[NASA-TN-82615] p0140 A81-24994
- Advanced subsonic transport propulsion
[NASA-TN-82696] p0019 A81-31195
- An introduction to NASA's turbine engine hot
section technology (HOST) project
p0019 A81-31206
- ENGINE FAILURE**
- High-response measurements of a turbofan engine
during nonrecoverable stall
[NASA-TN-81759] p0017 A81-25064
- ENGINE INLETS**
- Optimum subsonic, high-angle-of-attack naceller
p0005 A81-11646
- Three-dimensional turbulent boundary layer
development and separation in V/STOL engine
inlets at incidence with small-cross flow and
curvature influences
[AIAA PAPER 81-0254] p0005 A81-20703
- Design and development of the combustor inlet
diffuser for the NASA/G2 energy efficient engine
[ASME PAPER 81-GT-129] p0020 A81-30033
- Effect of a part-span variable inlet guide vane on
the performance of a high-bypass turbofan engine
[AIAA PAPER 81-1362] p0022 A81-40842
- Some aspects of calculating flows about
three-dimensional subsonic inlets
[AIAA PAPER 81-1361] p0007 A81-42177
- Low-speed aerodynamic performance of
50.8-centimeter-diameter noise-suppressing
inlets for the Quiet, Clean, Short-haul
Experimental Engine (QCEE) --- Lewis 9- by
15-foot low speed wind tunnel tests
[NASA-TP-1178] p0013 A81-11037
- Some aspects of calculating flows about
three-dimensional subsonic inlets
[NASA-TN-82678] p0004 A81-28054
- Fiber optics for aircraft engine/inlet control
[NASA-TN-82654] p0012 A81-31190
- Acoustic performance of inlet suppressors on an
engine generating a single mode
[NASA-TN-82697] p0127 A81-32968
- ENGINE MONITORING INSTRUMENTS**
- Experimental analysis of IMEP in a rotary
combustion engine --- Indicated Mean Effective
Pressure
[SAE PAPER 810150] p0079 A81-41732
- Modular instrumentation system for real-time
measurements and control on reciprocating engines
[NASA-TP-1757] p0071 A81-11315
- Engine diagnostics program: CP6-50 engine
performance deterioration
[NASA-CR-159867] p0024 A81-12085
- Aircraft Engine Diagnostics
[NASA-CR-2190] p0019 A81-31196
- ENGINE NOISE**
- Core noise measurements from a small, general
aviation turbofan engine
p0019 A81-22531
- A theoretical approach to sound propagation and
radiation for ducts with suppressors
p0128 A81-38061
- Comparison of predicted engine core noise with
proposed FAA helicopter noise certification
requirements
p0128 A81-38062
- New technique for the direct measurement of core
noise from aircraft engines
[AIAA PAPER 81-1587] p0128 A81-40962
- Turbomachinery noise studies of the AiResearch
QCGAT engine with inflow control --- acoustic
performance
[AIAA PAPER 81-2049] p0023 A81-48621
- Effects of blade-vane ratio and rotor-stator
spacing on fan noise with forward velocity
[AIAA PAPER 81-2032] p0024 A81-48628
- Comparison of predicted engine core noise with
current and proposed aircraft noise
certification requirements
[AIAA PAPER 81-2053] p0024 A81-48635
- Minor nozzle aeroacoustic characteristics for the
energy efficient engine
[AIAA PAPER 81-1994] p0128 A81-48639
- A model for the acoustic impedance of linear
suppressor materials bonded on perforated plate
[AIAA PAPER 81-1999] p0129 A81-49741
- Core noise measurements from a small, general
aviation turbofan engine
[NASA-TN-81610] p0125 A81-11769
- Analysis of pressure spectra measurements in a
ducted combustion system
[NASA-TN-81583] p0125 A81-15768
- Improved methods for fan sound field determination
[NASA-CR-165188] p0129 A81-15769
- VCE early acoustic test results of General
Electric's high-radius ratio conical plug nozzle
p0029 A81-17999
- Design of an exhaust mixer nozzle for the
Avco-Lycoming Quiet Clean General Aviation
Turbofan (QCGAT)
[NASA-CR-159426] p0029 A81-19120
- A theoretical approach to sound propagation and
radiation for ducts with suppressors
[NASA-TN-82612] p0130 A81-22837

- Comparison of predicted engine core noise with proposed FAA helicopter noise certification requirements
[NASA-TN-81739] p0130 N81-22839
- New technique for the direct measurement of core noise from aircraft engines --- YF 102 turbofan engine
[NASA-TN-82634] p0126 N81-26844
- Comparison of predicted engine core noise with current and proposed aircraft noise certification requirements
[NASA-TN-82659] p0126 N81-29922
- Effects of blade-vane ratio and rotor-stator spacing of fan noise with forward velocity
[NASA-TN-82690] p0126 N81-31956
- Acoustic performance of inlet suppressors on an engine generating a single mode
[NASA-TN-82697] p0127 N81-32968
- ENGINE PARTS**
- Thermal barrier coatings for heat engine components
p0056 A81-12920
- Cost/benefit analysis of advanced materials technologies for future aircraft turbine engines
[NASA-CN-165225] p0027 N81-15006
- Heat pipes to reduce engine exhaust emissions
[NASA-CASE-LEW-12590-1] p0049 N81-19245
- Traction drive for cryogenic boost pump --- hydrogen oxygen rocket engines
[NASA-TN-81704] p0101 N81-23188
- Hostile environmental conditions facing candidate alloys for the automotive Stirling engine
[NASA-TN-82632] p0054 N81-26236
- ENGINE STARTERS**
- An experimental evaluation of the performance deficit of an aircraft engine starter turbine
[SAE PAPER 801137] p0021 A81-34168
- Samarium cobalt (SMCO) generator/engine integration study
[AD-A092904] p0029 N81-17087
- Reasons for low aerodynamic performance of 13.5-centimeter-tip-diameter aircraft engine starter turbine
[NASA-TN-1810] p0016 N81-20076
- ENGINE TESTS**
- AT SPACE ELECTRIC ROCKET TESTS**
- Results of the Mission Profile Life Test first test segment - Thruster J1
[AIAA PAPER 81-0716] p0043 A81-29552
- Magneto-electrostatic thruster physical geometry tests
[AIAA PAPER 81-0753] p0044 A81-29566
- Evaluation of advanced combustors for dry NO_x/suppression with nitrogen bearing fuels in utility and industrial gas turbines
[ASME PAPER 81-GT-125] p0087 A81-30029
- An automated procedure for developing hybrid computer simulations of turbofan engines
p0020 A81-32544
- High temperature electronic requirements in aeropropulsion systems
p0072 A81-32547
- Description of the vane core turbine facility and the vane annular cascade facility recently installed at NASA Lewis Research Center
[SAE PAPER 801122] p0031 A81-34158
- Characteristics of 30-centimeter mercury ion thrusters
[AIAA PAPER 81-0715] p0041 A81-37569
- Particle and field measurements on two J-series 30-centimeter thrusters
[AIAA PAPER 81-0728] p0042 A81-38072
- JT9D performance deterioration results from a simulated aerodynamic load test
[AIAA PAPER 81-1588] p0022 A81-40963
- Turbine bypass engine - A new supersonic cruise propulsion concept
[AIAA PAPER 81-1596] p0023 A81-40971
- Experimental analysis of INEP in a rotary combustion engine --- Indicated Mean Effective Pressure
[SAE PAPER 810150] p0079 A81-41732
- Mixing effectiveness test of an exhaust gas mixer in a high bypass turbofan at altitude
[AIAA PAPER 81-1495] p0023 A81-44225
- Vehicle testing of Cummins turboprop and diesel engine
[NASA-CN-159840] p0140 N81-13803
- Experimental analysis of INEP in a rotary combustion engine
- [NASA-TN-81662] p0015 N81-16054
- Survey of aircraft icing simulation test facilities in North America
[NASA-TN-81707] p0009 N81-19078
- Retrofit and verification test of a 30-cm ion thruster
[NASA-CN-165233] p0042 N81-20174
- Design concepts for low-cost composite turbofan engine frame
[NASA-CN-165217] p0030 N81-22053
- Comparison of NASA and contractor results from aeroacoustic tests of QCSB OTW engine
[NASA-TN-81761] p0017 N81-25079
- JT9D performance deterioration results from a simulated aerodynamic load test
[NASA-TN-82640] p0017 N81-25082
- Test results of the Chrysler upgraded automotive gas turbine engine: Initial design
[NASA-TN-81660] p0107 N81-30562
- Aircraft Engine Diagnostics
[NASA-CN-2190] p0019 N81-31196
- High-power baseline and motoring test results for the GPU-3 Stirling engine
[NASA-TN-82646] p0139 N81-32087
- ENGINEERING DEVELOPMENT**
- U PRODUCT DEVELOPMENT**
- ENGINEERING MANAGEMENT**
- Engineering management and innovation
p0036 A81-20400
- ENGINES**
- AT AIR BREATHING ENGINES**
- AT DIESEL ENGINES**
- AT ELECTRIC ROCKET ENGINES**
- AT ELECTROSTATIC ENGINES**
- AT GAS TURBINE ENGINES**
- AT HELICOPTER ENGINES**
- AT HYDROGEN ENGINES**
- AT HYDROGEN OXYGEN ENGINES**
- AT INTERNAL COMBUSTION ENGINES**
- AT ION ENGINES**
- AT J-85 ENGINE**
- AT JET ENGINES**
- AT LIQUID PROPELLANT ROCKET ENGINES**
- AT MERCURY ION ENGINES**
- AT PISTON ENGINES**
- AT PIT ENGINES**
- AT ROCKET ENGINES**
- AT TP-34 ENGINE**
- AT TURBINE ENGINES**
- AT TURBOFAN ENGINES**
- AT TURBOJET ENGINES**
- AT TURBOPROP ENGINES**
- AT VARIABLE CYCLE ENGINES**
- AT VARIABLE STREAM CONTROL ENGINES**
- AT WANKEL ENGINES**
- EXPANSION**
- ENTROPY**
- T-S diagram for gadolinium near the Curie temperature
p0135 A81-43004
- ENVIRONMENT POLLUTION**
- AT AIR POLLUTION**
- ENVIRONMENT PROTECTION**
- Advanced technology for controlling pollutant emissions from supersonic cruise aircraft
p0001 N81-18004
- ENVIRONMENT SIMULATION**
- AT ALTITUDE SIMULATION**
- ENVIRONMENTAL QUALITY**
- AT AIR QUALITY**
- ENVIRONMENTAL TESTS**
- AT COMBUSTION TESTS**
- AT HIGH TEMPERATURE TESTS**
- Properties of FRP polyimide composites made with improved high strength graphite fibers
p0047 A81-43603
- The role of the micro environment on the tribological behavior of materials
p0087 A81-44693
- Fretting wear and fretting fatigue: How are they related?
[NASA-TN-82633] p0054 N81-26235
- Qualification testing of secondary sterilizable silver-zinc cells for use in the Jupiter atmospheric entry probe
[NASA-TN-82638] p0108 N81-30563
- Environmental effects on graphite fiber reinforced FRP-15 polyimide

- [NASA-TN-82625] p0046 N81-32194
- ENVIRONMENT**
- NT AEROSPACE ENVIRONMENTS**
- NT HIGH TEMPERATURE ENVIRONMENTS**
- NT JUPITER ATMOSPHERE**
- EPOXIES**
- U EPOXY COMPOUNDS**
- EPOXY COMPOUNDS**
- Ultra-high modulus organic fiber hybrid composites
[NASA-CN-165226] p0048 N81-21130
- EPOXY RESINS**
- Curing agent for polyepoxides and epoxy resins and composites cured therewith --- preventing carbon fiber release
[NASA-CASE-18W-13226-1] p0060 N81-17260
- Stress concentration in the vicinity of a hole defect under conditions of Hertzian contact
[NASA-TN-82649] p0084 N81-28443
- EQUATIONS OF MOTION**
- NT EULER EQUATIONS OF MOTION**
- NT NAVIER-STOKES EQUATION**
- NT REYNOLDS EQUATION**
- On the propagation of long waves in acoustically treated, curved ducts
[NASA-TN-81712] p0125 N81-19875
- EQUIPMENT SPECIFICATIONS**
- Spacecraft transmitter reliability
[NASA-CN-2159] p0037 N81-16119
- EROSION**
- The effect of mechanical surface and heat treatments on the erosion resistance of 6061 aluminum alloy
p0057 N81-27944
- Effect of mechanical surface and heat treatments on erosion resistance
[NASA-TN-81540] p0051 N81-11178
- The role of oxidation in the fretting wear process
[NASA-TN-81570] p0051 N81-12210
- Effects of erodant particle shape and various heat treatments on erosion resistance of plain carbon steel
[NASA-TP-1755] p0052 N81-16210
- Program to develop sprayed, plastically deformable compressor shroud seal materials
[NASA-CN-165237] p0088 N81-17434
- Synergistic erosion/corrosion of superalloys in PFB coal combustor effluent
[NASA-TN-81715] p0101 N81-23245
- ERROR ANALYSIS**
- Backward deletion to minimize prediction errors in models from factorial experiments with zero to six center points
p0122 N81-14999
- ERROR DETECTION CODES**
- Structural dynamics verification facility study
[NASA-TN-82675] p0092 N81-33497
- ESTIMATES**
- NT COST ESTIMATES**
- ESTIMATING**
- NT PARAMETER IDENTIFICATION**
- Numerical trials of HISS
[N81-10069] p0094 N81-13425
- ETCHING**
- Ion beam sputter etching of orthopedic implant alloy MP35N and resulting effects on fatigue properties
[AIAA PAPER 81-0671] p0057 N81-38069
- Ion beam sputter etching of orthopedic implanted alloy MP35N and resulting effects on fatigue
[NASA-TN-81747] p0045 N81-21174
- ETHERS**
- NT POLYPHENYL ETHER**
- EUCLIDEAN GEOMETRY**
- NT ANGLE OF ATTACK**
- EULER EQUATIONS OF MOTION**
- Surrogate-equation technique for simulation of steady inviscid flow
[NASA-TP-1866] p0005 N81-31129
- EUTECTIC ALLOYS**
- The effect of thermal cycling to 1100 C on the alpha /No/ phase in directionally solidified gamma/gamma-prime-alpha alloys
p0057 N81-32546
- The effect of thermal cycling to 1100 degree C on the alpha (No) phase in directionally solidified gamma/gamma prime-alpha alloys
[NASA-TN-81688] p0052 N81-18165
- EUTECTICS**
- NT EUTECTIC ALLOYS**
- EVACUATING (VACUUM)**
- Evacuation-induced pressure differentials in multilayer insulation systems
p0078 N81-18021
- EVALUATION**
- Status of commercial phosphoric acid fuel cell system development
[NASA-TN-81641] p0096 N81-13464
- Acceptance tests and manufacturer relationships for 20 ampere-hour sealed nickel-cadmium cells using discharge parameters
[NASA-TN-81619] p0049 N81-17189
- Turbine bypass engine: A new supersonic cruise propulsion concept
[NASA-TN-82608] p0018 N81-26145
- EVAPORATIVE COOLING**
- NT FILM COOLING**
- EXECUTIVE AIRCRAFT**
- U GENERAL AVIATION AIRCRAFT**
- EXHAUST DIFFUSERS**
- Mixing effectiveness test of an exhaust gas mixer in a high bypass turbofan at altitude
[AIAA PAPER 81-1495] p0023 N81-44225
- EXHAUST EMISSION**
- Fuel/air nonuniformity - Effect on nitric oxide emissions
[AIAA PAPER 81-0327] p0019 N81-20834
- Design and preliminary results of a fuel flexible industrial gas turbine combustor
[ASME PAPER 81-GT-108] p0087 N81-30013
- Evaluation of advanced combustors for dry NO_x/suppression with nitrogen bearing fuels in utility and industrial gas turbines
[ASME PAPER 81-GT-125] p0087 N81-30029
- Evaluation of concepts for controlling exhaust emissions from minimally processed petroleum and synthetic fuels
[ASME PAPER 81-GT-157] p0067 N81-30055
- Exhaust emission survey of an F100 afterburning turbofan engine at simulated altitude flight conditions
[NASA-TN-81656] p0016 N81-21078
- Analysis of effect of flameholder characteristics on lean, premixed, partially vaporized fuel-air mixtures quality and nitrogen oxides emissions
[NASA-TP-1842] p0016 N81-24065
- Effects of fuel-injector design on ultra-lean combustion performance
[NASA-TN-82624] p0104 N81-24533
- Test results of the Chrysler upgraded automotive gas turbine engine: Initial design
[NASA-TN-81660] p0107 N81-30562
- EXHAUST FLOW SIMULATION**
- NT FLIGHT SIMULATION**
- EXHAUST GASES**
- Development of a low NO_x/lean premixed annular combustor
[ASME PAPER 81-GT-40] p0020 N81-29954
- Effect of fuel nitrogen and hydrogen content on emissions in hydrocarbon combustion
[ASME PAPER 81-GT-63] p0057 N81-29973
- Advanced technology for controlling pollutant emissions from supersonic cruise aircraft
p0001 N81-18004
- Heat pipes to reduce engine exhaust emissions
[NASA-CASE-18W-12590-1] p0049 N81-19245
- An integrated exhaust gas analysis system with self-contained data processing and automatic calibration
[NASA-TN-81592] p0102 N81-23435
- Mixing effectiveness test of an exhaust gas mixer in a high bypass turbofan at altitude
[NASA-TN-82663] p0018 N81-27095
- Supercritical fuel injection system
[NASA-CASE-18W-12990-1] p0018 N81-29129
- Performance tests of a gas blending system based on mass-flow controllers
[NASA-TP-1896] p0066 N81-29246
- EXHAUST JETS**
- U EXHAUST GASES**
- EXHAUST NOZZLES**
- NT PLUG NOZZLES**
- Mixer nozzle aeroacoustic characteristics for the energy efficient engine
[AIAA PAPER 81-1994] p0128 N81-48639
- Model aerodynamic test results for two variable cycle engine annular exhaust systems at simulated takeoff and cruise conditions. Comprehensive data report. Volume 1: Design

- layouts
[NASA-CR-159819-VOL-1] p0028 N81-17081
Model aerodynamic test results for two variable
cycle engine coaxial exhaust systems at
simulated takeoff and cruise conditions.
Comprehensive data report. Volume 2: Tabulated
aerodynamic data book 1
[NASA-CR-159819-VOL-2-BK-1] p0028 N81-17002
Model aerodynamic test results for two variable
cycle engine coaxial exhaust systems at
simulated takeoff and cruise conditions.
Comprehensive data report. Volume 2: Tabulated
aerodynamic data book 2
[NASA-CR-159819-VOL-2-BK-2] p0028 N81-17083
Model aerodynamic test results for two variable
cycle engine coaxial exhaust systems at
simulated takeoff and cruise conditions.
Comprehensive data report. Volume 2: Tabulated
aerodynamic data book 3
[NASA-CR-159819-VOL-2-BK-3] p0028 N81-17084
Model aerodynamic test results for two variable
cycle engine coaxial exhaust systems at
simulated takeoff and cruise conditions.
Comprehensive data report. Volume 3: Graphical
data book 1
[NASA-CR-159819-VOL-3-BK-1] p0028 N81-17085
Model aerodynamic test results for two variable
cycle engine coaxial exhaust systems at
simulated takeoff and cruise conditions.
Comprehensive data report. Volume 3: Graphical
data book 2
[NASA-CR-159819-VOL-3-BK-2] p0028 N81-17086
Aerodynamic/acoustic performance of J3101/Double
bypass VCE with coaxial plug nozzle
[NASA-CR-159869] p0129 N81-17046
QCGAT mixer compound exhaust system design and
static big model test report
[NASA-CR-135386] p0029 N81-19119
Design of an exhaust mixer nozzle for the
Avco-Lycoming Quiet Clean General Aviation
Turboshaft (QCGAT)
[NASA-CR-159826] p0029 N81-19120
Mixing effectiveness test of an exhaust gas mixer
in a high bypass turbofan at altitude
[NASA-TN-82663] p0018 N81-27095
- EXHAUST SYSTEMS**
Model aerodynamic test results for two variable
cycle engine coaxial exhaust systems at
simulated takeoff and cruise conditions ---
Lewis 8 by 6-foot supersonic wind tunnel tests
[NASA-CR-159818] p0026 N81-13057
Model aerodynamic test results for two variable
cycle engine coaxial exhaust systems at
simulated takeoff and cruise conditions.
Comprehensive data report. Volume 1: Design
layouts
[NASA-CR-159819-VOL-1] p0028 N81-17081
Model aerodynamic test results for two variable
cycle engine coaxial exhaust systems at
simulated takeoff and cruise conditions.
Comprehensive data report. Volume 2: Tabulated
aerodynamic data book 1
[NASA-CR-159819-VOL-2-BK-1] p0028 N81-17082
Model aerodynamic test results for two variable
cycle engine coaxial exhaust systems at
simulated takeoff and cruise conditions.
Comprehensive data report. Volume 2: Tabulated
aerodynamic data book 2
[NASA-CR-159819-VOL-2-BK-2] p0028 N81-17083
Model aerodynamic test results for two variable
cycle engine coaxial exhaust systems at
simulated takeoff and cruise conditions.
Comprehensive data report. Volume 2: Tabulated
aerodynamic data book 3
[NASA-CR-159819-VOL-2-BK-3] p0028 N81-17084
Model aerodynamic test results for two variable
cycle engine coaxial exhaust systems at
simulated takeoff and cruise conditions.
Comprehensive data report. Volume 3: Graphical
data book 1
[NASA-CR-159819-VOL-3-BK-1] p0028 N81-17085
Model aerodynamic test results for two variable
cycle engine coaxial exhaust systems at
simulated takeoff and cruise conditions.
Comprehensive data report. Volume 3: Graphical
data book 2
[NASA-CR-159819-VOL-3-BK-2] p0028 N81-17086
- EXPANSION**
BT THERMAL EXPANSION
- Method for alleviating thermal stress damage in
laminates
[NASA-CASR-LEU-12493-2] p0046 N81-26179
- EXPERIMENTAL DESIGN**
BT FACTORIAL DESIGN
Backward deletion to minimize prediction errors in
models from factorial experiments with zero to
six center points
[NASA-TN-81524] p0123 N81-10778
- EXPLOSIVE CONDUCTION CIRCUITS**
U CIRCUIIS
- EXTRAPOLATION**
NEGA16 - Computer program for analysis and
extrapolation of stress-rupture data
[NASA-TP-1809] p0102 N81-23486
- EXTRATERRESTRIAL ENVIRONMENTS**
BT JUPITER ATMOSPHERE
- EXTRATERRESTRIAL RADIATION**
BT SOLAR RADIATION
BT SUNLIGHT
- EXTREMELY HIGH FREQUENCIES**
Advanced communications satellites
[AAS PAPER 80-206] p0069 N81-33532
K-band high power latching switch ---
communication satellite system
[NASA-CR-165159] p0073 N81-16389
- F**
- FAB (PROGRAMMING LANGUAGE)**
U FORTRAN
- FABRICATION**
GaAs shallow-homojunction solar cells
[NASA-CR-165167] p0110 N81-15463
High voltage V-groove solar cell
[NASA-CASR-LEU-13401-1] p0098 N81-16529
Coplanar back contacts for thin silicon solar cells
[NASA-CR-165272] p0112 N81-18495
Development program on a cold cathode electron gun
[NASA-CR-159570] p0073 N81-19395
Cell module and fuel conditioner development
[NASA-CR-165190] p0112 N81-19573
Heat exchanger and method of making
[NASA-CASR-LEU-12441-3] p0104 N81-24519
- FABRICS**
BT FELTS
Composition and method for making polyimide
resin-reinforced fabric
[NASA-CASR-LEU-12933-1] p0061 N81-19296
- FACTORIAL DESIGN**
Backward deletion to minimize prediction errors in
models from factorial experiments with zero to
six center points
[NASA-TN-81524] p0123 N81-10778
Backward deletion to minimize prediction errors in
models from factorial experiments with zero to
six center points
[NASA-TN-81524] p0122 N81-14999
- FACTORIES**
U INDUSTRIAL PLANTS
- FAIL-SAFE SYSTEMS**
Apparatus for sensor failure detection and
correction in a gas turbine engine control system
[NASA-CASR-LEU-12907-2] p0015 N81-19115
- FAILURES**
BT ENGINE FAILURES
BT SYSTEM FAILURES
- FAILURE ANALYSIS**
Effect of substrate surface finish on the
lubrication and failure mechanisms of polybismuth
disulfide films
[ASLE PREPRINT 81-AM-50-1] p0064 N81-33859
Method for estimating crack-extension resistance
curve from residual strength data
[NASA-TP-1753] p0091 N81-11417
Some effects of thermal-cycle-induced deformation
in rocket thrust chambers
[NASA-TP-1834] p0038 N81-20176
NEGA16 - Computer program for analysis and
extrapolation of stress-rupture data
[NASA-TP-1809] p0102 N81-23486
- FAILURE MODES**
Lubrication of rolling element bearings
p0086 N81-18738
Investigation of performance deterioration of the
CP6/JT9D high bypass ratio turbofan engines
p0016 N81-24086
- FAIRCHILD MILITARY AIRCRAFT**
U MILITARY AIRCRAFT

FAN BLADES

Mean rotor wake characteristics of an aerodynamically loaded 0.5 m diameter fan [AIAA PAPER 81-0208] p0006 A81-20830
 Superhybrid composite blade impact studies [ASME PAPER 81-GT-24] p0020 A81-29940
 Interactive multi-scale blade impact analysis [ASME PAPER 81-GT-79] p0030 A81-29967
 Superhybrid composite blade impact studies [NASA-TN-81597] p0091 A81-11412
 Rotor redesign for a highly loaded 1800 ft/sec tip speed fan, 2 [NASA-CN-159879] p0024 A81-12087
 Low-cost directionally-solidified turbine blades, volume 2 --- TFI731-3 turbofan engine [NASA-CN-159562] p0024 A81-12088
 Cold-air investigation of first stage of 4-1/2-stage, fan drive turbine with average stage-loading factor of 4.66 [NASA-TP-1780] p0015 A81-16050
 Composite containment systems for jet engine fan blades [NASA-TN-81675] p0092 A81-17480

FARM CROPS

WT ALFALFA
 WT BARLEY
 WT CORN
 WT COTTON
 WT GRAINS (FOOD)
 WT HAY
 WT LEGUMINOUS PLANTS
 WT MILLET
 WT OATS
 WT POTATOES
 WT RICE
 WT SORGHUM
 WT SUGAR BEETS
 WT SUNFLOWERS
 WT WHEAT

FASTENERS

WT PINS

FATIGUE (MATERIALS)

WT METAL FATIGUE
 WT THERMAL FATIGUE
 Comparisons of modified Vasco X-2 and AISI 9310 gear steels [NASA-TP-1731] p0080 A81-14322
 Ion beam sputter etching of orthopedic implanted alloy HP35N and resulting effects on fatigue [NASA-TN-81747] p0045 A81-21174
 Fretting wear and fretting fatigue: How are they related? [NASA-TN-82633] p0054 A81-26235

FATIGUE LIFE

Ion beam sputter etching of orthopedic implant alloy HP35N and resulting effects on fatigue properties [AIAA PAPER 81-0671] p0057 A81-38069
 Life analysis of multiregular planetary traction drive [NASA-TP-1710] p0082 A81-20423
 Prolonging thermal barrier coated specimen life by thermal cycle management [NASA-TN-81742] p0102 A81-23417
 Assessment of variations in thermal cycle life data of thermal barrier coated rods [NASA-TN-81743] p0102 A81-23418
 Effects of Ultra-Clean and centrifugal filtration on rolling-element bearing life [NASA-TN-82660] p0085 A81-29440
 Ball bearing mechanics [NASA-TN-81691] p0085 A81-31550

FATIGUE TESTING MACHINES

NASA five-ball fatigue tester - Over 20 years of research p0087 A81-44659

FATIGUE TESTS

Cyclic behavior of turbine disk alloys at 650 C p0056 A81-12266
 Ion beam sputter etching of orthopedic implant alloy HP35N and resulting effects on fatigue properties [AIAA PAPER 81-0671] p0057 A81-38069
 Creep and residual mechanical properties of cast superalloys and oxide dispersion strengthened alloys [NASA-TP-1781] p0053 A81-19273
 The fracture morphology of nickel-base superalloys tested in fatigue and creep-fatigue at 650 C

[NASA-TN-81740] p0101 A81-23244
 NASA five-ball fatigue tester: Over 20 years of research [NASA-TN-82589] p0102 A81-23462
 Stress concentration in the vicinity of a hole defect under conditions of Hertzian contact [NASA-TN-82649] p0084 A81-28443
 Endurance tests with large-bore tapered-roller bearings to 2.2 million DM [NASA-TN-82669] p0084 A81-29439
FEASIBILITY ANALYSIS
 Feasibility of Kevlar 49/PMR-15 polyimide for high temperature applications p0047 A81-43602
 Goals of thermionic program for space power p0133 A81-44656
FEEDBACK CONTROL
 Analysis and design of an adaptive multi-loop controlled two winding buck/boost regulator p0073 A81-21675
 Application handbook for a Standardized Control Module (SCM) for DC-DC converters, volume 1 [NASA-CN-165172] p0072 A81-10301
FELTS
 Preparation and characterization of electrodes for the NASA Redox storage system [NASA-TN-82702] p0107 A81-30522
FERRITALLOYS
 U IRON ALLOYS
FIBER COMPOSITES
 WT CARBON FIBER REINFORCED PLASTICS
 WT GLASS FIBER REINFORCED PLASTICS
 Prediction of composite thermal behavior made simple [NASA-TN-81618] p0045 A81-16132
 Computer code for intraply hybrid composite design [NASA-TN-82593] p0046 A81-25151
FIBER OPTICS
 Fiber optics for aircraft engine/inlet control [NASA-TN-82654] p0012 A81-31190
FIBER REINFORCED COMPOSITES
 Feasibility of Kevlar 49/PMR-15 polyimide for high temperature applications p0047 A81-43602
 Acousto-ultrasonic characterization of fiber reinforced composites p0090 A81-44660
 Computer code for intraply hybrid composite design p0047 A81-44662
 Tungsten fiber reinforced superalloys - A status review p0047 A81-44665
 Laminates and reinforced metals [NASA-TN-81591] p0045 A81-12171
 Fabrication development of alumina/aluminum composites [NASA-CN-165195] p0048 A81-19233
 Composition and method for making polyimide resin-reinforced fabric [NASA-CASE-LEW-12933-1] p0061 A81-19296
 Environmental effects on graphite fiber reinforced FHR-15 polyimide [NASA-TN-82625] p0046 A81-32194
FIBER RELEASE
 Curing agent for polyepoxides and epoxy resins and composites cured therewith --- preventing carbon fiber release [NASA-CASE-LEW-13226-1] p0060 A81-17260
FIBER STRENGTH
 CVD-produced boron filaments p0048 A81-11336
 Properties of PMR polyimide composites made with improved high strength graphite fibers p0047 A81-43603
 Oxidation-induced contraction and strengthening of boron fibers p0047 A81-44664
 Oxidation-induced contraction and strengthening of boron fibers [NASA-TN-82599] p0046 A81-25150
FIBERS
 WT BORON FIBERS
 WT METAL FIBERS
 WT REINFORCING FIBERS
FIELD STRENGTH
 WT ELECTRIC FIELD STRENGTH
 WT MAGNETIC FLUX
MILLERS
 Control of volume resistivity in inorganic-organic separators --- for alkaline batteries

- Polyvinyl alcohol battery separator containing inert filler --- alkaline batteries
[NASA-CASE-LEW-13556-1] p0108 A81-11034
- FILE COOLING**
Full-coverage film cooling. I - Three-dimensional measurements of turbulence structure. II - Prediction of the recovery-region hydrodynamics p0078 A81-15537
- Analysis for predicting adiabatic wall temperatures with single hole coolant injection into a low speed crossflow
[ASME PAPER 81-GT-91] p0077 A81-29998
- Curved film cooling admission tube
[NASA-CASE-LEW-13174-1] p0074 A81-12363
- Analysis for predicting adiabatic wall temperatures with single hole coolant injection into a low speed crossflow
[NASA-TN-81620] p0074 A81-13301
- FILE THICKNESS**
Some limitations in applying classical EHD film thickness formulas to a high-speed bearing
[ASME PAPER 80-C2/LUB-13] p0068 A81-18667
- Elastohydrodynamic lubrication of elliptical contacts
[NASA-TN-81647] p0080 A81-13358
- Measurement of rod seal lubrication for Stirling engine
[NASA-CR-165158] p0088 A81-13359
- Recent developments in lightweight solar cell modules --- with protective glass cover
p0099 A81-17571
- Analysis of starvation effects on hydrodynamic lubrication in nonconforming contacts
[NASA-TN-82668] p0084 A81-29438
- FILES**
Ion plating for the future
[NASA-TN-82630] p0054 A81-25189
- FILTRATION**
U FILTRATION
FILTRATION
Effects of Ultra-Clean and centrifugal filtration on rolling-element bearing life
[NASA-TN-82660] p0085 A81-29440
- FINITE DIFFERENCE THEORY**
Some modifications to, and operational experiences with, the two-dimensional, finite-difference, boundary-layer code, STAN5
[ASME PAPER 81-GT-89] p0077 A81-29996
- Factors which influence the behavior of turbofan forced mixer nozzles
[AIAA PAPER 81-0274] p0021 A81-32549
- Application of 'steady' state finite element and transient finite difference theory to sound propagation in a variable duct - A comparison with experiment
[AIAA PAPER 81-2016] p0128 A81-48622
- Factors which influence the behavior of turbofan forced mixer nozzles
[NASA-TN-81668] p0074 A81-15240
- Surface roughness effect on finite oil journal bearings
[NASA-TN-82639] p0084 A81-27526
- Influence of exit impedance on finite difference solutions of transient acoustic mode propagation in ducts
[NASA-TN-82666] p0126 A81-30905
- Surrogate-equation technique for simulation of steady inviscid flow
[NASA-TP-1866] p0005 A81-31129
- FINITE ELEMENT METHOD**
Finite element analysis of inviscid subsonic boattail flow
[AIAA PAPER 81-0276] p0006 A81-20831
- Application of 'steady' state finite element and transient finite difference theory to sound propagation in a variable duct - A comparison with experiment
[AIAA PAPER 81-2016] p0128 A81-48622
- Finite element analysis of inviscid subsonic boattail flow
[NASA-TN-81650] p0003 A81-18977
- Aeroelastic and dynamic finite element analyses of a bladder shrouded disk
[NASA-CR-159728] p0092 A81-19479
- A method of selecting grid size to account for Bertz deformation in finite element analysis of spur gears
[NASA-TN-82623] p0083 A81-27525
- FINIS**
BT COOLING FINIS
FLAMES
BT DIFFUSION FLAMES
FLAP CONTROL
U AIRCRAFT CONTROL
FLASHBACK
Ignition of lean fuel-air mixtures in a premixing-prevaporizing duct at temperatures up to 1000 K
[NASA-TN-81645] p0096 A81-13465
- FLAN DETECTION**
U NONDESTRUCTIVE TESTS
FLIGHT CONDITIONS
Effect of time-dependent flight loads on turbofan engine performance deterioration
[ASME PAPER 81-GT-203] p0030 A81-30093
- FLIGHT HAZARDS**
An analytical approach to airfoil icing
[AIAA PAPER 81-0403] p0117 A81-20810
- FLIGHT SIMULATION**
An experimental study of transmission, reflection and scattering of sound in a free jet flight simulation facility and comparison with theory
p0129 A81-28943
- JT9D performance deterioration results from a simulated aerodynamic load test
[AIAA PAPER 81-1588] p0022 A81-40963
- Exhaust emission survey of an F100 afterburning turbofan engine at simulated altitude flight conditions
[NASA-TN-81656] p0016 A81-21078
- FLIGHT SIMULATIONS**
A nonlinear propulsion system simulation technique for piloted simulators
p0022 A81-38064
- A nonlinear propulsion system simulation technique for piloted simulators
[NASA-TN-82600] p0101 A81-23085
- FLIGHT TESTS**
Diagnostic system design for the Ion Auxiliary Propulsion System (IAPS) - Flight test of two 8 cm mercury ion thrusters
[AIAA PAPER 81-0666] p0041 A81-38070
- Diagnostic system design for the Ion Auxiliary Propulsion System (IAPS). Flight tests of two 8 cm mercury ion
[NASA-TN-81702] p0037 A81-20172
- FLOW CHARACTERISTICS**
BT FLOW DISTRIBUTION
BT FLOW STABILITY
BT FLOW VELOCITY
BT MAGNETOHYDRODYNAMIC STABILITY
Analytical investigation of critical phenomena in MHD power generators
[NASA-CR-165143] p0109 A81-12546
- Prediction of laminar and turbulent primary and secondary flows in strongly curved ducts
[NASA-CR-3386] p0007 A81-16976
- High-frequency sound propagation in a spatially varying mean flow
[NASA-TN-81751] p0126 A81-20831
- Pumping power considerations in the designs of NASA-Bedox flow cells
[NASA-TN-82598] p0106 A81-28519
- FLOW DISTORTION**
Inlet flow distortion in turbomachinery
[ASME PAPER 80-GT-20] p0005 A81-17952
- FLOW DISTRIBUTION**
Calculation of the flow field in supersonic inlets using a bicharacteristics method with shock wave fitting
p0006 A81-21212
- Flow separation in inlets at incidence angles
p0006 A81-29114
- Laser-velocimeter flow-field measurements of an advanced turboprop
[AIAA PAPER 81-1568] p0007 A81-42211
- Laser-velocimeter flow-field measurements of an advanced turboprop
[NASA-TN-82677] p0004 A81-27041
- Analysis of starvation effects on hydrodynamic lubrication in nonconforming contacts
[NASA-TN-82668] p0084 A81-29438
- Stall flutter experiment in a transonic oscillating linear cascade
[NASA-TN-82655] p0004 A81-31126
- FLOW FIELDS**
U FLOW DISTRIBUTION

FLOW GEOMETRY

Solution of plane cascade flow using improved surface singularity methods
[ASME PAPER 81-GT-169] p0006 A81-30068
An electrostatic analog for generating cascade grids p0122 N81-14695

Turbine modeling technique to generate off-design performance data for both single and multistage axial-flow turbines
[NASA-CR-145244] p0027 N81-17078

FLOW MEASUREMENT

Laser-velocimeter flow-field measurements of an advanced turboprop
[AIAA PAPER 81-1568] p0007 A81-42211
Laser-velocimeter flow-field measurements of an advanced turboprop
[NASA-TN-82677] p0004 N81-27041

FLOW PATTERNS

U FLOW DISTRIBUTION

FLOW RATE

U FLOW VELOCITY

FLOW SEPARATION

O BOUNDARY LAYER SEPARATION

U SEPARATED FLOW

FLOW STABILITY

NT MAGNETOHYDRODYNAMIC STABILITY

The coupling between flow instabilities and incident disturbances at a leading edge
p0010 A81-28682

TF34 engine compression system computer study --- simulation of flow stability
[NASA-CR-159889] p0027 N81-15005

FLOW VELOCITY

Laser-velocimeter flow-field measurements of an advanced turboprop
[AIAA PAPER 81-1568] p0007 A81-42211

RHD generator off-design performance and non-chemical kinetics analysis. Volume 1: Analysis of the off-design performance of the Engineering Test Facility RTF RHD generator flow train
[NASA-CR-145187] p0133 N81-11834

Effect of hole geometry and Electric-Discharge Machining (EDM) on airflow rates through small diameter holes in turbine blade material
[NASA-TF-1716] p0013 N81-12089

Flow through axially aligned sequential apertures of the orifice and Borda types
[NASA-TN-81681] p0075 N81-21314

An experimental evaluation of oil pumping rings
[NASA-CR-145271] p0088 N81-21355

Pumping power considerations in the designs of NASA-Bedox flow cells
[NASA-TN-82598] p0106 N81-28519

Experiments on flow through one to four jets of the orifice and Borda type
[NASA-CR-82680] p0077 N81-30391

FLOW VISUALIZATION

NT NUMERICAL FLOW VISUALIZATION

Evaluation of a method for heat transfer measurements and thermal visualization using a composite of a heater element and liquid crystals
[ASME PAPER 81-GT-93] p0079 A81-30000
Holographic flow visualization of time-varying shock waves
p0079 A81-47642

Evaluation of a method for heat transfer measurements and thermal visualization using a composite of a heater element and liquid crystals --- thermal performance of turbine blade cooling configurations
[NASA-TN-81639] p0075 N81-21313

Some flow phenomena associated with aligned, sequential apertures with Borda-type inlets --- inlet pressure and flow separation
[NASA-TF-1792] p0076 N81-24387

FLOWING

Performance of high resistivity n-type silicon solar cells under 1 MeV electron irradiation
[NASA-TN-82610] p0103 N81-23620

FLUID BOUNDARIES

NT LIQUID-SOLID INTERFACES

FLUID DYNAMICS

NT AERODYNAMICS

NT AEROTHERMODYNAMICS

NT COMPUTATIONAL FLUID DYNAMICS

NT ELASTOHYDRODYNAMICS

NT HYDRODYNAMICS

NT MAGNETOHYDRODYNAMICS

NT ROTOR AERODYNAMICS

NT VORTEX SHEDDING

An electrostatic analog for generating cascade grids
p0122 N81-14695

A four-cylinder Stirling engine controls model
[NASA-TN-81648] p0075 N81-15241

A RHD channel study for the RTF conceptual design
[NASA-TN-81764] p0132 N81-24927

FLUID FILMS

Lubrication fundamentals
[NASA-TN-81762] p0103 N81-23490

FLUID FLOW

NT AIR FLOW

NT ANGULAR FLOW

NT AXIAL FLOW

NT AXISYMMETRIC FLOW

NT BOUNDARY LAYER FLOW

NT BOUNDARY LAYER SEPARATION

NT CAPILLARY FLOW

NT CASCADE FLOW

NT CHANNEL FLOW

NT COAXIAL FLOW

NT COMPRESSIBLE FLOW

NT CONVECTIVE FLOW

NT CRITICAL FLOW

NT CROSS FLOW

NT DUCTED FLOW

NT FUEL FLOW

NT INCOMPRESSIBLE FLOW

NT INLET FLOW

NT INVISCID FLOW

NT ISOTHERMAL FLOW

NT JET FLOW

NT KNUDSEN FLOW

NT LAMINAR FLOW

NT MAGNETOHYDRODYNAMIC FLOW

NT MULTIPHASE FLOW

NT NONUNIFORM FLOW

NT NOZZLE FLOW

NT ONE DIMENSIONAL FLOW

NT ORIFICE FLOW

NT POTENTIAL FLOW

NT RADIAL FLOW

NT SECONDARY FLOW

NT SEPARATED FLOW

NT SUBSONIC FLOW

NT THREE DIMENSIONAL FLOW

NT TRANSONIC FLOW

NT TURBULENT FLOW

NT TWO DIMENSIONAL FLOW

NT TWO PHASE FLOW

NT UNSTEADY FLOW

NT VISCOUS FLOW

NT WATER FLOW

icing tunnel tests of a glycol-exuding porous leading edge ice protection system on a general aviation airfoil
[AIAA PAPER 81-0405] p0011 A81-20837

Self-acting geometry for noncontact seals
[NASA-TN-81659] p0081 N81-16474

Fundamental heat transfer research for gas turbine engines
[NASA-CP-2178] p0016 N81-24063

GRID30: Computer program for fast generation of multilevel, three-dimensional boundary-conforming O-type computational grids
[NASA-TF-1920] p0005 N81-31128

FLUID INJECTION

Analysis for predicting adiabatic wall temperatures with single hole coolant injection into a low speed crossflow
[ASME PAPER 81-GT-91] p0077 N81-29998

FLUID JETS

NT FREE JETS

Capillary and acceleration wave breakup of liquid jets in axial-flow airstreams
[NASA-TF-1791] p0075 N81-16417

FLUID MECHANICS

NT AERODYNAMICS

NT AEROTHERMODYNAMICS

NT COMPUTATIONAL FLUID DYNAMICS

NT ELASTOHYDRODYNAMICS

NT FLUID DYNAMICS

NT HYDRODYNAMICS

NT MAGNETOHYDRODYNAMICS

NT ROTOR AERODYNAMICS

NT VORTEX SHEDDING

Biography of Lewis Research Center technical publications announced in 1980
[NASA-TN-82661] p0137 N81-29026

FLUID PRESSURE

- Self-stabilizing radial face seal
[NASA-CASE-LBN-12991-1] p0083 N81-24442
Experiments on flow through one to four inlets of
the orifice and Forda type
[NASA-TN-82680] p0077 N81-30391

FLUIDIZED BED PROCESSORS

- Synergistic erosion/corrosion of superalloys in
PFB coal combustor effluent
[NASA-TN-81715] p0101 N81-23245

FLUORIDES

UT POLYVINYL FLUORIDE

FLUORINE COMPOUNDS

NT FLUOROPOLYMERS

NT POLYTETRAFLUOROETHYLENE

NT POLYVINYL FLUORIDE

FLUORINE ORGANIC COMPOUNDS

NT FLUOROPOLYMERS

NT POLYVINYL FLUORIDE

FLUORO COMPOUNDS

NT FLUOROPOLYMERS

NT POLYTETRAFLUOROETHYLENE

FLUOROPOLYMERS

NT POLYTETRAFLUOROETHYLENE

NT POLYVINYL FLUORIDE

- Texturing polymer surfaces by transfer casting ---
carotidvascular prosthesis
[NASA-CASE-LBN-12120-1] p0068 N81-16327

FLUTTER

NT SUBSONIC FLUTTER

NT SUPERSONIC FLUTTER

NT TRANSONIC FLUTTER

- Effects of mistuning on bending-torsion flutter
and response of a cascade in incompressible flow
--- turbofan engines
[NASA-TN-81674] p0091 N81-16494
NASTRAN level 16 user's manual updates for
aeroelastic analysis of bladed discs
[NASA-CR-159824] p0093 N81-19481
Measurement of aerodynamic work during fan flutter
[NASA-TN-82652] p0017 N81-25080

FLUTTER ANALYSIS

- Effects of mistuning on blade torsional flutter
p0092 N81-29095
Effects of mistuning on bending-torsion flutter
and response of a cascade in incompressible flow
[AIAA 81-0602] p0092 N81-29465
NASTRAN level 16 theoretical manual updates for
aeroelastic analysis of bladed discs
[NASA-CR-159823] p0093 N81-19480
NASTRAN level 16 programmer's manual updates for
aeroelastic analysis of bladed discs
[NASA-CR-159825] p0093 N81-15462

FLUX (RATE PER UNIT AREA)

U FLUX DENSITY

FLUX (RATE)

NT MAGNETIC FLUX

- Environmental charging effects monitors for
operational satellites
[NASA-TN-81669] p0037 N81-17127

FLUX DENSITY

NT CURRENT DENSITY

NT RADIANCE

NT SOUND INTENSITY

- Particle and field measurements on two J-series 30
centimeter thrusters
[NASA-TN-81741] p0039 N81-22084

FLUX MAPPING

U FLUX DENSITY

U MAPPING

FLUXMETERS

U MEASURING INSTRUMENTS

FLYING PLATFORM STABILITY

U AERODYNAMIC STABILITY

FOCUSING

- Gyrotron transmitting tube
[NASA-CASE-LBN-13429-1] p0071 N81-16384

FOKKEBOND TESTERS

U ADHESION TESTS

FORECASTING

NT PERFORMANCE PREDICTION

NT PREDICTION ANALYSIS TECHNIQUES

NT TECHNOLOGICAL FORECASTING

FORM

U SHAPES

FORMING TECHNIQUES

NT CASTING

NT INJECTION MOLDING

NT ROLL FORMING

Fabrication development of alumina/alumina
composites

[NASA-CR-165195]

p0048 N81-19233

POSTHEAT

KONFIG and RHECHFIG: Two interactive
preprocessing to the Navy/NASA Engine Program
(NHEP)

[NASA-TN-82636]

p0120 N81-25698

FOULING

Combustion system processes leading to corrosive
deposits
[NASA-TN-81752]

p0101 N81-23243

FRACTURE RESISTANCE

U FRACTURE STRENGTH

FRACTURE STRENGTH

On the equivalence between semispherical fracture
analyses and R-curves

p0092 N81-18792

Fracture toughness of brittle materials determined
with chevron notch specimens

p0064 N81-32545

Method for estimating crack-extension resistance
curve from residual strength data
[NASA-TP-1753]

p0091 N81-11417

Experimental compliance calibration of the compact
fracture toughness specimen
[NASA-TN-81665]

p0091 N81-16492

The fracture morphology of nickel-base superalloys
tested in fatigue and creep-fatigue at 650 C
[NASA-TN-81740]

p0101 N81-23244

FRACTURE TOUGHNESS

U FRACTURE STRENGTH

FREE JETS

An experimental study of transmission, reflection
and scattering of sound in a free jet flight
simulation facility and comparison with theory

p0129 N81-28943

FREE RADICALS

Free radical propulsion concept

[AIAA PAPER 81-0676]

p0041 N81-32905

Free radical propulsion concept

[NASA-TN-81770]

p0039 N81-20180

FREQUENCIES

NT BROADBAND

NT EXTREMELY HIGH FREQUENCIES

NT HIGH FREQUENCIES

NT IONIZATION FREQUENCIES

NT MAXIMUM USABLE FREQUENCY

Satellites using the 30/20 GHz band

[NASA-TN-81600]

p0069 N81-10241

FREQUENCY BANDS

U FREQUENCIES

FREQUENCY MODULATION

Carrier - Interference ratios for frequency
sharing between satellite systems transmitting
frequency modulated and digital television signals

p0069 N81-21911

FRETTING

The role of oxidation in the fretting wear process
[NASA-TN-81570]

p0051 N81-12210

Fretting wear and fretting fatigue: How are they
related?

[NASA-TN-82633]

p0054 N81-26235

FRICTION

NT SLIDING FRICTION

NT STATIC FRICTION

Changes in surface chemistry of silicon carbide
(0001) surface with temperature and their effect
on friction

[NASA-TP-1756]

p0060 N81-14079

Evaluation of boundary lubricants using
steady-state wear and friction

[NASA-TN-81601]

p0061 N81-17265

Surface chemistry and friction behavior of the
silicon carbide (0001) surface at temperatures
to 1500 deg C

[NASA-TP-1813]

p0061 N81-19300

FRICTION COEFFICIENT

U COEFFICIENT OF FRICTION

FRICTION MEASUREMENT

Tribological properties of silicon carbide in
metal removal process

p0085 N81-17900

Friction and wear results from sputter-deposited
chrome oxide with and without nichrome metallic
binders and interlayers

[ASME PAPER 80-C2/LUB-49]

p0089 N81-18693

FUEL CELL CATALYSTS

U ELECTROCATALYSTS

FUEL CELLS

- Status of commercial phosphoric acid fuel cell system development
[AIAA PAPER 81-0396] p0108 A81-20805
- Status of commercial phosphoric acid fuel cell system development
[NASA-TN-81641] p0096 A81-13464
- Study of component technologies for fuel cell on-site integrated energy systems
[NASA-CR-165152-VOL-1] p0110 A81-15461
- Study of component technologies for fuel cell on-site integrated energy system. Volume 2: Appendices
[NASA-CR-165152-VOL-2] p0110 A81-15462
- Preparation and evaluation of advanced electrocatalysts for phosphoric acid fuel cells
[NASA-CR-165179] p0111 A81-17527
- Cell module and fuel conditioner
[NASA-CR-165189] p0112 A81-18494
- Preparation and evaluation of advanced electrocatalysts for phosphoric acid fuel cells
[NASA-CR-165245] p0112 A81-18496
- Non-noble catalysts and catalyst supports for phosphoric acid fuel cells
[NASA-CR-165221] p0112 A81-18497
- Cell module and fuel conditioner development
[NASA-CR-165190] p0112 A81-19573
- Study of fuel cell on-site, integrated energy systems in residential/commercial applications
[NASA-CR-165144] p0112 A81-21533
- Technology development for phosphoric acid fuel cell powerplant, phase 2
[NASA-CR-165317] p0113 A81-21536
- Technology development for phosphoric acid fuel cell powerplant (phase 2)
[NASA-CR-165316] p0113 A81-21547
- Stabilizing platinum in phosphoric acid fuel cells
[NASA-CR-165311] p0113 A81-22473
- Technology development for phosphoric acid fuel cell powerplant (phase 2) --- on site integrated energy systems
[NASA-CR-165318] p0113 A81-22475
- FUEL COMBUSTION**
- Pressure spectra and cross spectra at an area contraction in a ducted combustion system
[ASME PAPER 80-C2/AREC-9] p0077 A81-18638
- Requirements and preliminary concept of a Zero-Gravity Combustion Facility for Spacelab
[AIAA PAPER 81-0165] p0032 A81-20642
- Ultra-lean combustion at high inlet temperatures
[ASME PAPER 81-GT-44] p0086 A81-29958
- Effect of fuel nitrogen and hydrogen content on emissions in hydrocarbon combustion
[ASME PAPER 81-GT-63] p0057 A81-29573
- Low NO_x/ combustion systems for burning heavy residual fuels and high-fuel-bound nitrogen fuels
[ASME PAPER 81-GT-109] p0089 A81-30014
- Combustion experimentation aboard the space transportation system
p0032 A81-46068
- Deposition and material response from Mach 0.3 burner rig combustion of SRC 2 fuels
[NASA-TN-81634] p0051 A81-15069
- High-density fuel combustion and cooling investigation --- engine design
[NASA-CR-165177] p0050 A81-16177
- Experimental evaluation of catalytic combustion with heat removal at near stoichiometric conditions
[NASA-TN-81748] p0103 A81-23609
- Selected results from combustion research at the Lewis Research Center
[NASA-TN-82627] p0017 A81-25083
- Material response from Mach 0.3 burner rig combustion of a coal-oil mixture
[NASA-TN-81686] p0055 A81-27258
- Compatibility of alternative fuels with advanced automotive gas turbine and stirling engines. A literature survey
[NASA-TN-81754] p0105 A81-27604
- FUEL CONSUMPTION**
- Advanced fuel system technology for utilizing broadened property aircraft fuels
p0066 A81-11612
- Effect of time-dependent flight loads on turbofan engine performance deterioration
[ASME PAPER 81-GT-203] p0030 A81-30093
- Improved components for engine fuel savings
[SAE PAPER 801116] p0027 A81-34152
- Performance deterioration of commercial high-bypass ratio turbofan engines
[SAE PAPER 801118] p0021 A81-34154
- A status report on the Energy Efficient Engine Project
[SAE PAPER 801119] p0021 A81-34155
- Cogeneration Technology Alternatives Study (CTAS) Volume 5: Analytical approach and results
[NASA-CR-159763] p0109 A81-10517
- Vehicle testing of Cummins turbocompound diesel engine
[NASA-CR-159840] p0140 A81-13733
- Energy efficient engine diffuser/combustor model technology
[NASA-CR-165157] p0026 A81-15002
- Ceramic applications in turbine engines --- for improved component performance and reduced fuel usage
[NASA-CR-159865] p0029 A81-19118
- Energy efficient engine flight propulsion system: Aircraft/engine integration evaluation
[NASA-CR-159584] p0030 A81-22051
- The B3 combustors: Status and challenges --- energy efficient turbofan engines
[NASA-TN-82684] p0018 A81-28095
- Test results of the Chrysler upgraded automotive gas turbine engine: Initial design
[NASA-TN-81660] p0107 A81-30562
- FUEL CONTAMINATION**
- Accuracy of trace element determinations in alternate fuels
p0056 A81-22530
- FUEL CONTROL**
- A model for the analysis of premixing-prevaporizing fuel-air mixing passages
[AIAA PAPER 81-0345] p0030 A81-20767
- Selected results from combustion research at the Lewis Research Center
[AIAA PAPER 81-1392] p0022 A81-40859
- Propellant management for low thrust chemical propulsion systems
[AIAA PAPER 81-1453] p0042 A81-42198
- FUEL FLOW**
- Small gas-turbine combustor study: Fuel injector evaluation
[NASA-TN-82641] p0018 A81-26146
- FUEL INJECTION**
- A model for the analysis of premixing-prevaporizing fuel-air mixing passages
[AIAA PAPER 81-0345] p0030 A81-20767
- Ultra-lean combustion at high inlet temperatures
[NASA-TN-81649] p0097 A81-14398
- Fuel injector characterization studies
[NASA-CR-165200] p0026 A81-15003
- Capillary and acceleration wave breakup of liquid jets in axial-flow airstreams
[NASA-TN-1791] p0075 A81-16417
- Acceleration wave breakup of liquid jets with airstreams
[NASA-TN-81717] p0075 A81-21310
- Effects of fuel-injector design on ultra-lean combustion performance
[NASA-TN-82624] p0104 A81-24533
- Small gas-turbine combustor study: Fuel injector evaluation
[NASA-TN-82641] p0018 A81-26146
- Supercritical fuel injection system
[NASA-CASE-LEN-12390-1] p0018 A81-29129
- FUEL OILS**
- HT LIQUID FUELS**
- Design and preliminary results of a fuel flexible industrial gas turbine combustor
[ASME PAPER 81-GT-108] p0087 A81-30013
- Experimental study of the stability of aircraft fuels at elevated temperatures
[NASA-CR-165165] p0067 A81-12255
- FUEL PRODUCTION**
- HT LIQUID FUELS**
- Effect of hydroprocessing severity on characteristics of jet fuel from OSCO 2 and Paraho distillates
[NASA-TP-1768] p0066 A81-24283
- FUEL PUMPS**
- Low-thrust chemical propulsion system pump technology
[NASA-CR-165210] p0088 A81-17437
- FUEL SYSTEMS**
- Advanced fuel system technology for utilizing broadened property aircraft fuels

- Supercritical fuel injection system p0066 A81-11612
[NASA-CASE-LEN-12990-1] p0018 N81-29129
- FUEL TESTS**
- Advanced fuel system technology for utilizing broadened property aircraft fuels p0066 A81-11612
- Experimental study of the stability of aircraft fuels at elevated temperatures p0067 N81-12255
[NASA-CR-165165]
- Effect of hydroprocessing severity on characteristics of jet fuel from CSCO 2 and Paraho distillates p0066 N81-24283
[NASA-TP-1768]
- FUEL-AIR RATIO**
- A model for the analysis of premixing-prevaporizing fuel-air mixing passages [AIAA PAPER 81-0345] p0030 A81-20767
- Fuel/air nonuniformity - Effect on nitric oxide emissions p0019 A81-20834
[AIAA PAPER 81-0327]
- Ultra-lean combustion at high inlet temperatures p0086 A81-29958
[ASME PAPER 81-GT-44]
- Prolonging thermal barrier coated specimen life by thermal cycle management p0065 A81-44658
- Ignition of lean fuel-air mixtures in a premixing-prevaporizing duct at temperatures up to 1000 K p0096 N81-13465
[NASA-TN-81645]
- Fuel injector characterization studies p0026 N81-15003
[NASA-CR-165200]
- Spectral flame radiance from a tubular-can combustor p0016 N81-19121
[NASA-TP-1722]
- Analysis of effect of flameholder characteristics on lean, premixed, partially vaporized fuel-air mixtures quality and nitrogen oxides emissions p0016 N81-24065
[NASA-TP-1642]
- FUELS**
- NT AIRCRAFT FUELS
- NT CHEMICAL FUELS
- NT CRYOGENIC ROCKET PROPELLANTS
- NT DIESEL FUELS
- NT FUEL OILS
- NT HIGH ENERGY FUELS
- NT HYDROCARBON FUELS
- NT JET ENGINE FUELS
- NT KEROSENE
- NT LIQUID FUELS
- NT LIQUID ROCKET PROPELLANTS
- NT SYNTHETIC FUELS
- Atomic hydrogen storage method and apparatus p0066 N81-14103
[NASA-CASE-LEN-12081-3]
- FUNCTIONS (MATHEMATICS)**
- NT COORDINATE TRANSFORMATIONS
- NT TRANSFER FUNCTIONS
- FURAN RESINS**
- NT Kevlar (TRADEMARK)
- FURNACES**
- High temperature cyclic oxidation furnace testing at NASA Lewis Research Center p0058 A81-44653
- High temperature cyclic oxidation furnace testing at NASA Lewis Research Center p0054 N81-26234
[NASA-TN-81773]
- GADOLINIUM**
- T-S diagram for gadolinium near the Curie temperature p0135 A81-43004
- GAGES**
- U MEASURING INSTRUMENTS
- GALERKIN METHOD**
- Perturbation solutions of combustion instability problems p0050 N81-16176
[NASA-CR-159643]
- GALLIUM ARSENIDES**
- Analysis of GaAs and Si solar cell arrays for earth orbital and orbit transfer missions p0109 A81-27254
- GaAs shallow-homojunction solar cells p0110 N81-15463
[NASA-CR-165167]
- GaAs homojunction solar cell development p0099 N81-17561
- Proton radiation damage in bulk n-GaAs p0059 N81-17564
- Analysis of costs of gallium arsenide and silicon solar arrays for space power applications p0038 N81-20173
[NASA-TP-1811]
- Determination of optimum sunlight concentration level in space for gallium arsenide solar cells p0040 N81-26173
[NASA-TN-82643]
- GALLIUM COMPOUNDS**
- NT GALLIUM ARSENIDES
- GALVANIC CELLS**
- U ELECTROLYTIC CELLS
- GAPS**
- High voltage V-groove solar cell p0098 N81-16529
[NASA-CASE-LEN-13401-1]
- GARP**
- U GLOBAL ATMOSPHERIC RESEARCH PROGRAM
- GAS ANALYSIS**
- NT OSCILLOMETRY
- An integrated exhaust gas analysis system with self-contained data processing and automatic calibration p0102 N81-23435
[NASA-TN-81592]
- GAS DISCHARGES**
- Adapting magnetoelectrostatic containment to inert gas thrusters p0043 A81-20625
[AIAA PAPER 81-0140]
- GAS DISSOCIATION**
- Free radical propulsion concept p0041 A81-32905
[AIAA PAPER 81-0676]
- GAS DYNAMICS**
- NT AERODYNAMICS
- NT AEROTHERMODYNAMICS
- NT ROTOR AERODYNAMICS
- GAS EVACUATING**
- U EVACUATING (VACUUM)
- GAS FLOW**
- NT AIR FLOW
- NT KNUDSEN FLOW
- GAS GENERATOR ENGINES**
- U GAS GENERATORS
- GAS GENERATORS**
- Effect of a part-span variable inlet guide vane on the performance of a high-bypass turbofan engine p0022 A81-40842
[AIAA PAPER 81-1362]
- GAS STREAMS**
- Effect of a semi-annular thermal acoustic shield on jet exhaust noise p0125 N81-11770
[NASA-TN-81615]
- GAS TURBINE ENGINES**
- NT HYDROGEN ENGINES
- NT J-85 ENGINE
- NT JET ENGINES
- NT TURBOFAN ENGINES
- NT TURBOJET ENGINES
- NT TURBOPROP ENGINES
- Thermal barrier coatings - Burner rig hot corrosion test results p0063 A81-12630
- Thermal barrier coatings for heat engine components p0056 A81-12920
- Calculated and experimental data for a 11d-mm bore roller bearing to 3 million DB p0085 A81-19663
[ASME PAPER 80-C2/LUB-14]
- Ultra-lean combustion at high inlet temperatures p0086 A81-29958
[ASME PAPER 81-GT-44]
- Some modifications to, and operational experiences with, the two-dimensional, finite-difference, boundary-layer code, STAN5 p0077 A81-29996
[ASME PAPER 81-GT-89]
- Low MC/x/ and fuel flexible gas turbine combustors p0020 A81-30006
[ASME PAPER 81-GT-99]
- Evaluation of advanced combustors for dry MC/x/ suppression with nitrogen bearing fuels in utility and industrial gas turbines p0087 A81-30029
[ASME PAPER 81-GT-125]
- A study of external fuel vaporization --- for aircraft gas turbine engines p0020 A81-30057
[ASME PAPER 81-GT-158]
- Boundary layer development on turbine airfoil suction surfaces p0008 A81-30094
[ASME PAPER 81-GT-204]
- Loss model for off-design performance analysis of radial turbines with pivoting-vane, variable-area stators p0021 A81-34166
[SAE PAPER 801135]
- Composite wall concept for high-temperature turbine shrouds - Heat transfer analysis p0021 A81-34169
[SAE PAPER 801138]
- Some advantages of methane in an aircraft gas turbine

- [SAE PAPER 801154] p0022 A81-34177
Selected results from combustion research at the
Lewis Research Center
[AIAA PAPER 81-1392] p0022 A81-40859
New technique for the direct measurement of core
noise from aircraft engines
[AIAA PAPER 81-1587] p0128 A81-40962
Tungsten fiber reinforced superalloys - A status
review p0047 A81-44665
Thermal barrier coatings for superalloys p0058 A81-49217
Comparisons of four alternative powerplant types
for future general aviation aircraft
[NASA-TN-81584] p0013 A81-10067
Engine diagnostics program: CF6-50 engine
performance deterioration p0024 A81-12085
[NASA-CR-159867]
Effect of hole geometry and Electric-Discharge
Machining (EDM) on airflow rates through small
diameter holes in turbine blade material
[NASA-TP-1716] p0013 A81-12089
Progress in materials and structures at Lewis
Research Center p0142 A81-12982
Applicability of advanced automotive heat engines
to solar thermal power p0097 A81-14397
[NASA-TN-81658]
Ultra-lean combustion at high inlet temperatures
[NASA-TN-81640] p0097 A81-14398
Curved centerline air intake for a gas turbine
engine p0014 A81-14999
[NASA-CASE-LEW-13201-1]
Cost/benefit analysis of advanced materials
technologies for future aircraft turbine engines
[NASA-CR-165225] p0027 A81-15006
Apparatus for sensor failure detection and
correction in a gas turbine engine control system
[NASA-CASE-LEW-12907-2] p0015 A81-19115
Ceramic regenerator systems development program
[NASA-CR-165139] p0141 A81-22982
Fundamental heat transfer research for gas turbine
engines p0016 A81-24063
[NASA-CP-2178]
Tungsten fiber reinforced superalloys: A status
review p0045 A81-25148
[NASA-TN-82590]
Overview: DOE/NASA automotive gas turbine and
stirling projects p0105 A81-25487
[NASA-TN-82637]
Compatibility of alternative fuels with advanced
automotive gas turbine and stirling engines. A
literature survey p0105 A81-27604
[NASA-TN-81754]
Cold-air performance of compressor-drive turbine
of Department of Energy upgraded automobile gas
turbine engine. 1: Volute-manifold and stator
performance p0004 A81-28053
[NASA-TN-82682]
Test results of the Chrysler upgraded automotive
gas turbine engine: Initial design p0107 A81-30562
[NASA-TN-81660]
An introduction to NASA's turbine engine hot
section technology (HOST) project p0019 A81-31206
Structural dynamics verification facility study
[NASA-TN-82675] p0092 A81-33457
- GAS TURBINES**
Design and preliminary results of a fuel flexible
industrial gas turbine combustor p0087 A81-30013
[ASME PAPER 81-GT-108]
Prolonging thermal barrier coated specimen life by
thermal cycle management p0065 A81-44658
Catalytic combustion of coal-derived liquids
[NASA-TN-81594] p0097 A81-14396
Off-design analysis of a gas turbine powerplant
augmented by steam injection using various fuels
[NASA-TN-81611] p0098 A81-16571
Samarium cobalt (SMCO) generator/engine
integration study p0029 A81-17087
[AD-A092904]
Effects of fuel-injector design on ultra-lean
combustion performance p0104 A81-24533
[NASA-TN-82624]
High-response measurements of a turbofan engine
during nonrecoverable stall p0017 A81-25084
[NASA-TN-81759]
- Corrosion resistant thermal barrier coating ---
protecting gas turbines and other engine parts
[NASA-CASE-LEW-13088-1] p0054 A81-25188
Small gas-turbine combustor study: Fuel injector
evaluation p0018 A81-26146
[NASA-TN-82641]
Advanced aircraft engine materials trends
[NASA-TN-82626] p0055 A81-27259
Burner rig evaluation of thermal barrier coating
--- gas turbines p0055 A81-28231
[NASA-TN-81684]
Comparison of Integrated Gasifier-Combined Cycle
and AFB-steam turbine systems for industrial
cogeneration p0106 A81-28522
[NASA-TN-82648]
- GAS-METAL INTERACTIONS**
Deposition and material response from Mach 0.3
burner rig combustion of SMC 2 fuels p0051 A81-15069
[NASA-TN-81634]
Improved refractory coatings --- sputtered
coatings on substrates that form stable nitrides
[NASA-CASE-LEW-2169-2] p0052 A81-16209
- GAS-SOLID INTERACTIONS**
NT GAS-METAL INTERACTIONS
GASBOOS FUELS
NT LIQUID FUELS
GASEOUS ROCKET PROPELLANTS
Performance of a magnetic multipole line-cusp
argon ion thruster p0041 A81-38071
[AIAA PAPER 81-0745]
- GASES**
NT ARGON
NT ARGON FLASH
NT CARBON DIOXIDE
NT CARBON MONOXIDE
NT CHARGED PARTICLES
NT DISSOLVED GASES
NT ELECTRON PLASMA
NT EXHAUST GASES
NT GAS STREAMS
NT HIGH TEMPERATURE GASES
NT HYDROGEN
NT HYDROGEN ATOMS
NT LIQUID NITROGEN
NT LIQUID OXYGEN
NT NITROGEN
NT OZONE
NT RARE GASES
NT XENON
GASIFICATION
NT COAL GASIFICATION
GASOLINE
NT LIQUID FUELS
GASP
U GLOBAL AIR SAMPLING PROGRAM
- GEAR TESTS**
Optimal tooth numbers for compact standard spur
gear sets p0083 A81-27524
[NASA-TN-82614]
A method of selecting grid size to account for
Hertz deformation in finite element analysis of
spur gears p0083 A81-27525
[NASA-TN-82623]
- GEARS**
Comparisons of modified Vasco X-2 and AISI 9310
gear steels p0080 A81-14322
[NASA-TP-1731]
Design of spur gears for improved efficiency
[NASA-TN-81625] p0081 A81-17436
Advanced continuously variable transmissions for
electric and hybrid vehicles p0082 A81-19459
[NASA-TN-81718]
Surface geometry of circular cut spiral bevel gears
[NASA-TN-82622] p0083 A81-26459
A method of selecting grid size to account for
Hertz deformation in finite element analysis of
spur gears p0083 A81-27525
[NASA-TN-82623]
Simplified solution for stresses and deformation
[NASA-TN-82617] p0084 A81-28444
- GILDED ROCKET PROPELLANTS**
NT LIQUID FUELS
GENERAL AVIATION AIRCRAFT
An analytical approach to airfoil icing
[AIAA PAPER 81-0403] p0117 A81-20810
Icing tunnel tests of a glycol-exuding porous
leading edge ice protection system on a general
aviation airfoil p0011 A81-20837
[AIAA PAPER 81-0405]

- Core noise measurements from a small, general aviation turbofan engine p0019 A81-22531
- NASA research in aeropropulsion [ASME PAPER 81-G1-96] p0001 A81-30003
- Low and high speed propellers for general aviation - Performance potential and recent wind tunnel test results p0023 A81-42758
- An overview of general aviation propulsion research programs at NASA-Lewis Research Center [SAE PAPER 810624] p0023 A81-42778
- Light transport and general aviation aircraft icing research requirements [NASA-CR-165293] p0000 A81-19079
- General Aviation Turbine Engine (GATE) study [NASA-CR-159482] p0029 A81-19117
- Quiet Clean General Aviation Turbofan (QCGAT) technology study, volume 1 [NASA-CR-164222] p0030 A81-22052
- GENERAL DYNAMICS MILITARY AIRCRAFT**
- U MILITARY AIRCRAFT
- GEOMAGNETIC FIELD**
- U GEOMAGNETISM
- GEOMAGNETIC STORMS**
- U MAGNETIC STORMS
- GEOMAGNETISM**
- Environmental charging effects monitors for operational satellites p0037 A81-18057
- GEOMETRICAL HYDROMAGNETICS**
- U MAGNETOHYDRODYNAMICS
- GEOMETRY**
- NT ANGLE OF ATTACK
- NT COPLANARITY
- NT CRACK GEOMETRY
- NT CURVATURE
- NT DIFFERENTIAL GEOMETRY
- NT DUCT GEOMETRY
- NT FLOW GEOMETRY
- NT NOZZLE GEOMETRY
- NT TENSOR ANALYSIS
- NT TOPOLOGY
- Fast Generation of body conforming grids for 3-D p0122 A81-14706
- GRID30: Computer program for fast generation of multilevel, three-dimensional boundary-conforming O-type computational grids [NASA-TP-1920] p0005 A81-31128
- GEOSTATIONARY SATELLITES**
- U SYNCHRONOUS SATELLITES
- GLANDS (SEALS)**
- Circumferential shaft seal [NASA-CASE-LEW-12119-2] p0083 A81-26447
- GLASS**
- Electrostatic bonding of thin (cycle sine 3 mil) 7070 cover glass to Ta2O5 AR-coated thin (cycle sine 2 mil) silicon wafers and solar cells [NASA-CR-165240] p0111 A81-16582
- GLASS COATINGS**
- Recent developments in lightweight solar cell modules --- with protective glass cover p0099 A81-17571
- GLASS FIBER REINFORCED PLASTICS**
- Contact law and impact responses of laminated composites [NASA-CR-159884] p0048 A81-12172
- GLAUCOUS COEFFICIENT**
- U AERODYNAMIC FORCES
- GLOBAL AIR SAMPLING PROGRAM**
- Ozone contamination in aircraft cabins - Results from GASP data and analyses [AIAA PAPER 81-0305] p0010 A81-20740
- Cloud encounter and particle density variabilities from GASP data [AIAA PAPER 81-0308] p0117 A81-20742
- Tabulations of ambient ozone data obtained by GASP airliners, March 1975 to December 1977 [NASA-TN-81528] p0116 A81-13568
- Analysis of atmospheric ozone levels at commercial airplane cruise altitudes in winter and spring, 1976 - 1977 --- Global Atmospheric Sampling Program [NASA-TP-1807] p0117 A81-21685
- NASA Global Atmospheric Sampling Program (GASP) data report for tape VL0015, VL0016, VL0017, VL0018, VL0019, and VL0020 [NASA-TN-81661] p0115 A81-30657
- GLOBAL ATMOSPHERIC RESEARCH PROGRAM**
- Ozone contamination in aircraft cabins: Results from GASP data and analyses [NASA-TN-81671] p0009 A81-16021
- GLYCOLS**
- Icing tunnel tests of a glycol-exuding porous leading edge ice protection system on a general aviation airfoil [AIAA PAPER 81-0405] p0011 A81-20837
- GOVERNMENT/INDUSTRY RELATIONS**
- Aerospace in the future [NASA-TN-82664] p0143 A81-29063
- GOVERNMENTS**
- A methodology for fostering commercialization of electric and hybrid vehicle propulsion systems [NASA-TN-81575] p0140 A81-18933
- GRADIENTS**
- NT PRESSURE GRADIENTS
- GRADUATION**
- U CALIBRATING
- GRAINS (POOD)**
- NT BARLEY
- NT CORN
- NT OATS
- NT RICE
- NT SORGHUM
- NT WHEAT
- Normal crop calendars. Volume 2: The spring wheat states of Minnesota, Montana, North Dakota, and South Dakota [E81-10070] p0094 A81-13426
- GRAPHITE**
- NT PYROLYTIC GRAPHITE
- Dynamics of solid dispersions in oil during the lubrication of point contacts. I - Graphite [ASLE PREPRINT 81-AM-5D-3] p0064 A81-33860
- Acoustic hydrogen storage method and apparatus [NASA-CASE-LEW-12081-3] p0066 A81-14103
- Dynamics of solid dispersions in oil during the lubrication of point contacts. Part 1: Graphite [NASA-TN-81683] p0061 A81-17264
- Ion sputter textured graphite --- applications to electron tube devices [NASA-CASE-LEW-12919-1] p0046 A81-27198
- Environmental effects on graphite fiber reinforced FMB-15 polyimide [NASA-TN-82625] p0046 A81-32194
- GRAPHITE-EPPOXY COMPOSITES**
- Contact law and impact responses of laminated composites [NASA-CR-159884] p0048 A81-12172
- GRAPHITE-POLYIMIDE COMPOSITES**
- Properties of PBE polyimide composites made with improved high strength graphite fibers p0047 A81-43603
- Influence of excess diamine on properties of PBE polyimide resins and composites p0047 A81-43635
- GRASSES**
- NT HAY
- NT SORGHUM
- GRAVITATION**
- NT REDUCED GRAVITY
- GRAVITATION THEORY**
- Forced and natural convection in laminar-jet diffusion flames --- normal-gravity, inverted-gravity and zero-gravity flames [NASA-TP-1841] p0076 A81-24388
- GRAVITATIONAL EFFECTS**
- Combustion of solid carbon rods in zero and normal gravity [NASA-TN-81728] p0082 A81-22317
- GRAVITY GRADIENT SATELLITES**
- NT AIS
- GREEN WAVE EFFECT**
- Preliminary evaluation of the Environmental Research Institute of Michigan crop calendar shift algorithms for estimation of spring wheat development stage --- North Dakota, South Dakota, Montana, and Minnesota [E81-10071] p0094 A81-13427
- GRIDS**
- Fast Generation of body conforming grids for 3-D p0122 A81-14706
- GRINDING (MATERIAL REMOVAL)**
- Tritological properties of silicon carbide in metal removal process p0025 A81-17900

GROUND SUPPORT EQUIPMENT
Icing instrumentation

p0117 N81-14559

GROUPE

NT DIRECTIONAL SOLIDIFICATION (CRYSTALS)

GUIDE VANES

Design, durability and low cost processing
technology for composite fan exit guide vanes

p0089 A81-22664

Effect of a part-span variable inlet guide vane on
the performance of a high-bypass turbofan engine
[AIAA PAPER 81-1362] p0022 A81-40842

GYROPLANES

U HELICOPTERS

GYROTHONS

U CYCLOTRON RESONANCE DEVICES

H

HALL ACCELERATORS

High B-field, large area ratio MHD duct experiments
[NASA-TN-82673] p0132 N81-32026

HALL GENERATORS

Preliminary investigation of acoustic oscillations
in an H₂-O₂ fired Hall generator
[NASA-TN-81756] p0103 N81-23610

HALOGEN COMPOUNDS

NT FLUOROPOLYMERS

NT POLYTETRAFLUOROETHYLENE

HANDBOOKS

NT USER MANUALS (COMPUTER PROGRAMS)

HARDENING (MATERIALS)

NT PRECIPITATION HARDENING

HARDNESS TESTS

Comparisons of modified Vasco X-2 and AISI 9310
gear steels
[NASA-TP-1731] p0080 N81-14322

HARMONIC OSCILLATION

Experimental determination of unsteady blade
element aerodynamics in cascades. Volume 2:
Translation mode cascade
[NASA-CR-165166] p0007 N81-14976

HARMONICS

NT HARMONIC OSCILLATION

HAY

Normal crop calendars. Volume 2: The spring
wheat states of Minnesota, Montana, North
Dakota, and South Dakota
[E81-10070] p0094 N81-13426
Normal crop calendars. Volume 1: Assembly and
application of historical crop data to a
standard product
[E81-10075] p0095 N81-13431

HAZARDS

NT AIRCRAFT HAZARDS

NT FLIGHT HAZARDS

NT OPERATIONAL HAZARDS

NT RADIATION HAZARDS

NT TOXIC HAZARDS

HEALTH-EDUCATION TELECOMMUNICATIONS EXP

U NET EXPERIMENT

HEAT

NT PROCESS HEAT

HEAT DISSIPATION

U COOLING

HEAT DISSIPATION CHILLING

U COOLING

HEAT EFFECTS

U TEMPERATURE EFFECTS

HEAT EQUATIONS

U THERMODYNAMICS

HEAT EXCHANGERS

Improved ceramic heat exchanger materials
[NASA-CR-159678] p0065 N81-14082
Ceramic regenerator systems development program
[NASA-CR-165139] p0141 N81-22982
Heat exchanger and method of making
[NASA-CASE-LEW-12441-3] p0104 N81-24519

HEAT FLOW

U HEAT TRANSMISSION

HEAT GAIN

U HEATING

HEAT PIPES

High power densities from high-temperature
material interactions --- in thermionic energy
conversion and metallic fluid heat pipes
[AIAA PAPER 81-1161] p0070 A81-39144
High power densities from high-temperature
materials interactions --- thermionic energy

conversion and metallic fluid heat pipes
[NASA-TN-81626] p0131 N81-16900
Heat pipes to reduce engine exhaust emissions
[NASA-CASE-LEW-12590-1] p0009 N81-19245
Study of thermal management for space platform
applications
[NASA-CR-165238] p0033 N81-21106
Heat pipes containing alkali metal working fluid
[NASA-CASE-LEW-12253-1] p0076 N81-22310
SEP BISHOP variable conductance heat pipes
acceptance and characterization tests
[NASA-TN-82635] p0076 N81-30390

HEAT RADIATORS
Study of thermal management for space platform
applications
[NASA-CR-165238] p0033 N81-21106

HEAT REGULATION
U TEMPERATURE CONTROL

HEAT REJECTION DEVICES
U HEAT RADIATORS

HEAT RESISTANCE
U THERMAL RESISTANCE

HEAT RESISTANT ALLOYS
NT NICKEL-BASED ALLOYS
NT REFRACTORY METAL ALLOYS
NT TUNGSTEN ALLOYS

Cyclic behavior of turbine disk alloys at 650 C
p0056 A81-12266

Comparative evaluation of insulating properties of
plasma-sprayed ceramic coatings
p0064 A81-15984

Elevated temperature mechanical properties and
residual tensile properties of two cast
superalloys and several nickel-base oxide
dispersion strengthened alloys
p0057 A81-24104

Oxidation and hot corrosion of coated and bare
oxide dispersion strengthened superalloy MA-755E
p0058 A81-43384

Synergistic erosion/corrosion of superalloys in
PFB coal combustor effluent
p0058 A81-44663

Tungsten fiber reinforced superalloys - A status
review
p0047 A81-44665

Thermal barrier coatings for superalloys
p0056 A81-49217

Tungsten wire-reinforced superalloys for 1093 C
(2000 F) turbine blade applications
[NASA-CR-159720] p0047 N81-10112

Evaluation of candidate Stirling engine heater
tube alloys for 1000 hours at 760 C
[NASA-TN-81578] p0051 N81-15068

The effects of trace impurities in coal-derived
liquid fuels on deposition and accelerated high
temperature corrosion of cast superalloys
[NASA-TN-81678] p0052 N81-16211

Microstructure of Al₂O₃ scales formed on NiCrAl
alloys
[NASA-TN-81676] p0052 N81-16212

Creep and residual mechanical properties of cast
superalloys and oxide dispersion strengthened
alloys
[NASA-TP-1781] p0053 N81-19273

Heat pipes containing alkali metal working fluid
[NASA-CASE-LEW-12253-1] p0076 N81-22310

The fracture morphology of nickel-base superalloys
tested in fatigue and creep-fatigue at 650 C
[NASA-TN-81740] p0101 N81-23244

Synergistic erosion/corrosion of superalloys in
PFB coal combustor effluent
[NASA-TN-81715] p0101 N81-23245

Tungsten fiber reinforced superalloys: A status
review
[NASA-TN-82590] p0045 N81-25148

Material response from Mach 0.3 burner rig
combustion of a coal-oil mixture
[NASA-TN-81686] p0055 N81-27258

Advanced aircraft engine materials trends
[NASA-TN-82626] p0055 N81-27259

NASA's activities in the conservation of strategic
aerospace materials
[NASA-TN-81617] p0055 N81-29205

Cobalt: A vital element in the aircraft engine
industry
[NASA-TN-82662] p0055 N81-29206

An introduction to NASA's turbine engine hot
section technology (HOST) project

- Conservation of Strategic Aerospace Materials (COSAM) p0019 N81-31206
- A new diffusion-inhibited oxidation-resistant coating for superalloys [NASA-TN-82687] p0019 N81-31208
- HEAT STORAGE**
- Study of component technologies for fuel cell on-site integrated energy systems [NASA-CR-165152-VOL-1] p0110 N81-15461
- Study of component technologies for fuel cell on-site integrated energy system. Volume 2: Appendices [NASA-CR-165152-VOL-2] p0110 N81-15462
- Thermal energy storage for the Stirling engine powered automobile [NASA-CR-159561] p0113 N81-22467
- HEAT TESTS**
- U HIGH TEMPERATURE TESTS**
- HEAT TRANSFER**
- HT TURBULENT HEAT TRANSFER**
- Heat transfer from a row of impinging jets to concave cylindrical surfaces p0078 N81-24924
- Ion beam texturing of heat transfer surfaces [AIAA PAPER 81-0670] p0086 N81-29531
- Composite wall concept for high-temperature turbine shrouds - Heat transfer analysis [SAE PAPER 801138] p0021 N81-34169
- Heat transfer coefficients for staggered arrays of short pin fins [NASA-TN-81556] p0074 N81-13302
- High-density fuel combustion and cooling investigations --- engine design [NASA-CR-165177] p0050 N81-16177
- Thermal and flow analysis of a convection air-cooled ceramic coated porous metal concept for turbine vanes [NASA-TN-81749] p0016 N81-22056
- Heat pipes containing alkali metal working fluid [NASA-CASE-LEW-12253-1] p0076 N81-22310
- Fundamental heat transfer research for gas turbine engines [NASA-CP-2178] p0016 N81-24063
- Heat exchanger and method of making [NASA-CASE-LEW-12441-3] p0104 N81-24519
- HEAT TRANSFER COEFFICIENTS**
- Heat transfer coefficients for staggered arrays of short pin fins [ASME PAPER 81-GT-75] p0077 N81-29983
- Some modifications to, and operational experiences with, the two-dimensional, finite-difference, boundary-layer code, STANS [ASME PAPER 81-GT-89] p0077 N81-29996
- Evaluation of a method for heat transfer measurements and thermal visualization using a composite of a heater element and liquid crystals [ASME PAPER 81-GT-93] p0079 N81-30000
- Evaluation of a method for heat transfer measurements and thermal visualization using a composite of a heater element and liquid crystals --- thermal performance of turbine blade cooling configurations [NASA-TN-81639] p0075 N81-21313
- Influence of thermal boundary conditions on heat transfer from a cylinder in cross flow [NASA-TP-1894] p0076 N81-29384
- HEAT TRANSMISSION**
- HT HEAT TRANSFER**
- HT TURBULENT HEAT TRANSFER**
- Development and testing of heat transport fluids for use in active solar heating and cooling systems [NASA-TN-82395] p0098 N81-16584
- Heat transparent high intensity high efficiency solar cell [NASA-CASE-LEW-12892-1] p0105 N81-27598
- HEAT TREATMENT**
- HT ANNEALING**
- HT LASER ANNEALING**
- The effect of mechanical surface and heat treatments on the erosion resistance of 6061 aluminum alloy p0057 N81-27944
- Oxidation-induced contraction and strengthening of boron fibers p0047 N81-44664
- Effect of mechanical surface and heat treatments on erosion resistance [NASA-TN-81540] p0051 N81-11178
- Effects of erodent particle shape and various heat treatments on erosion resistance of plain carbon steel [NASA-TP-1755] p0052 N81-16210
- Oxidation-induced contraction and strengthening of boron fibers [NASA-TN-82599] p0046 N81-25150
- HEATING**
- HT RADIO FREQUENCY HEATING**
- HT SOLAR HEATING**
- A computer simulation of the transient response of a 4 cylinder Stirling engine with burner and air preheater in a vehicle [NASA-CR-165262] p0078 N81-22313
- HEATING EQUIPMENT**
- HT BOILERS**
- HT FURNACES**
- HEP (HIGH ENERGY FUELS)**
- U HIGH ENERGY FUELS**
- HELICOPTER ATTITUDE INDICATORS**
- U HELICOPTERS**
- HELICOPTER ENGINES**
- Comparison of predicted engine core noise with proposed FAA helicopter noise certification requirements p0128 N81-38062
- Comparison of predicted engine core noise with proposed FAA helicopter noise certification requirements [NASA-TN-81739] p0130 N81-22839
- HELICOPTER MOTORS**
- U ROTARY WINGS**
- HELICOPTER VANCES**
- Fluid mechanics mechanisms in the stall process of helicopters [NASA-TN-81956] p0003 N81-21027
- HELICOPTERS**
- Pneumatic boot for helicopter rotor deicing p0009 N81-19059
- Fluid mechanics mechanisms in the stall process of helicopters [NASA-TN-81956] p0003 N81-21027
- HELIX TUBES**
- U TRAVELING WAVE TUBES**
- HERMES SATELLITE**
- U COMMUNICATIONS TECHNOLOGY SATELLITE**
- HET EXPERIMENT**
- Applications Technology Satellite and Communications Technology Satellite user experiments for 1967 - 1980 reference book, volume 1 [NASA-CR-165169-VOL-1] p0033 N81-12135
- Applications Technology Satellite and Communications Technology Satellite user experiments for 1967-1980 reference book, volume 2 [NASA-CR-165169-VOL-2] p0033 N81-12136
- Applications Technology Satellite and Communications Technology Satellite user experiments for 1967-1980 reference book. Volume 3: User form surveys [NASA-CR-165169-VOL-3] p0033 N81-12137
- HIGH ENERGY FUELS**
- Safety management of complex research operators [NASA-TN-81772] p0068 N81-25263
- HIGH FREQUENCIES**
- High-frequency sound propagation in a spatially varying mean flow [NASA-TN-81751] p0126 N81-20831
- HIGH INTENSITY LASERS**
- U HIGH POWER LASERS**
- HIGH MELTING COMPOUNDS**
- U REFRACTORY MATERIALS**
- HIGH POWER LASERS**
- Safety management of complex research operators [NASA-TN-81772] p0068 N81-25263
- HIGH PRESSURE**
- JT8D-15/17 high pressure turbine root discharged blade performance improvement --- engine design [NASA-CR-165220] p0028 N81-17380
- HIGH STRENGTH ALLOYS**
- Effect of THF variables upon structure and properties in ODS alloy BDA 8077 sheet --- Thermochemical Processing of Oxide Dispersion Strengthened nickel alloy p0059 N81-10706

HIGH TEMPERATURE

Tungsten wire-reinforced superalloys for 1093 C (2000 F) turbine blade applications [NASA-CR-159720] p0047 N81-10112

Evaluation of candidate Stirling engine heater tube alloys for 1000 hours at 760 C [NASA-TN-81578] p0051 N91-15068

High temperature alkali corrosion in high velocity gases [NASA-TN-82591] p0054 N81-25191

HIGH TEMPERATURE ALLOYS
U HEAT RESISTANT ALLOYS

HIGH TEMPERATURE ENVIRONMENTS
High temperature electronic requirements in aeropropulsion systems p0072 A81-32547

Description of the vane core turbine facility and the vane annular cascade facility recently installed at NASA Lewis Research Center [SAE PAPER 801122] p0031 A81-34158

High temperature electronic requirements in aeropropulsion systems [NASA-TN-81682] p0071 N81-16388

High power densities from high-temperature materials interactions --- thermionic energy conversion and metallic fluid heat pipes [NASA-TN-81626] p0131 N81-16900

Corrosion resistant thermal barrier coating --- protecting gas turbines and other engine parts [NASA-CASE-LEW-13088-1] p0054 N81-25188

HIGH TEMPERATURE FLUIDS
U HIGH TEMPERATURE GASES

HIGH TEMPERATURE GASES
Composite wall concept for high-temperature turbine shrouds - Heat transfer analysis [SAE PAPER 801138] p0021 A81-34169

Curved film cooling admission tube [NASA-CASE-LEW-13174-1] p0074 N81-12363

HIGH TEMPERATURE LUBRICANTS
Steady-state boundary lubrication with formulated C-ethers to 260 C [NASA-TP-1812] p0053 N81-21193

HIGH TEMPERATURE MATERIALS
U REFRACTORY MATERIALS

HIGH TEMPERATURE TESTS
The effect of thermal cycling to 1100 C on the alpha /beta phase in directionally solidified gamma/gamma-prime-alpha alloys p0057 A81-32546

High power densities from high-temperature material interactions --- in thermionic energy conversion and metallic fluid heat pipes [AIAA PAPER 81-1161] p0070 A81-39144

Properties of PBR polyimide composites made with improved high strength graphite fillers p0047 A81-47603

High temperature cyclic oxidation furnace testing at NASA Lewis Research Center p0058 A81-44653

Experimental study of the stability of aircraft fuels at elevated temperatures [NASA-CR-165165] p0067 N81-12255

High temperature cyclic oxidation furnace testing at NASA Lewis Research Center [NASA-TN-81773] p0054 N81-26234

HIGH VOLTAGES
The effect of solar array voltage patterns on plasma power losses p0043 A81-19937

High voltage planar multi-junction --- solar cells [NASA-CASE-LEW-13400-1] p0098 N81-16528

The effect of sincity carrier mobility variations on the performance of high voltage silicon solar cells p0098 N81-17536

KILLER MILITARY AIRCRAFT
U MILITARY AIRCRAFT

BIGGED MOTOR BLADES
U ROTARY WINGS

HISTORIES
U CASE HISTORIES
History of ball bearings [NASA-TN-81689] p0081 N81-18391

HOLE DISTRIBUTION (MECHANICS)
Effect of hole geometry and Electric-Discharge Machining (EDM) on airflow rates through small diameter holes in turbine blade material [NASA-TP-1716] p0013 N81-12089

HOLE DISTRIBUTION (MECHANICS)

Stress concentration in the vicinity of a hole defect under conditions of Hertzian contact [NASA-TN-82649] p0084 N81-28443

HOLLOW CATHODES
Fluid model of plasma outside a hollow cathode neutralizer [AIAA PAPER 81-0739] p0134 A81-29560

HOLOGRAPHIC INTERFEROMETRY
Holographic flow visualization of time-varying shock waves p0079 A81-47642

HORIZONTAL ORIENTATION
Stability of large horizontal-axis axisymmetric wind turbines p0092 A81-22526

HOT CORROSION
U TEMPERATURE DEPENDENCE
Thermal barrier coatings - Burner rig hot corrosion test results p0063 A81-12630

Oxidation and hot corrosion of coated and bare oxide dispersion strengthened superalloy MA-755x p0058 A81-43384

Synergistic erosion/corrosion of superalloys in PFB coal combustor effluent p0058 A81-44663

An investigation of hot corrosion mechanisms in nickel base alloys p0058 N81-16208

The effects of trace impurities in coal-derived liquid fuels on deposition and accelerated high temperature corrosion of cast superalloys [NASA-TN-81678] p0052 N81-16211

Heat pipes containing alkali metal working fluid [NASA-CASE-LEW-12253-1] p0076 N81-22310

HOT GAS SYSTEMS
U HIGH TEMPERATURE GASES

HOT GASES
U HIGH TEMPERATURE GASES

HOT JET EXHAUST
U HIGH TEMPERATURE GASES

HOT JET EXHAUST
U JET EXHAUST

HOT JETS
U JET FLOW

HUGHES MILITARY AIRCRAFT
U MILITARY AIRCRAFT

HYBRID COMPUTERS
An automated procedure for developing hybrid computer simulations of turbofan engines p0020 A81-32544

An automated procedure for developing hybrid computer simulations of turbofan engines [NASA-TN-81605] p0037 N81-11688

HYBRID STRUCTURES
Superhybrid composite blade impact studies [NASA-TN-81597] p0091 N81-11412

HYDRAULIC ACTUATORS
U ACTUATORS

HYDRAULIC EQUIPMENT
U HYDRAULIC EQUIPMENT

HYDRAULIC EQUIPMENT
An experimental evaluation of oil pumping rings [NASA-CR-165271] p0088 N81-21355

HYDRAULIC HEATING SOURCES
U HYDRAULIC EQUIPMENT

HYDRAULIC PUMPS
U HYDRAULIC EQUIPMENT

U PUMPS

HYDRAULIC SYSTEMS
U HYDRAULIC EQUIPMENT

HYDRAULIC VALVES
U HYDRAULIC EQUIPMENT

HYDROAEROMECHANICS
U AERODYNAMICS

HYDROCARBON COMBUSTION
Effect of fuel nitrogen and hydrogen content on emissions in hydrocarbon combustion [ASME PAPER 81-GT-63] p0057 A81-29973

HYDROCARBON FUELS
U DIESEL FUELS

U JET ENGINE FUELS

U LIQUID FUELS
Effect of fuel nitrogen and hydrogen content on emissions in hydrocarbon combustion [NASA-TN-81612] p0097 N81-14399

Spectral flame radiance from a tubular-can combustor [NASA-TP-1722] p0016 N81-19121

An assessment of the use of antimisting fuel in turbofan engines

- [NASA-CR-165258] p0067 N81-19316
Safety management of complex research operators
[NASA-TN-81772] p0368 N81-25263
- HYDROCARBONS**
NT ALKENES
NT METHANE
NT PROPANE
NT TOLUENE
Infrared spectroscopy for the determination of hydrocarbon types in jet fuels
[NASA-TN-82674] p0066 N81-31380
- HYDRODYNAMIC COEFFICIENTS**
Surface roughness effect on finite oil journal bearings
[NASA-TN-82639] p0084 N81-27526
- HYDRODYNAMIC STABILITY**
U FLOW STABILITY
- HYDRODYNAMICS**
NT ELASTOHYDRODYNAMICS
NT MAGNETOHYDRODYNAMICS
Full-coverage film cooling. I - Three-dimensional measurements of turbulence structure. II - Prediction of the recovery-region hydrodynamics
p0078 N81-15537
Effect of surface roughness on hydrodynamic bearings
[NASA-TN-81711] p0082 N81-21356
- HYDROGEN**
NT HYDROGEN ATOMS
Effect of fuel nitrogen and hydrogen content on emissions in hydrocarbon combustion
[ASME PAPER 81-GT-63] p0057 N81-29973
Preparation and evaluation of advanced electrocatalysts for phosphoric acid fuel cells
[NASA-CR-165179] p0111 N81-17527
- HYDROGEN ATOMS**
Atomic hydrogen storage method and apparatus
[NASA-CASE-LBN-12081-3] p0066 N81-14103
- HYDROGEN ENGINES**
Free radical propulsion concept
[AIAA PAPER 81-0676] p0041 N81-32905
- HYDROGEN FUELS**
NT LIQUID FUELS
- HYDROGEN OXYGEN ENGINES**
High performance cryogenic engines for orbit transfer vehicles
[IAF PAPER 80-P-253] p0043 N81-18363
Traction drive for cryogenic boost pump --- hydrogen oxygen rocket engines
[NASA-TN-81704] p0101 N81-23188
- HYDROLYSIS**
Effect of hydroprocessing severity on characteristics of jet fuel from CSCO 2 and Paraho distillates
[NASA-TP-1768] p0066 N81-24263
- HYDROMAGNETIC FLOW**
U MAGNETOHYDRODYNAMIC FLOW
- HYDROMAGNETIC STABILITY**
U MAGNETOHYDRODYNAMIC STABILITY
- HYDROMAGNETICS**
U MAGNETOHYDRODYNAMICS
- HYDROMAGNETISM**
U MAGNETOHYDRODYNAMICS
- HYDROMECHANICS**
NT ELASTOHYDRODYNAMICS
NT HYDRODYNAMICS
NT MAGNETOHYDRODYNAMICS
- HYDROX ENGINES**
U HYDROGEN OXYGEN ENGINES
- HYDROXYL COMPOUNDS**
NT GLYCOLS
NT POLYVINYL ALCOHOL
- MIXAL PROPERTIES**
Computer code for intraply hybrid composite design
p0047 N81-44662
Computer code for intraply hybrid composite design
[NASA-TN-82593] p0046 N81-25151
- HYPERBOLIC ROCKET PROPELLANTS**
NT LIQUID FUELS
- ICE**
NT SEA ICE
- ICE FORMATION**
NT CLOUD GLACIATION
An analytical approach to airfoil icing
[AIAA PAPER 81-0403] p0117 N81-26819
Icing instrumentation
p0117 N81-14559
- Survey of aircraft icing simulation test facilities in North America
[NASA-TN-81707] p0009 N81-19078
Light transport and general aviation aircraft icing research requirements
[NASA-CR-165290] p0010 N81-19079
- ICE MAPPING**
Comparative analysis of sea ice features using Side-Looking Airborne Radar (SLAR) and LANDSAT imagery --- Beaufort Sea and Bering Sea
[R31-10044] p0095 N81-33539
- ICE PACKS**
U SEA ICE
- ICE PREVENTION**
Icing tunnel tests of a glycol-exuding porous leading edge ice protection system on a general aviation airfoil
[AIAA PAPER 81-0405] p0011 N81-20837
Survey of aircraft icing simulation test facilities in North America
[NASA-TN-81707] p0009 N81-19078
Evaluation of a pneumatic boot deicing system on a general aviation wing model
[NASA-TN-82363] p0011 N81-25065
- ICING**
U ICE FORMATION
- IDENTIFYING**
NT CROP IDENTIFICATION
NT PARAMETERS IDENTIFICATION
- IGNITION**
NT SPARK IGNITION
Ignition of lean fuel-air mixtures in a premixing-pretaporizing duct at temperatures up to 1000 K
[NASA-TN-81645] p0096 N81-13465
- ILLINOIS**
Evaluation of results of US corn and soybeans exploratory experiment: Classification procedures verification test --- Missouri, Iowa, Indiana, and Illinois
[R81-10076] p0095 N81-13432
- IMAGE PROCESSING**
Limited Area Coverage/High Resolution Picture Transmission (LAC/HRPT) tape IJ grid pixel extraction processor user's manual
[R81-10072] p0094 N81-13428
Limited Area Coverage/High Resolution Picture Transmission (LAC/HRPT) data vegetative index calculation processor user's manual
[R81-10073] p0094 N81-13429
LBOS to universal tape conversion processor
[R81-10074] p0095 N81-13430
- IMMISCIBILITY**
U SOLUBILITY
- IMPACT RESISTANCE**
Superhybrid composite blade impact studies
[NASA-TN-81597] p0091 N81-11412
Effects of erodant particle shape and various heat treatments on erosion resistance of plain carbon steel
[NASA-TN-1755] p0052 N81-16210
- IMPACT SENSITIVITY**
U IMPACT RESISTANCE
- IMPACT TESTS**
Superhybrid composite blade impact studies
[ASME PAPER 81-GT-24] p0020 N81-29940
Contact law and impact responses of laminated composites
[NASA-CR-159884] p0048 N81-12172
- IMPEDANCE**
NT ACOUSTIC IMPEDANCE
- IMPELLER BLADES**
U ROTOR BLADES (TURBOCHASINERY)
- IMPINGEMENT**
NT JET IMPINGEMENT
- IMPLANTATION**
NT ION IMPLANTATION
- INCENTIVES**
A methodology for fostering commercialization of electric and hybrid vehicle propulsion systems
[NASA-TN-81575] p0140 N81-18933
- INCIDENT RADIATION**
The coupling between flow instabilities and incident disturbances at a leading edge
p0010 N81-28682
- INCOMPRESSIBLE FLOW**
Turbulent solution of the Navier-Stokes equations
p0077 N81-19284

- The experimental verification of a streamline curvature numerical analysis method applied to the flow through an axial flow fan
[AIAA PAPER 81-0363] p0005 881-20782
- Effects of mistuning on bending-torsion flutter and response of a cascade in incompressible flow
[AIAA 8602] p0092 881-29465
- Effects of mistuning on bending-torsion flutter and response of a cascade in incompressible flow --- turbofan engines
[NASA-TN-81674] p0091 881-16494
- INDEXES (DOCUMENTATION)**
Bibliography of Lewis Research Center Technical Publications announced in 1978
[NASA-TN-79162] p0137 881-17943
- INDIANA**
Evaluation of results of US corn and soybeans exploratory experiment: Classification procedures verification test --- Missouri, Iowa, Indiana, and Illinois
[881-10076] p0095 881-13432
- INDICATING INSTRUMENTS**
NT DRAG FORCE ANEMOMETERS
NT LASER ANEMOMETERS
- INDUCED FLUID FLOW**
U FLUID FLOW
- INJECTION SYSTEMS**
U INTAKE SYSTEMS
- INDUSTRIAL ENERGY**
Conceptual design study of a coal gasification combined-cycle powerplant for industrial cogeneration
[NASA-TN-81687] p0105 881-25488
- Comparison of Integrated Gasifier-Combined Cycle and AFB-steam turbine systems for industrial cogeneration
[NASA-TN-82648] p0106 881-28522
- INDUSTRIAL MANAGEMENT**
NT ENGINEERING MANAGEMENT
- INDUSTRIAL PLANTS**
Conceptual design study of a coal gasification combined-cycle powerplant for industrial cogeneration
[NASA-TN-81687] p0105 881-25488
- INDUSTRIAL SAFETY**
Safety management of complex research operations
p0067 881-44661
- INDUSTRIES**
NT AEROSPACE INDUSTRY
A methodology for fostering commercialization of electric and hybrid vehicle propulsion systems
[NASA-TN-81575] p0140 881-18933
- INERT GASES**
U RARE GASES
- INFORMATION SYSTEMS**
NT MANAGEMENT INFORMATION SYSTEMS
- INFORMATION TRANSMISSION**
U DATA TRANSMISSION
- INFRARED INSTRUMENTS**
NT INFRARED SPECTROPHOTOMETRIES
- INFRARED SPECTROPHOTOMETRIES**
Infrared spectroscopy for the determination of hydrocarbon types in jet fuels
[NASA-TN-82674] p0066 881-31380
- INJECTION**
NT FLUID INJECTION
NT FUEL INJECTION
- INJECTION CARBURIZERS**
U FUEL INJECTION
- INJECTION WELDING**
Fabrication of injection molded sintered alpha SiC turbine components
[ASME PAPER 81-GT-161] p0089 881-30060
- INLET FLOW**
Inlet flow distortion in turbomachinery
[ASME PAPER 80-GT-20] p0005 881-17952
- Flow separation in inlets at incidence angles
p0006 881-29114
- Turbomachinery noise studies of the AResearch OGCAT engine with inlet control --- acoustic performance
[AIAA PAPER 81-2049] p0023 881-48621
- Some aspects of calculating flows about three-dimensional subsonic inlets
[NASA-TN-82678] p0004 881-28054
- Experiments on flow through one to four inlets of the orifice and Borda type
[NASA-TN-82680] p0077 881-30391
- INLET PRESSURE**
Some flow phenomena associated with aligned, sequential apertures with Borda-type inlets --- inlet pressure and flow separation
[NASA-TP-1792] p0076 881-24387
- INLET TEMPERATURES**
Ultra-lean combustion at high inlet temperatures
[ASME PAPER 81-GT-44] p0086 881-29958
- INLETS (DEVICES)**
U INTAKE SYSTEMS
- INORGANIC COATINGS**
NT CERAMIC COATINGS
Advanced inorganic separators for alkaline batteries and method of making same --- a polymeric coating applied to a porous flexible substrate
[NASA-CASE-LEN-13171-1] p0100 881-22466
- INORGANIC SULFIDES**
NT MOLYBDENUM DISULFIDES
- INSULATION**
NT MULTILAYER INSULATION
NT THERMAL INSULATION
- INTAKE SYSTEMS**
NT AIR INTAKES
NT ENGINE INLETS
NT SUPERSONIC INLETS
Ignition of lean fuel-air mixtures in a premixing-prevaporizing duct at temperatures up to 1000 K
[NASA-TN-81645] p0096 881-13465
- Experiments on flow through one to four inlets of the orifice and Borda type
[NASA-TN-82680] p0077 881-30391
- INTEGRATED CIRCUITS**
Solar cell system having alternating current output
[NASA-CASE-LEN-12806-2] p0096 881-12542
- Integrated IC-circuits in ALTA-technology on one substrate
[BNPT-FD-T-79-107] p0072 881-14227
- INTEGRATED ENERGY SYSTEMS**
Study of component technologies for fuel cell on-site integrated energy systems
[NASA-CR-165152-VOL-1] p0110 881-15461
- Study of component technologies for fuel cell on-site integrated energy system. Volume 2: Appendices
[NASA-CR-165152-VOL-2] p0110 881-15462
- Study of fuel cell on-site, integrated energy systems in residential/commercial applications
[NASA-CR-165144] p0112 881-21533
- Technology development for phosphoric acid fuel cell powerplant (phase 2) --- on site integrated energy systems
[NASA-CR-165318] p0113 881-22475
- INTEGRAL DIFFERENTIAL EQUATIONS**
U DIFFERENTIAL EQUATIONS
- INTERACTIVE GRAPHICS**
U COMPUTER GRAPHICS
- INTERFACES**
NT LIQUID-SOLID INTERFACES
NT SOLID-SOLID INTERFACES
- INTERFACIAL ENERGY**
Contact angle measurements of a polyphenyl ether to 190 C on M-50 steel
[NASA-TN-82628] p0063 881-27277
- INTERFACIAL STRAIN**
U INTERFACIAL TENSION
- INTERFACIAL TENSION**
Contact angle measurements of a polyphenyl ether to 190 C on M-50 steel
[NASA-TN-82628] p0063 881-27277
- INTERFEROMETRY**
NT MICROGRAPHIC INTERFEROMETRY
- INTERLAYERS**
NT MULTILAYER INSULATION
- INTERMETALLICS**
NASA's activities in the conservation of strategic aerospace materials
[NASA-TN-81617] p0055 881-29205
- Conservation of Strategic Aerospace Materials (COSAM)
p0019 881-31208
- INTERMODULATION**
Experimental investigation of intermodulation effects and related efficiencies associated with two- and three-signal operation of a traveling wave tube
[NASA-TN-81576] p0069 881-10240

INTERNAL COMBUSTION ENGINES

HT DIESEL ENGINES
 HT GAS TURBINE ENGINES
 HT HELICOPTER ENGINES
 HT HYDROGEN ENGINES
 HT J-85 ENGINE
 HT JET ENGINES
 HT TURBOPAN ENGINES
 HT TURBOJET ENGINES
 HT TURBOPROP ENGINES
 HT WANKEL ENGINES
 Low-thrust chemical propulsion system pump technology
 [NASA-CR-165210] p0088 N81-17437
 Supercritical fuel injection system
 [NASA-CASE-LEW-12990-1] p0018 N81-29129
 INTERPLANETARY PROPULSION
 U ROCKET ENGINES
 INVENTIONS
 Engineering management and innovation p0036 N81-20400

INVENTORIES

HT CROP INVENTORIES
 INVENTED CONVERTERS (DC TO AC)
 Solar cell system having alternating current output
 [NASA-CASE-LEW-12806-2] p0096 N81-12542

INVISCID FLOW

The experimental verification of a streamline curvature numerical analysis method applied to the flow through an axial flow fan
 [AIAA PAPER 81-0363] p0005 N81-20782
 Finite element analysis of inviscid subsonic boattail flow
 [AIAA PAPER 81-0276] p0006 N81-20831
 Solution of plane cascade flow using improved surface singularity methods
 [ASME PAPER 81-GT-169] p0006 N81-30068
 Finite element analysis of inviscid subsonic boattail flow
 [NASA-TN-81650] p0003 N81-14977
 Surrogate-equation technique for simulation of steady inviscid flow
 [NASA-TF-1866] p0005 N81-31129

ION BEAMS

Ion beam texturing of heat transfer surfaces
 [AIAA PAPER 81-0670] p0386 N81-29531
 Ion beam deposited protective films
 [AIAA PAPER 81-0672] p0086 N81-29532
 Ion beam applications research - A 1981 summary of Lewis Research Center programs
 [AIAA PAPER 81-0659] p0041 N81-38068
 Ion beam sputter etching of orthopedic implant alloy MP35N and resulting effects on fatigue properties
 [AIAA PAPER 81-0671] p0057 N81-38069
 Ion plating for the future p0087 N81-44654
 Ion beam deposited protective films
 [NASA-TN-81722] p0030 N81-19221
 Simultaneous ion sputter polishing and deposition
 [NASA-TN-81679] p0053 N81-19278
 Method of cold welding using ion beam technology
 [NASA-CASE-LEW-12982-1] p0081 N81-19455
 Ion beam applications research. A summary of Lewis Research Center Programs
 [NASA-TN-81721] p0044 N81-21129
 Sputtered protective coatings for die casting dies
 [NASA-TN-81735] p0053 N81-21173
 Ion beam sputter etching of orthopedic implanted alloy MP35N and resulting effects on fatigue
 [NASA-TN-81747] p0045 N81-21174

ION CRYSTALS

HT ION BEAMS

ION ENGINES

HT MERCURY ION ENGINES
 HT IIT ENGINES
 Simplified power supplies for ion thrusters
 [AIAA PAPER 81-0693] p0040 N81-29542
 Ion beam applications research - A 1981 summary of Lewis Research Center programs
 [AIAA PAPER 81-0669] p0041 N81-38068
 Performance of a magnetic multipole line-cusp argon ion thruster
 [AIAA PAPER 81-0745] p0041 N81-38071
 SEPT II thrusters - Still ticking after eleven years
 [AIAA PAPER 81-1539] p0042 N81-46934
 Electric propulsion - characteristics, applications, and status
 [NASA-TN-81630] p0033 N81-13079

Performance of a magnetic multipole line-cusp argon ion thruster
 [NASA-TN-81703] p0038 N81-19219
 Performance capabilities of the 8-cm mercury ion thruster
 [NASA-TN-81720] p0038 N81-19220
 Simplified power supplies for ion thrusters
 [NASA-TN-81725] p0039 N81-20177
 Goals of the ionic program for space power
 [NASA-TN-82616] p0132 N81-25808
 SEPT 2 thrusters: Still ticking after eleven years
 [NASA-TN-81774] p0040 N81-26174

ION EXCHANGE MEMBRANE ELECTROLYTES

New ion exchange membranes --- composed of radiation crosslinked polyacrylic resins
 [NASA-TN-81670] p0044 N81-16123
 Anion permselective membrane
 [NASA-CR-165223] p0111 N81-16583
 Advances in membrane technology for the NASA redox energy storage system
 [NASA-TN-82701] p0108 N81-33601

ION IMPLANTATION

Passivation of carbon steel through mercury implantation
 [NASA-CR-165292] p0059 N81-20244
 Reduced annealing temperatures in silicon solar cells
 [NASA-TN-82597] p0104 N81-23627

ION IRRADIATION

HT PROTON IRRADIATION
 Ion beam texturing of heat transfer surfaces
 [AIAA PAPER 81-0670] p0086 N81-29531
 Ion beam deposited protective films
 [AIAA PAPER 81-0672] p0086 N81-29532
 The self-consistent calculation of pseudo-molecule energy levels, construction of energy level correlation diagrams and an automated computation system for SCF-X(alpha)-SV calculations
 [NASA-TN-81710] p0130 N81-25779

ION PLATING

Frictional and morphological characteristics of ion plated soft, metallic films p0057 N81-38066
 Ion plating for the future p0087 N81-44654
 Sputtering and ion plating for aerospace applications p0087 N81-44655
 Thin-film coatings p0142 N81-12983
 Sputtering and ion plating for aerospace applications
 [NASA-TN-81726] p0082 N81-20424
 Ion plating for the future p0054 N81-25189
 Catalyst surfaces for the chromous/chromic redox couple
 [NASA-CASE-LEW-13148-2] p0107 N81-29524

ION PROPULSION

Adapting magnetoelectrostatic containment to inert gas thrusters
 [AIAA PAPER 81-0140] p0043 N81-20625
 Recent work on an RF ion thruster
 [AIAA PAPER 81-0676] p0041 N81-35625
 Ion beam applications research - A 1981 summary of Lewis Research Center programs
 [AIAA PAPER 81-0669] p0041 N81-38068
 Electric propulsion - characteristics, applications, and status
 [NASA-TN-81630] p0033 N81-13079
 Extended operating range of the 30-cm ion thruster with simplified power processor requirements
 [NASA-TN-81729] p0039 N81-20179
 Particle and field measurements on two J-series 30 centimeter thrusters
 [NASA-TN-81711] p0039 N81-22084

ION SOURCES

Ion beam deposited protective films
 [AIAA PAPER 81-0672] p0086 N81-29532
 Simultaneous ion sputter polishing and deposition
 [NASA-TN-81679] p0053 N81-19278
 Recent work on an RF ion thruster
 [NASA-TN-81736] p0039 N81-20178
 Passivation of carbon steel through mercury implantation
 [NASA-CR-165292] p0059 N81-20244

IONIC PROPELLANTS

U ION ENGINES

IONIZATION
 NT SURFACE IONIZATION
 IONIZATION PRELIMINARIES
 Recent work on an RF ion thruster
 [NASA-TN-81734] p0039 N81-20178
 IONIZED GASES
 NT ARGON PLASMA
 NT CHARGED PARTICLES
 NT ELECTRON PLASMA
 NT FLASMA JETS
 NT PLASMA SHEATHS
 IONS
 NT ANIONS
 IOWA
 Evaluation of results of US corn and soybeans
 exploratory experiment: Classification
 procedures verification test --- Missouri, Iowa,
 Indiana, and Illinois
 [N81-10076] p0095 N81-13432
 IP (IMPACT PREDICTION)
 U COMPUTERIZED SIMULATION
 IRON ALLOYS
 NT CARBON STEELS
 NT STEELS
 Mechanical properties of weldments in experimental
 Fe-12Mn-0.2Ti and Fe-12Mn-1Mo-0.2Ti alloys for
 cryogenic service p0058 N81-48143
 IRRADIATION
 NT ELECTRON IRRADIATION
 NT ION IRRADIATION
 NT PHOTON IRRADIATION
 Annealing of radiation damage in low resistivity
 silicon solar cells p0099 N81-17554
 Reduced annealing temperatures in silicon solar
 cells
 [NASA-TN-82597] p0104 N81-23627
 IRROTATIONAL FLOW
 U POTENTIAL FLOW
 ISING MODEL
 U MATHEMATICAL MODELS
 ISOTHERMAL FLOW
 The influence of isothermal annealing on the
 molybdenum fibers of a directed solid
 gamma/gamma prime - alpha alloy p0056 N81-10765
 ISOTROPIC MEDIA
 Theoretical model applicable to the experimental
 determination of surface anchoring energies of
 nematic liquid crystals
 [NASA-TN-81628] p0124 N81-12817
 ISOTOPE
 NT ISOTROPIC MEDIA
 ITERATION
 NT ITERATIVE SOLUTION
 ITERATIVE SOLUTION
 On the propagation of long waves in acoustically
 treated, curved ducts p0128 N81-38060
 Surrogate-equation technique for simulation of
 steady inviscid flow
 [NASA-TN-1866] p0005 N81-31129

J

J-85 ENGINE
 Aerodynamic stability analysis of NASA
 J85-13/plasma pressure pulse generator
 installation
 [NASA-CN-165141] p0027 N81-15004
 JEEPS
 U AUTOMOBILES
 JET AIRCRAFT
 NT BORING 747 AIRCRAFT
 NT TURBOFAN AIRCRAFT
 NT TURBOPROP AIRCRAFT
 JET AIRCRAFT NOISE
 Numerical techniques in linear duct acoustics - A
 status report
 [ASME PAPER 80-WA/NC-2] p0127 N81-21120
 New technique for the direct measurement of core
 noise from aircraft engines
 [AIAA PAPER 81-1587] p0128 N81-40962
 New interpretations of shock-associated noise with
 and without screech
 [NASA-TN-81590] p0125 N81-10807
 Core noise measurements from a small, general
 aviation turbofan engine

[NASA-TN-81610] p0125 N81-11769
 Effect of a semi-annular thermal acoustic shield
 on jet exhaust noise
 [NASA-TN-81615] p0125 N81-11770
 Aerodynamic/acoustic performance of IJ101/double
 bypass VCE with conannular plug nozzle
 [NASA-CN-159869] p0129 N81-17846
 Status of noise technology for advanced supersonic
 cruise aircraft p0001 N81-18002
 New technique for the direct measurement of core
 noise from aircraft engines --- YF 102 turbofan
 engine
 [NASA-TN-82634] p0126 N81-26844
 An improved prediction method for noise generated
 by conventional profile coaxial jets
 [NASA-TN-82712] p0127 N81-32964
 Computer program to predict aircraft noise levels
 [NASA-TN-1913] p0127 N81-33947
 JET DAMPING
 U DAMPING
 JET DRIVE
 U JET PROPULSION
 JET ENGINE FUELS
 NT LIQUID FUELS
 The use of Antihisting Kerosene (AHK) in turbojet
 engines p0009 N81-19063
 Effect of hydroprocessing severity on
 characteristics of jet fuel from OSCO 2 and
 Paraho distillates
 [NASA-TN-1768] p0066 N81-24283
 Infrared spectroscopy for the determination of
 hydrocarbon types in jet fuels
 [NASA-TN-82674] p0066 N81-31380
 JET ENGINES
 NT J-85 ENGINE
 NT TURBOFAN ENGINES
 NT TURBOJET ENGINES
 NT TURBOPROP ENGINES
 Composite containment systems for jet engine fan
 blades
 [NASA-TN-81675] p0092 N81-17480
 JT9D performance deterioration results from a
 simulated aerodynamic load test
 [NASA-TN-82640] p0017 N81-25082
 Selected results from combustion research at the
 Lewis Research Center
 [NASA-TN-82627] p0017 N81-25083
 JET EXHAUST
 An improved prediction method for noise generated
 by conventional profile coaxial jets
 [AIAA PAPER 81-1991] p0129 N81-49743
 Advanced technology for controlling pollutant
 emissions from supersonic cruise aircraft
 p0001 N81-18004
 JET FLAMES
 U JET FLOW
 JET FLOW
 Effect of a semi-annular thermal acoustic shield
 on jet exhaust noise
 [NASA-TN-81615] p0125 N81-11770
 Forced and natural convection in laminar-jet
 diffusion flames --- normal-gravity,
 inverted-gravity and zero-gravity flames
 [NASA-TN-1841] p0076 N81-24388
 JET FUELS
 U JET ENGINE FUELS
 JET IMPINGEMENT
 Heat transfer from a row of impinging jets to
 concave cylindrical surfaces p0078 N81-24924
 JET NOISE
 U JET AIRCRAFT NOISE
 JET PROPULSION
 Advanced subsonic transport propulsion
 [NASA-TN-82696] p0019 N81-31195
 JETAVATORS
 U GUIDE VANES
 JOINTS (ANATOMY)
 Ion beam sputter etching of orthopedic implanted
 alloy MP35N and resulting effects on fatigue
 [NASA-TN-81747] p0045 N81-21174
 JOINTS (MECHANICAL)
 NT WELDED JOINTS
 JOURNAL BEARINGS
 Dynamic characteristics of a high-speed rotor with
 radial and axial foil-bearing supports
 [ASME PAPER 80-C2/LUB-35] p0085 N81-18683

C-3

Friction and wear results from sputter-deposited
chrome oxide with and without nichrome metallic
binders and interlayers
[ASME PAPER 80-C2/LUB-49] p0089 A81-18693
Effect of surface roughness on hydrodynamic bearings
[NASA-TN-81711] p0082 A81-21356
Surface roughness effect on finite oil journal
bearings
[NASA-TN-82639] p0084 A81-27526
JOURNALS (SHAFTS)
U SHAFTS (MACHINE ELEMENTS)
JUPITER ATMOSPHERE
Qualification testing of secondary sterilizable
silver-zinc cells for use in the Jupiter
atmospheric entry probe
[NASA-TN-82638] p0108 A81-30563

K

K BAND
U EXTREMELY HIGH FREQUENCIES
KA BAND
U EXTREMELY HIGH FREQUENCIES
KEROSENE
BT LIQUID FUELS
KEROSENE
BT LIQUID FUELS
The use of Antisticking Kerosene (AKK) in turbojet
engines
p0009 A81-19063
An assessment of the use of antisticking fuel in
turbofan engines
[NASA-CR-165258] p0067 A81-19316
KEVLAR (TRADEMARK)
Feasibility of Kevlar 49/PBR-15 polyimide for high
temperature applications
p0047 A81-43602
KINETIC ENERGY
Performance prediction of straight two dimensional
diffusers
[NASA-CR-165186] p0133 A81-11833
The electric rail gun for space propulsion
[NASA-CR-165312] p0042 A81-22078
KINETIC FRICTION
BT SLIDING FRICTION
KINETIC THEORY
BT TRANSPORT THEORY
KINETICS
BT KINETIC ENERGY
BT REACTION KINETICS
KLYSTRONS
Analytical investigation of efficiency and
performance limits in klystron amplifiers using
multidimensional computer programs; multi-stage
depressed collectors; and thermionic cathode
life studies
p0098 A81-16552
KNUDSEN FLOW
Polytetrafluoroethylene transfer film studied with
X-ray photoelectron spectroscopy
[NASA-TP-1728] p0060 A81-11214
KNUDSEN NUMBER
U KNUDSEN FLOW

L

LABORATORIES
BT SPACE LABORATORIES
LAKES
A methodology for the design and calibration of
data based models of aggregate lake ecosystem
dynamics
p0111 A81-18482
LAMINAR FLOW
U LAMINAR FLOW
LAMINAR FLOW
Prediction of laminar and turbulent primary and
secondary flows in strongly curved ducts
[NASA-CR-3388] p0007 A81-16976
Forced and natural convection in laminar-jet
diffusion flames --- normal-gravity,
inverted-gravity and zero-gravity flames
[NASA-TP-1841] p0076 A81-24388
LAMINAR FLOW CONTROL
U BOUNDARY LAYER CONTROL
LAMINAR JETS
U JET FLOW
U LAMINAR FLOW

LAMINATED MATERIALS

U LAMINATES
LAMINATES
Evacuation-induced pressure differentials in
multilayer insulation systems
p0078 A81-18021
Nonlinear laminate analysis for metal matrix fiber
composites
[AIAA 81-0579] p0046 A81-29411
Laminates and reinforced metals
[NASA-TN-81391] p0045 A81-12171
Method for alleviating thermal stress damage in
laminates --- metal matrix composites
[NASA-CASL-LBN-12493-1] p0045 A81-17170
Test evaluation of a laminated wood wind turbine
blade concept
[NASA-TN-81719] p0104 A81-24535
Nonlinear laminate analysis for metal matrix fiber
composites
[NASA-TN-82596] p0046 A81-25149
Method for alleviating thermal stress damage in
laminates
[NASA-CASL-LBN-12493-2] p0046 A81-26179

LAMINATIONS

U LAMINATES
LANGMUIR PROBES
U ELECTROSTATIC PROBES
LANGUAGES
BT FORTRAN
LARGE AREA CROP INVENTORY EXPERIMENT
Normal crop calendars. Volume 2: The spring
wheat states of Minnesota, Montana, North
Dakota, and South Dakota
[881-10070] p0094 A81-13426
Evaluation of results of US corn and soybeans
exploratory experiment: Classification
procedures verification test --- Missouri, Iowa,
Indiana, and Illinois
[881-10076] p0095 A81-13432
LARGE SPACE STRUCTURES
Performance capabilities of the 8-cm Mercury ion
thruster
[AIAA PAPER 81-0754] p0044 A81-29567
Propellant management for low thrust chemical
propulsion systems
[AIAA PAPER 81-1453] p0042 A81-42198
Performance capabilities of the 8-cm mercury ion
thruster
[NASA-TN-81720] p0038 A81-19220

LASER ANEMOMETERS

Laser-velocimeter flow-field measurements of an
advanced turboprop
[AIAA PAPER 81-1568] p0007 A81-42211
LASER ANNEALING
Space Photovoltaic Research and Technology 1980.
High Efficiency, Radiation Damage and Blanket
Technology
[NASA-CF-2169] p0098 A81-17531
LASER APPLICATIONS
BT LASER FUSION
LASER DOPPLER VELOCIMETERS
Laser-velocimeter flow-field measurements of an
advanced turboprop
[NASA-TN-82677] p0004 A81-27041
LASER FUSION
Laser surface fusion of plasma sprayed ceramic
turbine seals
[NASA-CASL-LBN-13269-1] p0062 A81-22190

LASERS

BT HIGH POWER LASERS
LEACHING
Effect of silling and leaching on the structure of
sintered silicon
p0064 A81-22529
Effect of silling and leaching on the structure of
sintered silicon
[NASA-TN-81602] p0060 A81-13166
LEAD (METAL)
Catalyst surfaces for the chromous/chromic redox
couple
[NASA-CASL-LBN-13148-2] p0107 A81-29524
LEAD ACID BATTERIES
Characterization, performance, and prediction of a
lead-acid battery under simulated electric
vehicle driving requirements
[NASA-TN-81771] p0106 A81-28523
LEADING EDGES
Icing tunnel tests of a glycol-exuding porous
leading edge ice protection system on a general

- aviation airfoil
[AIAA PAPER 81-0405] p0011 A81-20837
The coupling between flow instabilities and
incident disturbances at a leading edge p0010 A81-28082
- LEAKAGE**
Self-acting geometry for noncontact seals
[NASA-TN-81639] p0081 A81-16474
- LEGISLATIVE CODES**
U COMPUTER PROGRAMMING
- LEGUMINOUS PLANTS**
Normal crop calendars. Volume 2: The spring
wheat states of Minnesota, Montana, North
Dakota, and South Dakota
[N81-10070] p0094 A81-13426
- LEPTONS**
NT ELECTRONS
LEVEL (QUANTITY)
NT MOLECULAR ENERGY LEVELS
LIFE (DURABILITY)
NT FATIGUE LIFE
NT SERVICE LIFE
Assessment of variations in thermal cycle life
data of thermal barrier coated rods p0058 A81-44657
Combustor liner durability analysis
[NASA-CN-165250] p0027 A81-17079
Effects of plasma spray parameters on two layer
thermal barrier
[NASA-TN-81724] p0053 A81-22161
An introduction to NASA's turbine engine hot
section technology (HOST) project p0019 A81-31206
- LIFE CYCLE COSTS**
Advanced propulsion system concept for hybrid
vehicles
[NASA-CN-159772] p0040 A81-18935
- LIFE SUPPORT SYSTEMS**
A methodology for the design and calibration of
data based models of aggregate lake ecosystem
dynamics p0111 A81-18482
- LIFETIME (DURABILITY)**
U LIFE (DURABILITY)
LIGHT (VISIBLE RADIATION)
NT SUNLIGHT
LIGHT AIRCRAFT
Light transport and general aviation aircraft
icing research requirements
[NASA-CN-165290] p0010 A81-19079
- LIGHT ALLOYS**
NT ALUMINUM ALLOYS
- LIGHTNING**
Lightning accommodation systems for wind turbine
generator safety
[NASA-TN-82601] p0105 A81-24539
- LINEAR EQUATIONS**
Numerical techniques in linear duct acoustics - A
status report
[ASME PAPER 80-WA/HC-2] p0127 A81-21120
- LINESS**
U LININGS
- LININGS**
Combustor liner durability analysis
[NASA-CN-165250] p0027 A81-17079
- LIQUEFIED GASES**
NT LIQUID NITROGEN
NT LIQUID OXYGEN
LIQUID AMMONIA
NT LIQUID FUELS
LIQUID ATOMIZATION
Capillary and acceleration wave breakup of liquid
jets in axial-flow airstreams
[NASA-TP-1791] p0075 A81-16417
Acceleration wave breakup of liquid jets with
airstreams
[NASA-TN-81717] p0075 A81-21310
- LIQUID COOLING**
NT FILM COOLING
- LIQUID CRYSTALS**
Evaluation of a method for heat transfer
measurements and thermal visualization using a
composite of a heater element and liquid crystals
[ASME PAPER 81-61-93] p0079 A81-30000
Theoretical model applicable to the experimental
determination of surface anchoring energies of
nematic liquid crystals
[NASA-TN-81620] p0124 A81-12817
- Evaluation of a method for heat transfer
measurements and thermal visualization using a
composite of a heater element and liquid crystals
--- thermal performance of turbine blade cooling
configurations
[NASA-TN-81639] p0075 A81-21313
- LIQUID DROPS**
U DROPS (LIQUIDS)
LIQUID FLOW
NT WATER FLOW
LIQUID FUELS
Some advantages of methane in an aircraft gas
turbine
[SAE PAPER 801154] p0022 A81-34177
- LIQUID HYDROGEN**
NT LIQUID FUELS
LIQUID MERCURY
U MERCURY (METAL)
LIQUID METALS
NT LIQUID SODIUM
NT MERCURY (METAL)
LIQUID NITROGEN
Depressurization and two-phase flow of water
containing high levels of dissolved nitrogen gas
[NASA-TP-1839] p0076 A81-28389
- LIQUID OXYGEN**
Self-acting geometry for noncontact seals
[ASME PREPRINT 81-AH-5B-2] p0090 A81-33867
- LIQUID PROPELLANT ROCKET ENGINES**
NT HYDROGEN OXYGEN ENGINES
Low-thrust chemical rocket engine study
[NASA-CN-165276] p0042 A81-21122
- LIQUID ROCKET PROPELLANTS**
NT CRYOGENIC ROCKET PROPELLANTS
NT LIQUID FUELS
Pressure spectra and cross spectra at an area
contraction in a ducted combustion system
[ASME PAPER 80-C2/ASMO-9] p0077 A81-18638
Propellant management for low thrust chemical
propulsion systems
[AIAA PAPER 81-1451] p0042 A81-42198
Perturbation solutions of combustion instability
problems
[NASA-CN-159643] p0050 A81-16176
Low-thrust chemical rocket engine study
[NASA-CN-165275] p0042 A81-21125
- LIQUID SODIUM**
Moderate temperature sodium cells. I - Transition
metal disulfide cathodes p0113 A81-15027
- LIQUID-SOLID INTERFACES**
Elastohydrodynamic lubrication of elliptical
contacts
[NASA-TN-81647] p0080 A81-13358
- LIQUIDS**
NT CRYOGENIC ROCKET PROPELLANTS
NT LIQUID FUELS
NT LIQUID NITROGEN
NT LIQUID OXYGEN
NT LIQUID ROCKET PROPELLANTS
NT LIQUID SODIUM
NT MERCURY (METAL)
- LITERATURE**
NT DOCUMENTATION
- LITHIUM**
Radiation damage in lithium-counterdoped n/p
silicon solar cells p0109 A81-27204
- LOAD DISTRIBUTION (FORCES)**
Continuous analysis of stresses from arbitrary
surface loads on a half space p0093 A81-14162
- LOAD FACTORS**
U LOADS (FORCES)
- LOADING FORCES**
U LOADS (FORCES)
- LOADING RATE**
Experimental compliance calibration of the compact
fracture toughness specimen
[NASA-TN-81665] p0091 A81-16492
- LOADING WAVES**
U LOADS (FORCES)
- LOADS (FORCES)**
NT AERODYNAMIC LOADS
NT CYCLIC LOADS
NT ROLLING CONTACT LOADS
NT THRUST LOADS
Method for estimating crack-extension resistance
curve from residual strength data

- [NASA-TP-1753] p0091 N81-11417
Cold-air investigation of first stage of
4-1/2-stage, fan drive turbine with average
stage-loading factor of 4.66
[NASA-TP-1780] p0015 N81-16050
J79D performance deterioration results from a
simulated aerodynamic load test
[NASA-TN-82640] p0017 N81-25082
- LONG TERM EFFECTS**
SEBT II thrusters - Still ticking after eleven years
[AIAA PAPER 81-1539] p0042 A81-40934
- LOW COST**
Development of low-cost directionally-solidified
turbine blades p0088 A81-10707
Design concepts for low-cost composite turbofan
engine frame [NASA-CR-165217] p0030 N81-22053
Comparative radiation testing of solar cells for
the shuttle power extension package
[NASA-TN-82656] p0105 N81-27605
- LOW DENSITY RESEARCH**
Polytetrafluoroethylene transfer film studied with
X-ray photoelectron spectroscopy
[NASA-TP-1728] p0060 N81-11214
- LOW GRAVITY**
U REDUCED GRAVITY
- LOW TEMPERATURES**
Radiation damage annealing mechanisms and possible
low temperature annealing in silicon solar cells
p0040 A81-27207
Atomic hydrogen storage method and apparatus
[NASA-CASE-LEW-12081-3] p0066 N81-14103
- LOW THRUST**
Low-thrust chemical rocket engine study
[NASA-CR-165276] p0042 N81-21122
Low-thrust chemical rocket engine study
[NASA-CR-165275] p0042 N81-21125
- LOW THRUST PROPULSION**
NT ELECTROSTATIC PROPULSION
NT ION PROPULSION
NT PLASMA PROPULSION
NT SOLAR ELECTRIC PROPULSION
Propellant management for low thrust chemical
propulsion systems
[AIAA PAPER 81-1453] p0042 A81-42198
Low-thrust chemical propulsion system pump
technology
[NASA-CR-165210] p0088 N81-17437
- LOX (OXYGEN)**
U LIQUID OXYGEN
- LOX-HYDROGEN ENGINES**
U HYDROGEN OXYGEN ENGINES
- LUBRICANT TESTS**
Lubrication of rolling element bearings
p0086 A81-18738
The role of the micro environment on the
tribological behavior of materials p0087 A81-46493
Evaluation of boundary lubricants using
steady-state wear and friction
[NASA-TN-81601] p0061 N81-17265
- LUBRICANTS**
NT HIGH TEMPERATURE LUBRICANTS
NT LUBRICATING OILS
NT SOLID LUBRICANTS
Some limitations in applying classical EHD film
thickness formulas to a high-speed bearing
[ASME PAPER 80-C2/LUB-13] p0068 A81-18667
Evaluation of boundary lubricants using
steady-state wear and friction
[NASA-TN-81601] p0061 N81-17265
NASA five-ball fatigue tester: Over 20 years of
research [NASA-TN-82589] p0102 N81-23462
- LUBRICATING OILS**
Dynamics of solid dispersions in oil during the
lubrication of point contacts. I - Graphite
[ASLE PREPRINT 81-AM-5D-3] p0064 A81-33860
Dynamics of solid dispersions in oil during the
lubrication of point contacts. Part 1: Graphite
[NASA-TN-81683] p0061 N81-17264
- LUBRICATION**
NT BOUNDARY LUBRICATION
Lubrication of rolling element bearings
p0086 A81-18738
Practical applications of surface analytic tools
in tribology p0086 A81-18739
- Effect of substrate surface finish on the
lubrication and failure mechanisms of molybdenum
disulfide films [ASLE PREPRINT 81-AM-5D-1] p0064 A81-33859
Elastohydrodynamic lubrication of elliptical
contacts [NASA-TN-81647] p0080 N81-13358
Measurement of rod seal lubrication for Stirling
engine [NASA-CR-165158] p0088 N81-13359
History of ball bearings [NASA-TN-81689] p0081 N81-18391
Introduction to ball bearings [NASA-TN-81690] p0081 N81-18392
Performance of jet- and inner-ring-lubricated 35
millimeter bore ball bearings operating to 2.5
million DM [NASA-TP-1808] p0082 N81-19458
Dynamics of solid dispersions in oil during the
lubrication of point of contacts. Part 2:
Molybdenum disulfide [NASA-TN-81709] p0062 N81-20275
Surface films and metallurgy related to
lubrication and wear [NASA-TN-82645] p0083 N81-27523
Analysis of starvation effects on hydrodynamic
lubrication in nonconforming contacts
[NASA-TN-82668] p0084 N81-29438
Effects of Ultra-Clean and centrifugal filtration
on rolling-element bearing life [NASA-TN-82660] p0085 N81-29440
- LUBRICATION SYSTEMS**
Self-lubricating composite materials p0142 N81-12984
Ball bearing mechanics [NASA-TN-81691] p0085 N81-31550
- LUBES BANDS**
U PLASTIC DEFORMATION

M

- MACHINE LIFE**
U SERVICE LIFE
- MACHINING**
NT MILLING (MACHINING)
Effect of hole geometry and Electric-Discharge
Machining (EDM) on airflow rates through small
diameter holes in turbine blade material
[NASA-TP-1716] p0013 N81-12089
- MAGNETIC COOLING**
T-S diagram for gadolinium near the Curie
temperature p0135 A81-43004
- MAGNETIC DISKS**
Disk HDD generator study
[NASA-CR-159872] p0111 N81-18491
- MAGNETIC DISTURBANCES**
NT MAGNETIC STORMS
- MAGNETIC FIELD INTENSITY**
U MAGNETIC FLUX
- MAGNETIC FILMS**
NT GEOMAGNETISM
Atomic hydrogen storage method and apparatus
[NASA-CASE-LEW-12081-3] p0066 N81-14103
- MAGNETIC FLUX**
T-S diagram for gadolinium near the Curie
temperature p0135 A81-43004
- MAGNETIC METALS**
U METALS
- MAGNETIC PROPERTIES**
NT CURIE TEMPERATURE
NT GEOMAGNETISM
Theoretical model applicable to the experimental
determination of surface anchoring energies of
nematic liquid crystals [NASA-TN-81628] p0124 N81-12617
- MAGNETIC STORAGE**
NT MAGNETIC DISKS
- MAGNETIC STORMS**
Environmental charging effects monitors for
operational satellites p0037 A81-38057
Development and design of three monitoring
instruments for spacecraft charging
[NASA-TP-1800] p0040 N81-31282
- MAGNETIC SUBSTORES**
U MAGNETIC STORMS

MAGNETIC TAPES

NT COMPUTER COMPATIBLE TAPES

MAGNETOACOUSTICS

O MAGNETOACOUSTICS

MAGNETOACOUSTIC FLOW

On the magnetoacoustic instability

[AIAA PAPER 81-0248]

p0133 A81-20698

MAGNETOACOUSTIC GENERATORS

The STD/MHD codes - Comparison of analyses with experiments at AEC/EPDE, Reynolds Metal Co., and Hercules, Inc --- for MHD generator flows

[AIAA PAPER 81-0173]

p0133 A81-20649

On the magnetoacoustic instability

[AIAA PAPER 81-0248]

p0133 A81-20698

MHD generator off-design performance and non chemical kinetics analysis. Volume 1: Analysis of the off-design performance of the Engineering Test Facility ETP MHD generator flow train

[NASA-CR-165187]

p0133 A81-11834

Analytical investigation of critical phenomena in MHD power generators

[NASA-CR-165143]

p0109 A81-12546

Engineering support for magnetohydrodynamic power plant analysis and design studies

[NASA-CR-159690]

p0110 A81-13444

Performance calculations for 1000 HPe MHD/steam power plants

[NASA-TN-81667]

p0098 A81-16570

Disk MHD generator study

[NASA-CR-159872]

p0111 A81-18491

Performance calculations for 200-1000 HPe MHD/steam power plants

[NASA-TN-81775]

p0100 A81-22476

Preliminary investigation of acoustic oscillations in an H₂-O₂ fired Hall generator

[NASA-TN-81756]

p0103 A81-23610

Assessment of disk MHD generators for a base load powerplant

[NASA-TN-82609]

p0103 A81-23611

Conceptual design of the MHD Engineering Test Facility

[NASA-TN-82621]

p0132 A81-24926

A MHD channel study for the ETP conceptual design

[NASA-TN-81764]

p0132 A81-24927

High B-field, large area ratio MHD duct experiments

[NASA-TN-82673]

p0132 A81-32026

MAGNETOACOUSTIC STABILITY

On the magnetoacoustic instability

[AIAA PAPER 81-0248]

p0133 A81-20698

MAGNETOACOUSTICS

Performance prediction of straight two dimensional diffusers

[NASA-CR-165186]

p0133 A81-11833

High B-field, large area ratio MHD duct experiments

[NASA-TN-82673]

p0132 A81-32026

MAGNETS

Electronically commutated dc motors for electric vehicles

[NASA-TN-81654]

p0097 A81-15464

MAINTENANCE

Aircraft Engine Diagnostics

[NASA-CP-2190]

p0019 A81-31196

MANAGEMENT

NT ENGINEERING MANAGEMENT

NT RESOURCES MANAGEMENT

NT SAFETY MANAGEMENT

MANAGEMENT INFORMATION SYSTEMS

Data acquisition and analysis in the DOE/NASA Wind

Energy Program

[NASA-TN-81603]

p0096 A81-13463

MANAGEMENT SYSTEMS

NT MANAGEMENT INFORMATION SYSTEMS

MAGNETIC ALLOYS

Mechanical properties of weldments in experimental

Fe-12Ni-0.2Ti and Fe-12Ni-18Co-0.2Ti alloys for

cryogenic service

p0058 A81-48143

MAGNETOACOUSTIC

NT SPACE SHUTTLES

MANOMETERS

Gauge calibration system based on piston manometer

p0079 A81-48950

MANUALS

NT USER MANUALS (COMPUTER PROGRAMS)

MANUFACTURING

Acceptance tests and manufacturer relationships

for 20 ampere-hour sealed nickel-cadmium cells

using discharge parameters

[NASA-TN-81619]

p0049 A81-17189

Acceptance tests and manufacturer relationships from the 20A standard cell data

p0100 A81-21515

MAPPING

NT ICE MAPPING

Numerical trials of HISSE

[N81-10069]

p0094 A81-13425

MARKET RESEARCH

Market definition study of photovoltaic power for

remote villages in developing countries

[NASA-CR-159880]

p0110 A81-14391

Highlights of NASA/DOE photovoltaic market

assessment visit to Morocco

[NASA-TN-82288]

p0138 A81-27976

Highlights of NASA/DOE photovoltaics market

assessment visit to Colombia

[NASA-TN-84011]

p0138 A81-32081

MARKETING

A methodology for fostering commercialization of

electric and hybrid vehicle propulsion systems

[NASA-TN-81575]

p0140 A81-18933

MASS FLOW RATE

Performance tests of a gas blending system based

on mass-flow controllers

[NASA-TP-1896]

p0066 A81-29246

MATERIAL REMOVAL (MACHINING)

O MACHINING

MATERIALS RECOVERY

NASA's activities in the conservation of strategic

aerospace materials

p0056 A81-22535

MATERIALS SCIENCE

High power densities from high-temperature

material interactions --- in thermionic energy

conversion and metallic fluid heat pipes

[AIAA PAPER 81-1161]

p0070 A81-39144

MATERIALS TESTS

Ultrasonic measurement of material properties

p0090 A81-19656

NASA five-ball fatigue tester - Over 20 years of

research

p0087 A81-44659

The role of the micro environment on the

tribological behavior of materials

p0087 A81-44693

Mechanical properties of weldments in experimental

Fe-12Ni-0.2Ti and Fe-12Ni-18Co-0.2Ti alloys for

cryogenic service

p0058 A81-48143

MATHEMATICAL LOGIC

NT ALGORITHMS

MATHEMATICAL MODELS

NT DIGITAL SIMULATION

Backward deletion to minimize prediction errors in

models from factorial experiments with zero to

six center points

p0122 A81-14999

Supersonic stall flutter of high-speed fans

[ASME PAPER 81-GT-184]

p0020 A81-30078

Thermodynamics. II - The extended thermodynamic

system

p0136 A81-31375

Loss model for off-design performance analysis of

radial turbines with pivoting-vane,

variable-area stators

[SAR PAPER 801135]

p0021 A81-34166

Backward deletion to minimize prediction errors in

models from factorial experiments with zero to

six center points

[NASA-TN-81524]

p0123 A81-10778

Multivariable identification using centralized

fixed nodes

p0014 A81-12091

The role of oxidation in the fretting wear process

[NASA-TN-81570]

p0051 A81-12210

An electrostatic analog for generating cascade grids

p0122 A81-14695

Propulsion system mathematical model for a

lift/cruise fan V/STOL aircraft

[NASA-TN-81663]

p0015 A81-16055

Turbine modeling technique to generate off-design

performance data for both single and multistage

axial-flow turbines

[NASA-CR-165244]

p0027 A81-17078

Combustor liner durability analysis

[NASA-CR-165250]

p0027 A81-17079

Extended frequency turbofan model

[NASA-CR-165261]

p0030 A81-20078

- An evaluation of a simplified near field noise model for supersonic helical tip speed propellers [NASA-TN-81727] p0130 N81-22836
- Synthetic battery cycling [NASA-TN-81757] p0049 N81-25168
- Serrogate-equation technique for simulation of steady inviscid flow [NASA-TN-1886] p0005 N81-31129
- MATHEMATICS (MATHEMATICS)**
- BT HIGHVALUES**
- MATRIX MATERIALS**
- Nonlinear laminate analysis for metal matrix fiber composites [NASA-TN-82596] p0046 N81-25149
- Computer code for intraply hybrid composite design [NASA-TN-82593] p0046 N81-25151
- MAXIMUM USABLE FREQUENCY**
- The 30/20 GHz experimental communications satellite system [NASA-TN-82683] p0035 N81-30172
- MEAN FIBER PATH**
- Polytetrafluoroethylene transfer film studied with X-ray photoelectron spectroscopy [NASA-TN-1728] p0060 N81-11214
- MEASURING INSTRUMENTS**
- BT AMMETERS**
- BT CYCLOTRON RESONANCE DEVICES**
- BT DRAG FORCE AMMETERS**
- BT ELECTROSTATIC PROBES**
- BT ENGINE ANALYZERS**
- BT ENGINE MONITORING INSTRUMENTS**
- BT INFRARED SPECTROPHOTOMETRIES**
- BT LASER ANEMOMETERS**
- BT LASER DOPPLER VELOCIMETERS**
- BT MANOMETERS**
- BT METEOROLOGICAL INSTRUMENTS**
- BT OPTICAL MEASURING INSTRUMENTS**
- BT POTENTIOMETERS (INSTANTANEOUS)**
- BT RADIATION PYROMETERS**
- BT SPECTROMETERS**
- BT STRAIN GAGES**
- BT THERMOCOUPLE PYROMETERS**
- BT VACUUM GAGES**
- BT VOLTMETERS**
- BT WATTMETERS**
- Evaluation of a method for heat transfer measurements and thermal visualization using a composite of a heater element and liquid crystals [ASAE PAPER 81-6T-93] p0079 A81-30000
- Diagnostic system design for the Ion Auxiliary Propulsion System (IAPS). Flight tests of two 8 cm mercury ion [NASA-TN-81702] p0037 N81-20172
- MECHANICAL DEVICES**
- Sputtering and ion plating for aerospace applications [NASA-TN-81726] p0082 N81-20424
- MECHANICAL DRIVES**
- BT TRANSMISSIONS (MACHINE ELEMENTS)**
- Axial force and efficiency tests of fixed center variable speed belt drive [NASA-TN-81652] p0080 N81-15367
- Experimental analysis of ISEP in a rotary combustion engine [NASA-TN-81662] p0015 N81-16054
- Design of spur gears for improved efficiency [NASA-TN-81625] p0081 N81-17436
- Advanced continuously variable transmissions for electric and hybrid vehicles [NASA-TN-81718] p0082 N81-19459
- Life analysis of multicracker planetary traction drive [NASA-TN-1710] p0082 N81-20423
- Traction drive for cryogenic boost pump --- hydrogen oxygen rocket engines [NASA-TN-81704] p0101 N81-23188
- MECHANICAL MEASUREMENT**
- BT FLOW MEASUREMENT**
- BT FRICTION MEASUREMENT**
- BT PRESSURE MEASUREMENT**
- BT VELOCITY MEASUREMENT**
- MECHANICAL PROPERTIES**
- BT ABRASION RESISTANCE**
- BT ANISOTROPY**
- BT ANISOTROPIC ELASTICITY**
- BT ANISOTROPIC ELASTICITY**
- BT COMPRESSIBILITY**
- BT CREEP PROPERTIES**
- BT CREEP RUPTURE STRENGTH**
- BT ELASTIC PROPERTIES**
- BT FATIGUE LIFE**
- BT FIBER STRENGTH**
- BT FRACTURE STRENGTH**
- BT SHEAR STRENGTH**
- BT STRESS RELAXATION**
- BT STRUCTURAL STABILITY**
- BT TENSILE STRENGTH**
- BT THERMAL RESISTANCE**
- Elevated temperature mechanical properties and residual tensile properties of two cast superalloys and several nickel-base oxide dispersion strengthened alloys p0057 A81-24104
- Influence of excess diamine on properties of PBR polyimide resins and composites p0047 A81-43635
- NASA five-ball fatigue tester - Over 20 years of research p0087 A81-44659
- Computer code for intraply hybrid composite design p0047 A81-44662
- Oxidation-induced contraction and strengthening of boron fibers p0047 A81-44664
- Mechanical properties of weldments in experimental Fe-12Mn-0.2Ti and Fe-12Mn-1Mo-0.2Ti alloys for cryogenic service p0056 A81-48143
- Synthesis of improved phenolic and polyester resins [NASA-CN-165180] p0065 N81-17263
- Introduction to ball bearings [NASA-TN-81690] p0081 N81-18392
- Creep and residual mechanical properties of cast superalloys and oxide dispersion strengthened alloys [NASA-TN-1781] p0053 N81-19273
- Microstructure and mechanical properties of bulk and plasma-sprayed Y2O3-partially stabilized zirconia [NASA-CN-165126] p0059 N81-22158
- Computer code for intraply hybrid composite design [NASA-TN-82593] p0046 N81-25151
- Effect of Yttria additives on properties of pressureless-sintered silicon nitride [NASA-TN-1899] p0063 N81-31366
- MEDICAL EQUIPMENT**
- BT PROSTHETIC DEVICES**
- Ion beam sputter-etched ventricular catheter for hydrocephalus shunt [NASA-CASE-LEN-13107-1] p0118 N81-27786
- MEDICAL SCIENCE**
- BT ORTHOPEDICS**
- Ion beam applications research. A summary of Lewis Research Center Programs [NASA-TN-81721] p0044 N81-21129
- MEETINGS**
- U CONFERENCES**
- MEETING**
- BT VACUUM MELTING**
- MEMBRANE ANALOGY**
- U MEMBRANE STRUCTURES**
- U STRUCTURAL ANALYSIS**
- MEMBRANE STRUCTURES**
- In-situ cross linking of polyvinyl alcohol --- application to battery separator films [NASA-CASE-LEN-13135-2] p0062 N81-24257
- MEMBRANE THEORY**
- U STRUCTURAL ANALYSIS**
- MEMBRANES**
- BT ION EXCHANGE MEMBRANE ELECTROLYTES**
- BT MEMBRANE STRUCTURES**
- MERCURY (METAL)**
- Extended operating range of the 30-cm ion thruster with simplified power processor requirements [NASA-TN-81729] p0039 N81-20179
- Pervaporation of carbon steel through mercury implantation [NASA-CN-165292] p0059 N81-20244
- MERCURY ION ENGINES**
- SERT II 1980 extended flight thruster experiments [AIAA PAPER 81-0665] p0040 A81-29528
- Results of the Mission Profile Life Test first test segment - Thruster J1 [AIAA PAPER 81-0716] p0043 A81-29552
- Performance capabilities of the 8-cm Mercury ion thruster [AIAA PAPER 81-0754] p0044 A81-29567
- Extended operating range of the 30-cm ion thruster with simplified power processor requirements

- [AIAA PAPER 81-0692] p0040 A81-32897
Free radical propulsion concept
[AIAA PAPER 81-0676] p0041 A81-32905
Characteristics of 30-centimeter mercury ion
thrusters
[AIAA PAPER 81-0715] p0041 A81-37569
Diagnostic system design for the Ion Auxiliary
Propulsion System (IAPS) - Flight test of two 8
cm mercury ion thrusters
[AIAA PAPER 81-0666] p0041 A81-38070
Particle and field measurements on two J-series
30-centimeter thrusters
[AIAA PAPER 81-0728] p0042 A81-38072
Diagnostic system design for the Ion Auxiliary
Propulsion System (IAPS). Flight tests of two 8
cm mercury ion
[NASA-TN-81702] p0037 A81-20172
Retrofit and verification test of a 30-cm ion
thruster
[NASA-CR-165233] p0042 A81-20174
Characteristics of 30-centimeter mercury ion
thrusters
[NASA-TN-81706] p0039 A81-21121
Particle and field measurements on two J-series 30
centimeter thrusters
[NASA-TN-81741] p0039 A81-22084
- MESE**
Generation of C-type cascade grids for viscous
flow computation p0122 A81-14721
- METAL BONDING**
NT METAL-METAL BONDING
Thermal barrier coating system having improved
adhesion
[NASA-CASE-LEU-13359-1] p0062 A81-24265
- METAL COATINGS**
An experimental investigation of silicon wafer
surface roughness and its effect on the
pull-strength of plated metals p0109 A81-38063
A new diffusion-inhibited oxidation-resistant
coating for superalloys
[NASA-TN-82687] p0056 A81-23273
- METAL CORROSION**
U CORROSION
- METAL FATIGUE**
Ion beam sputter etching of orthopedic implant
alloy MP35N and resulting effects on fatigue
properties
[AIAA PAPER 81-0671] p0057 A81-38069
Introduction to ball bearings
[NASA-TN-81690] p0081 A81-18392
Method for alleviating thermal stress damage in
laminates
[NASA-CASE-LEU-12493-2] p0046 A81-26179
Endurance tests with large-bore tapered-roller
bearings to 2.2 million DN
[NASA-TN-82669] p0084 A81-29439
- METAL FIBERS**
The influence of isothermal annealing on the
molybdenum fibers of a directed solid
gamma/gamma prime - alpha alloy p0056 A81-10765
Tungsten fiber reinforced superalloys - A status
review p0047 A81-44665
Tungsten wire-reinforced superalloys for 1093 C
(2000 P) turbine blade applications
[NASA-CR-159720] p0047 A81-10112
- METAL FILMS**
Adherence of ion beam sputter deposited metal
films on H-13 steel p0056 A81-14958
Ion beam deposited protective films
[AIAA PAPER 81-0672] p0086 A81-29532
Frictional and morphological characteristics of
ion plated soft, metallic films p0057 A81-38066
- METAL FORMING**
U FORMING TECHNIQUES
U METAL WORKING
- METAL JOINTS**
NT WELDED JOINTS
- METAL MATRIX COMPOSITES**
Nonlinear laminate analysis for metal matrix fiber
composites
[AIAA 81-0579] p0046 A81-29411
Tungsten fiber reinforced superalloys - A status
review
- Superhybrid composite blade impact studies
[NASA-TN-81557] p0047 A81-44665
Laminates and reinforced metals
[NASA-TN-81591] p0045 A81-12171
Method for alleviating thermal stress damage in
laminates --- metal matrix composites
[NASA-CASE-LEU-12493-1] p0045 A81-17170
Fabrication of aluminum oxide fiber reinforced
aluminum matrix composites
[NASA-CR-165184] p0048 A81-19229
Fabrication development of alumina/aluminum
composites
[NASA-CR-165195] p0048 A81-19233
Method for alleviating thermal stress damage in
laminates
[NASA-CASE-LEU-12493-2] p0046 A81-26179
- METAL OXIDES**
NT ALUMINUM OXIDES
NT CHROMIUM OXIDES
NT NICKEL OXIDES
NT TANTALUM OXIDES
NT YTTRIUM OXIDES
NT ZIRCONIUM OXIDES
Effect of TBP variables upon structure and
properties in ODS alloy NDA 8077 sheet ---
ThermoMechanical Processing of Oxide Dispersion
Strengthened nickel alloy p0059 A81-10706
Effect of CoO₂, H₂O and Y₂O₃ additions on the
sinterability of a sintered Si₃N₄ with 14.5 wt% SiO₂
p0064 A81-28974
Method for depositing an oxide coating ---
producing solar panels
[NASA-CASE-LEU-13131-1] p0054 A81-24230
Method of forming oxide coatings
[NASA-CASE-LEU-13132-1] p0106 A81-27616
- METAL PARTICLES**
Accuracy of trace element determinations in
alternate fuels p0056 A81-22530
- METAL POLISHING**
Simultaneous ion sputter polishing and deposition
[NASA-TN-81679] p0053 A81-19278
- METAL SHEETS**
Effect of TBP variables upon structure and
properties in ODS alloy NDA 8077 sheet ---
ThermoMechanical Processing of Oxide Dispersion
Strengthened nickel alloy p0059 A81-10706
On the equivalence between semiempirical fracture
analyses and R-curves p0092 A81-18792
- METAL SUBFACES**
Ion beam texturing of heat transfer surfaces
[AIAA PAPER 81-0670] p0086 A81-29531
Improved refractory coatings --- sputtered
coatings on substrates that form stable nitrides
[NASA-CASE-LEU-23169-2] p0052 A81-16209
Effects of erodent particle shape and various heat
treatments on erosion resistance of plain carbon
steel
[NASA-TN-1755] p0052 A81-16210
Method of cold welding using ion beam technology
[NASA-CASE-LEU-12982-1] p0081 A81-19455
Corrosion resistant thermal barrier coating ---
protecting gas turbines and other engine parts
[NASA-CASE-LEU-13088-1] p0054 A81-25188
Surface films and metallurgy related to
lubrication and wear
[NASA-TN-82645] p0083 A81-27523
- METAL WORKING**
Computer-aided roll pass design in rolling of
airfoil shapes p0088 A81-15796
Tribological properties of silicon carbide in
metal removal process p0085 A81-17900
- METAL-METAL BONDING**
Mechanical bonding of metal
[NASA-CASE-LEU-12941-1] p0068 A81-16329
Method of cold welding using ion beam technology
[NASA-CASE-LEU-12982-1] p0081 A81-19455
- METALLIZING**
Fabrication and testing of polyvinylidene fluoride
capacitors
[NASA-CR-159501] p0073 A81-22278
- METALLOIDS**
NT SILICON

METALS

NT ALKALI METALS
 NT ALUMINUM
 NT COBALT
 NT GADOLINIUM
 NT LEAD (METAL)
 NT LIQUID SODIUM
 NT LITHIUM
 NT MERCURY (METAL)
 NT METAL COATINGS
 NT METAL FILMS
 NT METAL MATRIX COMPOSITES
 NT MOLYBDENUM
 NT NICKEL
 NT PLATINUM
 NT TANTALUM
 NT TITANIUM
 NT TRANSITION METALS
 NT TUNGSTEN
 NT YTTRIUM
 NT ZIRCONIUM

Correlation of ideal and actual shear strengths of metals with their friction properties
 [NASA-TP-1891] p0063 N81-27282
 Conservation of Strategic Aerospace Materials (COSAM) p0019 N81-31208

Relationship between the ideal tensile strength and the friction properties of metals in contact with nonmetals and themselves
 [NASA-TP-1883] p0063 N81-33293

METROLOGICAL COMPRESSION TESTS

U MECHANICAL PROPERTIES

METROLOGICAL INSTRUMENTS

Icing instrumentation p0117 N81-14559

METROLOGY

Applications Technology Satellite and Communications Technology Satellite user experiments for 1967 - 1980 reference book, volume 1
 [NASA-CR-165169-VOL-1] p0033 N81-12135
 Applications Technology Satellite and Communications Technology Satellite user experiments for 1967-1980 reference book, volume 2
 [NASA-CR-165169-VOL-2] p0033 N81-12136
 Applications Technology Satellite and Communications Technology Satellite user experiments for 1967-1980 reference book, Volume 3: User form surveys
 [NASA-CR-165169-VOL-3] p0033 N81-12137
 Applications Technology Satellite and Communications Technology Satellite user experiments for 1967-1980 reference book, Volume 4: Abstracts
 [NASA-CR-165169-VOL-4] p0133 N81-12138

METRES

U MEASURING INSTRUMENTS

METHACRYLATE RESINS

U ACRYLIC RESINS

METHANE

Some advantages of methane in an aircraft gas turbine
 [SAE PAPER 801154] p0022 A81-34177

METHOD OF CHARACTERISTICS

Calculation of the flow field in supersonic inlets using a bicharacteristics method with shock wave fitting p0006 A81-21212

METROPOLITAN AREAS

U CITIES

MICROCIRCUITS

U MICROELECTRONICS

MICROCRACKS

Laser surface fusion of plasma sprayed ceramic turbine seals
 [NASA-CASE-LEW-1:269-1] p0062 N81-22190

MICROELECTRONICS

High voltage V-groove scler cell
 [NASA-CASE-LEW-1:401-1] p0098 N81-16529

MICROHARBOURS

U HARBOURS

MICROSTRUCTURE

The effect of mechanical surface and heat treatments on the erosion resistance of 6061 aluminum alloy p0057 A81-27944
 Microstructure of Al2O3 scales formed on NiCrAl alloys

[NASA-TN-81676] p0052 N81-16212
 Microstructure and mechanical properties of bulk and plasma-sprayed Y2O3-partially stabilized zirconia
 [NASA-CR-165126] p0059 N81-22158
 Computer code for intraply hybrid composite design
 [NASA-TN-82593] p0046 N81-25151

MICROWAVE AMPLIFIERS

NT CYCLOTRON RESONANCE DEVICES

MICROWAVE EQUIPMENT

NT KLYSTRONS

NT MICROWAVE TUBES

NT TRAVELLING WAVE TUBES

MICROWAVE FREQUENCIES

NT EXTREMELY HIGH FREQUENCIES

MICROWAVE SWITCHING

K-band high power latching switch ---

communication satellite system [NASA-CR-165159] p0073 N81-16389

MICROWAVE TRANSMISSION

Analytical investigation of efficiency and performance limits in klystron amplifiers using multidimensional computer programs; multi-stage depressed collectors; and thermionic cathode life studies p0098 N81-16552

MICROWAVE TUBES

NT KLYSTRONS

NT TRAVELLING WAVE TUBES

Three-axis electron-beam test facility [NASA-TP-1836] p0071 N81-20359

MIDAIR COLLISIONS

NT BIRD-AIRCRAFT COLLISIONS

MILITARY AIRCRAFT

NASA research in aeropropulsion [ASME PAPER 81-GT-96] p0001 A81-30003

NASA Research in aeropropulsion [NASA-TN-81633] p0014 N81-13056

MILLIT

Numerical trials of HISSE [E81-10069] p0094 N81-13425

MILLING (MACHINING)

Effect of milling and leaching on the structure of sintered silicon p0064 A81-22529

MINERALS

NT GRAPHITE

MINIMIZATION

U OPTIMIZATION

MINNESOTA

Normal crop calendars. Volume 2: The spring wheat states of Minnesota, Montana, North Dakota, and South Dakota [E81-10070] p0094 N81-13426

Preliminary evaluation of the Environmental Research Institute of Michigan crop calendar shift algorithm for estimation of spring wheat development stage --- North Dakota, South Dakota, Montana, and Minnesota [E81-10071] p0094 N81-13427

MISCIBILITY

U SOLUBILITY

MISSILE STABILIZATION

U STABILIZATION

MISSION PLANNING

Results of the Mission Profile Life Test first test segment - Thruster J1 [AIAA PAPER 81-0716] p0043 A81-29552

MISSISSIPPI

Normal crop calendars. Volume 1: Assembly and application of historical crop data to a standard product [E81-10075] p0095 N81-13431

MISSOURI

Evaluation of results of US corn and soybeans exploratory experiment: Classification procedures verification test --- Missouri, Iowa, Indiana, and Illinois [E81-10076] p0095 N81-13432

MIXED FLOW

U MULTIPHASE FLOW

MIXERS

Factors which influence the behavior of turbofan forced mixer nozzles [AIAA PAPER 81-0274] p0021 A81-32549

Mixer nozzle aerodynamic characteristics for the energy efficient engine [AIAA PAPER 81-1994] p0128 A81-48639

- Factors which influence the behavior of turbofan
forced mixer nozzles
[NASA-TN-81668] p0074 881-15240
- QC&AT mixer compound exhaust system design and
static big model test report
[NASA-CR-135386] p0029 881-10119
- Mixing effectiveness test of an exhaust gas mixer
in a high bypass turbofan at altitude
[NASA-TN-82663] p0018 881-27095
- MIXING**
- NT DISSOLVING
- NT FRESHING
- Performance tests of a gas blending system based
on mass-flow controllers
[NASA-TN-1896] p0066 881-29246
- MIXTURES**
- NT BINARY MIXTURES
- NT DISPERSIONS
- NT EUTECTIC ALLOYS
- NT METAL MATRIX COMPOSITES
- NT SOLID SUSPENSIONS
- MOBILITY**
- NT ELECTRON MOBILITY
- MODAL RESPONSE**
- Interactive multi-node blade impact analysis
[ASME PAPER 81-GT-79] p0030 881-29387
- Improved methods for fan sound field determination
[NASA-CR-165188] p0129 881-15769
- Nastran level 16 theoretical manual updates for
aeroelastic analysis of bladed discs
[NASA-CR-155823] p0093 881-19480
- MODE SHAPES**
- U MODAL RESPONSE
- MODELS**
- NT BRAINBOARD MODELS
- NT DIGITAL SIMULATION
- NT DYNAMIC MODELS
- NT MATHEMATICAL MODELS
- NT WIND TUNNEL MODELS
- MODES**
- NT COUPLED MODES
- NT FAILURE MODES
- NT PROPAGATION MODES
- MODULATION**
- NT FREQUENCY MODULATION
- NT INTERMODULATION
- NT PULSE MODULATION
- MODULES**
- NT ELECTRONIC MODULES
- MOLECULAR BONDS**
- U CHEMICAL BONDS
- MOLECULAR ENERGY LEVELS**
- The self-consistent calculation of pseudo-molecule
energy levels, construction of energy level
correlation diagrams and an automated
computation system for SCF-I(Alpha)-SW
calculations
[NASA-TN-81710] p0130 881-25779
- MOLECULAR STRUCTURES**
- The self-consistent calculation of pseudo-molecule
energy levels, construction of energy level
correlation diagrams and an automated
computation system for SCF-I(Alpha)-SW
calculations
[NASA-TN-81710] p0130 881-25779
- MOLYBDENUM**
- The effect of thermal cycling to 1100 degree C on
the alpha (Mo) phase in directionally solidified
gamma/gamma prime-alpha alloys
[NASA-TN-81688] p0052 881-18165
- MOLYBDENUM ALLOYS**
- NT BEEB 41
- The influence of isothermal annealing on the
molybdenum fibers of a directed solid
gamma/gamma prime - alpha alloy
p0056 881-10765
- The effect of thermal cycling to 1100 C on the
alpha /Mo/ phase in directionally solidified
gamma/gamma prime-alpha alloys
p0057 881-32546
- MOLYBDENUM COMPOUNDS**
- NT MOLYBDENUM DISULFIDES
- MOLYBDENUM DISULFIDES**
- Effect of substrate surface finish on the
lubrication and failure mechanisms of molybdenum
disulfide films
[ASLE PREPRINT 81-AM-5E-1] p0064 881-33859
- Effect of substrate surface finish on the
lubrication and failure mechanisms of molybdenum
disulfide films
[NASA-TN-81595] p0060 881-10170
- Atomic hydrogen storage method and apparatus
[NASA-CASR-12081-3] p0066 881-14103
- Dynamics of solid dispersions in oil during the
lubrication of point of contacts. Part 2:
Molybdenum disulfide
[NASA-TN-81709] p0062 881-20275
- MOLYBDENUM SULFIDES**
- NT MOLYBDENUM DISULFIDES
- MOMENTUM ENERGY**
- U KINETIC ENERGY
- MONITORS**
- Environmental charging effects monitors for
operational satellites:
p0037 881-38057
- MONOCRYSTALS**
- U SINGLE CRYSTALS
- MONOLITHIC CIRCUITS**
- U INTEGRATED CIRCUITS
- MONOMERS**
- Cross-linked polyvinyl alcohol and method of
making same
[NASA-CASR-13101-2] p0044 881-29160
- MONOPROPPELLANTS**
- NT LIQUID FUELS
- MONTANA**
- Normal crop calendars. Volume 2: The spring
wheat states of Minnesota, Montana, North
Dakota, and South Dakota
[881-10070] p0094 881-13426
- Preliminary evaluation of the Environmental
Research Institute of Michigan crop calendar
shift algorithms for estimation of spring wheat
development stage --- North Dakota, South
Dakota, Montana, and Minnesota
[881-10071] p0094 881-13427
- MOROCCO**
- Highlights of NASA/DOE photovoltaic market
assessment visit to Morocco
[NASA-TN-82288] p0138 881-27976
- MORPHOLOGY**
- Frictional and morphological characteristics of
ion plated soft, metallic films
p0057 881-38066
- MOTION EQUATIONS**
- U EQUATIONS OF MOTION
- MOTION PICTURES**
- Simulation and visualization of face seal motion
stability by means of computer generated movies
p0087 881-38059
- MOTION STABILITY**
- NT AERODYNAMIC STABILITY
- NT FLOW STABILITY
- NT MAGNETOHYDRODYNAMIC STABILITY
- NT ROTARY STABILITY
- Simulation and visualization of face seal motion
stability by means of computer generated movies
p0087 881-38059
- MOTOR VEHICLES**
- NT AUTOMOBILES
- NT ELECTRIC AUTOMOBILES
- NT ELECTRIC MOTOR VEHICLES
- NT TRUCKS
- MOTORS**
- NT ELECTRIC MOTORS
- MULTICHANNEL COMMUNICATION**
- Experimental investigation of intermodulation
effects and related efficiencies associated with
two- and three-channel operation of a traveling
wave tube
[NASA-TN-81576] p0069 881-10240
- MULTILAYER INSULATION**
- Evacuation-induced pressure differentials in
multilayer insulation systems
p0078 881-18021
- MULTILAYER STRUCTURES**
- U LAMINATES
- MULTIPHASE FLOW**
- NT TWO PHASE FLOW
- QC&AT mixer compound exhaust system design and
static big model test report
[NASA-CR-135386] p0029 881-19119
- MULTIPLE ACCESS**
- NT TIME DIVISION MULTIPLE ACCESS
- MULTISTAGE COMPRESSORS**
- U TURBOCOMPRESSORS
- MULTIVARIATE STATISTICAL ANALYSIS**
- NT REGRESSION ANALYSIS

MUSCULOSKELETAL SYSTEM
NT JOINTS (ANATOMY)

N

N-P JUNCTIONS

U P-N JUNCTIONS

NACELLES

Optimum subsonic, high-angle-of-attack nacelles
p0005 A81-11646

NASA PROGRAMS

NT GLOBAL ATMOSPHERIC RESEARCH PROGRAM

NT QUIET ENGINE PROGRAM

NT SUPERSONIC CRUISE AIRCRAFT RESEARCH

NASA's activities in the conservation of strategic aerospace materials
p0056 A81-22535

NASA research in aeropropulsion

[ASME PAPER 81-67-96] p0001 A81-30003

Advanced communications satellites

[AAS PAPER 80-206] p0069 A81-33532

The NASA high-speed turboprop program

[SAR PAPER 801120] p0021 A81-34156

Solar photovoltaics: stand alone applications ---
NASA Lewis Research Center research and development
p0143 A81-12990

An overview of general aviation propulsion

research programs at NASA Lewis Research Center
[NASA-TN-81666] p0015 A81-16052

NASA preprototype redox storage system for a

photovoltaic stand-alone application
[NASA-TN-82607] p0104 A81-24534

Bibliography of Lewis Research Center technical

publications announced in 1980
[NASA-TN-82661] p0137 A81-29026

Aerospace in the future

[NASA-TN-82664] p0143 A81-29063

NASA STRUCTURAL ANALYSIS PROGRAM

U NASTRAN

NASTRAN

Aeroelastic and dynamic finite element analysis of
a bladder shrouded disk
[NASA-CR-159728] p0092 A81-15479

Nastrian level 16 theoretical manual updates for

aeroelastic analysis of bladed discs
[NASA-CR-159823] p0093 A81-19480

NASTRAN level 16 user's manual updates for

aeroelastic analysis of bladed discs
[NASA-CR-159824] p0093 A81-19481

NASTRAN level 16 programmer's manual updates for

aeroelastic analysis of bladed discs
[NASA-CR-159825] p0093 A81-19482

NATIONS

NT DEVELOPING NATIONS

NAVIER-STOKES EQUATION

Turbulent solution of the Navier-Stokes equations
p0077 A81-19284

Turbulent solution of the Navier-Stokes equations

[NASA-TN-81621] p0074 A81-12358

NEAR FIELDS

An evaluation of a simplified near field noise

model for supersonic helical tip speed propellers
[NASA-TN-81727] p0130 A81-22836

NETWORK ANALYSIS

Analysis and design of an adaptive multi-loop

controlled two winding buck/boost regulator
p0073 A81-21675

NEUTRALIZERS

Fluid model of plasma outside a hollow cathode

neutralizer
[AIAA PAPER 81-0739] p0134 A81-29560

NEUTRON FLUX

U FLUX (RATE)

NICKEL

The effect of thermal cycling to 1100 degree C on
the alpha (Ni) phase in directionally solidified
gamma/gamma prime-alpha alloys
[NASA-TN-81688] p0052 A81-18165

NICKEL ALLOYS

NT BSE 41

Effect of TSP variables upon structure and

properties in ORS alloy NDA 8077 sheet ---
Thermomechanical Processing of Oxide Dispersion
Strengthened nickel alloy
p0059 A81-10706

Elevated temperature mechanical properties and

residual tensile properties of two cast
superalloys and several nickel-base oxide

dispersion strengthened alloys

The effect of thermal cycling to 1100 C on the
alpha /Ni/ phase in directionally solidified
gamma/gamma prime-alpha alloys
p0057 A81-24104

Synergistic erosion/corrosion of superalloys in
PFB coal combustor effluent
p0057 A81-32546

Low-cost directionally-solidified turbine blades,

volume 2 --- TP8731-3 turbofan engine
[NASA-CR-159562] p0024 A81-12088

Nickel ternary alloy having improved cyclic

oxidation resistance
[NASA-CASE-LEN-13339-1] p0051 A81-12211

An investigation of hot corrosion mechanisms in

nickel base alloys
p0058 A81-16208

The fracture morphology of nickel-base superalloys

tested in fatigue and creep-fatigue at 650 C
[NASA-TN-81740] p0101 A81-23244

Synergistic erosion/corrosion of superalloys in

PFB coal combustor effluent
[NASA-TN-81715] p0101 A81-23245

Burner rig evaluation of thermal barrier coating

--- gas turbines
[NASA-TN-81684] p0055 A81-28231

NASA's activities in the conservation of strategic

aerospace materials
[NASA-TN-81617] p0055 A81-29205

NICKEL CADMIUM BATTERIES

Acceptance tests and manufacturer relationships

for 20 ampere-hour sealed nickel-cadmium cells
using discharge parameters
[NASA-TN-81619] p0049 A81-17189

NICKEL COMPOUNDS

NT NICKEL OXIDES

NICKEL OXIDES

Elevated temperature mechanical properties and

residual tensile properties of two cast
superalloys and several nickel-base oxide
dispersion strengthened alloys
p0057 A81-24104

NICKEL ZINC BATTERIES

Response of nickel to zinc cells to electric

vehicle chopper discharge waveforms
[NASA-TN-81713] p0103 A81-23608

Additive for zinc electrodes

[NASA-CASE-LEN-13286-1] p0105 A81-27597

NITRIC OXIDE

Fuel/air nonuniformity - Effect on nitric oxide

emissions
[AIAA PAPER 81-0327] p0019 A81-20834

NITRIDES

NT SILICON NITRIDES

NT TITANIUM NITRIDES

NITROGEN

NT LIQUID NITROGEN

Effect of fuel nitrogen and hydrogen content on

emissions in hydrocarbon combustion
[ASME PAPER 81-GT-63] p0057 A81-29973

NITROGEN COMPOUNDS

NT NITRIC OXIDE

NT NITROGEN OXIDES

NT POLYIMIDES

NT SILICON NITRIDES

NT TITANIUM NITRIDES

NITROGEN OXIDES

NT NITRIC OXIDE

Development of a low NO_x/lean premixed annular

combustor
[ASME PAPER 81-GT-40] p0020 A81-29954

Low NO_x/ and fuel flexible gas turbine combustors

[ASME PAPER 81-GT-99] p0020 A81-30006

Design and preliminary results of a fuel flexible

industrial gas turbine combustor
[ASME PAPER 81-GT-108] p0087 A81-30013

Low NO_x/ combustion systems for burning heavy

residual fuels and high-fuel-bound nitrogen fuels
[ASME PAPER 81-GT-109] p0089 A81-30014

Evaluation of advanced combustors for dry NO_x/

suppression with nitrogen bearing fuels in
utility and industrial gas turbines
[ASME PAPER 81-GT-125] p0087 A81-30029

Exhaust emission survey of an F100 afterburning

turbofan engine at simulated altitude flight
conditions
[NASA-TN-81656] p0016 A81-21078

- Analysis of effect of flameholder characteristics on lean, premixed, partially vaporized fuel-air mixtures quality and nitrogen oxides emissions [NASA-TP-1042] p0016 N81-24065
- NOISE CASES**
- U CASE CASES**
- NOISE (SOUND)**
- UT AERODYNAMIC NOISE**
- UT AIRCRAFT NOISE**
- UT ENGINE NOISE**
- UT JET AIRCRAFT NOISE**
- NOISE ATTENUATION**
- U NOISE REDUCTION**
- NOISE ELIMINATION**
- U NOISE REDUCTION**
- NOISE GENERATORS**
- Core noise measurements from a small, general aviation turbofan engine p0019 A81-22531
- NOISE INTENSITY**
- Comparison of predicted engine core noise with proposed FAA helicopter noise certification requirements p0128 A81-38062
- NOISE MEASUREMENT**
- New technique for the direct measurement of core noise from aircraft engines [AIAA PAPER 81-1527] p0128 A81-40962
- Core noise measurements from a small, general aviation turbofan engine [NASA-TN-81610] p0125 N81-11769
- An evaluation of a simplified near field noise model for supersonic helical tip speed propellers [NASA-TN-81727] p0130 N81-22836
- New technique for the direct measurement of core noise from aircraft engines --- YF 102 turbofan engine [NASA-TN-82634] p0126 N81-26844
- NOISE PREDICTION**
- The NASA-LERC wind turbine sound prediction code [NASA-TN-81737] p0100 N81-21537
- NOISE PREDICTION (AIRCRAFT)**
- An experimental study of transmission, reflection and scattering of sound in a free jet flight simulation facility and comparison with theory p0129 A81-28943
- A theoretical approach to sound propagation and radiation for ducts with suppressors p0128 A81-38061
- Comparison of predicted engine core noise with proposed FAA helicopter noise certification requirements p0128 A81-38062
- Comparison of predicted engine core noise with current and proposed aircraft noise certification requirements [AIAA PAPER 81-2053] p0024 A81-48635
- An improved prediction method for noise generated by conventional profile coaxial jets [AIAA PAPER 81-1991] p0129 A81-49743
- A theoretical approach to sound propagation and radiation for ducts with suppressors [NASA-TN-82612] p0130 N81-22837
- Comparison of predicted engine core noise with proposed FAA helicopter noise certification requirements [NASA-TN-81739] p0130 N81-22839
- Comparison of predicted engine core noise with current and proposed aircraft noise certification requirements [NASA-TN-82659] p0126 N81-29922
- An improved prediction method for noise generated by conventional profile coaxial jets [NASA-TN-82712] p0127 N81-32964
- Computer program to predict aircraft noise levels [NASA-TP-1913] p0127 N81-33947
- NOISE REDUCTION**
- Numerical techniques in linear duct acoustics - A status report [ASME PAPER 80-WA/NC-2] p0127 A81-11120
- A theoretical approach to sound propagation and radiation for ducts with suppressors p0128 A81-38061
- Comparison of predicted engine core noise with current and proposed aircraft noise certification requirements [AIAA PAPER 81-2053] p0024 A81-48635
- Mixer nozzle aeroacoustic characteristics for the energy efficient engine [AIAA PAPER 81-1994] p0128 A81-48633
- A model for the acoustic impedance of linear suppressor materials bonded on perforated plate [AIAA PAPER 81-1999] p0129 A81-49741
- Low-speed aerodynamic performance of 50.8-centimeter-diameter noise-suppressing inlets for the Quiet, Clean, Short-haul Experimental Engine (QCSEE) --- Lewis 9- by 15-foot low speed wind tunnel tests [NASA-TP-1178] p0013 N81-11037
- Effect of a semi-annular thermal acoustic shield on jet exhaust noise [NASA-TN-81615] p0125 N81-11770
- Curved centerline air intake for a gas turbine engine [NASA-CASE-LEW-13201-1] p0014 N81-14999
- Aerodynamic/acoustic performance of YJ101/double bypass VCE with conical plug nozzle [NASA-CN-159869] p0129 N81-17846
- Status of noise technology for advanced supersonic cruise aircraft p0001 N81-18002
- Recent developments in aircraft engine noise reduction technology p0009 N81-19072
- Design of an exhaust mixer nozzle for the Avco-Lycoming Quiet Clean General Aviation Turbofan (CCGAT) [NASA-CN-159426] p0029 N81-19120
- The NASA-LERC wind turbine sound prediction code [NASA-TN-81737] p0100 N81-21537
- A theoretical approach to sound propagation and radiation for ducts with suppressors [NASA-TN-82612] p0130 N81-22837
- Rotor wake characteristics relevant to rotor-stator interaction noise generation [NASA-TN-82703] p0019 N81-30130
- Turbomachinery noise studies of the A12 research CCGAT engine with inflow control [NASA-TN-82694] p0127 N81-31957
- A model for the acoustic impedance of linear suppressor materials bonded on perforated plate --- noise reduction in aircraft engines [NASA-TN-82716] p0127 N81-32965
- Acoustic performance of inlet suppressors on an engine generating a single mode [NASA-TN-82697] p0127 N81-32968
- NOISE SPECTRA**
- Pressure spectra and cross spectra at an area contraction in a ducted combustion system [ASME PAPER 80-C2/AERO-9] p0077 A81-18638
- Analysis of pressure spectra measurements in a ducted combustion system [NASA-TN-81583] p0125 N81-15768
- NOISE SUPPRESSORS**
- U NOISE REDUCTION**
- NOMINAL VALUES**
- U APPROXIMATION**
- NONADIABATIC PROCESSES**
- U HEAT TRANSFER**
- NONDESTRUCTIVE TESTS**
- Surface flaw detection in structural ceramics by scanning photoacoustic spectroscopy p0079 A81-17906
- Ultrasonic measurement of material properties p0090 A81-19656
- Acousto-ultrasonic characterization of fiber reinforced composites p0090 A81-44660
- NONEUCLIDIAN GEOMETRY**
- U DIFFERENTIAL GEOMETRY**
- NONISOTROPY**
- U ANISOTROPY**
- NONLINEAR EQUATIONS**
- A rapid method for the approximate determination of nonlinear solutions Application to aerodynamic flows p0007 A81-11628
- NONLINEAR SYSTEMS**
- A nonlinear propulsion system simulation technique for piloted simulators [NASA-TN-82600] p0101 N81-23085
- NONUNIFORM FLOW**
- High-frequency sound propagation in a spatially varying mean flow p0129 A81-49913
- Factors influencing the predicted performance of advanced propeller designs [NASA-TN-82676] p0004 A81-27042

- NONVISCOUS FLOW**
U INVISCID FLOW
NORTH DAKOTA
 Normal crop calendars. Volume 2: The spring wheat states of Minnesota, Montana, North Dakota, and South Dakota [N81-10070] p0094 N81-13426
 Preliminary evaluation of the Environmental Research Institute of Michigan crop calendar shift algorithm for estimation of spring wheat development stage --- North Dakota, South Dakota, Montana, and Minnesota [N81-10071] p0094 N81-13427
- NOTCH TESTS**
 Fracture toughness of brittle materials determined with chevron notch specimens p0064 N81-32545
- NOTCHED METALS**
U NOTCH TESTS
NOZZLE COEFFICIENT
U NOZZLE FLOW
NOZZLE DESIGN
 QCGAT mixer compound exhaust system design and static big model test report [NASA-CN-135386] p0029 N81-19119
 Design of an exhaust mixer nozzle for the Avco-Lycoming Quiet Clean General Aviation Turbofan (QCGAT) [NASA-CN-159426] p0029 N81-19120
- NOZZLE FLOW**
 HSD generator off-design performance and non chemical kinetics analysis. Volume 1: Analysis of the off-design performance of the Engineering Test Facility E1F HSD generator flow train [NASA-CN-165187] p0133 N81-11834
 Application of computer generated color graphic techniques to the processing and display of three dimensional fluid dynamic data [NASA-TN-82658] p0119 N81-29782
- NOZZLE GEOMETRY**
 Acoustic transmission matrix of a variable area duct or nozzle carrying a compressible subsonic flow [NASA-TN-81614] p0125 N81-12821
 NASA contributions to radial turbine aerodynamic analyses [NASA-TN-81644] p0003 N81-13019
 Factors which influence the behavior of turbofan forced mixer nozzles [NASA-TN-81668] p0074 N81-15240
 The effect of inflow velocity profiles on the performance of supersonic ejector nozzles [NASA-TN-81673] p0075 N81-16421
- NUCLEAR AUXILIARY POWER UNITS**
NT SPACE POWER REACTORS
NUCLEAR ELECTRIC POWER GENERATION
NT SPACE POWER REACTORS
NUCLEAR POWER REACTORS
NT SPACE POWER REACTORS
NUCLEAR REACTIONS
NT ELECTRON SCATTERING
NUCLEAR REACTORS
NT SPACE POWER REACTORS
NUCLEATE BOILING
 Ion beam texturing of heat transfer surfaces [AIAA PAPER 81-0670] p0086 N81-29531
- NUMERICAL ANALYSIS**
NT APPROXIMATION
NT COMPUTATIONAL FLUID DYNAMICS
NT REGOR ANALYSIS
NT FINITE DIFFERENCE THEORY
NT FINITE ELEMENT METHOD
NT ITERATIVE SOLUTION
 Turbulent solution of the Navier-Stokes equations [NASA-TN-81621] p0074 N81-12358
 Analysis of starvation effects on hydrodynamic lubrication in noncavitating contacts [NASA-TN-82668] p0084 N81-29438
- NUMERICAL CONTROL**
 Propulsion control and control theory: A new research focus p0014 N81-12099
- NUMERICAL FLOW VISUALIZATION**
 Full potential solution of a transonic quasi-3-D flow through a cascade using artificial compressibility [AIAA PAPER 81-07-70] p0006 N81-29979
 Numerical simulation of flows in curved diffusers with cross-sectional transition using a three-dimensional viscous analysis [NASA-TN-81672] p0074 N81-15239
 Prediction of laminar and turbulent primary and secondary flows in strongly curved ducts [NASA-CN-3380] p0007 N81-16976
 Application of computer generated color graphic techniques to the processing and display of three dimensional fluid dynamic data [NASA-TN-82658] p0119 N81-29782
- NUMERICAL DIAGRAM**
 Multivariable sygnist array method with application to turbofan engine control p0026 N81-12101
- O RING SEALS**
 Self-acting geometry for noncontact seals [ASLE PREPRINT 81-AM-5B-2] p0090 N81-33867
 Self-stabilizing radial face seal [NASA-CASE-LEN-12991-1] p0083 N81-24442
 Circumferential shaft seal [NASA-CASE-LEN-12119-2] p0043 N81-26447
- OATS**
 Numerical trials of NISS2 [N81-10069] p0094 N81-13425
 Normal crop calendars. Volume 2: The spring wheat states of Minnesota, Montana, North Dakota, and South Dakota [N81-10070] p0094 N81-13426
 Normal crop calendars. Volume 1: Assembly and application of historical crop data to a standard product [N81-10075] p0095 N81-13431
- OCEANS**
NT ATLANTIC OCEAN
OIL ADDITIVES
 Dynamics of solid dispersions in oil during the lubrication of point contacts. I - Graphite [ASLE PREPRINT 81-AM-5B-3] p0064 N81-33860
- OILS**
NT FUEL OILS
NT LUBRICATING OILS
NT SHALE OIL
OLEFINS
U ALKENES
ONBOARD EQUIPMENT
NT AIRBORNE EQUIPMENT
NT AIRCRAFT EQUIPMENT
 Icing instrumentation p0117 N81-14559
- ONE DIMENSIONAL FLOW**
 Acoustic transmission matrix of a variable area duct or nozzle carrying a compressible subsonic flow p0128 N81-22533
- ONISOTROPY**
U ANISOTROPY
OPEN CIRCUIT VOLTAGE
 The effect of minority carrier mobility variations on solar cell spectral response [NASA-TN-82604] p0103 N81-23625
- OPSSINGS**
NT AFFERTURES
OPERATING TEMPERATURE
 Annealing of radiation damage in low resistivity silicon solar cells p0099 N81-17554
- OPERATIONAL MANASERS**
 Safety management of complex research operations p0067 N81-44661
 Safety management of complex research operators [NASA-TN-81772] p0068 N81-25263
- OPTICAL EQUIPMENT**
NT INFRARED SPECTROPHOTOMETERS
NT LASER DOPPLER VELOCIMETERS
NT OPTICAL MEASURING INSTRUMENTS
OPTICAL MEASURING INSTRUMENTS
NT INFRARED SPECTROPHOTOMETERS
 Fiber optics for aircraft engine/inlet control [NASA-TN-82654] p0012 N81-31190
- OPTICAL PROPERTIES**
NT PHOTOVOLTAIC EFFECT
NT RADIANCE
NT TRANSPARENT
 Heat transparent high intensity high efficiency solar cell [NASA-CASE-LEN-12892-1] p0105 N81-27598

OPTICAL SENSORS

U OPTICAL MEASURING INSTRUMENTS

OPTICAL CONTROL

Performance seeking controls

p0014 N81-12092

Road map to adaptive optical control --- jet
engine control

p0025 N81-12098

OPTIMIZATION

NT OPTICAL CONTROL

Performance of a magnetic multipole line-cusp

argon ion thruster

[NASA-TN-81703]

p0038 N81-19219

OPTIMUM CONTROL

U OPTICAL CONTROL

ORBIT TRANSFER VEHICLES

High performance cryogenic engines for orbit

transfer vehicles

[IAP PAPER 80-P-253]

p0043 N81-18363

Analysis of Goss and Si solar cell arrays for

earth orbital and orbit transfer missions

p0109 N81-27254

Performance of a magnetic multipole line-cusp

argon ion thruster

[AIAA PAPER 81-0745]

p0041 N81-36071

Shuttle compatible cryogenic liquid storage and

supply systems

[AIAA PAPER 81-1509]

p0037 N81-42207

Low-thrust chemical rocket engine study

[NASA-CN-165276]

p0042 N81-21122

The electric rail gun for space propulsion

[NASA-CN-165312]

p0042 N81-22078

ORBITS

NT EARTH ORBITS

ORIFICE FLOW

Flow through axially aligned sequential apertures

of the orifice and Borda types

[NASA-TN-81681]

p0075 N81-21314

Depressurization and two-phase flow of water

containing high levels of dissolved nitrogen gas

[NASA-TN-1639]

p0076 N81-28389

ORIPICES

Experiments on flow through one to four inlets of

the orifice and Borda type

[NASA-TN-82680]

p0077 N81-30391

ORTHOTOPPER AIRCRAFT

U RESEARCH AIRCRAFT

ORTHOPEDICS

Ion beam sputter etching of orthopedic implant

alloy MP35N and resulting effects on fatigue

properties

[AIAA PAPER 81-0671]

p0057 N81-38069

Ion beam sputter etching of orthopedic implanted

alloy MP35N and resulting effects on fatigue

[NASA-TN-81747]

p0045 N81-21174

OSCILLATIONS

NT HARMONIC OSCILLATIONS

Preliminary investigation of acoustic oscillations

in an M2-O2 fired Hall generator

[NASA-TN-81756]

p0103 N81-23610

OSCILLATORS

NT MICROWAVE TUBES

OTV

U ORBIT TRANSFER VEHICLES

OUTLETS

Performance prediction of straight two dimensional

diffusers

[NASA-CN-165186]

p0133 N81-11833

OVERCAST

U CLOUD COVER

OXIDATION

NT ELECTROCHEMICAL OXIDATION

Oxidation-induced contraction and strengthening of

boron fibers

p0047 N81-44664

The role of oxidation in the fretting wear process

[NASA-TN-81570]

p0051 N81-12210

Preparation and evaluation of advanced

electrocatalysts for phosphoric acid fuel cells

[NASA-CN-165179]

p0111 N81-17527

OXIDATION RESISTANCE

The effect of zirconium on the cyclic oxidation of

NiCrAl alloys

p0056 N81-15559

Oxidation and hot corrosion of coated and bare

oxide dispersion strengthened superalloy MA-755E

[NASA-TN-81589]

p0058 N81-43384

Properties of PBA polyimide composites made with

improved high strength graphite fibers

p0047 N81-43603

High temperature cyclic oxidation furnace testing

at NASA Lewis Research Center

p0058 N81-44651

NiCrAl ternary alloy having improved cyclic

oxidation resistance

[NASA-CASE-LEU-13339-1]

p0051 N81-12211

High temperature cyclic oxidation furnace testing

at NASA Lewis Research Center

[NASA-TN-81773]

p0054 N81-26234

Burner rig evaluation of thermal barrier coating

--- gas turbines

[NASA-TN-81684]

p0055 N81-28231

A new diffusion-inhibited oxidation-resistant

coating for superalloys

[NASA-TN-82687]

p0056 N81-33273

OXIDATION-REDUCTION REACTIONS

Improvement and scale-up of the NASA Redox storage

system

[NASA-TN-81632]

p0049 N81-13105

OXIDE FILMS

Ion beam deposited protective films

[AIAA PAPER 81-0672]

p0086 N81-25532

Method for depositing an oxide coating ---

producing solar panels

[NASA-CASE-LEU-13131-1]

p0054 N81-24230

Method of forming oxide coatings

[NASA-CASE-LEU-13132-1]

p0106 N81-27616

OXIDES

NT ALUMINUM OXIDES

NT CARBON DIOXIDE

NT CARBON MONOXIDE

NT CHROMIUM OXIDES

NT METAL OXIDES

NT NICKEL OXIDES

NT NITRIC OXIDE

NT NITROGEN OXIDES

NT SILICON DIOXIDE

NT TANTALUM OXIDES

NT TITANIUM OXIDES

NT ZINC OXIDES

OXIDISERS

NT LIQUID OXYGEN

OXYGEN

NT LIQUID OXYGEN

NT OZONE

OZONE

Ozone contamination in aircraft cabins: Results

from GASP data and analyses

[NASA-TN-81671]

p0009 N81-16021

OZONE/HEAT

Ozone contamination in aircraft cabins - Results

from GASP data and analyses

[AIAA PAPER 81-0305]

p0010 N81-20740

Tabulations of ambient ozone data obtained by GASP

airliners, March 1975 to December 1977

[NASA-TN-81528]

p0116 N81-13568

Analysis of atmospheric ozone levels at commercial

airplane cruise altitudes in winter and spring,

1976 - 1977 --- Global Atmospheric Sampling

Program

[NASA-TN-1807]

p0117 N81-21685

P

P-I-N DIODES

U P-I-N JUNCTIONS

P-I-N JUNCTIONS

Thin n-i-p silicon solar cell

p0114 N81-27097

P-N JUNCTIONS

Radiation damage in lithium-counterdoped n/p

silicon solar cells

p0109 N81-27204

Radiation damage in silicon MIP solar cells

p0099 N81-17557

P-TYPE SEMICONDUCTORS

Annealing of radiation damage in low resistivity

silicon solar cells

p0099 N81-17554

PANEL METHOD (FLUID DYNAMICS)

Solution of plane cascade flow using improved

surface singularity methods --- application of

panel method to internal aerodynamics

[NASA-TN-81589]

p0003 N81-14979

PANELS

Completion of evaluation of manufacturing

processes for S/Al composites containing 0.2mm

diameter boron fibers

[NASA-TN-81573] p0051 N81-11111
PARABOLIC REFLECTORS
Solar Thermal Power Systems parabolic dish project
[NASA-TN-82371] p0107 N81-28524
PARALLEL FLOW
NT THREE DIMENSIONAL FLOW
PARALLEL PLATES
Multiple plate hydrostatic viscous damper
[NASA-CASE-LBN-12465-1] p0083 N81-22360
PARALLEL PROCESSING (COMPUTERS)
An approach to real-time simulation using parallel processing
[NASA-TN-81731] p0121 N81-21803
PARAMETER IDENTIFICATION
Multivariable identification using centralized fixed codes
[NASA-TN-81764] p0014 N81-12091
A BMD channel study for the ETF conceptual design
[NASA-TN-81764] p0132 N81-24927
PARAMETERIZATION
NT PARAMETER IDENTIFICATION
A nonlinear propulsion system simulation technique for piloted simulators
p0022 N81-38064
PARTIAL PRESSURE
Conditioned pressure spectra and coherence measurements in the core of a turbofan engine
[NASA-TN-82688] p1126 N81-30907
PARTICLE BEAMS
NT ELECTRON BEAMS
NT ION BEAMS
PARTICLE EMISSION
NT SECONDARY EMISSION
PARTICLE FLUX
U FLUX (RATE)
PARTICLE SIZE DISTRIBUTION
Cloud encounter and particle density variabilities from GASP data
[AIAA PAPER 81-0308] p0117 N81-20742
Polyvinyl alcohol battery separator containing inert filler --- alkaline batteries
[NASA-CASE-LBN-13556-1] p0106 N81-27615
PARTICLES
NT ANIONS
NT ARGON PLASMA
NT CHARGED PARTICLES
NT DROPS (LIQUIDS)
NT ELECTRON BEAMS
NT ELECTRON PLASMA
NT ELECTRONS
NT METAL PARTICLES
NT PLASMA JETS
NT PLASMA SHEATHS
Dynamics of solid dispersions in oil during the lubrication of point contacts. Part 1: Graphite
[NASA-TN-81683] p0061 N81-17264
PASSENGER AIRCRAFT
NT BOEING 747 AIRCRAFT
PASSIVATION
U PASSIVITY
PASSIVITY
Passivation of carbon steel through mercury implantation
[NASA-CR-165292] p0059 N81-20244
PATTERN RECOGNITION
Numerical trials of HISSE
[E81-10069] p0094 N81-13425
Limited Area Coverage/High Resolution Picture Transmission (LAC/HRT) tape IJ grid pixel extraction processor user's manual
[E81-10072] p0094 N81-13428
Evaluation of results of US corn and soybeans exploratory experiment: Classification procedures verification test --- Missouri, Iowa, Indiana, and Illinois
[E81-10076] p0095 N81-13432
Acceptance tests and manufacturer relationships for 20 ampere-hour sealed nickel-cadmium cells using discharge parameters
[NASA-TN-81619] p0049 N81-17189
PAYLOADS
NT SPACE SHUTTLE PAYLOADS
NT SPACEBORNE EXPERIMENTS
NT SPACELAB PAYLOADS
PCM (MATERIALS)
U PHASE CHANGE MATERIALS

PERFORATED PLATES

A model for the acoustic impedance of linear suppressor materials bonded on perforated plate
[AIAA PAPER 81-1993] p0129 N81-49741
A model for the acoustic impedance of linear suppressor materials bonded on perforated plate --- noise reduction in aircraft engines
[NASA-TN-82716] p0127 N81-32965

PERFORMANCE

JT8D-15/17 high pressure turbine root discharged blade performance improvement --- engine design
[NASA-CR-165220] p0028 N81-17080
The effect of minority carrier mobility variations on the performance of high voltage silicon solar cells
p0098 N81-17536

PERFORMANCE PREDICTION

NT PREDICTION ANALYSIS TECHNIQUES

The STD/BMD codes - Comparison of analyses with experiments at AEDC/HPDE, Reynolds Metal Co., and Hercules, Inc --- for BMD generator flows
[AIAA PAPER 81-0173] p0133 N81-20649
An analytical approach to airfoil icing
[AIAA PAPER 81-0403] p0117 N81-20810
Supersonic stall flutter of high-speed fans
[ASME PAPER 81-GT-184] p0020 N81-30078
Self-acting geometry for noncontact seals
[ASLE PREPRINT 81-AN-58-2] p0090 N81-33867
Loss model for off-design performance analysis of radial turbines with pivoting-vane, variable-area stators
[SAR PAPER 801135] p0021 N81-34166
Factors influencing the predicted performance of advanced propeller designs
[AIAA PAPER 81-1564] p0007 N81-42210
Performance prediction of straight two dimensional diffusers
[NASA-CR-165186] p0133 N81-11833
Engine diagnostics program: CP6-50 engine performance deterioration
[NASA-CR-155867] p0024 N81-12085
Analytical investigation of critical phenomena in BMD power generators
[NASA-CR-165143] p0109 N81-12546
Performance of high resistivity n++ silicon solar cells under 1 MeV electron irradiation
[NASA-TN-82610] p0103 N81-23626
JT9D performance deterioration results from a simulated aerodynamic load test
[NASA-TN-82640] p0017 N81-25082
Factors influencing the predicted performance of advanced propeller designs
[NASA-TN-82676] p0004 N81-27042
The supersonic fan engine: An advanced concept in supersonic cruise propulsion
[NASA-TN-82657] p0018 N81-27094

PERFORMANCE TESTS

Heat transfer coefficients for staggered arrays of short pin fins
[ASME PAPER 81-GT-75] p0077 N81-29983
Characteristics of 30-centimeter mercury ion thrusters
[AIAA PAPER 81-0715] p0041 N81-37569
Performance of a magnetic multipole line-cusp argon ion thruster
[AIAA PAPER 81-0745] p0041 N81-38071
Performance of a steel spar wind turbine blade on the Mod-0 100 kW experimental wind turbine
[NASA-TN-81588] p0096 N81-11448
An assessment of the use of antimisting fuel in turbofan engines
[NASA-CR-165256] p0067 N81-19316
Performance of jet- oil inner-ring-lubricated 35 millimeter bore ball bearings operating to 2.5 million DM
[NASA-TP-1808] p0082 N81-19458
Acceptance tests and manufacturer relationships from the 20A standard cell data
p0100 N81-21515
Investigation of performance deterioration of the CP6/JT9D high bypass ratio turbofan engines
p0016 N81-24086
Effect of a part-span variable inlet guide vane on the performance of a high-bypass turbofan engine
[NASA-TN-82617] p0017 N81-25081
SBET 2 thrusters: Still ticking after eleven years
[NASA-TN-81774] p0040 N81-26174
Mixing effectiveness test of an exhaust gas mixer in a high bypass turbofan at altitude

- [NASA-TN-82663] p0018 N81-27095
Performance tests of a gas blending system based
on mass-flow controllers
- [NASA-TP-1896] p0066 N81-29246
SEP BIOD variable conductance heat pipes
acceptance and characterization tests
- [NASA-TN-82635] p0076 N81-30390
Qualification testing of secondary sterilizable
silver-zinc cells for use in the Jupiter
atmospheric entry probe
- [NASA-TN-82638] p0108 N81-30563
Turbo machinery noise studies of the AirResearch
OCGT engine with inflow control
- [NASA-TN-82694] p0127 N81-31957
- PERFUSION**
- U DIFFUSION**
- PERIODEIC PROCESSES**
- U CYCLES**
- PERIPHERAL EQUIPMENT (COMPUTERS)**
- NT COMPUTER COMPATIBLE TAPES**
- PERIPHERIES**
- U BOUNDARIES**
- PERMEABILITY**
- NT DIELECTRIC PERMEABILITY**
- PETURBATION THEORY**
- A rapid method for the approximate determination
of nonlinear soluticns Application to
aerodynamic flows
- p0007 A81-11628
- Perturbation solutions of combustion instability
problems
- [NASA-CN-159643] p0050 N81-16176
- A rapid perturbation procedure for determining
nonlinear flow solutions: Application to
transonic turbo machinery flows
- [NASA-CN-3425] p0001 N81-22012
- PETROLEUM PRODUCTS**
- NT DIESEL FUELS**
- NT LUBRICATING OILS**
- Evaluation of concepts for controlling exhaust
emissions from minimally processed petroleum and
synthetic fuels
- [ASME PAPER 81-GT-157] p0067 A81-30056
- PHASE CHANGE MATERIALS**
- Solar Thermal Power Systems parabolic dish project
- [NASA-TN-82371] p0107 N81-28524
- PHASE TRANSFORMATIONS**
- NT NUCLEATE BOILING**
- NT PREVAPORIZATION**
- NT VACUUM MELTING**
- NT VAPORIZING**
- The influence of isothermal annealing on the
molybdenum fibers of a directed solid
gamma/gamma prime - alpha alloy
- p0056 A81-10765
- PHENOLIC RESINS**
- Synthesis of improved phenolic and polyester resins
- [NASA-CN-165180] p0065 N81-17263
- PHENOLOGY**
- Normal crop calendars. Volume 2: The spring
wheat states of Minnesota, Montana, North
Dakota, and South Dakota
- [E81-10070] p0094 N81-13426
- Preliminary evaluation of the Environmental
Research Institute of Michigan crop calendar
shift algorithm for estimation of spring wheat
development stage --- North Dakota, South
Dakota, Montana, and Minnesota
- [E81-10071] p0094 N81-13427
- Normal crop calendars. Volume 1: Assembly and
application of historical crop data to a
standard product
- [E81-10075] p0095 N81-13431
- PHENOMENOLOGY**
- NT PHENOLOGY**
- PHOSPHORIC ACID**
- Status of commercial phosphoric acid fuel cell
system development
- [AIAA PAPER 81-0356] p0108 A81-20805
- Status of commercial phosphoric acid fuel cell
system development
- [NASA-TN-81641] p0096 N81-13464
- Preparation and evaluation of advanced
electrocatalysts for phosphoric acid fuel cells
- [NASA-CN-165179] p0111 N81-17527
- Cell module and fuel conditioner
- [NASA-CN-165189] p0112 N81-18494
- Preparation and evaluation of advanced
electrocatalysts for phosphoric acid fuel cells
- [NASA-CN-165245] p0112 N81-18496
Non-noble catalysts and catalyst supports for
phosphoric acid fuel cells
- [NASA-CN-165221] p0112 N81-18497
Technology development for phosphoric acid fuel
cell powerplant, phase 2
- [NASA-CN-165317] p0113 N81-21536
Technology development for phosphoric acid fuel
cell powerplant (phase 2)
- [NASA-CN-165316] p0113 N81-21547
Stabilizing platinum in phosphoric acid fuel cells
- [NASA-CN-165311] p0113 N81-22473
Technology development for phosphoric acid fuel
cell powerplant (phase 2) --- on site integrated
energy systems
- [NASA-CN-165318] p0113 N81-22475
- PHOSPHORUS**
- Phosphazene diamines
- [NASA-CN-165147] p0065 N81-10169
- PHOSPHORUS COMPOUNDS**
- NT PHOSPHORIC ACID**
- PHOTOACOUSTIC SPECTROSCOPY**
- Surface flaw detection in structural ceramics by
scanning photoacoustic spectroscopy
- p0079 A81-17906
- PHOTOCHEMICAL REACTIONS**
- NT RADICLYSIS**
- PHOTOELECTRIC CELLS**
- NT PHOTOVOLTAIC CELLS**
- PHOTOELECTRON SPECTROSCOPY**
- The transfer of polytetrafluoroethylene studied by
X-ray photoelectron spectroscopy
- p0087 A81-31238
- Surface chemistry and friction behavior of the
silicon carbide (0001) surface at temperatures
to 1500 deg C
- [NASA-TP-18113] p0061 N81-19300
- PHOTOGRAPHS**
- NT MOTION PICTURES**
- PHOTOLYSIS**
- NT RADIOLYSIS**
- PHOTOTHERMAL CONVERSION**
- Applicability of advanced automotive heat engines
to solar thermal power
- [NASA-TN-81658] p0097 N81-14397
- PHOTOTHERMOTROPISM**
- U ANISOTROPY**
- U TEMPERATURE EFFECTS**
- PHOTOVOLTAIC CELLS**
- High efficiency ultrathin coplanar back contact
cells
- p0114 A81-27092
- Global calibration of terrestrial reference cells
and errors involved in using different
irradiance monitoring techniques
- p0068 A81-27148
- The DOE photovoltaics program
- p0143 N81-12989
- High voltage planar multijunction --- solar cells
- [NASA-CASB-LEN-13400-1] p0098 N81-16528
- High voltage V-groove solar cell
- [NASA-CASB-LEN-13401-1] p0098 N81-16529
- NASA preprototype redox storage system for a
photovoltaic stand-alone application
- [NASA-TN-82607] p0104 N81-24534
- Laboratory evaluation of a pilot cell battery
protection system for photovoltaic applications
- [NASA-TN-81714] p0104 N81-24536
- Design description of the Schuchuli Village
photovoltaic power system
- [NASA-TN-82650] p0094 N81-28517
- Comparison of photovoltaic cell temperatures in
modules operating with exposed and enclosed back
surfaces
- [NASA-TN-81769] p0106 N81-28520
- Highlights of NASA/DOE photovoltaics market
assessment visit to Colombia
- [NASA-TN-84011] p0138 N81-32081
- PHOTOVOLTAIC CONVERSION**
- Photovoltaic applications - Past and future
- p0109 A81-27231
- Solar photovoltaics: Stand alone applications ---
NASA Lewis Research Center research and
development
- p0143 N81-12990
- Market definition study of photovoltaic power for
remote villages in developing countries
- [NASA-CN-155880] p0110 N81-14391

- Review of stand-alone photovoltaic application projects sponsored by US DOE and US AID
[NASA-TN-81738] p0100 N81-22477
- Highlights of NASA/DOE photovoltaic market assessment visit to Morocco
[NASA-TN-82288] p0138 N81-27976
- PHOTOVOLTAIC EFFECT**
Heat transparent high intensity high efficiency solar cell
[NASA-CASE-LEW-12892-1] p0105 N81-27598
- PISTON OSCILLATIONS**
PISTON PLANTS
A MHD channel study for the ETP conceptual design
[NASA-TN-81764] p0132 N81-24927
- PINS**
Heat transfer coefficients for staggered arrays of short pin fins
[NASA-TN-81596] p0074 N81-13302
- PISTON ENGINES**
NT DIESEL ENGINES
Comparisons of four alternative powerplant types for future general aviation aircraft
[NASA-TN-81584] p0013 N81-10067
- Modular instrumentation system for real-time measurements and control on reciprocating engines
[NASA-TP-1757] p0071 N81-11315
- Advanced Technology Spark-Ignition Aircraft Piston Engine Design Study
[NASA-CN-165162] p0026 N81-13963
- A four-cylinder Stirling engine controls model
[NASA-TN-81648] p0075 N81-15241
- PISTONS**
Multiple plate hydrostatic viscous damper
[NASA-CASE-LEW-12445-1] p0083 N81-22360
- PLANAR STRUCTURES**
Finite element analysis of inviscid subsonic boattail flow
[AIAA PAPER 81-0276] p0006 A81-20831
- High voltage planar multijunction --- solar cells
[NASA-CASE-LEW-13400-1] p0098 N81-16528
- PLANETARY ATMOSPHERES**
NT JUPITER ATMOSPHERE
PLANETARY ENVIRONMENTS
NT JUPITER ATMOSPHERE
PLANKTON
A methodology for the design and calibration of data based models of aggregate lake ecosystem dynamics
p0111 N81-18482
- PLANKTON BLOOM**
U PLANKTON
PLANNING
NT MISSION PLANNING
PLANT DESIGN
Conceptual design of the MHD Engineering Test Facility
[NASA-TN-82621] p0132 N81-24926
- PLANTING**
Normal crop calendars. Volume 2: The spring wheat states of Minnesota, Montana, North Dakota, and South Dakota
[N81-10070] p0094 N81-13426
- PLANTS (BOTANY)**
NT ALFALFA
NT BARLEY
NT CORN
NT HAY
NT OATS
NT SORGHUM
NT SUNFLOWERS
PLANTS (INDUSTRIES)
U INDUSTRIAL PLANTS
PLASMA ARCS
U PLASMA JETS
PLASMA COMBUSTION
U PLASMA CONTROL
PLASMA CONTROL
Adapting magnetoelectrostatic containment to inert gas thrusters
[AIAA PAPER 81-0140] p0043 A81-20625
- PLASMA DISCHARGES**
U PLASMA JETS
PLASMA ELECTRODES
Fluid model of plasma outside a hollow cathode neutralizer
[AIAA PAPER 81-0739] p0134 A81-29560
- PLASMA FLOW**
U MAGNETOHYDRODYNAMIC FLOW
- PLASMA INSTABILITY**
U MAGNETOHYDRODYNAMIC STABILITY
PLASMA INTERACTIONS
Review of biased solar array. Plasma interaction studies
[NASA-TN-82693] p0036 N81-32187
- PLASMA JETS**
Recent work on an RF ion thruster
[AIAA PAPER 81-0678] p0041 A81-35625
- Recent work on an RF ion thruster
[NASA-TN-81734] p0039 N81-20178
- PLASMA LAYERS**
NT PLASMA SHEATHS
PLASMA LOSS
Improved thermionic energy converters
[NASA-CASE-LEW-12443-1] p0099 N81-19561
- PLASMA PHYSICS**
MHD generator off-design performance and non chemical kinetics analysis. Volume 1: Analysis of the off-design performance of the Engineering Test Facility ETP MHD generator flow train
[NASA-CN-165187] p0133 N81-11834
- Preliminary investigation of acoustic oscillations in an M2-02 fired Hall generator
[NASA-TN-81756] p0103 N81-23610
- PLASMA POWER SOURCES**
Simplified power supplies for ion thrusters
[NASA-TN-81725] p0039 N81-20177
- PLASMA PROBES**
NT ELECTROSTATIC PROBES
PLASMA PROPULSION
SENT II 1980 extended flight thruster experiments
[AIAA PAPER 81-0665] p0040 A81-29528
- Fluid model of plasma outside a hollow cathode neutralizer
[AIAA PAPER 81-0739] p0134 A81-29560
- Parasitic current losses due to solar electric propulsion generated plasmas
[AIAA PAPER 81-0740] p0043 A81-29561
- PLASMA SHEATHS**
The effect of solar array voltage patterns on plasma power losses
p0043 A81-19937
- Analysis of the charging of the SCATHA (P78-2) satellite
[NASA-CN-165348] p0033 N81-27169
- PLASMA SPRAYING**
Comparative evaluation of insulating properties of plasma-sprayed ceramic coatings
p0064 A81-15984
- Ion plating for the future
p0087 A81-44654
- Effects of plasma spray parameters on two layer thermal barrier
[NASA-TN-81724] p0053 N81-22161
- Burner rig evaluation of thermal barrier coating --- gas turbines
[NASA-TN-81684] p0055 N81-28231
- PLASMA STABILITY**
U MAGNETOHYDRODYNAMIC STABILITY
PLASMA THEORY
U PLASMA PHYSICS
PLASMAS (PHYSICS)
NT AECM PLASMA
NT ELECTRON PLASMA
PLASTIC ANISOTROPY
NT ELASTIC ANISOTROPY
PLASTIC DEFORMATION
Mechanical bonding of metal
[NASA-CASE-LEW-12941-1] p0068 N81-16329
- PLASTIC FILMS**
U POLYMERIC FILMS
PLASTIC WELDING
U PLASTIC DEFORMATION
PLASTICISMS
Advanced inorganic separators for alkaline batteries and method of making same --- a polymeric coating applied to a porous flexible substrate
[NASA-CASE-LEW-13171-1] p0100 N81-22466
- PLASTICS**
NT ACRYLIC RESINS
NT CARBON FIBER REINFORCED PLASTICS
NT EPOXY RESINS
NT Kevlar (TRADIMARK)
NT PHENOLIC RESINS
NT POLYESTER RESINS
NT POLYTETRAFLUOROETHYLENE
NT POLYVINYL ALCOHOL

- NT POLYVINYL FLUORIDE
 PLATES (STRUCTURAL MEMBERS)
 NT ANNULAR PLATES
 NT PERFORATED PLATES
 PLATING
 NT ELECTROPLATING
 NT ION PLATING
 PLATINUM
 Stabilizing platinum in phosphoric acid fuel cells
 [NASA-CR-165311] p0113 N81-22473
 PLUG NOZZLES
 VCH early acoustic test results of General
 Electric's high-radius ratio conical plug nozzle
 p0029 N81-17999
 PNEUMATIC EQUIPMENT
 Pneumatic boot for helicopter rotor deicing
 p0009 N81-19059
 Evaluation of a pneumatic boot deicing system on a
 general aviation wing model
 [NASA-TN-82363] p0011 N81-25065
 POINT DEFECTS
 NT VACANCIES (CRYSTAL DEFECTS)
 POISSONVILLE FLOW
 U LAMINAR FLOW
 POLARIZATION (CHARGE SEPARATION)
 Preparation and characterization of electrodes for
 the NASA Redox storage system
 [NASA-TN-82702] p0107 N81-30522
 POLICIES
 NT ENERGY POLICY
 POLISHED METALS
 U METAL POLISHING
 POLISHING
 NT METAL POLISHING
 POLLUTION
 NT AIR POLLUTION
 POLLUTION CONTROL
 Evaluation of concepts for controlling exhaust
 emissions from minimally processed petroleum and
 synthetic fuels
 [ASME PAPER 81-GT-157] p0067 N81-30056
 Advanced technology for controlling pollutant
 emissions from supersonic cruise aircraft
 p0001 N81-18004
 Heat pipes to reduce engine exhaust emissions
 [NASA-CASE-LEW-12590-1] p0049 N81-19245
 Supercritical fuel injection system
 [NASA-CASE-LEW-12990-1] p0018 N81-29129
 POLYACRYLATES
 U ACRYLIC RESINS
 POLYAMIDE RESINS
 NT KEVLAR (TVALSHARK)
 POLYESTER RESINS
 Synthesis of improved phenolic and polyester resins
 [NASA-CR-165180] p0065 N81-17263
 POLYIMIDE RESINS
 Feasibility of Kevlar 49/FMB-15 polyimide for high
 temperature applications
 p0047 N81-43602
 Composition and method for making polyimide
 resin-reinforced fabric
 [NASA-CASE-LEW-12933-1] p0061 N81-19296
 Environmental effects on graphite fiber reinforced
 FMB-15 polyimide
 [NASA-TN-82625] p0046 N81-32194
 POLYIMIDES
 Lower-curing-temperature FMB polyimides
 [NASA-TN-81705] p0045 N81-17174
 Tribological properties and thermal stability of
 various types of polyimide films
 [NASA-TN-81765] p0102 N81-23275
 POLYMER CHEMISTRY
 In-situ cross linking of polyvinyl alcohol ---
 application to battery separator films
 [NASA-CASE-LEW-13135-2] p0062 N81-24257
 POLYMER MATRIX COMPOSITES
 Self-lubricating composite materials
 p0142 N81-12984
 Lower-curing-temperature FMB polyimides
 [NASA-TN-81705] p0045 N81-17174
 POLYMERIC FILMS
 Ion beam texturing of heat transfer surfaces
 [AIAA PAPER 81-0670] p0086 N81-29531
 Evaluation of a method for heat transfer
 measurements and thermal visualization using a
 composite of a heater element and liquid crystals
 [ASME PAPER 81-GT-93] p0079 N81-30000
 The transfer of polytetrafluoroethylene studied by
 X-ray photoelectron spectroscopy
 p0087 N81-31238
 Texturing polymer surfaces by transfer casting ---
 cardiovascular prosthesis
 [NASA-CASE-LEW-13120-1] p0068 N81-16327
 Advanced inorganic separators for alkaline
 batteries and method of making same --- a
 polymeric coating applied to a porous flexible
 substrate
 [NASA-CASE-LEW-13171-1] p0100 N81-22466
 Tribological properties and thermal stability of
 various types of polyimide films
 [NASA-TN-81765] p0102 N81-23275
 Cross-linked polyvinyl alcohol and method of
 making same
 [NASA-CASE-LEW-13101-2] p0044 N81-29160
 POLYPHENYL ETHER
 Steady-state boundary lubrication with formulated
 C-ethers to 260 C
 [NASA-TP-1812] p0053 N81-21193
 Contact angle measurements of a polyphenyl ether
 to 190 C on M-50 steel
 [NASA-TN-82628] p0063 N81-27277
 POLYTETRAFLUOROETHYLENE
 The transfer of polytetrafluoroethylene studied by
 X-ray photoelectron spectroscopy
 p0087 N81-31238
 Polytetrafluoroethylene transfer film studied with
 X-ray photoelectron spectroscopy
 [NASA-TP-1728] p0060 N81-11214
 POLYVINYL ALCOHOL
 Inexpensive cross-linked polymeric separators made
 from water soluble polymers
 [NASA-TN-82619] p0101 N81-23205
 In-situ cross linking of polyvinyl alcohol ---
 application to battery separator films
 [NASA-CASE-LEW-13135-2] p0062 N81-24257
 Cross-linked polyvinyl alcohol and method of
 making same
 [NASA-CASE-LEW-13504-1] p0063 N81-27279
 Polyvinyl alcohol battery separator containing
 inert filler --- alkaline batteries
 [NASA-CASE-LEW-13556-1] p0106 N81-27615
 Cross-linked polyvinyl alcohol and method of
 making same
 [NASA-CASE-LEW-13101-2] p0044 N81-29160
 Alkaline battery containing a separator of a
 cross-linked copolymer of vinyl alcohol and
 unsaturated carboxylic acid
 [NASA-CASE-LEW-13102-1] p0107 N81-29531
 POLYVINYL FLUORIDE
 Fabrication and testing of polyvinylidene fluoride
 capacitors
 [NASA-CR-159501] p0073 N81-22278
 POROUS WALLS
 Composite wall concept for high-temperature
 turbine shrouds - Heat transfer analysis
 [SAE PAPER 801138] p0021 N81-34169
 PORTABLE EQUIPMENT
 An economics systems analysis of land mobile radio
 telephone services
 [NASA-TN-81476] p0069 N81-10239
 POSITIONING DEVICES (MACHINERY)
 NT CAMS
 POTATOES
 Normal crop calendars. Volume 2: The spring
 wheat states of Minnesota, Montana, North
 Dakota, and South Dakota
 [EEI-10070] p0094 N81-13426
 POTENTIAL ENERGY
 NT ELECTRIC POTENTIAL
 NT OPEN CIRCUIT VOLTAGE
 POTENTIAL FIELDS
 Particle and field measurements on two J-series
 30-centimeter thrusters
 [AIAA PAPER 81-0728] p0042 N81-38072
 POTENTIAL FLOW
 Some aspects of calculating flows about
 three-dimensional subsonic inlets
 [AIAA PAPER 81-1361] p0007 N81-42177
 POTENTIOMETERS (INSTRUMENTS)
 Development and design of three monitoring
 instruments for spacecraft charging
 [NASA-TP-1800] p0040 N81-31282
 POWDER METALLURGY
 Effect of milling and leaching on the structure of
 sintered silicon
 p0064 N81-22529
 Oxidation and hot corrosion of coated and bare
 oxide dispersion strengthened superalloy MA-755B

- Advanced aircraft engine materials trends
[NASA-TN-82626] p0058 A81-43384
p0055 A81-27259
- POWER CONDITIONING**
Extended operating range of the 30-cs ion thruster
with simplified power processor requirements
[AIAA PAPER 81-0692] p0040 A81-32897
JPL's electric and hybrid vehicles project:
Project activities and preliminary test results
--- power conditioning and battery charge
efficiency p0143 A81-12987
- Electronically commutated dc motors for electric
vehicles [NASA-TN-81654] p0097 A81-15464
- POWER CONVERTERS**
Fabrication and testing of polyvinylidene fluoride
capacitors [NASA-CR-159501] p0073 A81-22278
- POWER EFFICIENCY**
High efficiency ultrathin coplanar back contact
cells p0114 A81-27092
- Analytical investigation of efficiency and
performance limits in klystron amplifiers using
multidimensional computer programs; multi-stage
depressed collectors; and thermionic cathode
life studies p0098 A81-16552
- Comparison of photovoltaic cell temperatures in
modules operating with exposed and enclosed back
surfaces [NASA-TN-81769] p0106 A81-28520
- High B-field, large area ratio HED duct experiments
[NASA-TN-82673] p0132 A81-32026
- POWER GENERATORS**
U ELECTRIC GENERATORS
- POWER PLANTS**
Technology development for phosphoric acid fuel
cell powerplant, phase 2 [NASA-CR-165317] p0113 A81-21536
- Conceptual design study of a coal gasification
combined-cycle powerplant for industrial
cogeneration [NASA-TN-81687] p0105 A81-25488
- POWER PROCESSING SYSTEMS**
U POWER CONDITIONING
- POWER SUPPLY CIRCUITS**
Simplified power supplies for ion thrusters
[AIAA PAPER 81-0693] p0040 A81-29542
- Simplified power supplies for ion thrusters
[NASA-TN-81725] p0039 A81-20177
- PRECAUTIONS**
U ACCIDENT PREVENTION
- PRECIPITATION HARDENING**
Effect of TNP variables upon structure and
properties in ODS alloy NDA 8077 sheet ---
ThermoMechanical Processing of Oxide Dispersion
Strengthened nickel alloy p0059 A81-10706
- Elevated temperature mechanical properties and
residual tensile properties of two cast
superalloys and several nickel-base oxide
dispersion strengthened alloys p0057 A81-24104
- The effect of mechanical surface and heat
treatments on the erosion resistance of 6061
aluminum alloy p0057 A81-27944
- Oxidation and hot corrosion of coated and bare
oxide dispersion strengthened superalloy MA-755E
p0058 A81-43384
- PREDICTION ANALYSIS TECHNIQUES**
Backward deletion to minimize prediction errors in
models from factorial experiments with zero to
six center points p0122 A81-14999
- Nonlinear laminate analysis for metal matrix fiber
composites [AIAA 81-0579] p0046 A81-29411
- Analysis for predicting adiabatic wall
temperatures with single hole coolant injection
into a low speed crossflow [ASME PAPER 81-GT-91] p0077 A81-29998
- Analysis for predicting adiabatic wall
temperatures with single hole coolant injection
into a low speed crossflow [NASA-TN-81620] p0074 A81-13301
- Prediction of composite thermal behavior made simple
[NASA-TN-81618] p0045 A81-16132
- PREDICTIONS**
U NOISE PREDICTION
U NOISE PREDICTION (AIRCRAFT)
U PERFORMANCE PREDICTION
- PREHEATING**
U HEATING
- PREMIXING**
A model for the analysis of
premixing-prevaporizing fuel-air mixing passages
[AIAA PAPER 81-0345] p0030 A81-20767
- Fuel-air nonuniformity - Effect on nitric oxide
emissions [AIAA PAPER 81-0327] p0019 A81-20834
- Ignition of lean fuel-air mixtures in a
premixing-prevaporizing duct at temperatures up
to 1000 K [NASA-TN-81645] p0096 A81-13465
- PRESSINTERING**
U SINTERING
- PRESSURE**
U FLUID PRESSURE
U HIGH PRESSURE
U INLET PRESSURE
U PARTIAL PRESSURE
U SOUND PRESSURE
U STATIC PRESSURE
U ULTRAHIGH VACUUM
- PRESSURE DISTRIBUTION**
Energy efficient engine diffuser/combustor model
technology [NASA-CR-165157] p0026 A81-15002
- Flow through axially aligned sequential apertures
of the orifice and Borda types [NASA-TN-81681] p0075 A81-21314
- An experimental evaluation of oil pumping rings
[NASA-CR-165271] p0088 A81-21355
- Analysis of starvation effects on hydrodynamic
lubrication in nonconforming contacts [NASA-TN-82668] p0084 A81-29438
- PRESSURE EFFECTS**
Core compressor exit stage study. Volume 2: Data
and performance report for the baseline
configuration [NASA-CR-159498] p0027 A81-16051
- PRESSURE FIELDS**
U PRESSURE DISTRIBUTION
- PRESSURE GAGES**
U MANOMETERS
U VACUUM GAGES
- PRESSURE GRADIENTS**
Evacuation-induced pressure differentials in
multilayer insulation systems p0078 A81-18021
- PRESSURE MEASUREMENT**
Evacuation-induced pressure differentials in
multilayer insulation systems p0078 A81-18021
- Pressure spectra and cross spectra at an area
contraction in a ducted combustion [ASME PAPER 80-C2/AERO-91] p0077 A81-18638
- Experimental analysis of mass flow in a rotary
combustion engine --- Indicated Mean Effective
Pressure [NASA-TN-81749] p0079 A81-41732
- PRESSURE RECOVERY**
Performance prediction of straight two dimensional
diffusers [NASA-CR-165186] p0133 A81-11833
- PRESSURE REDUCTION**
Thermal and flow analysis of a convection
air-cooled ceramic coated porous metal concept
for turbine vanes [NASA-TN-81749] p0016 A81-22056
- Depressurization and two-phase flow of water
containing high levels of dissolved nitrogen gas
[NASA-TN-1639] p0076 A81-28389
- PRESSURE REGULATORS**
Ion beam sputter-etched ventricular catheter for
hydrocephalus shunt [NASA-CASE-LEN-13107-1] p0118 A81-27786
- PREVAPORIZATION**
A model for the analysis of
premixing-prevaporizing fuel-air mixing passages
[AIAA PAPER 81-0345] p0030 A81-20767
- Ignition of lean fuel-air mixtures in a
premixing-prevaporizing duct at temperatures up
to 1000 K

[NASA-TN-81645] p0096 N81-13465
PREVENTION
 NT ACCIDENT PREVENTION
 NT ICE PREVENTION
PRIMARY BATTERIES
 NT ALKALINE BATTERIES
 NT NICKEL ZINC BATTERIES
 NT SODIUM SULFUR BATTERIES
PRIMERS (COATINGS)
 A sputtered zirconia primer for improved thermal shock resistance of plasma sprayed ceramic turbine seals [NASA-TN-81732] p0062 N81-21198
 Advanced inorganic separators for alkaline batteries and method of making same --- a polymeric coating applied to a porous flexible substrate [NASA-CASE-LEN-13171-1] p0100 N81-22466
 Thermal barrier coating system having improved adhesion [NASA-CASE-LEN-13359-1] p0062 N81-24265
PRIVATE AIRCRAFT
 U GENERAL AVIATION AIRCRAFT
PROBLEM SOLVING
 NT ITERATIVE SOLUTION
PROCEDURES
 NT FINITE ELEMENT METHOD
 NT PANEL METHOD (FLUID DYNAMICS)
PROCESS HEAT
 Coal gasifier cogeneration powerplant project p0143 N81-12988
 Solar Thermal Power Systems parabolic dish project [NASA-TN-82371] p0107 N81-28524
PRODUCT DEVELOPMENT
 Development of low-cost directionally-solidified turbine blades p0088 N81-10707
 GaAs homojunction solar cell development p0099 N81-17561
 A methodology for fostering commercialization of electric and hybrid vehicle propulsion systems [NASA-TN-81575] p0140 N81-18933
 Fabrication of aluminum oxide fiber reinforced aluminum matrix composites [NASA-CN-165184] p0048 N81-19229
 Development program on a cold cathode electron gun [NASA-CN-159570] p0073 N81-19395
 Comparative radiation testing of solar cells for the shuttle power extension package [NASA-TN-82656] p0105 N81-27605
 The Mod-2 wind turbine development project [NASA-TN-82681] p0106 N81-27606
PRODUCTION ENGINEERING
 The HEWAC pilot line experience p0111 N81-17574
PRODUCTION METHODS
 U PRODUCTION ENGINEERING
PRODUCTS
 NT PETROLEUM PRODUCTS
PROGRAMMING LANGUAGES
 NT FORTRAN
PROGRAMS
 NT AGRISTARS PROJECT
 NT GLOBAL ATMOSPHERIC RESEARCH PROGRAM
 NT NASA PROGRAMS
 NT QUIET ENGINE PROGRAM
 NT SUPERSONIC CRUISE AIRCRAFT RESEARCH
PROJECTS
 NT AGRISTARS PROJECT
PROP-PAD TECHNOLOGY
 Low and high speed propellers for general aviation - Performance potential and recent wind tunnel test results p0023 N81-42758
PROPAGATION (EXTENSION)
 NT CRACK PROPAGATION
PROPAGATION MODES
 Acoustic performance of inlet suppressors on an engine generating a single mode [NASA-TN-82697] p0127 N81-32968
PROPANE
 Effect of fuel nitrogen and hydrogen content on emissions in hydrocarbon combustion [NASA-TN-81612] p0097 N81-14399
PROPELLANT TESTS
 Performance of a magnetic multiple line-cusp argon ion thruster [NASA-TN-81703] p0038 N81-19219

PROPELLANTS
 NT CRYOGENIC ROCKET PROPELLANTS
 NT GASEOUS ROCKET PROPELLANTS
 NT LIQUID ROCKET PROPELLANTS
PROPELLER BLADES
 The NASA high-speed turboprop program [SAB PAPER 801120] p0021 N81-34156
 Laser-velocimeter flow-field measurements of an advanced turboprop [AIAA PAPER 81-1568] p0007 N81-42211
 Low and high speed propellers for general aviation: Performance potential and recent wind tunnel test results [NASA-TN-81745] p0003 N81-21028
 An evaluation of a simplified near field noise model for supersonic helical tip speed propellers [NASA-TN-81727] p0130 N81-22836
PROPELLER EFFICIENCY
 The NASA high-speed turboprop program [SAB PAPER 801120] p0021 N81-34156
 Factors influencing the predicted performance of advanced propeller designs [NASA-TN-82676] p0004 N81-27042
PROPELLER FANS
 Laser-velocimeter flow-field measurements of an advanced turboprop [NASA-TN-82677] p0004 N81-27041
PROPELLERS
 NT PROPELLER FANS
 NT SHROUDED PROPELLERS
 Factors influencing the predicted performance of advanced propeller designs [AIAA PAPER 81-1564] p0007 N81-42210
 Low and high speed propellers for general aviation - Performance potential and recent wind tunnel test results p0023 N81-42758
 The propeller tip vortex: A possible contributor to aircraft cabin noise [NASA-TN-81768] p0130 N81-22838
 Factors influencing the predicted performance of advanced propeller designs [NASA-TN-82676] p0004 N81-27042
PROPULSION
 NT AUXILIARY PROPULSION
 NT CHEMICAL PROPULSION
 NT ELECTRIC PROPULSION
 NT ELECTROSTATIC PROPULSION
 NT ION PROPULSION
 NT JET PROPULSION
 NT LOW THRUST PROPULSION
 NT PLASMA PROPULSION
 NT SOLAR ELECTRIC PROPULSION
 NT SPACECRAFT PROPULSION
 NASA Research in aeropropulsion [NASA-TN-81633] p0014 N81-13056
PROPULSION SYSTEM CONFIGURATIONS
 Magneto-electrostatic thruster physical geometry tests [AIAA PAPER 81-0753] p0044 N81-29566
 NASA research in aeropropulsion [ASME PAPER 81-GT-96] p0001 N81-30003
 A status report on the Energy Efficient Engine Project [SAB PAPER 801119] p0021 N81-34155
 NASA Research in aeropropulsion p0142 N81-12980
 Progress in materials and structures at Lewis Research Center p0142 N81-12982
 Propulsion system research and development for electric and hybrid vehicles p0142 N81-12985
 Advanced Technology Spark-Ignition Aircraft Piston Engine Design Study [NASA-CN-165162] p0026 N81-13963
 Progress with variable cycle engines p0001 N81-17997
 Energy efficient engine: Flight propulsion system preliminary analysis and design [NASA-CN-159583] p0029 N81-18056
 Advanced propulsion system concept for hybrid vehicles [NASA-CN-159772] p0140 N81-18935
 Comparison of NASA and contractor results from aeroacoustic tests of QCSSE OTW engine [NASA-TN-81761] p0017 N81-25079
 SEP BICCD variable conductance heat pipes acceptance and characterization tests

- [NASA-TN-82635] p0076 N81-30390
PROPULSION SYSTEM PERFORMANCE
 The future of aeronautical propulsion p0001 A81-29052
 Performance capabilities of the 8-cm Mercury ion p0044 A81-29567
 thruster [AIAA PAPER 81-0754]
 Effect of time-dependent flight loads on turbofan p0030 A81-30093
 engine performance deterioration [ASME PAPER 81-GT-203]
 An automated procedure for developing hybrid p0020 A81-32544
 computer simulations of turbofan engines
 Extended operating range of the 30-cm ion thruster p0040 A81-32897
 with simplified power processor requirements [AIAA PAPER 81-0692]
 Improved components for engine fuel savings p0021 A81-34152
 [SAE PAPER 801116]
 Performance deterioration of commercial p0021 A81-34154
 high-bypass ratio turbofan engines [SAE PAPER 801118]
 A nonlinear propulsion system simulation technique p0022 A81-38064
 for piloted simulators
 Diagnostic system design for the Ion Auxiliary p0041 A81-38070
 Propulsion System /IAPS/- Flight test of two 8
 cm mercury ion thrusters [AIAA PAPER 81-0666]
 Effect of a part-span variable inlet guide vane on p0022 A81-40842
 the performance of a high-bypass turbofan engine [AIAA PAPER 81-1362]
 Selected results from combustion research at the p0022 A81-40859
 Lewis Research Center [AIAA PAPER 81-1392]
 JT9D performance deterioration results from a p0022 A81-40963
 simulated aerodynamic load test [AIAA PAPER 81-1588]
 Turbine bypass engine - A new supersonic cruise p0023 A81-40971
 propulsion concept [AIAA PAPER 81-1596]
 The supersonic fan engine - An advanced concept in p0023 A81-40973
 supersonic cruise propulsion [AIAA PAPER 81-1599]
 Factors influencing the predicted performance of p0007 A81-42210
 advanced propeller designs [AIAA PAPER 81-1564]
 An overview of general aviation propulsion p0023 A81-42778
 research programs at NASA-Lewis Research Center [SAE PAPER 810624]
 Mixing effectiveness test of an exhaust gas mixer p0023 A81-44225
 in a high bypass turbofan at altitude [AIAA PAPER 81-1495]
 An approach to real-time simulation using parallel p0121 A81-44652
 processing
 Propulsion Controls, 1979 --- air breathing engine p0014 N81-12090
 control [NASA-CP-2137]
 Performance seeking controls p0014 N81-12092
 F100 multivariable control synthesis program: A p0014 N81-12093
 review of full scale engine altitude tests ---
 F100 engine
 Design of a multivariable integrated control for a p0025 N81-12094
 supersonic propulsion system --- variable stream
 control engine
 Propulsion controls p0025 N81-12095
 Future Air Force aircraft propulsion control p0025 N81-12096
 systems: The extended summary paper
 Impact for the 80's: Proceedings of a Conference p0142 N81-12978
 on Selected Technology for Business and Industry [NASA-CP-2149]
 JPL's electric and hybrid vehicles project: p0143 N81-12987
 Project activities and preliminary test results
 --- power conditioning and battery charge
 efficiency
 Electronically commutated dc motors for electric p0097 N81-15464
 vehicles [NASA-TN-81654]
 Characterization of the near-term electric vehicle p0097 N81-15465
 (ETV-1) breadboard propulsion system over the
 SAE J272A driving schedule D [NASA-TN-81664]
- Propulsion system mathematical model for a p0015 N81-16055
 lift/cruise fan V/STOL aircraft [NASA-TN-81663]
 Free radical propulsion concept p0039 N81-20180
 [NASA-TN-81770]
 Characteristics of 30-centimeter mercury ion p0039 N81-21121
 thrusters [NASA-TN-81706]
 Energy efficient engine flight propulsion system: p0030 N81-22051
 Aircraft/engine integration evaluation [NASA-CN-159584]
 A nonlinear propulsion system simulation technique p0101 N81-23085
 for piloted simulators [NASA-TN-82600]
 Turbine bypass engine: A new supersonic cruise p0018 N81-26145
 propulsion concept [NASA-TN-82608]
 Advanced subsonic transport propulsion p0019 N81-31195
 [NASA-TN-82696]
PROPELLER EFFICIENCY
 Performance of a magnetic multipole line-cusp p0038 N81-19210
 argon ion thruster [NASA-TN-81703]
 Performance capabilities of the 8-cm Mercury ion p0038 N81-19220
 thruster [NASA-TN-81720]
PROSTHETIC DEVICES
 Texturing polymer surfaces by transfer casting --- p0068 N81-16327
 cardiovascular prosthesis [NASA-CASE-LEU-13120-1]
PROTECTION
 NT CIRCUIT PROTECTION
 NT ENVIRONMENT PROTECTION
 NT RADIATION PROTECTION
 NT THERMAL PROTECTION
PROTECTIVE COATINGS
 NT CERAMIC COATINGS
 NT PRIMERS (COATINGS)
 Thermal barrier coatings for heat engine components p0056 A81-12920
 Friction and wear results from sputter-deposited p0089 A81-18693
 chrome oxide with and without nichrome metallic
 binders and interlayers [ASME PAPER 80-C2/LUB-49]
 Ion beam deposited protective films p0086 A81-29532
 [AIAA PAPER 81-0672]
 Sputtered protective coatings for die casting dies p0057 A81-38067
 Oxidation and hot corrosion of coated and bare p0058 A81-43384
 oxide dispersion strengthened superalloy SA-755E
 Sputtering and ion plating for aerospace p0087 A81-44655
 applications
 Thermal barrier coatings for superalloys p0058 A81-49217
 Curved film cooling admission tube p0074 N81-12363
 [NASA-CASE-LEU-13174-1]
 Thin-film coatings p0142 N81-12983
 Improved refractory coatings --- sputtered p0052 N81-16209
 coatings on substrates that form stable nitrides [NASA-CASE-LEU-23169-2]
 Program to develop sprayed, plastically deformable p0088 N81-17434
 compressor shroud seal materials [NASA-CN-165237]
 Ion beam deposited protective films p0038 N81-19221
 [NASA-TN-81722]
 Sputtered protective coatings for die casting dies p0053 N81-21173
 [NASA-TN-81735]
 Microstructure and mechanical properties of bulk p0059 N81-22158
 and plasma-sprayed Y2O3-partially stabilized
 zirconia [NASA-CN-165126]
 Prolonging thermal barrier coated specimen life by p0102 N81-23417
 thermal cycle management [NASA-TN-81742]
 Corrosion resistant thermal barrier coating --- p0054 N81-25188
 protecting gas turbines and other engine parts [NASA-CASE-LEU-13088-1]
 Ion plating for the future p0054 N81-25189
 [NASA-TN-82130]
 An introduction to NASA's turbine engine hot p0019 N81-31206
 section technology (HOST) project
PROTON IRRADIATION
 Proton radiation damage in bulk n-GaAs p0099 N81-17564

PROTOTYPES

Conceptual design of the NED Engineering Test Facility
[NASA-TN-82621] p0132 N81-24926

PULSATING FLOW
U UNSTEADY FLOW

PULSE MODULATION
User's design handbook for a Standardized Control Module (SCM) for DC to DC Converters, volume 2
[NASA-CR-165173] p0072 N81-11314

PULSED RADIATION
NT SYSTEM GENERATED ELECTROMAGNETIC PULSES
PULSES
NT SYSTEM GENERATED ELECTROMAGNETIC PULSES

PUMPS
NT ELECTROMAGNETIC PUMPS
NT FUEL PUMPS
NT TURBINE PUMPS
NT WINDPOWERED PUMPS
An experimental evaluation of oil pumping rings
[NASA-CR-165271] p0088 N81-21355
Traction drive for cryogenic boost pump --- hydrogen oxygen rocket engines
[NASA-TN-81704] p0101 N81-23188

PURITY
Effects of Ultra-Clean and centrifugal filtration on rolling-element bearing life
[NASA-TN-82660] p0085 N81-29440

PYROGRAPHALLOY
U COMPOSITE MATERIALS
U PYROLYTIC GRAPHITE
U REFRACTORY MATERIALS
PYROLYTIC GRAPHITE
Electron reflection and secondary emission characteristics of sputter-textured pyrolytic graphite surfaces
p0065 N81-38065
Electron reflection and secondary emission characteristics of sputter-textured pyrolytic graphite surfaces
[NASA-TN-81755] p0062 N81-22193

PYROLYTIC MATERIALS
NT PYROLYTIC GRAPHITE

PYROMETERS
NT RADIATION PYROMETERS
NT THERMOCOUPLE PYROMETERS
PYROMETRY
U TEMPERATURE MEASUREMENT

Q

QUALITY
NT AIR QUALITY

QUALITY CONTROL
Spacecraft transmitter reliability
[NASA-CR-2159] p0037 N81-16119
Reliability and quality assurance on the MOD 2 wind system
[NASA-TN-82717] p0090 N81-33492

QUANTITATIVE ANALYSIS
An integrated exhaust gas analysis system with self-contained data processing and automatic calibration
[NASA-TN-81592] p0102 N81-23435

QUATERNARY ALLOYS
Ion beam sputter etching of orthopedic implant alloy MP35N and resulting effects on fatigue properties
[AIAA PAPER 81-0671] p0057 N81-38069

QUIET ENGINE PROGRAM
Turbomachinery noise studies of the AirResearch QCEAT engine with inflow control --- acoustic performance
[AIAA PAPER 81-2049] p0023 N81-48621
Low-speed aerodynamic performance of 50.8-centimeter-diameter noise-suppressing inlets for the Quiet, Clean, Short-haul Experimental Engine (QCSSE) --- Lewis 9- by 15-foot low speed wind tunnel tests
[NASA-TP-1178] p0013 N81-11037
QCEAT mixer compound exhaust system design and static big model test report
[NASA-CR-135386] p0029 N81-19119
Comparison of NASA and contractor results from aerodynamic tests of QCSSE OTU engine
[NASA-TN-81761] p0017 N81-25079
Comparison of predicted engine core noise with current and proposed aircraft noise certification requirements

[NASA-TN-82659]

p0126 N81-29922

R

RADIAL FLOW
Loss model for off-design performance analysis of radial turbines with pivoting-vane, variable-area stators
[SAR PAPER 801135] p0021 N81-34166
Analytical design of an advanced radial turbine --- automobile engines
[NASA-CR-165170] p0140 N81-20958

RADIANCE
Spectral flame radiance from a tubular-can combustor
[NASA-TP-1722] p0016 N81-19121

RADIANT FLUX DENSITY
NT RADIANCE

RADIATION DAMAGE
Thin n-i-p silicon solar cell
p0114 N81-27097
Space solar cells - High efficiency and radiation damage
p0108 N81-27174
Radiation damage in lithium-counterdoped n/p silicon solar cells
p0109 N81-27204
Radiation damage annealing mechanisms and possible low temperature annealing in silicon solar cells
p0040 N81-27207
Space Photovoltaic Research and Technology 1980. High Efficiency, Radiation Damage and Blanket Technology
[NASA-CR-2169] p0098 N81-17531
Theoretical results on the double-collecting tandem junction solar cell --- radiation damage
p0099 N81-17538
Annealing of radiation damage in low resistivity silicon solar cells
p0099 N81-17554
Radiation damage in silicon NIP solar cells
p0099 N81-17557
Proton radiation damage in bulk n-GaAs
p0099 N81-17564
Computer program for pulsed thermocouples with corrections for radiation effects
[NASA-TP-1895] p0120 N81-33838

RADIATION EFFECTS
NT RADIATION DAMAGE
NT RADIOLYSIS
New ion exchange membranes --- composed of radiation crosslinked polyacrylic resins
[NASA-TN-81670] p0044 N81-16123

RADIATION HAZARDS
Safety management of complex research operators
[NASA-TN-81772] p0068 N81-25263

RADIATION MEASURING INSTRUMENTS
NT ELECTROSTATIC PROBES
NT INFRARED SPECTROPHOTOMETERS

RADIATION PRESSURE
NT SOUND PRESSURE

RADIATION PROTECTION
Recent developments in lightweight solar cell modules --- with protective glass cover
p0099 N81-17571

RADIATION PYROMETERS
Surface pyrometry in presence of radiation from other sources with application to turbine blade temperature measurement
[NASA-TP-1754] p0013 N81-11039

RADIATION RESISTANCE
U RADIATION TOLERANCE

RADIATION TOLERANCE
Radiation damage in lithium-counterdoped n/p silicon solar cells
p0109 N81-27204
Performance of high resistivity n++p silicon solar cells under 1 MeV electron irradiation
[NASA-TN-82610] p0103 N81-23626

RADICALS
NT FREE RADICALS

RADIO COMMUNICATION
NT TELEPHONE
NT TIME DIVISION MULTIPLE ACCESS
An economics systems analysis of land mobile radio telephone services
[NASA-TN-81476] p0069 N81-10239

RADIO EQUIPMENT
NT RADIOTELEPHONES

- RADIO FREQUENCIES**
 NT EXTREMELY HIGH FREQUENCIES
 NT HIGH FREQUENCIES
RADIO FREQUENCY DISCHARGE
 Recent work on an RF ion thruster
 [AIAA PAPER 81-0678] p0041 A81-35625
 Recent work on an RF ion thruster
 [NASA-TN-81734] p0039 A81-20178
 Analytical prediction and experimental
 verification of performance at various operating
 conditions of a dual-mode traveling wave tube
 with multistage depressed collectors
 [NASA-TP-1831] p0072 A81-28352
RADIO FREQUENCY HEATING
 Gyrotron transmitting tube
 [NASA-CASE-LUN-13429-1] p0071 A81-16384
RADIO RELAY SYSTEMS
 NT TIME DIVISION MULTIPLE ACCESS
RADIO TRANSMISSION
 NT MICROWAVE TRANSMISSION
RADIO TRANSMITTERS
 NT RADIOTELEPHONES
RADIO WAVES
 NT SUBMILLIMETER WAVES
RADIOFREQUENCY ION THRUSTOR ENGINES
 U IIT ENGINES
RADIOLYSIS
 New ion exchange membranes --- composed of
 radiation crosslinked polyacrylic resins
 [NASA-TN-81670] p0044 A81-16123
RADIOSENSITIVITY
 U RADIATION TOLERANCE
RADIOTELEPHONES
 An economic systems analysis of land mobile radio
 telephone services p0069 A81-22528
RARE EARTH ELEMENTS
 NT GADOLINIUM
 NT YTTRIUM
RARE GASES
 NT ARGON
 NT XENON
 The self-consistent calculation of pseudo-molecule
 energy levels, construction of energy level
 correlation diagrams and an automated
 computation system for SCP-X(Alpha)-SU
 calculations
 [NASA-TN-81710] p0130 A81-25779
RATE METERS
 U MEASURING INSTRUMENTS
RATES (PER TIME)
 NT ANGULAR ACCELERATION
 NT CRITICAL VELOCITY
 NT CURRENT DENSITY
 NT FLOW VELOCITY
 NT FLUX (RATE)
 NT FLUX DENSITY
 NT LOADING RATE
 NT MAGNETIC FLUX
 NT MASS FLOW RATE
 NT RADIANCE
 NT SOUND INTENSITY
 NT SUPERSONIC SPEEDS
 NT TRANSONIC SPEED
RATIOS
 NT FUEL-AIR RATIO
 NT SIGNAL TO NOISE RATIOS
RAY TRACING
 High-frequency sound propagation in a spatially
 varying mean flow p0129 A81-49913
RC CIRCUITS
 Integrated RC-circuits in ALTA-technology on one
 substrate
 [BNFT-PB-T-79-107] p0072 A81-14227
RC NETWORKS
 U RC CIRCUITS
REACTION JETS
 U JET FLOW
REACTION KINETICS
 RHD generator off-design performance and non
 chemical kinetics analysis. Volume 1: Analysis
 of the off-design performance of the Engineering
 Test Facility RTF RHD generator flow train
 [NASA-CR-165187] p0133 A81-11834
REACTION RATE
 U REACTION KINETICS
REAL TIME OPERATION
 A nonlinear propulsion system simulation technique
 for piloted simulators p0022 A81-38864
 An approach to real-time simulation using parallel
 processing p0121 A81-44652
 Experimental analysis of INRP in a rotary
 combustion engine
 [NASA-TN-81662] p0015 A81-16054
 An approach to real-time simulation using parallel
 processing
 [NASA-TN-81731] p0121 A81-21803
REAL VARIABLES
 NT COPLANABILITY
 NT DIFFERENTIAL EQUATIONS
 NT LINEAR EQUATIONS
 NT NONLINEAR EQUATIONS
RECEIVERS
 NT RADIOTELEPHONES
RECIPROCATING ENGINES
 U PISTON ENGINES
RECIPROCATION
 An experimental evaluation of oil pumping rings
 [NASA-CR-165271] p0088 A81-21355
RECLAMATION
 NT MATERIALS RECOVERY
RECOGNITION
 NT PATTERN RECOGNITION
RECOMBINATION REACTIONS
 Free radical propulsion concept
 [AIAA PAPER 81-0676] p0041 A81-32905
RECOMPRESSION
 U COMPRESSING
RECONNAISSANCE
 NT AERIAL RECONNAISSANCE
RECOVERABLE SPACECRAFT
 NT SPACE SHUTTLES
RECTIFIERS
 NT THYRISTORS
REGENERATORS
 U REGENERATORS
REDOX CELLS
 Anion permselective membrane
 [NASA-CR-165223] p0111 A81-16583
 NASA preprototype redox storage system for a
 photovoltaic stand-alone application
 [NASA-TN-82607] p0104 A81-24534
 Zirconium carbide as an electrocatalyst for the
 chromous/chromic redox couple
 [NASA-CASE-LUN-13246-1] p0049 A81-26203
 Pumping power considerations in the designs of
 NASA-Redox flow cells
 [NASA-TN-82598] p0106 A81-28519
 Catalyst surfaces for the chromous/chromic redox
 couple
 [NASA-CASE-LUN-13148-2] p0107 A81-29524
 Preparation and characterization of electrodes for
 the NASA Redox storage system
 [NASA-TN-82702] p0107 A81-30522
 Design and assembly considerations for Redox cells
 and stacks
 [NASA-TN-82672] p0049 A81-31308
 A Redox system design for solar storage applications
 [NASA-TN-82720] p0108 A81-32608
 Advances in membrane technology for the NASA redox
 energy storage system
 [NASA-TN-82701] p0108 A81-33601
REDUCED GRAVITY
 Shuttle compatible cryogenic liquid storage and
 supply systems
 [AIAA PAPER 81-1509] p0037 A81-42207
 Conceptual design of an in-space cryogenic fluid
 management facility, executive summary
 [NASA-CR-165279-EXEC-SUMM] p0137 A81-21212
 Conceptual design of an in-space cryogenic fluid
 management facility
 [NASA-CR-165279] p0067 A81-21213
REDUCTION (CHEMISTRY)
 NT HYDROGENATION
 Effect of sintering and leaching on the structure of
 sintered silicon
 [NASA-TN-81602] p0060 A81-13166
REDUCTION (MATHEMATICS)
 U OPTIMIZATION
REFERENCES (STANDARDS)
 U STANDARDS
REFLECTION
 NT WAVE REFLECTION
REFLECTORS
 NT PARABOLIC REFLECTORS

REFRACTED RADIATION

REFRACTED RADIATION

U REFRACTED WAVES

REFRACTED WAVES

U REFRACTED WAVES

REFRACTED WAVES

High-frequency sound propagation in a spatially
varying beam flow

p0129 A81-49913

REFRACTORY MATERIALS

REFRACTORY MATERIALS

U REFRACTORY METAL ALLOYS

REFRACTORY METAL ALLOYS

U REFRACTORY METAL ALLOYS

REFRACTORY METAL ALLOYS

U REFRACTORY METAL ALLOYS

REFRACTORY METAL ALLOYS

Fabrication of injectors sintered alpha SiC
turbine components

[ASME PAPER 81-GT-161] p0089 A81-30060

Improved refractory coatings --- sputtered
coatings on substrates that form stable nitrides

[NASA-CASE-LEW-23169-2] p0052 A81-16209

High power densities from high-temperature
materials interactions --- thermionic energy

conversion and metallic fluid heat pipes

[NASA-TN-81626] p0131 A81-16900

REFRACTORY METAL ALLOYS

REFRACTORY METAL ALLOYS

U REFRACTORY METAL ALLOYS

REFRACTORY METAL ALLOYS

The role of oxidation in the fretting wear process

[NASA-TN-81570] p0051 A81-12210

REFRACTORY METALS

REFRACTORY METALS

U REFRACTORY METALS

REFRACTORY METALS

REFRACTORY METALS

U REFRACTORY METALS

REFRACTORY METALS

REFRACTORY METALS

U REFRACTORY METALS

REFRACTORY METALS

U REFRACTORY METALS

Backward deletion to minimize prediction errors in
models from factorial experiments with zero to
six center points

p0122 A81-14999

Backward deletion to minimize prediction errors in
models from factorial experiments with zero to
six center points

[NASA-TN-81524] p0123 A81-10778

REGULATORS

REGULATORS

U REGULATORS

REGULATORS

Analysis and design of an adaptive multi-loop

controlled two winding buck/boost regulator

p0073 A81-21675

REHEATING

REHEATING

U REHEATING

REHEATING

REINFORCED MATERIALS

REINFORCED MATERIALS

U REINFORCED MATERIALS

REINFORCED MATERIALS

REINFORCED MATERIALS

U REINFORCED MATERIALS

REINFORCED MATERIALS

CVD-produced boron filaments

p0048 A81-11336

Laminates and reinforced metals

[NASA-TN-81591] p0045 A81-12171

Fabrication of aluminum oxide fiber reinforced

aluminum matrix composites

[NASA-CR-165184] p0048 A81-19229

Composition and method for making polyimide

resin-reinforced fabric

[NASA-CASE-LEW-12933-1] p0061 A81-19256

Ultra-high modulus organic fiber hybrid composites

[NASA-CR-165228] p0048 A81-11130

Tungsten fiber reinforced superalloys: A status

review

[NASA-TN-82590] p0045 A81-25148

RELAXATION (MECHANICS)

RELAXATION (MECHANICS)

U RELAXATION (MECHANICS)

RELAXATION (MECHANICS)

U RELAXATION (MECHANICS)

RELAXATION (MECHANICS)

RELIABILITY

RELIABILITY

U RELIABILITY

RELIABILITY ANALYSIS

NEGA16 - Computer program for analysis and

extrapolation of stress-rupture data

[NASA-TP-1869] p0102 A81-23486

Reliability and quality assurance on the MOD 2

wind system

[NASA-TN-82717] p0090 A81-33492

RELIABILITY CONTROL

U RELIABILITY CONTROL

RELIABILITY ENGINEERING

RELIABILITY ENGINEERING

Aircraft engine diagnostics

[NASA-CR-2190] p0019 A81-31196

RELIEF VALVES

Ion beam sputter-etched ventricular catheter for

hydrocephalus shunt

[NASA-CASE-LEW-13107-1] p0118 A81-27786

RESEARCH

Assessment of variations in thermal cycle life

data of thermal barrier coated rods

p0058 A81-44657

REPAIRING

U MAINTENANCE

REPUBLIC MILITARY AIRCRAFT

U MILITARY AIRCRAFT

RESEARCH

U LOW DENSITY RESEARCH

U MARKET RESEARCH

RESEARCH AIRCRAFT

An overview of general aviation propulsion

research programs at NASA-Levis Research Center

[SAE PAPER 810624] p0023 A81-42778

RESEARCH AND DEVELOPMENT

Engineering management and innovation

Large wind-turbine projects in the United States

wind energy program

p0108 A81-23694

Photovoltaic applications - Past and future

p0109 A81-27231

Simplified power supplies for ion thrusters

[AIAA PAPER 81-0693] p0040 A81-29542

NASA research in aeropropulsion

[ASME PAPER 81-GT-96] p0001 A81-30003

Goals of thermionic program for space power

p0133 A81-44656

Safety management of complex research operations

p0067 A81-44661

Electric and hybrid vehicle system R/D

[NASA-TN-81606] p0096 A81-11449

The DOE photovoltaics program

p0143 A81-12989

Bibliography of Lewis Research Center Technical

Publications announced in 1979

[NASA-TN-81525] p0137 A81-17942

Bibliography of Lewis Research Center Technical

Publications announced in 1978

[NASA-TN-79162] p0137 A81-17943

Fundamental heat transfer research for gas turbine

engines

[NASA-CR-2178] p0016 A81-24063

Aerospace in the future

[NASA-TN-82664] p0143 A81-29063

RESEARCH FACILITIES

High temperature cyclic oxidation furnace testing

at NASA Lewis Research Center

p0058 A81-44653

Survey of aircraft icing simulation test

facilities in North America

[NASA-TN-81707] p0009 A81-19078

Safety management of complex research operations

[NASA-TN-81772] p0068 A81-25263

RESEARCH VEHICLES

SEBT II 1980 extended flight thruster experiments

[AIAA PAPER 81-0665] p0040 A81-29528

RESIDENTIAL ENERGY

Study of fuel cell on-site, integrated energy

systems in residential/commercial applications

[NASA-CR-165144] p0112 A81-21533

A bedrock system design for solar storage applications

[NASA-TN-82720] p0108 A81-32608

RESIN BONDING

Effect of load, area of contact, and contact

stress on the wear mechanisms of a bonded solid

lubricant film

[NASA-TN-81563] p0060 A81-12226

RESIN MATRIX COMPOSITES

Superhybrid composite blade impact studies
[NASA-TN-81597] p0091 N81-11412

RESINS

NT ACRYLIC RESINS
NT EPOXY RESINS
NT KEVLAR (TRADEMARK)
NT PHENOLIC RESINS
NT POLYESTER RESINS
NT POLYIMIDE RESINS

RESISTIVITY

U ELECTRICAL RESISTIVITY

RESISTORS

Integrated RC-circuits in ALTA-technology on one
substrate
[BNFT-FB-T-79-107] p0072 N81-14227

RESONANCE PROBES

NT CYCLOTRON RESONANCE DEVICES

RESOURCES MANAGEMENT

NASA's activities in the conservation of strategic
aerospace materials p0056 N81-22535

RESPONSES

NT DYNAMIC RESPONSE
NT MODAL RESPONSE
NT TRANSIENT RESPONSE

RETROFITTING

Retrofit and verification test of a 30-cm ion
thruster
[NASA-CR-165233] p0042 N81-20174

REUSABLE SPACECRAFT

NT SPACE SHUTTLES

REYNOLDS EQUATION

Surface roughness effect on finite oil journal
bearings
[NASA-TN-82639] p0084 N81-27526

REYNOLDS LAW

U REYNOLDS EQUATION

RHEOLOGY

Influence of excess diiside on properties of PBE
polyimide resins and composites p0047 N81-43635

RICE

Normal crop calendars. Volume 1: Assembly and
application of historical crop data to a
standard product
[N81-10075] p0095 N81-13431

R. H. HARRISON-DUNHAM EQUATION

U TEMPERATURE EFFECTS

RING STRUCTURES

Ladder supported ring bar circuit
[NASA-CASE-LEU-13570-1] p0071 N81-24348

RIT ENGINES

Recent work on an RF ion thruster
[NASA-TN-81734] p0039 N81-20178

ROCKET CHAMBERS

U THRUST CHAMBERS

ROCKET ENGINE DESIGN

High performance cryogenic engines for orbit
transfer vehicles
[IAP PAPER 80-P-253] p0043 N81-18363

Characteristics of 30-centimeter mercury ion
thrusters
[AIAA PAPER 81-0715] p0041 N81-37569

Ion beam applications research - A 1981 summary of
Lewis Research Center programs
[AIAA PAPER 81-0669] p0041 N81-38068

Performance capabilities of the 8-cm mercury ion
thruster
[NASA-TN-81720] p0038 N81-19220

Retrofit and verification test of a 30-cm ion
thruster
[NASA-CR-165233] p0042 N81-20174

Characteristics of 30-centimeter mercury ion
thrusters
[NASA-TN-81706] p0039 N81-21121

Low-thrust chemical rocket engine study
[NASA-CR-165276] p0042 N81-21122

Low-thrust chemical rocket engine study
[NASA-CR-165275] p0042 N81-21125

ROCKET ENGINES

NT ELECTRIC ROCKET ENGINES
NT ELECTROSTATIC ENGINES
NT HYDROGEN OXYGEN ENGINES
NT ION ENGINES
NT LIQUID PROPELLANT SCRAM ENGINES
NT MERCURY ION ENGINES
NT RIT ENGINES

Results of the Mission Profile Life Test first
test segment - Thruster J1
[AIAA PAPER 81-0716] p0043 N81-29552

Recent work on an RF ion thruster
[AIAA PAPER 81-0678] p0041 N81-35625
Extended operating range of the 30-cm ion thruster
with simplified power processor requirements
[NASA-TN-81729] p0039 N81-20179

ROCKET PROPELLANTS

NT CRYOGENIC ROCKET PROPELLANTS
NT GASEOUS ROCKET PROPELLANTS
NT LIQUID FUELS
NT LIQUID ROCKET PROPELLANTS

RODS

Assessment of variations in thermal cycle life
data of thermal barrier coated rods p0058 N81-44657

ROLL FORMING

Computer-aided roll pass design in rolling of
airfoil shapes p0088 N81-15796

ROLLER BEARINGS

Kinematic correction for roller skewing
[ASME PAPER 80-DT-76] p0085 N81-18647
Calculated and experimental data for a 118-mm bore
roller bearing to 3 million DN
[ASME PAPER 80-C2/LUB-14] p0085 N81-18668
Lubrication of rolling element bearings p0086 N81-18738

History of ball bearings
[NASA-TN-81689] p0081 N81-18391

Life analysis of multiroller planetary traction
drive
[NASA-TF-1710] p0082 N81-20423

NASA five-ball fatigue tester: Over 20 years of
research
[NASA-TN-82589] p0102 N81-23462

Endurance tests with large-bore tapered-roller
bearings to 2.2 million DN
[NASA-TN-82669] p0084 N81-29439

Effects of Ultra-Clean and centrifugal filtration
on rolling-element bearing life
[NASA-TN-82660] p0085 N81-29440

ROLLERS

Kinematic correction for roller skewing
[ASME PAPER 80-DT-76] p0085 N81-18647

ROLLING CONTACT LOADS

Dynamics of solid dispersions in oil during the
lubrication of point contacts. I - Graphite
[ASLE PREPRINT 81-AM-5D-3] p0064 N81-33860
NASA five-ball fatigue tester - Over 20 years of
research p0087 N81-44659

Effect of tangential traction and roughness on
crack initiation/propagation during rolling
contact
[NASA-TN-81608] p0080 N81-11395

Effect of load, area of contact, and contact
stress on the wear mechanisms of a loaded solid
lubricant film
[NASA-TN-81563] p0060 N81-12226

NASA five-ball fatigue tester: Over 20 years of
research
[NASA-TN-82589] p0102 N81-23462

Stress concentration in the vicinity of a hole
defect under conditions of Hertzian contact
[NASA-TN-82649] p0084 N81-28443

SOLAR ARRAY ARRAYS

U SOLAR ARRAYS

ROTARY DRIVES

U MECHANICAL DRIVES

ROTARY STABILITY

Dynamic characteristics of a high-speed rotor with
radial and axial foil-bearing supports
[ASME PAPER 80-C2/LUB-35] p0085 N81-18683

ROTARY WING AIRCRAFT

NT HELICOPTERS

ROTARY WINGS

Application of unsteady airfoil theory to rotary
wings p0006 N81-39874
Pneumatic boot for helicopter rotor deicing
p0009 N81-19059

ROTATING MACHINERY

NT COMPRESSOR SECTIONS
NT ROTARY WINGS
NT ROTORS
NT TURBINE WHEELS

ROTATING GENERATORS

NT AC GENERATORS
NT TURBOGENERATORS

ROTATING SHAFTS

NT SHAFTS (MACHINE ELEMENTS)
Multiple plate hydrostatic viscous damper
[NASA-CASE-LBN-72445-1] p0083 N81-22360

ROTATIONAL FLOW

U FLUID FLOW
U VORTICES

ROTOR AERODYNAMICS

Mean rotor wake characteristics of an aerodynamically loaded 0.5 m diameter fan
[NASA-TN-81657] p0015 N81-16053
Fluid mechanics mechanisms in the stall process of helicopters
[NASA-TN-81956] p0003 N81-21027

ROTOR BLADES (TURBOMACHINERY)

Mean rotor wake characteristics of an aerodynamically loaded 0.5 m diameter fan
[AIAA PAPER 81-0208] p0006 A81-20830
Stability of large horizontal-axis axisymmetric wind turbines
p0092 A81-22526

Effects of mistuning on blade torsional flutter
p0092 A81-29095
Some modifications to, and operational experiences with, the two-dimensional, finite-difference, boundary-layer code, STAN5
[ASME PAPER 81-GT-89] p0077 A81-29996

Evaluation of a method for heat transfer measurements and thermal visualization using a composite of a heater element and liquid crystal
[ASME PAPER 81-GT-93] p0079 A81-30110
Effects of blade-vane ratio and rotor-stator spacing on fan noise with forward velocity
[AIAA PAPER 81-2032] p0024 A81-48622

Comparison of upwind and downwind rotor operations of the DOE/NASA 100-kW Rod-0 wind turbine
[NASA-TN-81744] p0100 N81-22472

Test evaluation of a laminated wood wind turbine blade concept
[NASA-TN-81719] p0104 N81-24535

Rotor wake characteristics relevant to rotor-stator interaction noise generation
[NASA-TN-82703] p0019 N81-30130

ROTOR DISKS

U TURBINE WHEELS

ROTOR HUBS

U ROTORS

ROTORS

NT COMPRESSOR ROTORS

NT ROTARY WINGS

NT TURBINE WHEELS

Dynamic characteristics of a high-speed rotor with radial and axial foil-tearing supports
[ASME PAPER 80-C2/LUB-35] p0085 A81-18683
Performance of a steel spar wind turbine blade on the Rod-0 100 kW experimental wind turbine
[NASA-TN-81588] p0096 N81-11448

NASTRAN level 16 demonstration manual updates for aerodynamic analysis of bladed discs
[NASA-CR-159826] p0093 N81-19483

Measurement of aerodynamic work during fan flutter
[NASA-TN-82652] p0017 N81-25080

GRID3C: Computer program for fast generation of multilevel, three-dimensional boundary-conforming O-type computational grids
[NASA-TF-1920] p0005 N81-31128

ROUGHNESS

NT SURFACE ROUGHNESS

RP-1 ROCKET PROPELLANTS

NT LIQUID FUELS

RUBBER

NT ELASTOMERS

S

SAFETY

NT INDUSTRIAL SAFETY

SAFETY MANAGEMENT

Safety management of complex research operations
p0067 A81-44661

Lightning accommodation systems for wind turbine generator safety
[NASA-TN-82601] p0105 N81-24539

System safety in Stirling engine development
[NASA-TN-82615] p0140 N81-24994

Safety management of complex research operations

[NASA-TN-81772] p0068 N81-25263

SAMPLED DATA

U DATA SAMPLING

SAMPLED DATA SYSTEMS

U DATA SAMPLING

SAMPLING

NT AIR SAMPLING

NT DATA SAMPLING

SATELLITE COMMUNICATION

U SPACECRAFT COMMUNICATION

SATELLITE NETWORKS

Second year technical report on-board processing for future satellite communications systems
[NASA-CR-165155] p0070 N81-10242

SATELLITE SOLAR ENERGY CONVERSION

Analysis of costs of gallium arsenide and silicon solar arrays for space power applications
[NASA-TF-1611] p0038 N81-20173

SATELLITE TELEVISION

Carrier - Interference ratios for frequency sharing between satellite systems transmitting frequency modulated and digital television signals
p0069 A81-21911

SATELLITE TRANSMISSION

Next generation communications satellites: Multiple access and network studies
[NASA-CR-165145] p0033 N81-12139

SATELLITES

NT ATS

NT COMMUNICATION SATELLITES

NT COMMUNICATIONS TECHNOLOGY SATELLITE

NT SCATHA SATELLITE

NT SOLAR POWER SATELLITES

NT SYNCHRONOUS SATELLITES

SCALE (CORROSION)

High temperature cyclic oxidation furnace testing at NASA Lewis Research Center
[NASA-TN-81773] p0054 N81-26234

SCAN PROGRAM

U SUPERSONIC CRUISE AIRCRAFT RESEARCH

SCARS (GEOLOGY)

U EROSION

SCAT

U SUPERSONIC COMMERCIAL AIR TRANSPORT

SCATHA SATELLITE

Analysis of the charging of the SCATHA (P78-2)

satellite

[NASA-TN-165348] p0033 N81-27169

SCATTERING

NT ACOUSTIC SCATTERING

NT ELECTRON SCATTERING

SCP

U SELF CONSISTENT FIELDS

SCHEDULING

NT PREDICTION ANALYSIS TECHNIQUES

SCIENTIFIC SATELLITES

NT ATS

SEA ICE

Comparative analysis of sea ice features using Side-Looking Airborne Radar (SLAR) and LANDSAT imagery --- Beaufort Sea and Bering Sea
[N81-10044] p0095 N81-33539

SEALING

NT SELF SEALING

SEALS (STOPPERS)

NT GLANDS (SEALS)

NT O RING SEALS

Simulation and visualization of face seal motion stability by means of computer generated movies
p0087 A81-38059

Measurement of rod seal lubrication for Stirling engine

[NASA-CR-165158] p0088 N81-13359

Self-acting geometry for noncontact seals

[NASA-TN-81659] p0081 N81-16474

Computer program documentation for the dynamic analysis of a noncontacting mechanical face seal

[NASA-TN-81636] p0081 N81-17435

A sputtered zirconia primer for improved thermal shock resistance of plasma sprayed ceramic turbine seals

[NASA-TN-81732] p0062 N81-21198

SEAS

NT BEAUFORT SEA (NORTH AMERICA)

NT BERING SEA

SECONDARY BATTERIES

U STORAGE BATTERIES

SECONDARY EMISSION

Electron reflection and secondary emission characteristics of sputter-textured pyrolytic graphite surfaces

p0065 A81-38065

Electron reflection and secondary emission characteristics of sputter-textured pyrolytic graphite surfaces
[NASA-TN-81755]

p0062 A81-22193

SECONDARY FLOW

On the magnetohydrodynamic instability

[AIAA PAPER 81-0248]

p0133 A81-20698

Core compressor exit stage study. Volume 2: Data and performance report for the baseline configuration

[NASA-CR-159492]

p0027 A81-16051

Prediction of laminar and turbulent primary and secondary flows in strongly curved ducts
[NASA-CR-1388]

p0007 A81-16976

SEMI-ANALYTICAL PERTURBATION

U LONG TERM EFFECTS

SEEDS

Normal crop calendars. Volume 2: The spring wheat states of Minnesota, Montana, North Dakota, and South Dakota

[NSI-10070]

p0094 A81-13426

SELF-CONSISTENT FIELDS

The self-consistent calculation of pseudo-molecule energy levels, construction of energy level correlation diagrams and an automated computation system for SCP-I(Alpha)-SV calculations

[NASA-TN-81710]

p0130 A81-25779

SELF-INDUCED VIBRATION

ST SUBSONIC FLUTTER

ST SUPERSONIC FLUTTER

ST TRANSONIC FLUTTER

SELF-REGULATING

U AUTOMATIC CONTROL

SELF SEALING

Self-acting geometry for noncontact seals

[NASA-TN-81659]

p0081 A81-16474

Self-stabilizing radial face seal

[NASA-CASE-LEU-12991-1]

p0083 A81-24442

SEMI-CONDUCTOR DEVICES

ST PHOTOVOLTAIC CELLS

ST THYRISTORS

ST TRANSISTORS

High temperature electronic requirements in aeropropulsion systems

[NASA-TN-81682]

p0071 A81-16388

Heat transparent high intensity high efficiency solar cell

[NASA-CASE-LEU-12892-1]

p0105 A81-27598

SEMI-CONDUCTOR JUNCTIONS

ST P-I-N JUNCTIONS

ST P-N JUNCTIONS

ST SILICON JUNCTIONS

High voltage planar multijunction --- solar cells

[NASA-CASE-LEU-13400-1]

p0098 A81-16528

Theoretical results on the double-collecting tandem junction solar cell --- radiation damage

[NASA-CR-17538]

p0099 A81-17538

GaAs homojunction solar cell development

[NASA-CR-17561]

p0099 A81-17561

The HERAC pilot line experience

[NASA-CR-17574]

p0111 A81-17574

SEMI-CONDUCTORS (MATERIALS)

ST P-TYPE SEMI-CONDUCTORS

Space Photovoltaic Research and Technology 1980.

High Efficiency, Radiation Damage and Blanket Technology

[NASA-CP-2169]

p0098 A81-17531

SENDER

U TRANSMITTERS

SENSITIVITY

ST IMPACT RESISTANCE

ST RADIATION TOLERANCE

SEPARATED FLOW

ST BOUNDARY LAYER SEPARATION

Flow separation in inlets at incidence angles

[NASA-CR-29114]

p0006 A81-29114

Some flow phenomena associated with aligned, sequential apertures with Borda-type inlets ---

inlet pressure and flow separation

[NASA-TP-1792]

p0076 A81-24387

SEPARATORS

Control of volume resistivity in inorganic-organic separators --- for alkaline batteries

p0108 A81-11034

Advanced inorganic separators for alkaline

batteries and method of making same --- a

polymeric coating applied to a porous flexible

substrate

[NASA-CASE-LEU-13171-1]

p0100 A81-22466

Inexpensive cross-linked polymeric separators made from water soluble polymers

[NASA-TN-82619]

p0101 A81-23205

Polyvinyl alcohol battery separator containing

inert filler --- alkaline batteries

[NASA-CASE-LEU-13556-1]

p0106 A81-27615

Alkaline battery containing a separator of a cross-linked copolymer of vinyl alcohol and unsaturated carboxylic acid

[NASA-CASE-LEU-13102-1]

p0107 A81-29531

SEPT (ROCKET TESTS)

U SPACE ELECTRIC ROCKET TESTS

SEPT 2 STACRAFT

SEPT II 1980 extended flight thruster experiments

[AIAA PAPER 81-0665]

p0040 A81-29528

SEPT II thrusters - Still ticking after eleven years

[AIAA PAPER 81-1539]

p0042 A81-40934

SEPT II 1980 extended flight thruster experiments

[NASA-TN-81685]

p0038 A81-19222

SERVICES LIFE

Results of the Mission Profile Life Test first

test segment - Thruster J1

[AIAA PAPER 81-0716]

p0043 A81-29552

Prolonging thermal barrier coated specimen life by thermal cycle management

p0065 A81-44658

Electric propulsion - characteristics,

applications, and status

[NASA-TN-81630]

p0033 A81-13079

SERIES

U SYSTEM GENERATED ELECTROMAGNETIC PULSES

SHAFTS (MACHINE ELEMENTS)

Computer program documentation for the dynamic

analysis of a noncontacting mechanical face seal

[NASA-TN-81636]

p0081 A81-17435

Circumferential shaft seal

[NASA-CASE-LEU-12119-2]

p0083 A81-26441

SHALE OIL

Effect of hydroprocessing severity on

characteristics of jet fuel from OSCO 2 and

Paraho distillates

[NASA-TP-1768]

p0066 A81-24283

SHAPES

ST ELLIPTICITY

Effects of erodant particle shape and various heat treatments on erosion resistance of plain carbon steel

[NASA-TP-1755]

p0052 A81-16210

SHEAR FATIGUE

U SHEAR STRESS

SHEAR PROPERTIES

ST SHEAR STRENGTH

SHEAR STRENGTH

Completion of evaluation of manufacturing processes for M/Al composites containing 0.2mm diameter boron fibers

[NASA-TN-81573]

p0051 A81-11111

Correlation of ideal and actual shear strengths of metals with their friction properties

[NASA-TP-1891]

p0063 A81-27282

SHEAR STRESS

ST TORSIONAL STRESS

Continuous analysis of stresses from arbitrary surface loads on a half space

p0093 A81-14162

Simplified solution for stresses and deformation

[NASA-TN-82647]

p0084 A81-28444

SHEARING STRESS

U SHEAR STRESS

SHEATHS

ST PLASMA SHEATHS

SHEET METAL

U METAL SHEETS

SHELLS (STRUCTURAL FORMS)

ST TORSIONAL SHELLS

SHOCK DIFFUSERS

U DIFFUSERS

U SHOCK WAVE ATTENUATION

SHOCK RESISTANCE

ST IMPACT RESISTANCE

Laser surface fusion of plasma sprayed ceramic turbine seals

[NASA-CASE-LEU-13269-1]

p0062 A81-22190

SHOCK WAVE ATTENUATION

Shockless design and analysis of transonic blade shapes
(NASA-TN-82611) p0004 N81-25036

SHOCK WAVES
Calculation of the flow field in supersonic inlets using a bicharacteristics method with shock wave fitting
p0006 N81-21212

Holographic flow visualization of time-varying shock waves
p0079 N81-87642

New interpretations of shock-associated noise with and without screech
(NASA-TN-81540) p0125 N81-10807

SHORT HAUL AIRCRAFT
Low-speed aerodynamic performance of 50.8-centimeter-diameter noise-suppressing inlets for the Quiet, Clean, Short-haul Experimental Engine (QCSSE) --- Lewis 9- by 15-foot low speed wind tunnel tests
(NASA-TP-1178) p0013 N81-11037

SHORT TAKEOFF AIRCRAFT
Optimum subsonic, high-angle-of-attack nacelles
p0005 N81-11646

SHORT WAVE RADIATION
UT SUBMILLIMETER WAVES
SHROUDED BODIES
U SHROUDS
SHROUDED PROPELLERS
Aeroelastic and dynamic finite element analyses of a bladder shrouded disk
(NASA-CN-159728) p0092 N81-19479

SHROUDED TURBINES
An experimental evaluation of the performance deficit of an aircraft engine starter turbine
(SAE PAPER 801137) p0021 N81-34162

Laser surface fusion of plasma sprayed ceramic turbine seals
(NASA-CASE-LEU-13269-1) p0062 N81-22190

SHROUDS
Composite wall concept for high-temperature turbine shrouds - Heat transfer analysis
(SAE PAPER 801138) p0021 N81-34169

Program to develop sprayed, plastically deformable compressor shroud seal materials
(NASA-CN-165237) p0088 N81-17434

SHUTTS
U CIRCUITS
SHUTTLE ORBITERS
U SPACE SHUTTLE ORBITERS
SIGNAL GENERATORS
Integrated control system for a gas turbine engine
(NASA-CASE-LEU-12594-2) p0015 N81-19116

SIGNAL PROCESSING
Second year technical report on-board processing for future satellite communications systems
(NASA-CN-165155) p0070 N81-10242

Application handbook for a Standardized Control Module (SCM) for DC-EC converters, volume 1
(NASA-CN-165172) p0072 N81-10301

User's design handbook for a Standardized Control Module (SCM) for DC to EC Converters, volume 2
(NASA-CN-165173) p0072 N81-11314

SIGNAL TO NOISE RATIOS
Carrier - Interference ratios for frequency sharing between satellite systems transmitting frequency modulated and digital television signals
p0069 N81-21911

SIGNAL TRANSMISSION
NT DATA TRANSMISSION
NT MICROWAVE TRANSMISSION
NT SATELLITE TRANSMISSION
NT TELEVISION TRANSMISSION
SIGNATURES
NT SPECTRAL SIGNATURES
SILICA
U SILICON DIOXIDE
SILICATES
NT ALUMINUM SILICATES
SILICON
Effect of milling and leaching on the structure of sintered silicon
(NASA-TN-81602) p0060 N81-13166

Electrostatic bonding of thin (cycle sine 3 mil) 7070 cover glass to Ta2O5 Au-coated thin (cycle sine 2 mil) silicon wafers and solar cells
(NASA-CN-165240) p0111 N81-16522

Space Photovoltaic Research and Technology 1980.

High Efficiency, Radiation Damage and Emission Technology
(NASA-CN-2169) p0092 N81-17531

The effect of minority carrier mobility variations on the performance of high voltage silicon solar cells
p0098 N81-17536

The HRSAC pilot line experience
p0111 N81-17574

Analysis of costs of gallium arsenide and silicon solar arrays for space power applications
(NASA-TP-1811) p0038 N81-20173

An experimental investigation of silicon wafer surface roughness and its effect on the full strength of plated metals
(NASA-TN-81763) p0100 N81-22478

The effect of minority carrier mobility variations on solar cell spectral response
(NASA-TN-82604) p0103 N81-23625

SILICON CARBIDES
Tribological properties of silicon carbide in metal removal process
p0085 N81-17900

The adhesion, friction, and wear of binary alloys in contact with single-crystal silicon carbide
(ASME PAPER 80-C2/LUB-53) p0086 N81-18695

Fabrication of injection molded sintered alpha SiC turbine components
(ASME PAPER 81-GT-161) p0089 N81-30060

The generation and morphology of single-crystal silicon carbide wear particles under adhesive conditions
p0064 N81-35045

Anisotropic tribological properties of silicon carbide
(NASA-TN-81547) p0080 N81-11394

Changes in surface chemistry of silicon carbide (0001) surface with temperature and their effect on friction
(NASA-TP-1756) p0060 N81-14079

Surface chemistry and friction behavior of the silicon carbide (0001) surface at temperatures to 1500 deg C
(NASA-TP-1813) p0061 N81-19300

A program-management plan with critical-path definition for Combustion Augmentation with Thermionic Energy Conversion (CATEC)
(NASA-TN-82670) p0132 N81-30974

SILICON COMPOUNDS
NT ALUMINUM SILICATES
NT SILICON CARBIDES
NT SILICON DIOXIDE
NT SILICON NITRIDES
Ceramic applications in turbine engines --- for improved component performance and reduced fuel usage
(NASA-CN-159865) p0029 N81-19118

SILICON DIOXIDE
Effect of CeO2, HgO and Y2O3 additions on the sinterability of a milled Si3N4 with 14.5 wt% SiO2
p0064 N81-28974

SILICON FILMS
Electrostatic bonding of thin (approximately 3 mil) 7070 cover glass to Ta2O5 Au-coated thin (approximately 2 mil) silicon wafers and solar cells
p0111 N81-17569

SILICON JUNCTIONS
Silicon solar cells with high open-circuit voltage
p0113 N81-27689

Radiation damage annealing mechanisms and possible low temperature annealing in silicon solar cells
p0040 N81-27207

Analysis of GaAs and Si solar cell arrays for earth orbital and orbit transfer missions
p0109 N81-27254

An experimental investigation of silicon wafer surface roughness and its effect on the full-strength of plated metals
p0109 N81-38063

SILICON NITRIDES
Effect of milling and leaching on the structure of sintered silicon
p0064 N81-22529

Effect of CeO2, HgO and Y2O3 additions on the sinterability of a milled Si3N4 with 14.5 wt% SiO2
p0064 N81-28974

- Fracture toughness of brittle materials determined with chevron notch specimens p0064 A81-32545
- Dissolution of bulk specimens of silicon nitride p0065 A81-42024
- Effect of milling and leaching on the structure of sintered silicon [NASA-TN-81602] p0060 A81-13166
- Effect of Yttria additives on properties of pressureless-sintered silicon nitride [NASA-TP-1899] p0063 A81-31366
- SILICON OXIDES**
- NT SILICON DIOXIDE
- SILICON SOLAR CELLS**
- U SOLAR CELLS
- SILVER OXIDE ZINC BATTERIES**
- U SILVER ZINC BATTERIES
- SILVER ZINC BATTERIES**
- Additive for zinc electrodes [NASA-CASE-LEW-13286-1] p0105 A81-27557
- Qualification testing of secondary sterilizable silver-zinc cells for use in the Jupiter atmospheric entry probe [NASA-TN-82638] p0108 A81-30563
- SIMULATED ALTITUDE**
- U ALTITUDE SIMULATION
- SIMULATION**
- NT ALTITUDE SIMULATION
- NT COMPUTERIZED SIMULATION
- NT DIGITAL SIMULATION
- NT FLIGHT SIMULATION
- NT SYSTEMS SIMULATION
- SIMULATORS**
- NT FLIGHT SIMULATORS
- SINGLE CRYSTALS**
- The generation and morphology of single-crystal silicon carbide wear particles under adhesive conditions p0064 A81-35045
- SINTERING**
- Effect of milling and leaching on the structure of sintered silicon p0064 A81-22529
- Effect of CeO₂, MgO and Y₂O₃ additives on the sinterability of a milled Si₃N₄ with 14.5 wt% SiO₂ p0064 A81-28974
- Effect of milling and leaching on the structure of sintered silicon [NASA-TN-81602] p0060 A81-13166
- Effect of Yttria additives on properties of pressureless-sintered silicon nitride [NASA-TP-1899] p0063 A81-31366
- SIZE DISTRIBUTION**
- NT PARTICLE SIZE DISTRIBUTION
- SKETCHES**
- Kinematic correction for roller skewing [ASME PAPER 80-ETP-76] p0085 A81-18647
- SLIDING FRICTION**
- Kinematic correction for roller skewing [ASME PAPER 80-DPT-76] p0085 A81-18647
- The adhesion, friction, and wear of binary alloys in contact with single-crystal silicon carbide [ASME PAPER 80-C2/LUE-53] p0086 A81-18695
- The transfer of polytetrafluoroethylene studied by X-ray photoelectron spectroscopy p0087 A81-31238
- Dynamics of solid dispersions in oil during the lubrication of point contacts. I - Graphite [ASLE PREPRINT 81-AM-50-3] p0064 A81-33860
- The generation and morphology of single-crystal silicon carbide wear particles under adhesive conditions p0064 A81-35045
- Effect of load, area of contact, and contact stress on the wear mechanisms of a bonded solid lubricant film [NASA-TN-81563] p0060 A81-12226
- Adhesion and friction of transition metals in contact with nonmetallic hard materials [NASA-TN-82605] p0055 A81-28233
- Analysis of starvation effects on hydrodynamic lubrication in nonconforming contacts [NASA-TN-82668] p0084 A81-29438
- Relationship between the ideal tensile strength and the friction properties of metals in contact with nonmetals and themselves [NASA-TP-1883] p0063 A81-33293
- SLURRY PROPELLANTS**
- NT LIQUID FUELS
- SODIUM**
- NT LIQUID SODIUM
- SODIUM COMPOUNDS**
- NT SODIUM SULFATES
- SODIUM SULFATES**
- Combustion system processes leading to corrosive deposits [NASA-TN-81752] p0101 A81-23243
- SODIUM SULFUR BATTERIES**
- Moderate temperature sodium cells. I - Transition metal disulfide cathodes p0113 A81-15027
- SOFTWARE (COMPUTERS)**
- U COMPUTER PROGRAMS
- SOLAR ARRAYS**
- The effect of solar array voltage patterns on plasma power losses p0043 A81-19937
- Analysis of GaAs and Si solar cell arrays for earth orbital and orbit transfer missions p0109 A81-27254
- Commercial (terrestrial) and modified solar array design studies for low cost, low power space applications [NASA-TN-81622] p0061 A81-17266
- NASA preprototype redox storage system for a photovoltaic stand-alone application [NASA-TN-82607] p0104 A81-24534
- Comparative radiation testing of solar cells for the shuttle power extension package [NASA-TN-82656] p0105 A81-27605
- Review of biased solar arrays. Plasma interaction studies [NASA-TN-82693] p0036 A81-32187
- SOLAR CELLS**
- Silicon solar cells with high open-circuit voltage p0113 A81-27089
- High efficiency wraparound contact solar cells /HEWACS/ p0114 A81-27094
- Thin n-i-p silicon solar cell p0114 A81-27097
- Global calibration of terrestrial reference cells and errors involved in using different irradiance monitoring techniques p0068 A81-27148
- Space solar cells - High efficiency and radiation damage p0108 A81-27174
- Radiation damage in lithium-counterdoped n/p silicon solar cells p0109 A81-27204
- Radiation damage annealing mechanisms and possible low temperature annealing in silicon solar cells p0040 A81-27207
- Photovoltaic applications - Past and future p0109 A81-27231
- Analysis of GaAs and Si solar cell arrays for earth orbital and orbit transfer missions p0109 A81-27254
- An experimental investigation of silicon wafer surface roughness and its effect on the pull-strength of plated metals p0109 A81-38063
- Solar cell system having alternating current output [NASA-CASE-LEW-12806-2] p0096 A81-12542
- GaAs shallow-homojunction solar cells [NASA-CR-165167] p0110 A81-15463
- High voltage planar multi-junction --- solar cells [NASA-CASE-LEW-13400-1] p0098 A81-16528
- High voltage V-groove solar cell [NASA-CASE-LEW-13401-1] p0098 A81-16529
- Electrostatic bonding of thin (cycle sine 3 mil) 7070 cover glass to Ta₂O₅ AR-coated thin (cycle sine 2 mil) silicon wafers and solar cells [NASA-CR-165240] p0111 A81-16582
- Space Photovoltaic Research and Technology 1980. High Efficiency, Radiation Damage and Blanket Technology [NASA-CF-2169] p0098 A81-17531
- The effect of minority carrier mobility variations on the performance of high voltage silicon solar cells p0098 A81-17536
- Theoretical results on the double-collecting tandem junction solar cell --- radiation damage p0099 A81-17538
- Annealing of radiation damage in low resistivity silicon solar cells

- Radiation damage in silicon HEP solar cells p0099 N81-17554
- GaAs homojunction solar cell development p0099 N81-17557
- Proton radiation damage in bulk n-GaAs p0099 N81-17561
- Evaluation of solar cell covers and encapsulant materials for space application p0099 N81-17564
- Electrostatic bonding of thin (approximately 3 mil) 7070 cover glass to Ta2O5 AR-coated thin (approximately 2 mil) silicon wafers and solar cells p0111 N81-17568
- Recent developments in lightweight solar cell modules --- with protective glass cover p0111 N81-17569
- The HEWAC pilot line experience p0099 N81-17571
- Coplanar back contacts for thin silicon solar cells [NASA-CN-165272] p0111 N81-17574
- Analysis of costs of gallium arsenide and silicon solar arrays for space power applications p0112 N81-18495
- [NASA-TP-1811] p0038 N81-20173
- The effect of minority carrier mobility variations on solar cell spectral response p0103 N81-23625
- [NASA-TN-82604] p0103 N81-23625
- Performance of high resistivity n-type silicon solar cells under 1 MeV electron irradiation [NASA-TN-82610] p0103 N81-23626
- Reduced annealing temperatures in silicon solar cells [NASA-TN-82597] p0104 N81-23627
- Determination of optimum sunlight concentration level in space for gallium arsenide solar cells [NASA-TN-82643] p0040 N81-26173
- Heat transparent high intensity high efficiency solar cell [NASA-CASE-LEW-12892-1] p0105 N81-27558
- Comparative radiation testing of solar cells for the shuttle power extension package [NASA-TN-82656] p0105 N81-27605
- SOLAR COLLECTORS**
- The DOE photovoltaics program p0143 N81-12989
- Development and testing of heat transport fluids for use in active solar heating and cooling systems [NASA-TN-82395] p0098 N81-16584
- Method of forming oxide coatings [NASA-CASE-LEW-13132-1] p0106 N81-27616
- SOLAR CONVERTERS**
- U SOLAR GENERATORS**
- SOLAR COOLING**
- Development and testing of heat transport fluids for use in active solar heating and cooling systems [NASA-TN-82395] p0098 N81-16584
- SOLAR ELECTRIC PROPULSION**
- Analysis of GaAs and Si solar cell arrays for earth orbital and orbit transfer missions p0109 N81-27254
- Parasitic current losses due to solar electric propulsion generated plasmas p0043 N81-29561
- [AIAA PAPER 81-0740] p0043 N81-29561
- Extended operating range of the 30-cm ion thruster with simplified power processor requirements [AIAA PAPER 81-0692] p0040 N81-32897
- Characteristics of 30-centimeter mercury ion thrusters [AIAA PAPER 81-0715] p0041 N81-37569
- Particle and field measurements on two J-series 30-centimeter thrusters [AIAA PAPER 81-0728] p0042 N81-38072
- Electric propulsion - characteristics, applications, and status [NASA-TN-81630] p0033 N81-13079
- SEP BINOD variable conductance heat pipes acceptance and characterization tests [NASA-TN-82635] p0076 N81-30390
- Review of biased solar array. Plasma interaction studies [NASA-TN-82693] p0036 N81-32167
- SOLAR ENERGY**
- Highlights of NASA/DOE photovoltaics market assessment visit to Calcutta [NASA-TN-84011] p0138 N81-32061
- A Redox system design for solar storage applications [NASA-TN-81720] p0108 N81-32606
- SOLAR ENERGY ABSORBERS**
- Method for depositing an oxide coating --- producing solar panels [NASA-CASE-LEW-13131-1] p0054 N81-24230
- SOLAR ENERGY CONVERSION**
- High efficiency wraparound contact solar cells /HEWAC/ p0114 N81-27094
- Solar photovoltaics: Stand alone applications --- NASA Lewis Research Center research and development p0143 N81-12990
- Coplanar back contacts for thin silicon solar cells [NASA-CN-165272] p0112 N81-18495
- Review of stand-alone photovoltaic application projects sponsored by US DOE and US AID [NASA-TN-81738] p0100 N81-22477
- Highlights of NASA/DOE photovoltaic market assessment visit to Morocco [NASA-TN-82288] p0138 N81-27976
- Design description of the Schuchuli Village photovoltaic power system [NASA-TN-82650] p0094 N81-28517
- SOLAR GENERATORS**
- HT SOLAR CELLS**
- Solar Thermal Power Systems parabolic dish project [NASA-TN-82371] p0107 N81-28524
- SOLAR HEATING**
- Development and testing of heat transport fluids for use in active solar heating and cooling systems [NASA-TN-82395] p0098 N81-16584
- SOLAR POWER GENERATION**
- U SOLAR GENERATORS**
- SOLAR POWER SATELLITES**
- Analytical investigation of efficiency and performance limits in klystron amplifiers using multidimensional computer programs; multi-stage depressed collectors; and thermionic cathode life studies p0098 N81-16552
- SOLAR POWER SOURCES**
- U SOLAR GENERATORS**
- SOLAR PROPULSION**
- HT SOLAR ELECTRIC PROPULSION**
- SOLAR RADIATION**
- HT SUNLIGHT**
- Global calibration of terrestrial reference cells and errors involved in using different irradiance monitoring techniques p0068 N81-27148
- SOLAR TERRESTRIAL INTERACTIONS**
- Global calibration of terrestrial reference cells and errors involved in using different irradiance monitoring techniques p0068 N81-27148
- SOLID LUBRICANTS**
- Effect of substrate surface finish on the lubrication and failure mechanisms of molybdenum disulfide films [NASA-TN-81595] p0060 N81-10170
- Effect of load, area of contact, and contact stress on the wear mechanisms of a bonded solid lubricant film [NASA-TN-81563] p0060 N81-12226
- Dynamics of solid dispersions in oil during the lubrication of point contacts. Part 1: Graphite [NASA-TN-81683] p0061 N81-17264
- Dynamics of solid dispersions in oil during the lubrication of point of contacts. Part 2: Molybdenum disulfide [NASA-TN-81709] p0062 N81-20275
- SOLID ROCKET PROPELLANTS**
- HT LIQUID FUELS**
- SOLID STATE DEVICES**
- HT PHOTOVOLTAIC CELLS**
- HT SEMICONDUCTOR DEVICES**
- HT THYRISTORS**
- HT TRANSISTORS**
- SOLID SURFACES**
- Elastohydrodynamic lubrication of elliptical contacts [NASA-TN-81647] p0080 N81-13358
- Surface films and metallurgy related to lubrication and wear [NASA-TN-82645] p0083 N81-27523

SOLID SUSPENSIONS

Dynamics of solid dispersions in oil during the lubrication of point contacts. I - Graphite
[ASLE PREPRINT 81-AM-5E-3] p0064 A81-33860

SOLID-SOLID INTERFACES

Effect of electronic structure of the diamond surface on the strength of the diamond-metal interface
[NASA-TN-82714] p0063 A81-32269

SOLUBILITY

Dissolution of bulk specimens of silicon nitride
p0065 A81-42024

SONIC FLOW**U TRANSONIC FLOW****SOYBEANS**

Normal crop calendars. Volume 1: Assembly and application of historical crop data to a standard product
[881-10075] p0095 A81-13431

SOUND**U ACOUSTICS****SOUND ABSORPTION****U SOUND TRANSMISSION****SOUND INTENSITY**

Computer program to predict aircraft noise levels
[NASA-TF-1913] p0127 A81-33947

SOUND MEASUREMENT**U ACOUSTIC MEASUREMENT****SOUND PRESSURES**

New interpretations of shock-associated noise with and without screech
[NASA-TN-81590] p0125 A81-10807
Analysis of pressure spectra measurements in a ducted combustion system
[NASA-TN-81583] p0125 A81-15768

SOUND PROPAGATION

Numerical techniques in linear duct acoustics - A status report
[ASME PAPER 80-WA/HC-2] p0127 A81-21120
On the propagation of long waves in acoustically treated, curved ducts
p0128 A81-38060

A theoretical approach to sound propagation and radiation for ducts with suppressors
p0128 A81-38061

Application of 'steady' state finite element and transient finite difference theory to sound propagation in a variable duct - A comparison with experiment
[AIAA PAPER 81-2016] p0128 A81-48622
High-frequency sound propagation in a spatially varying mean flow
p0129 A81-49913

On the propagation of long waves in acoustically treated, curved ducts
[NASA-TN-81712] p0125 A81-19875

High-frequency sound propagation in a spatially varying mean flow
[NASA-TN-81751] p0126 A81-20831

A theoretical approach to sound propagation and radiation for ducts with suppressors
[NASA-TN-82612] p0130 A81-22837

SOUND TRANSMISSION

An experimental study of transmission, reflection and scattering of sound in a free jet flight simulation facility and comparisons with theory
p0129 A81-28943

A model for the acoustic impedance of linear suppressor materials bonded on perforated plate
[AIAA PAPER 81-1999] p0129 A81-49741

Acoustic transmission matrix of a variable area duct or nozzle carrying a compressible subsonic flow
[NASA-TN-81614] p0125 A81-12821

SOUND WAVES**UT AERODYNAMIC NOISE****UT AIRCRAFT NOISE****UT ENGINE NOISE****UT JET AIRCRAFT NOISE**

The coupling between flow instabilities and incident disturbances at a leading edge
p0010 A81-28682

Improved methods for fan sound field determination
[NASA-CR-165188] p0129 A81-15769

Preliminary investigation of acoustic oscillations in an H2-O2 fired Ball generator
[NASA-TN-81756] p0103 A81-22610

SOUTH DAKOTA

Normal crop calendars. Volume 2: The spring

wheat states of Minnesota, Montana, North

Dakota, and South Dakota

[881-10070] p0094 A81-13426

Preliminary evaluation of the Environmental Research Institute of Michigan crop calendar shift algorithms for estimation of spring wheat development stage --- North Dakota, South Dakota, Montana, and Minnesota
[881-10071] p0094 A81-13427

SOYBEANS

Normal crop calendars. Volume 2: The spring wheat states of Minnesota, Montana, North Dakota, and South Dakota
[881-10070] p0094 A81-13426

Normal crop calendars. Volume 1: Assembly and application of historical crop data to a standard product
[881-10075] p0095 A81-13431

Evaluation of results of US corn and soybeans exploratory experiment: Classification procedures verification test --- Missouri, Iowa, Indiana, and Illinois
[881-10076] p0095 A81-13432

SPACE CHARGE

Diagnostic system design for the Ion Auxiliary Propulsion System (IAPS). Flight tests of two 8 cm mercury ion
[NASA-TN-81702] p0037 A81-20172

SPACE COMMUNICATION**UT SPACECRAFT COMMUNICATION****SPACE ELECTRIC SOCKET TESTS**

SERT II 1980 extended flight thruster experiments
[AIAA PAPER 81-0665] p0040 A81-29528

SERT II 1980 extended flight thruster experiments
[NASA-TN-81685] p0038 A81-19222

SPACE ENVIRONMENT**U AEROSPACE ENVIRONMENTS****SPACE LABORATORIES**

Overview study of combustion experiments in a space laboratory
p0032 A81-46059

SPACE PLATFORMS

Study of thermal management for space platform applications
[NASA-CR-165238] p0033 A81-21106

SPACE POWER REACTORS

Goals of thermionic program for space power
[NASA-TN-82616] p0132 A81-25808

SPACE PROCESSING

Requirements and preliminary concept of a Zero-Gravity Combustion Facility for Spacelab
[AIAA PAPER 81-0165] p0032 A81-20642
Materials processing in space: Future technology trends
p0143 A81-12991

SPACE SHUTTLE ORBITERS

Shuttle compatible cryogenic liquid storage and supply systems
[AIAA PAPER 81-1509] p0037 A81-42207

SPACE SHUTTLE PAYLOADS**UT SPACEBORNE EXPERIMENTS**

Materials processing in space: Future technology trends
p0143 A81-12991

Conceptual design of an in-space cryogenic fluid management facility, executive summary
[NASA-CR-165279-TRC-SUM] p0137 A81-21212

Conceptual design of an in-space cryogenic fluid management facility
[NASA-CR-165279] p0067 A81-21213

SPACE SHUTTLES

Comparative radiation testing of solar cells for the shuttle power extension package
[NASA-TN-82656] p0105 A81-27605

SPACE SYSTEMS ENGINEERING**U AEROSPACE ENGINEERING****SPACE TRANSPORTATION****UT SPACE SHUTTLE ORBITERS****UT SPACE TRANSPORTATION SYSTEM****SPACE TRANSPORTATION SYSTEM****UT SPACE SHUTTLE ORBITERS****UT SPACE SHUTTLES**

Combustion experimentation aboard the space transportation system
p0032 A81-46068

SPACEBORNE EXPERIMENTS

Overview study of combustion experiments in a space laboratory
p0032 A81-46059

Combustion experimentation aboard the space transportation system p0032 A81-46068

Materials processing in space: Future technology trends p0143 A81-12991

SPACECRAFT CHARGING

Modelling of environmentally induced discharges in geosynchronous satellites p0034 A81-19936

The effect of solar array voltage patterns on plasma power losses p0043 A81-19937

Environmental charging effects monitors for operational satellites p0037 A81-38057

Environmental charging effects monitors for operational satellites [NASA-TN-81669] p0037 A81-17127

Analysis of the charging of the SCATHA (P78-2) satellite [NASA-CR-165348] p0033 A81-27169

Development and design of three monitoring instruments for spacecraft charging [NASA-TP-1800] p0040 A81-31282

SPACECRAFT COMMUNICATION

An economic systems analysis of land mobile radio telephone services p0069 A81-22528

Satellites using the 30/20 GHz band [NASA-TN-81600] p0069 A81-10241

SPACECRAFT CONSTRUCTION MATERIALS

Feasibility of Kevlar 49/IMR-15 polyimide for high temperature applications p0047 A81-43602

SPACECRAFT DESIGN

Conceptual design of an in-space cryogenic fluid management facility, executive summary [NASA-CR-165279-EXEC-SUMM] p0137 A81-21212

Conceptual design of an in-space cryogenic fluid management facility [NASA-CR-165279] p0067 A81-21213

SPACECRAFT POWER SUPPLIES

Space solar cells - High efficiency and radiation damage p0108 A81-27174

Extended operating range of the 30-cm ion thruster with simplified power processor requirements [AIAA PAPER 81-0692] p0040 A81-32897

Goals of thermionic program for space power p0133 A81-44656

Commercial (terrestrial) and modified solar array design studies for low cost, low power space applications [NASA-TN-81622] p0061 A81-17266

SPACECRAFT PROPULSION

NT ELECTROSTATIC PROPULSION

NT ION PROPULSION

NT PLASMA PROPULSION

NT SOLAR ELECTRIC PROPULSION

High performance cryogenic engines for orbit transfer vehicles [IAP PAPER 80-P-253] p0043 A81-18363

Parasitic current losses due to solar electric propulsion generated plasmas [AIAA PAPER 81-0740] p0043 A81-29561

Performance capabilities of the 8-cm Mercury ion thruster [AIAA PAPER 81-0754] p0044 A81-29567

Free radical propulsion concept [AIAA PAPER 81-0676] p0041 A81-32905

Ion beam applications research - A 1981 summary of Lewis Research Center programs [AIAA PAPER 81-0669] p0041 A81-38068

Particle and field measurements on two J-series 30-centimeter thrusters [AIAA PAPER 81-0728] p0042 A81-38072

Propellant management for low thrust chemical propulsion systems [AIAA PAPER 81-1453] p0042 A81-42198

Performance of a magnetic multipole line-cusp argon ion thruster [NASA-TN-81703] p0038 A81-19219

SENT II 1980 extended flight thruster experiments [NASA-TN-81685] p0038 A81-19222

The electric rail gun for space propulsion [NASA-CR-165312] p0042 A81-22078

SENT 2 thrusters: Still ticking after eleven years [NASA-TN-81774] p0040 A81-26174

SPACECRAFT TELEVISION

NT SATELLITE TELEVISION

SPACELAS PAYLOADS

Requirements and preliminary concept of a Zero-Gravity Combustion Facility for Spacelab [AIAA PAPER 81-0165] p0032 A81-20642

Combustion experimentation aboard the space transportation system p0032 A81-46068

Materials processing in space: Future technology trends p0143 A81-12991

Conceptual design of an in-space cryogenic fluid management facility, executive summary [NASA-CR-165279-EXEC-SUMM] p0137 A81-21212

Conceptual design of an in-space cryogenic fluid management facility [NASA-CR-165279] p0067 A81-21213

SPALLING

High temperature cyclic oxidation furnace testing at NASA Lewis Research Center [NASA-TN-81773] p0054 A81-26234

Effect of Yttria additives on properties of pressureless-sintered silicon nitride [NASA-TP-1899] p0063 A81-31366

SPARKS BLOWING

NT BLOWING

SPARK IGNITION

Advanced Technology Spark-Ignition Aircraft Piston Engine Design Study [NASA-CR-165162] p0026 A81-13963

SPECIFICATIONS

NT EQUIPMENT SPECIFICATIONS

SPECTRA

NT NOISE SPECTRA

SPECTRAL ANALYSIS

NT SPECTRUM ANALYSIS

SPECTRAL EMISSION

Spectral flame radiance from a tubular-cann combustor [NASA-TP-1722] p0016 A81-19121

SPECTRAL SIGNATURES

Preliminary evaluation of the Environmental Research Institute of Michigan crop calendar shift algorithm for estimation of spring wheat development stage --- North Dakota, South Dakota, Montana, and Minnesota [E81-10071] p0094 A81-13427

SPECTROCHEMISTRY

Accuracy of trace element determinations in alternate fuels [NASA-TN-81609] p0049 A81-13106

SPECTROCHEMISTRY

U SPECTROCHEMISTRY

SPECTROPHOTOMETRY

NT INFRARED SPECTROPHOTOMETRY

SPECTROSCOPES

U SPECTROMETERS

SPECTROSCOPIC ANALYSIS

Practical applications of surface analytic tools in tribology p0086 A81-18739

Accuracy of trace element determinations in alternate fuels p0056 A81-22530

SPECTROSCOPY

NT ABSORPTION SPECTROSCOPY

NT AUGER SPECTROSCOPY

NT ELECTRON SPECTROSCOPY

NT PHOTOACOUSTIC SPECTROSCOPY

NT PHOTOELECTRON SPECTROSCOPY

NT SPECTROSCOPIC ANALYSIS

NT X RAY SPECTROSCOPY

SPECTRUM ANALYSIS

Accuracy of trace element determinations in alternate fuels [NASA-TN-81609] p0049 A81-13106

SPEED INDICATORS

NT DRAG FORCE ANEMOMETERS

NT LASER ANEMOMETERS

SPRAYED COATINGS

Comparative evaluation of insulating properties of plasma-sprayed ceramic coatings p0064 A81-15984

Program to develop sprayed, plastically deformable compressor shroud seal materials [NASA-CR-165237] p0028 A81-17434

Microstructure and mechanical properties of bulk and plasma-sprayed Y2O3-partially stabilized zirconia

[NASA-CR-165126] p0059 N81-22158
Thermal barrier coating system having improved adhesion
[NASA-CASR-LEW-13359-1] p0062 N81-24265
Burner rig evaluation of thermal barrier coating --- gas turbines
[NASA-TN-81684] p0055 N81-28231

SPRAYED PROTECTIVE COATINGS
U PROTECTIVE COATINGS
U SPRAYED COATINGS
SPRAYING
NT PLASMA SPRAYING
SPUTTERING
Friction and wear results from sputter-deposited chrome oxide with and without nichrome metallic binders and interlayers
[ASME PAPER 80-C2/LUE-45] p0089 N81-18693
Electron reflection and secondary emission characteristics of sputter-textured pyrolytic graphite surfaces p0065 N81-38065
Sputtered protective coatings for die casting dies p0057 N81-38067
Sputtering and ion plating for aerospace applications p0087 N81-44655
Thin-film coatings p0142 N81-12983
Ion beam deposited protective films
[NASA-TN-81722] p0038 N81-19221
Simultaneous ion sputter polishing and deposition
[NASA-TN-81679] p0053 N81-19278
Method of cold welding using ion beam technology
[NASA-CASR-LEW-12982-1] p0081 N81-19455
Sputtering and ion plating for aerospace applications
[NASA-TN-81726] p0082 N81-20424
Ion beam applications research. A summary of Lewis Research Center Programs
[NASA-TN-81721] p0044 N81-21129
Sputtered protective coatings for die casting dies
[NASA-TN-81735] p0053 N81-21173
Ion beam sputter etching of orthopedic implanted alloy MP35N and resulting effects on fatigue
[NASA-TN-81747] p0045 N81-21174
Electron reflection and secondary emission characteristics of sputter-textured pyrolytic graphite surfaces
[NASA-TN-81755] p0062 N81-22193
Ion plating for the future
[NASA-TN-82630] p0054 N81-25189
Ion sputter textured graphite --- applications to electron tube devices
[NASA-CASR-LEW-12919-1] p0046 N81-27198

SQUEEZING
U COMPRESSING
STABILITY
NT AERODYNAMIC STABILITY
NT COMBUSTION STABILITY
NT CONTROL STABILITY
NT DYNAMIC STABILITY
NT FLOW STABILITY
NT MAGNETOHYDRODYNAMIC STABILITY
NT MOTION STABILITY
NT ROTARY STABILITY
NT STRUCTURAL STABILITY
NT THERMAL STABILITY
STABILITY TESTS
Experimental study of the stability of aircraft fuels at elevated temperatures
[NASA-CR-165165] p0067 N81-12255

STABILIZATION
Stabilizing platinum in phosphoric acid fuel cells
[NASA-CR-165311] p0113 N81-22473
Self-stabilizing radial face seal
[NASA-CASR-LEW-12991-1] p0083 N81-24442

STACKS
Cell module and fuel conditioner
[NASA-CR-165189] p0112 N81-18494
Cell module and fuel conditioner development
[NASA-CR-165190] p0112 N81-19573
Design and assembly considerations for Redox cells and stacks
[NASA-TN-82672] p0049 N81-31308

STAGNATION POINT
Influence of thermal boundary conditions on heat transfer from a cylinder in cross flow
[NASA-TN-1894] p0076 N81-29384

STAGNATION REGION
U STAGNATION POINT
STANDARDIZATION
User's design handbook for a Standardized Control Module (SCM) for DC to DC Converters, volume 2
[NASA-CR-165173] p0072 N81-11314

STANDARDS
Modification of the ECAS reference steam power generating plant to comply with the EPA 1979 new source performance standards
[NASA-CR-159853] p0110 N81-13467

STARTERS
NT ENGINE STARTERS
STATIC DISCHARGES
Magneto-electrostatic thruster physical geometry tests
[AIAA PAPER 81-0753] p0044 N81-29566

STATIC FRICTION
Effect of electronic structure of the diamond surface on the strength of the diamond-metal interface
[NASA-TN-82714] p0063 N81-32269

STATIC PRESSURE
Performance prediction of straight two dimensional diffusers
[NASA-CR-165186] p0133 N81-11833

STATIC STABILITY
NT STRUCTURAL STABILITY
STATIONKEEPING
Performance capabilities of the 8-cm mercury ion thruster
[NASA-TN-81720] p0038 N81-19220

STATISTICAL ANALYSIS
NT REGRESSION ANALYSIS
Numerical trials of HISSE
[N81-10069] p0094 N81-13425

STATOR BLADES
Off-design performance loss model for radial turbines with pivoting, variable-area stators
[NASA-TN-1708] p0013 N81-11038
Effects of blade-vane ratio and rotor-stator spacing of fan noise with forward velocity
[NASA-TN-82690] p0126 N81-31956

STATORS
Loss model for off-design performance analysis of radial turbines with pivoting-vane, variable-area stators
[SAE PAPER 801135] p0021 N81-34166
Turbine modeling technique to generate off-design performance data for both single and multistage axial-flow turbines
[NASA-CR-165244] p0027 N81-17078
Cold-air performance of compressor-drive turbine of Department of Energy upgraded automobile gas turbine engine. 1: Volute-manifold and stator performance
[NASA-TN-82682] p0004 N81-28053

STEAM GENERATORS
U BOILERS
STEAM TURBINES
Off-design analysis of a gas turbine powerplant augmented by steam injection using various fuels
[NASA-TN-81611] p0098 N81-16571

STEELS
NT CARBON STEELS
Adherence of ion beam sputter deposited metal films on H-13 steel p0056 N81-14998
Contact angle measurements of a polyphenyl ether to 190 C on H-50 steel
[NASA-TN-82628] p0063 N81-27277

STEPP GRADIENT AIRCRAFT
U V/STOL AIRCRAFT
STIMULATED EMISSION DEVICES
NT HIGH POWER LASERS
STIRLING CYCLE
Automotive Stirling engine development program
[NASA-CR-165134] p0139 N81-11952
Measurement of rod seal lubrication for Stirling engine
[NASA-CR-165158] p0088 N81-13359
Applicability of advanced automotive heat engines to solar thermal power
[NASA-TN-81658] p0097 N81-14397
Evaluation of candidate Stirling engine heater tube alloys for 1000 hours at 760 C
[NASA-TN-81578] p0051 N81-15068
A four-cylinder Stirling engine controls model
[NASA-TN-81648] p0075 N81-15241

- Advanced propulsion system concept for hybrid vehicles
[NASA-CR-159772] p0140 N81-18935
- A computer simulation of the transient response of a 4 cylinder Stirling engine with burner and air preheater in a vehicle
[NASA-CR-165262] p0078 N81-22313
- Thermal energy storage for the Stirling engine powered automobile
[NASA-CR-159561] p0113 N81-22467
- System safety in Stirling engine development
[NASA-TN-82615] p0140 N81-24994
- Overview: DOE/NASA automotive gas turbine and Stirling projects
[NASA-TN-82637] p0105 N81-25467
- Hostile environmental conditions facing candidate alloys for the automotive Stirling engine
[NASA-TN-82632] p0054 N81-26236
- Compatibility of alternative fuels with advanced automotive gas turbine and Stirling engines. A literature survey
[NASA-TN-81754] p0105 N81-27604
- High-power baseline and motoring test results for the GPU-3 Stirling engine
[NASA-TN-82646] p0139 N81-32087
- STOICHIOMETRY**
Experimental evaluation of catalytic combustion with heat removal at near stoichiometric conditions
[NASA-TN-81748] p0103 N81-23609
- STOL AIRCRAFT**
U SHORT TAKEOFF AIRCRAFT
- STORABLE PROPELLANTS**
NT AIRCRAFT FUELS
- STORAGE BATTERIES**
NT LEAD ACID BATTERIES
NT NICKEL CADMIUM BATTERIES
NT NICKEL ZINC BATTERIES
NT SILVER ZINC BATTERIES
Moderate temperature sodium cells. I - Transition metal disulfide cathodes
p0113 N81-15027
- Toroidal cell and battery --- storage battery for high amp-hour load applications
[NASA-CASE-LEU-12918-1] p0104 N81-24521
- STORMS**
NT MAGNETIC STORMS
- STRAIN AGING**
U PRECIPITATION HARDENING
- STRAIN DISTRIBUTION**
U STRESS CONCENTRATION
- STRAIN FATIGUE**
U FATIGUE (MATERIALS)
- STRAIN GAGES**
Miniature drag-force anemometer
[NASA-TN-81680] p0079 N81-16428
- STRAIN SOFTENING**
U PLASTIC DEFORMATION
- STRATA**
NT SUBSTRATES
- STRATIFICATION**
Laboratory evaluation of a pilot cell battery protection system for photovoltaic applications
[NASA-TN-81714] p0104 N81-24536
- STREAMLINE FLOW**
U LAMINAR FLOW
- STREAMS**
NT GAS STREAMS
- STRENGTH OF MATERIALS**
U MECHANICAL PROPERTIES
- STRESS ANALYSIS**
Continuous analysis of stresses from arbitrary surface loads on a half space
p0093 N81-14162
- On the equivalence between semiempirical fracture analyses and R-curves
p0092 N81-18792
- Axial force and efficiency tests of fixed center variable speed belt drive
[NASA-TN-81652] p0080 N81-15367
- REGA16 - Computer program for analysis and extrapolation of stress-rupture data
[NASA-TP-1809] p0102 N81-23486
- Nonlinear laminate analysis for metal matrix fiber composites
[NASA-TN-82596] p0046 N81-25149
- Optimal tooth numbers for compact standard spur gear sets
[NASA-TN-82614] p0083 N81-27524
- STRESS CALCULATIONS**
U STRESS ANALYSIS
- STRESS CONCENTRATION**
Continuous analysis of stresses from arbitrary surface loads on a half space
p0093 N81-14162
- Stress concentration in the vicinity of a hole defect under conditions of Hertzian contact
[NASA-TN-82649] p0084 N81-28443
- STRESS DISTRIBUTION**
U STRESS CONCENTRATION
- STRESS INTENSITY FACTORS**
Experimental compliance calibration of the compact fracture toughness specimen
[NASA-TN-81665] p0091 N81-14492
- STRESS RELAXATION**
Method for alleviating thermal stress damage in laminates --- metal matrix composites
[NASA-CASE-LEU-12493-1] p0045 N81-17170
- STRESS RUPTURE STRENGTH**
U CREEP RUPTURE STRENGTH
- STRESS WAVES**
Acousto-ultrasonic characterization of fiber reinforced composites
p0090 N81-44460
- Acousto-ultrasonic characterization of fiber reinforced composites
[NASA-TN-82651] p0090 N81-28458
- STRESS-STRAIN DISTRIBUTION**
U STRESS CONCENTRATION
- STRESS-STRAIN RELATIONSHIPS**
Nonlinear laminate analysis for metal matrix fiber composites
[AIAA 81-0579] p0046 N81-29411
- Nonlinear laminate analysis for metal matrix fiber composites
[NASA-TN-82596] p0046 N81-25149
- STRESSES**
NT AXIAL STRESS
NT SHEAR STRESS
NT TENSILE STRESS
NT THERMAL STRESSES
NT TORSIONAL STRESS
Effect of load, area of contact, and contact stress on the wear mechanisms of a bonded solid lubricant film
[NASA-TN-81563] p0060 N81-12426
- STRUCTURAL ANALYSIS**
NT DYNAMIC STRUCTURAL ANALYSIS
NT FLUTTER ANALYSIS
Aeroelastic and dynamic finite element analyses of a bladder shrouded disk
[NASA-CR-159728] p0092 N81-19479
- MASTRAN level 16 programmer's manual updates for aeroelastic analysis of bladed discs
[NASA-CR-159825] p0093 N81-19482
- STRUCTURAL DESIGN CRITERIA**
User's design handbook for a Standardized Control Module (SCM) for DC to DC Converters, volume 2
[NASA-CR-165173] p0072 N81-11314
- Engineering support for magnetohydrodynamic power plant analysis and design studies
[NASA-CR-159690] p0110 N81-13466
- STRUCTURAL DYNAMICS**
U DYNAMIC STRUCTURAL ANALYSIS
- STRUCTURAL FATIGUE**
U FATIGUE (MATERIALS)
- STRUCTURAL MATERIALS**
U CONSTRUCTION MATERIALS
- STRUCTURAL MEMBERS**
NT ANNULAR PLATES
NT CANTILEVER BEAMS
NT MEMBRANE STRUCTURES
NT PERFORATED PLATES
- STRUCTURAL RIGIDITY**
U STRUCTURAL STABILITY
- STRUCTURAL STABILITY**
Stability of large horizontal-axis axisymmetric wind turbines
p0092 N81-22526
- STRUCTURAL VIBRATION**
NT BENDING VIBRATION
NT FLUTTER
NT SUBSONIC FLUTTER
NT SUPERSONIC FLUTTER
NT TRANSONIC FLUTTER
Effects of mistuning on blade torsional flutter
p0092 N81-29095

STRUCTURAL WEIGHT

Recent developments in lightweight solar cell
modules --- with protective glass cover
p0099 N81-17571

STS

U SPACE TRANSPORTATION SYSTEM

SUBCIRCUITS

U CIRCUITS

SUBGRAVITY

U REDUCED GRAVITY

SUBLATERS

U SUBSTRATES

SUBMILLIMETER WAVES

Ladder supported ring bar circuit
(NASA-CASE-LRU-13570-1) p0071 N81-24348

SUBSONIC FLOW

Finite element analysis of inviscid subsonic
boattail flow
(AIAA PAPER 81-0276) p0006 N81-20831

Calculation of three-dimensional turbulent
subsonic flows in transition ducts
p0008 N81-21199

Acoustic transmission matrix of a variable area
duct or nozzle carrying a compressible subsonic
flow
p0128 N81-22533

Some aspects of calculating flows about
three-dimensional subsonic inlets
(AIAA PAPER 81-1361) p0007 N81-42177

Finite element analysis of inviscid subsonic
boattail flow
(NASA-TN-81650) p0003 N81-14977

A three-dimensional turbulent compressible
subsonic duct flow analysis for use with
constructed coordinate systems
(NASA-CN-3389) p0077 N81-20383

Some aspects of calculating flows about
three-dimensional subsonic inlets
(NASA-TN-82678) p0004 N81-28054

SUBSONIC FLOW

Aeroelastic characteristics of a cascade of
mistuned blades in subsonic and supersonic flows
--- turbofan engines
(NASA-TN-82631) p0091 N81-26492

SUBSTRATES

Effect of substrate surface finish on the
lubrication and failure mechanisms of molybdenum
disulfide films
(NASA-TN-81595) p0060 N81-10170

SUCTION

Boundary layer development on turbine airfoil
suction surfaces
(ASME PAPER 81-GT-204) p0008 N81-30094

SUGAR BEETS

Normal crop calendars. Volume 2: The spring
wheat states of Minnesota, Montana, North
Dakota, and South Dakota
(881-10070) p0094 N81-13426

SULFATES

WT SODIUM SULFATES

SULFIDES

WT DISULFIDES

WT MOLYBDENUM DISULFIDES

SULFUR COMPOUNDS

WT DISULFIDES

WT MOLYBDENUM DISULFIDES

WT SODIUM SULFATES

SUNFLOWERS

Normal crop calendars. Volume 2: The spring
wheat states of Minnesota, Montana, North
Dakota, and South Dakota
(881-10070) p0094 N81-13426

SUNLIGHT

Determination of optimum sunlight concentration
level in space for gallium arsenide solar cells
(NASA-TN-82643) p0040 N81-26173

SUPERALLOYS

U HEAT RESISTANT ALLOYS

SUPERCHARGERS

Effect of a part-span variable inlet guide vane on
the performance of a high-bypass turbofan engine
(AIAA PAPER 81-1362) p0022 N81-40842
Effect of a part-span variable inlet guide vane on
the performance of a high-bypass turbofan engine
(NASA-TN-82617) p0017 N81-25081

SUPERCHARGING

U SUPERCHARGERS

SUPERHYBRID MATERIALS

WT GRAPHITE-EPoxy COMPOSITES

Superhybrid composite blade impact studies

(ASME PAPER 81-GT-24) p0020 N81-29940

SUPERSONIC AIRCRAFT

ST SUPERSONIC COMMERCIAL AIR TRANSPORT

Development of a low NO_x/lean premixed annular
combustor
(ASME PAPER 81-GT-40) p0020 N81-29954

The supersonic fan engine - An advanced concept in
supersonic cruise propulsion
(AIAA PAPER 81-1599) p0023 N81-40973

Progress with variable cycle engines
p0001 N81-17997

Turbine bypass engine: A new supersonic cruise
propulsion concept
(NASA-TN-82608) p0018 N81-26145

The supersonic fan engine: An advanced concept in
supersonic cruise propulsion
(NASA-TN-82657) p0018 N81-27094

SUPERSONIC AIRFOILS

Rotor redesign for a highly loaded 1800 ft/sec tip
speed fan, 2
(NASA-CN-159879) p0024 N81-12087

SUPERSONIC COMMERCIAL AIR TRANSPORT

Turbine bypass engine - A new supersonic cruise
propulsion concept
(AIAA PAPER 81-1596) p0023 N81-40971

Design of a multivariable integrated control for a
supersonic propulsion system --- variable stream
control engine
p0025 N81-12094

SUPERSONIC CRUISE AIRCRAFT RESEARCH

Model aerodynamic test results for two variable
cycle engine coaxial exhaust systems at
simulated takeoff and cruise conditions ---
Lewis 8 by 6-foot supersonic wind tunnel tests
(NASA-CN-159818) p0026 N81-13057

Variable stream control engine for advanced
supersonic aircraft design update
p0001 N81-17996

VCR early acoustic test results of General
Electric's high-radius ratio coaxial plug nozzle
p0029 N81-17999

Status of noise technology for advanced supersonic
cruise aircraft
p0001 N81-18002

Advanced technology for controlling pollutant
emissions from supersonic cruise aircraft
p0001 N81-18004

SUPERSONIC FLOW INLETS

U SUPERSONIC INLETS

SUPERSONIC FLOW

Supersonic stall flutter of high-speed fans
(ASME PAPER 81-GT-184) p0020 N81-30078

Experimental determination of unsteady blade
element aerodynamics in cascades. Volume 2:
Translation mode cascade
(NASA-CN-155166) p0007 N81-14976

SUPERSONIC ISLANDS

Calculation of the flow field in supersonic inlets
using a bicharacteristics method with shock wave
fitting
p0006 N81-21212

Supersonic stall flutter of high speed fans --- in
turbofan engines
(NASA-TN-81613) p0003 N81-14978

SUPERSONIC NOZZLES

The effect of inflow velocity profiles on the
performance of supersonic ejector nozzles
(NASA-TN-81673) p0075 N81-16421

Status of noise technology for advanced supersonic
cruise aircraft
p0001 N81-18002

SUPERSONIC SPEEDS

An evaluation of a simplified near field noise
model for supersonic helical tip speed propellers
(NASA-TN-81727) p0130 N81-22836

SUPERSONIC TRANSPORTS

U SUPERSONIC COMMERCIAL AIR TRANSPORT

SUPPORT SYSTEMS

U LIFE SUPPORT SYSTEMS

SUPERSTARS

A theoretical approach to sound propagation and
radiation for ducts with suppressors
p0128 N81-38061

SURFACE COOLING

Heat transfer from a row of impinging jets to
concave cylindrical surfaces
p0078 N81-24924

SURFACE CRACKS

SURFACE CRACKS

Continuous analysis of stresses from arbitrary surface loads on a half space

p0093 A81-14162

Fretting wear and fretting fatigue: How are they related?

[NASA-TN-82633]

p0054 A81-26235

SURFACE DEFECTS

Surface flaw detection in structural ceramics by scanning photoacoustic spectroscopy

p0079 A81-17906

SURFACE ENERGY

Contact angle measurements of a polyphenyl ether to 190 C on S-50 steel

[NASA-TN-82628]

p0063 A81-27277

Relationship between the ideal tensile strength and the friction properties of metals in contact with nonmetals and themselves

[NASA-TP-1883]

p0063 A81-33293

SURFACE FINISHING

The effect of mechanical surface and heat treatments on the erosion resistance of 6061 aluminum alloy

p0057 A81-27944

Ion beam texturing of heat transfer surfaces [AIAA PAPER 81-0670]

p0096 A81-29531

Effect of substrate surface finish on the lubrication and failure mechanisms of molybdenum disulfide films

[ASLE PREPRINT 81-AM-5C-1]

p0064 A81-33859

Sputtering and ion plating for aerospace applications

p0087 A81-44655

Method of cold welding using ion beam technology [NASA-CASE-LEW-12982-1]

p0081 A81-19455

Passivation of carbon steel through mercury implantation

[NASA-CR-165292]

p0059 A81-20244

Laser surface fusion of plasma sprayed ceramic turbine seals

[NASA-CASE-LEW-13269-1]

p0062 A81-22190

Evaluation of a pneumatic boot deicing system on a general aviation wing model

[NASA-TN-82363]

p0011 A81-25065

SURFACE INTERACTIONS

U SURFACE REACTIONS

SURFACE IONIZATION

Electron spectroscopy of the diamond surface

p0130 A81-27031

SURFACE LAYERS

Surface films and metallurgy related to lubrication and wear

[NASA-TN-82645]

p0083 A81-27523

SURFACE PROPERTIES

NT ADHESION

NT COEFFICIENT OF FRICTION

NT INTERFACIAL TENSION

NT SURFACE CRACKS

NT SURFACE DEFECTS

NT SURFACE ENERGY

NT SURFACE ROUGHNESS

NT SURFACE TEMPERATURE

NT WALL TEMPERATURE

Practical applications of surface analytic tools in tribology

p0086 A81-18739

Electron reflection and secondary emission characteristics of sputter-textured pyrolytic graphite surfaces

p0065 A81-38065

An investigation of hot corrosion mechanisms in nickel base alloys

p0058 A81-16208

Mechanical bonding of metal [NASA-CASE-LEW-12941-1]

p0068 A81-16329

Surface chemistry and friction behavior of the silicon carbide (0001) surface at temperatures to 1500 deg C

[NASA-TP-1813]

p0061 A81-19300

Surface films and metallurgy related to lubrication and wear

[NASA-TN-82645]

p0083 A81-27523

SURFACE REACTIONS

Effect of mechanical surface and heat treatments on erosion resistance

[NASA-TN-81540]

p0051 A81-11178

Changes in surface chemistry of silicon carbide (0001) surface with temperature and their effect on friction

[NASA-TP-1756]

p0060 A81-14079

Non-noble catalysts and catalyst supports for phosphoric acid fuel cells

[NASA-CR-165221]

p0112 A81-18497

SURFACE ROUGHNESS

Effect of tangential traction and roughness on crack initiation/propagation during rolling contact

[NASA-TN-81608]

p0080 A81-11395

Texturing polymer surfaces by transfer casting --- cardiovascular prosthesis

[NASA-CASE-LEW-13120-1]

p0068 A81-16327

Effect of surface roughness on hydrodynamic bearings [NASA-TN-81711]

p0082 A81-21356

An experimental investigation of silicon wafer surface roughness and its effect on the full strength of plated metals

[NASA-TN-81763]

p0100 A81-22478

Surface roughness effect on finite oil journal bearings

[NASA-TN-82639]

p0084 A81-27526

SURFACE ROUGHNESS EFFECTS

An experimental investigation of silicon wafer surface roughness and its effect on the pull-strength of plated metals

p0109 A81-38063

Effect of substrate surface finish on the lubrication and failure mechanisms of molybdenum disulfide films

[NASA-TN-81595]

p0060 A81-10170

SURFACE TEMPERATURE

NT WALL TEMPERATURE

Curved film cooling admission tube [NASA-CASE-LEW-13174-1]

p0074 A81-12363

SURFACE TENSION

U INTERFACIAL TENSION

SURFACE TREATMENT

U SURFACE FINISHING

SURFACE VEHICLES

NT AUTOMOBILES

NT ELECTRIC AUTOMOBILES

NT ELECTRIC HYBRID VEHICLES

NT ELECTRIC MOTOR VEHICLES

NT TRUCKS

SURFACE WAVES

NT CAPILLARY WAVES

SURFING WAVES

U TURBULENT WAVES

SWITCHES

NT SWITCHING CIRCUITS

K-band high power latching switch --- communication satellite system

[NASA-CR-165159]

p0073 A81-16389

SWITCHING

NT MICROWAVE SWITCHING

SWITCHING CIRCUITS

Specifying and calibrating instrumentations for wideband electronic power measurements --- in switching circuits

[NASA-TN-81545]

p0079 A81-16429

SWITCHING ELEMENTS

U SWITCHING CIRCUITS

SWITCHING THEORY

Next generation communications satellites: Multiple access and network studies

[NASA-CR-165145]

p0033 A81-12139

SYMMETRICAL BODIES

NT AXISYMMETRIC BODIES

NT CYLINDRICAL BODIES

SYNCHRONISM

Tests of an overrunning clutch in a wind turbine [NASA-TN-82653]

p0107 A81-29528

SYNCHRONIZATION

U SYNCHRONISM

SYNCHRONOUS SATELLITES

Modelling of environmentally induced discharges in geosynchronous satellites

p0034 A81-19936

Environmental charging effects monitors for operational satellites

p0037 A81-38057

SYNTHESIS

Synthesis of improved phenolic and polyester resins [NASA-CR-165180]

p0065 A81-17263

SYNTHESIS (CHEMISTRY)

Phosphazene diamines

[NASA-CR-165147]

p0065 A81-10169

Cross-linked polyvinyl alcohol and method of making same

- [NASA-CASE-LEW-13504-1] p0063 N81-27279
- SYNTHETIC FUELS**
- WT LIQUID FUELS**
- Evaluation of concepts for controlling exhaust emissions from minimally processed petroleum and synthetic fuels
- [ASME PAPER 81-GT-157] p0067 A81-30056
- Some advantages of methane in an aircraft gas turbine
- [SAE PAPER 801154] p0022 A81-34177
- Catalytic combustion of coal-derived liquids
- [NASA-TN-81594] p0097 N81-14396
- SYNTHETIC RESINS**
- WT ACRYLIC RESINS**
- WT EPOXY RESINS**
- WT Kevlar (TRADEMARK)**
- WT PHENOLIC RESINS**
- WT POLYESTER RESINS**
- SYNTHETIC RUBBERS**
- WT ELASTOMERS**
- SYSTEM FAILURES**
- Phosphazene diamines
- [NASA-CR-165147] p0065 N81-10165
- Apparatus for sensor failure detection and correction in a gas turbine engine control system
- [NASA-CASE-LEW-12907-2] p0015 N81-19115
- SYSTEM GENERATED ELECTROMAGNETIC PULSES**
- Development and design of three monitoring instruments for spacecraft charging
- [NASA-TF-1800] p0040 N81-31282
- SYSTEMS ANALYSIS**
- Study of component technologies for fuel cell on-site integrated energy systems
- [NASA-CR-165152-VOL-1] p0110 N81-15461
- Study of component technologies for fuel cell on-site integrated energy system. Volume 2: Appendices
- [NASA-CR-165152-VOL-2] p0110 N81-15462
- SYSTEMS DESIGN**
- U SYSTEMS ENGINEERING**
- SYSTEMS ENGINEERING**
- Shuttle compatible cryogenic liquid storage and supply systems
- [AIAA PAPER 81-1509] p0037 A81-42207
- Automotive Stirling engine development program
- [NASA-CR-165134] p0139 N81-11952
- Progress in materials and structures at Lewis Research Center
- p0142 N81-12982
- The DOE photovoltaics program
- p0143 N81-12989
- Engineering support for magnetohydrodynamic power plant analysis and design studies
- [NASA-CR-159690] p0110 N81-13466
- Disk MHD generator study
- [NASA-CR-159872] p0111 N81-18491
- Thermal energy storage for the Stirling engine powered automobile
- [NASA-CR-159561] p0113 N81-22467
- NASA prototype redox storage system for a photovoltaic stand-alone application
- [NASA-TN-82607] p0104 N81-24534
- Conceptual design of the MHD Engineering Test Facility
- [NASA-TN-82621] p0132 N81-24926
- Design description of the Schuchuli Village photovoltaic power system
- [NASA-TN-82650] p0094 N81-28517
- The 30/20 GHz experimental communications satellite system
- [NASA-TN-82683] p0035 N81-30172
- SYSTEMS INTEGRATION**
- Future challenges in V/STOL flight propulsion control integration
- [SAE PAPER 801140] p0022 A81-34170
- SYSTEMS SIMULATION**
- An approach to real-time simulation using parallel processing
- p0121 A81-44652
- A nonlinear propulsion system simulation technique for piloted simulators
- [NASA-TN-82600] p0101 N81-23085
- TANTALUM**
- Integrated IC-circuits in ALTA-technology on one substrate
- [BHPT-PB-T-79-107] p0072 N81-14227
- TANTALUM COMPOUNDS**
- WT TANTALUM OXIDES**
- TANTALUM OXIDES**
- Electrostatic bonding of thin (approximately 3 mil) 7070 cover glass to Ta2O5 AB-coated thin (approximately 2 mil) silicon wafers and solar cells
- p0111 N81-17569
- TAPER**
- U TAPERING**
- TAPERING**
- Endurance tests with large-bore tapered-roller bearings to 2.2 million DM
- [NASA-TN-82669] p0084 N81-29439
- TDMA**
- U TIME DIVISION MULTIPLE ACCESS**
- TECHNOLOGICAL FORECASTING**
- The future of aeronautical propulsion
- p0001 A81-29052
- Advanced communications satellites
- [AAS PAPER 80-206] p0069 A81-33532
- Propulsion controls
- p0025 N81-12095
- Future Air Force aircraft propulsion control systems: The extended summary paper
- p0025 N81-12096
- Materials processing in space: Future technology trends
- p0143 N81-12991
- Aerospace in the future
- [NASA-TN-82664] p0143 N81-29063
- TECHNOLOGIES**
- WT ENERGY TECHNOLOGY**
- TECHNOLOGY ASSESSMENT**
- High efficiency wraparound contact solar cells /HENAACS/
- p0114 A81-27094
- Photovoltaic applications - Past and future
- p0109 A81-27231
- An overview of general aviation propulsion research programs at NASA-Lewis Research Center
- [SAE PAPER 810624] p0023 A81-42778
- Comparisons of four alternative powerplant types for future general aviation aircraft
- [NASA-TN-81584] p0013 N81-10067
- Satellites using the 30/20 GHz band
- [NASA-TN-81600] p0069 N81-10241
- Energy overview
- p0142 N81-12979
- NASA Research in aeropropulsion
- p0142 N81-12980
- Synthesis of improved phenolic and polyester resins
- [NASA-CR-165180] p0065 N81-17263
- Commercial (terrestrial) and modified solar array design studies for low cost, low power space applications
- [NASA-TN-81622] p0061 N81-17266
- Recent developments in aircraft engine noise reduction technology
- p0009 N81-19072
- Technology development for phosphoric acid fuel cell powerplant, phase 2
- [NASA-CR-165317] p0113 N81-21536
- Technology development for phosphoric acid fuel cell powerplant (phase 2)
- [NASA-CR-165316] p0113 N81-21547
- Assessment of disk MHD generators for a base load powerplant
- [NASA-TN-82609] p0103 N81-23611
- Ion plating for the future
- [NASA-TN-82630] p0054 N81-25189
- The supersonic fan engine: An advanced concept in supersonic cruise propulsion
- [NASA-TN-82657] p0018 N81-27094
- The 30/20 GHz experimental communications satellite system
- [NASA-TN-82683] p0035 N81-30172
- Continuously variable transmission: Assessment of applicability to advance electric vehicles
- [NASA-TN-82700] p0085 N81-33484
- TECHNOLOGY TRANSFER**
- WT AEROSPACE TECHNOLOGY TRANSFER**
- Solar photovoltaics: Stand alone applications --- NASA Lewis Research Center research and development
- p0143 N81-12990
- A case history of technology transfer
- [NASA-TN-82618] p0040 N81-30182

TECHNOLOGY UTILISATION

Advanced fuel system technology for utilizing broadened property aircraft fuels p0066 A81-11612

Photovoltaic applications - Past and future p0109 A81-27231

Ion beam applications research - A 1981 summary of Lewis Research Center programs [AIAA PAPER 81-0669] p0041 A81-38068

Applications Technology Satellite and Communications Technology Satellite user experiments for 1967-1980 reference book. Volume 4: Abstracts [NASA-CR-165169-VOL-4] p0133 A81-12138

Ion beam applications research. A summary of Lewis Research Center programs [NASA-TN-81721] p0044 A81-21129

Review of stand-alone photovoltaic application projects sponsored by US DOE and US AID [NASA-TN-81738] p0100 A81-22477

Overview: DOE/NASA automotive gas turbine and stirling projects [NASA-TN-82637] p0105 A81-25487

A case history of technology transfer [NASA-TN-82618] p0040 A81-30182

TELECOMMUNICATIONS

NT NET EXPERIMENT

NT MULTICARRIER COMMUNICATION

NT RADIO COMMUNICATION

NT RADIOTELEPHONES

NT SATELLITE TELEVISION

NT SPACECRAFT COMMUNICATION

NT TELEPHONY

NT TIME DIVISION MULTIPLE ACCESS

Advanced communications satellites [AAS PAPER 80-206] p0069 A81-33532

Applications Technology Satellite and Communications Technology Satellite user experiments for 1967 - 1980 reference book, volume 1 [NASA-CR-165169-VOL-1] p0033 A81-12135

Applications Technology Satellite and Communications Technology Satellite user experiments for 1967-1980 reference book, volume 2 [NASA-CR-165169-VOL-2] p0033 A81-12136

Applications Technology Satellite and Communications Technology Satellite user experiments for 1967-1980 reference book. Volume 3: User forum surveys [NASA-CR-165169-VOL-3] p0033 A81-12137

Applications Technology Satellite and Communications Technology Satellite user experiments for 1967-1980 reference book. Volume 4: Abstracts [NASA-CR-165169-VOL-4] p0133 A81-12138

The 30/20 GHz experimental communications satellite system [NASA-TN-82683] p0035 A81-30172

TELECONFERENCING

NT NET EXPERIMENT

TELEPHONES

NT RADIOTELEPHONES

TELEPHONY

An economic systems analysis of land mobile radio telephone services p0069 A81-22528

An economics systems analysis of land mobile radio telephone services [NASA-TN-81476] p0069 A81-10239

TELEVISION SYSTEMS

NT SATELLITE TELEVISION

TELEVISION TRANSMISSION

Carrier - interference ratios for frequency sharing between satellite systems transmitting frequency modulated and digital television signals p0069 A81-21911

TELEVISION THEORY

U NETWORK ANALYSIS

TEMPERATURE

NT CURIE TEMPERATURE

NT HIGH TEMPERATURE

NT INLET TEMPERATURE

NT LOW TEMPERATURE

NT OPERATING TEMPERATURE

NT SURFACE TEMPERATURE

NT WALL TEMPERATURE

TEMPERATURE CONTROL

Shuttle compatible cryogenic liquid storage and supply system

[AIAA PAPER 81-1509] p0037 A81-42207

TEMPERATURE DEPENDENCE

T-S diagram for gadolinium near the Curie temperature p0135 A81-43004

TEMPERATURE EFFECTS

Cyclic behavior of turbine disk alloys at 650 C p0056 A81-12266

Effect of CeO₂, MgO and Y₂O₃ additions on the sinterability of a milled Si₃N₄ with 14.5 wt% SiO₂ p0064 A81-28974

Factors which influence the behavior of turbofan forced mixer nozzles [AIAA PAPER 81-0274] p0021 A81-32549

Cell module and fuel conditioner [NASA-CR-165189] p0112 A81-18494

Assessment of variations in thermal cycle life data of thermal barrier coated rods [NASA-TN-81743] p0102 A81-23418

TEMPERATURE INVERSIONS

NT INTERFACIAL TENSION

TEMPERATURE MEASUREMENT

Turbine blade temperature measurements using thin film temperature sensors [NASA-CR-165201] p0059 A81-19277

Comparison of photovoltaic cell temperatures in modules operating with exposed and enclosed back surfaces [NASA-TN-81769] p0106 A81-28520

TEMPERATURE MEASURING INSTRUMENTS

NT RADIATION PYROMETERS

NT THERMOCOUPLE PYROMETERS

TEMPERATURE SENSORS

Turbine blade temperature measurements using thin film temperature sensors [NASA-CR-165201] p0059 A81-19277

TENSILE STRENGTH

An experimental investigation of silicon wafer surface roughness and its effect on the pull-strength of plated metals p0109 A81-38063

An experimental investigation of silicon wafer surface roughness and its effect on the pull-strength of plated metals [NASA-TN-81763] p0100 A81-22478

Oxidation-induced contraction and strengthening of boron fibers [NASA-TN-82599] p0046 A81-25150

Relationship between the ideal tensile strength and the friction properties of metals in contact with nonmetals and themselves [NASA-TP-1883] p0063 A81-33293

TENSILE STRESS

Ion beam sputter etching of orthopedic implanted alloy MP35N and resulting effects on fatigue [NASA-TN-81747] p0045 A81-21174

TENSILE TESTS

Elevated temperature mechanical properties and residual tensile properties of two cast superalloys and several nickel-base oxide dispersion strengthened alloys p0057 A81-24104

Completion of evaluation of manufacturing processes for B/AI composites containing 0.2mm diameter boron fibers [NASA-TN-81573] p0051 A81-11111

TENSOR ANALYSIS

Geometric methods in computational fluid dynamics --- turbomachinery p0075 A81-18331

TERNARY ALLOYS

The effect of zirconium on the cyclic oxidation of NiCrAl alloys p0056 A81-18559

TERNARY SYSTEMS

NiCrAl ternary alloy having improved cyclic oxidation resistance [NASA-CASE-LEW-13339-1] p0051 A81-12211

TERNARY SYSTEMS (DIGITAL)

8 DIGITAL SYSTEMS

TERRESTRIAL MAGNETISM

U GEOMAGNETISM

TEST BEDS

U TEST EQUIPMENT

TEST CHAMBERS

NT ANECHOIC CHAMBERS

TEST EQUIPMENT

NASA five-ball fatigue tester - Over 20 years of research

- TEST FACILITIES**
HT / AMBROS C CHAMBERS
 Power spectra and cross spectra at an area
 interaction in a ducted combustion system
 [NASA PAPER 80-C2/ABRO-5] p0077 881-18638
 Description of the warm core turbine facility and
 the warm annular cascade facility recently
 installed at NASA Lewis Research Center
 [SAR PAPER 801122] p0031 881-34158
 Diagnostic system design for the Ion Auxiliary
 Propulsion System /IAFS/ - Flight test of two 8
 cm mercury ion thrusters
 [AIAA PAPER 81-0666] p0041 881-38070
- TESTERS**
U TEST EQUIPMENT
TESTING MACHINES
U TEST EQUIPMENT
- TEXTURES**
 Texturing polymer surfaces by transfer casting ---
 cardiovascular prosthesis
 [NASA-CASE-LEU-13120-1] p0068 881-16327
 Mechanical bonding of sctal
 [NASA-CASE-LEU-12941-1] p0068 881-16329
 Ion sputter textured graphite --- applications to
 electron tube devices
 [NASA-CASE-LEU-12919-1] p0046 881-27198
- TP-34 ENGINE**
 TP34 engine compression system computer study ---
 simulation of flow stability
 [NASA-CR-155889] p0027 881-15005
- THERMAL AGITATION**
U THERMAL ENERGY
THERMAL BOUNDARY LAYER
 Influence of thermal boundary conditions on heat
 transfer from a cylinder in cross flow
 [NASA-TP-1894] p0076 881-29384
- THERMAL CONTROL COATINGS**
 Thermal barrier coatings - Burner rig hot
 corrosion test results
 p0063 881-12630
 Thermal barrier coatings for heat engine components
 p0056 881-12920
 Assessment of variations in thermal cycle life
 data of thermal barrier coated rods
 p0058 881-44657
 Prolonging thermal barrier coated specimen life by
 thermal cycle management
 p0065 881-44658
 Cost/benefit analysis of advanced materials
 technologies for future aircraft turbine engines
 [NASA-CR-165225] p0027 881-15006
- THERMAL CURRENTS**
U CONVECTIVE FLOW
THERMAL CYCLING TESTS
 The effect of thermal cycling to 1100 C on the
 alpha /Mo/ phase in directionally solidified
 gamma/gamma-prime-alpha alloys
 p0057 881-32546
 High temperature cyclic oxidation furnace testing
 at NASA Lewis Research Center
 p0058 881-44653
 Assessment of variations in thermal cycle life
 data of thermal barrier coated rods
 p0058 881-44657
 Prolonging thermal barrier coated specimen life by
 thermal cycle management
 p0065 881-44658
 The effect of thermal cycling to 1100 degree C on
 the alpha (Mo) phase in directionally solidified
 gamma/gamma-prime-alpha alloys
 [NASA-TN-81688] p0052 881-18165
- THERMAL EFFECTS**
U TEMPERATURE EFFECTS
THERMAL EFFICIENCY
U THERMODYNAMIC EFFICIENCY
THERMAL ENERGY
 Study of component technologies for fuel cell
 on-site integrated energy systems
 [NASA-CR-165152-VOL-1] p0110 881-15461
 Study of component technologies for fuel cell
 on-site integrated energy system. Volume 2:
 Appendices
 [NASA-CR-165152-VOL-2] p0110 881-15462
 Study of thermal management for space platform
 applications
 [NASA-CR-165230] p0033 881-21106
- THERMAL ENERGY STORAGE**
U HEAT STORAGE
- THERMAL EXPANSION**
 Prediction of composite thermal behavior made simple
 [NASA-TN-81618] p0045 881-16132
- THERMAL FATIGUE**
 Some effects of thermal-cycle-induced deformation
 in rocket thrust chambers
 [NASA-TP-1834] p0038 881-20176
 Sputtered protective coatings for die casting dies
 [NASA-TN-81735] p0053 881-21173
- THERMAL INSTABILITY**
 On the magnetocerothermal instability
 [AIAA PAPER 81-0248] p0133 881-20698
- THERMAL INSULATION**
 Comparative evaluation of insulating properties of
 plasma-sprayed ceramic coatings
 p0064 881-15984
 Effects of plasma spray parameters on two layer
 thermal barrier
 [NASA-TN-81724] p0053 881-22161
- THERMAL POWER**
U TURBOGENERATORS
THERMAL PROPERTIES
U THERMODYNAMIC PROPERTIES
THERMAL PROTECTION
 Thermal barrier coatings for superalloys
 p0058 881-49217
 Thermal barrier coating system having improved
 adhesion
 [NASA-CASE-LEU-13359-1] p0062 881-24265
 Corrosion resistant thermal barrier coating ---
 protecting gas turbines and other engine parts
 [NASA-CASE-LEU-13088-1] p0054 881-25188
- THERMAL RESISTANCE**
 High temperature cyclic oxidation furnace testing
 at NASA Lewis Research Center
 p0058 881-44653
 A sputtered zirconia primer for improved thermal
 shock resistance of plasma sprayed ceramic
 turbine seals
 [NASA-TN-81732] p0062 881-21198
 Burner rig evaluation of thermal barrier coating
 --- gas turbines
 [NASA-TN-81684] p0055 881-28231
- THERMAL SHOCK**
 Laser surface fusion of plasma sprayed ceramic
 turbine seals
 [NASA-CASE-LEU-13269-1] p0062 881-22190
- THERMAL STABILITY**
U TEMPERATURE DEPENDENCE
 Properties of PBR polyimide composites made with
 improved high strength graphite fibers
 p0047 881-43603
 Assessment of variations in thermal cycle life
 data of thermal barrier coated rods
 p0058 881-44657
 Tribological properties and thermal stability of
 various types of polyimide films
 [NASA-TN-81765] p0102 881-23275
- THERMAL STRESSES**
 Prediction of composite thermal behavior made simple
 [NASA-TN-81618] p0045 881-16132
 Method for alleviating thermal stress damage in
 laminates --- metal matrix composites
 [NASA-CASE-LEU-12493-1] p0045 881-17170
 Assessment of variations in thermal cycle life
 data of thermal barrier coated rods
 [NASA-TN-81743] p0102 881-23418
 Method for alleviating thermal stress damage in
 laminates
 [NASA-CASE-LEU-12493-2] p0046 881-26179
- THERMIONIC CATHODES**
 Simplified power supplies for ion thrusters
 [AIAA PAPER 81-0693] p0040 881-29542
 Analytical investigation of efficiency and
 performance limits in klystron amplifiers using
 multidimensional computer programs; multi-stage
 depressed collectors; and thermionic cathode
 life studies
 p0098 881-16552
- THERMIONIC CONVERSION SYSTEMS**
U THERMIONIC POWER GENERATION
THERMIONIC CONVERTERS
 High power densities from high-temperature
 material interactions --- in thermionic energy
 conversion and metallic fluid heat pipes
 [AIAA PAPER 81-1161] p0070 881-39144
 Goals of thermionic program for space power
 p0133 881-44656

High power densities from high-temperature materials interactions --- thermionic energy conversion and metallic fluid heat pipes [NASA-TN-81626] p0131 N81-16900

THERMIONIC DIODES
NT CATHODE DIODES
THERMIONIC POWER GENERATION
 Improved thermionic energy converters [NASA-CASE-LBN-12443-1] p0099 N81-19561
 Thermionic Energy Conversion (TEC) topping thermoelectrics [NASA-TN-81677] p0132 N81-19920
 Goals of thermionic program for space power [NASA-TN-82616] p0132 N81-25808
 A program-management plan with critical-path definition for Combustion Augmentation with Thermionic Energy Conversion (CATIC) [NASA-TN-82670] p0132 N81-30973

THERMIONIC REACTORS
U ICE ENGINES
THERMOCHEMICAL PROPERTIES
 High power densities from high-temperature material interactions --- in thermionic energy conversion and metallic fluid heat pipes [AIAA PAPER 81-1161] p0070 A81-39144

THERMOCOUPLE PYROMETERS
 Surface pyrometry in presence of radiation from other sources with application to turbine blade temperature measurement [NASA-TP-1754] p0013 N81-11039

THERMOCOUPLES
 Computer program for pulsed thermocouples with corrections for radiation effects [NASA-TP-1895] p0120 N81-33838

THERMODYNAMIC CYCLES
NT STIRLING CYCLE
 Prolonging thermal barrier coated specimen life by thermal cycle management [NASA-TN-81742] p0102 N81-23417
 Assessment of variations in thermal cycle life data of thermal barrier coated rods [NASA-TN-81743] p0102 N81-23418
 KONFIG and BIRCHFIG: Two interactive preprocessing to the Navy/NASA Engine Program (NHRP) [NASA-TN-82636] p0120 N81-25658

THERMODYNAMIC EFFICIENCY
 Performance calculations for 1000 MWe MHD/steam power plants [NASA-TN-81667] p0098 N81-16570

THERMODYNAMIC PROPERTIES
NT ENTROPY
NT SURFACE ENERGY
NT THERMAL EXPANSION
NT THERMAL INSTABILITY
NT THERMAL STABILITY
NT THERMOCHEMICAL PROPERTIES
NT THERMOPHYSICAL PROPERTIES
 Computer code for intraply hybrid composite design p0047 A81-44662
 Combustor liner durability analysis [NASA-CN-165250] p0027 N81-17079
 Lower-curing-temperature IMR polyimides [NASA-TN-81705] p0045 N81-17174

THERMODYNAMICS
NT AEROTHERMODYNAMICS
NT COMBUSTION PHYSICS
 Thermodynamics. II - The extended thermodynamic system p0136 A81-31375
 Computer code for intraply hybrid composite design [NASA-TN-81593] p0046 N81-25151

THERMOELASTICITY
NT AEROTHERMOELASTICITY
THERMOELECTRIC CONVERSION SYSTEMS
U THERMOELECTRIC POWER GENERATION
THERMOELECTRIC GENERATORS
 Goals of thermionic program for space power [NASA-TN-82616] p0132 N81-25808
THERMOELECTRIC POWER GENERATION
 Thermionic Energy Conversion (TEC) topping thermoelectrics [NASA-TN-81677] p0132 N81-19920

THERMOMECHANICAL TREATMENT
 Effect of TSP variables upon structure and properties in ODS alloy NDA 8077 sheet --- Thermomechanical Processing of Oxide Dispersion Strengthened nickel alloy p0059 A81-10706

The effect of mechanical surface and heat treatments on the erosion resistance of 6061 aluminum alloy p0057 A81-27944

THERMOSCCHARICS
U THERMODYNAMICS
THERMOSTAT
U TEMPERATURE MEASUREMENT
THERMOPHYSICAL PROPERTIES
NT TEMPERATURE INDEPENDENCE
NT THERMAL STABILITY
 High power densities from high-temperature material interactions --- in thermionic energy conversion and metallic fluid heat pipes [AIAA PAPER 81-1161] p0070 A81-39144
 Aviation turbine fuel properties and their trends [NASA-TN-82603] p0066 N81-25232

THERMOPHYSICS
U THERMODYNAMICS
THERMOSTATING RESINS
NT EPOXY RESINS
NT KEVLAR (TRADEMARK)
NT PHENOLIC RESINS
THERMOSTABILITY
U THERMAL STABILITY
THERMOTROPISM
U ANISOTROPY
U TEMPERATURE EFFECTS
THIS FILMS
 Thin a-i-p silicon solar cell p0114 A81-27097
 The transfer of polytetrafluoroethylene studied by I-ray photoelectron spectroscopy p0087 A81-31238
 Effect of substrate surface finish on the lubrication and failure mechanisms of molybdenum disulfide films [ASLE PREPRINT 81-AM-5D-1] p0044 A81-33859
 Frictional and morphological characteristics of ion plated soft, metallic films p0057 A81-38066
 Polytetrafluoroethylene transfer film studied with I-ray photoelectron spectroscopy [NASA-TP-1728] p0060 N81-11214
 Thin-film coatings p0142 N81-12983
 Ion beam deposited protective films [NASA-TN-81722] p0038 N81-19221
 Turbine blade temperature measurements using thin film temperature sensors [NASA-CN-165201] p0059 N81-19277
 Sputtering and ion plating for aerospace applications [NASA-TN-81726] p0082 N81-20424

THREE DIMENSIONAL BOUNDARY LAYER
 Core compressor exit stage study. Volume 2: Data and performance report for the baseline configuration [NASA-CN-159498] p0027 N81-16051

THREE DIMENSIONAL FLOW
NT SECONDARY FLOW
 Three-dimensional turbulent boundary layer development and separation in V/STOL engine inlets at incidence with small-cross flow and curvature influences [AIAA PAPER 81-0254] p0005 A81-20703
 Calculation of three-dimensional turbulent subsonic flows in transition ducts p0008 A81-21199
 Full potential solution of a transonic quasi-3-D flow through a cascade using artificial compressibility [ASME PAPER 81-GT-70] p0006 A81-29979
 Some aspects of calculating flows about three-dimensional subsonic inlets [AIAA PAPER 81-1361] p0007 A81-42177
 Numerical simulation of flows in curved diffusers with cross-sectional transitioning using a three-dimensional viscous analysis [NASA-TN-81672] p0074 N81-15239
 A three-dimensional turbulent compressible subsonic duct flow analysis for use with constructed coordinate systems [NASA-CN-3389] p0077 N81-20383
 Application of computer generated color graphic techniques to the processing and display of three dimensional fluid dynamic data [NASA-TN-82658] p0119 N81-29762

- THREE DIMENSIONAL MOTION**
BT SECONDARY FLOW
BT THREE DIMENSIONAL FLOW
THRUST
BT LOW THRUST
 Performance capabilities of the 8-cm Mercury ion thruster
 [AIAA PAPER 81-0754] p0044 881-29567
 Extended operating range of the 30-cm ion thruster with simplified power processor requirements
 [NASA-TN-81729] p0039 881-20179
 The electric rail gun for space propulsion
 [NASA-CN-165312] p0042 881-22078
 Effect of a part-span variable inlet guide vane on the performance of a high-bypass turbofan engine
 [NASA-TN-82617] p0017 881-25081
- THRUST BEARINGS**
 Dynamic characteristics of a high-speed rotor with radial and axial foil-bearing supports
 [ASME PAPER 80-C2/LUB-35] p0085 881-18683
- THRUST CHAMBERS**
 Adapting magnetoelectrostatic containment to inert gas thrusters
 [AIAA PAPER 81-0140] p0043 881-20625
 Some effects of thermal-cycle-induced deformation in rocket thrust chambers
 [NASA-TP-1834] p0038 881-20176
- THRUST LOADS**
 Ball bearing mechanics
 [NASA-TN-81691] p0085 881-31550
- THRUST POWER**
U THRUST
THRUSTORS
U ROCKET ENGINES
THRISTORS
 Electronically commutated dc motors for electric vehicles
 [NASA-TN-81654] p0097 881-15464
- TIME DEPENDENCE**
 Holographic flow visualization of time-varying shock waves
 p0079 881-47642
 Evaluation of candidate Stirling engine heater tube alloys for 1000 hours at 760 C
 [NASA-TN-81578] p0051 881-15068
- TIME DIVISION MULTIPLE ACCESS**
 Next generation communications satellites: Multiple access and network studies
 [NASA-CN-165145] p0033 881-12139
- TIN ALLOYS**
BT BABBITT METAL
TIPS
BT BLADE TIPS
TITANIUM
 The role of oxidation in the fretting wear process
 [NASA-TN-81570] p0051 881-12210
- TITANIUM ALLOYS**
 Computer-aided roll pass design in rolling of airfoil shapes
 p0088 881-15796
 Effects of geometric variables on rub characteristics of Ti-6Al-4V
 [NASA-TP-1835] p0053 881-20245
- TITANIUM COMPOUNDS**
BT TITANIUM NITRIDES
TITANIUM NITRIDES
 Improved refractory coatings --- sputtered coatings on substrates that form stable nitrides
 [NASA-CASE-LEU-23169-2] p0052 881-16209
- TOLERANCES (PHYSIOLOGY)**
BT RADIATION TOLERANCE
TOLUENE
 Effect of fuel nitrogen and hydrogen content on emissions in hydrocarbon combustion
 [NASA-TN-81612] p0097 881-14399
- TOMOMETRY**
U PRESSURE MEASUREMENT
TOPOLOGY
 An electrostatic analog for generating cascade grids
 p0122 881-14655
- TOROIDAL SHELLS**
 Toroidal cell and battery --- storage battery for high amp-hour load applications
 [NASA-CASE-LEU-12918-1] p0104 881-24521
- TORSIONAL STRESS**
 Effects of mistuning on blade torsional flutter
 p0092 881-29095
 Effects of mistuning on bending-torsion flutter and response of a cascade in incompressible flow
- [AIAA 81-0602] p0092 881-29465
TOXIC DISCHARGES
BT GAS DISCHARGES
TOXIC HAZARDS
 Safety management of complex research operators
 [NASA-TN-81772] p0068 881-25263
- TRACE CONTAMINANTS**
 Accuracy of trace element determinations in alternate fuels
 [NASA-TN-81609] p0049 881-13106
 The effects of trace impurities in coal-derived liquid fuels on deposition and accelerated high temperature corrosion of cast superalloys
 [NASA-TN-81678] p0052 881-16211
- TRACE ELEMENTS**
 Accuracy of trace element determinations in alternate fuels
 p0056 881-22530
- TRACTION**
 Life analysis of multiroller planetary traction drive
 [NASA-TP-1710] p0082 881-20423
- TRAFFIC**
BT AIR TRAFFIC
TRAILING EDGES
 Heat transfer coefficients for staggered arrays of short pin fins
 [ASME PAPER 81-GT-75] p0077 881-29983
 Heat transfer coefficients for staggered arrays of short pin fins
 [NASA-TN-81596] p0074 881-13302
- TRAINING SIMULATORS**
BT FLIGHT SIMULATORS
TRANSBUCKERS
BT ULTRASONIC WAVE TRANSDUCERS
TRANSFER FUNCTIONS
 User's design handbook for a Standardized Control Module (SCM) for DC to DC Converters, volume 2
 [NASA-CN-165173] p0072 881-11314
 Multivariable identification using centralized fixed modes
 p0014 881-12091
 Multivariable synthesis with transfer functions --- applications to gas turbine engines
 p0026 881-12102
- TRANSFORMATIONS (MATHEMATICS)**
BT COORDINATE TRANSFORMATIONS
TRANSIENT RESPONSE
 Extended frequency turbofan model
 [NASA-CN-165261] p0030 881-20078
- TRANSISTORS**
 Electronically commutated dc motors for electric vehicles
 [NASA-TN-81654] p0097 881-15464
- TRANSITION METALS**
BT COBALT
BT MOLYBDENUM
BT NICKEL
BT PLATINUM
BT TANTALUM
BT TITANIUM
BT TUNGSTEN
BT YTTRIUM
BT ZIRCONIUM
 Adhesion and friction of transition metals in contact with nonmetallic hard materials
 [NASA-TN-82605] p0055 881-28233
- TRANSITION POINTS**
 Numerical simulation of flows in curved diffusers with cross-sectional transitioning using a three-dimensional viscous analysis
 [NASA-TN-81672] p0074 881-15239
- TRANSLATIONAL MOTION**
BT SECONDARY FLOW
BT THREE DIMENSIONAL FLOW
 Experimental determination of unsteady blade element aerodynamics in cascades. Volume 2: Translation mode cascade
 [NASA-CN-165166] p0007 881-14976
- TRANSMISSION**
BT ACOUSTIC PROPAGATION
BT DATA TRANSMISSION
BT ELECTRIC POWER TRANSMISSION
BT ELECTROMAGNETIC WAVE TRANSMISSION
BT HEAT TRANSFER
BT HEAT TRANSMISSION
BT MICROWAVE TRANSMISSION
BT SATELLITE TRANSMISSION
BT SOUND TRANSMISSION

- UT TELEPHONY
 UT TELEVISION TRANSMISSION
 UT TURBULENT HEAT TRANSFER
 Shell passenger car transmission test: Dodge Omni
 A-804 transmission
 [NASA-CN-165181] p0088 N81-15366
 TRANSMISSION LINES
 UT WAVEGUIDES
 TRANSMISSION LOSS
 Parasitic current losses due to solar electric
 propulsion generated plasmas
 [AIAA PAPER 81-0740] p0043 A81-29561
 TRANSMISSIONS (MACHINE ELEMENTS)
 Design studies of continuously variable
 transmissions for electric vehicles
 [NASA-TN-81642] p0080 N81-13357
 Comparisons of modified Vanco X-2 and AISI 9310
 gear steels
 [NASA-TP-1731] p0090 N81-14322
 Axial force and efficiency tests of fixed center
 variable speed belt drive
 [NASA-TN-81652] p0080 N81-15367
 Advanced continuously variable transmissions for
 electric and hybrid vehicles
 [NASA-TN-81718] p0082 N81-19459
 Continuously variable transmission: Assessment of
 applicability to advance electric vehicles
 [NASA-TN-82700] p0085 N81-33484
 TRANSMITTERS
 UT RADIOTELEPHONES
 Spacecraft transmitter reliability
 [NASA-CP-2159] p0037 N81-16119
 TRANSDUCERS
 Aircraft operating efficiency on the North
 Atlantic, a challenge for the 1980's
 p0009 N81-19060
 TRANSONIC AIRCRAFT
 U SUPERSONIC AIRCRAFT
 TRANSONIC COMPRESSORS
 Holographic flow visualization of time-varying
 shock waves
 p0079 A81-47642
 TRANSONIC FLOW
 Full potential solution of a transonic quasi-3-D
 flow through a cascade using artificial
 compressibility
 [AASR PAPER 81-07-70] p0006 A81-29979
 A rapid perturbation procedure for determining
 nonlinear flow solutions: Application to
 transonic turbomachinery flows
 [NASA-CN-8425] p0001 N81-22012
 Shockless design and analysis of transonic blade
 shapes
 [NASA-TN-82611] p0004 N81-25036
 Stall flutter experiment in a transonic
 oscillating linear cascade
 [NASA-TN-82655] p0004 N81-31126
 TRANSONIC FLUTTER
 Stall flutter experiment in a transonic
 oscillating linear cascade
 [NASA-TN-82655] p0004 N81-31126
 TRANSONIC INLETS
 U SUPERSONIC INLETS
 TRANSONIC SPEED
 Improved method for calculating transonic
 velocities on blade-to-blade stream surfaces of
 a turbomachine
 [NASA-TP-1772] p0004 N81-22017
 TRANSONICS
 U TRANSONIC FLUX
 TRANSPARENTS
 Heat transparent high intensity high efficiency
 solar cell
 [NASA-CASE-LEN-12892-1] p0105 N81-27598
 TRANSPARENT SATTELS
 U TRANSPARENT
 TRANSPORT AIRCRAFT
 UT BORING 747 AIRCRAFT
 UT SHORT JAIL AIRCRAFT
 The supersonic fan engine - An advanced concept in
 supersonic cruise propulsion
 [AIAA PAPER 81-1599] p0023 A81-40973
 Light transport and general aviation aircraft
 icing research requirements
 [NASA-CN-165290] p0010 N81-19079
 TRANSPORT PROPERTIES
 UT CARRIER MOBILITY
 UT ELECTRICAL RESISTIVITY
 UT ELECTRON MOBILITY
 TRANSPORT THEORY
 Development and testing of heat transport fluids
 for use in active solar heating and cooling
 systems
 [NASA-TP-82395] p0098 N81-16584
 TRANSPORTATION
 UT SPACE SHUTTLE ORBITERS
 UT SPACE TRANSPORTATION SYSTEM
 TRANSPORTATION ENERGY
 Vehicle testing of Cummins turbocompound diesel
 engine
 [NASA-CN-159840] p0140 N81-13803
 TRAVELING WAVE AMPLIFIERS
 Ladder supported ring bar circuit
 [NASA-CASE-LEN-13570-1] p0071 N81-24348
 TRAVELING WAVE TUBES
 Electron reflection and secondary emission
 characteristics of sputter-textured pyrolytic
 graphite surfaces
 p0065 A81-38065
 Experimental investigation of intermodulation
 effects and related efficiencies associated with
 two- and three-signal operation of a traveling
 wave tube
 [NASA-TN-81576] p0067 N81-10240
 Spacecraft transmitter reliability
 [NASA-CP-2159] p0037 N81-16119
 Electron reflection and secondary emission
 characteristics of sputter-textured pyrolytic
 graphite surfaces
 [NASA-TN-81755] p0062 N81-22193
 Analytical prediction and experimental
 verification of performance at various operating
 conditions of a dual-mode traveling wave tube
 with multistage depressed collectors
 [NASA-TP-1331] p0072 N81-28352
 Performance of computer-designed small-sized
 four-stage depressed collector for operation of
 dual-mode traveling wave tube
 [NASA-TP-1832] p0072 N81-30360
 TRIBOLOGY
 Practical applications of surface analytic tools
 in tribology
 p0086 A 1-18739
 The generation and morphology of single-crystal
 silicon carbide wear particles under adhesive
 conditions
 p0064 A81-35045
 Frictional and morphological characteristics of
 ion plated soft, metallic films
 p0057 A81-38066
 The role of the micro environment on the
 tribological behavior of materials
 p0087 A81-46493
 Anisotropic tribological properties of silicon
 carbide
 [NASA-TN-81547] p0080 N81-11394
 Effects of erodant particle shape and various heat
 treatments on erosion resistance of plain carbon
 steel
 [NASA-TP-1755] p0052 N81-16210
 Tribological properties and thermal stability of
 various types of polyimide films
 [NASA-TN-81765] p0102 N81-23275
 Correlation of ideal and actual shear strengths of
 metals with their friction properties
 [NASA-TP-1891] p0063 N81-27282
 Relationship between the ideal tensile strength
 and the friction properties of metals in contact
 with nonmetals and themselves
 [NASA-TP-1883] p0063 N81-33293
 TRIGGERS
 U ACTUATORS
 TRIPROPELLANTS
 U LIQUID ROCKET PROPELLANTS
 TURBULENCE
 U MAINTENANCE
 TRUCKS
 Vehicle testing of Cummins turbocompound diesel
 engine
 [NASA-CN-159840] p0140 N81-13803
 TRUNCATION (MATHEMATICS)
 U APPROXIMATION
 TUBES
 U SHAFT (MACHINE ELEMENTS)
 TUBE CATHODES
 UT COLD CATHODES
 UT THERMIONIC CATHODES

TUNGSTEN

- Tungsten wire-reinforced superalloys for 1093 C (2000 F) turbine blade applications
[NASA-CR-159720] p0047 N81-10112
- Tungsten fiber reinforced superalloys: A status review
[NASA-TN-82590] p0045 N81-25148
- TUNGSTEN ALLOYS**
- Tungsten fiber reinforced superalloys - A status review
p0047 A81-44665

TUNING

- Effects of mistuning on bending-torsion flutter and response of a cascade in incompressible flow --- turbofan engines
[NASA-TN-81674] p0091 N81-16494
- Aeroelastic characteristics of a cascade of mistuned blades in subsonic and supersonic flows --- turbofan engines
[NASA-TN-82631] p0091 N81-26492

TURBINE RESISTORS**U RESISTORS****TURBINE BLADES**

- Development of low-cost directionally-solidified turbine blades
p0088 A81-10707
- Thermal barrier coatings for heat engine components
p0056 A81-1292C
- Heat transfer from a row of impinging jets to concave cylindrical surfaces
p0078 A81-24924
- Effects of mistuning on bending-torsion flutter and response of a cascade in incompressible flow [AIAA 81-0602] p0092 A81-29465
- Full potential solution of a transonic quasi-3-D flow through a cascade using artificial compressibility
[ASME PAPERS 81-GT-70] p0006 A81-29979
- Heat transfer coefficients for staggered arrays of short pin fins
[ASME PAPERS 81-GT-75] p0077 A81-29983
- Fabrication of injection molded sintered alpha SiC turbine components
[ASME PAPERS 81-GT-161] p0089 A81-30060
- Solution of plane cascade flow using improved surface singularity methods
[ASME PAPERS 81-GT-169] p0006 A81-30068
- Synergistic erosion/corrosion of superalloys in PFB coal combustor effluent
p0058 A81-44663
- Tungsten wire-reinforced superalloys for 1093 C (2000 F) turbine blade applications
[NASA-CR-159720] p0047 N81-10112
- Surface pyrometry in presence of radiation from other sources with application to turbine blade temperature measurement
[NASA-TP-1754] p0013 N81-11039
- Performance of a steel spar wind turbine blade on the Rod-0 100 kW experimental wind turbine
[NASA-TN-81588] p0096 N81-11448
- Low-cost directionally-solidified turbine blades, volume 2 --- TFE737-3 turbofan engine
[NASA-CR-159562] p0024 N81-12088
- Heat transfer coefficients for staggered arrays of short pin fins
[NASA-TN-81596] p0074 N81-13302
- An electrostatic analog for generating cascade grids
p0122 N81-14695
- Mean rotor wake characteristics of an aerodynamically loaded 0.5 m diameter fan
[NASA-TN-81657] p0015 N81-16053
- JT8D-15/17 high pressure turbine root discharged blade performance improvement --- engine design
[NASA-CR-165220] p0028 N81-17080
- Turbine blade temperature measurements using thin film temperature sensors
[NASA-CR-165201] p0059 N81-19277
- A sputtered zirconia primer for improved thermal shock resistance of plasma sprayed ceramic turbine seals
[NASA-TN-81732] p0062 N81-21198
- Evaluation of a method for heat transfer measurements and thermal visualization using a composite of a heater element and liquid crystals --- thermal performance of turbine blade cooling configurations
[NASA-TN-81639] p0075 N81-21313
- Thermal and flow analysis of a convection air-cooled ceramic coated porous metal concept

- for turbine vanes
[NASA-TN-81749] p0016 N81-22056
- Test evaluation of a laminated wood wind turbine blade concept
[NASA-TN-81719] p0104 N81-24535
- Lightning accommodation systems for wind turbine generator safety
[NASA-TN-82601] p0105 N81-24539
- Aeroelastic characteristics of a cascade of mistuned blades in subsonic and supersonic flows --- turbofan engines
[NASA-TN-82631] p0091 N81-26492
- Effects of blade-vane ratio and rotor-stator spacing of fan noise with forward velocity
[NASA-TN-82690] p0126 N81-31956
- TURBINE ENGINES**
- BT GAS TURBINE ENGINES**
- BT J-85 ENGINE**
- BT JET ENGINES**
- BT TURBOFAN ENGINES**
- BT TURBOJET ENGINES**
- BT TURBOPROP ENGINES**
- Fabrication of injection molded sintered alpha SiC turbine components
[ASME PAPER 81-GT-161] p0089 A81-30060
- Description of the wara core turbine facility and the wara annular cascade facility recently installed at NASA Lewis Research Center
[SAE PAPER 801122] p0031 A81-34158
- Turbine bypass engine - A new supersonic cruise propulsion concept
[AIAA PAPER 81-1596] p0023 A81-40971
- Off-design performance loss model for radial turbines with pivoting, variable-area stators
[NASA-TP-1708] p0013 N81-11038
- Superhybrid composite blade impact studies
[NASA-TN-81597] p0091 N81-11412
- Cost/benefit analysis of advanced materials technology candidates for the 1980's, part 2
[NASA-CR-165176] p0139 N81-11953
- Multivariable identification using centralized fixed modes
p0014 N81-12091
- General Aviation Turbine Engine (GATE) study
[NASA-CR-159482] p0029 N81-19117
- Ceramic applications in turbine engines --- for improved component performance and reduced fuel usage
[NASA-CR-159865] p0029 N81-19118
- Reasons for low aerodynamic performance of 13.5-centimeter-tip-diameter aircraft engine starter turbine
[NASA-TP-1810] p0016 N81-20076
- Analytical design of an advanced radial turbine --- automobile engines
[NASA-CR-165170] p0140 N81-20958
- Combustion system processes leading to corrosive deposits
[NASA-TN-81752] p0101 N81-23243
- Aviation turbine fuel properties and their trends
[NASA-TN-82603] p0066 N81-25232
- KOMPIC and REKCOMPIC: Two interactive preprocessing to the Navy/NASA Engine Program (NNEP)
[NASA-TN-82636] p0120 N81-25698
- Turbine bypass engine: A new supersonic cruise propulsion concept
[NASA-TN-82608] p0018 N81-26145
- TURBINE PUMPS**
- Self-acting geometry for noncontact seals
[ASLE PREPRINT 81-AM-5B-2] p0090 A81-33867
- Low-thrust chemical propulsion system pump technology
[NASA-CR-165210] p0088 N81-17437
- TURBINE WHEELS**
- Cyclic behavior of turbine disk alloys at 650 C
p0056 A81-12266
- TURBINES**
- BT AXIAL FLOW TURBINES**
- BT GAS TURBINES**
- BT SHROUDED TURBINES**
- BT STEAM TURBINES**
- Large wind-turbine projects in the United States wind energy program
p0106 A81-23694
- Performance of a steel spar wind turbine blade on the Rod-0 100 kW experimental wind turbine
[NASA-TN-81588] p0096 N81-11448

- The NASA-LeRC wind turbine sound prediction code
[NASA-TN-81737] p0100 N81-21537
Comparison of upwind and downwind rotor operations
of the DOE/NASA 100-kW Mod-0 wind turbine
[NASA-TN-81744] p0100 N81-22472
Tests of an overrunning clutch in a wind turbine
[NASA-TN-82653] p0107 N81-29528
- TURBOCHARGERS**
U SUPERCHARGERS
U TURBOCOMPRESSORS
TURBOCOMPRESSORS
Inlet flow distortion in turbomachinery
[ASME PAPER 80-GT-20] p0005 A81-17952
Supersonic stall flutter of high-speed fans
[ASME PAPER 81-GT-184] p0020 A81-30078
Vehicle testing of Cummins turbocompound diesel
engine
[NASA-CR-159840] p0140 N81-13803
Supersonic stall flutter of high speed fans --- in
turbofan engines
[NASA-TN-81613] p0003 N81-14978
Aerodynamic stability analysis of NASA
J85-13/planar pressure pulse generator
installation
[NASA-CR-165141] p0027 N81-15004
TF34 engine compression system computer study ---
simulation of flow stability
[NASA-CR-159889] p0027 N81-15005
Compressor exit stage study. Volume 2: Data
and performance report for the baseline
configuration
[NASA-CR-159498] p0027 N81-16051
Mastran level 16 theoretical manual updates for
aeroelastic analysis of bladed discs
[NASA-CR-159823] p0093 N81-19480
MASTRAN level 16 demonstration manual updates for
aeroelastic analysis of bladed discs
[NASA-CR-159826] p0093 N81-19483
- TURBOCONVERTERS**
U TURBOGENERATORS
TURBOELECTRIC CONVERSION
U TURBOGENERATORS
TURBOFAN AIRCRAFT
The supersonic fan engine: An advanced concept in
supersonic cruise propulsion
[NASA-TN-82657] p0018 N81-27094
- TURBOFAN ENGINES**
HT TF-34 ENGINE
The experimental verification of a streamline
curvature numerical analysis method applied to
the flow through an axial flow fan
[AIAA PAPER 81-0363] p0005 A81-20782
Core noise measurements from a small, general
aviation turbofan engine
[NASA-TN-81610] p0125 N81-11769
Design, durability and low cost processing
technology for composite fan exit guide vanes
[ASME PAPER 81-GT-203] p0030 A81-30093
An automated procedure for developing hybrid
computer simulations of turbofan engines
[NASA-TN-81605] p0037 N81-11688
Improved components for engine fuel savings
[SAB PAPER 801116] p0021 A81-34152
Performance deterioration of commercial
high-bypass ratio turbofan engines
[SAB PAPER 801118] p0021 A81-34154
A status report on the Energy Efficient Engine
Project
[SAB PAPER 801119] p0021 A81-34155
Effect of a part-span variable inlet guide vane on
the performance of a high-bypass turbofan engine
[AIAA PAPER 81-1362] p0022 A81-40842
JT9D performance deterioration results from a
simulated aerodynamic load test
[AIAA PAPER 81-1588] p0022 A81-40963
The supersonic fan engine - An advanced concept in
supersonic cruise propulsion
[AIAA PAPER 81-1599] p0023 A81-40973
The B3 combustors - Status and challenges
[AIAA PAPER 81-1353] p0023 A81-42176
Mixing effectiveness test of an exhaust gas mixer
in a high bypass turbofan at altitude
[AIAA PAPER 81-1495] p0023 A81-44225
Turbomachinery noise studies of the A18 research
QCAT engine with inflow control --- acoustic
performance
- [AIAA PAPER 81-2049] p0023 A81-48621
Effects of blade-vane ratio and rotor-stator
spacing on fan noise with forward velocity
[AIAA PAPER 81-2032] p0024 A81-48628
An automated procedure for developing hybrid
computer simulations of turbofan engines
[NASA-TN-81605] p0037 N81-11688
Core noise measurements from a small, general
aviation turbofan engine
[NASA-TN-81610] p0125 N81-11769
Low-cost directionally-solidified turbine blades,
volume 2 --- TF34-3 turbofan engine
[NASA-CR-159562] p0024 N81-12088
F100 multivariable control synthesis program: A
review of full scale engine altitude tests ---
F100 engine
[NASA-TN-81613] p0014 N81-12093
Engine identification for adaptive control
[NASA-TN-81613] p0025 N81-12100
Multivariable nyquist array method with application
to turbofan engine control
[NASA-TN-81613] p0026 N81-12101
Supersonic stall flutter of high speed fans --- in
turbofan engines
[NASA-TN-81613] p0003 N81-14978
Improved methods for fan sound field determination
[NASA-CR-165188] p0129 N81-15769
Effects of mistuning on bending-torsion flutter
and response of a cascade in incompressible flow
--- turbofan engines
[NASA-TN-81674] p0091 N81-16494
Samarium cobalt (SMCO) generator/engine
integration study
[AD-A092904] p0029 N81-17087
Integrated control system for a gas turbine engine
[NASA-CASE-LEU-12594-2] p0015 N81-19116
Design of an exhaust mixer nozzle for the
Avco-Lycoming Quiet Clean General Aviation
Turbofan (QCAT)
[NASA-CR-159426] p0029 N81-19120
An assessment of the use of antimisting fuel in
turbofan engines
[NASA-CR-165258] p0067 N81-19316
Exhaust emission survey of an F100 afterburning
turbofan engine at simulated altitude flight
conditions
[NASA-TN-81656] p0016 N81-21078
Energy efficient engine flight propulsion system:
Aircraft/engine integration evaluation
[NASA-CR-159584] p0030 N81-22051
Quiet Clean General Aviation Turbofan (QCAT)
technology study, volume 1
[NASA-CR-164222] p0030 N81-22052
Design concepts for low-cost composite turbofan
engine frame
[NASA-CR-165217] p0030 N81-22053
Investigation of performance deterioration of the
CF6/JT9D high bypass ratio turbofan engines
[NASA-TN-81656] p0016 N81-24086
Measurement of aerodynamic work during fan flutter
[NASA-TN-82652] p0017 N81-25080
Effect of a part-span variable inlet guide vane on
the performance of a high-bypass turbofan engine
[NASA-TN-82617] p0017 N81-25081
High-response measurements of a turbofan engine
during nonrecoverable stall
[NASA-TN-81759] p0017 N81-25084
Aeroelastic characteristics of a cascade of
stunted blades in subsonic and supersonic flows
--- turbofan engines
[NASA-TN-82631] p0091 N81-26492
New technique for the direct measurement of core
noise from aircraft engines --- TF 102 turbofan
engine
[NASA-TN-82634] p0126 N81-26844
The supersonic fan engine: An advanced concept in
supersonic cruise propulsion
[NASA-TN-82657] p0018 N81-27094
Mixing effectiveness test of an exhaust gas mixer
in a high bypass turbofan at altitude
[NASA-TN-82663] p0018 N81-27095
The B3 combustors: Status and challenges ---
energy efficient turbofan engines
[NASA-TN-82684] p0018 N81-28095
Conditioned pressure spectra and coherence
measurements in the core of a turbofan engine
[NASA-TN-82688] p0126 N81-30907
Advanced subsonic transport propulsion
[NASA-TN-82696] p0019 N81-31195

- Effects of blade-vane ratio and rotor-stator spacing of fan noise with forward velocity [NASA-TN-82690] p0126 N81-31956
- Turbomachinery noise studies of the AilResearch QCGAT engine with inflow control [NASA-TN-82694] p0127 N81-31957
- Acoustic performance of inlet suppressors on an engine generating a single mode [NASA-TN-82697] p0127 N81-32968
- TURBOPANS**
- Factors which influence the behavior of turbofan forced mixer nozzles [AIAA PAPER 81-0274] p0021 A81-32549
- TF34 engine compression system computer study --- simulation of flow stability [NASA-CN-159889] p0027 N81-15005
- Factors which influence the behavior of turbofan forced mixer nozzles [NASA-TN-81668] p0074 N81-15240
- Extended frequency turbofan model [NASA-CN-165261] p0030 N81-20078
- Rotor wake characteristics relevant to rotor-stator interaction noise generation [NASA-TN-82703] p0019 N81-30130
- TURBOGENERATORS**
- Stability of large horizontal-axis axisymmetric wind turbines [NASA-TN-81623] p0091 N81-12446
- TURBOJET ENGINE CONTROL**
- Engine identification for adaptive control p0025 N81-12100
- Multivariable nyquist array method with application to turbofan engine control p0026 N81-12101
- Integrated control system for a gas turbine engine [NASA-CASE-LEN-12594-2] p0015 N81-19116
- TURBOJET ENGINES**
- NT J-85 ENGINE
- NT TURBOFAN ENGINES
- NT TURBOPROP ENGINES
- The use of AntiKistling Kerosene (AKK) in turbojet engines p0009 N81-19063
- TURBOMACHINE BLADES**
- NT COMPRESSOR BLADES
- NT ROTOR BLADES (TURBOMACHINERY)
- NT STATOR BLADES
- NT TURBINE BLADES
- Superhybrid composite blade impact studies [ASME PAPER 81-GT-24] p0020 A81-29940
- Supersonic stall flutter of high speed fans --- in turbofan engines [NASA-TN-81613] p0003 N81-14978
- Solution of plane cascade flow using improved surface singularity methods --- application of panel method to internal aerodynamics [NASA-TN-81589] p0003 N81-14979
- Aerodynamic stability analysis of NASA J85-13/planar pressure pulse generator installation [NASA-CN-165141] p0027 N81-15004
- Effects of mistuning on bending-torsion flutter and response of a cascade in incompressible flow --- turbofan engines [NASA-TN-81674] p0091 N81-16494
- MASTRAN level 16 user's manual updates for aeroelastic analysis of bladed discs [NASA-CN-159824] p0093 N81-19481
- MASTRAN level 16 programmer's manual updates for aeroelastic analysis of bladed discs [NASA-CN-159825] p0093 N81-19482
- Improved method for calculating transonic velocities on blade-to-blade stream surfaces of a turbomachine [NASA-TP-1772] p0004 N81-22017
- TURBOMACHINERY**
- NT AXIAL FLOW TURBINES
- NT GAS TURBINES
- NT SHROUDED TURBINES
- NT STEAM TURBINES
- NT TURBINE PUMPS
- NT TURBINES
- NT TURBOCOMPRESSORS
- NT TURBOPANS
- NT TURBOGENERATORS
- Fast Generation of body conforming grids for 3-D p0122 N81-14706
- Geometric methods in computational fluid dynamics --- turbomachinery
- A rapid perturbation procedure for determining nonlinear flow solutions: Application to transonic turbomachinery flows [NASA-CN-3425] p0001 N81-22012
- Turbomachinery noise studies of the AilResearch QCGAT engine with inflow control [NASA-TN-82694] p0127 N81-31957
- TURBOPROP AIRCRAFT**
- The NASA high-speed turboprop program [SAE PAPER 801120] p0021 A81-34156
- Low and high speed propellers for general aviation: Performance potential and recent wind tunnel test results [NASA-TN-81745] p0003 N81-21028
- TURBOPROP ENGINES**
- The NASA high-speed turboprop program [SAE PAPER 801120] p0021 A81-34156
- Factors influencing the predicted performance of advanced propeller designs [AIAA PAPER 81-1564] p0007 A81-42210
- Laser-velocimeter flow-field measurements of an advanced turboprop [AIAA PAPER 81-1568] p0007 A81-42211
- Low and high speed propellers for general aviation - Performance potential and recent wind tunnel test results p0023 A81-42758
- Laser-velocimeter flow-field measurements of an advanced turboprop [NASA-TN-82677] p0004 N81-27041
- TURBOPUMPS**
- U TURBINE PUMPS
- TURBOPUMP**
- U TURBINE WHEELS
- TURBULENCE EFFECTS**
- Factors which influence the behavior of turbofan forced mixer nozzles [AIAA PAPER 81-0274] p0021 A81-32549
- TURBULENT BOUNDARY LAYER**
- Three-dimensional turbulent boundary layer development and separation in V/STOL engine inlets at incidence with small-cross flow and curvature influences [AIAA PAPER 81-0254] p0005 A81-20703
- Boundary layer development on turbine airfoil suction surfaces [ASME PAPER 81-GT-204] p0008 A81-30094
- TURBULENT FLOW**
- Turbulent solution of the Navier-Stokes equations p0077 A81-19284
- Calculation of three-dimensional turbulent subsonic flows in transition ducts p0008 A81-21199
- Turbulent solution of the Navier-Stokes equations [NASA-TN-81621] p0074 N81-12358
- Prediction of laminar and turbulent primary and secondary flows in strongly curved ducts [NASA-CN-3388] p0007 N81-16976
- A three-dimensional turbulent compressible subsonic duct flow analysis for use with constructed coordinate systems [NASA-CN-3389] p0077 N81-20383
- TURBULENT HEAT TRANSFER**
- Full-coverage film cooling. I - Three-dimensional measurements of turbulence structure. II - Prediction of the recovery-region hydrodynamics p0078 A81-15537
- TURBULENT MIXERS**
- The propeller tip vortex. A possible contributor to aircraft cabin noise [NASA-TN-81768] p0130 N81-22838
- Rotor wake characteristics relevant to rotor-stator interaction noise generation [NASA-TN-82703] p0019 N81-30130
- TWO DIMENSIONAL BODIES**
- Extended frequency turbofan model [NASA-CN-165261] p0030 N81-20078
- TWO DIMENSIONAL BOUNDARY LAYER**
- Some modifications to, and operational experiences with, the two-dimensional, finite-difference, boundary-layer code, STAN5 [ASME PAPER 81-GT-89] p0077 A81-29996
- TWO DIMENSIONAL FLOW**
- Flow separation in inlets at incidence angles p0006 A81-29114
- TWO PHASE FLOW**
- Depressurization and two-phase flow of water containing high levels of dissolved nitrogen gas

U TUBES

SUBJECT INDEX

[NASA-TP-1839]

p0076 N81-28389

U

U TUBES

U MANOMETERS

ULTRAHIGH VACUUM

The adhesion, friction, and wear of binary alloys
in contact with single-crystal silicon carbide
[ASME PAPER 80-C2/LUB-53] p0086 A81-18695

ULTRASONIC FLAW DETECTION

Ultrasonic measurement of material properties
p0090 A81-19656

ULTRASONIC TESTS

Ultrasonic measurement of material properties
p0090 A81-19656

ULTRASONIC WAVE TRANSDUCERS

Acousto-ultrasonic characterization of fiber
reinforced composites
p0090 A81-44660

ULTRASONICS

Acousto-ultrasonic characterization of fiber
reinforced composites
[NASA-TN-82651] p0090 N81-28458

UNITED STATES OF AMERICA

UT ILLINOIS

UT INDIANA

UT IOWA

UT MINNESOTA

UT MISSISSIPPI

UT MISSOURI

UT MONTANA

UT NORTH DAKOTA

UT SOUTH DAKOTA

UNSTEADY FLOW

Application of unsteady airfoil theory to rotary
wings
p0006 A81-39874

UPPER SURFACE BLOWING

Comparison of NASA and contractor results from
aeroacoustic tests of CSEER OTW engine
[NASA-TN-81761] p0017 N81-25079

URBAN AREAS

U CITIES

USER MANUALS (COMPUTER PROGRAMS)

Limited Area Coverage/High Resolution Picture
Transmission (LAC/HRPT) tape IJ grid pixel
extraction processor user's manual
[E81-10072] p0094 N81-13428

Limited Area Coverage/High Resolution Picture
Transmission (LAC/HRPT) data vegetative index
calculation processor user's manual
[E81-10073] p0094 N81-13429

Limited Area Coverage/high Resolution Picture
Transmission, LAC/HRPT tape conversion processor
user's manual
[E81-10077] p0095 N81-13433

Turbine modeling technique to generate off-design
performance data for both single and multistage
axial-flow turbines
[NASA-CR-165244] p0027 N81-17078

NASTRAN level 16 user's manual updates for
aeroelastic analysis of bladed discs
[NASA-CR-159824] p0093 N81-19481

NASTRAN level 16 demonstration manual updates for
aeroelastic analysis of bladed discs
[NASA-CR-159826] p0093 N81-19483

UTILITIES

Status of commercial phosphoric acid fuel cell
system development
[AIAA PAPER 81-0396] p0108 A81-20805
Study of fuel cell on-site, integrated energy
systems in residential/commercial applications
[NASA-CR-165144] p0112 N81-21533

UTILIZATION

UT COAL UTILIZATION

UT LASER FUSION

UT WINDPOWER UTILIZATION

V

V BAND

V EXTREMELY HIGH FREQUENCIES

V/STOL AIRCRAFT

VT HELICOPTERS

VT SHORT TAKEOFF AIRCRAFT

Three-dimensional turbulent boundary layer
development and separation in V/STOL engine
inlets at incidence with small-cross flow and

curvature influences

[AIAA PAPER 81-0254] p0005 A81-20703

Future challenges in V/STOL flight propulsion

control integration p0022 A81-34170

[SAB PAPER 801140]

Propulsion system mathematical model for a

lift/cruise fan V/STOL aircraft p0015 N81-16055

[NASA-TN-81663]

VACANCIES (CRYSTAL DEFECTS)

Radiation damage annealing mechanisms and possible

low temperature annealing in silicon solar cells

p0040 A81-27207

VACUUM

VT ULTRAHIGH VACUUM

VACUUM APPARATUS

VT VACUUM GAGES

VACUUM GAGES

Gauge calibration system based on piston manometer

p0079 A81-48950

VACUUM BELTING

Comparisons of modified Vasco X-2 and AISI 9310

gear steels

[NASA-TP-1731] p0080 N81-14322

VACUUM SYSTEMS

Gauge calibration system based on piston manometer

p0079 A81-48950

VACUUM TUBE OSCILLATORS

VT KLYSTRONS

VT MICROWAVE TUBES

VT TRAVELING WAVE TUBES

VACUUM TUBES

VT KLYSTRONS

VT MICROWAVE TUBES

VT TRAVELING WAVE TUBES

VALVES

VT PRESSURE REGULATORS

VT RELIEF VALVES

VANADIUM ALLOYS

Effects of geometric variables on rub

characteristics of Ti-6Al-4V

[NASA-TP-1835] p0053 N81-20245

VANES

VT GUIDE VANES

VANS

V TRUCKS

VAPOR DEPOSITION

CVD-produced boron filaments

p0048 A81-11336

Ion plating for the future

[NASA-TN-82630] p0054 N81-25189

VAPORIZING

VT COAL GASIFICATION

VT NUCLEATE BOILING

VT PREVAPORIZATION

A study of external fuel vaporization --- for

aircraft gas turbine engines

[ASME PAPER 81-GT-158] p0020 A81-30057

VARIABLES

Backward deletion to minimize prediction errors in

models from factorial experiments with zero to

six center points

[NASA-TN-81524] p0123 N81-10778

Design studies of continuously variable

transmissions for electric vehicles

[NASA-TN-81642] p0080 N81-13357

VARIABLE CYCLE ENGINES

Model aerodynamic test results for two variable

cycle engine coannular exhaust systems at

simulated takeoff and cruise conditions ---

Lewis 8 by 6-foot supersonic wind tunnel tests

[NASA-CR-159818] p0026 N81-13057

Model aerodynamic test results for two variable

cycle engine coannular exhaust systems at

simulated takeoff and cruise conditions.

Comprehensive data report. Volume 1: Design

layouts

[NASA-CR-159819-VOL-1] p0028 N81-17081

Model aerodynamic test results for two variable

cycle engine coannular exhaust systems at

simulated takeoff and cruise conditions.

Comprehensive data report. Volume 2: Tabulated

aerodynamic data book 1

[NASA-CR-159819-VOL-2-BK-1] p0028 N81-17082

Model aerodynamic test results for two variable

cycle engine coannular exhaust systems at

simulated takeoff and cruise conditions.

Comprehensive data report. Volume 2: Tabulated

aerodynamic data book 2

[NASA-CR-159819-VOL-2-BK-2] p0028 N81-17083

- Model aerodynamic test results for two variable cycle engine annular exhaust systems at simulated takeoff and cruise conditions. Comprehensive data report. Volume 2: Tabulated aerodynamic data book 3 [NASA-CR-159819-VOL-2-BK-3] p0028 N81-17084
- Model aerodynamic test results for two variable cycle engine annular exhaust systems at simulated takeoff and cruise conditions. Comprehensive data report. Volume 3: Graphical data book 1 [NASA-CR-159819-VOL-3-BK-1] p0028 N81-17085
- Model aerodynamic test results for two variable cycle engine annular exhaust systems at simulated takeoff and cruise conditions. Comprehensive data report. Volume 3: Graphical data book 2 [NASA-CR-159819-VOL-3-BK-2] p0028 N81-17086
- Aerodynamic/acoustic performance of XJ101/double bypass VCE with annular plug nozzle [NASA-CR-159809] p0129 N81-17846
- VCE early acoustic test results of General Electric's high-radius ratio annular plug nozzle p0029 N81-17999
- VARIABLE GEOMETRY STRUCTURES**
- Acoustic transmission matrix of a variable area duct or nozzle carrying a compressible subsonic flow p0128 A81-22533
- Application of 'steady' state finite element and transient finite difference theory to sound propagation in a variable duct - A comparison with experiment [AIAA PAPER 81-2016] p0128 A81-48622
- Off-design performance loss model for radial turbines with pivoting, variable-area stators [NASA-TP-1708] p0013 N81-11038
- VARIABLE STREAM CONTROL ENGINES**
- Design of a multivariable integrated control for a supersonic propulsion system --- variable stream control engine p0025 N81-12094
- Variable stream control engine for advanced supersonic aircraft design update p0001 N81-17996
- Progress with variable cycle engines p0001 N81-17997
- VARIANCE (STATISTICS)**
- NT REGRESSION ANALYSIS**
- VCE**
- U VARIABLE CYCLE ENGINES**
- VECTOR ANALYSIS**
- NT COPLANARITY**
- VECTOR SPACES**
- NT EIGENVALUES**
- VEGETABLES**
- NT POTATOES**
- VEGETATION**
- Limited Area Coverage/High Resolution Picture Transmission (LAC/HAPT) data vegetative index calculation processor user's manual [N81-10073] p0094 N81-13429
- VELOCITY**
- NT CRITICAL VELOCITY**
- NT FLOW VELOCITY**
- NT SUPERSONIC SPEEDS**
- NT TRANSONIC SPEED**
- VELOCITY DISTRIBUTION**
- The effect of inflow velocity profiles on the performance of supersonic ejector nozzles [NASA-TN-81673] p0075 N81-16421
- Improved method for calculating transonic velocities on blade-to-blade stream surfaces of a turbomachine [NASA-TP-1772] p0004 N81-22017
- VELOCITY FIELDS**
- U VELOCITY DISTRIBUTION**
- VELOCITY MEASUREMENT**
- Beam rotor wake characteristics of an aerodynamically loaded 0.5 m diameter fan [AIAA PAPER 81-0208] p0006 A81-20830
- Beam rotor wake characteristics of an aerodynamically loaded 0.5 m diameter fan [NASA-TN-81657] p0015 N81-16053
- VELOCITY PROFILES**
- U VELOCITY DISTRIBUTION**
- VIBRATION**
- NT BENDING VIBRATION**
- NT FLUTTER**
- NT STRUCTURAL VIBRATION**
- NT SUBSONIC FLUTTER**
- NT SUPERSONIC FLUTTER**
- NT TRANSONIC FLUTTER**
- VIBRATION TESTS**
- Effects of mistuning on blade torsional flutter p0092 A81-29095
- VINYL POLYMERS**
- NT POLYVINYL FLUORIDE**
- VISCOUS DAMPING**
- Multiple plate hydrostatic viscous damper [NASA-CASR-LBN-12445-1] p0083 N81-22360
- VISCOUS FLOW**
- NT BOUNDARY LAYER FLOW**
- NT BOUNDARY LAYER SEPARATION**
- NT SECONDARY FLOW**
- NT SEPARATED FLOW**
- Calculation of the flow field in supersonic inlets using a bi-characteristics method with shock wave fitting p0006 A81-21212
- Generation of C-type cascade grids for viscous flow computation p0122 N81-14721
- Numerical simulation of flows in curved diffusers with cross-sectional transmuting using a three-dimensional viscous analysis [NASA-TN-81672] p0074 N81-15239
- VISUALIZATION OF FLOW**
- U FLOW VISUALIZATION**
- VOICE COMMUNICATION**
- NT TELEPHONE**
- VOLATILIZATION**
- U VAPORIZING**
- VOLT-AMPERE CHARACTERISTICS**
- Silicon solar cells with high open-circuit voltage p0113 A81-27089
- Space solar cells - High efficiency and radiation damage p0108 A81-27174
- VOLTAGE**
- U ELECTRIC POTENTIAL**
- VOLTAGE CONVERTERS (DC TO DC)**
- Application handbook for a Standardized Control Module (SCM) for DC-DC converters, volume 1 [NASA-CR-165172] p0072 N81-10301
- User's design handbook for a Standardized Control Module (SCM) for DC to DC Converters, volume 2 [NASA-CR-165173] p0072 N81-11314
- VOLTAGE GENERATORS**
- NT PHOTOVOLTAIC CELLS**
- VOLTAGE MEASUREMENT**
- U ELECTRICAL MEASUREMENT**
- VOLTAGE VARIATION INDICATORS**
- U VOLTMETERS**
- VOLTMETERS**
- Environmental charging effects monitors for operational satellites [NASA-TN-81669] p0037 N81-17127
- VORTEX COLUMNS**
- U VORTICES**
- VORTEX DISTURBANCES**
- U VORTICES**
- VORTEX FLOW**
- U VORTICES**
- VORTEX GENERATION**
- U VORTEX GENERATORS**
- VORTEX GENERATORS**
- Factors which influence the behavior of turbofan forced mixer nozzles [NASA-TN-81668] p0074 N81-15240
- VORTEX SHEDDING**
- Fluid mechanics mechanisms in the stall process of helicopters [NASA-TN-81956] p0003 N81-21027
- VORTEX TUBES**
- U VORTICES**
- VORTICES**
- The coupling between flow instabilities and incident disturbances at a leading edge p0010 A81-28682
- Factors which influence the behavior of turbofan forced mixer nozzles [AIAA PAPER 81-0274] p0021 A81-32549
- The propeller tip vortex. A possible contributor to aircraft cabin noise [NASA-TN-81768] p0130 N81-22838

W

WAPERS

An experimental investigation of silicon wafer surface roughness and its effect on the pull-strength of plated films p0109 A81-38063

High voltage planar multijunction --- solar cells [NASA-CASE-LEW-13400-1] p0098 A81-16528

High voltage V-groove solar cell [NASA-CASE-LEW-13401-1] p0098 A81-16529

Electrostatic bonding of thin (cycle sine 3 mil) 7070 cover glass to Ta2O5 Al-Coated thin (cycle sine 2 mil) silicon wafers and solar cells [NASA-CR-165240] p0111 A81-16582

WAKES

NT AIRCRAFT WAKES

NT HELICOPTER WAKES

NT TURBULENT WAKES

Mean rotor wake characteristics of an aerodynamically loaded 0.5 m diameter fan [AIAA PAPER 81-0208] p0006 A81-20830

WALL TEMPERATURE

Analysis for predicting adiabatic wall temperatures with single hole coolant injection into a low speed crossflow [ASME PAPER 81-GT-91] p0077 A81-29998

Curved film cooling addition tube [NASA-CASE-LEW-13174-1] p0074 A81-12363

Analysis for predicting adiabatic wall temperatures with single hole coolant injection into a low speed crossflow [NASA-TN-81620] p0074 A81-13301

WALLS

NT POROUS WALLS

WAKEFIELD REQUIREMENTS

Experimental analysis of IHFP in a rotary combustion engine --- Indicated Mean Effective Pressure [SAR PAPER 810150] p0079 A81-41732

WARMING

U HEATING

WATER FLOW

Acceleration wave breakup of liquid jets with airstreams [NASA-TN-81717] p0075 A81-21310

WATTMETERS

Specifying and calibrating instrumentations for wideband electronic power measurements --- in switching circuits [NASA-TN-81545] p0079 A81-16429

WAVE ATTENUATION

NT ACOUSTIC ATTENUATION

NT SHOCK WAVE ATTENUATION

WAVE PROPAGATION

NT ACOUSTIC PROPAGATION

WAVE REFLECTION

Note on reflection and transmission coefficients for converging-diverging ducts [NASA-TN-82679] p0126 A81-30906

WAVE SCATTERING

NT ACOUSTIC SCATTERING

WAVEFORMS

Acousto-ultrasonic characterization of fiber reinforced composites p0090 A81-44660

Response of nickel to zinc cells to electric vehicle chopper discharge waveforms [NASA-TN-81713] p0103 A81-23608

Acousto-ultrasonic characterization of fiber reinforced composites [NASA-TN-82651] p0090 A81-28458

WAVEGUIDES

K-band high power latching switch --- communication satellite system [NASA-CR-165159] p0073 A81-16389

Ladder supported ring bar circuit [NASA-CASE-LEW-13570-1] p0071 A81-24348

WAVELENGTHS

Surface pyrometry in presence of radiation from other sources with application to turbine blade temperature measurement [NASA-TP-1754] p0013 A81-11039

WEAR

Effects of geometric variables on rub characteristics of Ti-6Al-4V [NASA-TR-1835] p0053 A81-20245

Fretting wear and fretting fatigue: How are they related? [NASA-TN-82633] p0054 A81-26235

Surface films and metallurgy related to lubrication and wear [NASA-TN-82645] p0083 A81-27523

WEAR TESTS

Tribological properties of silicon carbide in metal removal process p0085 A81-17900

Friction and wear results from sputter-deposited chrome oxide with and without nichrome metallic binders and interlayers [ASME PAPER 80-C2/LUB-49] p0089 A81-18693

The adhesion, friction, and wear of binary alloys in contact with single-crystal silicon carbide [ASME PAPER 80-C2/LUB-53] p0086 A81-18695

Effect of substrate surface finish on the lubrication and failure mechanisms of molybdenum disulfide films [ASLE PREPRINT 81-AM-5D-1] p0064 A81-33859

The generation and morphology of single-crystal silicon carbide wear particles under adhesive conditions p0064 A81-35045

The role of the micro environment on the tribological behavior of materials p0087 A81-46493

Effect of load, area of contact, and contact stress on the wear mechanisms of a bonded solid lubricant film [NASA-TN-81563] p0060 A81-12226

Evaluation of boundary lubricants using steady-state wear and friction [NASA-TN-81601] p0061 A81-17265

WEIGHT (MASS)

NT STRUCTURAL WEIGHT

WEIGHTLESSNESS

Requirements and preliminary concept of a Zero-Gravity Combustion Facility for Spacelab [AIAA PAPER 81-0165] p0032 A81-20642

Overview study of combustion experiments in a space laboratory p0032 A81-46059

Materials processing in space: Future technology trends p0143 A81-12991

WELDED JOINTS

Mechanical properties of weldments in experimental Fe-12Mn-0.2Ti and Fe-12Mn-1Mo-0.2Ti alloys for cryogenic service p0058 A81-48143

WELDING

NT COLD WELDING

WHEAT

Numerical trials of HISSE [E81-10069] p0094 A81-13425

Normal crop calendars. Volume 2: The spring wheat states of Minnesota, Montana, North Dakota, and South Dakota [E81-10070] p0094 A81-13426

Preliminary evaluation of the Environmental Research Institute of Michigan crop calendar shift algorithm for estimation of spring wheat development stage --- North Dakota, South Dakota, Montana, and Minnesota [E81-10071] p0094 A81-13427

Normal crop calendars. Volume 1: Assembly and application of historical crop data to a standard product [E81-10075] p0095 A81-13431

WHEELS

NT TURBINE WHEELS

WHIRL INSTABILITY

U ROTARY STABILITY

WIDEBAND

U BECDBAND

WIND ENERGY

U WINDPOWER UTILIZATION

WIND TUNNEL MODELS

An experimental study of transmission, reflection and scattering of sound in a free jet flight simulation facility and comparison with theory p0129 A81-28943

WIND TUNNEL TESTS

Low and high speed propellers for general aviation - Performance potential and recent wind tunnel test results p0023 A81-42758

- Effects of blade-vane ratio and rotor-stator spacing on fan noise with forward velocity [AIAA PAPER 81-2032] p0024 A81-48628
- Low-speed aerodynamic performance of 50.8-centimeter-diameter noise-suppressing inlets for the Quiet, Clean, Short-haul Experimental Engine (QCSSE) --- Lewis 9- by 15-foot low speed wind tunnel tests [NASA-TP-1178] p0013 N81-11037
- Model aerodynamic test results for two variable cycle engine coaxial exhaust systems at simulated takeoff and cruise conditions --- Lewis 8 by 6-foot supersonic wind tunnel tests [NASA-CR-159818] p0026 N81-13057
- Model aerodynamic test results for two variable cycle engine coaxial exhaust systems at simulated takeoff and cruise conditions. Comprehensive data report. Volume 1: Design layouts [NASA-CR-159819-VOL-1] p0028 N81-17081
- Model aerodynamic test results for two variable cycle engine coaxial exhaust systems at simulated takeoff and cruise conditions. Comprehensive data report. Volume 2: Tabulated aerodynamic data book 1 [NASA-CR-159819-VOL-2-BK-1] p0028 N81-17082
- Model aerodynamic test results for two variable cycle engine coaxial exhaust systems at simulated takeoff and cruise conditions. Comprehensive data report. Volume 2: Tabulated aerodynamic data book 2 [NASA-CR-159819-VOL-2-BK-2] p0028 N81-17083
- Model aerodynamic test results for two variable cycle engine coaxial exhaust systems at simulated takeoff and cruise conditions. Comprehensive data report. Volume 2: Tabulated aerodynamic data book 3 [NASA-CR-159819-VOL-2-BK-3] p0028 N81-17084
- Model aerodynamic test results for two variable cycle engine coaxial exhaust systems at simulated takeoff and cruise conditions. Comprehensive data report. Volume 3: Graphical data book 1 [NASA-CR-159819-VOL-3-BK-1] p0028 N81-17085
- Model aerodynamic test results for two variable cycle engine coaxial exhaust systems at simulated takeoff and cruise conditions. Comprehensive data report. Volume 3: Graphical data book 2 [NASA-CR-159819-VOL-3-BK-2] p0028 N81-17086
- Survey of aircraft icing simulation test facilities in North America [NASA-TN-81707] p0009 N81-19078
- Low and high speed propellers for general aviation: Performance potential and recent wind tunnel test results [NASA-TN-81745] p0003 N81-21028
- Rotor wake characteristics relevant to rotor-stator interaction noise generation [NASA-TN-82703] p0019 N81-30130
- Effects of blade-vane ratio and rotor-stator spacing of fan noise with forward velocity [NASA-TN-82690] p0126 N81-31956
- WINDING**
WT WIRE WINDING
WINDMILLS (WINDPOWERED MACHINES)
Large wind turbines: A utility option for the generation of electricity p0142 N81-12981
- Comparison of upwind and downwind rotor operations of the DOE/NASA 100-kW Mod-0 wind turbine [NASA-TN-81744] p0100 N81-22472
- WINDPOWER UTILIZATION**
Stability of large horizontal-axis axisymmetric wind turbines [NASA-TN-81623] p0091 N81-12446
- Comparison of upwind and downwind rotor operations of the DOE/NASA 100-kW Mod-0 wind turbine [NASA-TN-81744] p0100 N81-22472
- The Mod-2 wind turbine development project [NASA-TN-82681] p0106 N81-27606
- Reliability and quality assurance on the MOD 2 wind system [NASA-TN-82717] p0090 N81-33492
- WINDPOWERED GENERATORS**
Stability of large horizontal-axis axisymmetric wind turbines p0092 N81-22526
- Large wind-turbine projects in the United States wind energy program p0100 A81-23694
- Performance of a steel spar wind turbine blade on the Mod-0 100 kW experimental wind turbine [NASA-TN-81588] p0096 N81-11448
- Data acquisition and analysis in the DOE/NASA Wind Energy Program [NASA-TN-81603] p0096 N81-13463
- The NASA-LeRC wind turbine sound prediction code [NASA-TN-81737] p0100 N81-21537
- Lightning accommodation systems for wind turbine generator safety [NASA-TN-82601] p0105 N81-24539
- The Mod-2 wind turbine development project [NASA-TN-82681] p0106 N81-27606
- Tests of an overrunning clutch in a wind turbine [NASA-TN-82653] p0107 N81-29528
- Reliability and quality assurance on the MOD 2 wind system [NASA-TN-82717] p0090 N81-33492
- WINDPOWERED PUMPS**
Low-thrust chemical propulsion system pump technology [NASA-CR-165210] p0088 N81-17437
- WINGS**
WT BCTARY WINGS
Evaluation of a pneumatic boot deicing system on a general aviation wing model [NASA-TN-82363] p0011 N81-25065
- GRID30: Computer program for fast generation of multilevel, three-dimensional boundary-conforming O-type computational grids [NASA-TP-1920] p0005 N81-31128
- WIRE WINDING**
Analysis and design of an adaptive multi-loop controlled two winding buck/boost regulator p0073 A81-21675
- WOOD**
Test evaluation of a laminated wood wind turbine blade concept [NASA-TN-81719] p0104 N81-24535
- WRAPAROUND CONTACT SOLAR CELLS**
U SOLAR CELLS
- X**
- X RAY SPECTROGRAPHY**
U X RAY SPECTROSCOPY
X RAY SPECTROMETRY
U X RAY SPECTROSCOPY
X RAY SPECTROSCOPY
The transfer of polytetrafluoroethylene studied by X-ray photoelectron spectroscopy p0087 A81-31238
- Polytetrafluoroethylene transfer film studied with X-ray photoelectron spectroscopy [NASA-TP-1728] p0060 N81-11214
- XENON**
Performance of a magnetic multipole line-cusp argon ion thruster [AIAA PAPER 81-0745] p0041 A81-38071
- Y**
- YIELD**
Preliminary evaluation of the Environmental Research Institute of Michigan crop calendar shift algorithm for estimation of spring wheat development stage --- North Dakota, South Dakota, Montana, and Minnesota [81-10071] p0094 N81-13427
- YJ-85 ENGINE**
U J-85 ENGINE
YTIUM
Effect of Yttria additives on properties of pressureless-sintered silicon nitride [NASA-TP-1899] p0063 N81-31366
- YTIUM COMPOUNDS**
WT YTIUM OXIDES
YTIUM OXIDES
Thermal barrier coatings - Burner rig hot corrosion test results p0063 A81-12630
- Microstructure and mechanical properties of bulk and plasma-sprayed Y₂O₃-partially stabilized zirconia [NASA-CR-165120] p0059 N81-22158

Z

ZERO GRAVITY

U WEIGHTLESSNESS
ZINC NICKEL BATTERIES
U NICKEL ZINC BATTERIES
ZINC SILVER BATTERIES
U SILVER ZINC BATTERIES
ZINC SILVER OXIDE BATTERIES
U SILVER ZINC BATTERIES
ZIRCONIUM

The effect of zirconium on the cyclic oxidation of
NiCrAl alloys

p0056 A81-18559

NiCrAl ternary alloy having improved cyclic
oxidation resistance

[NASA-CASE-LEW-13339-1]

p0051 A81-12211

ZIRCONIUM CARBIDES

Zirconium carbide as an electrocatalyst for the
chromous/chromic redox couple

[NASA-CASE-LEW-13246-1]

p0049 A81-26203

ZIRCONIUM COMPOUNDS

HT ZIRCONIUM CARBIDES

HT ZIRCONIUM OXIDES

ZIRCONIUM OXIDES

Thermal barrier coatings - Burner rig hot
corrosion test results

p0063 A81-12630

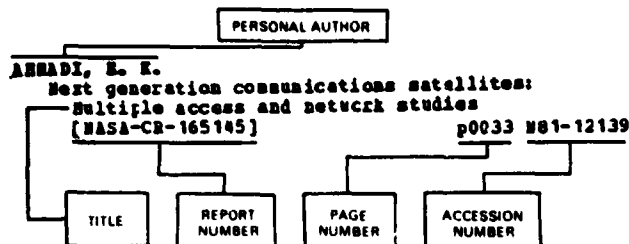
Microstructure and mechanical properties of bulk
and plasma-sprayed γ - ZrO_2 -partially stabilized
zirconia

[NASA-CR-165126]

p0059 A81-22158

PERSONAL AUTHOR INDEX

Typical Personal Author Index Listing



Listings in this index are arranged alphabetically by personal author. The title of the document provides the user with a brief description of the subject matter. The report number helps to indicate the type of document listed (e.g., NASA report, translation, NASA contractor report). The page and accession numbers are located beneath and to the right of the title. Under any one author's name the accession numbers are arranged in sequence with the /A4 accession numbers appearing first.

A

- ABBOTT, J. E.**
Low-speed aerodynamic performance of
50.8-centimeter-diameter noise-suppressing
inlets for the Quiet, Clean, Short-haul
Experimental Engine (QCSEE)
[NASA-TP-1178] p0013 N81-11037
Comparison of integrated Gasifier-Combined Cycle
and AFB-steam turbine systems for industrial
cogeneration
[NASA-TN-82648] p0106 N81-28522
- ABRAHAM, E. E.**
Moderate temperature sodium cells. I - Transition
metal disulfide cathodes
p0113 N81-15027
- ADAMCZYK, J.**
Full potential solution of a transonic quasi-3-D
flow through a cascade using artificial
compressibility
[ASME PAPER 81-GT-70] p0006 N81-29979
- ADAMCZYK, J. J.**
Inlet flow distortion in turbomachinery
[ASME PAPER 80-GT-20] p0005 N81-17952
Supersonic stall flutter of high-speed fans
[ASME PAPER 81-GT-184] p0020 N81-30078
An electrostatic analog for generating cascade grids
p0122 N81-14655
Supersonic stall flutter of high speed fans
[NASA-TN-81613] p0003 N81-14978
- AGARWAL, P. K.**
Ion beam texturing of heat transfer surfaces
[AIAA PAPER 81-0670] p0086 N81-29531
- ABRAHAM, E. E.**
Next generation communications satellites:
Multiple access and network studies
[NASA-CR-165145] p0033 N81-12139
- ABUJA, K. E.**
An experimental study of transmission, reflection
and scattering of sound in a free jet flight
simulation facility and comparison with theory
p0129 N81-28943
- AGERMAN, H.**
Computer-aided roll pass design in rolling of
airfoil shapes
p0088 N81-15796
- ALBRIGHT, A. E.**
Evaluation of a pneumatic boot deicing system on a
general aviation wing model
[NASA-TN-82363] p0311 N81-25065
- ALEXANDER, A.**
Interactive multi-node blade impact analysis
[ASME PAPER 81-GT-79] p0030 N81-29987

- ALGER, D. L.**
Applicability of advanced automotive heat engines
to solar thermal power
[NASA-TN-81658] p0097 N81-14397
- ALLEN, G. P.**
Self-acting geometry for noncontact seals
[ASLE PAPER 81-AM-5B-2] p0090 N81-33867
Self-acting geometry for noncontact seals
[NASA-TN-81659] p0081 N81-16474
A sputtered zirconia primer for improved thermal
shock resistance of plasma sprayed ceramic
turbine seals
[NASA-TN-81732] p0062 N81-21198
- ALLER, H.**
Automotive Stirling engine development program
[NASA-CR-165134] p0139 N81-11952
- ALLISON, J. F.**
Thin n-i-p silicon solar cell
p0114 N81-27097
- ALTAN, T.**
Computer-aided roll pass design in rolling of
airfoil shapes
p0088 N81-15796
- ANDERSON, B. E.**
Factors which influence the behavior of turbofan
forced mixer nozzles
[AIAA PAPER 81-0274] p0021 N81-32549
Numerical simulation of flows in curved diffusers
with cross-sectional transitioning using a
three-dimensional viscous analysis
[NASA-TN-81672] p0074 N81-15239
Factors which influence the behavior of turbofan
forced mixer nozzles
[NASA-TN-81668] p0074 N81-15240
Application of computer generated color graphic
techniques to the processing and display of
three dimensional fluid dynamic data
[NASA-TN-82658] p0119 N81-29782
- ANDERSON, D. E.**
Ultra-lean combustion at high inlet temperatures
[ASME PAPER 81-GT-44] p0086 N81-29958
Ultra-lean combustion at high inlet temperatures
[NASA-TN-81640] p0097 N81-14398
Effects of fuel-injector design on ultra-lean
combustion performance
[NASA-TN-82624] p0104 N81-24533
- ANDERSON, H. E.**
Design of spur gears for improved efficiency
[NASA-TN-81625] p0081 N81-17436
- ANDERSON, O. L.**
A model for the analysis of
premixing-prevaporizing fuel-air mixing passages
[AIAA PAPER 81-0345] p0030 N81-20767
- ANDERSON, R. C.**
An integrated exhaust gas analysis system with
self-contained data processing and automatic
calibration
[NASA-TN-81592] p0102 N81-23435
- ANDERSON, W. J.**
Dynamic characteristics of a high-speed rotor with
radial and axial foil-bearing supports
[ASME PAPER 80-C2/LUB-35] p0085 N81-18683
NASA five-ball fatigue tester - Over 20 years of
research
p0087 N81-44659
NASA five-ball fatigue tester: Over 20 years of
research
[NASA-TN-82589] p0102 N81-23462
- ANSON, L.**
Design of an exhaust mixer nozzle for the
Avco-Lycoming Quiet Clean General Aviation
Turbofan (QCGAT)
[NASA-CR-159426] p0029 N81-19120
- ANTL, R. J.**
Improved components for engine fuel savings

- [SAS PAPER 801116] p0021 A81-34152
ARIAS, A.
 Effect of CoO_2 , MgO and Y_2O_3 additions on the sinterability of a milled Si_3N_4 with 14.5 wt% SiO_2 p0064 A81-28974
 Effect of Yttria additives on properties of pressureless-sintered silicon nitride [NASA-TP-1899] p0063 A81-31366
ARNETT, B. A.
 Thin n-i-p silicon solar cell p0114 A81-27097
ARNETT, B. H.
 Engine identification for adaptive control p0025 A81-12100
ARPASI, B. J.
 An approach to real-time simulation using parallel processing p0121 A81-44652
 An approach to real-time simulation using parallel processing [NASA-TN-81731] p0121 A81-21803
ASTLEY, B. J.
 Application of 'steady' state finite element and transient finite difference theory to sound propagation in a variable duct - A comparison with experiment [AIAA PAPER 81-2016] p0128 A81-48622
AUER, R. H.
 Simulation and visualization of face seal motion stability by means of computer generated movies p0087 A81-38059
 Computer program documentation for the dynamic analysis of a noncontacting mechanical face seal [NASA-TN-81636] p0081 A81-17435
AYDELOTT, J. C.
 Propellant management for low thrust chemical propulsion systems [AIAA PAPER 81-1453] p0042 A81-42198
 Shuttle compatible cryogenic liquid storage and supply systems [AIAA PAPER 81-1509] p0037 A81-42207

B

- BACHALO, W. D.**
 Fuel injector characterization studies [NASA-CN-165200] p0026 A81-15003
BAHRT, C. F.
 General Aviation Turbine Engine (GATE) study [NASA-CN-159482] p0029 A81-19117
BARNHART, B.
 Ion beam sputter etching of orthopedic implant alloy MP35N and resulting effects on fatigue properties [AIAA PAPER 81-0671] p0057 A81-38069
 Ion beam sputter etching of orthopedic implanted alloy MP35N and resulting effects on fatigue [NASA-TN-81747] p0045 A81-21174
BAILLY, B. A.
 Boundary layer development on turbine airfoil suction surfaces [ASME PAPER 81-GT-204] p0008 A81-30094
BAIRD, J. E.
 Evaluation of results of US corn and soybeans exploratory experiment: Classification procedures verification test [B81-10076] p0095 A81-13432
BAKER, C. E.
 A study of external fuel vaporization [ASME PAPER 81-GT-156] p0020 A81-30057
BALDWIN, D. H.
 Large wind turbines: A utility option for the generation of electricity p0142 A81-12981
BALODIN, J. E.
 Rotor wake characteristics relevant to rotor-stator interaction noise generation [NASA-TN-82703] p0019 A81-30130
BANCROFT, C. D.
 The STD/HND codes - Comparison of analyses with experiments at AEDC/HPDE, Reynolds Metal Co., and Hercules, Inc [AIAA PAPER 81-0173] p0133 A81-20649
BANKAITIS, M.
 Lightning accommodation systems for wind turbine generator safety [NASA-TN-82601] p0105 A81-24539
 System safety in Stirling engine development [NASA-TN-82615] p0140 A81-24994
BANKS, B.
 Simultaneous ion sputter polishing and deposition [NASA-TN-81679] p0053 A81-19278
 Ion beam sputter-etched ventricular catheter for hydrocephalus shunt [NASA-CASE-LEW-13107-1] p0118 A81-27786
BANKS, B. A.
 Ion beam applications research - A 1981 summary of Lewis Research Center programs [AIAA PAPER 81-0669] p0041 A81-38068
 Texturing polymer surfaces by transfer casting [NASA-CASE-LEW-13120-1] p0068 A81-16327
 Mechanical bonding of metal [NASA-CASE-LEW-12941-1] p0068 A81-16329
 Ion beam applications research. A summary of Lewis Research Center Programs [NASA-TN-81721] p0044 A81-21129
BARAONA, C. E.
 Theoretical results on the double-collecting tandem junction solar cell p0099 A81-17538
 Comparative radiation testing of solar cells for the shuttle power extension package [NASA-TN-82656] p0105 A81-27605
BARBER, J. F.
 The electric rail gun for space propulsion [NASA-CN-165312] p0042 A81-22078
BARBER, T. A.
 JPL's electric and hybrid vehicles project: Project activities and preliminary test results p0143 A81-12987
BARIS, J.
 Preparation and evaluation of advanced electrocatalysts for phosphoric acid fuel cells [NASA-CN-165179] p0111 A81-17527
 Preparation and evaluation of advanced electrocatalysts for phosphoric acid fuel cells [NASA-CN-165245] p0112 A81-18496
BARNES, J. C.
 Comparative analysis of sea ice features using Side-looking Airborne Radar (SLAR) and LANDSAT imagery [B81-10044] p0095 A81-33539
BARNES, S. P.
 Carrier - Interference ratios for frequency sharing between satellite systems transmitting frequency modulated and digital television signals p0069 A81-21911
BARNETT, C. A.
 The effect of zirconium on the cyclic oxidation of NiCrAl alloys p0056 A81-18559
 High temperature cyclic oxidation furnace testing at NASA Lewis Research Center p0058 A81-44653
 NiCrAl ternary alloy having improved cyclic oxidation resistance [NASA-CASE-LEW-13339-1] p0051 A81-12211
 High temperature cyclic oxidation furnace testing at NASA Lewis Research Center [NASA-TN-81773] p0054 A81-26234
BARTER, M. J.
 Materials processing in space: Future technology trends p0143 A81-12991
BASSHAM, L. B.
 High performance cryogenic engines for orbit transfer vehicles [IAP PAPER 80-F-253] p0043 A81-18363
BATAKIS, A.
 Low NO_x / combustion systems for burning heavy residual fuels and high-fuel-bound nitrogen fuels [ASME PAPER 81-GT-109] p0089 A81-30014
BAUER, D. F.
 The electric rail gun for space propulsion [NASA-CN-165312] p0042 A81-22078
BAUNDICK, B. J.
 Fiber optics for aircraft engine/inlet control [NASA-TN-82654] p0012 A81-31190
BAUNHEIMER, E. J.
 Numerical techniques in linear duct acoustics - A status report [ASME PAPER 80-WA/HC-2] p0127 A81-21120
 Application of 'steady' state finite element and transient finite difference theory to sound propagation in a variable duct - A comparison with experiment [AIAA PAPER 81-2016] p0128 A81-48622

- Influence of exit impedance on finite difference solutions of transient acoustic mode propagation in ducts
[NASA-TN-82666] p0126 N81-30905
- BAUFORD, M.
Samarium cobalt (SMCO) generator/engine integration study
[AD-A092904] p0029 N81-17087
- BEAL, G. W.
Evaluation of concepts for controlling exhaust emissions from minimally processed petroleum and synthetic fuels
[ASME PAPER 81-GT-157] p0067 A81-30056
- BEATTIE, M. C.
Design of a multivariable integrated control for a supersonic propulsion system
p0025 N81-12094
- BECHTEL, R. T.
Results of the Mission Profile Life Test first test segment - Thruster J1
[AIAA PAPER 81-0716] p0043 A81-29552
- BENNING, F. P.
Cold-air investigation of first stage of 4-1/2-stage, fan drive turbine with average stage-loading factor of 4.66
[NASA-TP-1780] p0015 N81-16050
- BRITTON, M. S.
Energy efficient engine: Flight propulsion system preliminary analysis and design
[NASA-CR-159583] p0029 N81-18056
Integrated control system for a gas turbine engine
[NASA-CASE-LEW-12594-2] p0015 N81-19116
- BELL, J. C.
Continuous analysis of stresses from arbitrary surface loads on a half space
p0093 A81-14162
- BENFORD, S. M.
T-S diagram for gadolinium near the Curie temperature
p0135 A81-43004
Synergistic erosion/corrosion of superalloys in PFB coal combustor effluent
p0058 A81-44663
Synergistic erosion/corrosion of superalloys in PFB coal combustor effluent
[NASA-TN-81715] p0101 N81-23245
- BENSON, W.
Modification of the ECAS reference steam power generating plant to comply with the EPA 1579 new source performance standards
[NASA-CR-159853] p0110 N81-13467
- BENTZ, D. J.
Axial force and efficiency tests of fixed center variable speed belt drive
[NASA-TN-81652] p0080 N81-15367
Conceptual design of the NHD Engineering Test Facility
[NASA-TN-82621] p0132 N81-24926
- BENCAS, M. W.
Conceptual design of the NHD Engineering Test Facility
[NASA-TN-82621] p0132 N81-24926
- BERNHARD, D. G.
Applicability of advanced automotive heat engines to solar thermal power
[NASA-TN-81658] p0097 N81-14397
Overview: DOE/NASA automotive gas turbine and stirling projects
[NASA-TN-82637] p0105 N81-25487
- BERNATOVICH, B. T.
Space solar cells - High efficiency and radiation damage
p0108 A81-27174
- BRATE, S.
Advanced propulsion system concept for hybrid vehicles
[NASA-CR-159772] p0140 N81-18935
- BRODSKY, B.
Friction and wear results from sputter-deposited chrome oxide with and without nichrome metallic binders and interlayers
[ASME PAPER 80-C2/LUF-45] p0089 A81-18693
- BROTIANI, P. E.
VCE early acoustic test results of General Electric's high-radius ratio coaxial plug nozzle
p0029 N81-17999
- BIFANO, W. J.
Review of stand-alone photovoltaic application projects sponsored by US DOE and US AID
- [NASA-TN-81738] p0100 N81-22477
- BILL, R. C.
The role of oxidation in the fretting wear process
[NASA-TN-81570] p0051 N81-12210
Effects of geometric variables on rub characteristics of Ti-6Al-4V
[NASA-TP-1835] p0053 N81-20245
A sputtered zirconia primer for improved thermal shock resistance of plasma sprayed ceramic turbine seals
[NASA-TN-81732] p0062 N81-21198
Laser surface fusion of plasma sprayed ceramic turbine seals
[NASA-CASE-LEW-13269-1] p0062 N81-22190
Thermal barrier coating system having improved adhesion
[NASA-CASE-LEW-13359-1] p0062 N81-24265
Fretting wear and fretting fatigue: How are they related?
[NASA-TN-82633] p0054 N81-26235
- BIRCHENBOW, A. G.
Modular instrumentation system for real-time measurements and control on reciprocating engines
[NASA-TP-1757] p0071 N81-11315
- BISHOP, A. B.
Calculation of the flow field in supersonic inlets using a bicharacteristics method with shock wave fitting
p0006 A81-21212
The effect of inflow velocity profiles on the performance of supersonic ejector nozzles
[NASA-TN-81673] p0075 N81-16421
- BITTNER, D. A.
Effect of fuel nitrogen and hydrogen content on emissions in hydrocarbon combustion
[ASME PAPER 81-GT-63] p0057 A81-29973
Effect of fuel nitrogen and hydrogen content on emissions in hydrocarbon combustion
[NASA-TN-81612] p0097 N81-14399
- BLACKMORE, S. L.
QCGAT mixer compound exhaust system design and static big model test report
[NASA-CR-135386] p0029 N81-19119
- BLAMA, B. J.
Pneumatic boot for helicopter rotor deicing
p0009 N81-19059
- BLECH, R. A.
An approach to real-time simulation using parallel processing
p0121 A81-44652
An approach to real-time simulation using parallel processing
[NASA-TN-81731] p0121 N81-21803
- BLECHERMAN, S. S.
Design, durability and low cost processing technology for composite fan exit guide vanes
p0089 A81-22664
- BLOOMER, M. L.
Comparison of NASA and contractor results from aeroacoustic tests of QCSER OTU engine
[NASA-TN-81761] p0017 N81-25079
- BLOOMFIELD, M. S.
Coal gasifier cogeneration powerplant project
p0143 N81-12988
Conceptual design study of a coal gasification combined-cycle powerplant for industrial cogeneration
[NASA-TN-81687] p0105 N81-25488
- BLUE, J. W.
Proton radiation damage in bulk n-GaAs
p0099 N81-17564
- BOBER, L. J.
Factors influencing the predicted performance of advanced propeller designs
[AIAA PAPER 81-1564] p0007 A81-42210
Factors influencing the predicted performance of advanced propeller designs
[NASA-TN-82676] p0004 N81-27042
- BOBINGER, B. G.
Energy efficient engine: Flight propulsion system preliminary analysis and design
[NASA-CR-159583] p0029 N81-18056
- ROBULA, G. A.
Effect of a part-span variable inlet guide vane on the performance of a high-bypass turbofan engine
[AIAA PAPER 81-1362] p0022 A81-40F42
Mixing effectiveness test of an exhaust gas mixer in a high bypass turbofan at altitude
[AIAA PAPER 81-1495] p0023 A81-44225

- Effect of a part-span variable inlet guide vane on the performance of a high-bypass turbofan engine [NASA-TN-82617] p0017 N81-25081
Mixing effectiveness test of an exhaust gas mixer in a high bypass turbofan at altitude [NASA-TN-82663] p0018 N81-27095
- BOLDMAN, D. E.**
Stall flutter experiment in a transonic oscillating linear cascade [NASA-TN-82655] p0004 N81-31126
- BOLT, C. E.**
Rotor redesign for a highly loaded 1800 ft/sec tip speed fan, 2 [NASA-CR-159879] p0024 N81-12087
- BORDEN, E.**
Conceptual design of the NHD Engineering Test Facility [NASA-TN-82621] p0132 N81-24926
- BOULEY, C. J.**
Comparative analysis of sea ice features using Side-looking Airborne Radar (SLAR) and LANDSAT imagery [N81-10044] p0095 N81-33539
- BOYER, E.**
Road map to adaptive optimal control p0025 N81-12098
- BOYER, J. E.**
Characterization, performance, and prediction of a lead-acid battery under simulated electric vehicle driving requirements [NASA-TN-81771] p0136 N81-28523
- BRADLEY, E. J.**
Modification of the ECAS reference steam power generating plant to comply with the EPA 1979 new source performance standards [NASA-CR-159853] p0110 N81-13467
- BRACE, E. E.**
An analytical approach to airfoil icing [AIAA PAPER 81-0403] p0117 N81-20810
- BRADYARD, W. A.**
The effect of mechanical surface and heat treatments on the erosion resistance of 6061 aluminum alloy p0057 N81-27944
Improved refractory coatings [NASA-CASE-LEN-25169-2] p0052 N81-16209
- BRANDENBURY, E. E., JR.**
Space solar cells - High efficiency and radiation damage p0108 N81-27174
Radiation damage in lithium-counterdoped N/P silicon solar cells p0109 N81-27204
- BRANDON, E. T.**
Second year technical report on-board processing for future satellite communications systems [NASA-CR-165155] p0070 N81-10242
- BRANDS, E. C.**
Vehicle testing of Cummins turbocompound diesel engine [NASA-CR-159840] p0140 N81-13803
- BRANSON, J. P.**
VCE early acoustic test results of General Electric's high-radius ratio conical plug nozzle p0029 N81-17999
- BRIDAR, E.**
Simultaneous ion sputter polishing and deposition [NASA-TN-81679] p0053 N81-19278
- BRIDGES, E. E.**
Light transport and general aviation aircraft icing research requirements [NASA-CR-165290] p0010 N81-19079
- BRIDGE, E. E.**
Simplified solution for stresses and deformation [NASA-TN-82647] p0384 N81-28444
Analysis of starvation effects on hydrodynamic lubrication in nonconforming contacts [NASA-TN-82668] p0084 N81-29438
- BRIDEL, E.**
NASA Global Atmospheric Sampling Program (GASP) data report for tape V10015, V10016, V10017, V10018, V10019, and V10020 [NASA-TN-81661] p0115 N81-30657
- BRILEY, E. E.**
Calculation of three-dimensional turbulent subsonic flows in transition ducts p0008 N81-21199
Prediction of laminar and turbulent primary and secondary flows in strongly curved ducts
- [NASA-CR-3388] p0007 N81-16976
A three-dimensional turbulent compressible subsonic duct flow analysis for use with constricted coordinate systems [NASA-CR-3389] p0077 N81-20383
- BRODER, J. D.**
Recent developments in lightweight solar cell modules p0099 N81-17571
- BROMAN, C. E.**
Energy efficient engine: Flight propulsion system preliminary analysis and design [NASA-CR-159583] p0029 N81-18056
- BROWN, G. V.**
T-S diagram for gadolinium near the Curie temperature p0135 N81-43004
- BROWN, E. J.**
Safety management of complex research operations p0067 N81-44661
Safety management of complex research operations [NASA-TN-81772] p0068 N81-25263
- BRUTON, E. E.**
An automated procedure for developing hybrid computer simulations of turbofan engines p0020 N81-32544
- BUBSHY, E. E.**
Fracture toughness of brittle materials determined with chevron notch specimens p0064 N81-32545
- BUCHAR, C. E.**
Infrared spectroscopy for the determination of hydrocarbon types in jet fuels [NASA-TN-82674] p0066 N81-31380
- BUCHHEIM, D. E.**
Surface pyrometry in presence of radiation from other sources with application to turbine blade temperature measurement [NASA-TP-1754] p0013 N81-11039
- BUCKLEY, D.**
The effect of mechanical surface and heat treatments on the erosion resistance of 6061 aluminum alloy p0057 N81-27944
- BUCKLEY, D. E.**
Tribological properties of silicon carbide in metal removal process p0085 N81-17900
The adhesion, friction, and wear of binary alloys in contact with single-crystal silicon carbide [ASME PAPER 80-C2/L08-53] p0086 N81-18695
The generation and morphology of single-crystal silicon carbide wear particles under adhesive conditions p0064 N81-35045
The role of the micro environment on the tribological behavior of materials p0087 N81-46493
Effect of mechanical surface and heat treatments on erosion resistance [NASA-TN-81540] p0051 N81-11178
Anisotropic tribological properties of silicon carbide [NASA-TN-81547] p0080 N81-11394
Thin-film coatings p0142 N81-12983
Changes in surface chemistry of silicon carbide (0001) surface with temperature and their effect on friction [NASA-TP-1756] p0060 N81-14079
Effects of erodent particle shape and various heat treatments on erosion resistance of plain carbon steel [NASA-TP-1755] p0052 N81-16210
Surface chemistry and friction behavior of the silicon carbide (0001) surface at temperatures to 1500 deg C [NASA-TP-1813] p0061 N81-19300
Correlation of ideal and actual shear strengths of metals with their friction properties [NASA-TP-1891] p0063 N81-27282
Surface films and metallurgy related to lubrication and wear [NASA-TN-82645] p0063 N81-27523
Adhesion and friction of transition metals in contact with nonmetallic hard materials [NASA-TN-82605] p0055 N81-28233
Relationship between the ideal tensile strength and the friction properties of metals in contact

- with nonmetals and themselves
[NASA-TP-1003] p0063 N81-33293
- BUGGIE, A. B.
Stall flutter experiment in a transonic
oscillating linear cascade
[NASA-TN-82655] p0004 N81-31126
- BUJOLIS, M. P.
Small passenger car transmission test: Dodge Omni
A-404 transmission
[NASA-CN-165181] p0088 N81-15366
- BULLAN, D. L.
Catalytic combustion of coal-derived liquids
[NASA-TN-81594] p0097 N81-14396
Experimental evaluation of catalytic combustion
with heat removal at near stoichiometric
conditions
[NASA-TN-81748] p0103 N81-23609
- BURMAN, B. S.
Fabrication and testing of polyvinylidene fluoride
capacitors
[NASA-CN-159501] p0073 N81-22278
- BURKHARDT, L. A.
Effect of a part-span variable inlet guide vane on
the performance of a high-bypass turbofan engine
[AIAA PAPER 81-1362] p0022 N81-40842
Mixing effectiveness test of an exhaust gas mixer
in a high bypass turbofan at altitude
[AIAA PAPER 81-1495] p0023 N81-44225
Effect of a part-span variable inlet guide vane on
the performance of a high-bypass turbofan engine
[NASA-TN-82617] p0017 N81-25081
Mixing effectiveness test of an exhaust gas mixer
in a high bypass turbofan at altitude
[NASA-TN-82663] p0018 N81-27095
- BURKHART, J. A.
Conceptual design of the BHD Engineering Test
Facility
[NASA-TN-82621] p0132 N81-24926
- BURNS, R. E.
Comparison of Integrated Gasifier-Combined Cycle
and AFB-steam turbine systems for industrial
cogeneration
[NASA-TN-82648] p0106 N81-28522
- BURKE, B.
Frictional and morphological characteristics of
ion plated soft, metallic films
p0057 N81-38066
- BUZZARD, R. J.
Experimental compliance calibration of the compact
fracture toughness specimen
[NASA-TN-81665] p0091 N81-16492
- C**
- CARILLI, E. J.
Catalyst surfaces for the chromous/chromic redox
couple
[NASA-CASE-LEU-13148-2] p0107 N81-29524
- CAIRNELL, J.
Compatibility of alternative fuels with advanced
automotive gas turbine and stirling engines. A
literature survey
[NASA-TN-81754] p0105 N81-27604
- CALPO, F. D.
Material response from Mach 0.3 burner rig
combustion of a coal-oil mixture
[NASA-TN-81686] p0055 N81-27258
- CARL, D.
Low NO_x and fuel flexible gas turbine combustors
[ASME PAPER 81-GT-99] p0020 N81-36006
- CARLIN, C. E.
Should we attempt global (inlet engine airframe)
control design?
p0025 N81-12097
- CARLSON, A. E.
Engineering support for magnetohydrodynamic power
plant analysis and design studies
[NASA-CN-159690] p0110 N81-13466
- CARRUS, J. G.
Evaluation of results of 15 corn and soybeans
exploratory experiment: Classification
procedures verification test
[N81-10076] p0095 N81-13432
- CASSIDY, J. J.
Analysis of the charging of the SCATHA (P78-2)
satellite
[NASA-CN-165348] p0033 N81-27169
- CATALDO, R. L.
Response of nickel to zinc cells to electric
vehicle chopper discharge waveforms
[NASA-TN-81713] p0103 N81-23608
Laboratory evaluation of a pilot cell battery
protection system for photovoltaic applications
[NASA-TN-81714] p0104 N81-24536
- CHAI, A. Y.
High voltage planar multijunction
[NASA-CASE-LEU-13400-1] p0098 N81-16528
High voltage V-groove solar cell
[NASA-CASE-LEU-13401-1] p0098 N81-16529
- CHAIT, L. L.
Engineering support for magnetohydrodynamic power
plant analysis and design studies
[NASA-CN-159690] p0110 N81-13466
Modification of the BCAS reference steam power
generating plant to comply with the EPA 1979 new
source performance standards
[NASA-CN-159653] p0110 N81-13467
- CHAMBERLAIN, R.
Advanced subsonic transport propulsion
[NASA-TN-82696] p0019 N81-31195
- CHAMBERLIN, R.
Sixer nozzle aerodynamic characteristics for the
energy efficient engine
[AIAA PAPER 81-1994] p0128 N81-48639
- CHARIS, C. C.
Nonlinear laminate analysis for metal matrix fiber
composites
[AIAA 81-0579] p0046 N81-29411
Superhybrid composite blade impact studies
[ASME PAPER 81-GT-24] p0020 N81-29940
Computer code for intraply hybrid composite design
p0047 N81-44662
Superhybrid composite blade impact studies
[NASA-TN-81597] p0091 N81-11412
Laminates and reinforced metals
[NASA-TN-81591] p0045 N81-12171
Prediction of composite thermal behavior made simple
[NASA-TN-81618] p0045 N81-16132
Nonlinear laminate analysis for metal matrix fiber
composites
[NASA-TN-82596] p0046 N81-25149
Computer code for intraply hybrid composite design
[NASA-TN-82593] p0046 N81-25151
- CHAMPION, A. E.
Ultra-high modulus organic fiber hybrid composites
[NASA-CN-165228] p0048 N81-21130
- CHANG, L. K.
Factors influencing the predicted performance of
advanced propeller designs
[NASA-TN-82676] p0004 N81-27042
- CHANG, L.-K.
Factors influencing the predicted performance of
advanced propeller designs
[AIAA PAPER 81-1564] p0007 N81-42210
- CHAO, C. H. C.
A method of selecting grid size to account for
Bertz deformation in finite element analysis of
spur gears
[NASA-TN-82623] p0083 N81-27525
- CHARLSTON, J.
Preparation and characterization of electrodes for
the NASA Redox storage system
[NASA-TN-82702] p0107 N81-30522
Advances in membrane technology for the NASA redox
energy storage system
[NASA-TN-82701] p0108 N81-33601
- CHEN, H.
Advanced propulsion system concept for hybrid
vehicles
[NASA-CN-159772] p0140 N81-18935
- CHIAFFETTA, L.
A study of external fuel vaporization
[ASME PAPER 81-GT-158] p0020 N81-30057
- CHIAFFETTA, L. S.
A model for the analysis of
premixing-prevaporizing fuel-air mixing passages
[AIAA PAPER 81-0345] p0030 N81-20767
- CHINA, R. V.
Finite element analysis of inviscid subsonic
boattail flow
[AIAA PAPER 81-0276] p0006 N81-20831
Finite element analysis of inviscid subsonic
boattail flow
[NASA-TN-81650] p0003 N81-14977
- CHO, Y. C.
High-frequency sound propagation in a spatially
varying mean flow
p0129 N81-49913

CSOS, B. C.

PERSONAL AUTHOR INDEX

- High-frequency sound propagation in a spatially
varying mean flow
[NASA-TN-81751] p0126 N81-20831
- CSOS, B. C.
Three-dimensional turbulent boundary layer
development and separation in V/STOL engine
inlets at incidence with small-cross flow and
curvature influences
[AIAA PAPER 81-0254] p0005 A81-20703
- CSIKISTERN, L.
Technology development for phosphoric acid fuel
cell powerplant, phase 2
[NASA-CN-165317] p0113 N81-21536
Technology development for phosphoric acid fuel
cell powerplant (phase 2)
[NASA-CN-165316] p0113 N81-21547
Technology development for phosphoric acid fuel
cell powerplant (phase 2)
[NASA-CN-165318] p0113 N81-22475
- CHENSTORSEN, R.
Ion beam sputter etching of orthopedic implant
alloy MP35N and resulting effects on fatigue
properties
[AIAA PAPER 81-0671] p0057 A81-38069
Ion beam sputter etching of orthopedic implanted
alloy MP35N and resulting effects on fatigue
[NASA-TN-81747] p0045 N81-21174
- CHERUSKI, D. B.
Turbomachinery noise studies of the A18Research
QCGAT engine with inflow control
[NASA-TN-82694] p0127 N81-31957
- CHUBB, D. L.
Assessment of disk EHD generators for a base load
powerplant
[NASA-TN-82609] p0103 N81-23611
- CHUNG, K.
Aerodynamic stability analysis of NASA
J65-13/planar pressure pulse generator
installation
[NASA-CN-165141] p0027 N81-15004
- CICOM, D. B.
Improved methods for fan sound field determination
[NASA-CN-165188] p0129 N81-15769
- CIEPLOCK, C. C.
Advanced subsonic transport propulsion
[NASA-TN-82696] p0019 N81-31195
- CLAING, R. G.
Turbine blade temperature measurements using thin
film temperature sensors
[NASA-CN-165201] p0059 N81-19277
- CLARE, R. J.
Computer program to predict aircraft noise levels
[NASA-TP-1913] p0127 N81-33947
- CLARE, R. M.
Light transport and general aviation aircraft
icing research requirements
[NASA-CN-165290] p0010 N81-19079
- CLARK, R. M.
Spectral flame radiance from a tubular-can combustor
[NASA-TP-1722] p0016 N81-19121
- CHEWELSKI, D. B.
Turbomachinery noise studies of the A18Research
QCGAT engine with inflow control
[AIAA PAPER 81-2049] p0023 A81-48621
- COATS, J. W.
Comparison of NASA and contractor results from
aeroacoustic tests of QCS22 GTN engine
[NASA-TN-81761] p0017 N81-25079
- COCHRAN, R. P.
Effect of hole geometry and Electric-Discharge
Machining (EDM) on airflow ratios through small
diameter holes in turbine blade material
[NASA-TP-1716] p0013 N81-12089
- COCHRAN, T. B.
Overview study of combustion experiments in a
space laboratory
p0032 A81-46059
- COE, E. E.
Calculated and experimental data for a 114-mm bore
roller bearing to 3 million DN
[ASME PAPER 80-C2/LUE-14] p0085 A81-18668
- COHEN, R.
An experimental evaluation of oil pumping rings
[NASA-CN-165271] p0088 N81-21355
- COLE, G. L.
Propulsion system mathematical model for a
lift/cruise fan V/STOL aircraft
[NASA-TN-81663] p0015 N81-16055
- CONNELLY, R. E.
Traction drive for cryogenic boost pump
[NASA-TN-81704] p0101 N81-23188
- CONVERSE, G. L.
Turbine modeling technique to generate off-design
performance data for both single and multistage
axial-flow turbines
[NASA-CN-165244] p0027 N81-17078
- COOPER, L. F.
Analysis of effect of flameholder characteristics
on lean, premixed, partially vaporized fuel-air
mixtures quality and nitrogen oxides emissions
[NASA-TP-1842] p0016 N81-24065
Supercritical fuel injection system
[NASA-CASE-L3N-12990-1] p0018 N81-29129
- CORRETT, J. E.
Integrated control system for a gas turbine engine
[NASA-CASE-L3N-12594-2] p0015 N81-19116
- CORRIHAN, R. B.
Comparison of upwind and downwind rotor operations
of the DOE/NASA 100-kW Mod-0 wind turbine
[NASA-TN-81744] p0100 N81-22472
- COULDS, R. A.
Cyclic behavior of turbine disk alloys at 650 C
p0056 A81-12760
- COX, J. J.
Some limitations in applying classical EHD film
thickness formulas to a high-speed bearing
[ASME PAPER 80-C2/LUE-13] p0068 A81-18667
Life analysis of multiroller planetary traction
drive
[NASA-TP-1710] p0082 N81-20423
Surface geometry of circular cut spiral bevel gears
[NASA-TN-82622] p0083 N81-26459
Optimal tooth numbers for compact standard spur
gear sets
[NASA-TN-82614] p0083 N81-27524
A method of selecting grid size to account for
Hertz deformation in finite element analysis of
spur gears
[NASA-TN-82623] p0083 N81-27525
- COLLIER, R. E.
Mixing effectiveness test of an exhaust gas mixer
in a high bypass turbofan at altitude
[AIAA PAPER 81-1495] p0023 A81-44425
Exhaust emission survey of an F100 afterburning
turbofan engine at simulated altitude flight
conditions
[NASA-TN-81656] p0016 N81-21078
Mixing effectiveness test of an exhaust gas mixer
in a high bypass turbofan at altitude
[NASA-TN-82663] p0016 N81-27095
- CORREY, A. M.
Electron reflection and secondary emission
characteristics of sputter-textured pyrolytic
graphite surfaces
p0065 A81-38065
Electron reflection and secondary emission
characteristics of sputter-textured pyrolytic
graphite surfaces
[NASA-TN-81755] p0062 N81-22193
Ion sputter textured graphite
[NASA-CASE-L3N-12919-1] p0046 N81-27198
- CURTIS, R. E.
Global calibration of terrestrial reference cells
and errors involved in using different
irradiance monitoring techniques
p0068 A81-27148
Determination of optimum sunlight concentration
level in space for gallium arsenide solar cells
[NASA-TN-82643] p0040 N81-26173
- CUSABO, C.
Dynamics of solid dispersions in oil during the
lubrication of point contacts. I - Graphite
[ASLE PREPRINT 81-AM-5D-3] p0064 A81-33860
Dynamics of solid dispersions in oil during the
lubrication of point contacts. Part 1: Graphite
[NASA-TN-81683] p0061 N81-17264
Dynamics of solid dispersions in oil during the
lubrication of point of contacts. Part 2:
Bolybdenum disulfide
[NASA-TN-81705] p0062 N81-20275
- CUTMORE, R. E.
Evaluation of advanced combustors for dry HC/H/
suppression with nitrogen bearing fuels in
utility and industrial gas turbines
[ASME PAPER 81-GT-125] p0067 A81-30029

D

- DALE, B.
MASTRAN level 16 programmer's manual updates for
aeroelastic analysis of bladed discs
[NASA-CR-159825] p0093 N81-19482
- DANIELS, C. J.
A four-cylinder Stirling engine controls model
[NASA-TN-81648] p0075 N81-15241
- DAVIES, B. L.
Progress in materials and structures at Lewis
Research Center p0142 N81-12982
- DAVIS, R. E.
Cloud encounter and particle density variabilities
from GASP data
[AIAA PAPER 81-0308] p0117 A81-20742
- DAVIS, W. F.
Dissolution of bulk specimens of silicon nitride
p0065 A81-42024
- DAYTON, J. A., JR.
Three-axis electron-beam test facility
[NASA-TP-1836] p0071 N81-20359
Analytical prediction and experimental
verification of performance at various operating
conditions of a dual-mode traveling wave tube
with multistage depressed collectors
[NASA-TP-1831] p0072 N81-28352
- DEADHORN, D. J.
The effects of trace impurities in coal-derived
liquid fuels on deposition and accelerated high
temperature corrosion of cast superalloys
[NASA-TN-81678] p0052 N81-16211
- DEADHORN, D. L.
High temperature alkali corrosion in high velocity
gases
[NASA-TN-82591] p0054 N81-25191
- DEBOLT, M. E.
CVD-produced boron filaments
p0048 A81-11336
- DECKER, A. J.
Holographic flow visualization of time-varying
shock waves p0079 A81-47642
- DECORSO, S. M.
Low $W/O/x$ and fuel flexible gas turbine combustors
[ASME PAPER 81-GT-99] p0020 A81-30006
- DEISSLER, R. C.
Turbulent solution of the Navier-Stokes equations
p0077 A81-15284
Turbulent solution of the Navier-Stokes equations
[NASA-TN-81621] p0074 N81-12358
- DELABO, C. B.
Synthesis of improved phenolic and polyester resins
[NASA-CR-165180] p0065 N81-17263
- DELOMBARD, R.
Design description of the Schuchuli Village
photovoltaic power system
[NASA-TN-82650] p0094 N81-28517
- DELVIGES, P.
Lower-curing-temperature IMB polyimides
[NASA-TN-81705] p0045 N81-17174
Curing agent for polyepoxides and epoxy resins and
composites cured therewith
[NASA-CASE-LEN-12226-1] p0060 N81-17260
Composition and method for making polyimide
resin-reinforced fabric
[NASA-CASE-LEN-12933-1] p0061 N81-19296
- DREEL, H. F.
Samarium cobalt (SMCO) generator/engine
integration study
[AD-A092904] p0029 N81-17087
- DREETHLEARS, S. T.
The STD/MSD codes - Comparison of analyses with
experiments at AEDC/BPDE, Reynolds Metal Co.,
and Hercules, Inc.
[AIAA PAPER 81-0173] p0133 A81-20649
On the magnetoacoustic thermal instability
[AIAA PAPER 81-0248] p0133 A81-20698
- DRENNETT, J. T.
The Mod-2 wind turbine development project
[NASA-TN-82681] p0106 N81-27606
- DRENNIS, R. E.
Cost/benefit analysis of advanced materials
technology candidates for the 1980's, part 2
[NASA-CR-165176] p0139 N81-11953
Low-cost directionally-solidified turbine blades,
volume 2
- [NASA-CR-159562] p0024 N81-12088
- DRESCHE, R. E.
Propellant management for low thrust chemical
propulsion systems
[AIAA PAPER 81-1453] p0042 A81-42198
- DRESANO, R.
An assessment of the use of antimisting fuel in
turbofan engines
[NASA-CR-165258] p0067 N81-19316
- DEVULSTIAN, J. E.
Mechanical properties of weldments in experimental
Fe-12Mn-0.2Ti and Fe-12Mn-1Mo-0.2Ti alloys for
cryogenic service p0058 A81-48143
- DEWITT, R. L.
Requirements and preliminary concept of a
Zero-Gravity Combustion Facility for Spacelab
[AIAA PAPER 81-0165] p0032 A81-20642
Combustion experimentation aboard the space
transportation system p0032 A81-46068
- DEYO, J. E.
Photovoltaic applications - Past and future
p0109 A81-27231
Solar photovoltaics: Stand alone applications
p0143 A81-12990
- DICARLO, J. A.
Oxidation-induced contraction and strengthening of
boron fibers p0047 A81-44664
Oxidation-induced contraction and strengthening of
boron fibers
[NASA-TN-82599] p0046 N81-25150
- DIEDRICH, J. E.
Optimum subsonic, high-angle-of-attack nacelles
p0005 A81-11646
Low-speed aerodynamic performance of
50.8-centimeter-diameter noise-suppressing
inlets for the Quiet, Clean, Short-haul
Experimental Engine (QCSSE)
[NASA-TP-1178] p0013 N81-11037
- DIEHL, L. A.
Advanced technology for controlling pollutant
emissions from supersonic cruise aircraft
p0001 N81-18004
- DITTMAR, J. E.
An evaluation of a simplified near field noise
model for supersonic helical tip speed propellers
[NASA-TN-81727] p0130 N81-22836
The propeller tip vortex. A possible contributor
to aircraft cabin noise
[NASA-TN-81768] p0130 N81-22838
- DOCHAY, G.
Advanced propulsion system concept for hybrid
vehicles
[NASA-CR-159772] p0140 N81-18935
- DOBOSOFF, S. E.
Dynamic characteristics of a high-speed rotor with
radial and axial foil-bearing supports
[ASME PAPER 80-C2/LUB-35] p0085 A81-18683
- DORSON, D.
History of ball bearings
[NASA-TN-81689] p0081 N81-18391
Introduction to ball bearings
[NASA-TN-81690] p0081 N81-18392
Ball bearing mechanics
[NASA-TN-81691] p0085 N81-31550
- DOYLE, V. L.
VCE early acoustic test results of General
Electric's high-radius ratio conannular plug nozzle
p0029 N81-17999
- DRESHFIELD, R. L.
Advanced aircraft engine materials trends
[NASA-TN-82626] p0055 N81-27259
- DUERS, R. A.
Advanced technology for controlling pollutant
emissions from supersonic cruise aircraft
p0001 N81-18004
- DUGAN, J. F.
The NASA high-speed turboprop program
[SAB PAPER 801120] p0021 A81-34156
- DUGESOFF, C. E.
Characteristics of 30-centimeter mercury ion
thrusters
[NASA-TN-81706] p0039 N81-21121
- DULGEROFF, C. R.
Characteristics of 30-centimeter mercury ion
thrusters
[AIAA PAPER 81-0715] p0041 A81-37569

- Electric propulsion - characteristics, applications, and status
[NASA-TN-81630] p0033 N81-13079
- Retrofit and verification test of a 30-cm ion thruster
[NASA-CR-165233] p0042 N81-20174
- DOLIRAVICH, B. S.
Shockless design and analysis of transonic blade shapes
[NASA-TN-82611] p0004 N81-25036
- GRID30: Computer program for fast generation of multilevel, three-dimensional boundary-conforming C-type computational grids
[NASA-TP-1920] p0005 N81-31126
- DOLIRAVICH, G.
Fast Generation of body conforming grids for 3-D
p0122 N81-17706
- DURBIN, P. A.
Note on reflection and transmission coefficients for converging-diverging ducts
[NASA-TN-82679] p0126 N81-30906
- DUSTIN, R. G.
Characterization of the near-term electric vehicle (ETV-1) breadboard propulsion system over the SAE J227a driving schedule D
[NASA-TN-81664] p0097 N81-15465
- Results of the ETV-1 breadboard tests under steady-state and transient conditions
[NASA-TN-82667] p0108 N81-31627

E

- EDACKER, J. J.
Aerodynamic/acoustic performance of IJ101/double bypass VCE with conical plug nozzle
[NASA-CR-159869] p0129 N81-17846
- EDERHARDT, R. W.
Shuttle compatible cryogenic liquid storage and supply systems
[AIAA PAPER 81-1509] p0037 A81-42207
- EDIHARA, R. T.
Three-axis electron-beam test facility
[NASA-TP-1836] p0071 N81-20359
- EGHEMONT, B. W.
Electrostatic bonding of thin (cycle sine 3 mil) 7070 cover glass to Ta2O5 AR-coated thin (cycle sine 2 mil) silicon wafers and solar cells
[NASA-CN-165240] p0111 N81-16582
- Electrostatic bonding of thin (approximately 3 mil) 7070 cover glass to Ta2O5 AR-coated thin (approximately 2 mil) silicon wafers and solar cells
p0111 N81-17569
- EGUCHI, R.
Stress concentration in the vicinity of a hole defect under conditions of Hertzian contact
[NASA-TN-82649] p0084 N81-28443
- EISEMAN, P. A.
Geometric methods in computational fluid dynamics
p0075 N81-18331
- KESTERT, R. E.
Evaluation of advanced combustors for dry NO_x/suppression with nitrogen bearing fuels in utility and industrial gas turbines
[ASME PAPER 81-GT-125] p0087 A81-30029
- ELCHOURI, V.
Aerodynamic and dynamic finite element analyses of a bladder shrouded disk
[NASA-CN-159728] p0092 N81-19479
- Mastran level 16 theoretical manual updates for aerodynamic analysis of bladed discs
[NASA-CN-159823] p0093 N81-19480
- MASTRAN level 16 user's manual updates for aerodynamic analysis of bladed discs
[NASA-CN-159824] p0093 N81-19481
- MASTRAN level 16 demonstration manual updates for aerodynamic analysis of bladed discs
[NASA-CN-159826] p0093 N81-19483
- ELLIOTT, J. P.
A rapid method for the approximate determination of nonlinear solutions Application to aerodynamic flows
p0007 A81-11628
- A rapid perturbation procedure for determining nonlinear flow solutions: Application to transonic turbomachinery flows
[NASA-CN-3425] p0001 N81-22012
- ENGLISH, R. E.
Applications Technology Satellite and

- Communications Technology Satellite user experiments for 1967 - 1980 reference book, volume 1
[NASA-CR-165169-VOL-1] p0033 N81-12135
- Applications Technology Satellite and Communications Technology Satellite user experiments for 1967-1980 reference book, volume 2
[NASA-CR-165169-VOL-2] p0033 N81-12136
- Applications Technology Satellite and Communications Technology Satellite user experiments for 1967-1980 reference book, Volume 3: User forum surveys
[NASA-CR-165169-VOL-3] p0033 N81-12137
- Applications Technology Satellite and Communications Technology Satellite user experiments for 1967-1980 reference book, Volume 4: Abstracts
[NASA-CR-165169-VOL-4] p0133 N81-12138
- ENGLISH, R. E.
Goals of thermionic program for space power
[NASA-TN-82616] p0133 A81-44656
- Goals of thermionic program for space power
[NASA-TN-82616] p0132 N81-25808
- ENGLISH, C. E.
REGA16 - Computer program for analysis and extrapolation of stress-rupture data
[NASA-TP-1809] p0102 N81-23486
- An introduction to NASA's turbine engine hot section technology (HOST) project
p0019 N81-31206
- ETSION, I.
Simulation and visualization of face seal motion stability by means of computer generated movies
p0087 A81-38059
- Computer program documentation for the dynamic analysis of a noncontacting mechanical face seal
[NASA-TN-81636] p0081 N81-17435
- Self-stabilizing radial face seal
[NASA-CASE-LEW-12991-1] p0083 N81-24442
- EUSEPI, M. W.
An experimental evaluation of oil pumping rings
[NASA-CR-165271] p0088 N81-21355
- EVANICH, P.
Icing tunnel tests of a glycol-exuding porous leading edge ice protection system on a general aviation airfoil
[AIAA PAPER 81-0405] p0011 A81-20837
- Evaluation of a pneumatic boot deicing system on a general aviation wing model
[NASA-TN-82363] p0011 N81-25065
- EVANICH, P. L.
Pneumatic boot for helicopter rotor deicing
p0009 N81-19059
- EVANS, L., JR.
Performance tests of a gas blending system based on mass-flow controllers
[NASA-TP-1896] p0066 N81-29246
- EVANS, D. G.
Applicability of advanced automotive heat engines to solar thermal power
[NASA-TN-81658] p0097 N81-14397
- EVANS, J. C., JR.
Solar cell system having alternating current output
[NASA-CASE-LEW-12806-2] p0096 N81-12542
- High voltage planar multijunction
[NASA-CASE-LEW-13400-1] p0098 N81-16528
- High voltage V-groove solar cell
[NASA-CASE-LEW-13401-1] p0098 N81-16529
- Heat transparent high intensity high efficiency solar cell
[NASA-CASE-LEW-12892-1] p0105 N81-27598
- EVERSMAN, R.
Application of 'steady' state finite element and transient finite difference theory to sound propagation in a variable duct - A comparison with experiment
[AIAA PAPER 81-2016] p0128 A81-48622
- EVANSINHA, J. G.
Characterization, performance, and prediction of a lead-acid battery under simulated electric vehicle driving requirements
[NASA-TN-81771] p0106 N81-28523

F

- FADDOOBI, J. R.
Test evaluation of a laminated wood wind turbine blade concept
[NASA-TN-81719] p0104 N81-24535

- PARSH, D.**
Photovoltaic applications - Past and future
[NASA-TN-81680] p0109 N81-17231
- PAN, J. C.**
GaAs shallow-homojunction solar cells
[NASA-CN-165167] p0110 N81-15463
- PARNELL, C.**
Full potential solution of a transonic quasi-3-D
flow through a cascade using artificial
compressibility
[AIAA PAPER 81-67-70] p0006 A81-29979
- PARSONS, C. E.**
Recent developments in aircraft engine noise
reduction technology
p0009 N81-19072
- PARSONS, R. E.**
The DOE photovoltaics program
p0143 N81-12989
- PARSAULT, J.**
Practical applications of surface analytic tools
in tribology
p0086 A81-18739
- PASTER, D. A.**
Shuttle compatible cryogenic liquid storage and
supply systems
[AIAA PAPER 81-1509] p0037 A81-42207
- PAUGH, D. G.**
Analytical design of an advanced radial turbine
[NASA-CN-165170] p0140 N81-20958
- PIOMBERTO, A.**
An assessment of the use of antimisting fuel in
turbofan engines
[NASA-CN-165258] p0067 N81-19316
- PISCHE, G. K.**
Design studies of continuously variable
transmissions for electric vehicles
[NASA-TN-81642] p0080 N81-13357
- FISCHACH, L. E.**
ROMFIG and SHKCNFIG: Two interactive
preprocessing to the Navy/NASA Engine Program
(NNEP)
[NASA-TN-82636] p0120 N81-25698
- FISHER, D. E.**
Experimental compliance calibration of the compact
fracture toughness specimen
[NASA-TN-81665] p0091 N81-16492
- FLACK, J. E.**
Tungsten wire-reinforced superalloys for 1093 C
(2000 F) turbine blade applications
[NASA-CN-159720] p0047 N81-10112
- FLERINO, D. P.**
Structural dynamics verification facility study
[NASA-TN-82675] p0092 N81-33457
- FLOOD, D. J.**
GaAs homojunction solar cell development
p0099 N81-17541
Proton radiation damage in bulk n-GaAs
p0099 N81-17564
- FLORES, F. J.**
Effect of hydroprocessing severity on
characteristics of jet fuel from OSCO 2 and
Parabo distillates
[NASA-TN-1768] p0066 N81-24283
- FOGELSON, S. A.**
Modification of the ECAS reference steam power
generating plant to comply with the EPA 1979 new
source performance standards
[NASA-CN-159853] p0110 N81-13467
- FORRESTIERI, A. P.**
Recent developments in lightweight solar cell
modules
p0099 N81-17571
- FORMAN, L.**
Ion sputter textured graphite
[NASA-CASE-LEM-12919-1] p0046 N81-27198
- FORTINI, A.**
Heat exchanger and method of making
[NASA-CASE-LEM-12441-3] p0104 N81-24519
- FOX, T. A.**
Experimental investigation of intermodulation
effects and related efficiencies associated with
two- and three-signal operation of a traveling
wave tube
[NASA-TN-81576] p0049 N81-10240
Performance of computer-designed small-sized
four-stage depressed collector for operation of
dual-mode traveling wave tube
[NASA-TN-1832] p0072 N81-30360
- FRALICH, G. C.**
Miniature drag-force anemometer
[NASA-TN-81680] p0079 N81-16428
- FRANCISCU, L. C.**
Turbine bypass engine - A new supersonic cruise
propulsion concept
[AIAA PAPER 81-1596] p0023 A81-40971
The supersonic fan engine - An advanced concept in
supersonic cruise propulsion
[AIAA PAPER 81-1599] p0023 A81-40973
Turbine bypass engine: A new supersonic cruise
propulsion concept
[NASA-TN-82608] p0018 N81-26145
The supersonic fan engine: An advanced concept in
supersonic cruise propulsion
[NASA-TN-82657] p0018 N81-27094
- FRANK, T.**
An assessment of the use of antimisting fuel in
turbofan engines
[NASA-CN-165258] p0067 N81-19316
- FRICHTER, F. J.**
Fabrication of injection molded sintered alpha SiC
turbine components
[AIAA PAPER 81-67-161] p0089 A81-30060
- FRIEDMAN, G. I.**
Tungsten wire-reinforced superalloys for 1093 C
(2000 F) turbine blade applications
[NASA-CN-159720] p0047 N81-10112
- FRIEDMAN, B.**
Aviation turbine fuel properties and their trends
[NASA-TN-82603] p0066 N81-25232
- FRIEDRIC, G. C.**
Deposition and material response from Mach 0.3
burner rig combustion of SRC 2 fuels
[NASA-TN-81634] p0051 N81-15069
- FUCINARI, C. A.**
Ceramic regenerator systems development program
[NASA-CN-165139] p0141 N81-22982
- FUJIKI, M.**
Development of low-cost directionally-solidified
turbine blades
p0088 A81-10707
- FURST, D. G.**
General Aviation Turbine Engine (GATE) study
[NASA-CN-159482] p0029 N81-19117
- FUSARO, B. L.**
Effect of substrate surface finish on the
lubrication and failure mechanisms of molybdenum
disulfide films
[AIAA PREPRINT 81-AM-53-1] p0064 A81-33859
Effect of substrate surface finish on the
lubrication and failure mechanisms of molybdenum
disulfide films
[NASA-TN-81595] p0060 N81-10170
Effect of load, area of contact, and contact
stress on the wear mechanisms of a bonded solid
lubricant film
[NASA-TN-81563] p0060 N81-12226
Tribological properties and thermal stability of
various types of polyimide films
[NASA-TN-81765] p0102 N81-23275

G

- GADRE, J. G.**
Next generation communications satellites:
Multiple access and network studies
[NASA-CN-165145] p0033 N81-12139
- GANE, B. P.**
Zirconium carbide as an electrocatalyst for the
chromous/chronic redox couple
[NASA-CASE-LEM-13246-1] p0049 N81-26203
Preparation and characterization of electrodes for
the NASA Redox storage system
[NASA-TN-82702] p0107 N81-30522
- GALLO, A. B.**
NASTRAN level 16 user's manual updates for
aeroelastic analysis of bladed discs
[NASA-CN-159824] p0093 N81-19481
NASTRAN level 16 programmer's manual updates for
aeroelastic analysis of bladed discs
[NASA-CN-159825] p0093 N81-19482
NASTRAN level 16 demonstration manual updates for
aeroelastic analysis of bladed discs
[NASA-CN-159826] p0093 N81-19483
- GARDNER, W.**
Energy efficient engine diffuser/compressor model
technology
[NASA-CN-165157] p0026 N81-15002

- GAUGLER, R. E.**
Some modifications to, and operational experiences with, the two-dimensional, finite-difference, boundary-layer code, STAN5
[ASME PAPER 81-GT-89] p0077 A81-29996
- GAUTHIER, D. J.**
An introduction to NASA's turbine engine hot section technology (HST) project p0019 A81-31206
- GAUTHIER, D. J.**
Design and development of the combustor inlet diffuser for the NASA/GI energy efficient engine
[ASME PAPER 81-GT-129] p0020 A81-30033
- GAYDA, J.**
The fracture morphology of nickel-base superalloys tested in fatigue and creep-fatigue at 650 C
[NASA-TN-81740] p0101 A81-23244
- GENEY, M. A.**
Thermal barrier coatings - Burner rig hot corrosion test results p0063 A81-12630
Burner rig evaluation of thermal barrier coating
[NASA-TN-81684] p0055 A81-28231
A new diffusion-inhibited oxidation-resistant coating for superalloys
[NASA-TN-82687] p0056 A81-33273
- GERHART, P. E.**
Finite element analysis of inviscid subsonic boattail flow
[AIAA PAPER 81-0276] p0006 A81-20831
Finite element analysis of inviscid subsonic boattail flow
[NASA-TN-81650] p0003 A81-14977
- GIAMATI, C. C.**
Application of computer generated color graphic techniques to the processing and display of three dimensional fluid dynamic data
[NASA-TN-82658] p0119 A81-29782
- GILLANDERS, M.**
High efficiency wraparound contact solar cells /HEWACS/ p0114 A81-27094
The HEWACS pilot line experience p0111 A81-17574
- GIERE, J. D.**
Catalyst surfaces for the chromous/chromic redox couple
[NASA-CASE-LEN-13148-2] p0107 A81-29524
- GIULIANO, M.**
Coplanar back contacts for thin silicon solar cells
[NASA-CR-165272] p0112 A81-18495
- GISA, D. A.**
Conceptual design of the RHD Engineering Test Facility
[NASA-TN-82621] p0132 A81-24926
- GLASCOU, T. K.**
Effect of milling and leaching on the structure of sintered silicon
[NASA-TN-81602] p0060 A81-13166
- GLASER, P. E.**
Mean rotor wake characteristics of an aerodynamically loaded 0.5 m diameter fan
[AIAA PAPER 81-0208] p0006 A81-20830
Effects of blade-vane ratio and rotor-stator spacing on fan noise with forward velocity
[AIAA PAPER 81-2032] p0024 A81-48628
Mean rotor wake characteristics of an aerodynamically loaded 0.5 m diameter fan
[NASA-TN-81657] p0015 A81-16053
Effects of blade-vane ratio and rotor-stator spacing of fan noise with forward velocity
[NASA-TN-82690] p0126 A81-31956
- GLASCOU, J. C.**
Comparison of upwind and downwind rotor operations of the DOE/NASA 100-kW Mod-0 wind turbine
[NASA-TN-81744] p0100 A81-22472
- GLASCOU, T. K.**
Effect of milling and leaching on the structure of sintered silicon p0064 A81-22529
Oxidation and hot corrosion of coated and bare oxide dispersion strengthened superalloy MA-755E p0058 A81-43384
Progress in materials and structures at Lewis Research Center p0142 A81-12982
A new diffusion-inhibited oxidation-resistant coating for superalloys
[NASA-TN-82687] p0056 A81-33273
- GLASSFORD, A. P. E.**
Evacuation-induced pressure differentials in multilayer insulation systems p0078 A81-18021
- GLASSMAN, A. J.**
Loss model for off-design performance analysis of radial turbines with pivoting-vane, variable-area stators
[SAE PAPER 801135] p0021 A81-34166
Some advantages of methane in an aircraft gas turbine
[SAE PAPER 801154] p0022 A81-34177
Off-design performance loss model for radial turbines with pivoting, variable-area stators
[NASA-TP-1708] p0013 A81-11038
NASA contributions to radial turbine aerodynamic analyses
[NASA-TN-81644] p0003 A81-13019
- GLISSE, P. E.**
Mixer nozzle aeroacoustic characteristics for the energy efficient engine
[AIAA PAPER 81-1994] p0128 A81-48639
- GODFREY, M. P.**
The effect of minority carrier mobility variations on the performance of high voltage silicon solar cells p0098 A81-17536
The effect of minority carrier mobility variations on solar cell spectral response
[NASA-TN-82604] p0103 A81-23625
- GOLDSTEIN, M. E.**
The coupling between flow instabilities and incident disturbances at a leading edge p0010 A81-28682
- GONZALEZ-SANABRIA, O. D.**
Alkaline battery containing a separator of a cross-linked copolymer of vinyl alcohol and unsaturated carboxylic acid
[NASA-CASE-LEN-13102-1] p0107 A81-29531
- GOODYNCHETZ, J.**
Effect of a semi-annular thermal acoustic shield on jet exhaust noise
[NASA-TN-81615] p0125 A81-11770
- GOODENDY, A.**
Perturbation solutions of combustion instability problems
[NASA-CR-159643] p0050 A81-16176
- GOPAL, I. S.**
Next generation communications satellites: Multiple access and network studies
[NASA-CR-165145] p0033 A81-12139
- GORADIA, C.**
Theoretical results on the double-collecting tandem junction solar cell p0099 A81-17538
Radiation damage in silicon MIP solar cells p0099 A81-17557
Performance of high resistivity n⁺⁺p silicon solar cells under 1 MeV electron irradiation
[NASA-TN-82610] p0103 A81-23626
- GORADIA, C. P.**
High voltage planar multi-junction
[NASA-CASE-LEN-13400-1] p0098 A81-16528
High voltage V-groove solar cell
[NASA-CASE-LEN-13401-1] p0098 A81-16529
- GORDON, L. E.**
The Mod-2 wind turbine development project
[NASA-TN-82681] p0106 A81-27606
- GOYAL, A.**
Evaluation of advanced combustors for dry H₂/O₂ suppression with nitrogen bearing fuels in utility and industrial gas turbines
[ASME PAPER 81-GT-125] p0067 A81-30029
- GRABER, E. J.**
The NASA high-speed turboprop program
[SAE PAPER 801120] p0021 A81-34156
- GRANAN, E. E.**
Engineering management and innovation p0036 A81-20400
Analysis for predicting adiabatic wall temperatures with single hole coolant injection into a low speed crossflow
[ASME PAPER 81-GT-91] p0077 A81-29998
Some advantages of methane in an aircraft gas turbine
[SAE PAPER 801154] p0022 A81-34177
Curved film cooling admission tube
[NASA-CASE-LEN-13174-1] p0074 A81-12363

- Analysis for predicting adiabatic wall temperatures with single hole coolant injection into a low speed crossflow
[NASA-TN-81620] p0074 N81-13301
- GRANT, R. P.
Turbine blade temperature measurements using thin film temperature sensors
[NASA-CN-165201] p0059 N81-19277
- GRAVITT, R. D.
Energy efficient engine: Flight propulsion system preliminary analysis and design
[NASA-CN-159583] p0029 N81-18056
- GRAY, R. R.
Advanced aircraft engine materials trends
[NASA-TN-82626] p0055 N81-27259
- GREEN, W. K.
Second year technical report on-board processing for future satellite communications systems
[NASA-CN-165155] p0070 N81-10242
- GREENBAUMER-SHUG, L. A.
Accuracy of trace element determinations in alternate fuels
p0056 A81-22530
- Accuracy of trace element determinations in alternate fuels
[NASA-TN-81609] p0049 N81-13106
- GREGORIK, G. R.
An analytical approach to airfoil icing
[AIAA PAPER 81-0403] p0117 A81-20810
- GREYBALL, R. S.
Performance prediction of straight two dimensional diffusers
[NASA-CN-165186] p0133 N81-11833
- GROENBECK, D.
Comparison of predicted engine core noise with proposed FAA helicopter noise certification requirements
p0128 A81-38062
- GROENBECK, D. E.
Comparison of predicted engine core noise with current and proposed aircraft noise certification requirements
[AIAA PAPER 81-2053] p0024 A81-48635
- An improved prediction method for noise generated by conventional profile coaxial jets
[AIAA PAPER 81-1991] p0129 A81-49743
- Comparison of predicted engine core noise with proposed FAA helicopter noise certification requirements
[NASA-TN-81739] p0130 N81-22839
- Comparison of predicted engine core noise with current and proposed aircraft noise certification requirements
[NASA-TN-82659] p0126 N81-29922
- An improved prediction method for noise generated by conventional profile coaxial jets
[NASA-TN-82712] p0127 N81-32964
- GROBER, R. P.
Simplified power supplies for ion thrusters
[AIAA PAPER 81-0693] p0040 A81-29542
- Simplified power supplies for ion thrusters
[NASA-TN-81725] p0039 N81-20177
- GUTIERREZ, O. A.
Status of noise technology for advanced supersonic cruise aircraft
p0001 N81-18002
- H**
- HAS, J. R.
An experimental evaluation of the performance deficit of an aircraft engine starter turbine
[SAE PAPER 801137] p0021 A81-34166
- Reasons for low aerodynamic performance of 13.5-centimeter-tip-diameter aircraft engine starter turbine
[NASA-TP-1810] p0016 N81-20076
- Cold-air performance of compressor-drive turbine of Department of Energy upgraded automobile gas turbine engine. 1: Volute-manifold and stator performance
[NASA-TN-82682] p0004 N81-28053
- HACK, J. R.
Fabrication of aluminum oxide fiber reinforced aluminum matrix composites
[NASA-CN-165184] p0048 N81-19229
- HAGSDORN, W. R.
NASA preprototype redox storage system for a photovoltaic stand-alone application
[NASA-TN-82607] p0104 N81-24534
- A redox system design for solar storage applications
[NASA-TN-82720] p0108 N81-32608
- HAGGARD, J. R., JR.
Forced and natural convection in laminar-jet diffusion flames
[NASA-TP-1841] p0076 N81-24388
- HALFORD, G. R.
Progress in materials and structures at Lewis Research Center
p0142 N81-12982
- HANLON, E. M.
Propellant management for low thrust chemical propulsion systems
[AIAA PAPER 81-1453] p0042 A81-42198
- HANCOCK, B. J.
Elastohydrodynamic lubrication of elliptical contacts
[NASA-TN-81647] p0080 N81-13358
- History of ball bearings
[NASA-TN-81689] p0081 N81-18391
- Introduction to ball bearings
[NASA-TN-81690] p0081 N81-18392
- Effect of surface roughness on hydrodynamic bearings
[NASA-TN-81711] p0082 N81-21356
- Lubrication fundamentals
[NASA-TN-81762] p0103 N81-23490
- Surface roughness effect on finite oil journal bearings
[NASA-TN-82639] p0084 N81-27526
- Simplified solution for stresses and deformation
[NASA-TN-82647] p0084 N81-28444
- Analysis of starvation effects on hydrodynamic lubrication in nonconforming contacts
[NASA-TN-82668] p0084 N81-29438
- Ball bearing mechanics
[NASA-TN-81691] p0085 N81-31550
- HANNUK, M. P.
Some effects of thermal-cycle-induced deformation in rocket thrust chambers
[NASA-TP-1834] p0038 N81-20176
- HANSON, M. R.
Feasibility of Kevlar 49/PHR-15 polyimide for high temperature applications
p0047 A81-43602
- Environmental effects on graphite fiber reinforced PHR-15 polyimide
[NASA-TN-82625] p0046 N81-32194
- HART, P. R.
The effect of thermal cycling to 1100 C on the alpha /beta/ phase in directionally solidified gamma/gamma-prime-alpha alloys
p0057 A81-32546
- The effect of thermal cycling to 1100 degree C on the alpha (beta) phase in directionally solidified gamma/gamma prime-alpha alloys
[NASA-TN-81688] p0052 N81-18165
- HARKNEY, R. D.
Propulsion controls
p0025 N81-12095
- HARRIS, D. R.
Phosphazene diamines
[NASA-CN-165147] p0065 N81-10169
- HART, R. E., JR.
GaAs homojunction solar cell development
p0099 N81-17561
- Comparative radiation testing of solar cells for the shuttle power extension package
[NASA-TN-82656] p0105 N81-27605
- HATCH, A. M.
Conceptual design of the NHD Engineering Test Facility
[NASA-TN-82621] p0132 N81-24926
- HAVERSHAM, W. J.
Low NO_x and fuel flexible gas turbine combustors
[ASME PAPER 81-GT-99] p0020 A81-30006
- HAWKINS, C. R.
Free radical propulsion concept
[AIAA PAPER 81-0676] p0041 A81-32905
- Free radical propulsion concept
[NASA-TN-81770] p0039 N81-20180
- BRIDGES, L. J.
Acoustic performance of inlet suppressors on an engine generating a single mode
[NASA-TN-82697] p0127 N81-32968
- BRIDGES, E.
Energy efficient engine: Flight propulsion system preliminary analysis and design
[NASA-CN-159583] p0029 N81-18056

- HEITSAN, P. U.
Surface flaw detection in structural ceramics by scanning photoacoustic spectroscopy
p0079 A81-17906
- HEISINGER, J. A.
SEP BIOD variable conductance heat pipes acceptance and characterization tests
[NASA-TN-82635] p0076 A81-30390
- HEIDRICKS, E. C.
Some flow phenomena associated with aligned, sequential apertures with Borda-type inlets
[NASA-TP-1792] p0076 A81-24387
- HEIDRICKS, E. C.
Assessment of variations in thermal cycle life data of thermal barrier coated rods
p0058 A81-44657
Prolonging thermal barrier coated specimen life by thermal cycle management
p0065 A81-44658
Flow through axially aligned sequential apertures of the orifice and Borda types
[NASA-TN-81681] p0075 A81-21314
Prolonging thermal barrier coated specimen life by thermal cycle management
[NASA-TN-81742] p0102 A81-23417
Assessment of variations in thermal cycle life data of thermal barrier coated rods
[NASA-TN-81743] p0102 A81-23418
Experiments on flow through one to four inlets of the orifice and Borda type
[NASA-TN-82680] p0077 A81-30391
- HEIDRICKS, T. P.
Effect of milling and leaching on the structure of sintered silicon
p0064 A81-22529
Effect of milling and leaching on the structure of sintered silicon
[NASA-TN-81602] p0060 A81-13166
- HEIDRICKS, A. M.
Radiation damage in lithium-counterdoped W/P silicon solar cells
p0109 A81-27204
Radiation damage in silicon W/P solar cells
p0099 A81-17557
Performance of high resistivity n⁺⁺p silicon solar cells under 1 MeV electron irradiation
[NASA-TN-82610] p0103 A81-23626
- HEIDRICKS, P.
An experimental evaluation of the performance deficit of an aircraft engine starter turbine
[SAE PAPER 801137] p0021 A81-34168
Reasons for low aerodynamic performance of 13.5-centimeter-tip-diameter aircraft engine starter turbine
[NASA-TP-1810] p0016 A81-20076
- HILT, B. B.
Evaluation of advanced combustors for dry NO_x/suppression with nitrogen bearing fuels in utility and industrial gas turbines
[ASME PAPER 81-GT-125] p0087 A81-30029
- HIPPELSTEIN, S. A.
Evaluation of a method for heat transfer measurements and thermal visualization using a composite of a heater element and liquid crystals
[ASME PAPER 81-GT-93] p0079 A81-30000
Effect of hole geometry and Electric-Discharge Machining (EDM) on airflow rates through small diameter holes in turbine blade material
[NASA-TP-1716] p0013 A81-12089
Evaluation of a method for heat transfer measurements and thermal visualization using a composite of a heater element and liquid crystals
[NASA-TN-81639] p0075 A81-21313
- HIRSCHBERG, M. S.
Structural dynamics verification facility study
[NASA-TN-82675] p0092 A81-33457
- HIRSCHBERG, M. S.
Stability of large horizontal-axis axisymmetric wind turbines
p0092 A81-22526
Stability of large horizontal-axis axisymmetric wind turbines
[NASA-TN-81623] p0091 A81-12446
- HOBBEN, M. A.
Pumping power considerations in the designs of NASA-Redox flow cells
[NASA-TN-82598] p0106 A81-28519
- HOCKEY, J.
Preparation and evaluation of advanced electrocatalysts for phosphoric acid fuel cells
[NASA-CN-165245] p0112 A81-18496
- HODGSON, B. B.
Anion perselective membrane
[NASA-CN-165223] p0111 A81-16583
- HODGE, F. E.
Thermal barrier coatings - Burner rig hot corrosion test results
p0063 A81-12630
Thermal barrier coatings for heat engine components
p0056 A81-12920
Thermal barrier coatings for superalloys
p0058 A81-49217
Corrosion resistant thermal barrier coating
[NASA-CASE-LEW-13088-1] p0054 A81-25188
- HOFMEIER, J. L.
Vehicle testing of Cummins t ribocompound diesel engine
[NASA-CN-159840] p0140 A81-13803
- HOFFMAN, C. A.
Method for alleviating thermal stress damage in laminates
[NASA-CASE-LEW-12493-1] p0045 A81-17170
Method for alleviating thermal stress damage in laminates
[NASA-CASE-LEW-12493-2] p0046 A81-26179
- HOFFMAN, J. D.
Calculation of the flow field in supersonic inlets using a bicharacteristics method with shock wave fitting
p0006 A81-21212
- HOFFMAN, M.
Second year technical report on-board processing for future satellite communications systems
[NASA-CN-165155] p0070 A81-10242
- HOLDEN, J. D.
Ozone contamination in aircraft cabins - Results from GASP data and analyses
[AIAA PAPER 81-0305] p0010 A81-20740
Cloud encounter and particle density variabilities from GASP data
[AIAA PAPER 81-0308] p0117 A81-20742
Tabulations of ambient ozone data obtained by GASP airliners, March 1975 to December 1977
[NASA-TN-81528] p0116 A81-13568
Ozone contamination in aircraft cabins: Results from GASP data and analyses
[NASA-TN-81671] p0009 A81-16021
Analysis of atmospheric ozone levels at commercial airplane cruise altitudes in winter and spring, 1976 - 1977
[NASA-TP-1807] p0117 A81-21685
- HOLLOWAY, P. B.
Energy efficient engine: Flight propulsion system preliminary analysis and design
[NASA-CN-159583] p0029 A81-18056
- HOLMS, A. G.
Backward deletion to minimize prediction errors in models from factorial experiments with zero to six center points
p0122 A81-14999
Backward deletion to minimize prediction errors in models from factorial experiments with zero to six center points
[NASA-TN-81524] p0123 A81-10778
- HONYAK, L.
Turbomachinery noise studies of the AiResearch QCGAT engine with inflow control
[AIAA PAPER 81-2049] p0023 A81-48621
Turbomachinery noise studies of the AiResearch QCGAT engine with inflow control
[NASA-TN-82694] p0127 A81-31957
Acoustic performance of inlet suppressors on an engine generating a single mode
[NASA-TN-82697] p0127 A81-32968
- HOOPER, B. G., JR.
Cell module and fuel conditioner
[NASA-CN-165189] p0112 A81-18494
Cell module and fuel conditioner development
[NASA-CN-165190] p0112 A81-19573
- HOPKINS, G. S., III
Development of low-cost directionally-solidified turbine blades
p0088 A81-10707
Low-cost directionally-solidified turbine blades, volume 2
[NASA-CN-159562] p0024 A81-12088
- HORNE, W. L.
Electrostatic bonding of thin (approximately 3

- sil) 7070 cover glass to Ta205 Al-coated thin (approximately 2 mil) silicon wafers and solar cells
p0111 N81-17569
- KOVATH, B.**
Compatibility of alternative fuels with advanced automotive gas turbine and stirling engines. A literature survey
[NASA-TN-81754] p0105 N81-27604
Test results of the Chrysler upgraded automotive gas turbine engine: Initial design
[NASA-TN-81660] p0107 N81-30562
- KOSHY, E. M.**
Aerodynamic stability analysis of NASA J85-13/plane pressure pulse generator installation
[NASA-CR-165141] p0027 N81-15004
TF34 engine compression system computer study
[NASA-CR-159889] p0027 N81-15005
- KOUSER, M. J.**
Fuel injector characterization studies
[NASA-CR-165200] p0026 N81-15003
- KOWLETT, B. A.**
Variable stream control engine for advanced supersonic aircraft design update
p0001 N81-17996
- KRYCAR, P.**
Heat transfer from a row of impinging jets to concave cylindrical surfaces
p0078 N81-24924
- KSU, L. C.**
New ion exchange membranes
[NASA-TN-81670] p0044 N81-16123
Inexpensive cross-linked polymeric separators made from water soluble polymers
[NASA-TN-82619] p0101 N81-23205
In-situ cross linking of polyvinyl alcohol
[NASA-CASE-LBN-13135-2] p0062 N81-24257
Cross-linked polyvinyl alcohol and method of baking same
[NASA-CASE-LBN-13504-1] p0063 N81-27279
Polyvinyl alcohol battery separator containing inert filler
[NASA-CASE-LBN-13556-1] p0106 N81-27615
Cross-linked polyvinyl alcohol and method of baking same
[NASA-CASE-LBN-13101-2] p0044 N81-29160
Alkaline battery containing a separator of a cross-linked copolymer of vinyl alcohol and unsaturated carboxylic acid
[NASA-CASE-LBN-13102-1] p0107 N81-29531
- KUANG, Y. T.**
An investigation of hot corrosion mechanisms in nickel base alloys
p0058 N81-16208
- KUDSON, B. S.**
Ceramic applications in turbine engines
[NASA-CR-159865] p0029 N81-18118
- KUNT, B. B.**
Variable stream control engine for advanced supersonic aircraft design update
p0001 N81-17996
- KURLEY, J. P.**
Design of an exhaust mixer nozzle for the Avco-Lycoming Quiet Clean General Aviation Turbofan (QCGAT)
[NASA-CR-159426] p0029 N81-19120
- KURST, E. B.**
Diagnostic system design for the Ion Auxiliary Propulsion System (IAPS) - Flight test of two 8 cm mercury ion thrusters
[AIAA PAPER 81-0666] p0041 N81-38070
Diagnostic system design for the Ion Auxiliary Propulsion System (IAPS). Flight tests of two 8 cm mercury ion
[NASA-TN-81702] p0037 N81-20172
- KURST, L. G.**
Low-cost directionally-solidified turbine blades, volume 2
[NASA-CR-159562] p0024 N81-12088
- KURSH, P. I.**
Influence of excess diamine on properties of PBE polyamide resins and composites
p0047 N81-43635
- KUSTON, B. L.**
Surface geometry of circular cut spiral bevel gears
[NASA-TN-82622] p0083 N81-26459
- KUSTVEDT, D. C.**
Conceptual design of an in-space cryogenic fluid management facility, executive summary
[NASA-CR-165279-EMC-388M] p0137 N81-21212
Conceptual design of an in-space cryogenic fluid management facility
[NASA-CR-165279] p0067 N81-21213
- IGNACIAN, L. B.**
SST II 1980 extended flight thruster experiments [AIAA PAPER 81-0665] p0040 N81-29528
SST II 1980 extended flight thruster experiments [NASA-TN-81685] p0038 N81-19222
- INGERSO, B. B.**
Capillary and acceleration wave breakup of liquid jets in axial-flow airstreams
[NASA-TP-1791] p0075 N81-16417
Acceleration wave breakup of liquid jets with airstreams
[NASA-TN-81717] p0075 N81-21310
- ITO, Y. I.**
Phosphazene diamines
[NASA-CR-165147] p0065 N81-10169
- JABER, B. P.**
Extended frequency turbofan model
[NASA-CR-165261] p0030 N81-20078
- JAKUBOWSKI, A. E.**
Flow separation in inlets at incidence angles
p0006 N81-29114
- JAMES, B. L.**
Adapting magnetoelectrostatic containment to inert gas thrusters
[AIAA PAPER 81-0140] p0043 N81-20625
Results of the Mission Profile Life Test first test segment - Thruster J1
[AIAA PAPER 81-0716] p0043 N81-29552
- JANOVICH, M. A.**
Ceramic applications in turbine engines
[NASA-CR-159865] p0029 N81-19118
- JANUS, A. S.**
JT8D-15/17 high pressure turbine root discharged blade performance improvement
[NASA-CR-165220] p0028 N81-17080
- JAY, A.**
Effect of time-dependent flight loads on turbofan engine performance deterioration
[ASME PAPER 81-GT-203] p0030 N81-30093
- JEAN, P. B.**
Second year technical report on-board processing for future satellite communications systems
[NASA-CR-165155] p0070 N81-10242
- JEFFRIES, K. S.**
Analysis of GaAs and Si solar cell arrays for earth orbital and orbit transfer missions
p0109 N81-27254
Analysis of costs of gallium arsenide and silicon solar arrays for space power applications
[NASA-TP-1811] p0038 N81-20173
- JERACI, B. J.**
Low and high speed propellers for general aviation - Performance potential and recent wind tunnel test results
p0023 N81-42758
Low and high speed propellers for general aviation: Performance potential and recent wind tunnel test results
[NASA-TN-81745] p0003 N81-21028
The propeller tip vortex. A possible contributor to aircraft cabin noise
[NASA-TN-81768] p0130 N81-22838
- JOHNSON, G. M.**
Surrogate-equation technique for simulation of steady inviscid flow
[NASA-TP-1866] p0005 N81-31129
- JOHNSON, J. E.**
Deposition and material response from Mach 0.3 burner rig combustion of SRC 2 fuels
[NASA-TN-81634] p0051 N81-15069
- JONES, B. P.**
Energy efficient engine: Flight propulsion system preliminary analysis and design
[NASA-CR-159583] p0029 N81-18056
- JONES, B. G.**
Reliability and quality assurance on the MOD 2 wind system
[NASA-TN-82717] p0090 N81-33492

- JONES, R. E.
Selected results from combustion research at the
Lewis Research Center
[AIAA PAPER 81-1392] p0022 A81-40859
Selected results from combustion research at the
Lewis Research Center
[NASA-TN-82627] p0017 A81-25083
- JONES, W. E., JR.
Evaluation of boundary lubricants using
steady-state wear and friction
[NASA-TN-81601] p0061 A81-17265
Contact angle measurements of a polyphenyl ether
to 190 C on M-50 steel
[NASA-TN-82628] p0063 A81-27277
- JUTRAS, R.
Supersonic stall flutter of high-speed fans
[ASME PAPER 81-GT-184] p0020 A81-30078
Supersonic stall flutter of high speed fans
[NASA-TN-81613] p0003 A81-14978

K

- KAMPE, F.
Numerical trials of HISSE
[B81-10069] p0094 A81-13425
- KAQ, B. C.
Some aspects of calculating flows about
three-dimensional subsonic inlets
[AIAA PAPER 81-1361] p0007 A81-42177
Some aspects of calculating flows about
three-dimensional subsonic inlets
[NASA-TN-82678] p0004 A81-28054
- KAPLAN, S. I.
Photovoltaic applications - Past and future
p0109 A81-27231
- KARACHETTY, S.
Study of fuel cell on-site, integrated energy
systems in residential/commercial applications
[NASA-CR-165144] p0112 A81-21533
- KARCHNER, A.
Core noise measurements from a small, general
aviation turbofan engine
p0019 A81-22531
Core noise measurements from a small, general
aviation turbofan engine
[NASA-TN-81610] p0125 A81-11769
Conditioned pressure spectra and coherence
measurements in the core of a turbofan engine
[NASA-TN-82688] p0126 A81-30907
- KATZ, I.
The effect of solar array voltage patterns on
plasma power losses
p0043 A81-19937
Fluid model of plasma outside a hollow cathode
neutralizer
[AIAA PAPER 81-0739] p0134 A81-29560
Parasitic current losses due to solar electric
propulsion generated plasmas
[AIAA PAPER 81-0740] p0043 A81-29561
Analysis of the charging of the SCATHA (P78-2)
satellite
[NASA-CR-165348] p0033 A81-27169
- KAUSCH, E.
Integrated IC-circuits in ALTA-technology on one
substrate
[BNFT-PB-T-79-107] p0072 A81-14227
- KAYS, W. E.
Full-coverage film cooling. I - Three-dimensional
measurements of turbulence structure. II -
Prediction of the recovery-region hydrodynamics
p0078 A81-15537
- KASA, K. B. V.
Effects of mistuning on bending-torsion flutter
and response of a cascade in incompressible flow
[AIAA 81-0602] p0092 A81-29465
Application of unsteady airfoil theory to rotary
wings
p0006 A81-39874
Effects of mistuning on bending-torsion flutter
and response of a cascade in incompressible flow
[NASA-TN-81674] p0091 A81-16494
Aeroelastic characteristics of a cascade of
mistuned blades in subsonic and supersonic flows
[NASA-TN-82631] p0091 A81-26492
- KASABOFF, J. E.
Heat exchanger and method of making
[NASA-CASE-LEN-12441-J] p0104 A81-24519
- KRITH, T. G., JR.
Performance of a steel spar wind turbine blade on

- the Mod-0 100 kW experimental wind turbine
[NASA-TN-81588] p0096 A81-11448
- KERSLAGE, W. E.
SERT II 1980 extended flight thruster experiments
[AIAA PAPER 81-0665] p0040 A81-29528
SERT II thrusters - Still ticking after eleven years
[AIAA PAPER 81-1539] p0042 A81-40934
SERT II 1980 extended flight thruster experiments
[NASA-TN-81685] p0038 A81-19222
SERT 2 thrusters: Still ticking after eleven years
[NASA-TN-81774] p0040 A81-26174
- KHAN, A. S.
The effect of zirconium on the cyclic oxidation of
NiCrAl alloys
p0056 A81-18559
- KHANDLWAL, P. K.
Surface flaw detection in structural ceramics by
scanning photoacoustic spectroscopy
p0079 A81-17906
- KIEHL, R. E.
Effects of mistuning on bending-torsion flutter
and response of a cascade in incompressible flow
[AIAA 81-0602] p0092 A81-29465
Effects of mistuning on bending-torsion flutter
and response of a cascade in incompressible flow
[NASA-TN-81674] p0091 A81-16494
Aeroelastic characteristics of a cascade of
mistuned blades in subsonic and supersonic flows
[NASA-TN-82631] p0091 A81-26492
- KING, B. B.
Status of commercial phosphoric acid fuel cell
system development
[AIAA PAPER 81-0396] p0108 A81-20805
Status of commercial phosphoric acid fuel cell
system development
[NASA-TN-81641] p0096 A81-13464
- KIRALY, L. J.
Structural dynamics verification facility study
[NASA-TN-82675] p0092 A81-33497
- KIRKPATRICK, A. E.
Silicon solar cells with high open-circuit voltage
p0113 A81-27089
- KISSE, D. E.
Fabrication development of alumina/aluminum
composites
[NASA-CR-165195] p0048 A81-19233
- KLEN, J. S.
Energy efficient engine: Flight propulsion system
preliminary analysis and design
[NASA-CR-159583] p0029 A81-18056
- KNIP, G.
Comparisons of four alternative powerplant types
for future general aviation aircraft
[NASA-TN-81584] p0013 A81-10067
- KNOTT, P. E.
Aerodynamic/acoustic performance of YJ101/double
bypass VCE with conannular plug nozzle
[NASA-CR-155869] p0129 A81-17846
VCE early acoustic test results of General
Electric's high-radius ratio conannular plug nozzle
p0029 A81-17999
- KOHL, P. J.
Deposition and material response from Mach 0.3
burner rig combustion of SBC 2 fuels
[NASA-TN-81634] p0051 A81-15069
The effects of trace impurities in coal-derived
liquid fuels on deposition and accelerated high
temperature corrosion of cast superalloys
[NASA-TN-81678] p0052 A81-16211
Combustion system processes leading to corrosive
deposits
[NASA-TN-81752] p0101 A81-23243
Material response from Mach 0.3 burner rig
combustion of a coal-oil mixture
[NASA-TN-81686] p0055 A81-27258
- KORLMAN, S. L.
Icing tunnel tests of a glycol-exuding porous
leading edge ice protection system on a general
aviation airfoil
[AIAA PAPER 81-0405] p0011 A81-20837
Evaluation of a pneumatic boot deicing system on a
general aviation wing model
[NASA-TN-82363] p0011 A81-25065
- KOLECKI, J. C.
Commercial (terrestrial) and modified solar array
design studies for low cost, low power space
applications
[NASA-TN-81622] p0061 A81-17266

- KOSMAN, H. G.
Gyrotion transmitting tube
[NASA-CASE-LW-13429-1] p0071 N81-16384
Analytical investigation of efficiency and
performance limits in klystron amplifiers using
multidimensional computer programs; multi-stage
depressed collectors; and thermionic cathode
life studies p0098 N81-16552
Ladder supported ring bar circuit
[NASA-CASE-LW-13570-1] p0071 N81-24348
Analytical prediction and experimental
verification of performance at various operating
conditions of a dual-mode traveling wave tube
with multistage depressed collectors
[NASA-TP-1831] p0072 N81-28352
- KRAFT, G. A.
Advanced subsonic transport propulsion
[NASA-TN-82696] p0019 N81-31195
- KRAUSE, A. M.
Phosphazene diamines
[NASA-CR-165147] F0065 N81-10169
- KRAUSE, L. M.
Miniature drag-force anemometer
[NASA-TN-81680] p0079 N81-16428
- KRAUTER, A. I.
Measurement of rod seal lubrication for Stirling
engine
[NASA-CR-165158] p0088 N81-13359
- KREIN, M. J.
Comparison of NASA and contractor results from
aeroacoustic tests of QCSER OTW engine
[NASA-TN-81761] p0017 N81-25079
- KREJSA, S. A.
New technique for the direct measurement of core
noise from aircraft engines
[AIAA PAPER 81-1587] p0128 N81-40962
New technique for the direct measurement of core
noise from aircraft engines
[NASA-TN-82634] p0126 N81-26844
- KRESHOVSKI, J. P.
Prediction of laminar and turbulent primary and
secondary flows in strongly curved ducts
[NASA-CR-3388] p0007 N81-16976
A three-dimensional turbulent compressible
subsonic duct flow analysis for use with
constructed coordinate systems
[NASA-CR-3389] p0077 N81-20383
- KROSEL, S. M.
An automated procedure for developing hybrid
computer simulations of turbofan engines p0020 N81-32544
An automated procedure for developing hybrid
computer simulations of turbofan engines
[NASA-TN-81605] p0037 N81-11688
- KU, M. S.
Study of fuel cell on-site, integrated energy
systems in residential/commercial applications
[NASA-CR-165144] p0112 N81-21533
- KUBASCO, A. J.
Development of a low NO_x/lean premixed annular
combustor
[ASME PAPER 81-GT-40] p0020 N81-29954
- KURKOV, A.
Effects of mistuning on blade torsional flutter
p0092 N81-29095
- KURKOV, A. P.
Measurement of aerodynamic work during fan flutter
[NASA-TN-82652] p0017 N81-25080
- KVATERNIK, R. G.
Application of unsteady airfoil theory to rotary
wings p0006 N81-39674
- L**
- LABOTE, R. J.
High-density fuel combustion and cooling
investigation
[NASA-CR-165177] p0050 N81-16177
- LABOTTI, G. D.
Computer-aided roll pass design in rolling of
airfoil shapes p0088 N81-15796
- LARGE, G. D.
Analytical design of an advanced radial turbine
[NASA-CR-165170] p0140 N81-20958
- LARK, R. F.
Superhybrid composite blade impact studies
[ASME PAPER 81-GT-24] p0020 N81-29940
Superhybrid composite blade impact studies
[NASA-TN-81597] p0091 N81-11412
- LATSEN, W. C.
Particle and field measurements on two J-series
30-centimeter thrusters
[AIAA PAPER 81-0729] p0042 N81-38072
Particle and field measurements on two J-series 30
centimeter thrusters
[NASA-TN-81741] p0039 N81-22084
- LAUTER, R. W.
Progress in materials and structures at Lewis
Research Center p0142 N81-12982
- LECHNER, R. T.
Low NO_x/ combustion systems for burning heavy
residual fuels and high-fuel-bound nitrogen fuels
[ASME PAPER 81-GT-109] p0089 N81-30014
- LEE, D.
High-response measurements of a turbofan engine
during nonrecoverable stall
[NASA-TN-81759] p0017 N81-25084
- LEE, F. C.
Analysis and design of an adaptive multi-loop
controlled two winding buck/boost regulator
p0073 N81-21675
Application handbook for a Standardized Control
Module (SCM) for DC-DC converters, volume 1
[NASA-CR-165172] p0072 N81-10301
User's design handbook for a Standardized Control
Module (SCM) for DC to DC Converters, volume 2
[NASA-CR-165173] p0072 N81-11314
- LEE, R. Q.
Recent work on an RF ion thruster
[AIAA PAPER 81-0678] p0041 N81-35625
Recent work on an RF ion thruster
[NASA-TN-81734] p0039 N81-20178
- LEE, S. D.
Study of component technologies for fuel cell
on-site integrated energy systems
[NASA-CR-165152-VOL-1] p0110 N81-15461
Study of component technologies for fuel cell
on-site integrated energy system. Volume 2:
Appendices
[NASA-CR-165152-VOL-2] p0110 N81-15462
- LEHTINEN, R.
F100 multivariable control synthesis program: A
review of full scale engine altitude tests
p0014 N81-12043
- LEIBER, M. F.
Acceptance tests and manufacturer relationships
for 20 ampere-hour sealed nickel-cadmium cells
using discharge parameters p0049 N81-17189
Acceptance tests and manufacturer relationships
from the 20A h standard cell data p0100 N81-21515
- LEISINGER, G. G.
Multivariable nyquist array method with application
to turbofan engine control p0026 N81-12101
- LEONARD, R. G.
Engine identification for adaptive control
p0025 N81-12100
- LEROY, B. L.
An economic systems analysis of land mobile radio
telephone services p0069 N81-22528
An economic systems analysis of land mobile radio
telephone services
[NASA-TN-81476] p0069 N81-10239
- LESCO, D. J.
Specifying and calibrating instrumentations for
wideband electronic power measurements
[NASA-TN-81545] p0079 N81-16429
- LEVINE, S. S.
Thermal barrier coatings - Burner rig hot
corrosion test results p0063 N81-12630
Thermal barrier coatings for heat engine components
p0056 N81-12920
Thermal barrier coatings for superalloys
p0058 N81-49217
Corrosion resistant thermal barrier coating
[NASA-CASE-LW-13088-1] p0054 N81-25188
Advanced aircraft engine materials trends
[NASA-TN-82626] p0055 N81-27259
A new diffusion-inhibited oxidation-resistant
coating for superalloys

LEVY, B.

PERSONAL AUTHOR INDEX

- [NASA-TN-82687] p0056 N81-33273
LEVY, B.
Calculation of three-dimensional turbulent subsonic flows in transition ducts p0008 A81-21199
A three-dimensional turbulent compressible subsonic duct flow analysis for use with constructed coordinate systems [NASA-CN-3389] p0077 N81-20383
LEW, B. G.
Low NO_x and fuel flexible gas turbine combustors [ASME PAPER 81-61-99] p0020 A81-30006
LEWIS, B. L.
Effect of time-dependent flight loads on turbofan engine performance deterioration [ASME PAPER 81-61-203] p0030 A81-30093
LIGHT, L.
Dynamic characteristics of a high-speed rotor with radial and axial foil-bearing supports [ASME PAPER 80-C2/LUE-35] p0085 A81-18683
LIEBERMAN, A.
Design and assembly considerations for Redox cells and stacks [NASA-TN-82672] p0049 N81-31308
LIEBER, C. G.
Analytical design of an advanced radial turbine [NASA-CN-165170] p0140 N81-20958
LING, J. S.
Preparation and characterization of electrodes for the NASA Redox storage system [NASA-TN-82702] p0107 N81-30522
Advances in membrane technology for the NASA redox energy storage system [NASA-TN-82701] p0108 N81-33601
LINSCOTT, B. S.
The Mod-2 wind turbine development project [NASA-TN-82681] p0106 N81-27606
LIU, B. C.
Proton radiation damage in bulk n-GaAs p0099 N81-17564
LOEFFLER, I. J.
Comparison of NASA and contractor results from aerodynamic tests of QCSER OTW engine [NASA-TN-81761] p0017 N81-25079
LOMBARDI, S. E.
Kinematic correction for roller skewing [ASME PAPER 80-DRT-76] p0085 A81-18647
Design studies of continuously variable transmissions for electric vehicles [NASA-TN-81642] p0080 N81-13357
Design of spur gears for improved efficiency [NASA-TN-81625] p0081 N81-17436
Advanced continuously variable transmissions for electric and hybrid vehicles [NASA-TN-81718] p0082 N81-19459
Life analysis of multicracker planetary traction drive [NASA-TN-1710] p0082 N81-20423
Effects of Ultra-Clean and centrifugal filtration on rolling-element bearing life [NASA-TN-82680] p0085 N81-29440
Continuously variable transmission: Assessment of applicability to advance electric vehicles [NASA-TN-82700] p0085 N81-33484
LOONIS, W. B.
Evaluation of boundary lubricants using steady-state wear and friction [NASA-TN-81601] p0061 N81-17265
Steady-state boundary lubrication with formulated C-ethers to 260 C [NASA-TN-1812] p0053 N81-21193
LORENZO, C. F.
A four-cylinder Stirling engine controls model [NASA-TN-81648] p0075 N81-15241
LOUBSKY, S. J.
Assessment of disk MHD generators for a base load powerplant [NASA-TN-82609] p0103 N81-23611
LOUIS, J. F.
Assessment of disk MHD generators for a base load powerplant [NASA-TN-82609] p0103 N81-23611
LOVELL, C. E.
The effect of zirconium on the cyclic oxidation of NiCrAl alloys p0056 A81-18559
High temperature cyclic oxidation furnace testing at NASA Lewis Research Center p0058 A81-44653
Synergistic erosion/corrosion of superalloys in PFB coal combustor effluent p0058 A81-44663
The effects of trace impurities in coal-derived liquid fuels on deposition and accelerated high temperature corrosion of cast superalloys [NASA-TN-81678] p0052 N81-16211
Synergistic erosion/corrosion of superalloys in PFB coal combustor effluent [NASA-TN-81715] p0101 N81-23245
High temperature alkali corrosion in high velocity gases [NASA-TN-82591] p0054 N81-25191
High temperature cyclic oxidation furnace testing at NASA Lewis Research Center [NASA-TN-81773] p0054 N81-26234
LU, C. L.
Assessment of disk MHD generators for a base load powerplant [NASA-TN-82609] p0103 N81-23611
LUDWIG, L. E.
Composite wall concept for high-temperature turbine shrouds - Heat transfer analysis [SAE PAPER 801138] p0021 A81-34169
Multiple plate hydrostatic viscous damper [NASA-CASE-LBN-12445-1] p0083 N81-22360
Circumferential shaft seal [NASA-CASE-LBN-12119-2] p0083 N81-26447
LUIDEN, B. W.
Three-dimensional turbulent boundary layer development and separation in V/STOL engine inlets at incidence with small-cross flow and curvature influences [AIAA PAPER 81-0254] p0005 A81-20703
LUIDEN, B. W.
Optimum subsonic, high-angle-of-attack nacelles p0005 A81-11646
Flow separation in inlets at incidence angles p0006 A81-29114
LYONS, V. J.
Fuel/air nonuniformity - Effect on nitric oxide emissions [AIAA PAPER 81-0327] p0019 A81-20834

M

- MACIOCH, L. L.
A status report on the Energy Efficient Engine Project [SAE PAPER 801119] p0021 A81-34155
MACONBERG, M. L.
Photovoltaic applications - Past and future p0109 A81-27231
MARTINS, M. P.
Cost/benefit analysis of advanced materials technology candidates for the 1980's, part 2 [NASA-CN-165176] p0139 N81-11953
MARMOND, M. P.
Analysis and design of an adaptive multi-loop controlled two winding buck/boost regulator p0073 A81-21675
Application handbook for a Standardized Control Module (SCM) for DC-DC converters, volume 1 [NASA-CN-165172] p0072 N81-10301
MAIER, R. D.
Microstructure and mechanical properties of bulk and plasma-sprayed Y2O3-partially stabilized zirconia [NASA-CN-165126] p0059 N81-22158
MAJUMGI, B. L.
VCE early acoustic test results of General Electric's high-radius ratio conical plug nozzle p0029 N81-17999
MAJUMDAR, B. C.
Effect of surface roughness on hydrodynamic bearings [NASA-TN-81711] p0082 N81-21356
Surface roughness effect on finite oil journal bearings [NASA-TN-82639] p0084 N81-27526
MALOY, J. E.
Characteristics of 30-centimeter mercury ion thrusters [AIAA PAPER 81-0715] p0041 A81-37569
Electric propulsion - Characteristics, applications, and status [NASA-TN-81630] p0033 N81-13079
Characteristics of 30-centimeter mercury ion thrusters [NASA-TN-81706] p0039 N81-21121

- MANDELL, E. J.**
The effect of solar array voltage patterns on plasma power losses
p0043 A81-19937
- Fluid model of plasma outside a hollow cathode neutralizer**
[AIAA PAPER 81-0739] p0134 A81-29560
- Parasitic current losses due to solar electric propulsion generated plasmas**
[AIAA PAPER 81-0740] p0043 A81-29561
- Analysis of the charging of the SCATRA (P78-2) satellite**
[NASA-CR-165348] p0033 A81-27169
- MANTHERKEN, M. A.**
Performance capabilities of the 8-cm Mercury ion thruster
[AIAA PAPER 81-0754] p0044 A81-29567
- Performance capabilities of the 8-cm mercury ion thruster**
[NASA-TN-81720] p0038 A81-19220
- MARHO, M. A.**
Control of volume resistivity in inorganic-organic separators
p0108 A81-11034
- Cross-linked polyvinyl alcohol and method of making same**
[NASA-CASE-LEU-13504-1] p0063 A81-27279
- Polyvinyl alcohol battery separator containing inert filler**
[NASA-CASE-LEU-13556-1] p0106 A81-27615
- Qualification testing of secondary sterilizable silver-zinc cells for use in the Jupiter atmospheric entry probe**
[NASA-TN-82638] p0108 A81-30563
- MARCHMONT, G.**
Engineering support for magnetohydrodynamic power plant analysis and design studies
[NASA-CR-159690] p0110 A81-13466
- MAREK, C. J.**
Supercritical fuel injection system
[NASA-CASE-LEU-12990-1] p0018 A81-29129
- MARTINEY, P. J.**
Experimental study of the stability of aircraft fuels at elevated temperatures
[NASA-CR-165165] p0067 A81-12255
- MARTINI, V. R.**
A computer simulation of the transient response of a 4 cylinder Stirling engine with burner and air preheater in a vehicle
[NASA-CR-165262] p0078 A81-22313
- MARVIS, I. E.**
Integrated control system for a gas turbine engine
[NASA-CASE-LEU-12594-2] p0015 A81-19116
- MASLOUSKI, E. A.**
Electronically commutated dc motors for electric vehicles
[NASA-TN-81654] p0097 A81-15464
- MASON, J. E.**
Extended frequency turbofan model
[NASA-CR-165261] p0030 A81-20076
- MASON, W. E. B.**
Reliability and quality assurance on the MOD 2 wind system
[NASA-TN-82717] p0090 A81-33492
- MATHES, D. C.**
Improved methods for fan sound field determination
[NASA-CR-165188] p0129 A81-15769
- MATHIAS, S.**
Study of component technologies for fuel cell on-site integrated energy systems
[NASA-CR-165152-VOL-1] p0110 A81-15467
- Study of component technologies for fuel cell on-site integrated energy system. Volume 2: Appendices**
[NASA-CR-165152-VOL-2] p0110 A81-15462
- MATSUMO, K.**
Next generation communications satellites: Multiple access and network studies
[NASA-CR-165145] p0033 A81-12139
- MATTHEY, E. W.**
Silicon solar cells with high open-circuit voltage
p0113 A81-27689
- MATTHEY, M. D.**
Inlet flow distortion in turbomachinery
[ASME PAPER 80-GT-20] p0005 A81-17952
- MAXWELL, C. B.**
The STD/MHD codes - Comparison of analyses with experiments at AEDC/RPDR, Reynolds Metal Co., and Hercules, Inc
- [AIAA PAPER 81-0173]**
On the magnetothermal instability
[AIAA PAPER 81-0248] p0133 A81-20649
- MAY, C. E.**
New ion exchange membranes
[NASA-TN-81670] p0044 A81-16123
- MCALISTER, J. E.**
Structural dynamics verification facility study
[NASA-TN-82675] p0092 A81-33497
- MCALISTER, A. J.**
Non-noble catalysts and catalyst supports for phosphoric acid fuel cells
[NASA-CR-165221] p0112 A81-18497
- MCARDLE, J. G.**
Turbomachinery noise studies of the A1Research QCSAT engine with inflow control
[AIAA PAPER 81-2049] p0023 A81-48621
- Turbomachinery noise studies of the A1Research QCSAT engine with inflow control**
[NASA-TN-82694] p0127 A81-31957
- MCALRAY, J. E.**
Improved components for engine fuel savings
[SAE PAPER 801116] p0021 A81-34152
- MCBRIDE, E. F.**
Effect of voltage on the cost of an electric vehicle propulsion system
[NASA-TN-82592] p0140 A81-26986
- MCCARTHY, J. F., JR.**
Aerospace in the future
[NASA-TN-82664] p0143 A81-29063
- MCCORMICK, A.**
Silicon solar cells with high open-circuit voltage
p0113 A81-27089
- MCDONALD, G.**
Assessment of variations in thermal cycle life data of thermal barrier coated rods
p0058 A81-44657
- Prolonging thermal barrier coated specimen life by thermal cycle management**
p0065 A81-44658
- Prolonging thermal barrier coated specimen life by thermal cycle management**
[NASA-TN-81742] p0102 A81-23417
- Assessment of variations in thermal cycle life data of thermal barrier coated rods**
[NASA-TN-81743] p0102 A81-23418
- MCDONALD, G. E.**
Method for depositing an oxide coating
[NASA-CASE-LEU-13131-1] p0054 A81-24230
- Method of forming oxide coatings**
[NASA-CASE-LEU-13132-1] p0106 A81-27616
- MCDONALD, M.**
Calculation of three-dimensional turbulent subsonic flows in transition ducts
p0008 A81-21199
- Prediction of laminar and turbulent primary and secondary flows in strongly curved ducts**
[NASA-CR-3388] p0007 A81-16976
- A three-dimensional turbulent compressible subsonic duct flow analysis for use with constructed coordinate systems**
[NASA-CR-3389] p0077 A81-20383
- MCFARLAND, E. E.**
Solution of plane cascade flow using improved surface singularity methods
[ASME PAPER 81-GT-169] p0006 A81-30068
- Solution of plane cascade flow using improved surface singularity methods**
[NASA-TN-81589] p0003 A81-14979
- MCVEY, J. E.**
A model for the analysis of premixing-prevaporizing fuel-air mixing passages
[AIAA PAPER 81-0345] p0030 A81-20767
- MEADOWS, E. E.**
Next generation communications satellites: Multiple access and network studies
[NASA-CR-165145] p0033 A81-12139
- MEADVILLE, J. W.**
Low-thrust chemical propulsion system pump technology
[NASA-CR-165210] p0088 A81-17437
- MEHALIC, C. E.**
Performance deterioration of commercial high-bypass ratio turbofan engines
[SAE PAPER 801118] p0021 A81-34154
- MEITNER, P. L.**
Loss model for off-design performance analysis of radial turbines with pivoting-vane, variable-area stators

[SAE PAPER 801135] p0021 A81-34166
Off-design performance loss model for radial
turbines with pivoting, variable-area static
[NASA-TP-1708] p0013 A81-11038

RELIASON, R. T.
Advanced subsonic transport propulsion
[NASA-TN-82696] p0019 A81-31195

RELLIS, J. A.
Low-thrust chemical rocket engine study
[NASA-CN-165276] p0042 A81-21122

RENS, P. B.
Experimental analysis of ISEP in a rotary
combustion engine
[SAE PAPER 810150] p0079 A81-41732
Experimental analysis of ISEP in a rotary
combustion engine
[NASA-TN-81662] p0015 A81-16054

RENNIE, R. J.
Dissolution of bulk specimens of silicon nitride
p0065 A81-42024

RENNILL, G. S.
A program-management plan with critical-path
definition for Combustion Augmentation with
Thermonic Energy Conversion (CAIEC)
[NASA-TN-82670] p0132 A81-30973

RENNILL, R. C.
Multivariable identification using centralized
fixed modes
p0014 A81-12091

RETSCH, D. E.
Fundamental heat transfer research for gas turbine
engines
[NASA-CP-2178] p0016 A81-24063

REULEBERG, A., JR.
Thin n-i-p silicon solar cell
p0114 A81-27097

REYER, S.
Traction drive for cryogenic boost pump
[NASA-TN-81704] p0101 A81-23188

RICHALSON, G. E.
Stall flutter experiment in a transonic
oscillating linear cascade
[NASA-TN-82655] p0004 A81-31126

RINALONI, J.
Future challenges in V/STOL flight propulsion
control integration
[SAE PAPER 801140] p0022 A81-34170

RINALONI, J. E.
A nonlinear propulsion system simulation technique
for piloted simulators
p0022 A81-38064
A nonlinear propulsion system simulation technique
for piloted simulators
[NASA-TN-82600] p0101 A81-23085

RILES, J. E.
Pressure spectra and cross spectra at an area
contraction in a ducted combustion system
[ASME PAPER 80-C2/AEHC-5] p0077 A81-18638
Acoustic transmission matrix of a variable area
duct or nozzle carrying a compressible subsonic
flow
p0128 A81-22533
Acoustic transmission matrix of a variable area
duct or nozzle carrying a compressible subsonic
flow
[NASA-TN-81614] p0125 A81-12821
Analysis of pressure spectra measurements in a
ducted combustion system
[NASA-TN-81543] p0125 A81-15768

RILLEN, B. A.
The NASA high-speed turboprop program
[SAE PAPER 801120] p0021 A81-34156
The propeller tip vortex. A possible contributor
to aircraft cabin noise
[NASA-TN-81768] p0130 A81-22838

RILLEN, B. E.
Comparison of upwind and downwind rotor operations
of the DOE/NASA 100-kW Rod-O wind turbine
[NASA-TN-81744] p0100 A81-22472

RILLEN, R. A.
Thermal barrier coatings for heat engine components
p0056 A81-12920
Thermal barrier coatings for superalloys
p0058 A81-49217
Corrosion resistant thermal barrier coating
[NASA-CASE-LEW-13088-1] p0054 A81-25188

RILLEN, R. J.
Future challenges in V/STOL flight propulsion
control integration

[SAE PAPER 801140] p0022 A81-34170

RINER, R. V.
The fracture morphology of nickel-base superalloys
tested in fatigue and creep-fatigue at 650 C
[NASA-TN-81740] p0101 A81-23244

RINER, R. V., JR.
Cyclic behavior of turbine disk alloys at 650 C
p0056 A81-12266

RISBUCCI, J. A.
Silicon solar cells with high open-circuit voltage
p0113 A81-27089

RITICH, R. J.
Adherence of ion beam sputter deposited metal
films on H-13 steel
p0056 A81-14996
Ion beam deposited protective films
[AIAA PAPER 81-0672] p0086 A81-29532
Sputtered protective coatings for die casting dies
p0057 A81-38067
Ion beam deposited protective films
[NASA-TN-81722] p0038 A81-19221
Sputtered protective coatings for die casting dies
[NASA-TN-81735] p0053 A81-21173

RISBUCIE, J. A.
Evaluation of candidate Stirling engine heater
tube alloys for 1000 hours at 760 C
[NASA-TN-81578] p0051 A81-15068

RISBA, R.
Assessment of disk MHD generators for a base load
powerplant
[NASA-TN-82609] p0103 A81-23611

RITCHELL, G. A.
Low and high speed propellers for general aviation
- Performance potential and recent wind tunnel
test results
p0023 A81-42758
Low and high speed propellers for general
aviation: Performance potential and recent wind
tunnel test results
[NASA-TN-81745] p0003 A81-21028

RITCHELL, R. C.
Design concepts for low-cost composite turbofan
engine frame
[NASA-CN-165217] p0030 A81-22053

RIYOSHI, R.
Tribological properties of silicon carbide in
metal removal process
p0085 A81-17904
The adhesion, friction, and wear of binary alloys
in contact with single-crystal silicon carbide
[AFSE PAPER 80-C2/LUB-53] p0086 A81-18695
The generation and morphology of single-crystal
silicon carbide wear particles under adhesive
conditions
p0064 A81-35045
Anisotropic tribological properties of silicon
carbide
[NASA-TN-81547] p0080 A81-11394
Changes in surface chemistry of silicon carbide
(0001) surface with temperature and their effect
on friction
[NASA-TP-1756] p0060 A81-14079
Surface chemistry and friction behavior of the
silicon carbide (0001) surface at temperatures
to 1500 deg C
[NASA-TF-1813] p0061 A81-19300
Correlation of ideal and actual shear strengths of
metals with their friction properties
[NASA-TP-1891] p0063 A81-27282
Adhesion and friction of transition metals in
contact with nonmetallic hard materials
[NASA-TN-82605] p0055 A81-28233
Relationship between the ideal tensile strength
and the friction properties of metals in contact
with nonmetals and themselves
[NASA-TF-1883] p0063 A81-33293

RLINAB, R. J.
K-band high power latching switch
[NASA-CN-165159] p0073 A81-16389

ROFFAT, R. J.
Full-coverage film cooling. I - Three-dimensional
measurements of turbulence structure. II -
Prediction of the recovery-region hydrodynamics
p0078 A81-15537

ROFFITT, T. P.
Description of the warm core turbine facility and
the warm annular cascade facility recently
installed at NASA Lewis Research Center
[SAE PAPER 801122] p0031 A81-34158

- Cold-air investigation of first stage of
4-1/2-stage, fan drive turbine with average
stage-loading factor of 4.6e
[NASA-TP-1780] p0015 N81-16050
- MOORE, T. J.
Completion of evaluation of manufacturing
processes for B/Al composites containing 0.2mm
diameter boron fibers
[NASA-TN-81573] p0051 N81-11111
- MOOREHEAD, P. E.
Completion of evaluation of manufacturing
processes for B/Al composites containing 0.2mm
diameter boron fibers
[NASA-TN-81573] p0051 N81-11111
- MORRIS, V.
Combustor liner durability analysis
[NASA-CR-165250] p0027 N81-17079
- MORGAN, D. T.
Thermal energy storage for the Stirling engine
powered autocycle
[NASA-CR-159561] p0113 N81-22467
- MORGAN, J. L.
High B-field, large area ratio MHD duct experiments
[NASA-TN-8267] p0132 N81-32026
- MORRIS, J. P.
High power densities from high-temperature
material interactions
[AIAA PAPER 81-1161] p0070 A81-39144
High power densities from high-temperature
materials interactions
[NASA-TN-81626] p0131 N81-16900
Improved thermionic energy converters
[NASA-CASE-LEW-12443-1] p0099 N81-19561
Thermionic Energy Conversion (TEC) topping
thermoelectrics
[NASA-TN-81677] p0132 N81-19920
Heat pipes containing alkali metal working fluid
[NASA-CASE-LEW-12253-1] p0076 N81-22310
A program-management plan with critical-path
definition for Combustion Augmentation with
Thermionic Energy Conversion (CATEC)
[NASA-TN-82670] p0132 N81-30973
- MOSS, J. E.
Exhaust emission survey of an F100 afterburning
turbofan engine at simulated altitude flight
conditions
[NASA-TN-81656] p0016 N81-21078
- MOYER, D. E.
Effects of Ultra-Clean and centrifugal filtration
on rolling-element bearing life
[NASA-TN-82660] p0085 N81-29440
- MOZ, T. S.
Conceptual design of the MHD Engineering Test
Facility
[NASA-TN-82621] p0132 N81-24926
- MURPHY, W. B.
Integrated IC-circuits in ALTA-technology on one
substrate
[BNFT-FB-T-79-107] p0072 N81-14227
- MURZ, D.
Fracture toughness of brittle materials determined
with chevron notch specimens
p0064 A81-32545
- MURAYAMA, K.
Stress concentration in the vicinity of a hole
defect under conditions of Hertzian contact
[NASA-TN-82649] p0084 N81-28443
- MUSIAL, M. T.
A methodology for fostering commercialization of
electric and hybrid vehicle propulsion systems
[NASA-TN-81575] p0140 N81-18933
- N**
- NAGLE, W. J.
Toroidal cell and battery
[NASA-CASE-LEW-12918-1] p0104 N81-24521
Additive for zinc electrodes
[NASA-CASE-LEW-13286-1] p0105 N81-27597
- NATHIGER, J. J.
Comparison of Integrated Gasifier-Combined Cycle
and APB-steam turbine systems for industrial
cogeneration
[NASA-TN-82648] p0106 N81-28522
- NAKAMISHI, S.
Free radical propulsion concept
[AIAA PAPER 81-0676] p0041 A81-32905
Recent work on an RF ion thruster
[AIAA PAPER 81-0678] p0041 A81-35625
- Recent work on an RF ion thruster
[NASA-TN-81734] p0039 N81-20178
Free radical propulsion concept
[NASA-TN-81770] p0039 N81-20180
- NARENDRA, D.
Comparison of photovoltaic cell temperatures in
modules operating with exposed and enclosed back
surfaces
[NASA-TN-81769] p0106 N81-28520
- NASH, D. O.
Energy efficient engine: Flight propulsion system
preliminary analysis and design
[NASA-CR-159583] p0029 N81-18056
- NASH, J. P.
Applications Technology Satellite and
Communications Technology Satellite user
experiments for 1967 - 1980 reference book,
volume 1
[NASA-CR-165169-VOL-1] p0033 N81-12135
Applications Technology Satellite and
Communications Technology Satellite user
experiments for 1967-1980 reference book, volume 2
[NASA-CR-165169-VOL-2] p0033 N81-12136
Applications Technology Satellite and
Communications Technology Satellite user
experiments for 1967-1980 reference book.
Volume 3: User form surveys
[NASA-CR-165169-VOL-3] p0033 N81-12137
Applications Technology Satellite and
Communications Technology Satellite user
experiments for 1967-1980 reference book.
Volume 4: Abstracts
[NASA-CR-165169-VOL-4] p0133 N81-12138
- NASTROM, G. B.
Ozone contamination in aircraft cabins - Results
from GASP data and analyses
[AIAA PAPER 81-0305] p0010 A81-20740
Cloud encounter and particle density variabilities
from GASP data
[AIAA PAPER 81-0308] p0117 A81-20742
Tabulations of ambient ozone data obtained by GASP
airliners, March 1975 to December 1977
[NASA-TN-81528] p0116 N81-13568
Ozone contamination in aircraft cabins: Results
from GASP data and analyses
[NASA-TN-81671] p0009 N81-16021
Analysis of atmospheric ozone levels at commercial
airplane cruise altitudes in winter and spring,
1976 - 1977
[NASA-TN-1607] p0117 N81-21685
- NEAL, W. B.
Second year technical report on-board processing
for future satellite communications systems
[NASA-CR-165155] p0070 N81-10242
- NERDELIN, S. E.
Effects of Ultra-Clean and centrifugal filtration
on rolling-element bearing life
[NASA-TN-82660] p0085 N81-29440
- NELSON, D. P.
Model aerodynamic test results for two variable
cycle engine coannular exhaust systems at
simulated takeoff and cruise conditions
[NASA-CR-159818] p0026 N81-13057
Model aerodynamic test results for two variable
cycle engine coannular exhaust systems at
simulated takeoff and cruise conditions.
Comprehensive data report. Volume 1: Design
layouts
[NASA-CR-159819-VOL-1] p0028 N81-17081
Model aerodynamic test results for two variable
cycle engine coannular exhaust systems at
simulated takeoff and cruise conditions.
Comprehensive data report. Volume 2: Tabulated
aerodynamic data book 1
[NASA-CR-159819-VOL-2-BK-1] p0028 N81-17082
Model aerodynamic test results for two variable
cycle engine coannular exhaust systems at
simulated takeoff and cruise conditions.
Comprehensive data report. Volume 2: Tabulated
aerodynamic data book 2
[NASA-CR-159819-VOL-2-BK-2] p0028 N81-17083
Model aerodynamic test results for two variable
cycle engine coannular exhaust systems at
simulated takeoff and cruise conditions.
Comprehensive data report. Volume 2: Tabulated
aerodynamic data book 3
[NASA-CR-159819-VOL-2-BK-3] p0028 N81-17084
Model aerodynamic test results for two variable
cycle engine coannular exhaust systems at

- simulated takeoff and cruise conditions.
Comprehensive data report. Volume 3: Graphical
data book 1
[NASA-CN-159819-VOL-3-BK-1] p0028 N81-17085
Model aerodynamic test results for two variable
cycle engine conaxial exhaust systems at
simulated takeoff and cruise conditions.
Comprehensive data report. Volume 3: Graphical
data book 2
[NASA-CN-159819-VOL-3-BK-2] p0028 N81-17086
- NELSON, S. G.
Conceptual design study of a coal gasification
combined-cycle powerplant for industrial
cogeneration
[NASA-TN-81687] p0105 N81-25488
- NEUMANN, R. B.
Laser-velocimeter flow-field measurements of an
advanced turboprop
[AIAA PAPER 81-1568] p0007 N81-42211
Laser-velocimeter flow-field measurements of an
advanced turboprop
[NASA-TN-82677] p0004 N81-27041
- NEUSTADTER, R. E.
Data acquisition and analysis in the DOR/NASA Wind
Energy Program
[NASA-TN-81603] p0096 N81-13463
- NICH, A. W.
A reactor system design for solar storage applications
[NASA-TN-82720] p0108 N81-32608
- NIEDERDING, S. C.
High temperature electronic requirements in
aeropropulsion systems
p0072 N81-32547
High temperature electronic requirements in
aeropropulsion systems
[NASA-TN-81682] p0071 N81-16388
- NICH, C. Y.
Sputtered protective coatings for die casting dies
[NASA-TN-81735] p0053 N81-21173
- NICH, C.-Y.
Sputtered protective coatings for die casting dies
p0057 N81-38067
- NORRIS, D. L.
Advanced subsonic transport propulsion
[NASA-TN-82696] p0019 N81-31195
- NORMAN, C. T.
Small gas-turbine combustor study: Fuel injector
evaluation
[NASA-TN-82641] p0018 N81-26146
- NOTARDO, J.
Low NO_x and fuel flexible gas turbine combustors
[ASME PAPER 81-GT-99] p0020 N81-30006
Evaluation of advanced combustors for dry NO_x/
suppression with nitrogen bearing fuels in
utility and industrial gas turbines
[ASME PAPER 81-GT-125] p0087 N81-30029
- NOVICH, A. S.
Design and preliminary results of a fuel flexible
industrial gas turbine combustor
[ASME PAPER 81-GT-108] p0087 N81-30013
- OBRIEN, S. O.
Limited Area Coverage/High Resolution Picture
Transmission (LAC/HREP) tape IJ grid pixel
extraction processor user's manual
[N81-10072] p0094 N81-13428
Limited Area Coverage/High Resolution Picture
Transmission (LAC/HREP) data vegetative index
calculation processor user's manual
[N81-10073] p0094 N81-13429
EOS to universal tape conversion processor
[N81-10074] p0095 N81-13430
Limited Area Coverage/High Resolution Picture
Transmission, LAC/HREP tape conversion processor
user's manual
[N81-10077] p0095 N81-13433
- OBSON, R. S.
Fabrication of injectors molded sintered alpha sic
turbine components
[ASME PAPER 81-GT-161] p0089 N81-30060
- OLIVER, B. A.
The STD/HND codes - Comparison of analyses with
experiments at AEDC/EPDL, Reynolds Metal Co.,
and Hercules, Inc
[AIAA PAPER 81-0173] p0133 N81-20449
On the magnetoacoustic instability
[AIAA PAPER 81-0248] p0133 N81-20658
- OLSEN, B.
Icing instrumentation
p0117 N81-14559
Survey of aircraft icing simulation test
facilities in North America
[NASA-TN-81707] p0009 N81-19078
- ORJON, B.
High efficiency wraparound contact solar cells
/HEUACI/
p0114 N81-27094
The HEUAC pilot line experience
p0111 N81-17574
- ORANGE, T. E.
On the equivalence between semiempirical fracture
analyses and S-curves
p0092 N81-18792
Method for estimating crack-extension resistance
curve from residual strength data
[NASA-TP-1753] p0091 N81-11417
- ORIN, J. J.
Study of thermal management for space platform
applications
[NASA-CN-165238] p0033 N81-21106
- ORTIN, R. S.
Method for alleviating thermal stress damage in
laminates
[NASA-CASE-LEN-12493-1] p0045 N81-17170
Method for alleviating thermal stress damage in
laminates
[NASA-CASE-LEN-12493-2] p0046 N81-26179
- ORTIN, R.
Energy efficient engine: Pilot propulsion system
preliminary analysis and design
[NASA-CN-159583] p0029 N81-18056
- ORIN, R.
The influence of isothermal annealing on the
solvdenus fibers of a directed solid
gamma/gamma prime - alpha alloy
p0056 N81-10765
- PACIONE, R. L.
Phosphazene dianines
[NASA-CN-165147] p0065 N81-10169
- PAGLIARO, P.
Preparation and evaluation of advanced
electrocatalysts for phosphoric acid fuel cells
[NASA-CN-165179] p0111 N81-17527
Preparation and evaluation of advanced
electrocatalysts for phosphoric acid fuel cells
[NASA-CN-165245] p0112 N81-18496
- PAPILL, S. S.
Analysis for predicting adiabatic wall
temperatures with single hole coolant injection
into a low speed crossflow
[ASME PAPER 81-GT-91] p0077 N81-29998
Curved film cooling admission tube
[NASA-CASE-LEN-13174-1] p0074 N81-12363
Analysis for predicting adiabatic wall
temperatures with single hole coolant injection
into a low speed crossflow
[NASA-TN-81620] p0074 N81-13301
Influence of thermal boundary conditions on heat
transfer from a cylinder in cross flow
[NASA-TP-1894] p0076 N81-29384
- PAPTHANOS, L. C.
NASA Global Atmospheric Sampling Program (GASP)
data report for tape VL0015, VL0016, VL0017,
VL0018, VL0019, and VL0020
[NASA-TN-81661] p0115 N81-30657
- PARK, E. L., JR.
Ion beam texturing of heat transfer surfaces
[AIAA PAPER 81-0670] p0086 N81-29531
- PARK, J. E.
Extended frequency turbofan model
[NASA-CN-165261] p0030 N81-20074
- PARKER, J. C.
Development and testing of heat transport fluids
for use in active solar heating and cooling
systems
[NASA-TN-82395] p0098 N81-16584
- PARKER, R. J.
Lubrication of rolling element bearings
p0186 N81-18738
NASA five-ball fatigue tester - Over 20 years of
research
p0087 N81-44659

- Design studies of continuously variable transmissions for electric vehicles
[NASA-TN-81642] p0080 N81-13357
- NASA five-ball fatigue tester: Over 10 years of research
[NASA-TN-82589] p0102 N81-23462
- Endurance tests with large-bore tapered-roller bearings to 2.2 million DE
[NASA-TN-82669] p0084 N81-29439
- Continuously variable transmission: Assessment of applicability to advance electric vehicles
[NASA-TN-82700] p0085 N81-33484
- PARKS, D. E.
Fluid model of plasma outside a hollow cathode neutralizer
[AIAA PAPER 81-0739] p0134 N81-29560
- Parasitic current losses due to solar electric propulsion generated plasmas
[AIAA PAPER 81-0740] p0043 N81-29561
- Analysis of the charging of the SCATHA (P78-2) satellite
[NASA-CN-165348] p0033 N81-27169
- PART, S. F.
Energy efficient engine flight propulsion system: Aircraft/engine integration evaluation
[NASA-CN-159584] p0030 N81-22051
- PEARSON, C. V.
Conceptual design of the SRE Engineering Test Facility
[NASA-TN-82621] p0132 N81-24926
- PECZKOWSKI, J. L.
Multivariable synthesis with transfer functions
p0026 N81-12102
- PEDDIESON, J., JR.
Perturbation solutions of combustion instability problems
[NASA-CN-159643] p0050 N81-16176
- PEPPER, S. V.
Electron spectroscopy of the diamond surface
p0130 N81-27031
- Effect of electronic structure of the diamond surface on the strength of the diamond-metal interface
[NASA-TN-82714] p0063 N81-32269
- PETERS, C.
Numerical trials of HISSE
[N81-10069] p0094 N81-13425
- PETRASEK, D. E.
Tungsten fiber reinforced superalloys - A status review
p0047 N81-44665
- Tungsten fiber reinforced superalloys: A status review
[NASA-TN-82590] p0045 N81-25148
- PFANNKUCHE, H. G.
Tests of an overrunning clutch in a wind turbine
[NASA-TN-82653] p0107 N81-29528
- PHILLIPS, M. E.
New ion exchange membranes
[NASA-TN-81670] p0044 N81-16123
- In-situ cross linking of polyvinyl alcohol
[NASA-CASE-LEW-13135-2] p0062 N81-24257
- Cross-linked polyvinyl alcohol and method of making same
[NASA-CASE-LEW-13101-2] p0044 N81-29160
- Alkaline battery containing a separator of a cross-linked copolymer of vinyl alcohol and unsaturated carboxylic acid
[NASA-CASE-LEW-13102-1] p0107 N81-29531
- PHILLIPS, M.
Preliminary investigation of acoustic oscillations in an H2-O2 fired Ball generator
[NASA-TN-81756] p0103 N81-23610
- PHIBNEY, D. E.
Preliminary evaluation of the Environmental Research Institute of Michigan crop calendar shift algorithm for estimation of spring wheat development stage
[N81-10071] p0094 N81-13427
- PIAN, C. C. F.
Performance calculations for 1000 MWe MHD/steam power plants
[NASA-TN-81667] p0098 N81-16570
- PIERCE, W. S.
Fracture toughness of brittle materials determined with chevron notch specimens
p0064 N81-32545
- PIERCE, W. J.
The experimental verification of a streamline curvature numerical analysis method applied to the flow through an axial flow fan
[AIAA PAPER 81-0363] p0005 N81-20782
- PINEL, S. I.
Endurance tests with large-bore tapered-roller bearings to 2.2 million DE
[NASA-TN-82669] p0084 N81-29439
- PIOTROWSKI, S. S.
K-band high power latching switch
[NASA-CN-165159] p0073 N81-16389
- PITTS, L.
Moderate temperature sodium cells. I - Transition metal disulfide cathodes
p0113 N81-15027
- PLECHNER, R. M.
Comparisons of four alternative powerplant types for future general aviation aircraft
[NASA-TN-81584] p0013 N81-10067
- POESCHL, R. L.
Characteristics of 30-centimeter mercury ion thrusters
[AIAA PAPER 81-0715] p0041 N81-37569
- Electric propulsion - Characteristics, applications, and status
[NASA-TN-81630] p0033 N81-13079
- Retrofit and verification test of a 30-cm ion thruster
[NASA-CN-165233] p0042 N81-20174
- Characteristics of 30-centimeter mercury ion thrusters
[NASA-TN-81706] p0039 N81-21121
- PORTLANDER, M. W.
Integrated SC-circuits in ALIA-technology on one substrate
[BSFT-PB-T-79-107] p0072 N81-14227
- POOLOS, M. F.
Prolonging thermal barrier coated specimen life by thermal cycle management
p0065 N81-44658
- Prolonging thermal barrier coated specimen life by thermal cycle management
[NASA-TN-81742] p0102 N81-23417
- POPE, M. D.
Photovoltaic applications - Past and future
p0109 N81-27231
- POVINELLI, L. A.
Factors which influence the behavior of turbofan forced mixer nozzles
[AIAA PAPER 81-0274] p0021 N81-32549
- Factors which influence the behavior of turbofan forced mixer nozzles
[NASA-TN-81668] p0074 N81-15240
- POWELL, J. A.
High temperature electronic requirements in aeropropulsion systems
p0072 N81-32547
- High temperature electronic requirements in aeropropulsion systems
[NASA-TN-81682] p0071 N81-16388
- PPICH, M. G., JR.
Some effects of thermal-cycle-induced deformation in rocket thrust chambers
[NASA-TN-1834] p0036 N81-20176
- PROK, G. E.
Effect of hydroprocessing severity on characteristics of jet fuel from OSCO 2 and Paraho distillates
[NASA-TN-1768] p0066 N81-24283
- PROKOPIUS, P. E.
Status of commercial phosphoric acid fuel cell system development
[AIAA PAPER 81-0396] p0103 N81-20805
- Status of commercial phosphoric acid fuel cell system development
[NASA-TN-81641] p0096 N81-13464
- PRZYBYLUSKI, J. S.
Turbine blade temperature measurements using thin film temperature sensors
[NASA-CN-165201] p0059 N81-19277
- PUTT, C. E.
Application of computer generated color graphic techniques to the processing and display of three dimensional fluid dynamic data
[NASA-TN-82658] p0119 N81-29782
- QUASHEE, R.
Market definition study of photovoltaic power for

remote villages in developing countries
[NASA-CR-159880] p0110 N81-14391

R

RAFTOPOULOS, D. D.

Pressure spectra and cross spectra at an area
contraction in a ducted combustion system
[ASME PAPER 80-C2/1880-9] p0077 A81-18638

RAGSBALL, C.

Market definition study of photovoltaic power for
remote villages in developing countries
[NASA-CR-159880] p0110 N81-14391

RABENK, C. J.

Ceramic regenerator systems development program
[NASA-TP-165139] p0141 N81-22982

RABINS, P.

Analytical prediction and experimental
verification of performance at various operating
conditions of a dual-mode traveling wave tube
with multistage depressed collectors
[NASA-TP-1831] p0072 N81-28352
Performance of computer-designed small-sized
four-stage depressed collector for operation of
dual-mode traveling wave tube
[NASA-TP-1832] p0072 N81-30360

RABNEY, R. D.

Adapting magnetoelectrostatic containment to inert
gas thrusters
[AIAA PAPER 81-0140] p0043 A81-20625
Magnetoelectrostatic thruster physical geometry
tests
[AIAA PAPER 81-0753] p0044 A81-29566

RABD, R. R.

Study of fuel cell on-site, integrated energy
systems in residential/commercial applications
[NASA-CR-165144] p0112 N81-21533

RAO, V. D. N.

Ceramic regenerator systems development program
[NASA-CR-165139] p0141 N81-22982

RATAJCZAK, A. P.

Design description of the Schuchuli Village
photovoltaic power system
[NASA-TN-82650] p0094 N81-28517

RAUCH, R. R.

Improved ceramic heat exchanger materials
[NASA-CR-159678] p0065 N81-14082

RAUS, J. E.

K-band high power latching switch
[NASA-CR-165159] p0073 N81-16389

RAWLINS, V. K.

Extended operating range of the 30-cm ion thruster
with simplified power processor requirements
[AIAA PAPER 81-0692] p0040 A81-32857
Extended operating range of the 30-cm ion thruster
with simplified power processor requirements
[NASA-TN-81729] p0039 N81-20179

RECK, G. R.

Advanced fuel system technology for utilizing
broadened property aircraft fuels
p0066 A81-11612

REDDY, R. K.

A program-management plan with critical-path
definition for Combustion Augmentation with
Thermionic Energy Conversion (CATEC)
[NASA-TN-82670] p0132 N81-30973

REID, A.

Imp. vent and scale-up of the NASA Redox storage
system
[NASA-TN-81632] p0049 N81-13105

Zirconium carbide as an electrocatalyst for the
chromous/chronic redox couple
[NASA-CASE-LBN-15246-1] p0049 N81-26203

Preparation and characterization of electrodes for
the NASA Redox storage system
[NASA-TN-82702] p0107 N81-30522

RENNICK, R. J.

Stabilizing platinum in phosphoric acid fuel cells
[NASA-CR-165311] p0113 N81-22473

RESNOLTO, R.

Core noise measurements from a small, general
aviation turbofan engine
p0019 A81-22531

Core noise measurements from a small, general
aviation turbofan engine
[NASA-TN-81610] p0125 N81-11769

RESTALLICK, P. D.

Disk MHD generator study
[NASA-CR-159672] p0111 N81-18491

Assessment of disk MHD generators for a base load
powerplant
[NASA-TN-82609] p0103 N81-23611

RIBBLE, G. R., JR.

Test results of the Chrysler upgraded automotive
gas turbine engine: Initial design
[NASA-TN-81660] p0107 N81-30562

RICE, R. J.

A theoretical approach to sound propagation and
radiation for ducts with suppressors
p0128 A81-38061

A model for the acoustic impedance of linear
suppressor materials bonded on perforated plate
[AIAA PAPER 81-1999] p0129 A81-49741

High-frequency sound propagation in a spatially
varying mean flow
p0129 A81-49913

High-frequency sound propagation in a spatially
varying mean flow
[NASA-TN-81751] p0126 N81-20831

A theoretical approach to sound propagation and
radiation for ducts with suppressors
[NASA-TN-82612] p0130 N81-22837

A model for the acoustic impedance of linear
suppressor materials bonded on perforated plate
[NASA-TN-82716] p0127 N81-32965

Acoustic performance of inlet suppressors on an
engine generating a single mode
[NASA-TN-82697] p0127 N81-32968

RICE, R. J.

Experimental analysis of INEP in a rotary
combustion engine
[SAE PAPER 810150] p0079 A81-41732

Modular instrumentation system for real-time
measurements and control on reciprocating engines
[NASA-TP-1757] p0071 N81-11315

Experimental analysis of INEP in a rotary
combustion engine
[NASA-TN-81662] p0015 N81-16054

RICHTER, R.

Samarium cobalt (SMCO) generator/engine
integration study
[AD-A092904] p0029 N81-17087

RIDDLEBAUGH, S. R.

Small gas-turbine combustor study: Fuel injector
evaluation
[NASA-TN-82641] p0018 N81-26146

RIESEN, L. L.

Cross-linked polyvinyl alcohol and method of
making same
[NASA-CASE-LBN-13504-1] p0063 N81-27279

RIESEN, D. R.

Conceptual design of an in-space cryogenic fluid
management facility, executive summary
[NASA-CR-165279-EXEC-SUMM] p0137 N81-21212

Conceptual design of an in-space cryogenic fluid
management facility
[NASA-CR-165279] p0067 N81-21213

RIFFEL, R. R.

Experimental determination of unsteady blade
element aerodynamics in cascades. Volume 2:
Translation mode cascade
[NASA-CR-165166] p0007 N81-14976

RIGO, R. S.

Conceptual design of the MHD Engineering Test
Facility
[NASA-TN-82621] p0132 N81-24926

RILEY, T. J.

Commercial (terrestrial) and modified solar array
design studies for low cost, low power space
applications
[NASA-TN-81622] p0061 N81-17266

ROBBINS, R. R.

Large wind-turbine projects in the United States
wind energy program
p0108 A81-23694

Large wind turbines: A utility option for the
generation of electricity
p0142 N81-12981

ROBERTS, G. F.

A methodology for the design and calibration of
data based models of aggregate lake ecosystem
dynamics
p0111 N81-18482

ROBERTS, P. B.

Development of a low NO_x/lean premixed annular
combustor
[ASME PAPER 81-GT-40] p0020 A81-29954

- ROBINSON, R. S.
Passivation of carbon steel through mercury
implantation
[NASA-CN-165292] p0059 N81-20244
- ROCKWOOD, F. A.
Ceramic applications in turbine engines
[NASA-CN-159865] p0029 N81-19118
- ROELKE, R. J.
An experimental evaluation of the performance
deficit of an aircraft engine starter turbine
[SAR PAPER 801137] p0021 A81-34168
Reasons for low aerodynamic performance of
13.5-centimeter-tip-diameter aircraft engine
starter turbine
[NASA-TP-1810] p0016 N81-20076
Cold-air performance of compressor-drive turbine
of Department of Energy upgraded automobile gas
turbine engine. 1: Volute-manifold and stator
performance
[NASA-TN-82682] p0004 N81-28053
- ROGALLI, R.
Engineering support for magnetohydrodynamic power
plant analysis and design studies
[NASA-CN-159690] p0110 N81-13466
- ROBBIE, J. R.
The E3 combustors - Status and challenges
[AIAA PAPER 81-1353] p0023 A81-42176
The E3 combustors: Status and challenges
[NASA-TN-82684] p0018 N81-28095
- ROHN, R. A.
Life analysis of multicyclic planetary traction
drive
[NASA-TP-1710] p0082 N81-20423
- ROSENBERG, D. R.
Combustion system processes leading to corrosive
deposits
[NASA-TN-81752] p0101 N81-23243
- ROSTAPINSKI, S.
On the propagation of long waves in acoustically
treated, curved ducts
p0128 A81-38060
On the propagation of long waves in acoustically
treated, curved ducts
[NASA-TN-81712] p0125 N81-19875
- ROTUNBERG, M.
Analysis of the charging of the SCATNA (P78-2)
satellite
[NASA-CN-165348] p0033 N81-27169
- ROTH, S. P.
Future challenges in V/STOL flight propulsion
control integration
[SAR PAPER 801140] p0022 A81-34170
- ROTHMAN, R. P.
Effect of TNP variables upon structure and
properties in ODS alloy BSA 8077 sheet
p0059 A81-10706
- ROTHROCK, R. D.
Experimental determination of unsteady blade
element aerodynamics in cascades. Volume 2:
Translation mode cascade
[NASA-CN-165166] p0007 N81-14976
- ROUSAR, D. C.
High-density fuel combustion and cooling
investigation
[NASA-CN-165177] p0050 N81-16177
- RUERN, B. C.
Curved centerline air intake for a gas turbine
engine
[NASA-CASE-LEW-13201-1] p0014 N81-14999
- RUSSELL, D. A.
Evaluation of solar cell covers and encapsulant
materials for space application
p0111 N81-17568
- RUSSELL, L. M.
Evaluation of a method for heat transfer
measurements and thermal visualization using a
composite of a heater element and liquid crystals
[ASME PAPER 81-GT-93] p0079 A81-30000
Evaluation of a method for heat transfer
measurements and thermal visualization using a
composite of a heater element and liquid crystals
[NASA-TN-81639] p0075 N81-21313
- RUSSELL, P. L.
Evaluation of concepts for controlling exhaust
emissions from minimally processed petroleum and
synthetic fuels
[ASME PAPER 81-GT-157] p0067 A81-30056
- RUTLEDGE, S.
Simultaneous ion sputter etching and deposition
- [NASA-TN-81679] p0053 N81-19278
- SABLA, F. R.
Design and development of the combustor inlet
diffuser for the NASA/GE energy efficient engine
[ASME PAPER 81-GT-129] p0020 A81-30033
- SAGERSHED, D. A.
The NASA high-speed turboprop program
[SAR PAPER 801120] p0021 A81-34156
- SALIK, J.
The effect of mechanical surface and heat
treatments on the erosion resistance of 6061
aluminum alloy
p0057 A81-27944
Effect of mechanical surface and heat treatments
on erosion resistance
[NASA-TN-81540] p0051 N81-11178
Effects of erodent particle shape and various heat
treatments on erosion resistance of plain carbon
steel
[NASA-TP-1755] p0052 N81-16210
- SANDUSKEY, G. T.
Mixer nozzle aerodynamic characteristics for the
energy efficient engine
[AIAA PAPER 81-1994] p0128 A81-48639
- SANTORO, G. J.
Oxidation and hot corrosion of coated and bare
oxide dispersion strengthened superalloy MA-755B
p0058 A81-43384
Deposition and material response from Mach 0.3
burner rig combustion of SBC 2 fuels
[NASA-TN-81634] p0051 N81-15069
The effects of trace impurities in coal-derived
liquid fuels on deposition and accelerated high
temperature corrosion of cast superalloys
[NASA-TN-81678] p0052 N81-16211
Material response from Mach 0.3 burner rig
combustion of a coal-oil mixture
[NASA-TN-81686] p0055 N81-27258
- SARGENT, S. R.
Characterization of the near-term electric vehicle
(ETV-1) breadboard propulsion system over the
SAR J227a driving schedule D
[NASA-TN-81664] p0097 N81-15465
Results of the ETV-1 breadboard tests under
steady-state and transient conditions
[NASA-TN-82667] p0108 N81-31627
- SATHE, S. L.
Method of cold welding using ion beam technology
[NASA-CASE-LEW-12982-1] p0081 N81-19455
- SAUNDERS, A. A., JR.
Integrated control system for a gas turbine engine
[NASA-CASE-LEW-12594-2] p0015 N81-19116
- SAUNDERS, S. T.
A status report on the Energy Efficient Engine
Project
[SAR PAPER 801119] p0021 A81-34155
- SAVAGE, M.
Kinematic correction for roller skewing
[ASME PAPER 80-DET-76] p0085 A81-18647
Optimal tooth numbers for compact standard spur
gear sets
[NASA-TN-82614] p0083 N81-27524
- SANDY, D. T.
A theoretical approach to sound propagation and
radiation for ducts with suppressors
p0128 A81-38061
A theoretical approach to sound propagation and
radiation for ducts with suppressors
[NASA-TN-82612] p0130 N81-22837
- SCHARFEE, J. W.
A status report on the Energy Efficient Engine
Project
[SAR PAPER 801119] p0021 A81-34155
- SCHIBINE, A.
High efficiency ultrathin coplanar back contact
cells
p0114 A81-27092
Coplanar back contacts for thin silicon solar cells
[NASA-CN-165272] p0112 N81-18495
- SCHILL, J. D.
Program to develop sprayed, plastically deformable
compressor shroud seal materials
[NASA-CN-165237] p0088 N81-17434
Program to develop sprayed, plastically deformable
compressor shroud seal materials
[NASA-CN-165237] p0088 N81-17434

- SCHIFF, R.
Moderate temperature sodium cells. I - Transition metal disulfide cathodes
p0113 A81-15027
- SCHLINKER, R. H.
Boundary layer development on turbine airfoil suction surfaces
[ASME PAPER 81-GT-204]
p0008 A81-36094
- SCHLOSSER, R.
The self-consistent calculation of pseudo-molecule energy levels, construction of energy level correlation diagrams and an automated computation system for SCF-I(alpha)-SW calculations
[NASA-TN-81710]
p0130 N81-25779
- SCHMIDT, R. W.
The use of Antimisting Kerosene (AMK) in turbojet engines
p0009 N81-19063
- SCHMUELLER, G. W.
The effect of solar array voltage patterns on plasma power losses
p0043 A81-19937
Parasitic current losses due to solar electric propulsion generated plasmas
[AIAA PAPER 81-0740]
p0043 A81-29561
- SCHOCK, R. J.
Experimental analysis of INEP in a rotary combustion engine
[SAE PAPER 810150]
p0079 A81-41732
Experimental analysis of INEP in a rotary combustion engine
[NASA-TN-81662]
p0015 N81-16054
- SCHUELLER, D. G.
Photovoltaic applications - Past and future
p0109 A81-27231
- SCHUH, R. H.
Effect of voltage on the cost of an electric vehicle propulsion system
[NASA-TN-82592]
p0140 N81-26986
- SCHULLER, F. Z.
Calculated and experimental data for a 118-mm bore roller bearing to 3 million DN
[ASME PAPER 80-C2/LUE-14]
p0085 A81-18668
- SCHULLER, F. Z.
Performance of jet- and inner-ring-lubricated 35 millimeter bore ball bearings operating to 2.5 million DN
[NASA-TN-1808]
p0082 N81-19458
- SCHULTZ, R. F.
Heat pipes to reduce engine exhaust emissions
[NASA-CASE-LEW-12590-1]
p0049 N81-19245
- SCHUBB, J.
Low NO_x/ and fuel flexible gas turbine combustors
[ASME PAPER 81-GT-99]
p0020 A81-30006
- SCHWARTZ, R. J.
Electric and hybrid vehicle system R/D
[NASA-TN-81606]
p0096 N81-11449
Propulsion system research and development for electric and hybrid vehicles
p0142 N81-12585
The Federal electric and hybrid vehicle program
p0142 N81-12986
- SCHWARTZ, R.
Next generation communications satellites:
Multiple access and network studies
[NASA-CN-165145]
p0033 N81-12139
- SCHWIKHARD, W. G.
Icing tunnel tests of a glycol-exuding porous leading edge ice protection system on a general aviation airfoil
[AIAA PAPER 81-0405]
p0011 A81-20837
Evaluation of a pneumatic boot deicing system on a general aviation wing model
[NASA-TN-82363]
p0011 N81-25065
- SECORDE, R. H.
Electric vehicle motors and controllers
[NASA-TN-81760]
p0071 N81-21281
- SEDERQUIST, R. A.
Evaluation of concepts for controlling exhaust emissions from minimally processed petroleum and synthetic fuels
[ASME PAPER 81-GT-157]
p0007 A81-30056
- SEIDEL, R. S.
Inlet flow distortion in turbomachinery
[ASME PAPER 80-GT-20]
p0005 A81-17952
- SEIDEL, R. C.
Tests of an overrunning clutch in a wind turbine
[NASA-TN-82653]
p0107 N81-29528
- SEKAS, E. J.
Development of a low NO_x/ lean premixed annular combustor
[ASME PAPER 81-GT-40]
p0020 A81-29954
- SELDNER, E.
Performance seeking controls
p0014 N81-12092
- SELLERS, J. F.
Propulsion system mathematical model for a lift/cruise fan V/STOL aircraft
[NASA-TN-81663]
p0015 N81-16055
- SENG, G. T.
Effect of hydroprocessing severity on characteristics of jet fuel from OSCO 2 and Farah distillates
[NASA-TN-1768]
p0066 N81-24283
- SERAFINI, J. S.
Laser-velocimeter flow-field measurements of an advanced turboprop
[AIAA PAPER 81-1568]
p0007 A81-42211
Laser-velocimeter flow-field measurements of an advanced turboprop
[NASA-TN-82677]
p0004 N81-27041
- SERAFINI, T. Z.
Lower-curing-temperature PMV polyimides
[NASA-TN-81705]
p0045 N81-17174
Curing agent for polyepoxides and epoxy resins and composites cured therewith
[NASA-CASE-LEW-13226-1]
p0060 N81-17260
Composition and method for making polyimide resin-reinforced fabric
[NASA-CASE-LEW-12933-1]
p0061 N81-19296
Environmental effects on graphite fiber reinforced PMR-15 polyimide
[NASA-TN-82625]
p0046 N81-32194
- SHAFFER, J. L., JR.
Fracture toughness of brittle materials determined with chevron notch specimens
p0064 A81-32545
- SHARMA, O. P.
Boundary layer development on turbine airfoil suction surfaces
[ASME PAPER 81-GT-204]
p0008 A81-30094
- SHAW, L. S.
Mean rotor wake characteristics of an aerodynamically loaded 0.5 m diameter fan
[AIAA PAPER 81-0208]
p0006 A81-20830
Mean rotor wake characteristics of an aerodynamically loaded 0.5 m diameter fan
[NASA-TN-81657]
p0015 N81-16053
Rotor wake characteristics relevant to rotor-stator interaction noise generation
[NASA-TN-82703]
p0019 N81-30130
- SHAW, R. J.
An analytical approach to airfoil icing
[AIAA PAPER 81-0403]
p0117 A81-20810
- SHEILBY, D. W.
Control of volume resistivity in inorganic-organic separators
p0108 A81-11034
Advanced inorganic separators for alkaline batteries and method of making same
[NASA-CASE-LEW-13171-1]
p0100 N81-22466
Inexpensive cross-linked polymeric separators made from water soluble polymers
[NASA-TN-82619]
p0101 N81-23205
In-situ cross linking of polyvinyl alcohol
[NASA-CASE-LEW-13135-2]
p0062 N81-24257
Cross-linked polyvinyl alcohol and method of making same
[NASA-CASE-LEW-13504-1]
p0063 N81-27279
Additive for zinc electrodes
[NASA-CASE-LEW-13286-1]
p0105 N81-27597
Polyvinyl alcohol battery separator containing inert filler
[NASA-CASE-LEW-13556-1]
p0106 N81-27615
Cross-linked polyvinyl alcohol and method of making same
[NASA-CASE-LEW-13101-2]
p0044 N81-29160
Alkaline battery containing a separator of a cross-linked copolymer of vinyl alcohol and unsaturated carboxylic acid
[NASA-CASE-LEW-13102-1]
p0107 N81-29531
- SHIRAN, D.
Engineering support for magnetohydrodynamic power plant analysis and design studies
[NASA-CN-159690]
p0110 N81-13466
- SIOJI, J. S.
Low-thrust chemical rocket engine study

- [NASA-CN-165275] p0042 N81-21125
SHULTZ, B.
 Evaluation of concepts for controlling exhaust emissions from minimally processed petroleum and synthetic fuels
 [ASME PAPER 81-GT-157] p0067 A81-30056
- SHURE, L. I.**
 Coal gasifier cogeneration powerplant project
 p0143 N81-12988
- SIXKE, S. E.**
 High temperature alkali corrosion in high velocity gases
 [NASA-TN-82591] p0054 N81-25191
- SIGNER, R. E.**
 Performance of jet- and inner-ring-lubricated 35 millimeter bore ball bearings operating to 2.5 million DM
 [NASA-TP-1808] p0082 N81-19458
 Endurance tests with large-bore tapered-roller bearings to 2.2 million DM
 [NASA-TN-82669] p0084 N81-29439
- SIGNORELLI, R.**
 Advanced aircraft engine materials trends
 [NASA-TN-82626] p0055 N81-27259
- SIGNORELLI, R. A.**
 Tungsten fiber reinforced superalloys - A status review
 p0047 A81-44665
 Tungsten fiber reinforced superalloys: A status review
 [NASA-TN-82590] p0045 N81-25148
- SILVERSMITH, A. J.**
 Surface flaw detection in structural ceramics by scanning photoacoustic spectroscopy
 p0079 A81-17906
- SIMMONS, G. A.**
 MHD generator off-design performance and nox chemical kinetics analysis. Volume 1: Analysis of the off-design performance of the Engineering Test Facility ETP MHD generator flow train
 [NASA-CN-165187] p0133 N81-11834
- SIMON, P. F.**
 Comparison of photovoltaic cell temperatures in modules operating with exposed and enclosed back surfaces
 [NASA-TN-81769] p0106 N81-28520
- SIMONHAU, R. J.**
 Depressurization and two-phase flow of water containing high levels of dissolved nitrogen gas
 [NASA-TP-1839] p0076 N81-28389
- SIMONS, S. E.**
 Status of commercial phosphoric acid fuel cell system development
 [AIAA PAPER 81-0356] p0108 A81-20805
 Status of commercial phosphoric acid fuel cell system development
 [NASA-TN-81641] p0096 N81-13464
- SIMS, D. L.**
 Cyclic behavior of turbine disk alloys at 650 C
 p0056 A81-12266
- SINCLAIR, J. E.**
 Nonlinear laminate analysis for metal matrix fiber composites
 [AIAA 81-0579] p0046 A81-29411
 Superhybrid composite blade impact studies
 [ASME PAPER 81-GT-24] p0020 A81-29940
 Computer code for intraply hybrid composite design
 p0047 A81-44662
 Superhybrid composite blade impact studies
 [NASA-TN-81597] p0091 N81-11412
 Nonlinear laminate analysis for metal matrix fiber composites
 [NASA-TN-82596] p0046 N81-25149
 Computer code for intraply hybrid composite design
 [NASA-TN-82593] p0046 N81-25151
- SINK, L. E.**
 Development of low-cost directionally-solidified turbine blades
 p0088 A81-10707
- SITO, J. E.**
 Advanced communications satellites
 [AAS PAPER 80-206] p0069 A81-33532
 Satellites using the 30/20 GHz band
 [NASA-TN-81600] p0069 N81-10241
 The 30/20 GHz experimental communications satellite system
 [NASA-TN-82683] p0035 N81-30172
- SKIMA, C. A.**
 Future Air Force aircraft propulsion control systems: The extended summary paper
 p0025 N81-12096
- SLINBY, E. E.**
 Dynamics of solid dispersions in oil during the lubrication of point contacts. I - Graphite
 [ASLE PREPRINT 81-AM-5D-3] p0064 A81-33860
 Self-lubricating composite materials
 p0142 N81-12984
 Dynamics of solid dispersions in oil during the lubrication of point contacts. Part 1: Graphite
 [NASA-TN-81683] p0061 N81-17264
 Dynamics of solid dispersions in oil during the lubrication of point of contacts. Part 2: Molybdenum disulfide
 [NASA-TN-81709] p0062 N81-20275
- SLORE, E. G.**
 Energy overview
 p0142 N81-12979
- SMIALAK, J. L.**
 Microstructure of Al2O3 scales formed on NiCrAl alloys
 [NASA-TN-81676] p0052 N81-16212
- SMITH, E. E.**
 Curved centerline air intake for a gas turbine engine
 [NASA-CASE-LEU-13201-1] p0014 N81-14999
- SMITH, G. C. C.**
 Aeroelastic and dynamic finite element analyses of a bladder shrouded disk
 [NASA-CN-155728] p0092 N81-19479
 Nastran level 16 theoretical manual updates for aeroelastic analysis of bladed discs
 [NASA-CN-159823] p0093 N81-19480
- SMITH, G. Z.**
 Composite containment systems for jet engine fan blades
 [NASA-TN-81675] p0092 N81-17480
- SMITH, J. E.**
 A MHD channel study for the ETP conceptual design
 [NASA-TN-81764] p0132 N81-24927
 High B-field, large area ratio MHD duct experiments
 [NASA-TN-82673] p0132 N81-32026
- SOBIECHNY, E.**
 Shockless design and analysis of transonic blade shapes
 [NASA-TN-82611] p0004 N81-25036
- SOCKOL, P. E.**
 Generation of C-type cascade grids for viscous flow computation
 p0122 N81-14721
- SODA, E.**
 Effect of tangential traction and roughness on crack initiation/propagation during rolling contact
 [NASA-TN-81608] p0080 N81-11395
- SONDER, J. F.**
 F100 multivariable control synthesis program: A review of full scale engine altitude tests
 p0014 N81-12093
- SONDER, E. E.**
 Effect of a part-span variable inlet guide vane on the performance of a high-bypass turbofan engine
 [AIAA PAPER 81-1362] p0022 A81-40842
 Effect of a part-span variable inlet guide vane on the performance of a high-bypass turbofan engine
 [NASA-TN-82617] p0017 N81-25081
- SOPRIN, T. G.**
 Improved methods for fan sound field determination
 [NASA-CN-165188] p0129 N81-15769
- SOKOLOVSKI, B. E.**
 The E3 combustors - Status and challenges
 [AIAA PAPER 81-1353] p0023 A81-42176
 The E3 combustors: Status and challenges
 [NASA-TN-82684] p0018 N81-28095
- SOLTIS, D. G.**
 Additive for zinc electrodes
 [NASA-CASE-LEU-13286-1] p0105 N81-27597
- SOVEY, J.**
 A sputtered zirconia primer for improved thermal shock resistance of plasma sprayed ceramic turbine seals
 [NASA-TN-81732] p0062 N81-21198
- SOVEY, J. S.**
 Electron reflection and secondary emission characteristics of sputter-textured pyrolytic graphite surfaces
 p0065 A81-38065
 Performance of a magnetic multipole line-cusp argon ion thruster

- [AIAA PAPER 81-0745] p0041 A81-38071
Texturing polymer surfaces by transfer casting
[NASA-CASE-LEN-13120-1] p0068 N81-16327
Performance of a magnetic multipole line-cusp
argon ion thruster
[NASA-TN-81703] p0038 N81-19219
Electron reflection and secondary emission
characteristics of sputter-textured pyrolytic
graphite surfaces
[NASA-TN-81755] p0062 N81-22193
Thermal barrier coating system having improved
adhesion
[NASA-CASE-LEN-13359-1] p0062 N81-24265
Ion sputter textured graphite
[NASA-CASE-LEN-12919-1] p0046 N81-27198
- SPALVINS, T.**
Frictional and morphological characteristics of
ion plated soft, metallic films p0057 A81-38066
Ion plating for the future p0087 A81-44654
Sputtering and ion plating for aerospace
applications p0087 A81-44655
Sputtering and ion plating for aerospace
applications p0082 N81-20424
Ion plating for the future
[NASA-TN-82630] p0054 N81-25189
- SPANG, E. A., III**
Apparatus for sensor failure detection and
correction in a gas turbine engine control system
[NASA-CASE-LEN-12907-2] p0015 N81-19115
- SPIERS, G. D.**
An experimental investigation of silicon wafer
surface roughness and its effect on the
pull-strength of plated metals p0109 A81-38063
An experimental investigation of silicon wafer
surface roughness and its effect on the full
strength of plated metals [NASA-TN-81763] p0100 N81-22478
- SPINDT, C. A.**
Development program on a cold cathode electron gun
[NASA-CR-159570] p0073 N81-19395
- SPRITTER, J. E.**
A rapid method for the approximate determination
of nonlinear solutions Application to
aerodynamic flows p0007 A81-11628
A rapid perturbation procedure for determining
nonlinear flow solutions: Application to
transonic turbomachinery flows [NASA-CR-3425] p0001 N81-22012
- SPOCKLER, C. E.**
Combustion of solid carbon rods in zero and normal
gravity [NASA-TN-81728] p0082 N81-22317
- SRINIVASAN, A. V.**
Effects of mistuning on blade torsional flutter
p0092 A81-29095
- STABE, R. G.**
Description of the vane core turbine facility and
the vane annular cascade facility recently
installed at NASA Lewis Research Center
[SAE PAPER 801122] p0031 A81-34158
- STANARA, S. S.**
A rapid method for the approximate determination
of nonlinear solutions Application to
aerodynamic flows p0007 A81-11628
A rapid perturbation procedure for determining
nonlinear flow solutions: Application to
transonic turbomachinery flows [NASA-CR-3425] p0001 N81-22012
- STAIGER, P. J.**
Performance calculations for 200-1000 Hwe
MHD/steam power plants [NASA-TN-81775] p0100 N81-22476
A MHD channel study for the ETF conceptual design
[NASA-TN-81764] p0132 N81-24927
- STANOLICH, E. G.**
Effect of time-dependent flight loads on turbofan
engine performance deterioration
[ASME PAPER 81-GT-203] p0030 A81-30093
- JT9D performance deterioration results from a
simulated aerodynamic load test
[AIAA PAPER 81-1528] p0022 A81-40563
- JT9D performance deterioration results from a
simulated aerodynamic load test
[NASA-TN-82640] p0017 N81-25082
- STALHAMER, D. E.**
Design and assembly considerations for Redox cells
and stacks [NA A-TN-82672] p0049 N81-31308
- STANCHINA, E. E.**
Proton radiation damage in bulk n-GaAs
p0099 N81-17564
- STANKIEWICZ, E.**
Analytical prediction and experimental
verification of performance at various operating
conditions of a dual-mode traveling wave tube
with multistage depressed collectors
[NASA-TF-1831] p0072 N81-28352
- STANWARD, P. E.**
Analysis of the charging of the SCATHA (P78-2)
satellite [NASA-CR-165348] p0033 N81-27169
- STEARNS, C. A.**
Deposition and material response from Mach 0.3
burner rig combustion of SRC 2 fuels
[NASA-TN-81634] p0051 N81-15069
Combustion system processes leading to corrosive
deposits [NASA-TN-81752] p0101 N81-23243
- STECURA, S.**
Thermal barrier coatings - Burner rig hot
corrosion test results p0063 A81-12630
Effects of plasma spray parameters on two layer
thermal barrier [NASA-TN-81724] p0053 N81-22161
- STEEN, P. G.**
The effect of solar array voltage patterns on
plasma power losses p0043 A81-19937
Analysis of the charging of the SCATHA (P78-2)
satellite [NASA-CR-165348] p0033 N81-27169
- STERNBERG, E. G.**
Aerodynamic stability analysis of NASA
J85-13/planar pressure pulse generator
installation [NASA-CR-165141] p0027 N81-15004
TF34 engine compression system computer study
[NASA-CR-159889] p0027 N81-15005
- STEINBERG, R.**
Aircraft operating efficiency on the North
Atlantic, a challenge for the 1980's
p0009 N81-19060
- STELLA, E.**
Assessment of disk MHD generators for a base load
powerplant [NASA-TN-82609] p0103 N81-23611
- STEPHENS, G. E.**
Cost/benefit analysis of advanced materials
technologies for future aircraft turbine engines
[NASA-CR-165225] p0027 N81-15006
- STEPHENS, J. E.**
NASA's activities in the conservation of strategic
aerospace materials p0056 A81-22535
Mechanical properties of weldments in experimental
Fe-12Mn-0.2Ti and Fe-12Mn-1Mo-0.2Ti alloys for
cryogenic service p0058 A81-48143
Hostile environmental conditions facing candidate
alloys for the automotive Stirling engine
[NASA-TN-82632] p0054 N81-26236
NASA's activities in the conservation of strategic
aerospace materials [NASA-TN-81617] p0055 N81-29205
Cobalt: A vital element in the aircraft engine
industry [NASA-TN-82662] p0055 N81-29206
Conservation of Strategic Aerospace Materials
(CCSAM) p0019 N81-31208
- STEPHA, P. S.**
Evaluation of a method for heat transfer
measurements and thermal visualization using a
composite of a heater element and liquid crystals
[ASME PAPER 81-GT-93] p0079 A81-30000
Composite wall concept for high-temperature
turbine shrouds - Heat transfer analysis
[SAE PAPER 801138] p0021 A81-34169

- Evaluation of a method for heat transfer measurements and thermal visualization using a composite of a heater element and liquid crystals [NASA-TN-81639] p0075 N81-21313
- Thermal and flow analysis of a convection air-cooled ceramic coated porous metal concept for turbine vanes [NASA-TN-81749] p0016 N81-22056
- STERN, T. E.
Next generation communications satellites: Multiple access and network studies [NASA-CR-165145] p0033 N81-12139
- STETZ, T. T.
Flow through axially aligned sequential apertures of the orifice and Borda types [NASA-TN-81681] p0075 N81-21314
Some flow phenomena associated with aligned, sequential apertures with Borda-type inlets [NASA-TP-1792] p0076 N81-24387
Experiments on flow through one to four inlets of the orifice and Borda type [NASA-TN-82680] p0077 N81-30391
- STEVANS, W.
Supersonic stall flutter of high-speed fans [ASME PAPER 81-GT-184] p0020 A81-30078
- STEVENS, W. J.
Modelling of environmentally induced discharges in geosynchronous satellites p0034 A81-19936
Review of biased solar array. Plasma interaction studies [NASA-TN-82693] p0036 N81-32187
- STEVENS, W.
Supersonic stall flutter of high speed fans [NASA-TN-81613] p0003 N81-14978
- STEVENSON, S. E.
An economic systems analysis of land mobile radio telephone services p0069 A81-22528
An economics systems analysis of land mobile radio telephone services [NASA-TN-81476] p0069 N81-10239
- STEWART, W. L.
The future of aeronautical propulsion p0001 A81-29052
NASA research in aeropropulsion [ASME PAPER 81-GT-96] p0001 A81-30003
NASA Research in aeropropulsion p0142 N81-12980
NASA Research in aeropropulsion [NASA-TN-81633] p0014 N81-13056
- STOCHL, E. J.
Off-design analysis of a gas turbine powerplant augmented by steam injection using various fuels [NASA-TN-81611] p0098 N81-16571
- STOCKMAN, W. O.
Optimum subsonic, high-angle-of-attack nacelles p0005 A81-11646
Three-dimensional turbulent boundary layer development and separation in V/STOL engine inlets at incidence with small-cross flow and curvature influences [AIAA PAPER 81-0254] p0005 A81-20703
- STOPFER, L. J.
Design concepts for low-cost composite turbofan engine frame [NASA-CR-165217] p0030 N81-22053
- STONE, J. E.
An improved prediction method for noise generated by conventional profile coaxial jets [AIAA PAPER 81-1991] p0129 A81-49743
Status of noise technology for advanced supersonic cruise aircraft p0001 N81-18002
Recent developments in aircraft engine noise reduction technology p0009 N81-13072
An improved prediction method for noise generated by conventional profile coaxial jets [NASA-TN-82712] p0127 N81-32964
- STONEMAN, P.
Preparation and evaluation of advanced electrocatalysts for phosphoric acid fuel cells [NASA-CR-165179] p0111 N81-17527
Preparation and evaluation of advanced electrocatalysts for phosphoric acid fuel cells [NASA-CR-165245] p0112 N81-18496
- STONE, R. S.
Fabrication of injection molded sintered alpha SiC turbine components [ASME PAPER 81-GT-161] p0089 A81-30060
- STOTTI, G.
High efficiency ultrathin coplanar back contact cells p0114 A81-27092
Coplanar back contacts for thin silicon solar cells [NASA-CR-165272] p0112 N81-18495
- STRACE, W. C.
An overview of general aviation propulsion research programs at NASA-Levis Research Center [SAE PAPER 810624] p0023 A81-42778
Comparisons of four alternative powerplant types for future general aviation aircraft [NASA-TN-81584] p0013 N81-10067
An overview of general aviation propulsion research programs at NASA Levis Research Center [NASA-TN-81666] p0015 N81-16052
- STRAIGHT, R. P.
Conceptual design study of a coal gasification combined-cycle powerplant for industrial cogeneration [NASA-TN-81687] p0105 N81-25488
- STRANGE, J. D.
Applications Technology Satellite and Communications Technology Satellite user experiments for 1967 - 1980 reference book, volume 1 [NASA-CR-165169-VOL-1] p0033 N81-12135
Applications Technology Satellite and Communications Technology Satellite user experiments for 1967-1980 reference book, volume 2 [NASA-CR-165169-VOL-2] p0033 N81-12136
Applications Technology Satellite and Communications Technology Satellite user experiments for 1967-1980 reference book. Volume 3: User form surveys [NASA-CR-165169-VOL-3] p0033 N81-12137
Applications Technology Satellite and Communications Technology Satellite user experiments for 1967-1980 reference book. Volume 4: Abstracts [NASA-CR-165169-VOL-4] p0133 N81-12138
- STREMPER, G. C.
Fabrication of aluminum oxide fiber reinforced aluminum matrix composites [NASA-CR-165184] p0048 N81-19229
Fabrication development of alumina/aluminum composites [NASA-CR-165195] p0048 N81-19233
- STRONBERG, W. J.
JT9D performance deterioration results from a simulated aerodynamic load test [AIAA PAPER 81-1588] p0022 A81-40963
JT9D performance deterioration results from a simulated aerodynamic load test [NASA-TN-82640] p0017 N81-25082
- STUCKAS, E. J.
Advanced Technology Spark-Ignition Aircraft Piston Engine Design Study [NASA-CR-165162] p0026 N81-13963
- STURNAN, J. C.
Environmental charging effects monitors for operational satellites p0037 A81-38057
Environmental charging effects monitors for operational satellites [NASA-TN-81669] p0037 N81-17127
Development and design of three monitoring instruments for spacecraft charging [NASA-TP-1800] p0040 N81-31282
- SUBRAMANIAM, T. K.
Conceptual design study of a coal gasification combined-cycle powerplant for industrial cogeneration [NASA-TN-81687] p0105 N81-25488
- SULLIVAN, J. P.
Laser-velocimeter flow-field measurements of an advanced turboprop [AIAA PAPER 81-1568] p0007 A81-42211
Laser-velocimeter flow-field measurements of an advanced turboprop [NASA-TN-82677] p0004 N81-27041
- SULLIVAN, T. L.
Performance of a steel spar wind turbine blade on the Mod-0 100 kw experimental wind turbine [NASA-TN-81588] p0096 N81-11448
- SUNNERS, R. L.
An integrated exhaust gas analysis system with

self-contained data processing and automatic calibration
[NASA-TN-81592] p0102 N81-23435

SUN, C. T.
Contact law and impact responses of laminated composites
[NASA-CN-159884] p0048 N81-12172

SUPLINSKAS, R. D.
CVD-produced boron filaments p0049 A81-11336

SWARTZ, C. K.
Radiation damage in lithium-counterdoped N/P silicon solar cells p0109 A81-27204
Radiation damage annealing mechanisms and possible low temperature annealing in silicon solar cells p0040 A81-27207
Annealing of radiation damage in low resistivity silicon solar cells p0099 N81-17554
Radiation damage in silicon NIP solar cells p0099 N81-17557
GaAs homojunction solar cell development p0099 N81-17561
Performance of high resistivity n⁺⁺p silicon solar cells under 1 MeV electron irradiation [NASA-TN-82610] p0103 N81-23626
Reduced annealing temperatures in silicon solar cells [NASA-TN-82597] p0104 N81-23627
Comparative radiation testing of solar cells for the shuttle power extension package [NASA-TN-82656] p0105 N81-27605

SWEAN, T. P., JR.
The STD/HND codes - Comparison of analyses with experiments at AEDC/RPDE, Reynolds Metal Co., and Hercules, Inc [AIAA PAPER 81-0173] p0133 A81-20649
On the magnetoacoustic instability [AIAA PAPER 81-0248] p0133 A81-20658

SYTHIA, R. J.
A study of external fuel vaporization [ASME PAPER 81-GT-158] p0020 A81-30057

SEUCH, J. R.
An automated procedure for developing hybrid computer simulations of turbofan engines p0020 A81-32544
An automated procedure for developing hybrid computer simulations of turbofan engines [NASA-TN-81605] p0037 N81-11688

T

TACISA, R. E.
Ignition of lean fuel-air mixtures in a premixing-prevaporizing duct at temperatures up to 1000 K [NASA-TN-81645] p0096 N81-13465
Catalytic combustion of coal-derived liquids [NASA-TN-81594] p0097 N81-14396

TANNA, R. E.
An experimental study of transmission, reflection and scattering of sound in a free jet flight simulation facility and comparison with theory p0129 A81-28943

TANABAY, R. E.
Effect of IMF variables upon structure and properties in ODS alloy BIA 8077 sheet p0059 A81- 0706

TAYLOR, J. E.
Design and development of the combustor inlet diffuser for the NASA/GI energy efficient engine [ASME PAPER 81-GT-129] p0020 A81-30033

TEARE, J. D.
Assessment of disk HND generators for a base load powerplant [NASA-TN-82609] p0103 N81-23611

TEKUNALLA, V.
Study of fuel cell on-site, integrated energy systems in residential/commercial applications [NASA-CN-165144] p0112 N81-21533

TESTER, B. J.
An experimental study of transmission, reflection and scattering of sound in a free jet flight simulation facility and comparison with theory p0129 A81-28943

THALLER, L. E.
Improvement and scale-up of the NASA Redox storage system

[NASA-TN-81632] p0049 N81-13105
Synthetic battery cycling [NASA-TN-81757] p0049 N81-25168

THIEME, L. G.
High-power baseline and motoring test results for the GPU-3 Stirling engine [NASA-TN-82646] p0139 N81-32087

THOLLOT, P. A.
A methodology for fostering commercialization of electric and hybrid vehicle propulsion systems [NASA-TN-81575] p0140 N81-18933

THOMAS, G. L.
Diagnostic system design for the Ion Auxiliary Propulsion System /IAPS/ - Flight test of two 8 cm mercury ion thrusters [AIAA PAPER 81-0666] p0041 A81-38070
Diagnostic system design for the Ion Auxiliary Propulsion System (IAPS). Flight tests of two 8 cm mercury ion [NASA-TN-81702] p0037 N81-20172

THOMAS, B. D.
Laboratory evaluation of a pilot cell battery protection system for photovoltaic applications [NASA-TN-81714] p0104 N81-24536

THOMAS, B. L.
Large wind-turbine projects in the United States wind energy program p0108 A81-23694
Large wind turbines: A utility option for the generation of electricity p0142 N81-12981

THOMPSON, C. E.
QCGAT mixer compound exhaust system design and static big model test report [NASA-CN-135386] p0029 N81-19119

TINLING, B. E.
Propulsion system mathematical model for a lift/cruise fan V/STOL aircraft [NASA-TN-81663] p0015 N81-16055

TORRE, C. E.
Numerical simulation of flows in curved diffusers with cross-sectional transitioning using a three-dimensional viscous analysis [NASA-TN-81672] p0074 N81-15239

TORRESINO, D. P.
Comparisons of modified Vasco I-2 and AISI 9310 gear steels [NASA-TF-1731] p0080 N81-14322
Optimal tooth numbers for compact standard spur gear sets [NASA-TN-82614] p0083 N81-27524

TRIEBEL, C. F.
Samarium cobalt (SMCO) generator/engine integration study [AD-A092904] p0029 N81-17087

TRIVISONNO, R. J.
The effect of minority carrier mobility variations on solar cell spectral response [NASA-TN-82604] p0103 N81-23625

TROTH, B. L.
Design and preliminary results of a fuel flexible industrial gas turbine combustor [ASME PAPER 81-GT-108] p0087 A81-30013

TRUSCELLO, V. C.
Solar Thermal Power Systems parabolic dish project [NASA-TN-82371] p0107 N81-28524

V

VADYAN, J.
Calculation of the flow field in supersonic inlets using a bicaracteristics method with shock wave fitting p0006 A81-21212

VANLBERG, C. J.
The electric rail gun for space propulsion [NASA-CN-165312] p0042 N81-22078

VALENTINE, P. G.
Microstructure and mechanical properties of bulk and plasma-sprayed Y2O3-partially stabilized zirconia [NASA-CN-165126] p0059 N81-22158

VALLANCE, J. E.
Ceramic regenerator systems development program [NASA-CN-165139] p0141 N81-22982

VALLER, R. E.
High-density fuel combustion and cooling investigation [NASA-CN-165177] p0050 N81-16177

- VANFOSSHE, G. J.
Heat transfer coefficients for staggered arrays of short pin fins [ASME PAPER 81-GT-75] p0077 A81-29983
Heat transfer coefficients for staggered arrays of short pin fins [NASA-TN-81596] p0074 A81-13302
- VANNUCCI, M. B.
Properties of PBR polyimide composites made with improved high strength graphite fibers p0047 A81-43603
Lower-curing-temperature PBR polyimides [NASA-TN-81705] p0045 A81-17174
Curing agent for polyepoxides and epoxy resins and composites cured therewith [NASA-CASE-LEU-13226-1] p0060 A81-17260
- VARY, A.
Ultrasonic measurement of material properties p0090 A81-19656
Acousto-ultrasonic characterization of fiber reinforced composites p0090 A81-44660
Acousto-ultrasonic characterization of fiber reinforced composites [NASA-TN-82651] p0090 A81-28458
- VASICHEK, B. W.
Design description of the Schuchuli Village photovoltaic power system [NASA-TN-82650] p0094 A81-28517
- VAUGHN, J.
Theoretical results on the double-collecting tandem junction solar cell p0099 A81-17538
- VDOVIK, J. V.
Aerodynamic/acoustic performance of YJ101/double bypass VCE with conical plug nozzle [NASA-CR-159869] p0129 A81-17846
- VENTRICE, M.
Perturbation solutions of combustion instability problems [NASA-CR-159643] p0050 A81-16176
- VERNES, G.
Low NO_x and fuel flexible gas turbine combustors [ASME PAPER 81-GT-99] p0020 A81-30006
- VETTER, A. A.
The STD/HMD codes - Comparison of analyses with experiments at AEDC/HPDE, Reynolds Metal Co., and Hercules, Inc [AIAA PAPER 81-0173] p0133 A81-20649
- VIERHA, L. A.
Performance of a steel spar wind turbine blade on the Bod-0 100 kW experimental wind turbine [NASA-TN-81588] p0096 A81-11448
The NASA-LeRC wind turbine sound prediction code [NASA-TN-81737] p0100 A81-21537
- VON GLASS, U.
Comparison of predicted engine core noise with proposed FAA helicopter noise certification requirements p0128 A81-38062
- VON GLASS, U. E.
Comparison of predicted engine core noise with current and proposed aircraft noise certification requirements [AIAA PAPER 81-2053] p0024 A81-48635
- VOUGLASH, U.
New interpretations of shock-associated noise with and without screech [NASA-TN-81590] p0125 A81-10807
Comparison of predicted engine core noise with proposed FAA helicopter noise certification requirements [NASA-TN-81739] p0130 A81-22839
Comparison of predicted engine core noise with current and proposed aircraft noise certification requirements [NASA-TN-82659] p0126 A81-29922
- VRANOS, A.
Experimental study of the stability of aircraft fuels at elevated temperatures [NASA-CR-165165] p0067 A81-12255
- WAGNER, E. C.
Oxidation-induced contraction and strengthening of boron fibers p0047 A81-44664
- WAGNER, E. C.
Oxidation-induced contraction and strengthening of boron fibers [NASA-TN-82599] p0046 A81-25150
- WAITE, W. A.
Anion permeable membrane [NASA-CR-165223] p0111 A81-16583
- WAKEFIELD, M. A.
Study of fuel cell on-site, integrated energy systems in residential/commercial applications [NASA-CR-165144] p0112 A81-21533
- WAKEFIELD, T. D.
Surface flaw detection in structural ceramics by scanning photoacoustic spectroscopy p0079 A81-17906
- WALLACE, J. F.
Sputtered protective coatings for die casting dies p0057 A81-38067
Sputtered protective coatings for die casting dies [NASA-TN-81735] p0053 A81-21173
- WALSH, J.
An experimental evaluation of oil pumping rings [NASA-CR-65271] p0088 A81-21355
- WANG, C. B.
Analysis for predicting adiabatic wall temperatures with single hole coolant injection into a low speed crossflow [ASME PAPER 81-GT-91] p0077 A81-29998
Analysis for predicting adiabatic wall temperatures with single hole coolant injection into a low speed crossflow [NASA-TN-81620] p0074 A81-13301
- WANG, S.
Ion beam sputter etching of orthopedic implant alloy BP35N and resulting effects on fatigue properties [AIAA PAPER 81-0671] p0057 A81-38069
Ion beam sputter etching of orthopedic implanted alloy BP35N and resulting effects on fatigue [NASA-TN-81747] p0045 A81-21174
- WANG, S. Y.
A NHD channel study for the HTF conceptual design [NASA-TN-81764] p0132 A81-24927
High B-field, large area ratio NHD duct experiments [NASA-TN-82673] p0132 A81-32026
- WANGEN, E. P.
Apparatus for sensor failure detection and correction in a gas turbine engine control system [NASA-CASE-LEU-12907-2] p0015 A81-19115
- WARRINER, D. E.
Conceptual design of the NHD Engineering Test Facility [NASA-TN-82621] p0132 A81-24926
- WARREN, E. L.
Test results of the Chrysler upgraded automotive gas turbine engine: Initial design [NASA-TN-81660] p0107 A81-30562
- WARREN, J. E.
Cyclic behavior of turbine disk alloys at 650 C p0056 A81-12266
- WARSZAWSKY, I.
Gauge calibration system based on piston manometer p0079 A81-48950
- WARSZAY, M.
Status of commercial phosphoric acid fuel cell system development [AIAA PAPER 81-0396] p0108 A81-20805
Status of commercial phosphoric acid fuel cell system development [NASA-TN-81641] p0096 A81-13464
- WATNER, F. E.
CVD-produced boron filaments p0048 A81-11336
- WEBB, E. C.
Samarium cobalt (SMCO) generator/engine integration study [AD-A092904] p0029 A81-17087
- WEBB, E. J.
NASA research in aeropropulsion [ASME PAPER 81-GT-96] p0001 A81-30003
NASA research in aeropropulsion [NASA-TN-81633] p0014 A81-13056
- WERTON, J. E.
Method for alleviating thermal stress damage in laminates [NASA-CASE-LEU-12493-1] p0045 A81-17170
Method for alleviating thermal stress damage in laminates [NASA-CASE-LEU-12493-2] p0046 A81-26179

W

- WEIGAND, A. J.
Ion beam texturing of heat transfer surfaces
[AIAA PAPER 81-0670] p0086 A81-29531
Texturing polymer surfaces by transfer casting
[NASA-CASR-LEU-13120-1] p0068 A81-16327
- WEIKLE, R. E.
Specifying and calibrating instrumentation for
wideband electronic power measurements
[NASA-TN-81545] p0079 A81-16425
- WEINBERG, R.
Radiation damage in lithium-counterdoped N/P
silicon solar cells p0109 A81-27204
Radiation damage annealing mechanisms and possible
low temperature annealing in silicon solar cells
p0040 A81-27207
Annealing of radiation damage in low resistivity
silicon solar cells p0099 A81-17554
Radiation damage in silicon N/P solar cells
p0099 A81-17557
Performance of high resistivity n-type silicon
solar cells under 1 MeV electron irradiation
[NASA-TN-82610] p0103 A81-23626
Reduced annealing temperatures in silicon solar
cells p0104 A81-23627
[NASA-TN-82597]
- WEINER, V. G.
The effect of minority carrier mobility variations
on the performance of high voltage silicon solar
cells p0098 A81-17536
The effect of minority carrier mobility variations
on solar cell spectral response
[NASA-TN-82604] p0103 A81-23625
- WELLS, R. A.
Boundary layer development on turbine airfoil
section surfaces
[ASME PAPER 81-GT-204] p0008 A81-30094
- WERNER, J. E.
Vehicle testing of Cummins turbocompound diesel
engine
[NASA-CR-159840] p0140 A81-13803
- WEST, W. L., III
Normal crop calendars. Volume 2: The spring
wheat states of Minnesota, Montana, North
Dakota, and South Dakota p0094 A81-13426
[E81-10070]
Normal crop calendars. Volume 1: Assembly and
application of historical crop data to a
standard product p0095 A81-13431
[E81-10075]
- WESTONHILLAND, J. S.
Progress with variable cycle engines p0001 A81-17997
- WHEELER, D. R.
The transfer of polytetrafluoroethylene studied by
X-ray photoelectron spectroscopy p0087 A81-31238
Polytetrafluoroethylene transfer film studied with
X-ray photoelectron spectroscopy p0060 A81-11214
[NASA-TP-1728]
- WHITS, B. E.
Second year technical report on-board processing
for future satellite communications systems
[NASA-CR-165155] p0070 A81-10242
- WHITE, D. J.
Low NO_x/ combustion systems for burning heavy
residual fuels and high-fuel-bound nitrogen fuels
[ASME PAPER 81-GT-109] p0089 A81-30014
- WHITE, J. W.
Application of 'steady' state finite element and
transient finite difference theory to sound
propagation in a variable duct - A comparison
with experiment p0128 A81-48622
[AIAA PAPER 81-2016]
- WHITBOUGH, B.
High efficiency ultrathin coplanar back contact
cells p0114 A81-27092
Coplanar back contacts for thin silicon solar cells
[NASA-CR-165272] p0112 A81-18495
- WHITNEY, W. J.
Description of the vane core turbine facility and
the vane annular cascade facility recently
installed at NASA Lewis Research Center
[SAE PAPER 801122] p0031 A81-34158
Cold-air investigation of first stage of
4-1/2-stage, fan drive turbine with average
stage-loading factor of 4.66
[NASA-TP-1780] p0015 A81-16050
- WHITTENBERGER, J. D.
The influence of isothermal annealing on the
molybdenum fibers of a directed solid
gamma/gamma prime - alpha alloy p0056 A81-10765
Elevated temperature mechanical properties and
residual tensile properties of two cast
superalloys and several nickel-base oxide
dispersion strengthened alloys p0057 A81-24104
Creep and residual mechanical properties of cast
superalloys and oxide dispersion strengthened
alloys [NASA-TP-1781] p0053 A81-19273
- WICKENHUISSE, T. J.
Comparisons of four alternative powerplant types
for future general aviation aircraft
[NASA-TN-81584] p0013 A81-10067
- WILBUR, R. J.
Passivation of carbon steel through mercury
implantation [NASA-CR-165292] p0059 A81-20244
- WILL, E. A.
Computer program for pulsed thermocouples with
corrections for radiation effects p0120 A81-33838
[NASA-TP-1895]
- WILLER, G. S.
Conceptual design of an in-space cryogenic fluid
management facility, executive summary
[NASA-CR-165279-EXEC-SUMM] p0137 A81-21212
Conceptual design of an in-space cryogenic fluid
management facility [NASA-CR-165279] p0067 A81-21213
- WILLIAMS, R. C.
Low-speed aerodynamic performance of
50.8-centimeter-diameter noise-suppressing
inlets for the Quiet, Clean, Short-haul
Experimental Engine (QCEE) [NASA-TP-1178] p0013 A81-11037
- WILLIS, E. A.
An overview of general aviation propulsion
research programs at NASA-Lewis Research Center
[SAE PAPER 810624] p0023 A81-42778
An overview of general aviation propulsion
research programs at NASA Lewis Research Center
[NASA-TN-81666] p0015 A81-16052
- WILSON, C.
Design of an exhaust mixer nozzle for the
Avco-Lycoming Quiet Clean General Aviation
Turboprop (QCGAT) [NASA-CR-159426] p0029 A81-19120
- WILSON, D. B.
BHD generator off-design performance and nox
chemical kinetics analysis. Volume 1: Analysis
of the off-design performance of the Engineering
Test Facility BTF BHD generator flow train
[NASA-CR-165187] p0133 A81-11834
- WINKLEBLICK, R. G.
Conceptual design study of a coal gasification
combined-cycle powerplant for industrial
cogeneration [NASA-TN-81687] p0105 A81-25488
- WISTUCHY, L. G.
Electron reflection and secondary emission
characteristics of sputter-textured pyrolytic
graphite surfaces p0065 A81-38065
Ion beam sputter etching of orthopedic implant
alloy NP358 and resulting effects on fatigue
properties [AIAA PAPER 81-0671] p0057 A81-38069
Theoretical model applicable to the experimental
determination of surface anchoring energies of
nematic liquid crystals [NASA-TN-81628] p0124 A81-12817
Ion beam sputter etching of orthopedic implanted
alloy NP358 and resulting effects on fatigue
[NASA-TN-81747] p0045 A81-21174
Electron reflection and secondary emission
characteristics of sputter-textured pyrolytic
graphite surfaces [NASA-TN-81755] p0062 A81-22193
Ion sputter textured graphite
[NASA-CASR-LEU-12919-1] p0046 A81-27198
- WIRTH, G.
The influence of isothermal annealing on the
molybdenum fibers of a directed solid

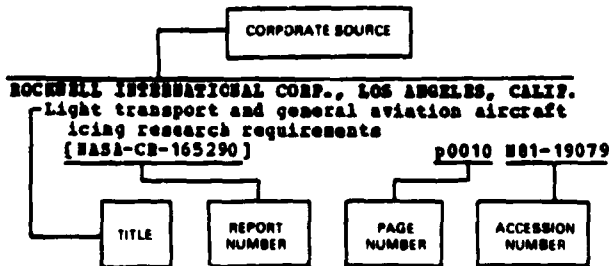
- gamma/gamma prime - alpha alloy p0056 A81-10765
- WISANBER, D. W.
Effects of geometric variables on rub characteristics of Ti-6Al-4V [NASA-TP-1835] p0053 A81-20245
Laser surface fusion of plasma sprayed ceramic turbine seals [NASA-CASE-LEN-13269-1] p0062 A81-22190
- WISLER, D. C.
Core compressor exit stage study. Volume 3: Data and performance report for screening test configurations [NASA-CR-159499] p0024 A81-12086
Core compressor exit stage study. Volume 2: Data and performance report for the baseline configuration [NASA-CR-159498] p0027 A81-16051
- WITERN, W. E.
Mechanical properties of weldments in experimental Fe-12Ni-0.2Ti and Fe-12Ni-1Mo-0.2Ti alloys for cryogenic service p0058 A81-48143
- WOHLGEMUTH, J.
High efficiency ultrathin coplanar back contact cells p0114 A81-27092
Coplanar back contacts for thin silicon solar cells [NASA-CR-165272] p0112 A81-18495
- WOLKE, J.
Effects of geometric variables on rub characteristics of Ti-6Al-4V [NASA-TP-1835] p0053 A81-20245
- WOLFGANG, G.
Effect of fuel nitrogen and hydrogen content on emissions in hydrocarbon combustion [ASME PAPER 81-GT-63] p0057 A81-29973
Effect of fuel nitrogen and hydrogen content on emissions in hydrocarbon combustion [NASA-TN-81612] p0097 A81-14399
- WOOD, J. C.
Test results of the Chrysler upgraded automotive gas turbine engine: Initial design [NASA-TN-81660] p0107 A81-30562
- WOOD, J. E.
Improved method for calculating transonic velocities on blade-to-blade stream surfaces of a turbomachine [NASA-TP-1772] p0004 A81-22017
- WOODWARD, R. F.
Effects of blade-vane ratio and rotor-stator spacing on fan noise with forward velocity [AIAA PAPER 81-2032] p0024 A81-48628
Effects of blade-vane ratio and rotor-stator spacing of fan noise with forward velocity [NASA-TN-82690] p0126 A81-31956
- WOOLLAN, J. A.
Atomic hydrogen storage method and apparatus [NASA-CASE-LEN-12081-3] p0066 A81-14103
- WRIGHT, C.
High efficiency ultrathin coplanar back contact cells p0114 A81-27092
Coplanar back contacts for thin silicon solar cells [NASA-CR-165272] p0112 A81-18495
- WULF, R. E.
Engine diagnostics program: CF6-50 engine performance deterioration [NASA-CR-159867] p0024 A81-12085
- Y**
- YACOBucci, E. G.
Design and preliminary results of a fuel flexible industrial gas turbine combustor [ASME PAPER 81-GT-108] p0087 A81-30013
Low NO_x/ combustion systems for burning heavy residual fuels and high-fuel-bound nitrogen fuels [ASME PAPER 81-GT-109] p0089 A81-30014
- YAMASOTO, Y.
Effect of tangential traction and roughness on crack initiation/propagation during rolling contact [NASA-TN-81608] p0080 A81-11395
Stress concentration in the vicinity of a hole defect under conditions of Hertzian contact [NASA-TN-82649] p0084 A81-28443
- YANG, C. Y.
Zirconium carbide as an electrocatalyst for the chromous/chromic redox couple [NASA-CASE-LEN-13246-1] p0049 A81-26203
- YANG, S. S.
Contact law and impact responses of laminated composites [NASA-CR-155884] p0048 A81-12172
- YANG, S.-J.
Three-dimensional turbulent boundary layer development and separation in V/STOL engine inlets at incidence with small-cross flow and curvature influences [AIAA PAPER 81-0254] p0005 A81-20703
- YAVUZKURT, S.
Full-coverage film cooling. I - Three-dimensional measurements of turbulence structure. II - Prediction of the recovery-region hydrodynamics p0078 A81-15537
- YEN, M. C.
Effect of milling and leaching on the structure of sintered silicon p0064 A81-22529
Effect of milling and leaching on the structure of sintered silicon [NASA-TN-81602] p0060 A81-13166
- YOUNG, M. L.
Stability of large horizontal-axis axisymmetric wind turbines p0092 A81-22526
Stability of large horizontal-axis axisymmetric wind turbines [NASA-TN-81623] p0091 A81-12446
- YOUNG, W. H., JR.
Fluid mechanics mechanisms in the stall process of helicopters [NASA-TN-81956] p0003 A81-21027
- YOUNGBLANK, J. L.
Curved centerline air intake for a gas turbine engine [NASA-CASE-LEN-13201-1] p0014 A81-14999
- YU, Y.
Application handbook for a Standardized Control Module (SCM) for DC-DC converters, volume 1 [NASA-CR-165172] p0072 A81-10301
- Z**
- ZAPLATYNSKY, I.
Thermal barrier coatings - Burner rig hot corrosion test results p0063 A81-12630
Comparative evaluation of insulating properties of plasma-sprayed ceramic coatings p0064 A81-15984
- ZARETSKY, B. V.
Some limitations in applying classical EHD film thickness formulas to a high-speed bearing [ASME PAPER 80-C2/LUB-13] p0068 A81-18667
NASA five-ball fatigue tester - Over 20 years of research p0087 A81-44659
Comparisons of modified Vasco I-2 and AISI 9310 gear steels [NASA-TP-1731] p0080 A81-14322
NASA five-ball fatigue tester: Over 20 years of research [NASA-TN-82589] p0102 A81-23462
- ZELINSKY, F. J.
Thermodynamics. II - The extended thermodynamic system p0136 A81-31375
- ZELLARS, G. E.
Synergistic erosion/corrosion of superalloys in PFB coal combustor effluent p0058 A81-44663
Synergistic erosion/corrosion of superalloys in PFB coal combustor effluent [NASA-TN-81715] p0101 A81-23245
- ZELLS, J. E.
Propulsion control and control theory: A new research focus p0014 A81-12099
- SIZEMAN, J. A.
Performance deterioration of commercial high-bypass ratio turbofan engines [SAE PAPER 801118] p0021 A81-34154
Investigation of performance deterioration of the CF6/JT9D high bypass ratio turbofan engines p0014 A81-24086

ZOLA, C. L.
An improved prediction method for noise generated
by conventional profile coaxial jets
(AIAA PAPER 81-1991) p0125 A81-49743
An improved prediction method for noise generated
by conventional profile coaxial jets
(NASA-TN-82712) p0127 N81-32964

**ORIGINAL PAGE IS
OF POOR QUALITY.**

CORPORATE SOURCE INDEX

Typical Corporate Source Index Listing



The title of the document is used to provide a brief description of the subject matter. The page number and NASA or AIAA accession number are included in each entry to assist the user in locating the abstract in the abstract section. If applicable, a report number is also included as an aid in identifying the document.

A

ACUREX CORP., MOUNTAIN VIEW, CALIF.
Synthesis of improved phenolic and polyester resins
[NASA-CR-165180] p0065 N81-17263

ARJOJET LIQUID ROCKET CO., SACRAMENTO, CALIF.
High performance cryogenic engines for orbit transfer vehicles
[IAP PAPER 80-P-253] p0043 N81-18363

High-density fuel combustion and cooling investigation
[NASA-CR-165177] p0050 N81-16177

Low-thrust chemical rocket engine study
[NASA-CR-165276] p0042 N81-21122

AIR FORCE ARMO PROPULSION LAB., WRIGHT-PATTERSON AFB, OHIO.
Future Air Force aircraft propulsion control systems: The extended summary paper
p0025 N81-12096

AIRSEARCH MFG. CO., PHOENIX, ARIZ.
Development of low-cost directionally-solidified turbine blades
p0088 N81-10707

Cost/benefit analysis of advanced materials technology candidates for the 1980's, part 2
[NASA-CR-165176] p0139 N81-11953

Low-cost directionally-solidified turbine blades, volume 2
[NASA-CR-159562] p0024 N81-12088

General Aviation Turbine Engine (GATE) study
[NASA-CR-159482] p0029 N81-19117

QCGAT mixer compound exhaust system design and static big model test report
[NASA-CR-135386] p0029 N81-19119

AKRON UNIV., OHIO.
Kinematic correction for roller skewing
[ASME PAPER 80-DET-76] p0085 N81-18647

Finite element analysis of inviscid supersonic boattail flow
[AIAA PAPER 81-0276] p0006 N81-20831

ARGONNE NATIONAL LAB., ILL.
Thermal energy storage for the Stirling engine powered automobile
[NASA-CR-159561] p0113 N81-22467

ARMY AVIATION RESEARCH AND DEVELOPMENT COMMAND, CLEVELAND, OHIO.
An experimental evaluation of the performance deficit of an aircraft engine starter turbine
[SAE PAPER 801137] p0021 N81-34168

The role of oxidation in the fretting wear process
[NASA-TN-81570] p0051 N81-12210

Design of spur gears for improved efficiency
[NASA-TN-81625] p0081 N81-17436

Effects of geometric variables on rub characteristics of Ti-6Al-4V
[NASA-TP-1835] p0053 N81-20245

Life analysis of multiroller planetary traction drive
[NASA-TP-1710] p0082 N81-20423

A sputtered zirconia primer for improved thermal shock resistance of plasma sprayed ceramic turbine seals
[NASA-TN-81732] p0062 N81-21198

Fretting wear and fretting fatigue: How are they related?
[NASA-TN-82633] p0054 N81-26235

Optimal tooth numbers for compact standard spur gear sets
[NASA-TN-82614] p0033 N81-27524

A method of selecting grid size to account for Hertz deformation in finite element analysis of spur gears
[NASA-TN-82623] p0083 N81-27525

Simplified solution for stresses and deformation
[NASA-TN-82647] p0084 N81-28444

Analysis of starvation effects on hydrodynamic lubrication in nonconforming contacts
[NASA-TN-82668] p0084 N81-29438

ARMY AVIATION RESEARCH AND DEVELOPMENT COMMAND, SANFORD, VA.
Fluid mechanics mechanisms in the stall process of helicopters
[NASA-TN-81956] p0003 N81-21027

ARMY MOBILITY EQUIPMENT RESEARCH AND DEVELOPMENT COMMAND, FORT BELVOIR, VA.
Photovoltaic applications - Past and future
p0109 N81-27231

ARMY PROPULSION LAB., CLEVELAND, OHIO.
Some limitations in applying classical EHD film thickness formulas to a high-speed bearing
[ASME PAPER 80-C2/LUB-13] p0068 N81-18667

Loss model for off-design performance analysis of radial turbines with pivoting-vane, variable-area stators
[SAE PAPER 801135] p0021 N81-34166

Effect of a part-span variable inlet guide vane on the performance of a high-bypass turbofan engine
[AIAA PAPER 81-1362] p0022 N81-40842

Mixing effectiveness test of an exhaust gas mixer in a high bypass turbofan at altitude
[AIAA PAPER 81-1495] p0023 N81-44225

AVCO CORP., LOWELL, MASS.
CVD-produced boron filaments
p0048 N81-11336

AVCO LYCOMING DIV., STRATFORD, CONN.
Design of an exhaust mixer nozzle for the Avco-Lycoming Quiet Clean General Aviation Turbofan (QCGAT)
[NASA-CR-159426] p0029 N81-19120

B

BATTILLE COLUMBUS LABS., OHIO.
Continuous analysis of stresses from arbitrary surface loads on a half space
p0093 N81-14162

Computer-aided roll pass design in rolling of airfoil shapes
p0088 N81-15796

BESCH AIRCRAFT CORP., BOULDER, COLO.
Conceptual design of an in-space cryogenic fluid management facility, executive summary
[NASA-CR-165279-BESC-SUM] p0137 N81-21212

Conceptual design of an in-space cryogenic fluid management facility

(NASA-CR-165279) p0067 N81-21213
BENDIX CORP., DETROIT, MICH.
 Multivariable synthesis with transfer functions p0026 N81-12102

BOEING AEROSPACE CO., SEATTLE, WASH.
 Electrostatic bonding of thin (cycle sine 3 mil) 7070 cover glass to Ta2O5 AR-coated thin (cycle sine 2 mil) silicon wafers and solar cells
 [NASA-CR-165240] p0111 N61-16582
 Evaluation of solar cell covers and encapsulant materials for space application p0111 N81-17568

Electrostatic bonding of thin (approximately 3 mil) 7070 cover glass to Ta2O5 AR-coated thin (approximately 2 mil) silicon wafers and solar cells p0111 N81-17569

BOEING CO., WICHITA, KANS.
 A theoretical approach to sound propagation and radiation for ducts with suppressors p0128 N81-38061

BOEING MILITARY AIRPLANE DEVELOPMENT, SEATTLE, WASH.
 Should we attempt global (inlet engine airframe) control design? p0025 N81-12097

BURNS AND ROE, INC., WOODBURY, N. Y.
 Engineering support for magnetohydrodynamic power plant analysis and design studies [NASA-CR-159690] p0110 N81-13466
 Modification of the BCAS reference steam power generating plant to comply with the EPA 1979 new source performance standards [NASA-CR-159853] p0110 N81-13467

C

CABOT CORP., KOKOMO, IND.
 Effect of TSP variables upon structure and properties in ODS alloy BDA 8077 sheet p0059 N81-10706

CARBONUMBUD CO., NIAGARA FALLS, N. Y.
 Fabrication of injection sintered sintered alpha SiC turbine components [ASME PAPER 81-GT-161] p0089 N81-30060

CASE WESTERN RESERVE UNIV., CLEVELAND, OHIO.
 Sputtered protective coatings for die casting dies p0057 N81-38067

Ion beam sputter etching of orthopedic implant alloy MP35N and resulting effects on fatigue properties [AIAA PAPER 81-0671] p0057 N81-38069

Microstructure and mechanical properties of bulk and plasma-sprayed Y2O3-partially stabilized zirconia [NASA-CR-165126] p0059 N81-22156

CLEVELAND STATE UNIV., OHIO.
 Effect of milling and leaching on the structure of sintered silicon p0064 N81-22529

COLORADO STATE UNIV., FORT COLLINS.
 Passivation of carbon steel through mercury implantation [NASA-CR-165292] p0059 N81-20244

COLUMBIA UNIV., NEW YORK.
 Next generation communications satellites: Multiple access and network studies [NASA-CR-165145] p0033 N81-12139

COMMUNICATIONS SATELLITE CORP., CLARKSBURG, MD.
 Thin n-i-p silicon solar cell p0114 N81-27097

CONTROL DATA CORP., MINNEAPOLIS, MINN.
 Ozone contamination in aircraft cabins - Results from GASP data and analyses [AIAA PAPER 81-0305] p0010 N81-20740

Cloud encounter and particle density variabilities from GASP data [AIAA PAPER 81-0308] p0117 N81-20742

CUMMINS ENGINE CO., INC., COLUMBUS, IND.
 Vehicle testing of Cummins turbocompound diesel engine [NASA-CR-159840] p0140 N81-13803

D

DATON UNIV., OHIO.
 Applications Technology Satellite and Communications Technology Satellite user experiments for 1967 - 1980 reference book,

Volume 1 [NASA-CR-165169-VOL-1] p0033 N81-12135
 Applications Technology Satellite and Communications Technology Satellite user experiments for 1967-1980 reference book, Volume 2 [NASA-CR-165169-VOL-2] p0033 N81-12136
 Applications Technology Satellite and Communications Technology Satellite user experiments for 1967-1980 reference book, Volume 3: User form surveys [NASA-CR-165169-VOL-3] p0033 N81-12137
 Applications Technology Satellite and Communications Technology Satellite user experiments for 1967-1980 reference book, Volume 4: Abstracts [NASA-CR-165169-VOL-4] p0133 N81-12138

DELAWARE UNIV., WILMINGTON.
 Inlet flow distortion in turbomachinery [ASME PAPER 80-GT-20] p0005 N81-17952
 Stability of large horizontal-axis axisymmetric wind turbines p0092 N81-22526

DETROIT DIESEL ALLISON, INDIANAPOLIS, IND.
 Surface flaw detection in structural ceramics by scanning photoacoustic spectroscopy p0079 N81-17906
 Design and preliminary results of a fuel flexible industrial gas turbine combustor [ASME PAPER 81-GT-108] p0087 N81-30013
 Road map to adaptive optimal control p0025 N81-12098

Experimental determination of unsteady blade element aerodynamics in cascades. Volume 2: Translation mode cascade [NASA-CR-165166] p0007 N81-14976

Ceramic applications in turbine engines [NASA-CR-159865] p0029 N81-19118

DEUTSCHE FORSCHUNGS- UND VERSUCHSANSTALT FÜR LUFT- UND RAUMFAHRT, COLOGNE (WEST GERMANY).
 The influence of isothermal annealing on the molybdenum fibers of a directed solid gamma/gamma prime - alpha alloy p0056 N81-10765

DU PONT DE NEMOURS (E. I.) AND CO., WILMINGTON, DEL.
 Ultra-high modulus organic fiber hybrid composites [NASA-CR-165228] p0048 N81-21130

E

EATON ENGINEERING AND RESEARCH CENTER, SOUTHFIELD, MICH.
 Small passenger car transmission test: Dodge Omni A-404 transmission [NASA-CR-165181] p0088 N81-15366

EIC, INC., NEWTON, MASS.
 Moderate temperature sodium cells. I - Transition metal disulfide cathodes p0113 N81-15027

ENERGY RESEARCH CORP., DANBURY, CONN.
 Technology development for phosphoric acid fuel cell powerplant, phase 2 [NASA-CR-165317] p0113 N81-21536
 Technology development for phosphoric acid fuel cell powerplant (phase 2) [NASA-CR-165316] p0113 N81-21547
 Technology development for phosphoric acid fuel cell powerplant (phase 2) [NASA-CR-165318] p0113 N81-22475

ENVIRONMENTAL RESEARCH AND TECHNOLOGY, INC., CONCORD, MASS.
 Comparative analysis of sea ice features using Side-Looking Airborne Radar (SLAR) and LANDSAT imagery [E81-10044] p0095 N81-33539

F

FIBER MATERIALS, INC., BIDDEFORD, MAINE.
 Fabrication of aluminum oxide fiber reinforced aluminum matrix composites [NASA-CR-165184] p0043 N81-19229
 Fabrication development of alumina/aluminum composites [NASA-CR-165195] p0048 N81-19233

FORD MOTOR CO., DEARBORN, MICH.
 Ceramic regenerator systems development program [NASA-CR-165139] p0141 N81-22982

G

GARRETT CORP., FROENIA, ARIZ.
Analytical design of an advanced radial turbine
[NASA-CR-165170] p0140 N81-20958

GENERAL DYNAMICS/ASTRONAUTICS, SAN DIEGO, CALIF.
Study of thermal management for space platform applications
[NASA-CR-165238] p0033 N81-21106

GENERAL ELECTRIC CO., CINCINNATI, OHIO.
Mixer nozzle aeroacoustic characteristics for the energy efficient engine
[AIAA PAPER 81-1994] p0128 A81-48639
Core compressor exit stage study. Volume 3: Data and performance report for screening test configurations
[NASA-CR-159499] p0024 N81-12086
Curved centerline air intake for a gas turbine engine
[NASA-CASE-LEW-13201-1] p0014 N81-14999
Aerodynamic stability analysis of NASA J85-13/plasma pressure pulse generator installation
[NASA-CR-165141] p0027 N81-15004
TF34 engine compression system computer study
[NASA-CR-159889] p0027 N81-15005
Core compressor exit stage study. Volume 2: Data and performance report for the baseline configuration
[NASA-CR-159498] p0027 N81-16051
Turbine modeling technique to generate off-design performance data for both single and multistage axial-flow turbines
[NASA-CR-165244] p0027 N81-17078
Samarium cobalt (SMCO) generator/engine integration study
[AD-A092904] p0029 N81-17087
Program to develop sprayed, plastically deformable compressor shroud seal materials
[NASA-CR-165237] p0088 N81-17434
Aerodynamic/acoustic performance of YJ101/double bypass VCE with coannular plug nozzle
[NASA-CR-159869] p0129 N81-17846
VCE early acoustic test results of General Electric's high-radius ratio coannular plug nozzle
p0029 N81-17999
Apparatus for sensor failure detection and correction in a gas turbine engine control system
[NASA-CASE-LEW-12907-2] p0015 N81-19115
Integrated control system for a gas turbine engine
[NASA-CASE-LEW-12594-2] p0015 N81-19116
Energy efficient engine flight propulsion system: Aircraft/engine integration evaluation
[NASA-CR-159584] p0030 N81-22051

GENERAL ELECTRIC CO., EVANSTON, OHIO.
Evaluation of advanced combustors for dry NO_x/suppression with nitrogen bearing fuels in utility and industrial gas turbines
[ASME PAPER 81-GT-125] p0087 A81-30029
Design and development of the combustor inlet diffuser for the NASA/GI energy efficient engine
[ASME PAPER 81-GT-129] p0020 A81-30033
Supersonic stall flutter of high-speed fans
[ASME PAPER 81-GT-184] p0020 A81-30078
Engine diagnostics program: CF6-50 engine performance deterioration
[NASA-CR-159367] p0024 N81-12085
Energy efficient engine: Flight propulsion system preliminary analysis and design
[NASA-CR-159583] p0029 N81-18056
Design concepts for low-cost composite turbofan engine frame
[NASA-CR-165217] p0030 N81-22053

GENERAL ELECTRIC CO., LYNN, MASS.
Quiet Clean General Aviation Turbofan (QCGAT) technology study, volume 1
[NASA-CR-164222] p0030 N81-22052

GENERAL ELECTRIC CO., PHILADELPHIA, PA.
Improved ceramic heat exchanger materials
[NASA-CR-159678] p0065 N81-14082

GENERAL ELECTRIC CO., SCHENECTADY, N. Y.
Evaluation of advanced combustors for dry NO_x/suppression with nitrogen bearing fuels in utility and industrial gas turbines
[ASME PAPER 81-GT-125] p0087 A81-30029

GIER, INC., WALTHAM, MASS.

Catalyst surfaces for the chromous/chromic redox couple
[NASA-CASE-LEW-13148-2] p0107 N81-29524

GOULD, INC., CLEVELAND, OHIO.
The influence of isothermal annealing on the molybdenum fibers of a directed solid gamma/gamma prime - alpha alloy
p0056 A81-10765

H

HAMILTON STANDARD, HARTFORD, CONN.
Study of thermal management for space platform applications
[NASA-CR-165238] p0033 N81-21106

HARVARD UNIV., CAMBRIDGE, MASS.
Prolonging thermal barrier coated specimen life by thermal cycle management
p0065 A81-44658

HERCULES, INC., CUMBERLAND, MD.
Interactive multi-mode blade impact analysis
[ASME PAPER 81-GT-79] p0030 A81-29987

HOUSTON CHEMICAL CO., CORPUS CHRISTI, TEX.
Development and testing of heat transport fluids for use in active solar heating and cooling systems
[NASA-TN-82395] p0098 N81-16584

HOUSTON UNIV., TEX.
Numerical trials of HISSE
[81-10069] p0094 N81-13425

HUGHES AIRCRAFT CO., CULVER CITY, CALIF.
Fabrication and testing of polyvinylidene fluoride capacitors
[NASA-CR-159501] p0073 N81-22278

HUGHES AIRCRAFT CO., LOS ANGELES, CALIF.
Diagnostic system design for the Ion Auxiliary Propulsion System /IAPS/- Flight test of two 8 cm mercury ion thrusters
[AIAA PAPER 81-0666] p0041 A81-38070
Study of thermal management for space platform applications
[NASA-CR-165238] p0033 N81-21106

HUGHES RESEARCH LABS., MALIBU, CALIF.
Characteristics of 30-centimeter mercury ion thrusters
[AIAA PAPER 81-0715] p0041 A81-37569
Retrofit and verification test of a 30-cm ion thruster
[NASA-CR-165233] p0042 N81-20174

I

ILLINOIS UNIV., URBANA.
Dynamics of solid dispersions in oil during the lubrication of point contacts. I - Graphite
[ASLE PREPRINT 81-AN-50-3] p0064 A81-33860

INSTITUTE OF GAS TECHNOLOGY, CHICAGO, ILL.
Stabilizing platinum in phosphoric acid fuel cells
[NASA-CR-165311] p0113 N81-22473

INTERNATIONAL APPLIED PHYSICS, INC., DAYTON, OHIO.
The electric rail gun for space propulsion
[NASA-CR-165312] p0042 N81-22078

IONICS, INC., WATERTOWN, MASS.
Anion permselective membrane
[NASA-CR-165223] p0111 N81-16583

J

JET PROPULSION LAB., CALIFORNIA INST. OF TECH., PASADENA.
JPL's electric and hybrid vehicles project: Project activities and preliminary test results
p0143 N81-12987
The DOE photovoltaics program
p0143 N81-12989
Solar Thermal Power Systems parabolic dish project
[NASA-TN-82371] p0107 N81-28524

K

KANSAS UNIV., LAWRENCE.
Icing tunnel tests of a glycol-exuding porous leading edge ice protection system on a general aviation airfoil
[AIAA PAPER 81-0405] p0011 A81-20837

KARLSRUHE UNIV. (WEST GERMANY).
Fracture toughness of brittle materials determined with chevron notch specimens

KERNFORSCHUNGSZENTRUM, KARLSRUHE (WEST GERMANY).
Fracture toughness of brittle materials
determined with chevron notch specimens
p0064 A81-32545

L

LINCOLN LAB., MASS. INST. OF TECH., LEXINGTON.
Photovoltaic applications - Past and future
p0109 A81-27231
GaAs shallow-homojunction solar cells
[NASA-CR-165167] p0110 A81-15463
LITTLE (ARTHUR D.), INC., CAMBRIDGE, MASS.
Study of component technologies for fuel cell
on-site integrated energy systems
[NASA-CR-165152-VOL-1] p0110 A81-15461
Study of component technologies for fuel cell
on-site integrated energy system. Volume 2:
Appendices
[NASA-CR-165152-VOL-2] p0110 A81-15462
LOCKHEED ENGINEERING AND MANAGEMENT SERVICES CO.,
INC., HOUSTON, TEX.
Normal crop calendars. Volume 2: The spring
wheat states of Minnesota, Montana, North
Dakota, and South Dakota
[E81-10070] p0094 A81-13426
Preliminary evaluation of the Environmental
Research Institute of Michigan crop calendar
shift algorithm for estimation of spring wheat
development stage
[E81-10071] p0094 A81-13427
Limited Area Coverage/High Resolution Picture
Transmission (LAC/HRPT) tape IJ grid pixel
extraction processor user's manual
[E81-10072] p0094 A81-13428
Limited Area Coverage/High Resolution Picture
Transmission (LAC/HRPT) data vegetative index
calculation processor user's manual
[E81-10073] p0094 A81-13429
EROS to universal tape conversion processor
[E81-10074] p0095 A81-13430
Normal crop calendars. Volume 1: Assembly and
application of historical crop data to a
standard product
[E81-10075] p0095 A81-13431
Evaluation of results of US corn and soybeans
exploratory experiment: Classification
procedures verification test
[E81-10076] p0095 A81-13432
Limited Area Coverage/High Resolution Picture
Transmission, LAC/HRPT tape conversion
processor user's manual
[E81-10077] p0095 A81-13433
LOCKHEED-GEORGIA CO., MARIETTA.
An experimental study of transmission,
reflection and scattering of sound in a free
jet flight simulation facility and comparison
with theory
p0129 A81-28943
LOCKHEED MISSILES AND SPACE CO., PALO ALTO, CALIF.
Evacuation-induced pressure differentials in
multilayer insulation systems
p0078 A81-18021
LOCKHEED MISSILES AND SPACE CO., SUNNYVALE, CALIF.
Study of thermal management for space platform
applications
[NASA-CR-165238] p0033 A81-21106

M

MARTIN MARIETTA AEROSPACE, DENVER, COLO.
Propellant management for low thrust chemical
propulsion systems
[AIAA PAPER 81-1453] p0082 A81-42198
Shuttle compatible cryogenic liquid storage and
supply systems
[AIAA PAPER 81-1509] p0037 A81-42207
MARTINI ENGINEERING, RICHMOND, WASH.
A computer simulation of the transient response
of a 4 cylinder Stirling engine with burner
and air preheater in a vehicle
[NASA-CR-165262] p0078 A81-22313
MATTECH, INC., ARLINGTON, VA.
Study of fuel cell on-site, integrated energy
systems in residential/commercial applications
[NASA-CR-165144] p0112 A81-21533
MECHANICAL TECHNOLOGY, INC., LATHAM, N. Y.
Friction and wear results from sputter-deposited

chrome oxide with and without nichrome
metallic binders and interlayers
[ASME PAPER 80-C2/LUB-49] p0089 A81-18693
Automotive Stirling engine development program
[NASA-CR-165134] p0139 A81-11952
Advanced propulsion system concept for hybrid
vehicles
[NASA-CR-159772] p0140 A81-18935
An experimental evaluation of oil pumping rings
[NASA-CR-165271] p0088 A81-21355
MISSISSIPPI UNIV., UNIVERSITY.
Ion beam texturing of heat transfer surfaces
[AIAA PAPER 81-0670] p0086 A81-29531
MISSOURI UNIV. - ROLLA.
Application of 'steady' state finite element and
transient finite difference theory to sound
propagation in a variable duct - A comparison
with experiment
[AIAA PAPER 81-2016] p0128 A81-48622
MITRE CORP., BEDFORD, MASS.
Second year technical report on-board processing
for future satellite communications systems
[NASA-CR-165155] p0070 A81-10242
MONROE LTD., GAITHERSBURG, MD.
Photovoltaic applications - Past and future
p0109 A81-27231
MOTOROLA, INC., PHOENIX, ARIZ.
Market definition study of photovoltaic power
for remote villages in developing countries
[NASA-CR-159880] p0110 A81-14391

N

NATIONAL AERONAUTICS AND SPACE ADMINISTRATION.
LANGLEY RESEARCH CENTER, HAMPTON, VA.
Cloud encounter and particle density
variabilities from GASP data
[AIAA PAPER 81-0308] p0117 A81-20742
Application of unsteady airfoil theory to rotary
wings
p0006 A81-39874
Geometric methods in computational
fluid dynamics
p0075 A81-18331
Fluid mechanics mechanisms in the stall process
of helicopters
[NASA-TN-81956] p0003 A81-21027
NATIONAL AERONAUTICS AND SPACE ADMINISTRATION.
MARSHALL SPACE FLIGHT CENTER, HUNTSVILLE, ALA.
Results of the Mission Profile Life Test first
test segment - Thruster J1
[AIAA PAPER 81-C716] p0043 A81-29552
Development and testing of heat transport fluids
for use in active solar heating and cooling
systems
[NASA-TN-82395] p0098 A81-16584
NATIONAL BUREAU OF STANDARDS, WASHINGTON, D.C.
Non-noble catalysts and catalyst supports for
phosphoric acid fuel cells
[NASA-CR-165221] p0112 A81-18497
NEW JERSEY INST. OF TECH., NEWARK.
Heat transfer from a row of impinging jets to
concave cylindrical surfaces
p0078 A81-24924
NEW MEXICO UNIV., ALBUQUERQUE.
Three-dimensional turbulent boundary layer
development and separation in V/STOL engine
inlets at incidence with small-cross flow and
curvature influences
[AIAA PAPER 81-0254] p0005 A81-20703
NIELSEN ENGINEERING AND RESEARCH, INC., MOUNTAIN
VIEW, CALIF.
A rapid method for the approximate determination
of nonlinear solutions Application to
aerodynamic flows
p0007 A81-1528
A rapid perturbation procedure for determining
nonlinear flow solutions: Application to
transonic turbomachinery flows
[NASA-CR-3425] p0001 A81-22012
NOTRE DAME UNIV., IND.
Proton radiation damage in bulk n-GaAs
p0099 A81-17564

O

OAK RIDGE NATIONAL LAB., TENN.
Photovoltaic applications - Past and future
p0109 A81-27231

OFFICE OF NAVAL RESEARCH, ARLINGTON, VA.
Dynamic characteristics of a high-speed rotor
with radial and axial foil-bearing supports
[ASME PAPER 80-C2/LUB-35] p0085 A81-18683
OHIO STATE UNIV., COLUMBUS.
An analytical approach to airfoil icing
[AIAA PAPER 81-0403] p0117 A81-20810
OREGON GRADUATE CENTER FOR STUDY AND RESEARCH,
BHAVENTON.
Mechanical properties of weldments in
experimental Fe-12Mn-0.2Ti and
Fe-12Mn-1Mo-0.2Ti alloys for cryogenic service
p0058 A81-48143

P

PITTSBURG UNIV., PA.
An investigation of hot corrosion mechanisms in
nickel base alloys p0058 A81-16208
PRATT AND WHITNEY AIRCRAFT, EAST HARTFORD, CONN.
Energy efficient engine diffuser/combustor model
technology [NASA-CR-165157] p0026 A81-15002
Variable stream control engine for advanced
supersonic aircraft design update p0001 A81-17996
Progress with variable cycle engines p0001 A81-17997
PRATT AND WHITNEY AIRCRAFT, WEST PALM BEACH, FLA.
Extended frequency turbofan model [NASA-CR-165261] p0030 A81-20078
PRATT AND WHITNEY AIRCRAFT GROUP, EAST HARTFORD,
CONN.
JT9D performance deterioration results from a
simulated aerodynamic load test [AIAA PAPER 81-1588] p0022 A81-40963
Rotor redesign for a highly loaded 1800 ft/sec
tip speed fan, 2 [NASA-CR-159879] p0024 A81-12087
Design of a multivariable integrated control for
a supersonic propulsion system p0025 A81-12094
Propulsion controls p0025 A81-12095
Model aerodynamic test results for two variable
cycle engine coannular exhaust systems at
simulated takeoff and cruise conditions [NASA-CR-159818] p0026 A81-13057
Cost/benefit analysis of advanced materials
technologies for future aircraft turbine engines
[NASA-CR-165225] p0027 A81-15006
Improved methods for fan sound field determination
[NASA-CR-165188] p0129 A81-15769
Combustor liner durability analysis [NASA-CR-165250] p0027 A81-17079
JT8D-15/17 high pressure turbine root discharged
blade performance improvement [NASA-CR-165220] p0028 A81-17080
Model aerodynamic test results for two variable
cycle engine coannular exhaust systems at
simulated takeoff and cruise conditions.
Comprehensive data report. Volume 1: Design
layouts [NASA-CR-159819-VOL-1] p0028 A81-17081
Model aerodynamic test results for two variable
cycle engine coannular exhaust systems at
simulated takeoff and cruise conditions.
Comprehensive data report. Volume 2:
Tabulated aerodynamic data book 1 [NASA-CR-159819-VOL-2-BK-1] p0028 A81-17082
Model aerodynamic test results for two variable
cycle engine coannular exhaust systems at
simulated takeoff and cruise conditions.
Comprehensive data report. Volume 2:
Tabulated aerodynamic data book 2 [NASA-CR-159819-VOL-2-BK-2] p0028 A81-17083
Model aerodynamic test results for two variable
cycle engine coannular exhaust systems at
simulated takeoff and cruise conditions.
Comprehensive data report. Volume 2:
Tabulated aerodynamic data book 3 [NASA-CR-159819-VOL-2-BK-3] p0028 A81-17084
Model aerodynamic test results for two variable
cycle engine coannular exhaust systems at
simulated takeoff and cruise conditions.
Comprehensive data report. Volume 2:

Graphical data book 1 [NASA-CR-159819-VOL-3-BK-1] p0028 A81-17085
Model aerodynamic test results for two variable
cycle engine coannular exhaust systems at
simulated takeoff and cruise conditions.
Comprehensive data report. Volume 3:
Graphical data book 2 [NASA-CR-159819-VOL-3-BK-2] p0028 A81-17086
Turbine blade temperature measurements using
thin film temperature sensors [NASA-CR-165201] p0059 A81-19277
An assessment of the use of anti-icing fuel in
turbofan engines [NASA-CR-165258] p0067 A81-19316
PRATT AND WHITNEY AIRCRAFT GROUP, HARTFORD, CONN.
Design, durability and low cost processing
technology for composite fan exit guide vanes
p0089 A81-22664
PRATT AND WHITNEY AIRCRAFT GROUP, WEST PALM BEACH,
FLA.
Cyclic behavior of turbine disk alloys at 650 C
p0056 A81-12266
Future challenges in V/STOL flight
control integration [SAE PAPER 801140] p0022 A81-34170
PURDUE UNIV., LAFAYETTE, IND.
Calculation of the flow field in supersonic
inlets using a bicharacteristics method with
shock wave fitting p0006 A81-21212
Factors influencing the predicted performance of
advanced propeller designs [AIAA PAPER 81-1564] p0007 A81-42210
Laser-velocimeter flow-field measurements of an
advanced turboprop [AIAA PAPER 81-1568] p0007 A81-42211
Multivariable nyquist array method with
application to turbofan engine control p0026 A81-12101
Contact law and impact responses of laminated
composites [NASA-CR-159884] p0048 A81-12172

R

RENSSELAER POLYTECHNIC INST., TROY, N. Y.
A methodology for the design and calibration of
data based models of aggregate lake ecosystem
dynamics p0111 A81-18482
ROCKETDYNE, CANOGA PARK, CALIF.
Low-thrust chemical propulsion system pump
technology [NASA-CR-165210] p0088 A81-17437
Low-thrust chemical rocket engine study
[NASA-CR-165275] p0042 A81-21125
ROCKWELL INTERNATIONAL CORP., LOS ANGELES, CALIF.
Light transport and general aviation aircraft
icing research requirements [NASA-CR-165290] p0010 A81-19079

S

SANDIA LABS., ALBUQUERQUE, N. MEX.
Photovoltaic applications - Past and future
p0109 A81-27231
SCIENTIFIC RESEARCH ASSOCIATES, INC., GLASTONBURY,
CONN.
Calculation of three-dimensional turbulent
subsonic flows in transition ducts p0008 A81-21199
Prediction of laminar and turbulent primary and
secondary flows in strongly curved ducts
[NASA-CR-3389] p0007 A81-16976
A three-dimensional turbulent compressible
subsonic duct flow analysis for use with
constructed coordinate systems [NASA-CR-3389] p0077 A81-20383
SEAR RESEARCH CORP., BALLSTON LAKE, N. Y.
Measurement of rod seal lubrication for Stirling
engine [NASA-CR-165158] p0088 A81-13359
SIEBENS A.G., MUNICH (WEST GERMANY).
Integrated IC-circuits in ALTA-technology on one
substrate [BAFT-EE-T-79-107] p0072 A81-14227

SOLAR TURBINES INTERNATIONAL, SAN DIEGO, CALIF.

Development of a low NO_x/lean premixed annular combustor
[ASME PAPER 81-GT-40] p0020 A81-29954
Low NO_x/combustion systems for burning heavy residual fuels and high-fuel-bound nitrogen fuels
[ASME PAPER 81-GT-109] p0089 A81-30014

SOLARTEC CORP., ROCKVILLE, MD.

High efficiency ultrathin coplanar back contact cells
p0114 A81-27092
Coplanar back contacts for thin silicon solar cells
[NASA-CR-165272] p0112 A81-18495

SPECTROLAB, INC., SYLMAR, CALIF.

High efficiency wraparound contact solar cells /HEWAC/
p0114 A81-27094
The HEWAC pilot line experience
p0111 A81-17574

SPECTRON DEVELOPMENT LABS., INC., COSTA MESA, CALIF.

Fuel injector characterization studies
[NASA-CR-165200] p0026 A81-15003

SPIRE CORP., BEDFORD, MASS.

Silicon solar cells with high open-circuit voltage
p0113 A81-27089

SRI INTERNATIONAL CORP., MENLO PARK, CALIF.

Development program on a cold cathode electron gun
[NASA-CR-159570] p0073 A81-19395

STANFORD UNIV., CALIF.

A rapid method for the approximate determination of nonlinear solutions Application to aerodynamic flows
p0007 A81-11628
Full-coverage film cooling. I - Three-dimensional measurements of turbulence structure. II - Prediction of the recovery-region hydrodynamics
p0078 A81-15537

STD RESEARCH CORP., ALCADIA, CALIF.

The STD/HND codes - Comparison of analyses with experiments at AEDC/BPDE, Reynolds Metal Co., and Hercules, Inc.
[AIAA PAPER 81-0173] p0133 A81-20649
Of the magnetoaerothermal instability
[AIAA PAPER 81-0449] p0133 A81-20698
Analytical investigation of critical phenomena in MHD power generators
[NASA-CR-165143] p0109 A81-12546

STONEMAN ASSOCIATES, INC., BARTON, CONN.

Preparation and evaluation of advanced electrocatalysts for phosphoric acid fuel cells
[NASA-CR-165170] p0111 A81-17527
Preparation and evaluation of advanced electrocatalysts for phosphoric acid fuel cells
[NASA-CR-165245] p0112 A81-18496

SUNDSTAND CORP., ROCKFORD, ILL.

An experimental evaluation of the performance deficit of an aircraft engine starter turbine
[SAE PAPER 801137] p0021 A81-34168

SYSTEMS SCIENCE AND SOFTWARE, LA JOLLA, CALIF.

The effect of solar array voltage patterns on plasma power losses
p0043 A81-19937
Fluid model of plasma outside a hollow cathode neutralizer
[AIAA PAPER 81-0739] p0134 A81-25560
Parasitic current losses due to solar electric propulsion generated plasmas
[AIAA PAPER 81-0740] p0043 A81-29561
Analysis of the charging of the SCATHA (P78-2) satellite
[NASA-CR-165348] p0033 A81-27169

T**TECHNION RESEARCH AND DEVELOPMENT FOUNDATION LTD., HAIFA (ISRAEL).**

Self-stabilizing radial face seal
[NASA-CASE-LEN-12991-1] p0083 A81-24442

TELEDYNE C&E, TOLEDO, OHIO.

Effect of time-dependent flight loads on turbofan engine performance deterioration
[ASME PAPER 81-GT-203] p0030 A81-30093
Boundary layer development on turbine airfoil suction surfaces
[ASME PAPER 81-GT-204] p0008 A81-30094

TELEDYNE CONTINENTAL MOTORS, MOBILE, ALA.

Advanced technology Spark-Ignition Aircraft Piston Engine Design Study
[NASA-CR-165162] p0026 A81-13963

TENNESSEE TECHNOLOGICAL UNIV., COOKSVILLE.

Perturbation solutions of combustion instability problems
[NASA-CR-159643] p0050 A81-16176

TENNESSEE UNIV., KNOXVILLE.

Application of 'steady' state finite element and transient finite difference theory to sound propagation in a variable duct - A comparison with experiment
[AIAA PAPER 81-2016] p0128 A81-48622

TEXAS UNIV., ARLINGTON.

MHD generator off-design performance and non-chemical kinetics analysis. Volume 1: Analysis of the off-design performance of the Engineering Test Facility STF MHD generator flow train
[NASA-CR-165187] p0133 A81-11834

TEXTRON BELL AEROSPACE CO., BUFFALO, N. Y.

Aeroelastic and dynamic finite element analyses of a bladder shrouded disk
[NASA-CR-159728] p0092 A81-19479
Nastran level 16 theoretical manual updates for aeroelastic analysis of bladed discs
[NASA-CR-159823] p0093 A81-19480
Nastran level 16 user's manual updates for aeroelastic analysis of bladed discs
[NASA-CR-159824] p0093 A81-15481
Nastran level 16 programmer's manual updates for aeroelastic analysis of bladed discs
[NASA-CR-159825] p0093 A81-19482
Nastran level 16 demonstration manual updates for aeroelastic analysis of bladed discs
[NASA-CR-159826] p0093 A81-19483

THERMO ELECTRON CORP., WALTHAM, MASS.

Thermal energy storage for the Stirling engine powered automobile
[NASA-CR-159561] p0113 A81-22467

TOLEDO UNIV., OHIO.

Pressure spectra and cross spectra at an area contraction in a ducted combustion system
[ASME PAPER 80-C2/AE80-9] p0077 A81-18638
Effects of mistuning on bending-torsion flutter and response of a cascade in incompressible flow
[AIAA 81-0602] p0092 A81-29465
Application of unsteady airfoil theory to rotary wings
p0006 A81-39874

TRW DEFENSE AND SPACE SYSTEMS GROUP, REDONDO BEACH, CALIF.

Application handbook for a Standardized Control Module (SCM) for DC-DC converters, volume 1
[NASA-CR-165174] p0072 A81-10301
User's design handbook for a Standardized Control Module (SCM) for DC to DC Converters, volume 2
[NASA-CR-165173] p0072 A81-11314
Materials processing in space: Future technology trends
p0143 A81-12991

TRW, INC., CLEVELAND, OHIO.

Tungsten wire-reinforced superalloys for 1093 C (2000 F) turbine blade applications
[NASA-CR-159720] p0047 A81-10112

TRW SYSTEMS, REDONDO BEACH, CALIF.

Study of thermal management for space platform applications
[NASA-CR-165238] p0033 A81-21106

TRW SYSTEMS GROUP, REDONDO BEACH, CALIF.

K-band high power latching switch
[NASA-CR-165159] p0073 A81-16389

U**ULTRASISTEMS, INC., IRVINE, CALIF.**

Phosphazene diamines
[NASA-CR-165147] p0065 A81-10169

UNITED TECHNOLOGIES CORP., EAST HARTFORD, CONN.

Effect of time-dependent flight loads on turbofan engine performance deterioration
[ASME PAPER 81-GT-203] p0030 A81-30093
Boundary layer development on turbine airfoil suction surfaces
[ASME PAPER 81-GT-204] p0008 A81-30094
Experimental study of the stability of aircraft fuels at elevated temperatures
[NASA-CR-165165] p0067 A81-12255

UNITED TECHNOLOGIES CORP., SOUTH WINDSOR, CONN.

Evaluation of concepts for controlling exhaust emissions from minimally processed petroleum

and synthetic fuels
[ASME PAPER 81-GT-157] p0067 A81-30056
Cogeneration Technology Alternatives Study
(CTAS) Volume 5: Analytical approach and
results
[NASA-CR-159763] p0109 A81-10517
UNITED TECHNOLOGIES CORP., WEST PALM BEACH, FLA.
Evaluation of concepts for controlling exhaust
emissions from minimally processed petroleum
and synthetic fuels
[ASME PAPER 81-GT-157] p0067 A81-30056
UNITED TECHNOLOGIES RESEARCH CENTER, EAST HARTFORD,
CONN.
A model for the analysis of
premixing-prevaporizing fuel-air mixing passages
[AIAA PAPER 81-0345] p0030 A81-20767
Effects of mistuning on blade torsional flutter
p0092 A81-29095
A study of external fuel vaporization
[ASME PAPER 81-GT-158] p0220 A81-30057
Boundary layer development on turbine airfoil
suction surfaces
[ASME PAPER 81-GT-204] p0008 A81-30094

ORIGINAL PAGE IS
OF POOR QUALITY

V

VIRGINIA POLYTECHNIC INST. AND STATE UNIV., BLACKSBURG.

Analysis and design of an adaptive multi-loop
controlled two winding buck/boost regulator
p0073 A81-21675
Flow separation in inlets at incidence angles
p0006 A81-29114
Application handbook for a Standardized Control
Module (SCM) for DC-DC converters, volume 1
[NASA-CR-165172] p0072 A81-10301
User's design handbook for a Standardized
Control Module (SCM) for DC to DC Converters,
volume 2
[NASA-CR-165173] p0072 A81-11314
Engine identification for adaptive control
p0025 A81-12100

VIRGINIA UNIV., CHARLOTTESVILLE. CVD-produced boron filaments

p0048 A81-11336

VOUGHT CORP., DALLAS, TEX.

Study of thermal management for space platform
applications
[NASA-CR-165238] p0033 A81-21106

W

WESTINGHOUSE ELECTRIC CORP., RADISON, PA.

Low NO_x and fuel flexible gas turbine combustors
[ASME PAPER 81-GT-99] p0020 A81-30006

WESTINGHOUSE ELECTRIC CORP., PITTSBURGH, PA.

Low NO_x and fuel flexible gas turbine combustors
[ASME PAPER 81-GT-99] p0020 A81-30006

Disk MHD generator study
[NASA-CR-159872] p0111 A81-16491

WESTINGHOUSE RESEARCH AND DEVELOPMENT CENTER, PITTSBURGH, PA.

Cell module and fuel conditioner
[NASA-CR-165189] p0112 A81-18494

Cell module and fuel conditioner development
[NASA-CR-165190] p0112 A81-19573

WICHITA STATE UNIV., KANS.

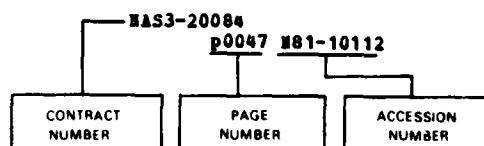
Performance prediction of straight two
dimensional diffusers
[NASA-CR-165186] p0133 A81-11833

X

IBROX ELECTRO-OPTICAL SYSTEMS, PASADENA, CALIF.

Adapting magneto-electrostatic containment to
inert gas thrusters
[AIAA PAPER 81-0140] p0043 A81-20625
Results of the Mission Profile Life Test first
test segment - Thruster J1
[AIAA PAPER 81-0716] p0043 A81-29552
Magneto-electrostatic thruster physical geometry
tests
[AIAA PAPER 81-0753] p0044 A81-29566

Typical Contract Number Index Listing



Listings in this index are arranged alphanumerically by contract number. Under each contract number, the accession numbers denoting documents that have been produced as a result of research done under that contract are arranged in ascending order with the /AA accession numbers appearing first. Preceding the accession number is the page number in the abstract section in which the citation may be found.

AF PROJ. 3145
p0029 N81-17087
AF-49(638)-1160
p0133 A81-20698
AGARD-OTAN-DPP-80-11067
p0075 N81-18331
DAAG29-77-G-0030
p0006 A81-20831
DAHC04-75-G-0026
p0006 A81-20831
DE-A101-76ET-20320
p0104 N81-24535
p0105 N81-24539
p0107 N81-29528
DE-A101-76ET-20366
p0100 N81-21537
LE-A101-77CS-51040
p0096 N81-13465
p0065 N81-14082
p0075 N81-15241
p0140 N81-20958
p0078 N81-22313
p0103 N81-23609
p0140 N81-24994
p0105 N81-25487
p0054 N81-26236
p0105 N81-27604
p0107 N81-30562
p0139 N81-32067
DE-A101-77CS-51044
p0096 N81-11449
p0097 N81-15464
p0097 N81-15465
p0082 N81-19459
p0071 N81-21281
p0103 N81-23608
p0140 N81-26586
p0106 N81-28523
p0085 N81-33484
DE-A101-77ET-10350
p0057 A81-29973
p0097 N81-14396
p0097 N81-14399
DE-A101-77ET-10769
p0133 N81-11833
p0110 N81-13467
p0103 N81-23610
p0103 N81-23611
p0132 N81-24926
p0132 N81-24927
p0132 N81-32026
DE-A101-79ET-20305
p0090 N81-33492
DE-A101-79ET-20485
p0100 N81-22477
p0104 N81-24536
p0094 N81-28517
p0106 N81-28520
DE-A101-80ET-17088
p0112 N81-19573
p0113 N81-22473
DE-A103-79ET-11272
p0096 N81-13464
p0112 N81-18494
p0112 N81-21533
p0113 N81-21547

p0113 N81-22475
DE-A103-80ET-11272
p0110 N81-15461
p0110 N81-15462
DE-A104-80AL-12726
p0049 N81-13105
p0111 N81-16583
p0106 N81-28519
p0107 N81-30522
p0049 N81-31308
p0108 N81-32608
p0108 N81-33601
DE-A101-80ET-17088
p0112 N81-18496
p0112 N81-18497
DE-A103-79ET-11272
p0113 N81-21536
DE-A104-81AL-16228
p0107 N81-28524
DE-A101-77CS-51040
p0104 N81-24533
DE-A101-77CS-51044
p0088 N81-15366
p0080 N81-15367
p0108 N81-31627
DE-A101-77ET-10769
p0098 N81-16570
p0111 N81-18491
DE-A101-79ET-20305
p0106 N81-27606
DE-A101-79ET-20485
p0110 N81-14391
DEN3-8 p0141 N81-22982
DEN3-17
p0079 A81-17906
p0089 A81-30060
p0029 N81-19118
DEN3-22
p0088 N81-13359
DEN3-30
p0109 N81-10517
DEN3-32
p0139 N81-11952
DEN3-43
p0089 A81-18697
DEN3-49
p0110 N81-1439
DEN3-67
p0113 N81-21547
p0113 N81-21547
p0113 N81-22475
DEN3-89
p0112 N81-21533
DEN3-92
p0140 N81-18935
DEN3-106
p0140 N81-20958
DEN3-107
p0110 N81-13466
p0110 N81-13467
DEN3-119
p0088 N81-21355
DEN3-121
p0110 N81-15461
p0110 N81-15462

DEN3-124
p0088 N81-15366
DEN3-137
p0111 N81-16583
DEN3-139
p0111 N81-18491
DEN3-146
p0020 A81-30006
DEN3-161
p0112 N81-18494
p0112 N81-19573
DEN3-167
p0089 A81-30060
DEN3-168
p0089 A81-30060
DEN3-176
p0111 N81-17527
p0112 N81-18496
DEN3-179
p0133 A81-20649
p0133 A81-20698
p0109 N81-12546
DEN3-202
p0133 A81-20649
p0133 A81-20698
DEN3-208
p0113 N81-22473
DEN3-226
p0078 N81-22313
DOT-FA78HAI-893
p0010 A81-20740
p0116 N81-13568
p0117 N81-21685
EC-77-A-01-2674
p0110 N81-13466
EC-77-A-31-1011
p0140 N81-13803
p0065 N81-14082
p0004 N81-28053
EC-77-A-31-1040
p0139 N81-11952
p0088 N81-13359
p0051 N81-15068
p0029 N81-19118
p0088 N81-21355
EC-77-A-31-1044
p0080 N81-13357
p0088 N81-15366
p0079 N81-16429
p0140 N81-18933
p0140 N81-18935
EC-77-A-31-1062
p0070 A81-39144
p0109 N81-10517
p0131 N81-16900
p0132 N81-19920
p0132 N81-30973
EC-77-A-31-1101
p0097 N81-14398
EC-77-A-01-2674
p0109 N81-12546
EF-A-01-2593
p0063 A81-12630
EF-77-A-01-2593
p0051 N81-15069
p0052 N81-16211
p0101 N81-23243
p0054 N81-25191
p0055 N81-27258
p0055 N81-28231
EF-77-A-01-2674
p0132 N81-24926
EN-78-C-02-4936
p0140 N81-13803
EX-76-A-29-1060
p0097 N81-14397
EX-76-I-01-1028
p0096 N81-11448
p0096 N81-13463
p0091 N81-16494
F19628-80-C-0001
p0070 N81-10242
F33615-72-C-1739
p0093 A81-14162

F33615-77-C-2018
p0029 N81-17087
NAG3-25
p0059 N81-20244
NAG3-28
p0117 A81-20810
NAG3-55
p0083 N81-27524
NASA ORDER C-2325
p0113 N81-22467
NASA ORDER C-30969-D
p0110 N81-15463
NASA ORDER C-46229-D
p0112 N81-18497
NAS1-15810
p0075 N81-18331
NAS3-71
p0011 N81-25065
NAS3-11175
p0078 A81-24924
NAS3-14336
p0078 A81-15537
NAS3-14377
p0078 A81-18021
NAS3-17522
p0008 A81-21199
NAS3-17760
p0093 A81-14162
NAS3-19429
p0030 N81-22052
NAS3-19698
p0065 N81-14082
NAS3-19699
p0033 N81-12135
p0033 N81-12136
p0033 N81-12137
NAS3-19856
p0008 A81-21199
NAS3-20048
p0001 N81-17997
NAS3-20050
p0129 A81-28945
NAS3-20054
p0088 N81-17434
NAS3-20055
p0007 N81-14976
NAS3-20061
p0026 N81-13057
p0028 N81-17081
p0028 N81-17082
p0028 N81-17083
p0028 N81-17084
p0028 N81-17085
p0028 N81-17086
p0001 N81-17997
NAS3-20065
p0114 A81-27094
NAS3-20070
p0024 N81-12086
p0027 N81-16051
NAS3-20072
p0059 A81-10706
p0027 N81-15006
NAS3-20073
p0088 A81-10707
p0139 N81-11953
p0024 N81-12088
NAS3-20084
p0047 N81-10112
NAS3-20091
p0030 A81-29987
NAS3-20096
p0073 N81-19395
NAS3-20102
p0073 A81-21675
p0072 N81-10301
p0072 N81-11314
NAS3-20380
p0088 A81-15796
NAS3-20382
p0092 N81-19479
p0093 N81-19480
p0093 N81-19481
p0093 N81-19482
p0093 N81-19483

CONTRACT NUMBER INDEX

NAS3-20392
 p0033 H81-12135
 p0033 H81-12136
 NAS3-20399
 p0043 A81-29552
 NAS3-20577
 p0048 A81-11336
 NAS3-20582
 p0129 H81-17846
 p0029 H81-17999
 NAS3-20584
 p0029 H81-19120
 NAS3-20585
 p0029 H81-19119
 NAS3-20591
 p0024 H81-12087
 NAS3-20599
 p0027 H81-15005
 NAS3-20602
 p0001 H81-17997
 NAS3-20630
 p0028 H81-17080
 NAS3-20631
 p0024 H81-12085
 NAS3-20632
 p0030 A81-30093
 NAS3-20643
 p0020 A81-30033
 p0029 H81-18056
 p0030 H81-22051
 NAS3-20646
 p0008 A81-30094
 p0026 H81-15002
 NAS3-20755
 p0029 H81-19117
 NAS3-20823
 p0113 A81-27089
 NAS3-20831
 p0059 H81-19277
 NAS3-20836
 p0007 A81-11628
 p0001 H81-22012
 NAS3-21013
 p0048 H81-19229
 NAS3-21020
 p0093 A81-14162
 NAS3-21030
 p0050 H81-16177
 NAS3-21037
 p0089 A81-22664
 NAS3-21042
 p0073 H81-22278
 NAS3-21052
 p0042 H81-20174
 NAS3-21250
 p0114 A81-27092
 p0112 H81-18495
 NAS3-21259
 p0027 H81-15004
 NAS3-21269
 p0030 A81-20767
 NAS3-21270
 p0114 A81-27094
 p0111 H81-17574
 NAS3-21272
 p0026 H81-13963
 NAS3-21280
 p0114 A81-27097
 NAS3-21288
 p0026 H81-15003
 NAS3-21345
 p0043 A81-20625
 p0044 A81-29566
 NAS3-21370
 p0033 H81-12135
 p0033 H81-12136
 p0033 H81-12137
 p0133 H81-12138
 NAS3-21389
 p0001 H81-17996
 NAS3-21391
 p0129 H81-15769
 NAS3-21593
 p0067 H81-12255
 NAS3-21603
 p0092 A81-29095
 NAS3-21607
 p0030 H81-20078
 NAS3-21608
 p0029 H81-17999

NAS3-21726
 p0113 A81-15027
 NAS3-21735
 p0077 H81-20383
 NAS3-21761
 p0073 H81-16389
 NAS3-21762
 p0043 A81-19937
 p0134 A81-29560
 p0043 A81-29561
 p0033 H81-27169
 NAS3-21836
 p0027 H81-17079
 NAS3-21837
 p0048 H81-21130
 NAS3-21844
 p0048 H81-19233
 NAS3-21924
 p0095 H81-33539
 NAS3-21940
 p0043 A81-18363
 p0042 H81-21122
 NAS3-21941
 p0042 H81-21125
 NAS3-21958
 p0088 H81-17437
 NAS3-21960
 p0043 A81-18363
 NAS3-21971
 p0020 A81-30057
 NAS3-21999
 p0027 H81-17078
 NAS3-22014
 p0007 H81-16976
 NAS3-22019
 p0065 H81-10169
 NAS3-22025
 p0065 H81-17263
 NAS3-22045
 p0067 H81-19316
 NAS3-22105-AE
 p0105 H81-25488
 NAS3-22117
 p0075 H81-18331
 NAS3-22160
 p0030 H81-22053
 NAS3-22186
 p0010 H81-19079
 NAS3-22216
 p0111 H81-16582
 p0111 H81-17569
 NAS3-22222
 p0111 H81-17568
 NAS3-22260
 p0137 H81-21212
 p0067 H81-21213
 NAS3-22264
 p0037 A81-42207
 NAS3-22270
 p0033 H81-21106
 NAS3-22475
 p0042 H81-22078
 NAS3-30292
 p0033 H81-12137
 NAS5-25759
 p0033 H81-12139
 NAS7-100
 p0107 H81-28524
 NAS8-32255
 p0098 H81-16584
 NAS8-32999
 p0043 A81-18363
 NAS8-33574
 p0043 A81-18363
 NAS9-14689
 p0094 H81-13425
 NAS9-15800
 p0094 H81-13426
 p0094 H81-13427
 p0094 H81-13428
 p0094 H81-13429
 p0095 H81-13430
 p0095 H81-13431
 p0095 H81-13432
 p0095 H81-13433
 MGR-15-005-162
 p0006 A81-21212
 MGR-15-005-191
 p0036 A81-21212
 MGR-43-003-015
 p0050 H81-16176

NSP C-727
 p0133 A81-20649
 p0133 A81-20698
 MSG-3073
 p0006 A81-29114
 MSG-3077
 p0085 A81-18647
 MSG-3119
 p0025 H81-12100
 MSG-3139
 p0091 H81-26492
 MSG-3185
 p0048 H81-12172
 MSG-3186
 p0133 H81-11833
 MSG-3188
 p0083 H81-26459
 MSG-3189
 p0005 A81-17952
 MSG-3252
 p0059 H81-22158
 MSG-3255
 p0133 H81-11834
 PROJ. AGRISTARS
 p0094 H81-13425
 p0094 H81-13426
 p0094 H81-13427
 p0094 H81-13428
 p0094 H81-13429
 p0095 H81-13430
 p0095 H81-13431
 p0095 H81-13432
 p0095 H81-13433
 SRI PROJ. 5413
 p0073 H81-19395
 W-31-109-38-4135
 p0113 H81-22467
 146-40-06
 p0095 H81-33539
 500-32-12
 p0119 H81-29782
 505-04
 p0013 H81-11039
 p0013 H81-12089
 505-04-42
 p0062 H81-21198
 505-04-82
 p0003 H81-14977
 505-05
 p0013 H81-11037
 505-05-92
 p0120 H81-25698
 505-23-6A
 p0018 H81-27095
 505-31-02
 p0130 H81-22837
 505-32
 p0015 H81-16050
 p0075 H81-21313
 505-32-2B
 p0004 H81-28053
 505-32-6A
 p0017 H81-25084
 505-32-02
 p0015 H81-16053
 p0126 H81-20831
 p0126 H81-26844
 p0126 H81-29922
 p0019 H81-30130
 p0126 H81-30905
 p0126 H81-30906
 p0126 H81-30907
 p0126 H81-31956
 p0127 H81-31957
 p0127 H81-32965
 p0127 H81-33947
 505-32-12
 p0074 H81-15239
 p0075 H81-16421
 p0127 H81-32964
 505-32-28
 p0074 H81-13301
 p0076 H81-29384
 505-32-32
 p0075 H81-16417
 p0016 H81-19121
 p0016 H81-24065
 p0017 H81-25083
 p0018 H81-26146
 505-32-42
 p0081 H81-16474
 p0081 H81-18391
 p0082 H81-19458
 p0053 H81-20245

p0062 H81-20275
 p0082 H81-20425
 p0053 H81-21193
 p0102 H81-23462
 p0054 H81-26235
 p0063 H81-27277
 p0084 H81-27526
 p0084 H81-29438
 p0085 H81-31550
 505-32-52
 p0001 H81-22012
 p0004 H81-25036
 p0005 H81-31129
 505-32-62
 p0012 H81-31190
 505-32-62
 p0017 H81-25080
 505-32-82
 p0071 H81-16388
 p0079 H81-16428
 p0066 H81-29246
 p0120 H81-33838
 505-32-92
 p0018 H81-27094
 505-33
 p0091 H81-11417
 505-33-02
 p0127 H81-32968
 505-33-12
 p0052 H81-16212
 p0045 H81-25148
 p0055 H81-27259
 p0056 H81-33273
 505-33-22
 p0091 H81-16492
 505-33-32
 p0045 H81-17174
 p0090 H81-28458
 p0046 H81-32194
 505-33-52
 p0091 H81-26492
 p0092 H81-33497
 505-33-62
 p0045 H81-16132
 p0046 H81-25149
 p0046 H81-25151
 505-33-82
 p0091 H81-16494
 505-41-22
 p0015 H81-16052
 p0015 H81-16054
 505-41-52
 p0003 H81-21028
 505-42-13-08
 p0003 H81-21027
 505-42-62
 p0017 H81-25079
 p0017 H81-25081
 p0004 H81-28054
 505-44-12
 p0009 H81-19078
 p0010 H81-19079
 505-44-22
 p0067 H81-19316
 p0117 H81-21685
 p0115 H81-30657
 505-53-12
 p0044 H81-16123
 p0054 H81-26234
 505-55
 p0040 H81-31282
 505-55-22
 p0049 H81-17189
 506-16
 p0080 H81-14322
 506-23-42
 p0033 H81-27169
 506-52-12
 p0038 H81-20176
 506-53
 p0060 H81-14079
 p0052 H81-16210
 506-53-12
 p0061 H81-19300
 p0082 H81-20424
 p0102 H81-23417
 p0102 H81-23418
 p0076 H81-24387
 p0046 H81-25150
 p0054 H81-25189
 p0130 H81-25779
 p0083 H81-27523
 p0055 H81-28233
 p0084 H81-28443
 p0077 H81-30391

CONTRACT NUMBER INDEX

ORIGINAL PAGE IS
OF POOR QUALITY

p0063 N81-32269
p0063 N81-33293
506-54-42
p0071 N81-20359
506-55-7A
p0132 N81-25808
506-55-7B
p0036 N81-32187
506-55-22
p0039 N81-20178
p0039 N81-21121
p0076 N81-24388
p0040 N81-30182
506-55-32
p0062 N81-22193
p0040 N81-26174
506-55-42
p0098 N81-17531
p0103 N81-23625
p0103 N81-23626
p0104 N81-23627
p0040 N81-26173
p0105 N81-27605
506-55-52
p0049 N81-25168
p0108 N81-30563
506-55-72
p0038 N81-20173
506-61-32
p0072 N81-30360
506-505-22
p0076 N81-30390
510-55-12
p0004 N81-31126
511-58-12
p0081 N81-17436
p0083 N81-26459
p0083 N81-27524
p0083 N81-27525
p0085 N81-33484
515-58-12
p0085 N81-29440
530-05-12
p0014 N81-13056
p0018 N81-26145
532-05-12
p0015 N81-16055
535-01-12
p0018 N81-28095
p0019 N81-31195
535-02-12
p0026 N81-13057
535-03-12
p0130 N81-22836
p0130 N81-22838
p0004 N81-27041
p0004 N81-27042
535-04-12
p0017 N81-25082
542-05-12
p0037 N81-20172
646-22-60
p0033 N81-12135
p0033 N81-12136
p0033 N81-12137
650-16-18
p0035 N81-30172
776-31-41
p0106 N81-27606
776-33-41
p0104 N81-24535
p0105 N81-24539
776-52-41
p0104 N81-24536
776-58-06
p0100 N81-22477
776-71-43
p0113 N81-22467
776-72-41
p0049 N81-13105
p0104 N81-24534
p0049 N81-31308
776-81-41
p0097 N81-14397
776-81-62
p0107 N81-28524
778-11-05
p0098 N81-16570
p0132 N81-24926
p0132 N81-24927
p0132 N81-32026

778-11-06
p0097 N81-14396
p0054 N81-25191
p0055 N81-27258
778-11-08
p0055 N81-28231
778-14-10
p0132 N81-30973
778-17-01
p0096 N81-13464
778-32-01
p0096 N81-13465
p0104 N81-24533
p0107 N81-30562
778-35-03
p0078 N81-22313
p0140 N81-24994
p0105 N81-25487
p0054 N81-26236
p0139 N81-32087
778-36-06
p0080 N81-13357
p0080 N81-15367
p0079 N81-16429
p0140 N81-18933
p0071 N81-21281
p0140 N81-26986
p0108 N81-31627
778-46-12
p0098 N81-16571
p0105 N81-25488
p0106 N81-28522
927-76-31
p0100 N81-21537
947-48-32
p0097 N81-14398

The diagram illustrates the relationship between a document symbol, a microfiche symbol, and their respective report, page, and accession numbers. At the top, two boxes are labeled "NASA DOCUMENT SYMBOL" and "MICROFICHE SYMBOL". Below them, a horizontal line contains the text "NASA-CR-159482 p0029 NS1-19117-0". The "NASA DOCUMENT SYMBOL" box is connected to the "p0029" part of the line. The "MICROFICHE SYMBOL" box is connected to the "NS1-19117-0" part of the line. Below the horizontal line, three boxes are labeled "REPORT NUMBER", "PAGE NUMBER", and "NASA ACCESSION NUMBER". The "REPORT NUMBER" box is connected to the "NASA-CR-159482" part of the line. The "PAGE NUMBER" box is connected to the "p0029" part of the line. The "NASA ACCESSION NUMBER" box is connected to the "NS1-19117-0" part of the line.

ATAA	PAPER	81-1509	p0037	81-42207**
ATAA	PAPER	81-1539	p0042	81-40934**
ATAA	PAPER	81-1564	p0007	81-42210**
ATAA	PAPER	81-1568	p0007	81-42211**
ATAA	PAPER	81-1587	p128	81-40962**
ATAA	PAPER	81-1588	p0022	81-40963**
ATAA	PAPER	81-1596	p0023	81-40971**
ATAA	PAPER	81-1599	p0023	81-40973**
ATAA	PAPER	81-1991	p129	81-49743**
ATAA	PAPER	81-1994	p128	81-48639**
ATAA	PAPER	81-1999	p129	81-49741**
ATAA	PAPER	81-2016	p128	81-48622**
ATAA	PAPER	81-2032	p0024	81-48628**
ATAA	PAPER	81-2049	p0023	81-48621**
ATAA	PAPER	81-2053	p0024	81-48635**
ATAA	81-0579		p0046	81-29411**
ATAA	81-0602		p0092	81-29465**

AIAA-81-1999 p0127 N81-32965*

ANL-K78-4135-1 p0113 181-22467*0

ASME	PAPER	80-C2/ARRO-9	p0077	AS1-18638**
ASME	PAPER	80-C2/LUB-13	p0068	AS1-18667**
ASME	PAPER	80-C2/LUB-14	p0085	AS1-18668**
ASME	PAPER	80-C2/LUB-35	p0085	AS1-18683**
ASME	PAPER	80-C2/LUB-49	p0089	AS1-18693**
ASME	PAPER	80-C2/LUB-53	p0086	AS1-18695**
ASME	PAPER	80-DRT-76	p0085	AS1-18647**
ASME	PAPER	80-GT-20	p0005	AS1-17952**
ASME	PAPER	80-BA/MC-2	p0127	AS1-21120**
ASME	PAPER	81-GT-24	p0020	AS1-29940**
ASME	PAPER	81-GT-40	p0020	AS1-29954**
ASME	PAPER	81-GT-44	p0086	AS1-29958**
ASME	PAPER	81-GT-63	p0057	AS1-29973**
ASME	PAPER	81-GT-70	p0006	AS1-29979**
ASME	PAPER	81-GT-75	p0077	AS1-29983**
ASME	PAPER	81-GT-79	p0030	AS1-29987**
ASME	PAPER	81-GT-89	p0077	AS1-29996**
ASME	PAPER	81-GT-91	p0077	AS1-29998**
ASME	PAPER	81-GT-93	p0079	AS1-30000**
ASME	PAPER	81-GT-56	p0001	AS1-30003**
ASME	PAPER	81-GT-99	p0020	AS1-30006**
ASME	PAPER	81-GT-108	p0087	AS1-30013**
ASME	PAPER	81-GT-109	p0089	AS1-30014**
ASME	PAPER	81-GT-125	p0087	AS1-30029**
ASME	PAPER	81-GT-129	p0020	AS1-30033**
ASME	PAPER	81-GT-157	p0067	AS1-30056**
ASME	PAPER	81-GT-158	p0020	AS1-30057**
ASME	PAPER	81-GT-161	p0089	AS1-30060**
ASME	PAPER	81-GT-169	p0006	AS1-30068**
ASME	PAPER	81-GT-184	p0020	AS1-30078**
ASME	PAPER	81-GT-203	p0030	AS1-30093**
ASME	PAPER	81-GT-204	p0008	AS1-30094**

AVRADCON-TB-80-C-13	p0013	881-11038**
AVRADCON-TB-80-C-15	p0051	881-12210**
AVRADCON-TB-80-C-16	p0082	881-20023**
AVRADCON-TB-80-C-17	p0016	881-20076**
AVRADCON-TB-80-C-19	p0053	881-20245**
AVRADCON-TB-80-C-20	p0004	881-28053**

REPORT/ACCHSSICN NUMBER INDEX

AVRADCON-TR-81-C-3 p0081 N81-17436**
 AVRADCON-TR-81-C-6 p0082 N81-21158**
 AVRADCON-TR-81-C-10 p0017 N81-25081**
 AVRADCON-TR-81-C-13 p0083 N81-26459**
 AVRADCON-TR-81-C-14 p0083 N81-27525**
 AVRADCON-TR-81-C-14 p0084 N81-28444**
 AVRADCON-TR-81-C-15 p0083 N81-27524**
 AVRADCON-TR-81-C-16 p0054 N81-26235**
 AVRADCON-TR-81-C-24 p0018 N81-27095**

 AVRADCON-81-C-17 p0084 N81-29438**

 BAB-ER-14967-EXHC-SUBH p0137 N81-21212**

 BAC-ER-14967 p0067 N81-21213**

 BEFT-FB-T-79-107 p0072 N81-14227 *

 CHL-80-1 p0048 N81-12172**

 CTR-0746-80002 p0140 N81-13803**

 DOE/JPL-1060-45 p0107 N81-28524**
 DOE/NASA/022-2 p0088 N81-13359**
 DOE/NASA/0008-12 p0141 N81-22582**
 DOE/NASA/0030-80/5 p0109 N81-10517**
 DOE/NASA/0032-80/8 p0139 N81-11952**
 DOE/NASA/0049-80/2 p0110 N81-14391**
 DOE/NASA/0067-79/2 p0113 N81-21547**
 DOE/NASA/0067-79/3 p0113 N81-21536**
 DOE/NASA/0067-79/6 p0113 N81-22475**
 DOE/NASA/0089-80/1 p0112 N81-21533**
 DOE/NASA/0092-80/1 p0140 N81-18935**
 DOE/NASA/0106-1 p0140 N81-20958**
 DOE/NASA/0107-1 p0110 N81-13466**
 DOE/NASA/0107-2 p0110 N81-13467**
 DOE/NASA/0119-81/1 p0088 N81-21355**
 DOE/NASA/0121-80/1-VOL-1 p0110 N81-15461**
 DOE/NASA/0121-80/1-VOL-2 p0110 N81-15462**
 DOE/NASA/0124-5 p0088 N81-15366**
 DOE/NASA/0137-1 p0111 N81-16583**
 DOE/NASA/0139-1 p0111 N81-18491**
 DOE/NASA/0161-5 p0112 N81-18494**
 DOE/NASA/0161-6 p0112 N81-19573**
 DOE/NASA/0176-80/3 p0111 N81-17527**
 DOE/NASA/0176-80/4 p0112 N81-18496**
 DOE/NASA/0179-1 p0109 N81-12546**
 DOE/NASA/0208-1 p0113 N81-22473**
 DOE/NASA/0226-1 p0078 N81-22313**
 DOE/NASA/1011-33 p0097 N81-14398**
 DOE/NASA/1011-34 p0004 N81-28053**
 DOE/NASA/1028-27 p0096 N81-11448**
 DOE/NASA/1028-25 p0091 N81-16494**
 DOE/NASA/1028-31 p0100 N81-22472**
 DOE/NASA/1040-18 p0051 N81-15068**
 DOE/NASA/1044-8 p0079 N81-16429**
 DOE/NASA/1044-10 p0140 N81-18933**
 DOE/NASA/1060-4 p0097 N81-14397**
 DOE/NASA/1062-0 p0132 N81-30973**
 DOE/NASA/1062-7 p0131 N81-16900**
 DOE/NASA/1062-8 p0132 N81-19920**
 DOE/NASA/2593-20 p0051 N81-15069**
 DOE/NASA/2593-22 p0052 N81-16211**
 DOE/NASA/2593-23 p0055 N81-27258**
 DOE/NASA/2593-26 p0054 N81-25191**
 DOE/NASA/2593-26 p0055 N81-28231**
 DOE/NASA/2593-27 p0101 N81-23243**
 DOE/NASA/3186-1 p0133 N81-11833**
 DOE/NASA/3255-1 p0133 N81-11834**
 DOE/NASA/4936-80/1 p0140 N81-13803**
 DOE/NASA/6229-1 p0112 N81-18497**
 DOE/NASA/9698-2 p0065 N81-14082**
 DOE/NASA/10350-19 p0057 N81-14399**
 DOE/NASA/10350-21 p0097 N81-14396**
 DOE/NASA/10444-12 p0080 N81-13357**
 DOE/NASA/10769-10 p0132 N81-32026**
 DOE/NASA/10769-13 p0098 N81-16570**
 DOE/NASA/10769-14 p0132 N81-24927**
 DOE/NASA/10769-15 p0103 N81-23610**
 DOE/NASA/10769-16 p0100 N81-22476**
 DOE/NASA/10769-17 p0103 N81-23611**
 DOE/NASA/10769-18 p0132 N81-24926**
 DOE/NASA/11272-2 p0056 N81-13464**
 DOE/NASA/12726-6 p0049 N81-13105**
 DOE/NASA/12726-7 p0106 N81-28519**
 DOE/NASA/12726-8 p0104 N81-24534**
 DOE/NASA/12726-10 p0049 N81-31308**
 DOE/NASA/12726-12 p0108 N81-33601**
 DOE/NASA/12726-13 p0107 N81-30522**

DOE/NASA/12726-14 p0108 N81-32608**
 DOE/NASA/20305-5 p0106 N81-27606**
 DOE/NASA/20305-6 p0090 N81-33492**
 DOE/NASA/20320-30 p0104 N81-24535**
 DOE/NASA/20320-31 p0105 N81-24539**
 DOE/NASA/20320-32 p0107 N81-29528**
 DOE/NASA/20366-1 p0100 N81-21537**
 DOE/NASA/20485-7 p0104 N81-24536**
 DOE/NASA/20485-8 p0100 N81-22477**
 DOE/NASA/20485-9 p0106 N81-28520**
 DOE/NASA/20485-10 p0094 N81-28517**
 DOE/NASA/51040-19 p0096 N81-13465**
 DOE/NASA/51040-21 p0075 N81-15241**
 DOE/NASA/51040-22 p0107 N81-30562**
 DOE/NASA/51040-23 p0103 N81-23609**
 DOE/NASA/51040-24 p0105 N81-27604**
 DOE/NASA/51040-25 p0140 N81-24994**
 DOE/NASA/51040-26 p0104 N81-24533**
 DOE/NASA/51040-28 p0105 N81-25487**
 DOE/NASA/51040-29 p0054 N81-26236**
 DOE/NASA/51040-31 p0139 N81-32087**
 DOE/NASA/51044-11 p0096 N81-11449**
 DOE/NASA/51044-13 p0080 N81-15367**
 DOE/NASA/51044-14 p0097 N81-15464**
 DOE/NASA/51044-15 p0097 N81-15465**
 DOE/NASA/51044-16 p0103 N81-23608**
 DOE/NASA/51044-17 p0082 N81-19459**
 DOE/NASA/51044-18 p0071 N81-21281**
 DOE/NASA/51044-19 p0106 N81-28523**
 DOE/NASA/51044-20 p0140 N81-26986**
 DOE/NASA/51044-21 p0108 N81-31627**
 DOE/NASA/51044-23 p0085 N81-33484**

 D180-26200-1 p0111 N81-16582**
 D2536-941001 p0092 N81-19479**
 D2536-941002 p0093 N81-19480**
 D2536-941003 p0093 N81-19481**
 D2536-941004 p0093 N81-19482**
 D2536-941005 p0093 N81-19483**

 E-PC-002 p0112 N81-21533**

 E-070 p0080 N81-14322**
 E-128 p0004 N81-22017**
 E-209 p0081 N81-18391**
 E-209 p0081 N81-18392**
 E-209 p0085 N81-31550**
 E-216 p0076 N81-28389**
 E-326 p0051 N81-11178**
 E-326 p0052 N81-16210**
 E-396 p0013 N81-11039**
 E-410-1 p0061 N81-17264**
 E-410-2 p0062 N81-20275**
 E-414 p0060 N81-11214**
 E-417 p0013 N81-12089**
 E-439 p0091 N81-11417**
 E-449 p0053 N81-20245**
 E-455 p0013 N81-11038**
 E-455 p0071 N81-11315**
 E-461 p0015 N81-16050**
 E-468 p0117 N81-21685**
 E-469 p0098 N81-17531**
 E-472 p0053 N81-19273**
 E-473 p0081 N81-16474**
 E-475 p0123 N81-10778**
 E-475 p0060 N81-14079**
 E-477 p0014 N81-12090**
 E-479 p0076 N81-24387**
 E-480 p0053 N81-21193**
 E-481 p0116 N81-13568**
 E-484 p0082 N81-20423**
 E-487 p0076 N81-24388**
 E-489 p0142 N81-12978**
 E-495 p0102 N81-23486**
 E-505 p0080 N81-11394**
 E-509 p0016 N81-19121**
 E-515 p0082 N81-19858**
 E-525 p0060 N81-12266**
 E-536 p0038 N81-20173**
 E-537 p0075 N81-16417**
 E-538 p0051 N81-12210**
 E-540 p0016 N81-20076**
 E-542 p0061 N81-12300**
 E-543 p0051 N81-11111**
 E-545 p0140 N81-18933**
 E-546 p0069 N81-10240**
 E-548 p0051 N81-15068**
 E-553 p0038 N81-20176**
 E-558 p0125 N81-15768**

E-561	p0013	N81-1006700	E-712	p0035	N81-202310
E-563	p0016	N81-2406500	E-715	p0054	N81-2623500
E-567	p0096	N81-1144800	E-716	p0061	N81-1726500
E-568	p0003	N81-1497900	E-717	p0106	N81-2852300
E-569	p0125	N81-1080700	E-718	p0055	N81-2725800
E-570	p0045	N81-1217100	E-720	p0102	N81-2346200
E-572	p0004	N81-2805300	E-723	p0105	N81-2548800
E-575	p0143	N81-2906300	E-725	p0052	N81-1816500
E-577	p0072	N81-2835200	E-726	p0084	N81-2943900
E-580	p0091	N81-1141200	E-727	p0037	N81-2017200
E-582	p0071	N81-2035900	E-728	p0083	N81-2752500
E-583	p0005	N81-3112900	E-729	p0038	N81-1921900
E-586	p0069	N81-1024100	E-730	p0101	N81-2318800
E-587	p0063	N81-3329300	E-733	p0127	N81-3394700
E-588	p0080	N81-1335700	E-734	p0045	N81-1717400
E-589	p0069	N81-1023900	E-735	p0039	N81-2112100
E-590	p0005	N81-3112800	E-736	p0009	N81-1907800
E-591	p0060	N81-1316600	E-738	p0108	N81-3360100
E-594	p0056	N81-1346300	E-739	p0107	N81-3052200
E-598	p0037	N81-1168800	E-740	p0130	N81-2577900
E-599	p0096	N81-1144900	E-742	p0062	N81-2119800
E-603	p0040	N81-3128200	E-744	p0101	N81-2324300
E-604	p0080	N81-1139500	E-745	p0125	N81-1987500
E-605	p0049	N81-1310600	E-746	p0103	N81-2360800
E-607	p0125	N81-1176900	E-747	p0104	N81-2453600
E-609	p0098	N81-1657100	E-748	p0101	N81-2324500
E-612	p0003	N81-1497800	E-750	p0075	N81-2131000
E-613	p0125	N81-1282100	E-751	p0063	N81-3136600
E-614	p0097	N81-1439900	E-752	p0082	N81-1945900
E-615	p0120	N81-3383800	E-753	p0104	N81-2453500
E-616	p0125	N81-1177000	E-755	p0038	N81-1922000
E-617	p0066	N81-2428300	E-756	p0044	N81-2112900
E-623	p0055	N81-2920500	E-759	p0038	N81-1922100
E-624	p0045	N81-1613200	E-763	p0046	N81-2514900
E-625	p0049	N81-1718900	E-764	p0053	N81-2216100
E-627	p0076	N81-2938400	E-765	p0039	N81-2017700
E-628	p0074	N81-1330100	E-767	p0101	N81-2320500
E-629	p0066	N81-2924600	E-768	p0130	N81-2283600
E-630	p0081	N81-1743600	E-771	p0082	N81-2331700
E-631	p0074	N81-1235800	E-772	p0039	N81-2017900
E-632	p0061	N81-1726600	E-773	p0084	N81-2943800
E-633	p0091	N81-1244600	E-778	p0082	N81-2042400
E-637	p0124	N81-1281700	E-782	p0045	N81-2117400
E-640	p0033	N81-1307900	E-786	p0102	N81-2343500
E-641	p0044	N81-1612300	E-787	p0121	N81-2180300
E-643	p0072	N81-3036000	E-791	p0130	N81-2283900
E-644	p0049	N81-1310500	E-792	p0105	N81-2760400
E-645	p0014	N81-1305600	E-793	p0101	N81-2324400
E-647	p0051	N81-1506900	E-794	p0039	N81-2208400
E-650	p0081	N81-1742500	E-795	p0102	N81-2341700
E-651	p0003	N81-1497700	E-796	p0102	N81-2341800
E-656	p0075	N81-2131300	E-797	p0126	N81-2083100
E-657	p0097	N81-1546400	E-798	p0100	N81-2247200
E-658	p0074	N81-1330200	E-799	p0003	N81-2102800
E-659	p0096	N81-1346400	E-802	p0039	N81-2017800
E-661	p0097	N81-1439600	E-803	p0053	N81-2117300
E-662	p0037	N81-1611900	E-808	p0100	N81-2153700
E-663	p0080	N81-1335800	E-809	p0100	N81-2247700
E-664	p0052	N81-1621200	E-813	p0039	N81-2018000
E-666	p0016	N81-2406300	E-814	p0103	N81-2360900
E-669	p0080	N81-1536700	E-815	p0016	N81-2205600
E-673	p0016	N81-2107800	E-818	p0062	N81-2219300
E-674	p0015	N81-1605300	E-819	p0103	N81-2361000
E-675	p0097	N81-1439700	E-820	p0049	N81-2516800
E-676	p0017	N81-3056200	E-821	p0130	N81-2283800
E-677	p0097	N81-1439800	E-822	p0017	N81-2508400
E-679	p0115	N81-3065700	E-823	p0071	N81-2128100
E-680	p0015	N81-1605400	E-824	p0017	N81-2507900
E-681	p0015	N81-1605500	E-825	p0103	N81-2349000
E-684	p0097	N81-1546500	E-826	p0100	N81-2247800
E-685	p0091	N81-1649200	E-827	p0132	N81-2492700
E-686	p0015	N81-1605200	E-831	p0106	N81-2852000
E-688	p0098	N81-1657000	E-832	p0068	N81-2526300
E-689	p0074	N81-1524000	E-835	p0040	N81-2617400
E-691	p0037	N81-1712700	E-836	p0100	N81-2247600
E-693	p0009	N81-1602100	E-837	p0045	N81-2514800
E-695	p0038	N81-1922200	E-838	p0054	N81-2519100
E-696	p0074	N81-1523900	E-839	p0140	N81-2698600
E-697	p0075	N81-1642100	E-841	p0046	N81-2515100
E-698	p0082	N81-2135600	E-842	p0104	N81-2362700
E-699	p0091	N81-1649400	E-845	p0019	N81-3119600
E-700	p0092	N81-1748000	E-846	p0046	N81-2515000
E-701	p0063	N81-2728200	E-847	p0101	N81-2308500
E-702	p0132	N81-1992000	E-848	p0105	N81-2453900
E-705	p0053	N81-1927800	E-849	p0103	N81-2361100
E-706	p0079	N81-1642800	E-851	p0066	N81-2523200
E-707	p0075	N81-2131400	E-852	p0103	N81-2362500
E-708	p0071	N81-1638800	E-853	p0055	N81-2823300
E-710	p0102	N81-2327500	E-854	p0104	N81-2453400

Z-855	p0018	N81-2614500	ZNC-18	p0113	N81-2153600
Z-856	p0103	N81-2362600			
Z-857	p0076	N81-3039000			
Z-859	p0126	N81-2684400	ZN-LO-00701	p0095	N81-1343300
Z-861	p0004	N81-2503600	ZN-LO-00702	p0094	N81-1342800
Z-863	p0130	N81-2283700	ZN-LO-00703	p0094	N81-1342900
Z-865	p0083	N81-2752400	ZN-LO-00705	p0095	N81-1343000
Z-867	p0140	N81-2499400			
Z-868	p0132	N81-2500800	Z81-10044	p0095	N81-3353900
Z-869	p0017	N81-2508100	Z81-10069	p0094	N81-1342500
Z-870	p0040	N81-3018200	Z81-10070	p0094	N81-1342600
Z-872	p0132	N81-2492600	Z81-10071	p0094	N81-1342700
Z-873	p0083	N81-2645900	Z81-10072	p0094	N81-1342800
Z-877	p0104	N81-2453300	Z81-10073	p0094	N81-1342900
Z-879	p0055	N81-2725900	Z81-10074	p0095	N81-1343000
Z-880	p0017	N81-2508100	Z81-10075	p0095	N81-1343100
Z-881	p0053	N81-2727700	Z81-10076	p0095	N81-1343200
Z-883	p0046	N81-3219400	Z81-10077	p0095	N81-1343300
Z-884	p0054	N81-2518900	Z833	p0054	N81-2623400
Z-886	p0091	N81-2649200			
Z-887	p0054	N81-2623600	FAA-ZX-43	p0116	N81-1356800
Z-889	p0100	N81-2565800	FAA-ZX-81-1	p0117	N81-2168500
Z-890	p0105	N81-2548700			
Z-891	p0118	N81-2614600	PC-LO-00423	p0095	N81-1343200
Z-893	p0108	N81-3056300			
Z-894	p0084	N81-2752600	FR-1	p0033	N81-1213900
Z-895	p0017	N81-2508200	FR-80-42/AS	p0065	N81-1726300
Z-898	p0040	N81-2617300	FR-40-76-952	p0073	N81-2227800
Z-900	p0083	N81-2752300	FR-13983	p0030	N81-2007800
Z-902	p0139	N81-3208700			
Z-904	p0018	N81-2809500	GR-4	p0112	N81-1849600
Z-905	p0084	N81-2844400			
Z-906	p0106	N81-2852200	IAP PAPER 80-P-253	p0043	N81-1836300
Z-907	p0084	N81-2844300			
Z-910	p0090	N81-2845800	ISSN-0340-7608	p0072	N81-1422700
Z-911	p0017	N81-2508000			
Z-914	p0107	N81-2952800	JPL-PUB-81-39	p0107	N81-2852400
Z-917	p0112	N81-3119000			
Z-918	p0004	N81-3112600	JSC-16339	p0095	N81-1343200
Z-922	p0105	N81-2760500	JSC-16373	p0095	N81-1343300
Z-923	p0018	N81-2709400	JSC-16374	p0094	N81-1342800
Z-926	p0119	N81-2978200	JSC-16375	p0094	N81-1342900
Z-927	p0126	N81-2952200	JSC-16377	p0094	N81-1342700
Z-929	p0085	N81-2944000	JSC-16382	p0095	N81-1343000
Z-934	p0055	N81-2920600	JSC-16813	p0095	N81-1343100
Z-938	p0018	N81-2709500	JSC-16814	p0094	N81-1342600
Z-940	p0126	N81-3090500			
Z-941	p0004	N81-2805400	KU-PRL-464-2	p0011	N81-2506500
Z-942	p0104	N81-2704200			
Z-943	p0004	N81-2704100	LENSCO-14386	p0095	N81-1343200
Z-944	p0108	N81-3162700	LENSCO-1-033	p0095	N81-1343100
Z-950	p0132	N81-3097300	LENSCO-15034	p0094	N81-1342600
Z-954	p0049	N81-3130800	LENSCO-15115	p0094	N81-1342700
Z-956	p0132	N81-3202600	LENSCO-15325	p0095	N81-1343300
Z-957	p0066	N81-3138000	LENSCO-15326	p0094	N81-1342800
Z-958	p0092	N81-3349700	LENSCO-15327	p0094	N81-1342900
Z-963	p0077	N81-3039100	LENSCO-15357	p0095	N81-1343000
Z-964	p0126	N81-3090600			
Z-965	p0106	N81-2766600	LYC-78-36	p0029	N81-1912000
Z-966	p0035	N81-3017200			
Z-968	p0056	N81-3327300	ME-MG80-1	p0133	N81-1183300
Z-970	p0126	N81-3090700			
Z-971	p0126	N81-3195600	NI-20ASE144QT9	p0133	N81-1195200
Z-973	p0036	N81-3218700	NI-80T825	p0140	N81-1893500
Z-977	p0127	N81-3195700	NI-81T83	p0088	N81-2135500
Z-979	p0019	N81-3119500			
Z-980	p0127	N81-3296800	NI-8164	p0070	N81-1024200
Z-983	p0085	N81-3348400			
Z-984	p0019	N81-3013000	NA-81-110	p0010	N81-1907900
Z-994	p0127	N81-3296400			
Z-998	p0063	N81-3226900	NASA-CASE-LEW-12081-3	p0066	N81-1410300
Z-1014	p0127	N81-3296500	NASA-CASE-LEW-12119-2	p0083	N81-2644700
Z-1015	p0090	N81-3349200	NASA-CASE-LEW-12253-1	p0076	N81-2231000
Z-1019	p0108	N81-3260800	NASA-CASE-LEW-12441-3	p0104	N81-2451900
Z-9356-1	p0003	N81-1301900	NASA-CASE-LEW-12443-1	p0099	N81-1956100
Z-9356-3	p0096	N81-1346500	NASA-CASE-LEW-12445-1	p0083	N81-2236000
Z-9356-7	p0075	N81-1524100	NASA-CASE-LEW-12493-1	p0045	N81-1717000
Z-9449-3	p0137	N81-1794300	NASA-CASE-LEW-12493-2	p0046	N81-2617900
Z-9449-4	p0137	N81-1794200	NASA-CASE-LEW-12590-1	p0049	N81-1924500
Z-9449-5	p0137	N81-2902600	NASA-CASE-LEW-12590-2	p0015	N81-1911600
Z-9542	p0013	N81-1103700	NASA-CASE-LEW-12806-2	p0096	N81-1254200
Z-9715	p0060	N81-1017000	NASA-CASE-LEW-12892-1	p0105	N81-2759800
			NASA-CASE-LEW-12907-2	p0015	N81-1911500
ZPB-1110	p0110	N81-1439100	NASA-CASE-LEW-12918-1	p0104	N81-2452100
EDU-10156	p0029	N81-1911800	NASA-CASE-LEW-12919-1	p0046	N81-2719800
EDR-10361-VOL-2	p0007	N81-1457600	NASA-CASE-LEW-12933-1	p0061	N81-1929600
			NASA-CASE-LEW-12941-1	p0068	N81-1632900
			NASA-CASE-LEW-12982-1	p0081	N81-1945500
BRC-LIB-80173	p0068	N81-1536600	NASA-CASE-LEW-12990-1	p0018	N81-2912900

NASA-CASE-LEW-12991-1	F0083	881-244420	NASA-CR-165141	p0027	881-1500400
NASA-CASE-LEW-13038-1	p0054	881-251800	NASA-CR-165143	p0109	881-1254600
NASA-CASE-LEW-13101-2	p0044	881-291600	NASA-CR-165144	p0112	881-2153300
NASA-CASE-LEW-13102-1	F0107	881-2953100	NASA-CR-165145	p0033	881-1213900
NASA-CASE-LEW-13107-1	F0118	881-2778000	NASA-CR-165147	p0065	881-1016900
NASA-CASE-LEW-13120-1	F0068	881-1632700	NASA-CR-165152-VOL-1	p0110	881-1546100
NASA-CASE-LEW-13131-1	F0054	881-2423000	NASA-CR-165152-VOL-2	p0110	881-1546200
NASA-CASE-LEW-13132-1	p0106	881-2761600	NASA-CR-165155	p0070	881-1024200
NASA-CASE-LEW-13135-2	F0062	881-242570	NASA-CR-165157	p0026	881-1500200
NASA-CASE-LEW-13148-2	p0107	881-2952400	NASA-CR-165158	p0088	881-1335900
NASA-CASE-LEW-13171-1	p0100	881-2246600	NASA-CR-165159	p0073	881-1638900
NASA-CASE-LEW-13174-1	F0074	881-1236300	NASA-CR-165162	p0026	881-1396300
NASA-CASE-LEW-13201-1	F0014	881-1499900	NASA-CR-165165	p0067	881-1225500
NASA-CASE-LEW-13226-1	F0060	881-1726000	NASA-CR-165166	p0007	881-1497600
NASA-CASE-LEW-13246-1	F0049	881-1620300	NASA-CR-165167	p0110	881-1546300
NASA-CASE-LEW-13269-1	p0062	881-2219000	NASA-CR-165169-VOL-1	p0033	881-1213500
NASA-CASE-LEW-13286-1	F0105	881-2759700	NASA-CR-165169-VOL-2	p0033	881-1213600
NASA-CASE-LEW-13339-1	p0051	881-1221100	NASA-CR-165169-VOL-3	p0033	881-1213700
NASA-CASE-LEW-13359-1	p0062	881-2426500	NASA-CR-165169-VOL-4	p0133	881-1213800
NASA-CASE-LEW-13400-1	PLC98	881-1652800	NASA-CR-165170	p0140	881-2095800
NASA-CASE-LEW-13401-1	PLC98	881-1652900	NASA-CR-165172	p0072	881-1030100
NASA-CASE-LEW-13429-1	p0071	881-1638400	NASA-CR-165173	p0072	881-1131400
NASA-CASE-LEW-13504-1	F0063	881-2727900	NASA-CR-165176	p0139	881-1195300
NASA-CASE-LEW-13556-1	p0106	881-2761500	NASA-CR-165177	p0050	881-1617700
NASA-CASE-LEW-13570-1	F0071	881-2434800	NASA-CR-165179	p0111	881-1752700
NASA-CASE-LEW-23169-2	p0052	881-1620900	NASA-CR-165180	p0065	881-1726300
NASA-CR-2137	p0014	881-1209000	NASA-CR-165181	p0088	881-1536600
NASA-CR-2149	p0142	881-1257800	NASA-CR-165184	p0048	881-1922900
NASA-CR-2159	F0037	881-1611900	NASA-CR-165186	p0133	881-1183300
NASA-CR-2169	PLC98	881-1753100	NASA-CR-165187	p0133	881-1183400
NASA-CR-2178	p0016	881-2406300	NASA-CR-165188	p0129	881-1576900
NASA-CR-2190	p0019	881-3119600	NASA-CR-165189	p0112	881-1849400
NASA-CR-3388	F0007	881-1697600	NASA-CR-165190	p0112	881-1957300
NASA-CR-3389	F0077	881-2038300	NASA-CR-165195	p0048	881-1923300
NASA-CR-3425	F0001	881-2201200	NASA-CR-165200	p0026	881-1500300
NASA-CR-135386	F0029	881-1911900	NASA-CR-165201	p0059	881-1927700
NASA-CR-159426	p0029	881-1912000	NASA-CR-165210	p0088	881-1743700
NASA-CR-159482	p0029	881-1911700	NASA-CR-165217	p0030	881-2205300
NASA-CR-159498	F0027	881-1605100	NASA-CR-165220	p0028	881-1708000
NASA-CR-159499	p0024	881-1206600	NASA-CR-165221	p0112	881-1849700
NASA-CR-159501	F0073	881-2227800	NASA-CR-165223	p0111	881-1656300
NASA-CR-159561	F0113	881-2246700	NASA-CR-165225	p0027	881-1500600
NASA-CR-159562	p0024	881-1203800	NASA-CR-165228	p0048	881-2113000
NASA-CR-159570	PLC73	881-1939500	NASA-CR-165233	p0042	881-2017400
NASA-CR-159583	F0029	881-1865600	NASA-CR-165237	p0088	881-1743400
NASA-CR-159584	p0030	881-2205100	NASA-CR-165238	p0033	881-2110600
NASA-CR-159643	p0050	881-1617600	NASA-CR-165240	p0111	881-1658200
NASA-CR-159678	p0065	881-1408200	NASA-CR-165244	p0027	881-1707800
NASA-CR-159690	F0110	881-1346600	NASA-CR-165245	p0112	881-1849600
NASA-CR-159720	p0047	881-1011200	NASA-CR-165250	p0027	881-1707900
NASA-CR-159728	p0092	881-1947900	NASA-CR-165258	p0067	881-1931600
NASA-CR-159763	PLC98	881-1051700	NASA-CR-165261	p0030	881-2007800
NASA-CR-159772	F0140	881-1953500	NASA-CR-165262	p0078	881-2231300
NASA-CR-159818	p0026	881-1305700	NASA-CR-165271	p0088	881-2135500
NASA-CR-159819-VOL-1	F0028	881-1708100	NASA-CR-165272	p0112	881-1849500
NASA-CR-159819-VOL-2-BK-1	p0028	881-1708200	NASA-CR-165275	p0042	881-2112500
NASA-CR-159819-VOL-2-BK-2	F0028	881-1708300	NASA-CR-165276	p0042	881-2112200
NASA-CR-159819-VOL-2-BK-3	F0028	881-1708400	NASA-CR-165279	p0067	881-2121300
NASA-CR-159819-VOL-3-BK-1	p0028	881-1708500	NASA-CR-165279-EXC-5088	p0137	881-2121700
NASA-CR-159819-VOL-3-BK-2	F0028	881-1706600	NASA-CR-165290	p0100	881-1907900
NASA-CR-159823	F0093	881-1948000	NASA-CR-165292	p0059	881-2028400
NASA-CR-159824	p0093	881-1948100	NASA-CR-165311	p0113	881-2247300
NASA-CR-159825	F0093	881-1948200	NASA-CR-165312	p0042	881-2207800
NASA-CR-159826	F0093	881-1948300	NASA-CR-165316	p0113	881-2154700
NASA-CR-159840	F0140	881-1380300	NASA-CR-165317	p0113	881-2153600
NASA-CR-159853	p0110	881-1346700	NASA-CR-165318	p0113	881-2247500
NASA-CR-159865	p0029	881-1911800	NASA-CR-165335	p0095	881-3353900
NASA-CR-159867	p0024	881-1208500	NASA-CR-165348	p0033	881-2716900
NASA-CR-159869	F0129	881-1784600	NASA-TN-79162	p0137	881-1794300
NASA-CR-159872	p0111	881-1849100	NASA-TN-81476	p0069	881-1023900
NASA-CR-159879	p0024	881-1208700	NASA-TN-81524	p0123	881-1077800
NASA-CR-159880	F0110	881-1439100	NASA-TN-81525	p0137	881-1794200
NASA-CR-159884	F0048	881-1217200	NASA-TN-81528	p0116	881-1356800
NASA-CR-159839	F0027	881-1500500	NASA-TN-81540	p0051	881-1117800
NASA-CR-160865	F0094	881-1342700	NASA-TN-81545	p0079	881-1642900
NASA-CR-160866	F0094	881-1342800	NASA-TN-81547	p0060	881-1139400
NASA-CR-160867	F0094	881-1342600	NASA-TN-81563	p0060	881-1222600
NASA-CR-160868	PLC95	881-1343100	NASA-TN-81570	p0051	881-1221000
NASA-CR-160869	PLC95	881-1343000	NASA-TN-81573	p0051	881-1111100
NASA-CR-160870	p0094	881-1342900	NASA-TN-81575	p0140	881-1893300
NASA-CR-160871	PLC95	881-1343300	NASA-TN-81576	p0069	881-1024000
NASA-CR-160873	PLC95	881-1343200	NASA-TN-81578	p0051	881-1506800
NASA-CR-160881	p0094	881-1342500	NASA-TN-81583	p0125	881-1576800
NASA-CR-164222	F0030	881-2245200	NASA-TN-81584	p0113	881-1006700
NASA-CR-165126	F0059	881-2215800	NASA-TN-81588	p0096	881-1144800
NASA-CR-165134	p0139	881-1195200	NASA-TN-81589	p0003	881-1497900
NASA-CR-165139	F0141	881-2258200	NASA-TN-81590	p0125	881-1010700
				NASA-TN-81591	p0045	881-1217100

NASA-TN-81592	p0102	N81-2343500	NASA-TN-81711	p0082	N81-2135600
NASA-TN-81594	p0057	N81-1439600	NASA-TN-81712	p0125	N81-1987500
NASA-TN-81595	p0060	N81-1017000	NASA-TN-81713	p0103	N81-2360800
NASA-TN-81596	p0074	N81-1330200	NASA-TN-81714	p0104	N81-2453600
NASA-TN-81597	p0091	N81-1141200	NASA-TN-81715	p0101	N81-2324500
NASA-TN-81600	p0069	N81-1024100	NASA-TN-81717	p0075	N81-2131000
NASA-TN-81601	p0061	N81-1726500	NASA-TN-81718	p0082	N81-1945900
NASA-TN-81602	p0060	N81-1316600	NASA-TN-81719	p0104	N81-2453500
NASA-TN-81603	p0056	N81-1346300	NASA-TN-81720	p0038	N81-1922000
NASA-TN-81605	p0037	N81-1168800	NASA-TN-81721	p0044	N81-2112900
NASA-TN-81606	p0096	N81-1144900	NASA-TN-81722	p0038	N81-1922100
NASA-TN-81608	p0080	N81-1139500	NASA-TN-81724	p0053	N81-2216100
NASA-TN-81609	p0049	N81-1310600	NASA-TN-81725	p0039	N81-2017700
NASA-TN-81610	p0125	N81-1176900	NASA-TN-81726	p0082	N81-2042000
NASA-TN-81611	p0098	N81-1657100	NASA-TN-81727	p0130	N81-2283600
NASA-TN-81612	p0097	N81-1439900	NASA-TN-81728	p0082	N81-2231700
NASA-TN-81613	p0003	N81-1497800	NASA-TN-81729	p0039	N81-2017900
NASA-TN-81614	p0125	N81-1282100	NASA-TN-81731	p0121	N81-2180300
NASA-TN-81615	p0125	N81-1177000	NASA-TN-81732	p0062	N81-2119900
NASA-TN-81617	p0055	N81-2920500	NASA-TN-81734	p0039	N81-2017800
NASA-TN-81618	p0045	N81-1613200	NASA-TN-81735	p0053	N81-2117300
NASA-TN-81619	p0049	N81-1718900	NASA-TN-81737	p0100	N81-2153700
NASA-TN-81620	p0074	N81-1330100	NASA-TN-81738	p0100	N81-2247700
NASA-TN-81621	p0074	N81-1235800	NASA-TN-81739	p0130	N81-2283900
NASA-TN-81622	p0061	N81-1726600	NASA-TN-81740	p0101	N81-2324400
NASA-TN-81623	p0091	N81-1244600	NASA-TN-81741	p0039	N81-2208400
NASA-TN-81625	p0081	N81-1743600	NASA-TN-81742	p0102	N81-2341700
NASA-TN-81626	p0131	N81-1690000	NASA-TN-81743	p0102	N81-2341800
NASA-TN-81628	p0124	N81-1281700	NASA-TN-81744	p0100	N81-2247200
NASA-TN-81630	p0033	N81-1307900	NASA-TN-81745	p0003	N81-2102800
NASA-TN-81632	p0049	N81-1310500	NASA-TN-81747	p0045	N81-2117400
NASA-TN-81633	p0014	N81-1305600	NASA-TN-81748	p0103	N81-2360900
NASA-TN-81634	p0051	N81-1506900	NASA-TN-81749	p0016	N81-2205600
NASA-TN-81636	p0081	N81-1743500	NASA-TN-81751	p0126	N81-2083100
NASA-TN-81639	p0075	N81-2131300	NASA-TN-81752	p0101	N81-2324300
NASA-TN-81640	p0097	N81-1439800	NASA-TN-81754	p0105	N81-2760400
NASA-TN-81641	p0096	N81-1346400	NASA-TN-81755	p0062	N81-2219300
NASA-TN-81642	p0080	N81-1335700	NASA-TN-81756	p0103	N81-2361000
NASA-TN-81644	p0003	N81-1301900	NASA-TN-81757	p0049	N81-2516800
NASA-TN-81645	p0096	N81-1346500	NASA-TN-81759	p0017	N81-2508400
NASA-TN-81647	p0080	N81-1335800	NASA-TN-81760	p0071	N81-2128100
NASA-TN-81648	p0075	N81-1524100	NASA-TN-81761	p0017	N81-2507900
NASA-TN-81650	p0003	N81-1497700	NASA-TN-81762	p0103	N81-2349000
NASA-TN-81652	p0080	N81-1536700	NASA-TN-81763	p0100	N81-2247800
NASA-TN-81654	p0097	N81-1546400	NASA-TN-81764	p0132	N81-2492700
NASA-TN-81656	p0016	N81-2107800	NASA-TN-81765	p0102	N81-2327500
NASA-TN-81657	p0015	N81-1605300	NASA-TN-81768	p0130	N81-2283800
NASA-TN-81658	p0057	N81-1439700	NASA-TN-81769	p0106	N81-2852000
NASA-TN-81659	p0081	N81-1647400	NASA-TN-81770	p0039	N81-2018000
NASA-TN-81660	p0107	N81-2056200	NASA-TN-81771	p0106	N81-2852300
NASA-TN-81661	p0115	N81-3065700	NASA-TN-81772	p0068	N81-2526300
NASA-TN-81662	p0015	N81-1605400	NASA-TN-81773	p0054	N81-2623400
NASA-TN-81663	p0015	N81-1605500	NASA-TN-81774	p0040	N81-2617400
NASA-TN-81664	p0057	N81-1546500	NASA-TN-81775	p0100	N81-2247600
NASA-TN-81665	p0091	N81-1649200	NASA-TN-81956	p0003	N81-2102700
NASA-TN-81666	p0015	N81-1605200	NASA-TN-82289	p0138	N81-2797600
NASA-TN-81667	p0098	N81-1657000	NASA-TN-82363	p0011	N81-2506500
NASA-TN-81668	p0074	N81-1524000	NASA-TN-82371	p0107	N81-2852400
NASA-TN-81669	p0037	N81-1712700	NASA-TN-82395	p0098	N81-1658400
NASA-TN-81670	p0044	N81-1612300	NASA-TN-82589	p0102	N81-2345200
NASA-TN-81671	p0009	N81-1602100	NASA-TN-82590	p0045	N81-2514800
NASA-TN-81672	p0074	N81-1523900	NASA-TN-82591	p0054	N81-2519100
NASA-TN-81673	p0075	N81-1642100	NASA-TN-82592	p0140	N81-2698600
NASA-TN-81674	p0091	N81-1649400	NASA-TN-82593	p0046	N81-2515100
NASA-TN-81675	p0092	N81-1740000	NASA-TN-82596	p0046	N81-2514900
NASA-TN-81676	p0052	N81-1621200	NASA-TN-82597	p0104	N81-2362700
NASA-TN-81677	p0132	N81-1992000	NASA-TN-82598	p0106	N81-2851900
NASA-TN-81678	p0052	N81-1621100	NASA-TN-82599	p0046	N81-2515000
NASA-TN-81679	p0053	N81-1927800	NASA-TN-82600	p0101	N81-2308500
NASA-TN-81680	p0079	N81-1642800	NASA-TN-82601	p0105	N81-2453900
NASA-TN-81681	p0075	N81-2131400	NASA-TN-82603	p0066	N81-2523200
NASA-TN-81682	p0071	N81-1638800	NASA-TN-82604	p0103	N81-2362500
NASA-TN-81683	p0061	N81-1726400	NASA-TN-82605	p0055	N81-2823300
NASA-TN-81684	p0055	N81-2823100	NASA-TN-82607	p0104	N81-2453400
NASA-TN-81685	p0038	N81-1922200	NASA-TN-82608	p0018	N81-2614500
NASA-TN-81686	p0055	N81-2725600	NASA-TN-82609	p0103	N81-2361100
NASA-TN-81687	p0105	N81-2548800	NASA-TN-82610	p0103	N81-2362600
NASA-TN-81688	p0052	N81-1816500	NASA-TN-82611	p0004	N81-2503600
NASA-TN-81689	p0081	N81-1839100	NASA-TN-82612	p0130	N81-2283700
NASA-TN-81690	p0081	N81-1839200	NASA-TN-82614	p0083	N81-2752400
NASA-TN-81691	p0085	N81-3155000	NASA-TN-82615	p0140	N81-2499400
NASA-TN-81702	p0037	N81-2017200	NASA-TN-82616	p0132	N81-2580800
NASA-TN-81703	p0038	N81-1921900	NASA-TN-82617	p0017	N81-2508100
NASA-TN-81704	p0101	N81-2318800	NASA-TN-82618	p0040	N81-3018200
NASA-TN-81705	p0045	N81-1717800	NASA-TN-82619	p0101	N81-2320500
NASA-TN-81706	p0039	N81-2112100	NASA-TN-82621	p0132	N81-2492600
NASA-TN-81707	p0009	N81-1907800	NASA-TN-82622	p0083	N81-2645900
NASA-TN-81709	p0062	N81-2027500	NASA-TN-82623	p0083	N81-2752500
NASA-TN-81710	p0130	N81-2577900	NASA-TN-82624	p0104	N81-2453300

NASA-TB-82625	p0046	N81-32194**	NASA-TP-1791	p0075	N81-16417**
NASA-TB-82626	p0055	N81-27259**	NASA-TP-1792	p0076	N81-24387**
NASA-TB-82627	p0017	N81-25083**	NASA-TP-1800	p0040	N81-31282**
NASA-TB-82628	p0063	N81-27277**	NASA-TP-1807	p0117	N81-21685**
NASA-TB-82630	p0054	N81-25189**	NASA-TP-1808	p0082	N81-19458**
NASA-TB-82631	p0091	N81-26492**	NASA-TP-1809	p0102	N81-23486**
NASA-TB-82632	p0054	N81-26236**	NASA-TP-1810	p0016	N81-20076**
NASA-TB-82633	p0054	N81-26235**	NASA-TP-1811	p0038	N81-20173**
NASA-TB-82634	p0126	N81-26094**	NASA-TP-1812	p0053	N81-21193**
NASA-TB-82635	p0076	N81-30390**	NASA-TP-1813	p0061	N81-19300**
NASA-TB-82636	p0120	N81-25658**	NASA-TP-1831	p0072	N81-20352**
NASA-TB-82637	p0105	N81-25487**	NASA-TP-1832	p0072	N81-30360**
NASA-TB-82638	p0108	N81-30563**	NASA-TP-1834	p0038	N81-20176**
NASA-TB-82639	p0064	N81-27526**	NASA-TP-1835	p0053	N81-20245**
NASA-TB-82640	p0017	N81-25082**	NASA-TP-1836	p0071	N81-20359**
NASA-TB-82641	p0018	N81-26146**	NASA-TP-1839	p0076	N81-20389**
NASA-TB-82643	p0040	N81-26173**	NASA-TP-1841	p0076	N81-20388**
NASA-TB-82645	p0083	N81-27523**	NASA-TP-1842	p0016	N81-24065**
NASA-TB-82646	p0139	N81-32087**	NASA-TP-1846	p0005	N81-31129**
NASA-TB-82647	p0084	N81-28444**	NASA-TP-1883	p0063	N81-33293**
NASA-TB-82648	p0106	N81-28522**	NASA-TP-1891	p0063	N81-27282**
NASA-TB-82649	p0084	N81-28443**	NASA-TP-1894	p0076	N81-29384**
NASA-TB-82650	p0094	N81-28517**	NASA-TP-1895	p0120	N81-33838**
NASA-TB-82651	p0090	N81-28458**	NASA-TP-1896	p0066	N81-29246**
NASA-TB-82652	p0017	N81-25080**	NASA-TP-1899	p0063	N81-31364**
NASA-TB-82653	p0107	N81-29528**	NASA-TP-1913	p0127	N81-33947**
NASA-TB-82654	p0012	N81-31190**	NASA-TP-1920	p0005	N81-31128**
NASA-TB-82655	p0004	N81-31126**				
NASA-TB-82656	p0105	N81-27605**	NEAR-TB-227	p0001	N81-22012**
NASA-TB-82657	p0018	N81-27094**				
NASA-TB-82658	p0119	N81-29782**	F-3970-F	p0095	N81-33539**
NASA-TB-82659	p0126	N81-29922**				
NASA-TB-82660	p0085	N81-29440**	PWA-5515-138	p0028	N81-17080**
NASA-TB-82661	p0137	N81-29026**	PWA-5523-92	p0024	N81-12087**
NASA-TB-82662	p0055	N81-29206**	PWA-5550-5-VOL-2-BK-3	p0028	N81-17084**
NASA-TB-82663	p0018	N81-27095**	PWA-5550-37	p0026	N81-13057**
NASA-TB-82664	p0143	N81-29063**	PWA-5550-50-VOL-1	p0028	N81-17081**
NASA-TB-82666	p0126	N81-30905**	PWA-5550-50-VOL-2-BK-1	p0028	N81-17082**
NASA-TB-82667	p0108	N81-31627**	PWA-5550-50-VOL-2-BK-2	p0028	N81-17083**
NASA-TB-82668	p0064	N81-29438**	PWA-5550-50-VOL-3-BK-1	p0028	N81-17085**
NASA-TB-82669	p0084	N81-29439**	PWA-5550-50-VOL-3-BK-2	p0028	N81-17086**
NASA-TB-82670	p0132	N81-30973**	PWA-5594-122	p0026	N81-15002**
NASA-TB-82672	p0049	N81-31308**	PWA-5604-31	p0059	N81-19277**
NASA-TB-82673	p0132	N81-32026**	PWA-5635-43	p0129	N81-15769**
NASA-TB-82674	p0066	N81-31380**	PWA-5684-19	p0027	N81-17079**
NASA-TB-82675	p0092	N81-33497**	PWA-5697-29	p0067	N81-19316**
NASA-TB-82676	p0004	N81-27042**	PWA-5755	p0027	N81-15006**
NASA-TB-82677	p0004	N81-27041**				
NASA-TB-82678	p0004	N81-28054**	QR-1	p0112	N81-18497**
NASA-TB-82679	p0126	N81-30906**	QR-1	p0113	N81-22473**
NASA-TB-82680	p0077	N81-30391**	QR-3	p0111	N81-17527**
NASA-TB-82681	p0106	N81-27606**	QR-4	p0112	N81-18494**
NASA-TB-82682	p0004	N81-28053**	QR-5	p0112	N81-19573**
NASA-TB-82683	p0035	N81-30172**	QR-5	p0113	N81-21547**
NASA-TB-82684	p0018	N81-28095**	QR-6	p0113	N81-21536**
NASA-TB-82687	p0056	N81-33273**	QR-7	p0113	N81-22475**
NASA-TB-82688	p0126	N81-30907**				
NASA-TB-82690	p0126	N81-31956**	REPT-2-53020/QR-52578	p0033	N81-21106**
NASA-TB-82693	p0036	N81-32187**	REPT-31-1653	p0140	N81-20958**
NASA-TB-82694	p0127	N81-31957**	REPT-80-9B6-NARED-B4	p0112	N81-18494**
NASA-TB-82696	p0019	N81-31195**	REPT-80-9B6-NARED-B5	p0112	N81-19573**
NASA-TB-82697	p0127	N81-32968**	REPT-34037	p0073	N81-16389**
NASA-TB-82700	p0065	N81-33484**	REPT-61051	p0113	N81-22473**
NASA-TB-82701	p0108	N81-33601**				
NASA-TB-82702	p0107	N81-30522**	RI/RD80-222	p0088	N81-17437**
NASA-TB-82703	p0019	N81-30130**	RI/RD80-237	p0042	N81-21125**
NASA-TB-82712	p0127	N81-32964**				
NASA-TB-82714	p0063	N81-32269**	RSC-3697-6	p0048	N81-21130**
NASA-TB-82716	p0127	N81-32565**				
NASA-TB-82717	p0090	N81-33492**	R75ARG026-VOL-1	p0030	N81-22052**
NASA-TB-82720	p0108	N81-32608**	R78ARG612	p0027	N81-15005**
NASA-TB-84011	p0138	N81-32081**	R79ARG123	p0029	N81-17087**
				R79ARG274	p0030	N81-22051**
NASA-TP-1178	p0013	N81-11037**	R79ARG623	p0029	N81-18056**
NASA-TP-1708	p0013	N81-11038**	R80-900007-12	p0007	N81-16976**
NASA-TP-1710	p0082	N81-20423**	R80-954440-17	p0067	N81-12255**
NASA-TP-1716	p0013	N81-12089**	R80ARG312-VOL-2	p0027	N81-16051**
NASA-TP-1722	p0016	N81-19121**	R80ARG313-VOL-3	p0024	N81-12086**
NASA-TP-1728	p0060	N81-11214**	R80ARG369	p0129	N81-17846**
NASA-TP-1731	p0080	N81-14322**	R80ARG429	p0027	N81-15004**
NASA-TP-1753	p0091	N81-11417**	R80ARG458	p0048	N81-17434**
NASA-TP-1754	p0013	N81-11039**	R81ARG219	p0027	N81-17078**
NASA-TP-1755	p0052	N81-16210**	R81ARG311	p0030	N81-22053**
NASA-TP-1756	p0060	N81-14079**				
NASA-TP-1757	p0071	N81-11315**	SAR PAPER 801116	p0021	N81-34152**
NASA-TP-1768	p0066	N81-24283**	SAR PAPER 801118	p0021	N81-34154**
NASA-TP-1772	p0004	N81-22017**	SAR PAPER 801119	p0021	N81-34155**
NASA-TP-1780	p0015	N81-16050**	SAR PAPER 801120	p0021	N81-34156**
NASA-TP-1781	p0053	N81-19273**	SAR PAPER 801122	p0031	N81-34158**

SAR PAPER 801135	p0021	A01-34166*	US-PATENT-APPL-SN-915050	p0096	H01-12542*
SAR PAPER 801137	p0021	A01-34168*	US-PATENT-APPL-SN-916654	p0018	H01-29129*
SAR PAPER 801138	p0021	A01-34169*	US-PATENT-APPL-SN-929084	p0081	H01-19455*
SAR PAPER 801140	p0022	A01-34170*	US-PATENT-APPL-SN-961832	p0083	H01-24442*
SAR PAPER 801154	p0022	A01-34177*	US-PATENT-APPL-SN-964754	p0107	H01-29524*
SAR PAPER 810150	p0079	A01-41732*	US-PATENT-APPL-SN-971473	p0044	H01-29160*
SAR PAPER 810624	p0023	A01-42778*	US-PATENT-APPL-SN-971475	p0062	H01-24257*
SDL-80-2122-13F	p0026	H01-15003*	US-PATENT-CLASS-44-78	p0066	H01-14103*
SN-8342-P	p0065	H01-10169*	US-PATENT-CLASS-55-2	p0066	H01-14103*
SN-80-00477	p0094	H01-13425*	US-PATENT-CLASS-60-39.06	p0018	H01-29129*
SN-LO-00476	p0094	H01-13427*	US-PATENT-CLASS-60-39.24	p0015	H01-19115*
SN-LO-00484	p0095	H01-13431*	US-PATENT-CLASS-60-204	p0104	H01-24519*
SN-LO-00485	p0094	H01-13426*	US-PATENT-CLASS-60-226B	p0015	H01-19116*
SNC-80-TR-62	p0088	H01-13359*	US-PATENT-CLASS-60-236	p0015	H01-19116*
SRI-5413	p0073	H01-19395*	US-PATENT-CLASS-60-238	p0015	H01-19116*
SSS-B-81-4798	p0033	H01-27169*	US-PATENT-CLASS-60-239	p0015	H01-19116*
STDR-80-22	p0109	H01-12546*	US-PATENT-CLASS-60-267	p0104	H01-24519*
TES484-66-79	p0113	H01-22467*	US-PATENT-CLASS-60-726	p0018	H01-29129*
TR-2	p0070	H01-10242*	US-PATENT-CLASS-60-737	p0018	H01-29129*
TRN-8R-8135	p0047	H01-10112*	US-PATENT-CLASS-62-12	p0066	H01-14103*
TRN-29922-6001-BU-01	p0072	H01-10301*	US-PATENT-CLASS-62-18	p0066	H01-14103*
TRN-29922-6001-BU-01-VOL-2	p0072	H01-11314*	US-PATENT-CLASS-62-40	p0066	H01-14103*
UDR-TR-80-99-VOL-1	p0033	H01-12135*	US-PATENT-CLASS-62-47	p0066	H01-14103*
UDR-TR-80-100-VOL-2	p0033	H01-12136*	US-PATENT-CLASS-136-249	p0096	H01-12542*
UDR-TR-80-101-VOL-3	p0033	H01-12137*	US-PATENT-CLASS-136-291	p0096	H01-12542*
UDR-TR-80-102-VOL-4	p0133	H01-12138*	US-PATENT-CLASS-137-15.1	p0014	H01-14999*
US-PATENT-APPL-SN-009887	p0066	H01-14103*	US-PATENT-CLASS-149-1	p0066	H01-14103*
US-PATENT-APPL-SN-027557	p0061	H01-19256*	US-PATENT-CLASS-156-292	p0045	H01-17170*
US-PATENT-APPL-SN-032307	p0104	H01-24519*	US-PATENT-CLASS-156-344	p0066	H01-14103*
US-PATENT-APPL-SN-038980	p0014	H01-14999*	US-PATENT-CLASS-181-214	p0014	H01-14999*
US-PATENT-APPL-SN-061555	p0107	H01-29524*	US-PATENT-CLASS-204-2.1	p0107	H01-29524*
US-PATENT-APPL-SN-065676	p0096	H01-12542*	US-PATENT-CLASS-204-192B	p0081	H01-19455*
US-PATENT-APPL-SN-070771	p0060	H01-17260*	US-PATENT-CLASS-228-116	p0081	H01-19455*
US-PATENT-APPL-SN-085779	p0054	H01-25188*	US-PATENT-CLASS-228-118	p0045	H01-17170*
US-PATENT-APPL-SN-102004	p0083	H01-26447*	US-PATENT-CLASS-228-118	p0046	H01-26179*
US-PATENT-APPL-SN-113014	p0062	H01-24257*	US-PATENT-CLASS-228-170	p0045	H01-17170*
US-PATENT-APPL-SN-122967	p0046	H01-26179*	US-PATENT-CLASS-228-174	p0045	H01-17170*
US-PATENT-APPL-SN-134855	p0104	H01-24521*	US-PATENT-CLASS-228-190	p0045	H01-17170*
US-PATENT-APPL-SN-145271	p0044	H01-25160*	US-PATENT-CLASS-228-190	p0046	H01-26179*
US-PATENT-APPL-SN-191746	p0052	H01-16209*	US-PATENT-CLASS-228-205	p0081	H01-19455*
US-PATENT-APPL-SN-199769	p0051	H01-12211*	US-PATENT-CLASS-239-127.1	p0104	H01-24519*
US-PATENT-APPL-SN-200634	p0074	H01-12363*	US-PATENT-CLASS-260-17.40C	p0044	H01-29160*
US-PATENT-APPL-SN-210632	p0060	H01-16329*	US-PATENT-CLASS-260-33.4B	p0061	H01-19296*
US-PATENT-APPL-SN-210587	p0068	H01-16327*	US-PATENT-CLASS-260-37EP	p0060	H01-17260*
US-PATENT-APPL-SN-219677	p0098	H01-16528*	US-PATENT-CLASS-260-326B	p0060	H01-17260*
US-PATENT-APPL-SN-219678	p0058	H01-16529*	US-PATENT-CLASS-260-326S	p0060	H01-17260*
US-PATENT-APPL-SN-220212	p0071	H01-16384*	US-PATENT-CLASS-261-28	p0018	H01-29129*
US-PATENT-APPL-SN-229233	p0062	H01-24265*	US-PATENT-CLASS-264-104	p0062	H01-24257*
US-PATENT-APPL-SN-229693	p0049	H01-19245*	US-PATENT-CLASS-264-104	p0044	H01-29160*
US-PATENT-APPL-SN-232577	p0099	H01-19561*	US-PATENT-CLASS-264-105	p0062	H01-24257*
US-PATENT-APPL-SN-236790	p0100	H01-22466*	US-PATENT-CLASS-277-96	p0083	H01-24442*
US-PATENT-APPL-SN-236887	p0083	H01-22360*	US-PATENT-CLASS-277-153	p0083	H01-26447*
US-PATENT-APPL-SN-242795	p0062	H01-22190*	US-PATENT-CLASS-277-193	p0083	H01-26447*
US-PATENT-APPL-SN-243682	p0076	H01-22310*	US-PATENT-CLASS-363-27	p0096	H01-12542*
US-PATENT-APPL-SN-246772	p0054	H01-24230*	US-PATENT-CLASS-363-60	p0096	H01-12542*
US-PATENT-APPL-SN-251009	p0071	H01-24348*	US-PATENT-CLASS-363-147	p0096	H01-12542*
US-PATENT-APPL-SN-264378	p0046	H01-27198*	US-PATENT-CLASS-364-106	p0015	H01-19115*
US-PATENT-APPL-SN-264380	p0105	H01-27598*	US-PATENT-CLASS-364-431	p0015	H01-19115*
US-PATENT-APPL-SN-266255	p0049	H01-26203*	US-PATENT-CLASS-423-648B	p0066	H01-14103*
US-PATENT-APPL-SN-272152	p0106	H01-27616*	US-PATENT-CLASS-427-221	p0061	H01-19296*
US-PATENT-APPL-SN-272233	p0106	H01-27615*	US-PATENT-CLASS-427-379	p0061	H01-19296*
US-PATENT-APPL-SN-272234	p0063	H01-27279*	US-PATENT-CLASS-428-139	p0044	H01-29160*
US-PATENT-APPL-SN-272406	p0105	H01-27597*	US-PATENT-CLASS-428-471	p0054	H01-25188*
US-PATENT-APPL-SN-272407	p0118	H01-27786*	US-PATENT-CLASS-428-632	p0054	H01-25188*
US-PATENT-APPL-SN-282298	p0107	H01-29531*	US-PATENT-CLASS-428-678	p0054	H01-25188*
US-PATENT-APPL-SN-672219	p0083	H01-26447*	US-PATENT-CLASS-428-679	p0054	H01-25188*
US-PATENT-APPL-SN-676432	p0066	H01-14103*	US-PATENT-CLASS-428-680	p0054	H01-25188*
US-PATENT-APPL-SN-741056	p0015	H01-19116*	US-PATENT-CLASS-429-27	p0062	H01-24257*
US-PATENT-APPL-SN-752050	p0015	H01-19115*	US-PATENT-CLASS-429-27	p0044	H01-29160*
US-PATENT-APPL-SN-837794	p0066	H01-14103*	US-PATENT-CLASS-429-28	p0062	H01-24257*
US-PATENT-APPL-SN-856462	p0104	H01-24519*	US-PATENT-CLASS-429-28	p0044	H01-29160*
US-PATENT-APPL-SN-893857	p0045	H01-17170*	US-PATENT-CLASS-429-94	p0104	H01-24521*
US-PATENT-APPL-SN-893857	p0046	H01-26179*	US-PATENT-CLASS-429-120	p0104	H01-24521*
US-PATENT-APPL-SN-909235	p0015	H01-19115*	US-PATENT-CLASS-429-139	p0062	H01-24257*
US-PATENT-APPL-SN-909608	p0015	H01-19116*	US-PATENT-CLASS-429-160	p0104	H01-24521*
			US-PATENT-CLASS-429-164	p0104	H01-24521*
			US-PATENT-CLASS-429-249	p0062	H01-24257*
			US-PATENT-CLASS-429-249	p0044	H01-29160*
			US-PATENT-CLASS-429-253	p0062	H01-24257*
			US-PATENT-CLASS-429-253	p0044	H01-29160*
			US-PATENT-CLASS-431-2	p0018	H01-29129*
			US-PATENT-CLASS-525-56	p0044	H01-29160*
			US-PATENT-CLASS-525-61	p0062	H01-24257*
			US-PATENT-CLASS-525-61	p0044	H01-29160*
			US-PATENT-CLASS-528-118	p0060	H01-17260*
			US-PATENT-CLASS-528-322	p0060	H01-17260*
			US-PATENT-CLASS-528-353	p0061	H01-19296*
			US-PATENT-CLASS-538-117	p0060	H01-17260*

REPORT/ACCESSION NUMBER INDEX

ORIGINAL PAGE IS
OF POOR QUALITY

US-PATENT-4,077,768	p0066	NO 1-14103*
US-PATENT-4,189,918	p0018	NO 1-29129*
US-PATENT-4,192,910	p0107	NO 1-29524*
US-PATENT-4,193,827	p0066	NO 1-14103*
US-PATENT-4,199,937	p0104	NO 1-24519*
US-PATENT-4,211,354	p0045	NO 1-17170*
US-PATENT-4,211,354	p0046	NO 1-26179*
US-PATENT-4,212,477	SCC63	NO 1-26447*
US-PATENT-4,217,633	p0096	NO 1-12542*
US-PATENT-4,220,171	p0014	NO 1-14999*
US-PATENT-4,229,196	p0066	NO 1-14103*
US-PATENT-4,242,864	p0015	NO 1-19116*
US-PATENT-4,244,853	p0061	NO 1-19296*
US-PATENT-4,244,857	p0060	NO 1-17240*
US-PATENT-4,245,449	p0104	NO 1-24519*
US-PATENT-4,245,768	p0081	NO 1-19455*
US-PATENT-4,249,238	p0015	NO 1-19116*
US-PATENT-4,255,495	p0054	NO 1-25180*
US-PATENT-4,260,164	p0083	NO 1-24442*
US-PATENT-4,262,044	p0104	NO 1-24521*
US-PATENT-4,262,067	p0062	NO 1-24257*
US-PATENT-4,266,788	p0063	NO 1-26447*
US-PATENT-4,267,953	p0046	NO 1-26179*
US-PATENT-4,270,584	p0107	NO 1-29524*
US-PATENT-4,272,470	p0044	NO 1-29160*
USAAVRA DCOR-TR-81-B-1	z0003	NO 1-21027*0
UTC-PCR-1333	p0109	NO 1-10517*0